ENGINEERING GEOLOGY PRACTICE IN NORTHERN CALIFORNIA

Edited by

Horacio Ferriz and Robert Anderson

2001

BULLETIN 210

SPECIAL PUBLICATION 12

ENGINEERING GEOLOGY PRACTICE IN NORTHERN CALIFORNIA

ISBN 0-9723388-0-2

ENGINEERING GEOLOGY PRACTICE IN NORTHERN CALIFORNIA

Edited by
Horacio Ferriz and Robert Anderson

2001

BULLETIN 210

SPECIAL PUBLICATION 12


ASSOCIATION OF ENGINEERING
AEG
GEOLOGISTS

CONTENTS

4....FACILITIES

5....TUNNELS AND TRANSPORTATION

6....RESIDENTIAL

7....KALEIDOSCOPE


ASSOCIATION OF ENGINEERING
AEG
GEOLOGISTS

FOREWORD

In the year 2000 California entered the third millennium and celebrated its one hundred and fiftieth year as a state. These milestones came at a time of significant surges in population growth and economic development, so the state is now confronted with unprecedented opportunities and challenges. It is an exciting time for the earth sciences in general, and for engineering geology in particular, for now more than ever we should exercise wisely our stewardship of the resources of the Golden State. In such a context, the Department of Conservation's Division of Mines and Geology is pleased to collaborate with the Association of Engineering Geologists in the publication of this important volume. All of those associated with its preparation hope that it will assist the engineering geology community in using the latest understanding of earth sciences and technology in its vital role to assure the general well being and safety of California's citizens.

California's geologic environment is and has been the basis for many of its opportunities. Gold, of course, was the initial stimulant to development, and mineral resources remain a cornerstone of our economy (the state regularly ranks among the top three for value of annual mineral production and was number one in the nation in 1999). In addition, climate, soil and water contribute to the state's preeminence in agriculture, and have attracted a host of industries and a vibrant population. However, California's geologic characteristics also contribute to many of the challenges that confront the state, generally arising from human activities competing for limited resources, such as water, and from exposure of the population to natural hazards. The challenges related to water availability, pollution control, toxic mineral occurrences (e.g., asbestos), earthquake and volcanic hazards, and landslide risk exposure are arguably greater in California than in any other part of our nation. They also make California an exhilarating place to practice engineering geology. I have no doubt that this volume will provide professionals with useful overviews of new developments in engineering geology technologies, and with a timely update of the efforts currently under way to characterize geologic hazards in Northern California. It is directed to both the new generation of engineering geologists, and the current practitioners of a profession that gallantly merges technology, social conscience, natural science and art. May it continue to thrive and prosper for the benefit of the residents of the Golden State.

JAMES F. DAVIS
CALIFORNIA STATE GEOLOGIST
DEPARTMENT OF CONSERVATION
DIVISION OF MINES AND GEOLOGY


ASSOCIATION OF ENGINEERING
AEG
GEOLOGISTS

PREFACE

Shortly before the turn of the millennium, a group of engineering geologists affiliated to the Sacramento and San Francisco sections of the Association of Engineering Geologists thought the time was ripe for a volume that would showcase our accomplishments as a profession. *Engineering Geology Practice in Northern California* arose out of that visionary idea, thousands of hours of voluntary work, the generous support of individual practitioners and local engineering firms, and the patient commitment of the Association of Engineering Geologists and the California Division of Mines and Geology.

Our hope in culminating this effort is that this collection of case studies, review papers, and how-to papers will be a useful summary of the state-of-practice of engineering geology in Northern California, and will set fruitful directions for future work. We also hope it will be a lasting gift of our generation to young engineering geologists, geologists who are not familiar with Northern California, civil engineers, law practitioners, educators, and interested citizens.

HONOR WHERE HONOR IS DUE

It is hard to describe our emotions now that this monumental project is done. Celebration and pats on the back are in order, but before we can relax and rest on our laurels it is well to remember and acknowledge the generous help of the many individuals and organizations that in one way or another made this project possible.

A Golden State partnership

It is with great pride that this volume carries the logos of two great organizations: The Association of Engineering Geologists and the California Division of Mines and Geology! AEG took care of all the editorial work, whereas CDMG performed the typesetting and final publication of the book.

The Association of Engineering Geologists started in June 1957, when twelve local engineering geologists met in Sacramento to discuss the need for a collegial society in the specific field of engineering geology. During the next eight months this group of founding members set up the framework of AEG by formulating the aims of the organization and membership qualifications. The association started recruiting members around three sections (Sacramento, San Francisco and Los Angeles) in 1958, and was formally incorporated according to the laws of the State of California on June 19, 1960. And the rest, as they say, belongs to history!

At a more local level, this book would not have been possible without the support of the Sacramento and San Francisco sections of AEG, to a large extent through the enthusiastic efforts of Chairs David Bieber (AEG Sacramento 1996-1998), Julia Turney (AEG Sacramento 1998-2000), Robert Anderson (AEG Sacramento 2000-2002), Roy Kroll (AEG Sacramento 2002-2004), and Gary Pishke (AEG San Francisco 1998-2000).

The California Division of Mines and Geology is a branch of the Department of Conservation, and traces its inception back more than 117 years. One of the oldest geological surveys in the United States, the CDMG has a variety of programs important to the future of California's environment, economy, and public safety. For example, CDMG generates maps related to geologic hazards such as earthquake faults and landslide-prone areas, and maps and interprets the availability of the state's mineral resources to assist in local land-use planning. It is also committed to the dissemination of geologic knowledge about California through publications such as the one you hold in your hands.

Our generous sponsors

The production of this volume was far from trivial, so our first accolade goes to the individuals and companies that helped fund the effort. We gratefully

list their names here, in the order in which they approached us, and in scanning the list realize that it could very well read as a who-is-who of geological engineering in Northern California:

- Youngdhal Consulting Group
- Horacio Ferriz, Ph.D.
- Bob Anderson
- Betsy Mathieson
- Louis Richardson
- Norman Janke
- Terrasearch
- Taber Consultants
- John Williams, Ph.D.
- AEG Engineering Geology Foundation
- San Jose State University
- Cotton Shires and Associates
- Wallace-Kuhl & Associates
- REG Review
- Gary Pischke
- Krazan & Associates
- Pacific Gas & Electric
- Dames & Moore, Sacramento
- Exponent Failure Analysis
- GEOCON
- Soil Tectonics
- Julia Turney
- URS Greiner Woodward Clyde
- Richard Thompson
- Jay Smith
- Roberta K. Smith
- EARTHTEC, Ltd.
- Redwood Geotechnical
- Robert H. Sydnor
- Cleary Consultants
- Christopher Palmer
- Glen Romig
- Kleinfelder, Inc.
- Roy C. Kroll

The Editorial Board

This volume includes 50 papers in every possible variety of engineering geology work, and the editorial work that went into putting all these papers into a coherent whole was a monumental task that could not have been accomplished without the dedication of a first rate Editorial Board. Everybody did a little bit of everything, but for the sake of associating a name with a field we present here a simplified list of the members of the Board, with our deep felt expression of gratitude for their time and effort. In alphabetical order:

- Bob Anderson, Chief Editor and Section Editor for Facilities
- Dave Bieber, Sub-section Editor for Facilities
- Richard Escandon, Section Editor for Tunnels
- Horacio Ferriz, Chief Editor and Section Editor for Kaleidoscope
- Charlene Herbst, Sub-section Editor for Facilities
- Roy Kroll, Section Editor for Residential
- Bill Lettis, Section Editor for Faults and Seismicity
- Steve Stryker, English Editor
- Gary Taylor, Production Editor
- Joan Van Velsor, Section Editor for Landslides

Our peer reviewers

Aside from the writing of the manuscript, the technical (critical) review is possibly the most important step in the transformation of research results into an effective, informative and readable paper. Review is at best a thankless job, done by people who would much rather pursue original research than review manuscripts by others, so it is with great pleasure that we praise our superb cadre of peer reviewers for their professional, disinterested, and generous help to the technical content of this volume. A standing ovation to:

- Lee Abramson
- Bob Anderson
- Art Arnold
- John Baldwin
- Dave Bieber
- Richard Blaugher
- Dave Boden
- John Boni
- Manuel Bonilla
- Glenn Borchardt
- Doug Boyer
- Bill Bryant
- Reid Buell
- Roland Burgman
- Gary Carver
- Kerry Cato
- Eric Chase
- Lloyd Cluff
- Bob Coleman
- Mark DeLisle
- John Dilles

- John Duffy
- John Edwards
- Richard Ely
- Horacio Ferriz
- Tom Flynn
- Bill Fraser
- Anita Grunder
- Lynn Giraudo
- Dave Gius
- Frank Glick
- Earl Hagadorn
- Dave Hayes
- Suzanne Hecker
- Bruce Hilton
- Dick Hilton
- Susan Hodges
- Eric Hubbard
- Robert Joslin
- John Juhrend
- Bill Kane
- George Kiersch
- Steve Klein
- Frank Kresse
- Roy Kroll
- Alan Kropp
- Ellis L. Krinitzky
- Bruce Lander
- Jim Lienkaemper
- Mike Majchrzak
- Tim McCrinck
- Elizabeth Miller
- Eldridge Moores
- Jim Morris
- Dennis Ostrom
- Jim Parsons
- Mark Petersen
- Richard Proctor
- Victor Romero
- Mark Schmoll
- Dave Sederquist
- Roy Shlemon
- David Simpson
- Pat Stevens
- Bob Tepel
- Joan Van Velsor
- John Williams
- Chris Wills
- Chuck Winterhalder
- Rob Witter
- Les Youd

The authors

And let us not forget the authors, who as a group are one of the most gifted and hard working group of professionals we have had the honor to work with. As luck would have it we called on their expertise at a time when construction was booming in California, so most of them worked on their papers late at night, after putting a full day's work at the office. And yet, they did a humdinger of a job!

We, the Chief Editors, want to take this opportunity to thank you all for all that hard work, apologize for being hard on your backs (then again, for us it was like herding cats!), and express our wishes that we will continue the professional relationship that has started so auspiciously. Thanks!

The production team

We have learned that putting together a book is like putting together a play. The end result is beautiful, and the actors deservedly take their bows. But there are many unsung heroes backstage that did a tremendous amount of work but never made it to the limelight. Our final salvo thus goes to the many secretaries that typed and re-typed the manuscripts, the artists that drafted the figures, Steve Stryker from California State University Stanislaus—our English Editor—who read and edited well over 1,200 manuscript pages, Gary Taylor from CDMG—our Production Editor— who coordinated the actual putting together of the book, Jim Williams, Lena Tabilio Dida, Jeff Tambert, and the rest of the production staff of CDMG for endless hours in front of the computer screen, and The University of California Press for their excellent work in printing the book.

IN RETROSPECT

The last 25 years have been an "interesting" time for California. We experienced explosive urban growth as high technology industries blossomed, environmental conscience rose to unprecedented levels, and we suddenly realized that we had inherited a piecemeal infrastructure that needed update and retrofit. Projects proposed to cope with these challenges ranged from the heroic to the comedic, and from the visionary to the tragic. Many of the success stories are chronicled in the pages of this book, but we are still trying to forget the wasted efforts to reclaim the Salton Sea, to build a nuclear waste repository, or to dam San Francisco Bay. We

have also learned bitter lessons from the collapse of the Oakland Freeway and the Bay Bridge, and from the loss that floodplain communities experienced during the 1996-1997 floods.

But *Engineering Geology Practice in Northern California* is more than a look into the past. The topics are so varied, and the approaches to the solution of problems are so imaginative, that we believe it will be a solid foundation on which the next generation of California geologists can build for the future.

THE FUTURE

The next ten years will probably see ebb and flow in the profession, closely linked to the increase in the population of the Golden State and the fluctuations of its economy. We will probably be called upon to build larger residential developments, develop new utility networks, and protect a larger population against the ravages of earthquakes, landslides and erosion. And each of these areas will pose new challenges and paradigms.

Imagine for a moment what the state will look like in 25 years. Estimates vary, but there is little doubt that services will have to be provided for 10 to 20 million additional people. Houses will have to be built for them, so many young engineering geologists will devote their professional lives to support residential construction, struggling with problems associated to natural asbestos, large scale grading, and sewage disposal into the geologic environment.

Water supply will be a second major area of employment. The time for construction of large dams or water conveyance projects may be past, but many young engineering geologists will probably learn their craft working for the Cal-Fed and Salinas Valley water projects, or in the retrofit and expansion of existing reservoirs and canals. The future is also promising for hydrogeologists, who will face the exciting challenge of managing the extensive use of a vital but finite resource.

In the area of utility networks, we understand that superconductor technologies are just around the corner, which may well lead to a complete restructuring of the power distribution networks. Engineering geologists will no doubt be called upon to site new power plants, perform foundation studies for new types of heavy equipment, and assure the reliability of power supply by honing existing approaches to natural hazard mitigation.

The assessment of earthquake hazards will undoubtedly continue to be a high priority for Northern California, and we forecast that the trend established over the last five years will continue into the future, as more and more engineering geologists become engaged in "earthquake geology". Much remains to be done in terms of detailed fault mapping, dating of soils exposed in trenches, and characterization of the seismogenic behavior of our myriad of faults.

Other geologic hazards, such as landsliding and erosion, will continue to grace the golden slopes of California, and there is little doubt that many young engineering geologists will cut their teeth helping homeowners protect their homes against slumps, mudflows, or coastal erosion. In this regard, we personally hope that practitioners will become more involved in public education, so that we see more preventive maintenance and less emergency "surgery".

In closing, we want to express our heartfelt belief that engineering geology has a brilliant future in California. Here's to a hard, fulfilling and noble profession!

HORACIO FERRIZ ,
ROBERT ANDERSON

GEOLOGY OF NORTHERN CALIFORNIA: AN OVERVIEW

DEBORAH R. HARDEN[1]

INTRODUCTION

Northern California's plate-tectonic setting has been largely responsible for shaping its geology. Since the early Mesozoic, an active plate boundary has existed along what is now California. Active subduction along the western edge of the North American plate resulted in the accretion of multiple terranes and formation of the Sierran arc during Jurassic and Cretaceous time. Beginning about 28 million years ago, development of the transform boundary between the Pacific and North American plates produced the active faults of the modern San Andreas fault system (Figure 1; Atwater et al., 1970). Growth of the transform boundary resulted in the northward migration of subduction and active volcanism into northern California during late Cenozoic time. The current position of the Mendocino triple junction limits subduction to the northwestern corner of California (Figure 2).

Plate tectonics is largely responsible for some obviously unwelcome aspects of life in California today. Earthquakes and landslides, geologic hazards directly tied to northern California's active tectonic setting, are discussed in detail in later articles in this volume. Less direct consequences of the tectonic setting of northern California with respect to engineering geology include: abundant landslide-prone, fault-controlled belts of serpentinite; weakly consolidated marine units uplifted in steep mountains; and high-gradient stream channels cut in easily eroded bedrock types normally associated with meandering floodplain settings.

[1]Department of Geology
San José State University
San José, CA 95192-0102
harden@geosun1.sjsu.edu

The purpose of this article is to summarize the geologic history of northern California and the tectonic factors, which have controlled this history, rather than presenting a systematic discussion of the geology of individual provinces or geologic units. The geology of northern California has been summarized in several excellent previous works, and although some of these publications pre-date plate tectonics theory, they provide invaluable descriptions of individual formations and localities, including much information that is important to engineering geologists. For the engineering geologist seeking an overall understanding of northern California geology, several are recommended, together with their comprehensive reference lists: Bailey (1966), Burchfiel et al. (1992), Ernst (1981), Wahrhaftig and Sloan (1989), and Wallace (1990). Readers will also find useful the California geologic map sheets and their cited sources (California Dept. of Conservation, scale 1:250,000) and the California fault map (Jennings, 1994). General overviews of California geology, written for beginning geologists, are provided by Harden (1998) and by Norris and Webb (1990). Items of topical and local interest to engineering geologists are discussed in the journal *California Geology*. A newly published volume (Moores et al., 1999) provides a compilation of the development of geologic concepts in California.

PALEOZOIC CALIFORNIA

The North American passive margin

During much of Paleozoic time, the western margin of North America was a stable continental platform. For about 350 million years, thousands of meters of Paleozoic sediments, mainly carbonates, accumulated in a shelf environment (Ernst, 1981; Cooper and Stevens, 1991; Burchfiel et al., 1992). Paleozoic rocks deposited along the passive margin are well exposed today in Nevada and in California's Basin and Range and Mojave Desert provinces. In northern California they are also preserved as meta-

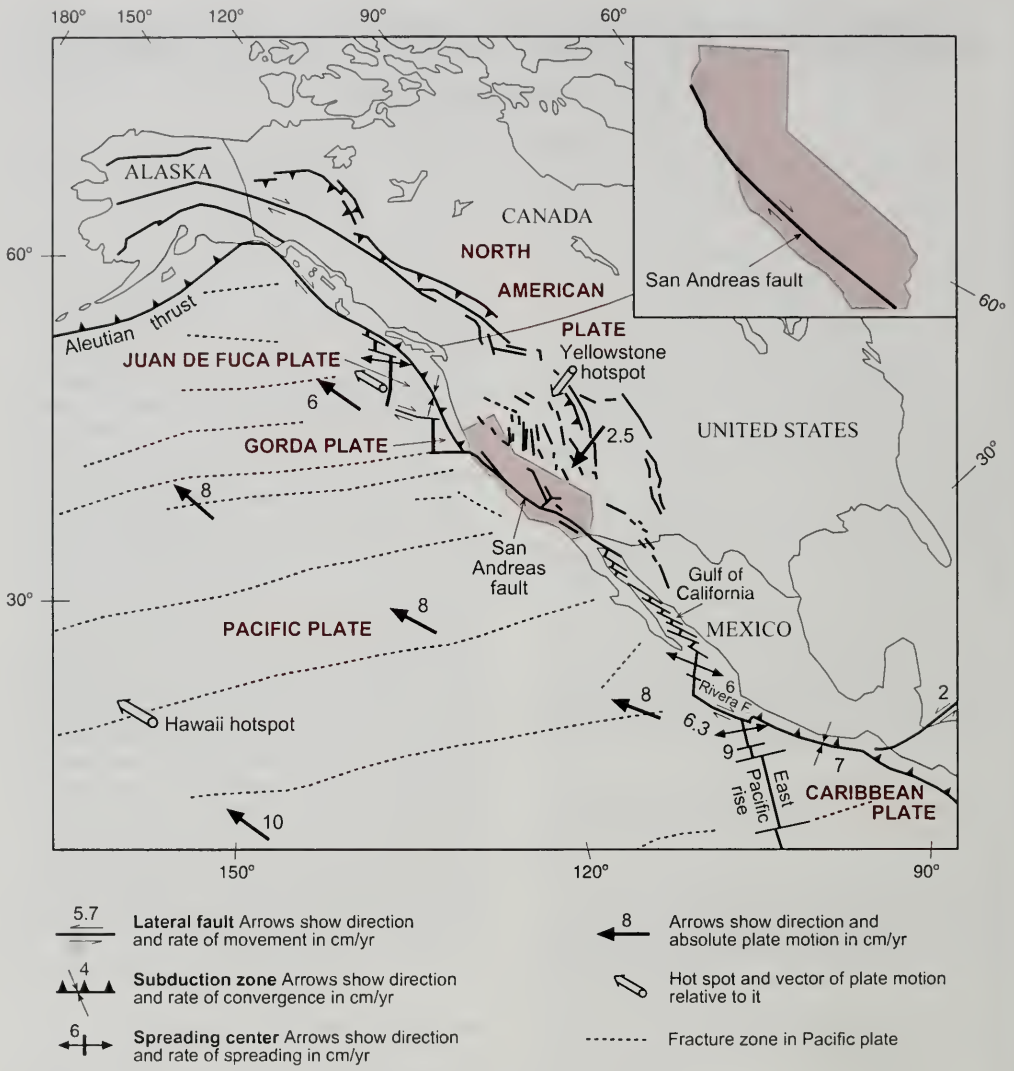

Figure 1. Major plate-tectonic features of western North America (Harden, 1998; modified from Wallace, 1990).

morphic roof pendants and septa of marble, quartzite, slate, and hornfels in the eastern Sierra Nevada (Figure 3). Localities where remnants of Paleozoic continental-margin rocks are present in the Sierra Nevada include the Saddlebag Lake, Mt. Morrison, and Bishop Creek roof pendants. Recent mapping and correlation of the eastern Sierran roof pendants by Stevens and Greene (1999) have identified them as the Morrison block, a fault-bounded block of Paleozoic continental-margin rocks with a common internal stratigraphy. Based on fossil evidence, the eastern Sierran roof pendants range in age

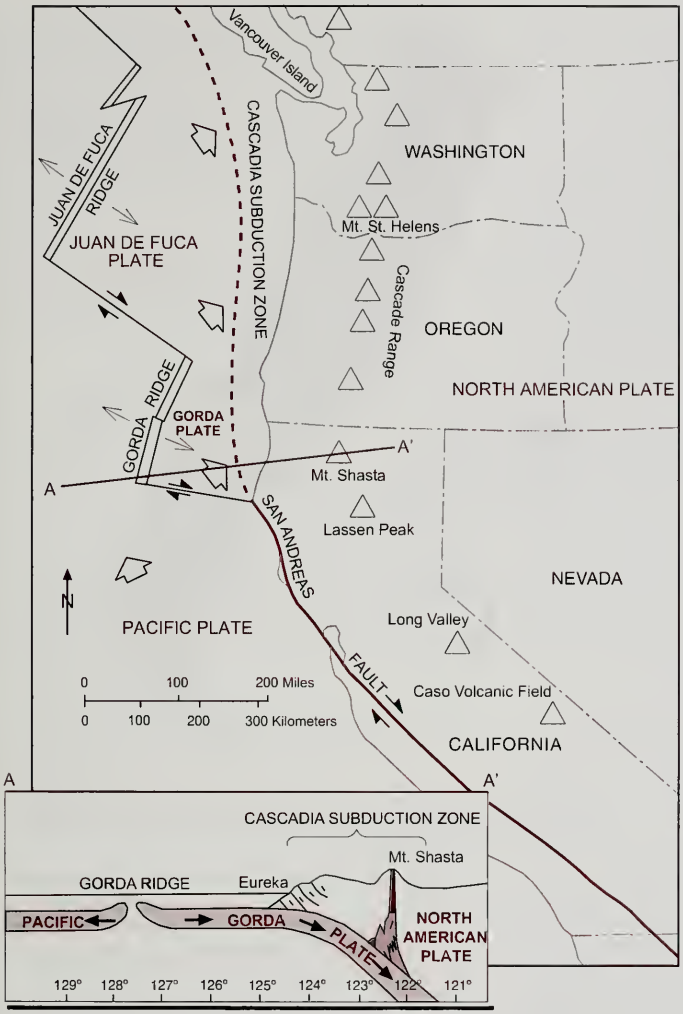

Figure 2. Map and cross section showing tectonic setting of northern California (Dengler et al.,1992).

from middle (?) Cambrian to middle (?) Permian. Although formed along the Paleozoic passive margin of North America, the Morrison block rocks were deposited in deeper-water environments than those exposed in the Inyo Mountains.

Paleozoic California's relatively quiet early tectonic setting was increasingly interrupted as the era progressed, most notably during the Mississippian Antler orogeny and the late Paleozoic Sonoma orogeny, which are recorded by Paleozoic rocks in western Nevada and in the Saddlebag Lake pendant west of Mono Lake (Schweikert and Lahren, 1987). These disturbances resulted in the accumulation of sediments shed from newly uplifted mountains, and in folding and faulting of preexisting sedimentary sequences.

Paleozoic terranes of Northern California

Beyond the stable continental margin, other oceanic rocks were forming west of North America during Paleozoic time. Remnants of these rocks would eventually be accreted to North America during Mesozoic time. Most of these rocks represent subduction-zone complexes, whereas others are remnants of oceanic island arcs.

Northern Sierra and Eastern Klamath terranes. During Mississippian and Permian time, a belt of island arcs lay west of the North American continent. Volcanoes from this chain erupted large volumes of andesite, and reefs ringed the volcanic islands. Today the ancient island arc system is preserved in the Paleozoic rocks of the northern Sierra Nevada and eastern Klamath Mountains (Harwood and Miller, 1990). The Northern Sierra terrane, a belt of Paleozoic rocks exposed in the northern Sierra Nevada, contains radiolarian chert and black shale of Mississippian and Permian age, as well as Permian metavolcanic rocks. Metamorphosed limestone associated with the volcanic rocks contains fossils of the McCloud fauna.

In the Klamath Mountains Province, the metamorphic rocks of the eastern Klamath terrane also contain metaandesitic rocks erupted from an oceanic arc and associated fringing carbonates. The Permian McCloud Limestone contains abundant corals, brachiopods, and fusulinids deposited as carbonate reefs fringing the eastern Klamath volcanic arc. The McCloud fauna is an assemblage distinct from both the Permian fauna of the North American margin and the Tethyan fauna of the Paleozoic subduction-zone complexes. It is found in a belt of Permian rocks that stretches from the Northern Sierra terrane north to British Columbia.

Paleozoic subduction zone complexes. On the California geologic map (Jennings, 1977), the western metamorphic belt of the Sierra Nevada province (Figure 3) appears as two continuous bands on the northwestern side of the Sierra Nevada. Mesozoic rocks on the west are separated from Paleozoic units on the east by an extensive fault system, and large fault-bounded slivers of ultramafic rock further accentuate the faults. In fact, each map unit is very complex and contains multiple accreted terranes. Most represent subduction-zone complexes containing metachert, oceanic metavolcanic rocks, and fragments of ophiolitic rocks. Rocks of both Paleozoic and early Mesozoic age can be found in the portion of the western metamorphic belt shown as Paleozoic on the State map.

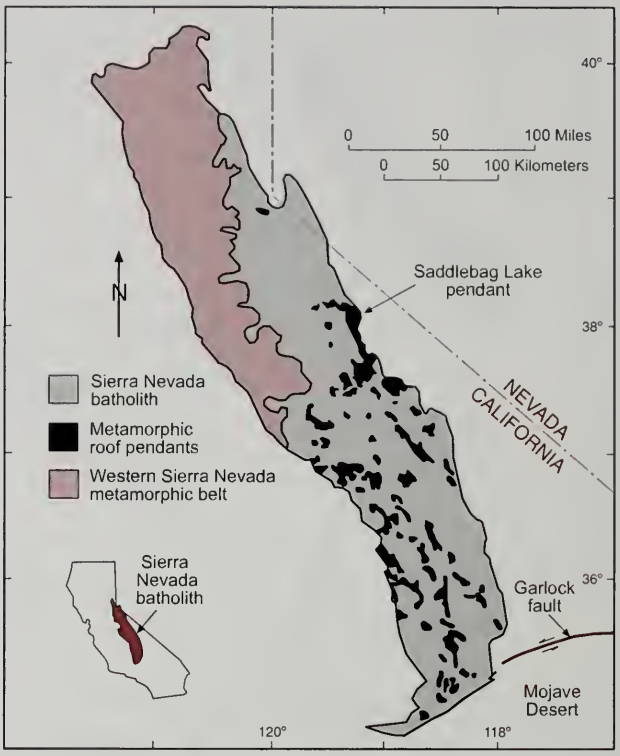

Figure 3. Map showing the western metamorphic belt, Sierran batholith, and roof pendants in the Sierra Nevada (Lahren and Schwiekert, 1994).

Further investigation of the State map reveals the similarity between the northwestern Sierra Nevada and the Klamath Mountains provinces. The metamorphic rocks of the Klamath Mountains also represent a composite of accreted oceanic terranes (Hacker et al., 1995), many of which can be matched with those of the northern Sierra Nevada. Overall, the geologic history of the northern Sierra Nevada during Paleozoic time appears to match well with that of the eastern Klamath Mountains (Davis, 1969).

Some of the oldest rocks in the northern Sierra Nevada are those of the Shoo Fly Complex, which is exposed in the northwestern Sierra Nevada. It contains metasedimentary and metavolcanic rocks of marine origin and has been subdivided by geologists into several units, possibly representing different oceanic terranes (Burchfiel et al., 1992). About 375 million years ago, during late Devonian time, a period of uplift and erosion is marked by an unconformity between the Shoo Fly Complex and all younger Paleozoic rocks in the northern Sierra Nevada. During this period of deformation, rocks of the Shoo Fly Complex were faulted and folded.

West of the Shoo Fly Complex and the northern Sierra terrane is the Calaveras Complex, a subduction-zone complex that appears to consist of multiple terranes containing rocks of Paleozoic age. Terranes correlative with those in the Calaveras Complex stretch discontinuously into British Columbia (Burchfiel et al., 1992).

At present, five major subduction-zone complexes are recognized in the Klamath Mountains, and several of these are subdivided into two or more units. They are systematically younger from east to west, reflecting the succession of plate collisions that added each oceanic slice to the North American continent. With the exception of the western Jurassic belt (discussed below), all contain Paleozoic rocks. From east to west they are the Central metamorphic belt, the Stuart Fork terrane, and the Western Paleozoic and Triassic belt, which has been subdivided into the Rattlesnake Creek - Marble Mountains, Hayfork, and the North Fork- Salmon River terranes (Irwin, 1981; Harwood and Miller, 1990).

MESOZOIC CALIFORNIA

Tectonic setting

By Jurassic time, about 160 million years ago, the breakup of Pangaea was well underway. The Atlantic Ocean was beginning to open, and North America moved west, away from the European continent. A north-south-trending subduction zone had developed along the western margin of the North American plate, roughly in the same area as today's Sierra Nevada. This was the beginning of the most important period of geologic "building" in California.

During Mesozoic time, belts of oceanic rock were accreted to northern California along the active subduction-zone margin (Howell and McDougall, 1978; Ernst, 1981; Howell, 1990). The earliest additions to western North America were the Paleozoic sedimentary and volcanic terranes discussed above, which were accreted during early Mesozoic time. In general, following each episode of accretion the subduction zone shifted westward, and accretion of a younger terrane began. The westernmost and youngest belts of accreted rocks in the Sierra Nevada and Klamath Mountains provinces are of Middle to Late Jurassic age. The westernmost belt of metamorphic rocks in the Sierra Nevada is the Foothills terrane, dated at about 160 million years. Along the central part of the Sierra foothills, the Foothills terrane is separated from the rocks of the older Calaveras Complex by the Melones fault, the easternmost branch of the Foothills fault system. In the Klamath Mountains, the youngest accreted terrane is known as the western Jurassic terrane and includes the Galice Formation, a long belt of metasedimentary rocks formed about 150 million years ago (Irwin, 1981). To the west, these rocks are separated from rocks of the Coast Ranges by the South Fork Mountain thrust.

The Franciscan Complex

Following the accretion of the Sierran and Klamath Mountains terranes, the subduction zone shifted west of the modern Great Valley. From about 140 million until about 28 million years ago, a subduction zone existed along the length of western North America. About 100 million years ago, the subduction zone was in the approximate position of today's Coast Ranges (Pakiser and Mooney, 1990). Fragments of the oceanic plates that collided with North America at that time are preserved in today's Coast Ranges as the Franciscan Complex. The plate whose fragments make up the Franciscan Complex has been named the Farallon Plate. The Franciscan Complex forms the heart of the Coast Range Province. Franciscan rocks are found in two northwest-trending belts, one extending almost the length of the province along the eastern edge of the San Andreas fault (Bailey et al., 1964). Related rocks extend north of California into southern Oregon, where they are recognized as the Dothan Formation. The second belt of Franciscan rocks crops out in the southern Santa Lucia Range, west of the Nacimiento fault.

The Franciscan Complex is composed of a number of individual geologic terranes juxtaposed and mixed during subduction and accretion along the North American margin. The rocks of the Franciscan have a variety of origins, including deep oceanic crust, sediments deposited in trenches, sediments accumulated on the deep ocean floor, and volcanic and sedimentary rocks formed on seamounts. The most abundant rocks in the Franciscan Complex are mudstone and graywacke, deposited as turbidite sequences. Volcanic rocks make up about 10 percent of exposed Franciscan rocks. These are altered submarine basalts, or greenstones, which display pillow structures at several localities. Radiolarian chert, which has yielded important stratigraphic and paleogeographic information, is another prominent component of the Franciscan. Limestone is a rare component of the Franciscan, occurring in northern Santa Clara County and in the vicinity of Laytonville, Mendocino County.

Metamorphic rocks of the Franciscan Complex include extensive exposures of blueschist in the northeastern Coast Range, as well as eclogitic rocks

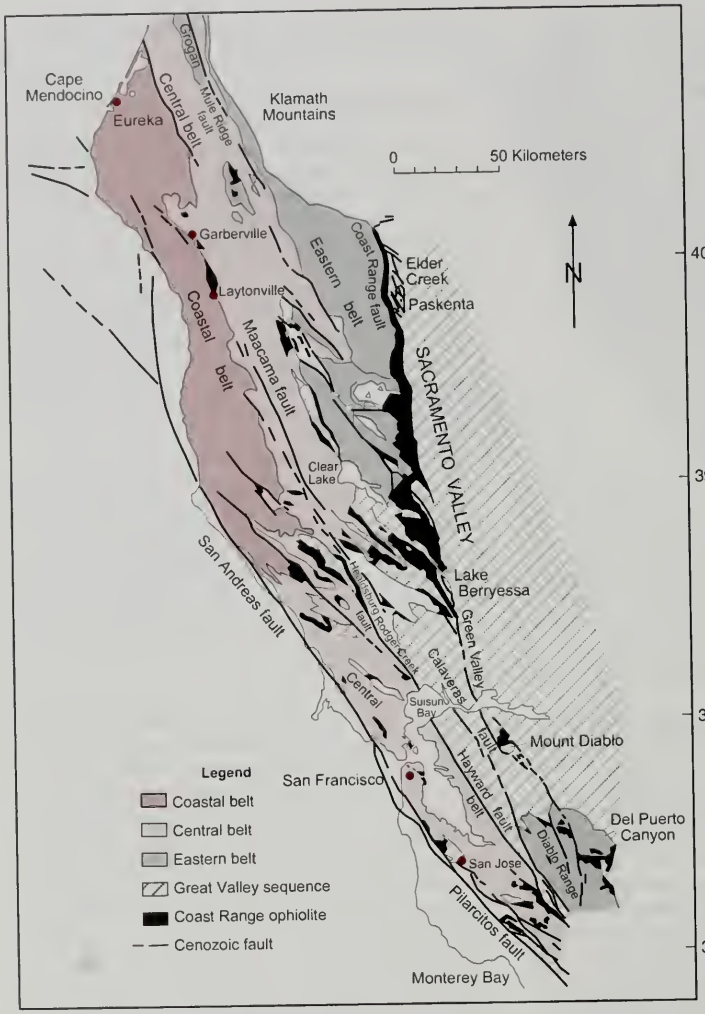

Figure 4. Major Franciscan belts, Coast Range ophiolite, and Great Valley sequence in the northern and central Coast Ranges (Harden, 1998; modified from McLaughlin et al., 1988).

on the Tiburon Peninsula in Marin County, and blueschist found near Cazadero in Sonoma County and in the eastern Diablo Range. Serpentinite in the Franciscan occurs along fault zones and in the matrix of melange units. The weak serpentinite of the Coast Ranges is notorious for creating landslide problems, and in outcrops it commonly shows an extreme degree of shearing and ductile deformation.

Franciscan rocks can be broadly divided into three units (Figure 4). The westernmost, termed the Coastal Belt, trends northwest between Eureka and the Russian River (Wahrhaftig and Sloan, 1989). In general, the Coastal Belt Franciscan is mainly graywacke and shale sequences that are not as disrupted as other parts of the Franciscan. The Central Belt, which includes the San Francisco Bay Area, is found east of the Coastal Belt. It is predominantly melange, with exotic blocks of greenstone, blueschist, chert, and resistant graywacke in a matrix of highly sheared mudstone. Several more coherent blocks have been recognized within the Franciscan Central Belt. These include the Marin Headlands terrane, which forms the resistant topography north of the Golden Gate Bridge and is composed of sequences of greenstone, chert, and sandstone, and the Nicasio Reservoir terrane, largely composed of pillow basalt. The Permanente terrane of the San Francisco Peninsula is notable for the Calera Limestone.

The Eastern Belt of the Franciscan extends east to the Coast Range thrust, the major fault boundary with rocks of the Great Valley sequence. Here the rocks are typically blueschist and related metamorphic rocks. Faulted slices of these rocks are also found on the Tiburon Peninsula of San Francisco Bay and west of Los Banos. The Eastern Belt is more highly metamorphosed because it was subducted to a deeper level than the Franciscan belts to the west. The Eastern Belt

and the melange matrix of the Central Belt are older than the blocks within the melange, and the Coastal Belt contains the youngest Franciscan rocks, with the entire Franciscan spanning a period of about 150 million years of accretion from Late Jurassic to early Tertiary time.

The Sierran batholith

Inland of the Mesozoic subduction zones, magma rose above the subducting plates, forming chains of andesitic volcanoes and granitoid plutons beneath them. At its maximum development, the Mesozoic magmatic arc extended along western North America from Baja California, Mexico, to British Columbia, Canada (Ernst, 1981). In California, the arc was located approximately in the position of today's Sierra Nevada range. Plutonic rocks representing the roots of the Mesozoic volcanic chain are found today throughout the Klamath Mountains, Sierra Nevada, Basin and Range, Mojave Desert, and Peninsular Ranges provinces (Figure 5). They are also exposed in the Coast Ranges' Salinian block, which was moved to its present position along the San Andreas fault, as discussed below. Mesozoic volcanic rocks, originally erupted along the arc, are also preserved in localities along the crest of the Sierra Nevada. The greatest volume of magma was generated about 100 million years ago, during the subduction of the Farallon Plate.

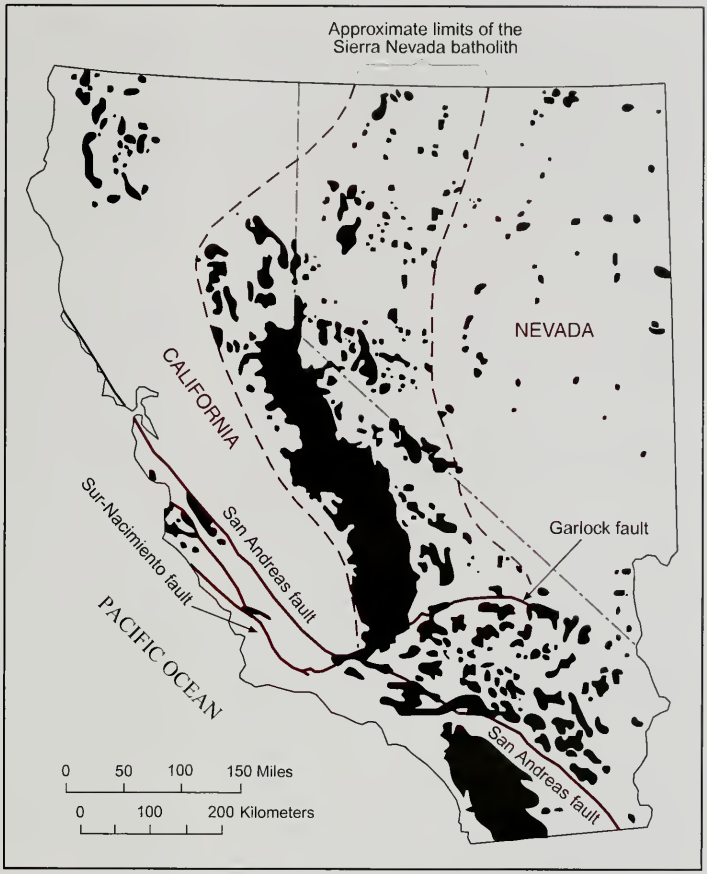

Figure 5. Map showing the extent of the Sierran batholith and plutonic rocks in the Klamath Mountains (Norris and Webb, 1990).

Mesozoic plutonic rocks of the batholith are the dominant rock type in the Sierra Nevada province. The oldest plutonic rocks are about 210 million years old, and the youngest plutons crystallized about 80 million years ago. Hundreds of individually emplaced plutons are ditsinguishable by their mineral components and ages. The most common plutonic rocks of the Sierra Nevada are granodiorite, granite, and tonalite. More mafic plutons of dioritic composition are also present, but are much less abundant than granitoids.

Rocks representing several different levels of the 100-million-year old magmatic arc are exposed today in different parts of the Sierra Nevada. In general, the depth of emplacement deepens from north to south. Cretaceous plutons in the central and northern Sierra Nevada appear to have been emplaced in the crust at depths of less than 10 kilometers, based on the aluminum content of horn-

blende, which is used as a geobarometer. Contacts between plutons of Cretaceous age in the northern and central Sierra Nevada are generally sharp, suggesting the emplacement of discrete magma batches into previously crystallized rock. Many of the intruding magmas ballooned outward as they rose within the crust, possibly because of decreased overburden confinement at higher levels.

In contrast, the characteristics of the southern Sierra Nevada batholith indicate that it crystallized at a much greater depth than the plutonic rocks in northern California. The mafic gneisses and plutons in the southwestern Sierran foothills indicate magma emplacement in the middle crust, at about 30 kilometers depth (Burchfiel et al., 1992).

Some of the Sierran roof pendants, including those exposed at Mt. Dana and the Minarets, are hornfels and schists whose protoliths were clearly volcanic. Metavolcanic rocks exposed in the peaks of the Minarets and the Ritter Range have been recognized as remnants of the 100-million-year-old Sierran volcanic arc. In the Minarets, a large caldera had about the same areal extent as the Pleistocene Long Valley caldera. Pyroclastic flows and breccias formed during the collapse of the caldera walls, as well as parts of the Mesozoic caldera rim, have been recognized by recent investigations (Fiske and Tobisch, 1994).

The oldest plutonic rocks, about 210 million years old, are found along the eastern edge of the Sierra Nevada, west of Mono Lake. Younger Jurassic plutons are found on both the western and eastern edges of the batholith (Bateman, 1985). However, the most voluminous plutons, accounting for over 90 percent of the batholith, were emplaced between about 120 and 80 million years ago (Burchfiel et al., 1992). These Cretaceous intrusions crop out in the center of the batholith and include the Half Dome granodiorite, the Cathedral Peak granodiorite, and other prominent units of the Yosemite area. About 80 million years ago the zone of magma generation shifted east of the Sierran arc. The likely cause of the change was an increase in the rate of subduction of the Farallon plate and a flattening of the subduction angle.

The Great Valley Sequence

Between the Mesozoic trench and the Sierran volcanic arc, a marine fore-arc basin extended along most of California's length. Sediments of the Great Valley Sequence, including marine rocks found today in the Transverse Ranges, accumulated in this elongate sedimentary basin, which occupied roughly the same area as today's Central Valley (Figure 4; Ernst, 1981). Most of the rocks were deposited during Jurassic and Cretaceous time, but deposition in the fore-arc basin continued into early Cenozoic time, after magmatic activity in the Sierra Nevada had ceased (Burchfiel et al., 1992).

Rocks of the Great Valley sequence are well exposed along the western margin of the Central valley and around the margins of Sutter Buttes, where they have been steeply upturned. Beneath the late Cenozoic alluvium of the Sacramento and San Joaquin rivers, as much as 20,000 meters of sediments fill the sedimentary basin. The Great Valley Sequence consists of marine sandstone, shale, and conglomerate ranging in age from Mesozoic to early Tertiary. Facies relationships, sedimentary features, and fossil evidence indicate that rocks along the eastern margin of the Great Valley generally formed under deltaic and shallow marine conditions. In contrast, those found on the western side of the valley are turbidites deposited in the deeper parts of the fore-arc basin. Sandstones in the older, lower formations of the Great Valley sequence are rich in volcanic rock fragments eroded from the Jurassic and early Cretaceous Sierran arc. Younger sandstones of the Great Valley Sequence are rich in feldspar and quartz eroded from the granitoid plutons (Dickinson and Rich, 1972; Ernst, 1981). In the northern Great Valley, the Klamath Mountains were also a sediment source for the Great Valley Sequence.

By the end of Mesozoic time, the northern part of the Great Valley fore-arc basin began to emerge, as basin sedimentation outpaced the rate of subsidence. By about 24 million years ago, terrestrial sediments were being deposited in the Sacramento Valley. Farther south, deep marine conditions persisted into middle Cenozoic time. The San Joaquin basin was very deep between 35 and 15 million years ago, and a shallow marine embayment persisted there until 2.5 to 3 million years ago (Bartow, 1991). Today the Cenozoic sediments are found overlying the Great Valley Sequence and underlying the alluvial deposits of the Sacramento and San Joaquin river system (the Late Cenozoic stratigraphy is summarized in the appendix of the paper by Ferriz, 2001, this volume).

The Coast Range ophiolite and other ophiolites of Northern California

The sedimentary rocks of the Great Valley Sequence accumulated on the Coast Range ophiolite, which is exposed along the western margin of the Central Valley (Figure 4), as well as at Point Sal in the southern Coast Ranges (Ernst, 1981). The ophiolite has been dated at about 165 million years, or mid-Jurassic. The best exposure of the base of the Great Valley sequence is along the banks of the South Fork of Elder Creek, about 10 kilometers northwest of the town of Paskenta. At this locality, mudstone of the Great Valley sequence was deposited on a sedimentary breccia containing ophiolite debris. Near Mt. Diablo, east of San Francisco Bay, is the only well-exposed section of sheeted dikes in the Coast Range ophiolite. The section is about 2,500 m thick and is overlain by about 1,500 m of pillow basalt.

Many of northern California's accreted terranes are also associated with ophiolite suites, as can be seen in the California geologic map. In the Klamath Mountains province, the rocks of the Eastern Klamath terrane rest on older ultramafic rocks of the Trinity Peridotite, the largest exposed body of ultramafic rock in North America. Farther west, belts of ultramafic rock form the base of several of the younger terranes of the Klamath Mountains; the Josephine ophiolite is the largest of these. The Feather River peridotite, the Smartville Complex, and the Kings-Kaweah ophiolite are examples of major bodies in the Sierran metamorphic terranes. Dismembered fragments of ophiolite are also found within the Franciscan Complex in the Coast Ranges. Considering California's long history as a convergent plate margin, it is not surprising that many fragments of oceanic basement are present in the accreted terranes of northern California.

CENOZOIC CALIFORNIA

Tectonic setting

About 28 million years ago, the Pacific and North American plates made direct contact when the closest part of Farallon Plate was completely consumed beneath North America, creating the San Andreas transform boundary (Figure 6; Ernst, 1981). The development of the transform margin has been the dominant factor in California's later Cenozoic history. Geologic events throughout California, even in provinces not directly at the plate boundary, have been strongly influenced by the San Andreas system. North and south of the newly created transform, subduction of the Farallon plate continued and, as increments of the Farallon plate were consumed in the subduction zones, the transform margin lengthened (Wallace, 1990). Subduction continues today where remnants of the Farallon plate and the East Pacific Rise still exist, north of the Mendocino triple junction and south of the Baja California peninsula.

Today the transform boundary between the Pacific and North American plates has lengthened to extend along most of California in the form of the San Andreas fault system (Wallace, 1990). North of Cape Mendocino, remnants of the Farallon plate, known as the Gorda and Juan de Fuca plates, are still being subducted beneath North America. As a result, a magmatic arc is still active north of Cape Mendocino, with the Cascades volcanic chain as its surface manifestation (Figure 2).

The development of the San Andreas transform has had major impacts on the geology of western California. Large crustal blocks have shifted by as much as 315 kilometers along the right-lateral faults of the San Andreas system. For example, crystalline rocks of the Salinian block, which probably formed as part of the Sierran batholith, moved northwestward along the San Andreas fault to their present position in the Coast Ranges.

The San Andreas system

The relative motion between the Pacific and North American plates has been calculated at about 4.9 centimeters per year during the past 3 to 4 million years. This rate is greater than the approximately 3.5 centimeters accounted for by combining the slip rates of all members of the San Andreas system (Wallace, 1990). The remaining plate motion is probably accommodated by faults along the eastern side of the Sierra Nevada and in the Basin and Range province. The location, earthquake history, and seismic potential of individual segments of the San Andreas system in northern California are discussed in other chapters of this volume.

The volcanic rocks at the Pinnacles volcanic field on the Pacific Plate provide the most definitive correlation between older rocks on opposite sides of the San Andreas fault and the corresponding rocks southeast of the San Andreas at the Neenach volcanic formation near Gorman. The units have been

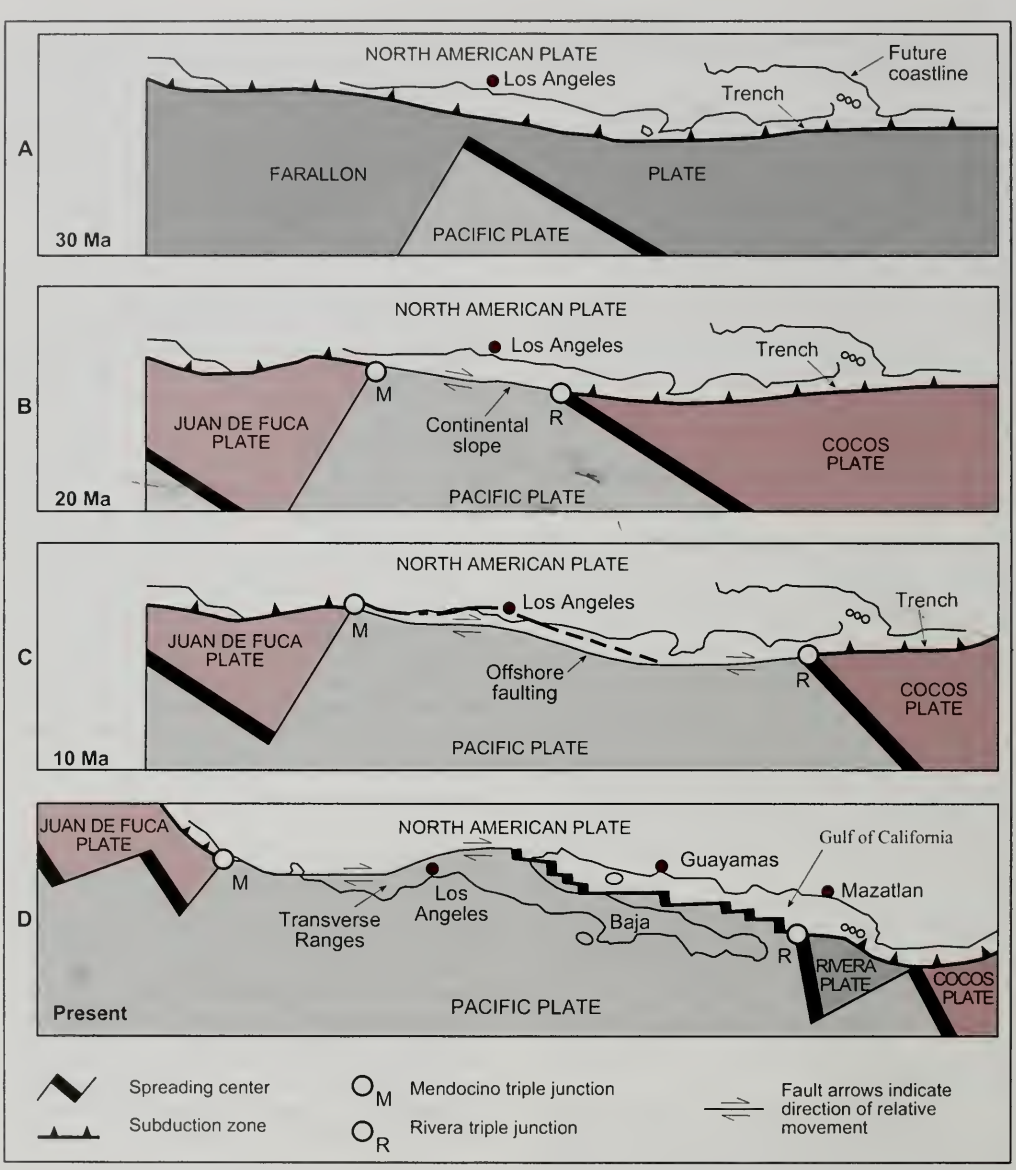

Figure 6. Development of the San Andreas transform boundary. The transform boundary has lengthened as the Pacific plate has increased its direct contact with North America (Wallace, 1990; after Atwater, 1970).

dated at 22 to 24 million years, with the currently accepted age placed at 23.5 million years. The offset between Pinnacles and Neenach is approximately 315 kilometers, yielding a long-term average slip rate of about 1.34 centimeters per year (Wallace, 1990). Along the entire San Andreas fault proper, all units older than the Pinnacles-Neenach volcanics show about the same amount of offset, indicating that the modern transform is no older than about 22 to 24 million years. Transform motion on earlier faults along the plate boundary began no earlier than 30 million years ago, as indicated by the patterns of magnetic anomalies in the oceanic crust (Atwater, 1970).

Cenozoic sedimentary basins

Cenozoic sedimentary rocks can be found in the Coast Ranges on both sides of the San Andreas fault (Figure 7). Most of the rocks were deposited in fault-bounded marine basins, such as those offshore basins that remain along the continental shelf today (Burchfiel et al., 1992). The formation of these basins, some of which received more than 6,000 meters of sediment, most likely resulted from extension during a period when the Pacific plate was moving in a more northwesterly direction relative to North America (Crouch and Backman, 1984; Graham et al., 1984).

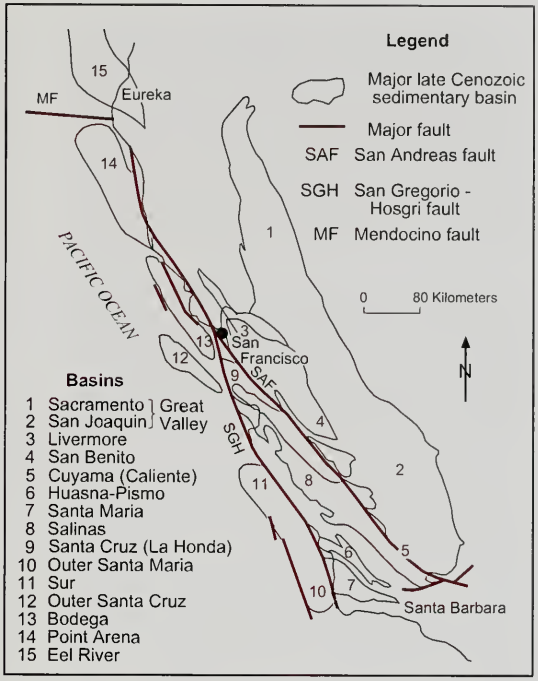

Figure 7. Late Cenozoic sedimentary basins of the Coast Ranges and adjacent offshore areas (Christiansen and Yeats, in Burchfiel et al., 1992).

Some of the older marine basins, which were being filled with sediment during Eocene time, were later separated by as much as 315 kilometers of right-lateral movement on the faults of the San Andreas system. Eocene sedimentary rocks seen today in the central and northern Coast Ranges west of the San Andreas fault were adjacent to the San Joaquin basin when the sediments were deposited (Page et al., 1998). Between about 22 and 11 million years ago, during Miocene time, the siliceous sediments of the Monterey Formation, including diatomaceous units, accumulated in deep, fault-bounded marine basins that were extensive along central California (Ernst, 1981). Today these sediments crop out throughout the central Coast Ranges and in portions of the northern Salinian block, as well as in southern California.

Cenozoic volcanic activity

Coast Ranges. Late Cenozoic volcanic rocks are found in the northern California Coast Ranges at several localities. East of the San Andreas fault, rocks from a series of volcanic fields get systematically younger from south to north along the Coast Ranges (Dickinson, 1997). Southernmost are the 9 to 15 million-year-old Quien Sabe Volcanics in the central Diablo Range, followed by the 12 to 8 million-year-old basalt and rhyolite in the Berkeley Hills. Volcanic rocks in the Sonoma volcanic field are between 8 and 3 million years old and, at the northern end of the series, the Clear Lake volcanics are between 2 million and 10,000 years old. The northward movement of volcanic activity during late Cenozoic time appears to be related to the northward migration of the Mendocino triple junction.

The southern Cascades and the Modoc Plateau. The Cascade Province is dominated by intermediate-composition volcanism, characteristic of its subduction-zone setting. North of Cape Mendocino, Mt. Shasta and Lassen Peak are forming as the Gorda

Plate undergoes subduction beneath the North American plate (Atwater, 1970; Ernst, 1981). Both pose potential volcanic hazards for northern Californians (Wright and Pierson, 1992). Volcanic rocks of the High Cascades Series were formed by eruptions during the past 3 million years, and Late Cenozoic volcanic rocks that pre-date the present volcanic cones, known as the Western Cascades Series, are evidence that active volcanoes were present in the California Cascade Range 20 to 30 million years ago.

To the east of the Cascades, recent mafic volcanic activity in the Modoc Plateau is related to crustal extension. Volcanic activity in the Long Valley area, discussed below, is also related to Basin-Range extension. There, silicic lavas are produced by magma rising through the thick crustal section of Sierra Nevada granitoids.

Mt. Shasta. Mount Shasta is a large stratovolcano built by eruptions from four main centers, mostly during Holocene time (Miller, 1980). During the past 4,500 years, the average recurrence interval between eruptions has been about 600 years. Two of Mt. Shasta's eruptive centers have been very active during Holocene time. Hotlum Cone at the summit has been constructed by at least 8 eruptions during the past 8,000 years. Shastina Cone, a subsidiary cone on the western flank of Mt. Shasta, was built by eruptions between 9,300 and 9,700 years ago. Older volcanic centers at Misery Hill, just south of the summit, and Sargeants Ridge, on the south flank of the mountain, show no evidence of postglacial activity.

About 300,000 to 400,000 years ago a debris avalanche from an ancestral Mt. Shasta traveled 49 kilometers northward from its source and covered 675 square kilometers of Shasta Valley. As estimated from records of water wells drilled in the valley, the debris avalanche filled the valley to a depth of 50 meters. The estimated volume of 45 km^3 makes it the largest volcanic debris avalanche measured in the United States (Crandell, 1989).

Mt. Lassen. At 5 p.m. on Memorial Day, May 30, 1914, a huge cloud of steam from Lassen Peak signaled the beginning of the first volcanic eruption of the 20th century in the conterminous states (Hill, 1970). During the first year, 170 eruptions of steam and ash were recorded. Between 1915 and 1922, volcanic activity produced lava flows, debris flows, and glowing avalanches. Today, hot springs and fumaroles remain active within Lassen National Park.

Lassen Peak itself is a plug dome of dacite that rose on the northern flank of an older Pleistocene stratovolcano, named Brokeoff cone (Turrin et al., 1998). Earlier eruptions from the Lassen area, centered west of today's Lassen Peak, destroyed a large stratovolcano and generated the Rockland ash 400,000 to 610,000 years ago. (The age of the Rockland is unresolved at the time of this writing.) The Rockland ash is an important marker bed in northern California and northwestern Nevada (Sarna-Wojcicki et al., 1985, 1991). Holocene and Pleistocene volcanic ashes can be extremely valuable for engineering geology studies, because they can be chemically fingerprinted and radiometrically dated.

The Mt. Lassen area has been the source of at least one other major explosion in the recent geologic past. Approximately 3.4 million years ago, a catastrophic eruption sent ash flows down the Sacramento Valley at least as far as present-day Willows, a distance of 130 kilometers. The resultant volcanic unit, the Nomlaki Tuff, is up to 90 meters thick at some localities east of Redding. Along the east side of the Sacramento Valley, the Nomlaki Tuff is found interlayered with volcanic flows and alluvial deposits of the Tuscan Formation (Sarna-Wojcicki et al., 1991). On the western side of the Sacramento Valley, the Nomlaki Tuff is found within alluvial deposits of the Tehama Formation. Much farther south, pumice and ash from the eruption are found in marine sedimentary deposits of the San Joaquin Formation in the Kettleman Hills near Coalinga.

Medicine Lake Highlands. Medicine Lake volcano is a recently active volcano located within the Medicine Lake Highlands, on the border between the Cascades and Modoc Plateau provinces, about 50 kilometers northeast of Mt. Shasta (Waters et al.,1990). Both basaltic and silicic eruptions have occurred at Medicine Lake during the past 700,000 years. The youngest flows occurred no more than a few hundred years ago. During the summer of 1989, thousands of micro-earthquakes caused concern about a possible eruption, but none occurred.

The Long Valley caldera. The Long Valley area is located on the western edge of the Basin and Range province, along the base of the Sierra Nevada Range. Volcanic activity began there about 3.6 million years ago, when mafic and andesitic lavas were erupted over a fairly wide area (Bailey, 1989). These flows were followed by the eruption of more silicic domes and flows near the northern edge of the pres-

ent caldera. About 760,000 years ago, the roof of the Long Valley magma chamber ruptured, causing a catastrophic eruption of about 600 km^3 of rhyolitic magma, today known as the Bishop Tuff. Ash flows covered 1,500 km^2 of the surrounding area to a depth of up to 200 meters. Airfall ash from this explosion is found in sediments as far east as Missouri and off the coast of California.

The Long Valley caldera resulted from the rapid evacuation of the magma chamber and collapse of the ground above it. The resulting oval depression measures about 17 by 32 kilometers and is 2 to 3 kilometers deep. The Mammoth Lakes resort lies within the rim of the caldera, and U.S. Highway 395 crosses through it. Post-caldera eruptions have produced domes and flows within the caldera, and the resurgent central dome is currently rising at about 2 to 3 centimeters per year. The presence of magma 5 to 15 kilometers beneath the central dome is suggested by seismic surveys and by continued swarms of earthquakes. During 1995, carbon dioxide gas leaked from the southwestern part of the caldera, killing large stands of trees. Concern about volcanic eruptions in the region has led to continuous monitoring of seismic and thermal activity in the Long Valley region by the U.S. Geological Survey (Hopson, 2001, this volume).

Mono-Inyo volcanic chain. Another center of recent volcanic activity on the east side of the Sierra Nevada is the Mono-Inyo volcanic chain. The Mono-Inyo chain is a system of vents 45 kilometers long that overlaps with the Long Valley caldera at the southern end and extends north to Mono Lake. The Mono Craters chain consists of at least 30 rhyolite domes, flows and craters whose ages range from about 40,000 to about 650 years BP; eruptions from Paoha Island on Mono Lake may be as recent as 150 years BP. The Inyo Craters chain, also comprised of rhyolite domes, flows and craters, extends south of the Mono Craters chain. The most recent eruptions from the Inyo Craters chain occurred as recently as 520 years ago.

Cenozoic volcanic rocks of the Sierra Nevada. Between about 28 and 22 million years ago, major ash flows erupted from the Great Basin and flowed westward to cover Mesozoic rocks in parts of today's Sierra Nevada province. The ash flows, some of which are preserved in the Valley Springs Formation, are found today in the northwestern Sierran foothills. Younger andesitic volcanoes erupted about 9 to 11 million years ago from the high Sierra Nevada to deposit the distinctive Mehrten Formation in the western foothills, west of Jamestown, and widespread volcanic flows in other areas (Huber, 1990). The distribution of these flows has been used to support the hypothesis that uplift of the modern Sierra Nevada must have post-dated the youngest of these rocks (Huber, 1990; Page and Sawyer, 2001, this volume).

Pleistocene climatic fluctuations

Evidence of Pleistocene glaciation in northern California can be found in much of the Sierra Nevada, in the higher parts of the Klamath Mountains, on the flanks of Mt. Shasta and Lassen Peak, and in the high parts of the northern Coast Ranges, including high peaks of the Yolla Bolly Wilderness west of Redding. The largest Pleistocene ice fields in the Sierra Nevada covered the upper Tuolumne, Merced, and San Joaquin rivers (Figure 8). Valley glaciers flowed as much as 100 kilometers down the western slope of the Sierra Nevada. Today, more than 100 small glaciers remain in the Sierra Nevada, most of them on the sun-sheltered northern sides of peaks. The largest, Palisade glacier, covers less than a square kilometer, compared with over 500 km^2 covered by the largest glaciers during late Pleistocene time (Bailey, 1966).

Two sets of glacial moraines are well preserved in the canyons of the eastern Sierra Nevada, and poorly preserved older glacial deposits remain from two or more earlier periods of glaciation. Geologists working on Pleistocene climate fluctuations currently correlate glacial events to worldwide climate events, as recorded by the oxygen isotope ratios of fossil tests in deep-sea sediment cores. The most recent glaciers, termed the Tioga glaciers in the Sierra Nevada, reached their maximum extent during Isotope Stage 2, the worldwide cooling between about 18,000 and 22,000 years BP. Prior to the Tioga glaciation, more extensive glaciers occupied northern California's alpine valleys. Termed the Tahoe glaciation in the Sierra Nevada, its age has been the subject of much dispute. Many workers believe that it correlates with Isotope Stage 6, between about 130,000 and 200,000 years ago, while others would place it during Stage 4, at about 60,000 to 100,000 BP. The moraines left by Tahoe glaciers form prominent ridges on the eastern side of the Sierra Nevada today. Evidence for pre-Tahoe glaciation is found at several Sierran localities, where older glacial tills no longer preserve any morainal topography. One world-famous locality where older Sierran till has

been preserved is along State Highway 395 near Sherwin Summit. At that locality, glacial till is buried by thick deposits of the Bishop Tuff. (Bailey, 1966). Older glacial deposits can also be seen farther north along Highway 395 near Bridgeport.

Northern California rivers with glaciated headwaters deposited enormous volumes of outwash in their lower reaches during glacial periods. In the Central Valley, at least four climatically controlled pulses of alluviation occurred during the past 2 million years (Marchand and Allwardt, 1981; Bartow, 1991). These are recorded by river terraces along the major streams flowing west from the High Sierra and by alluvial sequences in the subsurface sediments of the Central Valley. In the eastern Sierra Nevada, pluvial lakes formed or increased in volume during glacial periods (Bailey, 1966). Next to plate tectonics, recent climatic changes may be the most important natural factor controlling the California landscape.

San Francisco Bay

The current Sacramento-San Joaquin outlet was established sometime after about 600,000 years ago, following the breaching of a giant lake impounded in the Central Valley. Since that time, the San Francisco Bay estuary was episodically created by climatically controlled sea level rises. During glacial episodes, river valleys occupied the Bay. The oldest estuary existed approximately 400,000 years ago, based on the presence of the Rockland Ash in estuarine deposits identified in cores taken beneath the bay near Alameda.

Worldwide sea level was approximately 120 meters lower than at present during Isotope Stage 2, or the Tioga glacial period, 18,000 to 22,000 years ago. The lowering of sea level in the San Francisco area placed the shoreline just west of the Farallon Islands, about 32 kilometers west of today's beaches. At that time, the combined Sacramento and San Joaquin Rivers, as well as the smaller streams flowing from the Santa Clara Valley, flowed past today's Golden Gate onto what is now the continental shelf. River valleys occupied what is now the Bay, based on the presence of alluvial and associated eolian sediments in cores taken from beneath the bay (Figure 9; Atwater et al., 1977).

San Francisco Bay's present estuary formed less than 10,000 years ago, during the most recent postglacial rise in worldwide sea level. The estuary occupied its historic limit, and the Sacramento-San Joaquin delta occupied its current position by about 4,000 years ago (Atwater et al., 1977).

Topography

Most of northern and central California's major mountain ranges were elevated about 3 to 5 million years ago in response to increased compression along the plate boundary, caused by a change in plate motion (Page et al., 1998). The topography of northern California is young, with mountains con-

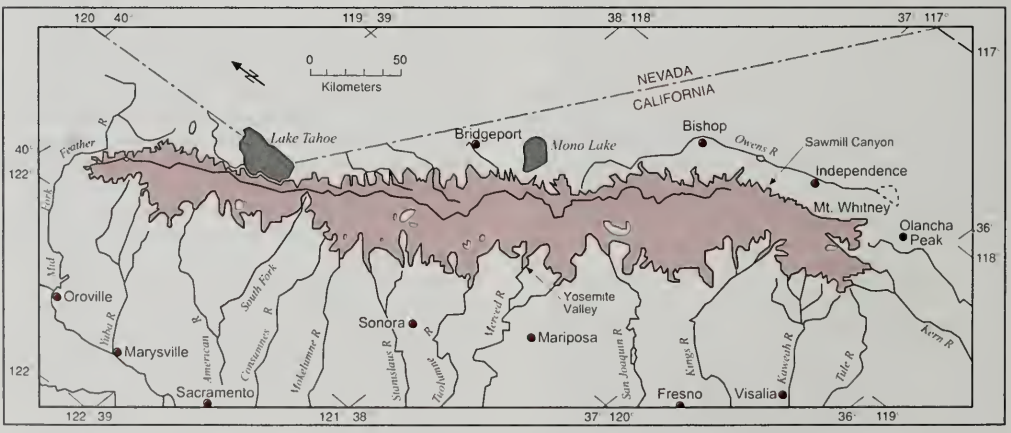

Figure 8. Approximate extent of ice in the Sierra Nevada 20,000 years ago during the Tioga glaciation (Bailey, 1966).

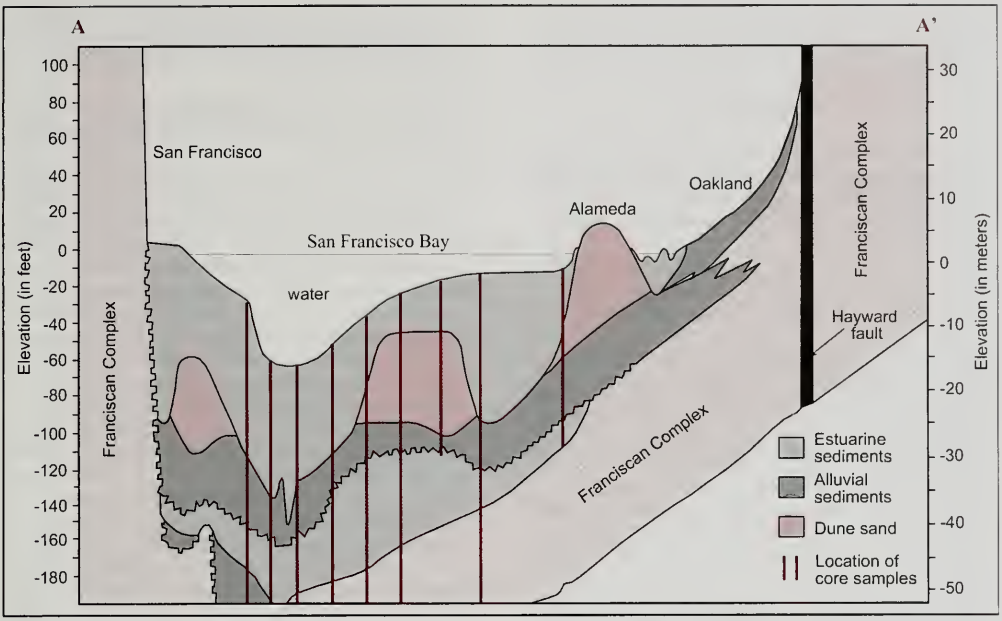

Figure 9. Cross section showing alluvial, eolian, and estuarine sediments beneath San Francisco Bay, between San Francisco and Alameda (Harden, 1998; modified from Atwater et al., 1977).

tinuing to rise today. The present Sierra Nevada range has risen in about the same position as the Mesozoic chain of volcanoes. The most recent uplift of the Klamath Mountains began approximately 5 to 6 million years ago.

Uplift of the southern and central Coast Ranges began about 3.5 million years ago, when most of western California emerged above sea level. Uplift rates increased about 500,000 years ago, giving rise to the modern Coast Ranges mountains (Page et al., 1998). (The timing of uplift is constrained by the Rockland Ash, whose age is estimated to be between 400,000 to 610,000 years BP.) Along the California coast, flights of marine terraces attest to ongoing uplift. Active folds and thrust faults throughout the central and northern Coast Ranges, of direct concern to engineering geologists, are further manifestations of convergence across the plate boundary.

ACKNOWLEDGEMENTS

Many people assisted with the compilation and writing of the textbook, *California Geology*, upon which this summary draws heavily. Among them are Calvin Stevens of San José State University, David Harwood, and Andrei Sarna-Wojcicki of the U.S. Geological Survey. Thanks also go to Patrick Lynch of Prentice Hall for help in obtaining the figures. I gratefully acknowledge the helpful reviews by Robert Coleman and Elizabeth Miller of Stanford University. Their comments and suggestions improved both the content and the clarity of this manuscript. Thanks also go to Chief Editor Horacio Ferríz for his editorial suggestions and for his patience.

AUTHOR PROFILE

Deborah R. Harden is a Professor of Geology at San José State University. Her specialty is geomorphology, with a particular interest in fluvial systems. She is the author of the textbook *California Geology*, published by Prentice Hall. Prior to her appointment at San José State, Dr. Harden was

employed as a geologist with Woodward Clyde Consultants and as a hydrologist with the U.S. Geological Survey.

REFERENCES

Atwater, B.F., Hedel, C.W., and Helley, E.J., 1977, Late Quaternary depositional history, Holocene sea-level changes, and vertical crustal movement, southern San Francisco Bay, California: U.S. Geological Survey, Professional Paper 1014, 15 p.

Atwater, T., 1970, Implications of plate tectonics for the Cenozoic tectonic evolution of western North America: Geological Society of America Bulletin, v. 81, p. 3513-3535.

Bailey, E.H., (ed.),1966, Geology of northern California: California Division of Mines and Geology, Bulletin 190, 507 p.

Bailey, E.H., Irwin, W.P., and Jones, D.L., 1964, Franciscan and related rocks and their significance in the geology of western California: California Division of Mines and Geology, Bulletin 183, 177 p.

Bailey, R.A., 1989, Geologic map of the Long Valley Caldera, Mono-Inyo Craters volcanic chain, and vicinity, eastern California: U.S. Geological Survey, Map I-1933, scale 1: 62,500.

Bartow, J.A., 1991, The Cenozoic evolution of the San Joaquin Valley, California: U.S. Geological Survey, Professional Paper 1501, 40 p.

Bateman, P. C., 1985, Plutonism in the central part of the Sierra Nevada batholith, California: U.S. Geological Survey, Professional Paper 1483, 186 p.

Burchfiel, B.C., Lipman, P. W., and Zoback, M.L., (eds..),1992, The Cordilleran Orogen: Conterminous U.S.: Geological Society of America, Geology of North America, Vol. G-3, 724 p.

California Department of Conservation, Division of Mines and Geology, various dates, regional geologic map sheets, scale 1:250,000.

Cooper, J.D., and Stevens, C.H., (eds.), 1991, Paleozoic paleogeography of the western United States: Society of Economic Paleontologists and Mineralogists, Pacific Section, pub. 67.

Crouch, J.K., and Backman, S.B., (eds.), 1984, Tectonics and sedimentation along the California margin: Society of Economic Paleontologists and Mineralogists, Pacific Section, vol. 38.

Davis, G.A., 1969, Tectonic correlations, Klamath Mountains and western Sierra Nevada: Geological Society of America Bulletin., v. 80, p. 1095-1108.

Dengler, L., Carver, G., and McPherson, R., 1992, Sources of North Coast seismicity: California Geology, v. 43, no. 3, p.40-53.

Dickinson, W.R.,1997, Overview: tectonic implications of Cenozoic volcanism in coastal California: Geological Society of America Bulletin., v. 109, no. 8, p. 936-954.

Dickinson, W.R., and Rich, E.R., 1972, Petrologic intervals and petrofacies in the Great Valley Sequence, Sacramento Valley, California: Geological Society of America Bulletin, v. 83, p. 1003-1024.

Ernst, W.G., (ed.),1981, The geotectonic development of California: Prentice-Hall, Upper Saddle River, New Jersey, 704 p.

Ferriz, H., 2001, Groundwater resources of northern California - an overview: in Ferriz, H., Anderson, R., (eds.), Engineering Geology Practice in Northern California: Association of Engineering Geologists Special Publication 12 and California Division of Mines and Geology Bulletin 210

Fiske, R.S., and Tobisch, O.T., 1994, Middle Cretaceous ash-flow tuff and caldera-collapse deposit in the Minarets Caldera, east-central Sierra Nevada, California: Geological Society of American Bulletin, v. 106, p. 582-593.

Graham, S.A., McCloy, C., Hitzman, M., Ward, R., and Turner, R., 1984, Basin evolution during change from convergent to transform continental margin in central California: American Association of Petroleum Geologists Bulletin, v. 68, p. 223-249.

Hacker, B.R., Donato, M.M., Barnes, C.G., McWilliams, M.O., and Ernst, W.G., 1995, Time scales of orogeny: Jurassic construction of the Klamath Mountains: Tectonics, v. 14, no. 3, p. 677-703.

Harden, D.R., 1998, California Geology: Prentice Hall, Upper Saddle River, New Jersey, 479 p.

Harwood, D.S., and Miller, M.M., 1990, Paleozoic and early Mesozoic paleogeographic relations; Sierra Nevada, Klamath Mountains, and related terranes: Geological Society of America, Special Paper 255, 422 p.

Hill, M.R., 1970, Mount Lassen is in eruption and there is no mistake about that: California Geology, November 1970, p. 211-227.

Hopson, R.F., 2001, Potential impact on water resources from eruptions near Mammoth Lakes, Mono County, California: in Ferriz, H., Anderson, R., (eds.), Engineering Geology Practice in Northern California: Association of Engineering Geologists Special Publication 12 and California Division of Mines and Geology Bulletin 210

Howell, D.G., (ed.), 1985, Tectonostratigraphic terranes of the Circum-Pacific region: Houston, Circum-Pacific Council for Energy and Mineral Resources, Earth Sci. Series no 1., p. 187-199.

Howell, D.G., and McDougall, K.A., (eds.), Mesozoic paleogeography of the western United States: Society of Economic Paleontologists and Mineralogists, Pacific Section, Symposium 2.

Huber, N. K., and Wahrhaftig, C., 1987, The geologic story of Yosemite National Park: U.S. Geological Survey Bulletin 1595, 64 p. (Reprinted, 1989, by the Yosemite Association, Yosemite National Park)

Huber, N. K., Bateman, P. C., and Wahrhaftig, C., 1989, Geologic map of Yosemite National Park and vicinity, California: U.S. Geological Survey, Miscellaneous Investigations Map I-1874, scale 1:125,000.

Irwin, W.P., 1981, Tectonic accretion of the Klamath Mountains: in Ernst, W.G., (ed.), The geotectonic development of California: Prentice-Hall, Upper Saddle River, N.J., p. 29-49.

Irwin, W.P., 1997, Preliminary map of selected post-Nevadan geologic features of the Klamath Mountains and adjacent areas, Oregon and California: U.S. Geological Survey, Open-file report 97-465.

Jennings, C.W., 1977, Geologic map of California: California Department of Conservation, Division of Mines and Geology, scale 1:750,000.

Jennings. C.W., 1994, Fault activity map of California: California Department of Conservation, Division of Mines and Geology, scale 1:750,000.

Lahren, M.M., and Schweikert, R.A., 1994, Sachse Monument Pendant, central Sierra Nevada, California: eugeoclinal metasedimentary rocks near the axis of the Sierra Nevada batholith: Geological Society of America Bulletin, v. 106, p. 186-194.

Marchand, D., and Allwardt, A., 1981, Late Cenozoic stratigraphic units, northeastern San Joaquin Valley, California: U.S. Geological Survey, Bulletin 1470, 70 p.

McLaughlin, R. , and others, 1988, Tectonics of formation, translation, and dispersal of the Coast Range ophiolite of California: Tectonics, v. 7., no. 5, p. 1,033-1,056.

Miller, C.D., 1980, Potential hazards from future eruptions in the vicinity of Mount Shasta volcano, northern California: U.S. Geological Survey Bulletin 1503, 43 p.

Moores, E.M., Sloan, D., and Stout, D.L., (eds.), 1999, Classic Cordilleran concepts: a view from California: Geological Society of America Special Paper 338, 500 p.

Norris, R.M. and Webb, R.W., 1990, California Geology, 2nd ed.: John Wiley and Sons, New York, N.Y., 541 p.

Page, B.M., Thompson, G.A., and Coleman, R.G., 1998, Late Cenozoic tectonics of the central and southern Coast Ranges of California: Geological Society of America Bulletin, v. 110, no. 7, p. 846-876.

Page, R.W., 1986, Geology of the fresh ground-water basin of the Central Valley: California, with texture maps and sections: U.S. Geological Survey, Professional Paper 1401-C, 54 p.

Page, W.D., Sawyer, T.L., 2001, Use of geomorphic profiling to identify Quaternary faults within the northern and central Sierra Nevada, California: in Ferriz, H., Anderson, R., (eds.), Engineering Geology Practice in Northern California: Association of Engineering Geologists Special Publication 12 and California Division of Mines and Geology Bulletin 210

Pakiser, L.C., and Mooney, W.D., 1990, Geophysical framework of the continental U.S.: Geological Society of America, Memoir 172, 836 p.

Sarna-Wojcicki, A.M., Meyer, C.E., Bowman, H.R., Hall, N.T., Russell, P.C., Woodward, M.J., and Slate, J.L., 1985, Correlation of the Rockland ash bed, a 400,000 year-old stratigraphic marker in northern California and western Nevada, and implications for middle Pleistocene paleogeography of central California: Quaternary Research, v. 23, p. 236-257.

Sarna-Wojcicki, A.M., Lajoie, K.L, Meyer, C.E., Adam, D.P., and Rieck, H.J., 1991, Tephrochronologic correlation of upper Neogene sediments along the Pacific margin, conterminous U.S.: in Morrison, R.B., (ed.), Quaternary nonglacial geology, Conterminous U.S., Geological Society of America, Geology of North America, vol. K-2, p. 117-140.

Stevens, C.H., and Greene, D.C., 1999, Stratigraphy, depositional history, and tectonic evolution of Paleozoic continental-margin rocks in roof pendants of the eastern Sierra Nevada, California: Geological Society of America Bulletin, v. 111, no. 6, p. 919-933.

Turrin, B.D., Christiansen, R.L., Clynne, M.A., Champion, D., Gerstel, W.J., Muffler, L.J.P., and Trimble, D.A., 1998, Age of Lassen Peak, California, and implications for the ages of late Pleistocene glaciations in the southern Cascade Range: Geological Society of America Bulletin, v. 110, no. 7, p. 931-945.

Wahrhaftig, C., and Sloan, D., (eds.), 1989, Geology of San Francisco and vicinity: American Geophysical Union, Washington, D.C., Field trip guidebook T105, 69 p.

Wallace, R.E., 1990, The San Andreas fault system, California: U.S. Geological Survey, Professional paper 1515, 283 p.

Waters, A.C., Donnelly-Nolan, J.M., and Rogers, B.W.,1990, Selected caves and lava-tube systems in and near Lava Beds National Monument, California: U.S. Geological Survey Bulletin 1673, 102 p.

Wright, T.L., and Pierson, T.C., 1992, Living with volcanoes: U.S. Geological Survey, Circular 1073, 57 p.


ASSOCIATION OF ENGINEERING
AEG
GEOLOGISTS

GROUNDWATER RESOURCES OF NORTHERN CALIFORNIA: AN OVERVIEW

HORACIO FERRIZ[1]

INTRODUCTION

California has substantial water resources; however, as more and more people compete for these resources, coordinated utilization and planning on a regional scale is becoming increasingly critical. Groundwater is a particularly important component in the water supply/demand equation, and continues to be an attractive source of water for individual farmers, agro-businesses, rural homeowners, land planners, and water purveyors. We geologists compete with the dowsers and experienced drilling outfits in the tasks of exploration and design of suitable wells for groundwater extraction; however, we take on almost the full burden of solving the problems generated by groundwater development, such as overdraft and progressive depletion of storage, declining water tables, deterioration of quality in freshwater aquifers due to seawater encroachment, and land subsidence due to the compaction of the underlying water-bearing sediments. In addition, we overlap considerably with civil and geotechnical engineers, land planners, and business managers insofar as groundwater basin management and protection are concerned.

This paper is intended to be a point of introduction to the hydrogeology of the major groundwater basins of Northern California (Figure 1), organized loosely by geologic province. The summaries presented are necessarily selective, as the database of California hydrogeology is vast. Hopefully, this overview will familiarize the new generation of hydrogeologists and engineering geologists with some of the basic, "classic" references that shaped much of our current understanding of California hydrogeology. In keeping with the theme of the volume, I have tried to include pertinent information on practical approaches to exploration and groundwater basin management. The interested reader will also want to refer to the excellent summaries prepared by Thomas and Phoenix (1983), and Planert and Williams (1995).

In preparing this summary I have drawn heavily on the work of the U.S. Geological Survey (USGS), the California Department of Water Resources (DWR) and the California Department of Conservation's Division of Mines and Geology (DMG), which, in my opinion, are three of the foremost geologic and hydrogeologic agencies in the world. Those of us that work in California are lucky to be able to stand on the shoulders of giants!

THE CENTRAL VALLEY

The Central Valley is the largest groundwater basin in the state, not only in terms of total storage capacity, but also in terms of its high utilization rate. A conservative estimate for the year 1995 puts the annual extraction rate at 9,000,000 acre-feet (~11 km^3), largely to support California's foremost industry—agriculture (DWR, 1998).

The basin is recharged by direct precipitation and infiltration along the beds of the San Joaquin and Sacramento river systems (which in turn receive most of their discharge from rainfall and snowmelt in the Sierra Nevada). Major withdrawals are through evapotranspiration, subflow into the Sacramento delta, and pumping. With regard to management of the groundwater resource, Bertoldi et al. (1991) have noticed that development of

[1]HF Geologic Engineering
1416 Oakdale-Waterford Hwy.
Waterford, CA 95386

Department of Physics and Geology
California State University, Stanislaus
Turlock, CA 95382
hferriz@geology.csustan.edu

the resource has greatly modified the total flow through the basin, increasing from an estimated 2 million acre-feet in the pre-development period (early 1900s) to nearly 12 million acre-feet in the late 1980s. In the mid 1980s, the total volume of fresh water storage in the upper 1,000 feet of the aquifer system was estimated at about 800 million acre-feet, with an estimated annual net-depletion rate of 800,000 acre-feet.

Stratigraphy and structure. The stratigraphic and structural setting of the fresh groundwater basin has been conveniently summarized by Page (1986). The valley is a synclinal trough that has a surface area of about 20,000 square miles (Figure 1). It is bound to the west by the Coast Ranges, and to the east by the Sierra Nevada, and is often divided into four areas: (1) A northern basin drained by the Sacramento River and its tributaries. (2) The delta region, where the Sacramento, American, and San Joaquin rivers join to empty into Suisun Bay (and from there into the bays of San Pablo and San Francisco). (3) A meridional basin drained by the San Joaquin River. (4) The southernmost Tulare basin, which under natural conditions had internal drainage into the now vanished Tulare Lake. A good percentage of the fluvial inflow into the Tulare basin is diverted toward agricultural irrigation, and the balance empties into the Central Valley aqueduct network.

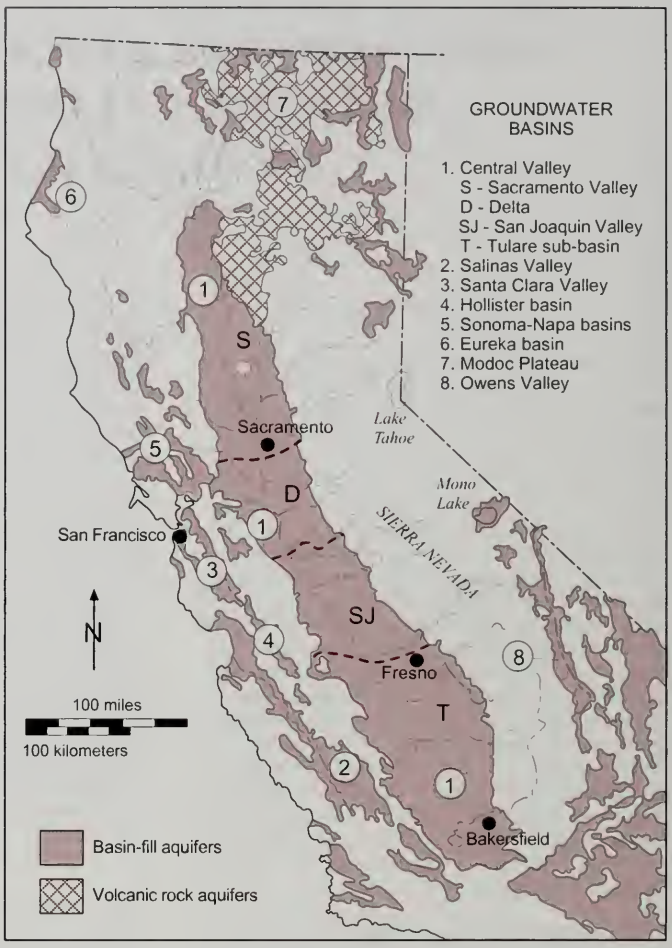

Figure 1. Main groundwater basins in Northern California (modified from Planert and Williams, 1995).

The trough is filled with a thick sequence of late Cretaceous to Holocene sediments, which at the axis of the syncline vary in thickness from 50,000 feet in the north to 30,000 feet in the south. The sedimentary section decreases in thickness toward the margins of the valley and, eventually, pinches out against the metamorphic foothills of the Sierra Nevada or against the fault-bound Franciscan basement of the Coast Ranges. Fresh groundwater aquifers are most often found in post-Eocene units, and the highest yields are obtained mainly from aquifers hosted by Miocene to Holocene units such as the Miocene Mehrten Formation; the Pliocene/Pleistocene Tuscan, Tehama, Laguna, Kern River,

and Tulare formations; and the Pleistocene/Holocene Victor, Turlock Lake, Riverbank, and Modesto formations. The Appendix contains summary descriptions and key bibliographic references to these formations.

Hydrogeology. When describing the aquifers of the Central Valley, it has been traditional to regard the Sacramento Valley basin as having a single unconfined aquifer, and the San Joaquin Valley basin as having an upper unconfined aquifer, an intervening aquitard (the Corcoran Clay), and a lower confined aquifer. This simplified conception is adequate for general description purposes, but Williamson et al. (1989) have convincingly argued that the continental deposits of the Central Valley form, in fact, a single heterogeneous aquifer system, in which lateral and vertical differences in hydraulic conductivity lead to local variations in the degree of aquifer confinement. Consequently, the exploration hydrogeologist should not be surprised to find only trivial head differences across the Corcoran Clay in west Fresno County, but a couple hundred feet difference across some of the minor clay lenses in Kings County. At depth, the freshwater aquifer boundary is "defined" by salinity contents higher than 2,000 milligrams per liter (obviously an arbitrary boundary, but a convenient one for defining the groundwater resource; Page, 1986, Plate 3). The base of the fresh water aquifer lies at an average depth of 3,000 feet in the southern San Joaquin Valley, 1,000 feet in the northern San Joaquin Valley, 200 to 2,000 feet in the Delta area, and 1,500 to 3,500 feet in the Sacramento Valley.

Williamson et al. (1989) reconstructed the likely configuration of the uppermost equipotential surface of the aquifer at the turn of the century, based

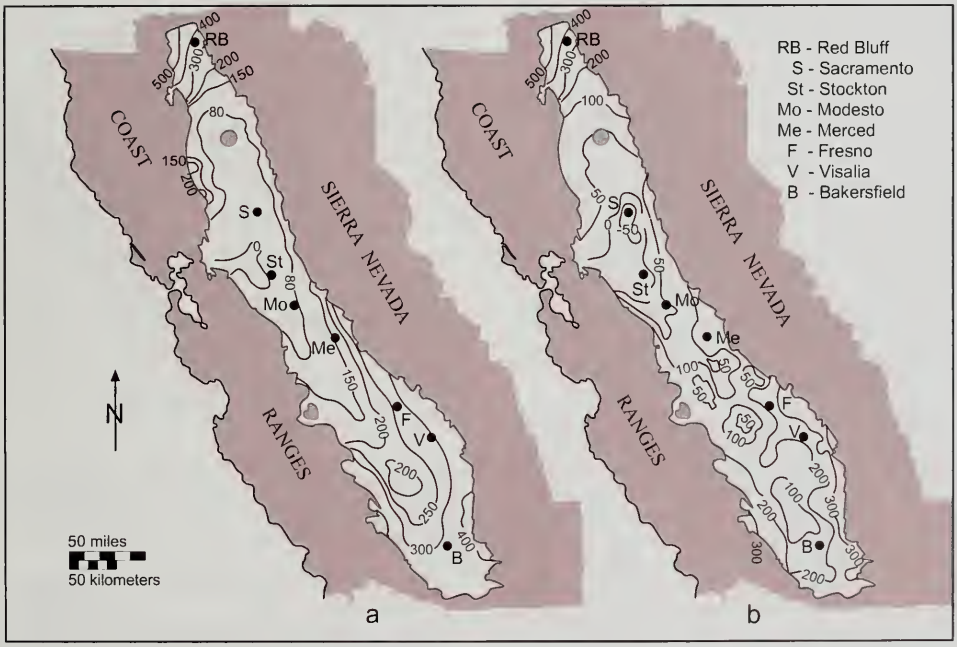

Figure 2. Elevation of the water table throughout the Central Valley. (a) Estimated configuration of the water table at the turn of the century (modified from Williamson et al., 1989). (b) Configuration of the water table in 1997. The contours for the San Joaquin Valley are based on data from DWR (1997a); the contours on the Sacramento Valley are loosely controlled from the data of DWR (1993, 1994, and 1997b).

on the data and observations of Hall (1889), Bryan (1915), and Mendenhall et al. (1916) (Figure 2a). At that time, groundwater generally moved from recharge areas in the higher ground at the edges of the basin toward its topographically lower axis, and from there to its discharge point at the Sacramento delta (or to the secondary discharge area of Tulare Lake). Prior to the development of large-scale agriculture and irrigation pumping, evapotranspiration along the many *tules* (marshes) that covered the floor of the valley was a major mechanism of aquifer discharge (*tule*, from the Nahuatl *tulli*, was the word used by the native inhabitants to describe the bulrushes growing in the saturated soils of the Central Valley). Otherwise groundwater was discharged to the streams as base flow, and eventually lost to the delta. Quite simply, the groundwater basin was "full to capacity".

Heavy pumpage from wells during the last 60 years has changed considerably the geometry of the equipotential surface. As shown in Figure 2b, water table levels have dropped considerably between Sacramento and Stockton, and deep, regional depression cones have formed north of Fresno and Bakersfield. Because of the lowering of the water table most of the *tule* marshes have disappeared, evapotranspiration losses of recharge water have become practically insignificant, and the rivers recharge the basin throughout most of their lengths. These changes have certainly modified the environment of the Central Valley; however, from the standpoint of utilization of the resource, groundwater extraction has certainly reduced the loss of precipitation and snowmelt water into the delta (at the same time that it has furthered the development of California's prime industry—agriculture).

Water quality. Bertoldi et al. (1991) summarized relevant issues regarding the quality of the groundwater resources. In general, the high level of recharge from Sierra streams contributes to lower total dissolved solids levels in the eastern portion of the basin, whereas groundwater in the western half of the basin has consistently higher salinities. Concentrations of dissolved solids are generally lower in the northern half of the Central Valley than in the southern part, perhaps due to the fact that marine sediments with saline connate waters form a larger proportion of the stratigraphic column in the San Joaquin Valley. (The last marine sediments in the Sacramento Valley are Eocene in age, whereas the southern half of the basin was the locus of localized marine deposition as recently as the Pliocene.) The basin is also subject to seawater intrusion in the Sacramento delta area.

Engineering geology. Shallow water table levels are of concern to civil works, particularly in the Sacramento delta area. For example, some portions of the delta are susceptible to liquefaction under seismic loading, largely due to the low consolidation of the sediments and shallow depths to the zone of saturation. Drainage of water-logged soils for agriculture has also led to oxidation of peat and subsidence. Levees have been built to protect the sinking ground from tidal flooding, but this in turn has created a potential hazard for catastrophic flooding in the event of levee failure.

Particularly high rates of groundwater extraction in the period between the early 1940s and the mid 1970s triggered extensive subsidence throughout the southern and central portions of the Central Valley. Poland et al. (1975) did an extensive study of the subsidence problem and concluded that nearly one-half of the area of the San Joaquin Valley (approximately 5,200 square miles) had been affected by subsidence, with as little as 1 foot of settlement in the less affected areas and as much as 30 feet in the Los Baños-Kettleman Hills area, 12 feet in the Tulare-Wasco area, and 10 feet in the Maricopa-Arvin area. Poland et al. (1975) were able to correlate the magnitude of subsidence with the local pumping rates and with the presence of thick lenses of montmorillonitic clays in the local stratigraphic column. Pumping-related subsidence has created agricultural drainage problems, has compromised roads and railroad tracks, and has triggered large expenditures for maintenance of the California Aqueduct (Poland et al.,1975). A recent review of the problem of subsidence in the San Joaquin Valley can be found in the paper by Swanson (1998).

A larger volume of surface water imports during the late 1970s and decreased rates of extraction during the last 20 years have contributed to a virtual cessation of subsidence in the Central Valley.

THE COAST RANGES

The narrow and elongated ranges and valleys of this province have a predominant north-northwesterly trend. Reed (1933) was the first to emphasize the presence of two types of "basements" within this province. Between the San Andreas fault and the Central Valley, the oldest exposed rocks belong to the Franciscan Series (Lawson, 1895), a subduc-

tion zone assemblage with a predominance of graywackes, submarine lavas, and serpentinites that have experienced low-temperature, high-pressure metamorphism. Between the San Andreas and Nacimiento faults (the Salinian Block of Compton, 1966), in contrast, the basement is formed by gneisses, schists, quartzites, marbles, and granulites that have been intruded by plutons of quartz diorite, granodiorite, adamellite, and granite. Finally, west of the Nacimiento fault and all the way to the coast, the basement is once again formed by Franciscan rocks. Clearly, the San Andreas and Nacimiento faults are major zones of structural discontinuity that have juxtaposed significantly different terranes.

A thick blanket of Upper Cretaceous and Cenozoic clastic rocks covers the basement rocks and bears record of intermittent but persistent crustal deformation. Folds, thrust faults, steep reverse faults, and strike-slip faults developed as a consequence of Cenozoic deformation, some of which continues to date (Page, 1966). Some of these deformed units host small-volume aquifers that can adequately supply small rural communities, but the truly significant aquifers of this province are found in Pliocene to Recent alluvial fill of active structural basins such as the Salinas Valley (a faulted synclinal structure between the Nacimiento and San Andreas faults) and the Santa Clara Valley (between the San Andreas and Hayward faults). Smaller groundwater basins such as the Sonoma and Napa valleys north of San Francisco Bay, or the Eureka basin in Humboldt County, have been formed by fluvial aggradation processes.

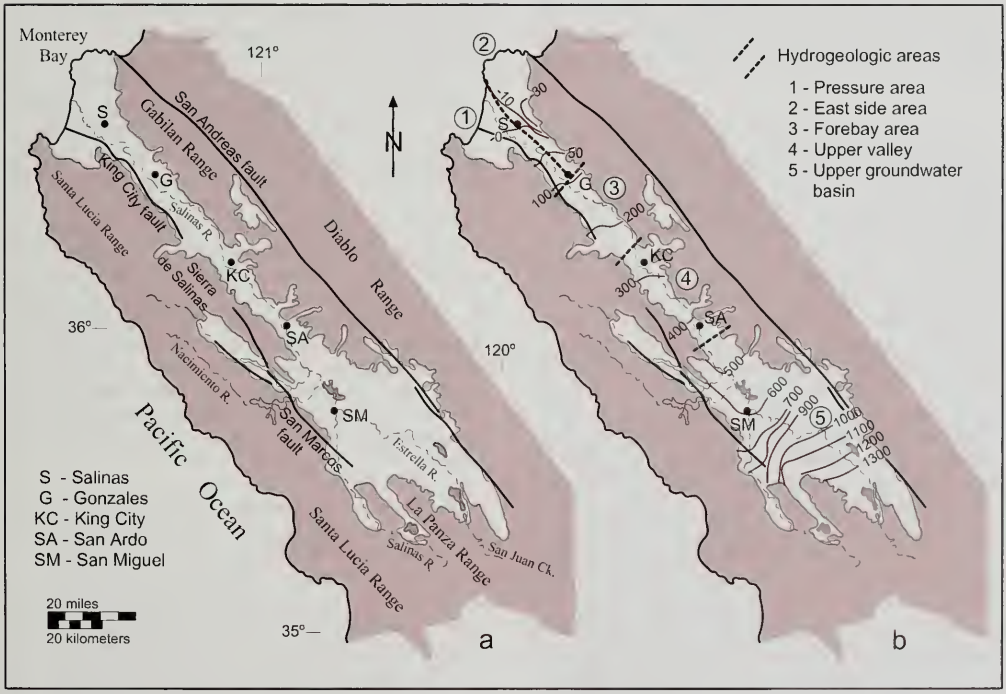

Figure 3. (a) General map of the Salinas Valley (modified from Planert and Williams, 1995, and from Durbin et al., 1978). (b) Hydrogeologic subdivisions of the Salinas groundwater basin, and general configuration of the water table in the early 1980's (modified from Planert and Williams, 1995, and from Showalter et al., 1983).

The Salinas Valley

Stratigraphy and structure. The Salinas Valley (Figures 1 and 3) is an elongated, intermontane fluvial valley formed by the Salinas River and its tributaries. The Salinas Valley groundwater basin has been divided into two sub-basins by Planert and Williams (1995). The first, called the upper basin, extends from the headwaters of the Salinas River and its tributaries (e.g., the Estrella River) to San Ardo. The groundwater resources of this basin have not been widely developed, so its hydrogeology is not well understood, but the unconsolidated deposits are reported to be as much as 1,750 feet in the alluvial deposits of the Estrella River. The second, lower basin, extends from San Ardo to Monterey Bay. The alluvial prism of the lower basin is 70 miles long, about 3 miles wide at San Ardo, and 10 miles wide at Monterey Bay. The lower basin has an average thickness of 1,000 feet of saturated sediments, but locally the alluvial prism is as much as 2,000 feet thick. It supports a thriving agricultural industry, and its groundwater resources are being actively utilized.

On the southwest, the Salinas Valley is separated from the Pacific Ocean by the Santa Lucia Range, and from the Carmel River by the Sierra de Salinas. On the northeast, it is separated from the San Joaquin Valley by the Diablo Range, and from the Hollister basin by the Gabilan Range. The history of structural deformation of these ranges, and of the intervening structural trough, is complex (e.g., Durham, 1974), but it appears that the basement under the valley has either been folded downward, down-dropped by faults, or both. The trough was invaded by the sea during the late Cretaceous, and was the site of intermittent marine deposition until the Pliocene. The marine deposits span the spectrum from conglomerates through mudstones, including the cherts and diatomites of the Miocene Monterey Formation. The ocean retreated during the Plio-Pleistocene, and the older marine deposits were widely blanketed by the sandstones and conglomerates (and subordinated mudstone, fresh-water limestone, and lignite) of the Paso Robles Formation. Durham (1974) classified sediments younger than the Paso Robles as alluvium, and differentiated it into: (a) old alluvium associated with old land surfaces in the hills, (b) old alluvium in valleys and lowland areas, (c) modern alluvium in stream beds, (d) debris-flow material, and (e) dune sand (described as the Aromas Sand by Dibblee (1973) and Dibblee et al. (1979)).

Hydrogeology. Durbin et al. (1978) followed local usage and divided the lower basin into four areas: the Pressure Area, the East Side Area, the Forebay Area, and the Upper Valley Area (Figure 3b). Groundwater moves from one area to another, so they are not sub-basins in a hydrogeologic sense; rather, they are a pragmatic way of recognizing variations in the degree of confinement of the aquifer, or regional variations in the specific capacity of production wells.

The Pressure Area extends from about 6 miles offshore beneath Monterey Bay to Gonzales. In this area of estuarine deposition massive clay units underlie much of the area between Monterey Bay and Salinas, and divide the unconsolidated deposits into an upper aquifer (the so-called 180-foot aquifer) a lower aquifer (the 400-foot aquifer), and a deep aquifer (the 900-foot aquifer). As the name of the area implies, within its footprint the aquifers are confined. The East Side Area encompasses the area east of the line that joins Gonzales and Salinas, up to the base of the Gabilan Range. Groundwater under semi-confined conditions is found in sand and gravel lenses that are interbedded with thick deposits of fine-grained sediments. Finally, groundwater in the Forebay and Upper Valley areas is mostly unconfined.

Specific capacity values (i.e., yield of the well divided by the drawdown) are smallest in the northern end of the basin, and tend to increase to the south. Average values of specific capacity are 25 gal/min/ft for the East Side Area and 60 gal/min/ft for the Pressure Area. In contrast, the average specific capacity of wells in the Forebay Area is 100 gal/min/ft. and 150 gal/min/ft in the Upper-Valley Area. Durbin et al. (1978) caution that the specific capacities of individual wells within each area are quite variable.

Recharge to the lower basin is largely by infiltration along the channel of the Salinas River (~30% of total recharge) and its tributaries (~20%). The second major source of recharge is irrigation return water (~40%). The remaining recharge is contributed by direct recharge from precipitation over the valley floor, subsurface inflow, and seawater intrusion. Outflow from the basin is dominated by pumping (~95%) and evapotranspiration by riparian vegetation (~5%). DWR (1995) estimated basin inflow at 532,000 acre-feet per year, and basin outflow at 550,000 acre-feet per year. The Salinas Valley Water Project is currently being implemented by the

Monterey County Water Resources Agency to mitigate groundwater overdraft and seawater intrusion. The project includes mitigation measures such as construction or retrofit of recharge dams, protection of recharge areas, and injection of recycled water into the impacted aquifers.

Not much information has been published on the hydrogeology of the upper basin, along the headwaters of the Salinas, Estrella, and San Juan Rivers. Showalter et al. (1983) state that groundwater in deep deposits is confined but that shallow groundwater is largely unconfined.

The general direction of groundwater flow is down the valley, from the headwaters of the Salinas and Estrella rivers, to San Ardo, to Monterey Bay (Figure 3b). Between San Ardo and Monterey Bay the average hydraulic gradient is 0.001 ft/ft, closely following the gradient of the Salinas River. Locally, however, pumping depression cones have imparted a distinctive cross-valley gradient to the potentiometric surface. Such is the case at the latitude of Gonzales, where water levels on the northeast side of the valley are about 30 feet lower than on the southwest side, or at the latitude of Salinas, where the difference is as high as 60 feet. Water levels in much of the Pressure and East Side areas are below sea level during a large part of the year. As a result, at Monterey Bay the direction of groundwater movement is inland and seawater intrusion is occurring (DWR, 1975).

Water quality. According to Planert and Williams (1995), groundwater in the Salinas Valley basin is generally acceptable for most uses, with dissolved solid concentrations ranging between 200 and 700 mg/liter. Exceptions are the Bitterwater area in the upper basin (high boron and arsenic), San Lorenzo Creek (high sulfate due to dissolution of gypsum beds), and the area between Soledad and Salinas (organic pollutants and high nitrate concentrations as a result of industrial and agricultural activity).

As reported by et al. (1978), seawater intrusion has considerably degraded water quality in the Pressure Area. Seawater intrusion was first noted in the 1930s and led to abandonment of several wells screened in the 180-foot aquifer. This degradation led to development of the 400-foot aquifer, but by the late 1960s this aquifer was also being degraded. By 1970 seawater intrusion had extended about 4 miles inland in the 180-foot aquifer, and about 2 miles in the 400-foot aquifer. The problem continues to affect the area, and as of 1995 seawater intrusion had extended up to 6 miles inland.

Engineering geology. The Salinas Valley has not been strongly affected by subsidence due to withdrawal of groundwater or by the problems commonly associated to shallow water tables. Nevertheless, this area promises to be a focus of engineering geology activity during the first few years of the new millennium. The works associated with the Salinas Valley Water Project will no doubt be the ground where many young engineering geologists will learn their craft. The planning horizon for the project is the year 2030, and it includes:

1. Spillway modifications at Nacimiento Dam to accommodate the probable maximum flood event, thus allowing full use of the capacity of the dam.
2. Operation of the Nacimiento and San Antonio reservoirs during the spring and summer months, first to increase recharge through the Salinas River bed, and ultimately for downstream diversion.
3. Storage and use of recycled water from the Monterey County water recycling projects.
4. Diversion of the Salinas River for direct delivery to agricultural users or to be stored in a newly-constructed reservoir for urban use.
5. Construction of treatment and water-conveyance facilities.

San Francisco Bay—Santa Clara Valley groundwater basin

Stratigraphy and structure. San Francisco Bay and the Santa Clara Valley occupy a linear, northwest-trending intermountain structural depression in the Central Coast Ranges (Figures 1 and 4). The depression is bound by the Mesozoic marine formations and Franciscan assemblage of the Santa Cruz Mountains and the San Francisco Peninsula on the west, and the Franciscan graywackes and serpentinite bodies of the Diablo Range on the east. The structural depression itself formed in response to movement along the San Andreas fault across the Santa Cruz Mountains and the San Francisco Peninsula, the Hayward fault along the eastern edge of the trough, and the Calaveras fault in the Diablo Range.

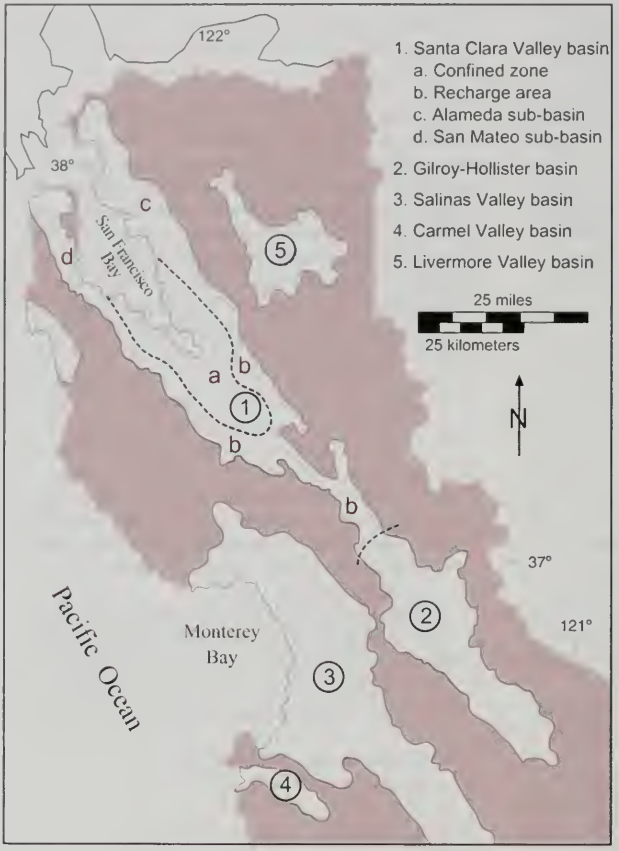

Figure 4. General map of the Bay Area, with hydrogeologic subdivisions (modified from Planert and Williams, 1995, Iwamura, 1995, and DWR, 1975).

Santa Clara Valley proper ends to the north against the San Francisco Bay, which occupies the northern end of the structural depression, but the alluvial fill "forks around" the Bay to merge with the plains and baylands of San Mateo on the west, and of Alameda on the east. The groundwater basin can thus be divided into five sub-basins (DWR, 1980): the Alameda Bay Plain and Niles Cone sub-basins east of San Francisco Bay, the San Mateo sub-basin west of San Francisco Bay, and the Santa Clara Valley and Coyote Valley sub-basins south of San Francisco Bay.

Hydrogeology. The hydrogeology of the Santa Clara Valley has been discussed recently by Iwamura (1995), who is the primary source of the following discussion. Other key references to the hydrogeology of the area are Clark (1924), and DWR (1967, 1975b, 1981).

For practical purposes, the aquifers of the Santa Clara Valley can be grouped into three hydrogeologic units: (1) a recharge area (called "forebay" by Iwamura, 1995), (2) an upper aquifer zone, and (3) a lower aquifer zone that hosts the primary drink-

Of these five, the Santa Clara Valley sub-basin is in many regards representative of the whole structural trough. Stratigraphically, its alluvial fill is divided into older, lightly consolidated Plio-Pleistocene alluvium of the Santa Clara Formation (Bailey and Everhart, 1964; Dibblee, 1966; Cummings, 1972), and younger, unconsolidated Pleistocene-Holocene alluvium. The Santa Clara Formation does not yield large volumes of water to wells along the margins of the structural trough, but it is water-yielding toward the center of the basin, where it becomes indistinguishable from young alluvium in terms of lithology and consolidation (or lack thereof).

The younger alluvium was deposited as a series of coalescing alluvial fan deposits off from the surrounding mountain ranges. The sediments of the upper fan areas are coarse-grained, and form thick accumulations of permeable gravels and sands. The finer-grained, distal fan deposits interdigitate with shallow marine and tidal deposits of San Francisco Bay. Hence, the sedimentary deposits near the axis and mouth of the valley show distinctive stratification and have marked variations in vertical hydraulic conductivity. Many of the sand and gravel bodies found in the axis of the basin represent buried stream channels with limited lateral continuity. These sinuous channels apparently carved their courses across the inderdigitating marine and distal fan deposits.

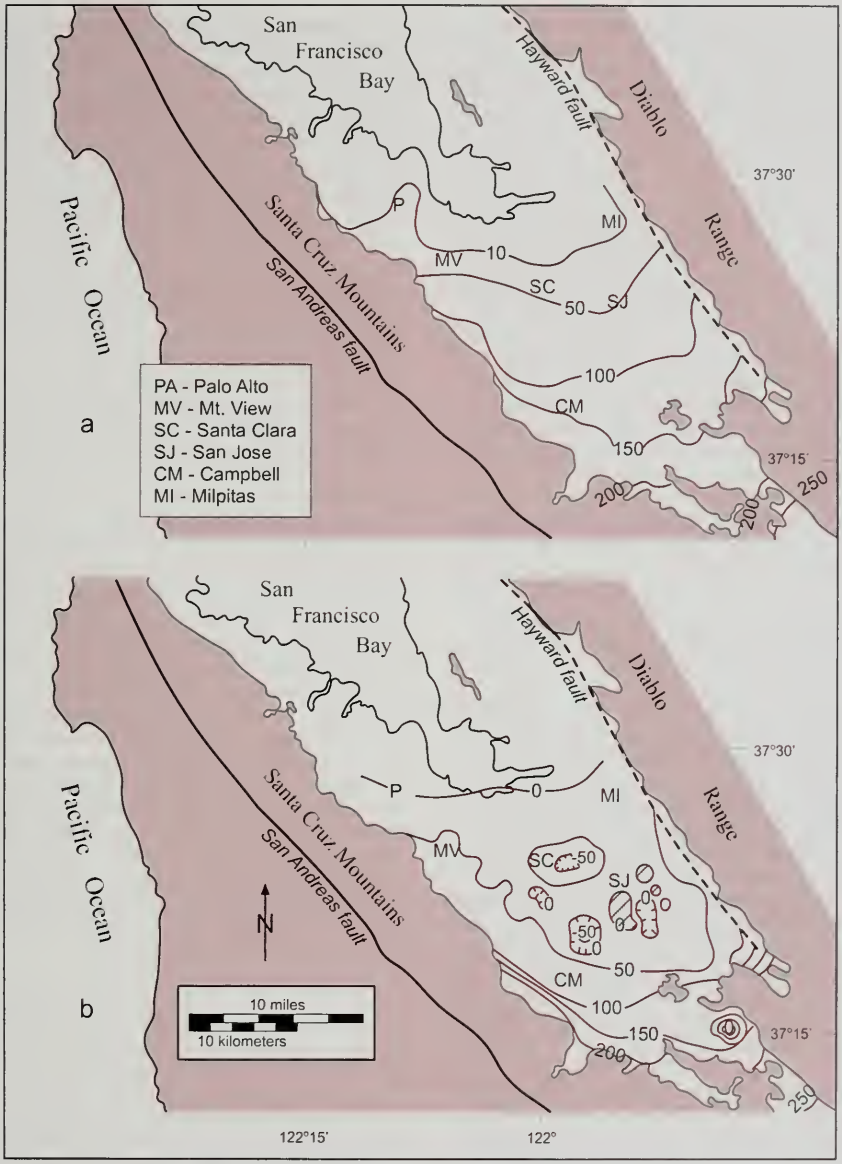

Figure 5. (a) Configuration of the water table throughout the Santa Clara Valley in the early 1900's (modified from Poland and Ireland, 1968 and from Planert and Williams, 1995). (b) Configuration of the water table throughout the Santa Clara Valley in September 1997 (modified from Moll, 1998).

ing water aquifers. The recharge area of the basin comprises the upper alluvial fan areas (including the foothills of Palo Alto/San Mateo on the west and of Alameda on the east). The sediments are highly permeable, though intervening leaky aquitards of small lateral extent are common.

Within the central portion of the basin the distal facies of the sloping alluvial fans become distinctively divided into discrete aquifers within a predominantly clayey section. The "upper aquifer zone" is the term used to group aquifers that occur within 150 feet from the surface. In contrast, the "lower aquifer zone" is the collective name given to aquifers that are deeper than 150 feet. The distinction is admittedly arbitrary, but it is also convenient because all the aquifers in the lower aquifer zone are confined. In the upper aquifer zone, groundwater is either unconfined or confined by leaky aquitards.

The two aquifer zones are separated by an extensive, thick, compacted aquitard that is essentially impermeable. The aquitard pinches out toward the medial portion of the alluvial fan apron, which enables recharge of both aquifer zones through lateral flow from the common recharge area in the upper reaches of the alluvial fans.

In the early 1900s, before significant development of the groundwater resource, groundwater flowed in a simple pattern, from the elevated recharge areas along the flanks of the basin toward San Francisco Bay (Figure 5a). Recent maps of the potentiometric surface (Moll, 1998) show a significant lowering of the water level and the hydraulic gradient in the urban area around San Jose (compare, for example, the change in the 50 foot elevation contour between Figures 5a and 5b). Wide depression cones have formed around the major pumping centers in the interior of the basin (e.g., around San Jose and Santa Clara in Figure 5b), and local recharge mounds have formed in response to local reinjection (e.g., hatched areas around San Jose in Figure 5b).

As previously mentioned, recharge to the basin occurs largely by infiltration from streams in the upper alluvial fan areas. However, return irrigation, infiltration of areal precipitation, and artificial recharge through the ponds operated by the Santa Clara Valley Water District are significant contributors to the inflow balance of the basin. Outflow is mainly by pumping withdrawal.

Many similarities exist between the hydrogeology of the Santa Clara Valley sub-basin and the Alameda Bay Plain, Niles Cone, and San Mateo subbasins, particularly with regard to the upper alluvial fan areas. For example, in the vicinity of Niles and Hayward one can recognize the shallow Newark aquifer, and the deeper Centerville aquifer. Saline water has advanced 2-5 miles into the shallow Newark aquifer on a broad front, so this aquifer is not widely utilized. The deeper Centerville aquifer is a viable resource, although faulty and abandoned wells appear to have allowed downward leakage of salty water from the Newark aquifer at some locations (DWR, 1960a; 1968).

Before development started in the early 1900s, the Santa Clara groundwater basin was essentially full to capacity, and surface streams emptied their "rejected recharge" into San Francisco Bay (Iwamura, 1995). Thus, the first wells drilled found groundwater at very shallow depths or, if drilled into the lower aquifer zone, were naturally flowing artesian wells. As groundwater production increased, however, the water table declined in the upper aquifer zone, and the artesian pressure decreased. The decline of the water table also led to a reversal in the gradient of the upper aquifer zone in the San Francisco bayfront area, which in turn led to saltwater intrusion into the upper aquifer (Tolman and Poland, 1940). The water levels and pressures started to rise in the mid-1930s after construction of several artificial recharge reservoirs. Water levels dropped again between 1944 and 1965 in response to pumping overdraft, and the accompanying pressure reduction in the lower aquifer zone triggered localized seawater intrusion, albeit not as extensive as in the upper aquifer zone. Overdraft ceased in 1965, when pumping decreased in response to water imports from the State Water Project and Hetch Hetchy Reservoir.

Currently, most groundwater is pumped from either the confined lower aquifer zone or from the unconfined gravels of the recharge area. Aquifers of the upper zone are little used, in part because the agricultural industry has declined significantly in the valley, and in part because of the high salinity triggered by seawater intrusion. Furthermore, local contamination plumes of organic solvents and fuels have affected the upper aquifer zone.

Water quality. The aquifers of the Santa Clara Valley basin have been partially affected by seawater intrusion, rise of deep-seated connate waters

with high contents of dissolved solids, nitrate and pesticide accumulation, gasoline and solvent leaks, and bacterial pollution due to poor disposal practices of sewage and refuse (Iwamura, 1980, 1995). The Santa Clara Valley Water District and the Regional Water Quality Control Board have given high priority to the investigation of these problems, and their remediation or containment will no doubt occupy the attention of a few generations of engineering geologists.

With respect to migration of contamination between the upper and lower aquifer zones, the intervening aquitard appears to be an effective barrier against natural migration. Unfortunately many wells are screened in both aquifers, so contaminant migration through the boreholes themselves, or through their gravel packs, is probably the main mechanism for dispersal of contaminants into the lower aquifer zone.

Engineering geology. The major claim to engineering geology fame of the Santa Clara Valley is the extensive subsidence that was induced by groundwater withdrawals between 1920 and 1969. Subsidence triggered a host of remedial actions, including levee construction along the bayfront and tributary stream banks to prevent inland encroachment of the waters of San Francisco Bay (Tolman and Poland, 1940). Construction of water conservation reservoirs in the mountainous watershed enhanced recharge of the aquifers, which led to a partial recovery of groundwater levels and pressures between 1935 and 1944, and to greatly diminished subsidence. The problem arose again in the mid 1940s. when increased pumping triggered anew the onset of subsidence, particularly in the area between southeast San Jose and downtown Mountain View. Poland and Ireland (1968) estimated up to 8 feet of subsidence for downtown San Jose for the 1945-1968 period, and a total aggregate subsidence of 13 feet for the 1935-1969 period (Poland, 1969). Recent reviews of the problem of subsidence in California can be found in the volume edited by Borchers (1998).

The import of water from the State Water Project and Hetch-Hetchy Reservoir led to decreased groundwater pumping and virtual cessation of land subsidence. Since water imports started, pressure in the lower aquifer zone has slowly increased, to the extent that some of the wells within the interior of the basin have recovered their artesian character.

Gilroy-Hollister groundwater basin

Stratigraphy and structure. In terms of stratigraphy and structure, the Gilroy-Hollister Valley is the southernmost extension of the Santa Clara and Coyote Creek Valleys (Figure 4). Topographically, the boundary between the two drainage basins is the apex of the Morgan Hill alluvial fan, which forms a drainage divide between the watershed of Coyote Creek (draining to San Francisco Bay), and that of the Pajaro River (draining to the Pacific Ocean). This drainage divide generally corresponds with the groundwater divide that forms the northwestern hydrogeologic boundary of the Gilroy-Hollister groundwater basin. The basin itself is hosted by the alluvial deposits of the headwater tributaries to the Pajaro River: the Llagas, Uvas, Pacheco, Tequisquita, and Santa Ana Creeks, and the San Benito River. The alluvial basin is about 20 miles long in the northwest direction and 6 miles wide, and is bound by the Franciscan of the Diablo Range to the northeast and faulted Tertiary sedimentary units to the southwest, within the zone of structural deformation of the San Andreas and Calaveras fault systems (Figure 6).

The thickness of the alluvial fill of the basin ranges between 500 feet at the Morgan Hill alluvial fan to more than 1,000 feet in the center and south of the basin, and 2,000 feet in the San Benito area. These thickness estimates include the underlying, slightly consolidated sands and gravels of the Santa Clara Formation and the San Benito Gravel. According to Kilburn (1972), the older sedimentary deposits have been subjected to several episodes of faulting and folding. The Holocene alluvium does not appear to be folded, but it is broken by currently active faults. The structural setting of the basin is complex: Two major faults, the San Andreas and Calaveras faults, dominate the tectonic fabric of the region, but a host of smaller faults cut the basin and act as groundwater barriers (e.g., the Park Hill West, Asuyama, Santa Ana Valley, Tres Pinos, and Bolado Park faults). Separating the Hollister and San Juan valleys are the faulted and folded sandstones of the Purisima Formation in the Lomerias Muertas and Flint Hills. For convenience, this zone of structural deformation is here referred to as the "Sargent anticline" (Figure 6).

Hydrogeology. From a hydrogeologic standpoint, the Gilroy-Hollister groundwater basin has been divided into four sub-basins (Kilburn, 1972; Iwamura, 1989): the Llagas sub-basin (a political

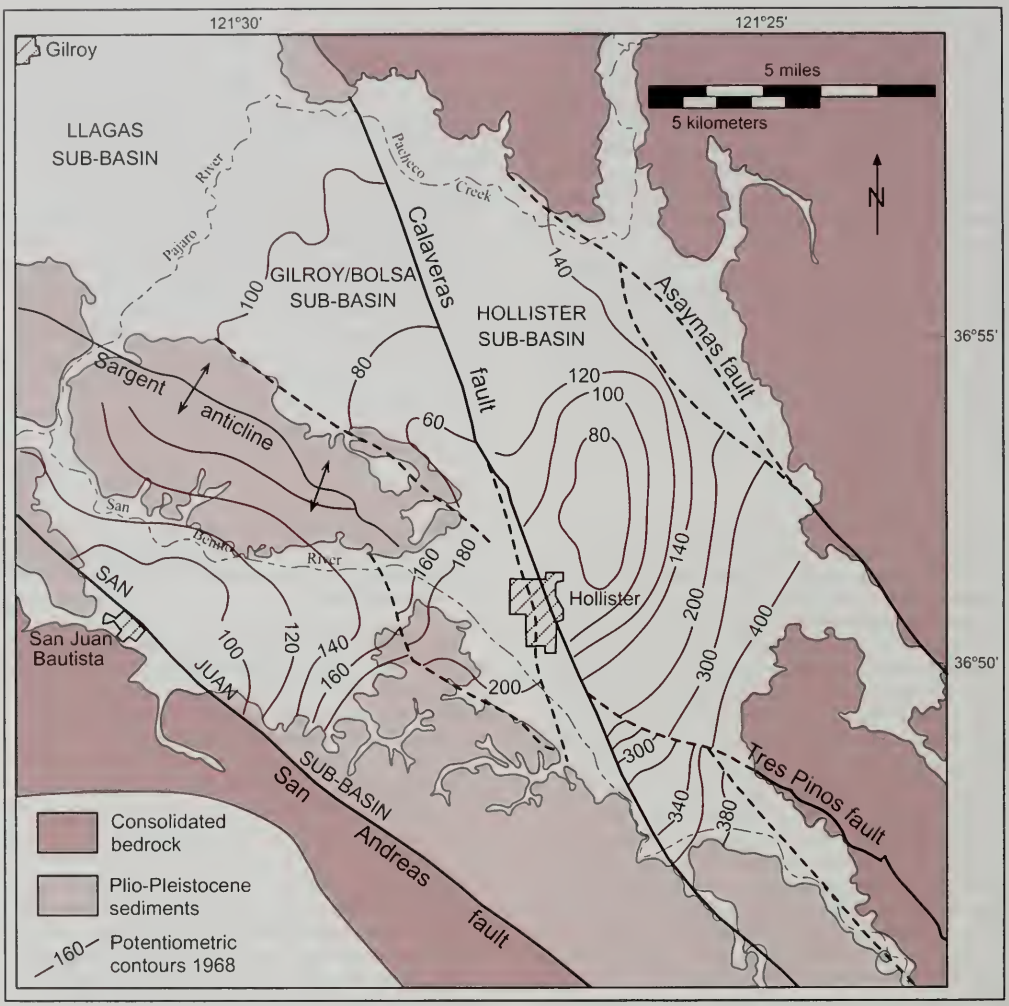

Figure 6. Map of the Gilroy-Hollister basin, with hydrogeologic subdivisions, and general configuration of the water table throughout the Gilroy-Hollister basin in 1968 (modified from Kilburn, 1972).

division used to refer to that part of the Gilroy-Hollister basin that is within Santa Clara County), the Gilroy-Bolsa sub-basin (which forms the natural extension to the southeast, into San Benito County, of the Llagas sub-basin), the Hollister sub-basin, and the San Juan sub-basin (Figure 6). Most of the sub-basin boundaries are defined by bedrock outcrops, the trace of the San Andreas or Calaveras faults, and the crest of the Sargent anticline (with the exception, of course, of the political boundary of Santa Clara and San Benito counties).

The combined Llagas-Gilroy-Bolsa sub-basin has a similar hydrostratigraphy to that found in the Santa Clara Valley groundwater basin (Iwamura, 1989): (1) A recharge area defined by the upper reaches of the alluvial fans, and (2) a flat interior portion where upper and a lower aquifer zones are

separated by an intervening aquitard. The recharge area has the typical stratigraphy of the proximal facies of an alluvial fan, with coarse gravel units interbedded with minor fine-grained lenses. The upper aquifer zone consists of several aquifers interbedded with thin aquitards. The uppermost aquifer is unconfined, whereas the others are confined or partially confined. The top of the intervening aquitard is found at depths that vary between 20 and 100 feet, and its thickness ranges between 40 and 100 feet. Numerous individual confined aquifers occur in the lower aquifer zone. Wells tapping into the lower zone south of Old Gilroy used to be flowing artesian wells, but agricultural pumping has decreased the aquifer pressures, and only very few wells retain their artesian character.

At its southeastern terminus, the Llagas-Gilroy-Bolsa sub-basin is bound by the "V" formed by the Calaveras fault and the axis of the Sargent anticline. The Pajaro River entrenched itself into the anticline as the latter formed during the Pleistocene-Holocene, forming a narrow gap that provides for surface drainage of the basin. However, the alluvial fill in the gap is not deep enough to allow for significant underflow discharge out of the basin. Prior to development of the groundwater resource in the early 1900s) groundwater discharge was chiefly by upward movement into the bed of the Pajaro River and evapo-transpiration from the marshy land between the Pajaro and Tequisquita Rivers (Clark, 1924). The sub-basin has now been extensively developed with irrigated agriculture, and pumping has created a broad depression cone at the southeastern end of the basin, a couple of miles west of the Hollister municipal airport (Figure 6).

The Hollister sub-basin is bound by the Calaveras fault to the west, and the front-range faults of the Diablo Range (Asuyamas and Santa Ana Valley faults) to the east. The boundary faults are relatively impermeable, with piezometric levels varying by as much as 100 feet across the faults. According to Kilburn (1972), prior to development groundwater moved generally to the northwest from recharge areas in the southern and eastern sides of the basin. Discharge was through artesian flow into the streams and marshes in the northern half of the basin. Probably little groundwater flowed across the Calaveras fault into the adjacent San Juan and Gilroy-Bolsa sub-basins. With the onset of irrigation pumping the piezometric surface changed, however, and the pattern of groundwater flow is now toward a broad depression centered 3 miles northeast of downtown Hollister and toward a secondary depression cone in the structural sliver formed between the Asuyamas and Santa Ana Valley faults.

The San Juan sub-basin is bound by the Sargent anticline to the north, the Calaveras fault to the east, the Bird Creek Hills to the south (formed by outcrops of folded sandstones of the Purisima Formation), and the San Andreas fault to the west. Based on a compilation of water-level records, Kilburn (1972) distinguished two aquifers in the San Juan and Hollister sub-basins: (1) a semi-confined aquifer that extends to a depth of as much as 300 feet below ground surface, and (2) an underlying confined aquifer of undetermined thickness. The basin appears to receive most of its recharge from streambed infiltration along the upper reach of the San Benito River, with perhaps some underflow from the Hollister sub-basin across the Calaveras fault. Before basin development, the San Benito River appears to have been a losing stream east of Hollister, and a gaining perennial stream west of Hollister. Groundwater flow at the time was to the northwest, toward the confluence of the Pajaro and San Benito Rivers. This configuration has changed considerably now that the basin is being actively pumped. For one thing, the San Benito River is now a losing stream throughout most of its extent and for most of the year, so the basin is now recharged whenever the river flows (in contrast, before development the groundwater basin was "full", and any additional recharge was "rejected" in the form of subflow to the lower reaches of the river). The general groundwater flow direction continues to be to the northwest but, instead of reaching the Pajaro River, it now gravitates toward a broad depression cone that has developed just east of San Juan Bautista.

Livermore groundwater basin

Livermore Valley is an intermontane valley nestled in the heart of the Diablo Range. The Livermore groundwater basin is hosted by the alluvial fill of the valley, and is elongated in an east-west direction (Figure 7). To the northwest it has a narrow extension that follows the trend of the Calaveras fault (the Dublin-San Ramon sub-basin). To the southeast it merges with Sunol Valley, but the latter has been traditionally considered a separate groundwater basin. The Livermore groundwater basin encompasses a surface area of approximately 100 square miles (~65 mi^2 underlain by Quaternary alluvium and 35 mi^2 underlain by Livermore Formation).

Major cities within the basin are Livermore on the east end, Pleasanton on the west end, and San Ramon Village and Dublin in the narrow northwestern extension.

Livermore Valley is drained by Arroyo de la Laguna and its tributaries (starting from the north and proceeding clockwise South San Ramon Creek, Alamo Creek, Tassajara Creek, Arroyo Las Positas, Arroyo Mocho, and Arroyo Valle). At the mouth of Livermore Valley, Arroyo de la Laguna joins Alameda Creek, which flows southerly through Sunol Valley (where it is impounded by Sunol Dam), cuts across the Diablo Range through Niles Canyon, and eventually reaches San Francisco Bay.

Stratigraphy. The Jurassic through Miocene formations that bound Livermore Valley are too indurated to host significant groundwater resources. The Pliocene Orinda Formation that crops out just north of Livermore Valley, and the Plio-Pleistocene Livermore Formation that crops out in the hills to the south are not indurated, and contain significant amounts of gravel and sand. Their yields are marginal and erratic, however, because of the relatively high proportion of fines. The Orinda Formation reaches a thickness of 9,000 feet north of the valley, whereas the Livermore can be up to 4,000 feet in thickness to the south. Locally, these units may play an important role in recharging the Quaternary alluvial aquifers.

The following summary of the Plio-Pleistocene geologic history of the area is largely based on Barlock (1988) and Andersen (1995) (see also Crittenden, 1951; Hall, 1958; DWR 1966, 1974; Dibblee, 1980a, 1980b): The Livermore intermontane basin between the Calaveras fault to the west and the Greenville fault to the east has been filled with continental detritus since the Late Miocene, in response to spasmodic Coast Range uplift. The lower portion of the Livermore Formation was deposited between 5 and 2.5 million years ago, by sand-dominated braided streams as a result of uplift in the Altamont Hills. 2.5 million years ago the sediments of the upper Livermore Formation record the uplift of the central Diablo Range and the development of an alluvial fan complex that reversed the direction of sediment transport. The braided streams and debris flows of this fan spreaded Franciscan detritus northward across Livermore valley. These deposits have been warped and tilted by Pleistocene deformation, so the Livermore Formation now dips 10 to 20° degrees to the north in the hills south of the valley.

The main aquifers of the Livermore basin are in Upper Pleistocene and Recent fluvial gravels and sands, which are collectively referred to as Quaternary alluvium. DWR (1966) "mapped" the changes in the paleogeography of the streams by contouring the proportion of sand and gravel in the 0 to 100, 100 to 200 and 200 to 300-foot depth intervals (the alluvium is as much as 500 feet thick along the axis of the valley). These contour maps, and a careful analysis of the stratigraphy of selected wells, have revealed a fascinating sedimentologic history: After northward tilting of the Livermore Formation in the mid-Pleistocene, streams draining the newly created highlands flowed north into the Livermore depression, crossed it from east to west while accumulating alluvium, and eventually flowed out through San Ramon Valley to empty into the ancestral Sacramento River into the area now occupied by Suisun Bay. The southern streams "cleaned up" gravels eroded from the Livermore Formation and spread them over nearly the entire floor of the valley. Gradually, great sheets of clean gravel accumulated as the streams worked their way back and forth over the valley floor.

The outlet to the northwest through San Ramon Valley seems to have been blocked from time to time, probably in response to rupture of the Calaveras fault and associated landsliding. At the times the outlet was blocked, the carrying capacity of the streams was reduced, and swamps and lakes formed in the western portion of the valley, so fairly continuous bodies of silt and clay accumulated on top of the previously deposited gravel layers. At least four thick layers separated by extensive gravel beds are known to be present in the western portion of the valley. The uppermost of these clay layers accumulated in recent time—a small remnant of the lake in which it accumulated persisted until the early 1900s in the area northwest of Pleasanton—and formed the 60-foot upper aquitard that extends to the ground surface.

The present stream outlet to the south through Sunol Valley was apparently established at the time when the uppermost gravel—called the upper aquifer—was being deposited. The upper gravel is considerably thicker in the southwest corner of the valley, parallel to the stream course of Arroyo de la Laguna, than it is in the San Ramon Valley. Accumulation of the upper aquifer gravel came to an end suddenly when the lake referred to in the last paragraph formed.

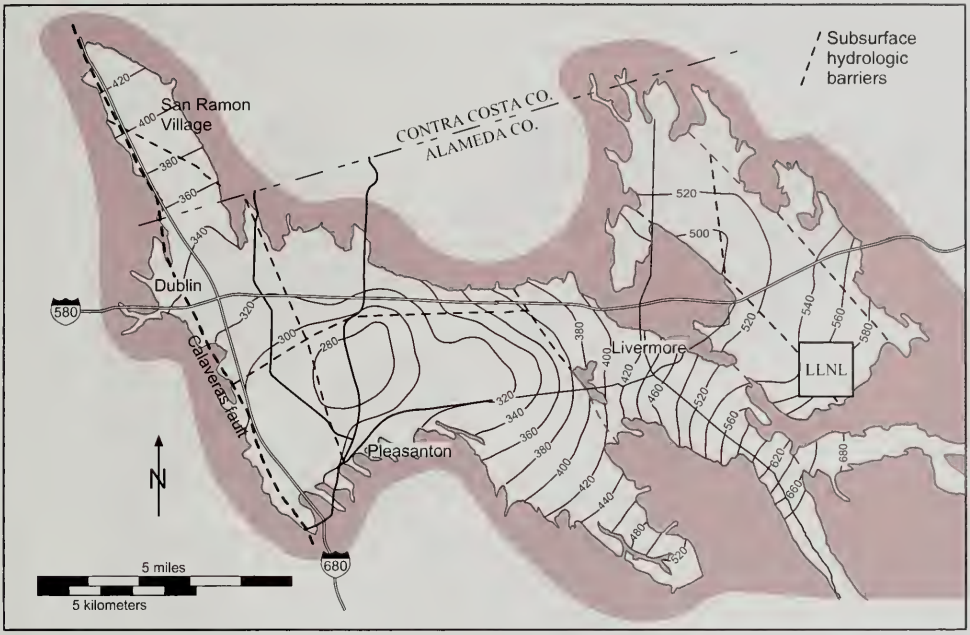

Figure 7. Configuration of the water table throughout Livermore Valley in October 1998 (modified from Gates, 1998). Thin unlabeled lines are major local roads for reference. LLNL marks the site of the Lawrence Livermore National Laboratory.

Hydrogeology. As shown in Figure 7, the potentiometric surface of the upper aquifer(s) indicates that
water moves from the periphery of the basin toward a depression cone located north of Pleasanton. Pumping in the Pleasanton area began as early as 1898, and large quantities of water have been produced ever since, both for local consumption and for exporting to the City of San Francisco.

Four distinct gravel aquifers can be recognized in the western and central portions of the basin, to an average depth of 400 feet. The highly permeable gravels are separated by four distinct clay aquitards. Originally, the upper aquifer was confined by the upper aquitard, and wells drilled into it had artesian flow. The pressure has declined considerably after nearly a century of pumping, however, so the upper aquifer is now a water-table aquifer. The deeper aquifers remain confined and are the ones from which most of the water is now pumped. The correlation of hydrostratigraphic units becomes less distinct to the east, but even as far as the Lawrence Livermore National Laboratory (LLNL on the far right of Figure 7) detailed stratigraphic work has revealed an alternance of hydrostratigraphic units of different permeability (LLNL, 1995).

DWR (1966) divided the basin into several subbasins, based on the presence of subsurface hydrologic barriers. These barriers are shown as dotted lines in Figure 7. They obviously do not have a marked effect in the potentiometric contours of the upper aquifer(s), but in the original work DWR (1966) reported differences of 10 to 50 feet in the levels of deep-screen wells on opposite sides of some of these barriers.

Typical yields from wells in the gravel aquifers range between 50 and 2,500 gallons per minute. The low values may reflect wells screened in the Livermore Formation, which is significantly less permeable than the Quaternary alluvium.

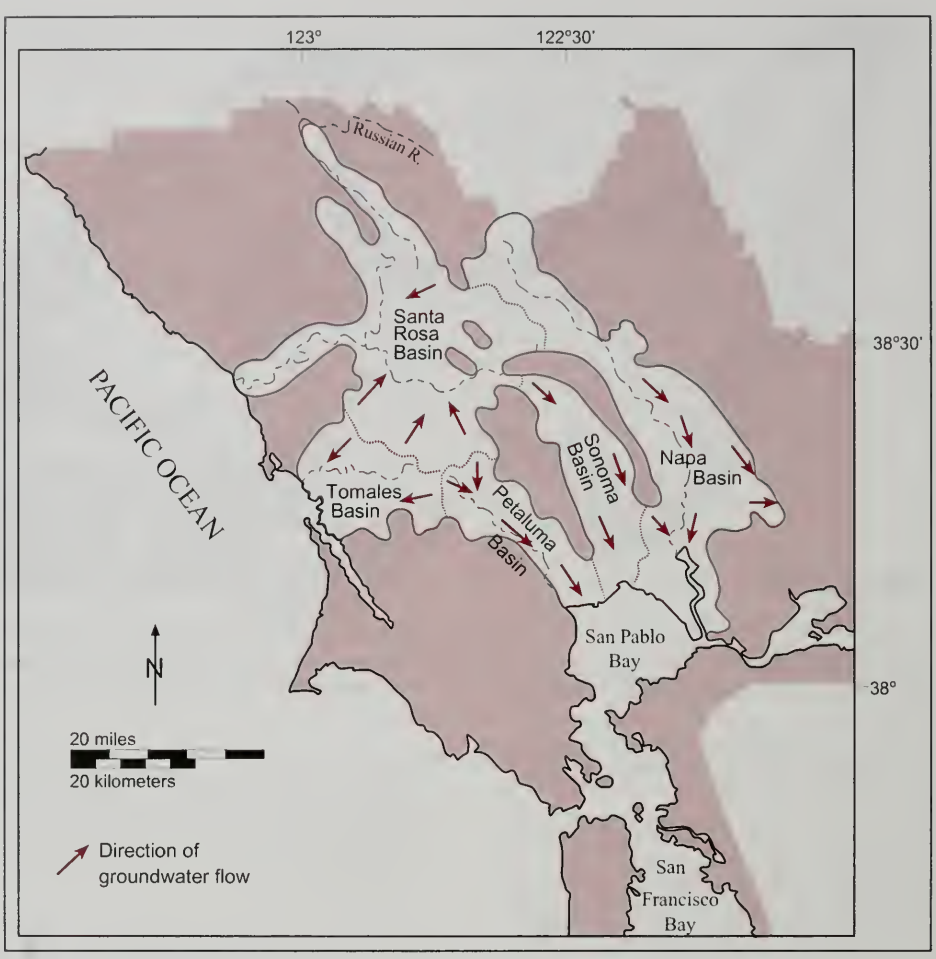

Figure 8. General map of the Petaluma, Sonoma and Napa Valleys (modified from Planert and Williams, 1995).

Water quality. Groundwater in the Livermore Valley is generally of good quality, although there are some areas in which relatively high contents of dissolved solids limit its domestic use (DWR, 1974). Pollution from point sources is a relatively minor concern in the west portion of the basin, where the upper aquiclude provides a significant amount of protection. On the east side of the basin, however, industrial pollution is of concern. The Lawrence Livermore National Laboratory has proved to be the source of several contaminant plumes of volatile organic compounds, hydrocarbons, chromium, and tritium, but active remediation efforts are ongoing and offsite plumes seem to have stabilized (LLNL, 1995).

The Petaluma, Sonoma, and Napa Valleys

The pleasant climate and fertile soils of the valleys north of San Francisco and San Pablo bays have made them a target for specialty agriculture (e.g., wine grapes) and for upscale rural residential development (Figure 8). This development has been aided by the availability of water from the Russian River for irrigation and urban consumption purposes. However, shallow wells are the basic source of water for rural residences, so thousands of shallow wells have been drilled in substrates that range from fractured Franciscan graywackes and Tertiary volcanic rocks to alluvial fill sediments. As in so many other California basins, the alluvial sediments have proved to be the most consistent target for groundwater exploration and development, even though the thickness of alluvial fill in these valleys is considerably less than in other valleys of the Coast Ranges (Cardwell, 1958; DWR, 1982a, 1982b). For example, DWR (1982c) reports an average thickness of only 250 feet for the alluvium of the Sonoma Valley.

The morphology of the Petaluma, Sonoma and Napa valleys appears to be less controlled by faulting than by volcanism, fluctuations in sea level, and normal fluvial processes. To be sure, the rocks that form the flanks of these valleys are cut by some prominent faults, but none of them seems to have promoted the accumulation of thick basin fills. Instead, volcanic activity during the Pliocene led to the formation of rhyolitic domes and andesitic/basaltic cinder cones, the emplacement of lava flows, and the accumulation of air-fall tuffs, ignimbrites, and volcaniclastic sediments (collectively known by the names of Sonoma Volcanics or Clear Lake Volcanics). These volcanic landforms controlled to some extent the development of drainage basins that became entrenched by fluvial erosion during periods of lowered sea level during the Pleistocene. The deepening of the valleys seems to have favored the accumulation of alluvial fan deposits along their flanks, now reflected in the Pleistocene gravels and sands of the Pleistocene Glen Ellen and Huichica Formations (Kunkel and Upson, 1960) (the sediments in these units are generally consolidated, so yields to wells can be quite low). Sea level rose during the Holocene, with the resulting encroachment of bay mud deposits into the valleys. In Sonoma Valley, for example, bay mud can be found as far inland as Schollville, 3 miles inland from the present shoreline of San Pablo Bay. The rise in sea level also triggered alluvial accumulation in the valleys, as the rivers adjusted their base profiles, eventually resulting in the fertile valley floors where wine grapes thrive today.

Because of the small volume of alluvial deposits, the storage capacity of the valleys is modest. For example, DWR (1982c) estimated the usable groundwater in storage in Sonoma Valley at about 472,000 acre-feet. Since the potential recharge is high, however, the basins have been able to support thousands of rural users without major depletion.

Maintenance of water quality should be a major consideration to major users, such as water companies, on three accounts. First, as in most coastal basins, these valleys are susceptible to salt water intrusion. Seawater has intruded into the pumped aquifers of the Petaluma, Sonoma and Napa Valleys, not by subsurface inflow from the bay, but by infiltration of surface water in tidal channels (Thomas and Phoenix, 1983). This problem is compounded by the encroachment of bay muds several miles inland from the present shoreline. These mud deposits contain entrapped saline water that "taints" the water chemistry of most wells near the shoreline. The second source of concern is thermal water associated with the volcanic centers of the Sonoma and Clear Lake Volcanics. The heat appears to be a remnant of the Pliocene pulse of volcanism, and meteoric groundwater that comes in close proximity to some of the Pliocene volcanic centers becomes hot enough to dissolve some of the ions contained in the surrounding rocks. The result is thermal water with high contents of boron, sodium, and total dissolved solids, which could conceivably impact the low salinity water characteristic of the valleys (and of many wells screened in fractured volcanic rocks). Third, the valleys are subject to intense agricultural exploitation, and this industry often requires the use of fertilizers and pesticides. No extensive contamination by these compounds has been recognized to date, but users of the basin are aware that they pose a latent threat.

THE BASIN AND RANGE PROVINCE

Owens Valley

Owens Valley is a narrow, north-trending graben bound by the Sierra Nevada to the west and the White and Inyo Mountains to the east. The valley extends for about 200 miles from the Nevada border just north of Mono Lake south to Haiwee Reservoir. A drainage divide south of the reservoir separates

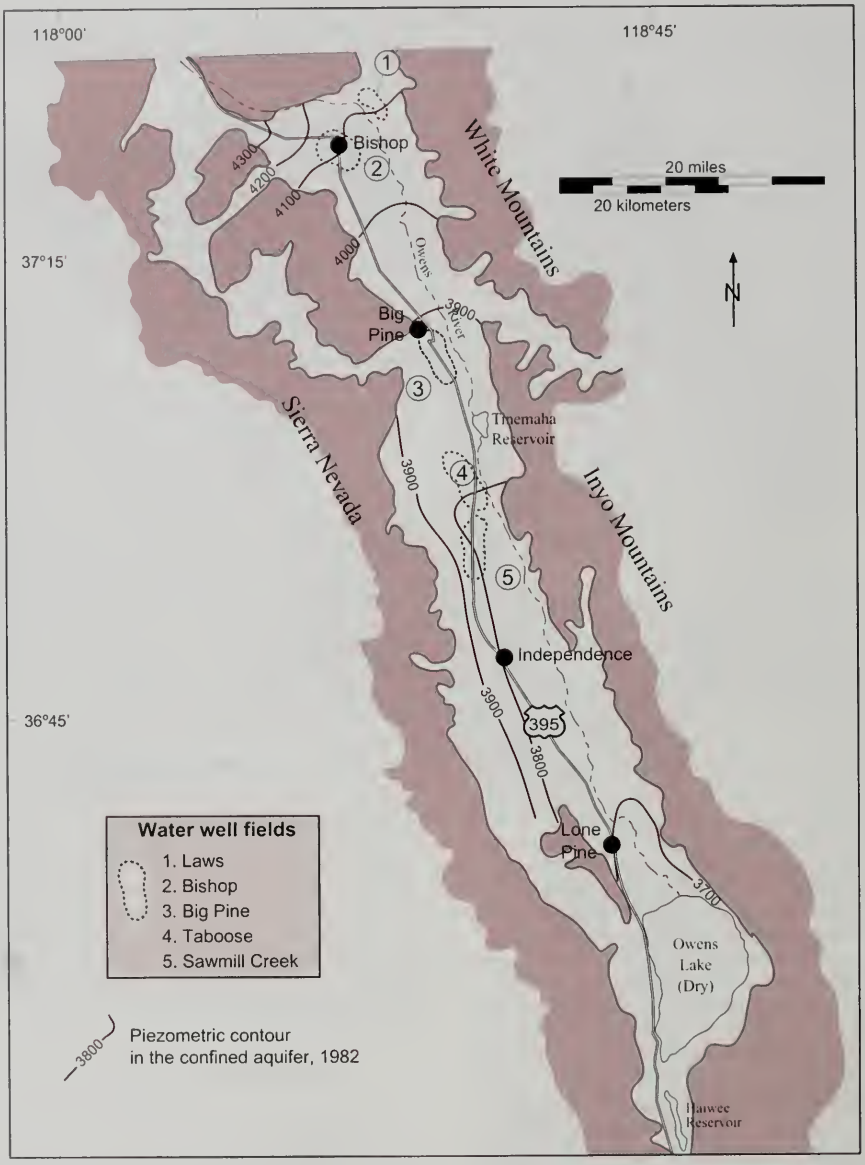

Figure 9. Map of the Owens Valley, with general configuration of the water table throughout the Owens Valley in 1985 (modified from Rogers et al., 1987).

the Owens Valley closed-drainage basin from the China Lake drainage basin to the south. Located in the rain shadow of the Sierra Nevada, the valley has an arid climate with an annual average of less than 6 inches of precipitation. However, because of the streamflow from the Sierra Nevada, the valley plays a crucial role in supplying water to the City of Los Angeles, 230 miles to the south.

The assessment of the water resources of the basin has been a matter of concern ever since the early 1900s, when the City of Los Angeles started acquiring much of the property and water rights along the axis of the valley. Key studies include those of Lee (1906, 1912), DWR (1960b), Griepentrog and Groenveld (1981), LADWP (1972, 1979 among many others), and Rogers et al. (1987). The following discussion is largely based on this last reference.

In terms of its hydrologic budget, inflow to the basin comes largely from partial infiltration of streamflow from the Sierra Nevada, with minor contributions from areal precipitation. Outflow is dominated by pumping (to boost the water supply to the City of Los Angeles) and evapotranspiration (discharge to surface springs was significant prior to development, but pumping has reduced spring discharge to an insignificant level).

The initial export of water from Owens Valley started with completion of the first aqueduct in 1913. Average export volume was about 300,000 acre-feet per year, out of which only a modest 10,000 acre-feet was derived from wells tapping the groundwater resource. A second aqueduct was completed in 1970, and the average annual export increased to about 500,000 acre-feet, with nearly 100,000 acre-feet currently produced by groundwater pumping. In 1987 the City of Los Angeles operated 92 deep wells distributed in nine well fields (but the total number of wells and test holes is in excess of 475). Nearly 50% of the yield was derived from two fields, Big Pine-Crater Mountain and Taboose-Aberdeen, in which production was largely from fractured volcanic rocks that are interbedded with the alluvial fill of the valley (Figure 9). Some of these wells yield as much as 9,000 gpm (in contrast, wells screened in sedimentary units have characteristic yields between 1,000 and 5,000 gpm).

The Owens Valley graben is filled with alluvial-fan gravel and sand deposits that interdigitate with lacustrine clay layers, air-fall tuffs, ignimbrites, and lava flows. The valley fill deposits range in thickness between 1,000 and 8,000 feet along the axis of the valley and, in the case of the alluvial-fan units, thicken considerably toward the bounding mountain ranges. Prominent among the volcanic units is the Bishop Tuff, which includes rhyolitic air-fall and ignimbrite units erupted from the Long Valley silicic volcanic center (in the northern third of the Owens Valley) 700,000 years ago (Bailey et al., 1976). Smaller in volume, but more significant in terms of groundwater production, are the basaltic scoria and lava flows of the Big Pine cinder cone field, south of the town of Bishop. Interbedded fine-grained lakebed deposits, like the ones exposed in the dry bed of Owens Lake, serve as confining units for the aquifers developed in the coarse-grained alluvial deposits and the fractured volcanic units.

Groundwater moves from the flanks of the surrounding mountains toward the center of the valley and then southward toward Owens Lake (Figure 9). The lake is now dry, but apparently still functions as the ultimate "sink" for groundwater flow due to intense evaporation. Pumping creates local depression cones, but none of these cones seems to have affected the general pre-development flow pattern. As to vertical movement, the presence of interbedded lacustrine clays often leads to confined conditions in the deep aquifers, so most deep wells and springs have some artesian pressure.

OTHER AQUIFERS

My intent in this overview paper was not to make an exhaustive inventory of the groundwater resources of California, partly because of my own limited stamina and knowledge, and partly because much work remains to be done to characterize other aquifers. However, the following key references may be useful as a starting point for practitioners interested in the hydrogeology of Shasta Valley (DWR, 1964), Eureka Valley (Evenson, 1959), the basin-fill aquifers of northernmost California (Wood, 1960; U.S. Department of the Interior, 1980), the volcanic-rock aquifers of the Cascades and the Modoc Plateau (Planert and Williams, 1995), and Death Valley (Hunt and Robinson, 1966).

In addition to the high-yield alluvial and volcanic-rock aquifers referred to above, much remains to be learned about the fractured-rock "aquifers" of the Sierra Nevada and the Klamath Mountains. These "aquifers" are comparatively small in terms of total storage, and are often hosted by fractured igneous and metamorphic rocks. Fortunately surface water

is comparatively abundant in these regions, and agricultural and urban demands are low, so groundwater extraction is modest and often limited to rural homesteads. Nevertheless, the exploration and development of fractured-rock groundwater resources remain two of the most challenging professional tasks for California hydrogeologists.

EXPLORATION METHODS

Alluvial aquifers. Finding groundwater in basins such as the Central Valley or the Santa Clara Valley basins is not the problem. Just dig and you will eventually find it. The real challenge faced by the exploration hydrogeologist is to site and design high yield wells. For example, in the northern San Joaquin Valley a typical domestic well would be less than 200 feet deep, would be screened in the lower 40 feet (8-inch diameter), and would have a safe yield of about 100 gpm. In contrast, an agricultural well equipped with an electric pump (and operated rationally during the low-tariff times of 10 pm to 10 am) would need to have a safe yield of about 2,000 gpm to service an orchard area of up to 300 acres. A farmer's dream would be a well that is no more than 500 feet deep, and is screened in the lower 200 feet (16-inch diameter).

How do we go about finding this dream well? My prime exploration strategies are careful surveys of neighbors' wells and thorough interviews with local drilling companies. Borehole geophysical surveys could be very useful for characterization of local aquifer conditions, but most existing wells have steel casing (which eliminates most types of resistivity logs) and active-source radioactive methods would be unadvisable because of the hazard that a loss of the active-source tool could represent to the aquifers. Natural gamma logs are very helpful and allow good discrimination of clay and sand units.

Vertical resistivity soundings remain the prime exploration tool in areas where neighboring wells are scarce, but the method cannot discriminate between low-yield and high-yield horizons. Ultimately, at least one pilot hole has to be drilled and carefully logged to characterize local aquifer conditions.

Fractured-rock aquifers. My prime exploration strategies when dealing with fractured-rock aquifers are lineament studies, surface fracture surveys (for both orientation and spacing of the fractures), surface geophysics, and drilling. The best aquifer management tool, in turn, is borehole geophysics.

The detailed analysis of surface fractures is a task that would try the patience of Job, but it is of crucial importance for pinpointing and characterizing zones of intense fracturing. Data must be collected, in a systematic way, about the orientation of each fracture, the spacing between fractures, and characteristics such as openness, mineral fill, or annealing. The interpretation of structural orientations requires the use of stereographic projections to represent and analyze the three-dimensional data in two dimensions. Fractures and other discontinuities (e.g., dikes or veins) are plotted in the pole format in order to detect the presence of preferred orientations, thus defining discontinuity sets, and to determine mean values for the orientations of these sets. This process can be facilitated by contouring to accentuate and distinguish the repetitive features from the random features. I believe that careful analysis of structural data eventually leads to the recognition of fracture directions that make "good geologic sense", in that they can be reconciled with the tectonic stress regime of the region. It is these regional fracture sets that I normally look for in an exploration program.

Spacing between discontinuities, and patterns of spatial distribution, can be characterized through the use of standard statistical techniques (e.g., Swan and Sandilands, 1995). For example, spacing between fractures can be easily represented, and visualized, by simple frequency histograms. Modal spacings of less than 1 foot are often indicative of a zone of intense fracturing.

Surface geophysics can be of some assistance in locating fracture clusters with high hydraulic conductivity, but it can hardly be considered a surefire method. The most promising approach is the so-called VLF method (short for very low frequency electromagnetic surveying). The VLF method relies on the fact that the U.S. and other coastal nations operate long wavelength, or very low frequency, radio stations for communication with submarines. The electromagnetic emissions from the VLF antennas propagate as air, water, and groundwaves, with magnetic and electric field components. Far away from the transmitter, the VLF field can be regarded as a uniform electromagnetic field that is oriented parallel to the surface of the ground and perpendicular to the bearing of the transmitter. In the ground, the primary (source) field propagates vertically away from the transmitter. Upon encountering an electrical conductor (e.g., a fluid-filled fracture), the propagation of the source field causes the flow

of secondary electrical currents, which in turn generate a secondary magnetic field that adds its strength to the total magnetic field. In the presence of a lateral change in conductivity, the secondary field is shifted in phase relative to the primary field. To the extent that the observed VLF anomalies are caused by relatively vertical and narrow structures elongated parallel to the bearing to the transmitter, the interpretation of the data is straightforward: the surface trace of the structure is inferred to be where there is a positive anomaly in the total magnetic field and where the in-phase response changes sign (the crossover point). Interpretation is complicated, however, by non-geologic conditions (e.g., power lines or grounded metal fences), topography, or departures from the ideal assumption that the conductor is narrow, steeply dipping, and parallel to the bearing to the transmitter.

Ultimately, the exploration program has to be put to the test by drilling. We have identified a lineament that coincides with a cluster of fractures, the fractures appear to have formed in response to a large scale tectonic stress regime, and surface geophysics suggests that a vertical, narrow conductive zone can be found at depth. Hence, we advise the property owner that it is time to retain a driller, and our client reasonably asks "How deep should we drill?" Personally, I feel inclined to abandon a hole that is more than a few hundred feet in favor of a new location. Chasing fractures can be an extremely costly proposition, as witnessed by many "dusters" drilled to depths of two or three thousand feet. Page et al. (1984) reached a similar conclusion after analyzing more than 200 well records from Nevada County in the Sierra Nevada. They found that most producing wells had depths of less than 180 feet, with yields commonly in the range between 5 and 60 gpm. In contrast, wells that had been advanced more than 215 feet in search of a producing fracture had yields that were often less than 5 gpm. In a separate study, Davis and Turk (1964) compiled the yields of 239 wells in crystalline rocks of the Sierra Nevada, and found that the median flow for wells with a depth of less than 100 feet was 10 gpm or more, but less than that in wells that had been advanced more than 200 feet. I stress the fact that these are empirical observations, to which no doubt many exceptions can be found. After all, fluid-filled fractures can remain open under lithostatic loads of tens of thousands of feet. If only we had the budget to keep looking for them!

Great advances have been made in recent years in the analysis of fractured-rock aquifers by borehole geophysics. For example, a pilot study at the Raymond site, in the foothills of the Sierra Nevada (Cohen et al., 1996), used impeller flowmeter logging, thermal-pulse flowmeter logging, hydrophysical logging, and straddle-packer injection profiling to determine the location of fluid-bearing fractures and their respective transmissivities. Cohen et al. (1996) concluded that the hydro-physical logging measurements were the most precise and enabled confident assessment of the relative magnitudes of the hydraulic conductivity of individual fractures. Hydrophysical logging is based on a variant of the borehole dilution method (Drost et al., 1968; Freeze and Cherry, 1979). The horizontal average linear velocity of groundwater moving through a fracture, or group of fractures, is estimated through the introduction of a "tracer" in an isolated interval of the well and periodic measurements of the concentration as the tracer is diluted by groundwater flowing through that interval. The rate of concentration decay is related to the average velocity of groundwater moving through the formation and across the borehole. In hydrophysical logging, deionized water is used as the tracer and fluid electric conductivity is measured repeatedly with a fluid conductivity probe to keep track of changes in the "concentration" of the tracer. Interpretation of the data is accomplished using the methods presented in Anderson et al. (1993), Tsang et al. (1990), Pedler et al. (1988), and Drost et al. (1968).

EPILOGUE

Preparing this summary started as a short project and ended being a never-ending story. Nevertheless, I enjoyed myself and greatly increased my admiration for the tremendous work performed by the "old guard" of California geologists. I hope our generation is remembered in the same light, and that our combined works will be a source of inspiration and encouragement to young engineering geologists and hydrogeologists. I can see that they will face unique challenges, such as the management of an enormous volume of accumulated data and the extensive use of a vital but finite resource. I feel we need to help them in what will be a difficult task by maintaining the highest standards in our colleges (yes, Physics and Field Geology are still essential in the Geology curriculum); by providing internship and professional training opportunities; by becoming involved, as a profession, in the management

of this resource; and by applying our ebullient scientific imagination to the solution of meaningful hydrogeologic problems. Here's to a wonderful profession!

ACKNOWLEDGMENTS

Grateful thanks to Bob Anderson, who encouraged me to write this paper, and to the superb team of Section Editors who kept things going when my mind was elsewhere. John S. Williams, Robert E. Tepel, and Steve B. Stryker provided invaluable advice as peer reviewers, Don Miller generously shared his knowledge of Central Valley stratigraphy with me, and Lauren Moll provided up to date unpublished data on the Santa Clara groundwater basin. Thank you!

AUTHOR PROFILE

Dr. Horacio Ferriz is a Certified Engineering Geologist with 20 years of geologic, geotechnical, hydrogeologic, and environmental experience. He is the Principal of HF Geologic Engineering, and the instructor of Applied Geology and Hydrogeology at California State University Stanislaus. His specialties include groundwater exploration and development, vadose zone hydrology, groundwater flow modeling, seismic engineering, and slope stability and rockfall analysis. Dr. Ferriz is the author of several research papers dealing with the volcanic geology of California and Mexico.

REFERENCES

Andersen, D.W., 1995, Neogene evolution of the Liver-more basin in the California Coast Range: Bulletin of the American Association of Petroleum Geologists, v. 79, p. 577-578.

Anderson, F. M., 1905, A stratigraphic study in the Mount Diablo Range of California: in California Academy of Sciences, Proceedings, p. 155-248.

Anderson, W.P., Evans, D.G., Pedler, W.H., 1993, Inferring horizontal flow in fractures using borehole fluid electrical conductivity logs: EOS, Transactions of the American Geophysical Union Fall Meeting v. 74, no. 43, p. 305, Dec. 1993.

Bailey, E.H., Everhart, D.L., 1964, Geology and quicksilver deposits of the New Almaden district, Santa Clara County, California: U.S. Geological Survey Professional Paper 360, 206 p.

Bailey, R.A., Dalrymple, G.B., Lanphere, M.A., 1976, Volcanism, structure, and geochronology of Long Valley Caldera, Mono County, California: Journal of Geophysical Research, v. 81, no. B5, p. 725-744.

Bailey, E.H., Irwin, W.P., Jones, D.L., 1964, Franciscan and related rocks, and their significance in the geology of western California: California Division of Mines and Geology Bulletin 183, 177 p.

Barlock, V.E., 1988, Sedimentology of the Livermore gravels (Miocene-Pleistocene), Southern Livermore Valley: M.Sc. Thesis, San Jose State University, (San Jose, California), 110 p.

Bartow, J. A., 1991, The Cenozoic evolution of the San Joaquin Valley, California: U.S. Geological Survey Professional Paper 1501, 40 p.

Bartow, J. A., Pittman, G. M., 1983, The Kern River Formation, southeastern San Joaquin Valley, California: U.S. Geological Survey Bulletin 1529 D, 17 p.

Bertoldi G.L, Johnston, R.H., Evenson, K.D., 1991, Ground water in the Central Valley, California—A summary report: U.S. Geological Survey Professional Paper 1401-A, 44 p.

Borchers, J.W. (ed.), 1998, Land subsidence—Case studies and current research: Association of Engineering Geologists Special Publication no. 8, Star Publishing Company (Belmont, California), 576 p.

Bryan, K., 1915, Ground water for irrigation in the Sacramento Valley, California: U.S. Geological Survey Water-Supply Paper 375-A, 49 p.

Cardwell, G.T., 1958, Geology and ground water in the Santa Rosa and Petaluma Valley areas, Sonoma County, California: U.S. Geological Survey Water-Supply Paper 1427, 273 p.

Clark, W.O., 1924, Ground water in Santa Clara Valley, California: U.S. Geological Survey Water-Supply Paper 519, 209 p.

Cohen, A.J.B., Karasaki, K., Benson, S., and others, 1996, Hydrogeologic characterization of fractured rock formations: A guide for groundwater remediators—Project summary: US EPA, Publication EPA/600/S-96/001.

Compton, R.R., 1966, Granitic and metamorphic rocks of the Salinian block, California Coast Ranges: in Bailey, E.H., (ed.), Geology of Northern California, California Division of Mines and Geology Bulletin 190, p. 277-287.

Crittenden, M.D., 1951, Geology of the San Jose-Mount Hamilton area, California: California Division of Mines and Geology Bulletin 157.

Croft, M. G., 1972, Subsurface geology of the Late Tertiary and Quaternary water bearing deposits of the southern part of the San Joaquin Valley, California: Contributions to the hydrology of the United States, U.S. Geological Survey Water Supply Paper 1999 H, p. 1-29.

Cummings, J.C., 1972, The Santa Clara Formation on the San Francisco Peninsula: in Frizzell, V., Helley, E.J., Adam, D.P. (eds.), Progress report on the USGS Quaternary studies in the San Francisco Bay area: Friends of the Pleistocene Guidebook, Oct. 6-8, p. 3-10.

Davis, G.H., Coplen, T.B., 1989, Late Cenozoic paleohydrologeology of the western San Joaquin Valley, California, as related to structural movements in the Central Coast Ranges: Geological Society of America, Special Paper 234, 40 p.

Davis, G.H., Green, J.H., Olmsted, F.H., Brown, D.W., 1959, Ground-water conditions and storage capacity in the San Joaquin Valley, California: U.S. Geol. Survey Water-Supply Paper 1469, 277 p.

Davis, S.N., Hall, F.R., 1959, Water quality of eastern Stanislaus and northern Merced Counties, California: Stanford University Publications, Geological Science, v. 6, no. 1, 112 p.

Davis, S.N., Turk, L.S., 1964, Optimum depth of wells in crystalline rocks: Ground Water, v. 2, no. 2, p. 6-11.

Dibblee, T.W., Jr., 1966, Geologic map of the Palo Alto quadrangle: California Division of Mines and Geology, Map Sheet 8, scale 1:24,000.

Dibblee, T.W., Jr., 1973, Geologic map of the Salinas quadrangle: U.S. Geological Survey Open File Map (no map number assigned), scale 1:62,500.

Dibblee, T.W., Jr., 1980a, Preliminary geologic map of the Livermore quadrangle, Alameda County, California: U.S. Geological Survey Open File Report 80-533b, scale 1: 24,000.

Dibblee, T.W., Jr., 1980b, Preliminary geologic map of the Niles quadrangle, Alameda County, California: U.S. Geological Survey Open File Report 80-533c, scale 1:24,000.

Dibblee, T.W., Jr., Nielsen, T.H., Brabb, E.E., 1979, Preliminary geologic map of the San Juan Bautista quadrangle, San Benito and Monterey Counties: U.S. Geological Survey Open File Report 79-375, scale 1:24,000.

Drost, W., Klotz, D., Koch, A., Moser, H., Neumaier, F., Rauert, W., 1968, Point dilution methods of investigating groundwater flow by means of radioisotopes: Water Resources Research, v. 4, p.125-146.

Durbin, T.J., Kapple, G.W., Freckleton, J.R., 1978, Two-dimensional and three-dimensional digital flow models of the Salinas Valley ground-water basin, California: U.S. Geological Survey Water-Resources Investigations 78-113, 134 p.

Durham, D.L., 1974, Geology of the southern Salinas Valley area, California: U.S. Geological Survey Professional Paper 819, 107 p.

DWR, 1946, Salinas Basin investigation: California Department of Water Resources (Sacramento, California), Bulletin 52, 246 p.

DWR, 1949, Salinas Basin investigation, basic data: California Department of Water Resources (Sacramento, California), Bulletin 52a, 432 p.

DWR, 1960a, Intrusion of salt water into groundwater basins of Southern Alameda County: California Department of Water Resources (Sacramento, California), Bulletin 81.

DWR, 1960b, Reconnaissance investigation of water resources of Mono and Owens Basins, Mono and Inyo Counties: California Department of Water Resources (Sacramento, California), 92 p.

DWR, 1964, Shasta Valley investigation: California Department of Water Resources (Sacramento, California), Bulletin 87, 170 p.

DWR, 1967, Livermore and Sunol valleys—Evaluation of ground water resources: California Department of Water Resources (Sacramento, California), Bulletin 118-2, Appendix A: Geology, 79 p.

DWR, 1967, Evaluation of ground water resources, South Bay: California Department of Water Resources (Sacramento, California), Bulletin 118-1, Appendix A: Geology, 153 p.

DWR, 1968, South San Francisco Bay - South Bay, Fremont Study Area: California Department of Water Resources (Sacramento, California), Bulletin 118-1, v. 1

DWR, 1971, Nitrates in ground waters of the Central Coast area: California Department of Water Resources (Sacramento, California), Memo. rept., 15 p.

DWR, 1973, South San Francisco Bay - Additional Fremont Study Area: California Department of Water Resources (Sacramento, California), Bulletin 118-1, v. 2

DWR, 1974, Evaluation of groundwater resources— Livermore and Sunol valleys: California Department of Water Resources (Sacramento, California), Bulletin 118-2, 153 p.

DWR, 1975a, Sea-water intrusion in California, Inventory of coastal groundwater basins: California Department of Water Resources (Sacramento, California), Bulletin 63-5, 394 p.

DWR, 1975b, South San Francisco Bay - Northern Santa Clara County Area: California Department of Water Resources (Sacramento, California), Bulletin 118-1, v. 3

DWR, 1975c, California's Ground Water: California Department of Water Resources (Sacramento, California), Bulletin 118.

DWR, 1978, Sacramento Valley: California Department of Water Resources (Sacramento, California), Bulletin 118-6, 136 p.

DWR, 1980, Ground Water Basins in California: California Department of Water Resources (Sacramento, California), Bulletin 118-80.

DWR, 1981, South San Francisco Bay—South Santa Clara County Area: California Department of Water Resources (Sacramento, California), Bulletin 118-1, v. 4.

DWR, 1982a, Sonoma County—Santa Rosa Plain: California Department of Water Resources (Sacramento, California), Bulletin 118-4, v. 2.

DWR, 1982b, Sonoma County—Petaluma Valley: California Department of Water Resources (Sacramento, California), Bulletin 118-4, v. 3.

DWR, 1982c, Sonoma County—Sonoma Valley: California Department of Water Resources (Sacramento, California), Bulletin 118-4, v. 4.

DWR, 1983, Sonoma County—Alexander Valley and Healdsburg Area: California Department of Water Resources (Sacramento, California), Bulletin 118-4, v. 5.

DWR, 1993, Groundwater levels in the Sacramento Valley groundwater basin—Tehama County: California Department of Water Resources (Northern District, Red Bluff, CA), District Report, 100 p.

DWR, 1994, Groundwater levels in the Sacramento Valley groundwater basin—Colusa County: California Department of Water Resources (Northern District, Red Bluff, CA), District Report, 82 p.

DWR, 1995, California's Ground Water - Salinas groundwater basin: California Department of Water Resources (Sacramento, California), Bulletin 118 - Basin number: 3-4.

DWR, 1996a, Adjudicated groundwater basins in California: Water Facts No. 3, California Department of Water Resources (Sacramento, California), 4 p.

DWR, 1996b, Groundwater management districts or agencies in California: Water Facts No. 4, California Department of Water Resources (Sacramento, California), 4 p.

DWR, 1997a, Lines of equal elevations in wells - Unconfined aquifer of the San Joaquin Valley: California Department of Water Resources (San Joaquin District, Fresno, CA), Map, scale 1" = 2 miles.

DWR, 1997b, Groundwater levels in the Sacramento Valley groundwater basin - Glenn County: California Department of Water Resources (Northern District, Red Bluff, CA), District Report, 204 p.

DWR, 1998, California Water Plan Update: California Department of Water Resources (Sacramento, California), Bulletin 160-98, three volumes.

Evenson, R.E., 1959, Geology and ground-water features of the Eureka area, Humboldt County, California: U.S. Geological Survey Water-Supply Paper 1470, 80 p.

Faye, R.E., 1973, Ground-water hydrology of northern Napa Valley, California: U.S. Geological Survey Water-Resources Investigations 73-0013, 64 p.

Freeze, R. A., Cherry, I. A., 1979, Groundwater: Prentice Hall (Englewood Cliffs, NJ) 604 p.

Frink, J. W., and Kues, H. A., 1954, Corcoran Clay — A Pleistocene lacustrine deposit in the San Joaquin Valley, California: American Association of Petroleum Geologists Bulletin, v. 38., p. 2,359-2,371.

Galehouse, J. S., 1967, Provenance and paleocurrents of the Paso Robles Formation, California: Geological Society of America Bulletin, v. 78, p. 951-978.

Gates, G., 1998, Groundwater level contours in the Livermore basin: Unpublished map of the Zone 7 Water Agency, Pleasanton, California, scale 1: 72,000.

Graham, S.A., Carroll, A.R., and Miller, G.E., 1988, Kern River Formation as a recorder of uplift and glaciation of the southern Sierra Nevada: in Graham, S.A., (ed.), Studies of the Geology of the San Joaquin Basin: Pacific Section, Society of Economic Paleontologists and Mineralogists, v. 60, p. 319-331.

Griepentrog, T.E., Groeneveld, D.P., 1981, The Owens Valley water management report: County of Inyo, 273 p.

Hackel, O. and others, 1965, Geology of southeastern San Joaquin Valley, California: Pacific Section, American Association of Petroleum Geologists; Society for Exploration Geophysics; Society of Economic Paleontologists and Mineralogists Guidebook, 40 p.

Hall, C.A., Jr., 1958, Geology and paleontology of the Pleasanton area, Alameda and Contra Costa Counties, California: University of California Publications in the Geological Sciences, v.34, no. 1.

Hall, W.H., 1889, Irrigation in California: National Geographic, v.2, no. 4, p.281.

Harwood, D.S., Helley, E.J., Doukas, M.P., 1981, Geologic map of the Chico Monocline and northeastern part of the Sacramento Valley: U.S. Geological Survey Miscellaneous Investigations Series Map I-1238, scale 1:62,500.

Hotchkiss, W.R., Balding, G.O., 1971, Geology, hydrology, and water quality of the Tracy-Dos Palos area, San Joaquin Valley, California: U.S. Geological Survey Open-File Report, 107 p.

Hunt, C.B., Robinson, T.W., 1966, Hydrologic basin, Death Valley, California: U.S. Geological Survey Professional Paper 494-B, 103 p.

Iwamura, T.I., 1995, Hydrogeology of the Santa Clara and Coyote Valleys groundwater basins: in Sanginés, E.M., Andersen, D.W., Buising, A.B. (eds.), Recent Geologic Studies in the San Francisco Bay Area: Pacific Section of the Society of Economic Paleontologists and Mineralogists Book 76 (May 3-5, 1995).

Iwamura, T.I., 1989, Geology and groundwater quality: in SCVWD (Santa Clara Valley Water District), 1989, Standards for the construction and destruction of wells and other deep excavations in Santa Clara County: Santa Clara Valley Water District, 5750 Almaden Expwy., San Jose, CA 95118, Appendix A, 21 p.

Iwamura, T.I., 1980, Saltwater intrusion investigation in the Santa Clara County Baylands Area, California: Santa Clara Valley Water District, 5750 Almaden Expwy., San Jose, CA 95118.

Johnson, M.J., 1977, Ground-water hydrology of the lower Milliken-Sarco-Tulucay Creeks area, Napa County, California: U.S. Geological Survey Water-Resources Investigations 77-0082.

Kapple, G.W., 1979, Digital model of the Hollister Valley ground-water basin, San Benito County, California: U.S. Geological Survey Water-Resources Investigations 79-32, 17 p.

Kilburn, C., 1972, Ground-water hydrology of the Hollister and San Juan Valleys, San Benito County, California, 1913-68: U.S. Geological Survey Open-File Report.

Kuespert, J. G., 1990, Kern River Formation along Alfred Harrell Highway, eastern Kern County: in Kuespert, J. G., and Reid, S. A., (eds.), Structure, Stratigraphy and Hydrocarbon Occurrences of the San Joaquin Basin, California: Pacific Section, Society of Economic Paleontologists and Mineralogists, v. 64, p. 293-300.

Kuespert, J. G., and Sanford, S. J., 1990, Kern River Field history and geology: in Kuespert, J. G., and Reid, S.A., (eds.), Structure, Stratigraphy and Hydrocarbon Occurrences of the San Joaquin Basin, California: Pacific Section, Society of Economic Paleontologists and Mineralogists, v. 64, p. 55-58.

Kunkel, F., Upson, J.E., 1960, Geology and ground-water in Napa and Sonoma valleys, Napa and Sonoma counties, California: U.S. Geological Survey Water-Supply Paper 1495, 252 p.

LADWP (Los Angeles Department of Water and Power), 1979, Increased pumping of the Owens Valley groundwater basin—Final Environmental Report: City of Los Angeles, 2 volumes.

LADWP (Los Angeles Department of Water and Power), 1972, Report on water resources management plan, Owens Valley groundwater basin: City of Los Angeles, 160 p.

Lawson, A.C., 1895, Sketch of the geology of the San Francisco Peninsula, California: U.S. Geological Survey 15th Annual Report, p.349-476.

Lee, H., 1912, An intensive study of the water resources of a part of Owens Valley, California: U.S. Geological Survey Water-Supply Paper 294, 135 p.

Lee, H., 1906, Geology and water resources of Owens Valley, California: U.S. Geological Survey Water-Supply and Irrigation Paper 181, 28 p.

Lennon, R. B., 1976, Geological factors in steam soak projects on the west side of the San Joaquin basin: Journal of Petroleum Technology, v. 5, p. 741-748

Lettis, W. R., 1982, Late Cenozoic stratigraphy and structure of the western margin of the central San Joaquin Valley, California: U.S. Geological Survey Open-File Report 82-526, 203 p.

Lettis, W. R., 1988, Quaternary geology of the northern San Joaquin Valley: in Graham, S. A., (ed.), Studies of the geology of the San Joaquin basin: Pacific Section SEPM, 60, p. 333-351.

LLNL (Lawrence Livermore National Laboratory), 1995, Environmental restoration at the Livermore site, Cali-fornia—Management summary: U.S. Department of Energy, Lawrence Livermore National Laboratory, UCRL-AR-122289, 14 p.

Lofgren, B.E., 1969, Field measurement of aquifer-system compaction, San Joaquin Valley, California: Internat. Assoc. Sci. Hydrology, Colloque de Tokyo, p. 273-284.

Loomis, K. B., 1990, Late Neogene depositional history and paleoenvironments of the west central San Joaquin basin, California: [Ph.D. Dissertation] Stanford University, 499 p.

Lydon, P.A., 1969, Geology and lahars of the Tuscan Formation, northern California: Geological Society of America Memoir 116, p. 441-475.

Marchand, D.E., Allwardt, A., 1981, Late Cenozoic stratigraphic units, northeastern San Joaquin Valley, California: U.S. Geological Survey Bulletin 1470, 70 p.

Mendenhall, W.C., Dole, R.B., Stabler, H., 1916, Groundwater in the San Joaquin Valley, California: U.S. Geological Survey Water-Supply Paper 398, 310 p.

Miller, D.D., Graham, S.A., 1995, Sedimentologic controls and stratigraphic architecture of the Kern River Formation, central California: in Blair, T.C., McPherson, J.G. (eds.), Alluvial fans—Processes, forms, controls, facies models, and use in basin analysis, Proceedings and abstracts of an International Research Conference, Society for Sedimentary Geology (SEPM), Death Valley, California (October 17-21, 1995), p. 68

Miller, D. D., McPherson, J. G., and Covington, T. E., 1990, Fluviodeltaic reservoir, South Belridge Field, San Joaquin Valley, California: in Barwis, J. H., McPherson, J. G., and Studlick, J. R. J., (eds.), Sandstone Petroleum Reservoirs, Springer Verlag, New York, p. 109-130.

Miller, D. D., Negrini, R., McGuire, M., Huggins, C., Minner, M., Hacker, B., Sarna-Wojcicki, A., Meyer, C., Fleck, R. J., Reid, S. A., 1998, New upper age constrain on the Kern River Formation: in Reid, T., (ed.), Outcrops of the Eastern San Joaquin Basin, v.2, San Joaquin Geological Society, p. 23-31.

Miller, G. E., 1986, Sedimentology, depositional environment, and reservoir characteristics of the Kern River Formation, Southeastern San Joaquin Basin, [M.S. thesis]: Stanford University, 80 p.

Miller, R.E., Green, J.H., Davis, G.H., 1971, Geology of the compacting deposits in the Los Banos-Kettleman City subsidence area, California: U.S. Geological Survey Professional Paper 497-E, 46 p.

Moll, L., 1998, Groundwater level in monitoring wells—September 1997: Santa Clara Valley Water District, 5750 Almaden Expwy., San Jose, CA 95118. Map in two sheets, Scale 1 inch = 5,000 feet.

Nicholson, G. 1980, Geology of the Kern River oil field: Kern River Oil Field Fieldtrip Guidebook, Pacific Section American Association of Petroleum Geologists, p. 7-17.

Olmsted, F.H., Davis, G.H., 1961, Geologic features and ground-water storage capacity of the Sacramento Valley, California: U.S. Geological Survey Water-Supply Paper W1497, 241 p.

Olson, H. C., Miller, G. E., Bartow, J. A., 1986, Stratigraphy, paleoenvironment and depositional setting of Tertiary sediments, southeastern San Joaquin Basin: Annual meeting guidebook, Southeast San Joaquin Valley Field Trip, Kern County, California Part II, Structure and Stratigraphy, Pacific Section American Association of Petroleum Geologists, p. 18-46.

Pacific Geotechnical Associates, 1991, Study of the regional geologic structure related to groundwater aquifers in the southern San Joaquin Valley groundwater basin, Kern County, California: Consultant's report.

Page, B.M., 1966, Geology of the Coast Ranges of California: in Bailey, E.H., (ed.), Geology of Northern California, California Division of Mines and Geology Bulletin 190, p. 255-276.

Page, R.W., 1986, Geology of the fresh ground-water basin of the Central Valley, California, with texture maps and sections: U.S. Geological Survey Professional Paper 1401-C, 54 p.

Page, R.W., Anttila, P.W., Johnson, K.I., Pierce, M.J., 1984, Ground-water conditions and well yields in fractured rocks, Southwestern Nevada County, California: U.S. Geological Survey Water-Resources Investigation 83-4262.

Pedler, W.H., Urish, D.W., 1988, Detection and characterization of hydraulically conductive fractures in a borehole: The emplacement method: EOS, Transactions of the American Geophysical Union Fall Meeting v. 69, no. 44, p. 1186, Dec. 1988.

Piper, A.M., Gale, H.S., Thomas, H.E., Robinson, T.W., 1939, Geology and ground-water hydrology of the Mokelumne area, California: U.S. Geological Survey Water-Supply Paper 780, 230 p.

Planert, M, Williams, J.S., 1995, Ground water atlas of the United States, Segment 1, California-Nevada: U.S. Geological Survey Hydrologic Investigations Atlas 730-B, 28 p.

Poland, J.F., 1972, Subsidence and its control: in Underground waste management and environmental implications—A symposium: Am. Assoc. Petroleum Geologists Memoir 18, p. 50-71.

Poland, J.F., 1969, Land subsidence and aquifer-system compaction, Santa Clara Valley, California: Internat. Assoc. Sci. Hydrology, Colloque de Tokyo, p. 12-21.

Poland, J.F., Davis, G.H., 1969, Land subsidence due to withdrawal of fluids: Geol. Soc. America, Eng. Geol. Rev., v.2, p. 187-269.

Poland, J.F., Ireland, R.L., 1968, Land subsidence in the Santa Clara Valley, California, as of 1962: U.S. Geological Survey Professional Paper 497-F, 61 p.

Poland, J.F., Lofgren, B.E., Ireland, R.L., Pugh, R.G., 1975, Land subsidence in the San Joaquin Valley, California, as of 1972: U.S. Geological Survey Professional Paper 437-H, 78 p.

Poland, J.F., Evenson, R.E., 1966, Hydrogeology and land subsidence, Great Central Valley, California: in Bailey, E.H. (ed.), Geology of Northern California: California Division of Mines Bull. 190, p. 239-247.

Reed, R.D., 1933, Geology of California: American Association of Petroleum Geologists, 355 p.

Richardson, D., Rantz, S.E., 1961, Interchange of surface and ground water along tributary streams in the Central Valley, California: U.S. Geological Survey Open-File report, 253 p.

Rogers, L.S., Hollett, K.J., Hardt, W.F., Sorenson, S.K., 1987, Overview of water resources in Owens Valley, California: U.S. Geological Survey, Water-Resources Investigations Report 86-4357, 38 p.

Savage, D. E., Downs, T., and Poe, O. J., 1954, Cenozoic land life of southern California: in Jahns, R. H., (ed.), Geology of Southern California, California Division of Mines and Geology Bulletin, v. 170, p. 43-58.

Schwartz, D. E., 1990, Cross Section 27 San Joaquin valley from Cantua Creek to Transverse Range: American Association of Petroleum Geologists, Pacific Section, 1 sheet.

SCVWD (Santa Clara Valley Water District), 1989, Standards for the construction and destruction of wells and other deep excavations in Santa Clara County: Santa Clara Valley Water District, 5750 Almaden Expressway, San Jose, CA 95118, 48 p.

Showalter, P.E., Akers, J.P., Swain, L.A., 1983, Design of a ground-water monitoring network for the Salinas River Basin, California: U.S. Geological Survey Water-Resources Investigations Report 83-4049, 74 p.

Swan, A.R.H., Sandilands, M., 1995, Introduction to geological data analysis: Blackwell Science (Oxford, England), 446 p.

Swanson, A.A., 1998, Land subsidence in the San Joaquin Valley, updated to 1995: in Borchers, J.W. (ed.), Land subsidence—Case studies and current research: Association of Engineering Geologists Special Publication no. 8, Star Publishing Company (Belmont, California), p. 75-79.

Templin, W.E., Schluter, R.C., 1990, A water-resources data-network evaluation for Monterey County, California - Phase 3: Northern Salinas River drainage basin: U.S. Geological Survey Water-Resources Investigations Report 89-4123, 96 p.

Tolman, C.F., Poland, J.F., 1940, Groundwater, salt-infiltration, and ground-surface recession in Santa Clara Valley, Santa Clara County, California: Transactions of the American Geophysical Union.

Thomas, H.E., Phoenix, D.A., 1983, California region: in Todd, D.K. (ed.), Ground-Water Resources of the United States, Premier Press (Berkeley, California), p. 631-686.

Trask, P.D., 1926, Geology of the Point Sur quadrangle, California: California University, Department of Geological Sciences Bulletin, v. 16, no. 6, p. 119-186.

Tsang, C.F., Hale, F.V., Hufschmied, P., 1989, Determi-nation of fracture inflow parameters with a borehole fluid conductivity logging method: Water Resources Research, v. 26, p. 561-578.

U.S. Department of the Interior, 1980, Klamath project, Butte Valley division: U.S. Department of the Interior, Water and Power Resources Service, Feasibility—Appendix on ground-water geology and resources, 50 p.

Watts, W. L., 1894, The gas and petroleum yielding formations of the Central Valley of California: California State Mining Bureau Bulletin, v. 3, 100 p.

Williamson, A.K., Prudic, D.E., Swain, L.A., 1989, Groundwater flow in the Central Valley, California: U.S. Geological Survey Professional Paper 1401-D, 127 p.

Wood, P.R., 1960, Geology and ground-water features of the Butte Valley region, Siskiyou County, California: U.S. Geological Survey Water-Supply Paper 1491, 150 p.

Wood, P.R., Dale, R.H., 1964, Geology and ground-water features of the Edison-Maricopa area, Kern County, California: U.S. Geological Survey Water-Supply Paper 1656, 103 p.

Wood, P.R., Davis, G.H., 1959, Ground-water conditions in the Avenal-McKittrick area, Kings and Kern Counties, California: U.S. Geological Survey Water-Supply Paper 1457, 141 p.

Woodring, W. P., Stewart, R., and Richards, R. W., 1940, Geology of Kettleman Hills oil field, California: U.S. Geological Survey Professional Paper 195, 170 p.

APPENDIX

IMPORTANT STRATIGRAPHIC UNITS OF THE CENTRAL VALLEY

Sacramento Valley

Tuscan Formation. This formation crops out from Red Bluff to Oroville (Harwood et al., 1981), and can be recognized in the subsurface to a distance of about 5 miles west of the Sacramento River (Olmstead and Davis, 1961; DWR, 1978). The Tuscan Formation was accumulated as alluvial fan deposits off the Cascade Range, and thus thins from east to west from 1,600 feet at the Cascade Range to about 300 in the subsurface under the Sacramento Valley (Lydon, 1969; DWR, 1978). In the subsurface it consists largely of black volcanic sands and gravels, with interbedded layers of tuffaceous clay and tuff breccia. The Tuscan Formation yields large quantities of fresh water to wells (900 to 3,000 gallons per minute; DWR, 1978), often from aquifers confined by tuffaceous beds.

Tehama Formation. This formation crops out in the western flank of the Sacramento Valley basin, From Red Bluff to Vacaville. The Tehama Formation extends easterly from the west marging of the basin toward the trough of the valley, where it interfingers with the Tuscan and Laguna Formations. In areas where it is exposed it has an average thickness of 1,800 feet and consists of poorly-sorted, thick-bedded sandy silt and clay that yield poorly to wells. Gravel and sand interbeds are usually thin (< 50 feet) and discontinuous, but may host high-yield localized aquifers (200 to 2,500 gallons per minute) (Olmstead and Davis, 1961; DWR, 1978). Because of its extension and thickness, the Tehama Formation is the principal water-bearing formation in the western half of the Sacramento Valley (but aquifer development challenges the hydrogeologist because of facies changes and large proportions of low-yield silt and clay interbeds).

Laguna and Fair Oaks Formations. The Laguna Formation is well exposed in the southeastern part of the Sacramento Valley, where it forms many of the low, rolling foothills southeast of Sacramento and south of the American River (formally, the equivalent sediments north of the American River are grouped under the Fair Oaks Formation, but the sedimentology and hydrogeology of the two formations are very similar). DWR (1978) has described the Laguna and Fair Oaks Formations as a westward-thickening wedge that was deposited by streams draining the Sierra Nevada. In outcrop they are up to 180 feet thick and rest conformably over the Mehrten Formation. To the west they dip toward the valley trough, where they interdigitates with the Tehama and Tuscan Formations.

The Laguna Formation includes beds of silt, clay, and sand with lenticular bodies of gravel. Some of the sands are clean and well sorted, whereas some of the gravels are silty and poorly sorted. Where fine-grained, the Laguna Formation yields poorly to wells, but in areas where well-sorted arkosic sands predominate the yields can be quite high (~1,750 gallons per minute).

Victor Formation. The Victor Formation overlies the Laguna and Fair Oaks Formations, and forms most of the valley floor east of the Sacramento River. According to DWR (1978) it was deposited on a plain of aggradation, now partly dissected, so it is composed of a heterogeneous assemblage of fluvial sediments deposited by streams that drained the Sierra Nevada. These streams left sand and gravel that grade laterally and vertically into silt and clay, which results on laterally-discontinuous, thin aquifers that are difficult to correlate. The Victor Formation is the most important water-bearing formation for domestic and shallow irrigation wells on the eastern half of the Sacramento Valley basin, even though yield to wells is generally modest (< 1,000 gallons per minute).

Northern San Joaquin Valley

Mehrten Formation. This formation crops out discontinuously along the eastern flank of the valley, between the Bear and Chowchilla rivers, and dips gently to the southwest beneath the valley. The formation was originally defined by Piper et al. (1939) to refer to a 190-foot section of clay, silt, and lithic sandstone and breccia (with characteristic black andesite detrital grains) in the Mokelumne area, laid down by streams carrying andesitic debris from the Sierra Nevada (see also Marchand and

Allwardt, 1981). The detailed makeup of the stratigraphic section changes markedly from one location to another, but the comparative abundance of andesitic detrital grains remains a diagnostic characteristic. In the Sacramento Valley the formation is as much as 200 feet thick where exposed, and in the subsurface it ranges in thickness from 400 to 500 feet. The unit apparently thickens to the south: in the northeastern part of the San Joaquin Valley Davis and Hall (1959) report an aggregate outcrop thickness of more than 700 feet, and a subsurface thickness of nearly 1,200 feet. The "black sands" of the Mehrten Formation generally yield large quantities of water to wells (3,000 to 4,000 gallons per minute being common), which makes them a preferred exploration target in the eastern half of the Central Valley (Davis and Hall, 1959).

Turlock Lake, Riverbank, and Modesto Formations. These formations are easily differentiated from the underlying Mehrten Formation because the silts, sands, and gravels that form them contain large proportions of quartz and feldspar (i.e., they are arkosic or quartz-feldspathic sediments), which give them a light color. In contrast, the underlying Mehrten is characterized by dark-colored andesitic clasts. The change in sediment type, from andesitic to granitic, was brought forth by the enormous supply of sediments "released" by the Pleistocene glaciation of the High Sierra. Technically, then, most of the sediments found in the Turlock Lake, Riverbank, and Modesto Formations are glacial outwash sediments.

Mapping of the poorly exposed sediments has traditionally been based on degree of soil development. Because the Turlock Lake sediments have been exposed for a longer period of time than the Riverbank or Modesto sediments, their soil profiles have developed thicker, more compact B horizons (local farmers refer to these compact soil horizons as "hardpan"). According to Davis and Hall (1959), the Turlock Lake Formation forms dissected, rolling hills with up to 60 feet of local relief. The Riverbank Formation, in contrast, forms low, slightly dissected hills with 10 to 20 feet of local relief to nearly flat land. Finally, the Modesto Formation has a nearly flat topographic relief with a gentle westward slope. The distinction between the three units is not practical in the subsurface, where the total combined thickness of these Pleistocene units can be as much as 1,000 feet. Typical yields for agricultural wells vary between 2,000 and 3,500 gallons per minute.

Southern San Joaquin Valley

Kern River Formation. Miocene marine and nearshore deposits at the southern end of the Central Valley (e.g., the Jewett and Olcese Formations) are overlain by Plio-Pleistocene sediments transported by streams draining westward from the Sierra Nevada. These sediments are grouped as the Kern River Formation, which is dominated by stacked channel-fill sands that includes lenses and layers of cobbly, locally bouldery gravels with sand/clay matrix, interbedded with medium- to very coarse-grained sands, clayey sands, and sandy clays. Some of the sandy clays contain minor layers of very fine pebbles (Hackel et al. 1965); Nicholson, 1980; Bartow and Pittman, 1983; Miller, 1986; Olson et al., 1986; Graham et al., 1988; Kuespert, 1990; Kuespert and Sanford, 1990; and Bartow, 1991). Borehole data and surface exposures indicate that the Kern River Formation ranges in thickness from 50 to 750 feet. According to Miller and Graham (1995), the depositional setting of the Kern River Formation evolved from a coarse-grained marine delta that fed deep-water, coarse clastic deposits during the Late Miocene, to a system of glaciogenic fluvial deposits and lacustrine deltas during the Plio-Pleistocene. The presence of Hemphillian (late Miocene-early Pliocene) vertebrate fossil assemblages found near the base of the formation (Savage et al., 1954; Bartow, 1991) constrain the lower age for the Kern River Formation at about 8.2 Ma. The upper age constraint of the Kern River Formation is based on a volcanic ash with a radiometric age of 6.13 Ma (Miller et al., 1998).

The Kern River Formation dips gently (<10°) toward the San Joaquin Valley, and overlies the easternmost end of the Bakersfield Arch (a broad, southwest plunging anticline). These uplifted and tilted strata are incised by the present day Kern River and are exposed in outcrops along either side of the river valley. Several faults cut through these sediments. Most are normal faults that strike either north-northwest or west-northwest (Nicholson, 1980; Bartow, 1991).

The Kern River reservoir sands have produced more than 1 billion barrels of oil from a 4 billion barrel resource, which, of course, makes them useless as a fresh-water aquifer at or near the oil fields. Away from the oil fields, however, the formation provides valuable groundwater storage and supports high yields to wells.

Tulare Formation. The Pliocene-Pleistocene-Recent(?) Tulare Formation is a widespread nonmarine unit that crops out along the western margin of the San Joaquin basin (Watts, 1894; Anderson, 1905). It consists of diverse sedimentary facies ranging from alluvial fan (Lennon, 1976; Lettis, 1988) to fluviodeltaic (Miller et al., 1990) and lacustrine units (Woodring et al., 1940; Lennon, 1976). Sediments range from conglomerates to silts and clays.

The Tulare Formation contains at least three major units in the southern San Joaquin Valley basin, which are separated by clay units deposited during widespread lacustrine flooding of the basin. The base of the Tulare is the *Amnicola* sand (named for the common occurrence of the freshwater gastropod) that ranges in age from 3.4 Ma to 2.2 Ma. Overlying the *Amnicola* sand are the Paloma Clay (Pacific Geotechnical, 1991), and an unnamed sand of varying thickness and extent. The latter is in turn overlain by the Corcoran Clay (Frink and Kues, 1954; Croft, 1972; Lettis, 1982, 1988), which is also referred to as the "E-clay" in the hydrogeologic literature (Page, 1986). Finally, extending from the Corcoran Clay to the present surface are Upper Pleistocene and Holocene alluvial sands.

The maximum reported thickness of the Tulare Formation along the western basin margin is 3,500 ft (Loomis, 1990; Woodring et al., 1940), with a similar thickness of equivalent section (3,800 ft) occurring in the southernmost part of the basin (Schwartz, 1990). Beneath the valley the thickness ranges from about 200 feet at North Belridge to about 5,000 feet beneath the Kettleman Plains (Wood and Davis, 1959). The Corcoran member of the Tulare Formation is recognized along the western San Joaquin Valley basin as far north as the San Luis Reservoir.

Three Pliocene-Pleistocene fluvial depositional systems provided sediment to the San Joaquin Valley basin prior to the deposition of the Corcoran Clay. The largest volume of sediment was contributed from the basin's southern margin as a combination of fluvial deposits from the Mojave province and the Sierra Nevada (e.g., Kern River). The second system represents sediment transport from the Sacramento Valley, as documented by paleocurrent measurements in the conglomerates of northernmost Kettleman Hills. Transport direction reversed itself after deposition of the lacustrine Corcoran Clay. The third and smallest depositional system originated in the Salinas basin, west of the present San Andreas fault, where paleocurrent directions in braided gravel deposits of the Pliocene-Pleistocene Paso Robles Formation indicate eastward transport of sediment and connection with the San Joaquin Valley basin across the present trace of the San Andreas fault (Galehouse, 1967). Deposition after the Corcoran Clay formed the alluvial fan and lacustrine systems that persist to the present day.

Along the western side of the valley, south of Tulare Lake, the Tulare Formation contains mostly saline water, whereas north of Tulare Lake it contains mostly fresh water (Hotchkiss and Balding, 1971; Miller et al., 1971). Because of the large proportion of clay in the deposits, yield to wells is generally low (< 500 gallons per minute), but Hotchkiss and Balding (1971) have reported average yields of more than 1,000 gallons per minute for wells in the Tracy-Dos Palos area.

INTRODUCTION TO THE LANDSLIDES SECTION

JOAN E. VAN VELSOR[1]

GRAVITY. IT'S NOT JUST A GOOD IDEA; IT'S THE LAW.

Earthquakes, liquefaction, debris flows, floods, sea cliff retreat, erosion, soft soils, rugged cliffs shedding huge boulders, volcanic eruptions, slumps, slides and slips: California has it all for the engineering geologist. It doesn't get any better than this anywhere else on earth.

The practice of engineering geology in Northern California is a continuous adventure and challenge. If an exciting geologic process exists, you will face it during your California career.

This section contains ten papers discussing the effects of gravity on unstable materials and how the engineering geologist can best advise property owners how to avoid, repair or abandon unstable ground. California has very large areas underlain by geologic materials destabilized by the combined forces of tectonic shearing, regional uplift, and periodic strong weather conditions. Landslides, debris flows, rockfalls, slumps, slides, and slips occur every winter, even when climactic conditions are benign. When extreme rainfall events occur, the number and size of instabilities is usually catastrophic.

Evaluation of landslide potential is essential to good land use planning. McCrink (2001) presents an interesting regional application of the Newmark method of dynamic slope stability analysis to predict seismic induced slope failures. Working at the 7.5-minute quadrangle level, the method is used in combination with a geographic information system to highlight potentially unstable ground using general quadrangle mapping, a digital elevation model, and general assumptions about representative seismic events.

One of the greatest geologic challenges in Northern California is site characterization in chaotic materials. We can map very well on the surface, and we can log our boreholes just fine, but correlation of subsurface information in chaotic terrain is a nightmare. Many of us have thrown up our hands, used an empirical rule of thumb or "professional judgement" (fancy word for guess in this context), to characterize such formidable formations as the Franciscan. Earthwork following the recommendations of the geologic report often unearths humbling surprises, and yet another opportunity to exercise the changed site conditions clause in our contracts. Medley (2001) flings a vital life ring to those floundering in the sea of boulders, inclusions, rippability estimates, percent blasting estimates and similar tough calls in hard-to-characterize *melanges*. He presents a very workable, practical method to finally get a grip on this extremely slippery problem.

It is vital that the accumulated wisdom of experienced practitioners be put into plain-language explanations for the guidance of those new to this challenging field. Three papers in this section address this challenge. First, the paper by Upp (2001) is a golden example of a well thought out and implemented exploration and analysis, and discusses all of the information needed for a standard-of-practice investigation. Second, Johnson and Cole (2001) present a very clear and useful explanation of the exciting art of down-hole logging. There are substantial advantages to meeting the earth up close by going down hole, and some equally substantial safety concerns that must be given serious consideration. New practitioners and old timers will find this paper valuable. It should be re-read every time you go underground. Finally, Van Velsor (2001) tackles the very practical aspects of dealing with the public and the press in the course of a landslide remediation project. Landslides by definition involve

[1] California Department of Transportation
5900 Folsom Blvd.
Sacramento, CA 95819-4612
joan.van.velsor@dot.ca.gov

displacement of soil and rock, which means that someone's property achieves a new—probably less valuable—configuration and lifelines are damaged. These events will bring the immediate attention of the public, press and legal profession, and their scrutiny during an emergency can be unsettling. You will want to go back to this paper for advice on working with your many external "partners"!

Monitoring of existing or suspected landslide movement is an indispensable part of a good geotechnical evaluation. The paper by Kane and Beck (2001) provides a wealth of information on the cost effective, valuable new method of time domain reflectometry (TDR), as well as a very readable overview of old-reliable techniques such as inclinometers, wireline piezometers, and extensometers.

Case histories are the lifeblood of professional information exchange. Only by selfless sharing of real project problems, analysis, and outcomes can the profession advance. The winter of 1996/1997 brought extreme rainfall to California; landslides of all types were numerous. This section contains excellent case studies of different types of landslides that were triggered by the 1996/1997 storms: Starting with fast moving debris flows, which are among the most destructive of landslides, DeGraff (2001) describes the Sourgrass debris flow in the Sierra Nevada. The forensic investigation determined that this debris flow reached velocities in excess of twelve miles per hour as it scoured the bottom of a small ravine, destroyed part of the Sourgrass campground, and temporarily dammed the South Fork of the Stanislaus River. Following on the theme of fast-moving land movements, Kroll et al. (2001) provide a good example of the current standard of practice for rockfall mapping, evaluation, and net design methodology. Rockfall evaluation and control is challenging, and until recently mitigation was largely limited to posting signs, scaling, construction of catchment ditches or slope flattening. Fortunately, recent advances in rock net technology have added some exciting new tools to the armory of the engineering geologist.

Two additional case studies illustrate the type of emergency work performed by engineering geologists when landslides occur. Hilton (2001) presents an evaluation of the Highway 50 landslide, which closed a vital highway link to Lake Tahoe in 1997, and gives an interesting summary of the fast-track repairs performed and their post-construction performance. McCormick and Rice (2001) present a case study of the complex Rio Nido landslide, triggered by the 1996-1997 storms. The landslide involved both debris flows and translational movement, and its description demonstrates the complexity of many of the landslides that California engineering geologists have to deal with in our beautiful but unstable state.

SELECTED REFERENCES

DeGraff, J.V., 2001, Sourgrass debris flow - A landslide triggered in the Sierra Nevada by the 1997 New Year storm: This volume.

Hilton, B.R., 2001, Stabilization of the Mill Creek landslide complex, El Dorado County, California: This volume.

Johnson, P.L., and Cole, W.F., 2001, The use of large-diameter boreholes and downhole logging methods in landslide investigations: This volume.

Kane, W.F., and Beck, T.J.,2001, Instrumentation for slope monitoring: This volume.

Kroll, R.C., Sederquist, D.C., and Rorem, E.J., 2001, Rockfall hazards mitigation - An emergency case study of Mosquito Bridge Road crossing in El Dorado County, California: This volume.

McCormick, W.V., and Rice, J.D., 2001, Rio Nido landslide, Sonoma County, California—Engineering geology and emergency response: This volume.

McCrink, T.P., 2001, Regional earthquake-induced landslide mapping using Newmark displacement criteria, Santa Cruz County, California: This volume.

Medley, E.W., 2001, Characterization of Franciscan melanges and other heterogeneous rock/soil mixtures: This volume.

Upp, R.R., 2001, Scenic Drive landslide, San Mateo County, California: This volume.

Van Velsor, J., 2001, Engineering geology in the public eye - Devil's Slide: This volume.

STABILIZATION OF THE MILL CREEK LANDSLIDE COMPLEX, EL DORADO COUNTY, CALIFORNIA

BRUCE R. HILTON[1]

ABSTRACT

The El Niño Storms of 1997 severely impacted Northern California, triggering flooding and slope failures. In January 1997, slope failures and roadway washouts resulted in a 28-day closure of Highway 50 between Sacramento and South Lake Tahoe. Over 30 slopes failures occurred along a 15-mile segment of the highway. Road damage sites were evaluated and repaired on the basis of traffic safety and the potential for long-term highway closure. One of these failures, the Mill Creek landslide complex, was considered the highest priority condition, because it had buried Highway 50 beneath 12 meters of debris. This debris flow originated more than 500 m above the roadway and is estimated to have resulted in accumulation of more than 700,000 cubic meters of debris.

Emergency repairs by Caltrans removed that portion of the debris flow that had buried the highway, but left almost two-thirds of the debris flow in place. Potential instability of this residual debris triggered a geotechnical investigation aimed at the design of stabilization measures to be constructed before the next rainy season.

The 5-month investigation, repair, and bid schedule imposed due to the needs of local businesses along Highway 50 and in South Lake Tahoe required an ambitious, time-efficient exploration, design, and construction support program. The investigation concluded that a thick sequence of residual slide debris and colluvium remained on a highly unstable condition.

The selected stabilization measure was a combination of three shear-keys with large-diameter subdrains and extensive surface drainage controls.

Construction of the stabilization systems required close interaction between the contractor, engineering geologist, and geotechnical and civil engineers. Repairs were completed in October 1997 and have been monitored since. Visual and remote monitoring systems remain in use. Although predictably large quantities of surficial sloughing of fill and disturbed soil occurred during early rains, no severe slide movement has been reported over the past four years.

INTRODUCTION

The winter storms of 1997, known as El Niño, severely impacted California properties and facilities. During December 1996 and January 1997, monthly rainfall totals exceeded previous totals by nearly 400%. Road damage was primarily the result of flooding, erosion, and slope failures. California Department of Transportation (Caltrans) battled to keep highways and bridges open despite the disastrous influence of El Niño. The more severely struck area in northern California was Highway 50, a primary transportation route between South Lake Tahoe and Sacramento. In January 1997, a "Pineapple Express" storm struck the northern Sierra Nevada. This unseasonably warm winter storm system developed from tropical moisture originating in the South Pacific and rapidly melted the deep snowpack in the Sierra. Flows along the American River reached unprecedented levels, and the river overtopped its embankments along Highway 50. Hundreds of embankments and both natural and cut slope failures resulted from scouring of toes, deep saturation, and denudation of natural slopes by recent fires. Given the location of Highway 50

[1]Kleinfelder, Inc.
3077 Fite Circle
Sacramento, CA 95827
Bhilton@Kleinfelder.com

at the bottom of a deeply-incised canyon shared with the American River, road damage rendered the highway essentially impassable since there were no detour opportunities.

MILL CREEK LANDSLIDE CONDITIONS

The most severe failure along the Highway 50 corridor was the January 27, 1997 Mill Creek landslide - a 1,600-foot long debris flow that buried Highway 50 and closed the road for 28 days (Figure 1). This landslide is located between Whitehall and Kyburz, along Highway 50 (Figure 2), and briefly dammed the American River, destroying homes and public facilities (Figure 3). The river scoured a channel through the toe of the debris flow after only two hours. Caltrans immediately began emergency repairs to re-open the highway, including removal of about 250,000 cubic meters of slide debris while re-directing surface drainage from the slide mass. The lower third of the slope was excavated to bedrock. Following the failure, much of the middle and upper surface of the landslide exhibited severe tension cracks. The surface of the slide was graded in an effort to reduce surface water infiltration through these tension cracks. In addition, V-ditches were constructed to channel surface water off the slide mass and into a natural drainage to the west (At least two drainages flow onto the upper slide mass, and a stream flows seasonally along the west of the landslide in a natural bedrock channel.)

Figure 1. Oblique aerial view of the Mill Creek landslide shortly after January, 1997 (Photo courtesy of Robert Sydnor).

Emergency repairs of the Mill Creek landslide were performed to temporarily stabilize it, so that the roadway could be reopened without significant risk to traffic. Due to the absence of appreciable rainfall following the failure, the slope remained temporarily stable. However, there remained a high potential for the landslide to reactivate because of the unstable nature of the residual slide debris and disturbed soils on the upper slope. The removal of toe debris left the remaining upper two-thirds of this slide mass, colluvium, and uncompacted fill unsupported. Extensive rain, snow melt, or uncontrolled surface water from seepage could again saturate and reactivate the slide.

The roadway embankment at the toe consisted of landslide debris remaining after the roadway surface was re-exposed and uncompacted debris hauled from upslope excavations. Rock slope protection was temporarily placed on the embankment adjacent to the river during the emergency repairs. Despite this effort to protect the embankment from scouring, the embankment continued to erode through the remainder of the winter and spring until the river dropped to a lower (summer) level.

HISTORY OF THE HIGHWAY 50 CORRIDOR

Wagon trails in the canyon of the South Fork of the American River date back to the early 1850's. The first established roadway, Olgolby Road, was constructed in 1861. The first winter after construction, severe winter storms reportedly triggered landslides that damaged several sections of the new route (Boyd, 1997). Automobile use in the canyon began shortly after the turn of the century, and paving of the canyon roadway was initiated in the 1930s. In the mid 1940's, Highway 50 was improved from Placerville to South Lake Tahoe to enable winter travel (Supernowicz, 1997). Excerpts from the Sacramento Bee on February 4, 1952 demonstrate the chronic slope stability problems that have plagued the canyon during severe winter storms:

"In addition to the (3,800 ton) rock, the highway was covered with almost 9 feet of debris. The slide came on the heels of one a few hours earlier, four miles west of Kyburz."

Between Placerville and South Lake Tahoe, Highway 50 traverses primarily public lands, managed by the El Dorado National Forest. Several forest fires have occurred in the South Fork of the American River and severely denuded steep slopes throughout this portion of the canyon. Significant fires in the area include the 1959 Icehouse fire, the 1973 Pelican fire, the 1981 Wright's Lake fire, and the 1992 Cleveland Corral fire. This denudation played a major role in reducing the stability of slopes in three ways: (1) destruction of deep root systems in soil and rock vital to shear resistance, (2) increased runoff velocity without vegetation to impede energy, and (3) absence of evapo-transpiration resulting in deeper saturation.

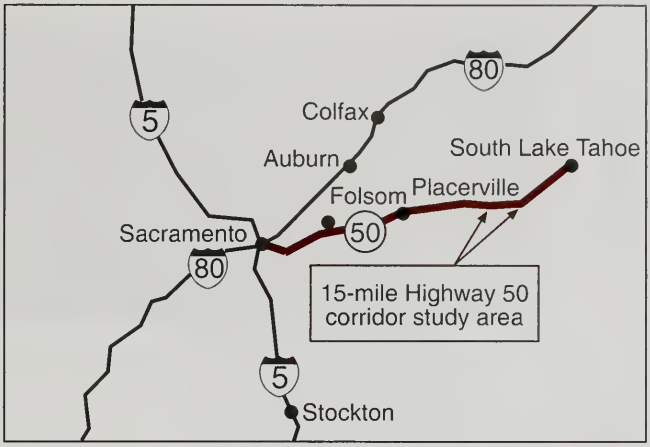

Figure 2. Site location map.

Figure 3. Side view of the toe of the Mill Creek landslide immediately post-failure, in January, 1997 (Photo courtesy of Anne Boyd).

Streamflow records for the South Fork of the American River are shown on Figure 4. Peak river flows clearly coincide with movement of the Mill Creek landslide. In the vicinity of Whitehall, the winter 1997 storms produced monthly rainfall totals for December 1996 and January 1997 of 353% and 234% of average year-to-date totals. December storms dropped much of the precipitation in the form of snow with snowlines as low as 2,000 meters (7,000 feet). In contrast, January storms were unusually warm. The heavy snowpack that developed in December, followed by the warm rainfall in January, resulted in catastrophic runoff and river flows. During the first week of January 1997, the South Fork of the American River exceeded its flood stage, resulting in severe erosion and scour of embankments along Highway 50.

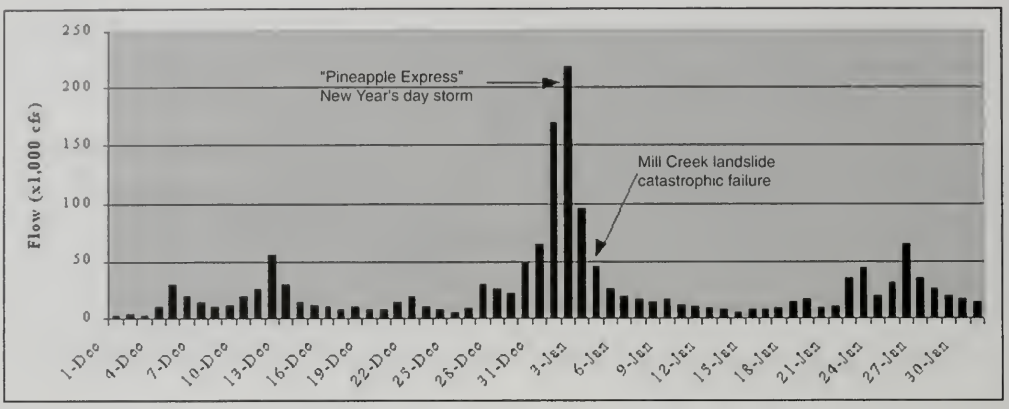

Figure 4. American River flow hydrograph. Note the coincidence of peak flows with the occurrence of the Mill Creek landslide.

GEOLOGIC CONDITIONS

Site geology

The Mill Creek landslide occurred on the north wall of the canyon of the South Fork of the American River (Figure 5), where highly weathered bedrock and soil had accumulated to depths of up to 30 meters and at an average slope gradient of 1V:2.9H. USFS personnel reported the presence of tension cracks in the area of the present headscarp in May 1996 (Boyd, 1996). Heavy and extended rainfall that began in late December 1996 and continued through January 1997 saturated this thick layer of soil and weathered bedrock and created seepage uplift forces above the bedrock.

Engineering geology and geotechnical studies were performed to evaluate the causes of road damage and recommend design repair methods to Caltrans. The initial geologic site assessment included review of "before" and "after" aerial photographs and detailed geologic mapping using a GPS to provide prompt data with reasonable accuracy. Slide geology and all subsurface data are shown on Figure 6. Seismic refraction profiles were obtained along the axis of the landslide, and along several transverse profiles coincident with boring locations for correlation. Refraction profiles proved particularly useful in mapping the soil-bedrock interface due to the pronounced seismic velocity differential (Figure 7). Six hollow-

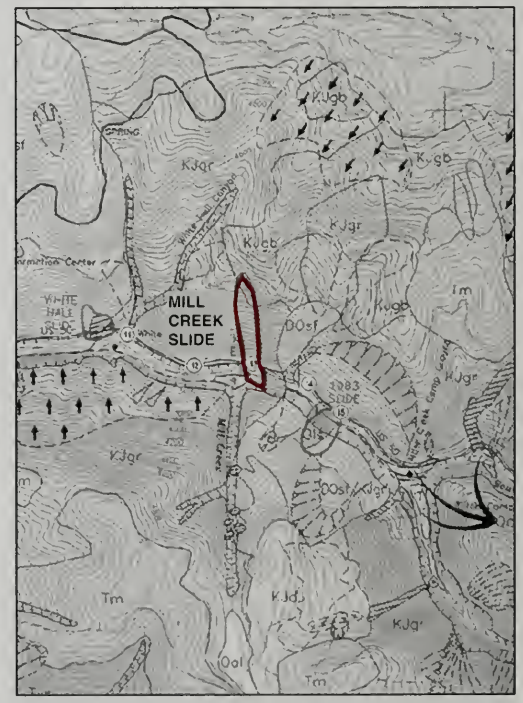

Figure 5. Regional geologic map of the portion of the Highway 50 corridor along which the Mill Creek landslide occurred.

stem auger borings were drilled within the accessible portions of the slide mass, to install downhole extensometers, TDR (time domain reflectometry) deformation sensors, and slope inclinometers for future monitoring (Figure 8). All collected data was compiled onto an isopach map and a bedrock topography map to ascertain maximum soil/residual debris thicknesses (Figure 9). Geologic cross-sections were prepared on the basis of these 3-D isopach and topographic models (Figure 10).

GEOLOGIC FINDINGS

The Mill Creek landslide is a large debris slide and flow in which oversteepened and thickly accumulated soil, colluvium, and weathered bedrock were "daylighted" at the toe by the road cut for Highway 50. The wedge of material that failed consisted of a layer of colluvium overlying variably weathered pyroxenite and diorite. The significant content of mafic (i.e. magnesium- and iron-rich) minerals in the underlying pyroxenite makes it weather more pervasively than the adjacent diorite. The natural stream channel running along the western boundary of the failure exposes competent diorite bedrock. The pyroxenite/diorite contact beneath the slide mass results in an asymmetrically weathered wedge with greater colluviation to the east than to the west. The failed section reflects this asymmetric trough, with its axis nearly coincident with a tributary to the American River. This bedrock trough coincides with the January 1997 debris flow, and we believe that flow of groundwater along the axis of the trough combined to create an extraordinary additional driving force, resulting in rapid failure of over 800,000 cubic meters of soil. A sequence of shallow landslides occurred along the eastern flank of the Mill Creek landslide, where the colluvial wedge thins onto the bedrock surface inclined to the east.

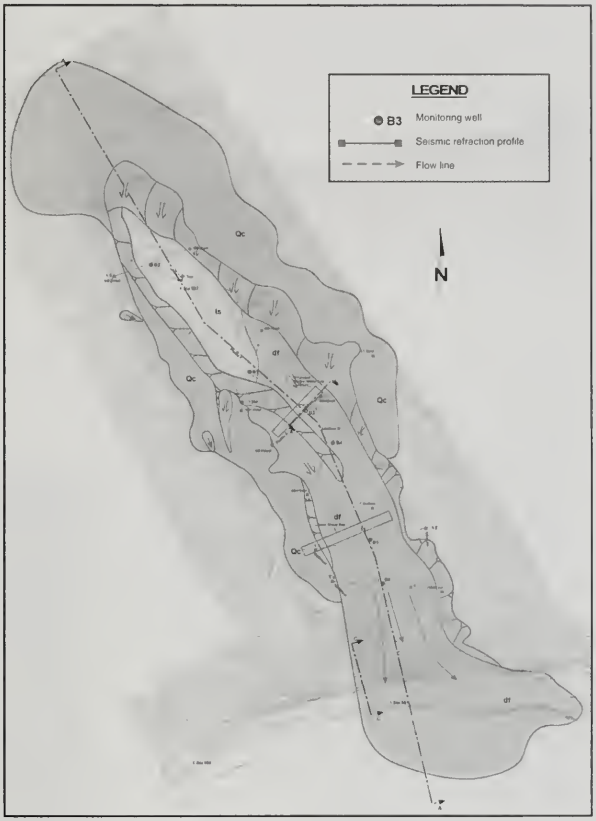

Figure 6. Geologic map of the Mill Creek landslide and adjacent terrain.

LANDSLIDE MECHANISMS

The failure occurred rapidly and consisted of saturated colluvium and portions of the weathered bedrock unit primarily in the lower two-thirds of the current failure area. Observers present during and immediately following failure reported that slide debris on the road was unexpectedly dry. It appears that the slope movement occurred in three progressive stages. The initial stage, saturated debris flow, was more mobile and temporarily extended into the river, which eventually eroded it. The second stage consisted of a more viscous, drier debris flow and debris slide that resulted in progressive (headward) failure of the slope extending several hundred meters above the highway. The debris generated by this stage of failure is probably the debris that was first reported by observers. The final stage of slope movement was primarily debris sliding (i.e. gradual downslope movement of discrete soil blocks) that resulted in little to no toe deposition but extensive

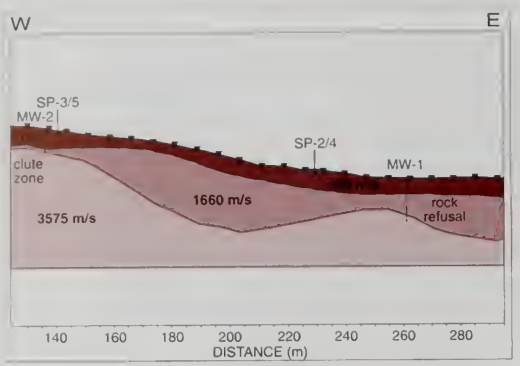

Figure 7. Transverse seismic refraction profile in the middle portion of the Mill Creek landslide.

distress to the upper portion of the slide-affected area. Concurrently, several lateral landslides occurred in the thick sequence of colluvium along the eastern flank of the upper slide mass. This upslope debris slide event produced an estimated 150,000 cubic meters of additional failure debris that remained on the slope face. The eventual head scarp of the overall failure sequence reached an elevation of 1,255 meters; approximately 500 m above the highway. Finally, these two failures removed lateral support of the slope along the northeast flank of the landslide, resulting in the formation of a complex of several adjoining landslides along the upper third to half of the eastern boundary of the slide area.

SLOPE STABILIZATION OPTIONS

Several repair options were considered, including buttressing, offloading, dewatering, shear key(s), retaining structures, and surface drainage controls.

Ultimately, the tight schedule and limited availability of funds led to the final selection of three subdrain shear keys excavated across the landslide. Large-diameter subdrains would be placed directly on the bedrock surface, draining to a gravity outlet system. Repairs included reconstructing surface drainage systems, installing horizontal drains along the "trough" and easterly scarp, and excavating debris catchment and desilting basins into bedrock at the toe. Neither funding nor time were available for mitigating the eastern flank landslides that remain prone to failure.

Mill Creek landslide repair recommendations were developed collaboratively by Kleinfelder, HDR, and Caltrans. The recommended repairs for the landslide included the following design elements:

- Removal of residual slide debris and fill in the lower slide area
- Middle and upper subdrain shear keys
- A lower buttress with subdrainage
- Surface drainage controls
- Three horizontal drain arrays along the upper eastern flank
- Two debris/desilting basins at the toe

Our initial recommendation for protection of the river embankment along the eastbound trav-

Figure 8. Total station system allowing remote website monitoring of slope inclinometers, piezometers, and downhole extensometers.

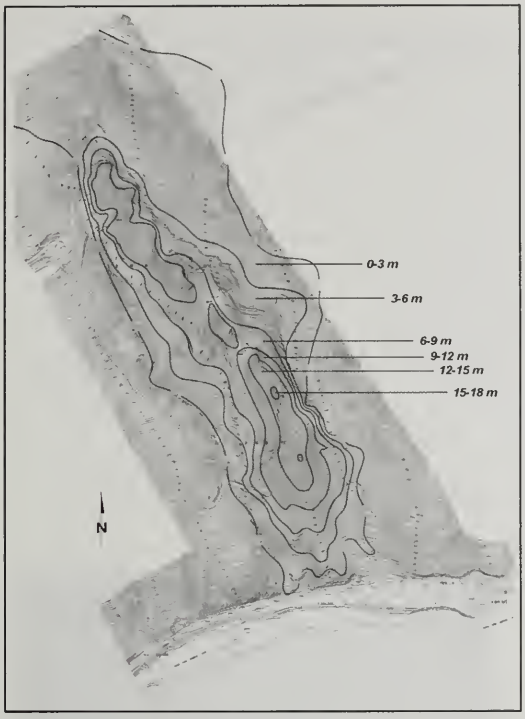

Figure 9. Isopach map of the Mill Creek landslide showing variations in thickness of residual slide debris and/or colluvial soils. This isopach map was used to identify landslide areas with the highest reactivation potential.

eled way was to excavate fill/debris extending into the river and thus modify the channel hydraulics. The remaining 1V:2H embankment would then be lined with rip-rap to protect it from future scour. However, this repair schedule was rejected by the Department of Fish and Game (DFG) due to the silt that would wash into the river during construction. Negotiations between Caltrans and DFG resulted in the final design, in which a slot would be excavated at a 1V:2H gradient into the east end of the existing fill/debris where it juts furthest into the river. The remaining embankment slope, west of the slot, would be laid back to 1V:2H and aligned with the slot.

Figure 10. Longitudinal geologic cross-section showing subsurface conditions related to the Mill Creek landslide.

Three subdrain keys were designed solely as gravity subdrains, which have lower maintenance and greater reliability than other drainage methods (Figure 11). These subdrains were backfilled as shear keys but were not designed to provide lateral support (however, they do provide some degree of horizontal support).

STABILITY MODELING OF PROPOSED REPAIRS

The potential for failure through and above each of the shear key fill embankments was evaluated using the Bishop method. The pre-failure slope condition was evaluated to calculate soil and groundwater properties at the time of failure that would produce a factor of safety of 1. These back-calculations suggest that the piezometric level (water pressure in the soil) was slightly below the ground surface elevation at the time of failure, as shown on Figure 12. These water pressures in the soil were significant factors in the slope failure, as evidenced by a corresponding 50 to 75% increase in the factor of safety when unsaturated conditions are assumed. Clearly, the most cost-effective means of reducing the reactivation potential was to control subsurface saturation.

Back-calculation analysis was used to produce a graph of friction angle (ϕ) versus cohesion. These values were compared to laboratory shear test results and representative shear parameters were selected. Selected shear values for the colluvial-bedrock interface were $\phi = 15°$ and c = 200 psf, and $\phi = 25°$ and c = 350 psf were selected for isotropic shear within colluvium or slide debris.

Stability analyses were also performed to evaluate the potential for failure through the drainage

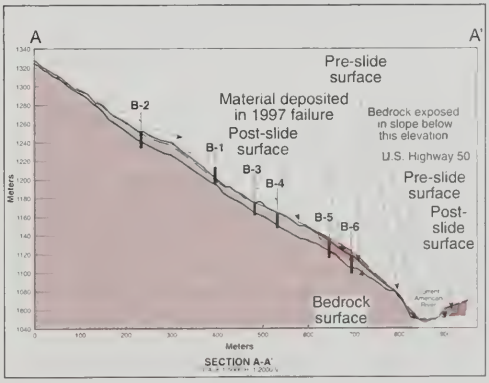

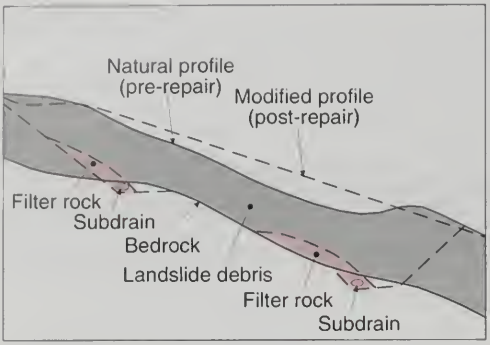

Figure 11. Recommended subdrain installation key detail included in plans and specifications (Courtesy of HDR).

keys, as well as failure above the three fill embankments under saturated and unsaturated conditions. These analyses suggest that if the proposed subdrain systems would effectively drain the residual slide mass, the probability of failure through or over the drainage keys and the corresponding fill embankments would be low (the calculated factor of safety is larger than 1.25 under these conditions). Conversely, should these subdrainage systems become ineffective, the factor of safety would be substantially reduced and failure might ensue. Monitoring and maintenance of these system are therefore crucial.

During our site reconnaissance and throughout our observations during construction, numerous seeps and several springs were noted along the top and perimeter of the slide, as well as within parts of the slide mass. These seeps indicate that groundwater continues to flow within the slide mass.

REPAIR CONSTRUCTION OBSERVATIONS

Construction observations were crucial to field modification of mitigation measures. During construction, constructability and safety issues associated with the backcut of the middle key were of concern (Figure 13). If the mid-slide shear key were not constructed, excessive hydrostatic forces within the middle portion of the landslide could exceed the ability of the lower key and buttress to support the slide. To mitigate this condition, a pumped vertical well dewatering system was installed. Constructability of the mid-slide shear key was reconsidered following observations that the slope had become

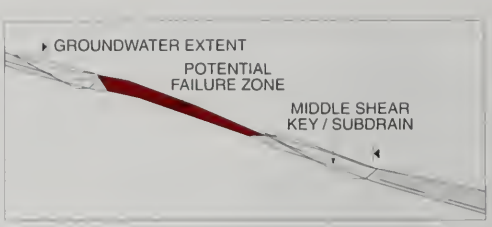

Figure 12. Slope stability modeling of backcut failure potential of recommended middle subdrain key.

less saturated. On October 3, 1997, the middle key grade was successfully reached and the subdrain system and backfill were completed shortly thereafter.

CONCLUSIONS

Repairs at the Mill Creek landslide were restricted by time and budget to "winterization"

Figure 13. Oblique aerial view of Mill Creek landslide near completion of repairs, in September, 1997.

and temporary repairs. The need for, and method of, future mitigation should be predicated on performance monitoring in view of the intensity or "test" of following winters. The 1997 repairs performed well through the 1998 and 1999 winters, but reconstruction of surface drainage systems was necessary in 1998. No measurable deflection of slope inclinometers and/or TDR extensometers has been detected to date. Groundwater monitoring wells showed only minor increases in groundwater levels despite substantial rainfall. This data suggests that dewatering systems also continue to perform well. Long-term or permanent mitigation will probably entail such methods as tunneling into bedrock or building a bridge at the toe to allow future debris flows to pass beneath the highway. If any observed or monitored movement is detected, we expect that an early warning system might be constructed to control traffic on Highway 50.

ACKNOWLEDGEMENTS

The Mill Creek landslide repairs were designed and constructed under one of several Caltrans design contract teams that Kleinfelder participated in. As the prime consultant, HDR Engineering of Folsom, California coordinated all subconsultants and provided the design and client liaison for this project. As the Kleinfelder Project Manager, I wish to express my sincere appreciation for the tremendous team work of HDR and the other design team members, including Jones and Stokes of Sacramento, Andregg Engineers, and Traffic Safety Consults. I also extend my appreciation to Spectrum Exploration, Norcal Geophysics, and PC Exploration, without whom our ambitious schedule could never have been met.

AUTHOR PROFILE

Bruce R. Hilton is an engineering geologist employed by Kleinfelder, Inc. and consults throughout the Western United States from Sacramento, California. He has over 20 years of experience as an engineering geologist. He specializes in landslide recognition and mitigation, as well as fault capability and hazards evaluation. Mr. Hilton earned his Bachelor of Science in Geology and completed all coursework in the Masters Program of California State University at Los Angeles.

SELECTED REFERENCES

Applied Earth Science, 1985, El Dorado National Forest geologic resource inventory: Consultant's report to the U.S. Forest Service, Scale 1:24,000.

Coyle, J., 1993, El Dorado forest bedrock geology map: Consultant's report by John Coyle and Associates to Kleinfelder, Scale 1:24,000.

Hilton, B.R., 1998, Geologic and geotechnical evaluation, 1997 storm damage, Highway 50 repairs: Consultant's report by Kleinfelder to HDR, 3 volumes, including geologic maps of damaged sites, Scale 1:200.

Jones, D., 1997, Bedrock geologic map of the vicinity of Mill Creek landslide: Consultant's report to Kleinfelder, Scale 1:6,000.

Sydnor, R.H., 1997, Reconnaissance engineering geology of the Mill Creek landslide of January 24, 1997: California Geology, v. 50, no. 3, p. 74-83.

USFS, 1994, Surficial stability map, Highway 50 corridor, El Dorado County, California: U.S. Forest Service, Scale 1:24,000.

USFS, 1997, Fire damage map, El Dorado National Forest: U.S. Forest Service, Scale 1:24,000.

Wagner, D.L., Jennings, C.W., Bedrossian, T.L., and Bortugno, E.J., 1981, Geologic map of the Sacramento Quadrangle, California: California Division of Mines and Geology Regional Geologic Map Series, Map No. IA, Sheet 1 of 4, Scale 1:250,000.

RIO NIDO LANDSLIDE, SONOMA COUNTY, CALIFORNIA: ENGINEERING GEOLOGY AND EMERGENCY RESPONSE

WILLIAM V. McCORMICK AND JOHN D. RICE[1]

ABSTRACT

A destructive landslide occurred in the Rio Nido canyon residential area of Sonoma County, California, on February 6-7, 1998. The landslide is complex, consisting of two types of slope failures. The upper portion of the landslide consists of a large rotational/translational block failure near the top of a ridge, approximately 600 feet above canyon floor elevation. Two debris flows were initiated from the east face of the block simultaneously with, or shortly after, the initial rotation of the block. The debris flows traveled down two separate drainages. The "southern" debris flow terminated in a residential area destroying three homes and damaging four others. The "northern" debris flow accumulated in a 20-foot-high debris dam in a remote drainage north of the residences. Prior to the occurrence of the slope failures, the area was subjected to prolonged and intense rainfall. Ever since the initial failure, the eastern face of the block has continued to fail during intense storm events, resulting in additional debris flow deposition in the canyon.

Initial emergency response consisted of helicopter and field reconnaissance by an engineering geologist, to determine the extent and character of the landslide complex, and to provide hazard assessment for the residential community. Residential areas were evacuated when the reconnaissance indicated substantial risk of additional debris flows and flooding associated with damming and breach of Rio Nido Creek by debris accumulation. Subsequent studies consisted of geologic mapping, topographic surveys, subsurface exploration, and real-time remote-sensing instrumentation. Detailed data from these studies were used for short- and long-term monitoring, development of potential future failure/hazard scenarios, establishing a schedule for residential re-occupation of evacuated areas, and mitigation design. Mitigation included construction of an underground creek diversion, a debris flow deflection berm, and a retention dam to collect future flows.

INTRODUCTION

Rio Nido is located approximately 1.75 miles northeast of the town of Guerneville, in western Sonoma County, California (Figure 1). The Rio Nido residential area is located within a series of narrow, steep-sided, incised canyons that drain southward into the Russian River, which is located at the south edge of the community. The Rio Nido area is drained by an unnamed ephemeral creek, which winds its way down the floor of the central canyon through a narrow courseway that meanders around and under residential structures.

Prior to the occurrence of the slope failures, the Rio Nido area was subjected to prolonged and intense rainfall associated with the El Niño weather pattern. Cumulative rainfall between November 1997 and the first week of February 1998 was 60 inches, with totals of 12.5 inches and 6.4 inches for the week and the two days prior to the failure, respectively. A destructive landslide occurred in the northern portion of the Rio Nido canyon residential area on February 6-7, 1998. According to eyewitness accounts, the initial slope failure (landslide) and subsequent mud/debris flow occurred at approximately 10:30 pm, followed by a larger debris flow at approximately 1:30 am on February 7, 1998. The debris flows were initiated from a steep, east-facing hillside and channeled into existing drainages with outflow and deposition in the Upper Canyon Three

[1]Kleinfelder, Inc.
2240 Northpoint Parkway
Santa Rosa, CA 95407
bmccormick@kleinfelder.com
jrice@kleinfelder.com

Figure 1. Location map.

residential area of Rio Nido (Figures 2 and 3). Debris flow deposition destroyed three homes and damaged at least four others.

In conjunction with local and state emergency personnel response, the Governor's Office of Emergency Services (OES) and the County of Sonoma Emergency Operations Center (EOC) requested that a certified engineering geologist evaluate the geologic conditions and assess the risk of additional slope failures.

EMERGENCY RESPONSE

Emergency response following a natural disaster typically involves, first and foremost, measures to protect human life and subsequently, measures to protect property. In general terms, response by emergency personnel include immediate evacuation of the residents in the area affected. Once residents are removed from the initially affected area, local or state emergency service agencies organize response teams to evaluate the conditions and develop strategies to protect citizens from further disaster. In the case of natural disasters involving landslides, an integral part of the response team is the engineering geologist. The role of the engineering geologist is to provide an evaluation of the geologic conditions and associated risks, so that emergency, as well as long-term actions, can be taken by governmental agencies to reduce the potential for loss of life or further property damage.

During emergency response to a landslide event, the primary goal of the engineering geologist is to evaluate the physical parameters of the landslide and to assess if additional failure might be imminent. Parameters to determine include: the type or mode of slope failure (i.e., rotational, translational, debris flow); the approximate dimensions of the landslide; estimation of the volume of the landslide debris and source area; estimation of landslide debris speed, direction and run-out path; and proximity of the landslide to existing development or sensitive areas (Wieczorek, 1984). In addition, it is of paramount importance to determine whether the landslide is still moving.

These parameters are used to assess the risk to life and property. Emergency risk (short-term) assessment involves making educated predictions of additional landsliding based on observed physical conditions, the geologist's previous landslide experience, and forecasted weather patterns. Since possible effects of landsliding may include loss of life, initial assessment by the geologist must be conservative. Long-term risk assessment involves modeling of the landslide for both static and dynamic conditions as additional subsurface geologic and laboratory test information becomes available.

Emergency response for the Rio Nido landslide started with a helicopter reconnaissance on the morning of February 7, 1998. During reconnaissance, it was determined that the landslide was complex; consisting of a large block failure and two debris flow channels. Initial rough estimation of the physical dimensions of the landslide block made from the helicopter (600 feet long, 200 feet wide, 50 to 100 feet thick) indicated that there was a potential debris flow source volume (i.e., the failed block) on the order of 250,000 cubic yards. Falling trees and crumbling debris from the front edge of the landslide block, and the forecast for continued heavy rains, indicated that additional failure was likely. Based on that information, the evacuation zone was extended further down canyon.

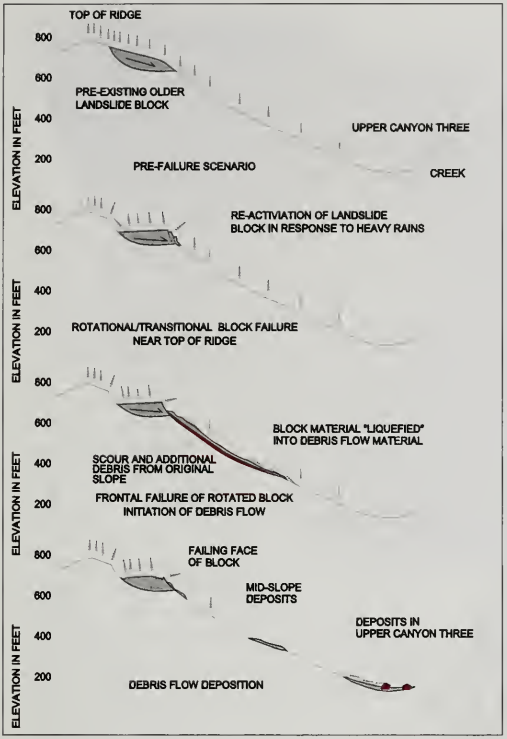

Figure 2. Schematic sections of the Rio Nido landslide failure sequence.

Following the initial response, helicopter reconnaissance was supplemented with field reconnaissance and mapping of the landslide. Geologic reconnaissance and mapping concentrated on identifying and measuring the limits and dimensions of the landslide to refine estimates of potential source volumes for additional failure, and on further evaluation of failure mode. Subdued geomorphic features, such as vegetated benches and concave, arcuate slopes, indicated this area was a pre-existing landslide. Portions of the slope had previously been mapped as containing landslide deposits (Huffman and Armstrong, 1980). From reconnaissance data, a model of the failure mechanism for this landslide was developed (Figure 2). Ground measurements indicated that the landslide block/source area was on the order of 150,000 cubic yards and that the volume of the debris flows that entered the residential canyon area was on the order of 15,000 cubic yards.

From the estimated source volume, potential debris flow failure scenarios of 30,000 and 150,000 cubic yards were developed to provide emergency planning information and relative risk assessment. These scenario volumes represent the most probable single large event (30,000 cubic yard failure of the fractured east face of the landslide block) and the worst case scenario (150,000 cubic yard failure of the entire block as a debris flow). These scenarios, presented as topographic plan maps to the local government agency, identified additional areas within the Rio Nido area that could be affected by subsequent debris flow "run-out" and impact. The "run-out" limits and approximate thickness of debris flow deposits were estimated by simple graphical methods using the physical characteristics of existing deposits observed and measured in the field (angle of repose and lateral limits of debris fan), and canyon width and gradient from existing topographic maps. During the first few months of the emergency, the 150,000 cubic yard scenario "run-out" limits were utilized by government agencies to establish subsequent evacuation zones. As weather patterns improved and additional geologic data became available, the 30,000 cubic yard scenario "run-out" limits were used as the boundary of permanent evacuation.

During field (ground) reconnaissance, it was determined that there was partial blockage of the creek channel that traversed the residential portion of the canyon bottom. Heavy rains and blockage of the channel produced flooding within the portion of the canyon where debris deposition occurred, as well as localized flooding downstream due to sediment transport from the debris fan. Based on the estimated volume and the potential for future failures of the landslide block, it was determined that there was a threat of catastrophic flooding throughout the canyon due to landslide/debris dam formation and subsequent breaching. As a result, the evacuation zone was extended further downstream along the potential flood route.

Based on evaluation of predicted weather patterns and the geologic data collected within the first five days after initial slope failure, three zones of staged, mandatory evacuations were implemented to reduce the potential for loss of life. These zones, depicted on Figure 3, were also later used in reverse order, as staged, voluntary re-entry zones for residents during favorable weather conditions. Permanent evacuation was established by county government within Zone 1.

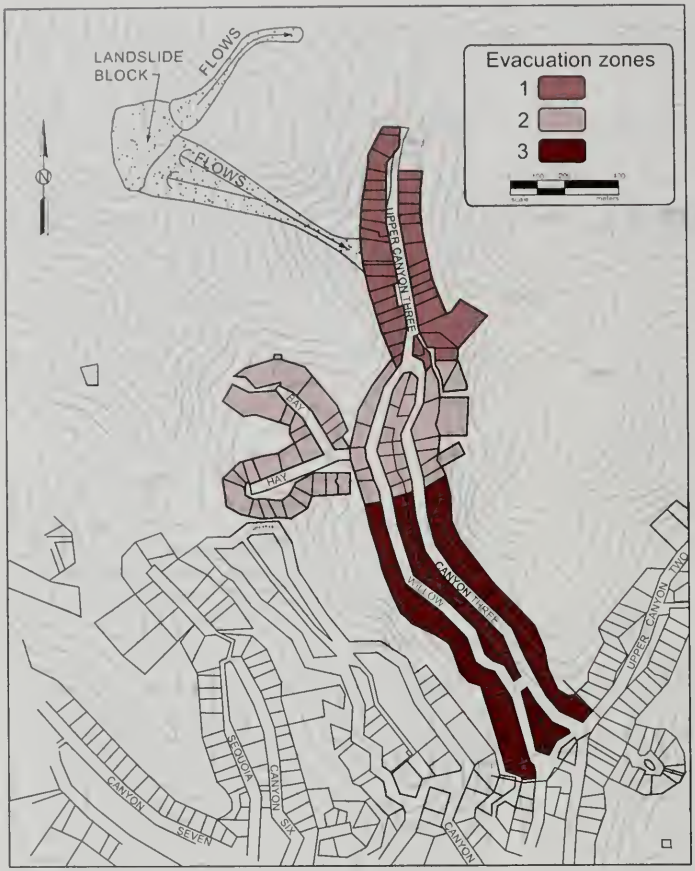

Figure 3. Staged residential evacuation zones in numerical order. Each successive zone was evacuated as additional geologic hazard and weather data became available. Re-occupation of the canyon was conducted in reverse order with favorable weather conditions (Zone 1 was permanently evacuated and is now the site of the debris flow retention basin).

SUPPLEMENTAL STUDY

Due to the continued instability of the landslide block and the forecasted El Niño weather patterns, observation, monitoring and evaluation of the geologic conditions continued for several months after the initial slope failure. Supplemental study included daily reconnaissance and detailed geologic mapping of the landslide block, establishment and monitoring of "low-tech" movement indicator arrays, a topographic survey of the landslide block, installation and monitoring of real-time remote-sensing instrumentation, and subsurface exploration.

Detailed geologic mapping is crucial in evaluating and refining the parameters of the landslide failure and the potential for future hazards. Detailed mapping of the geomorphic features of the landslide aid in evaluating the mode of failure, sense of movement, the geometry of the failure surface, and in determining which portions of the source area are likely to fail.

Geologic mapping and monitoring can be further refined with the assistance of a topographic survey. The limits and pertinent geomorphic features of the Rio Nido landslide block were surveyed in order to obtain a detailed map of the landslide block/debris source area (Figure 4) and to develop a more precise geologic cross-section through the block (Figure 5). The map and cross-section were used for both qualitative and quantitative analysis of potential hazards associated with future movement of the landslide block.

To provide an objective measurement of the rate and sense of movement of a landslide block for risk evaluation, a monitoring system needs to be implemented on the landslide block. Such systems can be of "low-tech" or "high-tech" design. During emergency situation, initial efforts typically consist of "low-tech" measures consisting of staking and distance measurements of pertinent geomorphic features or trees from fixed points beyond the limits of the landslide (crude extensometers) or placement of stake alignment arrays across landslide boundaries.

Figure 4. Detail map of geomorphic features and instrumentation on the landslide block.

Stake arrays (i.e., several stakes placed in a linear alignment from stable ground across the boundary onto the landslide block) were established shortly after the initial failure at Rio Nido and were subsequently measured for offset during daily reconnaissance.

Early in the emergency operations and preliminary geologic study, it was recognized that the Rio Nido event was complex, consisting of a large landslide block that exhibited both rotational and translational displacement, and two debris flow channels. The geologic conditions and destruction potential from debris flows at Rio Nido are unique in that a significant debris source remains in a potentially unstable configuration. Typically, debris flow source areas are colluvial-filled hollows (Reneau and Dietrich, 1987) and are usually completely evacuated at the time of failure, with little or no source materials remaining. During initial reconnaissance and observations, it was determined that it would be prudent to establish a "high-tech" equipment array to monitor the remnant landslide block/debris source for the remainder of the rainy season, and for the subsequent years.

Acting as the County's engineering consultant, Kleinfelder, Inc. coordinated efforts with the U.S. Geological Survey (USGS) to establish the placement of real-time, remote-sensing instrumentation on the landslide block to monitor displacement, groundwater levels, and precipitation. The instrumentation network consists of two instrumentation stations with radio transmitters powered by battery and solar panel energy sources; seven extensometers aligned into three arrays across different portions of the block to measure ground displacement; two piezometer transducers to measure groundwater pressures (levels) in the block; two geophones to detect ground motion vibrations; and one rain gauge to record rainfall (Figure 4). Instrumentation was installed within 3 weeks of the initial failure. Data can be accessed from a web site maintained at the County communication center. Data sets are transmitted every 5 minutes, unless pre-established signal threshold limits are exceeded, in which case data are transmitted at 1 minute intervals. Monitor-

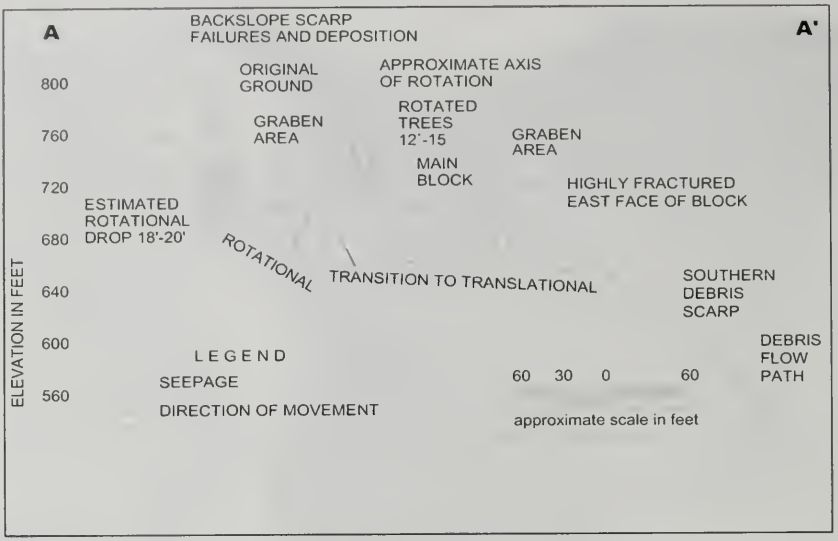

Figure 5. Cross section A-A' through the landslide block.

ing data were evaluated on a daily basis for the first six months following the initial failure and during the following winter.

Although the real-time instrumentation provides valuable data regarding the physical character of the landslide block, it is not intended to be a warning system for evacuation—especially for debris flow failures that can travel at relatively high speeds. The monitoring equipment provides data profiles that can be used to evaluate gradual changes in site physical conditions that have been interpreted as precursors to other failure events (Reid and LaHusen, 1998).

In order to obtain "ground truth" data to further quantify the depth, geometry, and physical character of the landslide failure surface, subsurface exploration needs to be performed. Test borings can be a reliable means of evaluating the subsurface geologic profile, particularly when continuous coring or sampling is utilized. This allows for a complete subsurface profile to be obtained, making identification of the landslide surface and subsurface geologic conditions possible. An additional approach that can be utilized to determine depth, as well as rate of movement of the landslide, is to install inclinometers within the limits of the landslide.

Two borings were drilled and sampled on top of the landslide block at Rio Nido. The borings were drilled with an all-terrain drill rig equipped with hollow-stem augers and sampled continuously by driving a core barrel. A zone of sheared clay, underlain by hard sandstone and siltstone bedrock, confirmed that the 50-foot depth of the landslide block estimated from the detailed geologic mapping and surveying was accurate. This data was used to confirm the estimated volume of the landslide block/debris flow source. In addition, samples collected from the slip surface were used for laboratory testing and subsequent slope stability analysis. Laboratory tests included Atterberg Limits and a 3-point staged residual direct shear test on a reconstituted sample of the slide plane material.

CONCLUSIONS

Data collected throughout the study period were used to evaluate the potential for future movement of the landslide block and generation of debris flows. Slope stability analyses were performed by geotechnical engineers for both static and pseudo-static conditions based on local and regional geologic conditions. Simplified seismic deformation analyses were performed to estimate the amount of potential movement, which in turn was used in refining debris flow volume estimates.

Mitigation alternatives developed in the course of the engineering geology study included removal of the large landslide block/debris flow source, permanent evacuation of a large part of the canyon, or construction of a retention facility in the northern part of the canyon to divert and collect future flows. Due to the constraints of the steep slopes, private ownership and the size of the landslide block, removal of the source was not considered to be legally or environmentally feasible by the government agencies. Construction of a retention facility was chosen as the mitigation alternative by the agencies. Construction of a retention facility includes a federal buy-out program and partial permanent evacuation of some of the residential properties, underground diversion of a creek, and construction of a deflection berm and earthen dam on those properties.

ACKNOWLEDGEMENTS

Thanks to all the emergency workers and staff of Sonoma County and California Department of Forestry who worked tirelessly to ensure the safety of the people of Rio Nido, provided crucial assistance and support to the geologic evaluation of this natural disaster, and procured State and Federal assistance for recovery. Special thanks to Chris Arnold and Eric Mays of the Sonoma County Permit and Resource Management Department for their support of our geologic engineering efforts during the emergency, which required many meetings, focused understanding and many hikes to the "top".

AUTHOR PROFILES

William V. McCormick has a M.Sc. degree in Geology from San Diego State University and is a California Certified Engineering Geologist with 15 years of geologic and geotechnical experience in Northern California. He is Geotechnical Manager of Kleinfelder, Inc. in Santa Rosa, California. His specialties include landslide investigation and mitigation design, and fault investigation and evaluation.

John D. Rice has a M.Sc. degree in Geotechnical Engineering from Utah State and is a registered California Civil and Geotechnical Engineer with 13 years of geotechnical experience. He is a Senior Project Engineer with Kleinfelder, Inc. in Santa Rosa California. His expertise includes slope stability analysis, geotechnical modeling, and alternative earth stabilization techniques.

SELECTED REFERENCES

Huffman, M. E. and Armstrong, C. F., 1980, Geology for planning in Sonoma County: California Division of Mines and Geology Special Report 120, scale 1:62,500.

Reid, M. and LaHusen, R., 1998, U.S. Geological Survey, personal communication and landslide monitoring network consultation to William McCormick.

Reneau, S. L. and Dietrich, W. E., 1987, The importance of hollows in debris flow studies; Examples from Marin County, California: Geological Society of America Reviews in Engineering Geology, Volume VII.

Wieczorek, G.F., 1984, Preparing a detailed landslide-inventory map for hazard evaluation and reduction: Bulletin of the Association of Engineering Geologists, v. 21, no. 3, p. 337-342.

SOURGRASS DEBRIS FLOW - A LANDSLIDE TRIGGERED IN THE SIERRA NEVADA BY THE 1997 NEW YEAR STORM

JEROME V. DeGRAFF[1]

ABSTRACT

The 1997 New Year storm triggered the Sourgrass debris flow in the Stanislaus River drainage of the Sierra Nevada, California. The storm was a rain-on-snow event that delivered 7.9 inches of precipitation in a 24-hour period to this area. Antecedent moisture conditions 4 days prior to the storm were already about 200 percent of normal. On New Year's Day, the Sourgrass debris flow occurred near the top of Summit Level Ridge as a debris slide. Slope movement occurred at the contact between weathered till and unweathered mudflow breccia. The initial slide mobilized rapidly into a debris flow that traveled about 2.4 miles downslope to the river. Its passage removed trees and eroded soil in a 200 to 500-foot-wide swath down the forested slope. Peak velocity of the debris flow was estimated to be 12 miles per hour. The final volume of material at the end of the runout path, estimated to be 191,000 cubic yards, temporarily dammed the Stanislaus River. Along its path, the debris flow destroyed a section of a 21-kV electric distribution line and severed a fiber optic telephone line before passing over California Highway 4, with little damage to the roadway. However, it became more destructive after it was channelized and its velocity increased. At the Stanislaus River it obliterated a paved Forest Service road, destroyed a steel-girder bridge over the river, and damaged Sourgrass Campground. Although the debris flow deposit temporarily dammed the North Fork of the Stanislaus River, the flood flow effectively removed the material in a matter of hours. Some material was transported to large channel bar deposits downstream. However, the bulk of the material was trapped in McKay Reservoir, which lost 10 percent of its storage capacity, or 200 acre-feet.

INTRODUCTION

During the last week of December 1996 a major storm struck northern California. The flood flows from major rivers draining the western slopes of the Sierra Nevada and subsequent flooding in the Central Valley were highly visible effects of this storm. A less well-known storm effect was the triggering of a major debris flow in the upper Stanislaus River watershed, within the Stanislaus National Forest (Figure 1). It was named the "Sourgrass debris flow" because of its impact to the Sourgrass Campground adjacent to the Stanislaus River.

An engineering geologist addressing natural hazards must be concerned with debris flows for several reasons. The most obvious is the destructive effect debris flows have on both natural systems and man-made structures. Another reason is the typically rapid onset of debris flows during a triggering event. Finally, their destructive effects are often delivered at some distance from the point of initiation.

Even though not widespread, debris flows are an important natural hazard in the Sierra Nevada. Steep canyon slopes are commonly the point of initiation for debris flows. Canyons through the Sierra Nevada are corridors where hydroelectric facilities, roads, pipelines, and telecommunication lines are concentrated. Together with increased recreational and residential development, there is an ever-greater potential for human and economic loss from debris flow occurrence in the Sierra Nevada. The ability to minimize debris flow hazard requires recognizing and better understanding their occurrence in this environment. Study of past debris flows can contribute to both recognition and understanding.

[1]USDA Forest Service
1600 Tollhouse Road
Clovis, CA 93611
jdegraff@fs.fed.us

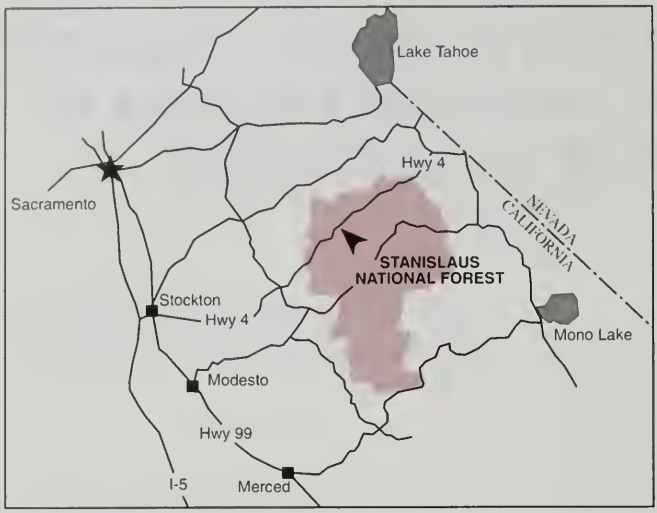

Figure 1. General location map for the Stanislaus National Forest and surrounding area. The black arrow points to the approximate location where the Sourgrass debris flow impacted California Highway 4.

TRIGGERING EVENT

Research on debris flows has identified several factors leading to their initiation during storm events. First, there must be sufficient antecedent moisture to bring earth materials to near saturation (Campbell, 1975). Second, the storm must have sufficient duration and include periods of greater intensity to produce pore-water pressures capable of inducing slope movement (Caine, 1980; Wieczorek, 1987).

Antecedent moisture conditions for the Sourgrass debris flow are inferred from nearby precipitation stations. By December 27, 1996, stations at 5,600-foot elevation within this part of the Sierra Nevada had received 200% of average precipitation (Frazier, 1997). This would seem to satisfy antecedent moisture requirements at the 6,000-foot elevation where the debris flow began.

The nearest precipitation station is at Calaveras Big Trees State Park, located about six miles west of the debris flow. The station is at 4,695 feet elevation compared to the 6,000-foot elevation where the debris flow occurred and only total daily precipitation values are available; however, it does provide insight to storm duration. Figure 2 shows precipitation at this station recorded on January 2, 1997, and the preceding three days. The total precipitation of 7.85 inches, recorded on January 2, 1997, represents the total rainfall from 0800 hours (8:00 am) on January 1, 1997 to 0800 hours (8:00 am) on January 2, 1997. The debris flow occurred at about 1830 hours (6:30 pm) during this period.

Lacking a recording precipitation station near the debris flow, periods of greater storm intensity can only be inferred. It is likely that rainfall intensity was higher during January 1, 1997 than during previous days, as suggested by the large rainfall total recorded at Calaveras Big Trees State Park. Also, the snowline in this area was

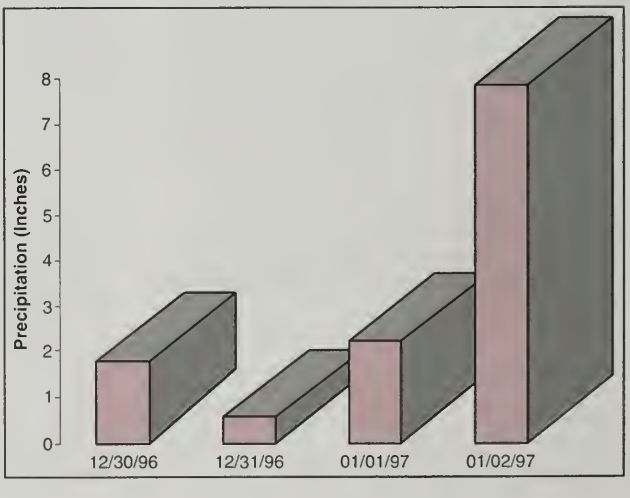

Figure 2. A graph showing the total daily precipitation received at Calaveras Big Trees State Park from December 30, 1996 to January 2, 1996. The amounts represent the 24-hour accumulation until 8:00 am of the day.

below 5,600 feet prior to January 1, 1997. Rainfall dominated on January 1,1997 leading to a rain-on-snow event at the debris flow location, where both precipitation and snowmelt water infiltrated the soil (Frazier, 1997). Rain-on-snow events create conditions comparable to periods of more intense rainfall. Triggering of debris flows by rain-on-snow events is documented for other debris flows occurrences in the Sierra Nevada (DeGraff et al., 1984; Bergman, 1987; Connelly, 1988).

THE SOURGRASS DEBRIS FLOW

The Sourgrass debris flow occurred at about 6:30 pm on New Year's Day. Two people travelling west on California Highway 4 between Bear Valley and Dorrington, California, were forced to stop after encountering water flowing across the highway. They turned back to Bear Valley upon hearing trees cracking and seeing flashes as the 21-kV electric transmission line fell on the slope above the highway. The time of the debris flow occurrence was pinpointed when it ruptured a fiber-optic cable buried in a shallow trench parallel to California Highway 4. The automated alarm system noted the cable break at 6:34 pm (Pacific Bell, 1997).

The debris flow started on the south-facing slope of Summit Level Ridge at an elevation of about 6,000 feet (Figure 3). There is an elevation difference of 2,000 feet from where the debris flow started to its deposition at the North Fork of the Stanislaus River. The runout distance for the Sourgrass debris flow was 2.4 miles from the point of initiation (Figure 4).

The Sourgrass debris flow initially occurred as a debris slide just below the crest of Summit Level Ridge (Figure 5). Summit Level Ridge is underlain by the Miocene Mehrten Formation: a volcanic mudflow breccia with interbedded tuff layers. At the head of the drainage, a thick, highly weathered unit of granitic gravels interpreted to represent glacial till (Tahoe?) mantles the Mehrten Formation. The till is estimated to be 50-feet thick within the debris slide scar area. The slip surface of the debris slide appears to be near the contact between the till and Mehrten Formation. This also represents a hydrogeologic boundary between a very permeable unit (till) over a much less permeable unit (Mehrten Formation). The contact between the Mehrten Formation and the underlying granitic bedrock is present just upslope from the lower timber access road upslope from Highway 4 (Figure 3).

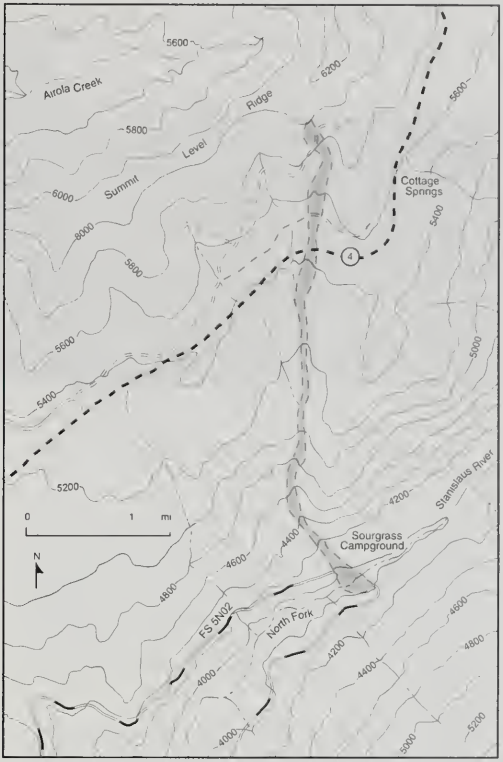

Figure 3. Part of the Boards Crossing 7.5-minute topographic map showing the Sourgrass debris flow and nearby features. The initial movement, debris flow path, and limits of the deposition area are shaded. The double dashed lines represent the timber access roads. The destroyed section of Forest Road (FS) 5N02 and bridge by Sourgrass campground are outlined across the shaded area.

The initial slope movement was on a south- to southwest-facing slope inclined between 26 to 40 percent within the broad headwater basin of an unnamed tributary to the North Fork of the Stanislaus River. A well-defined headscarp and lateral shear zones delineate an initial slide mass about 500 feet wide and 200 feet long. These dimensions, together with the inferred thickness, were employed to estimate the volume of the total debris slide mass. Part of the slide mass remains within the scar area. It is estimated that the part of the debris slide that mobilized as a debris flow was about 65,000

Figure 4. Aerial view of the entire length of the Sourgrass debris flow. The initiation point at Summit Level Ridge (on the skyline) is seen in the background. The North Fork of the Stanislaus River flows from right to the left in the foreground.

cubic yards. Howard et al. (1988) illustrated this transformation from debris slide to debris flow for slope movements near Pacifica, California.

The transition from a debris slide to a debris flow was evident where the sharp contact of the lateral shear zone became a smoothed, overridden margin with levees. The observed changes occur just upslope from the upper timber access road (Figure 3). For the first 1.2 miles, from the point of initial movement to downslope from Highway 4, the debris flow was within a broad basin (Figure 6).

The moderate slope and basin topography created a debris flow runout about 500 feet wide. Along the runout, most trees and vegetation were removed and soil scoured to an estimated average depth of 2 feet. The estimate of scour depth is based on the 3-foot depth to the fiber optic cable and the limited impact to the native surfaced roads and Highway 4. The shallow scouring over a large area added about 94,000 cubic yards to the debris flow volume.

The debris flow runout between 1.2 miles and 2.0 miles narrowed as the flow became confined within a more deeply incised stream channel. Passage of this channelized flow was more effective in scouring along the runout path. It eroded the channel gravels and banks to underlying granitic bedrock along many reaches. Average depth of erosion was determined to be 5 feet, and an additional volume of 35,000 cubic yards of material appears to have been added to the debris flow due to channel scouring. Prominent debris flow levees of uprooted trees, soil, and rock were deposited along the margins of the runout path (Figure 7). The presence of levees and matrix-supported deposits provide further evidence for a debris flow mode of emplacement (Costa and Jarrett, 1981; Cruden and Varnes, 1996).

From 2.0 to 2.4 miles, the stream channel was steeper and generally bedrock-lined prior to passage of the Sourgrass debris flow. It is estimated that only another 18,000 cubic yards of material was added to the volume of the debris flow along this part of its runout. Deposition occurred along much of the runout, which decreased the total volume reaching the North Fork of the Stanislaus River by about 10 percent. Therefore, the volume of the Sourgrass debris flow reaching the river was computed to be 191,000 cubic yards

At the North Fork of the Stanislaus River the debris flow deposit created a natural dam. Within the undamaged part of Sourgrass Campground a construction contractor had left a 40-foot equipment van; according to a workman, water impounded by the debris dam floated the van and turned it on its side. When the debris dam failed, the released water carried the van a short distance to where it became lodged in some trees. The remainder of the deposit was removed by the flood flows of the river.

Figure 5. The debris slide remnant and initial debris flow runout of the Sourgrass debris flow.

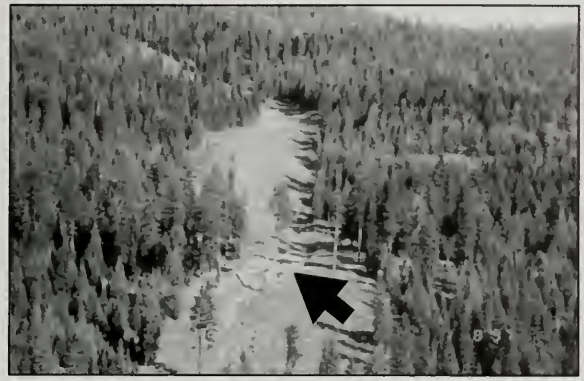

Figure 6. The upper part of the debris flow runout. California Highway 4 crosses the runout in the middle of this photo, where a Caltrans dump truck is visible (arrow).

McKays Reservoir, about eight miles downstream, has a spillway rated by the U. S. Geological Survey to provide flow data at values greater than 1,500 cubic feet per second. The hydrograph did not show the typical rapid drop and sharp rise associated with damming and later breaching (Costa and Jarret, 1981). However, it did show that the rising flow suddenly plateaued at 6:30 pm (1830 hrs) and then increased dramatically to a peak from 7:00 pm (1900 hrs) through 8:00 pm (2000 hrs) (Figure 8). This could indicate that the debris flow dam failed within an hour after its formation near Sourgrass Campground.

A remnant of the debris dam is present on the opposite bank from the debris flow runout (Figures 9 and 10). It consists of debris from the destroyed bridge intermixed with large woody debris and large rocks. Some transported material was deposited in channel bars along the river. These bars were noted for several miles downstream during aerial reconnaissance on January 8, 1997.

VELOCITY AND DAMAGE

The most obvious damages were the destruction of the trees along the debris flow path and damage to the 21-kV transmission line, which necessitated replacement of one pole and 1,300 feet of line. A Pacific Bell fiber-optic cable buried in a shallow trench adjacent to the upslope side of Highway 4 was ruptured and required repair. However, the damage within the first one-half mile resulted largely from impact to surface objects in the path of the debris flow. The debris flow passed over two native-surfaced timber access roads and Highway 4 but caused little damage. Erosional scour was limited to a shallow depth in areas underlain by soil.

Measurements just above the lower timber access road permitted determination of flow velocity, based on the super-elevation in bends or tendency to reach higher elevations on the outside bends than on the inside ones. Costa (1984) provides a detailed explanation for computing debris flow velocity from field measurements and calculations based on angular momentum. From the measurements, it is estimated that the debris flow was moving at a velocity between 2 and 3 miles per hour. This velocity combined with a small volume moving across a wide path, accounts for the limited scour and lack of damage to the timber access roads and Highway 4.

By the time the debris flow reached the North Fork of the Stanislaus River it was much more destructive. A two-lane paved Forest Service road and its bridge over the North Fork of the Stanislaus River were within the runout path of the Sourgrass debris flow. As in the upper flow path, surface objects such as large trees and the bridge across the

Figure 7. Debris flow levee consisting largely of large woody debris at margin of runout. This location is nearly 2.0 miles from the initial failure, at the point where the channel begins to steepen.

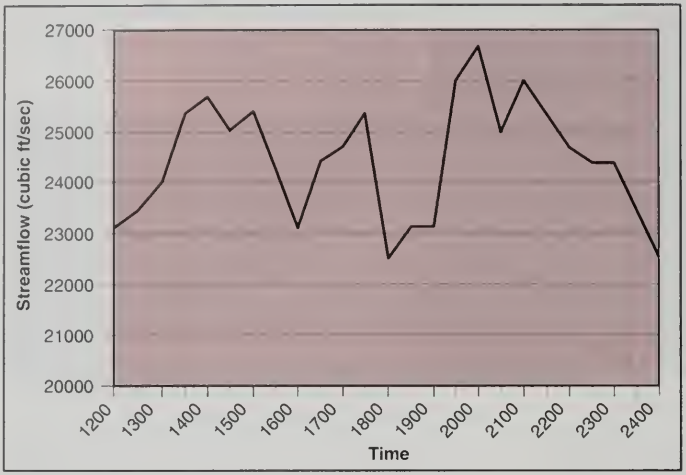

Figure 8. Flow through the spillway at Mckays Reservoir taken at 30-minute intervals. The spillway is rated to provide flow data at values greater than 1,500 cubic feet per second. Data provided by Northern California Power Administration.

Stanislaus River were destroyed. Erosional scour by the debris flow also destroyed the paved road across the debris flow path. Additionally, damage was sustained in the Sourgrass campground adjacent to the bridge. Nearly $1.25 million has been spent to restore these facilities.

Very rapid passage leading to the Stanislaus River is evident at several bends in the channel where super-elevation of the debris flow cleared vegetation high on the banks (Figure 8). Another velocity measurement was obtained near the Forest Service road next to the river. Velocity was determined by the velocity-head method, which involves measuring differences in the maximum height the debris flow reaches as it passes around a vertical obstacle. Webb et al. (1988) provide a detailed explanation of this approach. In this instance, a large tree was used. The computed velocity was just over 12 miles per hour. The greater velocity and mass of the debris flow confined to a narrower path at the end of the runout contributed to the greater impact to roads and structures at this location compared to Highway 4.

A less obvious impact, unrelated to the velocity of the debris flow, was the excess load of sediment delivered to the Stanislaus River. There is no information on the impact of the sediment on the fisheries habitat, but it appears that much of the debris flow volume reached McKays Reservoir. This small reservoir, about eight miles downstream, lost approximately 200 acre-feet of storage, which represents about 10 percent of its total storage capacity (Northern California Power Administration, 1997).

Figure 9. The deposition area for the Sourgrass debris flow at the North Fork of the Stanislaus River. The debris flow passed from the right across the river to the far bank on the left. A temporary road is partially constructed across the runout along the destroyed road alignment.

DISCUSSION AND CONCLUSIONS

Comparing the physical geomorphology of the Sourgrass debris flow to other Sierran debris flows reveals both typical and atypical aspects (DeGraff, 1997). A typical aspect was its being triggered by a rain-on-snow event (DeGraff, 1994). This type of precipitation event readily creates the pore-water pressures necessary to induce slope movement. Initial failure occurring at a hydrogeologic boundary was another typical feature. For the Sourgrass debris flow, this was the contact between permeable till and less permeable Mehrten Formation. It is also possible the till filled

Figure 10. A view from within the debris flow path looking across the North Fork of the Stanislaus River. Some of the woody debris seen at the base of the trees was carried across the river by the debris flow runout.

a bedrock hollow, which would further enhance the formation of elevated pore-water pressures leading to debris flow occurrence (Reneau and Dietrich, 1987). The higher velocity estimate of 12 miles per hour is average for recent debris flows in the Sierra Nevada (DeGraff, 1994).

An atypical aspect of the Sourgrass debris flow was its size. The final volume at the end of the runout was 191,000 cubic yards, which was nearly three times the initial volume. This volume greatly exceeded the hundreds to thousands of cubic yards more commonly associated with Sierra Nevada debris flows (DeGraff, 1994). Even though the runout distance of 2.4 miles was not unique for the Sierra Nevada, its width of 200 to 500 feet was uncommon (DeGraff, 1994). Natural dams are known to form from debris flow deposition (Costa and Schuster, 1988). The 1983 Strawberry Creek debris flow is an example that occurred in the Sierra Nevada (Connelly, 1988). However, other recent debris flows in the Sierra Nevada have been too small in volume to create landslide-dams (DeGraff, 1994).

Debris flows are an infrequent, but important, natural hazard in the Sierra Nevada (DeGraff, 1997). Even if infrequent, recognizing these hazards is important because of their destructive effect on both natural features and man-made structures. Debris flow hazard is also important because it has a rapid onset and can deliver impacts at some distance from the site of initiation (Connelly, 1988, DeGraff, 1994). The Sourgrass debris flow demonstrates the impacts that can result when a debris flow occurs where significant development exists. As increased development occurs in the Sierra Nevada, it will be important to recognize this natural hazard and develop a better understanding of its occurrence in this environment. Only in this way can actions be taken to minimize the risks posed to people and the built environment.

Figure 11. Part of the runout in the steeper channel section between 2.0 and 2.4 miles. Passage of the debris flow has cleared trees higher on the bend due to super-elevation.

ACKNOWLEDGEMENTS

The author wishes to thank J. David Rogers for suggesting that the Sourgrass debris flow might be an interesting contribution to this volume. Editing by Steve Stryker and Horacio Ferriz greatly enhanced the clarity and readability of this paper.

AUTHOR PROFILE

Mr. Jerome V. DeGraff has nearly 25 years of environmental and engineering geology experience with the USDA Forest Service in both Utah and California. He currently serves as the Province Geologist for the Stanislaus, Sierra, and Sequoia National Forests. Landslides and hazard mitigation are long-term professional interests. He was awarded the E.B. Burwell Jr. Award from the Engi-

neering Geology Division of the Geological Society of America and the Claire P. Holdredge Award from the Association of Engineering Geologists for his contributions to the field of engineering geology.

SELECTED REFERENCES

Bergman, J. A., 1987, Rain-on-snow and soil mass failure in the Sierra Nevada of California: *in* DeGraff, J. V. (ed.), Landslide activity in the Sierra Nevada during 1982 and 1983: Earth Resources Monograph 12, U. S. Forest Service, Pacific Southwest Region, San Francisco, p. 15-26.

Caine, N., 1980, The rainfall intensity-duration control of shallow landslides and debris flows: Geografiska Annaler, v. 62A, p. 23-27.

Campbell, R. H., 1975, Soil slips, debris flows, and rainstorms in the Santa Monica Mountains and vicinity, southern California: U.S. Geological Survey, Professional Paper 851, 51 p.

Connelly, S. F., 1988, The Strawberry Creek and Pyramid Guard Station landslides: Earth Resources Monograph 14, U. S. Forest Service, Pacific Southwest Region, San Francisco, 105 p.

Costa, J.E., 1984, Physical geomorphology of debris flows: in Costa, J.E. and Fleisher, P.J. (eds.), Developments and Applications of Geomorphology: Springer-Verlag (Berlin, Germany), p. 268-317.

Costa, J.E. and Jarrett, R.D., 1981, Debris flows in small mountain stream channels of Colorado and their hydrologic implications: Bulletin of the Association of Engineering Geologists, v. 18, p. 309-322.

Costa, J.E. and Schuster, R.L., 1988, The formation and failure of natural dams: Bulletin of the Geological Society of America, v.100, p.1,054-1,068.

Cruden, D.M. and Varnes, D.J., 1996, Landslide types and processes: *in* Turner, A.K. and Schuster, R.L. (eds.), Landslides, Investigation and Mitigation: Transportation Research Board Special Report 247, p.36-75.

DeGraff, J.V., 1994, The geomorphology of some debris flows in the southern Sierra Nevada, California: Geomorphology, v. 10, p. 231-252.

DeGraff, J. V., 1997, Sourgrass debris flow: a 1997 example of a dominant landslide mechanism in the southern Sierra Nevada: Association of Engineering Geologists, Abstracts and Program (Seattle, Washington), p. 95.

DeGraff, J.V., McKean, J., Watanabe, P.E., and McCaffery, W.F., 1984, Landslide activity and groundwater conditions: insights from a road in the central Sierra Nevada, California: Transportation Research Record no. 965, p. 32-37.

Frazier, J., 1997, Personal communication: USDA Forest Service, Sonora, CA.

Howard, T. R., Baldwin, J. E., III, and Donley, H. F., 1988, Landslide in Pacifica, California caused by the storm: *in* Ellen, S. D. and Wieczorek, G. F. (eds.), Landslides, floods, and marine effects of the storm of January 3-5, 1982, on the San Francisco Bay region, California: U. S. Geological Survey Professional Paper 1434, p. 163-183.

Northern California Power Administration, 1997, Personal communication by Mr. N. Worthington.

Pacific Bell, 1997, Personal communication by Mr. L. Tracy.

Reneau, S.L. and Dietrich, W.E., 1987, The importance of hollows in debris flow studies; examples from Marin County, California: *in* Costa, J.E. and Wieczorek, G.F., (eds.), Debris flows/avalanches: process, recognition, and mitigation: Geological Society of America, Reviews in Engineering Geology, v. 7, p. 165-180.

Webb, R.H., Pringle, P.T., Reneau, S.L., and Rink, G.R., 1988, Monument Creek debris flow, 1984: implications for formation of rapids on the Colorado River in Grand Canyon National Park: Geology, v. 16, p. 50-54.

Wieczorek, G. F., 1987, Effect of rainfall intensity and duration on debris flows in central Santa Cruz Mountains, California: *in* Costa, J. E. and Wieczorek, G. F. (eds.), Debris flows/avalanches: process, recognition, and mitigation: Geological Society of America, Reviews in Engineering Geology, v. 7, p. 93-104.

REGIONAL EARTHQUAKE-INDUCED LANDSLIDE MAPPING USING NEWMARK DISPLACEMENT CRITERIA, SANTA CRUZ COUNTY, CALIFORNIA

TIMOTHY P. McCRINK[1]

ABSTRACT

A dynamic slope stability method using Newmark displacement criteria is tested against 1989 Loma Prieta earthquake-induced ground failures in the Laurel 7-1/2 minute Quadrangle in the southern Santa Cruz Mountains, California. This study evaluates the methodology that will be used by the California Department of Conservation's Division of Mines and Geology in delineating zones of required investigation for earthquake-induced landslides. Test comparisons are first made using the procedure originally developed by the U.S. Geological Survey, and then with improvements to the input data and discrimination procedure. The tests show that about 50 percent of the Loma Prieta earthquake ground failures are included in areas identified by the original procedure with no improvements. Modifications made to improve the procedure include:

- Collection and analysis of laboratory-derived shear strength data.
- Inclusion of a new, pre-earthquake, landslide inventory.
- Preparation of a new 10-meter digital elevation model.
- Use of a near-field Loma Prieta earthquake strong-motion record.
- Recognition and removal of tectonic (fault-related) and ridge-top failures from the comparisons.

Model parameters are varied and repeatedly compared to the known slope failures to optimize the procedure for 1:24,000-scale mapping. With the modifications and optimized parameters, the procedure accounted for 84 percent of the Loma Prieta earthquake-induced landslides. The resulting calibrated computer model has been adopted by the Division of Mines and Geology for preparing seismic hazard zone maps throughout California.

INTRODUCTION

A decade ago, the M6.9 Loma Prieta earthquake struck the San Francisco Bay region. The earthquake was significant for the Division of Mines and Geology (DMG) and for development of a regional method to map earthquake-induced landslides. The earthquake led the California Legislature to pass the "Seismic Hazards Mapping Act of 1990" (Public Resources Code, Chapter 7.8, Division 2), the purpose of which is to reduce earthquake-related losses to life and property by identifying and mitigating secondary seismic hazards, such as landsliding. The Act requires DMG to delineate "Seismic Hazard Zones" or zones of required geotechnical investigation for areas susceptible to soil liquefaction and earthquake-induced landslides. It also authorized the State Mining and Geology Board to create a technical oversight committee to assist DMG with this task. The Seismic Hazards Mapping Act Advisory Committee concluded that there was no accepted method for delineating earthquake-induced landslides. The committee advised DMG to conduct a pilot study to test the Newmark (1965) displacement method as applied by the U.S. Geological Survey (USGS) in San Mateo County (Wieczorek et al., 1985). A separate analysis (Holden and Real, 1990) concluded that the most cost-effective way to prepare seismic hazard zone maps would be to

[1]California Department of Conservation
Division of Mines and Geology
801 K Street, MS 12-31
Sacramento, CA 95814-3531
tmccrink@consrv.ca.gov

produce them using a geographic information system (GIS).

Thus, the major purpose of this study was to develop a GIS-based computer model that could be used as a predictive tool to identify areas with a high probability for future earthquake instability. The DMG needed to determine whether the Newmark displacement method was adequate as a predictive tool at a regional scale (1:24,000). This determination required comparing the results of a Newmark analysis with the occurrence of known earthquake-induced landslides. The Loma Prieta earthquake, centered in the southern Santa Cruz Mountains (Figure 1), generated many landslides and provided a valuable data set to test this application of the Newmark displacement method.

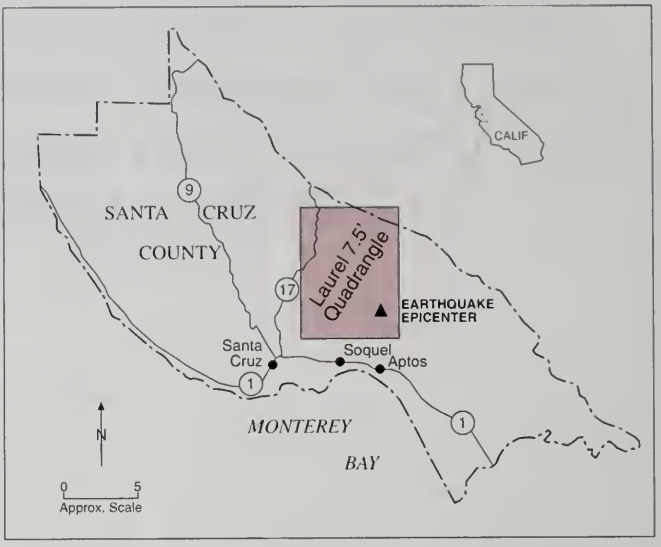

Figure 1. Location of the Laurel 7-1/2 minute Quadrangle, Santa Cruz County, California.

The Laurel 7-1/2 minute Quadrangle was chosen for the pilot study (Figure 1). The Loma Prieta earthquake epicenter was within the quadrangle, and a strong-motion seismic recording station was only 7 kilometers from the epicenter (Shakal et al., 1989). Also, the Laurel Quadrangle encompassed hundreds of earthquake-triggered landslides, most of which were mapped soon after the earthquake by geologists from public and private organizations. Furthermore, digital geologic and terrain data were available from the USGS. Finally, engineering geologic and geotechnical engineering consultant reports, documenting both earthquake ground failures and laboratory shear tests, were available at the Santa Cruz County Planning Department.

This study had three phases. First, the original USGS procedure was evaluated in the Laurel Quadrangle using existing or readily obtainable input information. This evaluation phase allowed identification of weaknesses in the procedure and areas in which data improvements were needed. Data and procedure improvements were applied in the second phase. The third phase determined the optimum combination of input parameters by varying the critical slope-stability parameters and identifying the combination that best encompassed, or "captured," the Loma Prieta earthquake-induced landslides. The resulting mapping procedure, approved by the Advisory Committee, has since been used to prepare more than 40 seismic hazard zone maps in both southern and northern California. Comparisons of released maps with slope failures triggered by the 1994 Northridge earthquake and implications of these maps on the practice of engineering geology will be discussed.

PHASE 1 - EVALUATION OF THE NEWMARK DISPLACEMENT METHOD

The Newmark slope stability method analyzes slopes that may fail during a seismic event. The method calculates the cumulative down-slope displacement of a rigid sliding block on an inclined plane for a given yield acceleration (defined as the inertial force that results in a factor of safety of 1.0) and a strong-motion time-history. The assumption is that, as long as the cumulative displacement does not exceed a certain value, structures on that slope may not be damaged. Thus, a carefully performed Newmark analysis provides usable design information beyond the knowledge that a particular slope may fail during an earthquake.

The Newmark method was developed for site-specific applications. The strength of this and other methods of stability analysis lies in the accurate determination of numerous geologic and geotechnical parameters, typically collected at a site and tested in the laboratory. To use the method for large areas, several key parameters need to be estimated or calculated over broad areas. These parameters include the strength of geologic materials, the ground surface slope gradient, the anticipated earthquake shaking, and the presence or absence of groundwater. The validity of any regional mapping method relies heavily upon the ability of these estimated parameters to characterize the actual conditions in nature.

The USGS first used the Newmark analysis for regional landslide mapping of "relative dynamic slope stability" in San Mateo County (Wieczorek et al., 1985). In brief, Wieczorek et al. (1985) divided the geologic units into three geologic strength categories, prepared a slope gradient map and characterized the anticipated earthquake shaking by selecting two strong-motion records to represent upper and lower bound earthquakes. They assumed that a calculated Newmark displacement of 5 centimeters was significant to structures. This displacement related to a yield acceleration range of 0.1 and 0.3g for the upper and lower bound earthquakes. They used an infinite-slope failure method of analysis considering saturated and unsaturated ground conditions. The geologic material strength values used by Wieczorek et al. (1985) are shown in Table 1, and landslide potential criteria are shown in Tables 2 and 3.

The Loma Prieta earthquake did not occur in San Mateo County and did not produce any triggered landslides in that county that could be used to test the mapping method. The evaluation phase of this study ran the USGS procedure, with no modifications, in Santa Cruz County, and compared the results to Loma Prieta earthquake-triggered ground failures. The goals of this phase were to identify the limitations of this application of the Newmark method and the input data, and to gain a familiarity with the capabilities of GIS technology.

Geologic unit category	ϕ (deg.)	C (lb/ft^2)
A. Crystalline rocks, well cemented sandstone	35	300
B. Unconsolidated and weakly cemented sandstone	35	0
C. Shales and clays	20	0

Table 1. Estimates of material strength for categories of geologic units in San Mateo County (after Wieczorek et al., 1985).

Loma Prieta earthquake ground failures

The USGS procedure was evaluated by comparison of the predictions with ground failures observed within the Laurel 7-1/2 minute Quadrangle following the Loma Prieta earthquake. The majority of the ground failures used in this study were compiled from maps and reports prepared by geologists from public and private organizations. Specifically, for the northern portion of the quadrangle, Spittler and Harp (1990) and the Technical Advisory Group on the Santa Cruz Geologic Hazard Investigation (1991) provided a comprehensive inventory of ground failures. In the northeastern quarter of the quadrangle, ground failures in the Soquel Demonstration Forest were compiled by Bedrossian (1989), and Bedrossian and Sowma (1991). The eastern part of the Laurel Quadrangle includes the Forest of Nisene Marks, where earthquake-triggered ground

Ground water condition	Yield acceleration	Slope movement	Susceptibility
wet or dry	< 0.1g	> 5cm for lower bound earthquake	High
dry	0.1 to 0.3g	≥ 5cm for upper bound earthquake	Moderate
dry	0.1 to 0.3g	≤ 5cm for lower bound earthquake	Moderate
wet or dry	< = 0.1g	> 5cm for lower bound earthquake	Moderate
dry	> = 0.3g	≤ 5cm for upper bound earthquake	Low
wet	0.1 to 0.3g	≥ 5cm for upper bound earthquake	Low
wet	0.1 to 0.3g	≤ 5cm for lower bound earthquake	Low
wet or dry	> 0.3g	< 5cm for upper bound earthquake	Very low

Table 2. Criteria for landslide potential in San Mateo County (after Wieczorek et al., 1985).

Lithologic category	Percent slope interval					
	I 0 to 5%	II 5 to 15%	III 15 to 30%	IV 30 to 50%	V 50 to 70%	VI > 70%
A	VL	VL	VL	VL	L	H
B	VL	VL	L	M	H	H
C	VL	L	M	H	H	H

Table 3. Landslide potential matrix for seismically-induced landslides in San Mateo County (after Wieczorek et al., 1985). VL = very low; L = low; M = moderate; H = high.

failures were mapped by Weber and Nolan (1989). Other ground failures in the quadrangle were derived from engineering geology and geotechnical engineering reports on file with the Santa Cruz County Planning Department. Additional ground failure locations and written descriptions were provided by Manson et al. (1991) and WCA (1993). The author also identified several ground failures in the field. Ground failures were compiled on an enlarged (1:12,000 scale) topographic base map. The ground failures were then digitized and given database attribution in the GIS (Figure 2).

Not all the ground failures were landslide-related (Plafker and Galloway, 1989). Accordingly, it was important to distinguish the landslide-related failures from tectonic or ridge-top spreading causes. Tectonic failures refer to those ground failures caused by co-seismic slip along existing faults and bedding planes. Ridge-top spreading failures have been attributed to earthquake triggered gravitational spreading of ridges (Hart et al., 1990). For ground failures in the north-central part of the quadrangle, the Technical Advisory Group on the Santa Cruz Geologic Hazard Investigation (1991) distinguished ground failure causes based on fracture orientation and trend variability. Other investigators (Bryant, 1991; Aydin et al., 1992; Ponti and Wells, 1991; Hart et al., 1990; Cotton et al., 1990), describe the nature and location of tectonic and ridge-top spreading failures in this area. In those portions of the Laurel Quadrangle where the ground failure cause was not already determined, failures were classified as either landslide-related or not landslide-related based on criteria shown in Table 4.

Ground failure information was not available in Santa Clara County in the northeast corner of the Laurel Quadrangle. Also, immediately south of the Forest of Nisene Marks in the southeast portion of the quadrangle, few post-earthquake rebuilding permits were filed, and the extent of ground failures is not known. Additionally, it was not determined if any ground failures occurred within the incorporated city area of Scotts Valley. Despite these shortcomings, the final map was the most complete and detailed set of ground failures ever collected from a single seismic event. The data set represents the "ground truth" used to evaluate the regional application of the Newmark method and formed the basis for improvements to the mapping procedure.

Digital geologic data

The spatial distribution of geologic materials was based on an unpublished digital geologic map of the Laurel Quadrangle (Wentworth, 1993; Clark et al., 1989). Each geologic formation shown on the digital geologic map was given an appropriate material strength category and converted to a raster format (i.e., the area was divided into 30 by 30 meter elements, called pixels) for the analysis. Because most geologic formations in the Laurel Quadrangle occur in San Mateo County, the evaluation used the same geologic material strength values and landslide potential criteria used by Wieczorek et al. (1985) (Tables 1 to 3). Geologic formations not common to both areas were placed in strength categories based on age and lithologic characteristics.

Criteria	Tectonic/ridge-top failures	Landslide failures
Shape/orientation	Straight; northwest-trending	Arcuate; variable orientation
Spatial relationships	Not associated with landslide features	On or near existing landslide features
Location	Tops of ridges; on and parallel to sharp ridges	Hillsides

Table 4. Criteria used to distinguish tectonic and ridge-top versus landslide-related ground failures. Tectonic failures refer to those ground failures caused by co-seismic slip along existing faults and bedding planes. Ridge-top spreading failures have been attributed to earthquake triggered gravitational spreading of ridges.

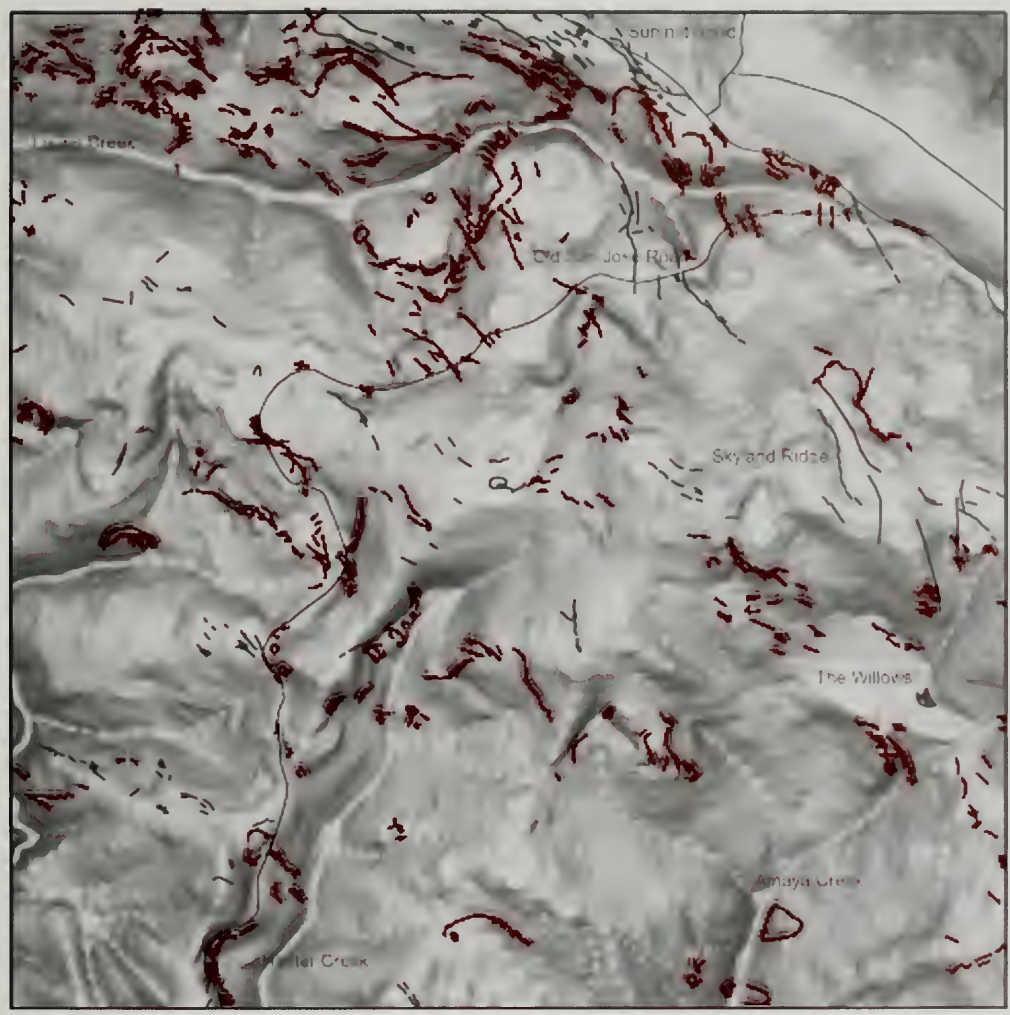

Figure 2. Representative Loma Prieta earthquake-induced ground failures, Laurel Quadrangle. Failures shown in red are landslide-related; those shown in black are tectonic or ridge-top spreading failures.

Digital terrain data

A USGS 30-meter horizontal resolution digital elevation model (DEM) was used to calculate slope gradient in the Laurel Quadrangle. This Level-1 DEM has a vertical accuracy of 7.5 meters, or about one half the topographic map contour interval. Slope gradient values calculated for each pixel were lumped into categories according to the intervals shown in Table 3.

Results of the evaluation

A landslide potential map was prepared on the GIS by an overlay of the material strength category

map and the slope gradient category map according to the landslide potential matrix shown in Table 3. The potential map was then compared, also on the GIS, to the map of all Loma Prieta earthquake ground failures. The results of this comparison showed that predictions of high, moderate, and low landsliding potential captured 50 percent of the ground failures. A seismic hazard zone map prepared from this analysis would cover 27 percent of the quadrangle area (Table 5).

Landslide potential level	Ground failures captured (Cumulative %)	Quadrangle area included (Cumulative %)
High	26.5	12.7
Moderate	42	19.9
Low	50.5	27.4
Very low	100	100

Table 5. Comparison of the USGS approach with ground failures in the Laurel Quadrangle resulting from the Loma Prieta earthquake.

This evaluation showed that predictions from the unmodified USGS procedure would encompass only half of the Loma Prieta ground failures. In addition, the ground failure map showed that the procedure missed many ground failures underlain by relatively strong geologic materials with low slope gradients. These proved to be either existing landslides not identified on the digital geologic map or ridge-top failures not directly attributable to landsliding.

Not all pre-existing landslides were shown on the geologic map for two reasons. First, because they were part of a traditional geologic map, only the most obvious landslides were identified. Second, the landslides shown typically included only the deposit and rarely the main scarp areas. Many ground failures triggered by the Loma Prieta earthquake occurred in the main scarp areas of old landslides, even where the geomorphic expression of the scarp had been subdued by erosion. Therefore, it was recognized that a detailed landslide inventory map, including the main scarp areas, would improve the method.

The three strength categories, which may be adequate at a scale of 1:62,500, appear to have been too simplistic for mapping at 1:24,000 scale. It was determined that a more detailed assessment of material strength properties was needed to characterize the geologic materials.

The 30-meter DEM and derivative slope map presented two GIS-related problems. First, the slope calculation caused a loss of information at the edges of the quadrangle, resulting in a map that did not reach the quadrangle boundaries. Second, the visual appearance of the resulting landslide potential and zone maps was poor. A seismic hazard zone map prepared from such coarse data would contain many pixel-sized polygons difficult to portray as zones of required investigation.

PHASE 2 – DATA IMPROVEMENTS AND PROCEDURE MODIFICATIONS

To address some of the shortcomings identified in the evaluation phase, several data and procedure improvements were made. These included (1) use of laboratory shear test data to characterize geologic units, (2) a strong-motion record from the Loma Prieta earthquake, (3) an improved landslide inventory that included the main scarp areas, and (4) a higher resolution DEM. These are discussed in more detail below.

Geologic material strength parameters

Nearly 300 direct shear and triaxial shear tests were collected from reports on file with the Santa Cruz County Planning Department. Single-parameter shear tests, such as unconfined compression tests, were not collected. Laboratory test data were available for 19 of the 35 mapped geologic formations in the Laurel Quadrangle.

The laboratory test data were compiled in a database and statistically evaluated. It was observed that the strength parameters from tests on unsaturated (field moisture) samples were unrealistically high, and these test values were removed. Some geotechnical reports did not indicate whether samples were saturated or unsaturated prior to shear testing. Those samples were compared to the population of other tests for that geologic unit, and obvious "outliers" were removed.

About one-third of the shear tests were performed on colluvial or fill materials above the undisturbed bedrock. A review of the geologic and tographic maps showed, in most cases, the same geologic units up-slope from locations of the colluvial samples. It was assumed, therefore, that the colluvial materials could be treated as the weathering product of the underlying bedrock material. Boring logs showed that the fills were relatively shallow

and were likely derived from minor cuts on the site. Their strength values were therefore included with the underlying rock unit.

The consultant's reports showed that many shear tests from landslide deposits did not represent the strength of the landslide slip surface. In these cases, the parent bedrock contained in the landslide was determined and the shear test values were compared with others from intact materials for that formation. In every case, the strength parameters were very similar to test values from the non-landslide materials.

Many geotechnical reports provided both peak and residual shear-strength values. It was found that the differences between peak and residual strength parameters, especially averages, were minor. However, for conservatism, where both peak and residual strength parameters were reported, the statistical analyses used residual values.

The shear test data showed that many marine clastic sedimentary deposits in the Laurel Quadrangle contain both fine- and coarse-grained lithologies. Accordingly, a distinct bimodal distribution of internal friction angle (phi) values was apparent in the shear tests. However, these lithologies were seldom depicted on the geologic map because of scale. One approach would have been to average the shear strength values for all lithologies within the mapped formations. However, this would result in unrealistically large landslide zones. In order to use both the fine-grained and coarse-grained shear strength values, it was assumed that fine-grained material strengths would be critical to slope stability in adverse bedding areas; that is, where bedding dips out of the slope. In contrast, coarse-grained material strengths were assumed to dominate in favorable bedding conditions, where the bedding dips into the slope. Structural geologic information, provided with the digital geologic map, was used to categorize areas of common bedding dip direction and magnitude, similar to the method of Brabb (1983). This information was then used to subdivide mapped geologic units into areas where fine-grained and coarse-grained strengths would be used.

To combine geologic units into "material strength groups," a procedure was developed to use the shear strength data. Descriptive statistics were first run on the shear strength parameters for each geologic unit. Because of its statistical distribution characteristics (Smith, 1986), average phi was used to assign geologic units to different strength groups. Average phi values were sequentially compared for each geologic unit. If the average phi values were within 2 degrees, the units were combined to form a strength group. Statistics were re-run on the new strength group and the next geologic unit was compared. To limit the size of any one strength group, it was judged that the range of average phi values for all geologic units within a group should not exceed 4 degrees. For geologic units whose average phi straddled strength-group boundaries, Student's-t statistical tests were performed to determine in which group they should be placed. Geologic formations with little or no shear test data were added to existing strength groups based on lithologic and stratigraphic similarities. After all the geologic units were placed into groups, the digital geologic map was converted into a raster-format geologic-material-strength map. Summary statistics for the shear strength groups are presented in Table 6.

Stability analyses, using the compiled strength parameters for each group, were performed on a computer spreadsheet at slope gradient increments of 1-degree. An infinite-slope failure model was used to calculate yield acceleration (a_y) from Newmark's equation 20 (Newmark, 1965):

$$a_y = (FS - 1)g \sin\theta$$

where FS is the static factor of safety, g is the acceleration due to gravity, and θ is the direction of movement of the slide mass, in degrees measured from the horizontal, when displacement is initiated (Newmark, 1965). For an infinite-slope failure θ is the same as the slope angle. The resulting yield acceleration values represent the susceptibility of the material strength groups at a range of slope angles.

Earthquake ground motions

The USGS's approach in San Mateo County used two strong-motion records to characterize the expected range of earthquake shaking. Wieczorek et al. (1985) held displacement constant at 5 centimeters and defined landslide potential in terms of yield acceleration. Because the purpose of this study was to compare the mapping procedure to Loma Prieta earthquake ground failures, a single representative strong-motion record from the Loma Prieta earthquake was used. With only one record to consider, landslide potential could be defined in terms of displacement values. The use of displacement to

SHEAR STRENGTH GROUP STATISTICS

Geologic material group	Formation name	Number tests	Mean/Median ϕ (deg.)	Group Mean/Median ϕ (deg.)	Group Mean/Median c(psf)	No data: Similar lithology	No data: Similar published values
A	Tp-fbc	60	36/35				Kgrd,Kgrm
	Tlo	5	36/38			Tsm	db,Tvb,Jodi,Jodb
	Tv-fbc	16	36/34	37.4/37	647/500		Jo,Jog,Jou,Jos
	Tb-fbc	12	35/33			Tbs	
	Tsr-fbc	26	42/42.6				
B	Tm	2	29.5/29.5			Tsc,Kuc,Kus	sch
	Tst	5	27.4/27			Tz,Tsl	
	Tbc	3	28.7/29	27.3/28	857/530		
	Te2-fbc	5	29.7/30				
	Tv-abc	6	26/25				
	Qal,Qof,Qcu	5	29.6/25			Qoa,Qa	
C	Tp-abc	19	24/23				
	Tb-abc	6	20.4/21				
	Tme	1	23	23.8/23	829/605		
	Tbm	5	24.6/28				
	Te2-abc	3	21/22			Te1,Kjs	
D	Tla	6	12.8/8	15.3/10.5	2212/750		Qls
	Tsr-abc	9	14.2/10				

abc = adverse bedding condition
fbc = favorable bedding condition

Abbreviations used above:

MAP SYMBOL	GEOLOGIC MAP UNIT	MAP SYMBOL	GEOLOGIC MAP UNIT	MAP SYMBOL	GEOLOGIC MAP UNIT
Qal	Alluvium	Tvb	Vaqueros Basalt		**Cretaceous units:**
Qls	Landslide deposit	Tz	Zayante Sandstone	Kus	Lithic wacke
Qof	Older floodplain	Tsl	San Lorenzo Formation	Kuc	Conglomerate
Qoa	Older alluvium	Tsr	Rices Mudstone Member	Kjs	Shale and sandstone
Qcu	Coastal terrace	Tst	Twobar Shale Member	db	Diabase
Qa	Aromas Sand	Tb	Butano Formation	Kgrd/Kgrm	Salinian intrusive rocks
Tp	Purisima Formation	Tbm	Butano Mudstone	Sch	Pelitic schist
Tsc	Santa Cruz Mudstone	Tbs	Butano Sandstone		**Coast Range Ophiolite:**
Tsm	Santa Margarita Sandstone	Tbc	Butano Conglomerate (w. ss)	Jo	Undivided
Tm	Monterey Formation	Tme	Marine sh/ss (Miocene to Eocene)	Jodi	Diorite dikes
Tlo	Lompico Sandstone	Te2	Marine ss/sh (Eocene)	Jodb	Diabase sills
Tla	Lambert Shale	Te1	Marine mudst/ss (Lower Eocene)	Jog	Gabbro cumulates
Tv	Vaqueros Sandstone			Jou	Ultramafic cumulates

Table 6. Shear strength data for the Laurel Quadrangle.

define landslide potential was considered preferable to yield acceleration for conceptual reasons.

The record selected was the DMG Strong-Motion Instrumentation Program (SMIP) Corralitos record (Shakal et al., 1989). The Corralitos Station is about 7 kilometers northeast of the Loma Prieta earthquake epicenter in the Santa Cruz Mountains. It is a free-field station on landslide deposits. The station produced a peak horizontal ground acceleration of 0.64g, the highest free-field acceleration recorded during the Loma Prieta earthquake.

The Corralitos record was integrated twice for a given yield acceleration to find the corresponding displacement, and the process was repeated for a range of yield accelerations. The resulting curve shows the full range of Newmark displacements that can be expected for the Corralitos record (Figure 3). It provides the crucial link between the "potential" for a landslide to be damaging (amount of displacement), and the landslide "susceptibility" (material strength and slope angle), in terms of yield acceleration calculated independently using Newmark's equation.

Inventory of pre-existing landslides

An inventory of pre-existing landslides for the Laurel Quadrangle was initiated by the author and completed by Wills (1995). This inventory was more complete than the digital geologic map, and an earlier compilation of CCA (1974). The landslide inventory used the same methods as employed elsewhere

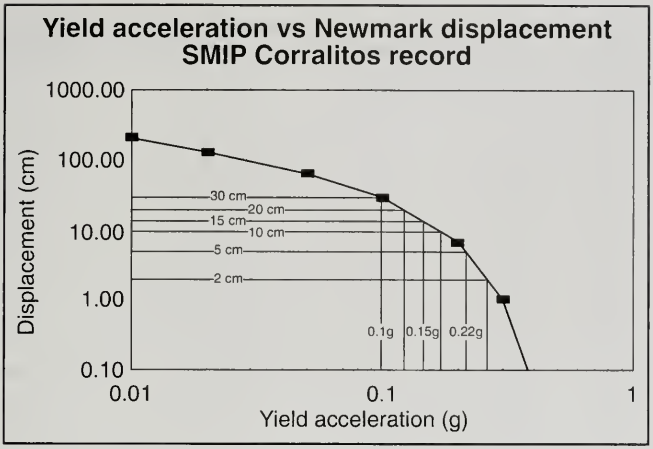

Figure 3. Yield acceleration versus Newmark displacement for the SMIP Corralitos strong-motion record.

for the DMG Landslide Hazard Identification Program, emphasizing stereo-aerial photographic interpretation and field reconnaissance. The photographs used were taken in 1931, 1939, 1943, 1975, and 1985 at scales ranging from 1:12,000 to 1:30,000. Both the landslide deposit and scarp areas of each landslide were mapped. Landslides were classified by type, recency of movement, and confidence of interpretation using a modification of the Wieczorek (1984) system. As in San Mateo County, questionable landslides in the new inventory were removed, and only definite and probable landslides were included in the analysis.

Digital terrain model

A new Level-2, 10-meter DEM was created from topographic contour lines, spot elevations and stream lines. The 10-meter DEM included a strip of elevation data from adjacent quadrangles to accommodate the data loss associated with slope gradient calculations. The resulting DEM more accurately reflects the terrain in the Laurel Quadrangle, both on the hillsides and along stream banks, and solved the problem of data loss at the DEM edges.

PHASE 3 – PARAMETER OPTIMIZATION AND MODEL SELECTION

The main purpose of this phase of the study was to derive a calibrated procedure that the DMG could apply statewide for predictive earthquake-induced landslide mapping. This purpose was accomplished by optimizing the parameters used in the analysis to maximize the number of landslides captured by the mapping procedure, while minimizing the amount of area that would be included in the seismic hazard zone.

Parameter optimization

Variations in phi, cohesion, thickness, and saturation were the main parameters varied in the analyses. To define landslide potential, different combinations of Newmark displacement thresholds at 2, 5, 10, 15, 20 and 30 centimeters were considered. It was assumed for this study that the Corralitos strong-motion record was representative of the expected ground motions that triggered the known ground failures, so this parameter was not varied. The optimization process was first performed by comparing the results to the complete set of Loma Prieta ground failures, and then only to those failures that were identified as landslide-related.

A set of 53 parameter combinations was initially run through the stability calculation. Each combination was then categorized by displacement thresholds, converted to a digital map, and compared to the full set of Loma Prieta ground failures. The best cases for this initial run captured about 71 percent of the ground failures and covered 48 percent

Case number	ϕ value used	c value used	Failure thickness (ft)	Saturation condition considered	Hazard potential criteria
60	Mean	c = 0	N/A	Sat and Unsat	5/30 cm
61	Mean	c = 0	N/A	Unsaturated	5/10/20/30 cm
62	Mean	c = 0	N/A	Unsaturated	5/15/30 cm
63	Mean	Median	20	Sat and Unsat	5/10/20/30 cm
64	Mean	Median	20	Unsaturated	5/30 cm
65	Mean	Median	30	Sat and Unsat	5/30 cm
66	Mean	Median	30	Unsaturated	5/10/20/30 cm
67	Mean	Median	30	Unsaturated	5/15/30 cm
68	Mean	Median	40	Sat and Unsat	5/30 cm
69	Mean	Median	40	Unsaturated	5/10/20/30 cm
70	Mean	Median	40	Unsaturated	5/15/30 cm
71	Mean	Medain	50	Sat and Unsat	5/30 cm
72	Mean	Median	50	Unsaturated	5/10/20/30/ cm
73	Mean	Median	50	Unsaturated	5/15/30 cm
74	Mean -1σ	Median	20	Sat and Unsat	5/30 cm
75	Mean -1σ	Median	20	Unsaturated	5/10/20/30 cm
76	Mean -1σ	Median	20	Unsaturated	5/15/30 cm
77	Mean -1σ	Median	30	Sat and Unsat	5/30 cm
78	Mean -1σ	Median	30	Unsaturated	5/10/20/30 cm
79	Mean -1σ	Median	30	Unsaturated	5/15/30 cm
80	Mean -1σ	Median	40	Sat and Unsat	5/30 cm
81	Mean -1σ	Median	40	Unsaturated	5/10/20/30 cm
82	Mean -1σ	Median	40	Unsaturated	5/15/30 cm
83	Mean -1σ	Median	50	Sat and Unsat	5/30 cm
84	Mean -1σ	Median	50	Unsaturated	5/10/20/30 cm
85	Mean -1σ	Median	50	Unsaturated	5/15/30 cm

Note: 1σ = one standard deviation
N/A = not applicable

Table 7. Parameter settings for model calibration.

of the Laurel Quadrangle. Thus, the addition of detailed landslide, terrain, ground-motion, and shear strength data improved the capture rate of the Newmark method by about 21 percent (but also increased by 21 percent the area of the quadrangle that would be included in the seismic hazard zone).

A significant observation was made at this point. The parameter combinations that performed the best were those that used lower than average shear strengths or had greater assumed landslide thickness (greater driving forces). This observation indicated that either average strength values were too high or the ground motion was too low. As mentioned above, the Corralitos strong-motion record was judged as representative of the ground motion that triggered the landslides, so later analyses focused on methods to lower the strength of the geologic materials. This adjustment to the strength parameters appeared to be justified because other studies have indicated that typical small diameter borehole sampling may result in laboratory shear

tests that overestimate the dynamic strength of geologic materials (Cole et al., 1991).

A second set of 32 parameter combinations was run through the stability calculation using combinations of reduced strength parameters and increased landslide thickness. Ten cases were identified as poor performers; that is, they did not produce a complete range of landslide potential. These were removed from further evaluation leaving 22 parameter combinations (Table 7). Landslide potential maps were prepared on the GIS and compared to only those Loma Prieta ground failures that were identified as landslide-related. As expected, the cases compared to the landslide-related failures did considerably better than those compared to the complete set of ground failures.

Selecting the best case

Selecting the best combination of parameters required that each parameter combination be tested for "efficiency" (that is, the maximum number of ground failures within the least amount of quadrangle map area). Efficiency was evaluated by use of a simple metric that compared the percentage of ground failures captured by each case with the percentage of the total quadrangle area that would be included in the seismic hazard zone. The difference between these two percentages (the "efficiency" difference) became the measure of efficiency when plotted against the ground-failure-capture percentage (GFC) (Figures 4 and 5).

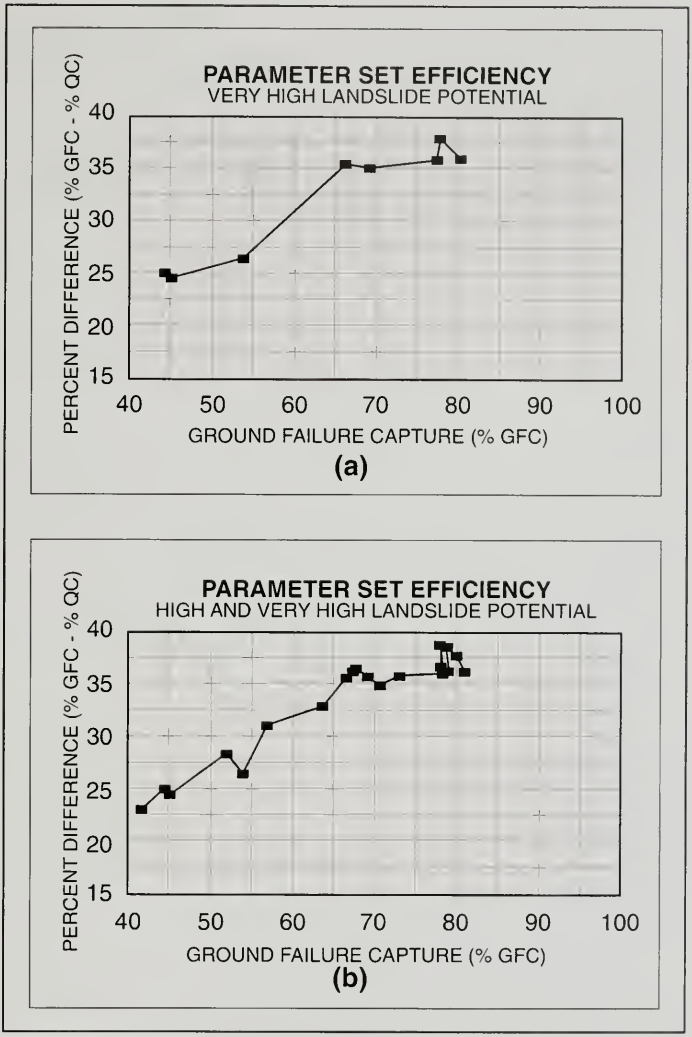

Figure 4. Parameter set "efficiency" for cases shown in Table 7. The percentage of ground failures captured for each set of stability parameters is shown on the x-axis. On the y-axis is shown the "efficiency" difference between the percentage of ground failures captured (%GFC) and the percentage of the quadrangle covered by seismic hazard zone (%QC). (a) Only "very high" level of landslide potential considered; (b) both "very high" and "high" levels of landslide potential included. For both landslide potential levels the peak efficiency occurs at about 78% ground failure capture.

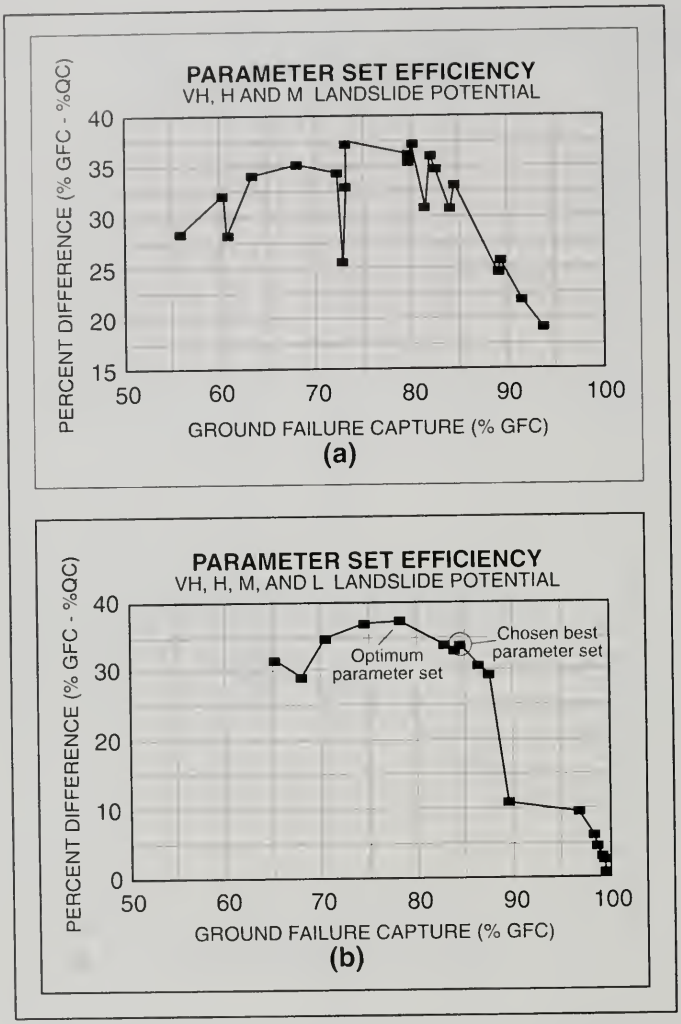

Figure 5. Parameter set "efficiency" for cases shown in Table 7. (a) "Very high," "high," and "moderate" levels of landslide potential included; (b) "Very high," "high," "moderate," and "low" levels of landslide potential included. Peak efficiency occurs at about 80% ground failure capture in (a) and 78% in (b). Case 62 (circled), though slightly off-peak, was selected in order to increase the number of failures captured.

For "very high" and "high" landslide potential levels (Figures 4a and 4b), the best cases captured about 78 percent of the Loma Prieta ground failures with up to a 38 percent "efficiency" difference. For "very high," "high" and "moderate" levels of landslide potential, the "efficiency" difference begins to drop off after about 80 percent GFC (Figure 5a). However, when "low" landslide potential is added, a maximum "efficiency" difference of about 38 percent and a GFC of about 78 percent were obtained (Figure 5b). Therefore, using only the efficiency criteria as defined, the procedure based on the Newmark method can encompass about 80 percent of the Loma Prieta ground failures (Figures 4 and 5). Nonetheless, DMG desired closer to 90 percent. Because seismic hazard zones are intended to prompt site-specific investigations, it was decided to compromise on efficiency to include more ground failures, and thereby expand the seismic hazard zone. Five cases were chosen as finalists in the best case selection. They are cases 61, 62, 78, 79, and 81 (Table 7).

From this group, case 62 was chosen as the best, mainly because it is easier to use. This case used mean phi and zero cohesion, unsaturated slope conditions, and displacement thresholds of 5, 15, and 30 centimeters. Because cohesion is assumed to be zero in this case, the thickness of the slide mass drops out of the stability calculation, making it simpler to apply. Case 62 captured 84 percent of the Loma Prieta landslide-related ground failures, and the resulting zone of required investigation covered 50 percent of the Laurel Quadrangle (Table 8, Figure 6), which resulted on an "efficiency" difference of 34 percent.

Geologic material group	SLOPE CATEGORY I 0-4%	II 5-9%	III 10-20%	IV 21-27%	V 28-31%	VI 32-37%	VII 38-42%	VIII 43-50%	IX 51-58%	X 59-63%	XI >63%
A	VL	VL	VL	VL	VL	VL	VL	VL	L	M	H
B	VL	VL	VL	VL	L	L	M	H	H	H	H
C	VL	VL	VL	L	M	H	H	H	H	H	H
D	L	M	H	H	H	H	H	H	H	H	H

Parameters used:
ϕ = Mean
c = 0
H = N/A
Displacement / Landslide potential criteria = 5, 15, and 30 cm

Capture Efficiency:
Ground failures captured = 84.2%
% of quadrangle covered (H, M, and L) = 50.3%
GFC - QC = 33.9%

Table 8. Landslide potential matrix for best case (case 62), Laurel Quadrangle. For this case, VL corresponds to displacement less than 5 cm, L to between 5 and 15 cm, M to between 15 and 30 cm, and H to greater than 30 cm. Shaded area indicates hazard potential levels included in the seismic hazard zone (i.e., all areas with greater than 5 cm displacement).

The removal of the tectonic/ridge-top ground failures from "ground truth" significantly affected the choice of the best set of parameters. When using the complete set of ground failures, the capture rate was about 71 percent, whereas capture rises to 84 percent when just the landslide-related failures are considered. This observation indicates that the procedure based on the Newmark method does not identify these complicated ground failures, for which alternative predictive procedures still need to be developed.

The 16 percent of the Loma Prieta earthquake slope failures not captured by the best case were evaluated. The "missed" ground failures were typically found to occur next to existing landslides where the slope gradient was low, on existing landslides that were not recognized in preparing the new inventory, or along road cuts and stream banks not accurately portrayed on the DEM. These observations indicate that continued improvement to the terrain and landslide inventory data can improve the method.

DISCUSSION

Summary of study results

This study evaluated the USGS application of the Newmark method for predictive analysis of landslides, and found that it could account for a maximum of about 50 percent of the ground failures generated by the 1989 Loma Prieta earthquake.

From the knowledge gained in the initial evaluation, input data were improved by (1) characterizing geologic units with shear strength data, (2) using a Loma Prieta earthquake strong-motion record, (3) including a detailed landslide inventory, and (4) calculating slope gradient from a higher resolution (10-meter) DEM. The mapping methodology was improved by (1) devising a procedure to analyze and incorporate shear test data, (2) identifying areas of adverse bedding, (3) using a single strong-motion record and displacement thresholds to define landslide potential, and (4) including scarp areas in the landslide inventory.

Through iterative testing of different parameter combinations, this study identified a set of parameters that captured 84 percent of the Loma Prieta slope failures while covering about 50 percent of the quadrangle with seismic hazard zones of required landslide investigation. This set of parameters used average phi values, zero cohesion, unsaturated slope conditions, and landslide potential levels defined by displacement thresholds of 5, 15 and 30 centimeters.

The selected best case model still has limitations. It cannot identify areas that are susceptible to ridge-top spreading or shattering, or to tectonic ground failure. Although the mapping procedure identifies where a slope failure is likely to initiate, it does not predict the potential for landslide run-out.

Applying the DMG procedure

The analysis procedure developed for the Laurel Quadrangle was first applied in southern California after the M6.9 Northridge earthquake of 1994.

Figure 6. Laurel Quadrangle landslide zones of required investigation for Case 62.

Over the following 5 years, DMG prepared 39 seismic hazard zone maps in Ventura, Los Angeles and Orange counties using the procedure. Some modifications were developed and added for consistent and repeatable map production. These include:

- Selecting a representative strong-motion record using probabilistic ground motion maps (Cramer and Petersen, 1996; CSMGB, 1997);
- Including all "definite" and "probable" landslides in the zones of required investigation;
- Using up-to-date DEM data to reflect recent large-scale earthwork.

Out of the 39 quadrangles completed in southern California, 14 contain Northridge earthquake-induced landslides (Harp and Jibson, 1995). These 14 quadrangles were used to validate the mapping procedure by first preparing earthquake-induced landslide zone maps, then comparing the known landslides to the zones. The current mapping procedure captured more than 85 percent of the mapped landslides in nine of the quadrangles and about 82 percent for two others (Table 9). The most commonly observed landslide features not included in the seismic hazard zones are the run-out debris fans at the toes of shallow, disrupted slope failures. Three quadrangles captured less than 80 percent of the Northridge failures. However, there is some question as to the accuracy of the inventories in these areas since they were prepared using high altitude (1:60,000) aerial photography, and the mapped landslides tend to be very small in these quadrangles.

Quadrangle name	Northridge earthquake landslide area within quadrangle (acres)	Northridge earthquake landslides within DMG landslide zones (% captured)
Calabasas	104	86
Canoga Park	40	76
Newhall	135	90
Oat Mountain	506	90
Simi Valley East	853	90
Simi Valley West	272	82
Topanga	72	88
Van Nuys	23	70
Beverly Hills	8	89
Burbank	8	89
Hollywood	<1	86
Mint Canyon	104	83
Pasadena	2	77
San Fernando	264	89

Table 9. Summary of the calibrated mapping procedure "capture statistics" for 1994 Northridge earthquake landslides.

The preparation of seismic hazard zone maps is ongoing in these three counties, and it is anticipated that 53 additional quadrangles will be completed by 2004. In northern California, zone maps have been prepared for the cities of Oakland and Piedmont, San Francisco, and portions of San Jose. Much of the southern San Francisco Bay area should be completed by 2005.

Implications to engineering geology practice in California

The release of seismic hazard zone maps by DMG has had a significant effect on engineering geology practice, and will continue to do so into the future. The Seismic Hazards Mapping Act requires that site-specific studies be prepared for developments within zones of required investigation before local governments can issue permits. Because landslide zones are prepared in a uniform manner throughout the State, the requirements for site-specific engineering geologic investigations will be similar regardless of where the project is located. Released zone maps have been improving the state-of-the-practice by promoting the use of better slope stability models, better ground-motion characterization, and better local government review of project reports (CSMGB, 1997).

Each seismic hazard zone map prepared by DMG requires the preparation of multiple GIS layers of geologic and engineering information. Compiled shear test data, revised geologic mapping, a strength parameters map, up-to-date terrain data and resulting slope maps, landslide inventories, adverse-bedding maps, and ground-motion maps are included in this package. This background data is intended to be a resource for engineering geologists preparing or reviewing site-specific investigation reports. Methods and procedures to make this information available, including internet access, are underway at DMG.

Over the next 10 years, seismic hazard zone maps will be prepared for many of the rapid-growth areas of California that are exposed to elevated earthquake risk. Therefore, at some point in their professional careers, most California engineering geologists will have reason to use a zone map in the course of their business, whether for landslide or liquefaction hazards, or in a consulting or review

capacity. DMG hopes that each seismic hazard zone map prepared, coupled with professional judgement derived from site-specific investigations, can contribute to mitigation of the many natural geologic processes so manifest in California.

CONCLUSIONS

Building on the foundation of an existing USGS methodology, a working GIS mapping procedure has been developed in this study that predicts areas with a high probability for earthquake instability. The mapping procedure has been calibrated to known earthquake-induced landslides from the 1989 Loma Prieta earthquake, and has been validated by comparisons with landslides from the 1994 Northridge earthquake.

A large-scale mapping program that uses the methodology developed in this study to delineate landslide zones of required investigation is in progress at DMG. These zone maps have regulatory implications that should improve the seismic safety of future structures, and will enhance the practice of engineering geology in California. Both the investigation discussed in this paper and the current mapping efforts at DMG have benefited significantly from the application of GIS technology.

ACKNOWLEDGMENTS

This study was partially funded by a U.S Geological Survey NEHRP grant, award number 1434-93-G-2334. It also benefited from the generous assistance of many people. The author would like to thank the following key contributors, without whose assistance the project would not have been possible. At the Division of Mines and Geology: Chuck Real, Chris Wills, Trinda Bedrossian, Michael Manson, Tom Spittler, Bob Moskovitz, Teri McGuire, and Oris Miller. At the U.S. Geological Survey: Carl Wentworth, Earl Brabb, Ray Wilson, and Dave Keefer. At the Santa Cruz County Planning Department: Joe Hanna, Paia Levine, Joel Schwartz, John Rosenthal, Dieter Beerman and Dave Johnson. In the consulting community: Gerald Weber of Weber and Associates, and Heidi Mack of William Cotton and Associates. Technical review of the methodology presented here was provided by Bruce Clark, Randy Jibson, Robert Larson, Scott Lindvall, and J. David Rogers, members of the State Mining and Geology Board's Seismic Hazards Mapping Act Advisory Committee Landslides Working Group. Special thanks to Roy Shlemon, Julia Turney, Bill Kane, and Dave Bieber, AEG technical reviewers, Joan Van Velsor, Section Editor, and Horacio Ferriz, Chief Editor.

AUTHOR PROFILE

Tim McCrink is a senior engineering geologist with the Division of Mines and Geology. With a staff of four engineering geologists, he is responsible for preparing earthquake-triggered landslide hazard zone maps in southern and northern California. Tim has been with the Division of Mines and Geology for the last 12 years. Before joining DMG, he worked in geotechnical engineering in California, petroleum exploration in Louisiana and Texas, and mineral exploration in Alaska. He earned Bachelor and Master's degrees in geology, and has completed numerous undergraduate and graduate civil engineering classes.

SELECTED REFERENCES

Aydin, A., Johnson, A.M. and Fleming, R.W., 1992, Right-lateral-reverse surface rupture along the San Andreas and Sargent faults associated with the October 17, 1989, Loma Prieta, California earthquake: Geology, v. 20, p. 1,063-1,067.

Bedrossian, T.L., 1989, Damage to Soquel Demonstration State Forest resulting from the October 17, 1989 Loma Prieta earthquake, Santa Cruz County, California: Memorandum to California Department of Forestry and Fire Protection, map scale 1:12,000.

Bedrossian, T.L. and Sowma, J.A., 1991, Earthquake damage in Soquel Demonstration State Forest, Santa Cruz County: California Geology, v. 44, no. 1, p. 3-9.

Brabb, E.E., 1983, Map showing direction and amount of bedding dip of sedimentary rocks in San Mateo County, California: U.S. Geological Survey Miscellaneous Investigations Series Map I-1257-C, 1 sheet, scale 1:62,500.

Bryant, W.A., 1991, San Andreas Fault ridge-top spreading fissures associated with the October 17, 1989 Loma Prieta earthquake, Santa Clara and Santa Cruz Counties, California: California Division of Mines and Geology Fault Evaluation Report, FER-225.

Clark, J.C., Brabb, E.E. and McLaughlin, R.J., 1989, Geologic map and structure sections of the Laurel 7-1/2' Quadrangle, Santa Clara and Santa Cruz counties, California: U.S. Geological Survey, Open-file Map 89-676, scale 1:24,000.

Cole, W.J., Marcum, D.R., Shires, P.O. and Clark, B.R., 1991, Investigation of landsliding triggered by the Loma Prieta earthquake and evaluation of analysis methods: Final Technical Report to U.S. Geological Survey, Contract No. 14-08-0001-G1860, 33 p.

Cramer, C.H. and Petersen, M.D., 1996, Predominant seismic source distance and magnitude maps for Los Angeles, Orange and Ventura counties, California: Bulletin

of the Seismological Society of America, v. 85, no. 5, p. 1,645-1,649.

CCA (Cooper-Clark and Associates), 1974, Preliminary map of landslide deposits in Santa Cruz County, California: Santa Cruz County Planning Department, Seismic Safety Element of the County General Plan, scale 1:62,500.

Cotton, W.R., Fowler, W.L. and Van Velsor, J.E., 1990, Coseismic bedding plane faults and ground fissures associated with the Loma Prieta earthquake of 17 October 1989: California Division of Mines and Geology Special Publication 104, p. 95-103.

CSMGB (California State Mining and Geology Board), 1997, Guidelines for evaluating and mitigating seismic hazards in California: California Department of Conservation, Division of Mines and Geology, Special Publication 117, 74 p.

Harp, E.L. and Jibson, R.W., 1995, Inventory of landslides triggered by the 1994 Northridge, California earthquake: U.S. Geological Survey Open-File Report 95-213, 17 p., Plate 1 scale 1:100,00; Plate 2 scale 1:50,000.

Hart, E.W., Bryant, W.A., Wills, C.J. and Treiman, J.A., 1990, The search for fault rupture and significance of ridgetop fissures, Santa Cruz Mountains, California: California Division of Mines and Geology Special Publication 104, p.83-94.

Holden, R. and Real, C.R., 1990, Seismic hazard information needs of the insurance industry, local government, and property owners in California: California Division of Mines and Geology Special Publication 108, 83 p.

Manson, M.W., Keefer, D.K. and McKittrick, M.A., 1991, Landslides and other geologic features in the Santa Cruz Mountains, California, resulting from the Loma Prieta earthquake of October 17, 1989: California Division of Mines and Geology Open File Report 91-5, 45 p.

Newmark, N.M., 1965, Effects of earthquakes on dams and embankments: Geotechnique, v. 15, no. 2, p. 139-160.

Plafker, G. and Galloway, J.P., editors, 1989, Lessons learned from the Loma Prieta, California, earthquake of October 17, 1989: U.S. Geological Survey Circular 1045, 48 p.

Ponti, D.J. and Wells, R.E., 1991, Off-fault ground ruptures in the Santa Cruz Mountains, California: ridge-top spreading versus tectonic extension during the 1989 Loma Prieta earthquake: Bulletin of the Seismological Society of America, v. 81, no. 5, p. 1,480-1,510.

Shakal, A., Huang, M., Reichle, M., Ventura, C., Cao, T., Sherburne, R., Savage, M., Darragh, R. and Petersen, C., 1989, CSMIP strong-motion records from the Santa Cruz Mountains (Loma Prieta), California earthquake of 17 October 1989: California Division of Mines and Geology OSMS 89-06, 196 p.

Smith, G.N., 1986, Probability and statistics in civil engineering: Nichols Publishing Company, New York, 244 p.

Spittler, T.E. and Harp, E.L., 1990, Preliminary map of landslide features and coseismic fissures in the Summit Road area of the Santa Cruz Mountains triggered by the Loma Prieta earthquake of October 17, 1989: California Division of Mines and Geology Open-File Report 90-6, 35 p., scale 1:4,800.

Technical Advisory Group on the Santa Cruz Geologic Hazard Investigation, 1991, Geologic hazards in the Summit Ridge area of the Santa Cruz Mountains, Santa Cruz County, California, evaluated in response to the October 17, 1989, Loma Prieta earthquake: Report of the Technical Advisory Group, U.S. Geological Survey Open-File Report 91-618, 427 p.

University of California, Berkeley, 1998, Evaluation and mitigation of seismic hazards: Short Course conducted by University Extension and College of Engineering, University of California, Berkeley, August 20-22, 1998.

Wentworth, C.M., 1993, unpublished digital version of the geologic map: Clark, J.C., Brabb, E.E. and McLaughlin, R.J., 1989, Geologic map and structure sections of the Laurel 7-1/2' Quadrangle, Santa Clara and Santa Cruz counties, California: U.S. Geological Survey, Open-file Map 89-676, scale 1:24,000.

Weber, G.E. and Nolan, J.M., 1989, Landslides and associated ground failure in the epicentral region of the October 17, 1989, Loma Prieta earthquake: Final Technical Report by Weber and Associates for U.S. Geological Survey Contract No. 14-08-0001-G1861, U.S. Geological Survey, Reston, Virginia, 24 p.

WCA (William Cotton and Associates), 1993, Personal communication between H. Mack and T. McCrink

Wieczorek, G.F., 1984, Preparing a detailed landslide-inventory map for hazard evaluation and reduction: Bulletin of the Association of Engineering Geologists, v. 21, no. 3, p. 337-342.

Wieczorek, G.F., Wilson, R.C. and Harp, E.L., 1985, Map of slope stability during earthquakes in San Mateo County, California: U.S. Geological Survey Miscellaneous Investigations Map I-1257-E, scale 1:62,500.

Wills, C.J., 1995, Aerial photo reconnaissance inventory of landslides in the Laurel Quadrangle, California: in, Year 1 Research and Development Status Report for GEOSAR Radar Based Terrain Mapping Project, California Department of Conservation/Jet Propulsion Laboratory/Calgis, Inc., U.S. Government's Advanced Research Projects Agency Contract Order No. B335/00, 135 p.

THE USE OF LARGE-DIAMETER BOREHOLES AND DOWNHOLE LOGGING METHODS IN LANDSLIDE INVESTIGATIONS

PHILIP L. JOHNSON[1] AND WILLIAM F. COLE[1]

ABSTRACT

Downhole logging of large-diameter borings provides distinct advantages over the logging of small-diameter borings or test pits in the subsurface investigation of landslides, in that it allows the mapping of three-dimensional structural components *in situ*. Because a key element in any landslide investigation is the identification of shear zones along which landslide movement has occurred, problems with core recovery during drilling severely limit the usefulness of small-diameter drilling methods. Backhoe test pits, on the other hand, allow detailed logging of *in situ* geologic conditions but are limited by excavation depth.

We propose a seven-step process to develop a downhole log that graphically depicts the geologic elements encountered by the borehole. This process entails: (1) drawing a preliminary cross section, (2) logging cuttings during drilling, (3) marking the intersection of the cross sectional plane with the borehole wall, (4) "hacking" the borehole wall to remove smeared materials, (5) graphically depicting the three-dimensional structure exposed on the borehole wall and describing the geologic conditions in writing, (6) sampling earth materials, and (7) modifying the cross section with data derived from the boring log.

The downhole logging method is limited, with respect to depth, by groundwater conditions, drilling rig depth capabilities, and borehole stability. Downhole logging is not advisable when there is potential for borehole caving, rockfall, noxious gases, oxygen-deficient atmosphere, or shallow groundwater. These constraints often can be mitigated through the use of specific downhole logging and drilling techniques combined with sound judgment on the part of an experienced downhole logger. However, under certain geologic and hydrogeologic conditions, downhole logging may not be suitable.

A landslide investigation at a winery in Napa County provides an example of the successful use of downhole logging of large-diameter borings. Downhole logging was used to confirm the existence of two ancient, deep-seated, static landslides, to determine the depth and lateral extent of static landslide deposits, and to delineate the depth of a recently active landslide.

Downhole logging of large-diameter boreholes has also been used for a variety of other purposes, such as investigation of faults that are covered with a significant thickness of unfaulted strata and the study of ground subsidence.

INTRODUCTION

The subsurface investigation of landslides provides unique challenges to the engineering geologist. Landslide exploration typically focuses on the depth of the basal rupture surface along which landslide movement has occurred, the geometry of the rupture surface, the direction of movement, the strength of sheared materials, and the underlying geology. Historically, engineering geologists in northern California have relied mostly upon the logging of small-diameter borings or backhoe test pits to gather subsurface information for landslide studies. Additional information regarding the depth and

[1]Cotton, Shires and Associates, Inc.
330 Village Lane
Los Gatos, CA 95030
pjohnson@cottonshires.com
bcole@cottonshires.com

direction of active landslide movement could be collected from slope inclinometers. However, these traditional methods have serious limitations in characterizing static landslides.

Test pits and trenches are helpful for investigating shallow landslides (i.e., less than 10 to 20 feet in depth) or shallow portions of deeper landslides but do not provide deep exposures. Small-diameter core borings have an excellent depth range, but are problematic because complete recovery of core samples from every interval of the boring is generally not possible, and complete information about the geologic structure cannot be acquired. The geologist cannot be certain that all of the sheared surfaces have been recovered in the core samples and may not be able to accurately determine the depth of landslide deposits solely from the core. Sampling at non-continuous intervals provides the worst results, because there is a low probability of sampling all of the sheared materials that the borehole intercepts.

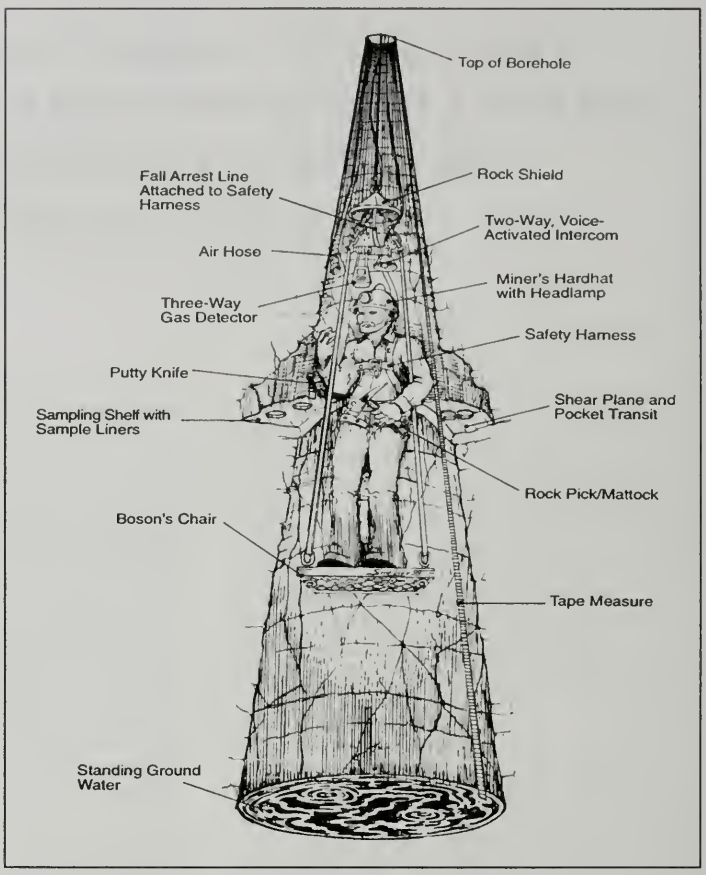

Figure 1. Downhole logging of a large-diameter borehole. Note the array of equipment utilized for downhole logging.

Slope inclinometers are also widely used for subsurface investigation of landslides. Although useful in actively moving landslides, slope inclinometers do not yield instructive data regarding the depth of static landslide deposits. To bypass these limitations, engineering geologists in northern California are turning to downhole logging of large-diameter boreholes for the subsurface investigation of landslides.

A large-diameter borehole is considered to be a boring with sufficient diameter (generally 24 inches or greater) to allow entry by a geologist. Large-diameter borings are usually drilled with a bucket auger or flight-auger drilling rig.

We define downhole logging as the act of logging the walls of a large-diameter borehole (Scullen, 1994) by a geologist who is lowered into a borehole (Figure 1). Because it is an *in situ* method, a more complete and accurate description of three-dimensional stratigraphic and structural geometry is possible than with any sampling method. In landslide investigations, the downhole logging technique provides the greatest measure of certainty when attempting to define the depth of the basal rupture surface (Leighton, 1976; Hutchinson, 1983).

In this article, we discuss successful downhole logging procedures, briefly explain relevant safety issues, discuss the limitations of downhole logging methods, describe an example of the use of downhole logging for landslide investigation in northern California, and provide examples of other uses for downhole logging.

DOWNHOLE LOGGING PROCEDURES AND SAFETY METHODS

Downhole logging procedures

Downhole logging methods can be divided into two groups: graphic logging and descriptive logging. Graphic logs provide a two-dimensional graphic depiction of the geology exposed in the borehole wall. Descriptive logs provide a written description of soil and bedrock materials, the contacts between these materials, joints, faults and stratification. The most useful downhole logs combine both graphic depiction and detailed description of the materials, contacts and geologic structure.

We recommend the following seven-step downhole logging process:

1. *Preliminary (pre-drilling) geologic cross sections* - The first step is to draw preliminary geologic cross sections through the landslide. These cross sections should be oriented parallel to the likely direction of landslide movement, and should cross through or near the anticipated boring locations. The cross sections should be based on detailed geologic field mapping and any existing subsurface information.

The preliminary cross section represents the best approximation of the subsurface geology that can be inferred from geologic field mapping and aerial photograph interpretation. One must keep in mind that the inferred depth of landsliding depends upon the selected model of slope instability (e.g., translational block sliding, rotational failure, or earth flow) and geomorphic evolution of the slope (e.g., stream incision at the toe of the slope, development of graben features at the head of the landslide). A reasonable set of working hypotheses is essential to the development of a preliminary cross section. The appropriate depths of the expected geologic features (under one or more hypotheses) should be shown on the cross section. The locations of large-diameter borings should be chosen to confirm the predicted subsurface geology or to disprove a particular hypothesis regarding that geology.

2. *Borehole drilling and cuttings log* - The second step is to drill the boring through the identified targets, to the desired depth, and log the cuttings produced by the drilling process. Typically, the boring will be drilled deeper than the anticipated targets, to allow for logging the material below the target features and to allow for accumulation of spoils in the lower portion of the borehole. For the purpose of logging cuttings, bucket augers are superior to flight augers, because the bucket auger retrieves a finite amount of material from a discrete depth with a minimum of mixing. The cuttings log is constructed in a manner similar to that of a small-diameter boring log and should emphasize the lithology or soil types encountered, color, oxidation, weathering, moisture content, and the presence of sheared materials. If gouge is observed in the cuttings, the depth should be noted on the log, and further investigation of potential shear zones should focus on this depth during downhole logging. If a portion of the borehole is inaccessible due to groundwater or caving conditions, the cuttings log may provide the only record of the materials encountered at those depths. The cuttings log can be used to construct a preliminary skeleton log in a large (typically 36 inch by 24 inch) format. This format allows the development of a detailed downhole graphic log at a suitable scale, such as 1 inch equals 2 feet, and provides room for an accompanying written description; this skeleton log can then be modified with details from downhole logging during later steps.

3. *Selection of borehole side wall for downhole logging* - Third, the geologist should select for logging the vertical plane that bisects the borehole and is oriented parallel to the plane of the cross section. The two vertical lines that form the intersections of this plane with the borehole walls can then be marked in the borehole. Typically, one of these intersection lines will be marked with a 100- to 200-foot long measuring tape that provides depth measurements from the ground surface. These intersection lines should be checked downhole with a compass, because boreholes frequently deviate from a vertical orientation.

4. *Side wall cleaning* - The fourth step is to clean one side of the borehole between the two intersection lines (the "side wall"). The cleaning process should expose an area that corresponds to 180° of the circumference of the borehole. Usually, the side of the borehole that corresponds to the direction of view of the cross-section is chosen for cleaning. Borehole cleaning is typically accomplished by "hacking"

or chipping the borehole surface with the pick end of a weeding tool or mattock. Cleaning the borehole is essential for thorough exposure of critical features and conditions such as shear zones, lithologic contacts and raveling ground. If the cleaning portion of the downhole logging process were done inadequately, the resulting boring logs would be deficient in detail and might omit significant shear zones.

A typical bucket auger will leave the borehole wall smeared with a 1- to 2-inch thick rind of cuttings and disturbed geologic materials. The selection of the proper cleaning methods and tools is essential for the complete exposure of the underlying geology. For unconsolidated sediments, a lightweight weeding tool with a series of fork-like tines provides good results. In rock and well-consolidated deposits, the pick end of a heavy mattock is a better tool. The mattock has a single stout pick that is heavy enough to chip the surface of the borehole and strong enough to withstand pounding against competent geologic materials. When wielded with sufficient force, these tools provide a ripping action that removes the smeared material. A common putty knife is also useful for removing gouge materials to expose the bounding surfaces of a shear zone.

Strength contrasts become readily apparent during the process of cleaning the borehole and can be important in identifying shear zones. While hacking the wall of the borehole, the contrast between very strong to weak bedrock materials (or dense sediments) and very soft to soft gouge materials is very noticeable. In addition, the cleaning tool often becomes mired in the cohesive gouge. Where sheared materials are encountered, the full circumference of the borehole should be cleaned to determine whether the shear zone is continuous around the borehole. Once a shear zone is exposed, the gouge materials should be excavated to expose the bounding surfaces (Figure 2). The lower bounding surface is best exposed by hacking from above to remove the gouge, and the upper surface is best exposed by hacking from below.

5. *Downhole logging* - The fifth step is graphic logging and detailed description of the geology exposed in the borehole wall. Our logging method uses the graphic depiction of the detailed geology exposed in the borehole wall between the intersection lines (Figure 3). The two-dimensional depiction of the borehole geology is recorded on a large format log, typically constructed at a scale of 1 inch equals 2 feet. The log contains a graphic "stick log" and a corresponding area for written description (Figure 4). The geology can be verbally described by the downhole logger to a person on the surface, or it can be recorded directly by the logger onto a clipboard sheet that is taken into the borehole and transferred later to the final log. In the case of two-way communication, a coordinate system is necessary, and planar elements must be drawn from several points that are placed on the log. The downhole clipboard method is especially useful, because it allows direct sketching or mapping of complex geologic features.

Figure 2. Photograph looking upward at gouge materials exposed below a polished bounding surface within a large-diameter borehole.

With the graphic method, planar elements (such as bedding, joints, faults and shear zones) that intersect the borehole are represented as parabolic or hyperbolic curves, just as these elements are seen in the borehole wall (Figure 3). Contacts are

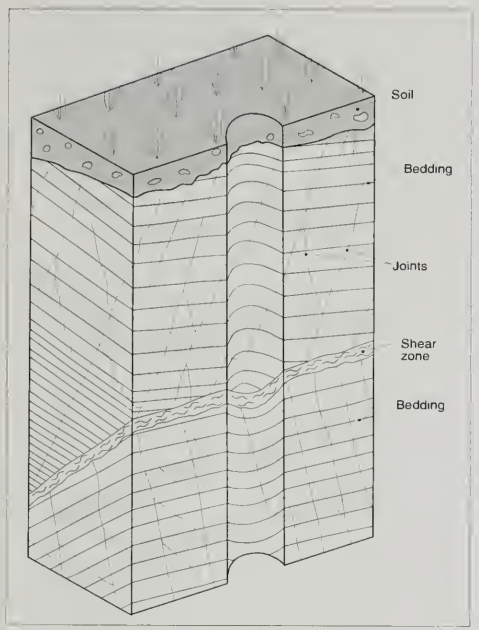

Figure 3. A schematic drawing depicting the intersection of planar structural elements (bedding, joints and a shear zone) with a hypothetical borehole and the plane of cross section. These elements produce a roughly v-shaped intersection with the borehole wall that point either in an updip or downdip direction, depending on the direction of view.

graphically depicted and rock types are represented with standard symbols or colors that correspond to the color of the rock. The stratification or foliation of the rock is also graphically depicted and orientations annotated onto the descriptive portion of the log (Figure 4).

The written description of the geology includes a detailed description of the earth materials encountered, contacts between material types, shear zones, faults, folds, joints, soil development features, soft sediment deformation features, and seepage. Rock-unit descriptions should include color, grain size, sorting, fining or coarsening upward, bed thickness, stratification types, clast composition, moisture, weathering, hardness, strength, fracture spacing and any other relevant characteristics. Contacts should be described as planar or irregular in appearance, sharp or gradational in transition, and depositional, erosional or sheared in origin. In addition, if the contact were sufficiently planar, its orientation should be measured and recorded. Fractures should be described in terms of orientation, filling material, oxidation, and width of open or filled space. A systematic explanation of engineering geologic description can be found in USBR (1998).

A thorough description of shear zones is particularly important, because the interpretation of these shear zones is key to the understanding of the depth and mechanics of landslide deformation, as well as the possible mode of origin. Many shear zones consist of shear gouge bounded by surfaces that are polished and striated; these two elements should be

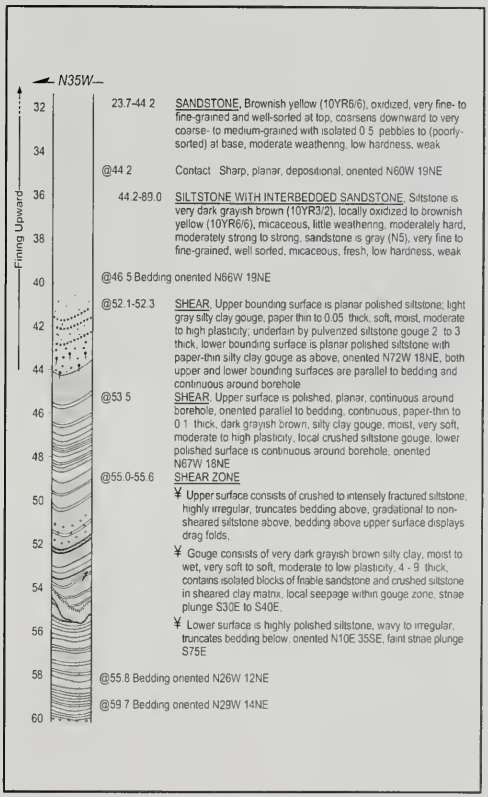

Figure 4. An example of a typical downhole log showing the graphical log and description of lithologic units, stratification, shears, and orientation of bedding.

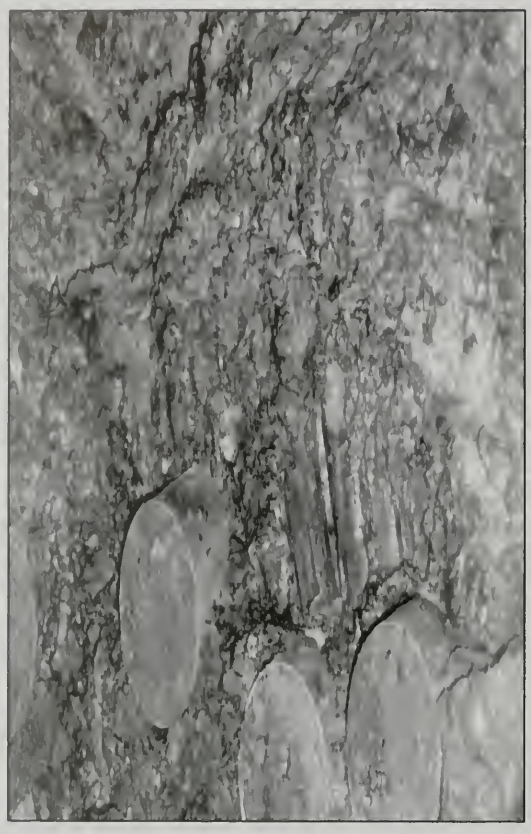

Figure 5. A photograph of shear zone samples. In this case, brass sample liners were driven into gouge materials that overlie a striated bounding surface.

described separately. The pertinent parameters for the bounding surfaces include surface polishing, degree of striae development (faint, weakly developed, moderately developed, well developed), striae orientation, appearance of surfaces (e.g., planar, irregular, wavy), continuity around the borehole, and orientation. The geologist should describe striae that can be confidently ascribed to a natural origin, rather than those that were created during excavation of the gouge. The gouge should be described in terms of grain size, color, plasticity, moisture, and consistency. Shear gouges typically consist of clay, crushed rock or a cohesive, heterogeneous mixture of crushed rock and clay. The geologist should also describe any polished surfaces within the gouge materials, especially those that are continuous around the borehole. Any distinct sense of slip indicators, such as offset beds or other piercing points, should be described and the amount and sense of slip should be noted.

6. *Downhole sampling and testing* - The sixth step is the subsurface sampling and *in situ* testing of materials. Samples of shear gouge material are collected for direct shear, torsional shear or Atterberg limits testing, and samples of other representative materials are typically collected for triaxial, direct shear, dry density, and moisture testing. Sampling is usually accomplished by directly driving a brass sample liner into a surface excavated into the borehole wall (Figure 1). A steel driver is utilized to hold the liner and protect it from the impact of the hammer. Samples for direct shear testing of gouge materials are typically driven normal to the surface of the shear zone (Figure 5). The gouge materials may also be collected as bag samples for determination of Atterberg limits or torsional shear testing. *In situ* testing of cohesive materials using a Torvane and pocket penetrometer is performed to acquire additional data that can be used to correlate physical properties of different materials and geologic units.

7. *Refine geologic cross sections* – The final step is to add the data from the borehole to the preliminary cross sections and to modify them to reflect the subsurface geologic conditions observed in the borehole.

DOWNHOLE SAFETY METHODS

The primary safety concerns for the downhole logger involve falling within the borehole, caving of the borehole walls, rock fall, noxious gases and oxygen-deficient atmosphere. These issues can be effectively addressed by the use of the proper safety equipment combined with sound geologic judgment regarding the stability of the borehole (Table 1). Because large-diameter boreholes are not generally shored and may extend to depths of 200 feet or greater, many geologists who are inexperienced in downhole methods may regard them as unsafe. However, a geologist who is trained to recognize potential caving conditions and assess the relevant hazard, and who is equipped with the necessary downhole safety equipment (as required by Cal-OSHA) can successfully downhole log many

POTENTIAL HAZARD	MITIGATION MEASURE
Sloughing of soil and loose sediments near the surface	• Loose earth materials should be removed from the perimeter of the borehole. • The entrance of the borehole should be protected with a short length (4 or 5 feet) of casing that extends 1 to 2 feet above the ground surface.
Caving and spalling of the borehole wall	• As the experienced geologist slowly descends through the borehole, the potential for caving or raveling ground is assessed and the presence of sheared material and free water is monitored. • If caving is confined to a specific interval within the borehole, that portion of the borehole may be reamed to a larger diameter and stabilized by inserting steel casing to seal off the caving interval. • If caving is severe, downhole logging may not be feasible below the caving interval.
Rockfall	• While descending through the borehole, the geologist checks for unstable blocks, especially those that rest along discontinuities that are inclined into the borehole. • Remove unstable blocks before proceeding deeper into the borehole. • Deflect rockfall by using a rock shield mounted above the logging platform (boson's chair, Figure 1). • Use an aluminum logging cage (Figure 6). Although the logging cage provides the best protection against rockfall and caving hazards, it should not be used as a means of entering a caving borehole.
Falling within the borehole	• The logger is lowered into the borehole via a steel cable connected to a power winch. • If the logger slips off the platform, he or she is prevented from falling by a separate fall arrest line that is connected to a body harness.
Noxious gases and oxygen-deficient atmosphere	• A three-way gas detector measures levels of oxygen, hydrogen sulfide, and explosive gasses (i.e., methane) in the logger's breathing space (Figure 1). • The borehole atmosphere is also monitored prior to downhole logging. • The borehole is continuously ventilated with an air blower and flexible plastic hose during downhole logging.
Poor lighting	• The logger typically clips a miner's headlamp to his or her hardhat. The headlamp is powered by a belt-mounted wet cell battery.
Difficulty communicating with the downhole logger	• The logger should communicate with the rig operator and others at the surface via a voice-activated, two-way communication system (Figure 1).

Table 1. Downhole safety methods.

large-diameter borings without the threat of injury. After drilling is completed, a geologist who is experienced with downhole logging methods should assess the potential for caving or rock fall. The experienced geologist should slowly descend through the borehole and monitor stability prior to downhole logging by less experienced personnel (Table 1).

The natural arching properties of rock and sediments surrounding a borehole provide considerable support to the borehole wall. These arching properties favor the stability of smaller diameter boreholes. For downhole logging, we prefer the use of a 24"- to 27"-diameter borehole rather than a 30"- to 36"-diameter borehole. These intermediate diameter boreholes provide both optimum stability and adequate room for the geologist to enter and work.

LIMITATIONS OF DOWNHOLE LOGGING

Although downhole logging of large-diameter boreholes has proven very effective for subsurface investigation of landslides, certain geological conditions may severely complicate or prevent the use of downhole logging. Downhole logging is very difficult or impossible where running or fast raveling ground is encountered, where concentrations of noxious gases are high, or where standing groundwater is very shallow. To some extent, all of these problems can be addressed with the use of specific drilling and downhole logging techniques (Table 2). However, in severe cases these problems may make downhole logging impractical.

Figure 6. A geologist entering a borehole in an aluminum logging cage.

CASE STUDY

In 1995, we conducted an investigation of an active landslide that threatened a winery building located on a hillside flanking the Carneros Valley, west of the town of Napa, California. Our review of historical aerial photographs indicated that the southeast flank of the hill was underlain by a well-defined ancient landslide mass, and the active landslide appeared to represent the reactivation of a sizable portion of this mass (Landslide A in Figure 7). A more subtly-defined ancient landslide mass was identified north of Landslide A.

The local stratigraphy included Quaternary alluvium and terrace deposits, the Pleistocene Huichica Formation, and the Miocene Neroly Sandstone. The Huichica Formation consists of discontinuous beds of highly oxidized, interbedded pebble to boulder conglomerate, sandstone, siltstone, and claystone; this unit is typically weak to friable. The underlying Neroly Sandstone consists of olive gray, well-sorted, fine- to medium-grained sandstone that is moderately strong to strong.

During our investigation, downhole logging of bucket auger borings was used for two purposes: (1) to define the lateral extent of landslide debris; and (2) to define the nec-

CONSTRAINT	MITIGATIVE PROCEDURE
Running sands or fast-raveling unconsolidated sediments	• Attempt to stabilize caving interval with steel casing. • If severe caving occurs before casing can be inserted, attempt to drill at an alternate location or utilize small diameter coring methods.
Shallow groundwater (Vadose zone)	• Slow seepage on the borehole walls does not present a serious problem unless accompanied by caving. • The boring can be drilled past the intended depth to allow the water to collect below the intended interval of interest.
Shallow groundwater table (Saturated zone)	• Use a submersible pump to temporarily lower the groundwater level in the borehole. This method is most effective where the borehole is drilled in moderately strong to very strong rock that has low permeablilty (primarily fracture permeability) and widely-spaced fractures of narrow width.
Exploration depth	• The depth of exploration is limited by groundwater conditions, borehole stability, and the depth range of the drilling rigs; most bucket auger rigs cannot drill deeper than 200 feet.

Table 2. Common constraints to downhole logging.

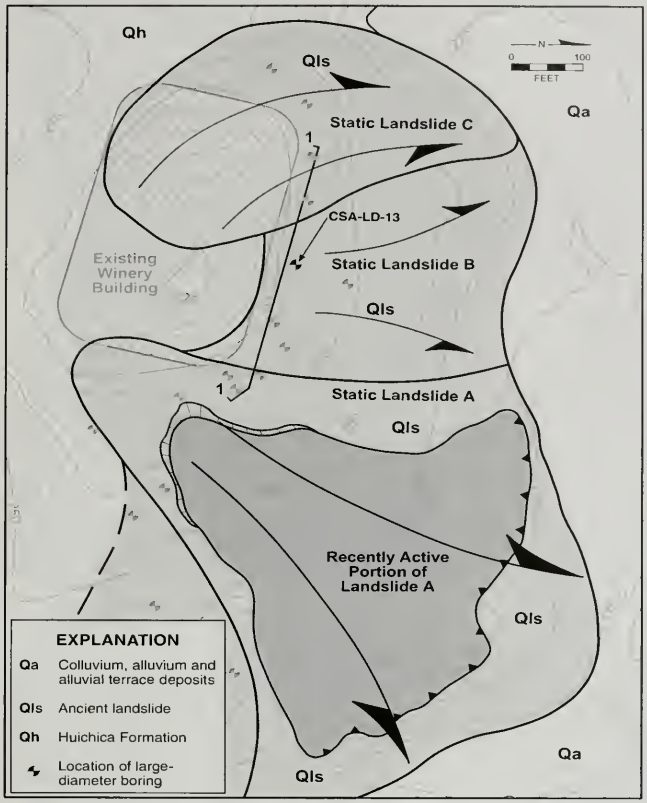

Figure 7. A simplified map of the Napa winery site showing the location of static and recently active landslides, large-diameter borings and the existing winery building.

essary design depths for potential landslide mitigation measures.

Active landsliding. Initially, our efforts focused on the active landslide. We used downhole logging to define its depth and lateral extent, which is the first step in the design of slope mitigation measures. A total of three large-diameter borings were drilled within the boundaries of the active portion of Landslide A (Figure 7). The basal rupture surface observed in the borings was defined as a zone of clay gouge that was bounded by polished surfaces. In order to protect the winery structure at the top of the hill, a row of tied-back, steel-reinforced concrete shear pins was installed at the head of the active landslide. The toe of the landslide was excavated and replaced with an engineered-fill buttress.

Static landslides. Following completion of slope repair activities for Landslide A, slope inclinometers were installed within two suspected ancient landslides that were identified through photogeologic analysis (Landslides B and C in Figure 7). The westernmost of the two static landslides (i.e., Landslide C), displayed an arcuate headscarp and a bulging downslope profile, but its margins appeared to be old and geomorphologically denuded. Landslide B, a weakly-defined ancient landslide, underlies the northern flank of the hill, between Landslide C and Landslide A.

In 1998, the two inclinometers nearest to the former active landslide area began to show discrete deflections at depths of 18 to 35 feet, and continued to show deflections over a period of several months. The remaining slope inclinometers did not experience any deflection, indicating that most of the ancient landslide mass remained static. In response to the results of inclinometer monitoring, a total of eight large-diameter borings were drilled and logged within the area of the two static landslides. Well-developed shear zones, with gouge varying in thickness from a few millimeters to two meters, were encountered in all of the borings. The striae on the polished surfaces that bounded these shear zones were generally oriented in a downslope direction. These features were interpreted to be the basal rupture surfaces of the two static landslides.

The simplified log of borehole CSA-LD-13 provides a good example of the stratigraphy and structure of the static landslides (Figure 8). The upper 4.7 feet consist of colluvial soil, and from 4.7 feet to 31.0 feet, Huichica Formation-derived landslide debris was encountered. The deepest shear that was logged in this boring separates the Huichica Formation landslide materials from the Neroly Sandstone

and was interpreted as the basal rupture surface of the static landslide (Figure 9). The Neroly Sandstone appeared to be unaffected by landsliding.

The information gained from logs, such as that shown in Figure 8, allowed the successful characterization of the static landslide complex and design of specific slope-stabilization measures. The final mitigation design consisted of a series of tied-back, steel-reinforced concrete shear pins (Figure 10) that were designed to protect the existing structure located on the hilltop.

OTHER USES OF DOWNHOLE LOGGING

Downhole logging is also useful in investigations of faulting and post-construction geotechnical conditions. Fault investigations are typically conducted by trenching through Holocene sediments where the critical sedimentary units are located at shallow depths. However, in cases where the thickness of young, unfaulted sediments is greater than the depth range for trench excavation, downhole logging of large-diameter borings has been used to extend the geologist's view of subsurface conditions to perform paleoseismic investigations (Dolan et al., 1997).

A fault investigation conducted in Saratoga (Santa Clara County), provides a good example of the use of downhole logging. The Berrocal fault is a northeast-vergent thrust fault that juxtaposes the Cretaceous and Jurassic Franciscan Complex over Plio-Pleistocene Santa Clara Formation in the Saratoga region (Sorg and McLaughlin, 1975). In the vicinity of a proposed building site, a relatively thick mantle of Holocene alluvial fan deposits covers the trace of the Berrocal fault. Previous investigations had used trenching, coring and shallow seismic refraction techniques to attempt to locate the trace of the fault at the building site. Trenches were not able to penetrate the alluvial fan deposits, and coring and seismic refraction methods did not yield data with sufficient resolution to precisely locate the fault traces. The two traces of the fault were finally defined by downhole logging of a series of large-diameter boreholes along a transect aligned perpendicular to the fault trace, as determined from geomorphology (Manzagol and Milstone, 1995).

Southwest of the fault, Franciscan Complex sandstone was encountered, whereas bedded Santa Clara Formation mudstone was encountered northeast of the fault. The central borehole penetrated, in descending order: alluvial fan deposits, weathered Franciscan sandstone, a zone of crushed rock and shears dipping to the southwest (the main trace of the Berrocal fault), and Santa Clara Formation mudstone. Downhole measurements of fault- orientation

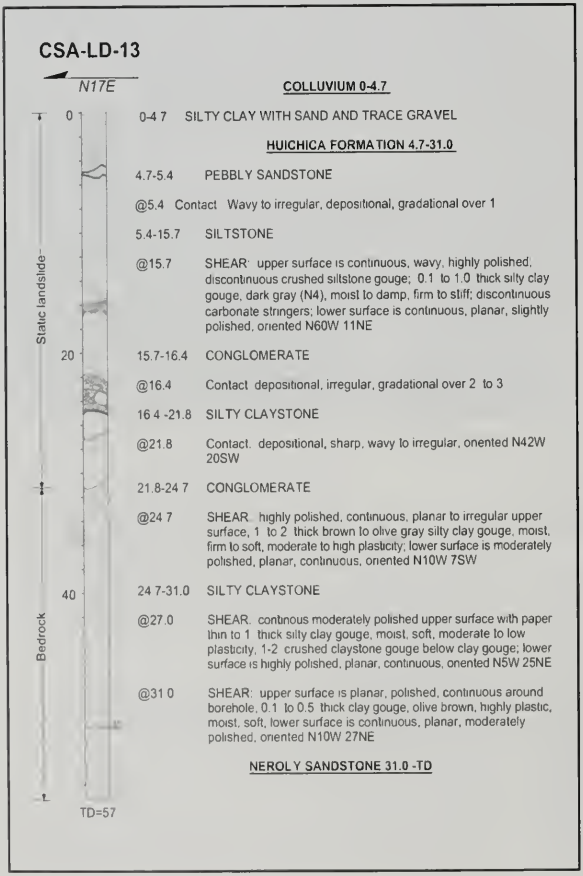

Figure 8. The simplified log of boring CSA-LD-13 from the Napa winery site. Note the multiple shear zones logged in this borehole; the deepest shear separates landslide debris derived from the Huichica Formation from bedrock of the Neroly Sandstone.

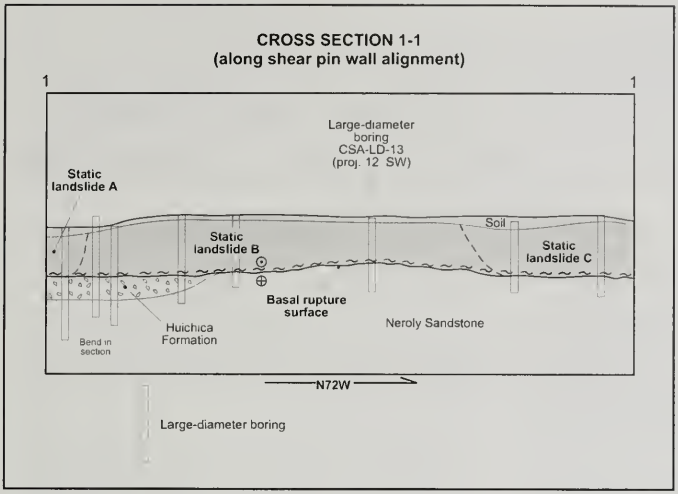

Figure 9. A simplified cross section along the alignment of the series of large-diameter borings drilled at the Napa winery site. This cross section is based upon data from a series of large-diameter borings within landslides B and C.

were used to project the trace to the ground surface, and additional downhole logging resulted in the identification of a second fault trace further to the east.

In Los Angeles, downhole logging of large-diameter boreholes was the only investigative method that successfully addressed the nature of alluvial deposits overlying twin subway tunnels. Ground subsidence over the tunnels and allegations of damage to buildings in the vicinity triggered a series of investigations. It was recognized that the largest magnitude of ground subsidence was associated with the distribution and thickness of Holocene alluvial fan deposits and the presence of subsurface water. However, direct observation of the alluvial deposits in large-diameter boreholes enabled the geologists to accurately iden-

Figure 10. A portion of a tied-back, reinforced concrete shear pin wall installed at the Codorniu Napa site to protect the upslope winery facilities. This shear pin wall roughly follows the alignment of cross-section 1 shown in Figure 7.

tify and evaluate erosional and depositional events, paleosols associated with the Holocene-Pleistocene contact, the absence of "voids" that had been postulated to explain the subsidence mechanism, and seepage properties of the heterogeneous alluvial deposits.

CONCLUSIONS

Downhole logging of large-diameter borings is particularly useful in the subsurface investigation of landslides. The primary advantage of this method is that it allows a complete description of geologic conditions, including the shear zones that form the basal element of a landslide. Small-diameter drilling and sampling methods are often ineffective in defining the depth and character of a landslide basal shear zone, and trenching methods are only useful at relatively shallow depths.

We propose the use of a seven-step process for development of a detailed downhole log. These steps include drawing preliminary cross sections, logging cuttings during drilling, selection of borehole side wall for downhole logging, cleaning of the side wall to expose the geology, logging of the geology exposed in the side wall, downhole sampling and testing, and refining of the cross sections with data from the boring.

The use of downhole-logging methods is limited by the potential for falling within the borehole, rockfall, caving conditions, noxious gases, oxygen-deficient atmosphere, shallow groundwater, and the depth range of the bucket auger drilling rig. These constraints can be addressed in many cases by the use of specific safety equipment and downhole logging techniques. The use of sound geologic judgement and experience in assessing the potential for borehole instability is an essential part of the downhole logging method. Under extreme circumstances downhole logging may not be suitable.

A landslide investigation in Napa County provides an example of the use of downhole-logging methods to precisely determine the depth and lateral extent of static landslide deposits; these methods also provided the opportunity to confirm aerial photograph interpretation and field mapping of landslides. Downhole logging methods have also been used effectively to locate fault traces beneath a significant thickness of unfaulted strata, perform paleoseismic studies, and evaluate potential ground subsidence.

ACKNOWLEDGEMENTS

We would like to thank Mark Smelser for providing original artwork and Julia Lopez for drafting the illustrations. We gratefully acknowledge the support provided by Bill Cotton and Patrick Shires. Roy Kroll, Horacio Ferriz and Steve Stryker provided helpful comments regarding this paper.

AUTHOR PROFILES

Philip L. Johnson, RG, CEG, is a Senior Engineering Geologist with Cotton, Shires and Associates. He has over 12 years of experience working on a variety of engineering geologic projects, including landslide, dam site, and seismic hazard investigations.

William F. Cole, RG, CEG, CHG, has 20 years of experience as a consulting engineering geologist. He has worked on a variety of geologic projects in domestic and international settings, with particular expertise in slope stability and evaluation of construction-related geotechnical issues.

SELECTED REFERENCES

Dolan, J. F., Sieh, K., Rockwell, T. K., Guptill, P., and Miller, G., 1997, Active tectonics, paleoseismology and seismic hazards of the Hollywood fault, Northern Los Angeles basin, California: Geological Society of America Bulletin, v. 109, p.1595-1616.

Hutchinson, J. N., 1983, Methods of locating slip surfaces in landslides: Bulletin of the Association of Engineering Geologists, v. XX, no. 3, p. 235-252.

Leighton, F.B., 1976, Geomorphology and engineering control of landslides: in Coates, D. R. (ed.), Geomorphology and engineering, proceedings of 7th geomorphology symposium, George Allen & Unwin, London, p. 273-287.

Manzagol, T.J. and Milstone, B.S., 1995, A geologic and geotechnical investigation, Lot 13 Teerlink Subdivision Tract 6781, Heber Way, Saratoga, California: Consultant's report to Mr. Steve Sheng.

Scullen, C. M., 1994, Subsurface exploration using bucket auger borings and down-hole geologic inspection: Bulletin of the Association of Engineering Geologists, v. XXXI, p. 91-105.

Sorg, D.H. and McLaughlin, R.J., 1975, Geologic map of the Sargent-Berrocal fault zone between Los Gatos and Los Altos Hills, Santa Clara County, California: U.S. Geological Survey Miscellaneous Field Investigations, MF-643.

USBR, 1998, Engineering geology field manual: United States Department of the Interior, Bureau of Reclamation, (Denver, Colorado), second edition, 496 p.

CHARACTERIZATION OF FRANCISCAN MELANGES AND OTHER HETEROGENEOUS ROCK/SOIL MIXTURES

EDMUND W. MEDLEY[1]

INTRODUCTION

Engineering geologists and geotechnical engineers commonly encounter weak, heterogeneous and geologically complex mixtures of strong blocks of rock embedded in soil-like matrices. Such rock/soil mixtures are well represented in Northern California by Franciscan Complex melanges (French: *mélange* or mixture, such as in Figure 1), fault breccias, lahar deposits, decomposed granites, glacial tills, and colluvium. Given their considerable spatial, lithological and mechanical variability, adequate geotechnical characterization of melanges and other rock/soil mixtures is challenging. Accordingly, practitioners often make the simplifying assumption that the mechanical behavior of rock/soil mixtures is adequately represented by the properties of the weak matrix materials and that there is no need to consider the contribution of blocks.

This paper has three purposes. First, the paper shows that blocks *do* influence the mechanical behavior of melanges and other rock/soil mixtures. Second, the paper describes a scheme for the systematic characterization of block lithologies, block proportions and block size distributions to reduce inconvenient and expensive surprises during tunneling, earthwork and foundation construction. Third, the paper summarizes recent research and practical experience on the geotechnical and geological characterization of melanges and other rock/soil mixtures.

[1]Edmund W. Medley
Exponent Failure Analysis Associates
149 Commonwealth Drive
Menlo Park, CA 94025
emedley@exponent.com

MELANGES AND OTHER BIMROCKS

Bimrocks

Melanges contain competent blocks of varied lithologies, embedded in sheared matrices of weaker rock (Figure 1). The word "melange" is included in over 1,000 geological terms for rock mixtures and fragmented rocks (Laznicka, 1988). Also, there are more than 20 aliases for melanges, such as olistostromes, argille scagliose, complex formations, friction carpet and polygenetic breccia. Because of the vast collection of geological terms describing the fundamental fabric of mixed strong blocks in weak matrix, Medley (1994a) introduced the term *bimrocks* (from "block-in-matrix rocks", based on Raymond's (1984) description of "block-in-matrix" melanges). The word "bimrock" has no geological or genetic connotations and is defined as "a mixture of rocks, composed of geotechnically significant blocks within a bonded matrix of finer texture". The expression "geotechnically significant blocks"

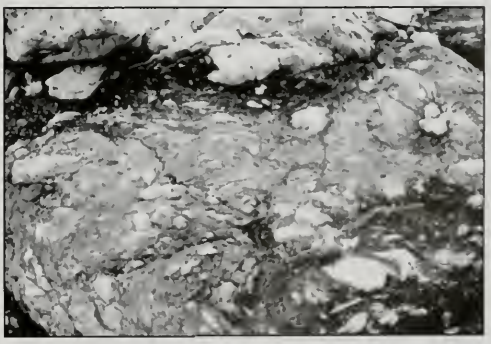

Figure 1. Franciscan melange at Shelter Cove, Point Delgada, Northern California. Matrix is dark gray sheared shale/argillite. Light colored blocks are graywacke. Outcrop is about 1m wide.

means that there is mechanical contrast between blocks and matrix, and the proportion and size range of the blocks influences the mechanical properties of the strong block/weak matrix mixture at the scale of interest (see Medley, 1994a, for details on the basis for the definition). In this paper, the term "bimrock" is used wherever the results obtained from studies of melanges can be applied to the characterizations of other rock/soil mixtures that conform to the definition of bimrocks.

GEOLOGICAL ASPECTS OF FRANCISCAN MELANGES

Melange bodies are present in over 60 countries. Medley (1994a, Appendix A) lists references and shows maps of worldwide locations of melange bodies. Although there are over 2,000 geological references on melanges, there are few references on the engineering geology or geotechnical engineering aspects other than the works of Medley (1994a, 1994b, 1995, 1997, 1998 and 1999), Medley and Goodman (1994), Medley and Lindquist (1995), Lindquist (1994a, 1994b), Lindquist and Goodman (1994), Goodman et al. (1994) and Goodman and Ahlgren (2000). Some geotechnical research on melanges has been performed in Italy by AGI (1977), Aversa et al. (1993), and D'Elia et al. (1986).

Melanges are abundant in the jumbled Franciscan Complex (the Franciscan) that covers about one-third of Northern California. Blake (1984), Raymond (1984), Cowan (1985), and Hsü (1985) described the geology of Franciscan melanges, and Wahrhaftig (1984), Blake and Harwood (1989), and Wakabayashi (1999) prepared useful field guides. Figure 2 illustrates the mapped appearance of the Franciscan at the scale of Marin County, north of San Francisco.

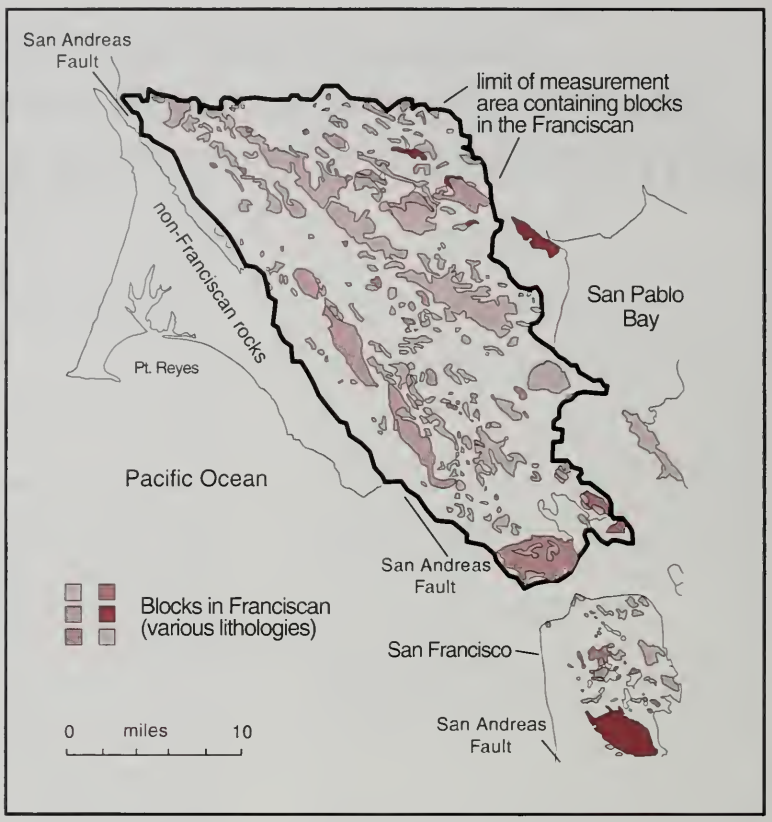

Figure 2. The Franciscan Complex in Marin County, north of San Francisco. Mapped blocks range to nearly 20 km in length. Area of interest within indicated boundary is about 1,000 km^2. (After Medley, 1994a; base map after Ellen and Wentworth, 1995).

The matrix of Franciscan melanges is composed of shale, argillite, siltstone, serpentinite or sandstone, and may be pervasively sheared to the consistency of soil. Savina (1982) measured as many as 800 shears per meter. Blocks are not evenly distributed within melanges and congregate to form block-rich and block-poor zones (Figures 2 and 10). The most intense shearing within melanges is often

in block-poor zones adjacent to the largest blocks, which is where earth flow landslides commonly occur. The weakest elements in a melange are the contacts between blocks and matrix. Contacts may be marked by a lustrous surface on the blocks and a wafer of sheared material that weathers to a slick film of clay. Shear surfaces generally pass around blocks via the block/matrix contacts, as shown in Figure 11. Blocks within the shears may be entrained within, and oriented parallel to, the shears as shown in Figures 1 and 10.

Medley (1994a) estimated that in the Franciscan of Marin County, California (Figure 2), as mapped by Ellen and Wentworth (1995), about 60 to 70% of blocks are graywacke, 15 to 20% are volcanic, 15 to 20% are serpentinite, 5 to 10% are chert, and the remaining blocks are rare limestone and exotic metamorphic rock. Blocks may also be composed of intact siltstone and sandstone/siltstone sequences. Large blocks in Franciscan melanges range between smoothly ellipsoidal to irregular in shape and, where measured, have major/minor axis lengths in the approximate ratio of about 2:1 (Medley, 1994a).

BLOCK SIZES

Block measurements from field mapping or drilling are invariably shorter than the true "diameter" of a block, as illustrated in Figure 3. Block sizes are indicated by the length d_{mod} (the maximum observed dimension) of blocks exposed in two dimensions (outcrops or geological maps). In one dimension, block sizes are also measured from sampling lines traversing outcrops ("scanlines" of Priest, 1993), or in drill core, by the chord length formed from the interception between the block and the core.

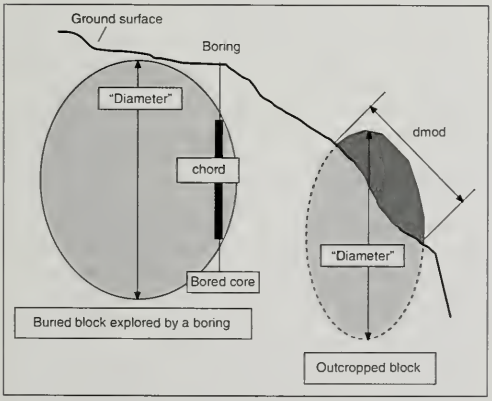

Figure 3. In two dimensions a block has apparent block size of d_{mod}, the *m*aximum observed *d*imension. In one dimension, the block size is indicated by the chord length, or intercept between a boring and a block. Only rarely are d_{mod} or a chord length equivalent to the actual diameter or maximum dimension of a block.

SCALE INDEPENDENCE OF BLOCK SIZE DISTRIBUTIONS

Many rock/soil mixtures contain a few large blocks and increasing numbers of smaller blocks, and the block size distributions tend to be fractal (negative power law) or "well graded" as explained by Medley (1994a) and Medley and Lindquist (1995). Fractal distributions have been observed at many scales of geological interest in Franciscan melanges (Medley, 1994a; Medley and Lindquist, 1995), fault gouges (Sammis and Beigel, 1989) and fractured rock masses (Nagahama, 1993). In Franciscan melanges, the range in block sizes is extreme, exceeding seven orders of magnitude, to range between sand (millimeters) and mountains (tens of kilometers) as illustrated in Figure 4. Despite the considerable difference in scales, the melanges depicted in Figure 1 and Figure 2 show block size distributions with similar well-graded appearances.

The block size distributions of Franciscan melanges are also scale independent, meaning that blocks will always be found, regardless of the scale of interest or observation. Over a smaller range of scales, the block size distributions of other rock/soil mixtures also show scale independence. Because blocks will always be found in melanges, the distinction between blocks and matrix depends solely on the scale of interest. Small blocks at one scale (e.g., 1: 1,000) are part of the matrix at a larger scale (1:10,000) (Figure 5). Likewise, large blocks at one scale of interest (e.g., 1:10,000) are not geotechnically significant blocks at a smaller scale (e.g., 1:1,000) because they are too large to be considered as individual blocks within the rock/soil mixture. Instead, they can be considered as strong, massive and unmixed rock masses (Figure 5).

CHARACTERISTIC ENGINEERING DIMENSION (L_c)

Because of scale independence, any reasonable dimension can be used to scale a melange rock mass for the problem at hand. Medley (1994a) called such

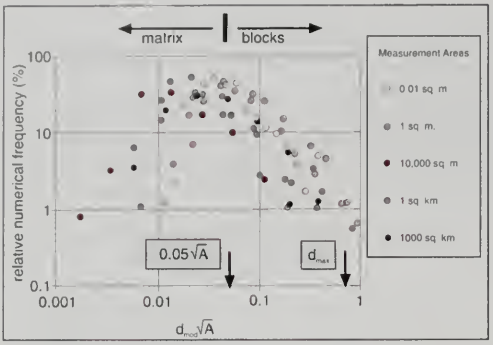

Figure 4. Normalized block size distribution curves for 1,928 blocks measured from outcrops and geological maps of several Franciscan melanges ranging over seven orders of magnitude in scale, ranging from centimeters to kilometers (after Medley, 1994a). The sizes of blocks are characterized by d_{mod}, the maximum observed dimension of the blocks in the outcrops and maps. The measurements of the block sizes are divided by the square root of the area ($\sqrt{A}$) containing the measured blocks to yield the dimensionless block size $d_{mod}/\sqrt{A}$. The normalizing parameter $\sqrt{A}$ is an indicator of the scale of the outcrop or geological map being measured. The relative frequency of blocks in each of the measured areas is the number of blocks in any size class divided by the total number of blocks in the measured area. The use of normalized block size and normalized numerical frequency allows the comparison of block size distributions over the extreme range in measurement scales. The data from each measurement area forms graphed plots that are similar in shape to each other, regardless of the size of the measured area. The similarity in shapes indicates that the block size distributions are scale independent. The plots peak at about $0.05d_{mod}/\sqrt{A}$, which is defined as the block/matrix threshold size at any scale. Blocks smaller than $0.05d_{mod}/\sqrt{A}$ tend to be too small to measure, are undercounted, and are assigned to the matrix. The largest indicated block size is approximately equivalent to $\sqrt{A}$ (at $d_{mod}/\sqrt{A}=1$), but 99% of the blocks are smaller than about $0.75\sqrt{A}$, which is defined as the maximum block size (d_{max}) at the scale of interest.

a descriptive length the *characteristic engineering dimension*, L_c (the "*ced*" of Medley, 1994a). The use of a characteristic engineering dimension is analogous to showing a coin, measuring tape, or spouse in a photograph, to give the observer the ability to appreciate the scale of the image. For example, Figure 1 could represent a melange at any scale, since it contains no clear scaling feature other than the information provided in the caption. L_c may variously be (1) an indicator of the size of a site, such as $\sqrt{A}$, where A is the area of the site, (2) the size of the largest mapped or estimated largest block (d_{max}) at the site, (3) the thickness of a failure zone beneath a landslide, (4) a tunnel diameter, (5) a footing width or (6) the dimension of a laboratory specimen. The characteristic engineering dimension changes as scales of interest change on a project (Figure 5).

LARGEST AND SMALLEST GEOTECHNICALLY SIGNIFICANT BLOCKS

The largest geotechnically significant block (d_{max}) within any given volume of Franciscan melange is about $0.75L_c$. Blocks greater than $0.75L_c$ result in such a diminished proportion of matrix in a local volume of rock mass, that the volume can be considered to be massive, unmixed rock composed mostly of the block.

In Figure 4, the square root of the area ($\sqrt{A}$) is the characteristic engineering dimension (L_c) for outcrops and geologic maps at scales of measurement that range from less than 0.01 square meters (portion of an outcrop) to more than 1,000 square kilometers (Marin County, Figure 2). Figure 4 shows that, at all the scales of measurement, the largest blocks (d_{mod}) are equivalent in size to $\sqrt{A}$, but about 99% of blocks are smaller than about $0.75\sqrt{A}$ (in other words, smaller than $0.75L_c$. [In Figure 4, block sizes for each set of data are normalized by the square root ($\sqrt{A}$) of the measured area of each outcrop or area of geologic map, and the relative frequency is the proportion of blocks in each size class divided by the total number of blocks in each of the measured maps or outcrops.]

At all scales of measurement in Figure 4, the graphed data plots of normalized block sizes have peak relative frequencies at about $0.05\sqrt{A}$ (equivalent to $0.05L_c$). At block sizes smaller than $0.05L_c$ the blocks become too small to be observed and tend to be undercounted, although in reality there are a myriad of them, and they become obvious once the scale of observation becomes smaller. For any given volume of Franciscan melange, blocks less than $0.05L_c$ in size comprise more than 95% of the total number of blocks, but contribute less than 1% to the total volume of melange and thus have negligible effect on the mechanical behavior of the melange. For these reasons, the threshold size

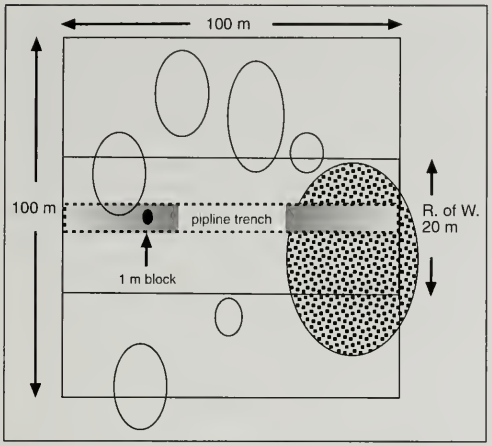

Figure 5. Sketch showing various scales of interest for an area in which a 20 m wide road and a 2 m wide, 2 m deep pipeline trench will be excavated in a melange. (1) The 100 m by 100 m geological map has an area (A) of 10, 000 m^2, and hence a $\sqrt{A}$ of 100 m, which is taken as the characteristic engineering dimension (L_c) at the large scale of interest of the overall site. The block/matrix threshold at this scale is 5 m ($0.05L_c$ or $0.05\sqrt{A}$). Hence the 1 m block in the center of the sketch is part of the matrix. In contrast, at the scale of overall site, the large speckled rock mass at the right of the sketch is a block since it is less than 0.75Lc (75 m) in size. (2) At the scale of the right of way of the road, L_c is the 20 m width. At this scale of interest, the 1 m block is at the block/matrix threshold ($0.05L_c$) and the largest geotechnically significant block is 15 m (0.75Lc). The large speckled block is massive rock at this scale of interest. Massive rock and blocks greater than about 1 m in size will present difficulties during mass grading of the road. (3) At the scale of the 2 m wide, 2 m deep pipeline trench, L_c can be taken as the depth of the trench. The block/matrix threshold will be 0.1 m, and the largest geotechnically significant block 1.5 m. At the local scale of interest of the trench represented by the trench depth, the 1 m block may present a problem for the trenching contractor. However, at the scale of the overall length of the trench, the speckled block is considered massive rock and will be more challenging since a significant portion of it must be excavated.

between blocks and matrix at any scale is taken to be $0.05L_c$ (equivalent to $0.05\sqrt{A}$).

Figure 5 illustrates how a block at one scale of interest can be part of matrix at a larger scale, but massive rock at a smaller scale. Figure 5 shows that it is essential to consider the possibility of having to penetrate very large blocks when constructing linear facilities such as roads, pipelines and tunnels. Figure 5 also illustrates examples of the selection of L_c for various scales of interest.

BLOCK SIZE DISTRIBUTIONS BASED ON CHORDS

True three-dimensional (3-D) block size distributions in bimrocks are poorly estimated by one-dimensional chord length distributions obtained from the limited linear sampling of typical geotechnical exploration core drilling. The degree to which chord length distributions match actual 3-D block size distributions is dependent on the orientation of blocks relative to the boring, volumetric block proportion and total length of drilling. Since observed chord lengths are almost invariably smaller than the actual block diameters (Figure 3), larger blocks are mischaracterized as smaller blocks and spuriously contribute to the lower end of the cumulative size distribution curve, as shown in Figure 6b. For this reason, it is unlikely that drilling and coring into a melange can recover an actual 3-D block size distribution curve, because the frequency of larger block sizes tends to be underestimated and the frequency of smaller sizes overestimated. The practical consequences of underestimating block sizes from exploration drilling are unpleasant and costly surprises during excavation and tunneling of bimrocks.

MECHANICAL CONTRAST BETWEEN BLOCKS AND MATRIX

The mechanical contrast between competent blocks and weaker matrix forces failure surfaces to negotiate tortuously around the perimeters of blocks (Figure 11). Sufficient contrast is afforded by friction angle ratios— (tanϕ of weakest block)/ (tanϕ of matrix) —between 1.5 and 2.0, as suggested by the work of Lindquist (1994a) and Volpe et al. (1991). Another means of identifying strength contrasts is to use rock stiffness, measured by Young's modulus, E. Lindquist (1994a) used a ratio of block stiffness to matrix stiffness— (E_{block}/E_{matrix}) —of 2.0 to generate block/matrix contrasts for physical models of melange. For strength or stiffness ratios less than

the lower bounds described above, there will be an increased tendency for shears and failure surfaces to pass through blocks rather than around them.

A wide range of block sizes tends to force failure surfaces to negotiate through matrix and along block/matrix contacts in contorted, tortuous paths. The tortuosity of pre-existing and induced shear surfaces increases shear resistance, as demonstrated by Savely (1990) for bouldery Gila Conglomerate in Arizona; Irfan and Tang (1993) for boulder-rich colluvium in Hong Kong; and Lindquist (1994a) for physical model melanges. When blocks are uniformly sized, failure surfaces tend to have smoother, undulating profiles (Medley 1994a, fig. 4.4), and hence the mixed rock mass has less shear resistance.

RELATION OF VOLUMETRIC BLOCK PROPORTION TO MELANGE STRENGTH

The overall strength of a melange is independent of the strength of the blocks. As long as there is mechanical contrast between blocks and matrix, the presence of blocks with a range of sizes adds strength by forcing tortuous failure surfaces to negotiate around blocks. Strength and deformation properties of a rock/soil mixture increase directly and simply with increasing volumetric block proportions as shown in Figure 7, which is compiled from the results of Irfan and Tang (1993) for boulder-rich colluvium in Hong Kong, and Lindquist (1994a) and Goodman et al. (1994) for physical model melanges and melange from Scott Dam, Northern California.

Using physical model melanges, Lindquist (1994a) determined a conservative relationship between volumetric block proportion and increased strength (Figure 7). Below about 25% volumetric block proportion, the strength and deformation properties of a melange are those of the matrix; between about 25% and 75%, the friction angle and modulus of deformation of the melange mass proportionally increase; and beyond 75% block proportion the blocks tend to touch and there is no further increase in melange strength. Lindquist's results for model melanges closely matched the findings of Irfan and Tang (1993) for boulder colluvium. As shown in Figure 7, some rock/soil mixtures may have different strength/volumetric proportion relationships, as indicated by the data for weathered Scott Dam melange. Nevertheless, the important feature of Figure 7 is that there is a simple and direct dependence between volumetric block proportions and bimrock strengths.

Lindquist (1994a) also determined that cohesion tends to decrease with increasing volumetric block proportion for physical model melanges. However, Goodman and Ahlgren (2000) observed that cohesion inexplicably increased with volumetric block proportion for Franciscan melange in the foundation of Scott Dam in Northern California. Because of the currently unresolved contradiction between these findings, it is prudent to neglect any benefit of uncertain increased cohesion with increased volumetric block proportion.

ESTIMATION OF VOLUMETRIC BLOCK PROPORTION

As described above, the volumetric block proportion of a melange is necessary to predict the geomechanical properties. The volumetric block proportion is approximated by measuring areal block propo-

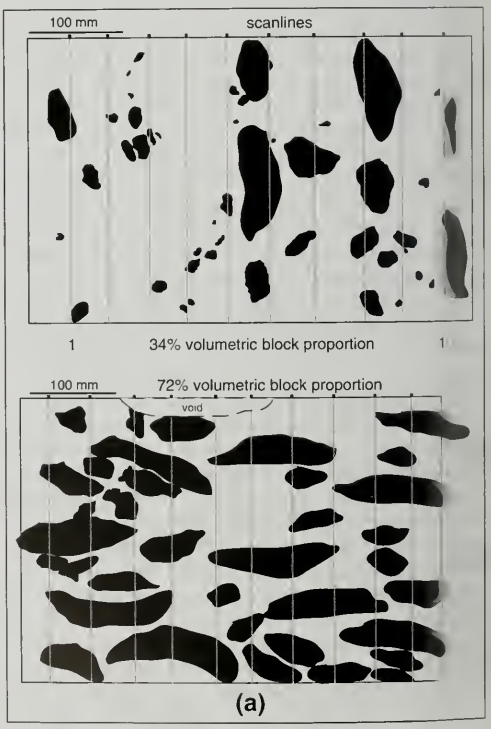

tios from outcrops, or linear block proportions from scnlines and exploration drilling. The linear block proortion is the ratio of the total length of chord leths to the total length of sample lines. The asmption that measured linear or areal block propzions are equivalent to the required volumetric blck proportions is only valid if there is enough saipling. Such equivalence is one of the fundamotal laws of *stereology*, an empirical and mathemtical study relating point, line and planar observations the true geometric properties of objects (Underwood, 1970; Weibel, 1980). Since blocks in melanges are not uniformly sized or distributed, the volumetric block proportion cannot be accurately determined from a few borings, but if there are sufficient total lengths of sampling lines (at least $10d_{max}$), the linear block proportion approaches the volumetric block proportion (Medley, 1994a, 1994b, 1997), with an error, or uncertainty, that can be roughly estimated.

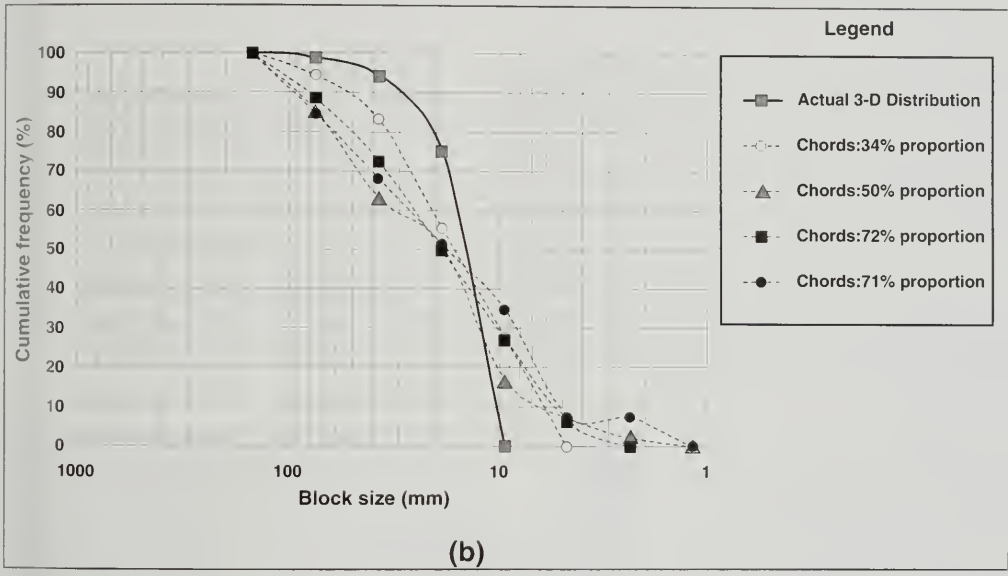

Figu 6. Comparisons are shown between actual and known three dimension (3-D) block size distributions and one-dimesion (chord length) distributions measured from tracings of physical model melanges (Medley, 1994a, after Linduist, 1994a). Fig 6a (on previous page) shows tracings of two models. One model has a relatively low volumetric bloc proportion (34%) where the model exploratory borings ("scanlines") are parallel to the orientation of the ellipsoidal block. When volumetric block proportion is low, there is less probability that a boring will intersect a block at all, and evenss that it will intercept the actual maximum dimension of blocks. The other model has a high volumetric block proprtion (72%) with blocks oriented approximately horizontal and the exploratory borings oriented vertical. Clearly, in the later case, even though the probability is high that borings will intersect blocks, the chord length distribution cannot matc the actual block size distribution since the vertical chords are always shorter than the horizontal maximum block dimesions. In Figure 6b, the data graphed are all for physical melange models with blocks oriented vertical and parallel tohe model borings. Block size data are plotted in the style of "particle size distributions". However, the y axis shows numrical frequency rather than particle weights. Actual block sizes in the models ranged between about 150 mm and 10 mi. The chord length distributions always under-estimate the larger block sizes and over-estimate the smaller sizes. Indee, blocks sizes are indicated that do not exist in the actual physical model melange. Although the chord length distriutions appear to estimate the largest actual block, it is unlikely that there were any chords that were 150 mm long. This ibecause data are plotted at the upper end of each size class, and the class interval for the largest chords is 75 mm to 15 mm. Hence, if the largest chord was, for example, actually 80 mm long, it would plot at the 150 mm location.

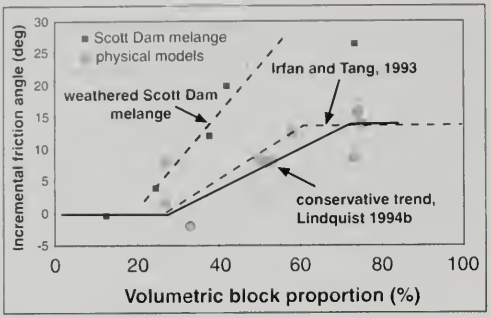

Figure 7. The strength of bimrocks increases directly with volumetric block proportion. The increase in friction is added to the frictional strength of the matrix. There is marked similarity between the data of Lindquist (1994b), for physical model melanges, and that of Irfan and Tang (1993), for Hong Kong boulder colluvium. However, the data obtained from laboratory testing of weathered Franciscan melange from Scott Dam (Goodman et al., 1994) shows that for some bimrocks blocks may provide considerably more incremental strength than indicated by the Lindquist and Irfan and Tang experiments. The "conservative trend" of Lindquist (1994b) could be used in lieu of site-specific testing of Franciscan melanges. (After Medley, 1999).

Although the desirable minimum total length of exploration drilling is equivalent to at least $10d_{max}$, optimum geotechnical exploration is rarely performed, even when subsurface conditions are relatively straightforward. Medley (1997) considered the error in estimates of volumetric block proportion based on the assumption that they are the same as the measured linear block proportions. He fabricated physical models of melange with known block size distributions and volumetric block proportions, and "explored" the models with hundreds of model boreholes. The experiments showed that measured linear block proportions had to be adjusted by an uncertainty factor to yield an appropriate estimate of the volumetric block proportion.

Uncertainty depends on both the total length of the linear measurements, such as from drilled core, and the linear block proportion itself. The uncertainty factor to be applied to the linear block proportion is both positive and negative. The actual volumetric block proportion may lie anywhere within the range defined by the adjusted lower and upper volumetric block proportions. As described by Medley (1997), it is prudent and conservative to apply the uncertainty adjustment to reduce (negative adjustment) the calculated estimates of volumetric block proportions for the purpose of assigning strength parameters for a bimrock. On the other hand, because of the economic consequences of under-estimating volumetric block proportions to be excavated by tunneling or earthwork construction, it is prudent and conservative to increase (positive adjustment) the calculated estimates of volumetric block proportions. (The uncertainty factor is shown in Figure 14, the use of which is described later in this paper).

GUIDELINES FOR CHARACTERIZATION

Elements in a program to characterize a volume of Franciscan melange or other rock/soil mixture include (1) establishing characteristic engineering dimensions (L_c), (2) estimating the sizes of smallest and largest blocks, (3) mapping, (4) exploration drilling, (5) geologic interpretation, (6) laboratory testing, (7) estimating rock mass volumetric block proportion, (8) estimating rock mass strength, and (9) estimating block size distributions. Guidelines for performing each of these nine elements are provided in the following sections. The guidelines are derived from case histories and work by Medley (1994a, 1998, 1999a).

ESTABLISHING CHARACTERISTIC ENGINEERING DIMENSIONS (L_c)

Flexibility is exercised in the selection of L_c, as illustrated in Figure 5. For an entire *site* or *outcrop*, determine the area of interest (A), and choose L_c as equivalent to $\sqrt{A}$ (Figure 5). For an *excavation* or *trench* use the height of the excavation. At the scale of the entire excavation or trench, measure the explored area (A) and use $\sqrt{A}$ (Figure 5). For a *landslide* use a critical cross-section depth or the thickness of the failure zone, as described by Medley (1994a, 1999) for the Lone Tree Landslide in Marin County, Northern California. For *foundation footings* use the foundation width. If piles or caissons will be driven or drilled through the bimrock, use the pile diameter. For *tunnels*, at the scale of the entire tunnel length, measure the explored area (A) and use $\sqrt{A}$. At the scale of the tunnel face, use the tunnel diameter. Medley (1994a, 1999) provided examples of the use of characteristic engineering dimensions for the Richmond Transport Tunnel excavated in 1994 through Franciscan melange in San Francisco (Klein et al., 2001, this volume). For

dam foundations use the most critical of dam width, dam height, $\sqrt{A}$ of footprint area, or some minimum design dimension such as the thickness of a critical shear failure zone, as described by Medley (1994a) and Goodman and Ahlgren (2000).

ESTIMATING THE SIZES OF SMALLEST AND LARGEST BLOCKS

As described above, geotechnically significant blocks that influence bimrock strength range between about $0.05L_c$ at the block/matrix threshold and $0.75L_c$ for the largest block (d_{max}). Select the most conservative block/matrix threshold that can be justified. As shown in Figure 5, blocks smaller than $0.05L_c$ are demoted to matrix at an overall site scale of interest, but may still be of substantial size at a contractor's smaller scale of interest, and where excavation equipment capabilities must be considered.

MAPPING

Block-poor zones in Franciscan melange landscapes are geomorphologically expressed as valleys and landslides. Block-rich regions and individual blocks form erosion-resistant outcroppings, hills, rocky protuberances and stacks and craggy headlands along rivers and coastlines (Figure 8), where they act as buttresses. Blocks may be vegetated with trees, whereas surrounding mobile, creep-prone matrix soils are sparsely vegetated. The sandier soils above blocks lose moisture more quickly than clayey matrix soils, and in the spring and early summer large blocks at shallow depths may be identified by the browning grasses and shrub vegetation overlying them. Matrix soils host greener vegetation. In air photos, the presence of near-surface blocks shows as tonal mottling (Figure 9).

At outcrops, the mechanical contrast between blocks and matrix can be established using a rock pick. Friction angles of blocks and matrix can be estimated using standard strength scales such as those provided by the Geological Society Engineering Geology Working Party (1995). The geologist should observe the nature of exposed block/matrix contacts, the matrix fabric, the block lithologies, and the array and nature of the discontinuities in the blocks (Medley, 1994a). A highly fractured block is a weak block that may have little mechanical contrast and should be assigned to the matrix. Zones of weakness in large blocks may also act as "channels" for developed failures. Shearing at different scales is common in melanges and should be mapped.

Figure 8. Franciscan melange at Coleman Beach, Sonoma County, Northern California. Blocks form erosion-resistant headlands and also buttress upslope weaker block-poor melange. Several homes are threatened by cliff-top retreat of block-poor melange. The near shore is strewn with relict blocks.

Photographs of outcrops should be taken at different scales with an indicator of the scale, such as a tape measure, included in the photograph (e.g., Figure 10). The procedure was described in more detail by Medley (1994a). The maximum observable dimensions (d_{mod}) of exposed blocks can later be measured, either manually or using image analysis software, as described by Medley (1994a) and Medley and Lindquist (1995).

EXPLORATION DRILLING

There should be no expectation that exploration drilling will adequately intercept all, or even many, of the blocks within a mass of bimrock. As indicated above, the desirable minimum total length of exploration core drilling

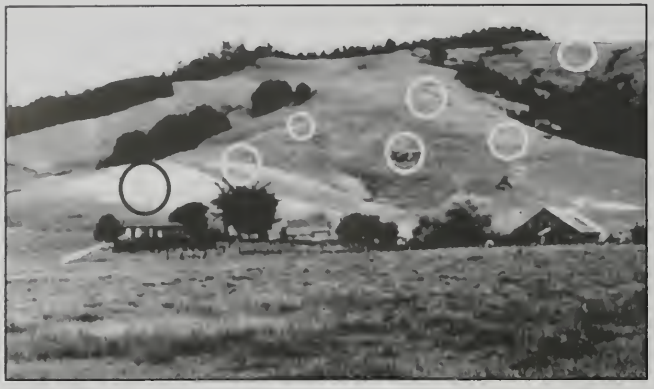

Figure 9. Franciscan melange photographed in the spring/early summer. Mottling of lighter tones indicate blocks underlying the hillside (circled).

GEOLOGIC INTERPRETATION

The problems of characterizing Franciscan melanges and other rock/soil mixtures are compounded by inappropriate use of geologic terms. For example, a succession of shale matrix and sandstone blocks in drill core may result in Franciscan melange being logged as *interbedded sandstones and shales* (Figure 11, BH-2), which incorrectly suggests lateral continuity. True blocks of coherent sequences of shales and sandstones are generally unsheared and the shales lack small blocks as described by Medley (1994a, fig. 5.16). Melanges also contain juxtaposed blocks of diverse lithologies that represent improbable depositional environments, such as eclogites adjacent to limestones (logged in BH-2, Figure 11), which are good clues to the presence of melange. A mental picture of the spatial and lithologic variety of bimrocks, similar to Figure 11, will reduce errors in geological interpretations.

is about $10d_{max}$. For example, at a site where $\sqrt{A}$, equivalent to L_c, is 100 m, the largest block will be about 75 m in size. Hence, at least 750 m of drilled core is preferable, but is unlikely to be drilled due to cost and time constraints. In most cases conservative adjustments to the linear block proportion must be made to provide prudent estimates of volumetric block proportions and block size distributions.

It is difficult to recover good quality core in melanges and similar rock/soil mixtures because of the abrupt variations between blocks and matrix, varying block lithologies (Figure 11), extensive shearing and highly fractured small blocks. Goodman and Ahlgren (2000) describe the poor sample recovery of Franciscan melange at Scott Dam, Northern California, even when using triple-barrel samplers and the integral sampling method of Rocha (1971) (a method in which friable rock is pregrouted and then cored).

When logging core, measure all block/core intercepts (chord lengths) greater than 2 cm long, even if the block/matrix threshold is larger. The information on small blocks will be useful for work performed at laboratory scale. Estimates of the linear block proportions should be made during core logging and the core should be photographed. Wrap the core promptly since matrix, particularly in sheared melanges, may dry and slake. Examples of suggested practice in the logging of melange core is provided by several case histories described by Medley (1994a).

Melanges should not be described as *soil with boulders*, a term that can mean different things to the geologist, who encounters blocks during exploration, and the contractor, who has to construct through or around them. Boulders are often considered to range in size between 200 mm to 2 m. A practitioner may observe blocks in outcrops or in a boring and call them "boulders", which implies to a contractor that they can be excavated and can be considered "soil". However, an unexpectedly large block that substantially fills a tunnel face will not likely be considered "soil" by the tunnel contractor, as pointed out by Attewell (1997). Furthermore, since chord lengths usually underestimate the true diameter of blocks, the apparent diameter of observed "boulders" may actually be chord lengths close to the edge of large blocks (Figures 3 and 11; BH-2). The excavation or penetration of blocks larger than about 1.5 m to 2 m diameter may require expensive blasting or jack hammering.

Borings are commonly terminated about 1 to 2 m into "*bedrock*" as shown in Figures 11 and 12. But logging the material encountered in the borings as *soil* above *bedrock* increases the probability that the blocks will later be interpreted as continuous bed-

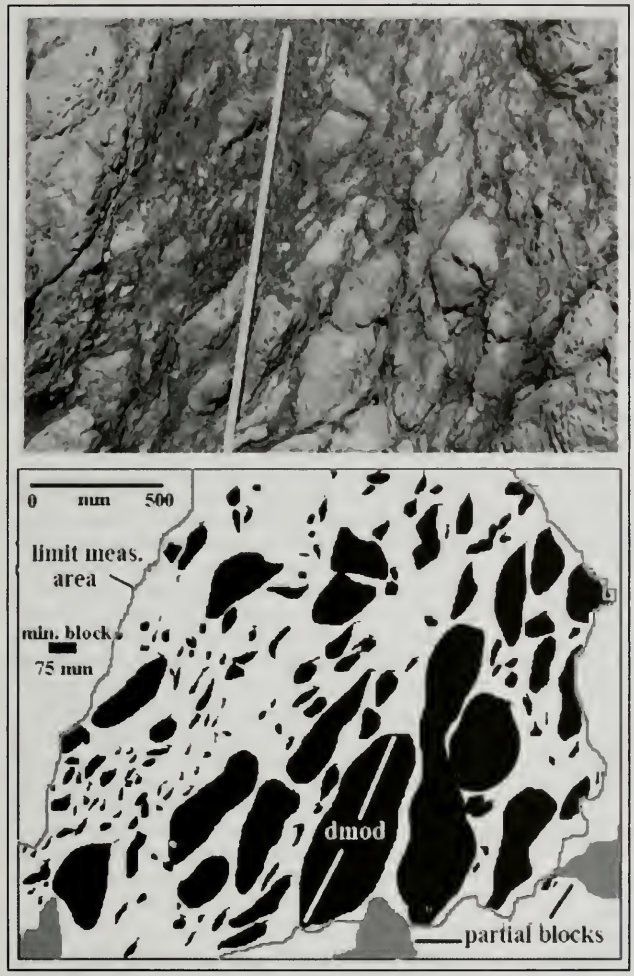

Figure 10. Photograph and sketch of outcrop of Franciscan melange at Caspar Headlands, Mendocino County, Northern California. The stadia rod in the photograph is 1.5 m (5 feet) long. The sketch shows the blocks discriminated by image analysis software. Block sizes are characterized by d_{mod} (maximum observed dimension). The area of measurement excludes two partial blocks at the lower right of the outcrop. At the scale of the outcrop, the size of blocks at the block/matrix threshold (75 mm) is shown by the black bar midway on left side of sketch. Note block-poor and block-rich areas. From Medley (1994a) and Medley and Lindquist (1995).

rock, which could result in erroneous slope design and troublesome excavation, as shown in Figure 12. In Marin County, Northern California, a mischaracterization similar to the one depicted in Figure 12 resulted in a landslide repair costing ten times as much as originally estimated.

LABORATORY TESTING

Because of scale independence, laboratory specimens of melange are scale models of melange at rock mass scale. The results of laboratory testing are thus more directly applicable to *in situ* melange rock masses than for many other geological materials. Lindquist (1994a, 1994b), Lindquist and Goodman (1994) and Goodman and Ahlgren (2000) described how specimens of melange with varying block proportions were tested to develop relationships between block proportions and strengths at laboratory scale. Specimen testing should be performed by laboratories experienced in rock testing, using multistage testing methods in which specimens of melange are subjected to several loads, each applied to the onset of increased strain at peak stress (Lindquist, 1994a; Bro, 1996, 1997; and Goodman and Ahlgren, 2000). For each specimen tested, a series of Mohr's circles can be drawn to identify the effective friction angle and cohesion.

The volumetric block proportions of each specimen can be determined after carefully disaggregating and wash seiving them to retrieve the blocks. Given that the characteristic engineering dimensions of the laboratory specimens are their diameters, blocks are those intact inclusions that have maximum dimension between about 5% and 75% of the diameter of the specimens. The volume of blocks (and hence the volumetric block proportion)

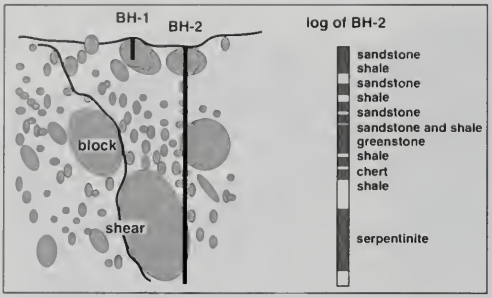

Figure 11. Shears in melanges typically tortuously negotiate around blocks at the block/matrix contacts. Sketch also shows exploration of a bimrock by borings (BH). BH-1 terminates in a block, a situation that, in Northern California, often results because the investigator identifies the block as "bedrock". The log of BH-2, shows a sequence of rocks that is not "interbedded sandstones and shales", because the juxtaposed presence of chert, greenstone and serpentinite suggests the presence of Franciscan melange. Note that BH-2 only rarely penetrates the diameter of a block.

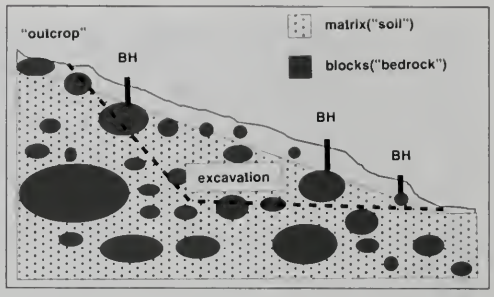

Figure 12. Borings in melange. Borings have been terminated in rock interpreted as continuous bedrock rather than blocks, and the matrix as soil or "soil with boulders". Because of this misinterpretation, the excavation of the designed slope will be troublesome.

is measured by weighing the blocks once the specific gravity of the blocks is known. The testing of specimens with different proportions of blocks yields plots of effective friction angle as a function of volumetric block proportion, such as that shown in Figure 13. Plots can also be developed for cohesion and deformation parameters a shown by Lindquist (1994a, 1994b) and Goodman and Ahlgren (2000).

ESTIMATING ROCK MASS VOLUMETRIC BLOCK PROPORTION

For the selected characteristic engineering dimension (L_c), identify the block/matrix threshold size as $0.05L_c$, and ignore all chord lengths shorter than the threshold size. Calculate the linear block proportion by dividing the sum of the chord lengths by the total scanline or total length of borings. To estimate the volumetric block proportion, the linear block proportion must be adjusted for uncertainty using a plot such as that shown in Figure 14. To use Figure 14, first estimate d_{max} (size of largest expected block), calculate multiples (N) of d_{max} by dividing the total length of sampling by d_{max}, and enter the graph at N. For the estimated linear block proportion (bold diagonal lines) identify uncertainty at the left axis, interpolating between the diagonal lines if necessary. To obtain the range of volumetric block proportions, multiply the linear block proportion by the uncertainty, and subtract the product from the linear block proportion (for the lower bound) and add for the upper bound. The lower bound is used for purposes of estimating bimrock strength and the upper for estimating block proportion for earthwork construction.

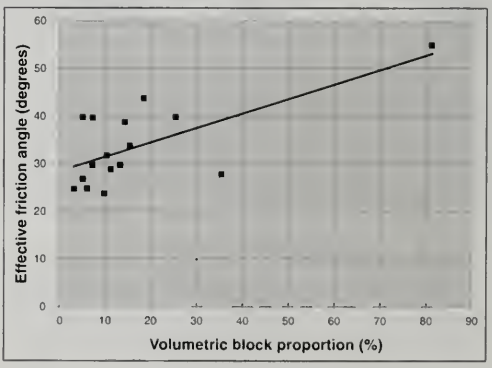

Figure 13. Plot of effective friction angle as a function of volumetric block proportion, generated from laboratory testing of Franciscan melange specimens obtained from core drilling at Scott Dam, Northern California (after Goodman and Ahlgren, 2000). The correlation is not good, but a straight line fit is appropriate given prior experience with laboratory testing of bimrocks (see Figure 7). Inclusion of the sole data point at 80% volumetric block proportion renders the best-fit line more conservative.

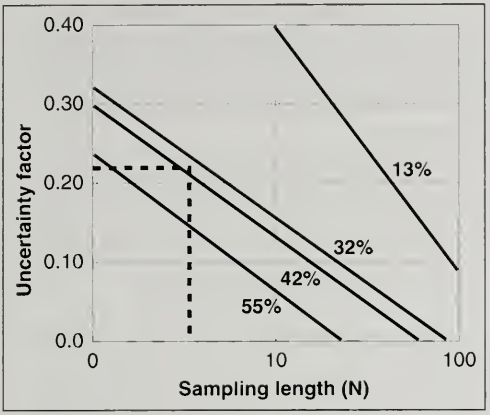

Figure 14. Uncertainty in estimates of volumetric block proportion as a function of the length of linear measurement, expressed as a multiple (N) of the length of the largest block (d_{max}), and the measured linear block proportion (13 percent to 55 percent). (From Medley, 1997). The dashed line shows the use of the graph for an example (provided in the text) at Scott Dam, where the 150 m of drill core (sampling length) was equivalent to 5 times the size of the largest block expected in the region of the dam (30 m). Hence, N is 5. The measured liner block proportion was 40 percent. Entering the graph at N of 5, and intersecting the linear volumetric proportion of 40% (interpolating between 42 percent and 32 percent diagonal lines), gives an uncertainty factor of 0.22 (dimensionless). The uncertainty in assuming that the linear block proportion is the same as the volumetric block proportion is estimated as 40% ± (0.23) (40%) ± 9%, giving upper and lower bounds of 31 percent and 49 percent. The actual volumetric block proportion will generally lie within the range of the lower and upper bounds. It is prudent to use the lowest estimate if the volumetric block proportion will be used to estimate bimrock strength. On the other hand, if the volumetric block proportion will be used for excavation purposes, it may be appropriate to over-estimate the block proportion, in which case the upper bound could be used.

At Scott Dam, Northern California, the likely mode of dam failure was considered to be sliding along an assumed 3 m-thick shear zone within the melange adjacent to the base of the dam. The size of the largest block (d_{max}) in the area was estimated to be about 30 m long. The 3 m thickness of the shear zone was selected as the characteristic engineering dimension (L_c) and the block/matrix threshold was calculated as 0.15 m (i.e., 5% of 3 m). About 360 m of exploratory drilling had been performed during the life of the dam, but only about 150 m of core had been recovered. Accordingly, the total length of coring was equivalent to about $5d_{max}$ (i.e., N = 5). Inspection of drill logs and photographs of core penetrating the assumed potential failure zone indicated that the linear block proportion, for blocks greater than 0.15 m, was about 40%. As shown in Figure 14, for a linear block proportion of 40%, and a relative sampling length of N = 5, the uncertainty factor is about 0.23. Hence, the estimated range of volumetric block proportion was 40%±(0.23)(40%), or about 40%±(9%) to yield a lower bound of 31% and an upper bound of 49%. Since it is prudent to take the lowest estimate of the volumetric block proportion for the purposes of estimating melange strength, the 31% estimate was actually adopted as a conservative estimate of the average block proportion in the Franciscan melange at the base of the dam (Goodman and Ahlgren, 2000).

ESTIMATING ROCK MASS STRENGTH

The overall strength of Franciscan melange rock masses is determined by using the estimates of *in situ* volumetric block proportion and the laboratory test plots of effective friction angle and cohesion as a function of volumetric block proportion, such as the one shown in Figure 13. It may be necessary to determine strengths for block-poor and block-rich zones within the rock mass, which may vary significantly from the overall average. In the case of Scott Dam, the friction angle was estimated to be 39 degrees for the overall volumetric block proportion of 31% (Goodman and Ahlgren, 2000).

ESTIMATING BLOCK SIZE DISTRIBUTIONS

Although the strength of the blocks does not influence the overall strength, the lithology, discontinuity fabric, number and size distribution of blocks are of concern to tunneling or earthwork contractors. For example, blocks greater than about 0.6 m in diameter are too large to be plucked by scrapers and must be excavated by bulldozers; blocks larger than about 1.5 m must be blasted. Encountering blocks complicates tunneling, so there is some value in making pre-construction estimates of possible block sizes. For example, between 1994 and 1995, while tunneling through Franciscan melange for the Richmond Transport Tunnel in San Francisco, the contractor had to traverse 200 m through an unexpected graywacke block. Medley (1994a) had earlier

predicted that the tunnel could encounter a block as large as 600 m.

Although the estimation of block size distributions from drilling data is unreliable (Figure 6), very approximate estimations can be made for Franciscan melanges using a method described by Medley and Lindquist (1995). First establish d_{max} at the appropriate scale of interest, then construct a first approximation for the block size distribution using the finding that, for some number of blocks (n) within a certain size class, there will be about 5n in the previous size class and 0.2n in the following size class. Size classes are constructed so that the span of each class is twice that of the previous class. Next, starting with d_{max}, work backwards through the size distribution. For example, if d_{max}, is thought to be 3.0 m, then initially assume that there is 1 block in the 2.0 m to 4.0 m class. Hence there will be about 5 blocks in the 1.0 m to 2.0 m class, about 25 blocks in the 0.5 m to 1.0 m class, about 125 blocks in the 0.25 m to 0.5 m class, and 625 blocks in the 0.125 m to 0.25 m class. The latter class contains the block/matrix threshold size, 0.15 m (i.e., 5% of 3 m or $0.05d_{max}$). The volume of individual blocks can be estimated assuming spherical or ellipsoidal blocks. The volume of all blocks in any particular class can be estimated by determining the volume of a single block with a dimension equivalent to the average size in the class, and multiplying that volume by the number of estimated blocks in the class. Finally, the total volume of blocks in all classes, divided by the volume of bimrock being considered, should match the estimated volumetric block proportion (preferably an upper bound estimate that incorporates uncertainty). If there is a difference, make adjustments to the assumed block size distribution (e.g., by doubling the number of blocks in the classes) and repeat the calculations until the volumetric block proportions match. This method gives approximate and conservative estimates but is useful for pre-excavation planning (Medley, 1995).

CONCLUSIONS

Engineering geologists and geotechnical engineers working in Northern California cannot avoid encountering and working with chaotic bimrocks such as Franciscan melange and other rock/soil mixtures. However, despite their heterogeneity, such mixtures can be reasonably characterized for the purpose of geological engineering design and construction. Even where there is great uncertainty in the characterization, the work performed to produce broad estimates of block proportions, block sizes, lithologic proportions, bimrock strengths and deformation properties will focus the attention of geologists, engineers, owners and contractors on the difficulties that may be encountered during design and construction.

As a final comment, the author hopes that practitioners will use more caution the next time they have occasion to use the expressions "interbedded" or "soil with boulders" in boring logs or reports.

ACKNOWLEDGMENTS

Richard E. Goodman and Pacific Gas & Electric Company supervised and funded much of the research summarized in this paper. I am indebted to Joan Van Velsor, who was sufficiently interested in my Ph.D. research to provide me with tons of Lone Tree Slide drill core and encouraged me to write this paper, which has benefited from her comments and patient prodding. Thanks to David Bieber, Horacio Ferriz, Betsy Mathieson, Steve Stryker and Dana Willis for their thorough reviews of the several generations of manuscripts of this paper.

AUTHOR PROFILE

Dr. Edmund Medley, PE, CEG, is a geological engineer with over 20 years of international experience in geological and geotechnical engineering. His career includes chapters as a mineral exploration prospector, teacher, university lecturer, vagabond and bimrock researcher. He is a Principal Engineer in the Geo^3 Group (Geological, Geotechnical and Geoenvironmental Engineering) at Exponent Failure Analysis Associates in Menlo Park, California, where he performs geo-forensic investigations. Dr. Medley is a Certified Engineering Geologist in California and Registered as a Civil Engineer in California and Hawaii. He also holds professional geologist and professional engineer registrations in British Columbia and the United Kingdom.

SELECTED REFERENCES

AGI, 1977, Proceedings of the International Symposium on the Geotechnics of Structurally Complex Formations: Associazone Geotechnica Italiana (Capri, Italy).

Attewell, P.B., 1997, Tunnelling and site investigation: Proceedings of the International Conference on Geotechnical Engineering of Hard Soils-Soft Rocks, A.A. Balkema (Rotterdam, Netherlands), v. 3, p. 1767-1790.

Aversa, S., Evangelista, A. Leroueil, S., and Picarelli, L., 1993, Some aspects of the mechanical behavior of "structured" soils and soft rocks: Proceedings of the International Symposium on Geotechnical Engineering of Hard Soils-Soft Rocks, Athens, Greece, A.A. Balkema, (Rotterdam, Netherlands), v. 1, p. 359-366.

Blake, M.C., 1984, Franciscan geology of Northern California: The Pacific Section of the Society of Economic Paleontologists and Mineralogists, (Los Angeles, California), 254 p.

Blake, M.C. and Harwood, D.S., 1989, Tectonic evolution of Northern California: Field trip guidebook for Trip 108, American Geophysical Union (Washington, DC).

Bro, A., 1996, A weak rock triaxial cell; Technical note: International Journal of Rock Mechanics and Mining Science, v. 33, no. 1, p. 71-74.

Bro, A., 1997, Analysis of multi-stage triaxial test results for a strain-hardening rock: International Journal of Rock Mechanics and Mining Science, v. 34, no. 1, p. 143-145.

Cowan, D.S., 1985, Structural styles in Mesozoic and Cenozoic melanges in the Western Cordillera of North America: Bulletin of the Geological Society of America, v. 96, p. 451-462.

D'Elia, B., Distefano, D., Esu, F. and Federico, G, 1986, Slope movements in structurally complex formations: in Tan Tjong Kie, Chengxiang, L., and Lin, Y. (eds.), Proceedings of the International Symposium on Engineering in Complex Rock Formations, (Beijing, China).

Ellen, S. D., and Wentworth, C.M., 1995, Hillside bedrock materials of the San Francisco Bay Region: United States Geological Survey Professional Paper 1357.

Geological Society Engineering Geology Working Party, 1995, The description and classification of weathered rocks for engineering purposes: Quarterly Journal of Engineering Geology, v. 28, no. 3, p. 207-242.

Goodman, R.E., Medley, E.W., and Lindquist, E.S., 1994, Final R&D Report: Characterization of dam foundations on melange-type mixtures - A methodology for evaluating the shear strength of melange, with application to the foundation rock as Scott Dam, Lake Pillsbury, Lake County, California: unpublished report prepared for Pacific Gas & Electric Company, San Francisco, California; University of California at Berkeley, Department of Civil Engineering, (UC Award Number Z10-5-581-93), 43 p.

Goodman, R.E. and Ahlgren, C.S., 2000, Evaluating safety of concrete gravity dam on weak rock: Scott Dam: Journal of Geotechnical and Geoenvironmental Engineering, American Society of Civil Engineers, v. 126, no. 5, p. 429-442.

Hsü, K.J., 1985, A basement of melanges: A personal account of the circumstances leading to the breakthrough in Franciscan research: in Drake, E.T. and Jordan, W.M. (eds.), Geologists and Ideas: a history of North American geology, Geological Society of America, (Centennial Special Volumes), v. 1, p. 47-64.

Irfan, T.Y. and Tang, K.Y., 1993, Effect of the coarse fraction on the shear strength of colluvium in Hong Kong: Hong Kong Geotechnical Engineering Office, TN 4/92, 128 p.

Klein, S., Kobler, M., Strid, J., 2001, Overcoming difficult ground conditions in San Francisco - The Richmond Transport Tunnel, San Francisco County, California: *in* Ferriz, H., Anderson, R., (eds.), Engineering Geology Practice in Northern California: Association of Engineering Geologists Special Publication 12 and California Division of Mines and Geology Bulletin 210

Laznicka, P., 1988, Breccias and coarse fragmentites: Petrology, environments, ores: in Developments in Economic Geology, Elsevier, v. 25, 832 p.

Lindquist, E.S., 1994a; The strength and deformation properties of melange: Ph.D. Dissertation, Department of Civil Engineering, University of California at Berkeley, California, 262 p.

Lindquist, E.S., 1994b, The mechanical properties of a physical model melange: Proceedings of 7th Congress of the International Association Engineering Geology, Lisbon, Portugal,; A.A. Balkema, (Rotterdam, Netherlands).

Lindquist, E.S. and Goodman, R.E., 1994; The strength and deformation properties of a physical model melange: in Nelson, P.P. and Laubach, S.E. (eds.), Proceedings of the first North American Rock Mechanics Conference (NARMS), Austin, Texas; A.A. Balkema, (Rotterdam, Netherlands).

Medley, E.W, 1994a, The engineering characterization of melanges and similar block-in-matrix rocks (bimrocks): Ph.D. Dissertation, Dept. of Civil Engineering, University of California at Berkeley, California, 387 p.

Medley, E.W, 1994b, Using stereologic methods to estimate the volumetric block proportion in melanges and similar block-in-matrix rocks (bimrocks): Proceedings of 7th Congress of the International Association of Engineering Geologists, Lisbon, Portugal; A.A. Balkema, (Rotterdam, Netherlands)

Medley, E.W, 1995, Estimating block sizes in Franciscan melanges: Abstracts of 38th Annual Meeting of the Association of Engineering Geologists, Sacramento, California.

Medley, E.W, 1997, Uncertainty in estimates of block volumetric proportion in melange bimrocks: Proceedings of the International Symposium of International Association of Engineering Geologists, Athens, Greece, A.A. Balkema (Rotterdam, Amsterdam), p. 267-272.

Medley, E.W, 1998, Order in chaos: The geotechnical characterization of melange bimrocks: Proceedings of First International Conference on Site Characterization, Atlanta, Georgia; (American Society of Civil Engineers, New York), p. 210-206.

Medley, E.W, 1999a, Systematic characterization of melange bimrocks and other chaotic soil/rock mixtures: *Feldsbau Rock and Soil Engineering*, Journal for Engineering Geology, Geomechanics and Tunnelling, Austrian Society for Geomechanics; v 17, no. 3, p. 152-162.

Medley, E.W, 1999b, Relating the complexity of geological mixtures to the scales of practical interest: Abstracts of the Annual Meeting of the Association of Engineering Geologists, Salt Lake City, Utah, September,1999.

Medley, E.W. and Goodman, R.E., 1994, Estimating the block volumetric proportion of melanges and similar block-in-matrix rocks (bimrocks): in Nelson, P.P. and Laubach, S.E., (eds.), Proceedings of the First North American Rock Mechanics Conference (NARMS), Austin, Texas; A.A. Balkema (Rotterdam, Netherlands), p. 851-858.

Medley, E.W. and Lindquist, E.S., 1995, The engineering significance of the scale-independence of some Franciscan melanges in California, USA: in Daemen, J.K. and Schultz, R.A (eds.), Proceedings of the 35th US Rock Mechanics Symposium; A.A Balkema, (Rotterdam, Netherlands), p. 907-914.

Nagahama, H., 1993, Technical note: Fractal fragment size distribution for brittle rocks: International Journal of Rock Mechanics and Geomechanics Abstracts, v. 30, p. 173-175.

Priest, S.D., 1993, Discontinuity analysis for rock engineering: Chapman & Hall, (New York, New York), 473 p.

Raymond, L.A., 1984, Classification of melanges: in Raymond L.A. (ed.), Melanges: Their nature, origin and significance: Geological Society of America Special Publication 228, p.7-20.

Rocha, M. 1971, A method of integral sampling of rock masses: Journal of Rock Mechanics, v.3, p. 1-12.

Sammis, C.G. and Biegel, R.L., 1989, Fractals, fault gouge and friction: Journal of Pure and Applied Geophysics, v. 131, p. 255-271.

Savely, J.P., 1990, Comparison of shear strength of conglomerates using a Caterpillar D9 ripper and comparison with alternative methods: International Journal of Mining and Geological Engineering, v.8, p. 203-225.

Savina, M. E., 1982, Studies in bedrock lithology and the nature of down slope movement: Ph.D. Dissertation, Department of Geological Sciences, University of California at Berkeley, California, 298 p.

Underwood, E.E., 1970, Quantative stereology: Addison Wesley Publishing Company, 272 p.

Volpe, R.L., Ahlgren, C.S., and Goodman, R.E., 1991, Selection of engineering properties for geologically variable foundations: in *Question 66*, Proceedings of the 17th International Congress on Large Dams, Vienna; ICOLD - International Committee on Large Dams, (Paris, France), p. 1087-1101.

Wakabayashi, J., 1999, The Franciscan complex, San Francisco Bay Area: A record of subduction complex processes: in Wagner, D.L. and Graham, S.A., (eds.), Geologic Field Trips in Northern California, Centennial Meeting of the Cordilleran Section of the Geological Society of America; Special Publication 119, California Division of Mines and Geology, (Sacramento, California), p. 1-21.

Wahrhaftig, C., 1984, Streetcar to subduction: American Geophysical Union, (Washington, D.C), 76 p.

Weibel, E.R., 1980, Stereological methods, Volume 2: Theoretical foundations: Academic Press, (New York, New York), 340 p.

ENGINEERING GEOLOGY IN THE PUBLIC EYE - DEVIL'S SLIDE

JOAN VAN VELSOR[1]

INTRODUCTION

One of the most rewarding challenges facing the engineering geologist is emergency response to catastrophic events. When a geologic process closes a vital public facility, the pressures for immediate analysis, recommendations, and repair mount quickly. This paper discusses such an event, the 1995 landslide recurrence at Devil's Slide in San Mateo County on State Route 1, and provides methods for responding to public scrutiny.

HISTORICAL BACKGROUND

Devil's Slide is a large coastal landslide that extends from sea level to the ridge crest at an approximate elevation of 900 feet. The landslide is approximately 2000-feet wide, and contains a smaller active slide, which is about 500-feet wide. There are multiple slide planes below the roadway, at depths of 40 to 300 feet. Underlying bedrock is formed by steeply dipping (dip direction parallel to the slope face) Paleocene sedimentary rocks that overly Cretaceous granitic rocks. The relationship between the two rock types is complex due to past faulting, folding and landslide movement. The slide is visible on an 1866 topographic map of the coast (Figure 1), and has frustrated all transportation efforts since 1897, disrupting in turn a county road, a railroad and a state highway.

The 1906 earthquake on the San Andreas fault resulted in substantial damage to the railroad project then under construction. "Just north of the point known as Devil's Slide, there was a landslide of the whole face of the west end of Montara Mountain. It started at about 800 feet above the sea, and swept down carrying many hundred feet of roadbed along with it. The material that slid was sandstone and granite, but it seemed to be much weathered and softened in places, so that it was loose ground" (Lawson, 1908, p. 252) (Figure 2).

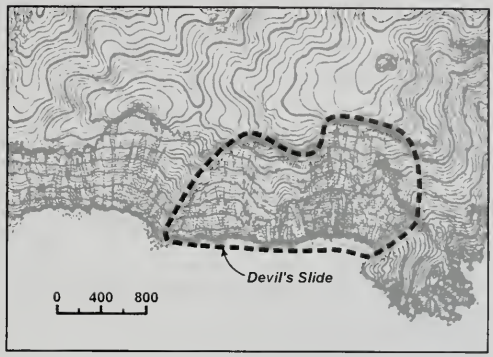

Figure 1. 1866 topographic map of the coast, clearly showing the existence of the slide.

The Ocean Shore railroad was constructed and operated until the early 1920's when high operating expenses, in part due to frequent landslide movement at Devil's Slide, forced abandonment of the railroad project (Figure 3). The Devil's Slide area was described as a "nightmare of unstable earth and numerous landslides, particularly during the rainy season, which frequently caused the road to close down for as long as three or four months at a time" (Wagner, 1974, p.42). In the 1930's, the State Highway Department constructed Route 1, then known as Route 56, across Devil's Slide, acquiring the Ocean Shore alignment by condemnation. State Route 56 was opened in 1937, after massive landslides during construction. In 1940 a very

[1]California Department of Transportation
5900 Folsom Blvd.
Sacramento, CA 95819-4612
jaan.van.velsor@dat.ca.gov

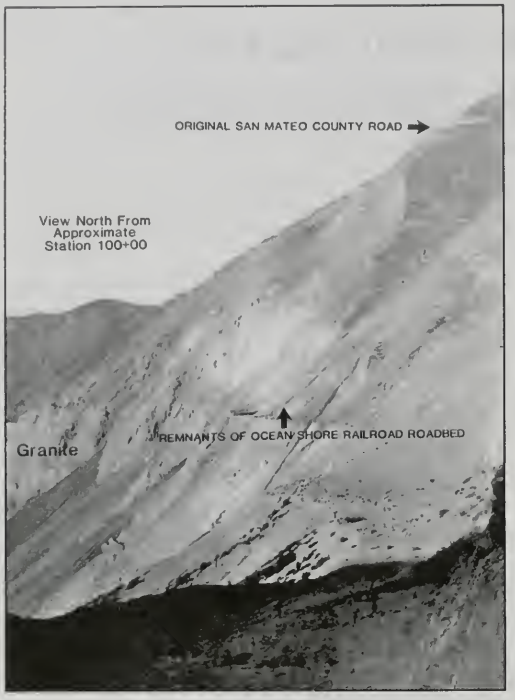

Figure 2. Condition of the slide after the 1906 earthquake on the San Andreas fault. Looking North from south saddle cut. Photograph by W.H. Coverdale.

large landslide resulted in protracted road closure (Figure 4). In the 1950's, after repeated subsidence of the roadway, the State Highway Department (now Caltrans) began developing alternative routes for State Route 1. Environmental groups, who disputed the need to relocate the highway into undeveloped open space, instituted lawsuits against the proposed bypass in 1970, invoking the recently passed environmental laws of CEQA and NEPA. They were successful in stopping the project and work was discontinued.

In 1980 and 1983, substantial slide movement closed the road (Figure 5) and triggered $50 million dollars of Federal Emergency Storm Damage funding for a permanent solution. Realignment studies and environmental analysis were resumed. A bypass alignment was again pursued, and environmental groups renewed their litigation against that solution, preferring no relocation of the existing highway.

By late 1994, the latest round of environmental litigation over the Caltrans environmental document was nearing completion, having been carried to the Federal Supreme Court. Federal, State and local officials, and residents on both ends of this troubled stretch of highway, weary of intermittent road closures and protracted acrimonious debate about alternatives, were looking forward with varying degrees of optimism to a final resolution.

In January of 1995, landsliding recurred, resulting in a five-month road closure (Figure 6). Caltrans engineers and engineering geologists responded to the renewed slide movement, conducting studies, preparing expedited contracts, and working with contractors to reopen the highway in June. The author was the principal engineering geologist for the project.

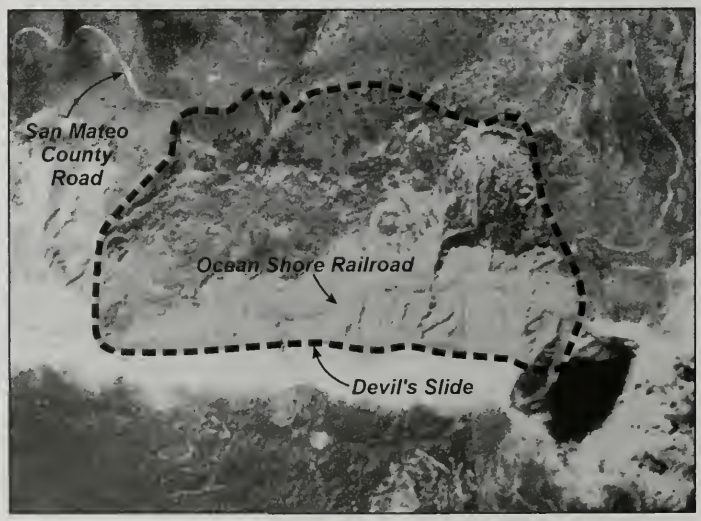

Figure 3. Photomosaic of the Devil's Slide area, 1928-1929. Photomosaic by G. E. Russel.

1995 LANDSLIDE EPISODE

Roadway cracks were reported on January 20, 1995, and the road was closed on January 22nd. Protracted road closures at Devil's Slide have severe financial and life style impacts on coastal residents. Businesses dependent on tourism have been forced into bankruptcy, emergency services compromised, and commuters across the slide have experienced 45 minute to 2-hour detours in response to road closures. It was urgent to reopen the road as quickly as possible. The questions faced by the geotechnical team quickly distilled into the following:

Figure 4. Protracted road closure of State Route 56 after the 1940 landslide episode. Photograph by H.A. Simard.

1. Will the landslide stop moving, as it had in the past, after about 5 feet of vertical movement, or was this the "final event" that would result in disintegration of the active slide block? Is this the end of Route 1 at this site? There were powerful stakeholders concerned with the final outcome; some that wished to see the existing road closed forever, perhaps forcing swifter action on other alternatives; others who did not believe it was seriously damaged. Because of the many decades of litigation, there was profound distrust between many of the key players.

2. If the landslide stabilizes, can it be repaired and reopened to traffic? If it can be repaired, what measures are appropriate? When can the contractor safely begin work? How much will it cost? How soon can it be completed?

It was clear that not only did these questions have to be answered quickly, but also the credibility of the results would be a major concern, particularly if the final recommendation were permanent abandonment of this alignment.

This project had been controversial for decades, and regional interest was high (Figure 7). We heard from the public in person, as well as via e-mail, letters, radio talk shows and phone calls. Regardless of road closure signs, gates, fences, and warning signs, pedestrian traffic continued (Figure 8). Parents climbed fences, passing children, strollers and infants over the chain link fence to continue through the site. The passing sightseers were admiring, curious, disbelieving or hostile. When critical construction activities were taking place, guards had to be posted to stop this traffic.

The geotechnical team first prepared a site map identifying the slide boundaries and major cracks within the subsiding block, and surveyors were assigned to collect data on a daily basis. Data was collected daily from pre-existing instrumentation (inclinometers, piezometers, survey monuments) and compiled with the survey data.

Devil's Slide complex contains multiple slide planes, and identifying the depth of sliding for this event was critical. New inclinometers were needed inside the dropping block to identify the depth of this slide event. The decision of when a drill rig could move onto the subsiding block was difficult. A daily barrage of phone calls, office visits, newspaper

Figure 5. 1983 aerial photo of Devil's slide. Photograph by Lynn Harrison.

articles, radio commentary and letters came from management, the public and public officials, inquiring about the movement status of the landslide and demanding faster action. However, regard for the safety of the drill rig and crew precluded mobilizing until the subsiding block stabilized.

This portion of roadway had subsided numerous times over the past 50+ years, and the opinion that it should "just be repaved and opened up" was widespread. Owners of 4x4 vehicles demanded the opportunity to drive through as it was. The roadway was severely cracked and deformed, and rockfalls had brought rocks up to 8 feet in diameter onto the roadbed. The view from the roadway was daunting. The view from offshore was even more so, as it revealed that the dropped block was not only severely broken, but was also undermined in several areas, with the roadway unsupported (Figure 9). These photographs proved invaluable in providing a sobering perspective to those urging precipitous action.

Figure 6. Photograph of the slide after the 1995 landsliding episode, which resulted in a five-month road closure. Photograph by Robert Colin.

The 1995 landslide event mobilized only a portion of the larger slide, so permanent repair of the landslide was not feasible. The best that could be hoped for was a reconstruction that would provide a reasonably safe interim solution until the ultimate project was selected and constructed. The possibility that a permanent single traffic lane or a summer only route might be the end result was recognized. Bypass advocates, some outside and some inside Caltrans, wished for the determination that the road was not repairable and should be abandoned.

ANALYSIS OF ALTERNATIVES

The geotechnical team considered the following alternatives for mitigation:

1. *Retaining wall with piles and tiebacks* - This alternative was rejected due to the great depth of the slide. The depth of the 1995 actively sliding block was approximately 110 feet below road level. Piles are increasingly costly as the depth of landsliding increases.

Figure 7. Can't say we didn't try just about everything! Cartoon by Phil Farley, San Francisco Chronicle.

At depths approaching 100 feet, the required diameter and close spacing of the piles, and multiple rows of tiebacks generally exclude this as a practical alternative because of increasing cost and diminishing reliability. The pile alternative would only reinforce shallower slide planes. The known deeper slide planes beyond 100 feet would remain unsupported.

2. *Regrading the upper slopes* - This rockfall mitigation alternative was rejected because of the considerable slope height above the road (>400 feet) and stability concerns. Any slope work short of a massive regrading to a conventionally analyzed and stable configuration was viewed by the geotechnical team as akin to poking around in a hibernating bear's den with a sharp stick. Something best not attempted if there were any other alternatives, since we did not know just exactly what would be unleashed, but could be fairly certain it was likely to be unwelcome.

3. *Restoring the grade with lightweight fill* - Over the 50 years since roadway construction, the roadway has subsided more than 40 feet in the active slide area. There was too little confidence in the degree of residual stability present to consider adding weight to the dropped block. Additional weight could tip the balance and send the entire mass crashing downslope.

4. *Other ideas* - Public input suggested the following alternatives: abandon the roadway; suspension bridge; grade beams tied back into the slope; do nothing - just smooth out and repave. Each suggestion required consideration and a written response.

Figure 8. Regardless of road closure signs, gates, fences, and warning signs, pedestrian and bicycle traffic continued. Photograph by Robert Colin.

Figure 9. Offshore view of the slide. The dropped block was not only severely broken, but was also undermined in several areas, with the roadway unsupported. Photograph by Robert Colin.

5. *Reinforcement and anchoring of the sliding block* - Ultimately the following combination of techniques was selected to restore the roadway:

• *Rock net:* A double layer of gabion wire was secured to the slope with a network of wire ropes, restrained by rock anchors on 30 foot centers, as the first order of work (Figure 10).

• *Rock dowels:* The 500-foot wide subsiding roadway block was fissured into a number of smaller blocks. To tie the mass together, several rows of 30-foot long rock dowel triplets were placed in the roadway, one vertical, one inclined at 45° into the slope and another inclined at 45° toward the sea cliff. Rock dowels were initially used in the early 1980's at this site, and consisted of #9 grade 60 reinforcing bar inserted into a 4 inch diameter grouted hole. Centralizers were placed at 10-foot increments. The rock dowels are passive reinforcing elements, and are not tensioned. A total of 300 dowels were installed (Figure 11).

• *Rock anchors:* Seventy rock anchors, up to 60 feet in unbounded length, were installed at three levels below the roadway (Figure 12). Upon completion of the rock anchor installation, fiber reinforced shotcrete was applied to the upper 30 feet of slope below the road to prevent "dribble" of smaller material, and consequent progressive undermining of the roadway.

Both the rock dowels and rock anchors served to tie together only the upper 30' to 50' of the dropping block, and addressed only the problem of disintegration of the upper portion of the actively sliding block. They did not address global slope stability.

• *Roadbed regrading:* After installation of the rock net, rock dowels and tie backs, the roadway on either side of the dropped block was regraded to conform to the subsiding block.

• *Warning system:* During construction, Caltrans management asked the geotechnical and

Figure 10. Rock net formed by a double layer of gabion wire secured to the slope with a network of wire ropes, restrained by rock anchors on 30 foot centers. Photograph by Robert Colin.

design team to develop a warning system. Extensometers were placed in conduit just under the roadway pavement and across the rock net. These were wired into data acquisition systems with automated responses. When slide movement exceeds threshold values, they will turn on emergency lights and message systems on both sides of the roadway notifying motorists that the road is closed, and send an automated notice to Caltrans 24 hour Emergency Response Center.

Caltrans public information officers provided daily press briefings during the emergency proceedings. They requested a daily status report from the geotechnical team, and assistance in responding to the many inquiries and suggestions received. The geotechnical team compiled data into tables and charts, preparing maps, photo boards and exhibits for briefings to management, the press and local officials.

Figure 11. Several rows of 30-foot long rock dowel triplets were placed in the roadway, one vertical, one inclined at 45° into the slope and another inclined at 45° toward the sea cliff. Rock dowels consisted of #9 grade 60 reinforcing bar inserted into a 4 inch diameter grouted hole. Photograph by Robert Colin.

Elected and appointed officials requested and received briefings and tours of the landslide site from the geotechnical team. A twelve-member delegation of local geolo-

Figure 12. Seventy rock anchors, up to 60 feet in unbounded length, were installed at three levels below the roadway. Photograph by Robert Colin.

gists and engineering geologists were given a briefing and site tour at the request of the San Mateo County Board of Supervisors. A number of public meetings were held, and the geotechnical team was a participant in these very lively events, where citizens weary of decades of frustration freely spoke their opinions of each other, elected officials, and the State Highway Department. At one event, a bomb threat was called in and dogs were escorted through the building to check for explosives. The McNeil-Lehrer news hour aired a lengthy segment on the landslide, the 30-year history of litigation, and the status of repair efforts.

Reconstruction was completed by June 30, 1995 (Figure 13). A day later, an opening ceremony was held, with ribbon-cutting and great sighs of relief.

METHODS FOR RESPONDING THE PUBLIC INTEREST

The response team learned a lot during the 1995 emergency. Some of the lessons were technical, but there were many about interaction with the public and the media. In retrospect, I offer the following suggestions for those of you that will have the opportunity of handling the next emergency.

1. Identify a project spokesperson that is not actively working on the project, and provide him or her with frequent updates for release to the press. Give clear instructions on his or her range of authority; which information and opinions are to be released, and which questions require direct response from management or the design team. Establish a location where information can be reviewed by the media and the public during normal office hours, such as raw data, photographs, and prior reports. Post a monitor to prevent disappearance of materials, provide a mechanism for copies, including collection of fees if appropriate.

2. Explaining real or apparent discrepancies in information, time estimates, cost, or project plans, will be a major time drain and will erode your credibility. In other words, be consistent and cautious in your professional work. Keep team members and management clients informed so a consistent message is communicated throughout.

3. Create databases, with suitable charts and graphs for monitoring project timelines. This will be time consuming when setting up, but there will be ample pay back in subsequent swift response to inquiries. Keep them updated, using non-project staff if at all possible.

4. Establish a policy about what information will be released, and when. In government work, all information is available for public access, but the release of ongoing work products is not required, nor is it generally advisable since release of incomplete analysis or preliminary conclusions can at best lead to confusion. On the other hand,

refusal to respond to all inquiries by claiming "ongoing studies" will lead to justifiable accusations of non-responsiveness, escalating pressure as requesters go higher up the political food chain, and creation of unnecessarily adversarial conditions. Expeditiously release all information you can, and give reasonable predictions about the date when studies will be completed and released.

Figure 13. View of the reconstructed section, which was completed on June 30, 1995. Photograph by Robert Colin.

5. Expect review of your work by outside engineering geologists representing other public agencies, project advocates and opponents, and those that are professionally curious. Make as much beneficial use of this as you can; you will receive other people's insights and opinions, which may assist you in your work. In my experience, most of this input will be professional and courteous. Consulting engineering geologists can be very helpful in explaining the problem, range of solutions, and likely outcomes to their clients. When you gain their trust and concurrence, they can be invaluable in reconciling their clients to unwelcome geologic realities. Those acting from unworthy motives may also appear. Do not dwell on their negative comments; time and exposure usually reveal all. Your severest critics, whatever their motives, may have useful insights.

6. Be forthcoming to the press and your peers, but be prudent. Revealing confidential information in the context of a friendly discussion can have severe adverse results.

7. Respect the power of the media; with selective editing they have the ability to make you sound like an extraordinarily wise geotechnical practitioner, or an unmitigated fool. Most are committed to fair, factual reporting, but a bad apple falling prey to the lure of sensationalism can leave your reputation in ruins.

8. Expect a public meeting. Prepare thoroughly, have your peers, friends or spouse put you through a practice grilling. They will find it entertaining, and you will get

valuable preparation if they are sufficiently ruthless. Have background information with you, summarized for quick reference—count on the fact that your memory will fail you. Regardless of preparation, you will be asked a question you cannot answer. Admit you do not know, write down the name and telephone number of the person asking the question, commit to finding out and providing an answer, and follow up. The public will forgive you (eventually) for not having an answer at hand in a difficult situation, but they will never forgive you for making one up or lying (often charitably referred to as "winging it"). Develop a thick skin. When issues affect people's lives closely, they may speak harshly of opinions they do not want to hear. Remember you will walk away from this project. Those directly affected will have to live with the results. Refuse to respond to personal abuse.

9. Protect the site, instrumentation and yourself. In difficult situations, instrumentation will have to be protected with cages, locks, metal cans or concrete bunkers. Instrumentation has been damaged by gun fire, rain gauges punched out after climbing on top of chain link cages, survey monuments removed, rocks dropped down inclinometers and piezometers, extensometers cut. It can happen to you and the loss of both time and database is severe; protect your field installations. Attention to personal security is strongly advised. Take a buddy with you into the field (in some cases you may want one that bites!). Do not release your home phone number or address. Receive mail at the office; receive messages via pager or cell phone.

10. Above all keep your sense of perspective. You are privileged to work on a project that is challenging and important. Your work will make a difference in people's lives. In six months or a year, no one will remember your trivial mistakes, or the rude things said about you. A good solution to a hard problem will be remembered, and you will have been instrumental in developing it.

ACKNOWLEDGEMENTS

A Caltrans team accomplished the 1995 repair of Devil's Slide. Some of the team members were Grant Wilcox, Engineering Geologist; Heng Tay, Design Engineer; Wyatt Kaelin, Construction Engineer; and the author. Construction was performed by Ford Construction Co., and Jensen Drilling Co. Slide monitoring has been admirably conducted and maintained for many years by De Wayne Nakayama, John Morgan, Wendy Conway, Robert Banks and Jim Cunningham (all with Materials and Research Engineering Associates). Subsurface exploration has benefited greatly from the wisdom and guidance of DeWitt Thompson from Materials and Research Engineering. David Heyes, engineering geologist, has provided mentoring, consultation and guidance to the author on this landslide as well as many others, since 1983. Caltrans photographer Robert Collins provided the 1995 construction photographs.

Roy Kroll and Horacio Ferriz provided invaluable peer review for this paper. Their advice, encouragement and constructive comments are gratefully acknowledged.

AUTHOR PROFILE

Joan Van Velsor is a California Certified Engineering Geologist with 20 years of geotechnical experience with the California Department of Transportation. She is Chief of Caltrans Geotechnical Services.

SELECTED REFERENCES

Beeston, H.E. and Gamble, J.H. 1980 Engineering geology of the Devil's Slide at San Pedro Mountain, San Mateo County, California: California Department of Transportation, 111 Grand Ave, Oakland, California.

Brabb, E.E. and Pampeyan, E.H., 1972, Preliminary geologic map of San Mateo County California: U.S. Geological Survey Miscellaneous Field Studies Map MF-344

Coverdale, W.H. 1906. Report on the Ocean Shore Railway San Francisco to Santa Cruz California: W.H.Coverdale & Company, Inc. (New York, New York).

Lawson, A.C., 1908, The California earthquake of April 18, 1906, Report of the State Earthquake Investigation Commission: Carnegie Institution, (Washington, D.C.) ,v.1, 451 p, v.2, 192p, 25 maps, 146 plates, 15 plates

Pampayaen, E.H., 1981, Geology of the Montara Mountain quadrangle, San Mateo County, California: U.S. Geological Survey Open File Report OFR-81-451, Scale 1:12,000

Wagner, J.R., 1974 The Last Whistle (Ocean Shore Railroad): Howell-North Books, (Berkeley, California), 135 p.

For further information about this fascinating project, the reader may want to visit the following web pages: *www.dot.ca.gov/dist4/dslide/dsdeis.html*, *www.dot.ca.gov/dist4/dslide*, *www.tunnel.org/*, *www.montara.com/* (has a 24 mini cam directed at Devil's slide, but is frequently fogged in), *www.montara.com/NuMontara/LatestMountainNews.html*


ASSOCIATION OF ENGINEERING
AEG
GEOLOGISTS

INSTRUMENTATION FOR SLOPE MONITORING

WILLIAM F. KANE[1] AND TIMOTHY J. BECK[2]

ABSTRACT

Remote monitoring of slope movement using electronic instrumentation can be an effective approach for many unstable or potentially unstable slopes. Water levels can be observed using vibrating wire piezometers. Movements and deformation can be determined with "in-place" electrolytic bubble inclinometers and tiltmeters, extensometers, and time domain reflectometry (TDR). All of these instruments can be attached to a programmed on-site datalogger. If pre-determined movement thresholds are exceeded, the datalogger can collect readings at selected time intervals and trigger an alarm or initiate a telephone message or page. These systems are self-contained using cellular telephone communications and batteries charged by solar panels.

Five case studies in Central and Northern California illustrate the use and flexibility of this technology in monitoring slope stability problems. In the first two, TDR is used as a field method to determine the depth to slide planes and determine the extent of the landslide. The other three case studies use a variety of instrumentation installed on-site and monitored remotely using dataloggers. Two studies used the datalogger to trigger an alarm to notify personnel of significant slope movement.

[1] KANE GeoTech, Inc.
P.O. Box 7526
Stockton, CA 95267-0526
wkane@kanegeotech.com

[2] California Dept. of Transportation
Transportation Laboratory
5900 Folsom Boulevard
P.O. Box 19128-0128
Sacramento, CA 95819
Tim_Beck@dot.ca.gov

INTRODUCTION

Many options are available for monitoring unstable and potentially unstable slopes. These options range from inexpensive, short-term surveys to more costly, long-term monitoring programs. The remote location of many unstable slopes has created a need for systems that can be accessed remotely and provide immediate warning in case of failure. Advances in electronic instrumentation and telecommunications now make it possible to monitor these slopes economically.

Slope stability and landslide monitoring involves selecting certain parameters and observing how they change with time. The two most important parameters are groundwater levels and displacement. Slope displacement can be characterized by depth of failure planes, direction, magnitude, and rate. One or all of these variables may be monitored. Conventional slope monitoring utilizes a single method or a combination of methods. Piezometers allow the determination of water levels. Surveying fixed surface monuments, extensometers, inclinometers, and tiltmeters allows determination of direction and rate of slope movement and depth, and areal extent of the failure plane. Extensometers provide an indication of displacement magnitude. Manually operated probe inclinometers are the most common means of long-term monitoring of slopes.

Available electronic instrumentation includes vibrating wire piezometers, electrolytic bubble inclinometers and tiltmeters, and time domain reflectometry (TDR) for sensing changes in slope conditions. This instrumentation can be monitored by technicians in the field, or remotely by dataloggers and telemetry. By combining instrumentation types, a full array of stability parameters can be observed. Computer software is available to quickly plot data, allowing immediate assessment of slope conditions.

Critical facilities (e.g., dams, quarries, highways, housing developments) adjacent to unstable slopes have created a need for monitoring systems that can provide immediate warning when movement occurs. Advances in telecommunications and electronic instrumentation now make it possible to economically monitor slope movements remotely. Many types of sensors and data transmission systems are available.

The purpose of this paper is to present case studies of monitoring programs and systems installed in Central and Northern California. These systems use electronic sensors such as extensometers, tiltmeters, inclinometers, and TDR. Telemetry was by either cell phone or hard-wire phone. Power was provided by rechargeable lead/acid batteries and solar panels.

INSTRUMENTATION FOR LANDSLIDE MONITORING

The critical data required from a slope monitoring program are the water levels in the slope, and the depth and rate of deformation and movement.

Water Levels

The simplest method of monitoring water levels in a slope is to drill and case a borehole. The water surface is located by dropping a measuring tape down the boring. Although useful for simple water table situations and where monitoring is required on an infrequent basis, other methods may be more desirable. These methods involve the use of more sophisticated mechanical or electrical instruments.

Vibrating wire piezometers. A vibrating wire piezometer (Figure 1) works on the same principle as tuning a guitar or piano (SINCO, 1994). A steel wire is stretched over a distance. One end of the sensing wire is attached to a diaphragm that can be deformed by water pressure entering through a porous tip. The natural frequency of the wire is a function of the tension it is under. The wire is set to vibrate by "plucking" it with an electromagnetic field. The wire is plucked using variable excitation frequencies and then allowed to return to its natural frequency. The magnetic coil then acts as a sensor that is used to "count" the number of vibrations. As the tension in the wire changes, the frequency becomes lower or higher. The frequency of vibration can be sensed by the electromagnetic coil and is transmitted to a readout device. The output signal is then converted into units of pressure or head.

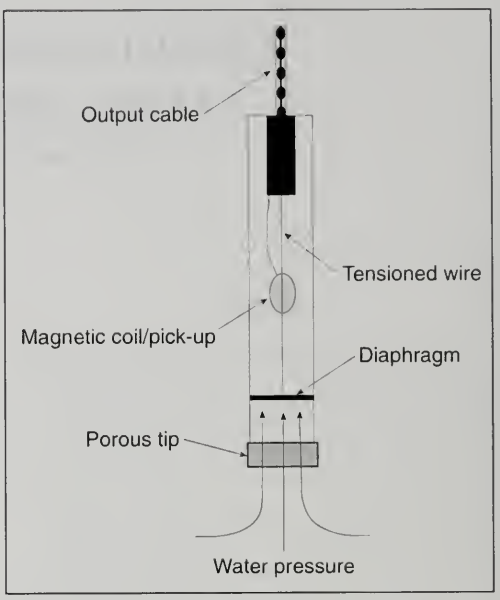

Figure 1. Schematic of a vibrating wire piezometer.

Because some changes in the diaphragm could result from changes in barometric pressure, two piezometers are required to make accurate groundwater measurements. One should read atmospheric pressure and the other downhole pressure. By subtracting the atmospheric from the downhole pressure, the true changes due to water level fluctuations can be obtained.

Vibrating wire piezometers should be considered at sites where frequent groundwater measurements are required. For example, a site where rapid groundwater fluctuations are suspected or where measurements are required during a critical event (e.g., rainfall, dam release) is ideal for using the device. Vibrating wire piezometers cost approximately US $350 to $500 each.

Slope Displacement/Movement Measurement

Probe inclinometers, "in-place" inclinometers, tiltmeters, extensometers, and TDR can be used alone or in combination to monitor slope movement (Dunnicliffe, 1993). Probe inclinometers require manual operation, whereas the other sensors can

be read electronically. The electronic sensors can be coupled with a datalogger for automated data collection. These automated systems also can be combined with telemetry to allow remote data collection. Additional programming of the remote data collection system can be used to trigger a warning of critical situations.

"In-place" inclinometers and tiltmeters. In-place inclinometers and tiltmeters can detect new movement, an acceleration of movement, and the direction of movement. In-place inclinometers are installed in a borehole cased with inclinometer casing. The wiring for the inclinometer can be buried and the boring covered with a locking cap to vandal-proof the installation. Tiltmeters are mounted at the ground surface. They are an option for those sites that are too steep for a drill rig or if the project budget does not allow for drilling. Tiltmeters also can be covered with a vandal-proof enclosure, and wires can be buried.

Electrolytic bubbles are used in tiltmeters and "in-place" inclinometers. An electrolytic bubble is similar to an ordinary "bull's eye" level, as seen in Figure 2. The fluid in this level, however, is an electrical conductor that moves between three electrical nodes. One node is located at the base of the vial (B), and two are located on the top (A and C) at an equal distance from node B. An electrical current is applied to the nodes and the resistance through the fluid is measured. As the vial tilts clockwise, the resistance between A and B increases and the resistance between B and C decreases. The change in resistance can be measured, and is directly proportional to the angle of tilt. Prices for tiltmeters and "in-place" inclinometers range from US $400 to $1,000.

Extensometers. Simple mechanical extensometers use a steel wireline firmly connected to a fixed location on the slope face on one end and to a track-mounted weight, located off the slide, on the other end. Movement of the slope pulls the weight along the graduated track. The amount and rate of movement can then be measured manually. Extensometers are very inexpensive, but critical events can be missed if readings are not taken in a timely fashion. These installations are also susceptible to vandalism and animal damage.

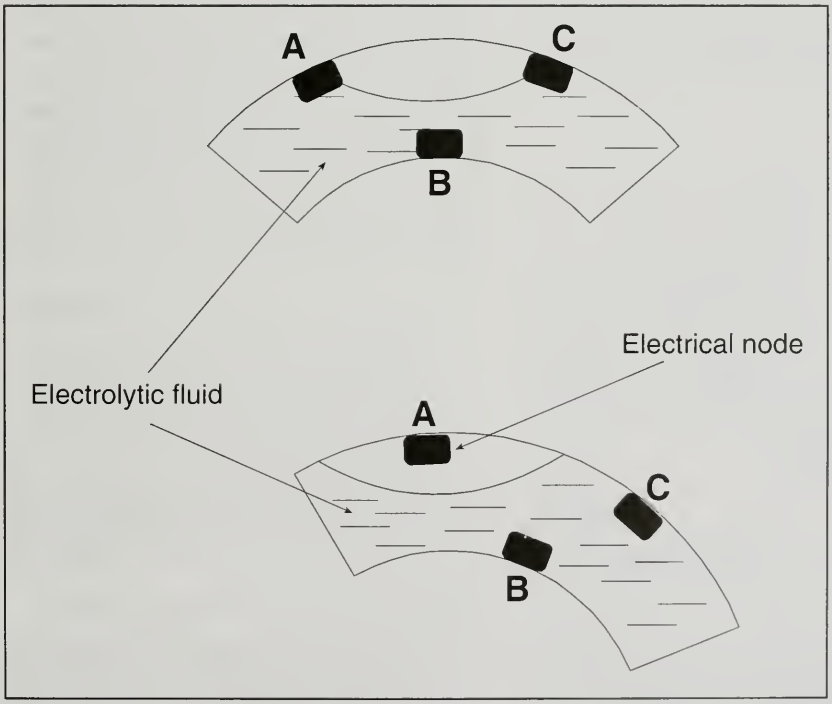

Figure 2. Schematic of an electrolytic bubble level.

Extensometers can also use potentiometers to measure movement. Much like the rheostat controls of a model electric train, the extensometer uses a vari-

able resistance mechanism to measure the amount of displacement. A moveable arm makes an electrical contact along the fixed resistance strip as shown in Figure 3. The resistance of the circuit is based on the position of the slider arm on the resistance strip. A regulated DC current is applied and the output voltage corresponds to the amount of displacement along the resistor due to ground movement. The wiring and sensor can be buried to make it vandal and animal proof. Potentiometer-based extensometers cost approximately US $800.

Time domain reflectometry (TDR). Time domain reflectometry (TDR) is a relatively new approach to monitoring slope movement (Beck and Kane, 1996; Kane and Beck, 1994, 1996a, 1996b; Mikkelsen,1996; O'Connor and Dowding, 1999). Originally developed to locate breaks and faults in communication and power lines, its first geotechnical application was around 1980 when it was used to locate shear zones in underground coal mines (Wade and Conroy, 1980). This technology uses a coaxial cable and a cable tester. The basic principle of TDR is similar to that of radar. The cable tester sends an electrical pulse down a coaxial cable grouted in a borehole (Figure 4). When the pulse encounters a break or deformation in the cable, a portion of the energy is reflected. The reflection shows as a "spike" in the cable signature. The relative magnitude and rate of displacement and the location of the zone of deformation can be determined immediately and accurately. When compared to previous cable readings, the size of the spike increase (i.e., the amount of energy reflected) correlates roughly with the magnitude of movement, although there is limited research on exact correlations (O'Connor and Dowding, 1999). A laptop computer is connected to the tester and cable signatures are transferred to disk for future reference.

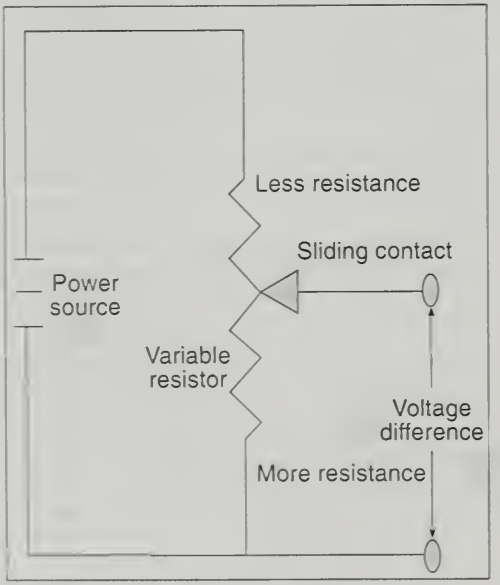

Figure 3. Schematic diagram of a variable resistance potentiometer used in a slope to monitor movement. The sliding contact moves within joint to change the voltage output of the extensometer as the slope moves.

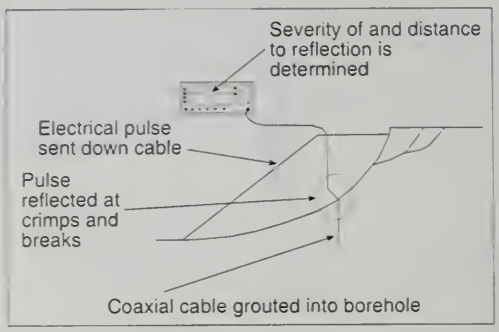

Figure 4. Principle of time domain reflectometry, showing how a deformed cable results in a signature "spike" on the cable tester screen.

Some of the advantages of TDR over probe inclinometers are the following:

1. Coaxial cable costs less than inclinometer casing.
2. TDR readings take minutes, whereas inclinometer readings can take over an hour to complete.
3. The coaxial cable can be extended to a convenient reading location off the slope or away from a highway.
4. TDR readings can easily be automated.
5. Slope movement can be determined immediately during data collection, rather than waiting until data is plotted on computer.

TDR does have some disadvantages as well:

1. TDR cannot determine the actual amount of movement. Relative amounts are estimated by comparing increases in signature spike size over time.

2. The direction of movement cannot be ascertained from a TDR signature.
3. The cable must be deformed before movement can be located. Simple bending of the cable, without damage, will not indicate any movement.
4. If water infiltrates a TDR cable, it will change the cable's electrical properties and may make signatures difficult to interpret.

Coaxial cable costs from US $0.20 to $2.50 per foot. Cable testers for reading cable signatures vary from about US $3,500 for a used unit to about US $10,000 for a new one.

TDR may also be used as a piezometer to monitor water levels by allowing water to enter the cable through holes drilled in the cable jacket. Experience to date is limited, and it appears that it cannot measure deformation beneath the water surface because of changes in the electrical properties of the cable due to water infiltration (Kane and Parkinson, 1998).

AUTOMATED AND REMOTE DATA ACQUISITION

Automated data acquisition can be done with a datalogger and electronic sensors. This type of system requires periodic visits to the site to download the data. Remote data acquisition equipment includes a datalogger, multiplexer, communication devices, and a power source. In addition, software is necessary to program and interact with the datalogger.

Datalogger

A datalogger is essentially a small computer and voltmeter with memory. It is programmed to do certain tasks. The Campbell Scientific CR10X logger used for this work can be programmed to output specified voltages over certain durations, read voltages, and store values (CSI, 1991a, 1991b). It can also be programmed to do calculations and store the results, for example, converting the readings of a piezometer to feet of head. Dataloggers cost about US $1,200.

Instruments are wired to connections, or "ports", on the logger. Control ports and excitation ports can be programmed to turn on peripheral equipment, such as cell phones or cable testers. Other ports are wired to the sensors and are used to measure output voltages.

The greatest advantage in using electronic instrumentation is the fact that dataloggers can be programmed to perform different tasks automatically. For example, a threshold magnitude of sensor movement can be programmed into the datalogger. If this threshold were exceeded, then the datalogger would trigger an action, such as activating a siren or a flashing-light alarm. In most cases this action is a phone call using an automatic telephone dialer, such as those commonly used for home security systems. They are readily available and cost around US $400. They can be programmed to deliver a recorded message or page multiple telephone numbers.

Multiplexer

A multiplexer allows many sensors to be attached to a single datalogger. A single multiplexer can have as many as sixteen instruments attached to it, and multiplexers can be wired to one another for a theoretically unlimited number of instrument hook-ups. The multiplexer is wired to a single set of ports on the datalogger. A set of contacts in the multiplexer switches between each sensor attached to it. The data is collected sequentially by the logger. Multiplexers can be purchased for about US $600.

Communications

There are several alternatives for communication with a datalogger. "Hardwired" telephone lines are the most reliable, but not always available. Alternatively, cellular and satellite telephones can be used, as well as radio transceivers. A telephone line only requires a modem to transmit data and receive instructions. The other methods require modems and cell phones or radio transceivers. Modems cost about US $400, whereas cellular telephones with antennas can be purchased for about US $750 plus monthly service fees. Radio and satellite systems can run about US $2,000 and $5,000 respectively.

Power

Power requirements vary depending on the number of instruments and the communication device. Ideally, power is available at the site but that is often not the case. A small system with a phone line and one or two sensors requires only a small rechargeable gel-type battery. A larger system with cellular phone and cable tester requires a 12V deep cycle marine battery. The battery is recharged by regulated solar panels. Regulated solar panels cost approximately US $250. Batteries run from US $25 to $100.

Software

Specialized software is required to process the raw data. When TDR cables are read in the field, TDR cable "signatures" (i.e., analog readings) can be digitized and downloaded to a laptop computer using the software from Tektronix (1994) or CSI (2000). Plotting several TDR signatures as a function of depth on the same plot requires the user to either write a specialized spreadsheet or use a commercially available program such as TDRPlot2000 (Kane and Parkinson, 1998). Piezometer data are best viewed with a spreadsheet. Electrolytic bubble tiltmeters and inclinometers used in the work described here were plotted using TBASEII (AGI, 1997).

The PC208W software package was developed to program, and communicate with, dataloggers (CSI, 1997). The program allows the user to write code for datalogger control, to contact the remote station automatically or manually, to monitor instrument readings, and to download data.

Security

When selecting a monitoring approach, one has to take instrument security in consideration. Weather and vandalism destroy equipment, so it is worthwhile to invest on protective measures. Weatherproofing the instrumentation can be done using a fiberglass enclosure that is sealed to the elements. These are available from instrument manufacturers at prices ranging from US $200 up to about $800. A protective enclosure often is necessary to prevent vandalism. An enclosure can be as simple as a 2-ft (0.6-m) corrugated metal pipe with a steel plate lid. Commercially available steel control boxes, costing about US $800, provide excellent protection.

INSTRUMENTATION CASE STUDIES

El Niño storms of January and February 1998 caused a large number of landslides in California (DMG, 1998; USGS, 1998; Bedrossian and Etzold, 1999). Repair of these landslides required immediate action in often hazardous conditions. At some locations, the relative ease and cost-effectiveness of TDR allowed the determination of the depth to the shear plane. At other locations, remote automated monitoring/warning systems were required during slope reconstruction to assure the safety of workers and the general public. The locations of the sites described below are shown in Figure 5.

Figure 5. Location map of case studies.

Mussel Rock landslide, San Mateo County

Continued long-term movement of the Mussel Rock landslide necessitated its repair before construction of a park and golf course complex. Repair measures required determining the location of the depth to the failure. Initial plans called for a site investigation of five borings and the installation of a single inclinometer to monitor movement. Because of cost advantages, however, it was decided to use TDR cables in all five borings. The TDR was monitored periodically for a fraction of the cost of monitoring the single inclinometer hole. Because five borings were monitored, instead of a single inclinometer casing, the depth and areal extent of the slide plane was determined precisely, as shown in Figure 6

Figure 7 contains an example of TDR signatures from two cables. Cable failure occurred in cable B-15 accompanied by a small deformation in cable B-18. Subsequently, deformation increased in cable B-18 over time. Cable B-19 showed a similar pattern indicating progressive movement along the slide plane up the slope. Cables B-16 and B-17 showed no change, thus constraining the location of the head and toe of the slide, as shown in Figure 7.

Highway 1, Mendocino County

A portion of California Highway 1 crosses a landslide complex approximately 200-m (650-ft) wide, just north of the town of Elk. The depth to the

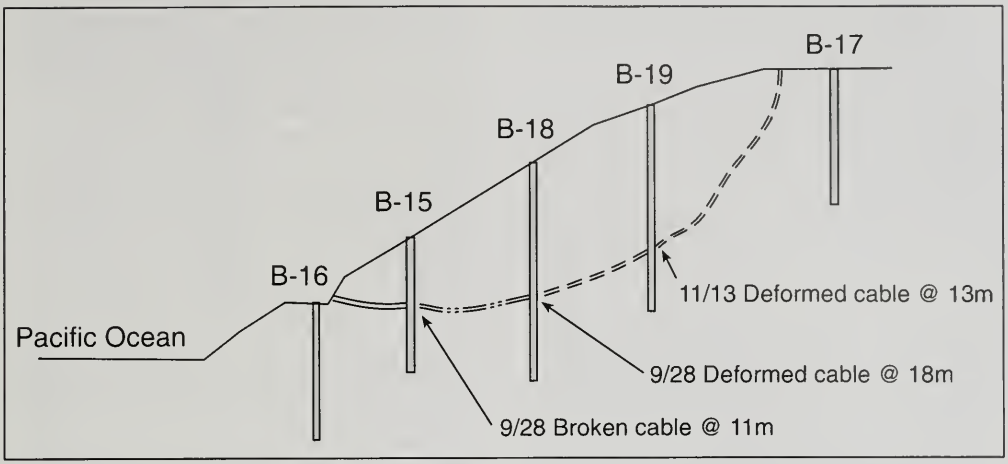

Figure 6. Relative location of TDR boreholes in the Mussel Rock landslide, San Mateo County.

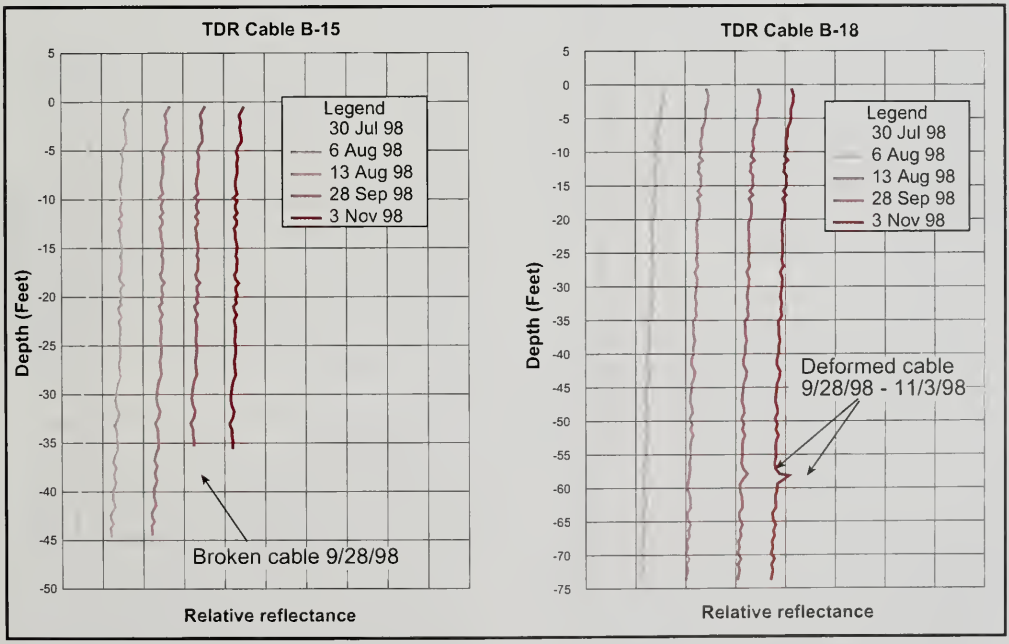

Figure 7. TDR cable signatures from the Mussel Rock landslide. The cable signatures are separated to show changes over time more clearly; ordinarily the cable signatures would plot on top of each other because relative reflectance of the cable does not change with time.

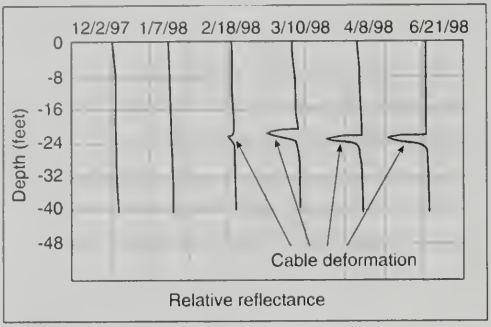

Figure 8. TDR cable signatures from Mendocino County. The cable signatures are separated to show changes over time more clearly; ordinarily the cable signatures would plot on top of each other because relative reflectance of the cable does not change with time.

failure plane was required to design the fix for this slide. In November 1997, a TDR cable was grouted in a borehole drilled in the center of the southbound lane. The cable was extended within a groove in the pavement off the shoulder of the road, allowing readings to be taken without stopping traffic. This saved a significant amount of labor cost and increased worker safety. The slide complex was activated as the winter rains infiltrated into the slide mass. The cable deformed at a depth of 6.4-m (21-ft), as shown in Figure 8, accurately locating the depth to the shear zone at the soil/rock interface. A second cable was installed in the slide later that winter. It failed to detect any movement, indicating that the slide movement had ceased.

Interstate 15, Riverside County, California

The California Department of Transportation (Caltrans) installed a monitoring system in oversteepened slopes in a sand pit adjacent to Interstate 15 in Riverside County. Two TDR cables 52-m (170-ft) deep and two vibrating wire piezometers were installed between Interstate 15 and the pit. A remote data collection system was also installed, including a datalogger, piezometer signal conditioner, a multiplexer connected to the TDR cables, and a cell phone and modem for data transmission. Power was supplied by a 12-volt battery and 20-watt solar panel. Because the cell phone required significant current, it could not be kept on at all times without draining the battery completely. Instead, it was turned on for intervals during the day for automated data acquisition.

The system was programmed to read the two piezometers every morning, calculate the head of water present in the slope, and store the values in memory. It then turned on the cable tester and sequentially accessed and digitized the cable signatures from the TDR installations. After data collection, the cell phone was turned on and a computer in Sacramento, about 560-km (350-mi) away, dialed the cell phone number and downloaded the data. The piezometer data was plotted using a spreadsheet program and the TDR data with TDRPlot2000. Data was collected for over a year before the system was removed for installation at another site. The data showed no change in slope conditions during the monitoring period.

State Highway 17, Santa Cruz County, California

In January 1998, a landslide/debris flow destroyed a small Santa Cruz County road adjacent to California Highway 17. Caltrans constructed a soldier pile wall at the head of the slide to protect Highway 17 from future movement. Caltrans was concerned that progressive failure at the head scarp would jeopardize the stability of the wall.

A monitoring system consisting of a datalogger, cell phone, and phone dialer was installed. The system monitored a tiltmeter attached to the wall, and an extensometer. The extensometer was attached to the wall at one end and anchored near the head scarp at the other, similar to the diagram shown in Figure 3b. The datalogger was programmed to monitor both instruments and determine threshold movement. If the threshold were exceeded, the phone dialer would immediately notify personnel by means of pagers. The system also was automated to download data everyday to an office computer. No significant movement of the wall had occurred to January 2000.

State Highway 1, Monterey County, California

Numerous slides along California Highway 1 in San Luis Obispo and Monterey Counties closed portions of the road throughout the winter of 1998. Grandpa's Elbow landslide in Monterey County was a reactivated older landslide complex. To protect motorists and clean-up crews, Caltrans instrumented the slide with four downhole, "in-place", electrolytic bubble inclinometers attached to a coaxial cable in a 200-ft borehole. The inclinometers were positioned at depths of 150, 100, 50, and 10

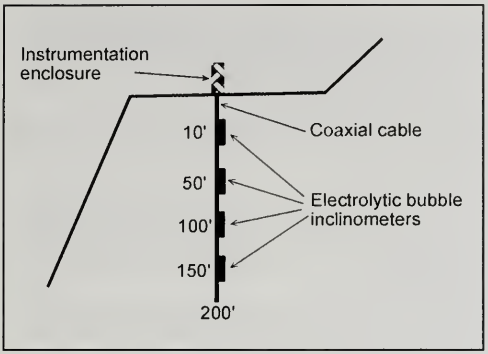

Figure 9. Schematic diagram showing the positions of electrolytic bubble inclinometers attached to the coaxial cable.

feet (Figure 9). Any movement of the slide changed the tilt of the inclinometers and triggered a warning

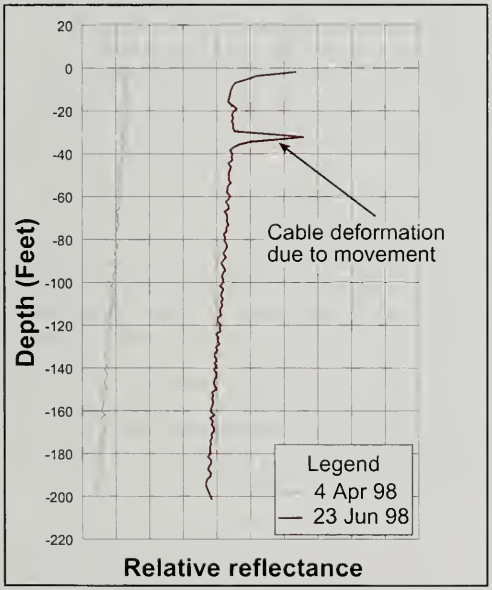

Figure 10. TDR cable signatures showing the deformation that activated the alarm on State Highway 1, Monterey County. The cable signatures are separated to show changes over time more clearly; ordinarily the cable signatures would plot on top of each other because relative reflectance of the cable does not change with time.

by hard-wire telephone line. The system could also be monitored remotely by computer and modem.

Soon after installation, slight movement of the inclinometers triggered the telephone dialer, and personnel were paged. TDR cable readings showed the development of a spike in the cable at a depth of 9-m (30-ft), indicating movement (Figure 10). Observation of tension cracks in the ground surface verified the fact that some movement had taken place. Because of the shallow nature of the movement and its location relative to the roadway, there was no imminent danger, and no action was taken.

CONCLUSIONS

Case studies have shown that basic TDR slope monitoring, using TDR cables alone at a fraction of the cost of inclinometers, can delimit sliding zones and determine the depth to a failure plane. Other examples showed how TDR can be combined with other instrumentation to collect almost real-time data remotely, and also trigger alarms when slope movement occurs.

Sensors, including vibrating wire piezometers, electrolytic bubble inclinometers and tiltmeters, and TDR are readily available to monitor groundwater and ground movement for slope stability. Advances in electronic technology, coupled with economical prices, make remote monitoring cost-effective and a powerful tool in slope stability work. This instrumentation will provide much of the information necessary not only to monitor slopes, but to obtain some of the necessary parameters for mitigation and remediation.

Although there are many manufacturers of various instruments described in this paper, the authors do not specifically endorse any of these products. Design philosophies combined with suitability to particular problems will dictate the appropriate method.

AUTHOR PROFILES

Dr. William F. Kane holds a B.A. degree in geology and M.Sc. and Ph.D. degrees in civil engineering. He is President of KANE GeoTech, Inc., Stockton, California, which he founded in 1997. Dr. Kane has consulted and done research in the areas of rock and soil mechanics, ground subsidence, and slope stability. He has taught civil engineering at the University of the Pacific, the University of Alabama,

and the University of Tennessee, where he founded and served as the first director of their Institute for Geotechnology. He has authored or co-authored approximately 80 technical papers and reports. Dr. Kane is a registered professional engineer in the State of California and a registered professional geologist in the State of Tennessee.

Timothy J. Beck is an engineering geologist with KANE GeoTech, Inc., Stockton, California. He also has worked for the California Department of Water Resources and has 15 years of service with the California Department of Transportation as an engineering geologist. He is one of the pioneers in using time domain reflectometry for monitoring slope movements. He has authored or co-authored approximately 10 technical papers and reports on engineering geology and instrumentation. Mr. Beck is a registered geologist and certified engineering geologist in the State of California.

SELECTED REFERENCES

AGI (Applied Geomechanics), 1997, TBASEII user's manual: Applied Geomechanics, Inc. Santa Cruz, CA.

Bedrossian, T. L. and Etzold, R., 1999, The 1998 storm-related events, a response: California Geology, v. 52, p. 4-12.

Beck, T. J. and Kane, W.F., 1996, Current and potential uses of time domain reflectometry for geotechnical monitoring: Proceedings, 47th Highway Geology Symposium (Cody, Wyoming), Wyoming Department of Transportation, p. 94-103.

CSI (Campbell Scientific), 1991a, CR10X measurement and control module operator's manual: Revised 5/97, Campbell Scientific, Inc. (Logan, UT).

CSI (Campbell Scientific), 1991b, Campbell Scientific TDR soil moisture measurement system manual: Revised 2/92, Campbell Scientific, Inc. (Logan, UT).

CSI (Campbell Scientific), 1997, PC208W datalogger support software instruction manual: Revision: 5/97, Campbell Scientific, Inc. (Logan, UT).

CSI (Campbell Scientific), 2000. PCTDR software instruction manual: Campbell Scientific, Inc. (Logan, UT).

CDMG (California Division of Mines and Geology), 1998, Landslide reports from various state offices between February 3,1998 and April 30,1998: California Division of Mines and Geology Web Page, http://www.consrv.ca.gov/dmg/minerals/98landslide/24.htm.

Dunnicliff, J., 1993, Geotechnical instrumentation for monitoring field performance: John Wiley & Sons, Inc., (New York, New York) 577 p.

Huang, F.-C., O'Connor, K. M., Yurchak, D. M., and Dowding, C. H., 1993, NUMOD and NUTSA: software for interactive acquisition and analysis of time domain reflectometry measurements: U. S. Bureau of Mines Information Circular 9346, 42 p.

Kane, W. F. and Beck, T. J., 1994, Development of a time domain reflectometry system to monitor landslide activity: Proceedings, 45th Highway Geology Symposium (Portland, Oregon), p. 163-173.

Kane, W. F. and Beck, T. J., 1996a, Rapid slope monitoring: Civil Engineering, American Society of Civil Engineers, New York, v. 66, p. 56-58.

Kane, W. F. and Beck, T. J., 1996b, An alternative monitoring system for unstable slopes: Geotechnical News, v. 143, p. 24-26.

Kane, W. F. and Parkinson, W. A., 1998, Remote landslide monitoring including time domain reflectometry: Short Course Manual, KANE GeoTech, Inc. (Stockton, CA).

Mikkelsen, P. E., 1996, Field instrumentation: in Turner, A. K., and Schuster, R. L. (eds.), Landslides. Investigation and Mitigation: Transportation Research Board, Special Report 247, National Academy Press, Washington, DC, p. 278-316.

O'Connor, K. M. and Dowding, C. H., 1999, Geomeasurements by pulsing TDR cables and probes: CRC Press (Boca Raton, Florida), 402 p.

SINCO (Slope Indicator Company), 1994, Applications guide: Slope Indicator Company (Bothell, WA), 2nd Edition.

Tektronix, 1994, 1502B metallic time domain reflectometer operator manual: Textronix, Inc., 070-6266-01 (Redmond, OR).

USGS (U. S. Geological Survey), 1998, El Niño and recent landslides: U.S. Geological Survey Web Page, http://geohazards.cr.usgs.gov/elnino/elninols.html.

Wade, L. V. and Conroy, P. J., 1980, Rock mechanics study of a longwall panel: Mining Engineering, p. 1,728-1,734.

SCENIC DRIVE LANDSLIDE, SAN MATEO COUNTY, CALIFORNIA

R. REXFORD UPP[1]

ABSTRACT

In the winter of 1997-98, the Scenic Drive landslide in the community of La Honda in San Mateo County, California, destroyed or damaged nine homes and a county road. This article presents the results of an investigation conducted to characterize the landslide, with emphasis on the methodology of landslide studies, and recommendations on how best to reopen and maintain the road. The study showed that this landslide is a portion of a much larger ancient landslide complex that developed in an area where Purisima Formation sandstone overlies Mindego Basalt. The landslide was reactivated by the heavy 1997-98 El Niño rainfall, following several years of above normal rainfall. There are insufficient data to determine with certainty the base of the older landslide complex, but it is probably located at the interface with the hard basalt that caused drilling refusal. Inclinometer monitoring shows that landslide creep movement continues, but the stability analysis suggests that the landslide would be stable under static conditions if it could be dewatered. By the fall of 1999, the road was reopened and, with Federal Government financial assistance, the County purchased the damaged properties. The landslide itself has been dedicated to open space.

INTRODUCTION

The subject site is located in the Santa Cruz Mountains, a range within the northwest-trending California Coast Ranges geomorphic province that forms the spine of the San Francisco Peninsula (Figure 1), with peak elevations of about 2,000 feet (600 m). These mountains receive the full force of Pacific storms. Annual precipitation averages approximately 30 inches (76 cm), with most precipitation occurring during the winter months. The mountains, which are predominantly underlain by Tertiary sedimentary rocks, have been scarred by numerous landslides triggered by the high rainfall (Brabb and Pampeyan 1972; Wieczorek 1982). Many of the larger landslides are thousands of years old and have been considered stable under current climatic conditions. Houses have been built on many of these landslides.

The community of La Honda, with over 100 homes, is located within one of these large ancient landslides, known as the La Honda landslide complex. The El Niño winter of 1997-98 produced

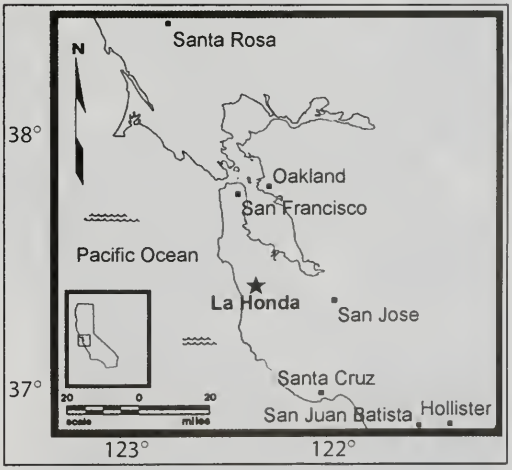

Figure 1. Location map.

[1]Upp Geotechnology
750 Camden Ave.
Campbell, CA 95008
rex@uppgeo.com

unusually high rainfall in the Santa Cruz Mountains, with over 40 inches (100 cm) recorded at the La Honda fire station. During this El Niño event a portion of the La Honda landslide reactivated. Movement of this portion, now referred to as the Scenic Drive landslide, destroyed or damaged nine homes and closed Scenic Drive, a county road that traverses the landslide (Figure 2).

San Mateo County was obligated to reopen the county road and retained me and my staff to conduct an investigation to characterize the landslide, including its dimensions, dynamics, past history, and the risk of further movement. The purpose of this article is to present a summary of that work, with emphasis on the methodology of landslide investigations. A detailed description of the investigation can be found in Upp Geotechnology (1998).

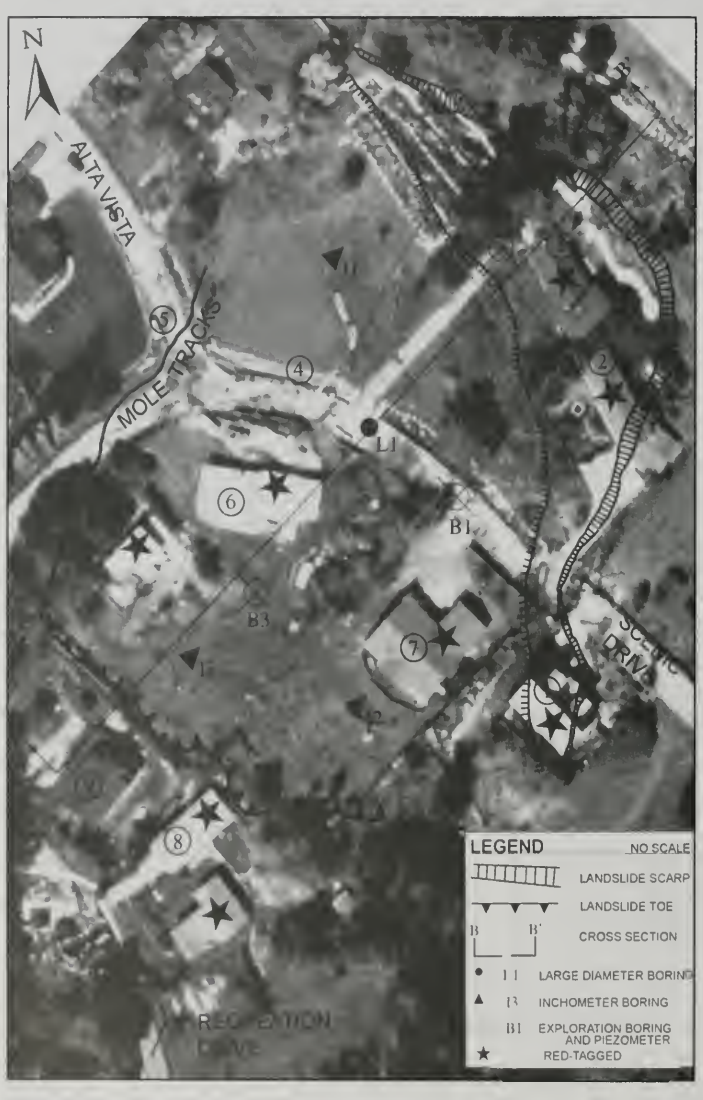

Figure 2. Aerial photograph showing the extent of the Scenic Drive landslide, the location of the head scarp and the toe of the slide, residences tagged as uninhabitable, and the location of the cross section of Figure 6. For map location consult Figure 4.

Our investigation did not start until after the landslide had fully developed, so we relied on information gathered by the County Geologist and geologists with the US Geological Survey (USGS) to characterize the history and surficial expression of the landslide.

METHODOLOGY

Geologic Mapping

The characterization of a landslide includes identifying the lateral limits and the depth to the slide surface, as well as the engineering properties of the soil and rock material and the groundwater conditions. The lateral limits of an active landslide can usually be established by good field mapping. Subsurface exploration is required to locate the slide surface and to collect samples to determine

the engineering properties. Piezometers should be installed to monitor the equilibrium groundwater levels. The determination of past landslide history utilizes several techniques, but the primary analysis for a landslide of this magnitude is based on aerial photograph interpretation.

By the time we were contacted, the lateral limits of the active slide had already been mapped by the San Mateo County Geologist and geologists with the USGS (Jayko et al., 1998). We used their maps throughout our investigation.

INCLINOMETERS

Although other methods are available to determine the depth of an active landslide, slope inclinometers were the most practical and economical, as long as slow movement continued. In mid-April we installed three inclinometers at the locations shown on Figure 2. Using the County's base topographic map, we first constructed a preliminary cross-section through the slide to estimate a most likely landslide depth of 25 to 30 feet (7.8 to 9.5 m). The inclinometers were then installed to a depth of 50 feet (15.6 m) to insure they would penetrate well below the slide surface. Inclinometer measurements taken throughout the summer showed no landslide movement and, therefore, did not reveal the slide surface at that time.

DOWNHOLE LOGGING

By the end of July, it had become apparent from the inclinometer data that the landslide was no longer moving. Therefore, we decided to down-hole log large diameter borings to characterize the depth of the landslide, using the technique described by Johnson and Cole (2001, this volume). Because of its easy access and central location, we selected a site on Scenic Drive itself for the first large-diameter boring (Figure 2). We also wanted to compare the subsurface conditions of the portion of the slide that had moved with the portion that had not, so we drilled the second large-diameter boring just below the toe bulge.

Our inclinometer borings had shown that the landslide material was highly fractured and blocky, and that groundwater was high. These conditions complicated the downhole logging and required heavy-duty pumping and steel casing to shield the upper portion of the holes while we logged the lower portion.

SHEAR STRENGTH TESTING

In addition to the landslide geometry, shear strength parameters of the soil and rock units are needed to perform a slope stability analysis. A variety of test methods is available to measure different types of shear strength, such as peak, residual, and torsional. Our analysis of aerial photos showed that the La Honda landslide had a long history of translational movement. Therefore, the lower strength value of the torsional shear strength was selected for analysis. This strength was obtained by use of the Bromley Ring shear test on a sample of clay gouge obtained from the landslide shear zone. Since the sample is tested in the remolded condition, undisturbed samples are not required and the clay samples were simply dug out of the shear zone exposed in the large diameter boring and preserved in a sealed plastic bag.

PIEZOMETERS

A third element commonly needed for a slope stability analysis is the location of the water table. A zone of clay gouge frequently develops along a slide surface by the grinding action of the landslide mass moving over the in-place material. This gouge zone can act as an aquitard that can create conditions necessary to develop artesian water pressure: that is, conditions where the water pressure below the slide mass is greater than the water pressure within the mass. To evaluate the groundwater conditions, we installed three sets of paired standpipe piezometers. One of each pair extended to depths well below the slide surface, and the second was terminated well above.

The piezometers were constructed by extending a 2-inch diameter PVC pipe to the bottom of the 8-inch diameter drilled holes. The lower 5 feet of each pipe were screened (slotted) and backfilled with pea gravel. A 2-foot thick bentonite seal was placed above the gravel. Above the seal, the annulus around the pipe was grouted with a portland cement mixture. The locations of the piezometers are shown in Figure 2.

SMALL DIAMETER BORINGS

To obtain additional data on the soil and rock characteristics within the slide, we intermittently collected both bulk and undisturbed ring samples from all the small diameter borings. In order to help evaluate any differences between the reacti-

vated Scenic Drive landslide and apparently stable portions of the La Honda landslide, we drilled and sampled four additional borings at locations beyond the limits of the active landslide.

ANALYSIS OF AERIAL PHOTOGRAPHS

We analyzed several stereographic pairs of black and white and color infrared aerial photographs to evaluate the landslide history. This type of analysis is based largely on a study of topographic features, changes in slope inclination, drainage patterns, and vegetation patterns. Relative landslide age is determined based on a subjective assessment of how sharp or subdued a feature appears, the maturity of vegetation, and whether one feature truncates another. Drainage patterns are altered by landslide movement, and vegetation patterns often indicate the location of surface and subsurface water. Infrared photos were particularly useful in analyzing shallow soil moisture patterns through the effect that moisture has on plant health. Contrasting patterns can help to distinguish different ages of landslide activity.

GEOLOGIC SETTING

The topography in the study area is characterized by narrow, steep-sided ridges and valleys. The community of La Honda is located in a ridge-bounded, bowl-shaped valley on the east side of the southerly-flowing La Honda Creek (Figure 3). According to the geologic map of the area (Brabb, 1980), the "bowl" is underlain by the Mio-Pliocene Tahana member of the Purisima Formation, which consists predominantly of glauconitic sandstone and siltstone with some silty mudstone. Where fresh, the sandstone and siltstone have a distinctive greenish-gray color, weathering to white or buff (Ellen et al., 1972). The mudstone generally is dark gray. Pebble conglomerate occurs near the base of the formation. This formation is in unconformable depositional contact with the underlying Mindego Basalt of Miocene or Oligocene age.

Upslope, to the north of the "bowl", the ridge is underlain by rocks mapped as Mindego Basalt. This unit includes both extrusive and intrusive mafic rocks. The extrusive rocks appear as dark gray blocks of basalt set in a matrix of pyroclastics and calcite. The blocks are hard but the matrix is soft due to weathering that extends to depths as great as 50 feet. The intrusive rocks are dark greenish gray and hard where fresh, weathering to orange brown.

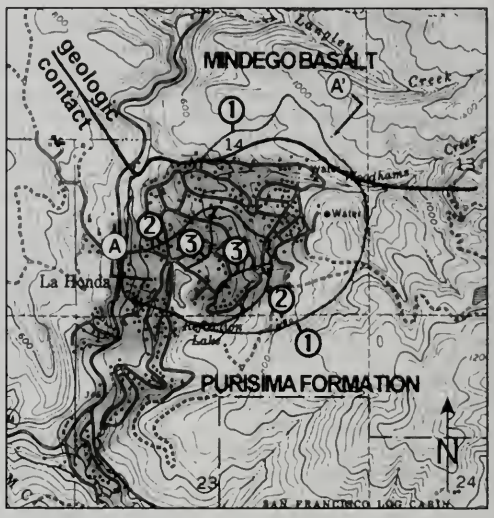

Figure 3. Geology of the immediate surroundings of the La Honda landslide complex, showing the relative ages of prehistoric landslides, and the location of the cross section of Figure 5. Because of the scale, the figure only shows the three oldest prehistoric landslides (1 through 3, with 1 being the oldest). See Figure 4 for the outline of the fourth prehistoric landslide and the four historic landslides.

LA HONDA LANDSLIDE

Aerial photographs, taken from 1941 through 1995, show that the topography of the La Honda area has a pronounced landslide influence. We could identify six generations of landslides within the La Honda landslide complex (Figures 3 and 4; the prehistoric landslides are labeled from 1 to 4, and the historic landslides are labeled with the dates of activity). The limits of the older landslides are less well defined than those of the younger landslides.

The oldest landslide, Landslide 1, extends from near the bases of the ridges surrounding the community of La Honda down to La Honda Creek. The second oldest landslide, Landslide 2, is located in the southwestern portion and entirely within Landslide 1. Landslide 3 is located within the central portion of Landslide 2 and represents a partial reactivation of Landslide 2 (Landslide 3 has a coincident headscarp but is narrower than Landslide 2; Figure 3). Based on topographic expression, the limits of Landslide 3 are defined with much greater certainty than are the limits of Landslides 1 and 2.

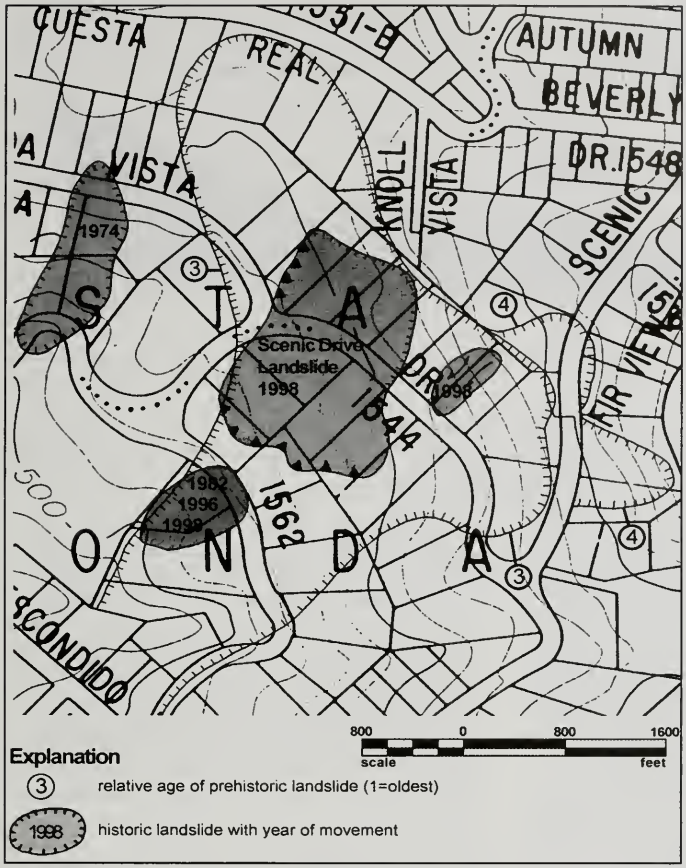

Figure 4. Outline of two prehistoric landslides (3 and 4, with 4 being the youngest), and the four historic landslides (labeled with the years in which movement took place).

Landslides labeled as 4 (Figure 4) are peripheral enlargements of Landslide 3, and apparently represent the last landslide movement before the community was developed and the roadways constructed.

The 1974 landslide disrupted Cañada Vista at its headscarp and Scenic Drive at its toe (Figure 4). This landslide was partially repaired and apparently has had no further movement.

A landslide that developed below Recreation Drive in 1982 damaged the road and a house on the lot below the road. The road was reopened and the house was relocated. Renewed landslide movement again damaged the road in 1996. The road was reopened again, only to be damaged by landslide movement a third time in 1998 (Figure 4).

The 1998 Scenic Drive landslide (the subject of this paper), which is also shown on Figure 4, is discussed in the section below.

The landslide configurations are very complex, particularly because of the multiple episodes of landslide movement. Our interpretation of subsurface conditions of the La Honda landslide complex is presented on Figure 5.

SCENIC DRIVE LANDSLIDE

Landslide history

The Santa Cruz Mountains experienced above-normal rainfall for the three years preceding the 1997-98 El Niño winter. By late January 1998, following a period of abnormally high rainfall beginning in late November 1997, residents within the landslide noted minor structural deformations in their homes (Jayko et al., 1998). The San Mateo County Geologist made periodic visits to the site to document and map the changing conditions. Several USGS geologists who live in the area also mapped and photographed the changing conditions. By the end of March, the USGS published a map of the landslide superimposed on an aerial photograph (Figure 2) (Jayko et al., 1998).

Distress first appeared as a crack across the road. Within days, the scarp had severed and displaced the road. The scarp continued to grow and, with time, enlarged to about 4 to 5 feet (1.5 m) high. The head scarp developed under, or in close proximity to,

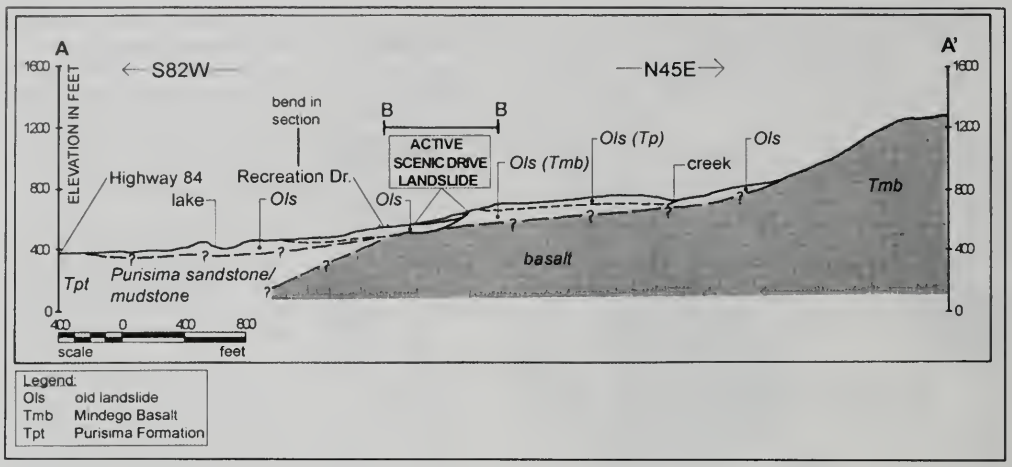

Figure 5. Geologic cross section across the La Honda landslide complex. See Figure 3 for location.

three houses (Figure 2) that were severely damaged. The damage was less severe to the three houses that were more centrally located in the landslide mass.

A small compression "mole track" first appeared in Scenic Drive near the intersection with Cañada Road in January 1998. The bulge continued to grow until an imposing thrust ridge developed. The toe of the slide bulged up behind the three houses on Recreation Drive, causing some damage. By the summer of 1998, the landslide had caused damage to Scenic Drive, nine residences, and several vacant parcels. Eight of the residences were tagged as uninhabitable by the County (Figure 2).

DESCRIPTION

The Scenic Drive landslide is roughly rectangular in plan view, with maximum dimensions of about 360 feet (110 m) by 500 feet (150 m) (Figures 2 and 4). The distance from the headscarp to the toe in the general direction of movement is about 525 feet (160 m). The elevation difference between the top of the headscarp to the base of the toe is about 80 feet (25 m). Our interpretation of the subsurface conditions of the Scenic Drive Landslide is presented in Figure 6.

The headscarp has an arcuate shape with the right end trending northwest-southeast and the left end trending north-south (Figure 2). The headscarp shows about 11 feet (3.3 m) of vertical displacement behind the carport of a destroyed home. The headscarp at this location has a dip of about 65 to 75 degrees and exposes volcanic rock of the Mindego Basalt. The northwest-southeast trending portion of the active headscarp is a part of an older headscarp that extends for about 1,500 feet (450 m) to the southeast (Figure 4). The north-south portion of the active headscarp crosses Scenic Drive with 4 to 5 feet (1.2 to 1.5 m) of vertical offset. Colluvial deposits representing older landslide material are exposed in this scarp. Earth movement across the headscarp severely damaged three houses.

The toe of the landslide is marked by a bulge of earth up to 5 feet (1.5 m) high. The toe has a convex downslope configuration (Figures 2 and 4), and its movement distressed at least two houses on Recreation Drive.

On each flank of the landslide, between the headscarp and the toe bulge, is a neutral zone. Displacements along both ends of the headscarp and toe bulge decrease to zero towards the neutral zone, although minor distortion of the pavement at the intersection of Scenic Drive and Cañada Vista developed.

Overall, the landslide exhibits complex movement with many internal structures between the head and toe. Upslope of the neutral zones, features are largely extensional. A distinct back-tilting graben developed below the headscarp and tilted

the houses in this area down toward the headscarp. Downslope of the neutral zone, features are generally compressional in nature, although some extensional features also developed. Internal structures have occurred within the landslide mass, including thrust ridges and associated grabens. Numerous extensional cracks developed in the landslide mass, particularly in its lower portion.

SUBSURFACE CONDITIONS

Twelve exploration borings were drilled as part of this investigation: seven within the Scenic Drive landslide and five outside its limits. Two large diameter borings were downhole logged and provided the most complete descriptive records of subsurface conditions. Boring L1, drilled near the center of the landslide mass (Figure 2), exposed active landslide debris consisting mostly of dark greenish gray, fine-grained, glauconitic sandstone fragments in a clay matrix originating from the Tahana member of the Purisima Formation. Included with this material, however, are fragments from the upslope Mindego Basalt. This landslide material is weaker and generally wetter than materials encountered below.

At a depth of about 27 feet (8 m), a 3-inch (7.5 cm) thick layer of very soft and wet clay landslide gouge was encountered, at what appears to be the base of the active landslide. Below this active shear zone is a stronger, dark greenish gray sandstone breccia. This lower unit consists of sandstone blocks in a clayey matrix, and is interpreted to be old landslide debris consisting of disturbed Purisima Formation sandstone. This boring met drilling refusal on hard Mindego Basalt at a depth of about 40 feet (12.3 m).

The other large diameter boring, L2, was drilled just below the toe of the active landslide. The active shear zone was not encountered in this boring. Disturbed Purisima Formation sandstone with multiple, old, inactive shear surfaces was exposed throughout the boring. Drilling refusal was met on the hard Mindego Basalt at a depth of about 38 feet (11.7 m).

GROUNDWATER

Pairs of standpipe piezometers were installed at three locations within the landslide to monitor the stabilized water table. Each pair included a deep and a shallow piezometer, to measure water level (pressure) both below and above the landslide surface. These piezometers show that the active shear zone gouge forms a barrier to upward migration of groundwater, creating artesian conditions below the active landslide mass. Groundwater rose to ground level in the borings that penetrated through the landslide shear surface, but was well below ground level in the shallow borings. This phenomenon was observed in the paired piezometers in the main body of the landslide, as well as in the upper large diameter boring.

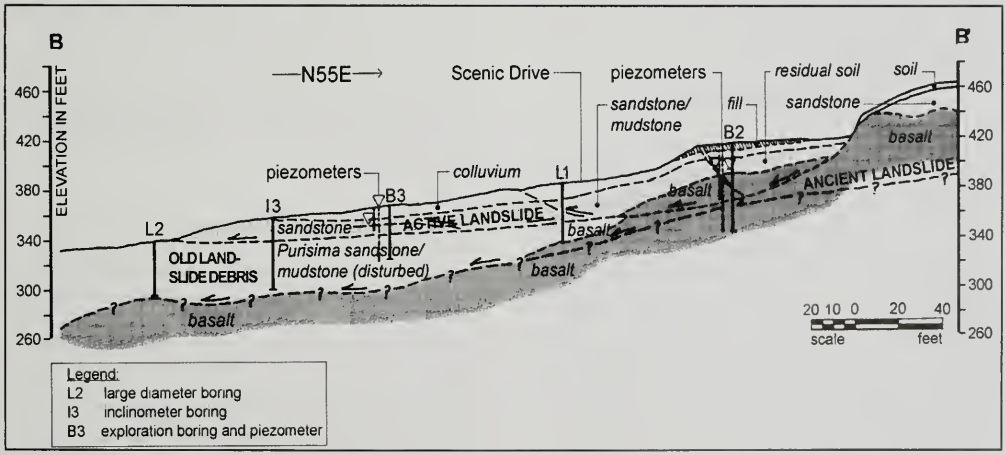

Figure 6. Geologic cross section across the Scenic Drive landslide. See Figure 2 for location.

The piezometers installed closer to the head scarp did not show the artesian conditions. At this location, both piezometers encountered water within the fractured basalt and no clay gouge barrier had developed.

INCLINOMETERS

Slope inclinometer casings were installed in three borings and 11 sets of readings were taken between April 1998 and November 1999. The data shows virtually no movement between the April and June 1998 readings, but small measurable movement between June and November 1998. The depth of measurable movement was consistent with the depth of the active landslide interpreted from the exploration borings (between 15 to 25 feet). The direction of movement, however, was in the upslope direction. We interpret this movement as a "relaxation" of the landslide mass backward into the tension cracks and grabens.

Between November 1998 and April 1999, however, all the inclinometers showed measurable downslope movement of up to 0.5 inches at depths of 31 to 45 feet. No surface movement of the active slide was observed in this period. It appears that movement occurred on a deeper slide surface, possibly the bottom of the La Honda landslide itself.

Between April 1999 and November 1999, minor movement continued in the upper 15 feet of the landslide. Again, the movement has been predominantly in the upslope direction. By July 2000, all three inclinometers had sheared off at the depths of deepest recorded movement.

SLOPE STABILITY ANALYSIS

Quantitative slope stability analysis was performed to evaluate the relative stability of the Scenic Drive landslide. The analysis used the Simplified Bishop method to evaluate the failure surface as it was identified in November 1998 and to calculate the factor of safety. Soil strength characteristics used were based on torsional and direct shear testing of selected representative samples of the landslide material, collected from the large and small diameter test borings. The analysis took in consideration both saturated and drained groundwater conditions, to estimate the stability of the landslide mass under natural conditions, and following the installation of a proposed dewatering system.

The analysis was also performed under static conditions and under several pseudo-static earthquake accelerations. The static saturated analysis yielded a factor of safety of 0.8, indicating a failed condition consistent with the actual landslide movement. The static drained analysis yielded a factor of safety of 1.3. The pseudostatic analyses all yielded safety factors of less than 1.0, suggesting that landslide movement is likely during a strong earthquake.

CONCLUSIONS

The Scenic Drive landslide is located in a geologically sensitive area with evidence of multiple episodes of landsliding. Older, deep-seated landslide movement may have transported and juxtaposed bedrock units, creating complex subsurface geology. The subsurface conditions include disturbed Purisima sandstone overlying Mindego Basalt. Bedrock units have been transposed by the landslide movement, as shown on geologic cross-sections A-A' and B-B' (Figures 5 and 6). This prior earth movement has greatly reduced the shear strength of the slope material. Several portions of the older landslides have become reactivated in historic times. Prior to 1998, however, the area now occupied by the Scenic Drive landslide may not have been active since the area was developed.

During the prior three or four consecutive years of above-normal rainfall, the ground underlying La Honda became saturated. The source of the groundwater is probably the fractured basalt underlying the ridges to the east as depicted on geologic cross-section A-A' (Figure 5). With above-normal rainfall beginning in November 1997, the groundwater pressure built up sufficiently by January 1998 to cause the Scenic Drive landslide to become active. Subsequent movement destroyed several houses and disrupted the roadway.

The area has had shallow groundwater and springs over the years. Acts of man (e.g., grading, leachfields) and acts of nature (e.g., earthquakes, climate) have altered the shallow water and vegetation patterns over historic time. In my opinion, however, surface run-off and shallow water were not significant contributors to the reactivation of the landslide. There is not enough data to define with certainty the base of the older landslides, but it is likely that the very hard basalt that caused drilling refusal in several of the borings is the undisturbed base of old landslide movement. It is also apparent

that only the upper portion of the older landslide material became reactivated as the Scenic Drive landslide.

Our stability analysis shows that the landslide is unstable under high groundwater conditions, including the artesian conditions observed during the investigation, and the inclinometer readings suggest that slow creep movement is ongoing. The stability analysis also revealed that if the landslide could be dewatered, then it should remain stable under static conditions.

By the fall of 1999, the County had reopened Scenic Drive by grading across the scarps and ridges, and will simply perform future road maintenance as needed. In addition, with federal financial assistance (FEMA), the County has purchased the eight red-tagged properties and will convert the landslide to open space.

ACKNOWLEDGEMENTS

I wish to acknowledge and express my appreciation for the help that I have received from others in conducting this investigation. Earl Brabb and Ray Wells of the U.S. Geological Survey provided invaluable assistance in identifying rock samples from the test borings. Jean DeMouthe, in her role as County Geologist, made the initial observations and maps of the landslide movement. Carol Prentice, Ray Wells, Angela Joyko, Michael Rymer, and Ray Wilson of the U.S. Geological Society provided initial observations and photographs of the landslide.

AUTHOR PROFILE

R. Rexford Upp received his BA degree in Geology from Humboldt State University and a Ph.D. in Engineering Geology from Stanford University. He is the Principal of Upp Geotechnology, Inc., a San Jose area-based consulting firm, and is a past President of the Association of Engineering Geologists.

SELECTED REFERENCES

Brabb, E.E. and Pampeyan, E.H., 1972, Preliminary map of landslide deposits in San Mateo County, California: U.S. Geological Survey, Miscellaneous Field Studies Map MF-344, Scale 1:62,500.

Brabb, E.E. 1980, Preliminary geologic map of the La Honda and San Gregorio quadrangles, San Mateo County, California: U.S. Geological Survey, Open File Report 80-245, Scale 1:24,000

Ellen, S., Wentworth, C.M., Brabb, E.E., and Pampeyan, E.H. 1972, Description of geologic units, San Mateo County, California: U.S. Geological Survey, text to accompany Miscellaneous Field Studies Map MF-328.

Jayko, A.S., Rymer, M.J., Prentice, C.S., Wilson, R.C., and Wells, R.E., 1998, Scenic Drive Landslide of January-March 1998, La Honda, San Mateo County, California: U.S. Geological Survey, Open File Report 98-229.

Johnson, P.L. and Cole, W.F., 2001, The use of large-diameter boreholes and downhole logging methods in landslide investigations: in Ferriz, H., Anderson, R., (eds.), Engineering Geology Practice in Northern California: Association of Engineering Geologists Special Publication 12 and California Division of Mines and Geology Bulletin 210.

Upp Geotechnology, 1998, Geotechnical investigation [for] landslide mitigation, Scenic Drive, San Mateo County, California: Consultant's report to San Mateo County Environmental Services Agency, 510 Hamilton Street, Redwood City, California.

Wieczorek, G.F. 1982. Map showing recently active and dormant landslides near La Honda, central Santa Cruz Mountains, California: U.S. Geological Survey, Miscellaneous Field Studies Map MF-1422, Scale 1:4,800.

ROCKFALL HAZARDS MITIGATION: AN EMERGENCY CASE STUDY OF MOSQUITO BRIDGE ROAD CROSSING IN EL DORADO COUNTY, CALIFORNIA

ROY C. KROLL[1], DAVID C. SEDERQUIST[1], AND ERIK J. OREM[2]

ABSTRACT

The "Pineapple Express" storm sequence of the winter of 1996-97 produced heavy Sierra Nevada snowfall in early December, followed by warm rains and rapid run-off that started on Christmas Eve. On 26 December, El Dorado County Department of Transportation personnel discovered heavy road damage to Mosquito Road, caused by a large rockfall adjacent to the historic, wooden suspension bridge that spans the south fork of the American River and provides primary access to the rural, upscale community of Swansboro. We conducted an emergency assessment of further rockfall potential and concluded that other boulders posed a further threat to life and property. The road was therefore closed while mitigation options were evaluated and implemented.

Blasting, mechanical dislodging, direct rock-bolt anchoring, and anchored wire-rope netting were each considered as options, as continuing storms resulted in the near isolation of Swansboro. Anchored wire-rope netting, in tandem with a localized cable net barrier fence, was chosen to protect the road and bridge, based upon a reasonable time frame and acceptable cost. Design and construction sequences overlapped to allow the contractor to order materials and secure specialty installation equipment in a timely manner. Geologic input on the mass and height above the bridge abutment of two suspect boulders were used to specify rock energy and pull-out strengths for both cable-net and barrier-fence anchors. Field rock cores were then retrieved and rated for both rock quality designation (RQD) and rock mass rating (RMR) to estimate tentative anchor depths. Field anchors were then set at various depths and pull-tested with various bonding agents. Final design parameters were then set, and installation was started. Several proposed anchor locations encountered unexpected conditions that required a consensus modification on local anchor criteria agreed upon by the manufacturer, consultant, and contractor. Installation of the cable-rope netting on the slope and local barrier fence was completed on 13 March 1997, less than three months after the initial catastrophic rockfall.

INTRODUCTION

The "Pineapple Express" storm sequence of the winter of 1996-97 produced heavy Sierra Nevada snowfall in early December, followed by warm rains and rapid run-off that started on Christmas Eve. At the request of the El Dorado County Department of Transportation (D.O.T.), on 26 and 27 December 1997, an emergency geologic safety inspection of unstable rock above and adjacent to the south abutment of the Mosquito Bridge on Mosquito Road, north of Placerville, California, was performed (Figure 1). Mosquito Bridge is a single lane, historic, wooden suspension bridge, built in the late

[1]Youngdahl Consulting Group
1234 Glenhaven Court
El Dorado Hills, CA 95762
moil@youngdahl.net

[2]Brugg Cable Products
11807 NE 99th Street, Suite 1160
Vancouver, WA 98682
geobrugg@aol.com

Figure 1. Vicinity map.

1800's, that crosses the South Fork of the American River.

Roadway pavement cratering and guardrail destruction, caused by the rockfall of large boulders, were observed (Figure 2). A focused inspection, at D.O.T.'s request, of two remaining perched boulders (estimated at 40 and 120 tons in weight, respectively), revealed pronounced open joints and centers of gravity near their hinge points. The potential for these boulders to fall and damage or disable the cable anchors and south bridge abutment was considered high. Such a condition could make the bridge unstable for motorists entering onto the bridge from the north side. Additionally, other individual boulders above the roadway approach to the bridge were observed weathering out of the underlying granitic parent rock along joints and fractures. This parent rock mass was also geologically evaluated for future random rockfall releases that would impact the roadway. The weathering was considered to be due to water infiltration and freeze-thaw processes gradually opening up the fracture sets into the underlying rock mass. D.O.T. personnel asked for a geologic opinion as to whether an immediate potential hazard to public safety existed and needed mitigation. In light of the observed field conditions, the geologic investigators confirmed the existence of hazards. Consequently, D.O.T. closed the road, pending mitigation.

This article will describe the rapid assessment of the rockfall hazard using classic rock mechanics methodology and procedures for cost estimating, accelerated field testing, and subsequent quick mitigation of the hazard using both cable-rope netting and a cable-net barrier fence.

MITIGATION OPTIONS

Options considered for mitigation were:

- removal of the two unstable boulders by mechanically dislodging (blasting or pulling) them;
- immobilization of the unstable boulders using rock bolts, and

Figure 2. View south across American River after rockfall. Note the skid path left of the bridge, and the large angular boulder in the bottom left.

- control of future random rockfall through use of an anchored cable net and high-impact cable barrier fence.

At a meeting on 31 December 1997 with representatives of the El Dorado County D.O.T., it was determined that, due to difficult equipment-access onto the slope and estimated boulder weights of 40 and 120 tons, the two unstable boulders could only be removed through blasting. Such a course of action would then likely increase the overall number of hazardous boulders by enlarging or increasing fracture sets in the adjoining rock mass, thus adding to the problem.

The site geology and working conditions (Figure 3), the steep and smooth exfoliation surfaces, the large amounts of active deep fractures, large boulder sizes, and wet and slippery moss-covered rock faces, were not amenable to immobilization of the unstable boulders. The cost for drilling moderately deep anchors for each boulder in the parent rock mass was judged to be prohibitive and impractical, given equipment-access problems on the steep slope.

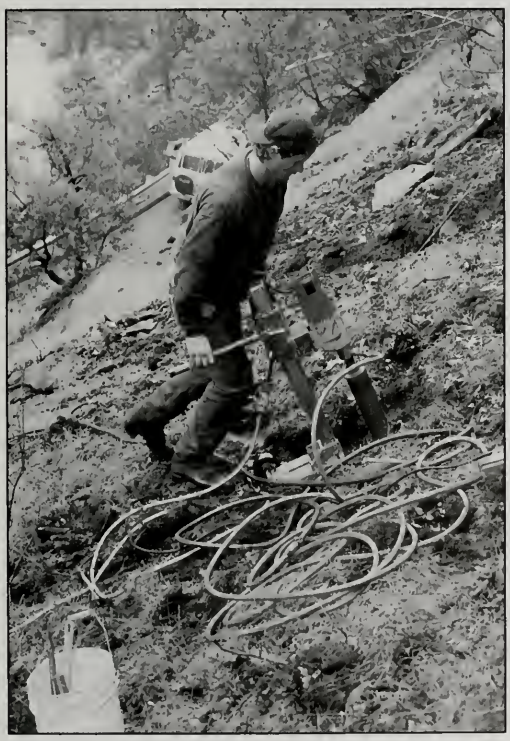

Figure 3. Contractor drilling for net anchor. Note the steep, loose terrain.

The mitigation measure judged most cost- and time-effective was use of a wire-rope net fastened to rock anchors above and below the entire parent outcrop and secondary construction of a high impact wire-rope rock protection barrier above the south bridge abutment.

DESIGN EXPLORATION

A critical component of the rock-slope protection system was the design of the rock anchors that were to support the net and the weight of boulders against the net. Brugg Cable Products (Brugg) specified that the anchors for the rock net be capable of withstanding a 15-ton pullout and that the up-slope tieback anchors for the rock fence be capable of withstanding a 20-ton pullout.

The basal granitic mass underlying the unstable boulders contained widely spaced joints and fractures. Weathering along these joints and fractures was the mechanism by which the unstable boulders had been formed. These fractures extended deep into the underlying rock mass. An evaluation of the rock quality resulting from these fractures provided a means to assess the suitability of the rock for the planned rock-anchor systems.

In order to evaluate the capacity of the rock to withstand the specified pullouts, the geologic investigators evaluated one rock core collected from the area of the up-slope tieback anchors for the fence (core #1) and one rock core from a proposed upper net anchor hole (core #2). Core #1 was cut at 1 5/8 inch (4.1 cm) diameter to a depth of 3.3 feet (102 cm) into granodiorite in the area designated for the up-slope tieback anchors for the rock fence (Figure 3). Core #2, with a diameter of 1 5/8 inches (4.1 cm) was advanced to a depth of 8.1 feet (246 cm). Fracture voids and rubble were encountered at approximately 5 feet in depth during drilling of the second core. Both RQD (rock quality designation) and RMR (rock mass rating) were determined for both cores in accordance with Goodman (1989), as shown in Table 1.

Goodman (1989) recommends the use of the RMR classification over the RQD designation due to the additional physical factors considered by RMR. The

FACTOR	CORE #1	CORE #2
Total core length (cm)	102	246
Core length recovered	102	240
Rock quality designation (RQD)	100	97
RQD quality	Good	Good
RMR drill core quality (DCQ)	20	20
Jn	4	9
Jr	4	1.5
Ja	1	4
Jw	1	1
SRF	1	2.5
Q	20	0.33
RMR rating*	56	40
RMR class	III (fair)	IV (poor)

*RMR rating (Goodman, 1989) = 9log(Q)+44

Table 1. Summary of rock quality data.

number of joint sets (Jn), the roughness of joints (Jr), the joint alteration/filling (Ja), the presence of water in joints (Jw), and the stress reduction factor (SRF) collectively allow the determination of the rock mass quality for tunneling (Q), which in turn is used to quantitatively categorize the rock's mass rating and place the rock mass in one of five engineering rock mechanics categories, ranging from I (very good) to V (very poor). As can be seen from Table 1, the higher number of joint sets, lower roughness of the joints, the lack of joint infilling, and the degree of openness (SRF) all contributed to a much lower "Q" value for Core #2.

The geologic investigators were unable to rule out the possibility that rubble and deeply weathered rock encountered at a depth of 5.2 feet (158 cm) in Core #2 represented penetration of a floating rock sheet or boulder. Anchoring into such a deeply buried large rock fragment could have provided a substantial deadman anchor for the cable net. However, the rubbly material did not quantitatively meet the pullout resistance requirements for the anchors.

Anchor location conditions were observed during the subsurface exploration activities to be non-uniform across the rock mass. The lower row of nine cable net anchors were located in granitic rock characteristic of the test core drilled in the rock barrier fence area. The upper nine cable net anchors, however, were programmed for installation in areas covered by slopewash, which complicated the evaluation of anchor locations within the underlying granitic rock. Consequently, the contractor probed and hand-excavated each selected upper net-anchor location to verify that sound rock was present at each anchor point.

LABORATORY TESTING

In order to develop some measured rock-strength characteristics applicable to the site, two core sections were tested for unconfined compressive strength (ASTM C-42). One unfractured section of core was cut to a length of 6.5 inches (16.5 cm) and reached compressive failure at 10,441 pounds per square inch (psi), which is equivalent to 752 tons per square foot. The second core section, cut to a 6.75 inch (17.1 cm) length and containing a single diagonal fracture, failed at 4,679 psi (337 tons per square foot) along a portion of the fracture which was filled with iron hydroxides. Empirical tensile strength is traditionally given as one-half of the compressive strength (Goodman, 1989), so based on the test results, it was estimated at 2,300 to 5,200 psi. Such tensile strength values are typical of weathered granitic rock and are generally considered favorable for rock anchor pull-out resistance.

FIELD TESTING

The mitigation design specified that the anchors for the cable net had to be capable of withstanding a 15-ton pullout force, and that the up-slope tieback anchors had to be capable of withstanding a 20-ton pullout force. In order to verify that the materials used and installation method would meet these specifications, modified proof tests were performed on three of the anchor bolts. These tests were completed by stressing each test anchor to 125% of the design strength, using a center pull 60-ton hydraulic jack equipped with a pressure gauge (Figure 4). Each test bolt was subjected to incremental stages of increased pull at 25% of the specified pull-out until either a 125% design-strength pull showed no anchor failure for a 5 minute period, or the anchor failed.

Two of the upper net anchors were tested. One 1-inch (2.54 cm) diameter anchor was set in cement

Figure 4. Testing anchor pull-out resistance capacity, using a Williams Form 60-ton jack.

grout within a 2-inch (5 cm) diameter by 4.5-foot (137 cm) deep hole. A second 1-inch diameter anchor was set in epoxy in a 1.4-inch (3.5 cm) diameter by 3.8- foot (117 cm) deep hole. The first anchor was able to sustain an 18.75 ton pull for 5 minutes without showing signs of failure. The second anchor failed at a pull of approximately 14 tons. Based on these tests, only grout-bonded anchors in anchor holes 2-inches in diameter, by at least 4.5-feet deep, were recommended for installation.

One bolt was also tested for the up-slope tieback anchors for the rock fence. A 1-inch representative bolt, installed specifically for the test was epoxied into a 2-inch (5.1 cm) diameter by 5.1-feet (155 cm) deep hole in the vicinity of the anchor locations for the rock fence. This bolt was able to sustain a 25-ton pull for 5 minutes and thus met pull-out specifications. Based on the field-test results, construction specifications for the barrier fence and cable-net anchors were issued by the design team.

Based on the results of the field testing program, the design specifications were finalized to include an anchor pullout resistance of 15 tons, achievable with a 2-inch diameter hole at least 4.5 feet deep, and with the anchor set in high strength cement grout. Similarly, it was concluded that a 20-ton pullout resistance could be achieved with a 2-inch diameter anchor hole to a depth of 5.1 feet, utilizing high strength cement grout (Figure 5).

FIELD MONITORING OF INSTALLATION

The biggest logistical problem faced by the contractor involved slope access and shuttling of large, heavy equipment and personnel onto the slick, wet slope face (Figure 3). A heavy duty hydraulic tele-

Figure 5. Finished cable net anchor grouted in place with cable attached.

scoping platform lift was finally judged best suited to provide the necessary slope access for personnel, equipment and materials. Several anchor points had to be shifted, based upon subsurface field conditions encountered. A pronounced thickened soil horizon in the upper anchor area required extending a rope cable beyond the upper limits of the mass to a remote anchor point, in order to bypass the constraining soil layer. A final field visit to observe the completion of installation activities on 13 March 1997 confirmed that design specifications had been met and geotechnical recommendations had been suitably followed. Based upon field geologic observations during installation (suitable anchor-hole diameter and depth), laboratory testing, and installation inspection by the design engineer, the installed cable net system and cable barrier fence were judged suitable to protect the motoring public, the roadway section, and the bridge structure, thus allowing the access to Swansboro to be safely reopened (Figure 6).

CONCLUSIONS

Site access for equipment played a major role in prioritizing mitigation alternatives. The client quickly discarded several of the choices, due to equipment-access constraints and the time delays that their implementation would have involved. Seeing past the technical choices, and realizing that the public's perception of progress was a priority for the client, allowed the geologic investigators to expedite implementation of the chosen mitigation method.

From a technical aspect, the Rock Mass Rating (RMR) system proved to be a more thorough quantitative evaluation tool for rock engineering design than the Rock Quality Designation (RQD), which rated both cores as good, based only on percentage of recovered core. Pullout testing must still be performed during both design and construction to verify RMR derived specifications.

The presence of water in the rock played a role in the suitability of cement grout versus epoxy resin cement. We think that the epoxy resin is better suited for anchor bonding in a relatively dry environment with good (class II) to very good (class I) rock. If the rock is wet and class III to class V on the average, then a high strength cement grout bond is better suited to the application.

Figure 6. View south across historic Mosquito Bridge after corrective measures were completed. Cable net draped across exfoliating granodiorite, and short rock barrier fence to right of center protects bridge anchor abutment structure.

This case study confirms that both core classification (RQD) and rock mass rating (RMR) for the subject site should be performed by an experienced engineering geologist, knowledgeable in the system proposed by Goodman (1989). Training of staff personnel can occur coincidentally.

A summary of costs might be of interest to other engineering geologists engaged in rockfall mitigation: The cable net covered approximately 7,300 square feet of slope (120 feet wide by 60 feet top-to-bottom) when finished. The rock barrier fence spanned 20 feet laterally and was 10 feet high. The final cost to El Dorado County, including all labor, consultation, and monitoring, was on the order of $195,000. Of this total, approximately $35,000 was for materials and freight. The cable net unit price was approximately $4 per square foot. The rock barrier fence unit price was on the order of $275 per linear foot.

The greatest single cost to the client is typically in labor for the installation. The client is usually best served by the geologic consultant who finds the most experienced, reputable contractor, capable of efficiently installing these specialty products using the appropriate equipment and seasoned crews. Thus, the client will benefit in both cost-savings and an accelerated schedule. Furthermore, the public perception of a timely completion will benefit both the client and the consultant.

ACKNOWLEDGMENTS

Our sincere thanks to John Duffy as both a peer reviewer, and for pioneering the use of cable-wire nets in California, which inspired our approach to this project. Special thanks go to Joan Van Velsor for sharing her insight on how to write a highly technical paper and still make it readable. Her diplomatic patience will not be forgotten. Lastly, Dr. Horacio Ferriz deserves our gratitude for seeing past the technical complexities of our effort, and delicately guiding us through insightful editorial suggestions to produce a useful paper for the practicing engineering geologist.

AUTHOR PROFILES

Roy C. Kroll is the chief engineering geologist and environmental manager at Youngdahl Consulting Group. He was the county liaison and the lead technical evaluator on the Mosquito Bridge rockfall project. He has performed engineering geology, fault hazard, geotechnical, hydrogeologic, and environmental studies throughout both northern and southern California since 1981. His experience also includes extensive forensic studies of distress and defects resulting from geologic conditions.

David C. Sederquist is a senior engineering geologist and hydrogeologist with Youngdahl Consulting Group. His technical experience includes slope stability, hydrogeologic and geotechnical engineering studies, groundwater resources studies, onsite sewage disposal design, and Phase 2 environmental assessments. David performed detailed field mapping, provided design criteria input, and monitored installation efforts for the Mosquito Bridge rockfall project.

Erik J. Rorem is the west coast representative of Brugg Cable Products with extensive experience in field engineering evaluation of slope failures and distress. Erik served as the technical liaison between the consulting engineering geologists and the technical design team of Brugg Cable Products for the Mosquito Bridge rockfall project. When not looking at failed slopes for design mitigation, Erik is busy conducting product seminars with both private firms and public agencies.

SELECTED REFERENCES

Brugg Cable Products, 1996, Impact load chart, Rock fall retaining systems: Brugg Cable Products, Inc., 1 p.

Brugg Cable Products, 1996, Sample specification pertaining to high impact rock catchment barrier: Brugg Cable Products, Inc., Vancouver, Washington, and Santa Fe, New Mexico, 5 p.

Brugg Cable Products, 1996, Sample specification pertaining to slope protection systems: Brugg Cable Products, Inc., Vancouver, Washington, and Santa Fe, New Mexico, 5 p.

Brugg Cable Products, 1996, Sample specification pertaining to low impact rock catchment barrier: Brugg Cable Products, Inc., Vancouver, Washington, and Santa Fe, New Mexico, 5 p.

Brugg Cable Products, 1997, Layout and engineering drawings for Mosquito Bridge fence and rock slope protection: Consultant's report to All Counties Fence Company, 14 p.

Duffy, J.D., 1992, Field tests of flexible rockfall barriers: Consultant's report to Brugg Cable Products, Inc., Birr, Switzerland, and Santa Fe, New Mexico, 37 p.

Goodman, R.E., 1989, Introduction to rock mechanics: John Wiley & Sons (New York, New York), second edition, 562 p.

Kane, W.F. and Duffy, J.D., 1993, Brugg low energy wire rope rockfall net field tests: University of the Pacific, Department of Civil Engineering, Technical Research Report 93-01, Consultant's report to Brugg Cable Products, Inc., 88 p.

Kohler, S.L., 1983, Mineral land classification of the Georgetown 15-minute quadrangle, El Dorado and Placer Counties, California: California Department of Conservation, Division of Mines and Geology, Open-File Report 83-35, 85 p.

Y & A (Youngdahl & Associates, Inc.), 1997, Mosquito Bridge rockfall, summary of observations and recommendations: Consultant's report to El Dorado County Department of Transportation, 2 p.

Y & A (Youngdahl & Associates, Inc.), 1997, Final report - Mosquito Bridge rockfall construction monitoring services: Consultant's report to All Counties Fence Company, Inc., Sacramento, CA, 6 p.

INTRODUCTION TO THE FAULTS SECTION

WILLIAM LETTIS[1] AND DAVID SCHWARTZ[2]

Active faults pose a significant hazard to the population and built environment of Northern California. Displacements on active faults produce surface fault rupture and earthquakes. Earthquakes, in turn, can produce strong ground shaking, liquefaction, landslides, and tsunamis. All of these hazards are a known future risk to developed communities in Northern California.

The principal active faults in Northern California generally belong to one of four distinct fault systems: the San Andreas fault system, the Cascadia subduction zone in northwestern California, Quaternary faults that in some instances follow the alignment of the Mesozoic Sierra Nevada foothills fault system, and the Sierra Nevada frontal fault system. Most of these active faults have been documented through careful mapping by the U.S. Geological Survey (USGS) and the California Department of Conservation, Division of Mines and Geology (DMG). At least for the greater San Francisco Bay area, it is reasonable to assume that all strike slip faults with a slip rate of 1 mm/year or greater have been identified and characterized.

In addition, thrust faults have been identified beneath active folds in the greater San Francisco Bay area and along the western margin of the Sacramento-San Joaquin Valley and Delta. The larger of these thrust faults were identified through structural, geomorphic, and seismologic studies over the past decade or so, although it is likely that future studies will identify additional active thrust faults and greatly improve our understanding of the origin and rates of thrust fault deformation.

[1] William Lettis & Associates, Inc.
1777 Botelho Drive, Suite 262
Walnut Creek, CA 94596
lettis@lettis.com

[2] David Schwartz
U.S. Geological Survey
345 Middlefield Rd., MS 977
Menlo Park, CA 94025
dschwartz@usgs.gov

In this section, many of the active faults in Northern California are described. The authors of each paper provide a summary of our current knowledge about each fault, supplemented with additional detailed information on the location and seismic potential of the fault. The papers also include a thorough list of references that direct the reader to further information on structural setting, recency and rate of activity, segmentation, historic earthquake activity, maximum earthquake potential, and earthquake recurrence.

The USGS recently completed a new earthquake probability evaluation for the greater San Francisco Bay area (WGCEP, 1999). This evaluation included an updated analysis of seismic source characteristics for all faults in the region with a slip rate of 1 mm/year or more. Many of the papers in this section include the analysis and results of this seismic source characterization, and, thus, are the product of the collective thinking of many individuals with knowledge and expertise on each fault.

SAN ANDREAS FAULT SYSTEM

The San Francisco Bay urban area straddles the San Andreas fault system. Virtually every community in the Bay area lies within ten miles of one or more active faults. The principal faults of the San Andreas fault system include the San Andreas fault, Hayward-Rodgers Creek fault, Calaveras fault, and the Concord-Green Valley fault. Each of these faults is described in this section incorporating, in part, the results of the USGS Working Group on Earthquake Probabilities. Hall et al. (2001) describe the San Andreas fault, with an emphasis on recent studies conducted on the San Francisco Peninsula. They present mapping and paleoseismic trench results that document the location and paleoseismic history of the Peninsula segment of the San Andreas fault. Lettis (2001) describes the Hayward-Rodgers Creek fault system, Kelson (2001) describes the Calaveras fault system, and Borchardt and Baldwin (2001) describe the Concord-Green Valley fault system. Each of these papers emphasizes recent interpretations of the segmentation of each fault

zone, and the likelihood for future multi-segment fault ruptures

THRUST FAULTS

The occurrence of the Coalinga earthquake in 1983, Whittier Narrows earthquake in 1988, and Northridge earthquake in 1994 heightened our awareness of the seismic potential of blind thrust faults in California. In part because of these earthquakes, a major emphasis over the past decade has been placed on identifying and characterizing blind thrust faults in Northern California. In its evaluation of earthquake probabilities, the USGS incorporated for the first time the possibility of blind thrust faults in the Bay area. Unruh (2001) describes the potential for blind thrust faults in the San Francisco Bay area, with an emphasis on the recently identified Mount Diablo blind thrust fault. Fenton and Hitchcock (2001) describe the results of geomorphic and paleoseismic studies on active thrust faults in the Santa Clara Valley, south of San Francisco Bay.

CASCADIA SUBDUCTION ZONE

The Cascadia subduction zone dominates the structural setting of northwestern California. The subduction zone extends along the Pacific margin, from north of the Canadian border to the Mendocino escarpment in Northern California. Fault movement associated with the subduction zone is the dominant earthquake hazard in northwestern California. Sources of earthquakes include the subduction zone interface, thrust and strike slip faults in the overriding North American plate, and normal faults in the subducted slab. Kelsey (2001) provides a thorough summary of the tectonic environment and seismic potential of the Cascadia subduction zone, with an emphasis on northwestern California.

SIERRA NEVADA

Active faults in the Sierra Nevada include faults associated with both the Sierra Nevada frontal fault system, which forms the boundary between the Sierra Nevada and the Basin and Range and Modoc Plateau provinces to the east, and Quaternary faults that in some instances follow the alignment of the Mesozoic Sierra Nevada foothills fault system. Extensive studies have been performed to evaluate the distribution and seismic potential of these faults during the last two decades. Detailed mapping, paleoseismic trenching, and extensive geomorphic profiling have been conducted on faults throughout the central and northern Sierra Nevada. Many of the active faults identified during these studies have slip rates as low as 10^{-3} to 10^{-4} mm/year, and thus document some of the lowest slip rate faults known in the world. Page and Sawyer (2001) provide a summary of these studies, including a description of the geomorphic techniques used to detect these low slip-rate faults.

In summary, tremendous progress has been made over the past decade to identify and characterize active faults in Northern California. In particular, we have made great strides in characterizing the Cascadia subduction zone, Quaternary faults in the Sierra Nevada, and blind thrust faults in the San Francisco Bay area. Furthermore, we continue to refine and improve our understanding of the seismic potential of strike slip faults of the San Andreas fault system.

Our current state of knowledge of active faults enables engineering geologists to efficiently characterize earthquake hazards for existing and new projects in Northern California. It is unlikely that significant active faults have gone undetected, given that known faults account for over 95% of the documented plate motion rate. However, some less active faults—with slip rates of less than 1 mm/year—and secondary faults related to the more active faults may still remain undetected. It is incumbent on the engineering geologist to perform sufficient studies at any project location to demonstrate the absence of such faults.

Future research on active faults in Northern California will continue to improve our understanding of the paleoseismic history of specific faults, fault segmentation, and earthquake recurrence. The USGS is sponsoring an ongoing program called the Bay Area Paleoseismic Experiment (BAPEX) to develop new paleoseismic information on every significant strike slip fault in the San Francisco Bay area. In particular, studies will be performed to evaluate the "linkage" of earthquake activity on faults, and how and where creeping faults accumulate elastic strain, if any. In addition, new and refined fault location maps will continue to be published by DMG and the USGS as new information on fault location becomes available. Many of these maps will be digital products, available over the internet, and no doubt will be frequently updated. Engineering geologists in Northern California should stay abreast of these continually revised and

updated maps through participation in their local section of AEG and other professional organizations.

SELECTED REFERENCES

Borchardt, G. and Baldwin, J.N., 2001, Late Holocene behavior and seismogenic potential of the Concord-Green Valley fault system in Contra Costa and Solano counties, California: This volume.

Fenton, C.H. and Hitchcock, C.S., 2001, Recent geomorphic and paleoseismic investigations of thrust faults in the Santa Clara Valley, California: This volume.

Hall, N.T., Wright, R.H., and Prentice, C.S., 2001, Studies along the Peninsula segment of the San Andreas fault: This volume.

Kelsey, H.M., 2001, Active faulting associated with the Southern Cascadia subduction zone in Northern California: This volume.

Kelson, K.I., 2001, Geologic characterization of the Calaveras fault as a potential seismic source, San Francisco Bay area, California: This volume.

Lettis, W.R., 2001, Late Holocene behavior and seismogenic potential of the Hayward-Rodgers Creek fault system in the San Francisco Bay area, California: This volume.

Page, W.D. and Sawyer, T.L, 2001, Identifying Quaternary faulting within the Northern and Central Sierra Nevada, California: This volume.

Unruh, J.R., 2001, Seismic hazards associated with blind thrusts in the San Francisco Bay area: This volume.

WGCEP (Working Group on California Earthquake Probabilities), 1999, Earthquake probabilities in the San Francisco Bay Region: 2000 to 2030—a summary of findings: U.S. Geological Survey Open-file Report 99-517, 60 p.

LATE HOLOCENE BEHAVIOR AND SEISMOGENIC POTENTIAL OF THE HAYWARD-RODGERS CREEK FAULT SYSTEM IN THE SAN FRANCISCO BAY AREA, CALIFORNIA

WILLIAM R. LETTIS[1]

ABSTRACT

The Hayward-Rodgers Creek fault system (HRC) is the primary dextral slip fault within the San Andreas fault system in the eastern and northern San Francisco Bay area. In 1999, the fault system was re-evaluated by the Working Group on California Earthquake Probabilities (WGCEP, 1999). This paper summarizes, in part, the consensus of Working Group 1999 for characterizing the seismic potential of the HRC. In addition, information is provided on the potential for surface fault rupture, and the expected amount and width of ground deformation. The HRC is divided into three potential fault rupture segments, each capable of producing a M_W 6.75 to 7 earthquake: the Rodgers Creek fault segment and the northern and southern segments of the Hayward fault. Current earthquake rupture scenarios also allow for rupture of the entire fault system in a single M_W 7 to 7.25 event.

The Hayward fault extends from near Warm Springs, Fremont, on the south, to San Pablo Bay, on the north, for a total fault length of 87 ± 10 km. The fault is creeping aseismically at an average rate of 4 to 5 mm/year, with a local high rate of 9 mm/year near Fremont. The most recent event on the southern Hayward fault occurred in 1868 (M_W 7) and ruptured the fault from near Agua Caliente, on the south, to near Rocky Mound, Oakland, on the north, a distance of 50 to 55 km. The most recent event on the northern Hayward fault occurred sometime between 1640 and 1776. Paleoseismic trench studies at the Mira Vista Golf and Country Club in El Cerrito suggest that 4 to 7 earthquakes have occurred on the northern Hayward fault during the past 2,130 years, giving an average recurrence time of 270 to 710 years between surface-faulting earthquakes. The long-term slip rate on the Hayward fault is assumed to be 9 ± 2 mm/year based on the observed aseismic creep rate of 9 mm/year near Fremont and on offset Holocene alluvial fan channels near the Masonic Home in Fremont.

The Rodgers Creek fault extends from San Pablo Bay, on the south, to near Healdsburg, on the north, for a total fault length of 63 ± 10 km. Based on paleoseismic studies at the Beebe Ranch and Triangle G Ranch trench sites, the most recent event on the Rodgers Creek fault occurred sometime between 1640 and 1776. Thus, timing of the most recent event allows for the possibility of coeval rupture of the Rodgers Creek fault and northern Hayward

[1] William Lettis & Associates, Inc.
1777 Botelho Drive, Suite 262
Walnut Creek, CA 94596
lettis@lettis.com

fault in a single event. Offset Holocene paleo-channels at Beebe Ranch provide a slip rate of 8.4 ± 2 mm/year for the Rodgers Creek fault. Unlike the Hayward fault, the Rodgers Creek fault does not appear to be creeping.

INTRODUCTION

The Hayward-Rodgers Creek fault system (HRC) is the primary dextral slip fault within the San Andreas fault system in the eastern and northern San Francisco Bay area. The fault system constitutes the largest source of seismic risk in the Bay area, including hazards from strong ground motion, surface fault rupture, liquefaction, and earthquake-induced landsliding. In 1999, the seismic potential of this fault system was re-evaluated by the Working Group on California Earthquake Probabilities (WGCEP, 1999). This paper summarizes, in part, the consensus of the 1999 Working Group on seismic source parameters for the HRC, including slip rate, displacement per event, segmentation, maximum earthquake magnitude, and earthquake recurrence. In addition, the potential for surface fault rupture is discussed, including an estimate of the expected amount and width of surface deformation along the fault zone.

The HRC was characterized previously by the Working Group on California Earthquake Probabilities (WGCEP, 1990) and the Working Group on Northern California Earthquake Probabilities (WGNCEP, 1996). Each of these working groups characterized the fault system as consisting of two seismically independent faults, the Hayward fault and the Rodgers Creek fault. Although Working Group 1999 retained separate names for these faults, it now considers earthquake rupture models that allow for the possibility of rupture of the entire fault system. In the following sections, I discuss first the Holocene behavior and seismogenic potential of the Hayward fault, followed by the Rodgers Creek fault, and conclude with a discussion of alternative rupture models for the entire fault system.

THE HAYWARD FAULT

The Hayward fault extends from near Warm Springs, Fremont, on the south, to San Pablo Bay, on the north (Figure 1), for a total fault length of 87 ± 10 km. The fault is creeping at the surface along its entire length (Lienkaemper et al., 1991; Lienkaemper and Galehouse, 1998), although the rate of creep varies spatially along the fault trace. The average rate of observed creep is 4 to 5 mm/year, with a high of 9 mm/year observed locally near the southern end of the fault near Fremont. The fault produced one large historical earth-

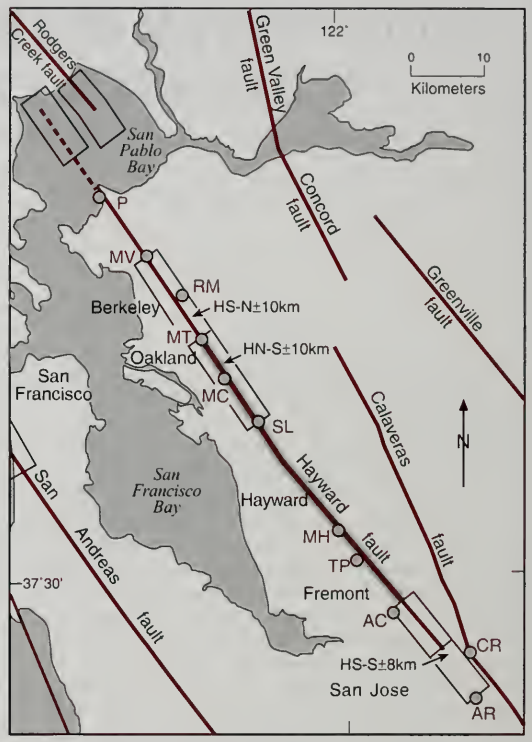

Figure 1. Location of the Hayward fault. Circles indicate localities mentioned in the text. Creeping trace extends at least 68 km from P (Point Pinole) to AC (Agua Caliente Creek). Trenching sites: MV, Mira Vista (Hayward Fault Paleoearthquake Group, 1997); MT, Montclair (Lienkaemper and Williams, 1999); MH, Masonic Home (Lienkaemper and Borchardt, 1996); TP, Tule Pond (Williams, 1992). Other localities: RM, Rocky Mound, key triangulation point of Yu and Segall (1996); SL, San Leandro, largest bend in fault and possible segment boundary; CR, near Calaveras Reservoir, the branching point of the northern Calaveras fault from the faster-creeping southern Calaveras fault; MC, Mills College; AC, Agua Caliente; and AR, Alum Rock. Minimum extent of 1868 surface rupture shown as gray band.

quake in 1868, with reported surface fault rupture generally of less than 0.5 m extending from near Agua Caliente, on the south, to San Leandro, on the north, and possibly as far north as Mills College, a distance of 32 to 41 km, respectively (Lawson, 1908). A paleoearthquake study in the Montclair District of Oakland (Lienkaemper and Williams, 1999) suggests that the 1868 surface rupture may have extended at least as far north as Montclair Park, indicating at least 45 km of surface rupture. Yu and Segall (1996) examined historical triangulation data from the 19th century to further evaluate the dimensions and size of the earthquake. They estimated the overall size of the 1868 earthquake to be M_W~7.0, and concluded that the rupture extended for 50 to 55 km from near Warm Springs, on the south, to near Rocky Mound, Oakland, on the north, with an average slip of 1.9 ± 0.4 m. At this time, we do not know how the magnitude and length of the 1868 event compares to earlier events on the southern Hayward fault because the paleoseismic record, to date, is not adequate to compare the size of events.

In 1836, another large earthquake struck the southern San Francisco Bay area. Early reports located this earthquake on the northern Hayward fault (Louderback, 1947). The occurrence of this earthquake was used to establish the timing of the most recent event on the northern Hayward fault and to demonstrate that the fault did not rupture simultaneously with the Rodgers Creek fault. More recently, Toppozada and Borchardt (1998) reexamined the intensity data and felt reports from the 1836 earthquake and concluded that the event occurred south of the southern Bay area and not on the northern Hayward fault. Thus, the most recent event for the northern Hayward fault is pre-1776, the date suggested by Toppozada and Borchardt (1998) for the start of the regional historical record. Determining that the 1836 earthquake did not occur on the northern Hayward fault, therefore, has removed constraints on elapsed time and segmentation for this part of the fault.

Seismicity (M_L 4.5) is occurring along nearly the entire length of the Hayward fault (Oppenheimer et al., 1992). Cross sections of the seismicity define a nearly vertical fault plane over most of the length of the fault, with a seismogenic zone extending down to 13 km. Focal mechanisms generally are consistent with right-lateral motion on a vertical fault, but near San Leandro secondary faults adjacent to the Hayward fault exhibit localized oblique slip and reverse motion. The focal mechanisms also are consistent with the presence of thrust or reverse faults along the western margin of the East Bay Hills between San Leandro and Oakland. In addition, preliminary results from a high-resolution seismicity analysis along the Hayward fault (Waldhauser and Ellsworth, 1999) identify a narrow zone of faulting from Berkeley to El Cerrito and from Hayward to Fremont, and a broad diffuse zone of faulting between Oakland and San Leandro. This area of localized convergence and broader zone of deformation along the Hayward fault in the San Leandro to Oakland area may be an indication of structural complexity and possible segmentation along the fault.

Previous seismic source characterizations (pre-1996)

In 1990, the Working Group divided the Hayward fault into two segments, the northern and southern Hayward fault. The two-segment model largely evolved from the assumed knowledge of two large historical earthquakes in 1836 and 1868 on the northern and southern segments, respectively. They assigned a slip rate of 9 ± 2 mm/year and slip-per-event of 1.5 ± 0.5 m to each segment. Based primarily on written accounts that the 1868 rupture extended only as far north as San Leandro (Lawson, 1908) and with no data on the extent of the 1836 rupture, the 1990 Working Group estimated lengths of 50 and 32 km for the northern and southern segments, respectively. In 1996, the Working Group retained a revised two-segment model but equally allowed for the scenario of rupture involving the entire fault length (one-segment model) (WGNCEP, 1996; Peterson et al., 1996). Given uncertainty in the northern extent of rupture of the 1868 earthquake and lack of a strong geometric basis for segmentation, the Working Group (1996) revised the 1990 characterization and defined two 43-km-long segments, each with a slip rate of 9 ± 2 mm/year and slip per event of 1.9 ± 0.4 m.

Information developed since 1996

Since publication of the Peterson et al. (1996) and WGNCEP (1996) summaries of source characteristics in the San Francisco Bay region, several seismologic and geologic studies have been performed on the Hayward fault. Toppozada and Borchardt (1998), in their study of the 1836 earthquake, present compelling information that the 1836 earth-

quake did not occur on the Hayward fault, although its precise location in the southern Bay area is not well established. The 1999 Working Group accepted the conclusion that the 1836 earthquake did not occur on the Hayward fault and should not be considered further in evaluating source characteristics of the Hayward fault.

Further research has been conducted on the structural character of San Pablo Bay. Gravity data reveal a prominent gravity low beneath the Bay (Jachens, 1999). The gravity low is sharply bounded on the west by the projected trace of the Hayward fault, suggesting that the fault extends nearly to the northern margin of San Pablo Bay. The gravity low is not similarly bounded on the east. The gravity low extends smoothly across the southern projected trace of the Rodgers Creek fault and does not reveal any internal structure or cross-faults between the Hayward and Rodgers Creek faults. In addition, BASIX acquired and processed seismic reflection data within the Bay and Chevron has released unpublished interpretations of proprietary seismic data in the Bay (Williams, 1999). These data do not show a prominent trace of the Hayward fault within the Bay; however, the quality of data is poor. A fault believed to be the southern extension of the Rodgers Creek fault is imaged on the Chevron seismic data extending about 4 km into the Bay.

Significant uncertainties in characterizing the Hayward fault include the depth that aseismic creep extends into the crust and the role of aseismic creep in releasing elastic strain along the fault. High-resolution seismicity studies reveal distinct horizontal seismicity lineations along parts of the Hayward fault (Waldhauser and Ellsworth, 1999). The lineations persist over time but with a slow repeat rate, suggesting high frictional resistance on the fault "stuck patch." High frictional resistance along the fault is consistent with findings from repeated geodetic surveys across the Hayward fault, indicating that the fault is frictionally locked between about 5 and 13 km depth (Savage and Lisowski, 1993). On the other hand, recent modeling of Interferometric Synthetic Aperture Radar (InSAR) measurements from 1992 to 1997 allows the possibility that the Hayward fault north of Berkeley could be creeping aseismically to a depth of 12 km (Burgmann, 1999). Lienkaemper and Galehouse (1998) recently reviewed evidence for creep along the fault and concluded that about 10% of the total movement rate on the fault is released by aseismic creep. Working Group 1999 concluded that, because the Hayward fault produced a large earthquake in 1868, the fault likely is storing elastic strain that will be released in future large earthquakes. Working Group 1999 reduced the full geologic slip rate of 9 mm/year by 20% (± 20%) on the southern Hayward fault and 40% (± 30%) on the northern Hayward fault in estimating the probability of future earthquakes on the fault. This reduction was treated in the Working Group 1999 model by proportionately reducing the width of the fault in the crust while maintaining a constant slip rate of 9 mm/year.

Two paleoseismic studies provide information on the number and timing of past earthquakes on the Hayward fault. Paleoseismic trenches were excavated at Mira Vista on the northern Hayward fault (Hayward Fault Paleoearthquake Group, 1999) and at the Tule Pond in Fremont on the southern Hayward fault (Williams, 1992) across sag ponds containing finely laminated, organic-rich silts and clays. At each site, upward fault terminations, tilted and disrupted strata, and discordant angular relations were used to identify past earthquakes. Liquefaction features also were preserved at the Tule Pond. At Mira Vista, four to seven surface-faulting events were identified during the past 1,630 to 2,130 years, providing a range in recurrence interval of 270 to 710 years. The 1868 event is not present at Mira Vista, providing limiting constraints on the maximum northern extent of the 1868 surface rupture. Timing of the most recent event is bracketed between 1640 and 1776 (the suggested starting point of the regional historic seismicity record). At the Tule Pond, at least six and up to eight surface faulting events were identified during the past 2,100 years, providing a range in recurrence interval of about 150 to 250 years.

Two other paleoseismic studies provide information on the Holocene slip rate on the Hayward fault. Paleoseismic trenches were excavated at the Masonic Home near Union City on the southern Hayward fault (Lienkaemper and Borchardt, 1996), and geomorphic analyses of offset paleochannels along Strawberry Creek were performed in Berkeley along the northern Hayward fault (Williams, 1999). At the Masonic Home, two offset alluvial fan deposits provide estimates of slip rate of 8.0 ± 0.7 and 9.2 ± 1.3 mm/year over the past 8,300 and 4,600 years, respectively. At Strawberry Creek, offset paleochannels provide a slip rate of 10 ± 2 mm/year (Williams, 1999). Both of these studies have uncertainty regarding the direction of stream flow and correlation of geomorphic features across the fault,

Fault segment	Slip rate (mm/year)	Length (km)	Width (km)	Slip/Event (m)	Most recent event	Geologic recurrence interval (yrs)[1]
Rogers Creek	9 ± 2	63	12	2 ± 0.5	1650-1776	100-679
Northern Hayward	9 ± 2	31	12	1.9 ± 0.4	1640-1776	270-710
Southern Hayward	9 ± 2	56	12	1.9 ± 0.4	1868	150-250

[1]Recurrence interval estimated from paleoseismic trench observations. Recurrence interval calculated by Working Group 1999 differs depending on recurrence model used and estimated range in maximum magnitude.

Table 1. Seismic source parameters for the HRC.

and on whether the studies captured the entire width of secondary deformation across the fault zone. These slip rates, therefore, should be regarded as tentative. More work is required to determine the Holocene geologic slip rate on the Hayward fault, and the variability in slip rate from south to north along the fault as slip decreases from south to north on the bordering Calaveras fault.

Seismic source characterization

Source characterization parameters used for estimating time-dependent earthquake probabilities include timing of the most recent event, slip rate, fault dimensions (length and width), segmentation, maximum magnitude, and recurrence. These parameters are provided in Table 1 for the HRC.

Most recent event. The most recent event on the Hayward fault is based on both historical seismicity data and paleoseismic information. The southern Hayward fault last ruptured during the 1868 earthquake. Lawson (1908) stated that surface rupture in 1868 extended at least from Agua Caliente Creek, on the south, to San Leandro, and less certainly to Mills College, on the north. Paleoseismic investigations by Lienkaemper and Williams (1999) suggest that slip may have extended at least as far north as the Montclair District of Oakland. Analysis of 19th-century triangulation data by Yu and Segall (1996) suggests that subsurface slip extended at least as far north as Rocky Mound near Berkeley. The study by Yu and Segall (1996) indicates a total rupture length of 50 to 55 m, with an average slip of 1.9 ± 0.4 m.

The 1868 event probably did not rupture the northern 30 to 35 m of the Hayward fault. Paleoseismic studies at Mira Vista in El Cerrito show that the most recent event at the trench site probably occurred between 1640 and 1776 (Hayward Fault Paleoearthquake Group, 1999). The work at Mira Vista, however, focused primarily on secondary deformation in a sag pond adjacent to the main trace of the fault. The Mira Vista trenches do not preclude the presence of the 1868 rupture along the main trace, although such a northern extent of the 1868 rupture is not supported by the historical triangulation data (Yu and Segall, 1996) or earthquake intensity data (Bakun, 1999).

Slip rate. Little new information has been developed since 1996 on the slip rate of the Hayward fault. Thus, Working Group 1999 retained the 1996 Working Group estimate of 9 ± 2 mm/year for the entire fault. Measurements of surface creep (Lienkaemper et al., 1991; Lienkaemper and Galehouse, 1997) show that the Hayward fault has an average creep rate of about 4 to 6 mm/year along most of the fault with a high of 9 mm/year noted near Fremont. Assuming that the rate of deep slip must at least equal the rate of surface creep, Working Group 1999 believed that an estimate of 9 mm/year is reasonably conservative for the fault. This estimate is supported by two minimum estimates of Holocene slip rate of 8.0 ± 0.7 and 9.2 ±1.3 mm/year at the Masonic Home near Union City (Lienkaemper and Borchardt, 1996) and an estimate of 10 ± 2 mm/year at Strawberry Canyon in Berkeley (Williams, 1999). The estimate of 9 ± 2 mm/year is intended to bracket these geologic uncertainties. The relation between surface creep and crustal stress accumulation was identified by the 1990 Working Group as an important issue that remains unresolved at this time. As described earlier, Working Group 1999 estimated that 20% (±20%) and 40%

(±30%) of the total moment rate on the southern and northern Hayward fault, respectively, is released by aseismic creep.

Slip per event. No new information has been obtained since 1996 on the amount of coseismic slip that occurs during large-magnitude Hayward fault earthquakes. Thus, Working Group 1999 retained the 1996 Working Group estimate of 1.9 ± 0.4 m based on the triangulation analysis of the 1868 earthquake by Yu and Segall (1996) of deep slip on the Hayward fault, and the assumption that the 1868 earthquake is the characteristic event for both the northern and southern segments of the fault. Observations of surface displacement reported in Lawson (1908) suggest that surface displacement along the Hayward fault during the 1868 event was about 50 cm or less. This would suggest that the deep slip of 1.9 m estimated by Yu and Segall (1996) attenuated toward the ground surface, and that the observed length of surface rupture may be significantly less than the length of subsurface rupture. The apparent attenuation of slip toward the ground surface also suggests that the Hayward fault was creeping during the seismic cycle culminating with the 1868 earthquake.

Surface fault rupture. The Hayward fault traverses the densely urbanized eastern Bay area. The fault generally consists of a single main creeping trace and, less commonly, two creep traces in a zone of faulting up to 200 to 500 m wide. Although the style of faulting is dominantly right-lateral strike slip, both normal and reverse faults occur within the fault zone, depending on the local fault orientation and on the geometry of overlapping fault strands. Reverse and oblique slip faults are especially prevalent along the fault zone between San Leandro and north Oakland. Most of the Holocene active Hayward fault zone is encompassed by the California Division of Mines and Geology Earthquake Fault Zone Special Studies maps. However, there are several notable exceptions in the San Lean-dro and Oakland areas, where Holocene and potentially Holocene fault traces of the Hayward fault zone extend outside the limits of the Special Studies Zone maps (e.g., McCormick et al., 1992).

Based on estimates of the maximum earthquake, coseismic fault rupture of up to 2 m may occur along the fault zone. Paleoseismic trench studies suggest that the rupture may be confined to a single primary trace or be distributed over a zone of faulting up to 200 m wide. In addition, because the fault is creeping, coseismic slip at depth may attenuate toward the ground surface; hence, the total expected amount of surface fault rupture is expected to be less than the coseismic slip at depth (i.e., less than 2 m).

Segmentation. The Hayward fault traditionally is divided into two segments, a northern segment and a southern segment. As noted earlier, this two-segment model originated largely from the belief that two large-magnitude historical earthquakes occurred on the northern and southern segment in 1836 and 1868, respectively. Other than this behavioral information, Working Group 1999 did not identify any significant physical, structural, or geometric basis for dividing the Hayward fault into two segments. Relocating the 1836 earthquake off of the Hayward fault (Toppozada and Borchardt, 1998) has removed behavioral constraints on segmentation of the Hayward fault and on the timing of the most recent event. However, it still appears that the 1868 event did not fully rupture the entire Hayward fault; thus, some form of segmentation may be occurring. In addition, analysis of seismicity shows that the character of deformation along the Hayward fault changes from a relatively simple, narrow fault plane with strike-slip motion north of Oakland and south of San Leandro, to a broader, more diffused zone of deformation with oblique and reverse motion on secondary faults between Oakland and San Leandro. This localized region of apparent structural complexity may reflect an unknown structural barrier to earthquake rupture.

The 1999 Working Group retained the two-segment model for the Hayward fault, partly based on the observation that the 1868 earthquake did not fully rupture the entire fault and partly out of tradition. However, it significantly revised the segment boundary locations and, thus, the lengths of the northern and southern segments of the fault.

As newly defined, the northern segment of the Hayward fault extends from San Pablo Bay, on the north, to near Montclair, on the south. The northern endpoint was judged to be near the northern end of San Pablo Bay, along the prominent gravity low beneath the Bay. Working Group 1999 assigned an uncertainty of ±5 km to the endpoint. The southern endpoint of the northern Hayward fault is not well constrained. There is no strong physical or behavioral basis for identifying a segment boundary. Initially, Working Group 1999 considered a possible southern endpoint anywhere between Mira Vista, on the north, and San Leandro, on the south, and

selected an endpoint mid-way between Montclair and Mills College with an uncertainty of ±10 km. For calculation of seismic movement, however, Working Group 1999 ultimately assigned an endpoint at Montclair, with an uncertainty of ±10 km, and made it the endpoint for both the northern and southern Hayward fault to avoid double counting of seismic movement.

The southern segment of the Hayward fault initially was interpreted by Working Group 1999 to be the extent of the 1868 rupture. As described above, the Working Group selected an endpoint to be at Montclair with an uncertainty of ±10 km. The southern endpoint was defined midway between the intersection of the Hayward fault with the Mission fault seismicity trend and the Alum Rock seismicity trend, with an uncertainty of ±8 km. This endpoint also allows for the possibility that the subsurface extent of the southern Hayward fault may extend toward a merger with the Calaveras fault near Calaveras Reservoir.

As newly defined, the lengths of the northern and southern segments of the Hayward fault are 35 ± 8 km and 52 ± 9 km, respectively. Further work is required to define the northern extent of the 1868 rupture. If the 1868 rupture were shown to extend north of the Montclair/Rocky Mound area, then the length of the northern and southern Hayward fault segments might shorten and lengthen, respectively, in future seismic source characterizations of the Hayward fault.

RODGERS CREEK FAULT

The Rodgers Creek fault extends from San Pablo Bay, on the south, to approximately 6 km southeast of Healdsburg, on the north, (Figure 2), for a total fault length of 63 ± 5 km. Unlike the Hayward fault to the south, the Rodgers Creek fault segment does not have any recognized surface creep (<2 mm/year, Galehouse, 1995) and appears to be entirely locked throughout the seismogenic zone. There is no evidence for a large historical surface-faulting earthquake on the Rodgers Creek fault. Based on intensity data and historical accounts, however, Toppozada et al. (1992) concluded that the 1898 Mare Island earthquake might have occurred on the southern Rodgers Creek fault, and assigned a M_W 6.5 to the event. Bakun (1999) also concluded that the 1898 earthquake occurred somewhere in the vicinity of San Pablo Bay and, if it were located on the southern Rodgers Creek fault, the intensity data

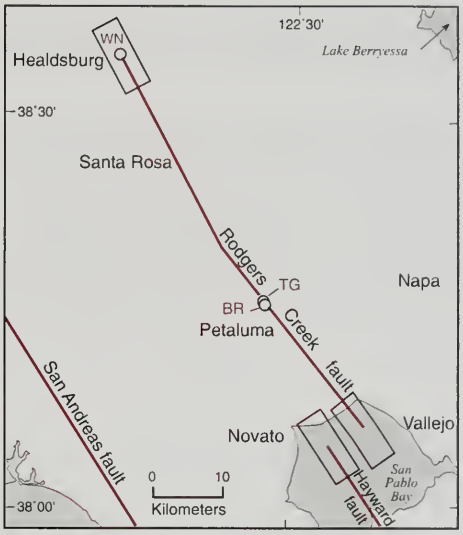

Figure 2. Location of the Rodgers Creek fault. Circles indicate localities mentioned in the text. Trenching sites: BR, Beebe Ranch; TG, Triangle G Ranch; WC, Windsor Creek.

suggest that the event might have had a M_W 6.3. This size earthquake is at the threshold of producing surface-fault rupture and, therefore, may not be recognized in paleoseismic trench investigations or as a distinct geomorphic feature.

Previous Working Group characterizations

In 1990, the Working Group characterized the Rodgers Creek as a single rupture segment, 63 km long, with a slip rate of 2.1 to 5.8 mm/year, a slip-per-event of 2 ± 0.3 m, and a recurrence interval of 248 to 679 years, based on initial results from the Beebe Ranch paleoseismic site (Budding et al., 1991). Between 1990 and 1996, additional paleoseismic studies were conducted at Beebe Ranch and at the Triangle G Ranch along the central reach of the Rodgers Creek fault (Schwartz et al., 1992; Budding et al., 1991). At Beebe Ranch, offset Holocene stream channels exposed in trenches across alluvial fan and debris flow deposits were used to estimate a slip rate of 8.4 ± 2 mm/year. Slip during the most recent event was 2 ± 0.5 m, based on an offset debris-flow levee and channel. At the Triangle G Ranch site, upward fault terminations and fissure infills pro-

vided evidence of the past three surface-faulting events with an average recurrence interval of 230 ± 130 years.

In 1996, The Working Group retained a single-segment rupture scenario for the Rodgers Creek fault and revised the source characterization to incorporate the results from Beebe Ranch and Triangle G Ranch. The 1996 Working Group adopted a slip rate of 9 ± 2 mm/year because it satisfies conservation of slip from the Hayward fault and is within the approximate uncertainty bounds of the slip rate estimated at Beebe Ranch. It also adopted a characteristic coseismic slip value of 2 m.

New information since 1996

No new paleoseismic data have been obtained on the Rodgers Creek since 1996. Unpublished modeling of geodetic data (Prescott, 1999) was used to calculate a slip rate of up to 12 m/year. However, these results are preliminary and are subject to revision based on further modeling. These data were not incorporated in the Working Group 1999 characterization of the Rodgers Creek fault.

In addition, further gravity and seismic reflection profiling have been performed within San Pablo Bay. These studies were performed, in part, to evaluate the structural association between the southern Rodgers Creek fault and the northern Hayward fault. As described earlier, a distinct gravity low is present within San Pablo Bay. The gravity low is abruptly truncated along the northern projection of the Hayward fault but extends smoothly across the Rodgers Creek fault. The Rodgers Creek fault, therefore, either does not extend beneath San Pablo Bay or, if present, does not significantly juxtapose basement rocks against a sedimentary basin. Nevertheless, unpublished seismic reflection data show disrupted and offset strata along the southern projection of the Rodgers Creek fault in central San Pablo Bay (Williams, 1999). Seismic reflection data obtained by BASIX do not image a fault in the southern San Pablo Bay along the projection of the Rodgers Creek fault, but the data quality in this area is poor. Rather, the BASIX data image an offshore fault along the northern projection of the Pinole fault. Williams (1999) hypothesizes that the Rodgers Creek fault may form a small left stepover to the Pinole fault beneath San Pablo Bay.

Seismic source characterization

Source characterization parameters used for estimating time-dependent earthquake probabilities include timing of the most recent event, slip rate, fault dimensions (length and width), segmentation, maximum magnitude, and recurrence (Table 1).

Most recent event. Paleoseismic data from Beebe Ranch and Triangle G Ranch indicate that the most recent event on the Rodgers Creek fault occurred after 1650. Although there has not been a large historical surface-faulting earthquake on the fault, Toppozada et al. (1992) suggest that the 1898 Mare Island earthquake occurred on the southern Rodgers Creek fault, with any possible ground rupture being south of the paleoseismic trenches. The 1898 event, however, does not appear to be the maximum potential earthquake on the fault, because it did not produce surface rupture. Thus, Working Group 1999 concluded that the most recent event on the Rodgers Creek fault occurred sometime between 1650 and 1776 (the beginning of the historical record).

Slip rate. No new information has been developed since 1996 on the geologic slip rate on the Rodgers Creek fault. Thus, Working Group 1999 retained a slip rate of 9 ± 2 mm/year based on the offset alluvial channels observed at Beebe Ranch (Schwartz et al., 1992).

Slip per event No new information has been developed since 1996 on slip-per-event on the Rodgers Creek fault. Thus, the 1996 Working Group estimate of 2 m per event was retained, with an assigned uncertainty of ±0.5 m based on the offset debris flow levee and channel observed at Beebe Ranch (Budding et al., 1991).

Segmentation. The Rodgers Creek fault terminates both to the north and south in distinct right stepovers of a few kilometers width (Figure 2). To the north, the fault is interpreted to end near Windsor Creek, where it forms an approximate 3-km-wide right stepover to the southern Maacama fault. To the south, the fault is interpreted to end in central San Pablo Bay, where it is imaged on seismic reflection data. The fault forms a 5- to 6-km-wide right stepover to the northern Hayward fault. The ends of both faults may run parallel and overlap one another by 5 to 10 km within San Pablo Bay. Both the northern and southern terminations of the Rodgers Creek fault have a location uncertainty of ±5 km. As defined, the Rodgers Creek fault is 63 ± 5 km long.

Working Group 1999 did not observe any structural, geometric, or behavioral changes along the Rodgers Creek fault that merit consideration for segmentation of the Rodgers Creek fault, so it did not consider any alternative segmentation models. The fault generally is very well-defined geomorphically as a strike-slip fault (e.g., beheaded drainages, pressure ridges, shutter ridges, deflected drainages) north of Highway 37 along the northern margin of San Pablo Bay to Windsor Creek, 6 m south of Healdsburg. It is not known, however, whether the Rodgers Creek fault ruptures solely as an independent seismic source or ruptures together with part or all of the Hayward fault. The timing of the most recent events on the northern Hayward fault and Rodgers Creek fault are 1640 to 1776 and 1650 to 1776, respectively, and the slip rate on both faults is comparable. Working Group 1999 strongly favored the interpretation that the Hayward and Rodgers Creek faults likely are separate, independent seismic sources, but it also considered the possibility that an earthquake may nucleate in the San Pablo Bay stepover and rupture bilaterally on both faults.

RUPTURE SCENARIOS FOR THE HAYWARD-RODGERS CREEK FAULT SYSTEM

As noted above, the HRC consists of the Hayward fault and the Rodgers Creek fault. The Hayward fault is further divided into two segments, a northern segment and a southern segment. The Rodgers Creek fault is considered to be one rupture segment. Working Group 1999 considered five rupture scenarios that involve these three fault segments. The various scenarios described below are shown on Figure 3.

- Scenario 1 (RC/NH/SH) envisions simultaneous rupture of all three segments, extending from the northern end of the Rodgers Creek fault to the southern end of the Hayward fault.
- Scenario 2 (RC/NH + SH) envisions simultaneous rupture of the Rodgers Creek fault with the northern Hayward fault and independent rupture of the southern Hayward fault.
- Scenario 3 (RC + NH/SH) envisions independent rupture of the Rodgers Creek fault and simultaneous rupture of the northern and southern Hayward fault.

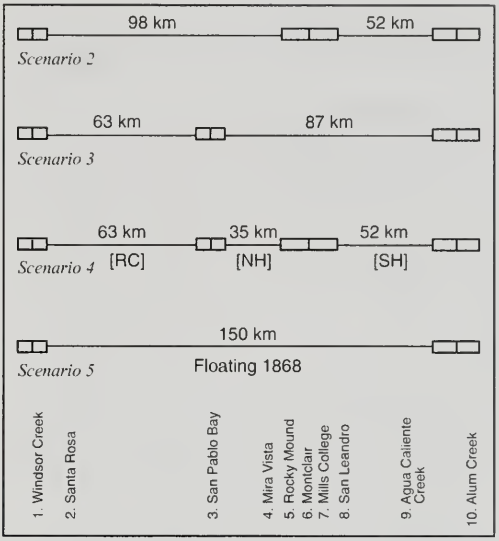

Figure 3. Segmentation scenarios for the Hayward-Rodgers Creek fault system. Open boxes depict uncertainty in segment boundaries. Not to scale. RC—Rodgers Creek segment, NH—North Hayward segment, SH—South Hayward segment.

- Scenario 4 (RC + NH + SH) envisions independent rupture of all three fault segments.
- Scenario 5 (Segments unknown). The fault system is segmented, but the segment boundaries are not known. Thus, the fault system ruptures in 1868-size events, spatially unconstrained along the entire fault (i.e., a floating 1868 earthquake).

EARTHQUAKE OCCURRENCE MODELS AND WEIGHTINGS

An earthquake occurrence model consists of various combinations of rupture scenarios with the relative frequency of their occurrence. Working Group 1999 considered four earthquake-occurrence models that describe the future earthquake behavior of the fault system, and assigned weightings to each model describing the likelihood that that model is correct. Each model consisted of various combinations of the five rupture scenarios identified for the HRC. The models and their relative weightings are summarized in Table 2. For example, Model A assigns a 9% likelihood that the entire fault system would

Rupture scenario	Model A (percent)	Model B (percent)	Model C (percent)	Model (percent)
1 (RC/NH/SH)	9	5	7	3
2 (RC/NH) + SH)	6	10	20	7
3 RC + (NH/SH)	55	40	10	15
4 RC + NH + SH	25	40	55	70
5 Segments unknown (floating 1868)	5	5	8	5
	100	100	100	100
Model weightings	22	36	11	31

Table 2. Working Group 1999 proposed models and weightings for the HRC.

rupture in a single event, a 6% likelihood that the Rodgers Creek and northern Hayward faults would rupture separately from the southern Hayward fault, a 55% likelihood that the Hayward fault in its entirety would rupture separately from the Rodgers Creek fault, a 25% likelihood that all three fault segments rupture separately, and a 5% likelihood that the fault system would rupture in 1868-size events spatially unconstrained along the fault. Model A was then given a 22% likelihood that it correctly describes the long-term occurrence of earthquakes on the fault system.

Overall, a strong preference was given to those models that favor independent rupture of the Rodgers Creek and both segments of the Hayward fault, and to independent rupture of the Rodgers Creek and the entire Hayward fault. Little preference was given to rupture of the entire fault system or to the concept of a floating "1868" earthquake.

ACKNOWLEDGMENTS

This paper summarizes, in part, the consensus of the Hayward-Rodgers Creek fault Seismic Source Characterization subgroup of the 1999 Working Group on California Earthquake Probabilities. Members of the subgroup included William Lettis, chairman, Keith Kelson, Gary Simpson, Kathryn Hanson, David Schwartz, Robert Wright, Bill Bryant, Bill Foxall, Jim Lienkaemper, Glen Borchardt, Chris Wills, Patrick Williams, Jim Hengesh, John Wesling, Bill Bakun, Dave Oppenheimer, Roland Bürgmann, and Dave Manaker. Each of these individuals attended one or more meetings of the subgroup and contributed valuable data, ideas, and discussion regarding our current understanding of the fault system. Not all members participated in the final segmentation and rupture model characterization of the fault system and some simplifications to the source model were made by the 1999 Working Group Oversight Committee. Mary Lou Zoback, Suzanne Hecker, Ivan Wong, Allan Lindh, and Tousson Toppozada also made valuable contributions to this group and thus this paper. This paper benefited significantly from the peer review of Jim Lienkaemper and Glenn Borchardt. Support for this paper, in part, was provided by the U.S. Geological Survey under award numbers 1434-HQ-99-GR-0004 and 99-HQ-GR-0102. The views and conclusions contained in this paper are those of the author and should not be interpreted as necessarily representing the official policies, either expressed or implied, of the U.S. Government.

AUTHOR PROFILE

Dr. William Lettis is a Certified Engineering Geologist with 23 years of experience in the assessment of seismic hazards. He is the Principal Geologist and President of William Lettis & Associates, Inc. He specializes in paleoseismic fault investigations and the characterization and mitigation of seismic hazards, including surface fault rupture, strong ground motions, liquefaction, and earthquake-induced slope failure.

SELECTED REFERENCES

Bakun, W.H., 1999, Seismic activity of the San Francisco Bay region: Bulletin of the Seismological Society of America, v. 89, p. 764-784.

Budding, K.E., Schwartz, D.P., and Oppenheimer, D.H., 1991, Slip rate, earthquake recurrence, and seismogenic potential of the Rodgers Creek fault zone, northern California—Initial results: Geophysical Research Letters, v. 18, p. 447-450.

Bürgmann, R., 1999, Preliminary geodetic findings on earthquake potential along the northern Hayward fault, California: Letter to Working Group 1999 reporting on work in progress, 9 .

Galehouse, J.S., 1995, Theodolite measurements of creep rates on San Francisco Bay region faults: U.S. Geological Survey Open-file Report 95-210, p. 335-346.

Hayward Fault Paleoearthquake Group, 1999, Timing of paleoearthquakes on the northern Hayward fault—preliminary evidence in El Cerrito, California: U.S. Geological Survey Open-file Report 99-318, 34 p.

Jachens, R., 1999, Presentation to Working Group 1999 reporting on work in progress.

Lawson, A.C., 1908, The earthquake of 1868: in Lawson, A.C. (ed.), The California Earthquake of April 18, 1906, Report of the State Earthquake Investigation Commission (Volume I), Carnegie Institution of Washington Publication No. 87, p. 434-448.

Lienkaemper, J.J. and Borchardt, G., 1996, Holocene slip rate of the Hayward fault at Union City, California: Journal of Geophysical Research, v. 101, p. 6,099-6,108.

Lienkaemper, J.J. and Galehouse, J.S., 1997, Revised long-term creep rates on the Hayward fault, Alameda and Contra Costa Counties, California: U.S. Geological Survey Open-file Report 97-690, 18 p.

Lienkaemper, J.J. and Galehouse, J.S., 1998, New evidence doubles the seismic potential of the Hayward fault: Seismological Research Letters, v. 69, p. 519-523.

Lienkaemper, J.J. and Williams, P.L., 1999, Evidence for surface rupture in 1868 on the Hayward fault in north Oakland and major rupturing in prehistoric earthquakes: Geophysical Research Letters, v. 26, p. 1,949-1,952.

Lienkaemper, J.J., Borchardt, G., and Lisowski, M., 1991, Historic creep rate and potential for seismic slip along the Hayward fault, California: Journal of Geophysical Research, v. 96, p. 18,261-18,283.

Louderback, G.D., 1947, Central California earthquakes of the 1830's: Bulletin of Seismological Society of America, v. 34, p. 33-74.

McCormick, W.V., Burkland, P.V., and Raynak, P.J., 1992, Subsidiary faulting east of the Hayward fault in southern Alameda County: California Division of Mines and Geology Special Publication 113, p. 189-196.

Oppenheimer, D.H., Wong, I.G., and Klein, F.W., 1992, The seismicity of the Hayward fault, California: California Division of Mines and Geology Special Publication 113, p. 91-100.

Peterson, M.D., Bryant, W.A., Cramer, C.H., Cao, T., Reichle, M.S., Frankel, A.D., Lienkaemper, J.J., McCrory, P.A., and Schwartz, D.P., 1996, Probabilistic seismic hazard assessment for the State of California: California Division of Mines and Geology with U.S. Geological Survey Open-file Report 96-706, 59 p.

Prescott, W., 1999, Report to Working Group 1999 reporting on work in progress.

Savage, J.C. and Lisowski, M., 1993, Inferred depth of creep on the Hayward fault, central California: Journal of Geophysical Research, v. 98, p. 787-793.

Schwartz, D.P., Pantosti, D., Hecker, S., Okumura, K., Budding, K.E., and Powers, T., 1992, Late Holocene behavior and seismogenic potential of the Rodgers Creek fault zone, Sonoma County, California: California Division of Mines and Geology Special Publication 113, p. 393-398.

Toppozada, T.R. and Borchardt, G., 1998, Re-evaluation of the 1836 "Hayward Fault" earthquake and the 1838 San Andreas fault earthquake: Bulletin of Seismological Society of America, v. 88, p. 140-159.

Toppozada, T.R., Bennett, J.H., Hallstrom, C.L., and Youngs, L.G., 1992, 1898 "Mare Island" earthquake at the southern end of the Rodgers Creek fault: California Division of Mines and Geology Special Publication 113, p. 385-392.

Waldhauser, F. and Ellsworth, W.L., 1999, Preliminary results from high-resolution seismicity analysis on the Hayward fault: Letter to Working Group 1999 reporting on work in progress, 7 p.

Williams, P.L., 1992, Geologic record of southern Hayward fault earthquakes: California Division of Mines and Geology Special Publication, v. 113, p. 171-179.

Williams, P.L., 1999, Seismic reflection profiles in San Pablo Bay: Presentation to Working Group 1999 on work in progress.

WGCEP (Working Group on California Earthquake Probabilities), 1990, Probabilities of large earthquakes occurring in the San Francisco Bay Region, California: U.S. Geological Survey Circular 1053, 51 p.

WGCEP (Working Group on California Earthquake Probabilities), 1999, Earthquake probabilities in the San Francisco Bay Region: 2000 to 2030—a summary of findings: U.S. Geological Survey Open-file Report 99-517, 60 p.

WGNCEP (Working Group on Northern California Earthquake Potential), 1996, Database of potential sources for earthquakes larger than magnitude 6 in northern California: U.S. Geological Survey Open-file Report 96-705, 53 p.

Yu, E. and Segall, P., 1996, Slip in the 1868 Hayward earthquake from the analysis of historical triangulation data: Journal of Geophysical Research, v. 101, p. 16,101-16,118.

GEOLOGIC CHARACTERIZATION OF THE CALAVERAS FAULT AS A POTENTIAL SEISMIC SOURCE, SAN FRANCISCO BAY AREA, CALIFORNIA

KEITH I. KELSON[1]

ABSTRACT

The 130-km-long Calaveras fault represents a significant seismic source in the southern and eastern San Francisco Bay region. It extends from an intersection with the Paicines fault south of Hollister, through the Diablo Range east of San Jose, and along the Pleasanton-Dublin-San Ramon urban corridor. The fault consists of three major sections: the 24-km-long southern Calaveras fault (from the Paicines fault to San Felipe Lake), the 64-km-long central Calaveras fault (from San Felipe Lake to Calaveras Reservoir), and the 42-km-long northern Calaveras fault (from Calaveras Reservoir to Danville). The poorly constrained slip rate on the southern section is interpreted to be 15 ± 2 mm/year, although some workers have postulated rates as high as 20 mm/year. The central and northern sections have geologic slip rates of 14 ± 5 mm/year and 6 ± 2 mm/year, respectively. The level of contemporary seismicity along the southern section is low, whereas the central section has generated numerous moderate earthquakes (as large as M_W6.2) in historic time. The northern section has a relatively low level of seismicity and may be locked, although it is associated with the M_W5.6 1861 San Ramon Valley earthquake. Geologic and seismologic data suggest that the northern section may produce earthquakes as large as M_W7.

Paleoseismologic studies suggest a recurrence interval for large ruptures of between 250 and 850 years on the northern fault section. The timing of the most-recent rupture on the northern Calaveras fault is unknown, but may be several hundred years ago.

Engineering geology and paleoseismic studies along the northern Calaveras fault suggest along-strike variations in local sense of slip, although the fault is dominated by dextral slip and may have a component of oblique reverse movement. Current characterization of the fault includes six possible rupture scenarios, which range from independent large ruptures along the three main fault sections to M_W6.2 earthquakes distributed randomly along the fault. Current unknowns important to seismic hazard assessment involve the magnitudes of possible earthquakes and the timing and recurrence of large earthquakes on the three fault sections.

INTRODUCTION

In the southern San Francisco Bay region, most of the relative motion between the North American and Pacific plates is accommodated along the dextral San Andreas and Calaveras faults (Figure 1). The 130-km-long active Calaveras fault traverses the eastern margin of the southern Santa Clara Valley, where it is a major structural boundary between the San Francisco Bay structural depression and the Diablo Range (Page, 1982). Over the last ten years new data have been collected on the long-term slip rate and timing of surface ruptures along some fault sections, and monitoring surface fault creep has been monitored at several localities. Some of these data were available for the compilation completed by WGNCEP (1996), and a more-recent compilation by WGCEP (1999). This

[1]William Lettis & Associates, Inc.
1777 Botelho Drive, Suite 262
Walnut Creek, California 94596
kelson@lettis.com

paper provides a general overview of the geologic, seismologic, and paleoseismologic characteristics of the Calaveras fault, summarizes recently developed data, and provides a geologic characterization of the fault as a potential seismic source. In addition, this paper presents a set of alternative rupture scenarios developed by WGCEP (1999) as part of an effort to estimate earthquake probabilities in the San Francisco Bay region.

The Calaveras fault forms the western border of the Diablo Range, and has had a long history of deformation, with a total dextral offset of as much as 200 km (Jones et al., 1994). Page et al. (1998) note that the Coast Ranges, which include the Diablo Range, underwent late Miocene deformation, followed by two more-recent generations of range building: (1) folding and thrusting beginning about 3.5 Ma, and (2) subsequent late Quaternary uplift of the ranges. In a regional sense, the Diablo Range lies east of the Calaveras fault and consists of the late Cretaceous Franciscan Complex and areas underlain by Franciscan rocks (Page et al., 1998). West of the fault, the Santa Clara Valley and the East Bay Hills (Figure 1) are composed of Neogene rocks and sediments.

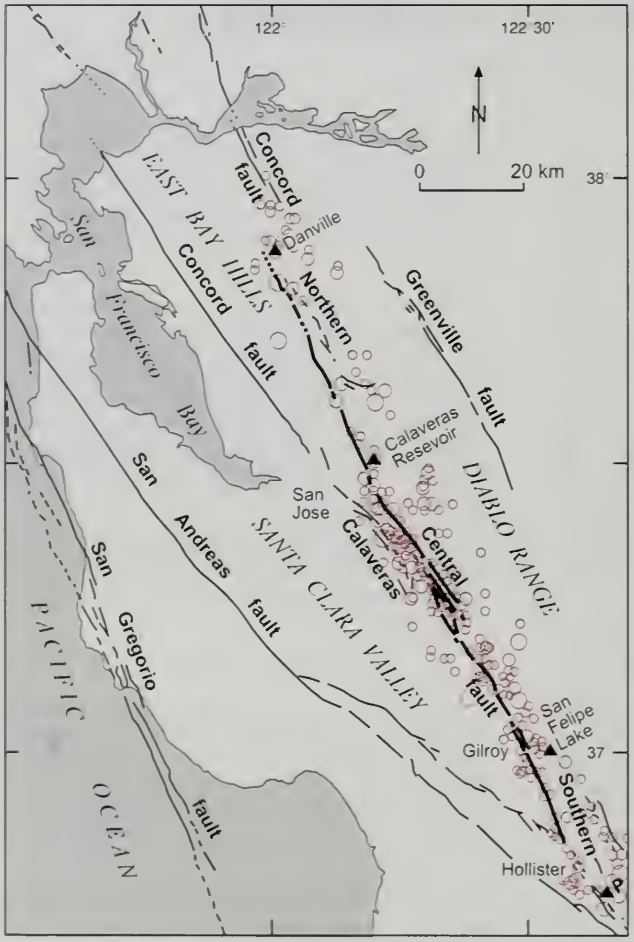

Figure 1. Regional map of the Calaveras fault (heavy lines) in the San Francisco Bay area, showing northern, central, and southern fault sections. Filled triangles show locations of fault section boundaries (±5 km), P = intersection with the Paicines fault. Seismicity along the Calaveras fault from the National Earthquake Information Center catalog.

PRIMARY FAULT SECTIONS

The Calaveras fault exhibits prominent geomorphic expression along its entire active length of 130 ± 10 km, and has generated small and moderate earthquakes during the last two hundred years of recorded history. Two independent fault sections have been identified based on differences in historical seismicity (e.g., Bakun, 1980; Oppenheimer et al., 1990): (1) a southern fault section extending from south of the town of Hollister to Calaveras Reservoir, and (2) a northern fault section extending from Calaveras Reservoir to the town of Danville (WGNCEP, 1996). Although these sections have been termed "segments" in the past, previous workers have not suggested that they are actual rupture segments. Based on review of structural relations with other major faults, contemporary seismicity, rate of present-day creep and geodetic deformation, and geomorphic expression, Kelson et al. (1998) and the WGCEP (1999) divided the previous "southern" Calaveras fault into the "central" and

"southern" fault sections (Figure 1). These sections, which may or may not reflect actual earthquake rupture segments, are defined as the:

- Southern Calaveras fault (from the Paicines fault, south of Hollister, to San Felipe Lake)
- Central Calaveras fault (from San Felipe Lake to Calaveras Reservoir)
- Northern Calaveras fault (from Calaveras Reservoir to the town of Danville)

Defining the endpoints of the three fault sections is important for adequately characterizing rupture segmentation models for the fault, maximum magnitude potential, and potential for surface rupture.

The northern endpoint of the northern Calaveras fault is judged herein to be near the town of Danville (Figure 1), with an uncertainty of ± 5 km to allow for possible rupture termination at either the 1970 Danville or 1990 Alamo earthquake swarms. The southern end of the northern Calaveras fault is interpreted herein to be located at the center of Calaveras Reservoir, which occupies a 7-km-long releasing stepover along the fault. This section boundary has an uncertainty of ± 5 km to capture the entire stepover, as well as zones of seismicity that intersect the fault south of the reservoir. As defined in this way, the northern Calaveras fault is 42 ± 10 km long (Table 1).

The central Calaveras fault extends from Calaveras Reservoir to San Felipe Lake, where the fault strike, level of instrumental seismicity, and fault-related geomorphology differ north and south of the

	NORTHERN CALAVERAS	CENTRAL CALAVERAS	SOUTHERN CALAVERAS
Instrumental seismicity	Low	Abundant	Low
Moderate-magnitude historical seismicity (M_w5 to 6.2)	1861	1911, 1943, 1949, 1955, 1979, 1984, 1988	none
Overall strike	N23W	N30W	N23W
General physiography	Borders East Bay Hills	Within Diablo Range	Alluvial plain
Geomorphology	Discontinuous, commonly covered by landslides	Prominent fault-related features, commonly covered by landslides	Prominent fault-related features
Map pattern	Single main strand	Multiple strands	Single main strand
Surface creep	2 to 4 mm/year	13 to 17 mm/year	6 to 18 mm/year
Geologic slip rate	6 ± 2mm/year	14 ± 5 mm/year	unknown
Length	42 ± 10km	64 ±10 km	24 ±10 km

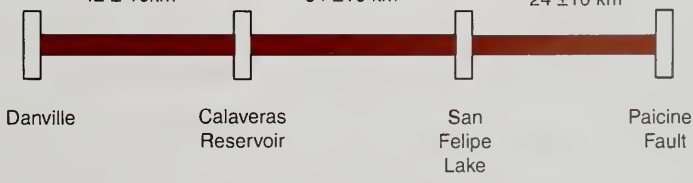

Table 1. General characteristics of the Calaveras fault sections, San Francisco Bay region.

lake (Table 1). The location uncertainty associated with this segment boundary is ± 5 km, to include the intersection between the Calaveras and Busch Ranch faults (4 km south of San Felipe Lake). This assessment suggests that the central Calaveras fault is 64 ± 10 km long.

The southern Calaveras fault extends from San Felipe Lake (± 5 km) to the intersection with the Paicines fault, about 7 km south of Hollister and near the San Benito River. This intersection is complex, with the two faults merging in a series of subparallel fault strands. As defined in this way, the southern Calaveras fault is 24 ± 10 km long (Table 1). The entire Calaveras fault, from Danville to the Paicines fault, is thus 130 ± 10 km long, which is comparable with the fault length interpreted by WGNCEP (1996).

Overall, the slip rate on the Calaveras fault decreases from south to north, with a relatively high slip rate along the southern and central fault sections and a lower rate along the northern fault section. Near the town of Hollister, roughly 15 to 20 mm/year of slip partitions onto the southern Calaveras fault from the San Andreas fault, in part via the Paicines fault (Perkins et al., 1989; Sims, 1991). South of the Paicines fault, the San Andreas fault has a long-term slip rate of about 34 mm/year (Sieh and Jahns, 1984), which leaves about 14 to19 mm/year on the San Andreas and other faults in the southern Santa Cruz Mountains. At a latitude of about 37°N (near the town of Gilroy; Figure 1), the central Calaveras fault had an average creep rate of about 16 mm/year between 1988 and 1999 (Galehouse, 1999) and a mid-Holocene slip rate of 14 ± 5 mm/year (Kelson et al., 1997, 1998). East of the city of San Jose, slip on the central Calaveras fault partitions onto the southern Hayward fault (9 ± 1 mm/year; Lienkaemper et al., 1991) and the northern Calaveras fault (6 ± 2 mm/year; Kelson et al., 1992a, 1992b, 1996; Simpson et al., 1999). Slip on the northern Calaveras fault, in turn, may be transferred eastward onto the Concord fault north of Danville, and/or westward onto the Hayward fault via distributed deformation within the East Bay Hills (Aydin and Page, 1984; Simpson et al., 1992; Kelson et al., 1993; Kelson and Simpson, 1995; Unruh and Lettis, 1998). The following paragraphs provide additional characteristics of the three Calaveras fault sections.

THE SOUTHERN CALAVERAS FAULT

As noted above, the 24-km-long southern Calaveras fault extends from a complex intersection with the San Andreas and Paicines faults in the area south of Hollister to San Felipe Lake (Figure 2). This fault section traverses the broad, low-relief Hollister Plain, which contains late Quaternary deposits laid down by the San Benito River and tributaries to the Pajaro River. South of Hollister, the fault consists of two to three subparallel strands that have moderate geomorphic expression. North of Hollister, the fault strikes N23°W and consists of one main strand that has prominent geomorphic expression (Table 1).

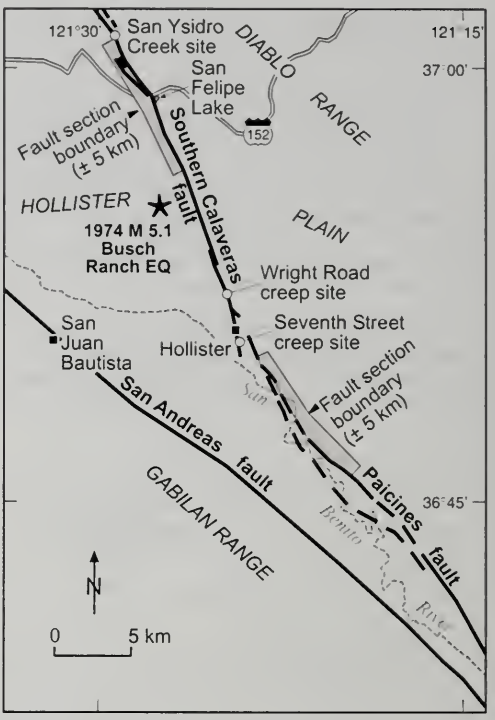

Figure 2. Simplified map of the southern Calaveras fault, showing fault section boundaries and existing creep measurement sites. Location of 1974 Busch Ranch earthquake (M_w5.1) from Oppenheimer et al. (1990).

Seismicity

The southern Calaveras fault exhibited a low level of microseismicity over the period 1963 to 1997 (Walter et al., 1999). The largest historical earth-

quake associated with this fault section was the 1974 Busch Ranch M_L 5.1 earthquake (Figure 2), which occurred on a northeast-trending subsidiary fault that intersects the southern Calaveras fault between Hollister and San Felipe Lake. This earthquake likely reflects the presence of complex interactions between the Calaveras, San Andreas, and Sargent faults. Relative to the central Calaveras fault (north of San Felipe Lake), the southern fault section exhibits comparatively low levels of contemporary seismicity (Table 1).

Slip rate

At the time of this writing, there are no data on the geologic slip rate or paleoseismic behavior of the southern Calaveras fault. Based on geodetic measurements (Savage et al., 1979; Matsu'ura et al., 1986; Lisowski and Prescott, 1981) and creep data (Harsh and Burford, 1982; Schulz et al., 1982; Galehouse, 1991), Kelson et al. (1992a) estimated the aseismic slip rate at 12 ± 6 mm/year. The degree of uncertainty assigned to this estimate was deliberately large, in order to capture the full range in all of the creep and geodetic measurements. As noted by Perkins et al. (1989) and Sims (1991), the southern Calaveras fault could have a geologic slip rate of as much as 20 mm/year. On the basis of existing geologic, paleoseismologic, geodetic, and creep data, WGNCEP (1996) and Petersen et al. (1996) interpreted that the slip rate on the "southern" Calaveras fault (as used by Oppenheimer et al., 1990) is 15 ± 2 mm/year.

Maximum earthquake magnitude

Regional seismic source characterizations by Petersen et al. (1996) and WGNCEP (1996) assumed that the 1984 Morgan Hill earthquake (M_w6.2) is a reasonable maximum magnitude event for the "southern" Calaveras fault (as referred to by Oppenheimer et al., 1990). However, this event occurred on the central Calaveras fault as defined herein. These workers concurred with previous assumptions that the fault does not generate large earthquakes because its high creep rate matches the assumed geologic slip rate (within the limits of uncertainty). WGNCEP (1996) calculated a repeat time of 60 years for a M_w6.2 earthquake on the "southern" Calaveras fault, which includes the southern fault section defined herein.

THE CENTRAL CALAVERAS FAULT

The central Calaveras fault extends from San Felipe Lake to Calaveras Reservoir (Figure 3), and is 64 ± 10 km long. This section of the fault strikes about N30°W and lies within the western part of the high-relief Diablo Range (Table 1). Subsidiary reverse faults west of the main fault zone, which probably merge at depth with the Calaveras fault (e.g., Coyle and Anderson, 1992), coincide with the western margin of the Diablo Range, and may be responsible for much of late Quaternary uplift of the range. Along most of this fault section (Figure 3), landslide deposits and colluvium within steep valleys obscure much of the main fault zone, although active fault strands have prominent geomorphic

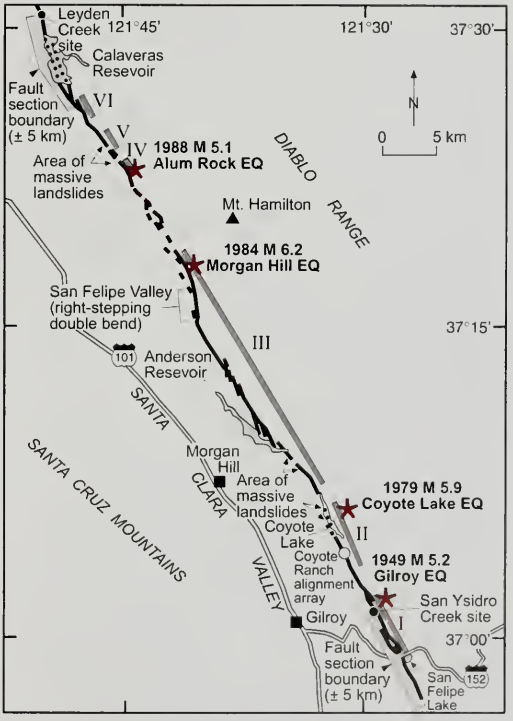

Figure 3. Simplified map of the central Calaveras fault, showing fault section boundaries, paleoseismic sites, and existing creep measurement sites. Earthquake locations (stars) and "stuck patches" (bars labeled I to VI) from Oppenheimer et al. (1990).

expression across stable alluviated areas. The presence of the fault within numerous linear valleys shows that the fault has had a strong influence on the geomorphic development of this part of the range block (Harden and Gallego, 1992).

Seismicity

The central Calaveras fault exhibits abundant microseismicity (Bakun, 1980, 1984; Reasenburg and Ellsworth, 1982; Bakun and Lindh, 1985; Oppenheimer et al., 1990; Du and Aydin, 1992). The fault also has generated several recent moderate-magnitude earthquakes (i.e., 1949 Gilroy M_W5.2, 1979 Coyote Lake M_W5.9, 1984 Morgan Hill M_W6.2, 1988 Alum Rock M_W5.1, and 1998 Gilroy M_W4.0). Oppenheimer et al. (1990) examined main shock and microearthquake data from the central Calaveras fault and qualitatively addressed the prospects for future earthquakes along the fault south of Calaveras Reservoir. Based on historical seismicity data, they concluded that deformation on the fault occurs through aseismic creep above 5 km, combined creep and microearthquakes between 5 and 10 km, and M_W>5 earthquakes between 8 and 10 km. Historical seismicity data also suggest the presence of six persistently aseismic zones along the fault, which range in length from about 3 to 27 km and apparently represent "stuck patches" that slip only during moderate-magnitude earthquakes (Figure 3). Five of these "stuck patches" have generated M_W>5 earthquakes since 1903. The northernmost of these six currently aseismic zones, which lies directly south of Calaveras Reservoir, has not slipped seismically since 1903 and is large enough to generate a M_W5.5 earthquake. The southernmost aseismic zone has not ruptured seismically since 1949 and also is identified as a likely site for a future M_W>5 earthquake (Oppenheimer et al., 1990). These observations, and the interpretation that the base of the seismogenic zone is at most 10 km deep, support the interpretation that the Calaveras fault can generate only small- to moderate-magnitude earthquakes. Oppenheimer et al. (1990), based on earthquake modeling by Hartzell and Heaton (1986) and Liu and Helmberger (1983), noted that there was a maximum coseismic slip of about 1 m at a depth of 8 km during the 1984 Morgan Hill earthquake, and a maximum slip of about 1.2 m during the 1979 Coyote Lake event. Finally, they estimated earthquake recurrence based on the observation that historical moderate shocks may have repeatedly ruptured the same segments of the fault. By dividing the amount of slip per event by an assumed slip rate of 17 mm/year, these workers estimated repeat times of 59 and 70 years for earthquakes similar to the Morgan Hill and Coyote Lake events, respectively.

Slip rates

The creep rate on the central fault section is best documented at the Coyote Ranch alignment array near Coyote Lake (Figure 3), which was measured intermittently between 1968 and 1988, and again starting in 1997 (Galehouse, 1999). As of mid-May, 1999, the simple average creep rate for 31 years of record, from 1968 to 1999, was 16.3 mm/year (Galehouse, 1999), although this value includes slip possibly triggered by the 1989 Loma Prieta earthquake (Galehouse, 1990). Detailed bimonthly measurements made since 1997 provide a simple average rate of 13.5 mm/year (Galehouse, 1999).

At a site about 5 km southeast of the Coyote Ranch array, Kelson et al. (1997, 1998) collected preliminary information on the middle to late Holocene slip rate along the central Calaveras fault. The investigation at San Ysidro Creek near Gilroy (Figure 3) included five trenches excavated across and parallel to the central Calaveras fault, in order to evaluate the age and displacement of four paleochannels that cross the main fault strand. The trench exposures provided evidence of about 37 to 45 m of cumulative dextral offset of the paleochannels, which range in age from about 2,500 to 4,100 years. These relations suggest that the geologic slip rate along the central Calaveras fault, based on the offset of individual channels, ranges from 11 ± 2 mm/year to 15 ± 4 mm/year. Encompassing the entire amount of uncertainty in the four slip-rate estimates, the average late Holocene rate is 14 ± 5 mm/year (Kelson et al., 1998). Within the uncertainty of the available geologic data, the long-term slip rate is consistent with the short-term slip rate derived from aseismic creep data and geodetic modeling. Thus, available geologic data support the interpretation by WGNCEP (1996) and Petersen et al. (1996) that the central Calaveras fault has a slip rate of 15 ± 2 mm/year.

Maximum earthquake magnitude

Recent models characterize the central Calaveras fault as being capable of producing earthquakes no larger than M_W6.2 (Peterson et al., 1996; WGNCEP, 1996). These models are founded mostly on the occurrence of several modeate-magnitude earthquakes during the past few decades (Bakun, 1980,

1984; Reasenburg and Ellsworth, 1982; Bakun and Lindh, 1985; Du and Aydin, 1992), the pattern of historical seismicity showing small "stuck patches" along the fault (Oppenheimer et al., 1990), and relatively high geodetic strain and creep rates (Savage et al., 1979; Matsu'ura et al., 1986; Galehouse, 1995). Agreement between the geodetic/creep rates and the regional slip-rate budget (Kelson et al., 1992a), supports the interpretation that there is little or no strain accumulation along the fault that might result in a large-magnitude earthquake. Based on these relations, WGNCEP (1996) assumed that the 1984 Morgan Hill earthquake (M_w6.2) is a reasonable maximum-magnitude event for the central Calaveras fault, and calculated a repeat time of 60 years for such an earthquake.

In contrast with the interpretation made by WGNCEP (1996), geologic relations exposed in the trenches at San Ysidro Creek (Figure 3) suggest the possibility that surface-rupturing earthquakes (M_w>6.2) may have occurred along the central Calaveras fault (Kelson et al., 1997, 1998). The relative position of each of four late Holocene paleochannels exposed in the trenches may be a direct result of coseismic offset along the fault. This would suggest the occurrence of at least three discrete surface-rupturing earthquakes between about 4,000 and 2,000 years ago, each of which produced dextral offset of 2 to 2.5 m (Kelson et al., 1997, 1998, 1999). In addition, the fault is associated with prominent geomorphic features (e.g., sag ponds, anti-slope scarps, offset streams) that commonly are present along strike-slip faults characterized by large surface-rupturing earthquakes.

THE NORTHERN CALAVERAS FAULT

The northern Calaveras fault extends from Calaveras Reservoir on the south to the town of Danville on the north (Figure 1), and is 42 ± 10 km long. The boundary between the northern and central Calaveras faults coincides with the complex intersection between the Calaveras and Hayward faults, as well as with a 7-km-long releasing double bend in the fault at Calaveras Reservoir (Figure 4). A prominent trend of microseismicity diverges to the northwest from near Calaveras Reservoir toward the Hayward fault (Wong and Hemphill-Haley, 1992), and probably reflects partial transfer of strain between the central Calaveras and southern Hayward faults (Andrews et al., 1993; Kelson et al., 1993). North of Calaveras Reservoir, the fault lies along the eastern margin of the East Bay Hills, where much of the fault trace is obscured by either latest Holocene floodplain deposits, landslide deposits, or urbanization. However, the fault has moderate geomorphic expression where it is not obscured, and it had moderate expression (as shown by historical photography) in several areas that are now urbanized. Because of this urbanization, the northern Calaveras fault has received a greater level of shallow subsurface investigation than either the central or southern fault sections.

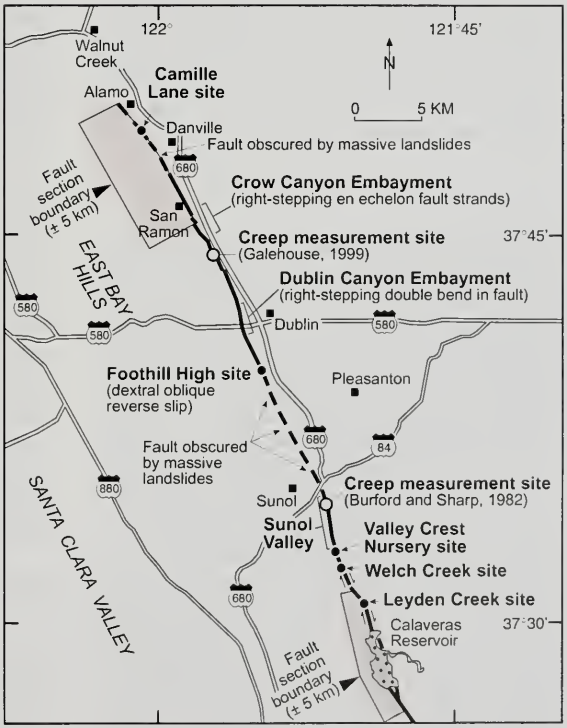

Figure 4. Simplified map of the northern Calaveras fault north of Calaveras Reservoir, showing existing paleoseismologic sites and creep-measurement sites.

Seismicity

The northern Calaveras fault exhibits little contemporary microseismicity compared to the central Calaveras fault (Figure 1; Oppenheimer and Lindh, 1992; Oppenheimer and MacGregor-Scott, 1992). Only one historic earthquake has occurred on the northern Calaveras fault, the 1861 M_W5.6 San Ramon Valley earthquake. This tremor was associated with surface cracking in the area that is now occupied by the cities of San Ramon and Dublin (Toppozada et al., 1981; Figure 4). The relative scarcity of contemporary microseismicity along the fault north of Calaveras Reservoir was interpreted by Oppenheimer and Lindh (1992) to suggest that the northern Calaveras fault is locked and could generate a M_W7 earthquake. Based on the occurrence of the 1861 earthquake, they interpreted that the northern Calaveras fault alternatively may rupture in M_W6 earthquakes along shorter sections of the fault (Oppenheimer and Lindh, 1992; Simpson et al., 1992). Oppenheimer and Lindh (1992) state that there are insufficient data to calculate the probability of a M_W7 event on the fault, but they estimate a 30-year probability of one or more events of $M_W \geq 6$ at 0.33.

Slip rates

The rates of creep and long-term (geologic) slip along the northern Calaveras fault are fairly well known, compared with the central and southern fault sections. Measurement of a 7-km-wide geodetic network at the southern end of Calaveras Reservoir shows about 6 mm/year of dextral motion at depth (Prescott et al., 1981). These data also suggest that fault creep relieves a large part of the crustal strain, and that the Calaveras fault slips at a rate of 2 to 3 mm/year above 3 km and at 6 mm/year at greater depths (Prescott et al., 1981). In addition, the historic slip rate on the fault in the Pleaanton-Sunol area (Figure 4) across short (£5 km) baselines is approximately 2.5 to 3.5 mm/year (Prescott et al., 1981; Burford and Sharp, 1982; Prescott and Lisowski, 1983). Farther north, in San Ramon, Galehouse and colleagues measured an average creep rate of 1.7 mm/year between 1981 and 1999 (Galehouse, 1999). Trenching and drilling at Leyden Creek provided a Holocene slip rate of 4 to 7 mm/year for the fault (Figure 4; Kelson et al., 1992b, 1996). Simpson et al. (1999) estimate a slip rate of 5 to 7 mm/year at Welch Creek. WGNCEP (1996) and Petersen et al. (1996) use a value of 6 mm/year for the slip rate on the northern Calaveras fault.

Paleoseismic chronology and earthquake recurrence

The current understanding of the Holocene earthquake behavior of the northern Calaveras fault is based primarily on data from the Leyden Creek and Welch Creek sites, which are about 2 and 5 km north of Calaveras Reservoir, respectively (Figure 4). The Leyden Creek site provided evidence of five or six surface ruptures within the past 2,500 years and an average recurrence interval of 250 to 850 years (Kelson et al., 1996). At Welch Creek (Figure 4), trenching by Simpson et al. (1999) documented three surface ruptures over approximately the same 2,500 year interval and a maximum recurrence interval of 1,375 to 3,425 years. The geologically based recurrence of 550 ± 300 years is larger than the recurrence of 192 years calculated by Oppenheimer and Lindh (1992) for a M_W6 earthquake based on historical seismicity and assumed rupture displacements. In a separate analysis, WGNCEP (1996) arbitrarily assigned a repeat time of 400 years for a M_W7 earthquake and calculated a repeat time of 200 years for a M_W6.1 earthquake based on historical seismicity.

There still are no well-constrained data on the timing of the most recent earthquake along the northern Calaveras fault. Based on radiometric dating of charcoal in sediments exposed in paleoseismologic trenches, the most recent scarp-producing rupture at Leyden Creek occurred after about A.D. 1160 (Kelson et al., 1996), and the most recent rupture at Welch Creek occurred before A.D. 1425 (Simpson et al., 1999). Preliminary data from the Valley Crest Nursery site, located 1 km northwest of Welch Creek (Figure 2), suggest that the most recent earthquake may have occurred prior to A.D. 1570, perhaps sometime between A.D. 1100 and 1300 (Baldwin et al., 1998). More work remains to be done to evaluate the timing of the most recent earthquake on the northern Calaveras fault.

Fault subsections

Several workers have addressed the lengths of possible earthquake rupture segments along the northern Calaveras fault. Simpson et al. (1992) divided the northern Calaveras fault into four subsections based primarily on geomorphic features along and adjacent to the fault. Of these, the southern, 7-km-long "Calaveras Reservoir" subsection approximates the uncertainty in the location of

the southern end of this fault section, as described herein. In addition, the northernmost subsection (the 9-km-long "Alamo" subsection) represents the uncertainty in the location of the northern end of the fault, as described herein. Simpson et al. (1992) also identified the 9-km-long "Sunol" subsection and the 23-km-long "San Ramon" subsection, and differentiated between them on the basis of the fault's location along the western and eastern margins, respectively, of uplifted range blocks. They also estimated maximum earthquake magnitudes of 6.25 to 7 for individual fault subsections and a maximum earthquake magnitude of 7.25 for rupture of the entire northern Calaveras fault.

WGNCEP (1996) divided the northern Calaveras fault into three subsections on the basis of simple geometric interpretation of the surface fault trace. Their fault model, which differs from that of Simpson et al. (1992), included a 14-km-long "Sunol Valley" subsection, a 13-km-long "Amador Valley" subsection on the south, and a 15-km-long "San Ramon Valley" subsection on the north. WGNCEP (1996) cited the presence of "distinct right-stepovers" in the surface fault trace as the locations of subsection endpoints, which is a different interpretation of the significance of fault-trace irregularities than that of Simpson et al. (1992). WGNCEP (1996) assumed that the "Sunol Valley" subsection only ruptures in conjunction with the other two subsections, and thus would only be involved in large (~M_w7) earthquakes. In contrast, WGNCEP (1996) assumed that the "San Ramon Valley" and "Amador Valley" subsections could produce moderate-magnitude (M_w6.1) earthquakes, on the basis of the 1861 M_w5.6 shock near San Ramon (Toppozada et al., 1981) and a possible moderate earthquake in 1864 whose location is unknown. These subsections could be involved in large (~M_w7) earthquakes, if the entire northern Calaveras fault were to rupture. It is important to note that the M_w6.1 value assumed by WGNCEP (1996) for a single-section rupture may be low considering the range of magnitude of 6.25 to 7 estimated from multiple empirical relations (Simpson et al., 1992).

Our recent unpublished detailed mapping of the fault, based on analysis of detailed recent and historical aerial photography, compilation of consultants' reports, and field observation, provides additional information on the character of the northern Calaveras fault and raises questions about the appropriateness of using small geometric changes in the fault trace to infer rupture segments. Overall, between Calaveras Reservoir and Danville, the fault is characterized by a series of alternating releasing stepovers and restraining bends or stepovers (Figure 4). These probably do not represent segment boundaries during large earthquakes. As noted by Page (1982), the southern end of the northern Calaveras fault coincides with a possible pull-apart basin occupied by Calaveras Reservoir (Figures 3 and 4). Directly north of the reservoir, paleoseismic studies at Leyden Creek show strike slip and a slight extensional component, with a ratio between horizontal and down-to-the-west vertical slip of about 10 to 1 (Kelson et al., 1996). A left-step in the fault trace directly north of Leyden Creek is about 0.5 km wide and may produce a restraining geometry. North of this stepover, paleoseismic studies at Welch Creek (Simpson et al., 1999) and Valley Crest Nursery (Baldwin et al., 1998) suggest nearly pure strike slip. For example, slickenslides preserved along the fault at the Valley Crest Nursery site plunge less than 10° to the northwest along the strike of the vertical fault (Baldwin et al., 1998). Between Valley Crest Nursery and Highway 680, the active fault strand lies beneath the floodplains of Alameda and San Antonio Creeks (Figure 4), and has poor geomorphic expression because of active alluviation and cultural activities.

North of Sunol Valley, the fault appears to exhibit up-on-the-west oblique reverse movement, where it is not obscured by abundant late Quaternary landsliding. At a trench site near Foothill High School (Figure 4), the west-dipping fault has had Holocene oblique reverse movement (Kelson and Randolph, 2000). The fault lies within a slightly restraining orientation that extends from Highway 680 on the south to Dublin Canyon on the north, and includes the Foothill High School site (Figure 4). Within the Dublin Canyon embayment in the East Bay Hills (Figure 4), previous consultants' reports and analysis of aerial photography suggest the presence of a right-stepping double bend across the alluviated embayment. This double bend is about 2 km long and about 0.5 km wide (Figure 4). This slightly releasing geometry across Dublin Canyon results in minor oblique extension. Between the Dublin Canyon embayment and the Crow Canyon embayment (Figure 4), multiple consultants' trenches have exposed gently west-dipping fault strands that are either: 1) strands of the northern Calaveras fault having a component of reverse movement, 2) landslide slip planes related to east-vergent mass movement, or 3) reverse fault strands that have been translated eastward by landslide movement.

Although generalizations are difficult, it seems reasonable to characterize the northern Calaveras fault between the Dublin Canyon and Crow Canyon embayments as having predominantly strike slip with a component of oblique reverse movement.

In northern San Ramon, the fault crosses a range-front embayment occupied by San Catanio and Crow Canyon Creeks, herein termed the Crow Canyon embayment (Figure 4). Multiple exploratory trenches completed by PRA (1976) showed that the fault contains a series of right-stepping, *en echelon* fault traces associated with sag ponds and discontinuous linear ridges. These sag ponds and linear ridges, although now destroyed by cultural development, are clearly visible on 1939 aerial photography and on an oblique aerial photograph presented by Rogers and Halliday (1992). Notably, these features coincide with the fault trace mapped by Herd (1978), and are east of the main trace of the Calaveras fault zone interpreted by Rogers and Halliday (1992). The right-stepping *en echelon* pattern of fault traces, coupled with the sag ponds within the range-front embayment, is evidence of slightly extensional strike slip. This minor right-stepover, which is approximately 2.2 km long and less than 0.5 km wide, is evidence of a slightly releasing fault geometry. North of the Crow Canyon embayment, the fault lies beneath a large landslide complex flanking Las Trampas Ridge. Northwest of the landslide, a trench across the northern Calaveras fault at the Camille Lane site in Alamo (Figure 4) exposed unfaulted latest Pleistocene alluvium (Simpson et al., 1994), suggesting that Holocene movement on the northern Calaveras fault may not extend as far northwest as Alamo.

In summary, it appears that the northern Calaveras fault consists of a series of subsections that have alternating restraining and releasing geometries, with the majority of the fault length characterized by fault geometries that promote local contraction and reverse faulting. Fault geometries that produce local extension appear to be present in Sunol Valley, at the Dublin Canyon embayment, and at the Crow Canyon embayment. Because these along-strike changes in fault geometry are slight, they probably are not significant barriers to rupture propagation along the fault, in contrast to the interpretation by WGNCEP (1996). However, the differences in near-surface slip vectors influence fault geomorphology and may affect interpretations of whether surface features are related to landslide or fault activity. In addition, these left- and right-stepping complications may make it difficult for site-specific geologic engineering studies to determine the locations of active fault strands based on extrapolation of fault locations from nearby trenches.

POSSIBLE RUPTURE SCENARIOS ALONG THE CALAVERAS FAULT

As part of an effort to calculate 30-year earthquake probabilities throughout the San Francisco Bay region, WGCEP (1999) considered several rupture scenarios for the Calaveras fault. These include rupture of various combinations of the northern, central, and southern fault sections (as defined herein), including rupture of the entire fault system. Given the three sections of the Calaveras fault (northern Calaveras, NCAL; central Calaveras, CCAL; southern Calaveras, SCAL), WGCEP (1999) assumed six scenarios that reasonably encompass the range in possible ruptures that may be associated with the Calaveras fault. These scenarios are summarized below.

- Scenario 1 (NCAL + CCAL + SCAL). Simultaneous rupture of all three sections, extending from the northern end of NCAL to the southern end of SCAL.
- Scenario 2 (NCAL + CCAL / SCAL). Simultaneous rupture of the NCAL and the CCAL, and independent rupture of the SCAL.
- Scenario 3 (NCAL / CCAL + SCAL). Independent rupture of the NCAL, and simultaneous rupture of the CCAL and the SCAL.
- Scenario 4 (NCAL / CCAL / SCAL). Independent ruptures of the NCAL, CCAL, and SCAL.
- Scenario 5 (NCAL / no sections). Independent rupture of the NCAL, coupled with characteristic ruptures of magnitude M_w6.2 that are spatially unconstrained ("floating") between the northern end of CCAL and the southern end of SCAL.
- Scenario 6 (no sections). Characteristic ruptures of magnitude M_w6.2 that are spatially unconstrained ("floating") along the entire fault between the northern end of NCAL and the southern end of SCAL.

These scenarios were grouped into different models of earthquake occurrence, and then used to

estimate the time-dependent probability of future earthquake occurrence (WGCEP, 1999). Each of these scenarios produces slightly different estimates of maximum earthquake magnitudes, each having a different probability of occurrence. For example, scenario 1 likely would generate a relatively large earthquake. However, the probability of such an event may be relatively low. In contrast, scenario 5 involves some moderate probability of a large, independent rupture of the northern Calaveras fault and a relatively high probability of a moderate earthquake along the central and southern fault sections. This scenario most closely reflects recent seismic source characterizations of the Calaveras fault (WGNCEP, 1996; Peterson et al., 1996). WGCEP (1999) addressed the relative weights each of these scenarios in four models of earthquake occurrence. The four fault models, each of which includes the six rupture scenarios, were weighted by WGCEP members. Based on these rupture scenarios and fault models, WGCEP (1999) calculated probabilities of 7%, 15%, and 18% for at least one $M_W \geq 6.7$ earthquake before 2030 on the southern, central, and northern Calaveras fault sections, respectively. We also calculated an 18% probability of a $M_W \geq 6.7$ earthquake on the Calaveras fault, as a whole.

Two critical issues involving possible rupture scenarios along the Calaveras fault remain unresolved at present. First, it is unclear whether recent interpretations of the central and southern sections of the Calaveras fault, which suggest that the fault is capable of producing only moderate-magnitude (M_W6.2) earthquakes (WGNCEP, 1996), are fully correct. These interpretations are founded mostly on the occurrence of several moderate-magnitude earthquakes during the past few decades (Bakun, 1980, 1984; Du and Aydin, 1992), the pattern of historical seismicity showing small "stuck" patches along the fault (Oppenheimer et al., 1990), and relatively high geodetic strain and creep rates (Matsu'ura et al., 1986; Galehouse, 1990). Agreement between the geodetic/creep rates and the regional slip-rate budget (Kelson et al., 1992a) supports an interpretation that there is little or no strain accumulation along the fault that might result in a large-magnitude earthquake. In addition, to date there is no definitive geologic evidence that these fault sections have produced earthquakes large enough to rupture the ground surface. However, trenches at San Ysidro Creek provided possible support for the occurrence of repeated large fault ruptures during the late Holocene (Kelson et al., 1997, 1998). As a result, WGCEP (1999) considered fault models in which the above scenarios 1, 2, 3, and 4 had relatively high weights, as well as fault models in which scenarios 5 and 6 had relatively high weights. Should future investigations support the occurrence of large earthquakes on the central or southern fault sections, the 15% and 7% probabilities (respectively) estimated by WGCEP (1999) might too low. Conversely, if it were shown that the fault sections have not generated large earthquakes in the recent past, these probabilities might be too high.

Second, the magnitudes of possible earthquakes along the northern Calaveras fault are important for seismic hazard assessments in the Danville-San Ramon-Pleasanton urban corridor. Engineering geology and geotechnical evaluations conducted by local practitioners often have not fully acknowledged the possibility that the northern Calaveras fault might produce a large (M_W7.0) earthquake. The fault "segments" (i.e., subsections) postulated by WGNCEP (1996) were characterized as having the potential for generating M_W6.1 earthquakes. This magnitude commonly is used in evaluating possible strong ground motions and in assessing dynamic stability of potentially unstable slopes. Because the "segments" defined by the WGNCEP (1996) are based mostly on minor strike changes in the fault and may not reflect actual rupture segments, the possibility of a large earthquake on the northern Calaveras fault may not be appropriately acknowledged in common geologic engineering and geotechnical practice. Because the structural complexities along the northern Calaveras fault probably are insufficient to arrest rupture propagation, the possibility of a large ($M_W \approx 7$) earthquake on the northern Calaveras fault should be considered in geologic engineering and geotechnical evaluations in the Danville-San Ramon-Pleasanton corridor.

CONCLUSIONS

The 130-km-long Calaveras fault represents a significant seismic source in the southern and eastern San Francisco Bay region. It extends from an intersection with the Paicines fault south of Hollister, through the Diablo Range east of San Jose, and along the Pleasanton-Dublin-San Ramon urban corridor. The fault consists of three major sections: the 24-km-long southern Calaveras fault (from the Paicines fault to San Felipe Lake), the 64-km-long central Calaveras fault (from San Felipe Lake to Calaveras Reservoir), and the 42-km-long northern Calaveras fault (from Calaveras Reservoir to Dan-

ville). The poorly constrained slip rate on the southern section is interpreted to be 15 ± 2 mm/year, although some workers have postulated rates as high as 20 mm/year. The central and northern sections have geologic slip rates of 14 ± 5 mm/year and 6 ± 2 mm/year, respectively.

The level of contemporary seismicity along the southern section is low, whereas the central section has generated numerous moderate earthquakes (as much as M_w6.2) in historic time. The northern section has a relatively low level of seismicity and may be locked. Geologic and seismologic data suggest that the northern section may produce earthquakes as large as ~M_w7.0.

Paleoseismologic studies suggest a recurrence interval for large ruptures of between 250 and 850 years on the northern fault section. The timing of the most-recent rupture on the northern Calaveras fault is unknown, but may be several hundred years ago. Engineering geology and paleoseismic studies along the northern Calaveras fault suggest along-strike variations in local sense of slip, although the fault is dominated by dextral slip and may have a component of oblique reverse movement.

Current characterization of the fault includes six possible rupture scenarios, which range from independent large ruptures along the three main fault sections to M_w6.2 earthquakes distributed randomly along the fault. Current unknowns important to seismic hazard assessment involve the magnitudes of possible earthquakes and the timing and recurrence of large earthquakes on the three fault sections.

ACKNOWLEDGMENTS

A summary paper such as this is the product of the efforts of many researchers, who are too numerous to name here. Members of the Working Group 1999 contributed much to the thoughts given herein. Collaboration with Bill Lettis and Gary Simpson helped formulate some early ideas, whereas later work with John Baldwin, Carolyn Randolph, David Schwartz, and Heidi Stenner have helped make sense of some complex relations. This paper was thoughtfully reviewed by Suzanne Hecker and John Baldwin, and figures were drafted by Jason Holmberg. Thanks also to Laura Paella and Deborah Ahrens for editorial help.

AUTHOR PROFILE

Keith Kelson is a Certified Engineering Geologist with 15 years of experience in seismic hazard assessment and surficial geology/water resources research. He is Vice-President of William Lettis & Associates, Inc. and has been principal investigator on more than 20 earthquake research grants funded by the U.S. Geological Survey, the National Science Foundation, and the Nuclear Regulatory Commission. Some of his current projects involve characterizing near-surface geology to assess ground water flow paths, slope stability issues, geotechnical constraints on pipeline installation, and liquefaction hazards.

SELECTED REFERENCES

Andrews, D.J., Oppenheimer, D.H., and Lienkaemper, J.J., 1993, The Mission link between the Hayward and Calaveras faults: Journal of Geophysical Research, v. 98, p. 12,083-12,095.

Aydin, A. and Page, B.M., 1984, Diverse Pliocene-Quaternary tectonics in a transform environment, San Francisco Bay region, California: Geological Society of America Bulletin,
v. 95, p. 1303-1317.

Bakun, W.H., 1980, Seismic activity on the southern Calaveras fault in central California: Bulletin of the Seismological Society of America, v. 70, p. 1181-1197.

Bakun, W.H., 1984, Seismic moments, local magnitudes, and coda duration magnitudes for earthquakes in central California: Bulletin of the Seismological Society of America, v. 74, p. 439-458.

Bakun, W.H. and Lindh, A.G., 1985, Potential for future damaging shocks on the Calaveras fault, California: U.S. Geological Survey Open-file Report 85-754, p. 266-279.

Baldwin, J.N., Kelson, K.I., and Randolph, C.E., 1998, Timing of the most-recent surface faulting event on the northern Calaveras fault, near Sunol, California [abs.]: American Geological Union 1998 Fall Meeting, EOS Supplement,
v. 79, no. 4.

Burford, R.O. and Sharp, R.V., 1982, Slip on the Hayward and Calaveras faults determined from offset powerlines: in Hart, E.W., et al. (eds.), California Division of Mines and Geology Special Publication 62, p. 261-269.

Coyle, J.M. and Anderson, P.C., 1992, Geologic and seismic hazards in the City of Morgan Hill, California: in Borchardt, G., et al. (eds.), California Division of Mines and Geology Special Publication 113, p. 305-310.

Du, Y. and Aydin, A., 1992, Northward progression of slip and stress transfer associated with three sequential earthquakes along the central Calaveras fault: in Borchardt,

G. et al. (eds.), California Division of Mines and Geology Special Publication 113, p. 241-247.

Galehouse, J.S., 1990, Effect of the Loma Prieta earthquake on surface slip along the Calaveras fault in the Hollister area: Geophysical Research Letters, v. 17, p. 1219-1222.

Galehouse, J.S., 1991, Creep rates on Bay area faults during the past decade [abs.]: Geological Society of America Abstracts with Program, v. 23, p. 27

Galehouse, J.S., 1995, Theodolite measurement of creep rates on San Francisco Bay region faults: U.S. Geological Survey Open-file Report 95-210, p. 335-346.

Galehouse, J.S., 1999, written communication to Keith Kelson.

Harden, D.R. and Gallego, A., 1992, Recent disruption of Packwood Creek by the Calaveras fault: in Borchardt, G., et al. (eds.), California Division of Mines and Geology Special Publication 113, p. 299-304.

Hartzell, S.H. and Heaton, T.H., 1986, Rupture history of the 1984 Morgan Hill, California, earthquake from the inversion of strong motion records: Bulletin of the Seismological Society of America, v. 76, p. 649-679.

Harsh, P.W. and Burford, R.O., 1982, Alignment-array measurements of fault slip in the eastern San Francisco Bay area, California: California Division of Mines and Geology Special Publication 62, p. 251-260.

Herd, D.G., 1978, Quaternary faulting along the northern Calaveras fault zone: U.S. Geological Survey Open-File Report 78-307, 5 map sheets.

Jones, D., Graymer, R. Wang, C., McEvilly, T., and Lomax, A., 1994, Neogene transpressive evolution of the California Coast Ranges: Tectonics, v. 13, p. 561-574.

Kelson, K.I. and Simpson, G.D., 1995, Late Quaternary deformation of the southern East Bay Hills, Alameda County, California [abs.]: American Association of Petroleum Geologists, Abstracts with Program, Pacific Section Convention, p. 37.

Kelson, K.I., Lettis, W.R., and Lisowski, M., 1992a, Distribution of geologic slip and creep along faults in the San Francisco Bay Region: in Borchardt, G. et al. (eds.), California Division of Mines and Geology Special Publication 113, p. 31-38.

Kelson, K.I., Lettis, W.R., and Simpson, G.D., 1992b, Late Holocene paleoseismic events at Leyden Creek, northern Calaveras fault: in Borchardt, G. et al. (eds.), California Division of Mines and Geology Special Publication 113, p. 289-297.

Kelson, K.I. and Randolph, C.E., 2000, Paleoseismic study of the northern Calaveras fault at 4120 Foothill Road, Pleasanton, California: unpublished technical report submitted to the U.S. Geological Survey, Bay Area Paleoseismological Experiment (BAPEX), Contract No. 98WRCN1012, 21 p.

Kelson, K.I., Simpson, G.D., Haraden, C.C., Sawyer, T.L., and Hemphill-Haley, M.A., 1993, Late Quaternary surficial deformation of the southern East Bay Hills, San Francisco Bay Region, California: Final Technical Report, U.S. Geological Survey, Award Number 1434-92-G-2209, 22 p., 1 plate.

Kelson, K.I., Simpson, G.D., Lettis, W.R., and Haraden, C., 1996, Holocene slip rate and earthquake recurrence of the northern Calaveras fault at Leyden Creek, northern California: Journal of Geophysical Research, v. 101, no. B3, p. 5961-5975.

Kelson, K.I., Baldwin, J.N., and Randolph, C.E., 1997, Geologic slip rate along the southern Calaveras fault at San Ysidro Creek, near Gilroy, California: EOS (Supplement), American Geophysical Union, v.78, no. 76, p. F439.

Kelson, K.I., Baldwin, J.N., and Randolph, C.E., 1998, Late Holocene slip rate and amounts of coseismic rupture along the central Calaveras fault, San Francisco Bay area, California: Final Technical Report submitted to the U.S. Geological Survey National Earthquake Hazard Reduction Program, Award Number 1434-HQ-97-GR-03151, 26 p.

Kelson, K.I., Tolhurst, J., and Manaker, D., 1999, Earthquakes on the Calaveras fault: Fact or fiction?—The geology, seismology and paleoseismology of the Calaveras fault: California Division of Mines and Geology Special Publication 119, Geological Society of America Field Trip Guidebook for Cordilleran Section, p. 58-73.

Lienkaemper, J.J., Borchardt, G., and Lisowski, M., 1991, Historic creep rate and potential for seismic slip along the Hayward fault, California: Journal of Geophysical Research, v. 96, p. 18,261-18,283.

Lisowski, M. and Prescott, W.H., 1981, Short-range distance measurements along the San Andreas fault system in central California, 1975 to 1979: Bulletin of the Seismological Society of America, v. 17, p. 1,607-1,624.

Liu, H. and Helmberger, D.V., 1983, The near-source ground motion of the 6 August 1979 Coyote Lake, California, earthquake: Bulletin of the Seismological Society of America, v. 73, p. 201-218.

Matsu'ura, M., Jackson, D.D., and Cheng, A., 1986, Dis-location model for a seismic crustal deformation at Hollister, California: Journal of Geophysical Research, v. 91, p. 12,661-12,674.

Oppenheimer, D.H. and Lindh, A.G., 1992, The potential for earthquake rupture of the northern Calaveras fault: in Borchardt, G. et al., (eds.), California Division of Mines and Geology Special Publication 113, p. 233-240.

Oppenheimer, D.H. and MacGregor-Scott, N., 1992, The seismotectonics of the eastern San Francisco Bay region: in Borchardt, G. et al., (eds.), California Division of Mines and Geology Special Publication 113, p. 11-16.

Oppenheimer, D.H., Bakun, W.H., and Lindh, A.G., 1990, Slip partitioning of the Calaveras fault, California, and prospects of future earthquakes: Journal of Geophysical Research, v. 95, no. B6, p. 8,483-8,498.

Page, B.M., 1982, The Calaveras fault zone of California, an active plate boundary element: in Hart, E.W., et al. (eds.),

California Division of Mines and Geology Special Publication 62, p. 175-184.

Page, B.M., Thompson, G.A., and Coleman, R.G., 1998, Late Cenozoic tectonics of the central and southern Coast Ranges of California: Geological Society of America Bulletin, v. 110, p. 846-876.

Perkins, J.A., Sims, J.D., and Sturgess, S.S., 1989, Late Holocene movement along the San Andreas fault at Melendy Ranch: Implications for the distribution of fault slip in central California: Journal of Geophysical Research, v. 94, no. B8, p. 10,217-10,230.

Petersen, M.D., Bryant, W.A., Cramer, C.H., Cao, T., Reichle, M.S., Frankel, A.D., Lienkaemper, J.J., McCrory, P.A., and Schwartz, D.P., 1996, Probabilistic seismic hazard assessment for the State of California: California Division of Mines and Geology Open-file Report issued jointly with U.S. Geological Survey, USGS 96-706, 52 p.

Prescott, W.H. and Lisowski, M., 1983, Strain accumulation along the San Andreas Fault system east of San Francisco Bay, California: Tectonophysics, v. 97, p. 41-56.

Prescott, W.H., Lisowski, M., and Savage, J.C., 1981, Geodetic measurement of crustal deformation on the San Andreas , Hayward, and Calaveras faults near San Francisco, California: Journal of Geophysical Research, v. 86, p. 10,853-10,869.

PRA (Purcell, Rhodes and Associates), 1976, Geologic investigation for a portion of the Bishop Ranch, San Ramon, California: Consultant's Report to Dame Construction Company, Dated July 15, 1976, 18 p., 13 sheets, (Alquist-Priolo Report AP-404).

Reasenberg, P. and Ellsworth, W.L., 1982, Aftershocks of the Coyote Lake, California, earthquake of August 6, 1979—a detailed study: Journal of Geophysical Research, v. 84, p. 7,599-7,615.

Rogers, J.D. and Halliday, J.M., 1992, Exploring the Calaveras-Las Trampas fault junction in the Danville-San Ramon area: in Borchardt, G. et al. (eds.), California Division of Mines and Geology Special Publication 113, p. 261-270.

Savage, J.C., Prescott, W.H., Lisowski, M., and King, N., 1979, Geodolite measurements of deformation near Hollister, California, 1971-1978: Journal of Geophysical Research, v. 84, p. 7,599-7,615.

Schulz, S.S., Mavko, G.M., Burford, R.O., and Stuart, W.D., 1982, Long-term fault creep observations in central California: Journal of Geophysical Research, v. 87, p. 6,977-6,982.

Sieh, K., and Jahns, R., 1984, Holocene activity of the San Andreas fault at Wallace Creek, California: Geological Society of America Bulletin, v. 95, p. 883-896.

Simpson, G.D., Lettis, W.R., and Kelson, K.I., 1992, Segmentation model for the northern Calaveras fault, Calaveras Reservoir to Walnut Creek: in Borchardt, G. et al. (eds.), California Division of Mines and Geology, Special Publication 113, p. 253-259.

Simpson, G.D., Lettis, W.R., Williams, C.R., Haraden, C.C., and Bachhuber, J.L., 1994, Paleoseismic investigation of the Northern Calaveras fault, Contra Costa and Alameda Counties, California: U.S. Geological Survey National Earthquake Hazard Reduction Program, Award Number 1434-93-G-2339, 26 p.

Simpson, G.D., Baldwin, J.N., Kelson, K.I., and Lettis, W.R., 1999, Late Holocene slip rate and earthquake history for the northern Calaveras fault at Welch Creek, eastern San Francisco Bay area, California: Bulletin of the Seismological Society of America, v. 89, p. 1,250-1,263.

Sims, J.D., 1991, Distribution and rate of slip across the San Andreas Transform boundary, Hollister Area, Central California [abs.]: Geological Society of America Cordilleran Section 1998 Meeting, Long Beach, California, v. 23, p. 98.

Toppozada, T.R., Real, C.R., and Parke, L., 1981, Preparation of isoseismal maps and summaries of reported effects for pre-1900 California earthquakes: California Division of Mines and Geology Open-file Report 81-11 SAC, 182 p.

Unruh, J.R. and Lettis, W.R., 1998, Kinematics of transpressional deformation in the eastern San Francisco Bay Region, California: Geology, v. 26, p. 19-22.

Walter, S.R., Oppenheimer, D.H., and Mandel, R.I., 1999, Significant earthquake clusters during 1967 to 1993 in the San Francisco-San Jose quadrangles, California: U.S. Geological Survey Miscellaneous Investigations Series, Map I-2580, 3 sheets.

Wong, I.G. and Hemphill-Haley, M.A., 1992, Seismicity and faulting near the Hayward and Mission faults: in Borchardt, G. et al. (eds.), California Division of Mines and Geology Special Publication 113, p. 207-215.

WGCEP (Working Group on California Earthquake Probabilities), 1990, Probabilities of large earthquakes occurring in the San Francisco Bay region, California: U.S. Geological Survey Circular 1053, 51 p.

WGCEP (Working Group on California Earthquake Probabilities), 1999, Earthquake probabilities in the San Francisco Bay region, 2000 to 2030 - A summary of findings: U.S. Geological Survey Open-file Report 99-517.

WGNCEP (Working Group on Northern California Earthquake Potential), 1996, Database of potential sources for earthquakes larger than magnitude 6 in northern California: U.S. Geological Survey Open-file Report 96-705, 40 p.

STUDIES ALONG THE PENINSULA SEGMENT OF THE SAN ANDREAS FAULT, SAN MATEO AND SANTA CLARA COUNTIES, CALIFORNIA

N. TIMOTHY HALL[1], ROBERT H. WRIGHT[1], AND CAROL S. PRENTICE[2]

ABSTRACT

The San Francisco Peninsula segment of the San Andreas fault zone extends approximately 90 km from offshore of the Golden Gate, near the 1906 epicenter, southeast to near Los Gatos. This paper summarizes private-sector geologic and geotechnical studies and fault-research investigations over the past 25 years along three reaches of the Peninsula segment. These investigations have generated significant new data on the Peninsula segment and advanced our understand-ing of the active traces, including the location, amount of slip, width of the zone of deformation, and late Holocene earthquake chronology.

Findings indicate that the currently active zone, which includes the 1906 ground rupture, was probably the location of the 1838 event, possibly a mid-17th Century 1906-type event, and likely ground rupture throughout the Holocene. The northwest reach, near Mussel Rock, may be wider and more complex, but the near-surface characteristics along linear reaches near Woodside typically include a 3- to 4-m-wide zone of shearing, expressed as a flower structure with a near-vertical southwest side, within a zone of ground deformation and cracking as much as 30 m wide, usually on the northeast side. Locally, the active zone consists of left-stepping, *en echelon* shears. In Portola Valley and several other locations, basins and sags occur where the zone steps or bends to the right.

In 1906, geologic slip on the central and northern Peninsula segment, from Woodside to Mussel Rock, varied from 2.4 to 2.7 m, but dropped to about 1.2 m in Portola Valley. We speculate that the seismic cycle on the Peninsula segment has a recurrence of 250 to 330 years between large-magnitude (M_w7.8) 1906-type events. The recurrence internal is shorter if one includes "smaller" earthquakes, such as the 1838 event (estimated magnitude M_w7.0 to 7.4), which may have triggered ground displacements of 1.6 ± 0.7 m near Woodside. The average late Holocene slip rate for the Peninsula segment is 17 ± 4 mm/yr, less than the 24 ± 3 mm/yr for the North Coast segment. Most of the apparent slip-rate deficit may be accommodated by the San Gregorio-Seal Cove fault.

INTRODUCTION

The San Andreas fault zone (SAF) traverses the densely populated San Francisco Peninsula from the coastline, at Mussel Rock in Daly City, southeast to Portola Valley, where the fault enters the Santa Cruz Mountains. The Peninsula segment of the SAF is defined as extending from offshore of the Golden Gate, near the epicenter of the 1906 earthquake, southeast to near the town of Los Gatos at the surface projection of the northwest limit of the 1989 Loma Prieta earthquake rupture zone, a distance of about 90 km (Figure 1; WGCEP, 1990, 1999).

The SAF is a N35°W-trending continuous zone of faulting, locally up to hundreds of meters wide, that separates basement rocks of the Jurassic and Cretaceous Franciscan Complex on the northeast,

[1] Geomatrix Consultants
2101 Webster Street, 12th Floor
Oakland, California 94612
thall@geomatrix.com
bwright@geomtrix.com

[2] U.S. Geological Survey
Western Earthquake Hazards
345 Middlefield Road, MS 977
Menlo Park, California 94025
cprentice@isdmnl.wr.usgs.gov

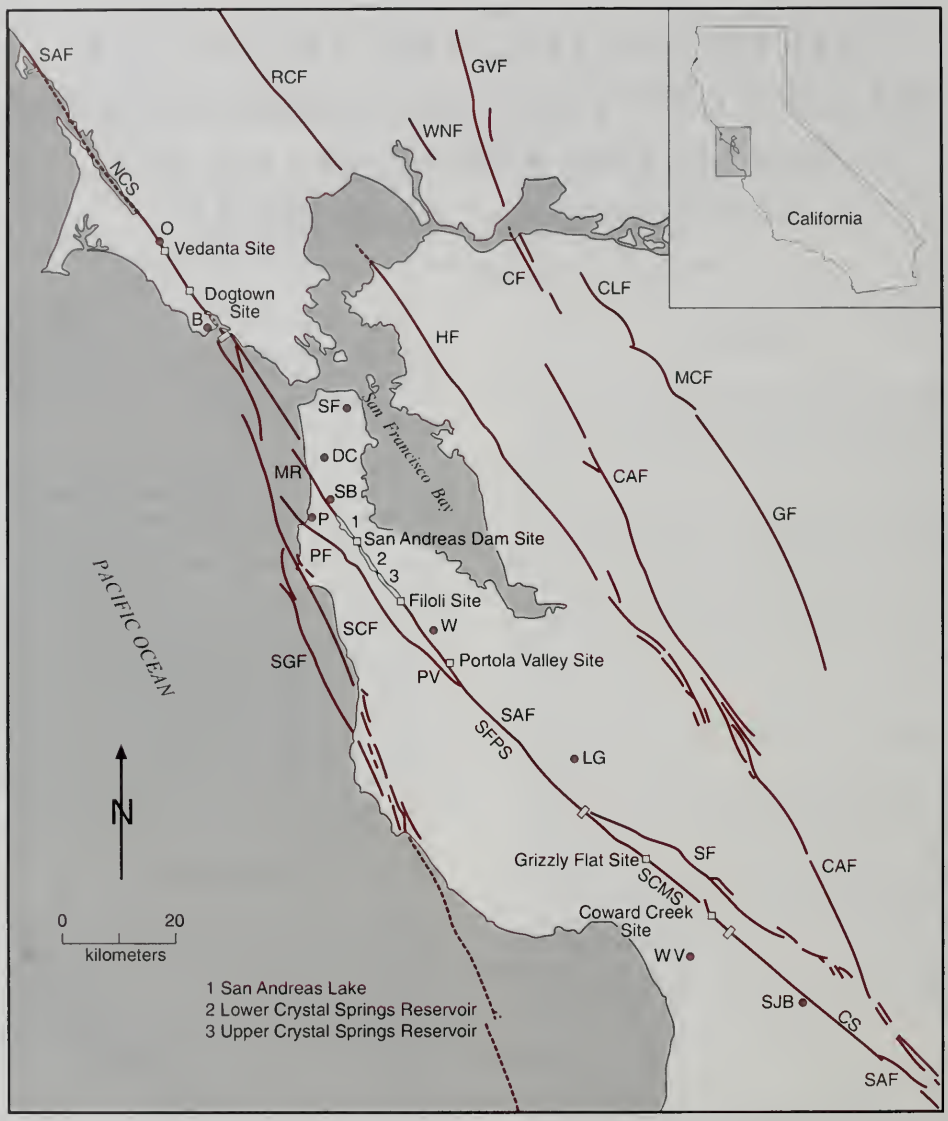

Geographic Locations: O=Olema, B=Bolinas, SF=San Francisco, DC=Daly City, P=Pacifica, W=Woodside, PV=Portola Valley, LG=Los Gatos, WV=Watsonville, SJB=San Juan Bautista, MR=Mussel Rock, SB=San Bruno
Faults: SAF=San Andreas, RCF=Rodgers Creek, WNF=West Napa, PF=Pilarcitos, CAF=Calaveras, GF=Greenville, SCF=Seal Cove, SGF=San Gregorio, SF=Sargent, MCF=Marsh Creek, CLF=Clayton, CF=Concord, GVF=Green Valley
Note: Open rectangles are the approximate location of segment boundaries of the Northern California section of the SAF and between the Northern California and Central California sections (NCS=North Coast, SFPS=San Francisco Peninsula, SCMS=Santa Cruz Mountains, CS=Central California; modified from WGCEP, 1990).

Figure 1. Regional fault map of the San Francisco Bay area showing key locations along the San Andreas fault.

from Salinian Block granitic basement rocks of comparable age on the southwest. At a more local scale, the Peninsula segment of the SAF contains the currently active zone, which is not always N35°W-trending nor geometrically simple. This zone was the location of his-torical slip during the April 18, 1906, earthquake (Schussler, 1906; Taber, 1907; Lawson, 1908), and likely was the source of the June 1838 earthquake (Louderback, 1947; Toppozada and Borchardt, 1998; Bakun, 1999; Hall et al., 1999). The active zone probably has been the location of surface rupture throughout the Holocene (Hall, 1984; Heingartner, 1995), and is the most likely location of future surface rupture and associated ground deformation.

This paper summarizes our findings along three reaches of the Peninsula segment of the SAF: (1) Mussel Rock to near San Andreas Lake, where the surface expression of the fault zone has been obscured by dense, minimally regulated development; (2) the Filoli Center, an essentially undisturbed paleoseismic site near Woodside; and (3) central Portola Valley, an area of low-density, highly regulated development.

MUSSEL ROCK TO SAN ANDREAS LAKE

The 7-km-long reach of the Peninsula segment from Mussel Rock, southeast through San Bruno to San Andreas Lake, is the most urbanized stretch of the SAF in northern California (Figure 1). Development in this part of the San Francisco Peninsula occurred largely in the 1950s, 1960s, and early 1970s before the advent of state regulations governing construction in active fault zones (Alquist-Priolo Fault-Rupture Hazard Zones Act of 1972; Hart, 1988). Although the general location of the SAF is well known in this region, it is difficult to locate active traces because of the cultural modification of the landscape.

Method of study

To locate active traces in the urbanized Daly City-San Bruno area, we used the following strategy: First, we assessed the pre-development topography in the vicinity of Mussel Rock as depicted on the 1853 U.S. Coast Survey map (scale 1:10,000). This map shows the locations and unmodified shapes of the scarps, linear drainages, knobs, saddles, and sag ponds that mark the surface expression of the active zone (Figure 2). Second, we reviewed the general location of ground ruptures plotted on the San Mateo Quadrangle after the 1906 earthquake (Lawson, 1908, Map No. 21; Lawson, 1914). These maps show the larger sag ponds and the approximate locations of the 1906 ground ruptures with respect to these ponds and other distinctive features. Third, using the 1950 edition of the San Francisco South Quadrangle (scale 1:24,000) and pre-development aerial photographs from the 1940s, we completed a photointerpretive map of the fault from unmodified fault-related topographic features. Fourth, we examined historical photographs taken after the 1906 earthquake, cataloged the distinctive natural features, and located the photographs using the pre-development maps and aerial photography. Cultural features such as houses, roads, fence lines, and groves of trees were used to locate approximately where each picture was taken and the direction the camera was pointing. Typically, these features changed little between 1906 and the early 1940s.

Geomorphic expression

Between Mussel Rock, a resistant outcrop of Franciscan Complex greenstone, and near the north boundary of San Andreas Reservoir, the SAF lies along or close to the crest of a northwest-trending ridge. The active traces lie just south of Fog Cap (Figure 2, elevation 222 m), the highest pointon the Pacific coast between San Francisco and Pacifica. Both north and south of Mussel Rock, marine terraces warp upward toward the fault zone, indicating it is the locus of local uplift as well as recurrent right-slip movement. The coincidence of the fault zone with a topographic high is unusual for northern California, where the zone typically is marked geomorphically by a broad "rift" or fault valley (Wallace, 1990). The N36°W to N40°W trend of the fault zone near Mussel Rock, which is up to 4° oblique to the N36°W trend of relative motion between the Pacific-North American plates according to the NUVEL-1 plate motion model (DeMets et al., 1990), may have resulted in a small component of fault-normal compression that is responsible for the observed uplift. Along this reach, 1906 ground ruptures typically lie along or near the bottoms of narrow, elongate sags or valleys incised into the ridge near its crest (Figure 2).

The most striking tectonic geomorphic features found near Mussel Rock were the ponds that marked the fault zone (U.S. Coast Survey, 1853). The largest of the ponds, located about 1.6 km southeast of Mussel Rock, was clearly fault-con-

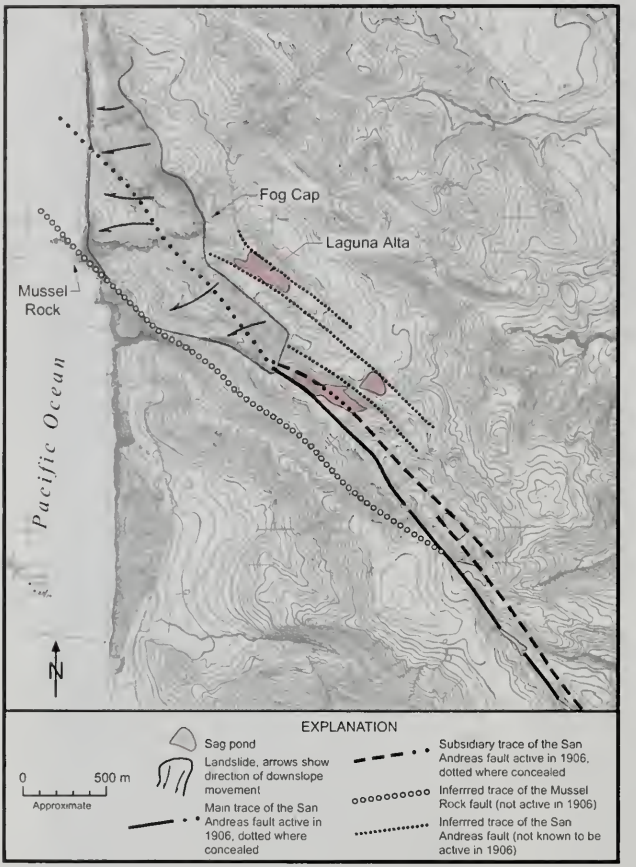

Figure 2. 1853 U.S. Coast Survey topographic map showing the unmodified expression of the San Andreas fault near Mussel Rock.

trolled. The northwest half of the pond was bounded by the main 1906 trace on the west and by a subsidiary trace on the east that also probably slipped at that time (Figure 2).

Laguna Alta, the northernmost and second-largest pond, was about 1,070 m east of Mussel Rock. Even though the sag containing this pond also appears to have been bounded by faults, its northwest trend was parallel to the strike of bedding in the Merced Formation (Bonilla, 1971, 1998) and may have been partly the result of differential erosion along a weak stratigraphic horizon. There is no mention in Lawson (1908) that the faults inferred to border this sag were active in 1906. The other large ponds also appear to have been fault-bounded (Pampeyan, 1995). Near Mussel Rock, strong ground shaking might have caused the highest parts of the cliff to move toward the free face, causing lateral spreading (Smith, 1981) and enhancing local settlement at Laguna Alta. However, such an explanation for the sags southeast of this pond becomes increasingly unlikely as the SAF diverges farther from the coast.

Most of the ponds appear to reflect local inhomo-genieties in the strike of the fault zone, where a small right step or a north-trending releasing bend caused local extension of the ground. We speculate that the faults bounding the sags near Mussel Rock might be part of a 3-km-wide right step-over in the SAF between Mussel Rock and the vicinity of Lake Merced to the north, as inferred from aeromagnetic data by Jachens and Zoback (1999).

1906 faulting

The main 1906 trace of the SAF near Daly City was described as a "furrow" that resulted from "shearing of the turf" (Wood, 1907). This trace, or furrow, was visible throughout the Daly City-San Bruno area as far north as a wagon road that crossed the fault about 1,400 m southeast of Mussel Rock. From here to the coast, however, fault-rupture features were obscured by the Mussel Rock landslides. Despite some controversy at the time, Wood (1907) interpreted that faulting continued on trend and intersected the shoreline about 1,220 m north of Mussel Rock, its trace marked by a debris flow that apparently was triggered by the earthquake and extended several hundred feet out into the Pacific Ocean. According to Wood (1907), this debris flow "lays too accurately in line with the projected path of the fault to be neglected. I regard it as movement of the loose material of the slide along the zone of shearing."

Because none of the cultural strain gauges Lawson (1908) and his colleagues used are preserved in the Daly City-San Bruno area, we relied on historical descriptions and photographs to assess the nature of the 1906 ground rupture. In general, the photographs indicate that as many as 3 to 4 traces defined a local zone of deformation that averaged 15 m wide. At one point, near what is now the intersection of Highway 35 and Sharp Park Boulevard, a fence crossed the fault zone at nearly a right angle (Figure 3). Photographic evidence indicates that the main trace, which lay just above the east edge of a well-defined swale, experienced about 2 m of right slip. Two subsidiary eastern traces, which extended as far as 15 m to the east, accounted for 0.6 to 1 m of additional right slip. According to Lawson (1908, p.4, Figure 29), bending of this fence may have extended westward from the fault more than 61 m, for a total displacement of 4 m. About 30 m southeast of the fence, the main trace apparently was confined to a furrow about 2 m wide between Franciscan Complex bedrock on the west and Merced Formation conglomerate on the east.

Historical photographs also show an active subsidiary trace about 120 to 180 m east of the main trace (Figure 2). The subsidiary trace branches from the main trace about 2.1 km southeast of the Mussel Rock landslide. Lawson (1908, p. 94) describes the subsidiary fault: "Southeast from this saddle [the modern Highway 35/San Andreas fault crossing] there is recognizable in the topography a distinct line of former movement, lying east of the fault. No furrow follows the line continuously, but an occasional short fissure or crack runs along it for a little way." Photographic evidence suggests this subsidiary fault may have experienced several centimeters of slip.

Lawson continues: "To the west of the place is a similar, but less well marked, topographic indication of a former movement. There is no evidence of any movement on this line at the time of the earthquake." Here Lawson appears to refer to the prominent linear drainage marking a fault that extends northwest to Mussel Rock. This fault locally forms the west boundary of the Merced Formation, cuts

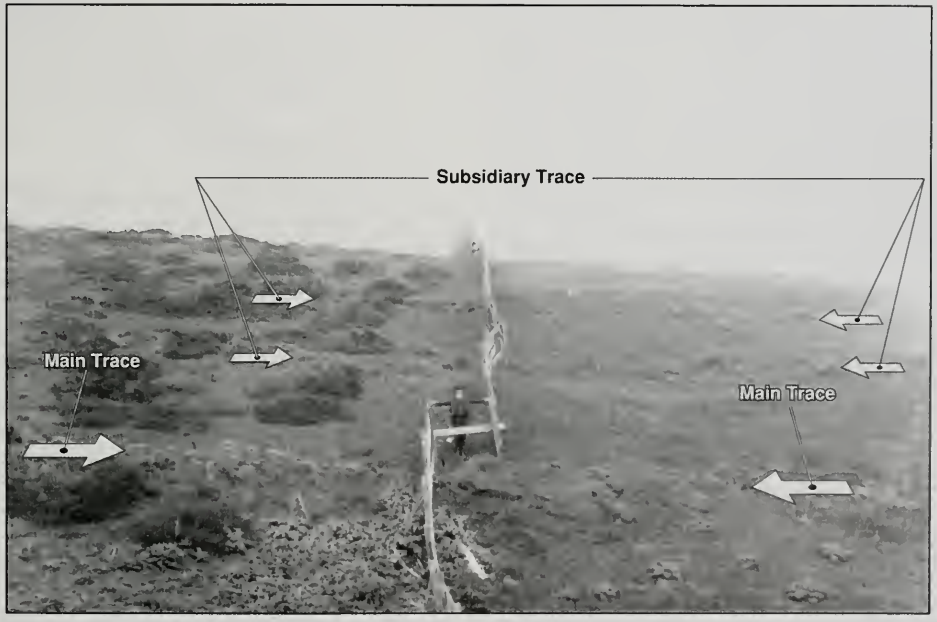

Figure 3. Fence in San Bruno deformed by 1906 faulting. View to northeast. H.O. Wood photograph No. 110, Bancroft Library, University of California, Berkeley. Courtesy of U.S. Geological Survey.

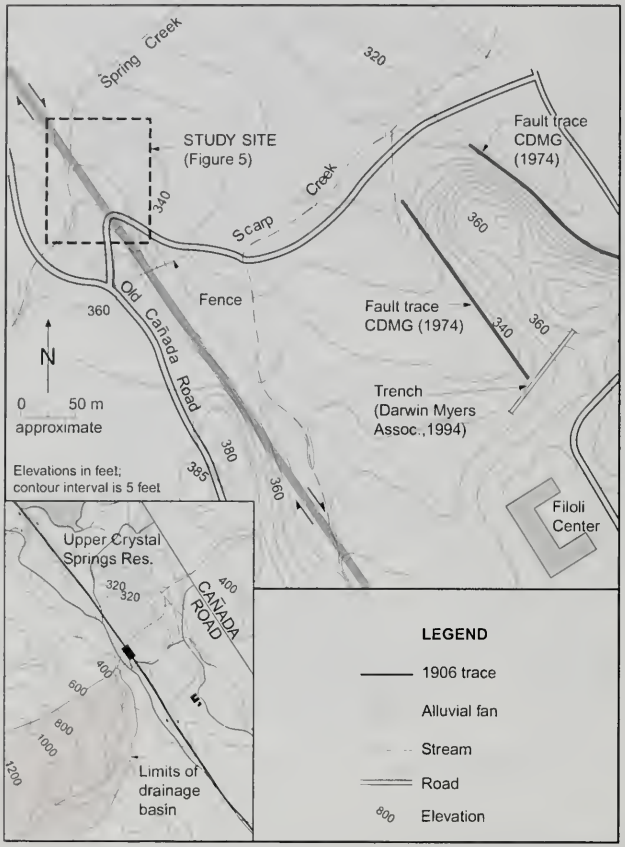

Figure 4. The Filoli Center site, Woodside, California.

Franciscan Complex greenstone, and offsets the overlying marine terrace deposits of possible Sangamon age (~125 ka) at the coastline. Kieffer (1999) informally named this potentially active trace of the SAF the Mussel Rock fault.

FILOLI CENTER SITE

The Filoli Center paleoseismic study site is 6.7 km northwest of central Woodside and about 1.5 km southeast of Upper Crystal Springs Reservoir (Figure 1). The authors have been performing paleoseismic research at the site since 1993 (Hall et al., 1995, 1999). Here the 1906 rupture is located along the southwest margin of a "rift" valley at the base of a 5- to 10-m-high, northeast-facing scarp. The scarp is breached by Spring Creek, an intermittent stream that drains an area of about 3 km^2 on the northeast flank of the Santa Cruz Mountains. Spring Creek has built an alluvial fan across the active fault zone (Figure 4) during the late Holocene. The fan contains several buried channels that cross the active fault zone at high angles, and one near-surface channel that follows the zone for 25 m or more. We matched several fault-normal channel deposits across the fault zone and dated them by radiocarbon analysis. These channels provide piercing points from which we estimated the amount and timing of historical and prehistoric slip events, as well as a geologic slip rate for the late Holocene. The fault-parallel channel provides evidence for a ground-rupturing earthquake that disrupted the fan surface sometime between the 15th and 17th centuries, temporarily deflecting the main channel. Results of our ongoing studies at the Filoli Center site are documented in Hall et al. (1999) and summarized below.

1906 faulting

An initial fault-normal trench (T-1) was centered on what was depicted as a single trace on regional-scale fault maps by Taber (1907) and Lawson (1908, Map No. 22). This trench and four additional fault-normal trenches (T-2, T-3, T-9, T-14; Figure 5) exposed several individual shears that define a zone ranging in width from 3 to 4 m. At each exposure of the zone, shears generally are steeply dipping to near vertical to within 1 to 2 m of the surface, where they typically begin to flatten and diverge, forming a flower structure having a near-vertical southwest side. In the fault-normal trenches, ground deformation features—including minor warping, infilled ground cracks, and fractures—were observed within about 30 m of the zone of active faulting on the eastern side only, forming an asymmetric rupture zone. Apparent vertical separation across these features does not exceed 0.3 m.

Maximum surface displacements reported in Lawson (1908) along the central San Francisco Peninsula near the Filoli Center were about half (2.4 to 2.7 m) of the 4.9 to 5.5 m displacements observed in western Marin County (Niemi, 1992). Rows of cypress trees and an adjacent fence line downstream (southeast) of San Andreas Dam, and 12.5 km northwest of Filoli, are offset 2.7 m (Hall, 1984; Lawson, 1908, Figure 32, Plate 61B). About 5 km northwest of Filoli, the causeway between Upper and Lower Crystal Spring reservoirs (now Highway 92) was offset 2.4 m (Lawson, 1908, p. 102-3, Figure 40). At the Folger Estate, about 9 km southeast of the Filoli site, two fences reportedly were offset 2.4 and 2.6 m (Lawson, 1908, p. 106, Plate 63B). Based on these observations, we estimate that maximum horizontal geologic displacements of 2.4 to 2.7 m also likely occurred at Filoli in 1906.

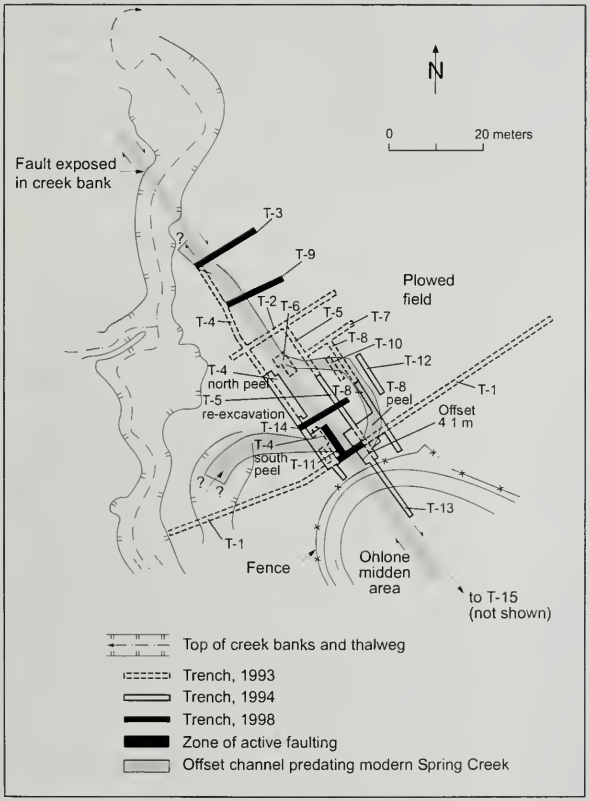

Figure 5. Filoli Center trenches showing channel offset by 1906 and 1838 (?) earthquakes.

Vertical and horizontal slip rates

J.C. Branner (in Lawson, 1908, p. 105) reports an up-on-the-west vertical slip of 0.15 m near old Cañada Road about 1.1 km northwest of Filoli Center. Using the range of maximum horizontal displacements of 2.4 to 2.7 m, the ratio of horizontal to vertical slip in 1906 in the vicinity of Filoli Center ranged from 16:1 to 18:1. This ratio compares well with the average of 17:1 measured for a Filoli Center channel deposit having a minimum calibrated AMS radiocarbon age of 2070 ± 120 years B.P. and a thalweg offset horizontally 30 ± 2 m and 1.8 m vertically across the fault (Hall et al., 1999). Based on these data, we estimate an average vertical slip rate for the Filoli Center site over the past 2,000 years of about 1 ± 0.2 mm/yr, west side up. From these data we also calculate an average horizontal (dextral) slip rate of about 17 ± 4 mm/yr, our preferred estimate for the late Holocene geologic slip rate for the Peninsula segment of the San Andreas fault. Our proposed slip-rate estimate from the Filoli Center site is about 30 percent lower than the minimum rate of 24 ± 3 mm/yr derived from studies north of San Francisco at the Vedanta site in Marin County (Niemi and Hall, 1992). The generally uniform maximum coseismic slip observed in 1906 between the Daly City–San Bruno area (Figure 3) and the Folger Estate in southern Woodside (Lawson, 1908, Plate 63B) indicates that the horizontal slip rate estimated from a Filoli Center site channel applies to most, if not all, of the Peninsula segment.

Paleoseismic chronology

In addition to using the approximately 2,000-year- old channel deposits to estimate the average late Holocene geologic slip rate for the Peninsula segment, we correlated two younger channel sequences across the zone of active faulting at the Filoli Center site. A near-surface sequence of three "nested" channel deposits at the same location, which is offset 2.5 m, probably records the 1906 surface rupture.

This sequence is incised at least 2 m into the fan surface, is older than the modern Spring Creek channel, and clearly predates the 1906 earthquake. The measured horizontal offset is consistent with the 2.4 to 2.7 m of maximum horizontal slip observed both north and south of Filoli after the 1906 earthquake.

Another nested sequence consisting of two channel deposits lies just below the sequence that records the 1906 faulting. The older sequence is offset 4.1 ± 0.5 m across the zone of active faulting. Calibrated AMS radiocarbon analyses indicate this channel was filled between 1476 and 1647 AD. We believe that the 4.1 ± 0.5 m offset recorded by this lower channel sequence is the sum of the coseismic slip observed near Filoli following the 1906 earthquake (2.5 ± 0.2 m) and the slip that occurred during the previous (penultimate) event on the Peninsula segment. We estimate that the penul-timate event produced an average slip of 1.6 ± 0.7 m at the Filoli Center site. This range of dextral slip is consistent with a range of single-event strike-slip earthquakes of magnitude M_W 7.0 to 7.4, and is also consistent with a single M_W 7.3 earthquake rupturing the approximately 90-km length of the Peninsula segment (Wells and Coppersmith, 1994). Based on its young radiocarbon age, a horizontal slip that is consistent with rupture length/magnitude relationships for the Peninsula segment, and the historical record (e.g., Louderback, 1947), we offer the working hypothesis that the penultimate earthquake recorded at the Filoli Center site is the San Francisco Peninsula earthquake of June 1838. We recognize that estimates of the extent of ground rupture and magnitude of this poorly documented earthquake vary. Readers are referred to Toppozada and Borchardt (1998), Schwartz et al. (1998), Bakun (1999), and Hall et al. (1999) for thorough discussions of this historical earthquake.

The channel sequence offset by the 1906 and 1838 (?) events crosses the active fault zone from west to east near the south end of the Filoli Center site and loops back to the west in an up-fan direction (Figure 5). This channel then follows the east margin of the active trace parallel to fan contours for at least 25 m. We speculate that fault-parallel channels are more likely to form on the Spring Creek fan after a surface-faulting event than at any other time. We envision a fan-head channel being deflected along the active trace by tectonic geomorphic features such as "mole tracks" (an elongate mound of heaved and broken ground), tension cracks, and grabens that form during a major slip event. Assuming that the fault-parallel channel formed in response to a SAF earthquake, and remembering that the channel was filled with gravel deposits within or shortly after the interval 1476 to 1647 AD, we suspect that a large pre-1906 earthquake occurred sometime between 353 and 552 years ago. (See also Prentice, 1989; Prentice et al., 1991; Niemi, 1992, Niemi and Hall, 1992; Heingartner and Schwartz, 1996; and Schwartz et al., 1998.)

In 1998, we re-excavated and deepened or extended four trenches (T-1, T-3, T-4, T-11; Figure 5), and opened two new ones (T-14, T-15; Figure 5) to clarify channel relationships and identify and date pre-1906 earthquakes marked by the upward erosional truncation of fault splays. The west margin of the fault-parallel channel coincides with the zone of shears active in 1906. The 1906 shears appear to have overprinted and obscured any older shears in this area. However, at least three shears were recognized that terminate at the base of the fault-parallel channel, which is consistent with our speculation that this channel developed along the fault after a ground-rupturing earthquake disrupted the fan surface (Figure 6).

CENTRAL PORTOLA VALLEY

Lawson (1908) and Taber (1907) both documented the effects of the 1906 earthquake in the Portola Valley area (Figures 1 and 7). Taber (1907) wrote: "Through the Portola Valley, and for about 3 miles northwest of Woodside, the fracture runs in a continuous and almost straight line. At a little distance, it looks as though a furrow had been run down the valley with a big plow. In places the earth has been piled up into ridges 2 or 3 feet high, and at other places fissures have been opened that measure 2-1/2 feet in width." Based in part on this report, Pampeyan (1970) map-ped the 1906 ground-rupture zone through this area as a single, continuous trace generally known as the Woodside trace (Dickinson, 1970). A second trace, generally known as the Trancos trace, is mapped northeast of and approximately parallel to the Wood-side trace on state and town maps (CDMG, 1987; TPV, 1984).

We summarize key observations of the SAF in Portola Valley beginning at the north end of town and moving southeast.

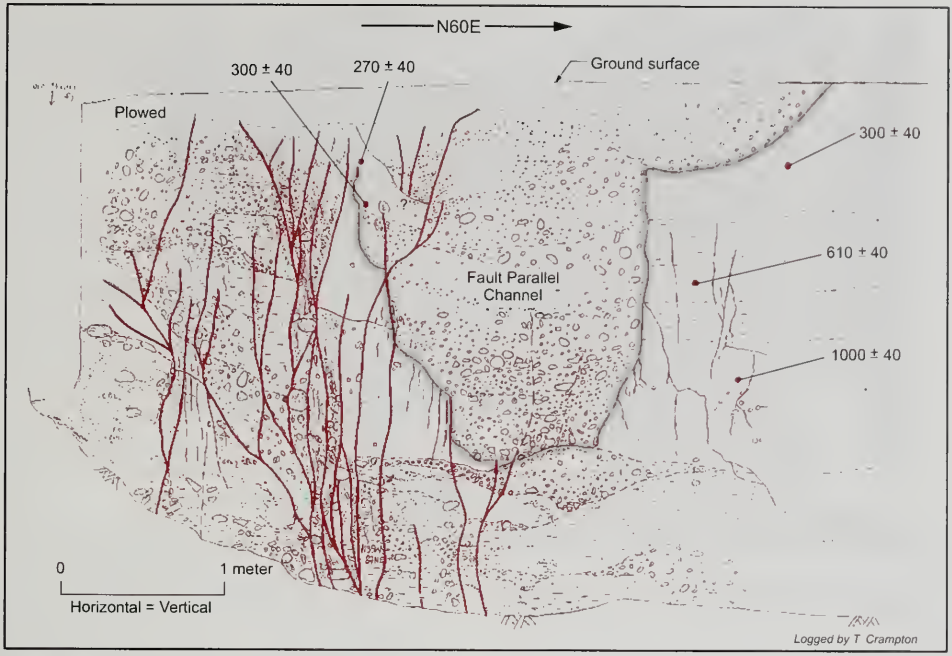

Figure 6. North wall of Filoli Trench T-9 showing fault-parallel channel and location of radiocarbon samples. Ages in radiocarbon years BP.

Portola Road

In the Portola Valley area, Lawson (1908) reported left-stepping, en echelon fault ruptures across Portola and Alpine roads and along the trace south of Alpine Road in what is now the Portola Valley Ranch subdi-vision: "The main fault fracture passes through the Portola Valley and crosses the public road in front of a small 1-story house southeast of the village store. Where the fault crosses the road, the fences on both sides were torn in two, and in the prune orchard south of the road the rows of trees were displaced in some instances about 2 feet. The cracks in the road were about 6 inches wide, approximately parallel, and running nearly north-south, while the direction of the fault line itself was about northwest-southeast."

A photograph of the 1906 rupture zone at Portola Road, looking southeast toward the location of the present baseball field, shows northeast-trending, left-stepping ruptures having vertical offsets of a few centimeters and a total right-lateral offset estimated from other nearby historical photos to be 1.0 to 1.2 m, distributed over a zone 6 to 7 m wide (Figure 8).

Portola Valley Town Center site

Woodward-Clyde Consultants (WCC, 1976a, 1976b; 1977; Taylor et al., 1980) investigated the location of the SAF at the Portola Valley School site, now the Portola Valley Town Center (PVTC) (Figure 7), by excavating five trenches and performing a magnetometer survey. The site is south and west of Portola Road, on the northwest margin of an oval-shaped basin that occupies the central portion of the SAF "rift" in this area. Although their trench T5 intersected the active Woodside trace, the other four WCC trenches yielded no definitive evidence for either the Woodside or Trancos traces at the PVTC.

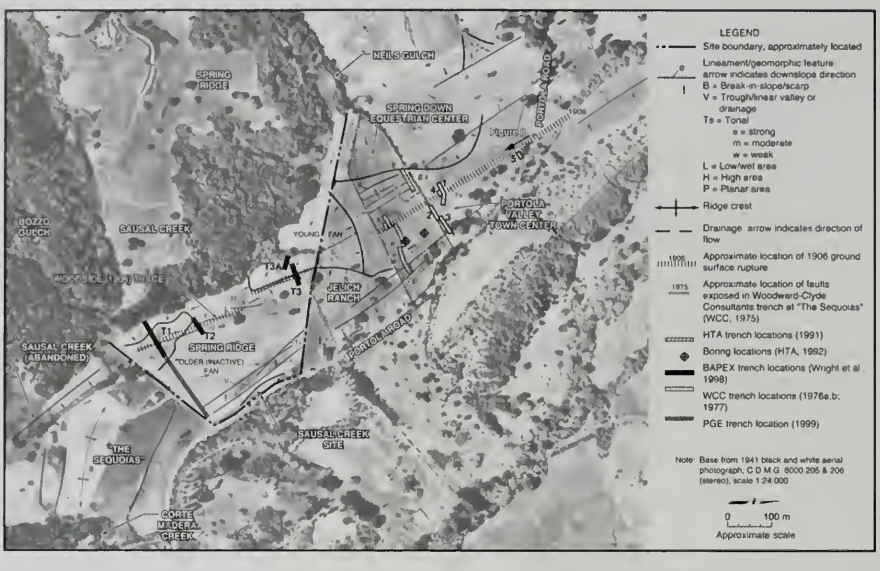

Figure 7. Aerial photograph showing tectonic geomorphology and exploration sites along the San Andreas fault in Portola Valley.

Spring Down Equestrian Center site

Harlan Tait Associates (HTA) investigated the SAF at Spring Down Equestrian Center (SDEC) in 1991 and 1992. The site, southeast of PVTC and southwest of Portola Road (Figure 7), includes the middle of the oval-shaped basin that occupies the central portion of the SAF "rift valley" in this area (Figure 9). The HTA investigations included six backhoe trenches and two borings, 15.4 and 27.3 m deep (HTA, 1991; Figure 7). The trenches encountered northeast-dipping alluv-ial fan deposits in the southwest part of the site, and southwest-dipping colluvial deposits in the northeast part of the site. In the center of the site, the alluvial and colluvial deposits interfinger with relatively flat-lying fluvial deposits, which in turn overlie marsh/lake deposits. The deposits and stratigraphic relationships encountered at the SDEC site are similar to those shown on the PVTC trench logs (WCC, 1976a, 1976b). We believe that a series of vertically aligned, down-to-the-west steps in HTA Trench 1 and a west-facing monocline in their Trench 6 mark the Woodside trace.

Radiocarbon analysis of detrital charcoal from the deeper HTA boring yielded an age date of 11,390 ±150 radiocarbon years B.P. at a depth of 27.1 m (Heingartner, 1995). The relatively thick sequence of Holocene deposits, which accumulated at an estimated average rate of 4.0 to 4.4 mm/yr, suggests relatively rapid subsidence and concurrent sedimentation within the Portola Valley basin throughout the Holocene.

Sausal Creek site

The Sausal Creek site includes the southern margin of the Portola Valley basin (Figure 9), and the gently northwest-sloping surface of the Sausal Creek fan. The Woodside trace, mapped along the southwest margin of the site, is marked by a zone of left-stepping lineaments evident on 1941 aerial photographs (HTA, 1991). Southeast of the site, the linear valley of Sausal Creek marks the Woodside trace. The Trancos trace is mapped along the northeast margin of the site, where several lineaments are visible on 1941 aerial photographs (Figure 7). Modern Sausal Creek, whose source area is Bozzo Gulch, forms the southwest boundary of the site and is entrenched as much as 10 m below the fan surface.

Figure 8. *En echelon* cracks of the Woodside trace crossing Portola Road in 1906. View to the south. Stanford University Archives, J.C. Branner collection. Courtesy of the U.S. Geological Survey.

An investigation funded by the Bay Area Paleoseis-mic Experiment (BAPEX) was conducted at the site in late 1998 (Wright et al., 1999; Clahan et al., 1999). The investigation included detailed logging and analysis of four backhoe trenches. Trench 1, excavated in the southwest corner of the site, exposed the Woodside trace in northwest-dipping alluvial fan deposits (Figure 7). Radiocarbon analyses of detrital charcoal from this trench indicate that fan sediments accumulated at a rate of about 8 mm/yr until as long ago as 900 radiocarbon years B.P., when deposition on the fan surface apparently ceased. Trench 1 was later extended northeast to within about 25 m of Portola Road by Pacific Geotechnical Engineering (PGE, 1999), but no additional evidence of faulting (i.e., the Trancos trace) was encountered.

Trench 2, excavated 100 m northwest of Trench 1, encountered fan deposits and a fan surface of similar age, further suggesting that Sausal Creek entrenched its channel about 900 radiocarbon years ago, starving the fan. In both Trenches 1 and 2, the Woodside trace is expressed as a zone of shearing about 6 to 8 m wide, with apparent down-to-the-southwest vertical displacements across individual shears that range from 1 cm to about 20 cm (Figure 10).

Trench 3 was excavated near the northwest corner of the site, across a southwest-facing scarp that marks the Woodside trace. East of the fault are northwest-dipping alluvial deposits having a radiocarbon age (based on detrital charcoal) of about 4,000 years B.P. To the west are alluvial deposits of the active Sausal Creek fan, which extends northwest to Jelich Ranch (Figure 7). These young deposits have a radiocarbon age of about 300 years B.P., are buttressed against the base of the fault scarp, and are separated from the older alluvium on the east by a complex 3-m-wide shear zone.

"The Sequoias"

"The Sequoias" retirement community is located on a northwest-trending ridge northeast of Sausal Creek (Figure 7). The Trancos trace is mapped bounding the northeast side of this ridge (TPV, 1984), approximately along the trend (N40°W) of a linear section of Corte Madera Creek (Figure 9). The Woodside trace is mapped as bounding the southwest side of the ridge, approximately along the trend (N35°W) of the linear valley of Sausal Creek, which is now occupied partly by a reservoir (TPV, 1984). Topographic relief across the ridge ranges from 15 to 45 m.

WCC (1975) excavated a backhoe trench near the northeast corner of "The Sequoias" that exposed a narrow shear zone entirely in bedrock of Eocene age (Whiskey Hill Formation), which they identified as the Trancos trace. In 1992, PGE excavated five backhoe trenches on the ridge and exposed fractured Santa Clara Formation of Plio-Pleistocene age. Most

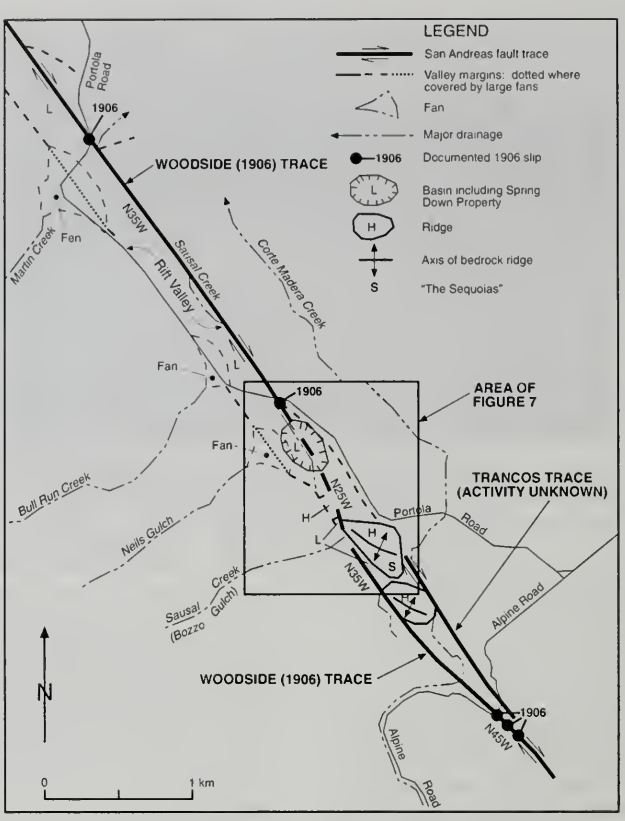

Figure 9. Tectonic model for the origin of geomorphic features along the San Andreas fault in Portola Valley.

fractures trend between N25°E and N45°E and dip 75°SE to vertical. The fractures might be the result of strong ground shaking.

Tectonic model of Portola Valley

The findings described in the previous paragraphs are consistent with a tectonic model (Figure 9) in which Holocene activity has been confined to the Woodside trace, where it takes a right (releasing) step or bend of about 150 m of fault-normal separation between the Portola Road crossing on the north and "The Sequoias" on the south. This step or bend, which results in local crustal extension, has been responsible for forming a pull-apart basin (Aydin and Nur, 1982; Hempton and Dunne, 1984; Hempton and Neher, 1986; Mann et al., 1983; ten-Brink and Ben-Avraham, 1989). Sediment has been accumulating in this basin at the SDEC at an average rate of about 4 mm/yr throughout the Holocene. This right-step or bend model is at variance with models suggested by WCC (1976b), Taylor et al. (1980), and Dickinson (1970), who postulated a left step from the Woodside trace to the Trancos trace in the vicinity of the PVTC site. Because WCC (1976b) was unable to follow the Woodside trace in trenches more than about 30 m southeast of the Portola Road crossing (Figure 9), they concluded that the 1906 slip must have stepped east to the Trancos trace.

Our model does not require a through-going, near-surface connection between the en echelon segments of the active Woodside trace, which could explain the lack of a clear fault signature in

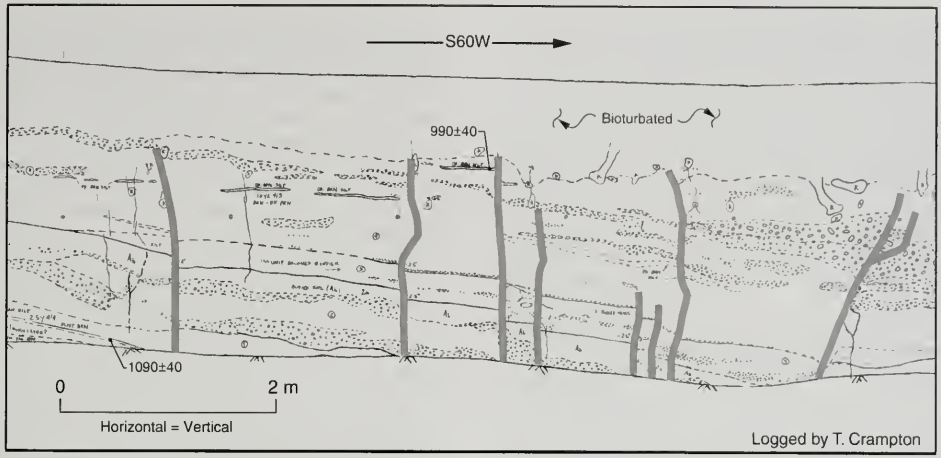

Figure 10. Field log of the south wall of Sausal Creek Trench T-1 showing multiple shears within the Woodside trace of the San Andreas fault.

trenches at the PVTC and SDEC sites. On the other hand, muted evidence for the 1906 ground rupture at the SDEC site may reflect the distributed nature of the shearing where the fault crosses the thick section of young sediments in the center of the Portola Valley basin.

As shown on Figure 9, the SAF "rift" in the Portola Valley area has a fairly consistent N35°W trend and a width of 245 to 275 m, with an apparent left bend in its boundaries in the vicinity of the SDEC site. Here trenching studies indicate that, moving from north to south, active faulting on the Woodside trace shifts from the northeast to the southwest side of the fault valley, and that the Trancos trace is either inactive or locally not present. From SDEC southeast to "The Sequoias," the fault zone is expressed as a relatively simple tectonic valley formed by subsidence across this releasing bend.

Southeast of "The Sequoias" to Alpine Road, the fault zone is more complex topographically, its boundaries largely defined by the channels of Sausal and Corte Madera creeks. Between these channels, the zone of faulting consists of a series of west-northwest-trending bedrock highs northeast of the Woodside trace, which appears to have been the only trace active in this area in 1906. The tectonic model shown on Figure 9 can also be used to explain the origin of these highs if slip has transferred partly from the Woodside trace to the Trancos trace between "The Sequoias" and Alpine Road. Compression associated with a restraining left step or bend could have produced the en echelon bedrock ridges. There is insufficient evidence at present to assess whether this inferred transfer of slip occurred only during the Pleistocene or into the Holocene as well. Additional fault-trenching studies are required to assess the existence and activity of the Trancos trace in Portola Valley.

The presence and timing of slip on the Trancos trace is one unresolved seismic hazard issue associated with the SAF in Portola Valley. Another issue concerns the origin of the linear southwest margin of the fault valley north of PVTC, which to date has not been identified as occurring along an active fault. A third unresolved issue involves the cause and seismic hazard implications of the apparent fifty percent or more drop in surface slip observed between Woodside (2.5 ± 0.2 m) and Portola Valley (~1.0 to 1.2 m) following the 1906 earthquake.

SUMMARY AND CONCLUSIONS

Based on the investigations summarized in this paper, which included review of numerous consultant's reports, we offer the following observations of the Peninsula segment of the SAF. We also suggest guidelines for improving the state of engineering geology practice for fault-rupture hazard investigations on the San Francisco Peninsula.

The currently active zone of the Peninsula segment of the SAF, which includes the 1906 ground rupture, probably experienced ground rupture during the June 1838 event and possibly during an event that may have occurred as recently as the mid-17th Century and been similar in extent to the 1906 earthquake (Hall et al., 1999). Both the thick section of Holocene sediments in the Portola Valley basin and deflected stream channels southeast (downstream) of San Andreas Dam (Hall, 1984) indicate that the currently active trace probably has been the location of ground rupture for most if not all of Holocene time. The near-surface characteristics along relatively linear reaches typically include a zone of intense shearing 3 to 4 m wide (e.g., at the Filoli Center). Often there is a zone of associated ground deformation and en echelon cracking as much as 30 m wide, usually located on the northeast side of the fault zone. Locally, as at the Sausal Creek site, the active fault trace is marked by left-stepping, north-trending en echelon shears that form a zone 6 to 8 m wide. Basins or sags of various sizes are present. Where the active fault zone has a major step or bend to the right, as near Daly City, the zone can reach 15 m wide.

Geologic slip observed on the Peninsula segment in 1906 (Filoli Center/Woodside reach) varied from 2.4 to 2.7 m, but dropped to about half that in Portola Valley. Slip possibly accompanying the June 1838 earthquake is estimated to have been 1.6 ± 0.7 m. These data suggest that the Peninsula segment may rupture in earthquakes of magnitudes as low as M_w7.0.

Our studies indicate that the average geologic slip rate for the Peninsula segment for the late Holocene is about 17 ± 4 mm/yr, compared with the 24 ± 3 mm/yr slip rate for the North Coast segment (Hall et al., 1999). Thus there may be a slip-rate gradient on the Northern California section of the SAF. The slip-rate deficit on the Peninsula segment, if real, may be accommodated by slip on nearby subparallel plate boundary faults, such as the San Gregorio-Seal Cove fault zone.

Finally, based on review of hundreds of private engineering geologic reports for sites along the Peninsula segment of the SAF and numerous visits to open trenches, we believe there is a need for standardization of trenching investigations. We suggest the following minimum guidelines:

1. All applicable OSHA trench safety regulations should be followed rigorously.

2. The trench investigation should include review of all previous fault investigations in the site vicinity and a stereoscopic assessment of fault-related geomorphic features at the site and vicinity using pre-development aerial photographs at a scale of 1:12,000 or larger, if available.

3. The trench should be at least 0.75 m wide and expose a minimum thickness of 2 m of native earth materials.

4. At least one wall of the trench should be cleaned of smeared soil to expose the native earth materials. Both walls and possibly the floor should be cleaned and evaluated across any zone of faulting and structural or stratigraphic complexity.

5. Earth materials should be categorized according to the Unified Soil Classification System (ASTM D2488) and colors described using the Munsell Soil Color Chart.

6. At least one wall of the trench should be accurately depicted on a graphical log by a Registered Geologist at a scale not smaller than 1:60.

7. Trenches in clayey soils should be kept open several days or long enough to allow the walls to dry sufficiently to reveal hidden shears.

8. Trench and field logs should be evaluated by the local reviewer, the official town, city, or county engineering geologist responsible for evaluating consultant reports, before the trench is backfilled.

A fault investigation is a highly specialized endeavor, the findings of which may have significant impacts for life safety and property values. Perhaps only qualified fault evaluation professionals, certified by the state the way geophysicists and hydrogeologists are, should perform fault investigations. However, in the absence of state regulation and given variable training by colleges and universities, the burden of improving the quality of fault investigations rests primarily with the local reviewer.

ACKNOWLEDGMENTS

The authors appreciate the thoughtful reviews provided by Dan Ponti and Pat McCrory of the U.S. Geological Survey. We are especially grateful to Kevin Clahan and Todd Crampton for the hours spent staring at trench walls to document active traces of the San Andreas fault. We also thank Ann

Taylor, Director of the Filoli Center, and Kirk Neely of Spring Ridge LLC, for providing access to their properties. The U.S. Geological Survey National Earthquake Hazard Reduction Program (NEHRP) awards 14-08-0001-G2081 and 1434-95-G-2581, and funding in FY 1998 from their Bay Area Paleoseismic Experiment program supported the research summarized in this paper. The findings and conclusions presented herein, however, are those of the authors and should not be interpreted as representing the official policies, either expressed or implied, of the U.S. Geological Survey.

AUTHORS' PROFILES

N. Timothy Hall is a Principal Engineering Geologist with Geomatrix Consultants. He was Professor of Geology at Foothill College in Los Altos Hills, California, for 21 years, and since 1981 has worked as an engineering geologist for private consulting firms. His experience includes paleoseismology and assessing the impact of active geologic processes on development. He earned a Ph.D. in Geology from Stanford University in 1984.

Robert H. Wright is Senior Consulting Engineering Geologist with Geomatrix Consultants, and is the Town Geologist of Woodside, California. He has 30 years of experience as an engineering geologist, including 5 years with the U.S. Geological Survey in Menlo Park, California, and the remainder with private consulting firms. His experience includes geologic hazards evaluations for land planning and development. He earned his Ph.D. in Earth Sciences from the University of California at Santa Cruz in 1982.

Carol Prentice is a Research Geologist with the U.S. Geological Survey. She has 13 years of experience as a geologist, including 3 years teaching high school science. Her experience includes paleoseismology and neotectonics, including faults of the San Andreas system in northern California and faults in Asia. She earned her Ph.D. in Geology from the California Institute of Technology in 1989.

SELECTED REFERENCES

Aydin, A., and Nur, A., 1982, Evolution of pull-apart basins and their scale independence: Tectonics, v. 1, p. 91-105.

Bakun, W.H., 1999, Seismic activity of the San Francisco Bay Region: Bulletin of the Seismologic Society of America, v. 89, no. 3, p. 764-784.

Bonilla, M.G., 1971, Preliminary geologic map of the San Francisco South quadrangle and part of the Hunters Point quadrangle, California: U. S. Geological Survey Miscellaneous Field Studies Map MF-311, scale 1:24,000.

Bonilla, M.G., 1998, Preliminary geologic map of the San Francisco South 7.5' quad and part of the Hunters Point 7.5' quadrangle, San Francisco Bay Area, California: U.S. Geological Survey Open-File Report 98-354, scale 1: 24,000.

CDMG (California Division of Mines and Geology), 1974, State of California special studies zones map, Woodside 7-1/2 minute quadrangle: California Division of Mines and Geology, Sacramento, Calif.

CDMG (California Division of Mines and Geology), 1987, Alquist-Priolo earthquake fault hazard zones, Mindego Hill quadrangle: California Division of Mines and Geology, scale 1:24,000.

Clahan, K. B., Hall, N. T. and Wright, R.H., 1999, Paleoseismic investigation of the San Andreas fault zone at Sausal Creek, Portola Valley, CA: Geological Society of America Cordilleran Section Annual Meeting, Berkeley, California, June 2-4, 1999 (Poster Session).

Darwin Myers Associates, 1994, Fault hazard investigation: Proposed visitors center, Filoli State Landmark, San Mateo County, Calif.: Consultant's report to Fioli Center.

DeMets, C., Gordon, R.G., Argus, D.F., and Stein, S., 1990, Current plate motions: Geophysical Journal International, v. 101, p. 425-478.

Dickinson, W. R., 1970, Commentary and reconnaissance photogeologic map, San Andreas Rift Belt, Portola Valley, California: Consultant's report to the Town of Portola Valley Planning Commission, dated July 6, 1970.

Hall, N.T., 1984, Holocene history of the San Andreas fault between Crystal Springs Reservoir and San Andreas Dam, San Mateo County, California: Bulletin of Seismological Society of America, v. 74, p. 281-299.

Hall, N.T., Wright, R.H., and Clahan, K.B., 1995, Paleoseismic investigations of the San Andreas fault on the San Francisco Peninsula, California: Final Technical Report for U.S. Geological Survey National Earthquake Hazards Reduction Program, Award No. 14-08-0001-G2091, unpublished report by Geomatrix Consultants.

Hall, N.T., Wright, R.H., and Clahan, K.B., 1999, Paleosesimic studies of the San Francisco peninsula segment of the San Andreas fault zone near Woodside, California: Journal of Geophysical Research, v. 104, no. B10, p. 23,215-23,236.

Harlan Tait Associates, 1991, Geologic and seismic hazards study, Spring Down Property, Portola Valley, California: Consultant's report to Spring Down Equestrian Center, 27 p.

Harlan Tait Associates, 1992, Supplemental geotechnical investigation, Goodstein Subdivision, X6D-175, Portola Road, Portola Valley, California: Consultant's report to Spring Down Equestrian Center, 2 p..

Hart, E.W., 1988, Fault-rupture hazard zones in California: California Division of Mines and Geology Special Publication 42, 24 p.

Heingartner, G.F., 1995, Written communication to N.T. Hall.

Heingartner, G.F., and Schwartz, D.P., 1996, Paleoseismic evidence for large magnitude earthquakes along the San Andreas fault in the southern Santa Cruz Mountains, California: EOS Transactions, American Geophysical Union, 77 (46), Fall Meeting Supplement, F462, 1996.

Hempton, M. R., and Dunne, L. A., 1984, Sedimentation in pull-apart basins; active examples in eastern Turkey: Journal of Geology, v. 92, p. 513-530.

Hempton, M. R., and Neher, K., 1986, Experimental fracture, strain and subsidence patterns over en-echelon strike-slip faults; implications for the structural evolution of pull-apart basins: Journal of Structural Geology, v. 8, no. 6, p 597-605.

Jachens, R.C., and Zoback, M.L., 1999, The San Andreas fault in the San Francisco Bay region, California: Structure and kinematics of a young plate boundary: International Geologic Review, v. 41, p. 191-205.

Kieffer, S., 1999, Implications of faulted marine terrace deposits of Mussel Rock, Daly City, California (abstract): Geological Society of America Abstracts with Programs, Berkeley, California, June.

Lawson, A.C. (ed.), 1908, The California earthquake of April 18, 1906; Report of the State Earthquake Investigation Commission: Carnegie Institution, Washington, D.C., Publication 87, v. 1, 451 p. (reprinted 1969).

Lawson, A.C., 1914, San Francisco folio–Tamalpais, San Francisco, Concord, San Mateo, and Hayward quadrangles: U.S. Geological Survey Folio No. 193, scale 1: 62,500.

Louderback, G.D., 1947, Central California earthquakes of the 1830s: Bulletin of the Seismological Society of America, v. 47, p. 33-74.

Mann, P., Hempton, M.R., Bradley, D.C., and Burke, K., 1983, Development of pull-apart basins: Journal of Geology, v. 91, p. 529-554.

Niemi, T.M., 1992, Late-Holocene slip rate, prehistoric earthquakes, and Quaternary neotectonics of the northern San Andreas fault, Marin County, California: Ph.D. dissertation, Stanford University, (Stanford, California), 199 p.

Niemi, T.M., and Hall, N.T., 1992, Late Holocene slip rate and recurrence of great earthquakes on the San Andreas fault in northern California: Geology, v.20, 195-198.

PG&E (Pacific Geotechnical Engineering), 1999, Fault location investigation, "The Sequoias", Portola Valley, for lodge addition and auxiliary power building, Portola Valley, California: Consultant's report, 20 p.

Pampeyan, E.H., 1970, Geologic map of the Palo Alto 7.5 minute quadrangle, San Mateo and Santa Clara counties, California: U.S. Geological Survey Open-File Report 70-254, scale 1:24,000.

Pampeyan E.H., 1995, Maps showing recently active fault breaks along the San Andreas fault from Mussel Rock to the central Santa Cruz Mountains, California: U.S. Geological Survey Open-File Report 93-684, scale 1:24,000.

Prentice, C.S., 1989, Earthquake geology of the northern San Andreas fault near Point Arena, California: Ph.D. dissertation, California Institute of Technology, (Pasadena, California), 252 p.

Prentice, C.S., Niemi, T.M., and Hall, N.T., 1991, Quaternary tectonics of the northern San Andreas fault, San Francisco Peninsula, Point Reyes, and Point Arena, California: in Sloan, D., and Wagner, D.L. (eds.), Geologic excursions in Northern California: San Francisco to the Sierra Nevada, California Division of Mines and Geology Special Report 109, p. 25-34.

Prentice, C.S., Hall, N.T., and Wright, R.W., in preparation, Strip map of the San Francisco Peninsula segment of the San Andreas fault: U.S. Geological Survey Miscellaneous Field Investigation Map.

Schussler, H., 1906, The water supply of San Francisco, California, before, during, and after the earthquake of April 18, 1906 and the subsequent conflagration: Martin B. Brown Press, (New York, New York), 103 p.

Schwartz, D.P., Pantosti, D., Okumura, K., Powers, T. J., and Hamilton, J., 1998, Paleoseismic investigations in the Santa Cruz Mountains, California: Implications for recurrence of large magnitude earthquake on the San Andreas fault: Journal of Geophysical Research, v. 103, p. 17,985-18,001.

Smith, T.C., 1981, Evidence of Holocene movement of the San Andreas fault zone, northern San Mateo County, California: California Division of Mines and Geology Open-File Report 61-6 SF, scale 1:24,000.

Taber, S., 1907, Some local effects of the San Francisco earthquake: in Jordan, D.S. (ed.), The California Earthquake of 1906: A.M. Robertson, (San Francisco, California), p. 303-315.

Taylor, C.L., Cummings, J.C., and Ridley, A.P., 1980, Discontinuous en echelon faulting and ground warping, Portola Valley, California: in Streitz, R., and Sherburne, R. (eds.), Studies of the San Andreas fault zone in northern California: California Division of Mines and Geology Special Report 140, p. 59-70.

ten-Brink, U. S., and Ben-Avraham, Z., 1989, The anatomy of a pull-apart basin; seismic reflection observations of the Dead Sea Basin: Tectonics, v. 8, p 333-350.

Toppozada, T.R., and Borchardt, G., 1998, Re-evaluation of the 1836 "Hayward fault" and the 1838 San Andreas fault earthquakes: Bulletin of the Seismological Society of America, v. 88, p. 140-159.

TPV (Town of Portola Valley), 1984, Geologic Map, Town of Portola Valley: William Cotton Associates (ed.), scale 1: 6,000.

Wallace, R.E. (ed.), 1990, The San Andreas fault system, California: U.S. Geological Survey Professional Paper 1515, 283 p.

Wells, D. L., and Coppersmith, K.J., 1994, New empirical relationships among magnitude, rupture length, rupture width, rupture area, and surface displacement: Bulletin of the Seismological Society of America, v. 84, p. 974-1,002.

Wright, R.H., Clahan, K.B., and Hall, N.T., 1999, Preliminary results: paleoseismic study of the Peninsula segment of the San Andreas fault at the Sausal Creek site, Portola Valley, California: Harlan Tait Assoc., San Francisco, Calif., unpub. BAPEX report to U.S. Geological Survey, 11 p.

Wood, H.O., 1907, Letter to A.C. Lawson dated 19 March 1907: Courtesy of Bancroft Library, University of California, Berkeley.

WCC (Woodward-Clyde Consultants), 1975, Geological evaluation, proposed Personal Care Facility, The Sequoias, Portola Valley, California: Consultant's report to The Sequoias.

WCC (Woodward-Clyde Consultants), 1976a, Results of fault study conducted for the Town of Portola Valley, Portola Valley Elementary School Site: Consultant's report to Portola Valley School District.

WCC (Woodward-Clyde Consultants), 1976b, Results of Phase II Fault Study, Portola Valley Elementary School Site: Consultant's report to Portola Valley School District.

WCC (Woodward-Clyde Consultants), 1977, Results of Phase III Fault Study, Portola Valley Elementary School Site, Consultant's report to Portola Valley School District.

WGCEP (Working Group on California Earthquake Probabilities), 1990, Probabilities of large earthquakes in the San Francisco Bay region, California: U.S. Geological Survey Circular 1053.

WGCEP (Working Group on California Earthquake Probabilities), 1999, Earthquake probabilities in the San Francisco Bay Region: 2000 to 2030 – a Summary of Findings: U.S. Geological Survey Open-File Report 99-517.


ASSOCIATED ENGINEERING
GEOLOGISTS

CHARACTERIZATION OF BLIND THRUST FAULTS IN THE SAN FRANCISCO BAY AREA, CALIFORNIA

JEFFREY R. UNRUH[1]

ABSTRACT

Oblique convergence along the boundary between the Pacific plate and the Sierra Nevada-Great Valley microplate at the latitude of the San Francisco Bay area is accommodated locally by uplift, folding and thrust faulting. As demonstrated by recent earthquakes on hidden or "blind" thrust faults in western California, areas of active crustal shortening may be source zones for moderate to large magnitude thrust-fault earthquakes. This paper synthesizes existing data to identify potential sources of thrust-fault earthquakes in the Bay area and characterize them in terms of maximum magnitude and average slip rate. In general, areas of active crustal shortening in the Bay area are associated with restraining bends or restraining stepovers among strike-slip faults of the San Andreas system. Examples include the Santa Cruz mountains (a left-restraining bend in the San Andreas fault) and the Mt. Diablo fold-and-thrust belt (a left-restraining stepover between the Greenville and Concord strike-slip faults). Based on the dimensions of individual thrust faults and folds within these stepover regions, most potential thrust-fault sources are capable of generating M_w5.5 to M_w6.5 earthquakes. Significant exceptions include the Foothills thrust system in the northeastern Santa Cruz mountains, which could generate an earthquake greater than M_w6.5 if multiple thrust-fault segments were to rupture simultaneously, and the blind Mt. Diablo thrust fault, which may be capable of producing a M_w6.75 earthquake. Slip rates on thrust faults, estimated indirectly from long-term average rates of surface uplift and horizontal shortening, range from several tenths of millimeters per year to about 1 mm/year. The most significant exception is the Mt. Diablo thrust fault, which probably has a long-term average slip rate of about 1 to 3 mm/year. In terms of contribution to regional seismic hazards in the Bay area, thrust faults are subordinate to strike-slip faults of the San Andreas system, which produce larger and more frequent earthquakes. However, because of their proximity to urbanized regions such as Silicon Valley and Livermore Valley, thrust faults may be significant local sources of strong ground shaking. The 1987 Whittier Narrows and 1994 Northridge earthquakes in southern California, which occurred on blind thrust faults beneath urbanized regions, may be analogs for thrust-fault earthquake scenarios in the Bay area.

INTRODUCTION

This paper draws on a collaborative analysis of late Cenozoic folds and thrust faults in the San Francisco Bay area by the Working Group on California Earthquake Probabilities (WGCEP, 1999). Unlike strike-slip faults of the San Andreas system, which are exposed at the surface and are thus amenable to detailed paleoseismic studies, active thrust faults commonly are not exposed and thus their seismic potential is much less understood. In the past three decades, several moderate magnitude earthquakes in California have occurred on thrust faults that were not recognized or evaluated as potential seismic sources prior to the earthquakes. Although the thrust-fault earthquakes were smaller than the anticipated "Big One" on the San Andreas fault, three of the earthquakes (1971 San Fernando earthquake, M_w6.6; 1987 Whittier Narrows earthquake, M_w6.0; 1994 Northridge earthquake, M_w6.7) struck highly urbanized areas of southern California and were very costly in terms of property damage and loss of life.

[1]William Lettis & Associates, Inc.
1777 Botelho Drive, Suite 262
Walnut Creek, CA 94596
unruh@lettis.com

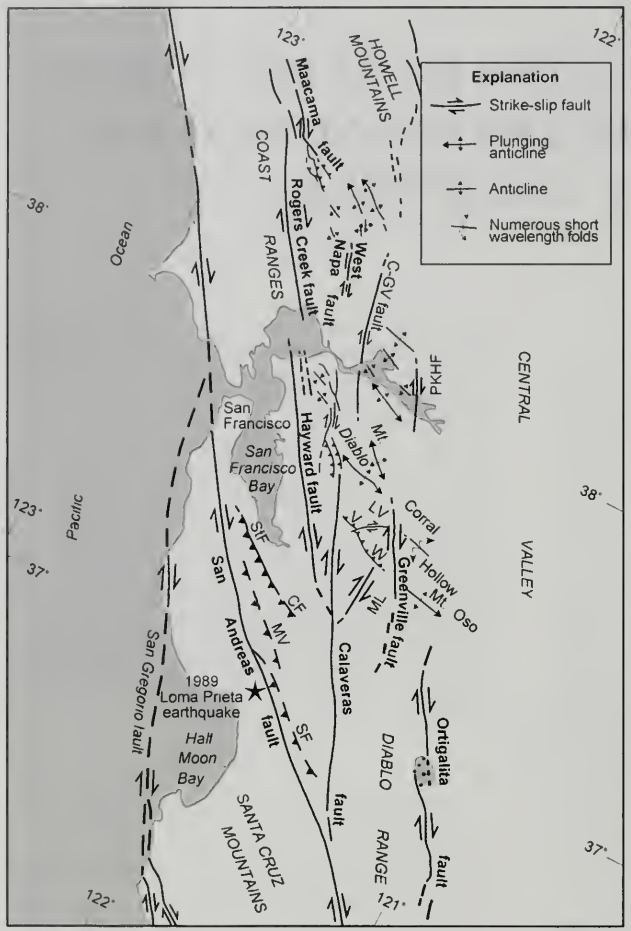

Figure 1. Major late Cenozoic strike-slip faults, folds and thrust faults in the greater San Francisco Bay area. Note that the thrust faults and folds typically are oriented about 45° to the strike-slip faults of the San Andreas system, and locally exhibit a right-stepping en echelon geometry typical of dextral wrench structures. Collectively, the strike-slip faults, thrust faults and folds accommodate about 40 mm/year of NW dextral shear between the Pacific plate on the west and the Sierra Nevada-Great Valley microplate on the east (see Figure 4). Abbreviations: StF = Stanford fault; CF = Cascade fault; MV = Monte Vista fault; SF = Sargent fault; LV = Livermore Valley; ML = Mt. Lewis fault; V = Verona fault; W = Williams fault; PKHF = Pittsburg-Kirby Hills fault.

These southern California earthquakes, as well as the 1989 Loma Prieta earthquake, which occurred on a southwest-dipping reverse-oblique slip fault beneath the Santa Cruz mountains (Bürgmann et al., 1994; Figures 1 and 2), have prompted a reassessment of the hazard from hidden or "blind" thrust faults in the San Francisco Bay area (WGCEP, 1999). This paper summarizes the current state of knowledge regarding thrust faults in the San Francisco Bay area. The paper first discusses the plate tectonic setting of the Bay Area and mechanisms by which active crustal shortening may occur, then reviews discrete areas of localized late Cenozoic uplift and crustal shortening that may be underlain by potentially seismogenic thrust faults. The evidence for active thrust faulting in these areas is summarized, and where sufficient data are available, individual thrust faults are identified and characterized as potential seismic sources. The paper concludes with an assessment of the contribution of thrust faults to regional seismic hazards in the Bay area.

TECTONIC SETTING OF ACTIVE CRUSTAL SHORTENING IN THE SAN FRANCISCO BAY AREA

Previous workers have noted that crustal shortening is a significant component of late Cenozoic deformation in the Bay area (Page, 1982; Aydin, 1982; McLaughlin et al., 1991; Jones et al., 1994; Crane, 1995; Unruh and Lettis, 1998). Crustal shortening is manifested in areas of rugged topography such as the Santa Cruz mountains (Figure 1), the East Bay hills, and the Mt. Diablo region (Figure 3), where young mountains are associated with late Cenozoic folds and thrust faults. The mountainous regions either straddle or are bounded by strike-slip faults of the San Andreas system (Figure 1).

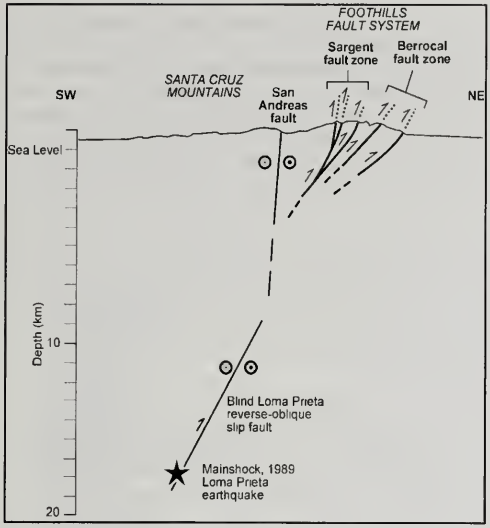

Figure 2. Cross-section across the Santa Cruz mountains showing the blind, southwest-dipping fault that produced the 1989 Loma Prieta earthquake, the surface trace of the San Andreas fault, and thrust faults of the Foothills system (modified from Bürgmann et al., 1994). No vertical exaggeration.

Coeval strike-slip and thrust faulting in the Bay area accommodates relative motion between the Pacific plate and the Sierra Nevada-Great Valley "Sierran" microplate (Figure 4). Although the two plates share a common boundary that passes through the Bay area, the plates are not moving parallel to each other along the boundary. Space-based geodesy indicates that the Sierran microplate has a more westerly direction of motion at this latitude (N57°W) than the average strike of the San Andreas and Hayward faults (N34°W) (Argus and Gordon, 1991). The oblique motion of the Sierran microplate relative to the strike of the San Andreas and Hayward faults results in a net component of convergence across the plate boundary, which is accommodated by both strike-slip and thrust faulting in the Bay area (Figure 4).

The relative importance of these two styles of faulting is controversial. Aydin (1982) compared the style of deformation in the eastern San Francisco Bay area to classic wrench-style tectonism, and concluded that crustal shortening is driven primarily by interactions among the major strike-slip faults of the San Andreas system (Figure 5a). In contrast, Jones et al. (1994) and Crane (1995) argued that large shortening strains are directed normal to the strike-slip faults, such that shortening and thrust faulting occur independently of strike-slip faulting (Figure 5b).

One test of these competing models is to compare the summed geologic slip-rate vectors of known strike-slip faults at a given latitude with the integrated motion across the Pacific-Sierran plate boundary (Kelson et al., 1992). The difference between the deformation accommodated by strike-slip faults and the global motion across the plate boundary places limits on the rate and direction of slip that may occur on unrecognized structures such as blind thrust faults. Vector velocity diagrams in Figure 6 illustrate this approach. The total motion between the Pacific plate and the North American plate is shown as a sum of Pacific-Sierran motion and Sierran-North American motion (Figure 6a). The integrated slip on all active faults in the Bay area accommodates Pacific-Sierran motion, which can be represented as 40 mm/year of right-lateral shear directed toward N31°W (Argus, 1999). The combined motion accommodated by the known active faults across the southern Bay area is shown as a vector sum of their velocities (Figure 6b), based on geologic estimates of slip rates adopted by WGCEP (1999).

The summation of geologic slip rates in Figure 6b shows that, within uncertainty, all of the integrated Pacific-Sierran motion at the latitude of the southern Bay area is accommodated by known strike-slip faults of the San Andreas system. The maximum residual or "available" motion that could be distributed among unrecognized thrust faults is no greater than the uncertainty in the measurements of Pacific-Sierran motion and the fault slip rates (i.e., on the order of a few millimeters per year). This result is consistent with a previous and more comprehensive analysis by Kelson et al. (1992), and appears to preclude the possibility that blind thrust faults, oriented subparallel to the major strike-slip faults and accommodating slip rates in excess of several mm/year, have gone undetected in the Bay area.

As noted by Kelson et al. (1992), blind thrust faults and zones of crustal shortening in the Bay area may be associated with restraining bends and restraining stepovers among strike-slip faults.

Restraining geometries may account for crustal shortening in the Santa Cruz mountains (a left-restraining bend in the San Andreas fault; Bürgmann et al., 1994; Figure 1), the East Bay hills (a restraining stepover between the Calaveras and Hayward strike-slip faults; Aydin, 1982; Figure 3), and the Mt. Diablo-Livermore Valley region (a restraining stepover between the Greenville and Concord strike-slip faults; Unruh and Sawyer, 1995, 1997; Figure 3). In all of these regions, most folds and thrust faults are oblique rather than parallel to the major strike-slip faults (Figures 1 and 3). In the East Bay hills and the Mt. Diablo-Livermore Valley region (Figure 3), the contractional structures exhibit a well-defined, right-stepping, en echelon pattern consistent with classic wrench-style tectonics (Unruh and Lettis, 1998).

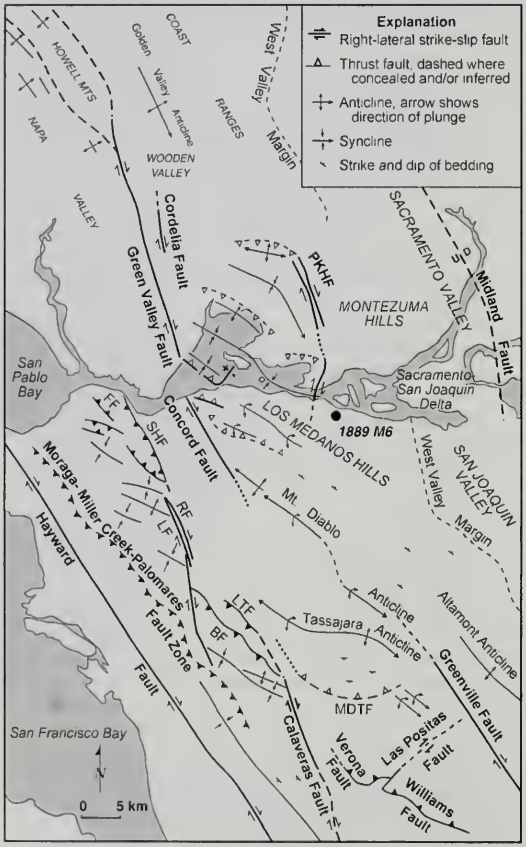

Figure 3. Late Cenozoic strike-slip faults, thrust faults and folds in the eastern San Francisco Bay region. Abbreviations: SHF = Southampton fault; FF = Franklin fault; RF = Reliez Valley fault; LF = Lafayette fault; LTF = Las Trampas thrust fault; BF = Bollinger thrust fault; MDTF = Mt. Diablo thrust fault (blind); PKHF = Pittsburg-Kirby Hills fault. Black dot shows estimated location of 1889 earthquake (Toppozada et al., 1981).

The interpretation that crustal shortening in the Bay area is more directly related to strike-slip kinematics, rather than to regional plate-boundary normal shortening, has several implications for seismic hazard assessment (Unruh and Lettis, 1998):

(1) The association of zones of active crustal shortening with restraining stepovers provides a predictive model for locating and identifying regions that potentially are underlain by seismogenic thrust faults.

(2) Individual thrust faults and folds are constrained in length, and thus seismic potential, by the dimensions of restraining stepover regions between strike-slip faults.

(3) Slip rates on thrust faults in restraining stepovers are more directly related to slip rates on the bounding strike-slip faults, rather than to the component of regional plate motion directed normal to the Pacific-Sierran plate boundary. If this is the case, then slip rates on the thrust faults may be constrained indirectly by evaluating slip rates on the strike-slip faults that border the stepover regions (Unruh and Lettis, 1998).

POTENTIALLY SEISMOGENIC THRUST FAULTS IN THE BAY AREA

The following sections focus on areas of localized Quaternary uplift, mountain building and crustal shortening in the Bay area that may be underlain by seismogenic thrust faults. In several cases, sufficient data are available to identify and characterize discrete thrust faults within these contractional areas as potential seismic sources. Where existing data are not sufficient to identify discrete thrust faults as sources, the contractional area is characterized as an areal source zone for thrust-fault earthquakes.

Northeastern Santa Cruz Mountains

The Santa Cruz Mountains are a rugged, youthful mountain range associated with a left-restraining bend in the San Andreas fault (Figure 1). Quaternary-active thrust faults have been recognized and mapped along the northeastern front of the range by numerous authors including Sorg and McLaughlin, 1975; McLaughlin et al., 1991, 1999; Bürgmann et al., 1994; Hitchcock et al., 1994; Angell et al., 1998; and Hitchcock and Kelson, 1999. A more detailed summary of this work is provided elsewhere in this volume by Fenton and Hitchcock (2001).

The range-front thrust faults, which are referred to collectively as the Foothills system (Bürgmann et al., 1994; Figure 2), include the Stanford fault, Cascade fault, Monte Vista fault and the Sargent fault (Figure 1). Long-term average vertical separation rates across faults of the Foothills system, estimated from offset and deformed fluvial terraces, range from about 0.15 mm/year to 0.4 mm/year (Sorg and McLaughlin, 1975; McLaughlin et al., 1991, 1999; Hitchcock et al., 1994; Angell et al., 1998; Hitchcock and Kelson, 1999). For a reasonable range of fault dips, slip rates to accommodate these shortening and uplift rates would need to be on the order 0.5 ± 0.3 mm/year (WGCEP, 1999). It is thus unlikely that any single fault within the Foothills system has a slip rate in excess of 1 mm/year. Based primarily on fault length, earthquakes ranging in magnitude from M_w6 to M_w7 may occur on the Foothills system, depending on whether the faults rupture individually or multiple fault segments rupture in a single event (WGCEP, 1999).

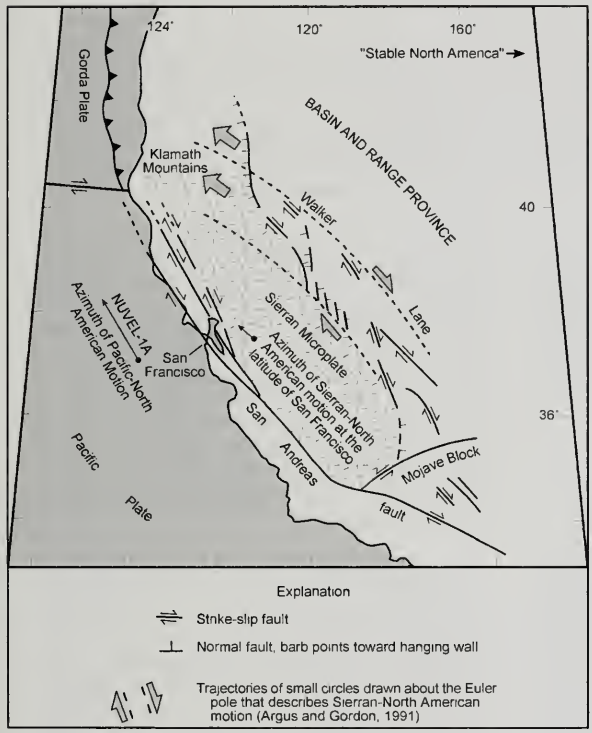

Figure 4. Major lithospheric plate boundaries in California. Black arrows show the motion of the Pacific plate and the Sierran microplate relative to stable North America at the latitude of the Bay area. Curving dashed lines show the trajectory of the Sierran microplate as determined by geodetic observations in eastern California (Argus and Gordon, 1991). Active strike-slip and normal faults in eastern California (i.e., the "Walker Lane") form the eastern tectonic boundary of the Sierran microplate. Note that the motion of the Sierran microplate becomes increasingly oblique to the strike of the San Andreas fault system with increasing latitude.

Cumulative Quaternary displacement on the range-front faults probably includes an unknown amount of aseismic slip. Following the Loma Prieta earthquake, Haugerud and Ellen (1990), Schmidt et al. (1995) and Langenheim et al. (1997) documented surface deformation concentrated along the Foothills thrust system, apparently due to triggered slip that occurred during or after the main shock (Figure 2). Based on analysis and modeling of geodetic data, Bürgmann et al. (1997) concluded that about 10 to 15 cm of transient aseismic creep occurred at depth on these structures following the 1989 earthquake. Given an assumed return period of about 400 years for Loma Prieta-type events, Hitchcock and Kelson (1999) observed that the average "aseismic" slip rate on the Foothills system faults may range from 0.25 to 0.4 mm/year, provided that the magnitude of triggered slip during each event were similar to that observed following the 1989 earthquake. If this estimate were correct, then about 50% or more of the long-term average slip rate for the

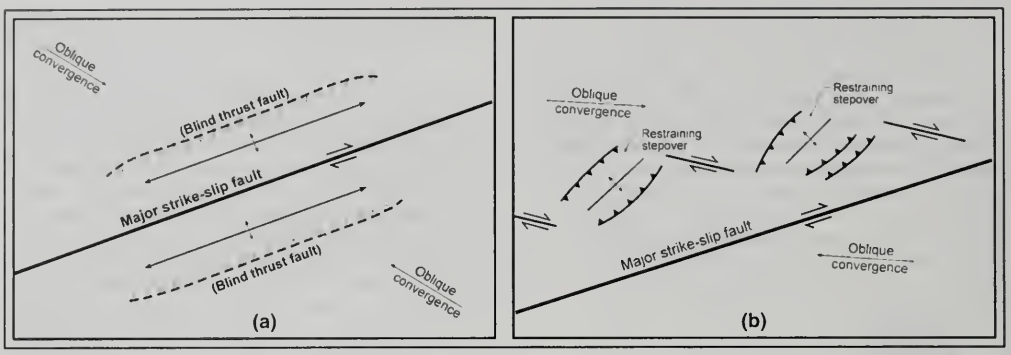

Figure 5. Models for the accommodation of oblique convergence along a transpressional plate boundary. (a) Oblique convergence partitioned onto subparallel strike-slip and thrust faults (i.e., "fault-normal compression"). (b) Oblique convergence distributed among strike-slip faults and thrust faults, with thrust faults primarily forming restraining stepovers among strike-slip faults. Note that neither the major strike-slip fault, nor the strike-slip faults between the stepover regions, are parallel to the direction of oblique convergence. This model is consistent with patterns of faulting in the eastern Bay area (Figure 3) and the vector velocity diagram for integrated fault motion in Figure 6b.

Foothills system would be accommodated by aseismic mechanisms. The implication for seismic hazard studies is that recurrence intervals for the Foothills system calculated directly from long-term average slip rates only constrain the minimum recurrence interval for surface-rupturing earthquakes (Hitchcock and Kelson, 1999).

The East Bay Hills

The East Bay hills constitute a region of youthful, elevated topography between the northern Calaveras and Hayward strike-slip faults (Figure 3). Thrust faults and folds that deform Pliocene-Pleistocene strata (Aydin, 1982; Crane, 1995) evidence late Cenozoic crustal shortening of this region. A report by Geomatrix (1998) documented late Pleistocene to Holocene (?) surface rupture on secondary structures related to the Franklin fault in the northern East Bay hills (Figure 3). Similarly, Wakabayashi and Sawyer (1998) obtained paleoseismic evidence for late Pleistocene to Holocene (?) surface rupture on the Miller Creek reverse-oblique fault in the west-central East Bay hills (Figure 3).

Based on the elevated topography, late Cenozoic folding, and paleoseismic evidence for surface-rupturing earthquakes, active thrust-related seismic sources probably are present within the East Bay hills (WGCEP, 1999). Given the limited number of structural geologic and paleoseismic studies in this region, however, WGCEP (1999) elected to define areal source zones within the East Bay hills rather than assign source characteristics (i.e., maximum earthquake magnitudes and slip rates) to discrete faults. Based on variations in fault and fold geometry, as well as assumptions about the possible distribution of dextral slip north of the termination of the Calaveras fault, WGCEP (1999) divided the East Bay hills into three areal source zones: (1) the western East Bay hills domain, (2) the southern East Bay hills domain, and (3) the northern East Bay hills domain.

The western East Bay hills domain is an elongated northwest-trending region bounded by the dextral Hayward fault on the west and by the Moraga-Miller Creek-Palomares reverse faults on the east (Figure 3). WGCEP (1999) considered two end-member models to explain the observed contractional deformation within this domain (Graymer, 1999). Both models invoke recent work on strain partitioning (Tapponnier et al., 1989; Richard and Cobbald, 1989; Lettis and Hanson, 1991; Teyssier and Tikoff, 1998) and assume that oblique motion on the Hayward fault is partitioned into strike-slip and dip-slip components. In one model (the "aseismic" model), reverse faults of the Moraga-Miller Creek-Palomares zone dip moderately to steeply west and root in the Hayward fault zone at depth. The "aseismic" model assumes that movement on these faults is accommodated primarily by triggered slip and/or

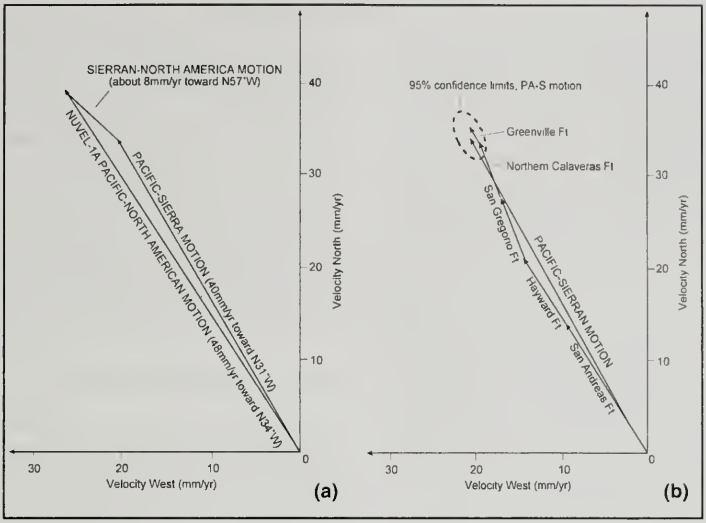

Figure 6. Velocity vector diagrams illustrating tectonic motions in the Bay area. (a) NUVEL-1A Pacific-North American motion at the latitude of the Bay area, expressed as the sum of Pacific-Sierran motion and Sierran-North American motion. Active faults in the Bay area collectively accommodate Pacific-Sierran motion. Note that, relative to North America, the motion of the Sierran microplate is about 20° more westerly than that of the Pacific plate. (b) Example of how combined movement on active strike-slip faults in the southern Bay area accommodates Pacific-Sierran motion. Note that none of the strike-slip faults are parallel to the global direction of dextral shear between the two plates. The dashed ellipse about the tip of the Pacific-Sierran velocity vector represents two-sigma uncertainty in the measured plate motion (Argus, 1999). A similar ellipse can be shown for the combined uncertainties associated with slip rates on the faults, but has been omitted for clarity.

post-seismic relaxation associated with moderate to large magnitude events on the Hayward fault to the west. The second model (the "seismic" model) assumes that the Hayward fault and the Moraga-Miller Creek-Palomares zones are independent seismic sources, each capable of producing earthquakes (Figure 3).

Given the sparse level of knowledge about the paleoseismic behavior of the Moraga-Miller Creek-Palomares system, WGCEP (1999) assigned equal weight to both the "aseismic" and "seismic" models in a probabilistic source characterization. For the "seismic" model, the range of potential earthquake magnitudes was estimated by first assessing the range in potential rupture area of thrust faults in the Moraga-Miller Creek-Palomares zone, then using the empirical relations of Wells and Coppersmith (1994) to estimate associated maximum earthquake magnitudes. Based on the results of this analysis, WGCEP (1999) concluded that earthquake magnitudes ranging from M_W5.5 to M_W6.5 are possible in the western East Bay hills domain, provided that the Moraga-Miller Creek-Palomares faults are independent seismic sources.

The southern East Bay hills domain is the roughly triangular region bounded by the western East Bay hills domain, the northern Calaveras fault on the east, and the Bollinger thrust fault on the north and northeast (WGCEP, 1999; Figure 3). The maximum length of mapped thrust faults within the southern East Bay hills is about 15 km, which WGCEP (1999) assumed to constrain the maximum potential rupture length for a thrust fault source in this zone. If it is assumed that the base of seismicity

is about 15 km in this region (Oppenheimer and Macgregor-Scott, 1992), and if it is assumed that the dip of seismogenic faults ranges between 30° and 45°, then simple geometric constraints placed on maximum source dimensions by the size and shape of the southern East Bay hills domain would limit rupture width to a maximum of about 21 km. The corresponding maximum earthquake magnitudes for this domain range between about M_W6.3 and M_W6.5 from regressions on magnitude versus rupture area (Wells and Coppersmith, 1994).

The northern East Bay hills domain lies north of the Bollinger fault and east of the western East Bay hills domain. Major thrust faults and reverse-oblique slip faults mapped in the northern East Bay hills include the Franklin fault and the Southhampton fault (Crane, 1995; Figure 3). Contractional deformation in the northern East Bay hills domain may be driven, in part, by transfer of dextral shear from the northern Calaveras fault westward to structures in the interior of this domain. This model was originally proposed in somewhat different form by Aydin (1982). For example, the Las Trampas and Bollinger thrust faults appear to form a restraining stepover between the northern Calaveras fault and the Lafayette and Reliez Valley strike-slip faults (Figure 3). Dextral slip on the Lafayette and Reliez Valley faults may in turn step northward onto the Franklin and Southhampton faults, or it may be consumed in the formation of west-northwest-trending folds directly to the west (Figure 3). Displaced stratigraphic contacts mapped by Crane (1995) indicate that several kilometers of dextral offset have been accommodated by the Lafayette and Reliez Valley faults. If all of this deformation has occurred in the past several million years, then strike-slip faults and associated thrust faults in the northern East Bay hills may have slip rates approaching 1 to 2 mm/year. Additional studies are required to fully evaluate the distribution, style and rate of deformation in the northern East Bay hills domain.

There are few constraints on the rate of horizontal shortening and surface uplift in the East Bay hills with which to estimate slip rates on blind thrust faults. Estimates of uplift rates for the southern and western East Bay hills from tectonic-geomorphic studies (Kelson and Simpson, 1995; Graymer, 1999) and geodetic leveling surveys (Gilmore, 1992), range between about 0.1 to 2.0 mm/year. If it is assumed that the surface uplift is accommodated by slip on thrust faults that dip 30° to 45°, then the corresponding range of slip rates on individual thrust faults necessary to generate the estimated uplift rates would be about 0.2 to 2.5 mm/year. WGCEP (1999) regarded the high values in this range as suspect, based on the observation that the average elevation and relief of the East Bay hills are less than that of the Santa Cruz mountains, which probably are rising at a long-term average rate of about 1.0 mm/year (Bürgmann et al., 1994). The order-of-magnitude range in estimated uplift rates clearly attests to uncertainty in the present state of knowledge regarding rates of tectonic activity in the East Bay hills; maximum thrust-fault slip rates in this region may be as high as 2 to 3 mm/year, but the true rates are probably lower.

Mt. Diablo fold-and-thrust belt

Mt. Diablo anticline is associated with a belt of late Cenozoic folds and thrust faults, collectively referred to as the "Mt. Diablo fold-and-thrust belt" (Crane, 1995; Unruh and Sawyer, 1995; 1997), that can be traced continuously for about 70 km from the northern Diablo Range to the western Sacramento-San Joaquin delta (Figures 1 and 3). Contractional structures within this belt are oriented WNW-ESE, exhibit a well-defined right-stepping *en echelon* pattern, and are bounded by the dextral Greenville fault to the southeast and the dextral Concord fault to the northwest (Figure 3). Unruh and Sawyer (1995; 1997) concluded that crustal shortening within this belt is driven primarily by a restraining transfer of dextral slip from the Greenville fault to the Concord fault. Based on analysis of stratigraphic, structural, geomorphic, and seismicity relations, Unruh and Sawyer (1997) identified and characterized several structures within the Mt. Diablo fold-and-thrust belt as potential seismic sources. From south to north, these structures include the Verona thrust fault, the Mt. Diablo thrust fault (blind), and the Los Medanos Hills thrust fault (Figure 3).

The Verona fault strikes northwest, dips northeast, and is approximately 7 to 9 km long. Field observations and exploratory trenching described by Herd and Brabb (1980) provide convincing evidence of late Quaternary surface-rupturing events on the fault. If it is assumed that the rupture length is equivalent to the length of the surface trace of the fault and that the rupture width is comparable to the rupture length (i.e., a 1:1 rupture aspect ratio; Nicol et al., 1996), then the Verona fault may be capable of generating M_W5.7 to M_W5.9 earthquakes (per Wells and Coppersmith, 1994). The only pub-

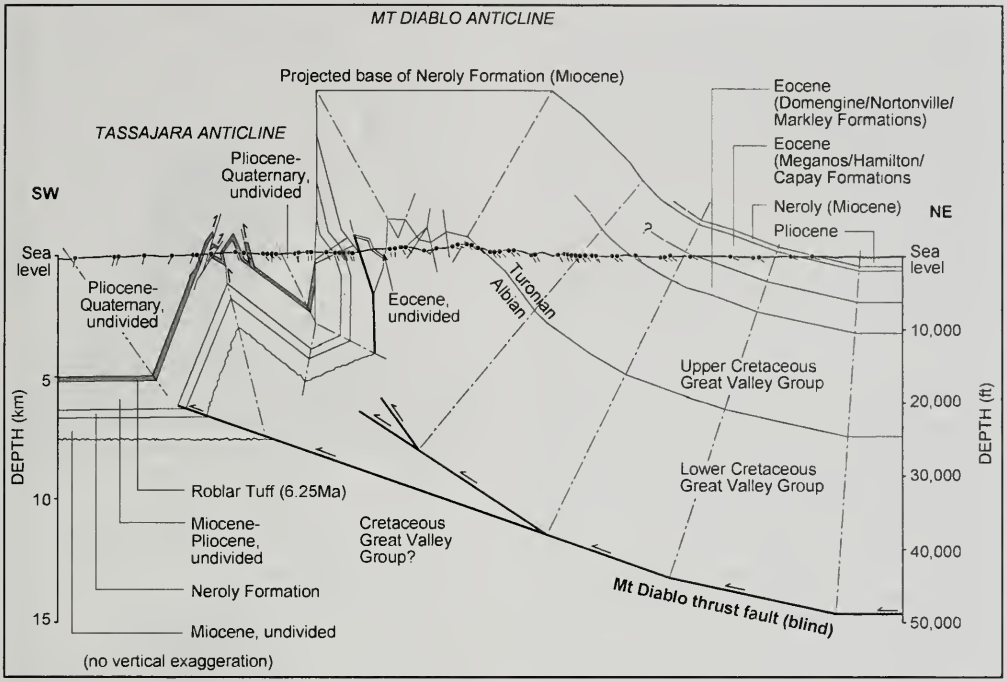

Figure 7. Geologic cross-section across the Mt. Diablo and Tassajara anticlines. The anticlines are interpreted to be asymmetric, southwest-vergent fault-propagation folds developed above the blind, northeast-dipping Mt. Diablo thrust fault. Figure modified from Unruh and Sawyer (1997).

lished estimate of slip rate on the Verona fault is in an abstract by Jahns and Harding (1982), which cites "offset horizons and marker units in a complex soil-stratigraphic section" as evidence for an average slip rate of 0.12 mm/year for the entire fault zone during the past 100,000 years. The Verona fault is separated from the northwest-striking, northeast-dipping Williams thrust fault by the northeast-striking Las Positas fault (Figure 3), which accommodated minor left-lateral triggered slip during the 1980 Livermore earthquake sequence (Bonilla et al., 1980). Although the Williams and Verona thrust faults have a common orientation, and possibly are linked at depth, independent data on the Quaternary activity of the Williams fault is not currently available.

The blind Mt. Diablo thrust fault is interpreted to underlie the asymmetric, southwest-vergent Mt. Diablo and Tassajara anticlines (Crane, 1995; Unruh and Sawyer, 1995; 1997; Figures 3 and 7). Based on estimates of the potential rupture area from construction of balanced cross sections, and from comparisons of the dimensions of the Mt. Diablo anticline to folds overlying the sources of the 1983 Coalinga and 1994 Northridge earthquakes (Figure 8), Unruh and Sawyer (1997) estimated that this structure may produce M_w 6.25 to M_w 6.75 earthquakes. The maximum magnitude in this range assumes that a continuous fault underlies the entire anticline and ruptures in a single event (Figure 8). The lower end of the magnitude range is intended to account for uncertainty regarding the presence of lateral ramps or tear faults that may subdivide the Mt. Diablo thrust fault into two or more discrete rupture segments (Unruh and Sawyer, 1997).

Balanced cross-sections provide a basis for evaluating a range of slip rates for the blind thrust fault beneath Mt. Diablo anticline (Figure 7). For the

range of values in horizontal shortening, fault dip and timing of deformation summarized in Unruh and Sawyer (1997), the minimum slip rate on the blind Mt. Diablo thrust fault would be about 1.3 mm/year (10 km total shortening; 30° fault dip; 9 Ma onset of shortening), and the maximum slip rate would be 7 mm/year (17 km total shortening; 45° fault dip; 3.4 Ma onset of shortening). Based on available data, WGCEP (1999) favored a long-term average slip rate in the range of 1 to 3 mm/year for the Mt. Diablo thrust fault. More recent and ongoing studies have focused on evaluating late Pleistocene and Holocene uplift and shortening rates in the Mt. Diablo fold-and-thrust belt (Sawyer, 1999).

The Los Medanos Hills thrust fault is interpreted to underlie the asymmetric, southwest-vergent Los Medanos Hills and Concord anticlines (Figures 2 and 3), analogous to the relationship between the Mt. Diablo thrust fault and the overlying Mt. Diablo and Tassajara anticlines to the south. Based on an estimate of potential rupture area from fold length and down-dip fault width from cross sections, Unruh and Sawyer (1997) estimated a maximum earthquake magnitude of M_w 6 for the Los Medanos thrust fault, and a long-term average slip rate of 0.3 to 0.7 mm/year.

Sacramento-San Joaquin Delta region

The pattern of right-stepping, *en echelon* anticlines that characterizes the Mt. Diablo fold-and-thrust belt continues north of the Los Medanos Hills anticline into the western Sacramento-San Joaquin Delta region (Figure 3). This region is a persistent source of small earthquakes (Ellsworth et al., 1982; Weber-Band, 1998), and historical accounts indicate that a moderate magnitude earthquake occurred near the town of Antioch in 1889 (Toppozada et al., 1981; Figure 3). Recent studies of the structure in this region by Weber-Band (1998) and Unruh and Hector (1999) identified several Quaternary faults.

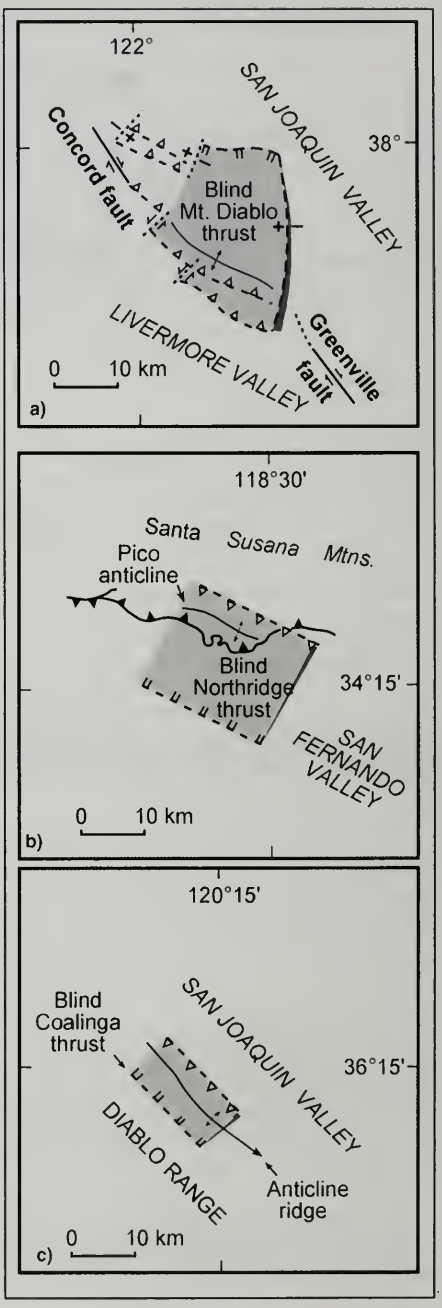

Figure 8. Plan-view maps showing dimensions of (a) the blind Mt. Diablo thrust fault (derived from data and analysis in Unruh and Sawyer, 1997), and the dimensions of the thrust faults that produced the (b) 1994 Northridge and (c) 1983 Coalinga earthquakes. All maps are plotted at the same scale to facilitate comparison. The interpreted size of the Mt. Diablo thrust fault is closer to that of the Northridge thrust fault (M6.7) than the Coalinga thrust fault (M6.2).

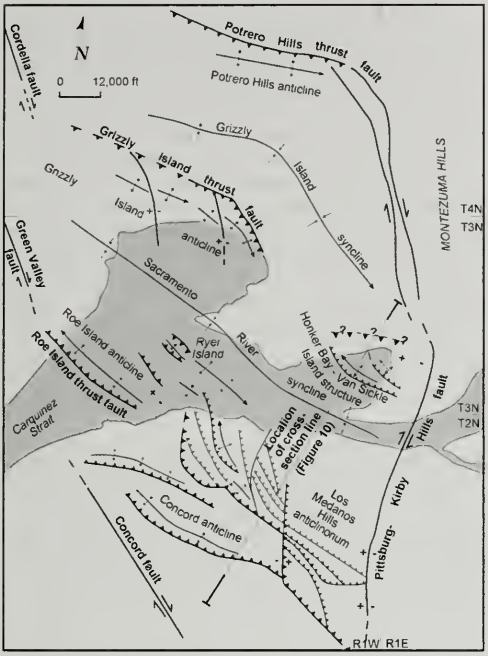

Figure 9. Late Cenozoic strike-slip faults, folds, and thrust faults in the western Sacramento-San Joaquin Delta region (modified from Unruh and Hector, 1999 and Hoffman, 1992). Note that the folds and thrust faults exhibit a right-stepping *en echelon* geometry and are oblique to strike-slip faults along the eastern and western borders of the map area. The Pittsburg-Kirby Hills fault forms the eastern tectonic boundary of this contractional domain and accommodates differential north-south shortening between the western and eastern areas of the Delta.

These structures include the Roe Island thrust fault, Potrero Hills thrust fault, Pittsburg-Kirby Hills fault zone, and the Midland fault (Figures 3 and 9).

The Roe Island thrust fault underlies the asymmetric, southwest-vergent Roe Island anticline in Suisun Bay, northwest of the Los Medanos Hills anticline (Figure 9). The vergence and asymmetry of the fold are well-documented by gas exploration efforts, and proprietary seismic reflection profiles appear to image reflections from a northeast-dipping thrust fault beneath the fold (Unruh and Hector, 1999). Based on an estimate of potential rupture area from fold length and down-dip fault width from cross sections, maximum earthquake magnitudes for this structure could range between M_W 5.5 to M_W 6.0 (WLA, 1999). The long-term average slip rate on the Roe Island thrust fault, estimated from horizontal shortening rates and deformed late Cenozoic stratigraphic markers visible in proprietary seismic reflection profiles, is about 0.3 to 0.7 mm/year (WLA, 1999).

North of the Los Medanos Hills and Roe Island anticlines, asymmetric folds in the western Delta region typically verge northeast to north-northeast such as Grizzly Island and Potrero Hills anticline (Figure 9). Based on construction of structure contour maps and analysis of seismic reflection profiles, Unruh and Hector (1999) interpreted that the Grizzly Island anticline and Honker Van Sickle Island anticlinorium (Figure 9) are fault-propagation folds underlain by southwest-dipping thrust faults. Downdip projection of these thrust faults indicates that they probably intersect the northeast-dipping Roe Island and Los Medanos Hills thrust faults in the upper 6 km (Figure 10). Because the amplitudes of the Grizzly Island and Honker Van Sickle structures are significantly less than those of the Roe Island and Los Medanos Hills anticlines, Unruh and Hector (1999) concluded that the southwest-dipping thrust faults are second-order structures that either splay into the northeast-dipping thrust faults or are rooted at shallow depths (Figure 10). Based on the interpretation that the southwest-dipping thrust faults beneath the Grizzly Island and Honker Van Sickle structures probably do not extend below about 6 km depth, WGCEP (1999) did not characterize them as independent seismic sources of moderate to large earthquakes.

The Potrero Hills thrust fault is interpreted to underlie the asymmetric, north-vergent Potrero Hills anticline in the south Fairfield area (Unruh and Hector, 1999; Figure 9). Minimum length of the anticline is 9 km. The fold and underlying south-dipping thrust fault are well documented at shallow depths by gas exploration well data (Unruh and Hector, 1999), but the down-dip geometry of the thrust fault is very uncertain. Based on estimates of potential rupture area, maximum earthquake magnitudes for this structure may range between M_W 5.75 to M_W 6.25 (WLA, 1999). The long-term average slip rate on the Potrero Hills thrust fault, based on horizontal shortening rates from balanced cross sections and stratigraphic relations, ranges from about 0.1 mm/year to 0.6 mm/year (WLA, 1999).

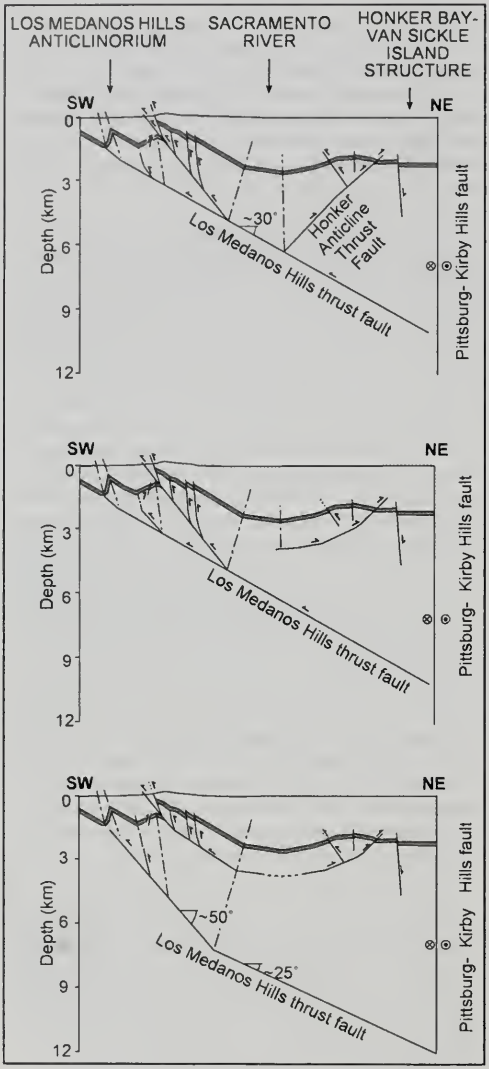

Figure 10. Kinematic models of the relationship between the northeast-dipping Los Medanos Hills thrust fault and the south-dipping thrust fault(s) beneath the Honker Bay-Van Sickle Island structure (modified from Unruh and Hector, 1999). The gray marker horizon is the Eocene Nortonville shale. The northeast-dipping thrust fault beneath the Los Medanos Hills anticline is interpreted to extend to depths of 10 km or greater, and thus may have sufficient rupture area to produce a moderate earthquake. In contrast, the antithetic thrust fault beneath the Honker Bay-Van Sickle Island structure is interpreted to be a second-order feature that does not extend to significant depths, and thus probably is not an independent source of moderate earthquakes. A similar relationship is inferred to exist between the northeast-dipping Roe Island thrust fault and the antithetic Grizzly Island thrust fault, both of which are located to the northwest of this cross section (Figure 9).

The NNE-striking Pittsburg-Kirby Hills fault can be traced from the town of Pittsburg northward through the Kirby Hills to the eastern end of the Potrero Hills anticline (Figures 3 and 9). Minimum length of the fault is 20 km. The mapped trace of the Pittsburg-Kirby Hills fault is associated with a north-northwest-trending alignment of small earthquakes in the western Delta region (McCarthy et al., 1994). However, Weber-Band (1998) argued that the epicenters are associated with a deep (18 to 22 km) seismic source zone that may not be associated with the surface trace of the Pittsburg-Kirby Hills fault. WGCEP (1999) thus considered two models for the Pittsburg-Kirby Hills fault as a potential seismic source:

(1) The Pittsburg-Kirby Hills fault is a subvertical strike-slip fault that accommodates differential NNE-SSW shortening and distributed dextral shear across the Delta region (Hector and Unruh, 1992; McCarthy et al., 1994; Unruh and Hector, 1999).

(2) The fault dips steeply east, possibly soling into the Midland fault (Figure 3) at depth. In this model, the fault formed in early Tertiary time as a normal fault, and currently is active as a reverse-oblique fault to accommodate uplift of the western Montezuma Hills (Weber-Band, 1998).

WGCEP (1999) estimated that the maximum earthquake on the Pittsburg-Kirby Hills fault may range between M_w6 and M_w7, and that the long-term average slip rate is about 0.1 to 0.7 mm/year. This range in magnitudes and slip rates encompasses both the strike-slip and thrust fault models described above, as well as uncertainty in geometric and structural segmentation of the fault that may limit rupture length.

The Midland fault is a west-dipping fault along the eastern margin of the Montezuma Hills (Figure 3) that accommodated extension and subsidence in the early Tertiary Sacramento Valley basin (Krug

et al., 1992). Seismic reflection profiles across the structure suggest that the fault has a downward-flattening or listric geometry (Weber-Band, 1998). Based on detailed analysis of seismic reflection data, Weber-Band (1998) documented late Cenozoic reactivation of the Midland fault to accommodate reverse slip and horizontal crustal shortening. The data presented by Weber-Band (1998) strongly imply that late Cenozoic uplift of the eastern Montezuma Hills can be attributed to movement on the Midland fault. WGCEP (1999) concluded that the Midland fault may be capable of generating M_W6 to M_W6.5 earthquakes, and that the long-term average slip rate on the fault probably ranges between 0.1 mm/year to 0.5 mm/year.

Howell Mountains

The Howell Mountains border eastern Napa Valley and are bounded on the southeast by the northern end of the Green Valley fault (Figures 1 and 3). Baldwin et al. (1998) investigated a series of folds and thrust faults in the Howell Mountains that deform the Pliocene Sonoma volcanics. In particular, fold limbs are very well-expressed topographically as dip slopes and "fold scarps". Contractional deformation in this region may be driven by a restraining transfer of some dextral slip from the Green Valley fault to the Sulphur Springs thrust fault and other thrust faults that form a contractional horsetail splay at the southern end of the Maacama strike-slip fault (Figure 1).

Based on a geometric analysis of the folds, Baldwin et al. (1998) suggested that the Howell Mountains may be underlain by one or more northeast-dipping blind thrust faults that collectively have accommodated about 2 to 3 km of horizontal shortening since deposition of the Sonoma volcanics, which have whole rock K-Ar ages of 2.9 Ma to 8 Ma in the northern Coast Ranges (Fox, 1983). The younger ages in this range (about 2.9 Ma) were obtained from rocks in the vicinity of the Howell Mountains. For the full range in ages of the Sonoma volcanics, the horizontal NE-SW shortening rate ranges between about 0.4 to 1.0 mm/year. If all of this shortening is accommodated by slip on a single blind thrust fault dipping 30° to 45°, then the extreme range in slip rates is from 0.5 mm/year to about 1.4 mm/year. Based primarily on the length of late Cenozoic folds and neotectonic lineament zones, Baldwin et al. (1998) concluded that potential thrust-fault sources of M_W6.25 and M_W6.5 earthquakes may be present in the Howell Mountains.

SUMMARY AND DISCUSSION

This review of late Cenozoic thrust faults and patterns of crustal shortening in the San Francisco Bay area prompts the following observations:

1) In nearly all of the examples discussed above, potentially seismogenic thrust faults and areal source zones of thrust-fault earthquakes are related to restraining bends and restraining stepovers among strike-slip faults of the San Andreas system. The folds and thrust faults are oblique rather than subparallel to the strike-slip faults, and thus do not appear to be accommodating shortening directed normal to the strike-slip faults (i.e., Figure 5a), as proposed for large areas of western California by Zoback et al. (1987). The best potential example of partitioning of oblique convergence onto subparallel strike-slip and thrust faults in the Bay area appears to be the Hayward fault and the Moraga-Miller Creek-Palomares faults in the western East Bay hills (Figure 3).

2) The maximum magnitude estimated for earthquakes on known or suspected thrust faults in the Bay area is M_W7. This value is associated with a multiple fault-segment rupture in the Foothills thrust belt, to which WGCEP (1999) assigned a low probability. The majority of maximum magnitude estimates for thrust faults in the Bay area ranges between M_W5.5 and M_W6.5.

3) In general, slip rates on individual thrust faults, and average shortening and uplift rates for contractional source zones, are on the order of tenths of a millimeter per year to a maximum of about 1 to 2 mm/year. The thrust fault with the highest estimated slip rate in the Bay Area is the Mt. Diablo thrust fault, which may have a slip rate of 1 to 3 mm/year. The Mt. Diablo thrust fault also is associated with the most dramatic topographic feature in the eastern Bay region - Mt. Diablo. Given this correlation between a relatively active thrust fault and tectonic topography, it is very unlikely that blind thrust faults with comparable slip rates remain undiscovered in the Bay area.

4) For the range of slip rates cited above, the average return periods for moderate magnitude events that release about 0.5 to 1.0 m of accumulated slip may range from 500 to 1,000 years (slip rate = 1.0 mm/year) to 2,500-5,000 years (slip rate = 0.2 mm/year). Return periods for moderate to large magnitude earthquakes that release about 1.5 to 2.0

m of accumulated slip are probably between 1,500 to 2,000 years (slip rate = 1.0 mm/year) and 7,500 to 10,000 years (slip rate = 0.2 mm/year).

Thrust faults in the Bay area appear to be subordinate to strike-slip faults of the San Andreas system in terms of overall contribution to regional seismic hazard. WGCEP (1999) found no evidence that thrust faults are capable of generating earthquakes as large, or as frequently, as the major strike-slip faults. However, because thrust faults and contractional source zones primarily are located in areas bounded by strike-slip faults, they may contribute significantly to the occurrence of "background" or "floating" earthquakes such as moderate magnitude events that do not occur on previously identified and well-characterized faults.

To estimate the average recurrence of thrust-fault earthquakes in the Bay area, one can consider a "background" source model that: (a) assumes that the average slip rate of blind thrust faults is about 0.5 mm/year, (b) assumes that the average thrust-fault earthquake releases about 1.0 m of accumulated slip, and (c) assumes that there are at least 12 thrust-fault sources distributed throughout the Bay area. These assumptions are consistent with observations discussed in this paper. On the average, each thrust fault might produce an earthquake within a 2,000-year period; if there are 12 such faults, then there will be 12 thrust-fault earthquakes in a 2,000-year period. This model thus predicts that, on the average, at least one moderate thrust-fault earthquake is likely to occur in a 167-year period in the Bay area. At least two potentially thrust-related earthquakes are documented by Toppozada et al. (1981) during the last 150 years: the M6 1889 Antioch earthquake, which occurred in the vicinity of the Pittsburg-Kirby Hills fault and structures of the western Delta region (Figure 3), and the M5.5 1891 earthquake, which occurred in the southern Napa Valley area (Figure 3). Both of these events are spatially associated with contractional source zones even though their sources were not confidently identified.

Although the contribution of thrust faults to regional hazard is low, they may be significant local sources of strong ground shaking in deterministic evaluations of seismic hazard, especially for urbanized regions, such as Silicon Valley and Livermore Valley, that are adjacent to contractional source zones (i.e., northeast Santa Cruz mountains and the Mt. Diablo fold-and-thrust belt, respectively). The 1987 Whittier Narrows and 1994 Northridge earthquakes in southern California, which occurred on blind thrust faults beneath urbanized regions, may be analogs for scenario thrust-fault earthquakes in the Bay area.

ACKNOWLEDGMENTS

This paper is based on the conclusions of the Thrust Fault subgroup of the 1999 Working Group on Northern California Earthquake Probabilities. Participants in the Thrust Fault Subgroup included Michael Angell (Geomatrix Consultants), Roland Bürgmann (University of California, Berkeley), Trevor Dumitru (Stanford University), Russell Graymer (U.S. Geological Survey), James Hengesh (Dames & Moore), George Hilley (Arizona State University), Christopher Hitchcock (William Lettis & Associates, Inc.), Robert Jachens (U.S. Geological Survey), Angela Jayko (U.S. Geological Survey), Robert McLaughlin (U.S. Geological Survey), Fabian Schonenberg (PartnerRe Services, Zurich, Switzerland), John Wakabayashi (Independent), Janine Weber-Band (Exponent - Failure Analysis Associates), Colin Williams (U.S. Geological Survey), Patrick Williams (University of California, Berkeley), Ivan Wong (Woodward-Clyde URS-Greiner), and Mary Lou Zoback (U.S. Geological Survey). Conversations with William Lettis and David Schwartz contributed significantly to the synthesis of data and seismic source characterization developed by the Thrust Fault subgroup. This paper was improved by constructive reviews from Eldridge Moores, Roland Bürgmann, Horacio Ferriz and Steve Stryker. Some of the research described in this paper was supported by U.S. Geological Survey National Earthquake Hazard Reduction Program grants to William Lettis & Associates (award numbers 1434-95-G-2611; 1424-HQ-96-GR-02738; 1434-HQ-96-GR-03146; 1434-HQ-96-GR-02724; 99-HQ-GR-0069). The views and conclusions contained in this paper are those of the author and should not be interpreted as necessarily representing the official policies, either expressed or implied, of the U.S. Government.

AUTHOR PROFILE

Dr. Unruh, Senior Geologist with William Lettis & Associates, Inc., is a Registered Geologist with over 14 years of research and professional experience in characterizing tectonically-active areas of the western United States. His specialties include seismic hazard assessment, structural geology, seis-

motectonics, Quaternary geology, geomorphology, and geophysics. Dr. Unruh also has a position as a Research Geologist at the University of California, Davis, and teaches part of UCD's Summer Field geology program.

SELECTED REFERENCES

Angell, M., Crampton, T., 1996, Quaternary contractional faulting and folding northeast of the San Andreas fault, Portola Valley-Palo Alto, California: U.S. Geological Survey Open-File Report 96-267, p. 51-64.

Angell, M., Hanson, K., Crampton, T., 1998, Characterization of Quaternary contractional deformation adjacent to the San Andreas fault, Palo Alto, California: Technical report submitted to U.S. Geological Survey, Award No. 1434-95-G-2586.

Argus, D.F., 1999, written communication.

Argus, D.F., and Gordon, R.G., 1991, Current Sierra Nevada-North American motion from very long baseline interferometry: Implications for the kinematics of the western United States: Geology, v. 19, p. 1085-1088.

Aydin, A., 1982, The East Bay hills, a compressional domain resulting from interaction between the Calaveras and Hayward-Rogers Creek faults: California Division of Mines and Geology Special Publication 62, p. 11-21.

Baldwin, J.N., Unruh, J.R., and Lettis, W.R., 1998, Neotectonic investigation of the northward extension of the Green Valley fault, Napa County, California: Technical report submitted to the U.S. Geological Survey, National Earthquake Hazards Reduction Program Award No. 1434-HQ-96-GR-02738, 27 p. plus maps.

Bonilla, M.G., Lienkaemper, J., and Tinsley, J.C., 1980, Surface faulting near Livermore, California, associated with the January 1980 earthquakes: U.S. Geological Survey Open-File Report 80-523, 27 p.

Bürgmann, R., Arrowsmith, R., Dumitru, T., and McLaughlin, R., 1994, Rise and fall of the Southern Santa Cruz Mountains, California, from fission tracks, geomorphology, and geodesy: Journal of Geophysical Research, v. 99, no. B10, p. 20,181-20,202.

Bürgmann, R., Segall, P., Lisowski, M., and Svarc, J., 1997, Postseismic strain following the 1989 Loma Prieta earthquake from GPS and leveling measurements: Journal of Geophysical Research, v. 102, p. 4,933-4,955.

Crane, R.C., 1995, Structural geology of the East Bay hills: in Sangines, E.M., Andersen, D.W., and Buising, A.V. (eds.), Recent geologic studies in the San Francisco Bay area: Pacific Section, Society of Economic Paleontologists and Mineralogists, v. 76, p. 87-114.

DeMets, C., Gordon, R.G., Argus, D.F., and Stein, S., 1994, Effect of recent revisions to the geomagnetic reversal time scale on estimate of current plate motions: Geophysical Research Letters, v. 21, no. 20, p. 2,191-2,194.

Ellsworth, W.L., Olson, J.A., Shijo, L.N., and Marks, S.M., 1982, Seismicity and active faults in the eastern San Francisco Bay region: California Division of Mines and Geology Special Publication 62, p. 83-91.

Fox, K., 1983, Tectonic setting of late Miocene, Pliocene, and Pleistocene rocks in part of the Coast Ranges north of San Francisco, California: U.S. Geological Survey Professional Paper 1239, 33 p.

Geomatrix Consultants, 1998, Walnut Creek water treatment plant expansion seismic study-Phase II: Consultant's report to the East Bay Municipal Utilities District, Oakland, California, 57 p. plus appendices.

Gilmore, T.D., 1992, Historical uplift measured across the eastern San Francisco Bay region: California Division of Mines and Geology Special Publication 113, p. 55-62.

Graymer, R., 1999, Written communication to Working Group on California Earthquake Probabilities.

Haugerud, R.A., and Ellen, S.D., 1990, Coseismic ground deformation along the northeast margin of the Santa Cruz Mountains: in Schwartz, D.P., and Ponti, D.J. (eds.), Field guide to neotectonics of the San Andreas fault system, Santa Cruz Mountains: U.S. Geological Survey Open-File Report 90-274, p. 32-37.

Hector, S. and Unruh, J., 1992, Late Cenozoic blind thrusting and transpressional kinematics, Potrero Hills region, Sacramento-San Joaquin Delta, California: in Cherven, V.B., and Edmondson, W.F. (eds.), The Structural Geology of the Sacramento Basin: Annual Meeting, Pacific Section, American Association of Petroleum Geologists, v. MP-41, p. 155.

Herd, D.G., and Brabb, E.E., 1980, Faults at the General Electric test reactor site, Vallecitos Nuclear Center, Pleasanton, California: A summary review of their geometry, age of last movement, recurrence, origin, and tectonic setting and the age of the Livermore Gravels: U.S. Geological Survey Administrative Report, 77 p.

Hitchcock, C.S., Kelson, K.I., and Thompson, S.C., 1994, Geomorphic investigations of deformation along the northeastern margin of the Santa Cruz Mountains: U.S. Geological Survey Open-File Report 94-187, 52 p.

Hitchcock, C.S., and Kelson, K.I., 1999, Growth of late Quaternary folds in southwest Santa Clara Valley, San Francisco Bay area, California: Implications of "triggered slip" for seismic hazard and earthquake recurrence: Geology, v. 26, p. 391-394.

Hoffman, R.D., 1992, Structural geology of the Concord area: in Cherven, V.B., and Edmondson, W.F. (eds.), The Structural Geology of the Sacramento Basin: Annual Meeting, Pacific Section, American Association of Petroleum Geologists, v. MP-41, p. 79-90.

Jahns, R.H., and Harding, R.C., 1982, Evaluation of the inferred Verona fault in Vallecitos Valley, California: California Division of Mines and Geology Special Publication 62, p. 185.

Jones, D.L., Graymer, R., Wang, C., McEvilly, T.V., and Lomax, A., 1994, Neogene transpressive evolution of the California Coast Ranges: Tectonics, v. 13, p. 561-574.

Kelson, K.I., Lettis, W.R., and Lisowski, M., 1992, Distribution of geologic slip and creep along faults in the San Francisco Bay region: California Division of Mines and Geology Special Publication 113, p. 31-38.

Kelson, K.I., and Simpson, G.D., 1995, Late Quaternary deformation of the southern East Bay Hills, Alameda County, California: Abstract in American Association of Petroleum Geologist Bulletin, v. 79, p. 39.

Krug, E.H., Cherven, V.B., Hatten, C.W., and Roth, J.C., 1992, Subsurface structure in the Montezuma Hills, southwestern Sacramento basin: in Cherven, V.B., and Edmondson, W.F. (eds.), Structural Geology of the Sacramento Basin: Annual Meeting, Pacific Section, Society of Economic Paleontologists and Mineralogists, v. MP-41, p. 41-60.

Langenheim, V.E., Schmidt, K.M., and Jachens, R.C., 1997, Coseismic deformation during the 1989 Loma Prieta earthquake and range-front thrusting along the southwestern margin of the Santa Clara Valley, California: Geology, v. 25, p. 1091-1094

Lettis, W.R., and Hanson, K.L., 1991, Crustal strain partitioning: Implications for seismic hazard assessment in western California: Geology, v. 19, p. 559-562.

Lettis, W.R., Wells, D.L., and Baldwin, J.N., 1997, Empirical observations regarding reverse earthquakes, blind thrust faults and Quaternary deformation: Are blind thrust faults truly blind?: Bulletin of the Seismological Society of America, v. 87, p. 1171-1198.

McCarthy, J., Hart, P.E., Anima, R., Oppenheimer, D., and Parsons, T., 1994, Seismic evidence for faulting in the western Sacramento Delta region: EOS (Transactions of the American Geophysical Union), v. 75, p. 684.

McLaughlin, R.J., Clark, J.C., Brabb, E.E., and Helley, E.J., 1991, Geologic map and structure sections of the Los Gatos 7.5' quadrangle, Santa Clara and Santa Cruz Counties, California: U.S. Geological Survey Open-File Report 91-593, 45 p., scale 1:24,000.

McLaughlin, R.J., Langenheim, V.E., Schmidt, K.M., Jachens, R.C., Standley, R.G., Jayko, A.S., McDougall, K.A., Tinsley, J.S., and Valin, Z.C., 1999, Neogene contraction between the San Andreas fault and the Santa Clara Valley, San Francisco Bay Region, California: International Geology Review, v. 41, p. 1-30.

Nicol, A., Watterson, J., Walsh, J.J., and Childs, C., 1996, The shapes, major axis orientations and displacement patterns of fault surfaces: Journal of Structural Geology, v. 18, p. 235-248.

Oppenheimer, D.H., and Macgregor-Scott, N., 1992, The seismotectonics of the eastern San Francisco Bay region: California Division of Mines and Geology Special Publication 113, p. 11-16.

Page, B.M., 1982, The Calaveras fault zone of California-an active plate boundary element: California Division of Mines and Geology Special Publication 62, p. 175-184.

Richard, R., and Cobbald, P.R., 1989, Mechanical reasons for partitioning of fault motions in continental convergent wrench zones: Abstract in International Workshop on Active and Recent Strike-Slip Tectonics, Florence, Italy, April 18-20, 1989.

Sawyer, T.L., 1999, Assessment of contractional deformation rates of the Mt. Diablo fold and thrust belt, eastern San Francisco Bay region, northern California: Technical report submitted to the U.S. Geological Survey National Earthquake Hazards Reduction Program, Award number 98-HQ-GR-1006, 53 p. plus maps.

Schmidt, K.M., Ellen, S.D., Haugerud, R.A., Peterson, D.M., and Phelps, G.A., 1995, Breaks in pavement and pipes as indicators of range-front faulting resulting from the 1989 Loma Prieta earthquake near the southwest margin of the Santa Clara Valley, California: U.S. Geological Survey Open-File Report 95-820, 33 p.

Sorg, D.H., and McLaughlin, R.J., 1975, Geologic map of the Sargent-Berrocal fault zone between Los Gatos and Los Altos Hills, Santa Clara County, California: U.S. Geological Survey Map MF-643, scale 1:24,000.

Tapponnier, P., Armijo, R., and Lacassin, R., 1989, Fault bifurcation and partition of strike-slip and dip-slip of mechanical interfaces in the continental lithosphere: Abstract in International Workshop on Active and Recent Strike-Slip Tectonics, Florence, Italy, April 18-20, 1989.

Teyssier, C. and Tikoff, B., 1998, Strike-slip partitioned transpression of the San Andreas fault system: A lithospheric-scale approach: in Holdsworth, R.E., Strachan, R.A., and Dewey, J.F. (eds.), Continental transpressional and transtensional tectonics: Geological Society, London, Special Publications, v. 135, p. 143-158.

Toppozada, T.R., Real, C.R., and Parke, D.L., 1981, Preparation of isoseismal maps and summaries of reported effects of pre-1990 California earthquakes: California Division of Mines and Geology Open-File Report 81-11, 182 p.

Unruh, J.R., and Sawyer, T.L., 1995, Late Cenozoic growth of the Mt. Diablo fold-and-thrust belt, central Contra Costa County, California, and implications for transpressional deformation of the northern Diablo Range: American Association of Petroleum Geologists, 1995 Pacific Section Convention Abstracts, p. 47.

Unruh, J.R., and Sawyer, T.L., 1997, Assessment of blind seismogenic sources, Livermore Valley, Eastern San Francisco Bay Region: Technical report submitted to the U.S. Geological Survey, National Earthquake Hazards Reduction Program, Award no. 1434-95-G-2611.

Unruh, J.R. and Lettis, W.R., 1998, Kinematics of transpressional deformation in the eastern San Francisco Bay region, California: Geology, v. 26, p. 19-22.

Unruh, J.R., and Hector, S.T., 1999, Subsurface characterization of the Potrero-Ryer Island thrust system, Western Sacramento-San Joaquin Delta, Northern California: Technical report submitted to the U.S. Geological Survey, National Earthquake Hazards Reduction Program, Award no. 1434-HQ-96-GR-02724, 32 p.

Wakabayashi, J. and Sawyer, T.L., 1998, Paleoseismic investigation of the Miller Creek fault, eastern San Francisco Bay area, California: Technical report submitted to U.S. Geological Survey, National Earthquake Hazards Reduction Program, Award no. 1434-HQ-97-GR-03141, 17 p., 7 figures, plate.

Weber-Band, J., 1998, Neotectonics of the Sacramento-San Joaquin Delta area, east-central Coast Ranges, California: Ph.D. dissertation, University of California, Berkeley, 216 p.

Wells, D.L., and Coppersmith, K.J., 1994, New empirical relationships among magnitude, rupture length, rupture width, rupture area, and surface displacement: Bulletin of the Seismological Society of America, v. 84, p. 974-1,002.

WLA (William Lettis & Associates, Inc.), 1999, Preliminary seismic source characterization, western Sacramento-San Joaquin Delta region, northern California: Consultant's report to the California Department of Water Resources, 32 p.

Woodward, N.B., Boyer, S.E., and Suppe, J., 1989, Balanced geological cross-sections: An essential technique in geological research and exploration: American Geophysical Union Short Course in Geology, Volume 6, 132 p.

WGCEP (Working Group on California Earthquake Probabilities), 1999, Probabilities of large earthquakes in the San Francisco Bay region, California: U.S. Geological Survey Open-File Report 99-517, 60 p.

Zoback, M.D., Zoback, M.L., Mount, V.S., Suppe, J., Eaton, J.P., Healy, J.H., Oppenheimer, D., Reasenberg, P., Jones, L., Raleigh, C.B., Wong, I.G., Scotti, O., and Wentworth, C., 1987, New evidence on the state of stress of the San Andreas system: Science, v. 238, p. 1105-1111.


ASSOCIATION OF ENGINEERING GEOLOGISTS
AEG

LATE HOLOCENE BEHAVIOR AND SEISMOGENIC POTENTIAL OF THE CONCORD-GREEN VALLEY FAULT SYSTEM IN CONTRA COSTA AND SOLANO COUNTIES, CALIFORNIA

GLENN BORCHARDT[1] AND JOHN N. BALDWIN[2]

ABSTRACT

The dextral strike-slip Concord-Green Valley fault (CGVF) system traverses the heavily populated I-680 and I-80 corridor in the eastern San Francisco Bay area. Recent paleoseismic studies at Galindo Creek and Lopes Ranch provide new insight into the seismic behavior of this fault system. The 16-to 24-km-long Concord fault appears to have a geologic slip rate (3.4 ± 0.3 mm/year) similar to the average "long-term" (18-year record) creep rate for the fault (3-4 mm/year). Based on the presence of ductile deformation at Galindo Creek, it appears likely that part of the Concord fault behaves primarily aseismically and seldom has catastrophic ground rupture associated with major earthquakes. Trench exposures on the northern part of the Concord fault and on the southern part of the Green Valley fault (GVF), however, suggest multiple episodes of surface faulting. Based on the occurrence of a M5.4 earthquake on the central part of the Concord fault in 1955, it appears that the fault is at least partly locked at depth. Paleoseismic studies at Lopes Ranch on the GVF suggest that multiple surface-rupturing events have occurred within the last 2,700 years. The preliminary minimum slip rate at Lopes Ranch is 3.8 to 4.8 mm/year (over the last 300 years)-similar to the 14-year average creep rate of 4.9 mm/year. The CGVF appears not to have produced an earthquake greater than M5.4 since 1776, when the written record began in the Bay area.

INTRODUCTION

The Concord-Green Valley fault (CGVF) is a major N25-30°W-striking, dextral, strike-slip fault system in the San Francisco Bay area (Figure 1). The CGVF is composed of at least two major fault segments: from south to north: the Concord fault (16 to 24-km long) and the Green Valley fault (29 to 43-km-long). The Concord fault traverses the heavily urbanized communities of Walnut Creek and Concord, beginning in the southeast at the base of Mount Diablo and continuing northwest to Suisun Bay. At Suisun Bay, geologic slip on the Concord fault is transferred to the Green Valley fault (GVF) across an apparent right bend (Figure 1). The GVF extends from Suisun Bay northwest to Wooden Valley, traversing the rapidly developing I-680 corridor in central and eastern Solano County, near Fairfield (Figure 1). Along its length, the GVF intersects several major transportation routes, rail lines, power transmission lines, pipelines, and levees. In addition, the Cordelia fault, located only 2 to 4 kilometers east of the GVF, may be a secondary trace of the GVF (Figure 1). It has a well-defined surface trace that strikes northerly and a late Holocene slip rate of <1 mm/year (Gilpin et al., 1999; HTA, 1994).

The presence or absence of a rupture segmentation boundary at Suisun Bay between the Concord fault and the GVF is poorly understood; however, many investigators currently interpret the CGVF as a single fault system capable of producing a M7.1

[1]Soil Tectonics
P.O. Box 5335
Berkeley, CA 94705
gborchardt@usa.net

[2]William Lettis & Associates
1777 Botelho Drive, Suite 262
Walnut Creek, CA 94596
baldwin@lettis.com

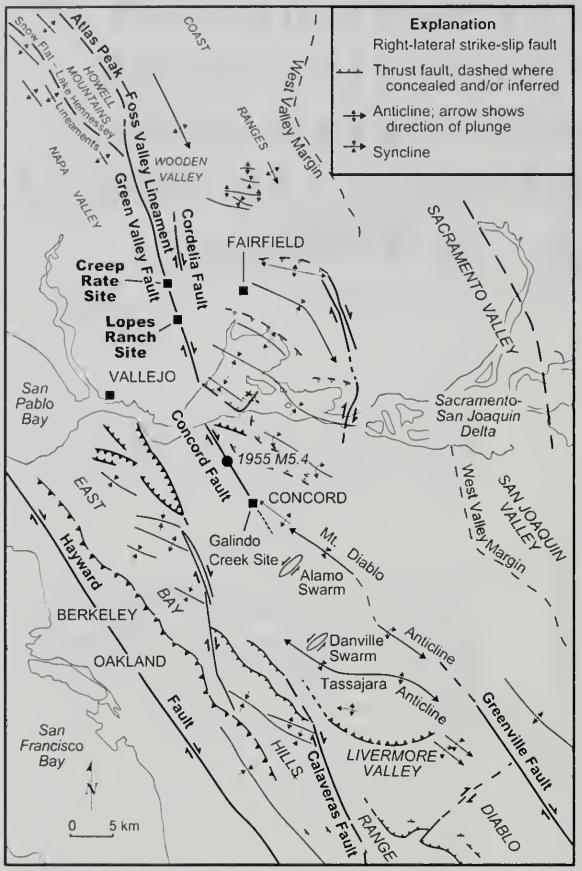

Figure 1. The Concord-Green Valley fault system.

earthquake (WGNCEP, 1996). Such an earthquake likely would severely impact the eastern part of the San Francisco Bay area through surface-fault rupture and strong ground shaking (ABAG, 1999). Currently the fault system is poorly characterized and we lack the necessary paleoseismic data to address the potential of a single continuous rupture, or smaller independent rupture segments. This paper presents the most recent paleoseismic information available on the CGVF system, and discusses some of the continuing uncertainties regarding its earthquake hazard potential.

Much of the information presented in this paper is based on recent mapping (Baldwin and Unruh, 1997; Baldwin et al., 1998) and paleoseismic studies conducted by the authors on the Concord fault (Borchardt et al., 1999) and Green Valley fault (Baldwin and Lienkaemper, 1999; Baldwin and Meyer, 1999). In addition, it includes compilation of existing geologic mapping (Bryant, 1992, 1991, 1982; Frizzell and Brown, 1972; and Wills and Hart, 1992) and trenching data from various geotechnical investigations conducted on the fault system.

TECTONIC SETTING

Most of the active faulting and seismicity in northwestern California can be related directly to the transpressional motion between the Pacific Plate and the Sierra Nevada-Central Valley microplate. Global motion between the Pacific and North American plates at the latitude of the northern San Francisco Bay region is estimated by the NUVEL-1A plate-motion model (Unruh, 2001, this volume) and geodetic analyses to be approximately 40 ± 3 mm/year, with an azimuth of N31°W ± 2.5° (Argus, 1999; Kelson et al., 1992; Gordon, 1993). Motion of the intervening Sierra Nevada-Central Valley microplate with respect to stable North America is different from that of the Pacific Plate (Argus and Gordon, 1991). Detailed geodetic studies employing both trilateration and satellite-based techniques indicate that 31 to 38 mm/year of northwest dextral shear between these two plates is accommodated by distributed deformation across a 100-km-wide zone in the northern Coast Ranges west of the Great Valley (Williams et al., 1994; Table 1).

Most of the dextral shear component of distributed plate motion in the San Francisco Bay area is accommodated by three major right-lateral strike-slip faults or fault systems that include: the San Andreas fault, the Hayward-Rodgers Creek-Healdsburg fault system, and the Concord-Green Valley-Cordelia fault system (Figure 1). At the latitude of the CGVF, the plate-boundary slip is partitioned between these three major right-lateral strike-slip fault systems. The San Andreas fault has a slip rate of about 24 ± 2 mm/year (Niemi and Hall, 1992; Prentice, 1989) and the Hayward-Rodgers Creek fault system has a slip rate of about 8 ± 2 mm/year

FAULT	AVERAGE	MINIMUM	MAXIMUM	REFERENCE
San Andreas	24	22	26	Niemi and Hall (1992); Prentice (1989)
Hayward-Rodgers Creek	8	6	10	Lienkaemper and Borchardt (1996); Schwartz et al. (1992)
Concord-Green Valley	4.5	2	8	Borchardt et al. (1999); Baldwin and Lienkaemper, 1999 WGCEP (1999)
Totals	**36.5**	**30**	**44**	
Bay Area Geodesy	34.5	31	38	Williams et al. (1994)

Table 1. Slip rates (in mm/year) across the San Andreas fault system at the latitude of the Concord-Green Valley fault in the San Francisco Bay area.

(Lienkaemper and Borchardt, 1996; Schwartz et al., 1992). The remaining slip predicted by the plate motion model (0 to 6 mm/year) is distributed across the CGVF and other faults.

There are at least two structural models that attempt to explain the origin of dextral slip on the CGVF system. These models differ significantly in the process of transferring slip between Bay area strike-slip faults. The models therefore imply different earthquake hazards for the eastern San Francisco Bay region. One model (Ellsworth et al., 1982; Oppenheimer and Lindh, 1992; WGNCEP, 1996) assumes that 4 to 7 mm/year (Kelson et al., 1996; Simpson et al., 1999) of slip from the northern Calaveras fault is transferred eastward between Danville and Walnut Creek across a right step-over to the Concord fault. This model assumes that the presence of a series of left-lateral faults, which were the source of earthquake swarms in 1970 and 1990 (Oppenheimer and Macgregor-Scott, 1992), help transfer slip between the Calaveras and Concord faults, and that Walnut Creek is a pull-apart basin. The second model (Unruh and Sawyer, 1997) hypothesizes that slip on the CGVF system originates to the southeast across a left-stepping restraining bend and the Mt. Diablo anticlinorium between the Concord and Greenville faults. Implications of this model are that: (1) slip on the CGVF is independent of the Calaveras fault; thus, slip on the northern Calaveras fault is partitioned northwesterly across contractional structures within the East Bay Hills (Simpson et al., 1992); (2) the slip rate on the CGVF is likely less than earlier estimates, and may be closer to the poorly assessed slip rate of the Greenville fault (see section on geologic slip rate).

Early slip rate estimates for the CGVF ranged from 8 ± 2 mm/year (Kelson et al., 1992) to 6 ± 2 mm/year (WGNCEP, 1996). These slip rates were based mostly on the aseismic creep rate of the GVF and the interpretation that slip on the northern Calaveras fault is partitioned on to the Concord fault. However, recent paleoseismic studies (Borchardt et al., 1999) suggest that the Concord fault has a geologic slip rate of only 3.4 ± 0.3 mm/year. Preliminary data collected on the GVF suggest a minimum late Holocene geologic slip rate of 3.8 to 4.8 mm/year. In addition, a poorly constrained dextral offset of 18 to 20 km of Pliocene Sonoma Volcanics across the fault (Bryant, 1992; Unruh, 1999) yield a minimum long-term slip rate of at least 3 mm/year for the Green Valley fault. WGCEP (1999) included the most recent slip and aseismic-creep rate data on the CGVF fault system in the new earthquake probability models of the Bay area, assigning revised slip rates of 4 ± 2 mm/year for the Concord fault and 5 ± 3 mm/year for the GVF, respectively.

HISTORICAL SEISMICITY

No earthquakes greater than M6 seem to have occurred on the CGVF system in the last 225 years (Toppozada et al., 1986). The system, nevertheless, is associated with microseismicity and historically

has experienced moderate-magnitude earthquakes. The largest of these was a M5.4 earthquake that occurred on the Concord fault on October 24, 1955. No earthquakes greater than M5 are known to have occurred along the GVF in historic time. However, recent paleoseismic studies south of Cordelia indicate that the GVF has produced multiple surface-fault ruptures within the last 2,700 years (Baldwin and Lienkaemper, 1999). Surface ground rupture normally occurs only during earthquakes with magnitudes greater than M5.5.

GEOMORPHOLOGY

The Concord fault consists of three sections, each having slightly different characteristics (northern, central, and southern). Each may or may not be associated with rupture segments on the basis of physiographic and creep-rate differences (Sharp, 1973). The southern termination of the Concord fault is mapped as several active strands along the base of Lime Ridge, which is a northwest trending extension of the Mount Diablo anticlinorium (Figure 1; Wills and Hart, 1992; Smith, 1992). It is poorly defined by the presence of discontinuous scarps, breaks in slope, and tonal lineaments. The central section of the Concord fault exhibits clear evidence of creep (e.g., offset streets and curbs), prominent tectonic geomorphology (e.g., tonal lineaments and west-facing scarps), and offset of Holocene strata in trenches excavated across it (Wills and Hart, 1992). Northwest of downtown Concord, the surface expression of the northern section of the fault becomes obscured as it crosses the modern flood plain and tidal sediments south of Suisun Bay.

At Suisun Bay, the Concord fault steps right or bends about 5 to 10° north to the southern GVF (Figure 1). The 29-to 43-km-long GVF consists of southern (22 ± 3-km-long) and northern (14 ± 4-km-long) segments separated by a slight right-step near the Green Valley Golf Course (WGCEP, 1999). The northern GVF continues northwesterly to at least Wooden Valley. Along its entire length, the GVF is delineated by prominent tectonic geomorphology (i.e., right-laterally offset drainages, closed depressions, scarps, and tonal and vegetation lineaments) expressed as a complex anastomozing fault zone of at least two to three active strands (Bryant, 1992). There is also an inferred down-to-the-east vertical component across the fault as suggested by stratigraphy, topography, and trench exposures. Near Wooden Valley, the tectonic geomorphology abruptly terminates and the northward projection of the fault becomes obscure. Recent mapping and aerial reconnaissance (Baldwin et al., 1998; Baldwin and Unruh, 1997) suggest that geologic slip is transferred, in part, northwest across a series of west-vergent folds and thrust-faults that are part of the Atlas Peak-Foss Valley and Snow Flat-Lake Hennessey lineaments (Figure 1). It is likely that some slip also continues northward, based on a linear trend of microseismicity that correlates with the Cedar Roughs fault (Wong, 1990).

ASEISMIC CREEP RATE

Aseismic creep rates increase from south to north along the CGVF, from about 3 mm/year in Concord to about 5 mm/year near Cordelia. Since 1981, Galehouse (1998) has monitored aseismic slip along the central part of the Concord fault near Ashbury Drive and Salvio Street in Concord (Figure 1). At these locations, creep has been between 3 and 4 mm/year over the last 18 years. It typically is expressed as episodes of rapid slip (7 to 10 mm over a few months), alternating with intervals of slow slip (1 to 2 mm/year over several years).

The GVF shows evidence of aseismic creep, primarily along the southern part of the fault. A pre-1862 fence is offset about 0.25 m, and a 1922 power line near the I-80/I-680 intersection is offset about 0.28 m, yielding long-term creep rates between 2.3 and 5.5 mm/year, respectively (Figure 1; Frizzell and Brown, 1976). These displaced cultural features have not been remeasured since 1975, but will be surveyed as part of the ongoing Bay Area Paleoseismological Experiment (BAPEX) to further evaluate the GVF (Baldwin and Lienkaemper, 1999). Theodolite measurements between North Brook Boulevard and Watt Drive, southwest of Cordelia, indicate an average dextral creep rate for the last 14 years of 4.9 mm/year for the GVF (Galehouse, 1999).

GEOLOGIC SLIP RATE AND PALEOSEISMIC DATA

The CGVF remains poorly studied compared to other regional dextral faults such as the San Andreas and Hayward faults. Slip rates used in earlier regional strain-rate studies (Kelson et al., 1992), probabilistic seismic hazard maps (Petersen et al., 1996) and earthquake recurrence (WGNCEP, 1996) usually assumed that the slip rate on the CGVF exceeded the aseismic creep rate. Early estimates of aseismic slip on the GVF suggested a creep rate of 5.5 mm/year (Galehouse, 1992), lead-

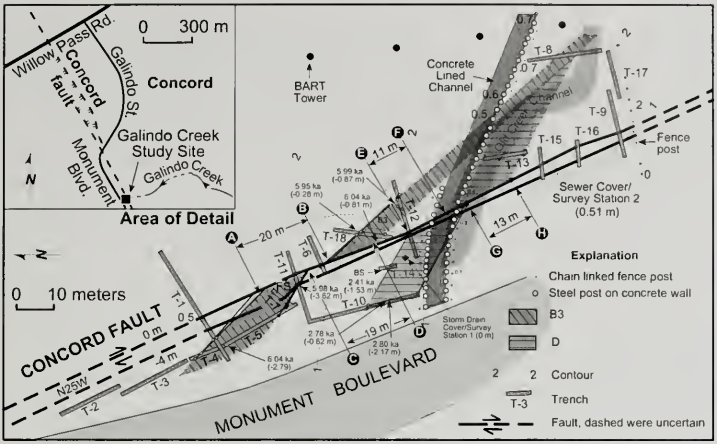

Figure 2. Site map of the Galindo Creek study site showing the locations of trenches excavated in 1994 (T-1 to T-7) and in 1997 (T-8 to T-18). The approximate 20-m offset of 6,000 year old channel B3 yields a geologic slip rate of 3.4 ± 0.3 mm/year. Offset along channel D constrains the slip rate to less than 5.4 mm/year during the last 2,400 years (from Borchardt et al., 1999).

ing investigators to assume that the geologic slip rate may be 6 mm/year. Findings from the recent paleoseismic and aseismic creep rate studies suggest that the geologic slip rate is less than 5 mm/year (Borchardt et al., 1999; Baldwin and Lienkaemper, 1999). WGCEP (1999) assigned a geologic slip rate of 4 ± 2 mm/year for the Concord fault and 5 ± 3 mm/year for the GVF, reflecting the findings of these recent geologic and aseismic creep studies.

Concord fault

The first paleoseismic study conducted on the Concord fault was completed recently along the southern section by Borchardt et al. (1999) at the Galindo Creek site, located directly south of downtown Concord (Figure 1). At Galindo Creek, the fault is expressed as a tonal lineament and a west-facing 2-m-high scarp. Trenches excavated at the site exposed four major Galindo Creek paleochannels that are dextrally offset along the fault. Detrital charcoal dates collected from Channel Fill B3, which is present on both sides of the fault, yielded an average calibrated age of 6.0 ± 0.1 ka (Figure 2). The northern channel margin of Channel Fill B3 is offset 20 m, and the southern margin is offset 19 m. The top of the channel fill is 2.7 m higher on the east than on the west. Thus, by using the age and amount of dextral and vertical offset of Channel Fill B3, a horizontal slip rate of 3.4 ± 0.3 mm/year and a vertical slip rate of 0.45±0.06 mm/year were calculated. Other channels were either too deep for satisfactory excavation or were observed only on one side of the fault. Channel Fill D, dated at 2.4 ka and only exposed on the west side of the fault, nonetheless provides useful information when coupled with data showing the historical location of Galindo Creek (Figure 2). By projecting the northern margin of Channel Fill D from the west and the historical location of Galindo Creek from the east, Borchardt et al. (1999) measured at least 13 m of dextral separation along the fault. Assuming that the historic channel is correlative with Channel Fill D, this gave a maximum slip rate of 5.4 mm/year (Figure 2).

The relatively large component of east-side-up vertical separation along the Concord fault is expressed as well-developed drag folds within the fault zone. Here, otherwise flat-lying sedimentary beds dip between 71° and 47°SW along the fault plane (Figure 3). Plastic deformation is intense within 0.75 to 1.5 m of the fault. The vertical component of deformation is probably due to the proximity of the Galindo Creek site to the actively growing Mt. Diablo anticlinorium, which is centered about 8 km to the southeast. Discrete offsets of individual sedimentary beds are rare at Galindo Creek, suggesting much of the deformation observed in the trenches is related to aseismic creep rather than past surface ruptures. Thin alluvial units at Galindo Creek typically have been drag-folded several meters along the main fault (Figure 3). Units deposited between 6 and 7 ka have been unaffected by offsets along secondary shears or by sedimentation that might have provided "event horizons". Event horizons are sedimentary beds or soils that show the passage of time following an earthquake. All of the fault-normal trenches at the site exhibited ductile rather than brittle deformation (Borchardt et al., 1999). Nevertheless, evidence for brittle deformation is present about 2.5 km to the north at Buchanan

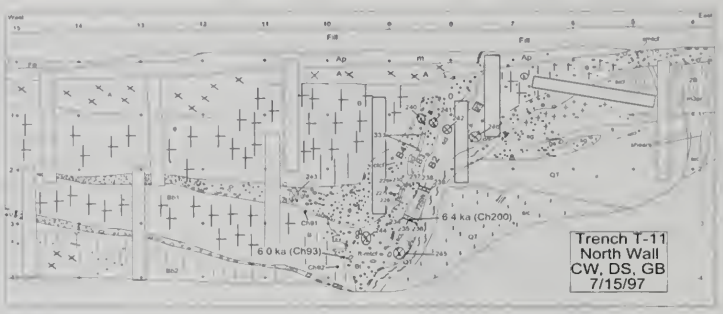

Figure 3. Log of trench across the Concord fault showing drag folding produced by uplift on the east (from Borchardt et al., 1999). Abbreviations: g=gravel, s=sand, si=silt, c=clay; Ap, A, B, Bb1, Bb2 = soil horizons; QT=Plio-Pleistocene Tulare Formation; cmtcf= common medium thick clay films; k=krotovinas. Numbers indicate locations of charcoal specimens or materials sampled for particle size distribution.

Airport, where consultant trenches excavated to fulfill the requirements of the State's fault zoning program (Hart and Bryant, 1997) show evidence of discrete offsets in alluvium. Therefore, it appears that at least the northern part of the Concord fault undergoes ground surface rupture from either moderate or large magnitude earthquakes.

Green Valley fault

The geologic slip rate of the GVF is poorly constrained. Bryant (1982, 1991) and Unruh (1999) estimate a long-term Quaternary slip rate of at least 3 mm/year, based on an unconstrained dextral separation (<20 km) of Pliocene Sonoma Volcanics. An unpublished preliminary paleoseismic study by Sims (1993) conducted on the southern part of the GVF at Lopes Ranch provides the only Holocene slip-rate data for the fault (Figure 4). Re-interpretation of the original (Sims, 1993) radiocarbon data, suggests that a buried 310-yr-old paleochannel is right-laterally offset 1.2 to 1.5 m across the GVF, yielding a slip rate of 3.8 to 4.8 mm/year (Baldwin and Lienkaemper, 1999). This slip rate is similar to the 14-year-creep rate average of 4.9 mm/year determined about 3 km northwest of the site. Additional studies at Lopes Ranch (Baldwin and Lienkaemper, 1999) and re-interpretation of Sims' trench logs show that the measured displacement of the 310-year-old paleochannel likely is a minimum due to the presence of additional fault traces at the site. It is unclear whether the paleochannel is offset from aseismic creep or the most recent surface-faulting event.

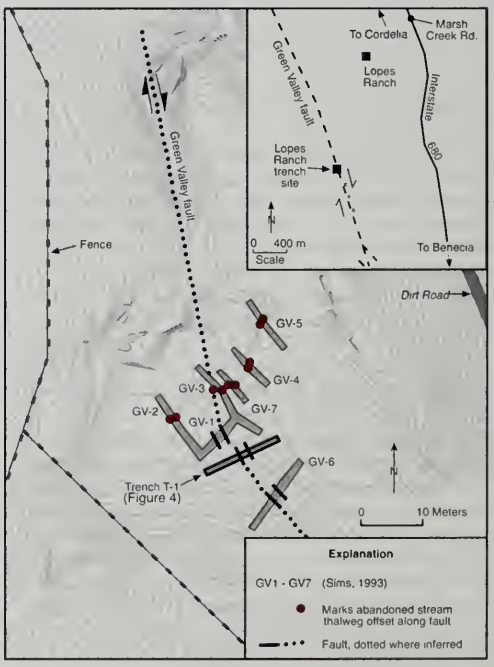

Figure 4. Trench and fault location map of the Lopes Ranch paleoseismic site, Solano County, California (from Baldwin and Lienkaemper, 1999).

On the basis of trench exposures, re-interpretation of Sims' (1993) trench logs, and radiometric analysis of charcoal samples collected from faulted deposits at Lopes Ranch, multiple surface-rupturing events have occurred on the GVF in the past 2,700 years (Baldwin and Lienkaemper, 1999; Figure 5). Evidence for paleoearthquakes is expressed in the trenches as (1) truncated units, (2) upward fault terminations, and (3) tilted stratigraphic deposits (Figure 5). Due to the preliminary nature of the work, and continuing investigation at Lopes Ranch and other possible sites along the GVF, we make no attempt to constrain the most recent surface-faulting event or earthquake recurrence.

SEISMIC HAZARD ASSESSMENT

It is uncertain whether the fault system behaves as a single seismic source capable of generating large earthquakes, or if the fault system consists of several independent rupture segments capable of producing only M5.5 to 6.25 earthquakes. WGCEP (1999) considered single, double, and triple segment rupture models for the CGVF. One model included the entire CGVF system rupturing, a second model included independent Concord fault and GVF rupture segments, and the third model considered an independent Concord fault and two (northern and southern) independent rupture segments on the GVF. New estimates of recurrence along the CGVF system exceed 700 years for a single CGVF rupture, and even greater intervals for independent segment ruptures along the Concord fault and GVF, respectively. Because no data is available on the most recent surface-rupturing event for these faults, it is not possible to assess where the CGVF may be within its earthquake cycle. Lopes Ranch provides the only timing data available for the CGVF, with preliminary results suggesting multiple earthquakes within the last 2,700 years.

Early assessments (WGNCEP, 1996) of the seismic hazard for the CGVF assumed a geologic slip rate of 6 ± 2 mm/year. Under a single-segment rupture model, WGNCEP (1996) estimated a M6.9 event every 180-330 years for the entire CGVF system. In a two-segment rupture model, which individually assesses the recurrence of surface rupturing segments on the Concord fault and the GVF, a M6.5 event would occur every 110 to 240 years on the Concord fault and a M6.7 event would occur every 150 to 330 years on the GVF.

SEISMIC INTENSITY DISTRIBUTION

The seismic shaking intensity caused by a M6.8 earthquake in the single rupture model shows that Concord, Suisun, parts of Walnut Creek, and artificial-fill along the margins of San Francisco Bay between San Pablo and San Jose can expect modified Mercalli intensities greater than VII (Figure 6). Sites within 5 km of the fault, and on unconsolidated saturated alluvium may experience modified Mercalli intensities as high as X. Thus, high-rise buildings, pipelines, and above-ground storage facilities at several local refineries would be especially affected by the near-field effects of such an earthquake.

CONCLUSIONS

Recent paleoseismic investigations at Galindo Creek and Lopes Ranch provide valuable new information on the seismic behavior of the CGVF system. Additional paleoseismic data is necessary to better constrain the recurrence, slip rate, and seismic hazard of the CGVF system. Their apparently similar geologic slip rates suggest that the Concord fault and GVF could act as a single structure capable of pro-

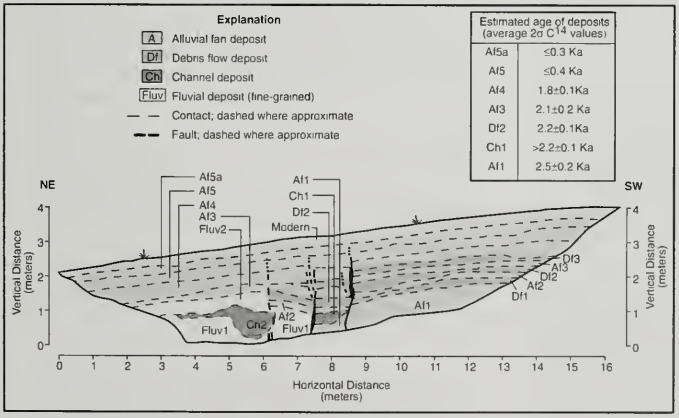

Figure 5. Log of paleoseismic trench across the GVF (from Baldwin and Lienkaemper, 1999).

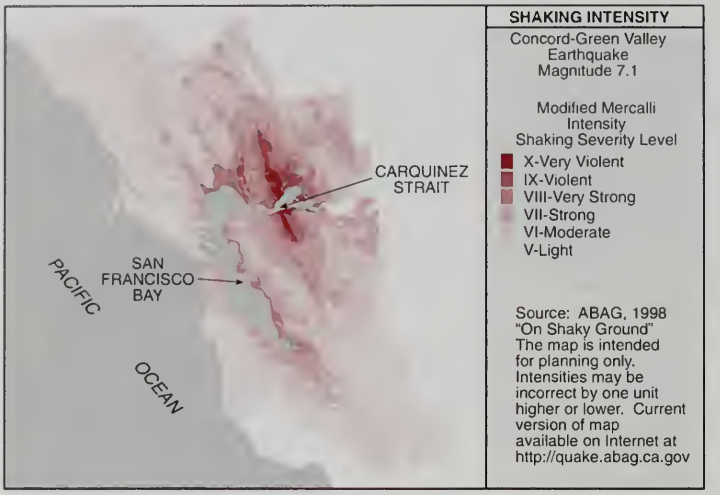

Figure 6. Seismic intensity for a M6.8 earthquake on the CGVF (ABAG, 1999).

ducing earthquakes up to M6.8. Paleoseismic studies along the central segment of the Concord fault yield a geologic slip rate of 3.4 ± 0.3 mm/year, which is similar to the local creep rate. In addition, preliminary results at Lopes Ranch on the GVF suggest a minimum geologic slip rate of 3.8 to 4.8 mm/year, which also is similar to the local creep rate. These results suggest that WGNCEP's (1996) geologic slip rate of 6 ± 2 mm/year for the CGVF was too high. Thus, WGCEP (1999) revised these earlier geologic slip rates for the CGVF, resulting in slip rates of 4 ± 2 mm/year for the Concord fault and 5 ± 3 mm/year for the GVF.

There is no indication of surface ground rupture at the Galindo Creek site. Nevertheless, the 1955 M5.4 earthquake provides evidence that the central Concord fault is at least capable of <M5.5 earthquakes and may be locked at depth. Preliminary findings from trench studies on the GVF at Lopes Ranch suggest that multiple surface-rupturing events (>M5.5) occurred there within the last 2,700 years. Such earthquakes could severely damage the infrastructure of the rapidly developing I-680 and I-80 corridors in Contra Costa and Solano Counties.

ACKNOWLEDGEMENTS

We are extremely grateful to our colleagues D.L. Snyder, C.J. Wills, J.J. Lienkaemper, and J.D. Sims without whom the investigations crucial to the above discussion would not have been performed. We thank the Bay Area Rapid Transit District and Silicon Valley Power for permission to access Galindo Creek and Lopes Ranch, respectively. We also thank the field crew from Rogers/Pacific and Snyder and Smith Associates and others who assisted with the work. We are grateful to the U.S. Geological Survey (USGS) for supporting this research under USGS awards number 1434-94-G-2483 and 1434-HQ-97-GR-03102 and Bay Area Paleoseismological Experiment Contract No. 98WRCN1012. Additional support for this study was provided by the Professional Development Program of William Lettis & Associates, Inc. The views and conclusions contained in this document are those of the authors and should not be interpreted as necessarily representing the official policies, either expressed or implied, of the U.S. Government.

AUTHOR PROFILES

Glenn Borchardt is the Principal of Soil Tectonics, a firm that specializes in pedochronology (dating through mapping stages of soil development) and paleoseismology. He has been involved in dozens of fault studies in both northern and southern California. The most important involved the proposed Auburn Dam, the proposed Point Conception LNG Terminal, the Vallecitos Reactor near Livermore, USGS-sponsored studies of the Raymond, San Gabriel, Hayward, and Concord faults, and numerous evaluations of faults for the state's fault zoning program. He is one of the co-authors of the CDMG earthquake planning scenarios involving the San Andreas, Hayward, Newport-Inglewood, San Jacinto, Rodgers Creek, and Cascadia faults.

John Baldwin is a a Senior Project Geologist at William Lettis & Associates, Inc. He has over eight years of combined professional and educational experience specializing in neotectonics and engineering/environmental geology. He has charac-

terized the geologic and geomorphic settings of landfills, private residences, public utility systems, and petroleum pipelines. He has also evaluated the foundations and slope stability of bridges located in Shasta County, California, and has conducted various USGS-NEHRP-funded paleoseismic investigations on the San Andreas and Calaveras, and Green Valley faults in the San Francisco bay area.

SELECTED REFERENCES

ABAG (Association of Bay area Governments), 1999, Earthquake hazard map for the entire Bay area, Scenario: Concord-Green Valley fault (http://quake.abag.ca.gov).

Argus, D.G., 1999, Personal communication to J.N. Baldwin.

Argus, D.G., and Gordon, R.G., 1991, Current Sierra Nevada-North American motion from very long baseline interferometry: Implications for the kinematics of the western United States: Geology, v. 19, p. 1,085-1,088.

Baldwin, J.N., and Lienkaemper, J.J., 1999, Paleoseismic investigations along the Green Valley fault, Solano County, California: Unpublished report - Bay Area Paleoseismological Experiment Contract No: 98WRCN1012, 18 p.

Baldwin, J.N., and Meyer, J., 1999, Preliminary geoarchaeological study at Green Valley Creek, Solano County, California: Unpublished Report - Bay Area Paleoseismological Experiment Contract No: 98WRCN1012, 10 p.

Baldwin, J.N., Unruh, J.R., and Lettis, W.R., 1998, Neotectonic investigation of the northward extension of the Green Valley fault, Napa County, California: Final Technical Report to the U.S. Geological Survey National Earthquake Hazards Reduction Program, 27 p., 2 plates (scale 1:24,000).

Baldwin, J.N., and Unruh, J.R., 1997, Neotectonic lineaments and Quaternary folds in the Howell Mountains, eastern Napa County, California: Restraining stepover at the northern termination of the Green Valley fault?: EOS-Transactions, American Geophysical Union, v. 78, no. 46, p. 632.

Borchardt, G., Snyder, D.L., and Wills, C.J., 1999, Holocene slip rate of the Concord fault at Galindo Creek in Concord, California: Final Technical Report for the U.S. Geological Survey National Earthquake Hazards Reduction Program, 30 p.

Bryant, W.A., 1992, Southern Green Valley fault, Solano County: California Division of Mines and Geology, unpublished Fault Evaluation Report FER-232, map scale 1: 24,000, 14 p.

Bryant, W.A., 1991, The Green Valley fault: in Figuers, S. (Chairman), Field trip guide to the geology of western Solano County: Northern California Geological Society, Association of Engineering Geologists, and Rogers/Pacific, p. 1-11.

Bryant, W.A., 1982, Green Valley fault zone, Cordelia and Mt. George quadrangles, California: California Division of Mines and Geology, unpublished Fault Evaluation Report FER-126, map scale 1:24,000.

DeMets, C., Gordon, R.G., Argus, D.F., and Stein, S., 1990, Current plate motions: Geophysical Journal International, v. 101, p. 424-478.

Frizzell, V.A., Jr., and Brown, R.D., Jr., 1976, Map showing recently active breaks along the Green Valley fault, Napa and Solano Counties, California: U.S. Geological Survey Miscellaneous Field Studies Map MF-743, scale 1:24,000.

Galehouse, J.S., 1999, Personal communication to J.N. Baldwin.

Galehouse, J.S., 1992, Creep rates and creep characteristics of Eastern San Francisco Bay area faults: 1979-1992: in Borchardt, G., Hirschfeld, S.E., Lienkaemper, J.J., McClellan, P., Williams, P.L., and Wong, I.G., (eds.), Proceedings of the Second Conference on Earthquake Hazards in the Eastern San Francisco Bay area: California Division of Mines and Geology Special Publication 113, p. 45-53.

Galehouse, J.S., 1998, Theodolite measurements of creep rates on San Francisco Bay region faults [abs.]: U.S. Geological Survey NEHRP Web Page; (http://erp-web.er.usgs.gov/reports/abstract/1998/nc/g3111fin.htm), 6 p.

Gilpin, L.M., Kennedy, D.G., McNeal, C.C., Zepeda, R.L., and Borchardt, G., 1999, Geomorphology of the Cordelia fault zone in volcanic uplands, Fairfield, Solano County, California [abs.]: Geological Society of America Abstracts with Programs, Cordilleran Section, v. 31, no. 6, p. A-57.

Gordon, R.G., 1993, Orbital dates and steady rates: Nature v. 364, p. 760-761.

HTA (Harlan Tait Associates), 1994, Fault and limited geotechnical investigation, North Fairfield site, Fairfield, California: Consultant's report to the City of Fairfield, 41 p.

Hart, E.W., and Bryant, W.G., 1997 (revised), Fault rupture hazard zones in California: California Division of Mines and Geology Special Publication 42, 34 p.

Kelson, K.I., Lettis, W.R., and Lisowski, M., 1992, Distribution of geologic slip and creep along faults in the San Francisco Bay region: in Borchardt, G., Hirschfeld, S.E., Lienkaemper, J.J., McClellan, P., Williams, P.L., and Wong, I.G., (eds.), Proceedings of the Second Conference on Earthquake Hazards in the Eastern San Francisco Bay area: California Division of Mines and Geology Special Publication 113, p. 31-38.

Kelson, K.I., Simpson, G.D., Lettis, W.R., and Haraden, C., 1996, Holocene slip rate and earthquake recurrence of the northern Calaveras fault at Leyden Creek, northern California: Journal of Geophysical Research, v. 101, no. B3, p. 5,961-5,975.

Lienkaemper, J.J., Borchardt, G., and Lisowski, M., 1991, Historic creep rate and potential for seismic slip along the Hayward fault, California: Journal of Geophysical Research, v. 96, no. B11, p. 18,261-18,283.

Lienkaemper, J.J., and Borchardt, G., 1996, Holocene slip rate of the Hayward fault at Union City, California: Journal of Geophysical Research, v. 101, no. B3, p. 6,099-6,108.

Niemi, T.M., and Hall, N.T., 1992, Late Holocene slip rate and recurrence of great earthquakes on the San Andreas fault in northern California: Geology, v. 20, no. 3, p. 195-198.

Oppenheimer, D.H., and Macgregor-Scott, N., 1992, The seismotectonics of the eastern San Francisco Bay region: in Borchardt, G., Hirschfeld, S.E., Lienkaemper, J.J., McClellan, P., Williams, P.L., and Wong, I.G., (eds.), Proceedings of the Second Conference on Earthquake Hazards in the Eastern San Francisco Bay area: California Division of Mines and Geology Special Publication 113, p. 11-16.

Petersen, M.D., Bryant, W.A., Cramer, C.H., Cao, T., Reichle, M.S., Frankel, A.D., Lienkaemper, J.J., McCrory, P.A., and Schwartz, D.P., 1996, Probabilistic seismic hazard assessment for the State of California: California Division of Mines and Geology Open File Report 96-08, 33 p.

Prentice, C.S., 1989, Earthquake geology of the northern San Andreas fault near Point Arena, California: Ph.D. Thesis, California Institute of Technology, (Pasadena, California), 246 p.

Schwartz, D.P., Pantosti, D., Hecker, S., Okumura, K., Budding, K.E., and Powers, T., 1992, Late Holocene behavior and seismogenic potential of the Rodgers Creek fault zone, Sonoma County, California: in Borchardt, G., Hirschfeld, S.E., Lienkaemper, J.J., McClellan, P., Williams, P.L., and Wong, I.G., (eds.), Proceedings of the Second Conference on Earthquake Hazards in the Eastern San Francisco Bay area: California Division of Mines and Geology Special Publication 113, p. 393-398.

Sharp, R.V., 1973, Map showing recent tectonic movement on the Concord fault, Contra Costa and Solano Counties, California: U.S. Geological Survey Miscellaneous Field Studies Map MF-505, scale 1:24,000.

Simpson, G.D., Baldwin, J.N., Kelson, K.I., and Lettis, W.R., 1999 (in review), Late Holocene slip rate and earthquake history for the northern Calaveras fault at Welch Creek, eastern San Francisco Bay area, California: Bulletin of Seismological Society of America.

Simpson, G.D., Lettis, W.R., and Kelson, K.I., 1992, Segmentation model for the Northern Calaveras fault, Calaveras Reservoir to Walnut Creek: in Borchardt, G., Hirschfeld, S.E., Lienkaemper, J.J., McClellan, P., Williams, P.L., and Wong, I.G., (eds.), Proceedings of the Second Conference on Earthquake Hazards in the Eastern San Francisco Bay area: California Division of Mines and Geology Special Publication 113, p. 253-259.

Sims, J.D., 1993, Parkfield area tectonic framework [abs.]: in Jacobson, M.L., (ed.), Summaries of technical reports, Volume XXXIV prepared by participants in the National Earthquake Hazards Reduction Program: U.S. Geological Survey Open-File Report 93-195, p. 682-684.

Smith, G.A., 1992, The Ygnacio segment and the southern terminus of the Concord fault: in Borchardt, G., Hirschfeld, S.E., Lienkaemper, J.J., McClellan, P., Williams, P.L., and Wong, I.G., (eds.), Proceedings of the Second Conference on Earthquake Hazards in the Eastern San Francisco Bay area: California Division of Mines and Geology Special Publication 113, p. 319-323.

Toppozada, T.R., Real, C.R., and Parke, D.L., 1986, Earthquake history of California: California Geology, v. 39, no. 2, p. 27-33.

Unruh, J.R., 1999, Personal communication to J.N. Baldwin.

Unruh, J.R., 2001, Characterization of blind thrust faults in the San Francisco Bay area: in Ferriz, H., Anderson, R., (eds.), Engineering Geology Practice in Northern California: Association of Engineering Geologists Special Publication 12 and California Division of Mines and Geology Bulletin 210

Unruh, J.R., and Sawyer, T.L., 1997, Assessment of blind seismogenic sources, Livermore Valley, eastern San Francisco Bay Region: Final Technical Report for NEHRP Award No. 1434-95-G-2611, p. 95.

WGCEP (Working Group on California Earthquake Probabilities), 1999, Earthquake probabilities in the San Francisco Bay Region: 2000 to 2030 - a summary of findings: U.S. Geological Survey Open-file Report 99-517, 60 p.

WGNCEP (Working Group on Northern California Earthquake Potential), 1996, Database of potential sources for earthquakes larger than magnitude 6 in northern California: U.S. Geological Survey Open-file Report 96-705, 40 p.

Williams, S.D.P., Svarc, J.L., Lisowski, M., and Prescott, W.H., 1994, GPS measured rates of deformation in the northern San Francisco Bay region, California, 1990-1993: Geophysical Research Letters, v. 21, p. 1,511-1,514.

Wills, C.J., and Hart, E.W., 1992, Progress in understanding the Concord fault through site specific investigations: in Borchardt, G., Hirschfeld, S.E., Lienkaemper, J.J., McClellan, P., Williams, P.L., and Wong, I.G., (eds.), Proceedings of the Second Conference on Earthquake Hazards in the Eastern San Francisco Bay area: California Division of Mines and Geology Special Publication 113, p. 311-317.

Wong, I.G., 1991, Contemporary seismicity, active faulting and seismic hazards of the Coast Ranges between San Francisco Bay and Healdsburg, California: Journal of Geophysical Research, v. 96, no. B12, p. 19,891-19,904.

RECENT GEOMORPHIC AND PALEOSEISMIC INVESTIGATIONS OF THRUST FAULTS IN SANTA CLARA VALLEY, CALIFORNIA

CLARK H. FENTON[1] AND CHRISTOPHER S. HITCHCOCK[2]

ABSTRACT

Santa Clara Valley is an intermontane valley bounded by the San Andreas and Calaveras/Hayward right-lateral strike-slip fault systems. Restraining bends in the strike-slip faults and partitioning of the oblique convergence between the Sierran and Pacific plates result in net shortening across this region. This crustal shortening is accommodated by belts of northeast- and southwest-vergent thrust faults on the southwest and northeast valley margins, respectively, resulting in uplift of the flanking ranges of the Santa Cruz Mountains and East Bay Hills. Although the marginal thrust faults exhibit much lower slip-rates than adjacent strike-slip faults, they are located within a major urban center and, thus, pose a potentially significant seismic hazard. Recent studies of these structures, most notably the Monte Vista-Shannon fault on the western side of the valley, and the Evergreen fault on the eastern side, indicate that they experienced movement during late Pleistocene and Holocene time. Detailed geomorphic and paleoseismic investigations indicate that not all faults pose a surface-faulting hazard; however, deformation of fluvial terraces and alluvial deposits indicate that they accommodate a significant portion of the contractional strain across the region. The proximal association with the faults of the San Andreas system indicates that the thrust faults may not be independent seismic sources, but they may accommodate triggered slip during large earthquakes on the nearby strike-slip faults. Without further detailed study of the thrust faults bordering Santa Clara Valley, we may be underestimating the seismic hazard in this region.

INTRODUCTION

Until relatively recently, Quaternary-active reverse faults of the San Francisco Bay area have received scant attention as potential seismic hazards, being overlooked by concerns over the next large earthquake on one of the major strike-slip faults of the San Andreas system (WGCEP, 1990; WGNCEP, 1996). Following the 1989 M_W6.9 Loma Prieta earthquake, which occurred on a northeast-verging blind reverse-oblique fault adjacent to the main trace of the San Andreas fault in the Santa Cruz Mountains and caused $8 billion in damage (Bürgmann et al., 1994), greater concern has been shown toward the seismic potential of the Bay Area's "secondary" faults. In addition to the strong ground motion, the Loma Prieta earthquake also produced triggered slip or secondary faulting on reverse faults along the northeastern side of the Santa Cruz Mountains (Aydin et al., 1992; Bürgmann et al., 1997; Langenheim et al., 1997). Along with the 1995 M_W6.7 Northridge earthquake in southern California, the Loma Prieta earthquake highlighted the need to identify and characterize reverse faults, including faults that may be poorly expressed at the surface (i.e., "buried" or "blind" structures) as potential seismic hazards.

[1]URS Corporation
500 12th Street, Suite 200
Oakland, CA 94607
Clark_Fenton@urscorp.com

[2]William Lettis & Associates, Inc.
1777 Botelho Drive
Walnut Creek, CA 94596
hitch@lettis.com

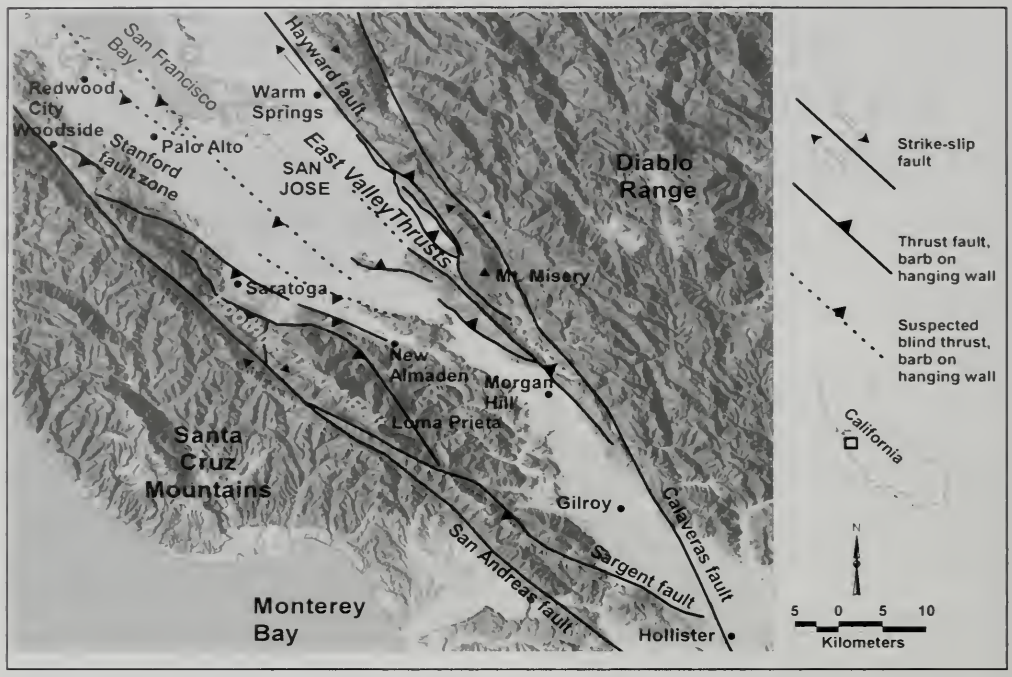

Figure 1. Location of major faults in the Santa Clara Valley region.

Because surface deformation associated with reverse faults may be distributed within zones up to several kilometers wide, it is difficult to identify these faults and predict their likely pattern of future surface deformation as part of regional and site-specific hazard characterization. Repeated displacements on reverse faults may only produce subtle surface deformation that often is not readily perceptible using conventional geologic, geomorphic, and paleoseismologic techniques. Currently, there are no established standards for the calculation of possible amounts of surface deformation (i.e., ground displacement and ruptures) from reverse faults during future earthquakes. In addition, the locations and dips of these structures typically are poorly constrained.

Potentially significant localized strong ground shaking and directivity effects associated with these faults may be important for site-specific studies. Therefore, it is critical that geologists and engineers carefully investigate and characterize the locations of late Quaternary uplift, folding, and ground deformation that may be associated with reverse faulting when such a fault is mapped in the vicinity of a site under investigation. Appraisal of these subtle clues may help provide vital information on the expected type and amount of ground disturbance associated with future episodes of reverse faulting.

Jayko and Lewis (1996) previously summarized some of the diverse geologic and geophysical studies that have been carried out in recent years in an attempt to locate contractional structures and characterize their seismogenic potential in the San Francisco Bay Area. This paper describes characteristics of reverse faults that bound, and previously have been mapped within, Santa Clara Valley in the southern San Francisco Bay area (Figure 1). The geomorphic and paleoseismic data and techniques used to locate and evaluate these faults also are discussed.

GEOLOGIC SETTING

The tectonic framework of the San Francisco Bay area is defined by the Pacific-Sierran plate boundary, marked by the right-lateral San Andreas fault

system. Since the Miocene (23 Ma), as much as 315 km of right-lateral strike-slip movement has occurred, juxtaposing the plutonic assemblage of the Salinian block to the southwest of the San Andreas, against the Franciscan terrane on the northeast side of the fault (Page et al., 1998). However, contemporary plate movement is not parallel to the strike of the San Andreas fault system. Following a change in relative plate motion approximately 3.5 Ma, the style of deformation altered, resulting in a component of convergence across the plate margin in the region of San Francisco Bay. Partitioning plate margin strain results in contractional strain being accommodated on a number of reverse and oblique reverse faults adjacent to the San Andreas system (Lettis and Hanson, 1991), resulting in a plate boundary that extends approximately 50 km inboard of the San Andreas fault (Lisowski et al., 1991). The plate boundary zone in the Bay Area includes the upland regions of the Santa Cruz Mountains and the Diablo Range, both areas of intense deformation, with reverse faulting and close to tight folding being the most common style of deformation (Crane, 1995; Graymer, 1995; Graymer et al., 1995; Page et al., 1998).

Santa Clara Valley is the southern continuation of the San Francisco Bay block, a structural and topographic low located between the San Andreas and Calaveras/Hayward fault systems (Olson and Zoback, 1998). Santa Clara Valley is an intermontane basin filled mainly with late Cenozoic terrigenous clastic sediments and less extensive shallow marine deposits in older sections. The margins of the San Francisco Bay block are relatively simple, being bounded by the linear surface traces of the right-lateral San Andreas and Hayward faults. In contrast, both the western and eastern margins of Santa Clara Valley are marked by narrow belts of thrust faults oriented oblique to the major strike-slip faults (Figure 1).

Recent geomorphic investigations of the thrust faults along the margins of Santa Clara Valley have provided a greater understanding of their activity and, hence, their contribution to seismic hazards in the San Francisco Bay area (e.g., Hitchcock et al., 1994; Angell et al., 1998). Previous "traditional" paleoseismic investigations, namely exploratory fault trenching carried out to satisfy the guidelines of the Alquist-Priolo Earthquake Fault Zone Act (Hart, 1994), revealed little or no data on the activity of these faults. However, field studies following recent blind thrust earthquakes have led to advances in our understanding of the morphotectonic features associated with blind thrust faults. The presence of subtle unconformities and minor colluvial wedges formed at fold scarps (the surface expression of fault-related folds) are now recognized as indicators of ground surface warping and tilting above blind thrusts (Dolan et al., 1997).

Hitchcock et al. (1994) applied geomorphic mapping and analysis to document deformation of fluvial terrace surfaces and, along with measurements of stream channel incision and sinuosity, have used these data to infer late Quaternary movement on the Monte Vista, Shannon, and Cascade faults. To date, paleoseismic trenching studies have not revealed any recurrence data for the thrust faults bounding Santa Clara Valley, and have had limited success in determining the timing of the most recent event on some faults (e.g., Fenton et al., 1995). Geophysical investigations, in particular gravity (Roberts and Jachens, 1993), microearthquake relocation (Fenton et al., 1995; Zoback et al., 1999), and satellite geodesy (Bürgmann et al., 1994, 1997) have all provided a wealth of data towards furthering our understanding of the thrusts in Santa Clara Valley. The results of these and other studies are presented in the following sections.

FAULTS ON THE SOUTHWEST SIDE OF SANTA CLARA VALLEY (FOOTHILLS THRUST BELT)

The southwestern margin of Santa Clara Valley is bounded by the rugged, young, southern Santa Cruz Mountains (Figure 1). Late Cenozoic uplift of the mountains has occurred, in part, along a series of northwest-striking reverse faults, known as either the Loma Prieta domain (Aydin and Page, 1984), or Foothills thrust belt (Bürgmann et al., 1994), bordering the northeastern margin of the range-front. Bounded by the main trace of the San Andreas fault to the west, this sequence of southwest-dipping thrusts, associated with a restraining left-bend in the San Andreas fault, has been responsible for the uplift of the Santa Cruz Mountains (Bürgmann et al., 1994). Structural relations and gravity data suggest that as much as 3 km of uplift has occurred within the past 4.6 million years via reverse slip within the Foothills thrust belt (McLaughlin et al., 1996). Fission track ages give an uplift rate of 0.8 mm/year over the last 4.6 million years (Bürgmann et al., 1994). The Foothills thrust belt dips to the southwest, toward the San Andreas fault, and it includes the Stanford, Monte Vista,

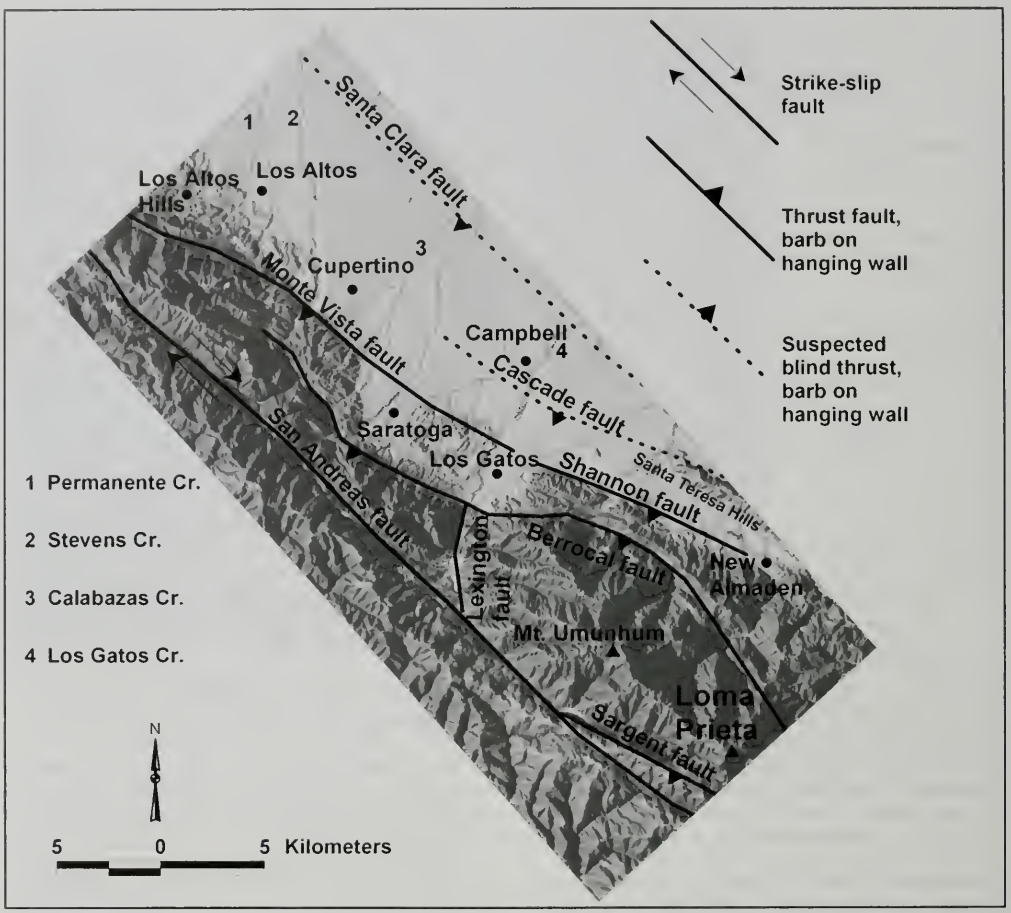

Figure 2. Location of faults in the Foothills thrust belt around the Saratoga embayment.

Shannon, Berrocal, and Sargent faults. These faults offset the Pliocene and Pleistocene Santa Clara Formation, and locally offset and deform younger overlying Quaternary sediments and geomorphic surfaces within the range-front communities of Palo Alto, Los Altos Hills, Cupertino, Saratoga, and Los Gatos, located along the southwestern margin of Santa Clara Valley (Sorg and McLaughlin, 1975; McLaughlin et al., 1991, 1999; Hitchcock et al., 1994; Angell et al., 1998).

The up-dip projection of the blind Loma Prieta fault, which is interpreted to have been the source of the 1989 M_w 6.9 Loma Prieta earthquake (Bürgmann et al., 1994), coincides with the Foothills thrust belt. Following the Loma Prieta earthquake, contractional surface deformation was observed to be concentrated along the Foothills thrust belt, apparently due to aseismic slip that occurred during or after the earthquake (Haugerud and Ellen, 1990; Schmidt et al., 1995; Langenheim et al., 1997). Bürgmann et al. (1997) inferred significant postseismic creep on these structures at depth from analysis and modeling of geodetic data.

Faults located northeast of the range-front, beneath Santa Clara Valley, include the Cascade and Santa Clara faults (DWR, 1975). These faults

were inferred on the basis of gravity data (Taylor, 1956) and apparent displacements of buried stream channels and bedrock interpreted from water well-logs (DWR, 1975). The faults are mapped as buried or concealed (Bortugno et al., 1991) and, prior to the 1989 Loma Prieta earthquake, few of the faults were considered significant seismic sources. Hitchcock et al. (1994) revealed evidence of late Quaternary deformation above the Monte Vista and Cascade faults, and Langenheim et al. (1997) showed that gravity and aeromagnetic anomalies coincide with the Foothills thrust belt along the range-front. Angell et al. (1998) demonstrated late Quaternary deformation on the Stanford and Pulgas faults in Palo Alto.

Offset and deformation of late Cenozoic deposits (Sorg and McLaughlin, 1975; McLaughlin et al., 1991, 1999), fission track evidence for rapid late Cenozoic uplift of the Santa Cruz mountain range (Bürgmann et al., 1994), geomorphic evidence of deformation of Quaternary deposits and surfaces (Hitchcock et al., 1994; Angell et al., 1998; Hitchcock and Kelson, 1999), and geophysical features coincident with the range-front faults (Langenheim et al., 1997), indicate that the Foothills thrust belt is tectonically active. Despite the dramatic range-front topography along the southwest side of Santa Clara Valley, individual faults are poorly expressed at the Earth's surface and, to date, paleoseismic investigations have not yielded data on past rupture events (Hitchcock et al., 1994). Thus, the seismic potential of the faults is poorly understood.

Historical records show that a M 6.5 earthquake in 1865 may have occurred on a fault east of the San Andreas fault, possibly along the northeastern flank of the Santa Cruz Mountains (Toppozada and Borchardt, 1998; Tuttle and Sykes, 1992). Focal mechanisms interpreted from instrumental microseismicity (Sorg and McLaughlin, 1975) and aftershocks of the 1989 earthquake (Bürgmann et al., 1994; Zoback et al., 1999) are consistent with motion on low-angle, southwest-dipping thrust faults. In addition, the 1989 Loma Prieta earthquake produced coseismic contractional deformation in several northwest-trending zones along the northeastern flank (Aydin et al., 1992; Schmidt et al., 1995). Based on the magnitude of aseismic deformation of the northeastern Santa Cruz mountains following the 1989 Loma Prieta earthquake, it is possible that a large component of the total slip on the Foothills thrust belt occurs aseismically in association with slip on the nearby San Andreas fault (Angell and Hall, 1993; Hitchcock et al., 1993; Hitchcock and Kelson, 1999).

Below, we describe some of the major faults within the Foothills thrust belt that bound the western margin of Santa Clara Valley.

Sargent fault

The 56-km-long Sargent fault zone (Figure 1) is a northwest-striking, northeast-verging, reverse-oblique fault zone that intersects the San Andreas fault to the north near Lake Elsman and the Calaveras fault to the south beneath the southern Santa Clara Valley near Hollister (Sorg and McLaughlin, 1975). The fault varies in dip from near vertical to less than 30°, averaging about 50°. The fault exhibits a prominent component of right-lateral slip, as shown by geomorphic offsets and fault plane slickensides exposed near Loma Prieta (Bryant et al., 1981). Alluvial gravels of unknown age in the hanging wall are tilted 45° to 50° to the southwest (Sorg and McLaughlin, 1975). The Sargent fault is the locus of contemporary microseismicity with both reverse and strike-slip focal mechanisms (Walter et al., 1996). Prescott and Burford (1976) measured 3 ± 1 mm/year creep along the southern third of the Sargent fault. As is the case with several of the faults in the Foothills thrust belt, the Sargent fault experienced triggered slip during the 1989 M_W 6.9 Loma Prieta earthquake (Aydin et al., 1992). Although a small component of right-normal slip was observed near Lake Elsman reservoir, the overall displacement was right-lateral reverse, southwest side up.

From a trenching investigation along the southern part of the fault, Nolan et al. (1995) calculated a preliminary slip-rate of only 0.6 mm/year and a recurrence interval of 1,200 years for the southernmost part of the fault. However, these estimates are based on poorly constrained stratigraphic data. Based on its proximity to the San Andreas fault, WGNCEP (1996) did not consider the northern two-thirds of the Sargent fault to be an independent seismic source. The southern third of the fault was considered to be a seismogenic structure capable of generating a maximum earthquake of M_W 6.8. To accommodate the uncertainty of whether the Sargent or any other fault in the Foothills thrust system is an independent seismic source, the WGCEP (1999) treated the Foothills thrust system as a source zone rather than discrete seismic sources.

Berrocal fault

The Berrocal fault is located along the Santa Cruz Mountains range-front, between Saratoga and Los Gatos, and extends for a total length of 55 km (Figure 1). Southeast of Los Gatos, the Berrocal fault intersects the Sargent fault. To the northwest, the fault either dies out or merges with the Monte Vista fault (Figure 2). The Berrocal fault is also linked to the San Andreas fault by the north-striking Lexington fault along Los Gatos Creek (McLaughlin et al., 1991). This short fault dips steeply to the east beneath Mt. Umunhum and Sierra Azul, juxtaposing Franciscan rocks and steeply dipping to overturned Plio-Pleistocene Santa Clara Formation. Small earthquakes and some Loma Prieta aftershocks may occur on the Lexington fault. The Berrocal fault dips moderately (35° to 50°) to the southwest, although some strands are steeply dipping and some dip moderately to the northeast, possibly due to rotation of fault planes (McLaughlin et al., 1999). At Wood Road, near downtown Los Gatos, the Berrocal fault displaces late Pleistocene fluvial deposits (McLaughlin et al., 1991). Scattered seismicity along and to the southwest of the mapped fault trace may be related to either the Berrocal fault or a related northeast-vergent blind thrust fault. Significant contractional surface deformation was observed along the Berrocal fault in the Los Gatos and Saratoga areas during the Loma Prieta earthquake (Haugerud and Ellen, 1990; Schmidt et al., 1995; Langenheim et al., 1997).

Monte Vista fault

The 54-km-long Monte Vista fault is one of the primary range-front faults and probably the most extensively studied fault in the Foothills thrust belt (Figure 2). Where exposed, the fault strikes northwest, dips southwest, and places Franciscan, Miocene sediments, Santa Clara Formation, and Pleistocene alluvium over Pleistocene and older strata (Sorg and McLaughlin, 1975; McLaughlin et al., 1991). To the south, the fault merges with the Shannon fault and at its northern end it intersects the San Andreas fault, via the Hermit fault, between Woodside and Redwood City (Angell et al., 1998). Within the towns of Los Altos and Palo Alto, the Monte Vista fault consists of a belt of imbricate northeast-vergent thrust faults dipping 35° to 60° to the southwest (Dibblee, 1966; Cotton and Associates, 1978). Within Cupertino, the Monte Vista fault lies at the base of a prominent northeast-facing escarpment between the towns of Los Altos Hills and Cupertino. Between Calabazas Creek and Saratoga, south of Cupertino, the range-front trends more southerly. In this area, to the west of the range-front, fold axes within the Santa Clara Formation also have southerly trends, suggesting that the Monte Vista fault changes strike, curves to the south, and joins the Berrocal fault along the range-front near Saratoga (Cotton et al., 1980; McLaughlin, 1974; Sorg and McLaughlin, 1975). However, well-logs show that a fault, possibly the southern extension of the Monte Vista fault, displaces bedrock and buried stream channels between Calabazas Creek and Vasona Reservoir, along the eastern edge of the Saratoga-Los Gatos embayment (DWR, 1975). Gravity data also suggest a bedrock offset beneath the alluvial cover between Calabazas Creek and Vasona Reservoir (Taylor, 1956). Therefore, the Monte Vista fault may extend southeastward from the range-front and join the Shannon fault mapped south of Vasona Reservoir by Bailey and Everhart (1964).

Limited exploratory trenching indicates that the Monte Vista fault has accommodated late Quaternary and possibly Holocene displacement (Hitchcock et al., 1994). Directly downstream of the range-front, Permanente Creek parallels the Monte Vista fault and is bordered on the southwest by a series of prominent linear fronts and faceted ridge spurs. The fault trace at the base of these facets thrusts colluvial deposits over fluvial gravel deposited by Permanente Creek. From its relatively poor development, the soil on the colluvial deposits was interpreted as being Holocene in age (McCormick, 1992). Four discontinuous fault traces, expressed as linear depressions or saddles within the Santa Clara Formation to the north of Cupertino, were trenched 0.8 km east of the main trace of the Monte Vista fault (Earth Science Associates, 1978). Northeast-dipping shear zones, exposed in two trenches, offset soil horizons estimated as 3,000 to 5,000 years old based on soil-profile development (Earth Science Associates, 1978). These shear zones may represent a southwest-vergent backthrust rooted in a thrust fault located east of the Monte Vista fault.

Geomorphic mapping by Hitchcock et al. (1994) shows that late Pleistocene fluvial terraces flanking Stevens Creek are deformed into a syncline-anticline pair (Figure 3) that coincides with folds in Tertiary bedrock in the hanging wall of the Monte Vista fault (Sorg and McLaughlin, 1975). The style of late Quaternary deformation affecting these ter-

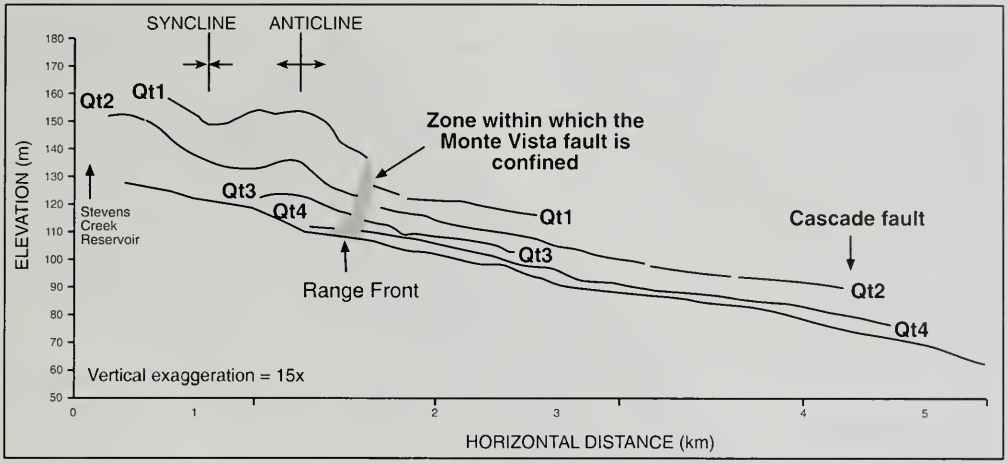

Figure 3. Longitudinal profile of geomorphic surfaces along Stevens Creek east of Stevens Creek Reservoir. Anticline and syncline traces shown on the profile are projected from mapping of Sorg and McLaughlin (1975).

race surfaces is consistent with contractional deformation associated with the Monte Vista or a closely related fault. Based on possible ages for a faulted Qt1 terrace of 60 to 180 ka (120 ± 60 ka), and for a Qf2 alluvial fan offset at the range-front of 11 to 35 ka (23 ± 12 ka), Hitchcock and Kelson (1999) determined a late Pleistocene uplift rate across the Monte Vista fault of 0.12 ± 0.06 mm/year. This is somewhat less than the rate of 0.36 mm/year estimated by Sorg and McLaughlin (1975), which was based on differences in projected stream-terrace heights across the fault, and compatible with rates of 0.1 to 0.2 mm/year similarly derived by McLaughlin et al. (1999). Assuming a 45° fault dip, constrained by the map pattern of the faulted terraces, Hitchcock and Kelson (1999) calculated an average late Pleistocene slip-rate of 0.17 ± 0.09 mm/year for the Monte Vista fault.

Shannon fault

The Shannon fault, which extends from near Saratoga, south to Coyote Creek near New Almaden (Figure 2), consists of several *en echelon*, southwest-dipping, thrust or reverse fault strands and several subsidiary northeast-dipping normal fault strands. Between Saratoga and Blossom Hill, the fault is a 2- to 3-km-wide zone, mapped as four parallel linear strands striking N50°W (Bailey and Everhart, 1964; McLaughlin et al., 1991). Geomorphic investigations provide evidence of probable late Pleistocene deformation associated with these southwest-dipping, northeast-vergent reverse fault strands (Hitchcock et al., 1994).

Southeast of Blossom Hill, the Shannon fault consists of several southwest-dipping reverse faults that strike N75°W and are located between the Santa Teresa Hills and the Berrocal fault (Bailey and Everhart, 1964). Trench exposures at the Senator mine, west of New Almaden, show that the southern segment of the Shannon fault offsets Miocene rock and cuts a paleosol with an estimated late Pleistocene age (McLaughlin et al., 1999). As with the Berrocal, Sargent, and Monte Vista faults, contractional surface deformation occurred along the Shannon fault in the Los Gatos and Campbell areas during the Loma Prieta earthquake.

Cascade fault

The Cascade fault underlies broad alluvial-fans bordering Santa Clara Valley, approximately 2 to 6 km northeast of the Santa Cruz Mountains range-front (Figure 2). Hitchcock et al. (1994) show a strong correlation between the mapped trace of the Cascade fault and fault-related geomorphic features, including vegetation lineaments, closed depressions, linear drainages, stream profile convexities, and high-sinuosity stream reaches, developed in late

Pleistocene and possibly Holocene deposits. Between Los Altos Hills and Los Gatos most of the major streams show longitudinal-profile convexities where they cross the mapped trace of the Cascade fault. In general, the crests of the convexities coincide with the zone of lineaments. These relations suggest late Pleistocene and possibly Holocene uplift associated with this section of the Cascade fault (Hitchcock et al., 1994). These observations provide only indirect information on the sense of slip and no information on the amount and direction of fault dip. Based on similar characteristics and proximity to other faults in the Foothills fault system, it is likely that the Cascade fault is a southwest-dipping, northeast-vergent reverse fault similar to the Monte Vista, Berrocal, and Shannon faults.

Stanford fault zone

Several short, northwest-striking, northeast-vergent thrust and reverse-oblique faults are located at the northern end of the Foothills thrust belt in the vicinity of Palo Alto (Figure 2). These include the Stanford, Hermit, Pulgas, Frenchman's Road, San Juan Hill, and Willow Road Bridge faults (Kovach and Beroza, 1993; Kovach and Page, 1995; Page et al., 1996; Angell et al., 1998). Collectively known as the Stanford fault zone, this is a series of left-stepping *en echelon* fault segments inferred from geomorphic evidence of localized uplift northeast of the range-front and associated faults exposed in bedrock (Angell et al., 1998). These faults apparently link the San Andreas and Monte Vista faults (Angell et al., 1998). The Stanford fault is inferred to be the causative blind thrust fault responsible for the region of uplift and folding affecting Plio-Pleistocene and younger gravels referred to by Kovach and Page (1995) and Page et al. (1996) as the Stock Farm monocline. The Willow Road Bridge fault comprises a zone of multiple shears that juxtapose Eocene and Paleocene mudstone to the southwest and upper Cretaceous mudstone to the northeast. These faults do not affect overlying Quaternary terrace gravels (Brabb and Olson, 1986). The San Juan Hill fault, which may be the southeast continuation of the Pulgas fault, similarly does not cut young terrace gravels and has no topographic expression. The Frenchman's Road fault dips 60° to 70° to the southwest, cutting a broad anticline developed in Miocene and Plio-Pleistocene rocks (Kovach and Page, 1995). The Hermit fault, although marked by a subtle northwest-trending linear topographic depression, shows no evidence for Holocene displacement.

Based on structural and geomorphic analysis of bedrock and Quaternary geologic relationships, seismicity, and quantitative cross section balancing, Angell et al. (1998) show the faults of the Stanford fault zone as a series of southwest-dipping structures, originating from shallow thrust ramps on a fault that roots into the San Andreas at depths greater than 12 to 8 km. Roering et al. (1996), using elastic half-space dislocation theory, model the Stanford fault as a southwest-dipping blind reverse fault beneath the Stock Farm monocline. The monocline folds Plio-Pleistocene Santa Clara Formation and ponds late Quaternary alluvium along its flanks (Angell et al., 1998).

FAULTS ON THE NORTHEAST SIDE OF SANTA CLARA VALLEY (EAST VALLEY THRUSTS)

The northeastern margin of Santa Clara Valley, including the Evergreen Valley, is marked by a northeast-dipping sequence of thrust faults that are part of the East Bay Hills structural domain (Aydin and Page, 1984) or Graymer's (1995) Fremont subzone of the southern Hayward fault (Figure 1). The faults include the Piercy, Coyote Creek, Silver Creek, Evergreen, Quimby, Berryessa, Crosley, and Warm Springs faults (Figure 4).

This series of reverse and reverse-oblique faults bounds the southwest margin of a region of rapid late Cenozoic uplift. Kelson and Simpson (1996) infer a late Pleistocene uplift rate of 1.5 ± 0.5 mm/year for the southern part of the East Bay Hills/Mission Peak area of the Diablo Range based on uplifted fluvial terraces. The Crosley, Berryessa and Warm Springs faults have been interpreted as structures that may transfer slip from the southern Hayward fault to the Calaveras fault (Graymer, 1995). Jones et al. (1994) interpret these faults as a steeply-dipping zone of thrusts that roots in the Calaveras fault at approximately 10 km depth. However, outcrop mapping suggests that many of these faults are moderate to relatively low-angle features that may root into the Calaveras fault at shallower depths. The thrust faults strike about 10° to 15° more westerly than the main strike-slip faults.

Although seismicity in this area is diffuse, cross-sections of relocated microearthquake hypocenters indicate that the seismogenic faults may dip moderately to the east (WCC, 1994). Earthquake focal mechanisms also indicate reverse motion on northwest-striking faults. No large, historical earthquakes have been conclusively attributed to the

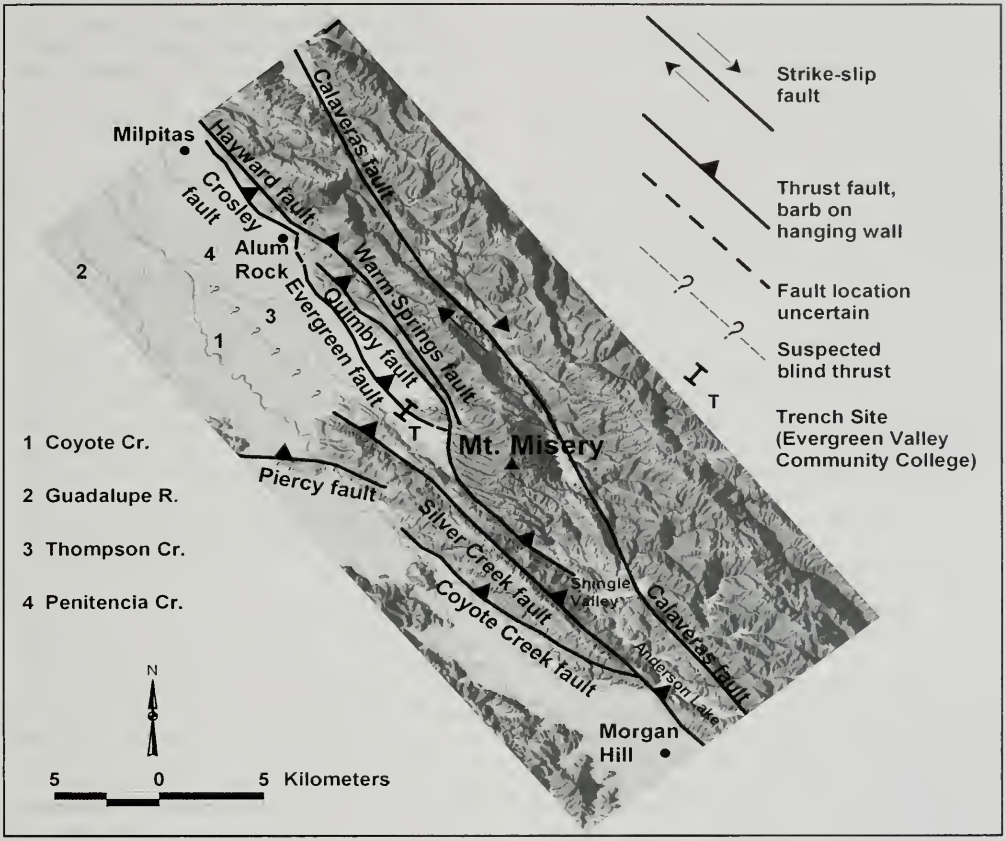

Figure 4. Location of faults in the East Valley thrust system. The location of the paleoseismic trenches shown in Figure 5 is marked.

thrust faults along the eastern Santa Clara Valley margin (Oppenheimer et al., 1990). Jaumé and Sykes (1996) suggest that the 1 July 1911, M 6.2 earthquake may have occurred on a thrust fault parallel to the Calaveras fault; however, anecdotal intensity data indicate that this event probably occurred on the Calaveras fault (Bakun, 1999; Toppozada, 1984).

The range-front that bounds the eastern side of Santa Clara Valley is modified by many large-scale slope failures. The character of the range-front changes from north to south. At its northern end it is relatively diffuse, being fronted by a broad zone of undulating topography. Heading south towards Mount Misery, the range-front becomes more linear and steeper, but is commonly covered by large landslides. The Evergreen Valley, which forms a prominent embayment in the range-front, is separated from the main Santa Clara Valley by a low ridge of hills between the Coyote Creek and Silver Creek faults (Figure 1). South of Evergreen, the range-front steps west and continues as a linear, steep, west-facing escarpment.

To date, there have been relatively few investigations of the thrust faults bounding the eastern side of Santa Clara Valley. Paleoseismic investigations of many of these faults have been inconclusive and, in some cases, it is unclear whether the mapped "fault" trace is of tectonic or landslide origin (e.g., Bryant, 1981b). The location of these reverse faults along the

base of a relatively linear, actively uplifting range-front (Figure 4) indicates that at least some of them are active, potentially seismogenic structures.

At the northern end of the range-front, between the Hayward fault and Evergreen Valley, offsets of geomorphic features, including stream deflections, observed along the faults indicate predominantly right-lateral strike-slip displacement (Bryant, 1980). The Evergreen Valley section of the range-front is marked by fold scarps and uplifted fluvial terrace fragments, indicating a greater component of vertical displacement.

The faults along the eastern margin of Santa Clara Valley are collectively known as the southeast extension of the Hayward fault (WGNCEP, 1996). Herein, these faults are called the East Valley thrust system (Figure 4). The location, geometry, and activity for these faults are discussed below.

Coyote Creek fault

The Coyote Creek fault (Figure 4) is a moderately west-dipping thrust fault that places Mesozoic serpentinite over gravels of the Plio-Pleistocene Santa Clara Formation. The fault extends from Coyote Reservoir east of Gilroy, where it splays from the Calaveras fault, to just south of Metcalf Canyon, where the fault trace dies out. Over much of its length, the Coyote Creek fault follows the range-front along the northeastern side of Santa Clara Valley. Much of the fault trace is obscured by landsliding. Dibblee (1973b) originally mapped the fault as displacing Holocene alluvium. However, Bryant (1981a) concluded that this offset was the result of landsliding and not tectonic faulting. In addition, Bryant (1981a) found no compelling geomorphic evidence for Holocene movement either along the fault trace mapped by Dibblee (1973b), or on parallel fault traces (e.g., the Metcalf fault).

The Piercy fault is located north of Metcalf Canyon, along strike from the Coyote Creek fault (Figure 4). This short, northwest-striking, northeast-dipping thrust fault places Jurassic-Cretaceous serpentinite of the Franciscan Formation over Pleistocene gravels (Rogers and Williams, 1974). As in the case of the Coyote Creek fault, the Piercy fault displays no obvious geomorphic evidence for Holocene or latest Pleistocene movement (Bryant, 1981b).

Despite the lack of paleoseismic evidence for Holocene displacement, the location of the Coyote Creek and Piercy faults along the range-front of the actively uplifting Diablo Range indicates that these are potentially active structures.

Silver Creek fault

The 70-km-long Silver Creek fault (Figure 4) is mapped as a steep, east-dipping oblique reverse fault with an exposed, well-documented southern fault section and an inferred northern section buried beneath late Quaternary sediments of Santa Clara Valley (Bortugno et al., 1991). The southern section of the Silver Creek fault extends approximately 30 km from Anderson Reservoir, northeast of Morgan Hill, where it splays from the Coyote Creek fault to the mouth of the Silver Creek Valley, southwest of the town of Evergreen (Hart et al., 1981). Based on geophysical and well-log data, DWR (1975) mapped the northern section as an approximately 40-km-long fault beneath Santa Clara Valley, extending from Silver Creek Valley to Alameda Creek in Fremont.

The southern section of the Silver Creek fault is geomorphically expressed as linear stream valleys and ridges and as short, discontinuous tonal lineaments in the Plio-Pleistocene Santa Clara Formation. Over 100 trenches have been excavated across the southern trace of the Silver Creek fault (Wiegers and Tryhorn, 1992). Several of these trenches show fault offset of the Plio-Pleistocene Santa Clara Formation. Displacement observed in the trenches includes both right-lateral and reverse faulting. However, identification of unfaulted late Pleistocene alluvium across the fault has been cited as evidence that the fault has not experienced Holocene activity (Bryant, 1981b; Wiegers and Tryhorn, 1992).

The northern section of the Silver Creek fault is mapped based on inferred offset of buried stream channels identified in water-well logs (DWR, 1975). This reach of the fault is buried under Holocene alluvium and has no documented geomorphic expression (Figure 4). There is no evidence that the Silver Creek fault and nearby secondary fault splays influence the flow of groundwater beneath Santa Clara Valley (DWR, 1975). The presence of this fault section remains speculative.

Recent investigations of the Silver Creek fault in Silver Creek Valley have shown that much of the fault is the structural contact at the base of the

Coast Range ophiolite (De Vito, 1995). Exposures in Sliver Creek, however, show a near vertical fault cutting Santa Clara Formation.

The absence of clear Holocene offset and a lack of youthful geomorphic features along the Silver Creek fault indicate that it is either inactive or has a very low slip-rate.

Evergreen fault

The Evergreen fault is an east-dipping reverse or reverse-oblique fault that strikes northwest across the piedmont of the Evergreen Valley, east of San Jose (Figure 4). The fault extends from the southern end of the Evergreen Valley, where it merges with the Quimby fault, northwest along the Evergreen Valley to Penitencia Creek, East San Jose, where it appears to merge with the Crosley fault. Dibblee (1972a, b) first mapped the Evergreen fault based on an exposure in Yerba Buena Creek where Upper Jurassic Knoxville Shale is faulted, northeast-side-up, over Plio-Pleistocene gravels of the Santa Clara Formation. Alluvial fan deposits in Yerba Buena Creek, considered by Dibblee to be Holocene, also were mapped as being vertically offset by the fault. Dibblee also mapped the fault about 5 km northwest of Yerba Buena Creek, where a west-facing scarp truncates late Pleistocene alluvial deposits. The Evergreen fault was mapped as a concealed feature between these two sites.

Subsequent studies have shown that the fault mapped by Dibblee (1972a, b) is more accurately represented as a complex reverse fault zone that may also show evidence of right-lateral slip during the late Quaternary (Reid, 1979; Bryant, 1981b). Herd (cited in Bryant, 1981b) mapped the Evergreen fault as a series of well-defined, but discontinuous, sinuous, east-dipping thrust faults. Aerial photographic interpretation by Bryant (1981b) confirmed the presence of a number of west-facing, discontinuous scarps crossing late Pleistocene fan surfaces, although he stated that some scarps may be erosional in origin. Page (1992) classified the East Evergreen fault as a "marginal thrust", stating that such "young thrusts will probably undergo slippage in the future, most likely in the subsurface but possibly at the surface."

Although marked by prominent scarps, some of which appear to offset Holocene alluvial fan surfaces, trenching studies have not accurately located the fault at its northern end (Bryant, 1981b). The sinuous trace of these scarps suggests that they may be the toes of landslides, and not tectonic features. The southern extent of the fault is marked by a prominent southwest-facing scarp on a late Pleistocene fan surface within the campus of Evergreen Valley Community College. Recent trenching at this site revealed that the Evergreen fault is a moderate to low-angle (less than 45°) thrust fault. The fault displaces Knoxville Shale east-side-up against Santa Clara Formation gravels (WCC, 1994; Fenton et al., 1995). The fault plane was observed to cut up through the Santa Clara Formation gravels and internal paleosol horizons estimated to be late Pleistocene in age (Figure 5). Overlying gravels of unknown age are also warped. WCC (1994) interpreted the trench exposures at Evergreen Valley Community College as indicating that the Evergreen fault experienced coseismic rupture during the late Pleistocene but that this rupture did not propagate to the surface. Rather, it just resulted in warping of the ground surface, creating a fold scarp (Figure 5). Slickensides on the fault surface indicated that fault-slip includes a small component of lateral movement in addition to reverse movement.

Quimby fault

The Quimby fault runs along the base of the range-front bounding the eastern side of the Evergreen Valley (Figure 4). This northeast-dipping fault has a sinuous trace, predominantly concave-east. Most of the fault trace is obscured by large landslides. At its northern end, near Alum Rock, the Quimby fault apparently merges with the Crosley fault beneath an area of extensive landslide deposits (Dibblee, 1972a,c; Helley and Wesling, 1990). At its southern end, the fault merges with the Warm Springs fault at the southern end of the Evergreen Valley. This combined fault then apparently dies out in the Shingle Valley. Some reaches of the Quimby fault are marked by prominent southwest-facing scarps, some of which may be the result of landsliding rather than tectonic faulting (Bryant, 1981b). Evidence for Holocene movement from trenching investigations along the Quimby fault is inconclusive (Bryant, 1981b).

Crosley fault

The Crosley fault was first identified by Dibblee (1973a) as a moderate to steeply northeast-dipping reverse to reverse-oblique fault that places Franciscan and Cretaceous rocks over Plio-Pleistocene

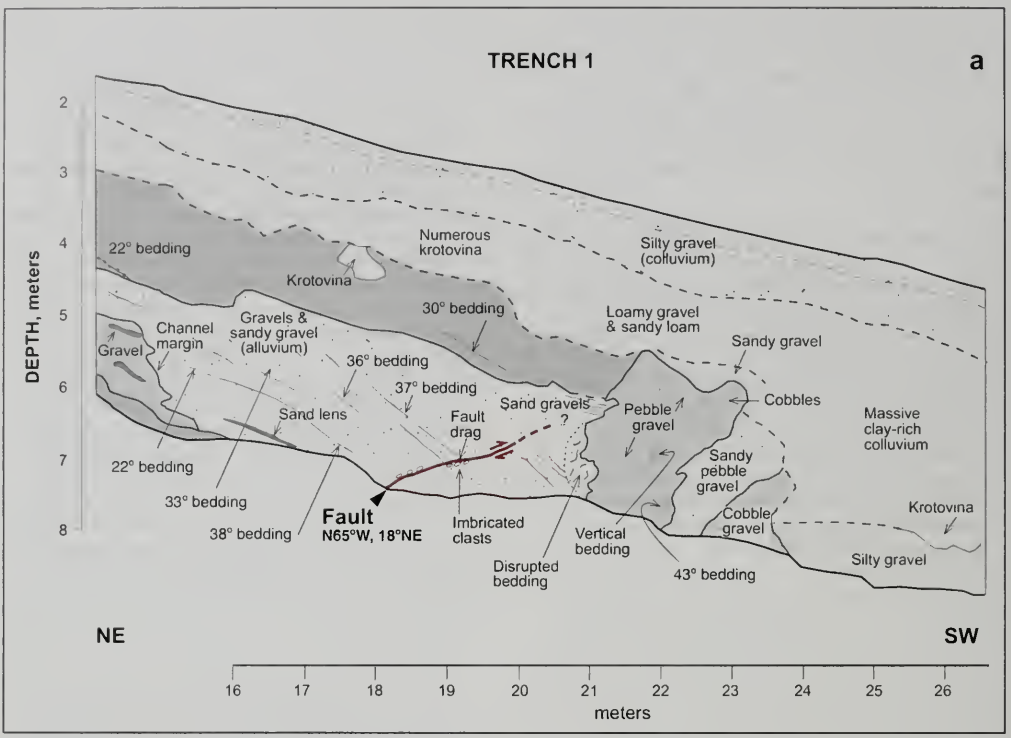

Figure 5. Detail of the Evergreen fault zone exposed in exploratory trenches. (a) Note the complex stratigraphic relationships in the footwall and the progressive steepening of bedding within Santa Clara Formation gravels towards the fault in the hangingwall of Trench 1. The small amount of displacement on the exposed fault (approximately 0.15 m) and the degree of deformation within the gravels to the southwest of the exposed fault plane suggests that there may be another thrust fault located below the reaches of the trench. (b) (on facing page) Trench 2 shows a broader, more complex fault zone in shale bedrock. One fault plane propagates up into overlying colluvium, warping the overlying colluvium-colluvium contact.

Santa Clara Formation (Figure 4). The fault extends from Milpitas, where it splays from the southeast extension of the Hayward fault (Warms Springs fault), to Alum Rock, where it apparently merges with the Quimby fault (Figure 4). The fault generally is located near the base of the west-sloping hills, and is mapped as a concealed fault buried beneath colluvium (Bryant, 1980). Hart et al. (1981) consider the Crosley fault to be active, based on geomorphology and offset Holocene deposits, and a southeast extension of the Hayward fault.

The Crosley fault is characterized by subdued fault scarps suggestive of late Pleistocene or younger surface-faulting, a sinuous map trace, and variations in dip-direction to both northeast and southwest. Trenches across the Crosley fault have exposed offset Holocene soil deposits along northeast-dipping fault planes but often are inconclusive as to the cause of faulting. In many cases, the fault may be associated with local or regional slope instabilities, and may be interpreted as a shallow thrust fault at the toe of a landslide (Bryant, 1980).

Berryessa fault

The Berryessa fault (Figure 4) juxtaposes Plio-Pleistocene Santa Clara Formation against serpen-

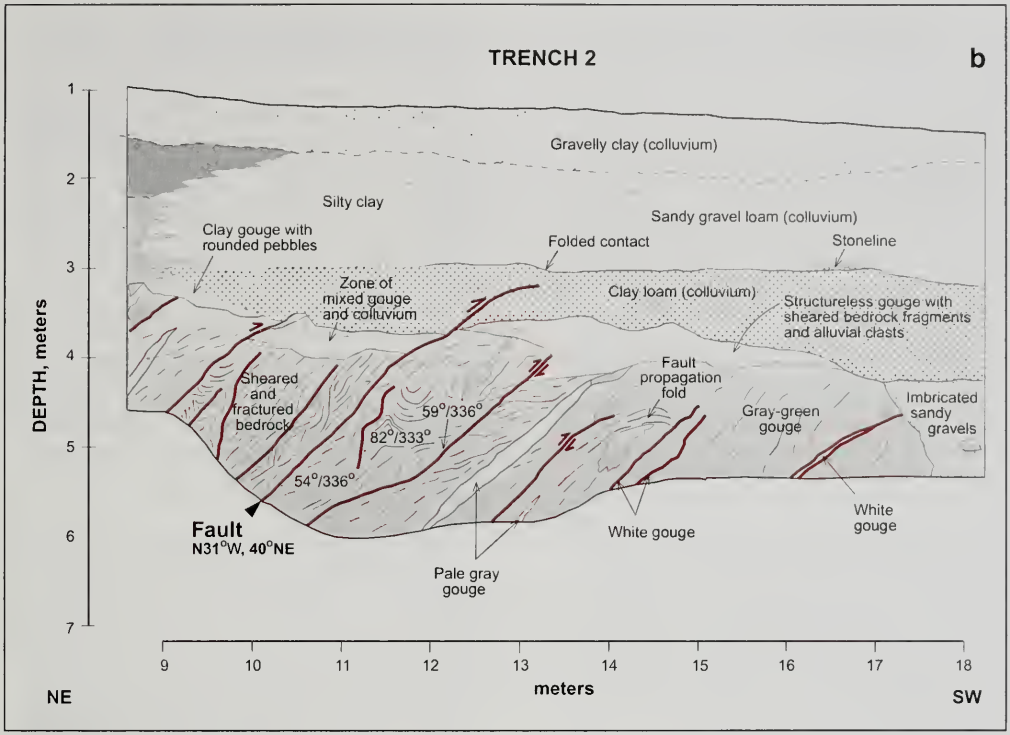

tine of the Franciscan Formation (Bryant, 1980). The fault is mapped by Dibblee (1973a) and Graymer (1995) as a predominantly strike-slip fault, although the mapped trace is characteristic of a moderate to steep east-dipping fault (Bryant, 1980). It is exposed in Berryessa Creek, where a well-developed shear plane striking N15°W and dipping 60° to the southwest thrusts serpentinite over Cretaceous Berryessa Formation. The fault is poorly defined geomorphically and commonly is masked by, or confused with, massive landslides along much of its mapped trace.

Numerous trench studies have found no displacement of Holocene soils by the Berryessa fault (Bryant, 1980). However, a study by Cotton and Associates (1978) mapped what is thought to be fault-related colluvium derived from the Santa Clara Formation. Studies by Norfleet (1995) provide additional data on the recency of faulting for the Berryessa fault. Trench exposures show a northeast-dipping fault zone comprised of clay fault gouge, which juxtaposes Santa Clara Formation on the east and colluvial surficial deposits on the west. However, after review of numerous consultant reports, limited site reconnaissance and aerial photography interpretation, Norfleet (1995) concluded that features associated with the inferred Berryessa fault are landslide-related and not of tectonic origin.

Warm Springs fault (Hayward fault)

The Warm Springs fault is considered to be the southeast extension of the Hayward fault (WGNCEP, 1996). Originally correlated with the Hayward fault by Dibblee (1973a), it was recently renamed the Warm Springs fault by Graymer (1995). Although south of Warm Springs it is mapped as a direct continuation of the Hayward fault, the character of this fault is quite different from that of the actively creeping Hayward fault. The Warm Springs fault runs through the undulat-

ing slopes at the base of the Mission Peak - Mount Misery range-front to the southern end of the Evergreen Valley, where it merges with the Quimby fault (Figure 4). The fault is almost entirely expressed in bedrock or obscured by landslides (Helley and Wesling, 1990). The geomorphic expression of the fault trace is much less well-developed than that of the Hayward fault and there is no evidence for contemporary aseismic creep. There is no clear geomorphic evidence for recent movement along the fault, and unlike the Hayward fault, there is no documented evidence of late Quaternary, right-lateral strike-slip faulting (Bryant, 1980, 1981b).

Evidence for late Pleistocene and Holocene movement on the Warm Springs and other East Valley thrusts is less clear-cut than that for the Foothill thrust belt. The association of these faults with the range-front of the actively uplifting Diablo Range and limited paleoseismic investigations do indicate that at least some of these faults are active and are potentially seismogenic. Trenching investigations indicate that these faults may not rupture to the surface (Figure 5); therefore, identification of individual paleo-events may be very difficult, if not impossible. In addition, extensive landsliding along the range-front has obscured or modified the traces of a number of the faults. Further investigations will be required to understand the seismotectonic character of the East Valley thrusts.

FAULT CHARACTERISTICS AND IMPLICATIONS FOR SEISMIC HAZARDS

The Foothills and East Valley thrust systems are areas of late Quaternary crustal shortening and, as such, are potential seismic sources impacting Santa Clara Valley and surrounding region. In order to quantify associated seismic hazards, it is necessary to characterize these faults in terms of their activity and the maximum earthquake that they can generate.

In the absence of data from historical seismicity, maximum credible earthquakes (MCE) are calculated from empirical relationships among magnitude, fault-rupture length, and fault-plane area (Wells and Coppersmith, 1994). This approach is standard practice in contemporary seismic hazards investigations (WGNCEP, 1996). The maximum earthquake for each fault or fault zone is shown in Table 1, along with parameters such as rupture length, and slip-rate that are used to estimate the MCE and earthquake recurrence.

Fault activity is expressed in terms of slip-rate or recurrence interval. Slip-rates have been determined for a number of faults by relating calculated uplift rates to slip on a planar subsurface fault (e.g. Hitchcock et al., 1994; Table 1). In most cases, these slip-rates are poorly constrained, but they provide order-of-magnitude estimates of fault activity (Table 1). To date, paleoseismic investigations have been unsuccessful in determining paleoevent chronologies for individual faults; thus, there are no direct data with which to calculate recurrence intervals. The lack of success in paleoseismic trenching investigations may be the result of some or all of these faults not producing distinct surface ruptures. Slip on these faults may be more commonly expressed as tilting or warping of the ground surface (Lettis et al., 1997). Paleoseismic investigations of the Evergreen fault show that, even when a discrete fault plane is identified, it may not propagate to the surface (Figure 5) but may die out in a zone of near-surface warping (Fenton et al., 1995).

The Loma Prieta earthquake triggered slip on a number of faults in the Foothills thrust belt (e.g., Bürgmann et al., 1997). If this coseismic displacement accounts for at least a portion of the overall movement recorded on these faults, then the return period for independent events on these thrusts is probably greater than that suggested by long-term averaged geologic slip-rates (Hitchcock and Kelson, 1999). The small amount of offset recorded on these faults following the Loma Prieta earthquake suggests that it may be very difficult to resolve individual events and perhaps impossible to discriminate between triggered slip and slip from independent earthquakes on these faults based on trench exposures alone.

Microseismicity in Santa Clara Valley is so sparse that it is difficult to relate it to specific faults (WCC, 1994; Zoback et al., 1999). Relocation of hypocenters along the northeast side of the San Andreas fault indicates that, in addition to the faults mapped at the surface, there may be active blind thrusts located 3 to 5 km to the northeast of the Foothills thrust belt (Zoback et al., 1999). These structures are located beneath the most densely populated part of Santa Clara Valley.

Based on fault geometry and fault length, Kovach and Beroza (1993) and Angell and Hall (1993) suggest that the thrust faults located to the northeast of the San Andreas fault in the Stanford area are capable of generating M 6+ earthquakes. Zoback et

FAULT	LENGTH (km)	SLIP RATE (mm/yr)	FAULT DIP AND SENSE OF SLIP	MAXIMUM EARTHQUAKE (M_w)	REFERENCES
Foothills thrust belt:					
Sargent	56	0.6 3.0*	30-90° SW reverse-oblique	6.75	Nolan et al. (1995); Prescott & Burford (1976); WGNCEP (1996)
Berrocal	55	0.36	35-50° SW reverse	6.75	Hitchcock et al. (1994)
Monte Vista	30-54	0.4	35-60° SW reverse	6.50-6.75	Hitchcock et al. (1994)
Shannon	48-63	<1.0	~75° SW reverse	6.75	Hitchcock et al. (1994)
Cascade	?	<1.0	<45° SW reverse	6.0+	Hitchcock et al. (1994)
Stanford	18	0.6	up to 70° SW reverse	6.0+	Angell et al. (1998); Kovach & Beroza (1993)
East Valley thrusts:					
Coyote Creek	75	Unknown	30-45° reverse	7.0-7.25	Bryant (1981a,b)
Silver Creek	70	Unknown	30-90° NE reverse	6.75-7.0	De Vito (1995)
Evergreen	30	<0.4	<45° NE reverse	6.50-6.75	Fenton et al. (1995)
Quimby	40-60	Unknown	<30° NE reverse	6.75	Bryant (1981b)
Crosley	20-25	Unknown	40-70° NE reverse-oblique	6.50	Bryant (1980); Hart et al. (1981)
Berryessa	20	Unknown	~60° NE reverse-oblique	6.50	Bryant (1980)
Warm Springs	26	3**	<90° NE reverse-oblique	6.50	WGNCEP (1996)

*contemporary creep rate measured along the southern end of the fault.
**right-lateral slip rate assigned to the SE extension of the Hayward fault (Working Group on Northern California Earthquake Potential, 1996).

Table 1. Fault characteristics for the Foothills thrust belt and East Valley thrusts

al. (1999) suggest that we cannot ignore the possibility of the entire length of the Foothills thrust belt rupturing in a single, complex event, generating a M 7+ earthquake. However, such an event is considered to be very unlikely (WGCEP, 1999). Although the largest and most prominent seismic hazard for Santa Clara Valley remains a large earthquake on either the San Andreas or a related strike-slip fault, the Foothills thrust belt and the East Valley thrust systems pose a significant seismic hazard to the region. The discordance between thrust fault seismicity and mapped thrust fault traces, in addition to the lack of geomorphic or seismologic indicators of the Loma Prieta rupture plane, raises the possibility that the next large, damaging earthquake in Santa Clara Valley may occur on a fault that we have yet to recognize.

The characterization of the active thrust faults of Santa Clara Valley is far from complete. Further detailed investigations are required to characterize the styles of fault deformation and the timing of fault movement.

CONCLUSIONS

The recent investigations described above have shown that the margins of Santa Clara Valley are flanked by a pair of distinct, active thrust or reverse-oblique fault systems. The Foothills thrust belt along the southwest margin of the valley bounds the northeast flank of the Santa Cruz Mountains uplift and consists of a series of northeast-verging thrust and reverse-oblique faults that display abundant geomorphic evidence for movement during the late Pleistocene and possibly Holocene. Individual faults are capable of generating MCEs of M_w 6.25 to

M_w 6.75. Slip-rates on individual faults, calculated from geomorphic offsets, are less than 1 mm/year. The northeastern valley margin is bounded by a series of northwest-striking, southwest-vergent thrust faults that occupy the restraining stepover between the Hayward and Calaveras faults. These faults have geomorphic and paleoseismic evidence of being active during the late Pleistocene. Evidence of Holocene movement on many of these faults is not clear. Although these faults have traditionally been thought of as being the southeast extension of the Hayward fault, the sense of slip on these structures is reverse faulting and the slip-rates on individual faults is considerably lower than that of the Hayward fault.

The thrust faults on both valley margins probably root into the adjacent strike-slip faults: the San Andreas for the Foothills thrust belt, and the Hayward and Calaveras for the East Valley thrusts. The proximity of some of the thrust faults to the main strike-slip faults, coupled with the moderate dip on the thrust fault planes, indicates that they may merge at depths of only a few kilometers. Thus, they may not be independent seismic sources. Triggered slip observed in the Foothills thrust belt following the 1989 Loma Prieta earthquake may be the dominant mode of deformation on these structures (Hitchcock and Kelson, 1999). The broad topographic warping and apparent lack of well-defined, discrete fault scarps along many of these faults indicate that they may not pose a surface-faulting hazard *per se*, but they may still cause localized warping associated with the coseismic growth of folds and fold scarps. However, it should be cautioned that investigations of these faults are still incomplete, and that further detailed geomorphic, paleoseismic, geological, and seismological studies are required to understand the potential seismic hazards associated with these thrusts.

ACKNOWLEDGMENTS

We thank Bill Lettis for encouraging us to write this paper. Jeff Unruh and Michael Angell provided helpful reviews and advice. Ivan Wong and Bill Lettis also reviewed earlier drafts of the manuscript. Horacio Ferriz, Robert Anderson, and Steve Stryker provided welcome editorial guidance. Fumiko Goss and Doug Wright prepared the figures. Fenton thanks Dave Simpson, Tom Sawyer, Janet Sawyer, Tom Kolbe, Carl Wentworth, Chris Wills, Ken Weaver, and George Ford for field assistance and useful discussions. Hitchcock wishes to thank Keith Kelson, Robert McLaughlin, Edward Helley, and Steve Thompson. Hitchcock's research was funded in part by the National Earthquake Hazards Reduction Program, under U.S. Geological Survey grant 1434-92-G-2220.

AUTHORS PROFILE

Dr. Clark Fenton is a Senior Seismic Geologist with URS Corporation with 9 years of geologic, paleoseismic, and seismic hazard experience. His areas of expertise include paleoseismology, probabilistic seismic hazard assessment, and fault rupture hazard analysis. He has carried out geologic and seismic hazard investigations on every continent with the exception of Antarctica.

Mr. Chris Hitchcock, Senior Project Geologist with William Lettis & Associates, Inc., is a Certified Engineering Geologist experienced in the application of geologic and hydrologic techniques to seismic hazard, water supply, and engineering geology investigations. He has evaluated seismic and engineering hazards, including earthquake-related ground failures and slope instability, for both regional hazard maps and site-specific investigations.

SELECTED REFERENCES

Angell, M. and Hall, N.T., 1993, Compressive structures along the San Andreas fault in northern California and implications for seismic hazard assessment: Seismological Research Letters, v. 64, p. 50.

Angell, M., Hanson, K. and Crampton, T., 1998, Characterization of Quaternary contractional deformation adjacent to the San Andreas fault, Palo Alto, California: Geomatrix Consultants, NEHRP Final Technical Report Award No. 1434-95-G-2586, 70 p.

Aydin, A. and Page, B.M., 1984, Diverse Pliocene-Quaternary tectonics in a transform environment, San Francisco Bay region, California: Geological Society of America Bulletin, v. 95, p. 1,303-1,317.

Aydin, A., Johnson, A.M. and Fleming, R.W., 1992, Right-lateral-reverse surface rupture along the San Andreas and Sargent faults associated with the October 17, 1989, Loma Prieta, California, earthquake: Geology, v. 20, p. 1,063-1,067.

Bailey, E.H. and Everhart, D.D., 1964, Geology and quicksilver deposits of the New Almaden District, Santa Clara County, California: U.S. Geological Survey Professional Paper 360, 260 p.

Bakun, W.H., 1999, Seismic activity of the San Francisco Bay region: Bulletin of the Seismological Society of America, v. 89, p. 764-784.

Bortugno, E.J., McJunkin, R.D. and Wagner, D.L., 1991, Map showing recency of faulting, San Francisco-San Jose Quadrangle, California: California Division of Mines and Geology, Geologic Map of the San Francisco-San Jose Quadrangle, 1:250,000.

Bryant, W.A., 1980, Southeast segment of the Hayward fault, Crosley fault, Berryessa fault, Clayton fault, SE segment of the Mission fault and inferred break of 1868: California Division of Mines and Geology, Fault Evaluation Report 105, 26 p.

Bryant, W.A., 1981a, Calaveras, Coyote Creek, Animas, San Felipe, and Silver Creek faults: California Division of Mines and Geology, Fault Evaluation Report 122, 13 p.

Bryant, W.A., 1981b, Southeast segment of the Hayward fault, Evergreen fault, Quimby fault, Silver Creek fault, and Piercy fault: California Division of Mines and Geology Fault Evaluation Report FER-106, 20 p.

Bryant, W.A., Smith, D.P. and Hart, E.W., 1981, Sargent, San Andreas and Calaveras fault zone - evidence for recency in the Watsonville East, Chittenden and San Felipe quadrangles, California: California Division of Mines and Geology, Open-File Report 81-7, 3 map sheets, 1:24,000 scale.

Bürgmann, R., Arrowsmith, R., Dumitru, T., and McLaughlin, R., 1994, Rise and fall of the Southern Santa Cruz Mountains, California, from fission tracks, geomorphology, and geodesy: Journal of Geophysical Research, v. 99, p. 20,181-20,202.

Bürgmann, R., Segall, P., Lisowski, M., and Svarc, J., 1997, Postseismic strain following the 1989 Loma Prieta earthquake from GPS and leveling measurements: Journal of Geophysical Research, v. 102, p. 4,933-4,955.

Cotton and Associates, 1978, Analysis of the geotechnical hazards of Los Altos Hills, Santa Clara County, California: Consultant's report to the Town of Los Altos Hills, 42 p.

Cotton, W.R., Hay, E.A., and Hall, N.T., 1980, Shear couple tectonics and the Sargent-Berrocal fault system in northern California: in Streitz, R. and Sherburne, R. (eds.), Studies of the San Andreas fault zone in Northern California, California Division of Mines and Geology Special Report 140.

Crane, R., 1995, Geology of the Mount Diablo region: in Crane, R. and Lyon, C., (eds.), Map accompanying Geology of the Mount Diablo Region Field Trip Guidebook, Northern California Geological Society, scale 1:48,000.

De Vito, L.A., 1995, Compressional folding and faulting in the vicinity of Silver Creek Valley, southeast San Jose, California: in Sangin,s, E.M., Andersen, D.W. and Buising, A.B. (eds.), Recent Geologic Studies in the San Francisco Bay Area, Society of Economic and Petroleum Geologists, Pacific Section, v. 76, p. 125-140.

Dibblee, T.W., 1966, Geologic map of the Palo Alto quadrangle, California: California Division of Mines and Geology Map Sheet 8, scale 1:62,500.

Dibblee, T.W., 1972a, Preliminary geologic map of the San Jose East quadrangle, Santa Clara County, California: U.S. Geological Survey Open-File Map, scale 1:24,000.

Dibblee, T.W., 1972b, Preliminary geologic map of the Lick Observatory quadrangle, Santa Clara County, California: U.S. Geological Survey Open-File Map, scale 1:24,000.

Dibblee, T.W., 1972c, Preliminary geologic map of the Milpitas quadrangle, Alameda and Santa Clara Counties, California: U.S. Geological Survey Open-File Map, scale 1:24,000.

Dibblee, T.W., 1973a, Preliminary geologic map of the Calaveras Reservoir quadrangle, Alameda and Santa Clara Counties, California, U.S. Geological Survey Open-File Map, scale 1:24,000.

Dibblee, T.W., 1973b, Preliminary geologic map of the Mt. Sizer quadrangle, Santa Clara County, California: U.S. Geological Survey Open-File Map, scale 1:24,000.

Dolan, J.F., Sieh, K., Rockwell, T.K., Guptill, P. and Miller, G., 1997, Active tectonics, paleoseismology, and seismic hazards of the Hollywood fault, northern Los Angeles basin, California: Geological Society of America Bulletin, v. 109, p. 1,595-1,616.

DWR (California Department of Water Resources), 1975, Evaluation of groundwater resources: South San Francisco Bay: California Department of Water Resources Bulletin 118-1, v. 3 (Northern Santa Clara County Area).

Earth Science Associates, 1978, West reservoir geotechnical feasibility investigation: Consultant's report to Santa Clara Water District.

Fenton, C.H., Wong, I.G., and Sawyer, J.E., 1995, Geological and seismological investigations of the Evergreen fault, southeastern San Francisco Bay area, California: American Association of Petroleum Geologists Bulletin, v. 79, p. 584.

Graymer, R., 1995, Geology of the southeast San Francisco Bay area hills, California: in Sangin,s, E.M., Andersen, D.W. and Buising, A.B. (eds.), Recent Geologic Studies in the San Francisco Bay Area, Society of Economic and Petroleum Geologists, Pacific Section, v. 76, p. 115-124.

Graymer, R.W., Jones, D.L. and Brabb, E.E., 1995, Geologic map of the Hayward fault zone, Contra Costa, Alameda, and Santa Clara Counties, California: A digital database: U.S. Geological Survey, Open-File Report, 1:50,000.

Hart, E.W., 1994, Fault-rupture hazard zones in California, Alquist-Priolo Earthquake Fault Zoning Act with index to Earthquake Fault Zones maps: California Division of Mines and Geology, Special Publication 42, 33 p.

Hart, E.W., Bryant, W.A., Smith, T.C., Bedrossian, T.L. and Smith, D.P., 1981, Summary report: fault evaluation program, 1979-1980 area (southern San Francisco Bay region): California Division of Mines and Geology Open File Report 81-3, 12 p.

Haugerud, R. A., and Ellen, S. D., 1990, Coseismic ground deformation along the northeast margin of the Santa Cruz Mountains: in Schwartz, D. P., and Ponti, D. J., (eds.), Field guide to neotectonics of the San Andreas fault system, Santa Cruz Mountains, U.S. Geological Survey Open-File Report 90-274, p. 32-37.

Helley, E.J. and Wesling, J.R., 1990, Quaternary geologic map of the San Jose East quadrangle, Santa Clara County, California: U.S. Geological Survey Open-File Report 90-427, 1:24,000 scale map + 14 p.

Hitchcock, C.S. and Kelson, K.I., 1999, Growth of late Quaternary folds in southwest Santa Clara Valley, San Francisco Bay area, California: Implications of triggered slip for seismic hazard and earthquake recurrence: Geology, v. 27, p. 387-390.

Hitchcock, C. S., Kelson, K. I., and Thompson, S. C., 1993, Geomorphic analyses of late Quaternary range-front deformation, northeastern margin of the Santa Cruz Mountains, California [abs]: EOS, v. 74, no. 43, p. 433.

Hitchcock, C. S., Kelson, K. I., and Thompson, S. C., 1994, Geomorphic investigations of deformation along the northeastern margin of the Santa Cruz Mountains: U.S. Geological Survey Open-File Report 94-187, 52 p.

Jaumé, S.C. and Sykes, L.R., 1996, Evolution of moderate seismicity in the San Francisco Bay region, 1850 to 1993: seismicity changes related to the occurrence of large and great earthquakes: Journal of Geophysical Research, v. 101, p. 765-789.

Jayko, A.S. and Lewis, S.D. (eds.), 1996, Toward assessing the seismic risk associated with blind faults, San Francisco Bay region: U.S. Geological Survey Open-File Report 96-267, 188 p.

Jones, D.L., Graymer, R., Wang, C., McEvilly, T.V. and Lomax, A., 1994, Neogene transpressive evolution of the California Coast Ranges: Tectonics, v. 13, p. 561-574.

Kelson, K.I. and Simpson, G.D., 1996, Late Quaternary deformation of the southern East Bay Hills, Alameda County, CA: in Jayko, A.S. and Lewis, S.D. (eds.), Toward assessing the seismic risk associated with blind faults, San Francisco Bay Region, U.S. Geological Survey Open-File Report 96-267, p. 110-118.

Kovach, R.L. and Beroza, G.C., 1993, Seismic potential from reverse faulting on the San Francisco peninsula: Bulletin of the Seismological Society of America, v. 83, p. 597-602.

Kovach, R.L. and Page, B.M., 1995, Seismotectonics near Stanford University: California Geology, v. 48, p. 91-98.

Langenheim, V.E., Schmidt, K.M. and Jachens, R.C., 1997, Coseismic deformation during the 1989 Loma Prieta earthquake and range-front thrusting along the southwestern margin of the Santa Clara Valley, California: Geology, v. 25, p. 1,091-1,094.

Lettis, W.R. and Hanson, K.L., 1991, Crustal strain partitioning: implications for seismic-hazard assessment in western California: Geology, v. 19, p. 559-562.

Lettis, W.R., Wells, D.L. and Baldwin, J.N., 1997, Empirical observations regarding reverse earthquakes, blind thrust faults, and Quaternary deformation: Are blind thrusts truly blind?: Bulletin of the Seismological Society of America, v. 87, p. 1,171-1,198.

Lisowski, M., Savage, J.C. and Prescott, W.H., 1991, The velocity field along the San Andreas fault in California: Geological Society of America Abstracts with Programs, v. 23, p. A313.

McCormick, W., 1992, Personal communication, Earth Systems Consultants.

McLaughlin, R.J., 1974, The Sargent-Berrocal fault zone and its relation to the San Andreas fault system in the southern San Francisco Bay region and Santa Clara Valley, California: U.S. Geological Survey Journal of Research, v. 2, p. 593-598.

McLaughlin, R.J., Clark, J.C., Brabb, E.E., and Helley, E.J., 1991, Geologic map and structure sections of the Los Gatos 7.5' quadrangle, Santa Clara and Santa Cruz Counties, California: U.S. Geological Survey Open-File Report 91-593, 45 p., scale 1:24,000.

McLaughlin, R. J., Sorg, D. H., and Helley, E. J., 1996, Constraints on slip histories of thrust faults of the southwestern San Francisco Bay area from geologic mapping investigations: in Jayko, A. S., and Lewis, S. D., (eds.), Toward assessing the seismic risk associated with blind faults, U.S. Geological Survey Open-File Report 96-267, p. 65-70.

McLaughlin, R.J., Langenheim, V.E., Schmidt, K.M., Jachens, R.C., Standley, R.G., Jayko, A.S., McDougall, K.A., Tinsley, J.S. and Valin, Z.C., 1999, Neogene contraction between the San Andreas and the Santa Clara Valley, San Francisco Bay region, California: International Geology Review, v. 41, p. 1-30.

Norfleet, 1995, Final report, Phase IA regional geologic study of the Special Geologic Hazard Study Area: Consultant's report for the City of San Jose, Norfleet Consultants Project Number 950902, 145 p.

Nolan, J.M., Zinn, E.N. and Weber, G.E., 1995, Paleoseismic study of the southern Sargent fault, Santa Clara and San Benito Counties, California: U.S. Geological Survey, NEHRP Final Technical Report Award No. 1434-94-G-2466, 23 p.

Olson, J.A. and Zoback, M.L., 1998, Source character of microseismicity in the San Francisco Bay block, California, and implications for seismic hazard: Bulletin of the Seismological Society of America, v. 88, p. 543-555.

Oppenheimer, D.H., Bakun, W.H. and Lindh, A.G., 1990, Slip partitioning of the Calaveras fault, California, and prospects for future earthquakes: Journal of Geophysical Research, v. 95, p. 8,483-8,498.

Page, B.M., 1992, Tectonic setting of the San Francisco Bay region: in Borchardt, G., Hirschfeld, S.E., Lienkaemper, J.J., McClellan, P., Williams, P.L. and Wong, I.G. (eds.), Proceedings of the Second Conference on Earthquake Hazards in the Eastern San Francisco Bay Area, California Department of Conservation, Division of Mines and Geology, p. 1-7.

Page, B.N., Ingle, J.C., jr. and Kovach, R.L., 1996, Quaternary diapir of claystone in faulted anticline, Stanford, California: California Geology, v. 49, p. 55-67.

Page, B.M., Thompson, G.A. and Coleman, R.G., 1998, Late Cenozoic tectonics of the central and southern Coast Ranges of California: Geological Society of America Bulletin, v. 110, p. 846-876.

Prescott, W.H. and Burford, R.O., 1976, Slip on the Sargent fault: Bulletin of the Seismological Society of America, v. 66, p. 1,013-1,016.

Reid, G.O., 1979, Faulting in the Evergreen area, San Jose, California: in Recent deformation along the Hayward, Calaveras, and other fault zones, Eastern San Francisco Bay Region, California: Geological Society of America Guidebook, 75th Annual Cordilleran Section Meeting, San Jose, California, p. 9-24.

Roberts, C.W. and Jachens, R.R., 1993, Isostatic residual gravity map of the San Francisco Bay area, California: U.S. Geological Survey Geophysical Investigation Map GP-1006,

Roering, J.J., Arrowsmith, J.R., and Pollard, D.D., 1996, Characterizing the deformation and seismic hazard of a blind thrust fault near Stanford, California: Coseismic elastic modeling: in Jayko, A.S. and Lewis, S.D. (eds.), Toward assessing the seismic risk associated with blind faults, San Francisco Bay Region, U.S. Geological Survey Open-File Report 96-267, p. 41-44.

Rogers, T.H. and Williams, J.W., 1974, Potential seismic hazards in Santa Clara County, California: California Division of Mines and Geology, Special Report 107, 39 p.

Schmidt, K. M., Elllen, S. D., Haugerud, R. A., Peterson, D. M., and Phelps, G. A., 1995, Breaks in pavement and pipes as indicators of range-front faulting resulting from the 1989 Loma Prieta earthquake near the southwest margin of the Santa Clara Valley, California: U.S. Geological Survey Open-File Report 95-820, 33 p.

Sorg, D. H., and McLaughlin, R. J., 1975, Geologic map of the Sargent-Berrocal fault zone between Los Gatos and Los Altos Hills, Santa Clara County, California: U.S. Geological Survey Map MF-643, scale 1:24,000.

Taylor, S. G., 1956, Gravity investigation of the southern San Francisco Bay area, California: Unpublished Ph.D. Thesis, Stanford University, 105 p.

Toppozada, T.R., 1984, History of earthquake damage in Santa Clara County and comparison of the 1911 and 1984 earthquakes: in Bennett, J.H. and Sherburne, R.W. (eds.), The 1984 Morgan Hill, California earthquake, California Division of Mines and Geology Special Publication No. 68, p. 237-248.

Toppozada, T.R. and Borchardt, G., 1998, Re-evaluation of the 1836 "Hayward fault" and 1836 San Andreas fault earthquakes: Bulletin of the Seismological Society of America, v. 88, p. 140-159.

Tuttle, M. and Sykes, L., 1992, Re-evaluation of the 1838, 1865, 1868, and 1890 earthquakes in the San Francisco Bay area: in Borchardt, G., Hirschfeld, S.E., Lienkaemper, J.J., McClellan, P., Williams, P.L. and Wong, I.G. (eds.), Proceedings of the Second Conference on Earthquake Hazards in the Eastern San Francisco Bay Area, California Department of Conservation, Division of Mines and Geology, p. 81-89.

Walter, S.R., Oppenheimer, D.H., and Mandel, R.I., 1996, Significant earthquake clusters, 1967-1993, San Francisco-San Jose quadrangle: U.S. Geological Survey Miscellaneous Investigation Series Map I-2580, scale 1: 250,000.

Wells, D.L. and Coppersmith, K.J., 1994, New empirical relationships among magnitude, rupture length, rupture width, rupture area, and surface displacement: Bulletin of the Seismological Society of America, v. 84, p. 974-1,002.

Wiegers, M.O. and Tryhorn, A.D., 1992, Fault rupture studies along the Silver Creek fault, south San Jose, California: in Borchardt, G., Hirschfeld, S.E., Lienkaemper, J.J., McClellan, P., Williams, P.L. and Wong, I.G. (eds.), Proceedings of the Second Conference on Earthquake Hazards in the Eastern San Francisco Bay Area, California Department of Conservation, Division of Mines and Geology, p. 225-230.

WCC (Woodward-Clyde Consultants), 1994, Geologic and Seismologic evaluation of the Evergreen fault, Evergreen Valley College, San Jose, California: Consultant's report to San Jose/Evergreen Community College District, 29 p.

WGCEP (Working Group on California Earthquake Probabilities), 1990, Probabilities of large earthquakes in the San Francisco Bay region, California: U.S. Geological Survey, Circular 1053, 51 p.

WGCEP (Working Group on California Earthquake Probabilities), 1999, Earthquake probabilities in the San Francisco Bay region: 2000 to 2030 - A summary of findings: U.S. Geological Survey Open-File Report 99-517, 52 p.

WGNCEP (Working Group on Northern California Earthquake Potential), 1996, Database of potential sources for earthquakes larger than magnitude 6 in northern California: U.S. Geological Survey, Open-File Report 96-705, 53 p.

Zoback, M.L., Jachens, R.C. and Olson, J.A., 1999, Abrupt along-strike change in tectonic style: San Andreas fault zone, San Francisco peninsula: Journal of Geophysical Research, v. 104, p. 10,719-10,742.

ACTIVE FAULTING ASSOCIATED WITH THE SOUTHERN CASCADIA SUBDUCTION ZONE IN NORTHERN CALIFORNIA

HARVEY M. KELSEY[1]

ABSTRACT

This review paper focuses on the Quaternary tectonics of northern California, from the California/Oregon border south to the latitude of Point Delgada, 30 km south of Cape Mendocino. There are five sources of seismic shaking in northern California: the Mendocino fault, faults within the Gorda plate, faults within the North American plate ("upper plate"), the Cascadia subduction zone, and faults belonging to the San Andreas fault system. The earthquakes felt most often come from Gorda plate and Mendocino fault sources, with epicenters offshore. However, the maximum potential for seismic shaking comes from thrust faults within the upper plate, the Cascadia subduction zone and faults of the San Andreas fault system, even though earthquakes from these sources occur less frequently. The greatest density of upper-plate faults and folds in northern California, and the greatest concentration of previous paleoseismic study, is in the Humboldt Bay region. Important upper-plate thrust faults include the Little Salmon fault and the five strands of the Mad River fault zone. The thrust faults have Holocene scarps, and trenches across these scarps yield information on earthquake recurrence in the late Holocene. Earthquakes on the Little Salmon fault recur hundreds of years apart and earthquakes on the individual thrust faults of the Mad River fault zone recur thousands of years apart. Together these thrust faults accommodate contraction of the upper plate, which reflects partial coupling of the upper plate to the subducting Gorda plate along the Cascadia subduction zone. Multiple episodes of coseismic subsidence have been documented through buried wetland soils along the margins of Humboldt Bay and in the Eel River valley immediately landward of the coastal dunes. This abrupt subsidence records intermittent earthquakes on the Cascadia subduction zone and on the upper-plate thrust faults that may rupture in conjunction with the subduction zone. Where the Cascadia subduction zone is closest to the coast, near Cape Mendocino, subduction-zone-related coseismic vertical deformation is uplift. However, going northward from the Cape Mendocino area, the Cascadia subduction zone diverges oceanward from the coast and coastal coseismic deformation is subsidence. The magnitude of coseismic subsidence probably is influenced, during some earthquakes, by deformation of upper-plate thrust faults and associated folds.

INTRODUCTION

The purpose of this paper is to describe active faulting associated with the southern Cascadia subduction zone in northern California (Figure 1). It constitutes a review of geologic investigations, available as of 1999, that discuss sources of seismic shaking and sources of coseismic ground rupture, subsidence and uplift and also reviews those localities where landforms, outcrops or subsurface logs form the basis for interpretations of ongoing fault-related deformation.

[1]Department of Geology
Humboldt State University
Arcata, CA 95521
hmk1@axe.humboldt.edu

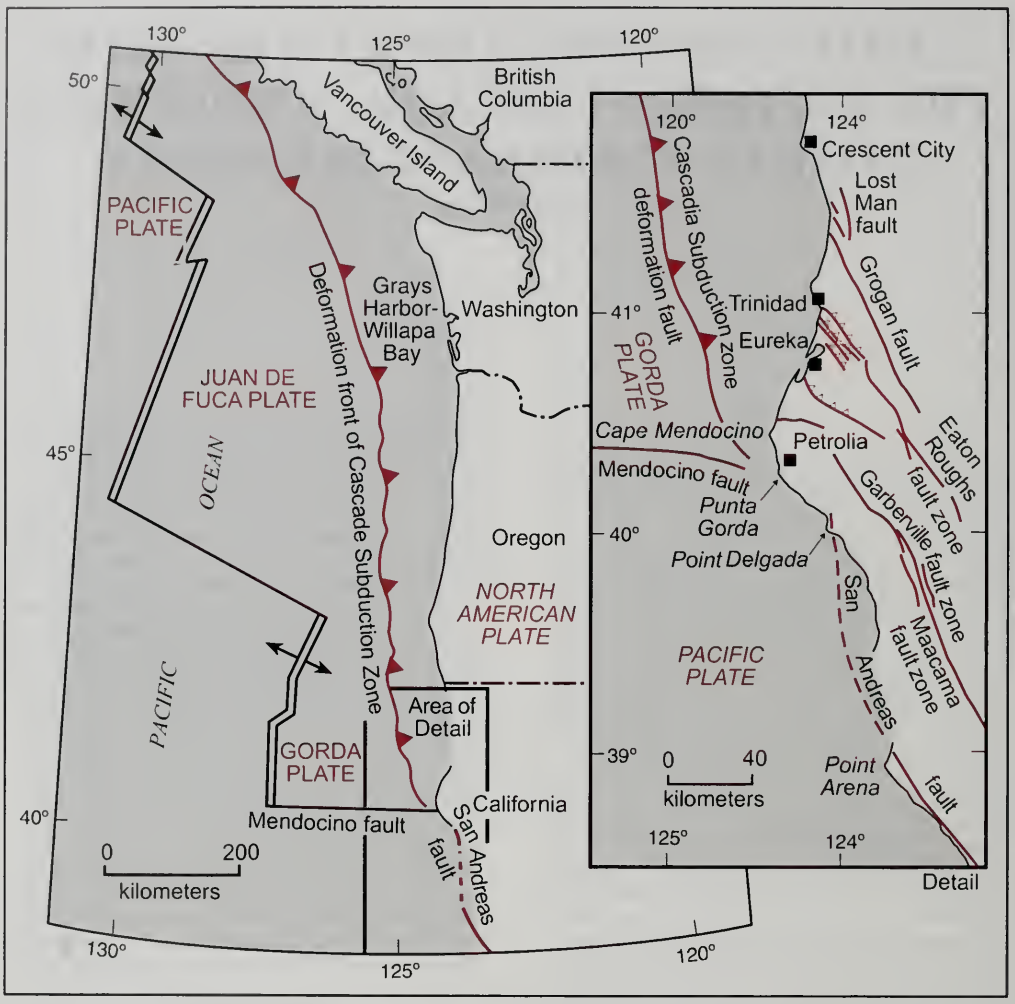

Figure 1. The map on the left shows the location of north coastal California at the southern end of the Cascadia subduction zone and at the northern terminus of the San Andreas fault. The northern terminus of the San Andreas fault, the western end of the Mendocino fault and the southern end of the Cascadia subduction zone meet at a triple junction of plates (Gorda, Pacific and North American plates) in the vicinity of Cape Mendocino. The map on the right depicts the area discussed in this paper, which is the California/Oregon border south to the latitude of Point Delgada (Figure 2); the map also shows the coastal region from Point Delgada south to Point Arena, where the San Andreas fault comes on land. Point Arena is the furthest northern location on the San Andreas fault where there is paleoseismic work (Prentice, 1989; Prentice et al., 1991) from which estimates have been made of recurrence of shaking from earthquakes on the San Andreas fault. Configuration of the subduction zone, Mendocino fault and San Andreas fault in the vicinity of the Mendocino triple junction is taken from Clarke and Carver (1992) and Oppenheimer et al. (1993).

The geographic scope of this review paper extends from the California/Oregon border south to the latitude of Point Delgada, 30 km south of Cape Mendocino (Figure 2). The area of mapped faults extends from the coast eastward to the trace of the Eaton Roughs, Grogan and Surpur Creek faults (Figure 2). The onland geology is integrally linked with the offshore geology and limiting the depiction of faults to structures east of the coast and north of Point Delgada (Figure 2) is an artifact of the paper's defined geographic scope. Excellent papers that describe and interpret the offshore geology include Clarke (1987, 1992), and Clarke and Carver (1992).

Northern coastal California is at the south end of the Cascadia subduction zone, where the Gorda plate is being subducted beneath the North American plate (Figure 1). Further south, the North American plate is juxtaposed against the Pacific plate along the strike-slip San Andreas fault zone. These three plates (Gorda, North American, Pacific) meet at a triple junction near Cape Mendocino (Figure 1). The Mendocino triple junction has migrated northward with time (Dickinson and Snyder, 1979a, 1979b; Furlong, 1993; Furlong and Govers, 1999), and this migration has resulted in the northward impingement into coastal California of the San Andreas and related strike-slip faults that accommodate Pacific/North American relative plate motion (Kelsey and Carver, 1988). The area covered in this paper, although almost entirely north of the latitude of the triple junction, is still subject to seismic shaking from San Andreas-fault-related earthquakes with epicentral locations south of the triple junction region.

Data presented in this paper come from two main sources. The first includes data not published in peer-reviewed literature and consists of U. S. Geological Survey open-file reports, symposium volumes, geotechnical reports with appendices, field trip guidebooks and M. Sc. theses from Humboldt State University, Arcata, California. These references are not readily available through libraries or government agencies, but may be consulted at the sponsoring institution. The second source of data are articles in peer-reviewed journals.

SOURCES OF SEISMICITY IN NORTHERN CALIFORNIA

Dengler et al. (1992) identify five sources of seismicity in north coastal California. Each of the five source regions is part of a seismogenic boundary between crustal plates (Figure 1). Following is a summary of the more extensive discussion of seismicity sources provided by Dengler et al. (1992).

Gorda plate

The Gorda plate, offshore of northern California, is the most common seismic source for earthquakes with Maximum Modified Mercalli intensities of >VII (Dengler et al., 1992). The seismic sources within the Gorda plate are strike-slip faults, and the dominant style of deformation is left-lateral strike-slip faulting. These faults manifest contraction and shear of the Gorda plate as it is subducted at the southern end of the subduction zone. A M_L 7.2 earthquake on the Gorda plate on Nov. 8, 1980, with its epicenter 50 km west of Trinidad, California, is the largest magnitude, historic earthquake caused by a Gorda plate seismic source.

Mendocino fault

The Mendocino fault (Figure 1) is a separate seismic source from the Gorda plate because seismicity on the Mendocino fault occurs on the plate boundary between the Pacific and Gorda plate. The largest historic earthquake clearly associated with the Mendocino fault was a M_W 6.9 on Sept. 1, 1994 (Dengler et al., 1995). However, in most cases it is difficult to ascribe an offshore earthquake definitively to the Mendocino fault or the Gorda plate when the seismic source is near the Mendocino fault. Dengler et al. (1992) estimate that the recurrence interval from combined Gorda and Mendocino fault sources for seismic shaking of Maximum Mercalli intensity VII or greater is 5.5 years, based on a period of observation of about 140 years.

San Andreas fault

The San Andreas fault terminates just south of the Mendocino triple junction (Figure 1). The San Andreas fault is capable of producing magnitude 8 plus earthquakes and did so in 1906 when the ground rupture from the 1906 earthquake extended at least as far north as Shelter Cove (Lawson, 1908; Prentice et al., 1999), 50 km southeast of Cape Mendocino. Although data on the severity of seismic shaking are limited, the 1906 earthquake probably produced the most severe seismic shaking in historic time north of the Mendocino triple junction. Modified Mercalli intensities in southern Humboldt County and the Humboldt Bay region ranged from

VII to IX (Lawson, 1908). The last event on the San Andreas fault prior to 1906 that probably produced severe shaking north of the triple junction occurred sometime after A. D. 1635, based on paleoseismic studies at Point Arena 120 km south of Shelter Cove (Prentice, 1989; Prentice et al. 1991) (Figure 1). The recurrence interval of San Andreas fault earthquakes (hundreds of years) is small compared to the average 5.5 year recurrence interval for earthquakes of Maximum Mercalli intensity >VII on the Gorda plate and Mendocino fault (Dengler et al., 1992). However, maximum Gorda plate and Mendocino fault earthquakes are a unit magnitude or more smaller than possible magnitude maxima for San Andreas fault-generated earthquakes.

The Garberville and the Lake Mountain-Eaton Roughs fault zones are two right-lateral, strike-slip fault zones that occur east of the San Andreas fault proper but are still part of the San Andreas fault system (Kelsey and Carver, 1988) (Figure 2). The two fault zones trend N30°W into the northwest-trending upper-plate thrust faults in the Eel River valley/Humboldt Bay area. Both of these fault zones have lineaments and sag ponds along their traces (Kelsey and Carver, 1988); and this fault-generated topography suggests, despite lack of historic seismicity M_L 5.5 along these traces, that the fault zones are capable of generating earthquakes with surface rupture.

North American plate ("upper plate")

Faults within the North American plate (Figure 2) are sources of seismicity in northern California. Most of these faults are thrust faults and accommodate contraction in the upper plate perpendicular to the direction of Pacific/Gorda plate convergence (Carver, 1987; Clarke and Carver, 1992). This contraction implies that the subduction zone is in part coupled to the upper plate, and that a portion of the convergence of the plates is accommodated by shortening of the upper plate, with the rest being accommodated by slip on the subduction zone. Upper-plate faults are well documented because they have displaced late Neogene sediments near the coast by hundreds of meters (WCA, 1980). Upper-plate faults are well located at the surface because they have moved multiple times in the late Holocene, creating mappable fault scarps (Carver, 1987; Clarke and Carver, 1992). Several of these faults have been identified in boreholes (WCA, 1980) or have been trenched (Carver and Burke, 1988), and details on slip rate and fault geometry are comparatively well known (Table 1). A question that remains unsolved is whether upper-plate thrust faults are independent sources of seismicity, or whether they only move in conjunction with earthquakes on the underlying subduction zone (Clarke and Carver, 1992).

Cascadia subduction zone

The southernmost 150 km of the 1,200-km-long Cascadia subduction zone are offshore of northern California (Figure 1). The subduction zone is capable of producing M_W 8 + earthquakes. During such earthquakes, the locked upper plate is displaced coseismically toward the deformation front, resulting in coseismic uplift nearest the deformation front and coseismic subsidence further landward from the deformation front (Thatcher, 1984).

In January, 1700, a $M_W \sim 9$ subduction zone earthquake affected the coastal zone from northern California to southern British Columbia (Satake et al., 1996; Jacoby et al., 1997; Yamaguchi et al., 1997). Buried tidal marshes along this stretch record the abrupt coastal subsidence that occurred during this earthquake (Atwater et al., 1995). The tidal marshes that were drowned as a consequence of coseismic subsidence were stratigraphically preserved by the buildup of tidal sediment above the subsided marsh.

The A. D. 1700 event may represent the maximum magnitude earthquake for the Cascadia subduction zone as a whole in recent time, and the M_S 7.1 Cape Mendocino earthquake of April 1992 is the strongest event confined to the southernmost extent of the Cascadia subduction zone (Oppenheimer et al., 1993). The Cape Mendocino earthquake caused Modified Mercalli intensities greater than VIII over a 900 km^2 area centered around Cape Mendocino, coseismic uplift of at least 0.5 m along a 25-km portion of the coast (Carver et al., 1994), and $66 million of damage in southern Humboldt County (Oppenheimer et al., 1993).

DISTRIBUTION OF ACTIVE FAULTS AND FOLDS IN NORTHERN CALIFORNIA

Figure 2 shows locations of onshore faults and fold axes of upper-plate structures inferred to be active in the Holocene. These structures extend from the Oregon border to 30 km south of Cape Mendocino. The coastal area in the vicinity of Humboldt Bay is underlain by folded and faulted late Neogene and Quaternary sediment (Figure 2), and it is in this

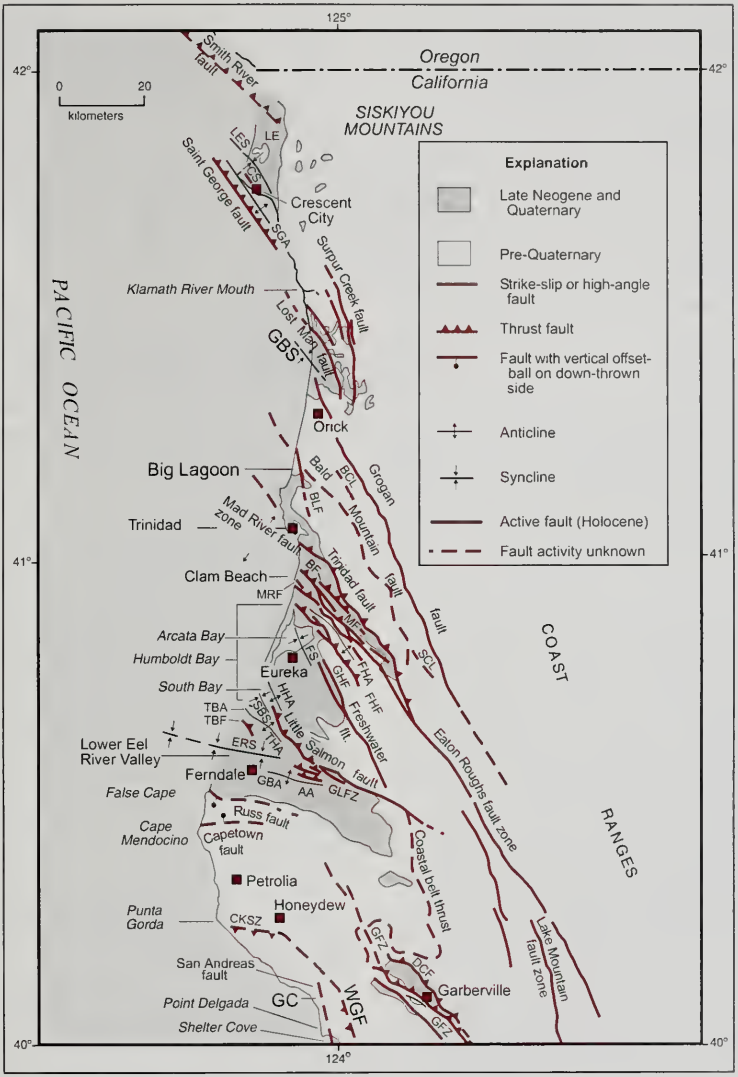

Figure 2. Tectonic map of northern California showing major faults and folds. Sources of data: Kelsey and Carver, 1988; Stone, 1993; Knudsen, 1993; Merritts, 1996; Polenz and Kelsey, 1999. LES, Lake Earl syncline; SGA, Saint George anticline; CS, Cemetery scarp; LE, Lake Earl; GBS, Gold Bluffs syncline; BCL, Bridge Creek lineament; SCL, Snow Camp lineament; BLF, Big Lagoon fault; BF, Blue Lake fault; MF, McKinleyville fault; MRF, Mad River fault; FHA, Fickle Hill anticline; FHF, Fickle Hill fault; GHF, Greenwood Heights fault; FS, Freshwater syncline; HHA, Humboldt Hill anticline; SBS, South Bay syncline; TBA, Table Bluffs anticline; THA, Tompkins Hill anticline; ERS, Eel River syncline; GLFZ, Goose Lake fault zone; AA, Alton anticline; GBA, Grizzly Bluffs anticline; CKSZ, Cooksie shear zone; WGF, Whale Gulch fault; GC, Gitchell Creek; GFZ, Garberville fault zone; DCF, Dean Creek fault.

Fault or fault zone	Time of initiation of faulting (Ma)*	Datum that is offset**	Vertical seperation of datum across fault (m)	Dip of fault	Average slip rate (mm/yr)
Mad River fault zone					
Trinidad fault	0.7	Franciscan/Falor contact	575	40°	1.3
Blue Lake fault	0.7	Franciscan/Falor contact	750-950	35°-40°	1.7-2.4
McKinleyville fault	0.7	Franciscan/Falor contact	300	35°	0.7
Mad River fault	0.7	Franciscan/Falor contact	325	35°	0.8
Fickle Hill fault	0.7	Franciscan/Falor contact	350	25°	1.2
Mad River fault zone total	0.7	Franciscan/Falor contact	2010-2500	35°	5.0-6.4
Little Salmon fault zone					
Little Salmon fault zone	0.7	base of Hookton Formation	1700	25°	5.7
Little Salmon fault zone total at Tompkins hill	0.8-1.0	Franciscan/Wildcat Group contact	2000	25°	4.7-5.9

Note: Data for this table come from the following sources: Carver, 1987; Kelsey and Carver, 1988; Woodward-Clyde Associates, 1980; and Clark and Carver, 1992.

* See text for discussion of determinination of timing and faulting.

**Geology described by Manning and Ogle (1950) and Ogle (1953).

Table 1. Vertical seperation and slip rate data for upper-plate thrust faults, Cascadia Subduction zone, northern California

region that fault-slip magnitude data or fault-slip rate data are available as a result of outcrop investigations, trenches or borehole-derived stratigraphy. The region consists of two coastal lowland areas—the Eel River valley and the combined Humboldt Bay-Mad River estuary—, separated by the Table Bluff/Tompkins Hill uplands (TBA, Table Bluff anticline; THA, Tompkins Hill anticline; Figure 2). The Eel River valley is underlain by the Eel River syncline (ERS, Figure 2) (Ogle, 1953), in which are preserved nearly 4,000 m of Miocene to late Pleistocene sediments (Ingle, 1976; 1987). This sedimentary sequence is bordered on the south by the Russ fault (Ogle, 1953) (Figure 2). The Russ fault is a poorly exposed, east-trending, high-angle fault that is presumed to have been active in the late Quaternary, based on offset of late Pleistocene marine terraces, down to the south (Carver et al., 1986; McCrory, 1996), but shows no evidence of Holocene scarps.

The late Neogene and Quaternary sediments of the Eel River valley/southern Humboldt Bay area are bound to the north by the Little Salmon fault, which is discussed in more detail below. Between the Russ fault and the Little Salmon fault, the late Neogene and Quaternary sediments within the Eel River syncline are folded and faulted by structures superposed on the Eel River syncline. The most prominent fold is the Table Bluff/Tompkins Hill anticline, which is an anticlinal fold in the hanging wall of the Table Bluff thrust fault (TBF, Figure 2) (Berger et al., 1991; Clarke and Carver, 1992; McCrory, 1996). The Table Bluff fault trends subparallel to the Little Salmon fault to the north, and may merge with it at depth. Other folds and faults within the Eel River valley area are the Grizzly Bluff and Alton anticlines (GBA, AA, Figure 2) (Ogle, 1953) and the Goose Lake fault zone (GLFZ, Figure 2) (WCA, 1980; O'Dea, 1992). Cumulatively, these faults and folds manifest ongoing north-northeast-directed contraction in the Eel River Valley area in the Holocene.

The wide southern part of Humboldt Bay (South Bay) is inferred to be underlain by the South Bay syncline (SBS, Figure 2) (Valentine, 1992). South Bay is in the footwall of the Little Salmon fault and above the down-dip extension of the Table Bluff fault. To the north of the Little Salmon fault, Humboldt Bay is narrow because the coastal area is a region of uplift occupied by the Humboldt Hill anticline (HHA, Figure 2), which is a hanging wall anticline of the Little Salmon fault. Further north, the broad, wide northern part of Humboldt Bay (Arcata Bay) is wide because the inferred Freshwa-

ter syncline (FS, Figure 2) underlies Arcata Bay. Even though the Freshwater syncline is not mapped east of the bay where Knudsen (1993) mapped Neogene strata in the Freshwater Creek basin, the syncline is inferred to trend northwestward from the Freshwater Creek basin into Arcata Bay by Clarke and Carver (1992). Clarke and Carver (1992) infer that the syncline is the structure that accounts for sudden subsidence events recorded at Mad River Slough, on the north margin of Arcata Bay (see below).

The northern end of Humboldt Bay merges north with the broad floodplain and coastal plain of the lower Mad River. The multiple fault strands of the N35°W-trending Mad River fault zone intersect the coast north of Humboldt Bay (Figure 2).

Five north-northwest trending faults traverse the coastal region immediately north of the area of expansive Neogene and Quaternary cover sediment. The Big Lagoon fault (Wagner and Saucedo, 1987) (BLF, Figure 2) is an east-dipping reverse or thrust fault. The fault was exposed during highway excavations on the east side of Big Lagoon (observations of G. A. Carver and H. M. Kelsey, October 3, 1981); where exposed, the fault cuts Pliocene or Pleistocene sediment and dips 25° to the northeast. The Big Lagoon embayment occurs in the footwall block of the Big Lagoon fault. Immediately north of the Big Lagoon fault is the Bald Mountain fault (Manning and Ogle, 1950; Harden et al., 1981; Wagner and Saucedo, 1987) (Figure 2), an inactive, high angle fault (Cashman et al., 1986) separating Franciscan sandstone to the southwest from Franciscan schist to the northeast.

The Grogan fault (Figure 2) is a reverse fault (~ 55° NE dip) where it intersects the coast, juxtaposing Franciscan sandstone over Pliocene and Pleistocene sediment of the Gold Bluffs Formation (unpublished field observation of J. C. Young that is described in Kelsey and Trexler [1989]). Further inland, the Grogan fault is a straight, north-northwest-trending fault that separates Franciscan schist to the southwest from Franciscan sandstone to the northeast (Manning and Ogle, 1950; Harden et al., 1981; Wagner and Saucedo, 1987).

The Lost Man fault and Surpur Creek fault (Figure 2) were mapped by Kelsey and Cashman (1983) and Kelsey and Trexler (1989), who documented that the faults displace Pliocene and Pleistocene sediment and that the faults are associated with mesoscale (outcrop-scale) faults that are high angle and conjugate. Based on the straight fault traces over rugged topography and on the mesoscale fault data, they inferred that the Lost Man fault and Surpur Creek faults are high-angle faults. However, similar to the Grogan fault and the Mad River fault zone/Eaton Roughs fault system to the south, the Lost Man and Surpur Creek faults may become less steep in a north-northwest direction. The Lost Man fault trends toward the Saint George reverse fault, which is offshore of Crescent City (Figure 2). The Saint George reverse fault has been interpreted from offshore seismic data to be a thrust fault (Clarke, 1992; Clarke, personal communication, 1996).

The deformed Neogene and Quaternary sediments of the Crescent City coastal plain occur within the hanging wall of the Saint George thrust fault (Figure 2). Evidence of deformation includes tilted late Neogene deposits and late Neogene erosion surfaces within and east of the coastal plain (Stone, 1993) and deformed marine terraces (Polenz and Kelsey, 1999). The distribution and elevation of three late Pleistocene marine terraces, differentiated on the basis of soil development, led Polenz and Kelsey (1999) to infer the existence of two northwest-trending folds on the coastal plain within the hanging wall of the fault, the Lake Earl syncline and the Saint George anticline (LES and SGA, Figure 2). Based on landforms and stratigraphy derived from well logs, Polenz and Kelsey (1999) also infer that the backedge of one of the terraces may be a fault scarp (CS, Cemetery scarp, Figure 2) that displaces Late Pleistocene sediment.

MAD RIVER FAULT ZONE AND LITTLE SALMON FAULT: GEOMETRY OF FAULTING AND FAULT SLIP RATES

Little Salmon fault

The Little Salmon thrust fault is the primary upper-plate fault in the southern Humboldt Bay area (Figure 2). Ogle (1953) first described the amount of offset on the Little Salmon fault in his study of the late Neogene stratigraphy of the Lower Eel River valley. Further study of the Little Salmon fault was prompted by seismic hazard assessment of the Humboldt Bay Nuclear Power Plant, located on the east shore of Humboldt Bay about 10 km south of Eureka, California.

The Little Salmon fault dips 25° to 30° to the northeast where exposed in trenches and where the dip can be reconstructed from well log borings (Carver and Burke, 1988; WCA, 1980). Cumulative displacement on the fault appears to decrease in a northwestward direction toward the coast. For instance, the top of the early Pleistocene Rio Dell Formation (Ogle, 1953), at a locality on the east shore of Humboldt Bay 400 m northeast of the inferred trace of the Little Salmon fault, has a vertical separation of approximately 800 m across the fault (WCA, 1980). By contrast, the top of Rio Dell Formation, 3 km southeast of Humboldt Bay, has a vertical separation of 1,400 m across the fault (WCA, 1980). Further southeast, at Tompkins Hill, the vertical separation across the Little Salmon fault, at the Wildcat Formation/Franciscan Formation contact, is nearly 2,000 m (WCA, 1980) but G. A. Carver (written comm., 1999) notes that this vertical separation may also include displacement on the neighboring Table Bluff fault. Carver and Burke (1992) state that there are 1,700 m of vertical separation at the base of the Hookton Formation (Ogle, 1953) across the combined Little Salmon fault and Table Bluff anticline near Table Bluff (Figure 2). Assuming a total vertical separation of the basal contact of the Eel River Neogene section of 2,000 m, and a fault dip of 25°, the net horizontal crustal contraction across the Little Salmon fault and related structures is about 4,300 m.

Commencement of faulting on the Little Salmon fault probably occurred during the waning stages of deposition of the late Neogene Eel River stratigraphic section. The uppermost units of the Eel River group, the Scotia Bluffs sandstone and Carlotta sandstone and conglomerate, are separated from the overlying Hookton Formation by an angular unconformity (Ogle, 1953; WCA, 1980). On the basis of the angular unconformity, it appears deformation of the Eel River late Neogene section started prior to deposition of the basal sediment of the Hookton Formation. Paleomagnetic studies done by WCA (1980) suggest that the Bruhnes-Matuyama boundary (780,000 years BP) is near the top of the late Neogene Eel River group but not within the overlying Hookton Formation. Assuming deformation on the Little Salmon fault started several hundreds of thousands of years prior to cutting of the unconformity at the base of the Hookton Formation, then the Little Salmon fault might have first become active sometime between 0.8-1.0 Ma, which are the ages of fault initiation that are used for slip rate calculations in Table 1.

Trenching studies across the trace of the Little Salmon fault (Carver and Burke, 1988; Clarke and Carver, 1992; Carver and McCalpin, 1996) reveal that there have been three slip events on two imbricate strands (west and east fault traces) of the fault along the margins of Humboldt Bay in the last 1,700 years. Each event had a dip slip displacement of 3.6 to 4.5 m on the west trace (Clarke and Carver, 1992), and perhaps an additional 1 to 2 m on the east trace (G. A. Carver, written comm., 1999). Clarke and Carver (1992) suggest that the last two faulting events on the fault occurred 290 to 690 and 530 to 1,170 years BP. Based on an inferred 26 m of slip displacement (west trace only) of strata 2,150 to 4,800 years in age, Carver and Burke (1988) and Clarke and Carver (1992) calculate that the net late Holocene dip-slip rate on the Little Salmon fault at this site is 6 to 12 mm/year. The upper bound to this Holocene slip rate is twice the estimated slip rate based on vertical separation of the entire Eel River section across the Little Salmon fault (Table 1).

Mad River fault zone

The Mad River fault zone (Carver, 1987) is a N35°W-trending zone of thrust faults and associated folds that intersects the coast 4 to 20 km north of Humboldt Bay (Figure 2). The Mad River fault zone and the Little Salmon fault together comprise the two main contractional fault zones in the upper plate in the Humboldt Bay region. The Mad River fault zone is about 15 km wide and contains five principal thrust faults, the Trinidad, Blue Lake, McKinleyville, Mad River and Fickle Hill faults (Figure 2). Dips of thrust faults within the zone range from 15° to 25° near the coast and steepen to 35° to 45° at the southeastern end of the zone. At the southeast end of the Mad River fault zone, 20 to 25 km inland along strike, the thrust faults appear to merge into steeply dipping to vertical strike-slip faults associated with the northern end of the Eaton Roughs fault zone (Kelsey and Carver, 1988).

Vertical separation across the faults of the Mad River fault zone can be measured across the contact of the Franciscan Formation with the Falor Formation (Manning and Ogle, 1950). The Falor Formation is a late Neogene to Quaternary unit composed of marine and fluvial sediment (Manning and Ogle, 1950; Carver, 1987). An ash near the base of the unit is correlated with the 1.8 to 2.0 Ma Huckleberry Ridge ash (Sarna-Wojcicki et al., 1987). The age of the top of the Falor Formation is not well known but at the coast near Trinidad, *Balanophyllia elegans*

coral from near the top of the Falor Formation radiometrically dates at 0.35 to 1.0 Ma (personal communication from W. Miller, as cited in Kelsey and Carver, 1988). Therefore the period of deposition of the Falor Formation was roughly from 1.8 Ma to 0.3-1.0 Ma. Because of the lack of evidence of syndeformational deposition in the Falor Formation sediment, Carver (1987) and Kelsey and Carver (1988) assumed that faulting in the Mad River fault zone started after the Falor Formation deposition was completed; therefore they assumed that the commencement of faulting on the Mad River fault zone was around 0.7 Ma (average of 0.35 to 1.0 Ma). Table 1 shows magnitudes of vertical separation of the Falor Formation/Franciscan Formation contact across each of the thrust faults of the Mad River fault zone and the average dip of the faults where the vertical separation was measured. Data on fault dip come from outcrop exposures in the case of the Trinidad, Blue Lake and Fickle Hill faults (Carver, 1987).

Carver and Burke (1988) conducted a trenching program across scarps of thrust faults of the Mad River fault zone. For the McKinleyville and Mad River fault scarps, the trenches were located where the scarps cut across marine terrace surfaces. The trenches either reveal a low angle 20° to 30° fault or a fold that presumably is above a blind thrust fault.

The Mad River fault (MRF, Figure 2) at McKinleyville cuts the 80,000 year old marine terrace in three to four separate low-angle faults. The total width of the fault at this site is about 1 km and the net vertical separation of the marine terrace surface is 40 m (Carver, 1987). Assuming a fault dip of 25°, the slip rate of the fault in the last 80,000 years is 1.2 mm/year. At the Mad River fault trench site, Franciscan Formation bedrock and overlying marine terrace sand together were folded into a recumbent anticline over as many as five layers of colluvium, each colluvial layer being interpreted as having derived from the fault scarp after a slip event (figure 5.13 in Carver and McCalpin, 1996). Carver and Burke (1988) interpret the recumbent fold overlying the colluvial layers to be a hanging wall anticline above a blind thrust fault.

Radiocarbon dating of fault-scarp derived colluvial wedges within trenches at the Mad River fault (discussed above) and the McKinleyville fault trench sites indicate at least two or three slip events on each of these faults during the Holocene (Carver and Burke, 1988). Therefore, recurrence of slip events on individual thrust faults within the Mad River fault zone may be on the order of 3,000 to 4,500 years.

REGIONS WITH INFERRED COSEISMIC SUBSIDENCE

Two coastal regions of documented subsidence have been investigated in northern California, Humboldt Bay and the lower Eel River valley. At both sites, investigations attribute instances of buried peaty tidal wetland soils to coseismic subsidence accompanying upper-plate thrust earthquakes and/or Cascadia subduction zone earthquakes (Vick, 1988; Clarke and Carver, 1992; Valentine, 1992; Valentine et al., 1992). Other coastal sites between Humboldt Bay and the California/Oregon border also have buried wetland soils (e.g., Redwood Creek estuary at Orick, California, personal communication, G. A. Carver) but these sites have been only cursorily examined.

Humboldt Bay

Buried tidal wetland soils have been observed in outcrop and core along the margins of Humboldt Bay, including Mad River Slough (northernmost part of Humboldt Bay), the sloughs near Eureka (narrow, middle portion of Humboldt Bay) and South Bay (Figure 2). In Mad River Slough, four buried soils occur in the upper 1,600 years of stratigraphic time (Vick, 1988). The most widespread of the four buried soils is the upper one, which can be traced continuously along 5.5 km of cutbank in a north-south direction. This buried soil includes buried Sitka spruce tree trunks to the north and buried herbaceous plants in growth position to the south (Jacoby et al., 1995). Jacoby et al. (1995) inferred that the trees were killed by coseismic subsidence about 300 years ago. Clarke and Carver (1992) suggest that the subsidence history at Mad River Slough reflects periodic abrupt subsidence in the axis of the Freshwater syncline, which they infer is a broad syncline that trends northwest across the northern part of the bay (Figure 2).

In the narrow middle portion of Humboldt Bay, along the margins of tidal sloughs near Eureka, there are multiple buried peaty soils, at least two of which probably correlate to buried soils at Mad River Slough (Valentine, 1992; Valentine et al., 1992). In addition, there are at least two buried soils that are older than the oldest buried soil at

Mad River Slough (Valentine, 1992; Valentine et al., 1992). The oldest of the buried soils in the sloughs of the Eureka area is about 4,200 years BP (Valentine, 1992; Valentine et al., 1992).

The South Bay record of buried soils shows no more than four buried soils in any one core, but at least three of the buried soils are older than the oldest buried soil at Mad River Slough (Valentine, 1992; Valentine et al., 1992). Because of the difficulty of correlating buried soils from one core to the next, it is uncertain how many distinct buried soils are present in the South Bay (Valentine et al., 1992). In the vicinity of the Little Salmon fault at Hookton Slough, three soils have been buried and preserved in the last 1,300 years, and Valentine et al. (1992) suggest that two of these episodes of soil burial correlate with the two most recent earthquakes on the Little Salmon fault. The two most recent earthquakes, temporally constrained from trenching studies, occurred at 290 to 690 years BP and 530 to 1170 years BP (Clarke and Carver, 1992). Valentine et al. (1992) also suggest that only two of the three subsidence events observed at Hookton Slough are present in the northern part of the bay at Mad River Slough, from which they infer that one of the three younger-than-1,300 years events in the southern part of Humboldt Bay did not affect the northern part of Humboldt Bay. Clarke and Carver (1992) argue, based on the magnitude of fault slip inferred in fault trenches across the Little Salmon fault, that the two inferred slip events on the Little Salmon fault within the last 1,170 years occurred synchronously with earthquakes on the southern part of the Cascadia subduction zone.

To summarize, Valentine et al. (1992) infer that ten subsidence events have occurred in the Humboldt Bay region in the last 4,200 years, and that at least one and perhaps more of these events did not affect the entire Humboldt Bay area. Although paleoseismic studies of subsidence in Humboldt Bay cover the entire bay and entail at least 26 logged cores and 46 ^{14}C age determinations, these studies are not exhaustive in comparison with Atwater and Hemphill-Haley's (1997) paleoseismic investigation of subsidence events on the outer Washington coast in the vicinity of Grays Harbor and Willapa Bay (Figure 1). Further work in Humboldt Bay is needed to better substantiate the chronology and extent of individual subsidence events. Specifically, coring could be done at more sites, as well as more comprehensive coring at sites already investigated, in order to determine how widespread are specific buried soil horizons. More biostratigraphic work is needed to assess the occurrence and magnitude of subsidence. More ^{14}C age determinations are needed on fossil plants that were killed by the purported seismic events. At present, many of the ^{14}C age determinations are on bulk peat samples from the buried soils. More detailed work will establish more accurate return periods for subsidence events and further evaluate the suggestion that some subsidence events are confined to only the South Bay portion of Humboldt Bay.

Lower Eel River valley

Li (1992) investigated late Holocene wetland stratigraphy in the lowermost Eel River valley, within the axial region of the Eel River syncline (Ogle, 1953) (Figure 2). Li (1992) completed three vibracore transects immediately landward of the coastal dunes, with one transect on the south side of the valley and two on north side of the valley.

Horizons of peaty soil are buried within the late Holocene sediment of the lower Eel River valley. Through correlation of cores based on lithology, depth and ^{14}C age, Li (1992) interpreted that there are five buried wetland soils in the upper 3 to 4 m of fine-grained fluvial and estuarine mud. Although the uppermost buried wetland soil had in situ tree trunks preserved within it, the lower four buried soils were difficult to correlate across the valley because one to three of the buried soils were missing in most cores. Li (1992) determined, based on ^{14}C age determinations on bulk peat samples, that the five buried wetland soils were all younger than 2,300 years BP.

Li (1992) used foraminiferid biostratigraphy, in conjunction with data on elevational zonation of foraminifera relative to tidal datum, to infer that the burial of the peaty soils was accompanied by an elevation change of the marsh surface from high marsh to tidal flat. The elevation change was apparently rapid, based on sharpness of the contact at the top of the buried soils and based on abrupt change from high marsh foraminiferid species to tidal flat foraminiferid species at this contact. Li (1992) inferred that the abrupt change was caused by coseismic subsidence of the lower Eel River valley.

REGIONS WITH INFERRED UPLIFT OF COSEISMIC ORIGIN

Coastline south of Cape Mendocino

During the 1992 Ms 7.1 Cape Mendocino earthquake, the coast from Cape Mendocino 25 km south to Punta Gorda underwent as much as 1.4 m of coseismic uplift, documented by the die-off of intertidal marine organisms (Carver et al., 1992). Evidence of prehistoric, rapid and probably coseismic emergence of Holocene wave-cut bedrock platforms occurs along the same stretch of coast (Merritts, 1996). The candidate, coseismically uplifted platforms are wave-cut because the bore holes of the pholadid *Penitella penita*, typical of the intertidal zone, are present on the bedrock terrace surfaces (Merritts, 1996). Evidence of prehistoric, rapid emergence of Holocene wave-cut bedrock platforms also can be seen further south in the coastal stretch from Punta Gorda approximately 30 km southeastward to the area of Gitchell Creek (GC, Figure 2), 8 km north of Point Delgada and Shelter Cove (Merritts, 1996). Along the Cape Mendocino-to-Gitchell Creek stretch of coastline, episodic emergence, interpreted as coseismic uplift, has occurred at least four times between 600 and 7,000 years ago. Some of the coseismic uplift events had uplift magnitudes as large as 2.5 m. There may have been more than four uplift events if some of the risers between wave-cut platforms represent more than one coseismic uplift event (Merritts, 1996).

Coseismic uplift of the coast south of Cape Mendocino probably occurred as a consequence of rupture of the southernmost part of the Cascadia subduction zone (Merritts, 1996), similar to the case for the 1992 M_s 7.1 Cape Mendocino earthquake (Oppenheimer et al., 1993). However, Merritts (1996) suggests that some of the coseismic uplift near Point Delgada may be occurring on the upper plate due to active thrust faults associated with a restraining bend at the northernmost terminus of the San Andreas fault (Figure 2).

Clam Beach area north of Humboldt Bay

Clarke and Carver (1992) and Carver and McCalpin (1996) infer that there have been two instances of coseismic uplift at Clam Beach, a 200 to 300-m-wide and nearly 7-km-long beach on the coast 9 to 16 km north of Humboldt Bay (Figure 2). The Mad River fault and the McKinleyville fault intersect the coast along the Clam Beach coastal reach. The southern part of Clam Beach is periodically occupied by the Mad River, as it migrates to the north in front of (west of) the modern sea cliff (Borgeld et al., 1993; Scalici, 1993).

The first instance of tectonic uplift at Clam Beach is inferred based on the elevation of a strath (flat erosion-cut surface) cut into late Pleistocene marine sand that underlies the modern beach. The strath is 3 m above mean tide level and is buried by beach sand. Clarke and Carver (1992) infer that the strath was planated by waves 960 to 1,260 years ago based on ^{14}C dating of driftwood in the beach sand 20 to 70 cm above the strath. The strath and overlying beach sand are buried by dune sand. Clarke and Carver (1992) infer that the source of the dune sand is nearshore sand that became subaerially exposed, and thereby available for wind transport, after the first of two inferred instances of coseismic uplift of the coast. After deposition, the dune sand stabilized, a weak soil developed on the dune surface, trees colonized the dunes, and peaty mud accumulated in undrained depressions within the dunes.

The evidence for the second instance of coseismic uplift at Clam Beach is a deposit of dune sand that buries the trees and peat on the surface of the vegetated dune. Four ^{14}C age determinations on these trees and the peat have ages of 0 to 300 years BP. Similar to the argument for the first episode of coseismic uplift, Clarke and Carver (1992) infer that the earlier dune is buried by dune sand that was transported landward from an emergent nearshore sand plain, exposed after the second instance of coseismic uplift. Although both Clarke and Carver (1992) and Carver and McCalpin (1996) infer that the stratigraphy at Clam Beach is the result of two coseismic uplift events, they do not specify the structure that they infer to be the cause of coseismic uplift.

PREDICTED EARTHQUAKE-INDUCED GROUND ACCELERATIONS AND SHAKING DURATION AT HUMBOLDT BAY

A set of three bridges span the narrow, central portion of Humboldt Bay and the California Department of Transportation commissioned an engineering study (Geomatrix, 1992) to assess seismically induced ground acceleration and duration of shaking that could be expected at the bridge sites. As a result of evaluation of all seismic sources, including

an earthquake on the northern San Andreas fault, Geomatrix (1992) determined that three maximum credible earthquake scenarios were a structural threat to bridges over Humboldt Bay. These maximum credible earthquakes are a M_W7.5 earthquake on the Little Salmon fault, a M_W7.5 intraplate earthquake within the Gorda plate, and a M_W8.4 to M_W 9 interplate earthquake on the Cascadia subduction zone (minimum epicentral distances of 5, 20 and15 km, respectively, from Humboldt Bay bridges).

Using models of seismic energy attenuation from these maximum credible earthquakes, Geomatrix (1992) calculated that the Little Salmon fault could produce median horizontal peak ground accelerations in central Humboldt Bay of 0.68 g (g = gravitational acceleration), whereas a Gorda intraplate earthquake could produce median horizontal peak ground accelerations of 0.26 g and a subduction zone earthquake event could produce median horizontal peak ground accelerations of 0.26 to 0.33 g. Duration of strong shaking (duration of time between the first and last acceleration exceeding 0.05 g) for the maximum credible earthquake could be 25 sec in the case of an earthquake on the Little Salmon fault or within the Gorda plate and >40 seconds in the case of a subduction zone event.

DISCUSSION

A useful perspective for seismic hazard assessment in northern California is to qualitatively review the recurrence of coseismic shaking, levels of shaking intensity, and earthquakes for the different seismic sources, utilizing geologic and paleoseismic data. Northern California is most likely to feel shaking from Gorda plate and Mendocino fault seismic sources, and less likely to feel shaking from a San Andreas, Cascadia subduction zone or upper plate source. However, the strongest ground motion in the Humboldt Bay area, based on predictions of peak horizontal acceleration, would be from an upper-plate thrust fault source (Little Salmon fault or Mad River fault zone). The next most intense shaking would be from a Cascadia subduction zone source that ruptures at least the length of the subduction zone offshore of northern California. Intense shaking would also be generated from a San Andreas fault source, as exemplified by the reported Modified Mercalli intensities of VII to IX for the 1906 earthquake. Expected duration of shaking is slightly greater for an earthquake from the subduction zone than for an earthquake from an upper crustal or Gorda plate source. Based on paleoseismic studies to date, earthquakes on the Little Salmon fault, the San Andreas fault or the Cascadia subduction zone are about equally as likely to occur (recurrence interval of hundreds of years). An earthquake on one of the thrust faults of the Mad River fault zone is a less likely source of intense shaking by an order of magnitude because individual earthquakes on thrust faults of the Mad River fault zone recur on the order of thousands of years.

The magnitude of the seismic hazard posed by upper-plate faults, in terms of intensity and duration of shaking, is unclear because it is uncertain whether upper-plate thrust faults in the Humboldt Bay region are an independent seismic source or just move when triggered by an earthquake on the underlying Cascadia subduction zone. But even if the sources were linked, the Little Salmon fault might not break every time a Cascadia subduction zone earthquake occurs because the rate of strain accumulation on the Little Salmon fault is less than on the subduction zone. The same argument could be made for individual faults of the Mad River fault zone.

The Holocene stratigraphic and geomorphic record of the coastal lowland argues for instances of coseismic land-level change. Vertical deformation consists of coseismic uplift of the southernmost part of the coast near Cape Mendocino, where the coast is only 15 km east of the subduction zone deformation front. Further north, the subduction zone deformation front diverges seaward relative to the coastline (Figure 1), and the coseismic form of displacement at the coast is subsidence. Three tectonic models could account for these changes. The first model is that coastal, coseismic land-level displacements are caused by slip displacement on upper-plate reverse and thrust faults. The second model is that coseismic land-level displacements are caused by displacement of faults within the subduction zone. The third model, a combination of the first two, is that instances of coseismic land level change sometimes just involve rupture of the subduction zone and at other times entail concurrent rupture of upper-plate reverse and thrust faults and the subduction zone. Which model or models are most appropriate along a specified coastal segment would depend on the position of upper-plate faults, and on whether upper-plate faults are an independent seismic source or only move in conjunction with movement on the subduction zone.

In the Cape Mendocino coastal area, from Cape Mendocino south 25 km to Punta Gorda, inferred coseismic uplift events (Merritts, 1996) are probably a result of earthquakes on the subduction zone. Such causal relationship is demonstrated to be feasible by the coseismic uplift of the intertidal zone on the Mendocino coast after the 1992 M_S7.1 Cape Mendocino earthquake (Oppenheimer et al., 1993; Carver et al., 1994). Further south, from Punta Gorda to Point Delgada, prehistoric coseismic uplift events may be the result of earthquakes on upper-plate thrust faults in the region where the San Andreas fault bends as it trends northward into the Mendocino triple junction region (Merritts, 1996) (Figure 1).

In the Eel River valley area, subsidence events (Li, 1992) could be the result of earthquakes on the subduction zone or within the upper plate or both. The deformation front is 40 km west of the mouth of the Eel River at this latitude (Figure 1), therefore the coseismic signal at the coast during a subduction zone earthquake probably is subsidence, thus accounting for Li's (1992) sequence of buried wetland soils. Another mechanism that could cause abrupt coseismic subsidence is slip on a fault beneath or within the Eel River basin. A candidate fault would be the Russ fault, which bounds the Eel River Neogene section on the south (Ogle, 1953) (Figure 2).

South Bay, the southern, wide embayment within Humboldt Bay, is the site of multiple buried wetland soils. Valentine (1992, p. 184) ascribed the subsidence to "earthquakes associated with the southern end of the Cascadia subduction zone fold-and-thrust belt". Carver (written communication, 1999) interprets these instances of subsidence to be coseismic land-level changes during earthquakes on the Table Bluff thrust fault caused by extension of the fault's hanging wall at the down-dip terminus of the seismogenic segment of the fault. Abrupt subsidence, however, also could be triggered by earthquakes on the subduction zone, the locked, seismogenic portion of which probably underlies South Bay.

The margins of Arcata Bay, including Mad River Slough and the tidal sloughs near Eureka, all have stratigraphic evidence of multiple buried soils. However, the region between Arcata Bay on the north and South Bay on the south (the city of Eureka and vicinity) consists of uplifted late Pleistocene marine terraces flanked on the west by the narrow, middle portion of Humboldt Bay. The uplifted marine terraces in Eureka could reflect repeated coseismic uplift of the hanging wall of the Little Salmon fault. Carver (written communication, 1999) interprets the buried soils along the margins of Arcata Bay (within what Clarke and Carver [1992] call the "Freshwater syncline") to be the result of earthquakes on the Little Salmon fault. The hanging wall of the Little Salmon fault coseismically uplifts near the fault (Eureka area) but coseismically drops in the down-dip direction (northward, in the vicinity of Arcata Bay) because the hanging wall attenuates over the down-dip terminus of the seismogenic segment of the fault.

The hypothesis that coseismic uplift and subsidence in the middle to northern part of Humboldt Bay are caused by earthquakes on the Little Salmon fault is reasonable for some of the earthquakes that affect this region, but not for all of them. Vick (1988) and Valentine (1992) together infer that there have been eight to ten subsidence events in the northern Humboldt Bay region in the last 4,500 years. Incorporating the best inferred data for the slip magnitude and slip recurrence on the Little Salmon fault from Clarke and Carver (1992), about 6 m of coseismic slip every 500 years, then the Humboldt Bay region shortens in a direction perpendicular to plate convergence at a rate of about 10 mm/year as a consequence of upper-plate thrust faults. This shortening rate is only 25 to 33 percent of the Juan de Fuca-North American plate convergence rate of 30 to 40 mm/year (Heaton and Kanamori, 1984), so clearly most of the deformation is accommodated along the Cascadia subduction zone. Subsidence patterns documented by Vick (1988) and Valentine (1992) in Humboldt Bay cannot therefore be exclusively the product of hanging wall deformation during thrust earthquakes, but must also reflect strain accumulation and release on the subduction zone. A corollary of this conclusion is that, despite the presence of uplifted late Pleistocene marine terraces along the middle portion of Humboldt Bay, the middle portion of the bay could be the site of subsidence during some or all of the earthquakes that affect the region. The observed long-term uplift of marine terraces in the Eureka area could be the product of interseismic rock uplift that is not entirely recovered during coseismic subsidence. Multiple, uplifted late Pleistocene marine terraces within a coastal reach that has late Holocene buried soils is also characteristic of the southern Oregon coast at Cape Blanco and within the Coquille River estuary (Kelsey et al., 1998; Witter, 1999). Therefore, northern California coastal areas within

embayments and atop synclines (Eel River valley, South Bay, Arcata Bay) may have net coseismic subsidence greater than coastal areas removed from synclinal axes, but all of the California coast north of the Eel River valley probably has experienced instances of coseismic subsidence.

The structural cause of the inferred instances of coseismic uplift at Clam Beach (Clarke and Carver, 1992; Carver and McCalpin,1996) are difficult to fit into a tectonic model. Because Clam Beach is 65 km east of the deformation front, the site is unlikely to coseismically uplift during an earthquake on the subduction zone. Alternatively, the uplift could be the result of folding of the hanging wall of the McKinleyville thrust fault during slip on this fault. However, based on recurrence interval estimates for slip on the individual strands of the Mad River fault zone (Carver and Burke, 1988), it appears unlikely that there would be as many as two instances of coseismic slip on the McKinleyville fault zone in the last 1,000 to 1,200 years. Furthermore, coseismic uplift on a thrust hanging wall is inconsistent with the argument that even the hanging wall of upper-plate thrust faults may coseismically subside during subduction zone earthquakes. Non-tectonic explanations for the Clam Beach stratigraphy cannot be ruled out because the position of paleo sea level is not identified in the Clam Beach strata, and the stratigraphic section is non marine except for the basal beach sand. The other possibility is that the Clam Beach site does not record coseismic uplift but rather records migration and deposition of dune sand as a consequence of beach erosion by the Mad River and the ocean, in concert with aseismic uplift of the coast caused by strain buildup on the upper plate of the subduction zone.

ACKNOWLEDGMENTS

I thank Bill Lettis for encouraging me to undertake this review article and serving as section editor. The manuscript was improved as a result of careful reviews by Robert C. Witter and Gary A. Carver. Jason Holmberg produced the two figures. Chief Editor Horacio Ferriz provided editorial support.

AUTHOR PROFILE

Dr. Harvey Kelsey is a Research Associate at Humboldt State University. His research interests range from late Quaternary deformation and paleoseismicity at active convergent margins to particle size distribution in channels and sediment budgets of forested watersheds. Presently, he is most active in projects that use the tools of Quaternary stratigraphy to decipher paleoseismic history on the Cascadia subduction zone.

SELECTED REFERENCES

Atwater, B., Nelson, A., Clague, J., Carver, G., Yamaguchi, D., Bobrowsky, P., Bourgeois, J., Darienzo, M., Grant, W., Hemphill-Haley, E., Kelsey, H., Jacoby, G., Nishenko, S., Palmer, S., Peterson, C., and Reinhart, M., 1995, Summary of coastal geologic evidence of great earthquakes at the Cascadia subduction zone: Earthquake Spectra, v. 11, p. 1-17.

Atwater, B.F., and Hemphill-Haley, E., 1997, Recurrence intervals for great earthquakes of the past 3500 years at northeastern Willapa Bay, Washington: U.S. Geological Survey Professional Paper 1576, 108 p.

Berger, G.W., Burke, R.M., Carver, G.A., and Easterbrook, D.J., 1991, Test of thermoluminescence dating with coastal sediments from northern California: Chemical Geology, v. 87, p. 21-37.

Borgeld, J.C., Scalici, M.J., Lorang, M., Komar, P.D. and Burrows, F.G.A., 1993, Final project evaluation report: Mad River mouth migration: Report prepared for the California Department of Highways, Hydraulics Division, Eureka, California, 81 p.

Carver, G.A., 1987, Late Cenozoic tectonics of the Eel River basin region, coastal northern California: in H. Schymiczek, and Suchland, R. (eds.), Tectonics, sedimentation and evolution of the Eel River and other coastal basins of northern California: San Joaquin Geological Society, Miscellaneous Publication v. 37, p. 61-72.

Carver, G.A., Burke, R.M., and Kelsey, H.M., 1986, Quaternary deformation in the region of the Mendocino triple junction: National Earthquake Hazard Reduction Program Final Technical Report, 48 p. and 6 maps.

Carver, G.A. and Burke, R.M., 1988, Trenching investigations of northwestern California faults, Humboldt Bay region: U.S. Geological Survey, National Earthquake Hazard Reduction Program Final Technical Report, 53 p.

Carver, G.A. and Burke, R.M., 1992, Late Cenozoic deformation on the Cascadia subduction zone in the region of the Mendocino triple junction: in Pacific Cell Friends of the Pleistocene guidebook for the field trip to north coastal California, p. 31-63.

Carver, G.A., Jayko, A.S., Valentine, D.W., and Li, W.H. 1994, Coastal uplift associated with the 1992 Cape Mendocino earthquake, northern California: Geology, v. 22, p. 195-198.

Carver, G.A. and McCalpin, J.P., 1996, Paleoseismology of compressional tectonic environments: in McCalpin, J.P. (ed.), Paleoseismology, Academic Press, New York, 183-270.

Cashman, S.M., Cashman, P.H., and Longshore, J.D., 1986, Deformational history and regional tectonic significance of the Redwood Creek schist, northwestern California: Geological Society of America Bulletin, v. 97, p. 35-47.

Clarke, S.H., 1987, Geology of the California continental margin north of Cape Mendocino: in Scholl, D.W., Grantz, A., and Vedder, J.G. (eds.), Geology and resource potential of the continental margin of western North America and adjacent ocean basins - Beaufort Sea to Baja California, Circum-Pacific Council for Energy and Mineral Resources, Earth Science Series, p. 15A1-15A8.

Clarke, S.H., 1992, Geology of the Eel River basin and adjacent region: implications for late Cenozoic tectonics of the southern Cascadia subduction zone and Mendocino triple junction: American Association of Petroleum Geologists Bulletin, v. 76, p. 199-224.

Clarke, S.H., Jr., and Carver, G.A., 1992, Late Holocene tectonics and paleoseismicity, southern Cascadia subduction zone: Science, v. 255, p. 188-192.

Dengler, L., Carver, G., and McPherson, R., 1992, Sources of north coast seismicity: California Geology, March/April, 1992, p. 40-53.

Dengler, L., Moley, K., McPherson, R., Pasyanos, M., Dewey, J., and Murray, M., 1995, The September 1, 1994 Mendocino fault earthquake: California Geology, March/April, 1995, p. 43-53.

Dickinson, W.R. and Snyder, W.S., 1979a, Geometry of triple junctions related to San Andreas transform: Journal of Geophysical Research, v. 84, p. 561-572.

Dickinson, W.R. and Snyder, W.S., 1979b, Geometry of subducted slabs related to San Andreas transform: Journal of Geology, v. 87, p. 609-627.

Furlong, K.P., 1993, Thermal-rheological evolution of the upper mantle and the development of the San Andreas fault system: Tectonophysics, v. 223, p. 149-164.

Furlong, K.P. and Govers, R., 1999, Ephemeral crustal thickening at a triple junction: the Mendocino crustal conveyor: Geology, v. 27, p. 127-130.

Geomatrix (Geomatrix Consultants), 1992, Seismic ground motion study for Humboldt Bay bridges on Route 255, Humboldt County, California: Contract No.59N772, San Francisco, California, 8 sections and 5 appendices.

Harden, D., Kelsey, H.M., Stephens, T., and Morrison, S., 1981, Geologic Map of the Redwood Creek Basin: U.S. Geological Survey, Water Resources Division, Open-File Report 81-496, geologic map scale 1:62,500.

Heaton, T.H. and Kanamori, H., 1984, Seismic potential associated with subduction in the northwestern United States: Bulletin of the Seismological Society of America, v. 74, p. 933-941.

Ingle, J.C., 1976, Late Neogene paleobathymetry and paleoenvironments of the Humboldt basin, northern California: in Fritsche, A.E., TerBest, H., and Wornhardt, W. (eds.), The Neogene symposium, Soc. Econ. Paleon. Mineral., Pacific Section, p. 53-61.

Ingle, J.C., 1987, The depositional, tectonic and paleogeographic history of the Eel River (Humboldt), Point Arena, and Bodega (Point Reyes) basins of northern California, a summary of stratigraphic evidence: in Schymiczek, H., and Suchland, R. (eds.), Tectonics, sedimentation and evolution of the Eel River and other coastal basins of northern California, San Joaquin Geological Society, Miscellaneous Publication v. 37, p. 49-54.

Jacoby, G.C., Bunker, D.E., and Benson, B.E., 1997, Tree-ring evidence for an A.D. 1700 Cascadia earthquake in Washington and northern Oregon: Geology, v. 25, p. 999-1002.

Kelsey, H.M. and Cashman, S.M., 1983, Wrench faulting in northern California and its tectonic implications: Tectonics, v. 2, p. 565-576.

Kelsey, H.M. and Trexler, J.H., 1989, Pleistocene deformation of a portion of the southern Cascadia forearc: Prairie Creek Formation, northern California: Journal of Geophysical Research, v. 94, p. 14027-14039.

Kelsey, H.M. and Carver, G.A., 1988, Late Neogene and Quaternary tectonics associated with northward growth of the San Andreas transform fault, northern California: Journal of Geophysical Research, v. 93, p. 4797-4819.

Kelsey, H.M., Witter, R.C., and Hemphill-Haley, E., 1998, Response of a small Oregon estuary to coseismic subsidence and postseismic uplift in the past 300 years: Geology, v. 26, p. 231-234.

Knudsen, K., 1993, Geology and stratigraphy of the Freshwater Creek watershed, Humboldt County, California: M.S. thesis, Arcata, California, Humboldt State University, 85 p.

Lawson, A.C., 1908, The California earthquake of April 18, 1906: Carnegie Institute, Washington, D.C., vol. 1, p. 54-59 and p. 165-170.

Li, Wen-Hao, 1992, Evidence for the late Holocene coseismic subsidence in the lower Eel River Valley, Humboldt County, northern California: an application of foraminiferal zonation to indicate tectonic submergence: M.S. thesis, Arcata, California, Humboldt State University, 87 p.

Manning G.A. and Ogle, B.A., 1950, Geology of the Blue Lake Quadrangle, California: Bulletin of the California Division of Mines and Geology, Bulletin No. 148, 35 p.

McCrory, P.A., 1996, Evaluation of fault hazards, northern coastal California, U.S. Geological Survey Open-File Report 96-656, 87 p., 2 plates.

Merritts, D.J., 1996, The Mendocino triple junction: active faults, episodic coastal emergence, and rapid uplift: Journal of Geophysical Research, v. 101, p. 6,051-6,070.

O'Dea, K.M., 1992, Terrace formation and deformation on Yager Creek, Humboldt County, California: in Pacific Cell Friends of the Pleistocene guidebook for the field trip to north coastal California, Department of Geology, Humboldt State University, Arcata, p. 229-234.

Ogle, B.A., 1953, Geology of the Eel River valley area, Humboldt County, California: Bulletin of the California Division of Mines, Bulletin No. 164, 128 p.

Oppenheimer, D., Beroza, G., Carver, G., Dengler, L., Eaton, J., Gee, L., Gonzalez, F., Jayko, A., Li, W.H., Lisowski, M., Magee, M., Marshall, G., Murray, M., McPherson, R., Romanowicz, B., Satake, K., Simpson, R., Somerville, P., Stein, R., and Valentine, D., 1993, The Cape Mendocino, California, earthquakes of April 1992: Subduction at the triple junction: Science, v. 261, p. 433-438.

Polenz, M. and Kelsey, H.M., 1999, Development of a late Quaternary marine terraced landscape during on-going tectonic contraction, Crescent City coastal plain: Quaternary Research, v. 52, p. 217-228.

Prentice, C.S., 1989, Earthquake geology of the northern San Andreas fault near Point Arena, California: Ph.D. Dissertation, California Institute of Technology, 252 p.

Prentice, C.S., Niemi, T.M., and Hall. N.T., 1991, Quaternary tectonics of the northern San Andreas fault, San Francisco Peninsula, Point Reyes, and Point Arena, California: in Geologic Excursions in Northern California: San Francisco to the Sierra Nevada, Sloan, D. and Wagner, D.L. (eds.), California Division of Mines and Geology Special Publication 109, p. 25-35.

Prentice, C.S., Merritts, D.J., Beutner, E.C., Bodin, P., Schill, A., and Muller, J.R., 1999, Northern San Andreas fault near Shelter Cove, California: Geological Society of America Bulletin, v. 111, p. 512-523.

Sarna-Wojcicki, A.M., Morrison, S.D., Meyer, C.E., and Hillhouse, J.W., 1987, Correlation of upper Cenozoic tephra layers between sediments of the western United States and eastern Pacific Ocean and comparison with biostratigraphic and magnetostratigraphic age data: Geological Society of America Bulletin, v. 98, p. 207-233.

Scalici, M.J., 1993, Mad River mouth monitoring project, Appendices: Historical review of the events shaping the Mad River delta and estuary northwest California, 1850-1941: report prepared for the California Department of Highways, Hydraulics Division, Eureka, California, 100 p.

Satake, K., Shimazaki, K., Tsuji, Y., and Ueda, K., 1996, Time and size of a giant earthquake in Cascadia inferred from Japanese tsunami records of January 1700: Nature, v. 379, p. 246-249.

Stone, L., 1993, Pliocene-Pleistocene sedimentary and tectonic history of the Crescent City/Smith River region, Del Norte County, California: M.S. thesis, Arcata, California, Humboldt State University, 185 p.

Thatcher, W., 1984, The earthquake deformation cycle at Nankai Trough, southwest Japan: Journal of Geophysical Research, v. 89, p. 3087-3101.

Valentine, D.W., 1992, Late Holocene stratigraphy as evidence for late Holocene paleoseismicity of the southern Cascadia subduction zone, Humboldt Bay, California: M.S. thesis, Arcata, California, Humboldt State University, 84 p.

Valentine, D.W., Vick, G.S., Carver, G.A. and Manhart, C.S., 1992, Late Holocene stratigraphy and paleoseismicity, Humboldt Bay, California: in Pacific Cell Friends of the Pleistocene guidebook for the field trip to north coastal California, Department of Geology, Humboldt State University, Arcata, p. 182-187.

Vick, GS., 1988, Late Holocene paleoseismicity and relative sea level changes of the Mad River Slough, northern Humboldt Bay, California: M. S. thesis, Arcata, California, Humboldt State University, 87 p.

Wagner, D.L. and Saucedo, G.J., 1987, Geologic map of the Weed quadrangle; California Division of Mines and Geology, Regional Map Series, Map 4A, 1:250,000 map sheet.

Witter, R.C., 1999, Late Holocene paleoseismicity, tsunamis and relative sea-level changes along the south-central Cascadia subduction zone, southern Oregon, U.S.A.: Ph.D. dissertation, Eugene, University of Oregon, 178 p.

WCA (Woodward-Clyde Associates), 1980, Evaluation of the potential for resolving the geologic and seismic issues at the Humboldt Bay Power Plant Unit no. 3: Appendices, Woodward-Clyde Consultants, Walnut Creek, California.

Yamaguchi, D.K., Atwater, B.F., Bunker, D.E., Benson, B.E., and Reid, M.S., 1997, Tree-ring dating the 1700 Cascadia earthquake: Nature, v. 389, p. 922-923.

USE OF GEOMORPHIC PROFILING TO IDENTIFY QUATERNARY FAULTS WITHIN THE NORTHERN AND CENTRAL SIERRA NEVADA, CALIFORNIA

WILLIAM D. PAGE[1] AND THOMAS L. SAWYER[2]

ABSTRACT

Although late Cenozoic faulting in the Sierra Nevada north of the Tuolumne River was recognized more than a century ago, it took the 1975 Oroville earthquake (M_L5.7) near the northern end of the Foothills fault system to bring attention to the potential for active faults within the Sierra Nevada. Since then more than thirty major studies have shown that, because they have low to very low degrees of activity, active faults in this area are difficult to recognize and require extensive investigations to characterize. Because identification of the late Cenozoic faults using geomorphic profiles has proved effective to help locate potentially active faults, we constructed 32 geomorphic profiles on late Cenozoic deposits in the northern and central Sierra Nevada. From these we identified 135 late Cenozoic geomorphic anomalies, of which we interpret 110 to be late Cenozoic faults. We find that down-to-the-east anomalies are commonly late Cenozoic faults. Paleogeographic reconstructions are useful to confirm non-tectonic origins for some anomalies and analysis of adjacent profiles help limit the lengths of the late Cenozoic faults (generally less than 20 kilometers). The profiles show that many late Cenozoic faults coincide with sections of the Mesozoic Foothills fault system, but most Mesozoic faults are not late Cenozoic faults. Additional detailed investigations, particularly trenching, are needed to evaluate the anomalies. Thus far investigations of 29 anomalies have confirmed that three out of four reflect Quaternary faults.

INTRODUCTION

The northern and central Sierra Nevada north of the Tuolumne River and west of the range crest has about 450 dams large enough to be under the jurisdiction of the California Division of Safety of Dams (DWR, 1988). Most of these dams were constructed more than 50 years ago with little consideration to earthquake hazards. To assess whether or not these dams and other critical facilities in the region are safe from earthquakes, the potential seismic sources need to be identified and characterized so that potential ground motions can be estimated.

Although late Cenozoic faulting in the northern and central Sierra Nevada ("the Sierra Nevada") was recognized more than a century ago (Browne, 1890; Lindgren, 1911), and was later noted at Tuolumne Table Mountain near Sonora (Eric et al., 1955; Hudson, 1965; Bateman and Wahrhaftig, 1966; WCC, 1975), it took the 1975 Oroville earthquake (M_L5.7) near the northern end of the Foothills fault system to bring attention to the potential for active faults within the Sierra Nevada. Studies of the surface rupture along the Cleveland Hill fault documented several centimeters of oblique faulting (normal west-side-down, right-slip) associated with the earthquake (Hart and Rapp, 1975; Clark et al., 1976). Trenches across the fault revealed similar,

[1]Geosciences Department
Pacific Gas and Electric Company
P.O. Box 770000, Mail Code N4C
San Francisco, California 94177
wdp7@pge.com

[2]Piedmont Geosciences, Inc.
10235 Blackhawk Drive
Reno, Nevada 89506
piedmont@reno.quik.com

older displacements, showing that significant earthquakes had occurred repeatedly on the fault (WCC, 1976, 1978a; Schwartz et al., 1977; Page et al., 1978b).

As a result of the 1975 earthquake, more than thirty major studies were conducted to investigate the activity of faults in various parts of the range. (Although many references are "gray literature", the important ones are referred to because they are commonly the only sources of information available; they are in the files of facility owners and the regulatory agencies):

- California Department of Water Resources - for Oroville Dam (DWR, 1977, 1979, 1989)

- California Department of Conservation, Division of Mines and Geology - for Alquist-Priolo studies (Bryant, 1983a, 1983b, 1983c)

- Nevada County Water Agency - for one dam (BGC, 1995)

- Oroville-Wyandotte Irrigation District - for two dams (Hamilton and Harlan, 1998)

- Pacific Gas and Electric Company (PG&E) - for a proposed nuclear power plant site (WCC, 1978a, 1978b, 1978c) and their 170 dams (WCC,1978c; PG&E, 1994b)

- Placer County Water Agency - for one dam (PG&E, 1994a)

- Sacramento Municipal Utility District - for two dams (Hamilton, 1994)

- U.S. Army Corps of Engineers - for nine dams (WCC, 1976; USACOE, 1977, 1982, 1994; Biggar et al., 1978; TEC, 1983; HTA, 1987; Haynes-Griffin, 1987; D&M, 1993)

- U.S. Bureau of Reclamation - for two dams (Alt et al., 1977; Schwartz et al., 1977; USBR, 1978)

- Yuba County Water Agency - for two dams (WCC, 1981; PG&E, 1991, 1992a, 1992b)

Since the earliest fault studies, the investigations have shown that, because active faults have low to very low degrees of activity in the Sierra Nevada, they are difficult to recognize and require extensive investigations to characterize. Jennings (1994) evaluated the information interpreted from the geomorphic profiles presented in this paper and created a separate category for late Cenozoic faults within the Sierra Nevada. Erosion by streams, rivers, and slope processes complicates the assessments: (1) the ~0.1 mm/year incision rates of the rivers and the corresponding erosion rates on the mountain slopes (Page and Noryko, 1977; Huber, 1981) are much faster than the 0.001 to 0.01 mm/year faulting rates, leaving the generally narrow interfluves where the ~0.001 mm/year erosion rates (Page and Noryko, 1977) are low enough for preservation of faulting, (2) the amount of displacement per event is small (5 to 50 cm), and (3) the recurrence interval between events on individual faults can be tens of thousands, or even hundreds of thousands of years. Thus, except in areas of very low erosion rates, erosion commonly destroys the features indicative of active faulting. Furthermore, differential erosion along the regional metamorphic foliation, particularly along the bedrock shears and faults in the Mesozoic Foothills fault system, has produced striking lineaments that have nothing to do with active faulting.

This paper focuses on identification of the late Cenozoic faults using the geomorphic profiling method, a technique that involves plotting geomorphic surfaces on a geologic cross-section to illustrate the relationship between a paleo landscape and the geologic features. The geomorphic profiling technique is discussed in detail because it is specific (but not unique) to the Sierra Nevada. The other methods for assessing fault activity (lineament analysis, geologic mapping, and exploratory trenching) are widely used in studies of Quaternary faults, but are only briefly presented with respect to issues encountered in the Sierra Nevada.

TECTONIC SETTING

The Sierra Nevada, together with the Central Valley, form the Sierran block, a tectonic subplate between the Coast Ranges and the Basin and Range (Figure 1) that is being subjected to right shear as the Pacific Plate moves northwest past the North American plate (Argus and Gordon, 1991). The block has been tilted westward approximately 1.5 degrees north of Fresno and the headwaters of the San Joaquin River (Christensen, 1966; Huber, 1981; Unruh, 1991). The Sierran block is bounded on the east by the 650-kilometer-long Sierra Nevada frontal fault system (Jennings, 1994), which is characterized by oblique slip faulting (normal east-side-down, right-slip). The Sierra Nevada frontal fault system forms the western border of the Walker Lane belt, a dif-

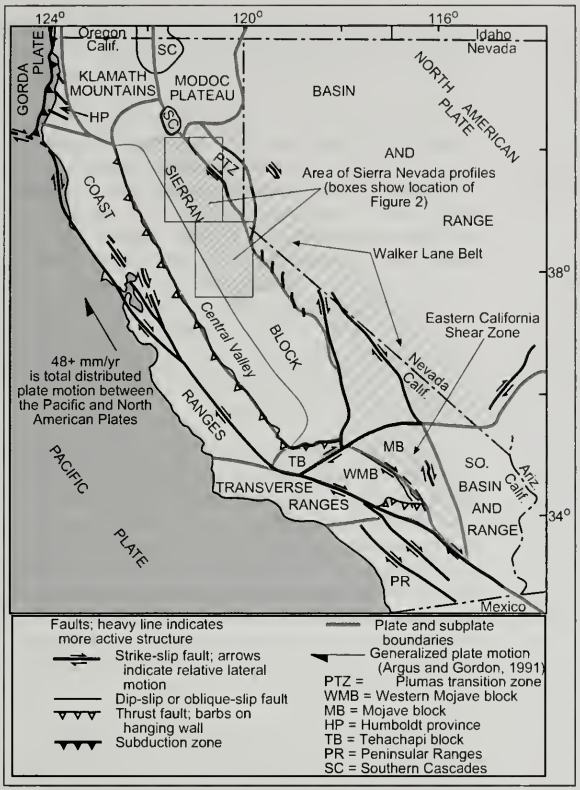

Figure 1. The Sierra Nevada in the current plate tectonic framework.

fuse zone of right-slip faulting that extends from Las Vegas, Nevada into Oregon (Stewart, 1988). The west side of the Sierran block is bounded by contractional deformation along reverse faults at the margin of the Coast Ranges and the Central Valley (Wong and Ely, 1983; Wong et al., 1988; Wentworth and Zoback, 1989; Unruh and Moores, 1992).

The ancestral Sierra Nevada was uplifted in the Cretaceous, but uplift had stopped by 57 million years (Ma) ago and erosion and degradation has proceeded since then (House et al., 1998). During the early to middle Miocene a second phase of tectonics produced moderate uplift of the range (Ely, 1991, 1992). The phase of uplift and tilting of the Sierran block that formed the present range started in the latest Miocene or earliest Pliocene, about 5 million years ago (Axelrod, 1957; Bateman and Wahrhaftig, 1966; Christensen, 1966; Grant et al., 1978; Chase and Wallace, 1986; Unruh, 1991; Wakabayashi and Sawyer, in press), and continues to date. During this last phase of uplift the Sierran block generally has acted as a "rigid body" of the earth's crust, although small amounts of deformation have occurred on short faults within it. The slip rates on these faults (0.001 to 0.01 mm/year) are one or more orders of magnitude lower than the deformational rates along the Sierra Nevada Frontal faults (0.1 - 3 mm/year)(Clark et al., 1984).

Regional seismicity

The Sierran block generally has a low level of seismic activity. The historical record of seismicity in the northern and central parts of the block, south of Lassen Peak and north of the Merced River (the area investigated for this paper), confirms this. The USGS/UC Berkeley on-line catalog of earthquakes for the period 1928 though December 1999 shows that 81 earthquakes of magnitude 4 and greater occurred within the region. The catalog includes fourteen magnitude 5 events. The Toppozada and Parke (1982) catalog reports one magnitude 5 event in 1909, and the Toppozada et al. (1981) catalog of pre-1900 California earthquakes reports three magnitude 5 and seven magnitude 4 events. The largest event reported was a magnitude 5.8 earthquake on 24 October, 1998, near the western shore of Mono Lake. Earthquake focal mechanisms show primarily right slip on northwest-striking faults, left slip on northeast-striking faults, and normal dip slip on faults that strike north (Hill et al., 1991; Uhrhammer, 1991).

GEOLOGIC FRAMEWORK

Pre-Cenozoic rocks

Paleozoic and Mesozoic basement rocks in the Sierran block represent several metamorphic terrains that were accreted to western North America and intruded by Cretaceous plutons (Schweickert, 1981; Edleman and Sharp, 1989; Edleman et al., 1989; Jayko, 1990). The terrains are fragments of oceanic crust, parts of volcanic arcs, and various

continental-margin deposits that range from latest Precambrian to Late Jurassic, 600 to 150 Ma old (Saleeby, 1990). The metamorphic grade ranges from sub-greenschist to amphibolite (Day et al., 1988; Schweickert et al., 1988). The granitic to ultramafic plutons are a product of volcanic-arc activity and range from Devonian to Late Cretaceous, 380 to 80 Ma ago (Stern et al., 1981; Saleeby, 1983, 1990; Sharp, 1988).

The metamorphic rocks have a northerly striking, steeply dipping structural grain that formed during accretion of the terrains. Zones of concentrated deformation are commonly associated with melange units or ultramafic bodies, and represent major pre-Cenozoic fault zones (Saleeby, 1983; Day et al., 1985; Schweickert et al., 1988; Edelman and Sharp, 1989). The Mesozoic Foothills fault system, defined by Clark (1960), includes some, but not all, of these zones of deformation. Because the basement rock is strongly anisotropic, basement shear zones and faults have localized portions of some late Cenozoic faults where they are oriented favorably to the current stress regime (Schwartz et al., 1977). The late Cenozoic faulting, however, commonly diverges from these trends and cuts across the regional fabric and, in places, crosses plutonic rocks.

Foliation is most strongly developed in metasedimentary rock (Day et al., 1985; Schweickert et al., 1988). Pre-Cenozoic basement shear zones and faults are dominantly, but not exclusively, ductile features in the southern and central part of the range. The proportion of brittle structures, related to the generally lower metamorphic grade, increases to the north (Schweickert et al., 1988). Consequently, brittle deformation along a shear zone is not a sufficient criterion to identify late Cenozoic faults in the basement rock. As is typical of rock associated with convergent plate margins, hundreds of basement faults, many of which are not shown on published maps, exist in the Sierra Nevada; most have not been reactivated in the late Cenozoic.

Cenozoic deposits

During the Late Cretaceous and early Tertiary, erosion reduced the region of the present Sierra Nevada to low hills that locally reached 500 meters above broad valleys (Ely, 1991; Yeend, 1974), and the region was deeply weathered (Bateman and Wahrhaftig, 1966). Uplift of the ancestral range in the early to middle Miocene was accompanied by erosion, river incision, and valley formation, followed by widespread deposition of volcanic rocks. By the beginning of the Pliocene, the northern Sierra Nevada was a wide piedmont in front of a string of volcanoes east of what is now the range crest (Curtis, 1954; Slemmons, 1966); hills and ridges of the earlier landscape locally projected above the volcanic deposits. Westerly flowing rivers carved wide valleys, and shallow canyons into the volcanic agglomerates of the Mehrten Formation (Bateman and Wahrhaftig, 1966). During the Pliocene and Pleistocene, in response to the increased gradient due to the regional uplift and westward tilting of the range, the west-flowing rivers incised through the volcanic deposits and into the underlying basement rocks, forming canyons that are commonly a kilometer or more deep. The interfluves were left capped by the Cenozoic deposits.

Individual beds and volcanic flows in the Cenozoic deposits—and their geomorphic surfaces—, as well as the Eocene erosion surface, have proved to be important markers that help to discriminate ancient bedrock faults from Quaternary faults in the Sierra Nevada. The deposits commonly filled ancient valleys and canyons, so the basal unconformities are very irregular. For this reason, and because they are not well exposed, the basal contacts of the deposits are less useful as a stratigraphic marker to locate late Cenozoic faults.

The following Cenozoic deposits have proved useful for geomorphic profiling:

"Auriferous gravel". The channels of the Eocene "auriferous gravel" record an ancient river system in the northern Sierra Nevada (Browne, 1890; Lindgren, 1911; Yeend, 1974). The surface and base of the deposit, where preserved, are smooth and generally make excellent markers (PG&E, 1991).

Valley Springs Formation. The late Oligocene and early Miocene Valley Springs Formation was deposited as volcanic and volcaniclastic rocks in stream valleys within the foothills north of Yosemite (Piper et al., 1939; Slemmons, 1966; Ely, 1991). Individual tuff beds make excellent stratigraphic markers (WCC, 1978a, 1978b; D&M, 1993).

Lovejoy Formation. The Miocene Lovejoy Formation (Durrell, 1966) consists of a sequence of basalt flows that followed rather narrow ancient channels of the ancestral Feather River as it crossed the Sierra Nevada. Extensive remnants now cap the ridges and make good markers (Page et al., 1995); in

addition the uppermost porphyritic basalt (Durrell, 1987), where preserved, is a distinctive mapable stratum.

Mehrten Formation. The Miocene Mehrten Formation, including the Penman Formation (Wagner and Saucedo, 1990), consists generally of a monotonous sequence of andesitic agglomerate and sandstone (Slemmons, 1966; Wagner, 1981) that now cap drainage divides north of the Tuolumne River. The depositional and erosional surfaces on the Mehrten are good markers horizons (Alt et al., 1977; WCC, 1978a; PG&E, 1994a). The top of the Table Mountain latite, a member of the formation near the Stanislaus River, is also an excellent datum (Slemmons, 1953, WCC, 1978a; Rhodes, 1987).

Tusean Formation. The Pliocene Tuscan Formation blankets much of the northernmost Sierra Nevada east of Chico. Its geomorphic surface and the distinctive Nomlaki Tuff within the deposit are useful markers (Alt et al., 1977; Harwood et al., 1981).

Laguna Formation. The Pliocene Laguna Formation occurs as fluvial terraces along the eastern margin of the Central Valley (Lindgren, 1911; Piper et al., 1939; Olmstead and Davis, 1961). Its geomorphic surface is a good geomorphic datum (WCC, 1978a; PG&E, 1991).

Other basalt flows. North of the North Fork of the Feather River the upper surfaces of several Pliocene and Quaternary basalt flows (Cohasset Ridge, Deer Creek, Rock Creek, and Warner Valley basalt) are commonly preserved and make good stratigraphic markers (WLA and PG&E, 1996).

IDENTIFYING QUATERNARY FAULTS USING GEOMORPHIC PROFILING

Analysis of Cenozoic strata and geomorphic surfaces, whether they are the surface on a depositional landform, a stripped structural surface, or the remnants of a relict erosional surface, provides an effective means to distinguish late Cenozoic faults in the northern Sierra Nevada. Such analysis helps to distinguish potentially active faults from the thousands of bedrock faults that form the Foothills fault system. Geomorphic profiles that show the original erosional and depositional surfaces, and in places the strata within the Cenozoic units, help locate late Cenozoic faulting from displacements on the profile.

The use of geomorphic profiles and cross-sections to illustrate the relationships of Cenozoic stratigraphy in the Sierra Nevada is a technique pioneered by Browne (1890) and Lindgren (1911), and used by Bateman and Wahrhaftig (1966). More recently, geomorphic profiling has been used as a strain gauge to help locate late Cenozoic deformation for project-specific investigations (Alt et al., 1977; WCC, 1978a; Page et al., 1978a; Ely, 1992; D&M, 1993).

We have expanded on the earlier work, and have profiled all the major interfluves north of the Tuolumne River where late Cenozoic volcanic and fluvial deposits either cap interfluves or delineate paleo stream courses (Figure 2). Interfluves are useful for this purpose because they are the locale of the lowest erosion rates in the Sierra Nevada, whereas paleo stream channels (particularly the "auriferous gravel") are useful because the channels are markers of limited thickness and generally were formed by graded streams with smooth, concave profiles. Lava flows are useful because, after they filled the ancient valleys and canyons, the tops of the flows formed smooth depositional surfaces.

We constructed 32 geomorphic profiles, using 1:24,000-scale U.S. Geological Survey topographic maps, primarily on the Mehrten and Tuscan formations; five of the profiles followed lava flows. The profiles were drawn as straight-line segments, placed along ridge crests to closely approximate the flow direction of paleo streams. A series of points that follow the geomorphic position of the least eroded part of the divide or ridge top were then projected perpendicular to the profile segment. To reduce projection anomalies, the turn points were placed on the geomorphic surface.

The geology along the profiles was projected onto the vertical plane of the cross-sections from published and unpublished maps and reports. The regional paleo flow directions were assessed from the distribution patterns and surface gradients of these deposits. Adjacent interfluves, rivers and streams, and geographic landmarks were projected perpendicular to the cross-section. In contrast, geologic structures and stratigraphic contacts were projected along their respective strike to the cross-section.

From the profiles, we identified stratigraphic and geomorphic anomalies where the projection of one surface or stratigraphic contact is more than 10 to 15 meters above or below the correlative datum

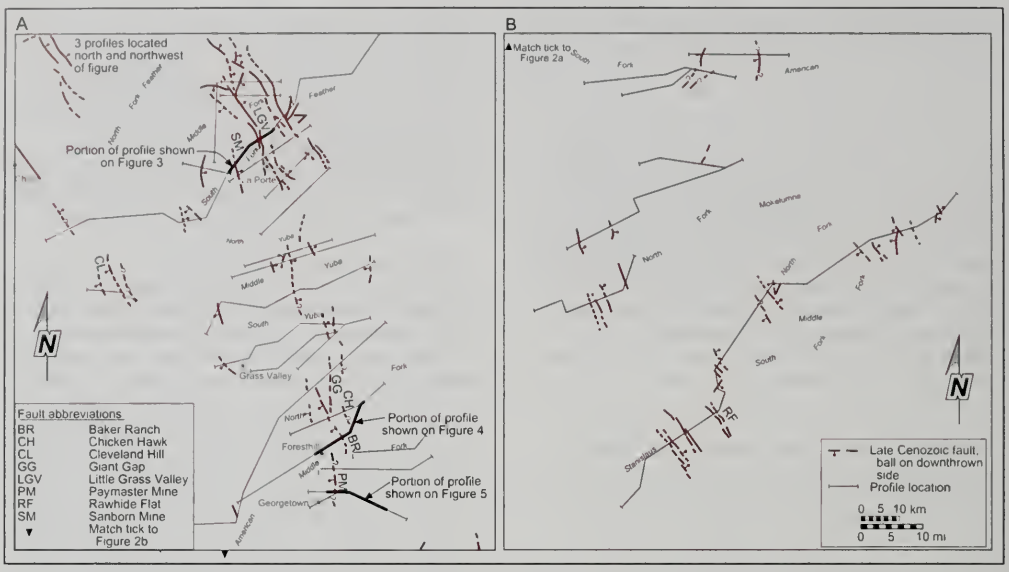

Figure 2. Map of geomorphic profiles and late Cenozoic faults in the Sierra Nevada. Faults were identified from analysis of geomorphic profiles.

(generally considered the resolution of the technique using 1:24,000-scale topographic maps), or the gradients on the surfaces differ by more than 5 meters per kilometer, provided that remnants are well preserved and extend for at least a kilometer on each side of the anomaly. The gradients of the geomorphic surfaces and the dips of Cenozoic stratigraphic contacts on the cross-sections are apparent, rather than true (attitudes have not been corrected for original orientation), but are considered representative. The amounts of vertical separation or gradient changes were measured directly from the profiles at each of the anomalies.

We evaluated each geomorphic anomaly by interpreting topographic maps and aerial photographs, by helicopter reconnaissance, and by selective field examination. The likelihood that an anomaly was a fault or the location of tectonic deformation was assessed based on the preservation and extent of the associated geomorphic surfaces and on the lengths of the projections of these surfaces. Stratigraphic anomalies were evaluated using the quality of exposures and the amount of depositional relief on the contact. At the significant anomalies, we inspected aerial photographs and topographic and geologic maps for geomorphic evidence of bedrock faults (aligned side-hill benches and ridge-top saddles, linear drainages, small alluvial basins, vegetation lineaments, bedrock faults). Using this information we inferred faults and suspected faults 5 kilometers in either direction from the anomaly (Figure 2), unless the data permitted longer extensions.

Assumptions and limitations

The technique of identifying and characterizing late Cenozoic faults from geomorphic profiles involves a number of assumptions and has limitations. The underlying premise is that most displacement along the faults postdates deposition of the marker unit (e.g., late Miocene Mehrten Formation) or the formation of the geomorphic surface (e.g., the Eocene erosion surface). Another assumption is that the faulting is temporally and structurally related to uplift and westward tilting of the range, which began about 5 million years ago, and was not significant prior to then.

The fundamental assumption in the technique is that the geomorphic surface or stratigraphic contact on one side of an anomaly is correlative on the opposite side. (Although we believe this generally to be true, aerial and field reconnaissance in some

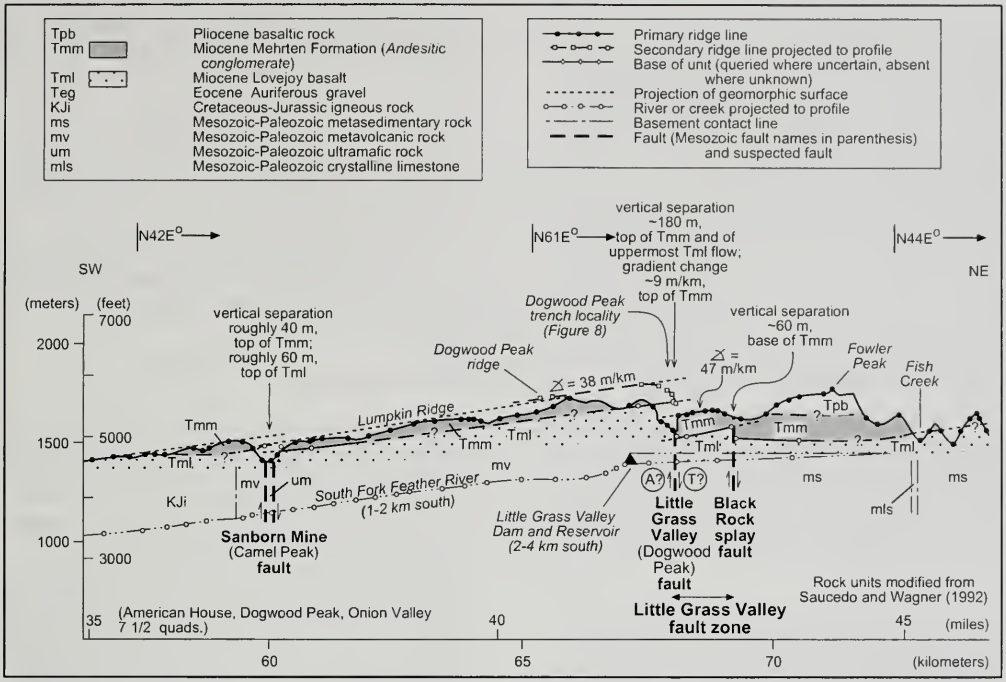

Figure 3. Profile on the Lovejoy basalt (Tml) and the Mehrten Formation (Tmm) at Lumpkin Ridge.

areas showed the geomorphic surfaces do not always correlate; in several cases, we found anomalies where a younger erosion surface has cut into the older surface, or a younger depositional surface lies below an older one.) We assumed that when the projections of two surfaces are closely concordant (their cumulative vertical separations are less than about 10 to 15 meters, and their gradients are within 5 meters per kilometer), the surfaces correlate, and no late Cenozoic fault exists between the two remnants.

Our profiling technique has several specific limitations. It generally cannot detect faults that have had small displacements. For example, relatively minor displacements along faults in late Cenozoic strata identified in field studies by Strand (1972), and Alt et al. (1977) were not detected using the technique applied in this study. The technique does not work where geomorphic surfaces are poorly preserved or widely discontinuous, because the exact position of the surfaces is uncertain. For example, at the higher elevations of the Sierra, glaciers have commonly destroyed the old surfaces. An area where a stratigraphic contact is not well constrained, or has considerable relief, precludes correlation with enough precision to identify tectonic effects. Typically, for example, the basal contact of a valley or canyon fill is unreliable, unless the ancient channel thalweg is identified and used as the marker unit.

Our technique is sensitive to vertical displacement but is not sensitive to lateral offset. Earthquake focal mechanisms (Uhrhammer, 1991; Hill et al., 1991), paleoseismic trenching studies (PG&E, 1994b; USACOE, 1994; Sawyer and Page, in preparation), and field mapping (Lahren and Schweickert, 1991) indicate that some late Cenozoic faults in the Sierra Nevada have a lateral component.

Non-tectonic processes may explain many anomalies that have a sense of vertical separation down in the direction of the flow (west side down). Most commonly, these anomalies are where the Mehrten Formation has been deposited around paleo highlands. Our profiles follow the regional, not necessar-

ily the local, paleo flow direction. Thus, by projecting the meandering flows onto the profile line, gradients may appear steepened and result in vertical separations that are artifacts of the profiling method. The Tunnel Hill anomaly east of Georgetown is an example (discussed below). Down-gradient vertical separations of the Mehrten surface across the highlands are a function of the amplitude of the meander that encircles each highland; therefore, the associated anomalies appear to be non-tectonic in origin. Careful evaluation of such anomalies is needed, however, because paleoseismic trenching of the Baker Ranch fault (PG&E, 1994a) showed that an anomaly could result from a combination of diversion of flows around a paleo highland and vertical separation along a fault (discussed below).

Most of our profiles follow northeast-trending interfluves on the western slope of the Sierra Nevada; thus, northeasterly striking faults that parallel the interfluves are difficult to identify. However, where geologic information can be projected from one interfluve to another, profile-parallel faults have been identified.

Some anomalies are caused by differential erosion on beds in the Mehrten or other formations, rather than Quaternary faulting. Careful mapping of stratigraphic contacts usually can identify these. If required, the anomaly can be trenched and detailed topographic profiling done across it, as was done for the Mount Hope anomaly on the ridge near Volcanoville, northeast of Georgetown (PG&E, 1994a).

In spite of the assumptions and limitations, geomorphic profiling is useful as a reconnaissance technique to identify relatively significant late Cenozoic faults and distinguish them from inactive bedrock faults of the Foothills fault system. The method allows the focusing of more detailed studies, such as field mapping and trenching. Field and exploratory trench studies have confirmed many anomalies as Quaternary faults.

Lineament analysis

Analysis of lineaments on maps, aerial photographs, and other imagery has been an effective tool to help identify active faults in many areas of the world. In the Sierra Nevada, however, the ancient shear zones and faults of the Foothills fault system are the locus of hundreds to thousands of lineaments (Schwartz et al., 1977; WCC, 1978a). Most of these are caused by differential erosion along the weaker rocks that form the shear zones, and do not reflect recent displacements. Nonetheless, a few late Cenozoic faults locally have followed bedrock structures that are oriented favorably to the current tectonic stress regime (Schwartz et al., 1996), as has

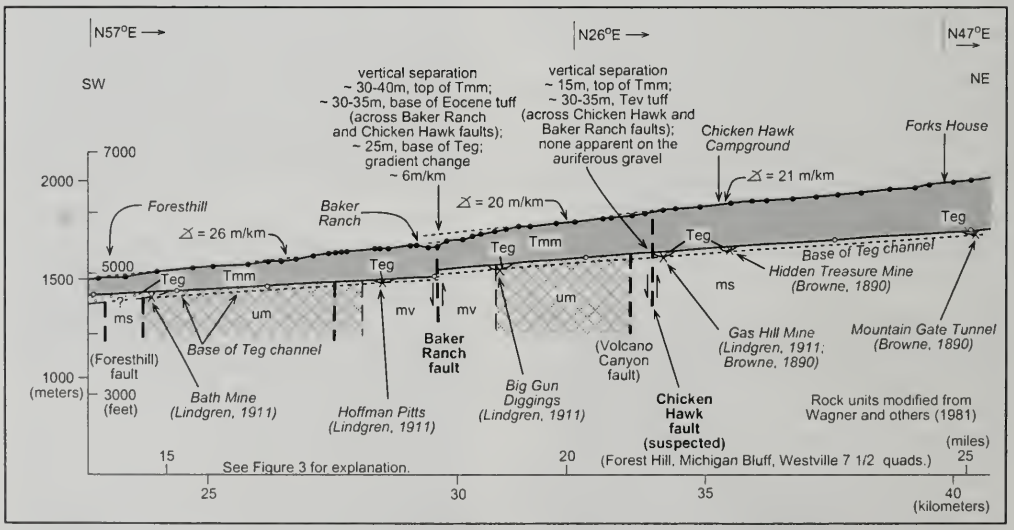

Figure 4. Profile on the Mehrten Formation along the Forest Hill Divide.

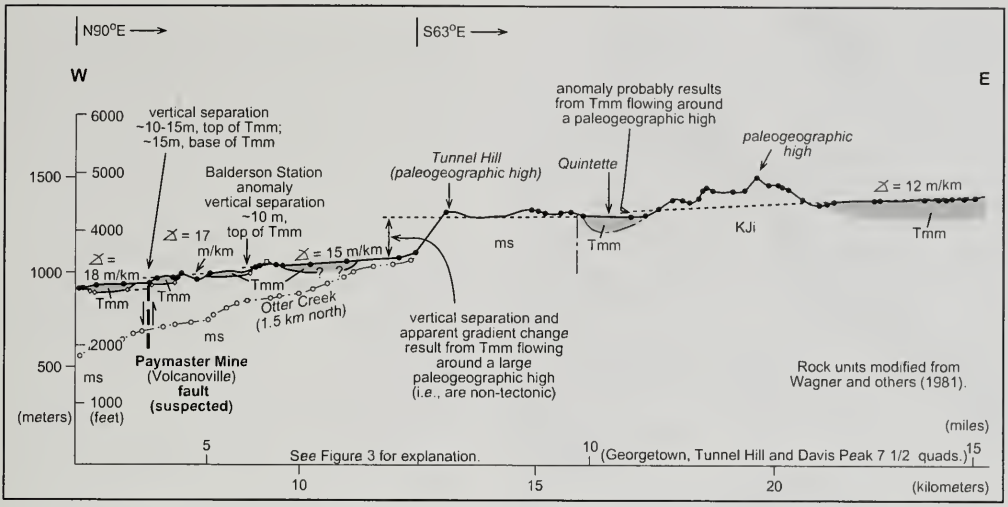

Figure 5. Georgetown Divide profile on the Mehrten Formation across Tunnel Hill.

been shown to be common elsewhere in the world (e.g., Sykes, 1978); thus, some lineaments, including those traversing old geomorphic surfaces, do depict Quaternary faults. Careful examination of areas of low erosion rates, particularly drainage divides and alluvial surfaces (the best locations to evaluate such lineaments), is an effective approach to discern the origin of geomorphic lineaments.

Detailed geologic mapping

Detailed geologic mapping can help verify the stratigraphic relationships at the geomorphic anomalies. Accurately delineating stratigraphic contacts and units within late Cenozoic deposits can prove or disprove faulting, provided the exposures are sufficient. Mapping of basement shear zones and contacts can help select trench sites as well as support the interpretations by identifying the basement structure underlying the geomorphic anomaly.

Two dating techniques provided useful information for the interpretation of the geomorphic profiles: (1) potassium-argon dates on the Mehrten and Tuscan formations helped constrain their ages (Saucedo et al., 1992) and (2) argon-argon measurements of volcanic flows were key in dating low potassium basalt as young as 60,000 years in the northern Sierra Nevada (Becker et al., 1994; Page and Renne, 1994).

Trenching

A successful method for evaluating fault activity is trenching across suspected late Cenozoic faults and logging the trench in detail to depict the stratigraphic relationships in the generally thin Quaternary deposits. Because faulting displacements are small and recur on long time periods (many thousands to tens of thousands of years), the trenches need to be sited in areas where the rates of erosion or deposition are low, such as at drainage divides. Typical features in trench exposures indicative of active faults include small steps in the bedrock surface, stepped or otherwise distorted stone lines, slickensided surfaces in pedogenic soils that extend downdip into the bedrock, and anomalous changes in stratigraphy across the fault. These commonly subtle, near-surface features tend to be quickly and easily destroyed or modified by surficial processes, such as soil creep, shrink-swell of expansive soils, animal burrows, and tree roots. These non-tectonic processes can produce features that resemble tectonic features, so trench exposures require careful interpretation (Swan and Hanson, 1977; Page et al., 1978b; WCC, 1978a).

Two dating methods were applied with success to dating of the trench stratigraphy. (1) Radiocarbon dates on charcoal were consistent and reproducible; however, the surficial deposits in the foothills only

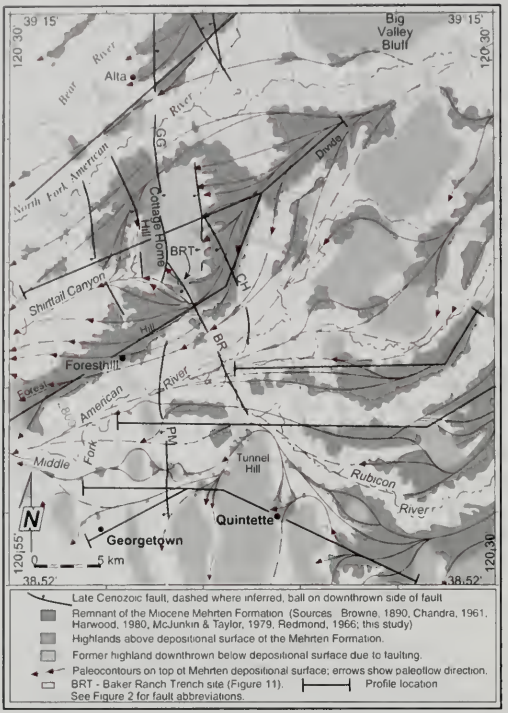

Figure 6. Paleogeographic reconstruction showing the flow paths of the Mehrten Formation in the Foresthill area.

locally contain such materials. Burned tree roots, charcoal in animal burrows, and mixing between deposits can complicate the interpretations. (2) Paleomagnetic measurements of the fine-grained depositional units proved useful in demonstrating that some colluvial and soil deposits are older than 780,000 years (the Bruhnes-Matuyama reversal) (Baksi et al., 1992). However, multiple magnetic directions—apparently resulting from weathering directions superimposed on depositional directions (Butler, 1991)—can complicate the interpretations (PG&E, 1991).

EXAMPLES OF GEOMORPHIC PROFILES AND ANOMALIES

We have chosen three profiles on late Cenozoic volcanic flow sequences in the northern and central Sierra Nevada to illustrate the geomorphic profiling technique. The Lumpkin Ridge profile (Figure 3) on the Lovejoy Formation follows this extensive sequence of Miocene basalt flows across part of the northern Sierra Nevada. The Forest Hill Divide profile (Figure 4) follows an extensive Mehrten depositional surface along the drainage divide between the North Fork and Middle Fork of the American River. The Georgetown Divide profile (Figure 5) follows eroded remnants of the Mehrten Formation on the divide south of the Middle Fork of the American River. The Forest Hill and Georgetown divides are in an area where the widespread and relatively uneroded depositional geomorphic surfaces provide the basis for a paleogeographic reconstruction of the depositional surface on the upper Mehrten Formation (Figure 6). Our reconstruction indicates that in the late Miocene the area was an expansive lahar/alluvial fan that issued from the ancestral canyon of the North Fork of the American River near Big Valley Bluff, and a smaller fan that had its source in the Rubicon River drainage east of Quintette.

Lumpkin Ridge profile - Little Grass Valley anomaly

Figure 3 is part of a very long profile on the Lovejoy Formation from Honey Lake to Oroville, that shows more than twenty faults within and bounding the Sierra Nevada and in the Diamond Mountains (Page et al., 1995). The portion of this profile that

Figure 7. Photograph of the Little Grass Valley fault. View is north along the fault (black arrows). The Black Rock splay of the Little Grass Valley fault follows the Black Rock arm of Little Grass Valley Reservoir in the center of the photograph. Dogwood Peak is in the middle distance; the Middle Fork Feather River Canyon is between them. The geomorphic profile (Figure 3) follows the ridgeline in the middle of the photograph. The Dogwood Peak trench site (Figure 8) is in the saddle to the right of Dogwood Peak.

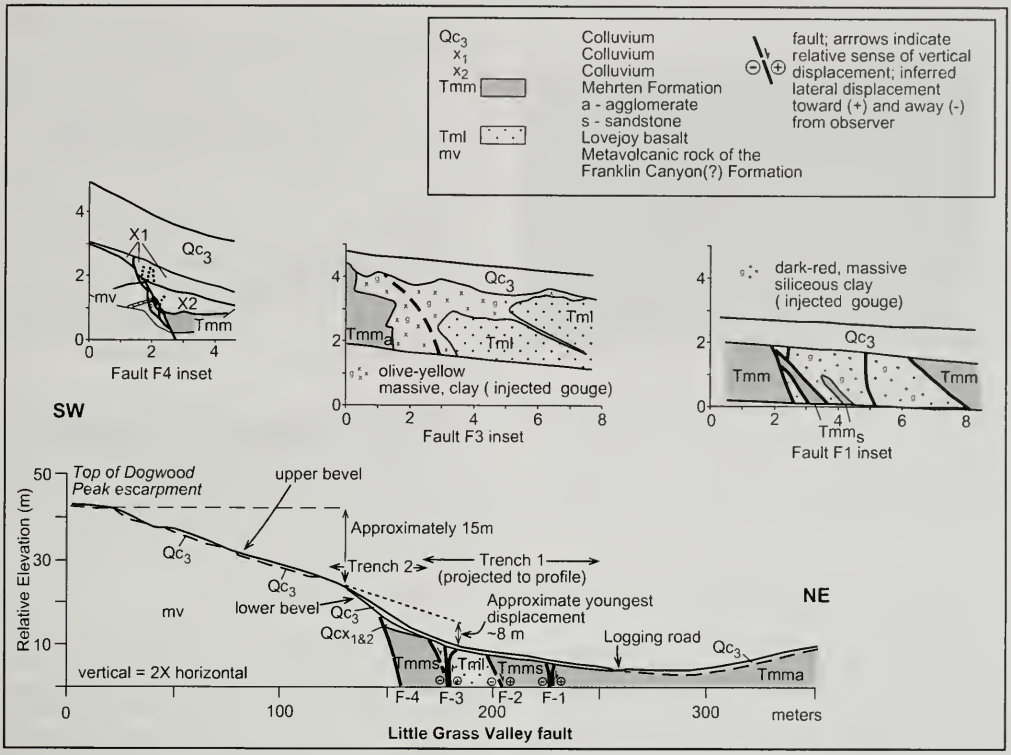

Figure 8. Cross-section at the Dogwood Peak trench locality.

crosses the northern Sierra Nevada near La Porte (Figure 2) illustrates three anomalies — one that coincides with the Sanborn Mine fault, and two that coincide with faults of the Little Grass Valley fault zone. The Little Grass Valley anomaly is discussed below because it (1) shows large down-on-the-east vertical separation of the Lovejoy and the overlying Mehrten formations, (2) is counter to the flow direction of these units, (3) is coincident with the Dogwood Peak bedrock fault, and (4) displaces both the base and top of the Lovejoy flow sequence.

The Little Grass Valley fault was first recognized as a late Cenozoic fault by Lindgren (1911), based on his early geomorphic analysis of the gold mines and tectonics at La Porte. Alt et al. (1977) extended the fault north to Spanish Peak. Our profile and detailed field mapping along the divide between the Middle and South forks of the Feather River for this study show that two faults, the Little Grass Valley fault and the Black Rock splay fault, vertically separate the geomorphic surface on the Lovejoy basalt a total of about 240 meters (Figure 3); the main Little Grass Valley fault displaces the Lovejoy about 160 meters.

The Little Grass Valley fault (Figure 7) was trenched at the divide to characterize its Quaternary activity (Page and Sawyer, 1992; Sawyer and Page, in preparation). (Herein, we informally refer to the section of the Mesozoic Dogwood Peak fault that is coincident with the late Cenozoic faulting as the Little Grass Valley fault.) Three trenches across the main fault at the saddle exposed four faults, F1 to F4 (Figure 8). F1 and F3 are massive, vertical, 2- to 4-meter-wide clay-filled gouge zones that appear to have been injected into the fault zone during at least three Quaternary surface-faulting events; F1 juxtaposes weathered sandstone and agglomerate beds within the Mehrten Formation; F2 is an east-

Figure 9. Photograph of the Baker Ranch fault. View is south from Shirttail Canyon along the fault (black arrows). The flat surface that forms the Forest Hill Divide (black, dash-dot arrows) is a relict depositional surface of the Mehrten Formation. The Baker Ranch trench locality is indicated by (white arrow). Cottage Home Hill is in the middle foreground.

dipping normal fault that places sandstone against Lovejoy basalt that has been weathered to saprolite; F3 juxtaposes sandstone against Lovejoy saprolite. F4 is sheared, foliated greenstone in fault contact with weathered Mehrten sandstone (Figure 8). Faults F1 to F3 do not displace the thin overlying colluvial deposits nor do the faults have any geomorphic expression at the trench site (Figure 8), indicating some antiquity to the most recent displacement on these faults. However, analysis of scarp-derived colluvium at fault F-4 in trench 2 indicates three, or possibly four, displacement events in the late Pleistocene (Figure 8). The uppermost colluvium that overlies F-4 is unfaulted and has yielded radiocarbon dates on detrital charcoal of 2,000 to 8,000 years BP.

The two bevels on the east-facing Dogwood Peak escarpment upslope of the trenches record two periods of tectonic activity of the fault (Figure 8). An older sequence of events formed a scarp with about 15 meters of cumulative displacement; during a quiescence period this scarp was eroded and degraded to form the upper bevel. A younger period of faulting formed the steeper lower bevel, and records about 8 meters of cumulative displacement (23 meters total cumulative displacement).

A narrow, latest Pleistocene lateral moraine at the base of the Dogwood Peak escarpment crosses the Little Grass Valley fault, 1.5 kilometers north of the trench site. A detailed longitudinal profile along the linear 300-meter-long moraine crest, based on a total station survey, shows no vertical displacement (Sawyer and Page, in preparation), tending to confirm the unfaulted Holocene deposits in the trenches.

Forest Hill profile - Baker Ranch anomaly

The profile on the Mehrten Formation along the Forest Hill divide (Figure 4), east of Auburn, and the associated paleogeographic reconstruction map (Figure 6) illustrates anomalies caused by faulting and by depositional patterns around paleogeographic highlands (PG&E, 1994a). The Forest Hill Divide profile shows two down-on-the-west faults near Foresthill: the Baker Ranch and the suspected Chicken Hawk faults.

The Baker Ranch fault was chosen as an example because it is less clearly the result of late Cenozoic faulting. The anomaly (1) has down-on-the-west displacement (in the flow direction of the Mehrten agglomerates, but where extensive remnants of an ancient surface that appears to be the preserved original "depositional surface" on the Mehrten generally remain), (2) is near paleo topographic highs that were never inundated by the Mehrten sedi-

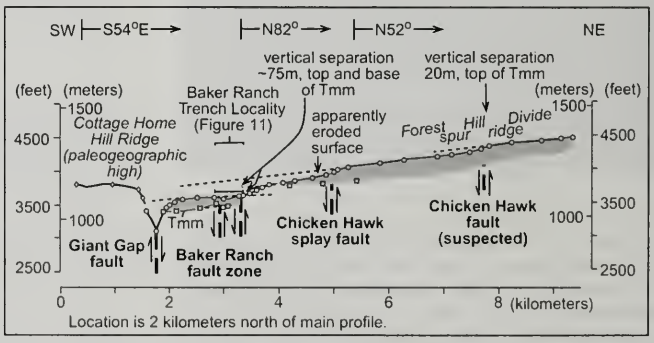

Figure 10. Profile at the Baker Ranch trench locality, 2 kilometers north of the Forest Hill Divide profile (Figure 4).

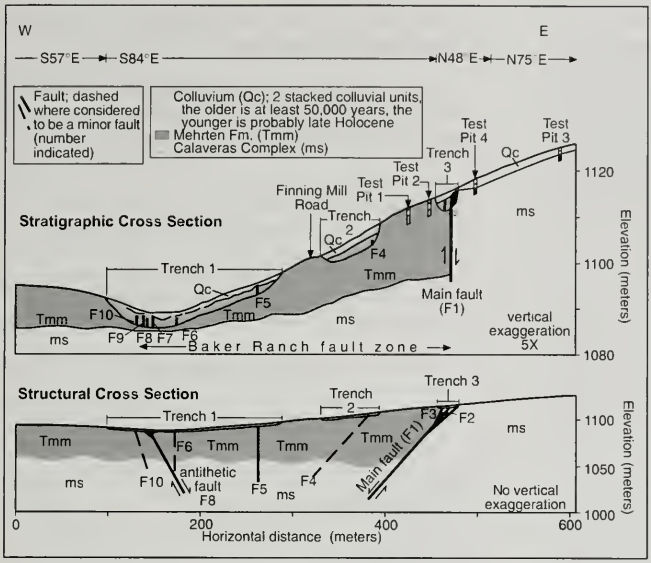

Figure 11. Cross-sections at the Baker Ranch trench locality.

ments, complicating the interpretations, and (3) is underlain by the "auriferous gravel" that is relatively well exposed in the canyon of the American River (Browne, 1890).

The Baker Ranch fault (Figure 9) appears to separate the surface of the Mehrten Formation 30 to 75 meters down on the west, as measured on two profiles along the Forest Hill Divide (Figure 4, Figure 10). In addition, detailed mapping of the base of the underlying "auriferous gravel" and analysis of the mapping by Browne (1890) show 25 meters of displacement across the Baker Ranch and Chicken Hawk faults, combined. The flow patterns of the Mehrten around a small paleo high on the Forest Hill Divide just north of Baker Ranch and around the larger paleo high at Cottage Home Hill influenced the depositional patterns of the Mehrten agglomerates. Apparently the Mehrten streams flowed mostly south of the paleo high north of Baker Ranch, but were blocked and ponded against the paleo high east of Cottage Home Hill. At the Baker Ranch trench locality, Mehrten agglomerate was deposited mostly from the south, but the final deposits appear to have inundated a paleo saddle east of the trenches and capped the earlier deposits. A portion of the apparent displacement on the Baker Ranch fault (Figure 4) is probably nontectonic, resulting from projecting the meandering flow onto the profile.

Three trenches excavated in a small saddle near the head of Shirttail Canyon exposed a Late Cenozoic fault and an antithetic zone of faults (PG&E, 1994a). The main fault does not have a discrete scarp at the surface, but is at the lower part of a smooth-sloping surface, the degraded fault scarp. In the trench, the fault juxtaposes weathered metavolcanic rock against highly weathered Mehrten agglomerate (Figure 11) along a narrow zone of faults and shears that cuts both bedrock units. The two overlying colluvial deposits, however, are unfaulted; the lower colluvium is estimated to be older than 100,000 years, based on weathering and comparison to other colluvial units in the Sierra Nevada foothills. The antithetic fault (faults F7 to F10) has a 4-meter-high scarp, and displaces units within the Mehrten Formation across a zone of small breccia and shears. Two equivalent colluvial units were exposed in the trench and, although the older is discontinuous, both are interpreted as unfaulted.

Neither the Giant Gap fault to the north, nor the suspected Paymaster Mine fault to the south, appear to displace the surface of the Mehrten Formation at the Forest Hill Divide. This relationship helps constrain the end points and, thus, the lengths of these late Cenozoic faults. Furthermore, it shows that the lengths of the bedrock faults cannot be used to estimate the lengths of the late Cenozoic fault segments when estimating earthquake magnitudes.

Georgetown Divide profile - Tunnel Hill anomaly

The Georgetown Divide profile (Figure 5) shows two down-on-the-west anomalies. One is at the suspected Paymaster Mine fault, suggesting late Cenozoic displacement coincident with a portion of the Mesozoic Volcanoville fault. The other is the major anomaly across a paleogeographic high at Tunnel Hill. This anomaly, a 300-meter-high, west-down step in the profile, is plotted using extensive rem-

nants of the Mehrten agglomerates. The flow patterns shown on Figure 6 indicate that Mehrten lahars had to flow about 10 kilometers around the northern end of the hill instead of taking the more direct 4-kilometer-long route across the hill. A profile (not shown) of the actual flow paths shows that the regional surface gradient is smooth around Tunnel Hill; thus, the apparent displacement is an artifact of the profiling method.

RESULTS OF THE PROFILING TECHNIQUE

Analysis of the 32 geomorphic profiles revealed 135 late Cenozoic geomorphic anomalies. We interpret 110 of these anomalies to be of late Cenozoic faulting origin (most of which are shown on Figure 2), and 25 to be of uncertain origin, possibly nontectonic.

Since 1975, 29 geomorphic anomalies have been investigated in detail, and trenches have been excavated to evaluate whether or not they are late Quaternary faults. Trenching studies sited on geomorphic anomalies have been more successful in identifying Quaternary faults than trenches sited on individual lineaments. Specifically, trenching results show that, on average, three out of four late Cenozoic anomalies reflect Quaternary faults; for those anomalies that are faults, one out of four has been active in the latest Pleistocene or Holocene (Page, 1999). In contrast, when lineaments reflecting bedrock faults are targeted as potential late Quaternary faults, only one in seven trenched lineaments coincide with latest Pleistocene/Holocene faults. Most, however, do not have suitable stratigraphy to allow evaluation of their activity prior to latest Pleistocene.

CONCLUSIONS

Geomorphic profiling is a highly effective tool for identifying late Cenozoic faults in the Sierra Nevada. Analysis of the profiles and paleogeographic reconstructions show the following:

- Down-to-the-east anomalies are usually late Cenozoic faults.

- In contrast, down-to-the-west anomalies are commonly depositional or erosional.

- Late Cenozoic faults have had repeated displacements to create the anomalies.

- The lengths of late Cenozoic faults are generally less than 20 kilometers.

- Many late Cenozoic faults, but not all, coincide with sections of the Mesozoic Foothills fault system. However, most Mesozoic faults are not late Cenozoic faults.

- Paleogeographic reconstructions are useful to confirm non-tectonic origins for some anomalies.

- Lineament analysis, detailed mapping, and trenching are needed to evaluate anomalies identified by geomorphic profiling.

ACKNOWLEDGMENTS

William Savage and Lloyd Cluff of PG&E's Geosciences Department initiated this study to identify active faults in the Sierra Nevada in the early 1990s. Pat Regan and Charles Ahlgren, the directors of PG&E's Dam Safety Program, endorsed the study. We greatly appreciate their support. John Wakabayashi, Steve Thompson, and Richard Ely helped with the preparation of the profiles and the initial analysis of the geomorphic anomalies. Although the authors have been involved in many investigations in the Sierra Nevada, we recognize that many other geologists have put in years of effort and made significant contributions to various aspects of the problem: Jack Alt, Norma Biggar, Lloyd Cluff, Richard Ely, Katherine Hanson, Jeff McCleary, Mike Perkins, David Schwartz, and Bert Swan. We appreciate these and the other geologists who have tried new methods and persevered in gathering enough data to make confident assessments of the activity of faults in the Sierra Nevada. Marcia McLaren helped with the seismicity analysis. Richard Ely and William Fraser provided peer review of this paper. Janet Cluff was the technical editor, and Janet Sawyer prepared the illustrations.

SELECTED REFERENCES

Alt, J.N., Schwartz, D.P., and McCrumb, D.R., 1977, Regional geology and tectonics: in Woodward-Clyde Consultants, Earthquake evaluation studies of the Auburn Dam area, v. 3: Consultant's report to the U.S. Bureau of Reclamation, Denver, 118 p. plus appendices.

Argus, D.F. and Gordon, R.G., 1991, Current Sierra Nevada-North American motion from very long baseline interferometry: Implications for the kinematics of the western United States: Geology, v. 19, p. 1085-1088.

Axelrod, D.I., 1957, Late Tertiary floras and the Sierra Nevadan uplift: Geological Society of American Bulletin, v. 68, p. 19-46, 1 plate.

Bateman, P.C. and Wahrhaftig, C., 1966, Geology of the Sierra Nevada: in Bailey, E.H., (ed.), Geology of Northern California: California Division of Mines and Geology Bulletin 190, p. 107-172.

Becker, T.A., Sharp, W.D., Renne, P.R., Turrin, B.D., Page, W.D., and Wakabayashi, J., 1994, 40Ar/39Ar dating of young low-K tholeiites: Examples from northeastern California, USA (abs.): in Lanphere, M.A., Dalrymple, G.B., and Turrin, B.D., (eds.), Abstracts of the Eighth International Conference on Geochronology, Cosmochronology, and Isotope Geology: U.S. Geological Survey Circular 1107, 24 p.

BCG (Berlogar Geotechnical Consultants), 1995, Giant Gap fault investigation, Yuba-Bear River Project, Nevada and Placer Counties, California: Consultant's report to the Nevada County Irrigation District, Colfax, California, 15 p. plus plates.

Biggar, N., Cluff, L.S., and Ewoldsen, H., 1978, Geologic and seismologic investigations, New Melones Dam Project, California: Consultant's report by Woodward-Clyde Consultants to the USACOE, Sacramento; 246 p. plus appendices.

Browne, R.E., 1890, Ancient river beds of the Forest Hill Divide: Tenth Report of the State Mineralogist, San Francisco, p. 435-465.

Bryant, W.A., 1983a, Bear Mountain fault zone north of Auburn: California Division of Mines and Geology, Fault Evaluation Report FER-146; 14 p. plus figures.

Bryant, W.A., 1983b, Bear Mountain fault zone, Auburn area: California Division of Mines and Geology Fault Evaluation Report FER-147; 14 p. plus figures.

Bryant, W.A., 1983c, Southern Foothills fault system, Amador, Calaveras, El Dorado, and Tuolumne Counties: California Division of Mines and Geology Fault Evaluation Report FER-148, 12 p. plus figures.

Burnett, J.L., 1963, Fracture traces in the Tuscan Formation, northern California: California Division of Mines and Geology Special Report 82, p. 33-40.

Butler, R.F., 1991, Paleomagnetism: magnetic domains to geologic terranes: Blackwell Scientific Publications, (Boston, Massachusetts), 319 p.

Chandra, D.K., 1961, Geology and mineral deposits of the Colfax and Forest Hill quadrangles, California: California Division of Mines and Geology, Special Report 67, 50 p.

Chase, C.G. and Wallace, T.C., 1986, Uplift of the Sierra Nevada, California: Geology, v. 14, p. 730-733.

Christensen, M.N., 1966, Late Cenozoic crustal movements in the Sierra Nevada of California: Geological Society of America Bulletin, v. 77, p. 163-182.

Clark, L.D., 1960, Foothills fault system, western Sierra Nevada, California: Geological Society of America Bulletin, v. 71, p. 483-496.

Clark, M.M., Sharp, R.V., Castle, R.O., and Harsh, P.W., 1976, Surface faulting near Lake Oroville, California, in August 1975: Seismological Society of America Bulletin, v. 66, p. 1101-1110.

Clark, M.M., Harms, K.K., Lienkaemper, J.J., Harwood, D.S., Lajoie, K.R., Matti, J.C., Perkins, J.A., Rymer, M.J., Sarna-Wojcicki, A.M., Sharp, R.V., Sims, J.D., Tinsley, J.C., and Ziony, J.L., 1984, Preliminary slip-rate table for late Quaternary faults of California: U.S. Geological Survey Open-File Report OFR84-106, 12 p.

Clark, W.B., 1979, Fossil river beds: California Geology, v. 32, no. 7, p. 143-149.

Curtis, G.H., 1954, Mode of origin of the pyroclastic debris in the Mehrten Formation of the Sierra Nevada, California: University of California Publications in Geological Sciences, v. 29, p. 253-502.

D&M (Dames and Moore), 1993, Photogeologic and imagery analysis for the geologic and seismologic investigation, New Hogan Dam, Calaveras County, California: Consultant's report to the U.S. Army Corps of Engineers, Sacramento District, Contract no. DACW05-92-0027, 51 p. plus tables and figures.

Dalrymple, G.B., 1964, Cenozoic chronology of the Sierra Nevada, California: University of California Publications in Geological Sciences, v. 47, 41 p.

Day, H.W., Moores, E.M., and Tuminas, A.C., 1985, Structure and tectonics of the northern Sierra Nevada: Geological Society of America Bulletin, v. 96, p. 436-450.

Day, H.W., Schiffman, P., and Moores, E.M., 1988, Metamorphism and tectonics of the northern Sierra Nevada: in Ernst, W.G., (ed.), Metamorphism and crustal evolution, western conterminous United States, Rubey Volume VII: Englewood Cliffs, Prentice-Hall, p. 737-763.

Diller, J.S., 1895, Lassen Peak Folio: U.S. Geological Survey Atlas Folio 15.

Durrell, C., 1966, Tertiary and Quaternary geology of the northern Sierra Nevada: in Bailey, E.H. (ed.), Geology of Northern California: California Division of Mines and Geology Bulletin 190, p. 185-197.

Durrell, C., 1987, Geologic history of the Feather River country, California: Berkeley, University of California Press, 337 p. plus appendix.

DWR (California Department of Water Resources), 1977, Performance of the Oroville Dam and related facilities during the August 1, 1975 Oroville earthquake: California Department of Water Resources Bulletin 203, 102 p.

DWR (California Department of Water Resources), 1979, The August 1, 1975 Oroville earthquake investigation: California Department of Water Resources Bulletin 203-78, p. 15-121.

DWR (California Department of Water Resources), 1988, Dams within the jurisdiction of the State of California: California Department of Water Resources Bulletin 17-88, Sacramento, 121 p.

DWR (California Department of Water Resources), 1989, The August 1, 1975 Oroville earthquake investigation: California Department of Water Resources Bulletin 203-88, 617 p.

Edelman, S.H. and Sharp, W.D., 1989, Terranes, early faults, and pre-Late Jurassic amalgamation of the western Sierra Nevada metamorphic belt, California: Geological Society of America Bulletin, v. 101, p. 1420-1433.

Edelman, S.H., Day, H.W., Moores, E.M., Zigan, S.M., Murphy, T.M., and Hacker, B.R., 1989, Structure across a Mesozoic ocean-continent suture zone in the northern Sierra Nevada, California: Geological Society of America Special Paper 224, 56 p.

Ely, R.W., 1991, Partially exhumed mid-Tertiary paleovalley along the lower Stanislaus River, Sierra Nevada, California (abs.): Geological Society of America, 1991 Abstracts with Program, v. 23, no. 23, p. 22.

Ely, R.W., 1992, Late Cenozoic uplift and faulting of the Sierra Nevada in the vicinity of Stanislaus Table Mountain, California (abs.): Geological Society of America, 1992 Abstracts with Program, v. 24, no. 5, p. 22.

Eric, J.H., Stromquist, A.A., and Swinney, C.M., 1955, Geology and mineral deposits of the Angels Camp and Sonora quadrangles, Calaveras and Tuolumne counties, California: California Division of Mines and Geology Special Report 41, 55 p.

Evernden, J.F., Savage, D.E., Curtis, G.H., and James, G.T., 1964, Potassium-argon dates and the Cenozoic mammalian chronology of North America: American Journal of Science, v. 262, no. 2, p. 145-198.

Grant, T.A., McCleary, J.R., and Blum, R.L., 1978, Correlation and dating of geomorphic and bedding surfaces on the east side of the San Joaquin Valley using dip: in Singer, M.J., (ed.), Soil development, geomorphology and Cenozoic history of the Northeastern San Joaquin Valley and adjacent areas, California: Guidebook for the joint field session, American Society of Agronomy, Soil Science Society of America, and Geological Society of America, University of California Press, p. 312-318.

Guffanti, M., Clynne, M.A., Smith, J.G., Muffler, L.J.P., and Bullen, T.D., 1990, Late Cenozoic volcanism, subduction, and extension in the Lassen region of California, southern Cascade Range: Journal of Geophysical Research, v. 95, p. 19,453-19,464.

Hamilton, D.H., 1994, Investigation of geological basis of seismic hazard to Slab Creek and Brush Creek dams: in Bolt, B.A., Ghanaat Y., Hamilton, D.H., and Leps, T.M., (Board of Consultants), Report on safety of Brush Creek and Slab Creek Dams: Federal Energy Regulatory Commission, project no. 2101, 20 p., Appendix A, 46 p. plus figures.

Hamilton, D.H. and Harlan, R.D., 1998, Seismotectonic investigation for the region of Lost Creek Dam, South Fork Feather River, California: Consultant's report to Oroville-Wyandotte Irrigation District, Oroville, 39 p. plus figures.

Hart, E.W. and Rapp, J.S., 1975, Ground rupture along the Cleveland Hill fault: in Sherburne, R.W. and Hauge, C.J. (eds.), Oroville, California, earthquake 1 August 1975: California Division of Mines and Geology Special Report 124, p. 61-72.

Harwood, D.S., 1980, Geologic map of the North Fork of the American River Wilderness Study Area and adjacent parts of the Sierra Nevada, California: U.S. Geological Survey Miscellaneous Field Studies Map MF-1177-A, scale 1: 62,500.

Harwood, D.S., Helley, E.J., and Doukas, M.P., 1981, Geologic map of the Chico monocline and the northeastern part of the Sacramento Valley: U.S. Geological Survey Miscellaneous Investigations Series, Map I-1238, scale 1: 62,500.

Haynes-Griffin, M.E., 1987, Seismic stability evaluation of Folsom Dam and Reservoir, Summary Report (report 1): U.S. Army Corps of Engineers Waterways Experiment Station, Vicksburg, MS, Technical Report GL-87-14 (draft), 64 p. plus tables and figures.

Hill, D.P., Eaton, J.P., Ellsworth, W.L., Cockerham, R.S., Lester, F.W., and Corbett, E.J., 1991, The seismotectonic fabric of central California: in Slemmons, D.B., Engdahl, E.R., Zoback, M.D., and Blackwell, D.D. (eds.), Neotectonics of North America: Geological Society of America, Decade Map Volume 1, p. 107-132.

House, M.A., Wernicke, B.P., and Farley, K.A., 1998, Dating topography of the Sierra Nevada, California, using apatite (U-Th)/He ages: Nature, v. 396, p. 66-69.

HTA (Harlan Miller Tait Associates), 1987, Photogeologic interpretation and imagery analysis, Hidden and Buchanan Dams near Merced, California: Consultant's report to the U.S. Army Corps of Engineers, Sacramento District, Contract no. DAC W05-87-R-0024, 53 p. plus appendix.

Huber, N.K., 1981, Amount and timing of late Cenozoic uplift and tilt of the central Sierra Nevada, California-Evidence from the upper San Joaquin River basin: U.S. Geological Survey Professional Paper 1197, 28 p.

Hudson, F.S., 1965, Measurement of the deformation of the Sierra Nevada, California, since middle Eocene: Bulletin of the Geological Society of America, v. 66, p. 835-870.

Jayko, A.S., 1990, Stratigraphy and tectonics of the Paleozoic arc-related rocks of the northernmost Sierra Nevada, California; the eastern Klamath and northern Sierra terranes: in Harwood, D.S. and Miller, M.M. (eds.), Paleozoic and early Mesozoic paleogeographic relations; Sierra Nevada, Klamath Mountains, and related terranes: Geological Society of America Special Paper 255, p. 307-323

Jennings, C.W., 1994, Fault activity map of California with locations and ages of recent volcanic eruptions: California Division of Mines and Geology, Geologic Data Map No. 6, scale 1:750,000.

Lahren, M.M. and Schweickert, R.A., 1991, Tertiary brittle deformation in the central Sierra Nevada, California: Evidence for late Miocene and possibly younger faulting: Geological Society of America Bulletin, v. 103, p. 898-904.

Lindgren, W., 1911, The Tertiary gravels of the Sierra Nevada of California: U.S. Geological Survey Professional Paper 73, 226 p.

Lydon, P.A., 1968, Geology and lahars of the Tuscan Formation, northern California: Geological Society of America Memoir 116, p. 441-475.

McJunkin, R.D., and Taylor, G.C., 1979, Geologic reconnaissance of the Saddle Mountain 15-minute quadrangle: unpublished field study for the State Map Project, scale 1: 62,500.

Olmsted, F.H. and Davis, G.H., 1961, Geologic features and ground water storage capacity of the Sacramento Valley, California: U.S. Geological Survey Water Supply Paper 780, 230 p.

Page, W. D., 1999, Quaternary faulting on strands of the Foothills fault system and other faults within the Sierra Nevada, California (abs.): Geological Society of America 1999, Abstracts with Programs, v. 31, 84 p.

Page, W. D., and Noryko, W., 1977, Erosion rates in the Sierra Nevada foothills near Sonora, California (abs.): in Abstracts with Programs, Geological Society of America, v. 9, no. 4, 479 p.

Page, W.D. and Renne, P.R., 1994, 40Ar/39Ar dating of Quaternary basalt, western Modoc Plateau, northeastern California: implications to tectonics (abs.): in Lanphere, M.A., Dalrymple, G.B. and Turrin, B.D., (eds.), Abstracts of the Eighth International Conference on Geochronology, Cosmochronology, and Isotope Geology: U.S. Geological Survey Circular 1107, 240 p.

Page, W.D. and Sawyer, T.L., 1992, Tectonic deformation of the Lovejoy Basalt, a late Cenozoic strain gauge across the northern Sierra Nevada, California (abs.): EOS, v. 73, 590 p.

Page, W.D., Gillam, M.L., McCleary, J.R., Lambert, R.S., and Blum, R.L., 1978a, Tectonic deformation of Table Mountain near Sonora, California (abs.): Earthquake Notes, Eastern Section, Seismological Society of America, v. 49, no. 1, 90 p.

Page W.D., Swan, F.H., III, Biggar, N., Harpster, R., Cluff, L.S., and Blum, R.L., 1978b, Evaluation of Quaternary faulting in colluvium and buried paleosols, western Sierran Foothills, California (abs.): in Abstracts with Program, Geological Society of America, v. 10, no. 3, 141 p.

Page, W.D., Sawyer, T.L., and Renne, P.R., 1995, Tectonic deformation of the Lovejoy Basalt, a late Cenozoic strain gage across the northern Sierra Nevada and Diamond Mountains, California: in Page, W.D. (ed.), Quaternary geology along the boundary between the Modoc Plateau, southern Cascade Mountains, and northern Sierra Nevada: Friends of the Pleistocene, 1995 Pacific Cell Field Trip, published by PG&E, San Francisco, Appendix 3-3, 11 p. plus tables and figures.

PG&E, 1991, Characterization of potential earthquake sources for Lake Francis Dam, State Dam No. 1034-009: Utility report to the Yuba County Water Agency, Marysville, for the California Division of Safety of Dams, 36 p. plus figures and plates.

PG&E, 1992a, Supplement to characterization of potential earthquake sources for Lake Francis Dam, State Dam No. 1034-009, Volume 1, Section 2, Stratigraphy in the Sierra Nevada Foothills: Utility report to Yuba County Water Agency, Marysville, for the California Division of Safety of Dams, p. 2-1 - 2-18, plus figures.

PG&E, 1992b, Supplement to characterization of potential earthquake sources for Lake Francis Dam, State Dam No. 1034-009, Volume 2, Section 5: Utility report to Yuba County Water Agency, Marysville, for the California Division of Safety of Dams, 9 p. plus figures, table, and attachments.

PG&E, 1994a, Characterization of potential seismic sources for Ralston Afterbay Dam, State Dam No. 1030-4: Utility report to Placer County Water Agency, Foresthill, for the Federal Energy Regulatory Commission, FERC project no. 2079, 93 p. plus appendix, tables, figures, and plates.

PG&E, 1994b, Characterization of potential earthquake sources for Rock Creek (Drum) Dam: Utility report for the California Division of Safety of Dams, Sacramento, 93 p. plus figures and plates.

Piper, A.M., Gale, H.S., Thomas, H.E. and Robinson, T.W., 1939, Geology and ground-water hydrology of the Mokelumne area, California: U.S. Geological Survey Water Supply Paper 780, 230 p.

Redmond, J.L., 1966, Structural analysis of the Blue Canyon Formation in the Sierra Nevada, Placer Country, California: University of Oregon, Ph.D. dissertation, 198 p., plate 2, scale 1:62,500.

Rhodes, D.D., 1987, Table Mountain of Calaveras and Tuolumne Counties, California: Geological Society of America Centennial Field Guide, Cordilleran Section, p. 269-272.

Roberts, C.T., 1985, Cenozoic evolution of the northwestern Honey Lake-Eagle basin, Lassen County, California: Golden, Colorado School of Mines Quarterly, v. 80, no. 1, 64 p.

Saleeby, J.B., 1983, Accretionary tectonics of the North American cordillera: Annual Review of Earth and Planetary Sciences, v. 15, p. 45-73.

Saleeby, J.B., 1990, Geochronological and tectonostratigraphic framework of Sierran-Klamath ophiolitic assemblages: in Harwood, D.S. and Miller, M.M. (eds.), Paleozoic and early Mesozoic paleogeographic relations; Sierra Nevada, Klamath Mountains, and related terranes: Geological Society of America Special Paper 255, p. 93-114.

Saucedo, G.J., Fulford, M.M., Mata-Sol, A.R., and Lindquist, T.A., 1992, Radiometric ages of rocks in the Chico Quadrangle, California: California Division of Mines and Geology Regional Geologic Map Series, map no. 7, scale 1: 250,000, 21 p.

Saucedo, G.J., and Wagner, D.L., 1992, Geologic map of the Chico quadrangle, California: California Division of Mines and Geology, Sacramento, Regional Geologic Map Series, map no. 7, scale 1:250,000.

Sawyer, T.L. and Page, W.D., in preparation, Late Cenozoic activity of the Little Grass Valley fault, northern Sierra Nevada, California (data in PG&E files).

Sawyer, T.L., Page, W.D., Wakabayashi, J., Thompson, S.C., and Ely, R.W., 1993, Late Cenozoic internal deformation on the northern and central Sierra Nevada, California: a new perspective (abs.): American Geophysical Union, Fall Meeting Proceedings, Supplement to EOS, 609 p.

Schwartz, D.P., Swan F.H., Harpster, R.E., Rogers, T.H., and Hitchcock, D.E., 1977, Surface faulting potential: in Woodward-Clyde Consultants, Earthquake evaluation studies of the Auburn Dam area, v. 2: Consultant's report to the U.S. Bureau of Reclamation, Denver, 135 p. plus appendices.

Schweickert, R.A., 1981, Tectonic evolution of the Sierra Nevada: in Ernst, W.G. (ed.), The geotectonic development of California, Rubey Volume I: Englewood Cliffs, Prentice-Hall, p. 88-131.

Schweickert, R.A., Bogen, N.L., and Merguerian, C., 1988, Deformational and metamorphic history of Paleozoic and Mesozoic basement terranes in the western Sierra Nevada metamorphic belt: in Ernst, W.G. (ed.), Metamorphism and crustal evolution, western conterminous United States, Rubey Volume VII: Englewood Cliffs, Prentice-Hall, p. 789-822.

Sharp, W.D., 1988, Pre-Cretaceous crustal evolution in the Sierra Nevada region, California: in Ernst, W.G. (ed.), Metamorphism and crustal evolution, western conterminous United States, Rubey Volume VII: Englewood Cliffs, Prentice-Hall, p. 823-865.

Slemmons, D.B., 1953, Geology of the Sonora Pass region: California University, Berkeley, Ph.D. thesis, 201 p.

Slemmons, D.B., 1966, Cenozoic volcanism of the central Sierra Nevada, California: California Division of Mines and Geology Bulletin 190, p. 199-214.

Stern, T.W., Bateman, P.C., Morgan, B.A., Newell, M.F., and Peck, D.L., 1981, Isotopic U-Pb ages of zircon from the granitoids of the central Sierra Nevada: U.S. Geological Survey Professional Paper 1185, 17 p.

Stewart, J.H., 1988, Tectonics of the Walker Lane belt, western Great Basin: Mesozoic and Cenozoic deformation in a zone of shear: in Ernst, W.G. (ed.), Metamorphism and crustal evolution of the western United States, Rubey Volume VII: Prentice-Hall, Englewood Cliffs, p. 683-713.

Strand, R.L., 1972, Geology of a portion of the Blue Nose Mountain quadrangle and adjacent areas, Plumas and Sierra counties, California: Davis, University of California, M.S. thesis, 86 p., 1 plate, scale 1:24,000.

Swan, F.H., III, and Hanson, K., 1977, Quaternary geology and age dating: in Woodward-Clyde Consultants, Earthquake evaluation studies of the Auburn Dam area, v. 4: Consultant's report to the U.S. Bureau of Reclamation, Denver, 83 p. plus appendices.

Sykes, L.R., 1978, Intraplate seismicity, reactivation of preexisting zones of weakness, alkaline magmatism, and other tectonism postdating continental fragmentation: Reviews of Geophysics and Space Physics, v. 16, no. 4, p 621-688.

TEC (Tierra Engineering Consultants, Inc.), 1983, Geologic and seismologic investigations of the Folsom Dam, California area: Consultant's report to the U.S. Army Corps of Engineers, Sacramento District, contract no. DACW-05-82-C-0042, 146 p. plus figures, tables, and appendices.

Toppozada, T.R. and Parke, D.L., 1982, Areas damaged by California earthquakes, 1900-1949: California Division of Mines and Geology, Open-File Report 82-17 SAC, 64 p.

Toppozada, T.R., Real, C.R., and Parke, D.L., 1981, Preparation of isoseismal maps and summaries of reported effects for pre-1900 California earthquakes: California Division of Mines and Geology, Open-File Report 81-11 SAC, 182 p. plus figures.

USBR (U.S. Bureau of Reclamation), 1978, Seismic study of Sugar Pine damsite: Central Valley Project, American River Division, Auburn-Folsom South Unit, Division of Design and Construction, Geology Branch, 46 p., general geology and fault map.

USACOE (U.S. Army Corps of Engineers), 1977, Fault evaluation study, Marysville Lake Project, Parks Bar alternative, Yuba River, California: report by Sacramento District, 25 p.

USACOE (U.S. Army Corps of Engineers), 1982, Geologic reconnaissance of Englebright Dam and Lake area, California: report by Sacramento District, 5 p. plus plate and figures.

USACOE (U.S. Army Corps of Engineers), 1994, Geologic and seismologic investigation (fault study), New Hogan Dam and Reservoir (New Hogan Lake), Calaveras River, California: report by Sacramento District, 44 p. plus figures, sheets, tables, and appendices.

Unruh, J.R., 1991, The uplift of the Sierra Nevada and implications for late Cenozoic epeirogeny in the western cordillera: Geological Society of America Bulletin, v. 103, p. 1395-1404.

Unruh, J.R. and Moores, E.M., 1992, Quaternary blind thrusting in the southwestern Sacramento Valley, California: Tectonics, v. 11, p. 192-203.

Uhrhammer, R.A., 1991, Northern California seismicity: in Slemmons, D.B., Engdahl, E.R., Zoback, M.D., and Blackwell, D.D. (eds.), Neotectonics of North America: Geological Society of America, Decade Map Volume 1, p. 99-106.

Wagner, H.W., 1981, Geochronology of the Mehrten Formation in Stanislaus County, California: University of California, Riverside, Ph.D. dissertation, 342 p.

Wagner, D.L., Jennings, C.W., Bedrossian, T.L., and Bortugno, E.J., 1981, Geologic map of the Sacramento Quadrangle, California: California Division of Mines and Geology, Sacramento, scale 1:250,000.

Wagner, D.L. and Saucedo, G.J., 1990, Age and stratigraphic relationships of Miocene volcanic rocks along the eastern margin of the Sacramento Valley: in Ingersoll, R.V. and Nilsen, T.H., (eds.), Sacramento Valley symposium and guidebook: Pacific Section, Society of Economic Paleontologists and Mineralogists, v. 65, p. 143-151.

Wakabayashi, J., Page, W.D., Renne, P.R., Sharp, W.D., and Becker, T.A., 1994, Plio-Pleistocene volcanic rocks and incision of the North Fork Feather River, California: tectonic implications (abs.): in Lanphere, M.A., Dalrymple, G.B. and Turrin, B.D. (eds.), Abstracts of the Eighth International Conference on Geochronology, Cosmochronology, and Isotope Geology: U.S. Geological Survey Circular 1107, p.345.

Wakabayashi, J., Page, W.D., Renne, P.R., Sharp, W.D., and Becker, T.A., 1995, Quaternary faulting, incision of the North Fork Feather River, and neotectonics of the northeastern Sierra Nevada, California, in Page, W.D., trip leader, Quaternary geology along the boundary between the Modoc Plateau, southern Cascade Mountains, and northern Sierra Nevada: Friends of the Pleistocene, 1995 Pacific Cell Field Trip, published by PG&E, San Francisco, Appendix 3-2, 7 p. plus figures.

WCC (Woodward-Clyde Consultants), 1975, Phase II report: Regional seismicity and fault study, Foothills fault system study: Consultant's report to Pacific Gas and Electric Company, San Francisco, v. 6, 94 p. plus plate.

WCC (Woodward-Clyde Consultants), 1976, Evaluation of potential for earthquakes and surface faulting, Parks Bar Afterbay Dam, Yuba County, California: Consultant's report to the U.S. Army Corps of Engineers, Sacramento, 45 p. plus figures.

WCC (Woodward-Clyde Consultants), 1978a, Foothills fault system study: Stanislaus Nuclear Project, Site Suitability/ Site Safety Report: Consultant's report to Pacific Gas and Electric Company, San Francisco, Appendix C.4, v. 6, 166 p. plus tables and figures.

WCC (Woodward-Clyde Consultants), 1978b, Quaternary studies-Sierran Foothills: Stanislaus Nuclear Project, Site Suitability/Site Safety Report: Consultant's report to Pacific Gas and Electric Company, San Francisco, Appendix C.5, v. 7, 71 p. plus tables and figures.

WCC (Woodward-Clyde Consultants), 1978c, Significant faults and seismicity in the northern Sierra Nevada region of major PG&E dams: Consultant's report to Pacific Gas and Electric Company, San Francisco, 31 p. plus references, tables, and figures.

WCC (Woodward-Clyde Consultants), 1981, Appendix D, Seismic geology report, FERC 10-year safety inspection report, New Bullards Bar Dam and Reservoir, Yuba County, California: Consultant's report to Yuba County Water Agency, Marysville, 24 p. plus figures.

Wentworth, C.M. and Zoback, M.D., 1989, The style of late Cenozoic deformation at the eastern front of the California Coast Ranges: Tectonics, v. 8, p. 237-246.

WLA (William Lettis and Associates) and PG&E, 1996, Lake Almanor and Butt Valley dams, seismic stability assessment, Volume 1, Seismic source characterization and estimated ground motions: Consultant's report for Pacific Gas and Electric Company, San Francisco, 271 p. plus figures and appendices.

Wong, I.G. and Ely, R.W., 1983, Historical seismicity and tectonics of the Coast Ranges-Sierran Block boundary: implications to the 1983 Coalinga, California earthquake: in Bennett, J.H. and Sherburne, R.W., (eds.), The 1983 Coalinga, California earthquakes: California Division of Mines and Geology Special Publication 66, p. 98-104.

Wong, I.G., Ely, R.W., Killmann, A.C., 1988, Contemporary seismicity and tectonics of the northern and central Coast Ranges-Sierran block boundary zone, California: Journal of Geophysical Research, v. 93, no. B-7, p. 7813-7833.

Yeend, W.E., 1974, Gold-bearing gravel of the ancestral Yuba River, Sierra Nevada, California: U.S. Geological Survey Professional Paper 772, 44 p. plus plate, scale 1: 62,500.


ASSOCIATION OF ENGINEERING GEOLOGISTS
AEG

INTRODUCTION TO THE FACILITIES SECTION

ROBERT ANDERSON[1] AND HORACIO FERRIZ[2]

According to the initial returns of the census, in the year 2000 there were close to 33 million people living in California, with an annual population increase rate of half a million per year. This means that by the year 2020 there may be as many as 43 million people living in the Golden State (and we have heard estimates as high as 48 million). Since there is no new land being added to the state, and we cannot pave over all of our farms and ranches, we are going to face tremendous challenges to provide homes and services for all of our citizens. This section of the book deals with the solutions that we are developing to face these challenges, ranging from the provision of water to the planning of extensive power supply networks, and from the construction of landfills to the retrofit of transportation corridors.

DAMS

This section includes five papers that address past and current practice in the construction of dams. The paper by Simpson and Schmoll (2001) is an outstanding example of the role that engineering geologists play in the exploration, design, and construction of new dams. This excellent case study is nicely complemented by the papers by Fraser (2001a, 2001b), who provides some useful guidance for selecting foundation objectives and assessing faults.

[1]California Seismic Safety Commission
1755 Creekside Oaks Drive, Suite 100
Sacramento, CA 95833
banderson@quiknet.com

[2]HF Geologic Engineering
1416 Oakdale-Waterford Hwy.
Waterford, CA 95386
hferriz@geology.csustan.edu

Although the heyday of dam construction in California has come and gone, there are still some projects planned, under construction, or in need of refurbishment. The latter will become more and more important as the dams built in the last century age, for it is unlikely that existing dams will simply be taken out of service in a state where water is just as valuable as oil. And how does one refurbish and repair dams in areas where communities have encroached into the flood zones protected by the dams? The complementary papers by Kiersch (2001) and by Allen (2001) provide a good overview of the dams of the Folsom reservoir (built in 1948-56), and the refurbishing of the Mormon Island auxiliary dam as an impressive example of seismic remediation of a dam above a heavily populated area.

POWER FACILITIES

With a booming population and industrial development, California has an acute need for additional power plants and related infrastructure. Since there are not many new hydroelectric power projects being proposed, and no new nuclear power plants are in queue to be licensed (California will not allow any new nuclear power plants without a permanent high-level radioactive waste disposal site on line), power plants currently under consideration are primarily natural-gas thermal plants. The new power plants have to be fed natural gas extracted from local reservoirs, or piped in from out-of-state. In earthquake country, this means that the plants and their related facilities, including natural gas supply pipelines, must be able to withstand a certain amount of strong ground shaking and ground deformation. The paper by Anderson (2001) addresses some of the issues relevant to engineering geologists engaged in the power industry, and shows that the next generation will have plenty of room for innovation.

Savage and Anderson (2001) take a step further and look for new issues and opportunities in the development of the growing California power network. We can surely continue building thermal power plants, but how does one satisfy the demands of 35 to 48 million Californians without lowering the quality of service and still maintain the current level of environmental stewardship? These are pressing questions that we will have to live with in the 21st century

LANDFILLS

Landfills seem to be the black sheep of urban facilities. Most people imagine them as steaming, smelly heaps of decaying refuse (even as they throw that candy wrapper into the trash). We are not going to say that a landfill is where we want to spend our next vacation, but the modern sanitary landfill is a carefully planned engineering structure that deals with complications at least as formidable as those faced by the builders of the ancient pyramids of Teotihuacán, Chichen Itzá, or Giza. To make things even more interesting, these new "pyramids" are built atop a layer of slick plastic and with heterogeneous materials, so the challenges to their stability are formidable. Walker and Anderson (2001) do a great job at providing a panoramic view of the tasks that engineering geologists perform for this industry, and the tables in their article summarize the key characteristics of active landfills in Northern California

Similar to other facilities, many California landfills are "elderly" structures that were constructed at a time when we thought the environment could absorb it all. Alas, this was not the case, and a good number of these old landfills have leaked contaminants into groundwater. Reeder et al. (2001) present an interesting case study of a "leaky" southern California landfill, in which the assessment work had to deal with fracture-controlled flow.

BRIDGES

Northern Californians are inordinately proud of their bridges, so the failure of the East Bay Bridge during the 1989 Loma Prieta earthquake struck a deep chord. On an outstanding display of craftsmanship the bridge was re-opened in a matter of days, but the forensic investigation that followed showed that the 1937 bridge was not up to seismic performance standards. Buell et al. (2001) provide an interesting progress report on the work being performed to build a replacement for the East Bay Bridge along an alternative alignment. A once-in-a-century chance to learn how engineering geologists go about helping to build a majestic bridge!

SELECTED REFERENCES

Allen, M.G., 2001, Seismic remediation of Mormon Island auxiliary dam, Folsom dam and reservoir project, Sacramento County, California: This volume.

Anderson, R., 2001, Assessment of geologic resources and hazards in siting of non-nuclear thermal power plants and related facilities: This volume.

Buell, R., McNeilan, T.W., Prentice, C., 2001, Engineering geology studies for the San Francisco-Oakland Bay Bridge East span seismic safety project: This volume.

Fraser, W., 2001a, Engineering geology aspects of describing dam foundation objectives: This volume.

Fraser, W., 2001b, Fault activity guidelines of the California Division of Safety of Dams: This volume.

Kiersch, G.A., 2001, Engineering geoscience investigations for the construction of Folsom dam and reservoir, Sacramento County: This volume.

Reeder, T., Murphy, R., Finegan, J., 2001, Hydrogeologic investigation of the Yucaipa landfill, San Bernardino County, California: This volume.

Savage, W., and Anderson, R., 2001, New issues and opportunities for managing geohazard risks to electric power systems: This volume.

Simpson, D.T., and Schmoll, M., 2001, Exploration, design, and construction of Los Vaqueros dam, Contra Costa County, California: This volume.

Walker, S., and Anderson, R., 2001, Engineering geology overview of municipal solid waste landfills in Northern California: This volume.

EXPLORATION, DESIGN, AND CONSTRUCTION OF LOS VAQUEROS DAM, CONTRA COSTA COUNTY, CALIFORNIA

DAVID T. SIMPSON[1] AND MARK SCHMOLL[1]

ABSTRACT

Construction of the Los Vaqueros Dam, a 1,100-foot-long and 200-foot-high zoned embankment dam, was completed in 1997 in eastern Contra Costa County, California for the Contra Costa Water District. Exploration for the dam and appurtenant works started in 1970 and included geologic mapping, soil and rock borings, *in situ* bore-hole tests, geophysical surveys, test pits, and trenches. The dam is composed of upstream and downstream shell zones on either side of a vertical clay core. Engineering geologists were responsible for design exploration and site characterization, as well as for construction services such as assessing foundation suitability, foundation mapping, and confirming foundation shaping and final clean-up prior to embankment placement. A landslide on the upstream left abutment and a set of parallel open joints traversing the left abutment core foundation required investigation during construction and remedial design measures.

This article describes the results of the site exploration and summarizes the design of the zoned Los Vaqueros dam embankment. The major roles of engineering geologists during construction will also be discussed. Three specific issues arose during construction: (1) a landslide on the upstream left abutment, (2) some open joints across the left abutment core foundation, and (3) a shear zone traversing the valley bottom of the dam foundation; these will be discussed in detail.

INTRODUCTION

Initial exploration for a dam in eastern Contra Costa County, California was by Leeds, Hill, and Jewett, Inc. (LHJ, 1970). Later work was performed by the California Department of Water Resources (DWR, 1978, 1981) at the Los Vaqueros site. At least eleven alternative sites and dam designs, between about 70 and 420 feet in height and with storage capacities between 20,000 and 700,000 acre feet, were considered by Contra Costa Water District (District) (Woodward-Clyde Consultants; WCC, 1988a). After numerous geologic and geotechnical exploration and design studies, and more than twenty-seven years after the initial exploration was started, the Los Vaqueros project was completed (Figure 1).

The entire Los Vaqueros project involved much more than construction of the Los Vaqueros dam. It included construction of a 250 cubic feet/second capacity pump station on the San Joaquin River delta, construction of 20 miles of 6- to 8-foot-diameter buried transfer pipeline, reservoir inlet and outlet structures, a steel- and concrete-lined inlet/outlet tunnel, and a concrete chute spillway (Figure 2), as well as construction of environmental mitigation wetlands at several locations. This paper will discuss the engineering geology and construction aspects of the dam.

[1]URS Corporation
500 12th Street, Suite 200
Oakland, CA 94607
david_simpson@urscorp.com
mark_schmoll@urscorp.com

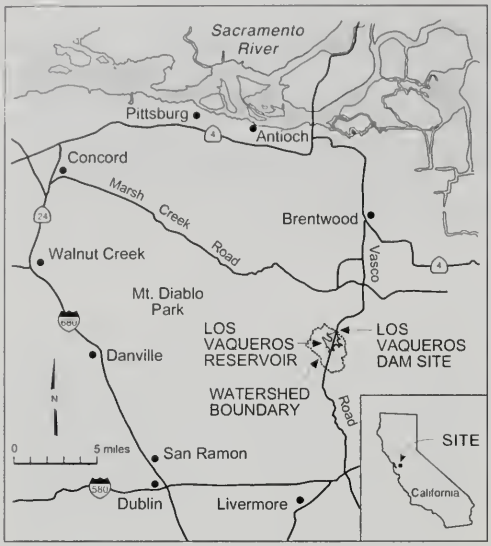

Figure 1. Los Vaqueros dam site location map.

The Los Vaqueros dam is a 1,100-foot-long and 200-foot-high zoned embankment dam. It required approximately 2.8 million cubic yards of earth material to construct, and provides 100,000 acre-feet of off-river storage for District customers in Contra Costa County in the eastern San Francisco Bay area.

The main goals of the Los Vaqueros project were to improve the year-round water quality and the reliability of the District's water supply system. Prior to completion of the project, the District obtained its water from the San Joaquin River delta. During summer and fall months the quality of the delta water was degraded slightly by salt water intrusion when the flow of the San Joaquin River was low. Following completion of the project, high quality water can now be pumped from the delta to the Los Vaqueros reservoir during periods of relatively high river discharge, generally in the winter and spring months. This water can then be pumped back out of the reservoir during the summer and fall to be blended with water coming directly from the delta to improve overall water quality. Another benefit of the reservoir is that it provides the District with several months of emergency storage should the pump station or upstream portions of the Contra Costa Canal become damaged or require shut down for maintenance.

SITE INVESTIGATIONS

Overview of regional and site geology and faulting

The site lies in the Coast Ranges geomorphic province, where regional structure has a northwest-southeast trend. This trend is consistent in the site vicinity, although the Mount Diablo piercement structure, located northwest of the site, creates a prominent interruption to the regional folding and faulting pattern. The San Andreas fault is the longest, most continuous structure in the Coast Ranges, and the Greenville fault is the easternmost major fault of the San Andreas system in the Los Vaqueros area. Holocene displacements have occurred on most of the major faults of the San Andreas system, including the Greenville fault system (Hart, 1981; Wesnousky, 1986).

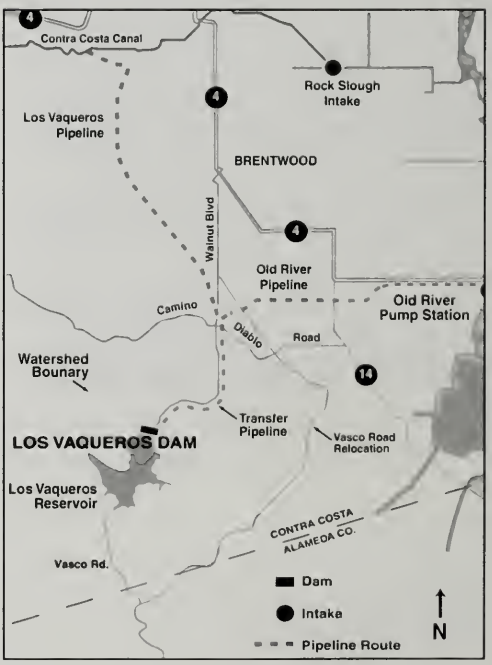

Figure 2. Map showing the locations of various features of the Los Vaqueros project.

Regional geologic mapping has been performed by Brabb et al. (1971), Dibblee (1980), Graymer et al. (1994), and Crane (1995). The Los Vaqueros dam site lies within an area underlain by generally eastward- to northeastward-dipping sedimentary rocks of the Great Valley Sequence. Brabb et al. (1971) mapped the bedrock in the site vicinity as the upper Cretaceous Marliff Shale: marine shale, siltstone, and sandstone. Dibblee's (1980) larger scale geologic map of the Byron Hot Springs 7.5 minute quadrangle indicates that bedrock at the dam site is the upper Cretaceous Panoche Formation. The type section of the Panoche Formation was described by Payne (1962) for an area south of the project site. Dibblee (1980) describes the Panoche in the vicinity of the dam as arkosic sandstone with large concretions, and minor interbedded shale and micaceous clay shale with thin sandstone interbeds. The formation is shown on the Byron Hot Springs quadrangle geologic map with a consistent northwest strike and dip between 15° and 40° to the northeast. The more recent regional compilation map by Graymer et al. (1994) shows bedrock at the dam site as upper Cretaceous sandstone and shale and does not assign formation names. After detailed exploration, WCC (1988a) concurred with Dibblee's original stratigraphic designation, and mapped the sequence at the site as the Panoche Formation. (The sequence included a thick claystone unit, which may be the reason why Brabb et al. (1971) assigned it to the Marliff Shale.)

The Brabb et al. (1971) map of the Mount Diablo-Byron area shows the southern end of the Davis fault about 1,200 feet east of the dam site. Dibblee (1980) maps an unnamed fault about 2,000 feet east of the dam. The Brentwood fault was originally mapped by DWR (1978) as a 7-mile-long structure recognizable in Tertiary and Cretaceous strata located about 1,000 feet east of the dam. In a seismic hazards assessment for the Los Vaqueros project, WCC (1988b) postulated that these faults may have been formed by the uplift of the Mount Diablo antiform, a large crustal upwarp that trends northwest; the bedrock at the dam site dips northeast and lies on the eastern flank of the antiform. WCC (1988b) extended the Brentwood fault 2 miles farther north under Sacramento delta alluvium. Biggar and Wong (1992) studied the Brentwood, Kellogg, Vaqueros, Davis, and Camino Diablo faults. Work for that study included a review of existing data from numerous borings drilled along these faults and excavation and detailed logging of seven exploratory trenches. Biggar and Wong (1992) found no evidence to indicate Holocene movement on any of these faults.

The nearest fault to the dam that is considered to be active by the State of California is the Marsh Creek segment of the Greenville fault (CDMG, 1982; Jennings, 1994), located about 3.8 miles to the southwest. The Marsh Creek segment was the source of the January, 1980 Livermore earthquake sequence (Bolt et al., 1981; Cockerham et al., 1980; Hart, 1981). Previously, the Antioch fault, the southern tip of which is near the site, had been thought to be active (CDMG, 1976), but more recent studies by Wills (1992) and WCC (1994) have shown that the Antioch fault is not active.

Summary and results of site exploration

As stated above, the initial exploration at the Los Vaqueros site was made in 1970 by LHJ. (The Los Vaqueros site was called the Upper Kellogg site at the time so that it could be differentiated from the Lower Kellogg site located several miles to the north.) Later, a fault and seismicity study (DWR, 1978) and an engineering feasibility study (DWR, 1981) were completed at the site. Exploration for the Los Vaqueros dam and appurtenant works by WCC (1988a, 1988b, 1989, 1992) included drilling of 90 core and auger borings, performing numerous borehole hydraulic conductivity tests, installing 16 piezometers, excavating 19 test pits, five trenches, three large diameter auger borings, numerous down-hole seismic velocity surveys, and more than 3,000 feet of seismic refraction and reflection survey lines (Figure 3). Previous investigators drilled numerous borings and excavated trenches as well (LHJ, 1970; DWR, 1978, 1981).

Detailed site-specific mapping (WCC, 1988a, 1992) indicated that the bedrock at the Los Vaqueros dam site consisted of a sequence of interbedded marine sandstone, siltstone, and claystone of the upper Cretaceous Panoche Formation. Five geologic units were mapped at the site: alluvium, landslide deposits, and three units of the Panoche Formation — claystone with interbedded siltstone, sandstone, and thinly interbedded sandstone, siltstone, and claystone (Figure 3). The sandstone was given the name "Ridge" sandstone because of its position capping the ridges that form the abutments of the dam. Bedrock orientation is generally consistent across the site: strike ranging from east-west to southeast-northwest and dip generally ranging from 15° to 40° to the north to northeast, in a downstream direction.

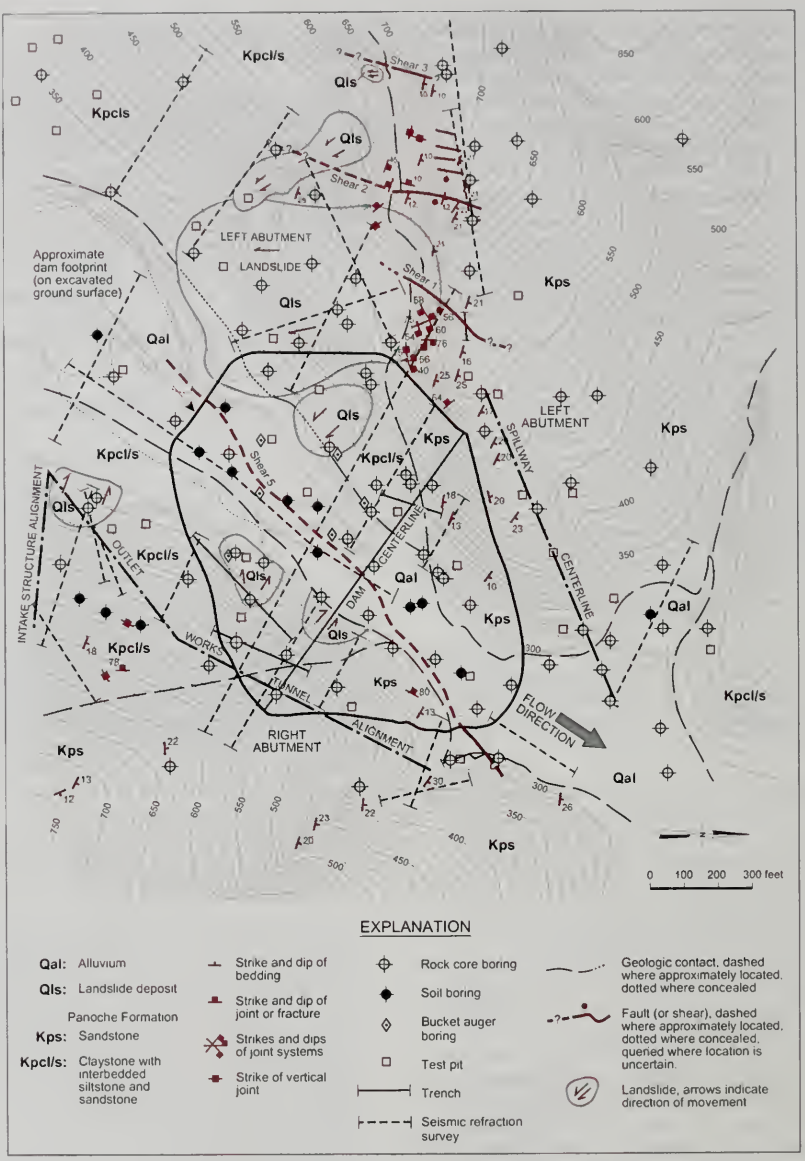

Figure 3. Surface geology and exploration locations map at the Los Vaqueros dam site prior to construction.

The dam was built across the channel of Kellogg Creek in a relatively narrow gap carved through a sandstone-capped ridge. The alluvium covering the valley floor within the dam footprint was found to be typically 20 to 30 feet thick, consisting of unconsolidated sands, silts, and clays.

Panoche Formation at the dam site. From oldest to youngest, the local stratigraphy of the Panoche Formation includes a claystone unit that underlies most of the reservoir and dam, a sandstone unit, and a sequence of thinly interbedded claystone, siltstone, and sandstone. The claystone unit of the Panoche Formation is composed mainly of weak to very weak, brown (weathered) to dark gray (fresh) claystone. The claystone is interbedded with weak to very weak, brown to light brown siltstone and occasional brown sandstone beds and minor gray, thin, very strong limestone lenses. The claystone and siltstone slake rapidly when exposed to air. This unit is moderately fractured and sheared. Most joints are tight to very narrow (0 to less than 1 mm wide), smooth, planar to slightly wavy, and some are slickensided.

The Ridge sandstone unit is composed of weak to medium-strong, brown (weathered) to light gray (fresh), fine- to medium-grained sandstone. The sandstone contains a few thin siltstone and claystone interbeds. Thin section analysis indicated that the sandstone is a feldspathic litharenite. Locally, the litharenite has been cemented into very strong, dark gray spheroidal concretions up to about 10 feet in diameter. Joints are common in the Ridge sandstone, and sets are often arranged perpendicular to, and parallel to, the regional bedding. These joints were found to generally range from tight to about 2 inches wide, although there are several joints in the left abutment that were found to be open as much as 12 inches or more (see discussion of left abutment below). Some zones in the sandstone have undergone shearing, but the rock does not display the pervasive shearing or slickensides found in the underlying claystone unit.

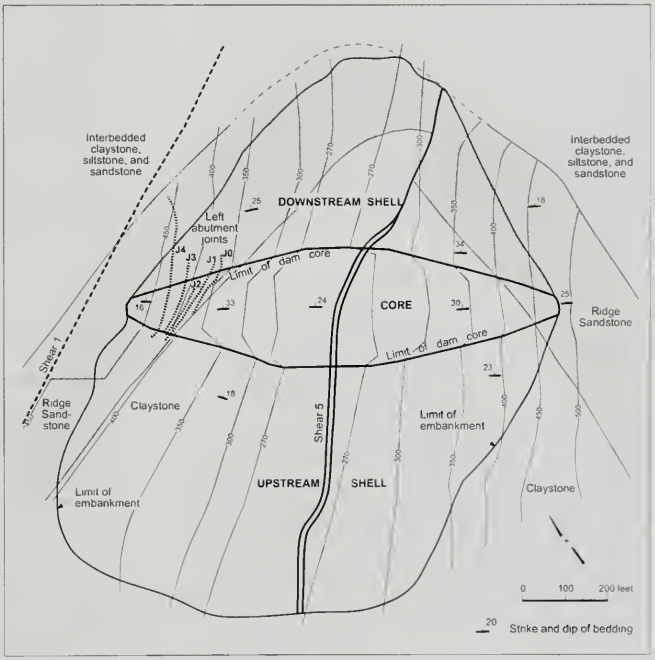

Figure 4. Simplified geologic map of the Los Vaqueros dam foundation.

The thinly interbedded claystone, siltstone, and sandstone unit stratigraphically overlies the Ridge sandstone and is very weak to weak, moderately to highly weathered, and locally tightly folded. Rhythmically interbedded 2- to 10-inch thick sandstone, siltstone, and claystone layers make up this unit.

Figure 4 is a simplified version of the dam foundation map showing the Ridge sandstone on the upper portions of the downstream abutments and beneath the downstream toe of the dam. The figure also shows the outcrop area of the underlying claystone unit. The thinly interbedded sandstone, siltstone, and claystone unit is not present within the footprint of the dam but is present beneath the spillway chute.

During design explorations at the site, five shear zones were identified (WCC, 1988a, 1989). Shears 1, 2, and 3 were observed offsetting the Ridge sandstone on the ridge above the left abutment, and Shear 5 was detected in a trench near the downstream toe of the dam (Figures 3 and 4). (Shear 4 was present west of Shear 3 on the left abutment

ridge and is not shown in Figure 3.) None of the five shear zones were found to offset surficial soils or alluvium, but because of its location beneath the dam, Shear 5 triggered additional exploration, as discussed in a later section.

Landslides. An ancient, large, rotational, predominantly bedrock landslide was identified on the left abutment early during the predesign phase of exploration (Figure 3). This location was near the proposed upstream toe of the dam. This feature created a terrace-like break in slope above a more steeply sloping toe that extended down to Kellogg Creek, where the channel made a sharp bend around the toe. It is possible that undercutting of the toe of the slope by Kellogg Creek had originally initiated the landslide movement. The top of the slide block, at the terrace-like break in slope, consisted of a roughly planar surface with a gentler slope than the adjacent hillside. This landslide, as well as the construction issues it raised, is discussed in more detail below. Several other relatively shallow landslides were identified in the dam abutments during the design exploration and mapping work (Figure 3).

Groundwater. Auger borings and piezometers placed in the flat valley bottom indicated that groundwater could be expected at depths as shallow as 10 to 12 feet below the ground surface. This meant that groundwater would be encountered in most of the valley bottom portion of the dam foundation excavation, which was designed to extend down to bedrock at 25 to 30 feet below the existing grade. Groundwater was much deeper on the dam abutments and was not expected to present a problem during construction.

DAM DESIGN

Foundation material requirements

Foundation material requirements varied depending on whether a concrete structure such as the spillway or intake structure was being supported, or whether the foundation was for the dam embankment. If the foundation was for the embankment, the requirements were dependent upon the portion of the dam to be supported. All excavation depths shown in the contract drawings were based upon subsurface data gathered from borings, test pits or trenches, seismic refraction surveys, and geologic mapping.

Structural excavations for the spillway, inlet structure, inlet/outlet tunnel, outlet structure, and for the concrete cutoff excavation beneath the core of the dam were required to be made to the lines and grades shown on the project drawings. These excavations generally extended down to slightly to moderately weathered bedrock. If localized zones of highly weathered, sheared, or otherwise unacceptable materials were encountered, the unacceptable materials were to be excavated and replaced with backfill concrete.

The upstream and downstream shell zones of the dam embankment were required to be founded on moderately weathered bedrock as defined in the contract specifications: "Less than half of the rock material is altered. Fresh or slightly discolored rock is present either as a discontinuous framework or as corestones." All soil, landslide materials, completely weathered and highly weathered rock, as defined in the specifications, were to be removed. The core of the dam embankment was required to be founded upon slightly weathered bedrock: "Rock is slightly discolored at and adjacent to discontinuities, but not noticeably lower in strength than fresh rock. Discontinuities are stained or discolored and may contain a thin filling of altered material." If localized zones of foundation rock were encountered that would be acceptable based upon the weathering requirements, but that were extensively fractured, sheared, or were otherwise unacceptable, these materials would be excavated.

Due to the rapid slaking observed in many of the siltstone and claystone core samples during the exploration phase of the project, the contractor was required, in portions of the foundation underlain by siltstone and claystone, to excavate an additional two feet of bedrock immediately prior to foundation surface treatment or placement of embankment materials, to remove all slaked rock.

Foundation grouting was performed beneath the core footprint. This consisted of a curtain with two rows of blanket grout holes upstream and two rows of blanket grout holes downstream. The rows of grout holes were spaced 12 feet apart. Adjacent rows of curtain holes were drilled parallel to the axis of the dam at opposing angles of 60 degrees to the horizontal. The curtain was designed to be 100 feet deep measured perpendicular to the foundation surface. The four rows of blanket holes were designed to provide a 30-foot-deep blanket upstream and downstream of the curtain. A detailed descrip-

tion of the grouting operations and results is beyond the scope of this paper.

Embankment design

Los Vaqueros Dam is a zoned 200-foot-high embankment with a 1,100-foot crest length. It required approximately 2.8 million cubic yards of material to construct. A schematic cross-section of the maximum dam section is shown in Figure 5. Table 1 lists the descriptions of the materials used in each zone of the embankment. The dam embankment was constructed with upstream and downstream slopes of 3:1 (horizontal:vertical) and 2.5:1, respectively. The central clay core was constructed with 0.5:1 upstream and downstream slopes.

The dam consists of upstream and downstream shell zones on both sides of a central core. The upstream shell of the dam was constructed of a central zone of compacted crushed siltstone, claystone, and some sandstone (Zone 4 in Figure 5) and an upstream zone of compacted sandstone, Zone 5. The upstream face of the dam is armored with sandstone riprap placed on imported granular bedding material. The downstream shell was constructed mainly of Zone 4 material that was surrounded by a sandy gravel drain blanket (Zone 3) sandwiched between two layers of a sand filter (Zone 2). The central clay core of the dam, Zone 1, was composed of compacted alluvial clay and is separated from the downstream shell by a 10-foot wide sand filter (Zone 2) and 10-foot wide sandy gravel chimney drain (Zone 3).

The riprap material and all other embankment construction materials, except the filter and drain, were locally derived. The Zone 1 clay core material was excavated from two upstream alluvial borrow areas. The Zones 4 and 5 materials were excavated from bedrock borrow areas on the upstream left

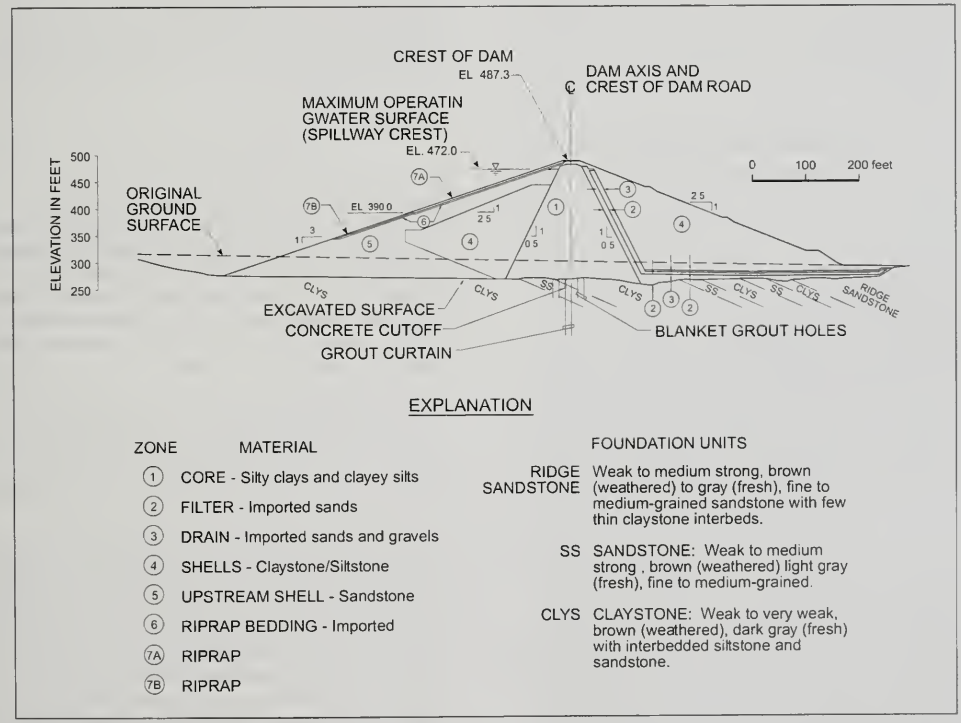

Figure 5. Maximum dam section showing internal embankment zoning and foundation geology.

ZONE	PORTION OF DAM	MATERIAL DESCRIPTION
1	CORE	SILTY CLAYS AND CLAYEY SILTS: locally derived from upstream alluvium
2	FILTER	IMPORTED SANDS
3	DRAIN	IMPORTED SANDS and GRAVELS
4	UPSTREAM AND DOWNSTREAM SHELLS	CRUSHED CLAYSTONE/SILTSTONE: locally derived from bedrock borrow areas
5	UPSTREAM SHELL	CRUSHED SANDSTONE: locally derived from bedrock borrow areas
6	RIPRAP BEDDING	IMPORTED DURABLE ROCK, SAND, and SILT
7A/7B	RIPRAP	DURABLE ANGULAR SANDSTONE: locally derived from sandstone concretions, 7A is slightly coarser than 7B to withstand potentially larger wave impact forces on upper portion of dam

Table 1. Descriptions of dam embankment material.

abutment and on a low hill in the reservoir inundation area. Upstream borrow areas were chosen so that visual impacts from the excavation operations would be minimized once the dam was completed and the reservoir was full.

ENGINEERING GEOLOGY DURING CONSTRUCTION

Assessment of foundation suitability

The primary responsibilities of the engineering geologists during construction of the Los Vaqueros Dam project were to assess the suitability of the foundation rock for each of the various structures at the site, which included recording significant features on foundation geologic maps, and to confirm that the shape of the foundation surfaces and the final clean-up met the contract requirements. A geologist was present during all excavation operations to observe that the design intent described in the contract specifications and shown on the contract drawings was being achieved. The drawings showed approximate depths of excavation for the individual foundations, but these depths were based upon observation of limited surface exposures and subsurface data. The geologist's presence was required because, if the actual conditions encountered during construction varied from those anticipated during the design, he would determine the most appropriate way to modify the excavation to address the conditions. In areas where the weathering criteria were met, but where excessive jointing or shearing made the foundation unacceptable, the geologist directed overexcavation until suitable foundation was exposed. The foundation excavations for the concrete inlet and outlet structures and the spillway did not typically require modifications, because they were designed to be placed well down into bedrock. However, to minimize the amount of soil and weathered rock excavated for the dam foundation, and to provide a basis for contractors to bid on the project, a reasonable foundation excavation plan was developed based upon available subsurface data. The actual depth of the dam foundation varied slightly from the original excavation plan contained in the contract drawings due to local variations in rock weathering and other geologic conditions.

Foundation mapping

Upon completion of the preliminary foundation clean-up, requiring the use of high-pressure air within the dam core zone and in the concrete structure foundations, the engineering geologist assessed the suitability of the foundation. The drafting of the foundation geologic maps was performed at this time in the construction sequence. The foundation geologic maps represent the as-built drawings of the foundation geology (WCC, 1998).

The maps for the core zone of the dam and for each of the concrete structures were drawn at a scale of 1 inch = 10 feet; mapping of the upstream and downstream shell foundations was performed at a scale of 1 inch = 20 feet. The foundation maps include details of the bedrock lithology, geologic contacts and bedding orientations, joints, shears, seeps and springs, as well as the limits of the foundation excavation. In addition to these typical features, the core foundation maps also included the outline of the top of the concrete cutoff wall. The cutoff wall was located 10 feet upstream of the axis of the dam and was excavated, and then backfilled with concrete, to a depth of 10 feet within the claystone unit across the valley bottom and up each abutment to the contact with the Ridge sandstone.

Confirmation of foundation shaping and clean-up

The contract drawings and specifications (WCC, 1995) provided requirements for shaping the foundation and for treatment of foundation defects beneath the core of the dam. Upon completion of the mass foundation excavation and the foundation grouting operations, the foundation for the core of the dam was required to be shaped "...so that a relatively uniformly varying profile is obtained free of sharp offsets, protruding points, edges, or breaks, and so that variations in elevation are gradual...". Sharp breaks in slope or steps in the foundation were not allowed, to prevent any cracks from forming within the clay core due to differential settlement. The drawings (WCC, 1995) also indicated that overhangs and protrusions with a height greater than 1 foot were to be removed. Cavities, depressions, and in some instances, steps in the core foundation could also be treated by placing concrete on the foundation. The removal of loose blocks, overhangs, and protrusions was done so that adequate compaction of the core material against the foundation could be achieved and so that no void spaces would be created at the core – foundation contact. It was the engineering geologist's responsibility to delineate areas requiring shaping.

In areas of the core foundation underlain by sandstone, the engineering geologist would outline narrow fractures, joints, and cavities requiring slush grout, and larger defects requiring concrete infill (dental or shaping concrete) and/or additional excavation to achieve an acceptable foundation. In areas of the core foundation underlain by claystone, this generally led to shaping by excavation only, because the claystone could easily be excavated to a suitable shape and it did not exhibit many open fractures requiring slush grout or concrete. Shaping and concrete infill were not generally required in the shell zones of the foundation.

Numerous small-scale bedrock shears were apparent, especially within the claystone mapping unit, once the foundation clean-up had been performed. These shears were observed along both bedding planes and across them. Typically, these small-scale shears were narrow (less than 1 inch wide), could be traced for several feet to several tens of feet, and tended to have several inches to several feet of displacement. Shear zones within the core foundation were required to be excavated to specific depths, based upon the width of the zone, and backfilled with concrete. For shear zones, cavities, and cracks that cross the core from the upstream side to the downstream side, treatment similar to that required for the core foundation was required to extend 20 feet beyond the core limits.

Immediately prior to placement of embankment core material, a final clean-up was performed so the final foundation surface could be reviewed and approved by the engineering geologist.

UPSTREAM LEFT ABUTMENT LANDSLIDE

Design investigations

During preliminary investigations, a large ancient rotational landslide was identified in the upstream portion of the left abutment. This landslide was initially mapped by LHJ (1970) and was investigated by drilling one core boring in its central portion. During later design studies by WCC (1985a, 1992) eight additional core borings were drilled within the landslide mass and additional geologic mapping was performed. These core borings identified displaced and sheared sandstone and claystone derived from the Panoche Formation. A remolded clay basal slip-plane was also identified in some of the borings. The landslide was found to be approximately 500 feet wide, 650 feet long, and up to 100 feet deep. The location of the landslide is shown on Figure 3.

Based on the results of these site investigations, the limits of the landslide were shown on the excavation and foundation plans, and on the left abutment excavation sections in the contract drawings. These drawings showed that the portion of the landslide underlying the footprint of the dam would be entirely removed as part of the dam foundation excavation. A small portion of the landslide, located upstream of the dam footprint, was to be left in-place.

Investigations during construction

During abutment stripping and foundation preparation, the base of the eastern margin of the landslide, underlying and adjacent to the dam footprint, was found to be up to 20 feet deeper than originally estimated. The basal slip surface of the landslide was identifiable in the foundation excavation as a 1/4- to 1-inch thick layer of dark gray remolded clay. The bedding orientation of the rock within the land-

slide was variable, contrasting with the relatively uniform bedding of the undisturbed rock underlying the slip plane.

Due to the immediate impact of the revised landslide limits on dam construction, a field investigation program was developed to characterize the depth and limits of the landslide near the dam. The basal slip-plane was mapped and the trace of this plane, where it was exposed within the excavation, was surveyed and plotted on a topographic map of the left abutment excavation. A 3-dimensional contour map showing the excavated surface and the estimated base of the landslide was drawn, utilizing the existing boring information and results of the field mapping. Two additional core borings were then drilled through the eastern portion of the slide to verify the interpretations. The results of these additional investigations showed the geometry of the landslide to be asymmetrical, with the deepest portion being along the eastern edge of the slide mass, under the dam footprint.

Construction impacts

Although the total volume of the landslide mass requiring removal increased only slightly due to the localized increase in depth, there were several impacts to the dam construction. The left abutment borrow area was located up slope of the landslide, and access to this borrow area was along two temporary haul roads that crossed the back scarp of the slide. Based on the revised shape and depth of the landslide, the cut to remove the additional slide material at the toe would result in an oversteepened slope below the borrow area and haul roads. A new back cut had to be made starting nearly 300 feet above the base of the slide to remove the landslide mass within the dam footprint and maintain a stable temporary cut. This 1:1 inclined cut removed the borrow area haul roads, effectively stopping the placement of fill in the dam. New haul roads had to be routed around the back cut, which resulted in a longer haul distance and a redesign of the borrow excavation plan.

Another significant impact was a redesign of the dam embankment. The shape of the dam footprint became larger in order to fill the increased excavation in the landslide area. This resulted in the requirement for additional Zone 5 (upstream shell sandstone) material. A revised borrow excavation plan was developed to increase the quantity of Zone 5 material, and the width of the Zone 5 portion of the upstream shell was revised to accommodate the quantity available.

A third impact to the project was a construction slope failure. The landslide mass within the dam footprint was completely removed by the contractor during the late summer and fall of 1996. However, the majority of the dam embankment was not placed back until the following spring. The eastern section of the 1:1 temporary back cut failed during a period of heavy rain in late December 1996. The new slide failed along a low angle, out-of-slope-dipping bedding plane shear. Although this new slide was relatively small (less than 10,000 cubic yards), it was completely within the footprint of the dam and had to be removed before embankment material could be placed in this area.

LEFT ABUTMENT CORE FOUNDATION JOINTS

Description of foundation defects

A sequence of five steeply dipping, open, northeast trending joints in Ridge sandstone in the left abutment core foundation was identified during the foundation excavation. The joints probably originated as incipient topple blocks of Ridge sandstone, rather than being tectonic in origin. Due to the linear extent and the width of these joints, they clearly represented a serious threat to the integrity of the dam, if left untreated. Upstream shell and core material could have been eroded through these subsurface openings once the reservoir was filled, leading to failure of the dam. Supplemental remedial measures were needed to address these defects.

Detailed mapping of this portion of the left abutment core foundation revealed that the five significant parallel joints had strikes approximately N70°E (approximately 55° off of the alignment of the axis of the dam) with dip between 70°SE and 90° (Figure 6). Nine inclined core borings were drilled into the left abutment to provide subsurface information about width, infilling material, and subsurface continuity of the joints that were visible at the surface, and to explore for other open joints in the subsurface that did not extend to the foundation surface. A video camera was lowered into several of the core holes to examine the width of the joints and the nature of the infilling materials.

The mapping indicated that the five main joints were open up to about 12 inches, and that they transected the entire core foundation from the upstream

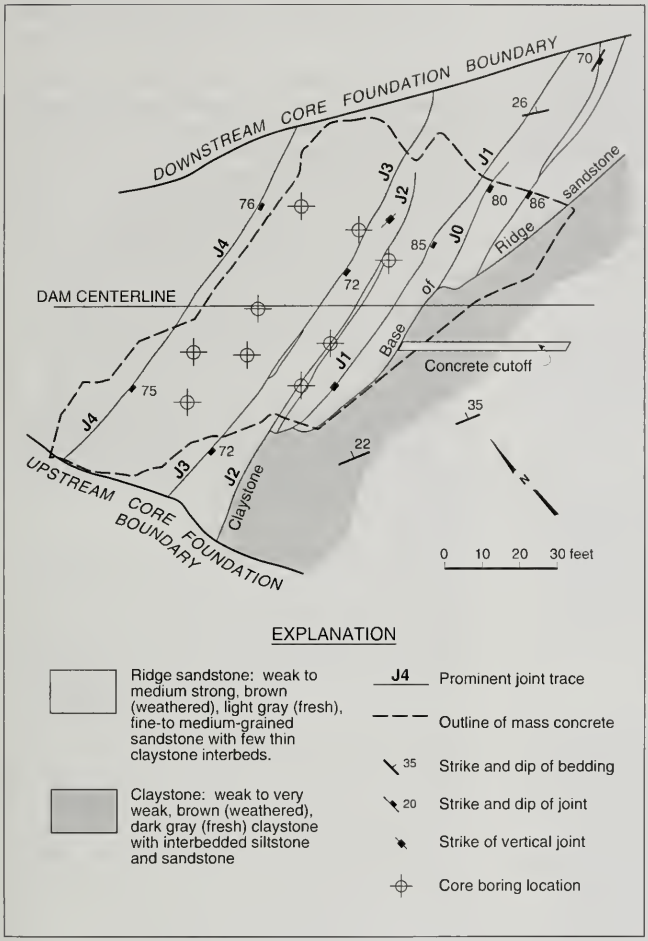

Figure 6. Map of significant joints in the left abutment core foundation. Also shown is the outline of the top of the excavation that was made across the joints and backfilled with mass concrete.

shell to the downstream shell. The joints were found to be either open, filled with sand (that was likely the product of sandstone weathering), or partially filled with slabs of sandstone that had apparently spalled from the sides of the joints.

The foundation mapping and drilling results showed that no significant joints were present in the subsurface that did not extend to the surface. Where two of the joints were observed to daylight at the foundation surface of the upstream shell, they did not extend into the claystone unit underlying the Ridge sandstone. Each of the joints was present only in the relatively more brittle sandstone and not in the more ductile claystone. The joints were found to extend down and terminate at the base of the Ridge sandstone, as much as about 45 feet. Based upon these findings a five-step left abutment joint remediation program was designed. The design was reviewed and accepted by the California Division of Safety of Dams.

Design and construction of remedial measures

The first step was to excavate, along the footprint of the core foundation, a large mass of the jointed sandstone down into the underlying claystone. The back of the excavation was extended into massive sandstone that was present behind the uppermost joint (identified as Joint J4 in Figure 6). The contractor was able to perform this work with a large track-mounted hoe ram and large track-mounted excavator. The side slopes of this excavation were cut at 1/2:1 slopes. The back slope of the excavation was to be the back surface of Joint J4. A 5-foot-wide and 1-foot-deep vertical keyway was chipped into the center of the back wall of the excavation. The bottom of the excavation extended 5 feet down into the underlying claystone. This excavation allowed close inspection of joints at the sandstone-claystone contact; the main joints did not extend down into the claystone.

The second step was to backfill the wedge-shaped excavation with mass concrete in 4-foot lifts. (Mass concrete is the name given to a large volume of unreinforced concrete that is placed in thick lifts.) The 10-foot-deep concrete cutoff wall was extended up across the bottom of the excavation prior to beginning the mass concrete placement. The outside face

of the mass concrete was formed to match the slopes of the adjacent foundation rock.

The third step was to excavate, to the maximum depth possible, the exposed length of each joint upstream and downstream of the mass backfill concrete. The contractor performed this work with hand tools, high pressure air and water lances, and heavy equipment. Following this detailed excavation work, the areas of the core and shell foundations adjacent to the excavated joints upstream and downstream of the mass backfill concrete were cleaned off with high-pressure air and water.

The fourth step was to fill the excavated joints with dental concrete. To allow the concrete to infiltrate to maximum depths, coarse sand was used as the aggregate and a small diameter vibrator was utilized.

For the fifth and final step, potential void spaces along each of the main joints beneath the dental concrete were stitch-grouted at a several locations upstream and downstream of the backfill concrete mass. Several of the stitch-grout holes were tight and did not accept any grout, whereas other locations accepted many cubic feet of grout.

VALLEY BOTTOM SHEAR 5

Five bedrock shear zones were identified during design investigations (WCC, 1988b, 1992). Four of the shear zones were located outside the dam excavation on the left abutment and one, Shear 5, was located in the valley bottom area. Shear 5 was found to extend from beyond the upstream shell of the dam through the dam footprint to beyond the downstream shell (Figure 4). The zone of shearing was about 30 feet wide where the shear entered the upstream shell in the claystone and narrowed to about 10 feet in width at the upstream edge of the core. The shear zone was generally about 15 to 20 feet wide within the core foundation area and quickly narrowed to 2 to 3 feet in width to the northeast, beneath most of the downstream shell in Ridge sandstone. Horizontal offset along Shear 5 was about 140 feet.

Materials within this shear zone consisted predominantly of intensely sheared claystone and clay. Groundwater seeps were present at many locations along this zone. Detailed mapping of the bedrock and the alluvial materials overlying Shear 5 at each end of the dam foundation excavation indicated that it was a bedrock feature and did not offset the alluvium.

Treatment of Shear 5 within the core foundation area involved excavation of sheared materials to a depth equal to three times the width of the zone and backfilling with dental concrete. Where the shear zone was greater than 1 foot wide, the excavation was extended to a minimum depth of 3 feet. Where Shear 5 crossed the downstream shell foundation, it was excavated to a depth equal to its width and backfilled with sand filter materials.

LESSONS LEARNED AT THE LOS VAQUEROS DAM SITE

Engineering geologists and geotechnical engineers must often explain the benefits of a complete site exploration program. This often involves justifying the scope (and associated cost) of the exploration program and the necessity of each part of the program.

It is the geologist's or engineer's responsibility, as a representative of his or her client, to invest a finite amount of financial resources in the most practical and beneficial way to the project. It is often a relatively simple matter to develop a reasonably accurate picture of a site's general geologic conditions merely by reviewing available literature and aerial photography and imagery, mapping surficial features and bedrock outcrops, and performing a limited amount of subsurface exploration, whether by drilling, trenching, or geophysical techniques. However, it is often the small abnormalities and local irregularities that can have a profound impact on the schedule and cost of a large construction project, when perhaps millions of dollars worth of heavy equipment could be put on stand-by while some previously unforeseen geologic feature or condition is explored, defined, and an acceptable solution developed.

For example, the result of a localized increase in the depth of the left abutment landslide caused significant schedule and cost impacts to the project. The preliminary and final design investigations included a reasonable number of borings to characterize a landslide of this size. However, due to its unusual asymmetrical shape, the deepest portion of the landslide was at the edge beneath the footprint of the dam. Even though a suitable effort had been applied to the problem of defining the limits of the large landslide, its ultimate configuration eluded

a complete characterization until it was exposed during the excavation for the dam foundation.

The set of joints in the Ridge sandstone that was exposed in the left abutment core foundation excavation was not recognized until the excavation was made. This was due partly to the difficulty of encountering and characterizing near-vertical features in typically vertical exploratory borings. The lack of recognition of the joints was also partly due to their location within rock that, prior to the commencement of construction, supported a band of low cliffs and the logistical difficulty in performing site exploration on such steep terrain. Perhaps additional mapping in this hard-to-drill area during the design phase of the project would have revealed the presence of other open joints at the surface and hinted at the possibility of additional parallel joints in the subsurface. As it is, many geologists associated with different consulting firms and California state agencies reviewed the site conditions and did not recognize these features, so they could not have been glaringly apparent. Even though recognition of these joints would not have eliminated all of the impacts that they had on the project, identification of the presence and magnitude of these joints prior to the design of the dam foundation excavation plan could have eliminated exploration during construction and delays to the foundation preparation and embankment fill placement.

Ultimately, it is the role of the engineering geologist and geotechnical engineer, during the exploration and design phases of a project, to collect, and correctly interpret and apply site-specific geologic information so that construction delays and the need for redesigns due to the presence of unanticipated conditions can be reduced or eliminated.

ACKNOWLEDGEMENTS

The authors would like to thank Doug Boyer and Frank Glick for their reviews of this paper.

AUTHOR PROFILES

David Simpson is a California Certified Engineering Geologist with 14 years of geologic and geotechnical experience. He is a Senior Geologist with URS Corporation where he has worked on numerous embankment and concrete dams throughout the western United States. His areas of expertise are engineering geology studies for dams, tunnels, pipelines, and landslides and soils and geomorphologic studies for geologic hazard assessments.

Mark Schmoll is a California Certified Engineering Geologist with 22 years of geologic and geotechnical experience and is the Engineering Geology group leader for the Oakland, California office of URS Corporation. His areas of expertise are engineering geology and geologic hazard assessment studies for tunnels, dams, pipelines and landslides.

SELECTED REFERENCES

Biggar, N.E. and Wong, I.G., 1992, Seismic hazard evaluation of the Vaqueros faults in eastern Contra Costa County, California: *in* Borchardt, G. et al. (eds.), Proceedings of the Second conference on Earthquake Hazards in the Eastern San Francisco Bay Area: California Division of Mines and Geology Special Publication 113, p.365-376.

Bolt, B.A., McEvilly, T.V., and Uhrhammer, R.A., 1981, The Livermore Valley, California sequence of January, 1980: Bulletin of the Seismological Society of America, v. 71, p. 451-463.

Brabb, E.E., Sonneman, H.S., and Switzer, J.R., 1971, Preliminary geologic map of the Mount Diablo—Byron area, Contra Costa, Alameda, and San Joaquin counties, California: U.S. Geological Survey Basic Data Contribution 28, scale 1: 62,500.

DWR (California Department of Water Resources), 1978, Faults and seismicity at Los Vaqueros Dam site, Preliminary report.

DWR (California Department of Water Resources), 1981, Los Vaqueros offstream storage unit, Engineering feasibility.

CDMG (California Division of Mines and Geology), 1976, Alquist-Priolo Special Studies Zone map of the Antioch South 7.5 minute quadrangle: California Department of Conservation, Division of Mines and Geology (Sacramento, California).

CDMG (California Division of Mines and Geology), 1982, Alquist-Priolo Special Studies Zone map of the Tassajara 7.5 minute quadrangle: California Department of Conservation, Division of Mines and Geology (Sacramento, California).

Cockerham, R.S., Lester, R.W., and Ellsworth, W.L., 1980, A preliminary report on the Livermore Valley earthquake sequence, January 24 - February 26, 1980: U.S. Geological Survey Open-File Report 80-714, 43 p.

Crane, R., 1995, Geology of the Mount Diablo region: Northern California Geological Society: Map accompanying Geology of the Mount Diablo Region Field Trip Guidebook, Crane, R., Lyon, C. (eds.), scale 1:48,000.

Dibblee, T.W., Jr., 1980, Preliminary geologic map of the Byron Hot Springs quadrangle, Alameda and Contra Costa counties, California: U.S. Geological Survey Open-File Report 80-534, scale 1: 24,000.

Graymer, R.W., Jones, D.L., and Brabb, E.E., 1994, Preliminary geologic map emphasizing bedrock formations in Contra Costa County, California: U.S. Geological Survey Open-File Report 94-622, scale 1: 75,000.

Hart, E.W., 1981, Recently active strands of the Greenville fault, Alameda, Contra Costa, and Santa Clara Counties, California: California Division of Mines and Geology Open-File Report 81-8, scale 1: 24,000.

Jennings, C.W., 1994, Fault activity map of California and adjacent areas with locations and ages of recent volcanic eruptions: California Division of Mines and Geology Geologic Data Map No. 6, scale 1: 750,000.

LHJ (Leeds, Hill, and Jewett, Inc.), 1970, Geologic investigations of Upper Kellogg Dam and Reservoir site: Consultant's report to Contra Costa Water District.

Payne, M.B., 1962, Type Panoche group (upper Cretaceous) and overlying Moreno and Tertiary strata on the west side of the San Joaquin Valley: California Division of Mines and Geology Bulletin No. 181, p. 165-175.

Wesnousky, S.G., 1986, Earthquakes, Quaternary faults and seismic hazard in California: Journal of Geophysical Research, v. 91, p. 12,587-12,631.

Wills, C.J., 1992, The elusive Antioch fault: *in* Borchardt, G. et al., (eds)., Proceedings of the Second conference on Earthquake Hazards in the Eastern San Francisco Bay Area: California Division of Mines and Geology Special Publication 113, p. 325-331.

WCC (Woodward-Clyde Consultants), 1988a, Damsite investigations report, Los Vaqueros Project: Consultant's report prepared for James M. Montgomery, Consulting Engineers, Inc., Walnut Creek, California.

WCC (Woodward-Clyde Consultants), 1988b, Seismic hazards assessment, Los Vaqueros Project: Consultant's report prepared for James M. Montgomery, Consulting Engineers, Inc., Walnut Creek, California.

WCC (Woodward-Clyde Consultants), 1989, Predesign investigations, damsite fault evaluation report: Consultant's report prepared for James M. Montgomery, Consulting Engineers, Inc., Walnut Creek, California.

WCC (Woodward-Clyde Consultants), 1992, Dam foundation design technical memorandum, Los Vaqueros Project, Predesign of dam and appurtenant works: Consultant's report prepared for Contra Costa Water District.

WCC (Woodward-Clyde Consultants), 1994, Geologic evaluation of the Antioch fault, proposed Kaiser Medical Center site, Antioch, California: Consultant's report prepared for Kaiser Foundation Health Plan, Inc., Oakland, California.

WCC (Woodward-Clyde Consultants), 1995, Los Vaqueros Dam drawings and specifications: Consultant's report prepared for Contra Costa Water District.

WCC (Woodward-Clyde Consultants), 1998, Los Vaqueros Dam foundation geology report: Consultant's report prepared for Contra Costa Water District.

ENGINEERING GEOLOGY CONSIDERATIONS FOR SPECIFYING DAM FOUNDATION OBJECTIVES

WILLIAM A. FRASER[1]

ABSTRACT

In dam construction, the actual depth to adequate foundation materials at a site is known with certainty only at the points of exploration. The foundation objective serves as a descriptive tool to convey design-intent information to construction engineering staff and the contractor. The selection of the most effective approach, or approaches, usually depends on site geology and the amount of available geologic and geotechnical data developed by the site investigation. The engineering geologist should be aware of the relevant approaches for defining a foundation objective prior to the initial site reconnaissance, so that the subsurface site investigation can be designed to yield sufficient and meaningful information. This paper summarizes the various ways in which a foundation objective can be described.

INTRODUCTION

Dam foundation requirements are based on the type of dam proposed and is largely dependent on the strength, deformation, and permeability characteristics of site materials. To determine the depth of excavation needed to achieve an adequate foundation, observation of site conditions in borings and test pits, field testing of soil and rock, laboratory testing of representative samples and, ultimately, design analysis are needed. A discussion of site investigation techniques and the influence of geology on dam design and construction are beyond the scope of this paper. For a discussion of site investigation techniques refer to Krynine and Judd (1957), Lowe and Zaccheo (1975), Hunt (1984), and USBR (1987). Discussions of the influence of geology on dams are found in Burnwell and Moneymaker (1950), Legget (1962), Best (1984), Janson (1988), and Goodman (1993). Janson (1983) provides a summary of the kinds of geologically related problems dams experience, as well as case histories of known dam failures.

This paper discusses various approaches for specifying a foundation objective. The foundation objective is a descriptive tool used to convey design intent information to both construction engineering staff and the contractor. The California Division of Safety of Dams generally requires the specification of a foundation objective for new dam projects. This paper illustrates the importance of engineering geology in developing a foundation objective that will be effective in controlling a dam foundation excavation. The various approaches have been utilized in dam construction practice observed by the author over the past 15 years. A number of recent Northern California dam projects, constructed under DSOD supervision, are presented to illustrate the importance of engineering geology in selecting an appropriate foundation objective approach.

THE FOUNDATION OBJECTIVE

Even at well-explored sites, the depth to adequate foundation materials is known with certainty only at the locations where exploration was actually performed. Foundation excavations must be responsive to unexpected, inadequate conditions. To assist

[1]Division of Safety of Dams
California Department of Water Resources
2200 X Street
Sacramento, CA 95814
billf@water.ca.gov

construction engineering staff, the specifications should contain a foundation objective; that is, a description of geologic or geotechnical conditions that meet foundation performance requirements. Other important foundation design details, such as shaping requirements and foundation treatment methods and expectations, are usually specified along with the foundation objective.

Contractors rely on the plans and specifications to determine the volume of excavation required and to select appropriate equipment for the excavation. Explicit direction to a contractor reduces the contractor's risk, and, therefore, more competitive bidding is possible. To provide a basis for contractor operations, an excavation contour map or other estimate of the expected occurrence of adequate conditions is often included in the plans and specifications. The contractor should be made aware that this is an estimate and that the final excavation must be based on the actual conditions encountered.

As a practical matter, the foundation objective must be recognizable in the foundation excavation. The selection of a particular descriptive approach is highly dependent on site geology as well as on the amount of geologic and geotechnical data developed by the site investigation. For the purposes of this discussion, geologic foundation materials are divided into four general categories: crystalline rock (intrusive and metamorphic), cemented stratified rock (sedimentary and volcanic), uncemented stratified rock (sedimentary and some pyroclastic deposits), and unconsolidated deposits (sedimentary). Because of this dependence on site geology, the engineering geologist plays an essential role in developing the foundation objective. The engineering geologist and the design engineer should consider possible approaches during the initial site reconnaissance, so that the detailed site investigation can be tailored to yield appropriate design information.

Figure 1. The cutoff trench excavation at Hardester North Dam encountered shale (sh) from the Great Valley Sequence. Embankment fill was placed downstream of the cutoff trench on a stiff to very stiff brown gravelly clay colluvium (Qc2) foundation. The black serpentinite-derived colluvium (Qc1) still visible upstream of the cutoff trench in the reservoir area was removed from dam foundation. [File photo by the author.]

Figure 2. Channel section and left abutment of Los Vaqueros Dam. The foundation objective of moderately weathered or better rock of the Panoche Formation has been reached in the channel section, the cutoff wall is completed, and curtain grouting is underway. Additional excavation was needed on the left abutment to obtain an acceptable foundation. [File photo by the author.]

APPROACHES FOR SPECIFYING FOUNDATION OBJECTIVES

Listed below are seven ways or approaches for specifying a foundation objective. The geologic and geotechnical observations needed for each approach, and the geologic environment for which each approach may be most applicable are discussed. Examples of the foundation objectives used in the construction of several recent California dam projects are given.

1. Attain a specific geologic unit

An example of this approach is a narrative goal such as *"extend the cutoff trench excavation completely through the alluvium and three feet into the underlying granitic rock"*. This approach requires sufficient exploration to identify a continuous geologic unit judged to possess adequate properties for the foundation. The foundation objective is usually described in the specifications, although an excavation contour map plan sheet could be provided based on known occurrences of the specified geologic unit. Typical applications for this approach are dam and appurtenant structure excavations at sites with clearly contrasting materials types, such as unconsolidated deposits overlying crystalline rock, stratified cemented rock, and stratified uncemented rock.

This approach was used at the 36-foot high Hardester North Dam, near Pope Valley, California, built in 1999. As can be seen in Figure 1, all colluvium was removed to provide a relatively impermeable, severely weathered rock foundation for the cutoff trench. In the shell foundation, an unacceptably weak serpentinite-derived black colluvium unit was removed and the embankment fill was placed on the underlying brown clay colluvium, determined by design-level evaluation to be acceptable.

2. Excavate to a grade based on field testing results

Two examples of this approach are the quantitative statements *"excavate the shell foundation to an*

elevation that encounters dense silty sand with an SPT $N_{1(60)}$ value of 30 blows per foot", and *"excavate the cutoff trench to an elevation that encounters crystalline rock with a permeability of less than 10 lugeons"*. This approach is typically used at well-explored sites where sufficient data exist to identify the materials with stated properties across the site. Specific geotechnical properties of acceptable foundation materials are stated explicitly and quantified, so the approach is often used for sites where the properties of a given foundation material need to be closely characterized. Field testing could include standard penetration tests, water tests, Goodman Jack deformation measurements, and seismic velocity measurements. Because of the repetitive measurements, the inferred target grade can be described as a well-constrained excavation contour map in contract documents. Typical applications are dam and appurtenant structure excavations in unconsolidated deposits, cemented and uncemented stratified rock, and crystalline rock.

This approach was used at the 285-foot high West Dam of the Diamond Valley reservoir near Hemet, California, completed in 2000. The three alluvial channels, which underlie a portion of the West Dam, were excavated to an elevation that removed alluvium with a SPT $N_{1(60)}$ value of less than 30.

3. Attain a specific rock quality

An example of this approach would be the narrative objective to *"excavate the dam foundation to slightly weathered granitic rock"*. Qualities of rock that are potentially significant to dam construction include degree of rock weathering and the density, orientation, aperture, and infilling of discontinuities. Strength, deformation, and permeability characteristics that are associated with a given rock quality are either measured or assumed, and those characteristics are evaluated for adequacy. Excavation to a given rock quality provides a foundation with those characteristics judged adequate. This approach requires that sufficient exploration be performed to identify the consistent presence of the rock quality specified, and to have reason to believe that rock with similar properties underlies the chosen surface. This approach requires that all observers recognize rock quality and are conversant with descriptive standards. Published rock descrip-

Figure 3. The right abutment of the McKays Point Diversion Dam. In this area the dam is founded on massive, slightly weathered granitic rock. [File photo by the author.]

Figure 4. The cutoff trench excavation for Bottoms Dam was taken several feet into siltstone and shale (s/sh) of the Great Valley Sequence. Five to seven feet of the overlying older alluvium (Qal) were found to be adequate for the upstream and downstream shell foundations. A serpentinite body (sp) was encountered on the knoll beyond the cutoff excavation. [File photo by the author.]

tive standards are available in GSA (1980) and USBR (1990). It should be confirmed during construction that the characteristics assumed to represent a given rock quality are, in fact, appropriate. Typical applications of this approach are dams and appurtenant structure excavations in crystalline and cemented stratified bedrock.

This approach was used at the 200-foot high Los Vaqueros Dam, near Byron, California, built in 1998 (Simpson and Schmoll, 2001, this volume). The foundation objective for the dam was specified as moderately weathered or better rock. Figure 2 shows the channel section at final grade and left abutment excavation nearing the foundation objective.

This approach can be more rigorous, essentially becoming somewhat of a hybrid of approach 2. A more rigorous qualitative assessment was done at the McKays Point Diversion Dam, a 233-foot high arch dam built in 1988, on the North Fork of the Stanislaus River in Calaveras County. The foundation objective for this highly loaded foundation was defined as a minimum of class III rock as defined by Bieniawski (1973). The Bieniawski rock-mass classification system evaluates, by assigning a rock quality rating, both the intact rock and the discontinuities within the rock mass using core samples. Foundation materials judged to possess acceptable deformation properties can be identified in each boring. A foundation excavation contour map estimating the excavation needed to reach acceptable foundation materials can be included in the contract drawings. Figure 3 shows the slightly weathered to fresh, massive rock encountered in the right abutment foundation excavation.

4. Achieve a surface that meets a construction control test

Two examples of this approach are *"excavate to a surface with a relative compaction of 95% ASTM D-1557"*, and *"excavate to a surface with an in-place dry density of 120 pounds per cubic foot"*. This approach is often used for poorly explored sites where prejudgments cannot be made with confidence. Estimates of the excavation needed to achieve adequate foundation material can be poorly constrained, potentially increasing excavation costs. It requires an ability to physically test the foundation materials during construction, and a belief that materials with adequate properties will underlie the chosen surface. This approach can also serve as a confirmatory evaluation, especially when exploration suggests variable or complex geologic conditions. Typical applications are dam and stability berm excavations in unconsolidated deposits.

This approach was used at the Bottoms Dam, a 47-foot high earth dam built in 1989, near Middletown, California. As can be seen in Figure 4, five to seven feet of older alluvium were left-in-place beneath the shells of the dam. To be considered acceptable for shell foundation, the older alluvium needed to have a density equal to the equivalent maximum dry density (100%) as determined using the ASTM D698-70 compaction standard. The older alluvium was found to meet that standard and was approved for shell foundation.

Figure 5. The excavation for the enlargement of the Homestake Tailings Dam encountered an unexpected occurrence of Quaternary lake deposits (Ql). Since the foundation objective called for highly weathered serpentinite (sp) rock, the unconsolidated silty deposits required visual examination to determine their adequacy. The fault contact between the serpentinite and the lake deposits was demonstrated to be inactive before fill placement could begin. [File photo by the author.]

5. Excavate to a surface based on the ability of excavation equipment

An example of this approach is *"excavate to blade refusal of a Caterpillar D-10N tractor dozer"*. This approach usually requires a calibration test between the capability of the equipment, the character of the material on which it refuses, and adequacy of that material for foundation. An example of an effective calibration demonstration, developed for the Diamond Valley Reservoir, is found in MWD (1995). Confirmation that the desired material has been actually encountered in the excavation is especially important because equipment refusal can occur on unrecognized unsuitable materials. Typical applications include dam and appurtenant structure excavations in weathered crystalline rock. This approach is not appropriate for stratified rock, where weaker materials might underlie a stronger layer.

This approach was used for the three dams at Diamond Valley reservoir, where ripper refusal and blade refusal of specific excavators were specified as the foundation objectives for cutoff trenches and shell foundations, respectively.

6. Excavate to a depth indicated by design analysis

This approach is often used when exploration indicates there is no expectation of material improvement within conventional excavation depth. The adequacy of the foundation is based on engineering analysis in conjunction with design solutions that mitigate the impact of the undesirable foundation materials. A common application of this approach is for low dams on weak alluvial foundations, where the foundation is taken to a specific depth, for example, a depth equal to twice the height of the dam. The foundation objective can be very clearly described in the plans as an excavation contour map. Although conventionally acceptable geologic materials may not be attained, this approach does require confirmation that the geologic conditions exposed in the foundation are consistent with

the assumptions made in the justifying design analysis. Differing conditions that invalidate the analysis and, therefore, the finding of adequacy, need to be recognized and evaluated prior to foundation acceptance. Typical applications are dam and appurtenant structure excavations in deep unconsolidated deposits.

7. Achieve a material judged adequate based on visual observation

An example of this approach is to *"excavate to a depth directed by the engineer"*. This approach requires the ability to make observations and judgments of strength and permeability during construction, and an expectation that adequate materials underlie the surface chosen. This approach is generally not used as the primary method of identifying adequate dam foundation materials, but should always be specified to confirm the adequacy of any surface indicated by other approaches, and to deal with unexpected foundation materials. Pocket penetrometers, geology hammers, or other hand probes can be used to calibrate and support judgments, but for critical judgments a construction control test contingency should be incorporated in the specifications. Without an exploratory basis for estimating the depth to adequate foundation materials, it would be difficult for a contractor to bid the work, which could result in higher excavation costs. Typical applications include dam and appurtenant structure excavations at poorly explored, highly variable, or ambiguously characterized sites.

This approach was used to evaluate an unexpected occurrence of lake deposits exposed in the foundation for the 1996 enlargement of the Homestake Tailings Dam in Lake County, California. As seen in Figure 5, the Pleistocene silty lake deposit was encountered over a 200-foot reach of the dam foundation. Since the foundation objective specified was a highly weathered rock, the lake deposit did not meet that objective. However, based on visual examination during construction, the dense silt deposit was judged to be an adequate foundation material.

CONCLUSION

The foundation objective is a descriptive tool used to convey information regarding the design intent of a dam foundation to construction staff and the contractor. Separate foundation objectives are usually needed to convey specific requirements for the various features of the project, such as the cutoff trench excavation, shell foundation excavations, outlet excavation, and spillway excavation. More than one approach may be needed to adequately describe some foundation surfaces.

The selection of the most appropriate approach or approaches is based largely on site geology, the amount of available geologic and geotechnical information, and the performance requirements of the foundation. The engineering geologist and design engineer should work together while planning the site investigation to identify the most effective approach for specifying a foundation objective at a given site. In this way, sufficient information can be gathered to estimate excavation requirements, while providing a framework to allow the excavation to be responsive to any unexpected geologic conditions.

Achieving the foundation objective indicates that a foundation with properties that are judged adequate based on design information has been obtained. The ultimate adequacy of the foundation must be confirmed as part of final foundation acceptance, to insure the foundation will perform as expected.

ACKNOWLEDGEMENTS

I wish to thank Jeffrey K. Howard for his helpful contributions in identifying the various approaches described in this paper. I also want to thank Steven W. Verigin, Ronald F. Delparte, Vernon H. Persson, David Simpson and Doug Boyer for their thoughtful review of the manuscript, and Elizabeth G. Brode for her assistance in preparing the photographs for this paper.

AUTHOR PROFILE

For the past 15 years William A. Fraser has been with the California Department of Water Resources, Division of Safety of Dams, in Sacramento, California. For the past 8 years he has been the Chief of the Division's Geology Branch, supervising a staff of five engineering geologists, involved in seismic hazard assessment, site exploration and characterization, and foundation design issues. The Division of Safety of Dams regulates the design, construction, and maintenance of more than 1,200 jurisdictional dams throughout California. Prior to working with the Division of Safety of Dams, Mr. Fraser served 7 years as a staff geologist with the Department of Water Resources, Division of Engineering, perform-

ing design and maintenance investigations on State Water Project facilities. Mr. Fraser is a Registered Geologist and a Certified Engineering Geologist in California.

SELECTED REFERENCES

Best, E., 1984, Dams, engineering geology: *in* Finkl, C. W., (ed.), The encyclopedia of applied geology, Van Nostrad Reinhold Company, (New York, New York), 644 p.

Bieniawski, Z.T., 1973, Engineering classification of jointed rock masses: Transactions South African Institute Civil Engineers, v. 15, p. 335-344.

Burwell, E.B. and Moneymaker, B.C., 1950, Geology in dam construction: *in* Paige, S., (ed.), Applications of geology to engineering practice, Berkey Volume, Geological Society of America, New York, 327 p.

GSA (Geological Society of America), 1980, Rock weathering classification: GSA Engineering Geology Division, Data Sheet 1, [Boulder, Colorado].

Goodman, R.E., 1993, Engineering geology-Rock in engineering construction: John Wiley & Sons, Inc., (New York, New York), 412 p.

Hunt, R.E., 1984, Geotechnical engineering investigation manual: McGraw-Hill Book Company, (New York, New York), 983 p.

Janson, R.B., 1983, Dams and public safety: U. S. Bureau of Reclamation, Water Resources Technical Publication, (Denver, Colorado), 332 p.

Janson, R.B., (ed.), 1988, Advanced dam engineering for design, construction, and rehabilitation: Van Nostrand Reinhold, (New York, New York), 811 p.

Krynine, D.P. and Judd, W.R., 1957, Principles of engineering geology and geotechnics: McGraw-Hill Book Company, (New York, New York), 730 p.

Legget, R.F., 1962, Geology and engineering: McGraw-Hill Book Company, (New York, New York), 884 p.

Lowe, J. and Zaccheo, P.F., 1975, Subsurface explorations and sampling: *in* Winterkorn, H.F., and Fang, H.Y., (eds.), Foundation engineering handbook, Van Nostrand Reinhold Company, (New York, New York), 751 p.

MWD (Metropolitan Water District of Southern California), 1995, Test excavation TE-1, Appendix C-3 of Domenigoni Valley Reservoir Project, East Dam Geotechnical Report: Metropolitan Water District, [Los Angeles, California], 5 p.

Simpson, D.T. and Schmoll, M., 2001, Exploration, design, and construction of Los Vaqueros Dam, Contra Costa County, California: *in* Ferriz, H., Anderson, R., (eds.), Engineering Geology Practice in Northern California: Association of Engineering Geologists Special Publication 12 and California Division of Mines and Geology Bulletin 210

USBR (U. S. Bureau of Reclamation), 1990, Engineering geology field manual: U. S. Bureau of Reclamation (Denver, Colorado), 598 p. [This manual does not have a publication date printed in it, and USBR does not recognize a formal date of publication]

USBR (U. S. Bureau of Reclamation), 1987, Design of small dams: U. S. Bureau of Reclamation, Water Resources Technical Publication, (Denver, Colorado), 860 p.

FAULT ACTIVITY GUIDELINES OF THE CALIFORNIA DIVISION OF SAFETY OF DAMS

WILLIAM A. FRASER[1]

ABSTRACT

This paper discusses the fault activity guidelines used by the California Division of Safety of Dams to evaluate faults in California. In California, earthquakes represent the most severe loading that some dams will experience. To provide a high degree of protection from earthquake-related dam failure, the seismic sources that could conceivably affect a dam must be identified. Clear and all-inclusive guidelines for assessing fault activity are needed by investigating geologists evaluating the seismic hazards. The California Department of Water Resources, Division of Safety of Dams, defines an *active* fault as having ruptured within the last 35,000 years. A *conditionally active* fault is defined as having ruptured in the Quaternary, but its displacement history during the last 35,000 years is unknown. Fault inactivity is demonstrated by a confidently located fault trace that is consistently overlain by unbroken geologic materials older than 35,000 years. Faults that have no indication of Quaternary activity are presumed to be *inactive*, except in regions of sparse Quaternary cover.

INTRODUCTION

In California, strong ground shaking can result in instability of the dam itself, strength loss of the foundation, instability of the natural reservoir rim, and release of the reservoir by seiche. Active faults within the foundation of the dam have the potential to cause damaging displacement of the structure. To prevent catastrophic release of water from the reservoir, appropriate design measures must be employed to resist earthquake-imposed loads.

To provide a high degree of protection from earthquake-related dam failure, identification of the seismic sources that could conceivably affect a project is needed. Seismotectonic investigations, often involving detailed field studies to determine the recency of fault activity and magnitude of paleoseismic earthquakes, are an important part of a site investigation for dams.

This paper discusses the fault activity guidelines used by the California Division of Safety of Dams (DSOD) to evaluate faults in California. In reviewing the safety of existing and proposed dams, the DSOD uses a deterministic method to estimate ground motion parameters for design analysis. In a deterministic seismic hazard assessment, the judgement as to which faults are active seismic sources is perhaps the most critical step. Clear guidelines to identify active faults are of interest to project planners, investigating geologists, and design engineers.

In developing these guidelines, the criteria used by other agencies, particularly agencies involved in dam design, were reviewed. Slemmons and McKinney (1977) provide an historical summary of the various definitions of the term "active fault", many of which are application specific.

DETERMINISTIC SEISMIC HAZARD ANALYSIS

In a deterministic seismic hazard assessment, faults within the proximity of the site are identified and assessed for activity. For each seismic source, an earthquake scenario, consisting of the maximum magnitude a fault is capable of generating at the

[1]California Division of Safety of Dams
2200 X Street
Sacramento, CA 95814
billf@water.ca.gov

closest distance to the site under consideration, is specified as the basis for the ground motion estimate. Statistically-based ground motion estimates for the several significant seismic sources are reported to engineering staff, who study the estimates and decide which to use in modeling the maximum loading for the structure.

A deterministic seismic hazard analysis is time-independent. The specified event is possible, but there is no consideration of the likelihood of occurrence within a given time frame, such as the life of the dam. This approach contrasts with the probabilistic seismic hazard analysis, which formally considers event likelihood and the uncertainty of the ground motion estimate.

The investigator compiles information on the known faults in the proximity of the site from previously published geologic maps and reports. Based on the results of this compilation, a detailed project-specific fault investigation may be required. Such investigations begin with evaluation of aerial photographs and other forms of remote sensing, such as infra-red or radar imagery, to locate faults and assess their activity. Historic aerial photographs may be especially helpful in recognizing fault-produced landforms in areas where construction or agriculture have altered the topography. Ground-based geophysical surveys, such as gravity, magnetism, and reflection or refraction seismology, may help determine fault locations. Once located, trench exposures are used to assess fault activity and character of expected movements. Maximum magnitude is determined through an evaluation of fault segmentation and displacement history. A comprehensive summary of techniques of fault activity evaluation has been compiled by Slemmons and dePolo (1986).

Active faults and conditionally active faults are used to develop the design ground motion. The faults judged to be inactive are eliminated from further consideration.

FAULT ACTIVITY GUIDELINES

Numerous definitions for active faulting have been proposed, but no one definition has been universally accepted (Slemmons and McKinney, 1977). In 1995, DSOD geology staff substantially revised their active fault guidelines. This process included detailed review by the DSOD Consulting Board for Earthquake Analysis (Housner et al., 1989, 1994)—a panel consisting of eminent experts in the fields of geology, seismology, and earthquake engineering. The goal of this revision was to develop clear guidelines for assessing fault activity, as well as precise categories of activity to provide a basis for design decisions. The guidelines also provide direction to geologists in planning fault investigations on behalf of dam owners.

A text of the guidelines is included in the Appendix and is discussed in some detail below. Three general categories of faults are defined: *active*, *inactive*, and *conditionally active*.

Figure 1. Holocene active fault. A recent investigation at Leyden Creek revealed evidence for as many as six surface ruptures along the Northern Calaveras fault during the last 2,500 years. The fault juxtaposes serpentinite (sp) and Holocene colluvium (Qc). Soil fissures within Holocene colluvium extend to within six inches of the surface. [Modified after Kelson et al. (1996); file photo by M.K. Merriam, Division of Safety of Dams.]

Figure 2. Latest Pleistocene active fault. A 1997 investigation of the Franklin fault near Walnut Creek has identified offset of 31,000 year old alluvium (Qal). [File photo by J.K. Howard, Division of Safety of Dams.]

Active seismic sources

An active seismic source is defined as a fault that has ruptured within the last 35,000 years. The 35,000-year value was selected based on the belief that Holocene activity (the last 11,000 years) is not a sufficiently conservative criterion for elimination of a fault when estimating ground motion for dam design. The 35,000-year criterion essentially defines a level of risk. Faults exhibit a wide range of average recurrence intervals, from a few tens of years to over several hundred thousand years, and a fault that has not moved in the last 35,000 years is assumed to have a ground-rupturing earthquake recurrence interval of more than 35,000 years. This low level of activity makes the likelihood of future events sufficiently improbable that the fault may be disregarded for design purposes.

This fault activity criterion is somewhat arbitrary by its very nature. There is no physical reason why a fault that has not moved during the last 35,000 years cannot move again. This point is illustrated by the October 16, 1999 M_w 7.1 Hector Mine earthquake. Much of the fault zone that produced this earthquake had not ruptured previously during the Holocene, clearly illustrating the need to design dams for a criterion more conservative than Holocene activity. The 35,000-year criterion was selected because it provides this conservatism, while retaining the practicality of having several age-dating techniques available to investigating geologists.

Two sub-categories of active faulting are defined: *Holocene active* and *Latest Pleistocene active*. At the present time the distinction between these sub-categories is descriptive only, and both categories are treated as active seismic sources for the purposes of design. These sub-categories conceivably could define separate criteria applicable to dams of different type, risk category, or location within California.

The guidelines provide examples of the lines of evidence that are used to classify a fault as Holocene active. Stratigraphic displacement of Holocene age materials is a primary way to identify a Holocene active fault. Other criteria used to demonstrate Holocene activity include geomorphic, geologic,

geodetic, and seismologic evidence. Holocene active faults are usually well-documented in the geologic literature. An example of a Holocene active fault is shown in Figure 1, in which a trench exposure at Leyden Creek reveals that the Calaveras fault has repeatedly offset Holocene colluvium (Kelson et al., 1996).

Faults of Latest Pleistocene age are usually not as well documented in the literature and may be more difficult to recognize. Age dating of geologic materials within this time frame is possible using radiocarbon and soil stratigraphic techniques. An example of a Latest Pleistocene active fault is shown in Figure 2, in which the Franklin fault offsets 31,000-year-old alluvium near Walnut Creek, California.

Inactive seismic sources

In planning and interpreting subsurface investigations, the investigating geologist needs to know the criteria by which a fault can be shown to be *inactive*. Inactivity is demonstrated by a confidently located fault trace that is consistently overlain by unbroken geologic materials 35,000 years or older, or other characteristics indicating lack of displacement within the last 35,000 years. Figure 3 shows a fault demonstrated to be inactive: The Waters Peak fault, near New Hogan Reservoir, is overlain by geologic materials greater than 35,000 years old (USACE, 1995).

Faults that have no suggestion of Quaternary activity are generally presumed to be *inactive*. However, in regions of sparse Quaternary cover, a fault lacking evidence for Quaternary activity cannot be assumed to be inactive. The presumption of inactivity requires a finding that there is no potential or expectation for activity. This may be demonstrated by fault characteristics inconsistent with the current tectonic regime.

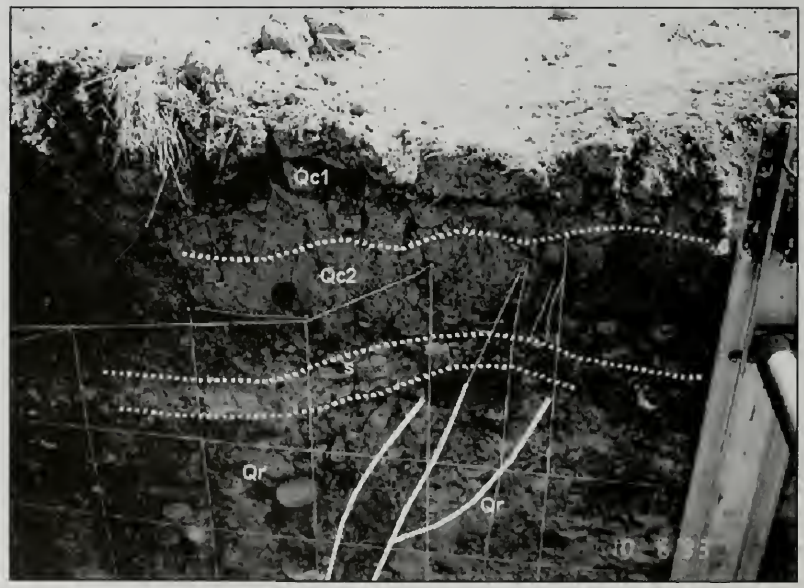

Figure 3. Inactive fault. A 1993 investigation by the U.S. Army Corps of Engineers demonstrated inactivity on the Waters Peak fault near Valley Springs, California. The down-to-the-east normal fault displaces Pleistocene Riverbank Formation (Qr). An unfaulted pedogenic silica horizon (s) developed on the alluvium—dated at more than 35,000 years old—and two younger unfaulted colluvium units (Qc1 and Qc2) overlie the fault. [File photo by author.]

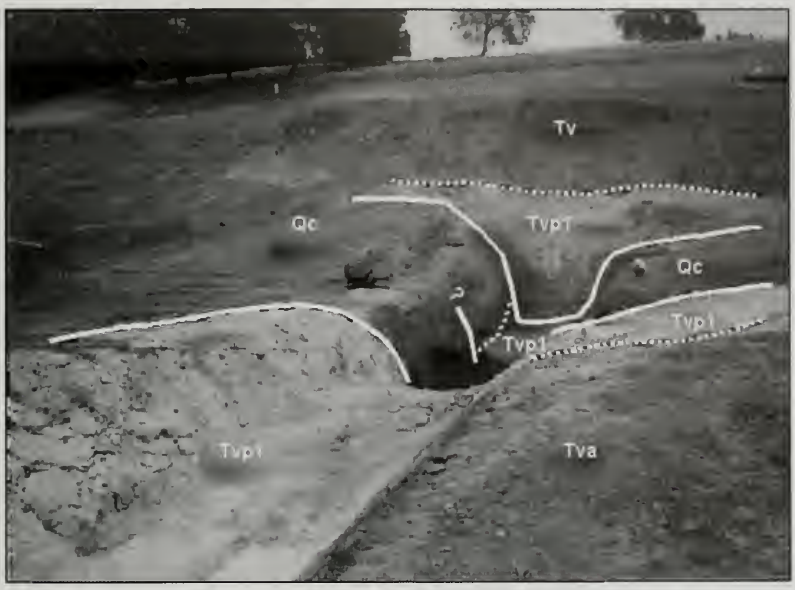

Figure 4. A conditionally active fault (shown by the white thick solid lines) is exposed in the foundation excavation for Shiloh Ranch Dam #2 near Santa Rosa. Tertiary white tuff (Tvp1) is in fault contact with Quaternary colluvium (Qc). The owner of the dam elected to design for fault offset rather than investigate the fault's displacement history during the last 35,000 years. Depositional contacts between the colluvium, white tuff, Tertiary andesite (Tva), and the undifferentiated volcanic unit (Tv) are shown by the dotted lines. [File photo by author]

Conditionally active seismic sources

The guidelines establish specific criteria for determining faults that require detailed investigation. In most areas of the State, demonstrated Quaternary activity is considered a reasonable and practical threshold for assuming that a fault may be associated with the current tectonic regime. A *conditionally active* fault is Quaternary active, but its displacement history during the last 35,000 years is not known well enough to determine activity or inactivity. The often misused and misunderstood term "potentially active fault" has been dropped from use. In regions of sparse Quaternary cover, such as the Sierra Nevada, pre-Quaternary faults that can be reasonably shown by Division staff to have attributes consistent with the current tectonic regime are also classified as conditionally active.

The DSOD treats *conditionally active* faults as seismic sources, with the understanding that additional investigation or analysis could change that designation. Figure 4 shows a conditionally active fault exposed in the foundation excavation for Shiloh Ranch Dam near Santa Rosa, California.

SUMMARY

To provide a high degree of protection from earthquake-related dam failure, the seismic sources that could conceivably affect a dam must be identified. However, there is no universally accepted definition for an active fault. The active fault criterion selected essentially defines an acceptable level of risk for the specific application. The DSOD has recently adopted a 35,000-year standard for determining fault activity for dam design and analysis. Clear and all-inclusive guidelines have been developed, that should assist geologists in California with planning fault investigations, as well as provide design engineers with an understanding of the implications of each fault activity class (see Appendix).

ACKNOWLEDGEMENTS

The author thanks Division of Safety of Dams staff members Jeffrey K. Howard, Robert J. Akers, and Vernon H. Persson for their helpful assistance in the development of the Fault Activity Guidelines. The author thanks the Division of Safety of Dams Consulting Board for Earthquake Analysis, especially board members Dr. Clarence R. Allen and Dr. Bruce A. Bolt, for their thoughtful review of the guidelines. The author thanks Frank L. Glick for his thorough peer review of the manuscript, and Elizabeth G. Brode and Jacob G. Summerhays for their assistance in preparing the photographs for this paper.

AUTHOR PROFILE

For the past 15 years, William A. Fraser has been with the California Department of Water Resources, Division of Safety of Dams, in Sacramento, California. For the last 8 years he has been the Chief of the Division's Geology Branch, supervising a staff of five engineering geologists, involved in seismic hazard assessment, site characterization, and foundation design issues. The Division of Safety of Dams regulates the design, construction, and maintenance of more than 1,200 jurisdictional dams throughout California. Prior to working with the Division of Safety of Dams, Mr. Fraser served 7 years as a staff geologist with the Department of Water Resources, Division of Engineering, performing design and maintenance investigations on State Water Project facilities.

SELECTED REFERENCES

Housner, G.W., Agbabian, M.S., Allen, C.R., Bolt, B.A., and Seed, H.B., 1989, Final Report: Consulting Board for Earthquake Analysis Meeting of June 1 and 2, 1988: California Division of Safety of Dams, Sacramento, California, 13 p.

Housner, G.W., Allen, C.R., Bolt, B.A., and Idriss, I.M., 1994, Final Report: Consulting Board for Earthquake Analysis Meeting of June 23 and 24, 1994: California Division of Safety of Dams, Sacramento, California, 17 p.

Kelson, K.I., Simpson, G.D., Lettis, W.R., and Haraden, C.C., 1996, Holocene slip rate and earthquake recurrence of the northern Calaveras fault at Leyden Creek, Northern California: Journal of Geophysical Research, v. 101, n B3, p. 5,961-5,975.

Slemmons, D.B. and dePolo, C.M., 1986, Evaluation of active faulting and associated hazards: in Wallace, R.E. (ed.), Studies in Geophysics, Active Tectonics, National Academy Press, 266 p.

Slemmons, D.B. and McKinney, R., 1977, Definition of "active fault": U.S. Army Engineer Waterways Experiment Station, Miscellaneous Paper S-77-8.

USACE (U.S. Army Corps of Engineers), 1995, Geologic and seismologic investigation, New Hogan dam and reservoir: U.S. Army Corps of Engineers Sacramento District [Sacramento, California], 50 p.

APPENDIX

DSOD FAULT ACTIVITY GUIDELINES FOR USE IN DETERMINISTIC FAULT ACTIVITY ASSESSMENTS

Active Seismic Sources (considered seismic sources for dam design or reevaluation)

Holocene Active Fault: is a fault on which surface or subsurface displacement has occurred within the Holocene epoch. Holocene activity is demonstrated by one or more lines of evidence including the following:

- Holocene (last 11,000 years) stratigraphic displacement
- geomorphic evidence of Holocene displacement or tectonism[1]
- geodetically measured tectonism or observations of fault creep
- well-located zones of seismicity

Latest Pleistocene Active Fault: is a fault on which no evidence of Holocene displacement is known, but which has experienced surface or subsurface displacement within the last 35,000 years. Latest Pleistocene activity is demonstrated by one or more of the following lines of evidence:

- stratigraphic displacement of units dated at 11,000 to 35,000 years
- geomorphic evidence of Latest Pleistocene displacement or tectonism[1]

[1]tectonism refers to crustal deformations which are indicative of faulting

Conditionally Active Seismic Sources (treated as a seismic source for dam design or reevaluation because of incomplete or inconclusive evidence, with the understanding that additional investigation or analysis could change the designation)

Conditionally Active Fault: a fault which meets one of the following criteria:

- a Quaternary active fault (one that has experienced surface or subsurface displacement within the last 1.6 million years) with a displacement history during the last 35,000 years that is not known with sufficient certainty to consider the fault an active or inactive seismic source

- a pre-Quaternary fault which can be reasonably shown to have attributes consistent with the current tectonic regime. For example, in the foothills of the Sierra Nevada geomorphic province, Mesozoic faults are considered Conditionally Active Seismic Sources unless proven otherwise

Inactive Seismic Sources (not considered for dam design or reevaluation)

Inactive Fault: a fault which has had no surface or subsurface displacement within the last 35,000 years. Inactivity is demonstrated by a confidently-located fault trace which is consistently overlain by unbroken geologic materials 35,000 years or older, or other observation indicating lack of displacement. Faults that have no suggestion of Quaternary activity are presumed to be inactive.


ASSOCIATION OF ENGINEERING
AEG
GEOLOGISTS

ENGINEERING GEOSCIENCE INVESTIGATIONS FOR THE CONSTRUCTION OF THE FOLSOM DAM AND RESERVOIR, SACRAMENTO COUNTY, CALIFORNIA

GEORGE A. KIERSCH[1]

ABSTRACT

The multi-purpose Folsom dam and reservoir project of 1948-56 used geologic guidance for the site selection, planning-design, and construction phases. The 4.8 miles of dams consist of a high concrete gravity dam with earthen wing embankments on the American River and nine saddle dams on small tributaries. To close the reservoir rim the Mormon Island auxiliary earthfill dam was built across the ancestral Blue Ravine channel of the south fork of the American River.

The main dam and most saddle embankments are founded on extensively fractured/sheared and weathered quartz diorite; on-site "outcrops" were in most instances residual weathered boulders underlain by highly weathered rock. Mapping of different weathering stages - slight, moderate, high - using petrographic and physical properties was used to estimate depths to suitable foundation rock. Subsurface exploration techniques used to investigate the main dam site included cored-borings, geophysical surveys, borehole photography, down-hole logging of man-sized openings, and 48-inch auger/calyx holes.

Foundation excavation for the main dam progressed in three separate contract stages, based on design investigations. Because of extensive weathering, additional exploration was required ahead of the second and third stages of excavation, using shallow percussion drill holes, shafts, adits, and man-sized holes. The degree and extent of weathered rock at each excavation level were compiled on three-dimensional diagrams, as were faults and zones requiring dental treatment.

Core trenches of most earthfill and saddle embankments were grouted on a split-center pattern. Grouting of permeable, highly weathered quartz diorite was difficult due to the abundance of clay-filled fractures. Impervious earthfill was "borrowed" from areas of highly weathered quartz diorite; permeable fill was supplied from alluvium deposits and rip-rap from the main dam excavations. The powerhouse was placed in a deep excavation below the river channel for additional power head. The exposed 250-foot open-cut, with clayey seams in fractured quartz diorite required dowels/rock bolts for stability.

The Mormon Island auxiliary dam is founded on metamorphic rocks that underlie the auriferous gravels of Blue Ravine channel. The core trench is excavated in deeply weathered and scoured schistose rocks cut by many small dikes. Springs issued from the core trench rocks and necessitated a grout curtain on 5-foot centers.

INTRODUCTION

The multiple-purpose Folsom project, situated in an area of extensively weathered intrusive and metamorphic rocks, involved several dam designs. Construction demonstrated the need for geologic guidance in site selection, foundation design-excavation,

[1]Deceased

location of sources of construction materials, diversion of the river, establishing the foundation grade, and remedial treatment of foundations and open-cut rock slopes.

NATURE OF THE PROJECT

The Folsom dam and reservoir project is located on the American River, 20 miles northeast of Sacramento (Figure 1), in the Sierra Nevada foothills of central California. The project consists of a concrete gravity dam 355 feet high and 1,400 feet long, with partially enveloping earthfill wing dams on the American River, the Mormon Island auxiliary earthfill dam across Blue Ravine (the ancient channel of the south fork of the American River) and eight smaller earthfill saddle dams. Together, these dams total 4.8 miles of structures. Development of the American River flood control and power generating facilities at Folsom were a joint undertaking by the U.S. Army Corps of Engineers and the U.S. Bureau of Reclamation.

PREVIOUS WORK

The earliest geologic work in the Folsom area was by Lindgren (1894), as part of his Mother Lode gold belt studies. The initial investigation for a dam near Folsom was performed in 1927 by the American River Hydroelectric Company with borings at a down stream site (Forbes, 1929). The Corps of Engineers completed a brief reconnaissance of the area in 1940 and, subsequently, received authorization for a concrete dam of 650,000 acre-feet capacity. The Bureau of Reclamation investigated a lower site and an upper site with borings and made reconnaissance geologic studies at the present site in 1942 (Gardner, 1942). Further reconnaissance investigations by the Corps were made in 1944-46 (Johnston, 1947) and led to authorization for a million acre-foot reservoir in 1947.

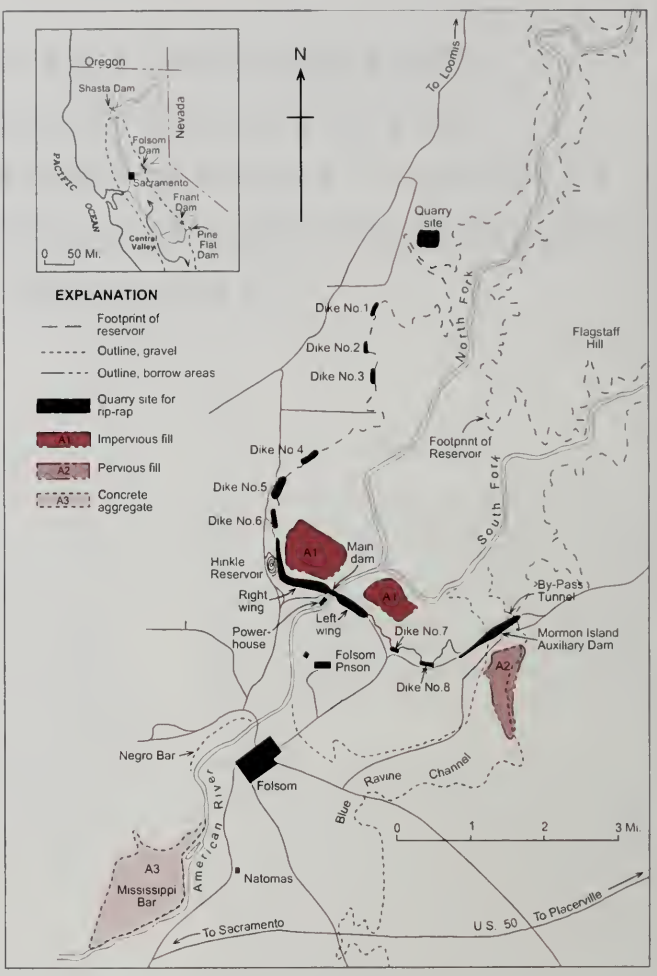

Figure 1. Location map of the Folsom project.

GEOLOGIC SETTING

The Folsom Project is located in the low westernmost foothills of the central Sierra Nevada. The upper "arms" of the reservoir extend eastward into the foothills where the streams are entrenched. Relief ranges from 1,242 feet near Flagstaff Hill to 150 feet near Folsom. The three tributaries of the American River drain some 2,000 square miles; the

Figure 2. Regional geologic map of the Folsom reservoir project. Geologic mapping by G. A. Kiersch (1949-50).

AGE		FORMATION or UNIT	THICKNESS (ft.)	GENERALIZED DESCRIPTION
SYSTEM	SERIES			
Quaternary	Recent	Stream gravels, (channel) (Qrc)	0-65	Hydraulic mining debris within stream channel. Angular to rounded gravel of quartzose, igneous, and metamorphic rock and occasional boulders. Lens "slickens".
	Upper Pleistocene	Intermediate alluvium (Qpal)	0-35	Gravel, sand, and silt. Unconsolidated, predominantly rounded quartzose material with some volcanic, granitic, and metamorphic rock.
	Upper Pleistocene (?) to Pleistocene	Old alluvium (Tqal)	0-90	Gravel with interbedded sand, silt, and clay. Weakly consolidated, sub-rounded to rounded, quartzose, granitic, and andesitic material. Includes a section of mudstone and siltstone overlaying gravels; patches of reworked Mehrten Formation.
Tertiary	Pliocene to Miocene	Mehrten Formation (Tms)	0-225	Interbedded gravel, cross-stratified sandstone, gray tuffaceous beds, channel gravel, mud flows of volcanic breccia, and a bouldery member. Predominantly andesitic volcanic debris.
	Miocene (?) to Eocene	Ione Formation (Te)	0-75	Undifferentiated non-marine and marine (?) clay, sand, gravel, and firmly cemented, channel-filling, white, quartz conglomerate. Includes thin beds possibly equivalent to Valley Springs Formation.
Mesozoic	Upper Cretaceous	Chico Group (Kc)	0-30	Sandstone (soft, fine-grained, greenish and gray beds), and thin bed of sandstone-conglomerate. Commonly fossiliferous.
	Upper Jurassic	Gabbro (gb)		A dark gray facies of quartz diorite. Occurs as small bodies Weathers bold outcrop. In part (?) Amador Group.
		Quartz diorite (qd) (Rocklin "granite")		Mottled gray, medium-to coarse-grained, composed primarily of andesine, quartz, and biotite. Locally, slight variation in composition and texture. Normally concealed by mantle soil grading into weathered rock.
		Ultramafics (s)		Serpentine and peridotite. Dunite and lherzolite is serpentinized, steatitized, and silicified in part.
		Mariposa Formation (Jms)		Black slates with associated quartzite, tuff, and sericite schist and numerous small igneous intrusives. Lithomarge zone at upper contact. Slates weather "knotty" surface.
	Upper-Middle Jurassic	Amador Group (Jmv)		Undifferentiated metamorphic and igneous rocks. Includes sericite schists, amphibolite schists, meta-sediments, meta-volcanics, augite andesite, meta-dacites, and tuffs.
Paleozoic	Permian to Carboniferous	Calaveras Formation (Cc)		Marmorized limestone, light-gray, coarse-grained, as faulted lens-shaped bodies. Reportedly fossiliferous.

Table 1. Rock units, ages, and engineering characteristics of the rocks in the Folsom area

Middle and North Forks join near Auburn, and the South and North Forks join one-half mile upstream from the main dam (Figure 1). The North and South Forks occupy broad, mature valleys up to 3 miles wide, with youthful entrenchment in a V-shaped inner valley 30 to 185 feet deep. The outer valley is bounded in part by low hills and erosional remnants with topographic saddles formed by the tributary drainages. These topographic lows required construction of eight saddle dams in order to create the desired reservoir capacity.

A late Plio-Pleistocene course of the American River, Blue Ravine channel, flowed through the Mormon Island area and joined the present river channel below the town of Folsom (Figures 1 and 2). This ancestral stream carved a broad, gently sloping valley, one to two miles wide.

Stratigraphy and lithology. The various formations that underlie the Folsom region have been described in detail by Kiersch and Treasher (1955). General descriptions of their characteristics, age, and properties are summarized in Table 1, and their areal distribution is shown in Figure 2.

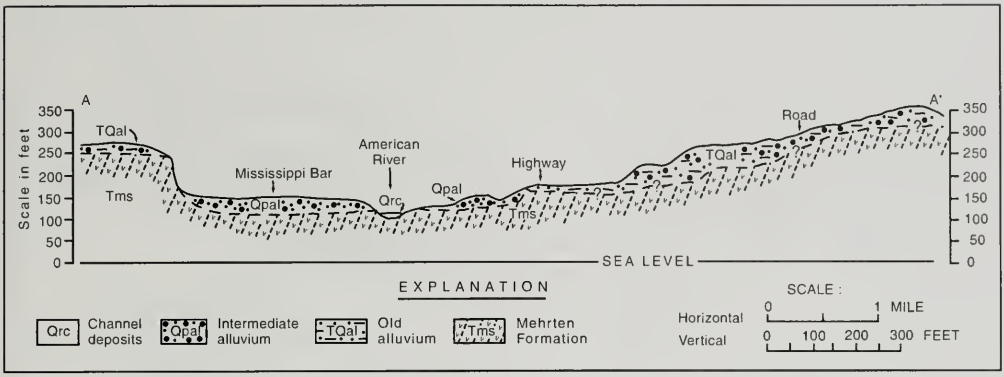

Figure 3. Geologic cross-section near Natomas, showing three ages of alluvium

The Folsom region is underlain by metamorphic rocks of the Calaveras Formation, the Lower Jurassic Amador Group, and the Upper Jurassic Mariposa Formation. These metamorphic rocks were intruded by the magmas of the Jurassic-Cretaceous Sierran batholith. Later, soft, fine-grained sediments of the Upper Cretaceous Chico Formation were deposited, followed by Eocene lone sediments and the tuffaceous Miocene Mehrten Formation. More recently, three epochs of alluviation led to accumulation of the informal units known as "old" alluvium, "intermediate" alluvium, and the Recent stream channel deposits (Figure 3).

Faults. Major faults trend both northeast and northwest. Northeast-trending faults dip steeply southward and are displaced up to 2,000 feet; northwest faults are not as pronounced. Quartz veinlets and mineralized stringers are abundant along northeast-trending breaks, and post-mineralization movements fracture these veinlets.

Shear zones. Regional shears strike generally east and are known to traverse all pre-Tertiary granitic and ultra-basic rocks. A major vertical shear zone, some 100 feet wide, is exposed in an abandoned quarry inside Folsom prison. Other shear zones, and particularly crudely sheeted fracture zones, were observed in the foundation excavations.

GEOLOGIC HISTORY

A brief summary of the geologic history of the Folsom area is helpful to explain conditions at the dam sites and their effect on the design and construction:

- Water-laid sediments with interbedded volcanic rocks were folded and uplifted at the close of the Paleozoic to form the Calaveras Formation. Prolonged erosion was followed by the widespread volcanism of the Amador Group and the deposition of the sediments of the Mariposa Group. An intense period of uplift with underthrusting followed during the late Jurassic.

- The underthrusting forces compressed the Calaveras, Amador, and Mariposa rocks into a series of northward-trending, steep repetitive folds, and the associated metamorphism formed slaty, schistose, and foliated structures. Underthrusting along the Foothills fault system incorporated slivers of ultramafic serpentinite, and felsic magmas intruded along this northward structural trend in the late Jurassic and early Cretaceous. Quartz diorite is the principal intrusive rock in the Folsom area.

- Closely associated with the intrusion of the Sierra Nevada batholith was the deposition of quartz and gold in northeastward-striking fractures.

- Prolonged erosion removed a large volume of the "bedrock series". The sediments derived from this erosion were deposited as the

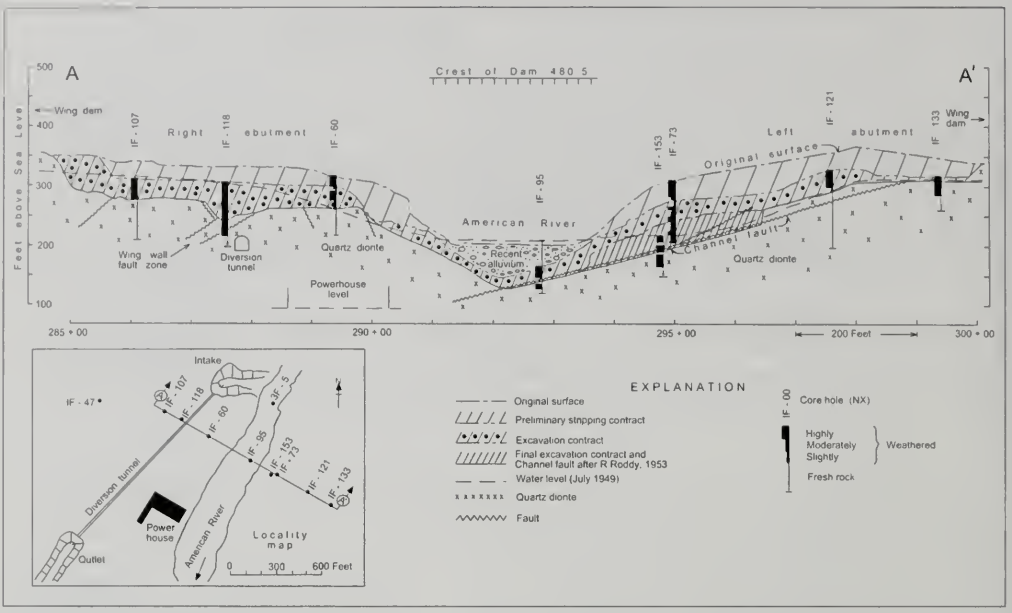

Figure 4. Geologic cross-section of the gravity section of the main dam, showing limits of excavation contracts, major faults, and final foundation grade.

Chico and Ione Formations. Erosion ultimately exposed the gold veins and led to widespread distribution of auriferous gravels in the ancient streambeds.

- Extensive volcanic activity started in the Oligocene and continued intermittently until the Pliocene. This intermittent activity led to accumulation of tuffs, lavas, and interbedded tuffaceous sediments of the Mehrten Formation. Tertiary stream channels with auriferous gravels were filled with lava flows and forced the former drainages to erode new channels.

- Uplift of the Sierra Nevada, which began in the Tertiary, reached its current approximate elevation by early Quaternary time. Westward tilt of the Sierran block is reflected in the dip directions of Tertiary strata in the Folsom area.

- Streams eroded and widened their valleys in several stages in response to the Sierran uplift. For example, the American River shows two clear stages in its wide, mature outer valley and its V-shaped inner channel (Figures 4 and 5). Down-cutting reached the gold-bearing veins in many places and re-worked the auriferous gravels throughout several of the drainage systems.

- Finally, the prolonged uplift of the Sierra Nevada resulted in a complex joint pattern: a major shallow-dipping east trending set and a northeast-trending set with high-angle dips.

PLANNING AND DESIGN INVESTIGATIONS

Geologic investigations for the planning and design phases of project began in late 1948 and were largely completed by early 1950. They included: (1) Regional mapping of parts of the Folsom and Auburn quadrangles (1:62, 500) and preliminary mapping of all dam sites (1" = 20 or 50 feet). (2) NX cored borings in the foundation area and proposed tunnel alignments of the gravity dam. (3) Two

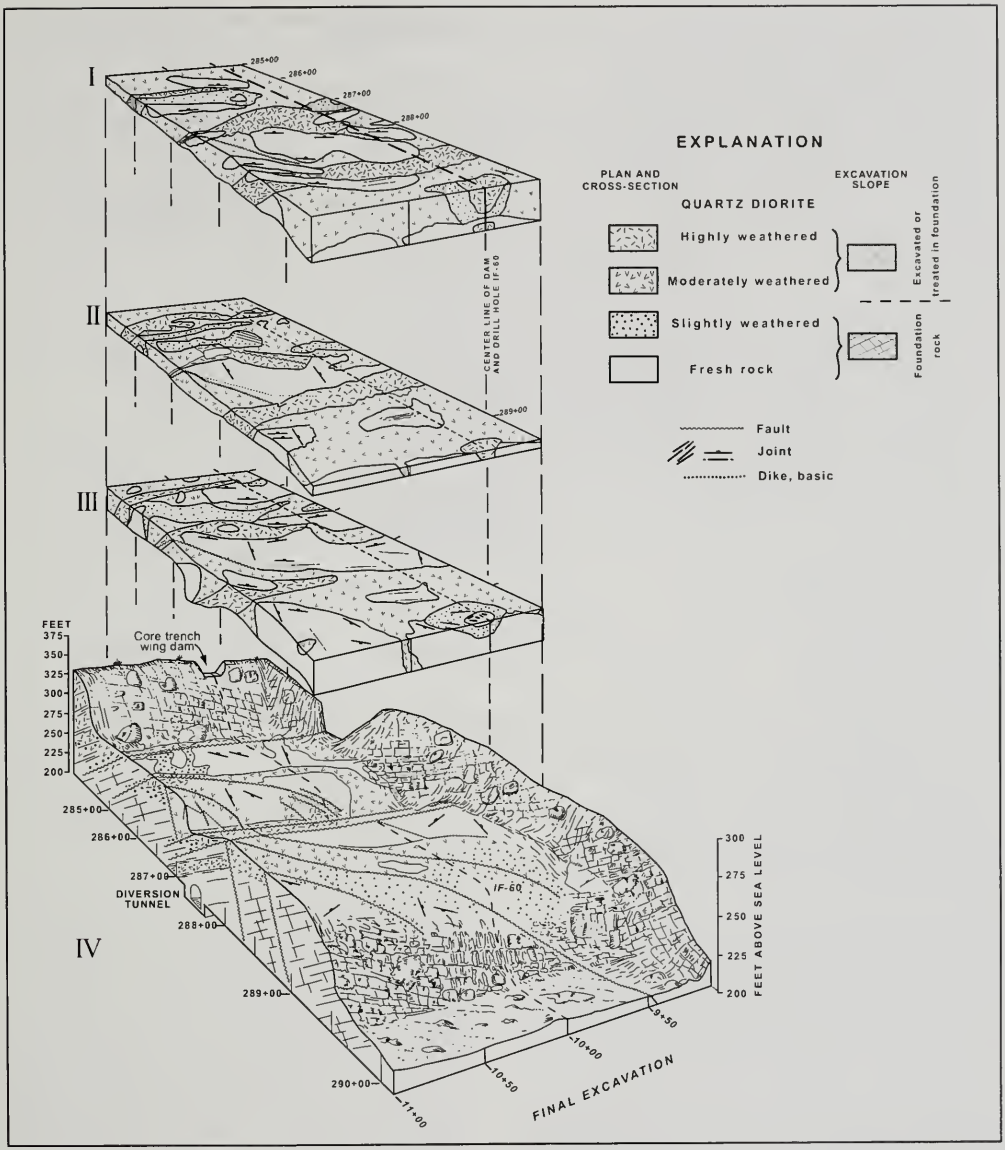

Figure 5. Block diagram showing the three stages of excavation of the right abutment of the main dam. The diagram illustrates the characteristics and weathering of the foundation rock.

48-inch auger borings through the weathered rock "blanket". (4) Additional shafts and test pits for the earthfill wing dams. The subsurface exploration data were used to estimate foundation conditions, select tunnel alignments, and locate construction material sources.

Scale	Essentially fresh	State of weathering		
		Slight	Moderate	High
Megascopic	Mottled. Light gray, medium-to coarse-grained. Unaltered, high quality and durable	Essentially as durable and high quality as rock in fresh state. ***Feldspars*** - "visibly" fractured, weakly bleached a whitish gray. ***Limonite*** - specks scarce. In logging cored borings, lighter colored feldspars used as criteria for separating from fresh rock.	Firmly coherent, somewhat friable, with original texture well preserved. ***Feldspars*** - moderately fractured, bleached grayish white. ***Quartz*** - very slightly rounded. ***Biotite*** - weakly bleached. ***Limonite*** - common, as specks coating minerals and along the boundaries of individual grains and cracks. Moisture content somewhat increased.	Loosely coherent, friable, with original texture and structure mostly preserved. ***Feldspars*** - highly fractured, bleached white. ***Quartz*** - rounded. ***Biotite*** - strongly bleached. ***Limonite*** - abundant, as specks and coating minerals, along grain boundaries and cracks. Moisture content increased. Rock very soft.
Microscopic	Fairly uniform texture; subhedral to euhedral crystals. Some fracturing of grains, but a "tight" welded appearance.	Weakly altered. ***Feldspars*** - mildly shattered, "tight" welded appearance, grains interlocked. Minor sericitization and "dusty" clay covering calcic "cores".	Only slightly altered. Grains shattered, particularly feldspars; many "open", others grains interlocked. ***Feldspars*** - sericitization and "dusty" clay covering part of calcic "cores". ***Biotite*** - partially altered to limonite. ***Quartz*** - slightly rounded. Some limonite along ramifying cracks and individual grain boundaries. Some ferrous iron oxidized to ferric iron.	Less altered than expected from iron stained, "rotten" appearance; grains highly shattered, particularly feldspars: more so in uniformly textured rocks. ***"Open" fractures*** - with limonite. ***Feldspars*** - sericitization and "dusty" clay covering calcic "cores". ***Quartz*** - partially rounded by solution of silica from grains at points of contact near surface. ***Biotite*** - bleached, appreciable alteration to limonite. ***Limonite*** - abundant as coating on mineral grains, in ramifying cracks, and along mineral boundaries. Ferrous iron oxidized to ferric oxide.

Table 2. Petrographic characteristics of quartz diorite (fresh and altered stages)

Further investigations for construction purposes began in late 1949 and continued intermittently through 1953. They included NX cored borings and percussion drill holes to explore successive excavation-lifts and tunnel alignments at the concrete dam, as well as two 36-inch calyx holes, and shafts/adits in the left abutment. This additional exploration assisted in selection of the final stripping limits, design and execution of required foundation treatment, preparation of "as-built" foundation and tunnel maps, and exploration/evaluation of sources for construction materials.

During this period the foundations for the earthfill dams and all saddle dikes were treated and covered, both diversion tunnels and three stages of foundation excavation at the gravity dam site were largely completed, and concrete pouring started. Details of the geologic investigations of 1948-1953 are given elsewhere (Kiersch and Treasher, 1955, p. 271-310).

FOUNDATION GEOLOGY OF SELECTED DAM SITES

Five rock formations in the vicinity of the dam sites are important: (1) The Rocklin quartz diorite that underlies the main dam and saddle embankments 1 to 7; (2) metamorphic rocks that are the foundation at Mormon Island auxiliary dam and saddle embankment 8; (3) a bouldery member of the Mehrten Formation that is the uppermost foundation material at saddle dam 5; (4) "old" alluvium within the Blue Ravine channel found at the Mormon Island site; and (5) Recent alluvium in the channel at the main dam. Colluvium derived from the weathered intrusive or metamorphic rocks comprises part of the overburden at all the sites.

Gravity section of the main dam

The American River is entrenched in a V-shaped inner-channel that is 200 feet wide and 185 feet

Operation			Essentially fresh	Weathered state		
				Slightly	Moderately	Highly
Geo-physical	Resistivity		1,800 ohm-ft	800—1,800 ohm-ft	600—800 ohm-ft	600 ohm-ft
	Seismic		14,000 - 10,000 ft./sec.		3,500—2,200 ft./sec.	
Rate of drilling	Diamond bit (NX)		6—12 ft/hr	6—12 ft/hr	25—30 ft/hr	30—40 ft/hr
	Percussion wagon drill (2 1/2" dia.)		15—20 ft/hr	25 ft/hr	35—45 ft/hr	Up to 50 ft/hr
Water-intake or "Pressure tests"			Only along "open" joints or quartz stringers		Moderate to large losses throughout	Large losses throughout
Blasting	Hole spacing	Highly fractured	Grid of 1/2 their depth (i.e., 12 ft holes on 6 ft. centers)		Grid of 10 foot centers	Grid of 10—12 foot centers
		Blocky	Grid of 1/3 their depth (i.e., 12 ft. holes on 4 ft. centers)		Grid of 7—10 foot centers	Grid of 10 foot centers
	Amount powder		3/4—1 lb./cu.yd. rock broken (60% special gelatin)		5/8—3/4 lb./cu.yd. rock broken	1/2—5/8 lb./cu.yd. rock broken (40% ammonia)
Rooting (hvy. duty 3 ft. deep)			No	No	Scarifies with effort	Scarifies easily
Loading			Blasted rock with power shovel		Blasted—Power shovel—Scarified—"Cat" and carryall —cuts excavated 50 feet deep	
Slope stability			Nearly vertical—1/2 to 1		1 to 1	1 to 1
Impervious earthfill material			Unfit	Unfit	Unfit	Satisfactory 8—10 passes sheepsfoot and 4—6 hvy. pneumatic roller
Groundwater percolation			Along joints, faults, shear zones and fractured quartz stringers only		Along inherent fractures; slower intergranular fractures	Along inherent fractures, inter- and intra-granular fractures. A coeff. of permeability 7 ft./day, within 6 ft of the surface
Grout "take"			Low	Moderate	Freely	Freely
Tunnel support			Not required, unless joints are closely spaced (4 foot centers or greater)		Required 2—4 foot centers	Required 2—3 foot centers
Rip-rap (dimension stone)			Excellent	Excellent	Unfit	Unfit
Adequacy - dam foundation			Concrete or earthfill		Earthfill	

Table 3. Engineering characteristics of quartz diorite (fresh and altered stages)

below the floor of the mature, outer-valley at the main dam site (Figures 4 and 5). The inner-channel is cut in quartz diorite. The uniform-textured quartz diorite is a mottled, light-gray, medium-to coarse-grained, massive aggregate of quartz, andesine-oligoclase, microcline and biotite, with subordinate amounts of hornblende, magnetite, and apatite. Deuteric alteration resulted in biotite developing at the expense of hornblende, and hydrothermal alteration is common throughout.

Weathering of the quartz diorite. The erratic depth of weathering became a serious foundation problem. "Outcrops" were in many instances nothing but residual weathered "corestones" underlain by decomposed rock to considerable depth. When cored in the early borings, such "corestones" were interpreted to be "sound rock." Subsequent excavation proved that the "corestones" represented less than 50 percent of the uppermost rock mass (Figure 5).

Weathering began with incipient alteration along the joints and fractures in the massive rock and progressed by stages until only residual "corestones" and jointed "ribs" of "fresh" rock remained in an otherwise highly weathered crumbly mass. Microscopic examination revealed that weathering began with the oxidation and partial hydration of the ferromagnesian minerals, and a consequent increase in volume. Hydration of the feldspars began after the breakdown of the mafic minerals and was appre-

ciable only in the advanced weathering stages as "dusty" clay (halloysite) films with grain boundaries invariably loosened; individual feldspar grains were microfractured and "expanded". Accelerated weathering occurred in closely spaced fracture zones. Advanced stages of deterioration were noted at depths of up to 140 feet below the surface, with less weathered rock continuing below. Where blanketed by terrace gravels, the quartz diorite was weathered to greater depths than elsewhere.

To facilitate the first estimate of excavation quantities and depths to an adequate foundation ("sound rock") from pre-construction borings, the erratically weathered rock observed in the cored borings was subdivided into three classes: highly, moderately, or slightly altered, based on the megascopic degree of weathering. The petrographic properties of the three classes are given in Table 2, and the engineering properties in Table 3. Kiersch and Treasher (1955, p. 282-86) presented a full description of the mineral composition and alteration products of each weathered class compared to fresh rock. The petrographic approach to evaluating complexly weathered rock masses later served as a basis for further research on weathering classifications by Dearman (1974, 1976, 1978).

Stream channel deposits. The 70-foot high pioneer hydroelectric dam of the Pacific Gas and Electric Company, constructed in 1894, is located some 4,700 feet downstream from the main dam. The reservoir ponded mining debris from earlier hydraulic and placer operations some 65 feet deep. The deposit extended upstream to the main damsite, and contained abundant blocks, boulders and cobbles of crystalline rocks.

Joints. The principal and most prominent joint sets strike N45E with 45° NW dip, and N88E with 72° SE dip. The N45E sets are spaced 5 to 10 feet apart and many showed distinct evidence of movement. On the left abutment, an additional set near stations 293 to 296 strikes roughly N40E with 70° - 80° NW dips. These joints permitted weathering to penetrate deeply, with highly weathered rock encountered at depth near the Channel fault (Figure 4). Near stations 296 to 300 a second set strikes about N60E with 20° NW dip. The Channel fault appears to parallel this joint set.

Faults. At least three faults seriously affected the foundation. One occurs near station 285 + 50 (Figures 4 and 5) and strikes roughly N45E with 45° NW dip. Quartz stringers and hydrothermal alteration are associated with the zone of highly weathered rock.

A major fault zone, about 50 feet wide, overlies the diversion tunnel (Figures 4 and 5); the rock is severely brecciated and softened. The zone is bounded by the northwest-dipping Wing Wall fault on the west and the northwest-dipping Penstock fault on the east (footwall), and nearly parallels the tunnel alignment. A dike, offset by the fault zone, indicates the hanging wall moved some 50 feet downstream relative to the footwall (Figure 5).

A third fault, the northeast-trending Channel fault, was exposed on the left abutment when excavation approached foundation grade near station 293 + 50 (Figure 4). The fault zone consists of highly fractured quartz, weathered rock, and unctuous clay in varying proportions, from one inch to three feet thick. Below the fault plane the rock generally was hard and fresh; above the fault plane the quartz diorite was severely fractured and highly decomposed locally, with decomposition decreasing up dip and becoming of minor importance near station 295 + 50.

Excavated bodies of moderately weathered rock exhibited several interesting features originally mapped as faults because of their closely sheared aspect. However, the "shears" flattened and died-out as the rock quality improved, so it was eventually concluded they were exfoliation planes due to weathering.

Wing dams and saddle embankments

The foundation rock on the left and right wings of the main dam (Figures 1 and 4), consists of highly weathered quartz diorite with scattered, boulder-like masses. Undoubtedly structural zones similar to those at the gravity section traverse the foundation of the wing dams and saddle embankments as suggested by structural patterns. However, excavation of the core trenches (3-10 feet) was not sufficiently deep to delineate these zones.

The saddle dams (Figure 1) are located in low, rolling foothills. The drainage valleys are hundreds of feet wide and tens of feet deep. Prominent joint sets, especially east trending fractures, controlled erosion of the topographic lows. The site of dike 5 is a steep-walled saddle, where deeply weathered quartz diorite underlies the channel and lower abut-

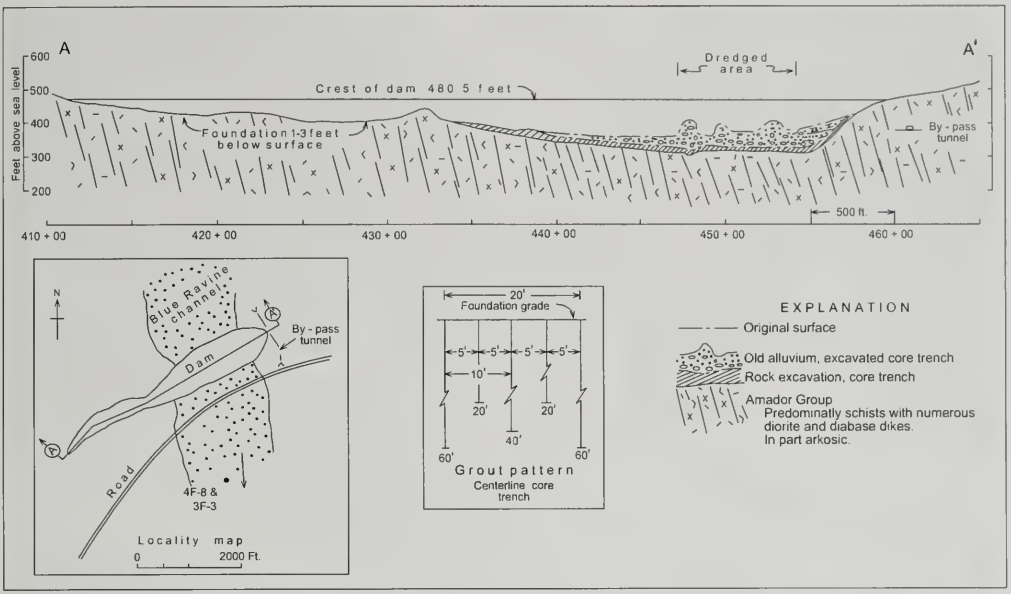

Figure 6. Geologic cross-section of the Mormon Island auxiliary dam, showing limits of excavation and typical grout hole pattern in core trench.

ments; a bouldery member of the Mehrten Formation forms the foundation of the uppermost abutments.

Mormon Island auxiliary dam

Blue Ravine channel is over one mile wide at the site of the Mormon Island auxiliary dam. The wide valley is underlain by metamorphic rocks of the Amador Group (Figure 6); the left abutment consists of arkosic and schistose rocks cut by thin diorite and diabase dikes, and the right abutment is mainly hornblende schist. The channel section is underlain by softer, schistose and arkosic members of Amador Group, which are deeply weathered and irregularly scoured. Furthermore, Blue Ravine channel was filled with auriferous gravels, and gold dredging disturbed the inner-channel gravels and stacked them as tailings.

The abutments of the dam site are blanketed by a thin mantle of non-uniform brownish soil grading into highly weathered metamorphic rock. Isolated fresh outcrops are cut-off at depth by "seams" of weathered material. The arkosic and schistose rocks weather more rapidly and to greater depths than the volcanic and plutonic rocks of the Amador Group. Schists and granitic dikes in the core trench excavation revealed the expected hard and soft variations due to weathering. The metamorphics were exceedingly soft and deeply weathered where overlain by channel gravels.

Along the alignment of the Natomas canal tunnel (Figure 6) the schistose and arkosic rocks are blocky, separated by "seams" of clayey material; the outer "shell" of a soft, highly altered rock-block progresses inward to the fresh "core". This spheroidal weathering was noted 75 feet below ground-level. Deep downcutting during Plio-Pleistocene time was followed by back-filling of the Blue Ravine channel, and a prolonged period of deep weathering in the underlying Amador Group rocks

Old alluvium. The gravels that back-filled the Blue Ravine channel are weakly cemented and crudely stratified (Table 1 and Figure 6). The dredged tailings were stacked in piles consisting of fine sand, silt, and gravel near the bottom, grading upward into coarser gravel and cobbles.

Figure 7. Aerial oblique view of the concrete gravity dam. Folsom Project under construction, showing the principal engineering features and related activities (9/28/53): (a) upstream cofferdam; (b) intake, diversion tunnel; (c) spoil area; (d) retaining wall to hold back earth-fill wing dam; (e) wing or abutment blocks (monoliths); (f) pumping plant; (g) river section of gravity dam, note monotiths (overpour spillway design); (h) wing or abutment monotiths; (i) trestle used to place concrete; (j) stilling basin; (k) tailrace; (l) power house in deep excavation, showing partial underground design; (m) sheet-piling; (n) conveyor belt, transporting concrete aggregate from pit to batching plant (from Kiersch, 1955).

CONSTRUCTION PHASE

Geological investigations for construction purposes began in late 1949 and continued through 1953. Seismic and resistivity surveys were conducted by Wantland (1950) on the right and left abutments of the main dam. The geophysical properties of the quartz diorite were correlated with the geologic data from cored borings. The recognizable differences between the materials tested paralleled the subdivisions of weathered rock pierced in the cored borings. The geophysical properties of fresh and weathered quartz diorite are given in Table 3.

Data assembled during the design phase of the geologic investigations were used to establish preliminary "sound rock" contours and possible foundation grades for all structures.

This database aided the Bureau of Reclamation geologists in their interpretation of resistivity data collected at the undrilled diversion dam sites located downstream.

Gravity section of the main dam

Both abutments of the main dam are relatively flat until the channel section is reached (Figures 4 and 7). This topographic condition allowed for early excavation of the abutments. Afterward, the coffer dams were closed, the river diverted, and the channel section was cleaned and excavated to foundation rock. The initial excavation contract covered a preliminary stripping of the abutments (1950), the

second contract removed another "lift" above foundation grade on both abutments (1950-51), and the third, or main, dam contract included completion of all excavation work to final foundation (1951-53).

Preliminary stripping of abutments. Geologic observations were directed toward establishing both the excavation characteristics of the weathered rock mass and the physical properties of suitable foundation rock. The geologic studies conducted included a map of all dam sites at 1 inch = 50 feet, an outcrop-and-joint-pattern map of the concrete dam area, detailed logging of all cored borings and test pits, correlation of boring logs with the surface maps, and interpretation of the aerial photographs.

The pre-construction investigations indicated that the preliminary excavation would encounter very erratic rock conditions (Figure 5). The surface mantle and uppermost highly weathered rock was classified as "common" excavation (blasting unnecessary). However, due to the variable nature of the weathering, it was decided that all material would be bid as "unclassifed" excavation. That meant that some blasting or rooting might be necessary to excavate even the highly weathered rock below an average depth of 10 feet. This classification proved wise and satisfactory to both the designers and the contractor.

A surface "lift" of 10 feet was excavated over parts of the abutments without blasting after the material was scarified by a heavy duty rooter (Stage 1, Figure 5). Power shovels or RD-8 dozers were used to load 12 cubic yard carryalls. Locally, rocky ridges required blasting, yet these ridges were usually underlain by highly weathered rock. Two successive deeper "lifts" were investigated on a grid with wagon drills and jackhammers. The engineering characteristics of each category of weathered and fresh quartz diorite, and their impact on the excavation equipment, are summarized in Table 3.

The initial excavation contract removed an average of 30 feet from the abutments. After cleaning, the stripped surface was mapped (scale 1 inch = 10 feet) to record attitudes of all structural features and the areal distribution of the weathered versus fresh quartz diorite (Figure 5). Additional subsurface information was obtained by drilling 222 percussion drill holes on 25-foot centers to a maximum depth of 30 feet. An analysis of the drill cuttings and performance of the drills aided in forecasting the type and extent of materials to be excavated (Table 3). A second program of NX cored borings aided in revising the estimated location-level of the foundation.

Excavation of abutments and channel. Two limits of excavation were used for the second excavation contract (Figure 5): an upper limit that included all rock subject to unquestionable removal and a lower limit to which excavation might be necessary. This classification allowed the contractor a definitive minimum volume of excavation, with the final foundation grade to be decided on the basis of the rock conditions exposed.

The second excavation followed the initial contract procedures calling for removal of a 10-foot "lift" (Stage 2) across the entire abutment (Table 3; Figure 5). Again, percussion holes were drilled and the geologist was aided by analyzing the cuttings, the drilling rates, and the results of blasting and removal of weathered rock. The decision to remove another 10 foot "lift" (Stage 3, Figure 5) was made based on these supplemental data and the earlier NX drill cores.

Although drill cores indicated that foundation quality rock could be reached at a depth of some 30 feet, excavation sometimes disproved this conclusion. The exposed "sound" rock was frequently a large residual "corestone" surrounded by weathered rock. Such errors occurred early-on because the originally soft and friable weathered drilling core had case-hardened while in storage and its physical character was misleading.

More material was excavated by the second contract than anticipated, due to the variable nature of the weathered rock mass. Eventually, the right abutment was excavated to near foundation grade, except for the Wing Wall fault zone (Figures 4 and 5). The left abutment was considered satisfactory, except for weathered rock on the edge of the channel (Figure 4).

After diverting the river, excavation of the hydraulic mining debris filling the channel behind the Pacific Gas and Electric diversion dam downstream was undertaken. Excavation disclosed the Channel fault zone, striking roughly perpendicular to the dam axis (Figure 4). This fault contained up to three feet of very plastic clay and highly weathered quartz diorite.

Several NX core borings had penetrated the fault zone, but no cores were recovered and the associated clay could not be sampled. Consequently the Channel fault zone was explored with a series of shafts, adits, and NX core borings that revealed a potentially serious structural zone. All rock overlying the fault was excavated (Figure 4) to expose foundation rock of unquestionable quality (80,000 cubic yards between stations 293 + 50 and 296 + 35). Exploratory drifts driven in the fault zone were plugged with 1,700 cubic yards of concrete. Rock bolts on 5-foot centers (14-feet long) were installed to stabilize the exposed steep 30-foot cut slope between the second and third excavation contracts (Figure 4).

On the right abutment several zones required "dental" treatment. For example, the Wing Wall fault zone treatment consisted of a "dental" shaft and the removal of poor-quality rock (Figure 4).

Diversion tunnel. Four possible alignments for a diversion tunnel were explored by NX cored borings. The alignment through the right abutment would be expected to find good-quality rock and offered superior hydraulic characteristics. The tunnel was directly below the Wing Wall fault zone, however, with the footwall of the fault only a short distance above the tunnel crown (Figure 4). The modified horseshoe tunnel cross-section (23 feet diameter) was driven wholly in quartz diorite, but an appreciable thickness of weathered rock at both portals and several sheet-like zones along the 1,650 foot tunnel resulted in considerable overbreak. Accordingly, steel supports were required throughout the tunnel, spaced on 4-, 3-, and 2-foot centers. Another typical problem involved joints spaced 2 to 5 feet apart that crossed the alignment and dipped 45° into the intake portal cut; clay "seams" filled the joints and caused rock creep.

Grouting. Foundation zones too small for "dental" treatment, or sections at depths greater than the treatment formula required, were sealed-off by extensive grouting. Most grouting was conducted from inspection galleries within the dam after concrete was placed to a pre-determined height. A cut-off curtain was placed along the upstream toe to consolidate the concrete-bedrock contact and seal-off underflow.

Left and right wing dams (earthfill)

Two earthfill wing dams were necessary at the main dam to create the desired reservoir capacity (Figure 1). The foundations were stripped (1 to 3 feet) to highly weathered undisturbed rock. The core trench was excavated deeper to firm, weathered quartz diorite and material able to hold a grout nipple—usually fractured, weathered rock-blocks that "took" grout.

Grouting. All earthfill dam foundations were grouted from the bottom of the core trench. Grout holes (EX – 1.5-inch diameter) were drilled along the center line of the core trench on a split-spacing method: primary holes on 20-foot centers with shallower holes at 10-foot and 5-foot centers (Figure 6, inset). Each zone was thoroughly pressure-washed with water to remove existing clay-fill of the joint-planes before attempting to grout. The stage method was used: drill and grout the first zone (0-20 feet) to refusal, then successively drill and grout each lower zone (20-40 and 40-60 feet), but circulate the grout from the top of the hole in each stage.

Good-quality rock was satisfactorily grouted, but highly weathered quartz diorite proved extremely difficult to grout satisfactorily. For example, a hole grouted to refusal might later take grout freely, even after several refusals. Throughout the middle zone (20-40 feet) there were surface leaks, and general grout consumption was high. Several tries were needed before each hole was finally grouted to refusal and the rock consolidated.

Water pressure tests gave erratic results; some holes took large amounts, others very little, with no regularity to the pattern (Table 3). The grouting record detected no correlation between water pressure tests and the grout "take" (details on grouting are given Kiersch and Treasher, 1955, p. 303-304).

Saddle embankments

The stripping, core trench excavation, and grouting procedures profited from experience gained at the wing dams. Core trenches were excavated deeper to reach better quality, weathered quartz diorite at dike 5. Consequently, grout consumption was lower and the time consumed was less; everything pointed to achieving an improved grout curtain compared to the wing dams. Exploration at dike 7 indicated "sound rocks" at depths of 70 to 100 feet. Weathered rock exposed in the core trench would not seat a grout packer, however, so the circuit-grouting method was used. The grout input pipe extended to the bottom of the hole, and slurry was circulated back to the collar under the required pressures.

The other saddle embankments, and part of the right wing dam, were built before the foundation was treated. Consequently, all these structures were grouted during 1953-54 through the completed earthfill to consolidate the foundation. Geologic conditions and grouting results were comparable to those obtained at other earthfill dams.

Mormon Island auxiliary dam (earthfill)

The Mormon Island auxiliary dam (Figures 1 and 6) has a crest length of 4,875 feet and is 165 feet high. The dam has two parts: the right abutment section (2,042 feet) is separated from the main dam and left abutment by a low knoll (Figure 6). Both parts are founded in metamorphic rocks of the Amador Group.

Exploration. Pre-construction exploration included ten drill holes through the channel alluvium, two deep shafts (along the centerline), five shallow test pits, and many bedrock probings (rods driven to bedrock) furnished by the Natomas Dredge Company. The metamorphic bedrock was not explored by cored borings. The distribution and thickness of gravels and overlying sediments in the channel near the left abutment are shown on the right side of Figure 6. After the core trench was excavated, three NX core borings were drilled in its floor; the foundation rock was severely fractured and weathered in the upper 50 feet.

Stripping and excavation of the core trench. The right abutment section was stripped of all overburden to weathered blocky schist. The core trench (5 feet deep) and foundation were covered with earthfill before curtain grouting of the foundation was deemed necessary.

The left abutment and main part of the auxiliary dam were stripped to weathered schist; the core trench was then excavated 5 feet deep and 12 feet wide. The undisturbed gravels in the "channel section" were non-uniform; some portions were well-cemented and stable, whereas others were soft and somewhat plastic. To improve stability, several additional feet of undisturbed gravels were stripped from the foundation area, and the disturbed channel gravels containing clay lenses were cut-back on a gentle slope. All foundation slopes were compacted with passes by a dozer before placing earthfill.

The core trench (50 feet wide) was taken to schist bedrock; the overlying gravels were in excess of 60 feet deep. The upper schist bedrock proved to be highly weathered so 5 to 10 feet of rock were removed in an effort to improve the foundation materials. Innumerable springs issued from the foundation along essentially vertical fractures; water inflow was heavy, and pumping averaged about 3 million gallons a week, which complicated the grouting.

Grouting. The grout holes were on 5-foot centers to a maximum depth of 60 feet (Figure 6, insert). Consumption of grout was high in the two upper zones, largely due to leakage along fractures at the surface. The initial grout curtain dried up or shifted a large number of springs outside the core trench. All holes were subsequently regrouted from the surface to improve consolidation of the foundation.

Bypass tunnel for the Natomas Canal. Nine trenches were excavated in 1949 to aid in selecting the intake and outlet locations for a bypass tunnel for the Natomas Canal (Figure 6). The canal served the downstream area (dredge ponds, and domestic and irrigation water) and had flowed for decades along the left abutment of site. During construction, the flow was diverted through the left abutment tunnel. When the Folsom Project became operational, the tunnel was plugged, and water was supplied to the downstream canal from the reservoir by means of a pumphouse.

The tunnel (6 x 6.5 feet) was driven from headings at both portals (2,200 feet long). Problems encountered included blocky rock with abundant clayey "seams" that was difficult to mine-out, drills becoming stuck and plugging easily in the soft material, and having to use timbering and spilling to secure the back against "raveling". The rock was highly broken due to its inherent bedding, foliation, and fracturing, except for 200 feet near the middle of the tunnel.

FOUNDATION MAPS

"As-built" maps of all foundations were prepared prior to back-filling, both as a permanent record and for future reference in case of maintenance problems. The concrete dam foundation was mapped at 1"=10 feet (1"=5 feet in critical areas), the earthfill dam foundations at 1"=160 feet (except for Mormon Island, which was mapped at 1"=20 feet), and the core trenches at 1"=20 feet (with parts of Mormon Island mapped at 1"=10 feet). These maps indicated (1) type and character of rock, (2) inherent structure

and associated mineralization, (3) areas of "dental" treatment and depth of backfilling, (4) location of all exploration below foundation grade with geologic logs, (5) water seeps and treatment, (6) grout holes and grout "take", and other details at specific locations.

CONSTRUCTION MATERIALS

Concrete aggregate. Extensive investigations proved that the "intermediate" alluvium deposit at Mississippi Bar (Figures 1 and 3) was suitable for concrete aggregate. These undredged gravels, averaging 20 to 25 feet thick, were blended with the coarser aggregate of the "old" alluvium (Figure 3).

Impervious earthfill. Highly weathered quartz diorite rock occurs throughout a large part of the reservoir and surrounding dam sites. Field tests determined that the weathered rock material near the surface was suitable for impervious fill. Consequently, this quality material was "borrowed" selectively from source-deposits near each dam site (Figure 1).

Adequate compaction of the material in lifts of 18-inches required 8 to 10 passes of a heavy-duty sheepsfoot roller, or 4 to 6 passes with a 100,000 pound 4-wheeled pneumatic roller. Best results were obtained by spreading 9-inch lifts and compacting with 2 to 3 passes of the pneumatic rollers.

Although highly weathered quartz diorite made satisfactory impervious earthfill, difficulties developed in borrowing and compacting this material. These difficulties included irregular quality in borrow areas, varied moisture content and, most importantly, the extremely rapid wear on the steel "feet" of the sheepsfoot rollers and of the teeth of graders, scrapers, and power shovel buckets due to the high quartz content.

Pervious earthfill. Large quantities of acceptable pervious fill were within reasonable distances of the dam sites, including (1) stream channel gravels of the American River removed from the tailrace section, (2) "old" alluvium of the Blue Ravine channel, and (3) highly weathered quartz diorite not suitable for impervious fill.

Rip-Rap. Quartz diorite was determined to be the best rock for rip-rap in the Folsom area. Large quantities of fresh and slightly weathered rock were excavated by the Bureau of Reclamation at the powerhouse site and tailrace channel. This material was used as rip-rap for all sites, including Mormon Island, along with rock from the diversion tunnel and abutments of the main dam. An alternate quarry site for rip-rap was explored by several NX diamond drill holes, and good quality rock was blocked-out, if needed (Figure 1).

SEISMIC RISKS

Faults and shear zones of sizeable displacement were mapped in the vicinity of the main dam site. However, in the 1940s and 1950s no major faults or shear zones along which recurring movement had been recorded were known within the region, so the Folsom project dams were not considered susceptible to seismic damage. In 1975, however, an earthquake occurred on the Cleveland Hill fault, a strand of the major Foothills fault system located northeast of Folsom. Shortly thereafter the State of California re-evaluated the Foothills system and declared it to be active and capable to generate earthquakes with Richter magnitude of 6.0 - 6.5. This lead to a seismic re-evaluation of the Folsom project and Mormon Island auxiliary dam that began in 1981 and extended into the mid-1990s. The remedial rehabilitation treatment undertaken at Mormon Island auxiliary dam since 1981 is reviewed by Allen (2001) in a companion paper in this volume.

LESSONS LEARNED

The Folsom project was one of the first large dams attempted in highly weathered rock, and it taught us much about the engineering geology of weathered materials. The extent of weathering in the quartz diorite was controlled by spacing of joints, the degree of microfracturing, and the geologic history of the near-surface area. Petrographic and physical properties of the weathered intrusive rock in distinct stages of deterioration (slight to highly) aided in final selection of foundation-levels.

We also learned that small-diameter cored borings were inadequate and led to a misleading model of the substrate. For example, "corestones" below grade were initially construed as shallow "outcrops" of fresh rock. Furthermore, severely weathered small-diameter drilling cores became case-hardened as they waited in the storage shed before being sent to the lab, which was misleading as to their in-situ characteristics. Fresh drilling cores remained soft and friable. Large openings/excavations that a geologist could inspect were clearly needed!

Finally, we learned that the highly-weathered material was difficult to grout and consolidate as foundation, but served as high-quality material for impervious earthfill.

ACKNOWLEDGMENTS

Preparation of this review of the original Folsom project has been aided and improved by the comments of reviewers Horacio Ferriz, Robert Anderson, Roy Kroll and Steve B. Stryker. Jane Hoffmann of Roadrunner Press, Tucson, skillfully assembled this abbreviated version of the 1955 publication.

AUTHOR PROFILE

Dr. George Kiersch was a Professor Emeritus from Cornell University and the Principal of Kiersch Associates, a consulting firm in Tucson, Arizona. Dr. Kiersch was the project geologist for the Folsom dam project, from 1949 to 1950, with the U.S. Army Corps of Engineers. Dr. Kiersch passed away on October 19, 2001.

SELECTED REFERENCES

Allen, M.G., 2001, Seismic remediation of Mormon Island auxiliary dam, Folsom dam and reservoir project, Sacramento County, California: *in* Ferriz, H. and Anderson, R., (eds.), Engineering Geology Practice in Northern California, Association of Engineering Geologists Special Publication 12 and California Division of Mines and Geology Bulletin 210.

Dearman, W. R., 1974, Weathering classification in the characterization of rock for engineering purposes in British practice: International Association of Engineering Geology Bulletin, v. 9, p. 33-42.

Dearman, W. R., 1976, Weathering classification in the characterization of rock - a revision: International Association of Engineering Geology Bulletin, v. 13, p. 123-127.

Dearman, W. W., et al., 1978, Engineering grading of weathered granite: Engineering Geology, v. 12, no. 4, p. 345-374.

Forbes, H., 1929, A proposed major development on the American River: California Department of Public Works, Division of Water Resources, Bulletin 24, p. 189-190.

Gardner, W.I., 1942. Preliminary geologic report on the Folsom Dam site: U.S. Bureau of Reclamation, Region II, Sacramento, California (unpublished).

James, L.B., and Kiersch, G.A., 1988, Geology of Reservoirs: *in* Jansen, R.B., (ed.), Advanced dam engineering for design, construction, and rehabilitation: Van Nostrand Reinhold, New York, p. 722-748.

Johnston, P.M., 1947, Preliminary geologic report on the Folsom Dam site: U.S. Army Corps of Engineers, Sacramento District, California (unpublished).

Kiersch, G. A., 1950, Geological investigations and problems - Folsom Dam Project, California: Bulletin of the Geological Society of America, v. 61, no. 12, pt II, p. 1526 (abstract).

Kiersch, G.A., 1955, Engineering geology: Colorado School of Mines Quarterly, v. 50, no. 3, 123 p.

Kiersch, G. A., and Treasher, R.A., 1955, Investigations, areal and engineering geology of the Folsom Dam Project, Central California: Economic Geology, v. 50, no. 3, p. 271-310.

Lindgren, W., 1894, Sacramento, California, folio: U.S. Geological Survey Geologic Atlas 5, 3 p., 4 maps.

TEC (Tierra Engineering Consultants), 1983, Geologic and seismologic investigations of the Folsom, California area: Consultant's report to the U.S. Army Corps of Engineers, Contract Report DACW05-82-C-0042, U.S. Army Corps of Engineers, Sacramento District, California.

Wantland, D., 1950, Geophysical investigations at the lower Ashland, Folsom, and Nimbus Dam sites - American River Divisions - Central Valley Project, California: Geology Report No. G-109, U.S. Bureau of Reclamation, Denver, Colorado.

SEISMIC REMEDIATION OF MORMON ISLAND AUXILIARY DAM, FOLSOM DAM AND RESERVOIR PROJECT, SACRAMENTO COUNTY, CALIFORNIA

MATTHEW G. ALLEN[1]

ABSTRACT

The Folsom dam and reservoir project was designed and constructed by the Corps of Engineers (the Corps), and then turned over to the Bureau of Reclamation in 1956 for operation and maintenance. The Corps conducted seismic stability studies of the project throughout the 1980's. These studies revealed potential instability of the earth embankment Mormon Island auxiliary dam. A portion of the upstream and downstream shells of the auxiliary dam is founded on alluvial soils that had been dredged for gold several times between 1927 and 1949. The remaining foundation consists of competent, undisturbed alluvium or metamorphic bedrock. The dredging process left the alluvium in a very loose condition, and thus susceptible to liquefaction under the maximum credible earthquake loading. Deformation analysis indicated that liquefaction of this material could lead to catastrophic release of the reservoir. Remediation of the potentially liquefiable foundation of the Mormon Island auxiliary dam was accomplished between 1990 and 1995. A block of dredged alluvium under the upstream shell was densified by dynamic compaction; another block of dredged alluvium under the downstream shell was densified and its drainage capacity improved by constructing stone-column drainage elements. This paper describes the site conditions and analyses leading to the conclusion of a seismic deficiency at the Mormon Island auxiliary dam and the construction that was performed to remediate the foundation.

INTRODUCTION

The Folsom dam and reservoir project is located on the American River in California, about 26 miles (42 km) upstream from its confluence with the Sacramento River. It borders the town of Folsom, about 20 miles (32 km) east-northeast of the city of Sacramento. The project consists of twelve water-retaining structures including a 340-foot high concrete gravity "main" dam constructed in the American River channel, right and left earth embankment "wing" dams that flank the concrete dam, eight earth embankment saddle dikes, and the Mormon Island auxiliary dam to close the reservoir perimeter. Figure 1 is an aerial photo showing the Mormon Island auxiliary dam during construction of the downstream seismic remediation.

The Folsom project was designed and constructed by the Corps in the 1940's and 1950's. After completion in 1956, ownership of the project was turned over to the Bureau of Reclamation for operation and maintenance. The Folsom project is a key element of the Bureau's Central Valley Project.

In 1981, the Bureau of Reclamation and the Corps entered into an agreement whereby the Corps would be responsible for seismic evaluation studies of the Folsom project under its Dam Safety Assurance Program. The Corps also retained responsibility for the design of any corrective measures that the two agencies agreed upon. The Bureau of Reclamation had responsibility for the construction of any corrective measures.

[1]U. S. Army Corps of Engineers
Sacramento District, Geotechnical Branch
1325 J Street
Sacramento, CA 95814-2922
matthew.allen@usace.army.mil

Figure 1. Folsom dam and reservoir project – Mormon Island auxiliary dam. Downstream seismic remediation activities in 1994.

THE MORMON ISLAND AUXILIARY DAM

The Mormon Island auxiliary dam is located about 2.5 miles (4 km) east of the main dam. It was constructed across Blue Ravine, an ancient channel of the American River. Figure 2 shows a typical cross section of the dam.

The auxiliary dam is a zoned embankment dam with a crest length of 4,820 feet (1,470 m) and a maximum height of 165 feet (50 m) from the bottom of the core trench to the crest. The slopes of the dam vary according to the foundation conditions, with the flattest slopes corresponding to the area founded on dredged alluvium. The downstream slopes of the dam vary between 1V on 2H and 1V on 3.5H and the upstream slopes vary between 1V on 2H and 1V on 4.5H. The embankment shells are constructed of dredge tailings from the Blue Ravine alluvium. The narrow, central impervious core is a well-compacted clayey mixture founded directly on rock over the entire length of the dam. The core is separated from the embankment shells, both upstream and downstream, by a double layer of transition and filter material. The transition and filter layers are each 12 feet (3.7 m) wide. The inner transition layer, in direct contact with the core, is well-compacted decomposed granite with the grain-size distribution of a silty sand. The outer transition layer, in contact with the shells, was constructed from the 2-inch (5 cm) minus fraction of the dredged alluvium.

The majority of the embankment is founded on rock. However, in the central area, between stations 441+50 and 456+50, a core trench was excavated up to 80 feet deep with 1V on 2H slopes, through both undisturbed and dredged alluvium, in order to found the core and most of the transition zones on rock. The embankment shells in this reach were founded on the alluvium. The dredged portion of the alluvium underlies the shells approximately between stations 446+00 and 455+00.

SITE PHYSIOGRAPHY AND GEOLOGY

In the geologic past, the American River flowed southward through the Blue Ravine channel to a point 2.5 miles (4 km) east of the gold-rush era town of Folsom. Then, turning abruptly westward, the river passed to the immediate southwest, intersecting the present channel of the American River downstream of the town. A broad valley, 1 to 1.5 miles (1.6-2.4 km) wide and bounded on either side by gentle slopes, was eroded by the ancient river. Sand, silt, gravel, and cobbles were deposited in the channel to a maximum depth of 80 feet (24.4 m) before the river established its present position by

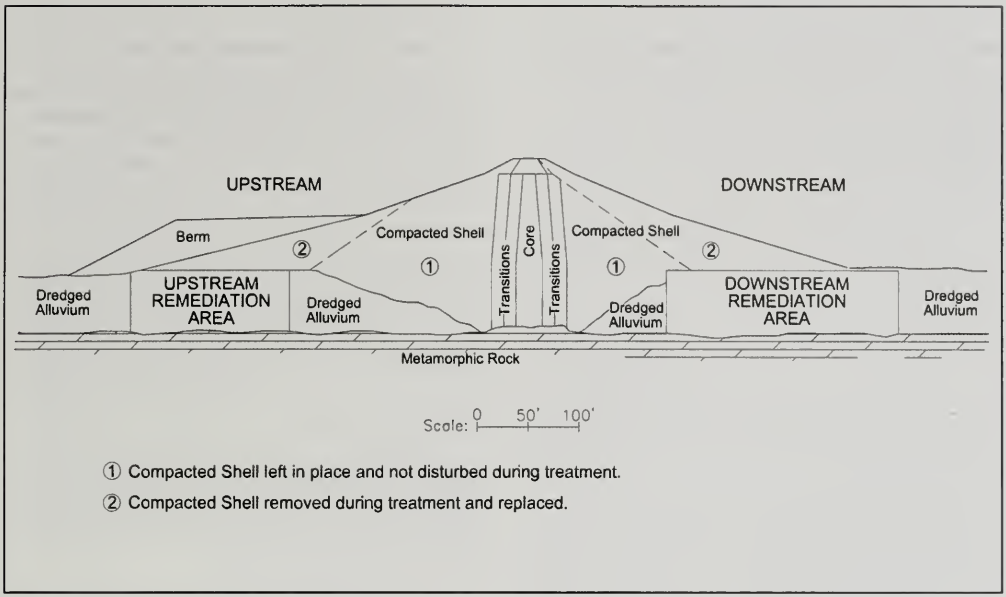

Figure 2. Typical cross section of the Mormon Island auxiliary dam with seismic remediation treatment areas.

headward erosion along the present course of the American River. Subsequent down-cutting left the former channel isolated above the level of the present American River.

The Mormon Island auxiliary dam is located in the gently sloping Blue Ravine valley. Bedrock at the site is formed by amphibolite-facies metavolcanics of the Calaveras and Amador Groups. The west abutment is largely underlain by schistose rock. The steeper east abutment is underlain by a harder, massive metabasalt. Outcrops on the abutments are scarce and bedrock is covered by 1 foot (0.3 m) of colluvial soil overlying intensely weathered metamorphic rock. Fresh metamorphic rock is found 6 to 15 feet (2-5 m) below the surface. The physical character of the metavolcanics is essentially uniform throughout the dam site for foundation purposes.

FOUNDATION ROCK

Within the foundation rocks the most pronounced discontinuity is schistosity, which varies in strike from N20°W to N20°E and dips westerly. Other jointing is closely spaced and separates the rock into blocks several inches to 2 feet (0.6 m) on the side. Prior to construction, many of the joints of the foundation were open, and many were filled with as much as 2 inches (5 cm) of clay and iron oxide.

Weathering of the metamorphic rocks resulted in rock that ranges from softened masses in the areas where schistosity is more pronounced to hard, dense, blocky greenstone containing only incipient planes of schistosity. Prolonged weathering progresses from the hard, dense, blocky schist to rock in which the amphiboles are weathered to clay, chlorite and limonite. In general, weathering of the bedrock is most pronounced in the soft rock beneath the dredged alluvium, and it is least notable in areas above the gravel-filled streambed (Kiersch and Treasher, 1955).

FOUNDATION ALLUVIUM

The maximum depth of the alluvium within Blue Ravine is between 65 and 80 feet (20-24m). Where it is undisturbed, the alluvium consists of basal gravels with fragments ranging from 1 inch to 12 inches (2.5 cm - 30 cm) in diameter, mixed with sand and clay, and is weakly to strongly cemented. Prior to construction of the dam, the deepest portion of

the channel was repeatedly dredged for its gold content. The dredging process tended to re-deposit the processed alluvium in a very loose condition, with irregular layering of the "fine" and "coarse" fractions. Exploration at this site has shown that the following depositional trends exist in the dredged alluvium:

1. Gravel, cobbles, and some boulders are present throughout the deposit, and there is an overall increase in the percentage of fines with depth.

2. The top 15 to 20 feet (4.6-6m) consist mainly of coarse sand to cobble sizes. The gravel and cobbles would dominate the dynamic response of this zone to earthquake shaking and, likewise, its response to vibratory remediation (discussed later in this paper).

3. A middle zone of irregular layers and lenses of silty sand with 15 to 25 percent fines and little or no cobbles is interbedded with sand and fine gravel with cobbles. The silty-sand layers varied in thickness up to the full 25-foot (7.6 m) thickness of the zone. The response of this zone to earthquake shaking would be dominated by the silty sand.

4. The bottom 10 to 20 feet (3-6 m) are significantly finer-grained. Laboratory testing of split spoon and dry core samples from this zone indicated low to non-plastic fines ranging from 10 to 77 percent and averaging about 30 percent. In this zone, the fines would dominate the response to earthquake shaking.

SEISMIC HAZARD AND DESIGN GROUND MOTIONS

Before 1975, the Foothills fault system was generally considered inactive, and the Sierra foothills were assessed as an area of relatively low seismic activity. Historically, there had not been any damaging earthquakes in this region. Then, on August 1, 1975, an earthquake with Richter magnitude 5.7 occurred near Oroville, California. This earthquake, located about 60 miles (96 km) north-northwest of Folsom Dam, generated intensive re-investigation of the Foothills fault system by the Bureau of Reclamation for their Auburn Dam site. These studies led to the now generally accepted conclusion that the fault system was active and capable of generating earthquakes of Richter magnitude 6 to 6.5.

A seismologic study of the local area (TEC, 1983) concluded that the maximum credible earthquake (MCE) applicable to the Folsom dam and reservoir project would have a Richter magnitude of 6.5 on the East Branch of the Bear Mountains fault zone. This fault is the closest known capable fault to the project, is in an extensional tectonic setting, and has a normal dip-slip seismic source mechanism. The hypothesized MCE has a focal depth of about 6 miles (9.6 km) and occurs about 8 miles (13 km) away from the Mormon Island auxiliary dam. This earthquake would produce more severe shaking at the project than earthquakes originating from other known potential sources. The study also concluded that reservoir-induced earthquakes are unlikely.

The results of the seismologic and geologic studies were used to determine appropriate ground motions for the seismic safety evaluation. The following design ground motion criteria were recommended (Bolt and Seed, 1983):

- Peak horizontal ground acceleration = 0.35 g
- Peak horizontal ground velocity = 20 cm/sec
- Bracketed duration ($\geq$ 0.05g) = 16 sec

Bolt and Seed (1983) then provided two time histories that meet the criteria and were representative of the 84-percentile level of ground motions that could be expected to occur at a rock outcrop from a magnitude 6.5 earthquake occurring 8 miles (13 km) from the site. These time histories were used for evaluation of all the structural features of the Folsom project and design of the auxiliary dam remediation. In 1995, the Bureau of Reclamation determined that advances in the state-of-practice suggested the ground motions should be re-evaluated. Their probabilistic seismic hazard analysis (LaForge and Ake, 1999) concluded that ground motions developed to represent a 35,000 year return period were generally consistent with those proposed by Bolt and Seed (1983). However, the peak velocity pulses, or "fling" effect, of their motions are higher than the peak velocities determined in 1983. As of 1999, a re-analysis of the structural performance of the auxiliary dam under the revised loads was pending.

SEISMIC STABILITY STUDIES

In 1980, the Corps' Waterways Experiment Station (WES) in Vicksburg, Mississippi, began a seis-

mic stability evaluation of the Folsom project. The evaluations were documented in a series of eight reports summarized by Hynes-Griffin (1988). Revisions were required to Reports 4 and 8 pertaining to the Mormon Island auxiliary dam, and were published in 1990 and 1992 respectively (Hynes et al., 1990; Wahl et al., 1992). All man-made water retaining structures were evaluated for the earthquake motions proposed by Bolt and Seed (1983). The seismic stability evaluation of the auxiliary dam included a review of construction records, field and laboratory investigations, static and dynamic stress analyses, evaluation for liquefaction potential, and post-earthquake slope stability analyses (Allen, 1984; Harder, 1986; Llopis, 1983 and 1984; Corps of Engineers, 1986).

The field investigations were conducted in stages, generally between 1983 and 1990, and included Standard Penetration Tests (SPT), Becker Penetration Tests (BPT), disturbed and undisturbed sampling, geophysical tests, and test pits with field density testing.

The BPT was developed to provide blowcount data in coarse-grained deposits for use in simplified liquefaction analyses. The BPT is performed by specialized equipment, whereby a double-walled steel casing is driven into the ground by a small pile-driving hammer. Most testing of this type performed in the United States uses a casing with an outside diameter of 6.6 inches (16.8 cm) and a closed end bit. The hammer is an ICE model 180, double-acting diesel hammer. Empirical correlations have been developed between blowcounts by BPT and SPT (Harder and Seed, 1986; Sy, 1993), making it possible to estimate the liquefaction potential of gravel and gravelly deposits.

An extensive laboratory testing program estimated the cyclic strengths of the shell and dredged foundation alluvium. The relative strength and pore pressure generation behavior of gravels in general, subjected to cyclic loads, were also investigated in the laboratory using samples of dredged alluvium from the Mormon Island auxiliary dam.

Finite element computer analyses were used to estimate the shear stresses induced in the dam and foundation by the MCE. These stresses were compared with the cyclic strengths measured in the laboratory to determine safety factors against liquefaction. Generally, the embankment materials were found to have safety factors against liquefaction averaging about 1.5. However, much of the foundation material had safety factors against liquefaction of 1.0 or less.

Based on the laboratory studies with gravel, relationships were developed between the safety factor against liquefaction and residual excess pore pressure, which led to estimates of the post-earthquake strength of the embankment and foundation materials. These strength parameters were then applied to determine the post-earthquake slope stability of the auxiliary dam. The resulting "critical" failure surface cut deeply through the upstream slope, through the core, and exited on the downstream side of the dam crest.

Based on these analyses, it was concluded that extensive liquefaction would probably occur in the dredged alluvium foundation and, to some extent, in the embankment shell material located adjacent to the core, deep in the core trench. This loss of strength could result in sliding deformations of both the upstream and downstream slopes large enough to cause a catastrophic loss of the reservoir. Therefore, remedial or hazard mitigating actions were recommended for immediate implementation.

SEISMIC REMEDIATION DESIGN

Remediation requirements for the auxiliary dam were developed using a limited deformation approach. The post-earthquake deformations were estimated for the MCE using the computer program TARA-3FL. These analyses showed that the area critical for controlling deformation was the foundation material just above bedrock, located directly beneath the exterior shells. This region is where the greatest stress and strain would develop. Without improvement, these materials could lose strength such that the embankment shells would drop vertically before spreading outward and separating from the core. The deformation model allowed designers to determine the size, location, and properties of improved blocks of foundation material under each shell, necessary to control the deformations and retain the reservoir. Figure 2 is a typical cross section showing the excavation lines and the treatment blocks for both the upstream and downstream remediation. Figure 3 is a plan view showing the foundation geology and layout of both the upstream and downstream treatment areas.

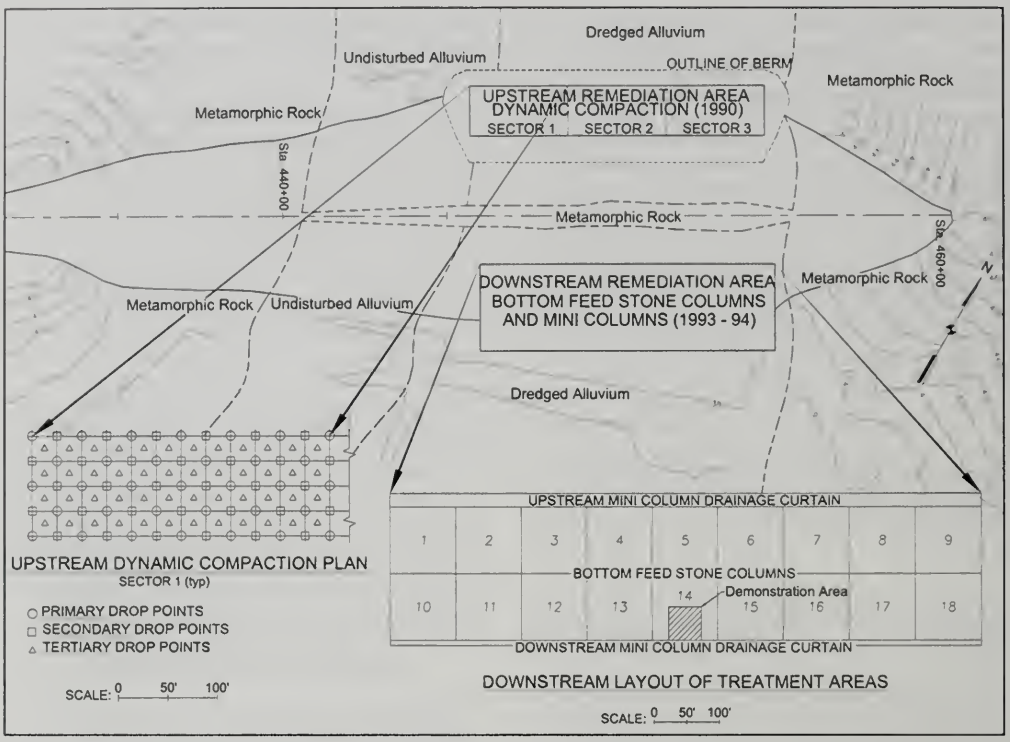

Figure 3. Foundation geology and layout of seismic remediation treatment areas of the Mormon Island auxiliary dam.

UPSTREAM REMEDIATION - DYNAMIC COMPACTION

A study of potential remediation techniques concluded that dynamic compaction might be effective, despite a lack of prior experience in the United States using this method to depths greater than 40 feet (12 m), and no known industry experience treating materials similar to the dredged alluvium at the auxiliary dam (Allen and Jones, 1990). However, the Bureau of Reclamation had used dynamic compaction in remediating Jackson Lake dam in Wyoming (Stevens et al., 1994), and due to drought conditions in 1989-1990, the Folsom reservoir was very low. The water had receded far away from the auxiliary dam, providing an unusual opportunity for access to the upstream foundation with groundwater at least 10 feet below the surface and continuing to drop. Based on the Bureau's belief that remediation using dynamic compaction would proceed quickly, and because there was only a small window of time available before the reservoir would rise, dynamic compaction was selected to begin remediation of the upstream side of the Mormon Island auxiliary dam.

The Bureau of Reclamation and the Corps jointly proceeded with preparation of the design and specifications in mid-May, 1990. The contract was advertised on June 17, 1990, and awarded in late July. Construction was completed by December of the same year. The contract included the construction of an upstream berm that would be used as a working pad for further explorations or remediation, if required, when the reservoir is at or below the flood control pool level (Bureau of Reclamation, 1990).

The remediation strategy for the upstream side of the auxiliary dam was to excavate part of the upstream embankment shell to expose an area of

the foundation surface about 300 feet (90 m) wide, measured perpendicular to the dam alignment, and about 1000 feet (305 m) long. Dynamic compaction was then performed on a treatment area measuring 150 feet (45 m) wide by 900 feet (275 m) long. The purpose of the dynamic compaction was to obtain as much densification as possible within the generally 60-foot (18 m) deep deposit of dredged alluvium. Based on the literature and the experience of the Bureau of Reclamation at Jackson Lake dam, the method was expected to perform well in the top 40 feet (12 m) or so. However, the lower portion of the deposit at the Mormon Island auxiliary dam was deeper and finer-grained than the industry's experience, and the results could not be predicted.

Compaction was performed using two dynamic compactors. These units were not cranes adapted for the purpose, but were specifically designed and built for dynamic compaction. The required compactive energy was specified as equivalent to 35 tons, free-falling 100 feet (30.5 m). Two 35-ton steel tampers were manufactured for this job. They were circular in shape, with a diameter at the base of about 7 feet (2 m). Prior to production work, a laser system was used to measure the velocity of the falling tamper just above the ground surface. The drop-height required to achieve the specified energy was determined to be 110 feet (33.5 m). Figure 4 is a photo showing the upstream excavation, the working surface for dynamic compaction, and the two compactors.

As shown in Figure 3, the treatment area was laid out as a grid with drop points identified by letter and number. Primary drop points were set on a grid spacing of 50 feet (15.2 m) and received 30 full-height impacts each. Secondary drop points were located to split the initial spacing and also received 30 full-height impacts each. Tertiary drop points split the previous spacing and received 15 full-height impacts each. A final "ironing" phase with two drops from 30-feet (9 m) on a continuous side-by-side pattern was also performed to densify

Figure 4. Upstream seismic remediation of the Mormon Island auxiliary dam – Embankment excavation and working surface for dynamic compaction.

the surface. Cycle times between drops were typically about 80 seconds.

The tampers produced holes or "craters" roughly 12 to 15 feet (3.7-4.6 m) in diameter. The typical procedure at each drop point was to tamp until the resulting hole was about 8 to 10 feet (2.4-3.0 m) deep. This would take as few as 6 drops early in the program and as many as 15 drops later on, as the site became more dense. The hole was filled with the alluvial borrow, then compaction would resume on that point. Craters would generally need filling 2 or 3 times in the course of 30 drops. After completing the specified number of drops, final filling of the crater took place while the compactor positioned for the next drop point.

PORE PRESSURE MONITORING

Vibrating-wire piezometers were installed in conjunction with pre-compaction SPT investigations. Typical responses recorded during the primary drop phase of 50-foot spacing indicated:

1. Pore pressures increased up to 4 feet (1.2 m) during the initial tamping.

2. Roughly 75% of this excess pressure dissipated during the 10 to 15 minutes required for crater backfilling.

3. Excess pressures completely dissipated in about 20 minutes, the time it took the compactor to move to another drop point.

None of the piezometers survived beyond the primary tamping, but the dissipation rates were encouraging and it was felt that the apparently temporary pore pressure increases would not hinder densification. Installing replacement piezometers was not considered necessary, especially considering the short time for construction.

Later in the program, however, physical evidence was observed of increased pore pressures that were not dissipating quickly. During the tertiary drop phase, there were a few isolated occurrences of groundwater appearing in the bottom of the compaction crater. This corresponded to an elevation about 10 feet (3 m) higher than the lake level. It was surmised that the groundwater had been raised locally because the pore pressures were dissipating more slowly than early in the program.

During the ironing phase, four or five mud boils appeared on the treatment surface. These were accompanied by "springy" ground within a radius of two to three feet (0.6-0.9 m) around the mud boil. Speculation was that pockets of high pore pressure were being created at depth between confining layers and lenses of silt and clay. The water under pressure would seek initial relief at the surface, carrying fine-grained soil with it.

EVALUATION OF PENETRATION TEST DATA AND REMEDIATION EFFECTIVENESS

The pre- and post-treatment characterization of the dredged alluvium was determined by field measurements of penetration resistance by SPT and BPT, and dynamic wave velocities by cross-hole tests and surface refraction tests. With time and experience, the drillers became adept at obtaining high-quality SPT data from sand and silt layers within the dredged alluvium deposit. However, because of the generally coarse-grained nature of the dredged alluvium and the speed of the Becker hammer drill, the BPT was selected as the primary tool for estimating the liquefaction potential of these materials and evaluating the effectiveness of remediation.

At first, the general correlation between BPT and SPT readings developed by Harder and Seed (1986) was used to convert BPT blowcount data to equivalent SPT $(N_1)_{60s}$. As high-quality SPT data in sand accumulated, site-specific refinements to the correlation were developed by Harder (1992) and used by the Corps and the Bureau of Reclamation throughout the upstream and downstream remediation programs.

The BPT yielded continuous blowcount and chamber pressure data through the entire depth of penetration. Production rates on the order of 250 linear feet (76 m) of penetration testing per 10 hour shift were common at this site. This large quantity of data was managed and processed to equivalent SPT $(N_1)_{60}$ blowcounts using a spreadsheet program. Using the computer in this way, BPT data were processed in the field literally as fast as they were generated. A total of 31 pre-compaction BPT's, 17 intermediate BPT's (intermediate tests followed completion of the primary dynamic compaction drops), and 42 post-compaction BPT's were performed. Locations for the tests were selected to provide a representative mix of conditions. Some were located where densification was presumed to be least, at the greatest distance from actual com-

paction points, in the center of the square grid pattern. Others were located where densification was presumed to be greater, along the lines of the square grid pattern, between dynamic compaction points.

Review of the data indicated that, in general, a dramatic increase in penetration resistance was achieved in the upper 30 to 40 feet (9-12 m) of the treatment block. A less dramatic but still significant increase was also observed in the bottom 10 to 20 feet (3-6 m) of the 60-foot (18 m) deposit. The improvement was not consistent across the site, but showed small random variations, presumably due to the heterogeneity of the deposit (Stevens et al., 1993).

Figure 5 shows the average of all BPT and SPT data, expressed as $(N_1)_{60}$'s, collected within the treatment zone before dynamic compaction (pre treatment), and after dynamic compaction (post treatment). The apparent improvement in the bottom 10 to 20 feet (3-6 m) is the result of two factors. First, it is partly a real increase in density due to the dynamic compaction. Second, it is also partly due to increased friction on the Becker casing from the dramatic density increase in the upper 30 to 40 feet (9-12 m).

PRELIMINARY CONCLUSIONS FROM UPSTREAM TREATMENT

BPT and SPT data indicated a high level of compaction effectiveness was achieved in the upper 30 to 40 feet (9-12 m) of the treatment zone. Below 40 feet (12 m), less dramatic but still significant increases in blowcount values were achieved. Generally, the middle third (as viewed in plan) of the 150-foot (46 m) wide treatment zone was adequately treated to preclude the occurrence of liquefaction. Areas that did not achieve the desired levels of treatment were along the dredged/undredged alluvium contact at both ends of the treatment area and at depth inside the perimeter of the treatment zone. Field observations indicated that high pore pressures did not have adequate time to dissipate during later phases of the compaction process. This may have resulted from confinement of water against the relatively impermeable undredged alluvium, lack of pore pressure control features, excessive energy input in the "shallower" areas, or any combination thereof.

Figure 5. Upstream seismic remediation of the Mormon Island auxiliary dam – Improvement of average $(N_1)_{60}$.

As of late 1999, treatment adequacy to preclude large deformations and the possible need for additional remediation in the bottom 20 to 30 feet (6-9 m) of the deposit were being studied by the Bureau of Reclamation and the Corps.

CONSIDERATIONS FOR FUTURE DYNAMIC COMPACTION

Based on this experience at the Mormon Island auxiliary dam, the following suggestions should be given careful consideration for implementation in any future projects using dynamic compaction for liquefaction remediation:

1. To the greatest extent possible, obtain sufficient data prior to design to better identify the treatment boundaries. It is particularly important to identify areas of reduced strata thickness.

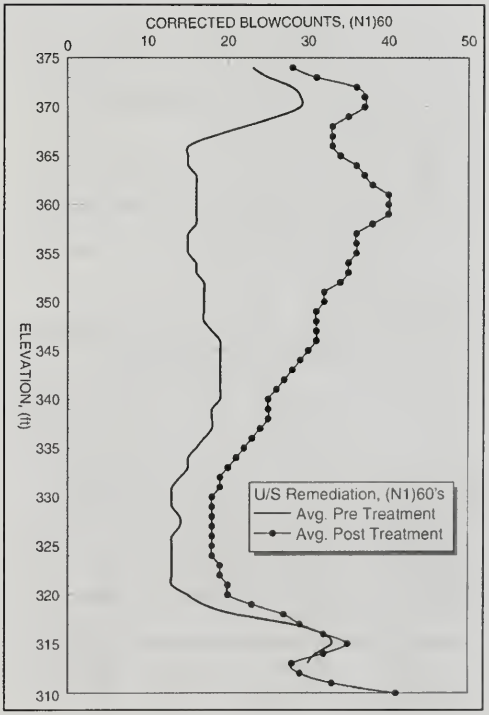

2. Evaluate the advantages of providing pore pressure relief by any or all of the following:

    a. Install wick drains to the full depth requiring treatment

    b. Construct drainage trenches around as much of the area as possible for surficial and perimeter pore pressure relief and water control, and as an exploratory and construction observation tool

    c. Specify the drop sequencing and pattern on a row by row basis

    d. Increase the number of phases of the compaction program, thus allowing areas to rest and pore pressure dissipation to occur as much as is practical

    e. Consider reductions of drop energy in confined areas

3. Install piezometers prior to the start of compaction, and reinstall as necessary to monitor pore pressure response during all phases of compaction and for some time after completion.

4. Consider reducing the drop energy during later phases of compaction if pore pressure instruments and/or field observations indicate induced pore pressures are restricting the compaction process.

TEST PROGRAM FOR POTENTIAL DOWNSTREAM REMEDIATION TECHNIQUES

With the completion of upstream remediation, dynamic compaction was initially considered for downstream remediation, but high groundwater led to rejecting this method. The anticipated cost of de-watering the site was too high. In the spring of 1991, preliminary designs to treat the downstream area were developed, employing vibratory-type methods to densify the treatment block and construct permeable stone column drainage elements through the embankment and foundation materials. These designs were unique because adequate treatment depended on both densification of the materials to reduce the generation of excess pore pressure, and a network of hydraulically connected, permeable, vertical drainage elements to control and dissipate excess pore pressure migrating from untreated areas of the foundation. A search of the literature and communications with researchers and industry specialists revealed there was little experience densifying and constructing stone columns in coarse gravel and cobbles such as those at the Mormon Island auxiliary dam. In addition, vibratory methods were generally considered ineffective at compacting clayey materials such as those also present at this site. Therefore, a test program was developed to evaluate vibratory treatment methods for constructing stone columns and for compacting the dredged alluvium at the auxiliary dam.

Separate contracts were awarded for ground improvement methods referred to as (a) bottom-feed stone columns, (b) rotary displacement stone columns, (c) vibropipe drain stone columns, and (d) vibrorod compaction. The test program was evaluated by the Bureau of Reclamation (1993b), which concluded that:

1. The test program made it clear that densification could be achieved to satisfy the analytical requirements.

2. Either the rotary displacement or bottom-feed methods would construct large diameter stone columns and would achieve the desired density. However, the rotary displacement method had considerable problems with penetration and would likely not be efficient in production.

3. The vibropipe method would efficiently construct small diameter stone columns in either the free field area or through the compacted embankment. No other method could penetrate the compacted embankment.

DOWNSTREAM MODIFICATIONS – BOTTOM-FEED STONE COLUMNS AND MINI COLUMNS

The initial concept design was based on the belief that a clean, free-draining stone column could be constructed to provide pore pressure relief during earthquake shaking. This concept was eventually modified, however, when it was determined from the test program that substantial densification of the foundation alluvium would be possible by vibratory

methods. Liquefaction remediation by densification is better understood and was considered more reliable than using drainage alone to control earthquake-generated pore pressure. Thus, a densification approach for treating the downstream foundation was adopted (Ledbetter et al., 1994; Nickell et al., 1994).

Deformation analyses indicated that a block of dredged alluvium measuring 900 feet (273 m) by 200 feet (60 m) in plan had to be treated to the full bedrock depth, generally 60-65 feet (18-20m). It was desirable to locate the treated block as far upstream (under the shell) as possible in order to minimize its size (Ledbetter et al., 1994). Even so, a wedge of dredged alluvium at the downstream base of the dam core could not be reached and would remain untreated, so the treated mass would be flanked, both upstream and downstream, by untreated alluvium (Figures 2 and 3). This material could liquefy during the design earthquake, and the design analyses showed that high pore pressures in the untreated areas would migrate into the treated material, weakening a significant volume.

To protect the treated mass from this weakening, 10-inch (0.25 m) diameter stone column drains, referred to as mini-columns, were constructed in multiple rows on 3.5-foot (1 m) spacing to form vertical drainage "curtains" along both the upstream and downstream sides of the treated mass. A 20-foot wide (6 m) curtain was constructed across the upstream face of the treated block and an 8-foot wide (2.4 m) curtain was constructed across the downstream face. Subsequent analyses at the WES indicated these curtains would successfully shield the treated mass from pore pressure migration. The entire system was connected at the surface by a blanket drain to provide free drainage under the slope of the dam. Figure 6 shows the embankment excavation, working surface, and one of the bottom-feed stone column rigs for the downstream remediation.

It was discovered in the test program, and confirmed in the first days of the downstream remediation program, that the vibratory probe could not consistently penetrate or adequately densify the full depth of the dredged alluvium deposit without constantly jetting water. Most of the difficulty occurred in the upper 20 feet (6 m) with its high concentration of gravel and cobbles mostly above the water table, and the lowermost 20 feet (6 m), which were predominantly silt and clay. The vibratory probe relies on developing a zone of liquefaction around itself in order to penetrate through soil. Apparently extra water was required in the gravel and cobbles to achieve this. In the fine-grained soils large quantities were washed to the surface in what was more of a replacement process than a densification process.

The bottom portion of the deposit required more time and backfill gravel to treat than the rest of the deposit. Typically, half of the total stone and working time were spent treating the bottom third of the deposit, resulting in average column diameters of about 6 feet (1.8 m) in this area. In the upper two thirds of the deposit column diameters averaged about 4 feet (1.2 m).

Stone columns were constructed on a triangular pattern at a spacing of 9 feet (2.7 m). Two rigs were used to construct a total of 2,900 columns in two alternating rows or passes, primary and secondary, where all primary rows were completed within a treatment area before beginning the secondary rows. All primary and secondary columns were constructed to the full 60-foot depth of the dredged alluvium deposit. Additional treatment in the form of a tertiary pass was required where densification objectives were not met after the secondary pass. Of the 20,000 square yards (16,722 m^2) treated, 3,200 square yards (16%) required additional treatment. Tertiary columns were constructed generally to 30 feet (9 m) depth at the centroid locations of the triangular pattern. Stone takes averaged about 0.8 tons per linear foot of column (Allen et al., 1995).

QUALITY CONTROL

Construction quality control was aided by an automated instrumentation system that monitored key functions of the stone column construction. The following parameters were continuously monitored and recorded versus time: depth of the tip of the probe or pipe, power consumption of the vibratory probe or hammer, weight of gravel backfill used, water flow rate, and air pressure. Extensive evaluation of these data provided field personnel with timely observations of construction progress and trends in quality. The system was invaluable in accurately monitoring the column construction. Similar systems have since become common on ground modification equipment. (See Kelsic et al. (1995) for a detailed description and analysis of these data).

Figure 6. Downstream seismic remediation of the Mormon Island auxiliary dam – Embankment excavation and working surface for bottom-feed stone columns and mini-columns.

TREATMENT ADEQUACY

Adequate treatment of the downstream alluvium was defined as a specified $(N_1)_{60}$ blowcount determined by the BPT. Generally, treated areas were approved if the average values from at least three BPT's were greater than 18 in the bottom third of the deposit and greater than 25 in the upper two thirds. The density requirement is less in the bottom because the finer-grained soils are inherently more resistant to liquefaction. A small number of data points less than the specified values were accepted, provided they were well distributed over the total depth and represented no more than 10% of the total number of data points. Figure 7 shows that, based on average values, pre-treatment $(N_1)_{60}$'s of 10 - 15 increased to at least 25, with most of the data being over 30. Figure 7 also shows that the middle third responded best to treatment efforts and the bottom third responded the least, although the increase in blowcount is still significant. These results are significant since this is the first known large-scale application of this method in coarse gravels and cobbles interbedded with silt and clay within the same deposit.

The BPT was viewed as an ideal tool for measuring treatment adequacy because it is fast compared to SPT's and provides a continuous indication of penetration resistance. The BPT yielded blowcount and chamber pressure data for every foot (0.3 m) of penetration. Approximately 53 BPT's, performed between 1983 and 1993, were used to define the pre-treatment condition of the site. During the downstream construction, 87 BPT's were performed to check treatment adequacy.

The locations for BPT testing within each approval area were selected based on a number of factors. As-built plan views provided by the contractor showed the "drift" of the individual columns. Drift was measured merely by noting the location of the probe at the ground surface upon completing a column compared to where it started the column. The automated data were reduced by the personnel of the Bureau of Reclamation, who also compared working time and amperage with stone takes. The effect of adjoining treatment areas was also con-

sidered. BPT's were conducted at the centroid of the triangular pattern. Areas displaying anomalous levels of effort (defined as working time divided by amperage achieved), either high or low, were specifically not tested; rather, locations were selected that represented the "typical" characteristics of each treatment area.

CONCLUSIONS FROM DOWNSTREAM TREATMENT

Based on the experience gained from this project and the evaluation of field test results, the following conclusions can be drawn:

1. The bottom-feed stone column, wet replacement method developed for this site provided large increases in density to remediate a wide variety of soil types from silty clay to gravel with cobbles.

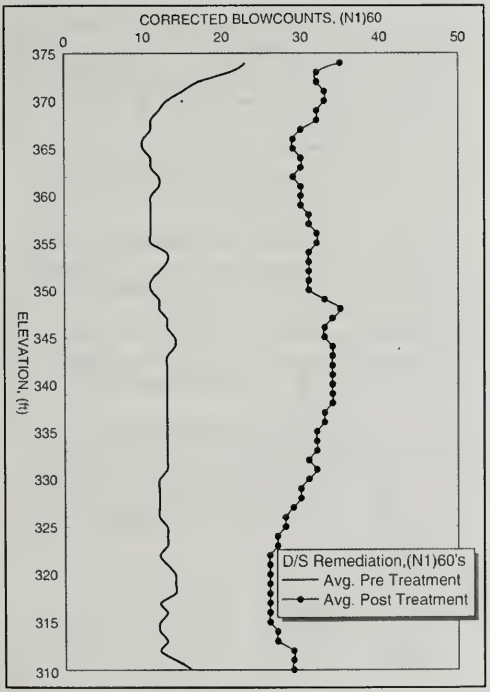

Figure 7. Downstream seismic remediation of the Mormon Island auxiliary dam – Improvement of average $(N_1)_{60}$.

2. The Becker penetration test was an effective tool for evaluating treatment adequacy at this site, and its use was validated by high quality SPT's.

3. The remediation results indicate that, by careful monitoring of critical parameters and adjusting construction techniques to fit a specific site, excellent improvement of materials previously thought to be untreatable by vibratory methods can be achieved.

AUTHOR PROFILE

Matthew Allen is a civil engineer employed by the U.S. Army Corps of Engineers in the Sacramento District. He has worked as a geotechnical engineer for 18 years on a variety of projects related to flood control and dam safety. His principal activities revolve around the dynamic stability evaluation of earth dams and the design and construction of remediation modifications. Mr. Allen holds BS and MS degrees in Civil Engineering from the California State University, Sacramento, and is a registered Professional Engineer in the State of California.

SELECTED REFERENCES

Allen, M.G., 1984, Liquefaction potential investigation of Mormon Island Auxiliary Dam, Folsom Project, California: Soil Design Section, U.S. Army Corps of Engineers, Sacramento District, CA.

Allen, M.G. and Jones, W.C., 1990, Proposed *in situ* ground remediation techniques at Mormon Island Auxiliary Dam: U.S. Army Corps of Engineers, Sacramento District, CA.

Allen, M.G., Jones, R., and Gularte, F.B., 1995, Bottom-feed stone columns, wet replacement construction method: Mormon Island Auxiliary Dam Modifications: ASCE Geotechnical Special Publication No. 49, Soil Improvement for Earthquake Hazard Mitigation, p. 82 - 95.

Bolt, B.A. and Seed, H.B., 1983, Accelerogram selection report for Folsom Dam Project, California: Contract Report DACW 05-83-Q-0205, U.S. Army Corps of Engineers, Sacramento District, CA.

Harder, L.F., 1986, Evaluation of Becker penetration tests performed at Mormon Island Auxiliary Dam in 1983: Technical Report GL-87-14, U.S. Army Corps of Engineers Waterways Experiment Station, Vicksburg, MS., Appendix A.

Harder, L.F., 1992, Evaluation of Becker hammer soundings performed at Mormon Island Auxiliary Dam in conjunction with upstream remediation: Prepared for the U.S. Army Corps of Engineers, Sacramento District, CA.

Harder, L.F. and Seed, H.B., 1986, Determination of penetration resistance for coarse-grained soils using the Becker hammer drill: UCB/EERC Report No. 86/06, University of California, Berkeley, CA

Hynes, M.E., Wahl, R.E., Donaghe, R.T., and Tsuchida, T., 1990, Seismic stability evaluation of Folsom Dam and Reservoir Project, Report 4, Mormon Island Auxiliary Dam – Phase I: Technical Report GL-87-14, U.S. Army Corps of Engineers Waterways Experiment Station, Vicksburg, MS.

Hynes-Griffin, M.E., 1987, Seismic stability evaluation of Folsom Dam and Reservoir Project, Report 1, Summary Report: Technical Report GL-87-14, U.S. Army Corps of Engineers Waterways Experiment Station, Vicksburg, MS.

Kelsic, R.H., Stevens, M.G., and McLean, F.G., 1995, Verification of stone column construction, Mormon Island Auxiliary Dam: ASCE Geotechnical Special Publication No. 49, Soil Improvement for Earthquake Hazard Mitigation, p. 111 - 126.

Kiersch, G.A. and Treasher, R.C., 1955, Investigations, areal and engineering geology - Folsom Dam Project, Central California: Economic Geology, v. 50, no. 3, p. 271-310.

LaForge, R. and Ake, J., 1999, Probabilistic seismic hazard analysis for Mormon Island Auxiliary Dam, Folsom Project, Central Valley Project, California: U.S. Bureau of Reclamation, Denver, CO

Ledbetter, R.H., Finn, W.D., Hynes, M.E., Nickell, J.S., Allen, M.G., and Stevens, M.G., 1994, Seismic safety improvement of Mormon Island Auxiliary Dam: 18'th Congress on Large Dams, International Commission on Large Dams, Durban, South Africa.

Ledbetter, R.H., Finn, W.D., Nickell, J.S., Wahl, R.E., and Hynes, M.E., 1991, Liquefaction induced behavior and remediation for Mormon Island Auxiliary Dam: Proceedings of the International Workshop on Remedial Treatment for Liquefiable Soils, U.S.-Japan Workshop on Wind and Seismic Effects, Tsukuba, Science City, Japan.

Llopis, J.L., 1983, Preliminary results of an *in-situ* seismic investigation of Folsom Dam, California: Draft Letter Report to U.S. Army Corps of Engineers, Sacramento District, CA, from U.S. Army Corps of Engineers Waterways Experiment Station, Vicksburg, MS.

Llopis, J.L., 1984, Preliminary results of *in situ* surface vibratory tests of Folsom Dam, California: Letter Report to Commander, U.S. Army Corps of Engineers, Sacramento District, CA, from U.S. Army Corps of Engineers Waterways Experiment Station, Vicksburg, MS.

Nickell, J.S., Allen, M.G., and Ledbetter, R.H., 1994, Seismic remediation for liquefiable gravels: Mormon Island Auxiliary Dam: Proceedings of the International Workshop on Remedial Treatment of Liquefiable Soils, 4'th U.S.-Japan Workshop on Soil Liquefaction, Tsukuba, Japan.

Stevens, M.G., Allen, M.G., and Farrar, J.A., 1993, Construction and verification of ground improvements at Mormon Island Auxiliary Dam: ASCE Geotechnical Publication No. 53., Geotechnical Practice in Dam Rehabilitation, p. 961 - 968.

Stevens, M.G., Dise, K., and Von Thun, J.L., 1994, Dynamic compaction to remediate liquefiable embankment foundation soils: Proceedings of the International Workshop on Remedial Treatment of Liquefiable Soils, 4'th U.S.-Japan Workshop on Soil Liquefaction, Tsukuba, Japan.

Sy, A., 1993, Energy measurements and correlations of the Standard Penetration Test (SPT) and the Becker Penetration Test (BPT): Ph.D. Thesis, Department of Civil Engineering, University of British Columbia, Vancouver.

TEC (Tierra Engineering Consultants), 1983, Geologic and seismologic investigations of the Folsom, California area: Contract Report DACW 05-82-C-0042, US Army Corps of Engineers, Sacramento District, CA.

U.S. Army Corps of Engineers, 1953, Foundation report, American River, California, Mormon Island Auxiliary Dam, Folsom Project: Sacramento District, CA

U.S. Army Corps of Engineers Laboratory, 1986, Report of soil tests, Folsom Dam laboratory program: South Pacific Division, Sausalito, CA.

U.S. Bureau of Reclamation, 1990, Modifications-Phase I, Mormon Island Auxiliary Dam, Folsom Unit, American River Division, Central Valley Project, California: Solicitation No. 0-SI-20-01140, Sacramento, CA.

U.S. Bureau of Reclamation, 1993a, Modifications-Phase II, Mormon Island Auxiliary Dam, Folsom Unit, American River Division, Central Valley Project, California: Solicitation No. 3-SI-20–2490, Sacramento, CA.

U.S. Bureau of Reclamation, 1993b, Report on ground improvement test section for Mormon Island Auxiliary Dam modifications: Technical Memorandum No. MM-3620-6, Denver, CO.

Wahl, R.E., Crawforth, S.G., Hynes, M.E., Comes, G.D., and Yule, D.E., 1992, Seismic stability evaluation of Folsom Dam and Reservoir Project, Report 8, Mormon Island Auxiliary Dam - Phase II: Technical Report GL-87-14, US Army Corps of Engineers Waterways Experiment Station, Vicksburg, MS.

ASSESSMENT OF GEOLOGIC RESOURCES AND HAZARDS IN SITING OF NON-NUCLEAR THERMAL POWER PLANTS AND RELATED FACILITIES

ROBERT ANDERSON[1]

ABSTRACT

One of the major engineering geology tasks in siting and constructing a non-nuclear thermal power plant is the assessment of geological resources and hazards around the proposed power plant location. In a normal sequence of events, a utility selects potential sites based upon several considerations (e.g., economic, political, land use, and environmental), and it is the job of its consulting engineering geologists to review each of the potential sites and rank them in terms of geologic suitability. To begin the assessment, published and unpublished geological literature regarding the site and linear facilities are reviewed, a site geological reconnaissance is conducted, a regional geologic map and site-specific geologic maps are prepared, and a recommendation of sites to be further evaluated is presented to the project developer. Geologic attributes and challenges are added to the decision matrix for selection of a primary site. After selection of the primary site, specific studies are completed to identify the geologic hazards at that location and their impacts on the project. During this phase the engineering geologist also looks at unique geologic resources and assesses the impacts that project development may have on these resources. Finally, the engineering geologist collects site-specific geologic data and observations that are used by engineers to plan grading, and in the design of foundations for power plants, substations and switchyards, and utility facilities (pipelines and electrical transmission systems).

In a complementary role, engineering geologists working for the pertinent regulatory agencies have the role of safeguarding public welfare and the environment by enforcing compliance with all applicable laws and regulations, particularly in the areas of geological hazard assessment and utilization and protection of geologic resources.

The consulting engineering geologist does not stop being involved with a thermal power plant once it is built. His or her role changes from siting and construction activities to water quality monitoring, monitoring of facility performance with respect to geohazards, and mitigation of geohazard damages (if necessary). During closure, the engineering geologist may be involved with a change in the land use or in regrading schemes to make the former facility site compatible with the post-closure land use.

Disclaimer: This paper does not represent a formal statement of policy or procedure by the California Energy Commission or the California Seismic Safety Commission. The views presented are exclusively those of the author.

INTRODUCTION

The siting and construction of new power plants is important to the well-being of Californians. At the same time, power plants are industrial facilities that place unique burdens on the environment, so they are subject to the environmental impact review process. The lead agency for this process is the California Energy Commission (CEC). The CEC has the

[1]California Seismic Safety Commission
1755 Creekside Oaks Drive, Suite 100
Sacramento, CA 95833
banderson@quiknet.com

charter of safeguarding life, property, public welfare and the environment by ensuring that energy facilities under CEC jurisdiction comply with all applicable laws, ordinances, regulations and standards (LORS). Several other entities might be involved in the process (Table 1), but the CEC is the state agency ultimately responsible for licensing thermal power plants that produce over 50 megawatts. The CEC uses the California Building Code (CBC) as a source of minimum requirements for its review of the preliminary design. The detailed final design of a proposed power plant project occurs only after the project has received certification from the CEC. In cases where the local agency is both willing and able, the CEC delegates to the local Chief Building Official (CBO) oversight authority for review of the final design and construction inspection of the project.

There were over 25 non-nuclear (natural gas-fired) thermal power plant siting cases brought before the CEC from 1998 through April 2001. As of the latter date, 19 of the power plant projects brought before the CEC had been licensed, one was suspended pending reassessment by the applicant, and the rest were under review.

The CEC staff has the responsibility of performing an independent assessment of each energy facility application, and works to ensure that the application is reviewed as thoroughly, consistently, and expeditiously as possible. Different teams from within the CEC work together when analyzing a proposal for siting or re-powering a thermal power plant. In this paper, the role of the engineering geology team is emphasized. Typical discipline team members with which the CEC engineering geologists interact include facility design, water resources, land use, transmission system engineering, waste management, alternative site analysis, air quality, and biology.

During a siting case assessment, the CEC engineering geology staff is to ensure that there will be no unreasonable exposure of people or property to geologic hazards, or significant adverse impacts to significant geological and paleontological resources during construction, operation and closure of a power plant. In addition, the engineering geologist may be asked to assess sites with regard to paleontological resources, surface water hydrology and water resources.

Descriptions of the typical kinds of information needed for the geological hazards and resources analysis of an Application for Certification (AFC) for a thermal power plant project are included in Tables 2 and 3.

TYPE OF FACILITY	FEDERAL	STATE	LOCAL
THERMAL POWER PLANT		California Energy Commission, (Title 20 California Code of Regulations for plants over 50 MW), California Water Resources Control Board	County or City Building Department
HYDROELECTRIC POWER PLANT	Federal Energy Regulatory Commission	Department of Water Resources, Division of Safety of Dams, California Water Resources Control Board	
GEOTHERMAL POWER PLANT		California Energy Commission, California Water Resources Control Board	County or City Building Department
NUCLEAR POWER PLANT	Nuclear Regulatory Commission, United States Environmental Protection Agency	California Energy Commission, California Water Resources Control Board	
SOLAR-ELECTRIC POWER PLANT	United States Bureau of Land Management	California Energy Commission, California Water Resources Control Board	County or City Building Department

Table 1. Regulatory entities responsible for power plant oversight in portions of California

REGIONAL GEOLOGY	SITE GEOLOGY AND TOPOGRAPHY	GEOLOGIC AND PALEONTOLOGIC RESOURCES	FAULTING AND SEISMICITY	LANDSLIDES AND EROSION POTENTIAL	WATER RESOURCES
DESCRIPTION OF MAJOR GEOLOGIC UNITS	Preparation of regional geologic map with cross sections depicting the generalized stratigraphic and hydrogeologic units in the vicinity of the proposed site	Nature and location of known geologic and paleontologic resources	Description of major active faults within 100 km of the proposed sites and the regional tectonic setting Description of method used to determine the seismic coefficient or peak horizontal ground acceleration for the project	Asses the slope and competency of soil and rock units making up slopes within 5 km of the proposed sites, or a regional description and assessment of the potential for landsliding	Assessment of the availability of surface and groundwater for use by the project
STRUCTURE AND STRATIGRAPHY OF THE REGION	Description of the topography of the proposed sites, and the regional geomorphic features	Potential impact—direct, indirect and cumulative— of the proposed project on geologic and paleontologic resources	Description and map depicting the location of major faults and related earthquakes, their magnitude and maximum credible earthquake	Presence of bedding and large joint or fracture sets	Description of aquifers and aquitards, and thier hydrogeologic properties
GEOLOGY OF STUDY AREAS	Relationship of location of project and linear facilities with respect to local and regional geology	Location of geologic resources and potential impacts of the project on the resources	Description of the regional tectonic setting and its relationship to the project and related linear facilities		Relationship of the local aquifers and aquitards to regional ground water conditions
GENERALIZED DESCRIPTION OF THE PROPOSED FACILITIES AND THEIR PROPOSED LOCATIONS	Relationship of project elements to site geologic hazards (if any)	Relationship of project elements to geologic and paleontologic resources (if any)	Description of anticipated strong ground shaking effects on project	Description of mitigation of landslides and erosion	Description of impact of project on water resources

Table 2. Regional engineering geology siting study

THE SITE EVALUATION PROCESS

A phased approach

The geologic hazards and resources siting component of the site evaluation process involves three stages or phases: (1) regional site selection study, (2) preliminary site assessment, and (3) engineering geology study. Phases two and three may be complemented with a site-specific geotechnical engineering report and an environmental site assessment. Before briefly discussing these phases, it is relevant to remember that, in addition to conducting a siting study for a thermal power plant and related facilities, applicants have to make sure that they are in compliance with applicable LORS of entities with jurisdiction over their project. There are no federal LORS with respect to mineral resources or geologic hazards, but there are some that address protection of paleontological resources for projects that encroach on lands owned by the United States government (e.g., the National Environmental Policy Act- Title 42, United States Code sections 4321-4327, the Federal Land Management and Policy Act- Title 43, United States Code sections 1701-1784), and state LORS regarding protection and stewardship of vertebrate paleontological resources (California Public Resources Code section 5097.5; California Environmental Quality Act Appendix "G" (V)(c)). In addition, the United States Bureau of Land Management (BLM, 1998) and the Society of Vertebrate Paleontologists (SVP, 1994) have guidelines for assessing and mitigating impacts to paleontological resources. The CEC engineering geology staff often uses the BLM and SVP guidelines in developing recommended conditions of certification with respect to paleontological resources.

The first phase of study concentrates on the review of available literature and maps at a regional scale (Table 2). The applicant selects potential sites based upon several considerations (e.g., economic, political, land use, and environmental), and it is the job of the applicant's engineering geologists to review each of the potential sites and rank them in terms of geologic suitability. To begin with, regional and site-specific geologic maps might be prepared, based on observations made during a geological reconnaissance of the site, and on a review of published and available unpublished geologic information. A description of the geology—including geologic hazards and significant geologic resources, if any—is prepared, and geologic attributes and challenges are added to the decision matrix for selection of a primary site. The Geological Hazards and Resources section of the AFC is then prepared for the primary site and related facilities. A limited discussion of the alternative sites is also included in the AFC.

The second phase of study starts after selection of the primary site. Site-specific studies are completed at this time, to identify the geologic hazards at the site and their impacts on the project. During this phase the engineering geologist also looks at unique geologic resources (such as water or paleontologic

ASPECT	TASK DESCRIPTION	USEFUL SOURCES OF PUBLISHED INFORMATION
GEOLOGY AND GEOLOGICAL RESOURCES	Compile and evaluate existing available geologic maps and reports, including subsurface geologic data for the project area. Prepare a geologic field map using topographic maps at a scale of 1:24,000, and aerial photos as appropriate. Prepare cross sections and a written description and analysis of the site geology, stratigraphy, structure, and surface water hydrology	California Division of Mines and Geology California Division of Oil, Gas and Geothermal Resources United States Geological Survey (USGS) Uniform Building Code/California Building Code Federal Emergency Management Agency
GEOLOGIC HAZARDS	Compile and evaluate existing geologic hazard data for the primary location and linear facilities. Acquire geologic hazards and resources data for alternate sites as needed to support alternative site assessment work by others. Conduct field investigations as needed to confirm and supplement existing data. Prepare geologic maps and cross sections, and reports on the impact of the project on geologic resources and of geological hazards on the project and linear facilities	California Division of Mines and Geology Available geologic and geotechnical reports of project site, related linear facilities and adjacent properties County Seismic Safety Element USGS
FAULTING AND SEISMICITY	Conduct literature review of seismic and fault studies for study area and linear facilities. Conduct same for alternative sites as asked by staff preparing alternatives analysis section of AFC. Determine appropriate seismic parameters. These may include peak ground acceleration, seismic zone designation per CBC, magnitude of design earthquake, distance and direction of design earthquake from project and related facilities. If a probabilistic analysis is done, use as a minimum 10% in 50-year return interval; if deterministic method is used use Maximum Credible Earthquake (MCE)	California Division of Mines and Geology Note 49 UBC/CBC Chapter 16 Available published and unpublished geologic literature

Table 3. General tasks regarding geological hazards and resources

resources), and assesses the impacts that project development may have on these resources. The second phase of geologic study usually includes (Table 3):

- Review of available geologic reports and maps, topographic maps and aerial photos of the project site and linear facilities
- Geologic mapping within two miles of the project site, and mapping along the alignment of linear facilities
- Drilling, trenching, logging, and sampling of subsurface geologic materials
- Testing of soils and geologic units (done in consultation with the project geotechnical engineer)
- Geophysical surveys, such as seismic refraction/reflection profiling and resistivity surveying
- Assessment of local and regional seismicity
- Liquefaction susceptibility analysis, if needed
- Assessment of potential cut-and-fill areas, grading impacts on geological resources, and site drainage (both run-off and run-on conditions)
- Preparation of an engineering geology report following section 1637A.1.2 of the CBC. The report includes a site geologic map at a scale of 1:24,000 showing the footprint of the proposed power plant and linear facilities, cut-and-fill areas, location of geological resources, and the location of potential geologic hazards (e.g., active faults, areas prone to collapsing or expansive soils, areas prone to liquefaction or lateral spreading, and landslides). The report should also include geologic cross sections of the project site and a description of geologic units and faults, an opinion as to the feasibility of the project with respect to geological hazards and resources, and preliminary recommendations regarding grading, drainage, and foundations.

The second phase of study could be further divided by the level of detail required by the type of facility. The most stringent class is for nuclear power plants, because they have a larger potential for a serious environmental and health-and-safety incident. Details regarding the types of studies needed for siting a nuclear power plant can be found

in Hatheway and McClure (1979). Next in level of detail are large hydro-electric power plants, because they often involve construction of a dam and inundation of a large area—with all the environmental impacts and potential hazards that they entail. Krynine and Judd (1957) remains an excellent reference for the types of studies that accompany dam projects. Next in the "sophistication" list are non-nuclear thermal power plants.

A third phase of study is sometimes needed using an investigation workplan based upon specific information regarding the facilities to be sited and any conditions of concern encountered after the AFC was submitted or the primary site was licensed. During this phase of study the engineering geologist provides site-specific geologic data and observations that are utilized by geotechnical engineers for foundation design, and by civil engineers for drainage and cathodic protection system design. Typical soils, rock, and water resources tests and activities include those listed below:

Soils

- Visual description of soils per USCS classification scheme ASTM D-2488
- Test method for penetration test and split-barrel sampling of soils ASTM D-1586
- Laboratory compaction testing using the 56,000 ft-lb/ft^3 method ASTM D-1557
- Grain size analysis ASTM D-422
- Atterberg limits ASTM D-4318
- Expansive index potential ASTM D-4829
- Liquefaction potential evaluation ASTM D-6066
- Bearing capacity of soils for static load and spread footings ASTM D-1194
- Seismic refraction profiling ASTM D-5777
- Resistivity surveys ASTM G-57
- Geological and geophysical logging of borings

Rock

- Seismic refraction profiling ASTM D-5777
- Resistivity surveys ASTM G-57
- Visual description of rock
- Rock quality designation (RQD)

Aquifer testing

- Determination of water level elevations, and estimated changes due to pumping or injection of cooling or waste water (if applicable)
- Groundwater flow direction and gradient
- Pumping tests (type depends on site conditions)
- Determination of transmissivity, hydraulic conductivity, and storativity
- Review of seismic refraction/reflection profiling with respect to aquifer test results

Water quality tests and analysis

- Chemical characterization of local aquifers and surface water
- Physical characterization of local aquifers and surface water
- Review of resistivity survey results and water quality results
- Analysis and interpretation of water quality test data and presentation of findings

Geologic setting and required maps

A regional and site specific description of the geologic setting is required under the geology and paleontological resources regulations found in Title 20 CCR Division 2, Article 6, Appendix "B". To begin with, the applicant needs to provide a 1:24,000 scale geologic map that shows the geology within a two-mile radius of the project site. The map must include the location of all geologic, stratigraphic, and structural features and a legend that names each feature or unit. Title 20 CCR regulations also call for a map showing the location of geologic resources. Both the Title 20 CCR regulations and the CEQA guidelines are vague as to what these are. Neither the regulations nor the guidelines are specific as to how far geologic mapping must extend from the center-line of an electric transmission line, water supply line, or a natural gas line. In practice, the appropriate professional staff determines if there are any geological hazards, geological resources, paleontological resources, or surface water hydrological aspects that can be impacted by, or impact, the proposed project, and mapping is extended as needed to cover these features.

Under the paleontological resources section of the Title 20 CCR regulations, a map showing paleontological resources at a scale of 1:24,000 is required. The map is submitted with a request for confidentially under separate cover to the CEC, which holds it confidentially due to the sensitive nature of paleontological resources.

Aerial photos and site visits

Aerial photos are a key tool of the geologist. A review of stereo-pair aerial photos may reveal sig-

nificant aspects about the distribution of soils and geologic units, and the relationship between the proposed project and relevant stratigraphic, geomorphic, and structural features, including landslides. If a site is located in an area that has been already developed, then aerial photos and maps that predate the current landuse activity should also be reviewed.

It is essential that the reviewing engineering geologist visit the primary power plant site and linear facilities early on in the review process. Observations made during the site visit help to clarify site conditions that may or may not be readily apparent from the AFC.

There have been several instances in which the interpretation of aerial photographs, coupled with a site reconnaissance, has proven instrumental in assessing geological conditions near the proposed power plants and linear facilities. For example, linear features observed in aerial photographs at a proposed site led a geologic consulting firm to label the features as possible faults. However, upon inspection in the field, the lineaments turned out to be bedding plane contacts and cuts made for oil field activities.

FAULTING AND SEISMICITY

When reviewing an application, the CEC engineering geologist looks for the answers to three groups of questions:

1. Are the project and related facilities planned to be built over an active or potentially active fault? Is the site located near the mapped termination of an active fault? If so, could the fault be projected through the project site?

2. In what seismic zone are the project and linear facilities located?

3. What is the estimated peak horizontal ground acceleration for the power plant and the linear facilities? How was the peak horizontal ground acceleration determined?

Title 20 CCR Division 2, Article 6, Appendix B regulations require an analysis of the likelihood of ground rupture, strong ground shaking, slope failure and liquefaction in the event of an earthquake. The LORS related to strong ground motion are found in chapter 16 of the CBC.

In order to help clarify the level of strong ground motion expected at a power plant, the following information should be included as a part of the Geological Hazards and Resources section

- The seismic zone designation (from Figure 16-2 of the CBC).
- A site specific seismic hazard analysis, which may include (1) a deterministic analysis of the strong ground motion for the maximum credible earthquake on the design fault for the project, (2) a probabilistic analysis of the strong ground motion for at least a 10 per cent in 50 year return interval earthquake, or (3) both deterministic and probabilistic analyses for the project and comparison of the results of the two analysis.

A description of the principal active faults in the vicinity of the project, and a detailed discussion of the fault associated with the design earthquake, also need to be prepared. Applicants are strongly encouraged to have a professional geologist do a search of the geologic literature, and to document active faults within 100 km of the project site with a standard reference list of professional papers. If the linear facilities extend outside of a 100 km (62.5 mile) radius from the project site, then all known faults that occur within 1,000 feet of the linear facilities are to be accounted for on the project geologic map. The Alquist-Priolo Earthquake Studies Zone Act of 1994 does not preclude the construction and operation of a thermal power plant on an active fault; however, elements of the project that are to have more than 2,000 man hours per year of occupancy are not to be sited on an active fault. In practice, thermal power plants, substations, and switchyards are not sited on active or potentially active faults. To date, no major power plant in California has suffered major damage from either strong ground shaking or fault rupture or soil failure (but see Schiff (1999) for a summary of the performance of electric power systems outside of California prior to the Kobe, Japan, earthquake of 1995).

FOUNDATION STUDIES

A thorough review of available boring logs, test pit and trench logs gives the engineering geologist a sense of the subsurface soil conditions. This is critical in addressing issues such as liquefaction, expansive soil, collapsing soil, bearing capacity of

soils, selection of preliminary foundation type, availability and quality of on-site fill, stability of slopes, the location and foundation layout with respect to cut and fill areas, and differential settlement under static or dynamic conditions.

Liquefaction and lateral spreading

Liquefaction and lateral spreading can have a significant effect on the alignment of power plant components. Measurements of the depth to groundwater, laboratory determination of the grain size distribution of soils encountered in soil borings or trenches, estimated ground acceleration during the design earthquake, and a review of local topography are very helpful in identifying soils that may be susceptible to liquefaction and lateral spreading (Ferriz, 2001, this volume). Liquefied soils were observed near the Moss Landing Power Plant after the Loma Prieta earthquake (Benuska, 1990); however, no liquefaction-related damage at the power plant or adjacent switchyard was reported. As of April 2001, lateral spreading after an earthquake had not been reported at a power plant in California.

Expansive soils

Soils with a high clay content and an expansive index of 30 or more are capable of impacting light weight structures when the soils are wetted. Expansive soils are present in certain areas of the state, such as the Bay Area, but the condition can be mitigated by excavation or soil amendment and has not presented a significant problem with construction of power plants.

Collapsing soils

There have been several power plant sites proposed in areas where collapsing soils have been noted in the geologic literature, such as the west margin of the Central Valley. A description of collapsing soil conditions can be found in the volume edited by Borchers (1998). ASTM D-5333 is a test method to determine the potential of a soil to collapse when hydrated, and fortunately collapsing soil is a condition that can be mitigated once it is recognized. For example, for construction of a natural gas-fired power plant site built in Southern California in the mid-1980's, the contractor first removed over eight feet of soil from the power plant footprint and then laid down the soil with adequate compaction and moisture conditioning to minimize the potential for soil collapse. The power plant has not experienced any significant settlement of the engineered fill or of structures located on the fill.

Bearing capacity and settlement

This is probably the most important soil property with respect to selection of the foundation type for a thermal power plant. For example, a combustion turbine generator (CTG) cannot operate when out of alignment with other elements of the power train. Some amount of settlement is tolerated, but not much. In Kosekoy, Turkey, a pile-supported General Electric Frame 6 CTG sited on semi-consolidated alluvium suffered 0.5 cm (0.2 inches) of settlement during the Koaceli, Turkey, earthquake of August 1999, but the 0.5 cm of foundation settlement was within tolerance and the alignment of the turbine shaft was not seriously affected.

Standard penetration blow counts, undrained compressive strength, and dry unit weight of soils are important indicators of the bearing capacity of the soil. In northern California, one must pay particular attention to siting in young Bay Mud and unconsolidated alluvium.

Availability and quality of on-site fill

Some thermal power plants have been proposed at brownfield sites. Siting a power plant on a brownfield can lead to problems with the quality of fill, as well as potential exposure to site-specific contaminants, but is otherwise a viable land use for what would alternatively be wasted real estate. One of the first steps in addressing potential problems are an engineering geology site investigation and an environmental site assessment. Reports that result from such investigations and assessments are especially useful when they include detailed boring logs, a boring location map, a detailed geologic map, soil test results, and geologic cross sections through the proposed power plant, substation, and switchyard footprints.

Slope stability

The applicant is to ensure that slopes are in compliance with the CBC and any local grading ordinances. Typical slopes for fill at thermal power plants vary from flatter than 5:1 (horizontal to vertical) to as steep as 1.75:1. The CEC reviews the proposed natural, cut and fill slopes for a project, as well as slopes adjacent to the site that may be

affected by construction activities. The CEC engineering geology and facility design staff uses the CBC and local agency requirements to establish minimum requirements for slope and foundation stability for non-nuclear thermal power plants, substations, and switchyards. Sites that contain a landslide within, or adjacent to, the footprint of the structure under consideration are generally screened out during review. A brief overview of a switchyard in Taiwan, where earthquake-induced landslides and differential settlement occurred, is presented in both the sections on electric transmission lines and substations.

GEOLOGIC RESOURCES

The applicant describes the geologic resources that are at or within the vicinity of the project. Geologic resources information is available from the Division of Mines and Geology (DMG) and the Department of Oil, Gas and Geothermal Resources (DOGGR). The mineral land classification from the DMG should be given. There are very few designated areas in California that qualify as areas of geologic recreation, and most of these sites are in federal, state, or county parks or monuments.

WATER RESOURCES

An applicant must submit in the AFC the information required by the Regional Water Quality Control Board to apply for Waste Discharge Requirements and a National Pollutant Discharge Elimination System permit. The submittal commonly includes an analysis of the quality and quantity of water available for the project and the impact of the project on available water. The information submitted is reviewed by CEC water resources staff, for compliance with the State Water Resources Control Board policy 75-58 (SWRCB, 1975). Other elements reviewed include the quality and disposition of water used for cooling. Guidelines for seismic evaluation of water transmission facilities useful in power plant siting may be found in Eidenger and Avila (1999).

Ground subsidence due to groundwater withdrawal. No thermal power plants have been adversely affected by ground subsidence due to groundwater withdrawal in California. However, there are areas of the state that have experienced significant (greater than one foot) ground subsidence in the past, such as the Central Valley and the Santa Clara Valley. Accounts of the most significant subsidence problems can be found in the volume edited by Borchers (1998). Subsidence should not be overlooked in areas where extensive pumping takes place or is planned as part of the project.

Groundwater injection. Groundwater injection is a source of potential concern on two counts. First, Nicholson and Wesson (1990) have reported that there are several cases where injection of large volumes of fluid has triggered small-to-moderate-size earthquakes. Second, concerned citizen groups often wonder if groundwater would be significantly degraded by mixing with the injected fluid.

For power plant projects where the use of injection wells to dispose of waste water is proposed, both the applicant and the CEC staff engineering geologist must consider whether or not the use of injection wells is likely to trigger local earthquakes. Nicholson and Wesson (1990) report that the key hydrologic factor in triggering earthquakes by fluid injection is an increase in pore pressure. For instance, if the target aquifer has high transmissivity and storativity, then as long as the injection well is not sited in a fault there should only be a minimal chance of triggering an earthquake by high pressure injection of waste water.

This issue was raised in a recent siting case for a proposed power plant. A consultant for a citizens group identified possible faults crossing the alignment of a waste water discharge line. The possible faults were up dip (up structure) from the proposed location of two wastewater injection wells critical to the project. The consultant, representatives from the applicant, and representatives from the CEC met in a workshop/field trip to view the features and assess their significance in light of the proposed injection wells, and to estimate the potential for mixing of waters from the aquifer proposed to receive injectate from the project (target aquifer) and an aquifer above the target aquifer. The concern was that if the features identified by the consultant turned out to be faults that dipped down structure, then injection under pressure could cause fault rupture and establish a path for water from one aquifer to mix with the other. There were three points that aided CEC staff in discounting the injection-induced earthquake scenario: (1) The lineaments identified in the aerial photos did not turn out to be faults, (2) the injection pressure proposed was not high enough to be of significance since the target aquifer had high transmissivity and storativity, and (3) the water quality of the target aquifer was not worse,

even with the injectate, than the water quality of the upper aquifer.

Drainage. The lack of adequate drainage and grading plans has, on occasion, slowed down the assessment of the geology and surface hydrology aspects of a siting project. Title 20 CCR requires a description of drainage facilities but not a map. Still, it is most helpful and expedient when the applicant includes a drainage plan in the submittal of the AFC. Precipitation and runoff patterns are also very useful (and they are required under the CEC's siting regulations). The former can be easily addressed by including in the AFC a chart for the average precipitation per month at a nearby weather station. The drainage run-on and run-off is affected by grading, disturbance of intact soils, and paving over of soils through which surface water would have otherwise percolated. Incidentally, although Title 20 of the CCR does not ask for a grading and drainage plan, it does require that the applicant comply with all applicable LORS. This requirement includes compliance with grading and drainage requirements under the CBC, the Regional Water Quality Control Board, and the local (usually county) building code.

Offsets from oil and gas wells

The local office of the DOGGR must be contacted by the applicant if oil or gas wells are located near the project or linear facilities. DOGGR requires that access to oil and gas wells be provided, so that maintenance, redevelopment or abandonment activities can take place at the well sites.

POST-CERTIFICATION INVOLVEMENT

After a site has been licensed and the final design has been approved for construction by the chief building official, the project engineering geologist begins a period of in-grade mapping and assessment and documentation of geologic conditions encountered. A final engineering geology report is prepared at the end of the construction project and follows the requirements set forth in the CBC. During the life of the facility the engineering geologist may monitor groundwater quality, changes in site conditions due to site operations, landslides or earthquakes, or changes due to continued development of the facility or adjacent properties. Should the site be expanded or re-powered, then the new project would need to go through a similar process of geologic assessment by the CEC.

LINEAR FACILITIES

Linear facilities include electric transmission lines, water supply and waste water discharge lines, and natural gas supply lines. For electric transmission lines, wind loading is typically seen as more of a problem than seismic loading of the lines and their towers or poles. Key geologic siting concerns for electric transmission poles and towers are siting on active faults, shear zones, soils prone to liquefaction or landslides, soil prone to collapse, and areas where strong ground shaking might be expected. Other concerns include channel scour and the potential to partially block surface water flow in drainages.

Electric transmission lines

California Public Utilities Commission General Order No. 95 contains some vague references to foundations for electric transmission line towers. Typically, a third party engineer working for the owner may serve as the inspector.

The CEC staff may review geologic maps, grading and drainage plans, boring logs, test pits and trench logs for electric transmission lines, and other linear facilities. Of particular interest are trench logs and geologic maps for areas where active faults are to be crossed, areas prone to liquefaction, or areas with collapsing soils.

For above ground electric transmission lines, soil and geologic unit parameters such as the dry unit weight, moisture content, cohesion, angle of internal friction, and (where available) corrected standard penetration blow counts should be compiled. These data are often found in the logs of borings and trenches excavated during an engineering geology or geotechnical investigation of a linear facility corridor. The data is then placed into context with respect to the site setting and the project. The applicant's engineer determines the depth of embedment for a tower or pole foundation, often with the help of a computer model such as the Moment Foundation Analysis and Design model (EPRI, 1999).

In the Chi-Chi, Taiwan, earthquake of September 1999, earthquake-induced landslides knocked down towers and pulled down electric transmission lines. In order to mitigate the effect of landsliding, electric transmission lines should either avoid crossing landslides, or cross the landslide area with a minimum of exposure (for example, by locating the towers outside of the footprint of the landslide).

SUBSTATIONS AND SWITCHYARDS

There have been several instances of seismic damage to substations and switchyards. The responsible earthquakes have ranged from moderate (such as the M_w 5.2 Tejon Ranch, California earthquake of June 1988 and the M_w 5.6 North Palm Springs, California earthquake of July 1986) to severe (such as the M_w 7.4 Koaceli, Turkey earthquake of August 1999 and the M_w 7.7 Chi-Chi, Taiwan earthquake). In the case of the earthquakes in the United States, damages have been minor, and no significant faulting or surface rupture failure has disrupted these kinds of facilities. The modest level of damage is partly due to the fact that seismic qualification testing of electrical equipment has been carried out in the United States for many years. IEEE-693-97 is used as a method to conduct seismic qualification testing of electrical equipment for substations and switchyards.

But damage can be severe, particularly during strong earthquakes. During the Chi-Chi earthquake, for example, the Chinglao switchyard was severely damaged due to both strong ground shaking and landsliding within the switchyard. The Chinglao switchyard was built on a cut-and-fill pad in an area prone to landsliding, and happened to be within ten kilometers of the epicenter of the Chi-Chi earthquake.

SUMMARY

The engineering geologist plays an important role in the siting of electric utility facilities. As with many large projects, the siting process is iterative and involves interaction between the engineering geologist and specialists from many other disciplines, especially geotechnical engineers, civil engineers, planners, and regulators. During the siting process the consulting engineering geologist assesses a site or sites with regard to geologic hazards, impact to geological and paleontological resources, surface water hydrology, impact to groundwater resources, and geotechnical issues relevant to project design. His or her counterpart in the regulatory community has the role of safeguarding public welfare and the environment by enforcing compliance with all applicable LORS related to geological hazards and resources. The consulting engineering geologist does not stop being involved with a non-nuclear thermal power plant once it is built. His or her role changes from siting and construction activities to water quality monitoring, monitoring of facility performance with respect to geohazards, and mitigation of geohazards. During closure, the engineering geologist may be involved with regrading schemes to make the former facility site compatible with the post-closure land use or with environmental restoration activities.

ACKNOWLEDGEMENTS

I wish to thank Robert Strand and Kisabuli from the Engineering Office of the California Energy Commission for their assistance in reviewing several drafts of this paper. I would also like to thank my fellow Editor, Horacio Ferriz, for encouraging me to write this paper in the first place, and for his editorial help.

AUTHOR PROFILE

Robert Anderson is a California Certified Engineering Geologist with 13 years of engineering geology and hydrogeology experience. He is a Senior Engineering Geologist at the California Seismic Safety Commission in Sacramento, California. Prior to joining the California Seismic Safety Commission he worked as an Associate Engineering Geologist with the California Energy Commission (1999-2001) and the California Integrated Waste Management Board (1990-1998). His specialties include geohazard assessment, and geologic engineering of power plants, landfills, waste water treatment plants, roads, bridges, and residential tracts.

SELECTED REFERENCES

Benuska, L. (ed.), 1990, Loma Prieta Earthquake reconnaissance report: *in* Earthquake Spectra, Earthquake Engineering Research Institute, Supplement to v. 6, p. 210.

BLM (Bureau of Land Management), 1998, General procedural guidance for paleontological resources management: U.S. Department of the Interior, Bureau of Land Management, Handbook H-8270-1, 34 p.

Borchers, J.W. (ed.), 1998, Land subsidence – Case studies and current research: Association of Engineering Geologists Special Publication No. 8, Star Publishing Company (Belmont, California), 576 p.

CEC (California Energy Commission), 1997, Rules of practice and procedure for power plant site certification regulations: California Energy Commission Report, p. 98-100.

Eidinger, J.M., Avila, E.A., (eds.) 1999, Guidelines for the seismic evaluation and upgrade of water transmission facilities: American Society of Civil Engineers, Technical Council on Lifeline Earthquake Engineering, Monograph No. 15, 199 p.

EPRI (Electric Power Research Institute), 1990, Moment foundation analysis and design (MFAD): User's Guide, 42 p. [revised 1999].

Ferriz, H., 2001, The basics of liquefaction analysis: *in* Ferriz, H., Anderson, R. (eds.), Engineering Geology Practice in Northern California: Association of Engineering Geologists Special Publication 12 and California Division of Mines and Geology Bulletin 210.

Hatheway, A.W. and McClure, C.R., 1979, Geology in the siting or nuclear power plants: Geological Society of America, Reviews in Engineering Geology, v. IV, 256 p.

Krynine, D.P. and Judd, W.R., 1957, Principles of engineering geology and geotechnics: McGraw-Hill Book Company, (New York, New York), 730 p.

Nicholson, C. and Wesson, R.L. 1990, Earthquake hazard associated with deep well injection: United States Geological Survey Bulletin 1951, 74 p.

Schiff, A.J., 1999, Guide to improved earthquake performance of electric power systems: American Society of Civil Engineers, Manuals and Reports on Engineering Practice No 96, 328 p.

SVP (Society of Vertebrate Paleontologists), 1994, Measures for assessment and mitigation of adverse impacts to nonrenewable paleontologic resources: Internal report, October 1994.

SWRCB (State Water Resources Control Board), 1975, Water quality control policy on the use and disposal of inland waters used for powerplant cooling: SWRCB Policy 75-58, dated June 19, 1975.

NEW ISSUES AND OPPORTUNITIES FOR MANAGING GEOHAZARD RISKS TO ELECTRIC POWER SYSTEMS

WILLIAM U. SAVAGE[1] AND ROBERT ANDERSON[2]

ABSTRACT

Electric power systems have generally performed well in recent years when affected by such geologic hazards (geohazards) as large earthquakes and major landslides. However, three issues drive a growing concern for achieving high levels of safety and reliability in the face of future geohazards: (1) increasing demand of high-technology manufacturers and users for high quality and highly reliable electric service, (2) economic and regulatory pressures to reduce costs of electric power, and (3) increasing urbanization leading to greater societal consequences of electric power interruption. Owners and regulatory overseers of electric power systems are now incorporating geohazards risk management strategies to assess exposure and vulnerability to geohazards, and to manage these risks through long-term mitigation and emergency response programs.

This paper identifies and discusses four important areas relevant to geohazard mitigation:

1. Improving identification of earthquake hazards through basic data collection, mapping hazard zones, and refined evaluations of extreme ground motions and levels of permanent ground deformation, by probabilistic and deterministic methods.

2. Improving vulnerability assessments of power systems by more accurately quantifying fragility curves for key components and facilities, and by developing models and tests for equipment interconnections.

3. Improving industry design practices through the development of consensus guidelines and protocols to optimize learning from future earthquakes or landslides.

4. Improving active risk management using new technologies to monitor and improve the response to geohazards as they occur.

These developments depend on the involvement of a broad range of talented earth scientists and engineers working closely with individuals from the electric power industry and government agencies. These collective efforts are of potential benefit to other utility and transportation systems, major users, and governmental agencies.

INTRODUCTION

Electric power generation, transmission, and distribution systems provide high-priority lifeline services to all of California. At the same time, however, geologic hazards (geohazards) can threaten the reliability of these services and can expose people to direct and indirect safety hazards. A practical geohazards risk management strategy that is being used by utilities to optimize public safety, customer service reliability, and business goals—while meeting regulatory requirements—is described in this paper. This paper builds on the lessons from earth-

[1]U.S. Geological Survey
345 Middlefield Rd., MS 977
Menlo Park, CA 94025
wusavage@usgs.gov

[2]California Seismic Safety Commission
1755 Creekside Oaks Drive, Suite 100
Sacramento, CA 95833
banderson@quiknet.com

quake and landslide case studies and on the body of practices used by the major California electric utilities to effectively address geohazards through individualized risk management. Additionally, the paper points to new developments in hazard assessment and engineering practice, utility-driven research, and public agency action. Finally, since new issues and concerns are arising due to demographic and regulatory changes in California and the nation, implications and opportunities associated with these new developments are also addressed.

GEOHAZARD THREATS TO A UTILITY NETWORK

Geohazards to man-made facilities are ubiquitous in California. They include natural and man-induced slope failures, soil foundation failures, surface faulting and earthquake shaking, and earthquake-induced ground failure. Other geohazards of concern include mass wasting, collapsing soils, rockfalls, volcanic eruptions, and tsunamis. The specific nature and severity of the geohazard at a given site depends on characteristics such as

- slope angle
- bedrock characteristics
- overlying soil characteristics
- presence of groundwater
- proximity and rate of activity of seismic sources
- proximity of active volcanic centers
- elevation of coastal sites with respect to potential inundation

A given site or locality may be exposed to multiple geologic hazards, so it is essential to consider the likelihood of exposure to the hazards as a function of time. Thus, minor surficial landsliding may occur at a site once per year on average, whereas a major deep-seated rotational landslide may happen on average only once in several thousand years. The assessment of geohazard exposure of a utility network is very difficult because of the large area such networks occupy. For example, the electric power transmission grid is intimately entwined with the major active faults in California, and the exposure of each element of the system to earthquake shaking may vary greatly depending on its location.

PERSPECTIVE OF UTILITY OWNER

Geohazards pose risks that a utility owner must successfully manage to stay in business and meet customer needs and public agency requirements. To be effective at risk management, they must understand the risk, prioritize actions in response to the risk, and monitor the risk exposure on the long term. In the "old days" of cost-plus regulatory electric rates, any damages due to natural hazard phenomena were viewed as "acts of God" and were compensated in the rate structure. Nowadays, such damages are increasingly viewed as the burden of the owner of the facilities, not the ratepayer. Experiences in the past decade have demonstrated that many threats to utility systems due to earthquakes, landslides, foundation failures, and related geohazards can be identified well before the occurrence of the event, and can be mitigated by generally well-understood engineering and emergency response practices. Thus, service disruptions due to these geohazards in large part may be considered "acts of man", so the owners of power plants, transmission lines, and distribution systems are increasingly having to deal with geohazards as part of their responsibilities as risk managers. Seismic hazards provide a good example of the way utilities have taken on these responsibilities.

For instance, the 1971 San Fernando earthquake clearly revealed the vulnerability of high-voltage (220 kV and above) substation components to seismic shaking. Major California utilities then began to investigate and to implement steps to reduce their vulnerability to earthquakes. Fifteen years later, the July 8, 1986, North Palm Springs earthquake, although small (M_L 5.6), did severe damage to Southern California Edison's Devers substation, a major link in the Southern California grid. Although customer power was restored quickly, the potential for widespread earthquake disruption to the backbone power transmission system was clearly revealed, and the major California utilities quickly instituted critical equipment upgrading programs. Although major earthquakes are relatively rare events, their damage potential and the societal disruption that can accompany them have focused utility attention on earthquake hazards and vulnerability reduction methods. Now, at the turn of the millennium, the electric power disruptions and damage in earthquakes in California (1987,1989, 1992, 1994) and elsewhere in the world (1995 Japan, 1999 Turkey, 1999 Taiwan) have motivated sustained statewide investments in earthquake risk reduction. The goals of these improvements in seismic performance of electric systems are to minimize health and safety hazards to workers, and to minimize interruption of electric power to the consumer.

SOCIETAL FACTORS THAT DRIVE RISK MANAGEMENT

Three major factors have increased the potential impact of earthquakes, landslides, and other geohazards to the economy and quality of life in California by the loss of electric power: 1) the growth of the California economy, 2) the rising demand for lower prices for electricity, 3) and population growth.

Growth of the California economy

The trillion-dollar California economy increasingly relies on continued growth of the high technology and business services sectors (Munroe, 1998). During the late 1990s, these sectors expanded their geographic extent in the coastal regions around San Francisco Bay, Los Angeles, and San Diego, and out into the Central Valley and Sierran foothills. In turn, the high technology and business services industries, as well as their customers and resellers, are increasingly dependent on a growing supply of reliable, high-quality electric power. High-technology marketplace competition is so intense that disruptions caused by even brief power outages can cause delivery schedules to be delayed or electronic communications to be missed, which could cause a customer to lose millions of dollars in business.

Rising demand for lower electric power prices

In parallel with the rising demand for quality and reliability of power, businesses are also demanding lower prices for their electricity. California is leading the way in the nation to a deregulated electric power market, in which customers can choose their electricity supplier and have it delivered by the interstate power grid and local electric utility. State or municipal regulation continue to oversee the local utilities, but the inter-utility grid is operated by an Independent System Operator under regulation by the Federal Energy Regulatory Commission (FERC), and power generators are free to compete in a largely unregulated economic environment. This new business environment for the utilities and their customers is changing the way each of these components of the electric system carries out its activities. For example, individual facility or system owners must accept increased responsibility for the reliability of customer service in order to stay competitive. (Concerns that price competitiveness may reduce the efforts of the power generators, transmission operator, and local utilities to maintain adequately safe and reliable service in the face of expensive design for mitigation of geohazards have been raised. Such concerns are almost certainly unfounded, since regulators continue to oversee safety and reliability issues.)

Population growth

A third critical element driving the need for reliable power supply in California is continued population growth, particularly along the coastal areas between the northern San Francisco Bay area and the Mexican border, and in the Central Valley. Initially, new population settles mainly in the cities and suburbs where jobs are to be found, leading to urban densification. Afterward, rising prices in the urban real estate market encourage expansion into more remote and often less desirable areas (from a geohazards perspective). Increases in population and population density raise the potential consequences when a hazardous event happens to occur, such as a major earthquake or the activation of a large number of landslides due to above-normal rainfall. The ever larger population compounds the consequences of utility service disruption by drawing more heavily on the emergency response resources of the affected region, and adding greater urgency to the restoration of utility services.

GEOHAZARD RISK MANAGEMENT APPROACH

Successful geohazard risk management needs to consider four fundamental issues described below.

Geohazard exposure

Geohazards vary regionally. For each individual facility or network of facilities, the exposure to geohazard phenomena is dependent on the foundation conditions, on the stability of slopes at or near the site, and on where, how often, and how big future earthquakes might be. A complete electric system typically has multiple generation sources located many hundreds of miles apart, which are connected by redundant high-voltage transmission lines to local distribution utility networks throughout a region (Figure 1). Because of this wide geographic distribution, different specific actions are needed to address high-hazard sites versus low-hazard sites.

Mixture of electric system components

Electric power systems today are composed of facilities and components that have been sited,

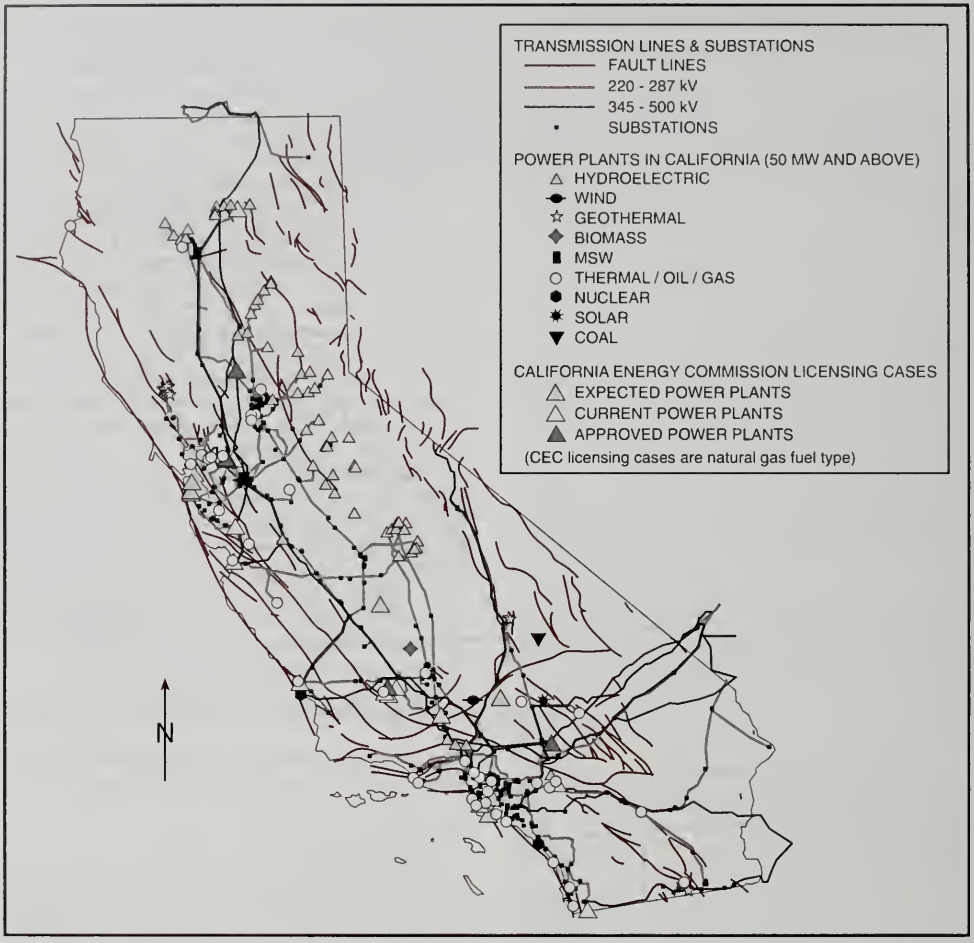

Figure 1. California electric transmission grid, with Holocene active faults. The transmission systems interconnect three large investor-owned electric utilities, two major municipal utilities, and a number of small municipal and out-of-state utilities. The figure also shows the location of major power plants.

designed, constructed, and maintained for as long as 100 years. These system elements have different geohazard performance capabilities, which are a function of the varied design criteria, fabrication materials, and construction practices used during this long time period. As a result, the current seismic vulnerability of customer service is largely a function of the weaker and typically older parts of the power system.

Electric system redundancy and reliability

Assessing the potential customer-service consequences of an individual geohazard event can be extremely complex. The damage to an electric system may be limited to a single facility that involves a direct economic loss to the owner of that facility, but with little impact on customer service. However, a large landslide or a strong earthquake could cause sufficient damage to overwhelm system redundancies and operational flexibility. This case was noted in the 1999 Taiwan earthquake, which caused shaking damage and triggered a landslide at the central switchyard for Taiwan's electric transmission system. The loss of function of the switchyard significantly reduced the amount of electric power available to portions of northern Taiwan for almost two weeks. Simply assessing the physical damage can be insufficient to forecast system functionality. Careful analysis of the details of the expected damage and extensive input from experienced operators of the system are needed to evaluate the operational consequences of extensive damage. If these operational factors are not taken into account, potential customer outages may be overestimated, potentially leading to overly extensive and expensive remediation efforts, or underestimated, leading to inadequate preparations.

Cost versus acceptable risk

As noted above, the changing business environment in California and the U.S. is leading to an ever greater reliance on uninterrupted electric power. Customers increasingly demand electric power to serve such critical business and personal services as instantaneous voice, text, and data communication, and computer-controlled manufacturing, distribution, and monitoring, to meet moment-to-moment timetables. At the same time, financial pressures are in place to drive down the cost of electric power as delivered to each customer. Power facility owners and relevant regulatory and law-making organizations struggle to establish the proper balance of acceptable risk in the face of such conflicting priorities.

For electric power facility owners, geohazard risk management should be systematically planned and carried out to obtain the maximum benefit for each dollar spent. Whether the risk management action be insurance, retrofitting components, or emergency response preparations, an objective analysis is needed to determine the best course of action. There are three hallmarks of an optimal approach. First, the approach must be long term, particularly for large systems. Although individual actions can be identified and completed in the short term, the overall approach needs to include cash-flow management, ongoing refinements in hazard and vulnerability assessments, and ongoing refinements of design criteria, new component specifications, and maintenance practices. Second, the approach must be carried out with annual priorities. Each annual budget should make best use of available funding at the time. Third, the approach should have the goal of "acceptable risk" as opposed to "no risk". Zero geohazard risk is probably not possible, and is economically unwarranted. Reducing risk and maintaining it at acceptable levels are the proper goals of a long-term geohazard risk-management program.

A SUGGESTED APPROACH

A five-step comprehensive approach to reduce the geohazard vulnerability of electric power systems is presented in Savage et al. (1995) and is summarized in the following paragraphs. These steps can be modified and individualized for systems of widely differing sizes and composition, from individual power plants to state-wide networks.

Identify geohazard sources and select appropriate scenarios

The geohazards affecting a facility or a system are assessed in an accurate, realistic, and quantitative manner. This includes site specific or regional assessments of such hazards as weak foundation conditions, landsliding potential, likely earthquake ground shaking, liquefaction and lateral spreading susceptibility, surface faulting, and tsunami inundation potential. Realistic hazard scenarios are selected that have a relatively high likelihood of occurrence, such as once every 500 years (longer time frames are used for dams and nuclear facilities). Each scenario is assumed to occur in locations

that expose a relatively large number of electric power customers to disruption due to damage to facilities. For example, some earthquake scenarios in the greater San Francisco Bay area have been proposed by WGCEP (1999), and these scenarios can be used by utilities as the starting point for their geohazard source characterization.

Assess the importance and vulnerability of important power system facilities and components

The importance of each facility and component is evaluated in terms of (1) its potential to threaten the life safety of owner, employees, or the general public if it is damaged or collapses, and (2) its criticality in maintaining or restoring customer service if it is damaged. The geohazard vulnerabilities of the important system elements are then evaluated. For example, high-voltage substations are important elements in delivering electric power, and past experience has demonstrated the vulnerability of some types of substation equipment to strong and even moderate levels of ground shaking. The vulnerability of substation components is typically described by fragility curves, that relate the probability of specific damage to the component (e.g. broken ceramic bushing in a transformer) to a particular ground motion parameter (e.g. peak ground acceleration). Each time there is a significant geohazard event, there is a valuable opportunity to collect data to evaluate past and current design practices, and to recommend improvements for the future. Professional organizations, such as the American Society of Civil Engineers (ASCE) and the Earthquake Engineering Research Institute (EERI), have established procedures for conducting post-earthquake investigations to optimize learning from earthquakes (Schiff, 1997 and 1999; EERI, 1996b). Evaluation reports that contain significant information on damage and performance of utilities have been prepared in the aftermath of the following earthquakes:

- Great Hanshin earthquake of 1995, Kobe, Japan, (Japanese Society of Civil Engineers, 1995).
- Northridge earthquake of 1994, California (DMG, 1995; EERI, 1996).
- Loma Prieta earthquake of 1989, California (EERI, 1990).
- Whittier Narrows earthquake of 1987, California (EERI, 1988).
- Morgan Hill earthquake of 1984, California (EERI, 1985).
- San Fernando earthquake of 1971, California (DMG, 1975).

Evaluate potential damage and operability in geohazard scenarios

For each selected scenario, the potential for damage and operability disruption associated with the facility or system are evaluated using the hazard vulnerabilities of the important facilities and components. For the particular geohazard being considered, fragility curves or other assessments are used to estimate likely damage states of the exposed facilities. Then power system personnel are asked to evaluate the impacts on operability of the assessed damage, a necessary process in evaluating the intangible aspects of daily operations. For example, in some cases serious damage may be easily handled by quickly bypassing it or by shifting operation to another facility that is not affected by the scenario.

Evaluate and prioritize alternative mitigation measures

Using the overall impact of the scenario analysis from step number three, the engineering, operations, and business staffs can objectively and quantitatively evaluate alternative mitigation measures to reduce geohazard risk. The alternatives may include, for example, replacing vulnerable equipment, preplanning emergency repairs, encouraging customers to acquire emergency generators, developing mutual aid plans, and obtaining insurance protection. The highest priority mitigation measures are those that reduce the most likely losses in the most rapid and cost-effective manner.

Implement a long-term geohazards safety program

Risk management requires continual vigilance. After carrying out the first four steps, the needs and priorities for risk management should be clear, and can be incorporated into a long-term plan. Each owner should determine the acceptable level of risk appropriate for the facilities or system under consideration. A significant element in a long-term safety program is using up-to-date standards for design and installation of new facilities and components. In many moderate and low hazard areas, most aspects of geohazard risk mitigation can be accomplished

at low or no additional cost simply by replacing or maintaining equipment and structures with hazard-resistant alternatives.

OPPORTUNITIES FOR IMPROVED RISK MANAGEMENT

Research and applications development by electric utilities, consulting engineers and geologists, university researchers, and state and federal government agencies are yielding a wide range of new data, advanced analysis techniques and tools, and improved strategies to sharpen the five-step risk management approach discussed above. In the following subsections, several important areas of advance are briefly described.

Improved identification of geohazards

Systematic regional and statewide mapping and characterization of landslide hazards and earthquake hazards (including both ground shaking and liquefaction) provide much improved means for the identification of hazard exposure of the networked components of the electric grid. It is simply infeasible for each utility operator to perform such an effort in a standardized and publicly accepted manner. These new databases are being presented in terms of hazards zones and in terms of probabilities of occurrence of the hazard. Even though the detail of these studies is not sufficient for engineering assessments at individual sites, they provide a previously unavailable means to assess relative hazard exposure and concentrate site-specific hazard assessment only at locations where they are needed. Examples of the regional approach to hazard mapping and related improvements include:

- The U.S. Geological Survey (USGS) has embarked on a major field effort to improve the characterization of earthquake sources in the San Francisco Bay area. The Bay Area Paleoseismic Experiment (BAPEX) program focuses on refining the recurrence model for Bay area faults over the past 2000 to 3000 years. These refinements will provide more accurate earthquake source parameters (e.g., fault rupture length, maximum magnitude, and recurrence interval) for use in seismic hazard assessments.

- Parallel with the initial BAPEX efforts, the USGS also led a reanalysis of the probabilities of future large earthquakes in the San Francisco Bay area (WGCEP, 1999). This study has been very useful to electric power utilities by specifying high-probability scenario earthquakes for use in earthquake risk assessments. It also provides a widely publicized, credible statement about severe earthquakes likely to occur in the next few decades in the Bay area.

- The California Department of Conservation, Division of Mines and Geology (DMG), in partnership with the USGS, has begun a systematic program to map earthquake hazard zones on a statewide basis, beginning with urban areas (Petersen et al., 1996; DMG, 1997; DeLisle, 2001, this volume). This activity was authorized by the Seismic Hazards Mapping Act of 1990, and maps have been released for liquefaction and landslide susceptibility zones for a few areas of northern and southern California, and statewide for probabilistic ground shaking. These maps serve as an important first step in characterizing ground motions and ground failure hazards for a region, although they are not sufficiently detailed for individual sites. Even though electric power systems are not covered by the required implementation of the zones, the data provide a significant advance in earthquake hazard information available for use in risk management.

- Additional studies currently in progress involve developing site-specific corrections for near-source ground motions involving fault rupture directivity and the ground-motion amplifications due to basin response effects. These refinements will be incorporated in both probabilistic ground motion computations and site-specific ground motion synthetic models for individual earthquake scenarios.

- Concern has recently been raised about the extremely high ground-motion values that are computed for highly active faults, such as the San Andreas. Brune (1999) suggests that the assumption of large ground-motion variances may not be warranted and that the largest earthquakes produce motions that are less than the values currently calculated. He supports this view with field investigations of geologically unstable rock formations. Strong motions recordings from the

1999 Turkey and Taiwan earthquakes exhibited lower than predicted ground shaking for earthquakes with magnitudes greater than 7.0. These results are significant for reassessing and potentially reducing earthquake hazard assessments within 20 to 40 km of major active faults for magnitude 7+ earthquakes.

- Investigations of permanent ground deformation associated with earthquake-induced liquefaction, and with landsliding, typically have focused on the more spectacular events, with displacements of multiple feet. Experiences with underground utilities in the 1994 Northridge and the 1995 Kobe earthquakes indicate that much underground damage occurs at small displacements, less than 0.5 m or so.

Improved assessment of power system vulnerabilities

Newer power system components generally incorporate modern foundation designs, but older installations were often built well below current standards, using building materials and equipment that makes them more vulnerable to damage due to tilting, settlement, lateral displacement, and seismic shaking. Recent systematic studies of older models of electric power equipment have revealed these vulnerabilities. With this knowledge, the utilities and manufacturers can develop retrofit modifications or can move the vulnerable equipment away from the hazards for cost-effective management of the risk without wholesale replacement of the equipment or facilities. Two areas of improvement in vulnerability characterization are discussed below.

1. Although critical ground motion data are often lacking at sites where substation equipment was damaged in past earthquakes, careful assembly and analysis of existing substation equipment damage data is taking place (Anagnos, 1999) using improved models for fragility functions (Der Kiureghian, 1999). Several West Coast utilities have been collaborating on shaking-table testing of commonly used substation equipment to directly determine the fragility curves for the equipment (Fujisaki et al., 1999). These data have already been used to make better decisions on deployment of certain equipment and are leading to improved retrofit techniques.

2. Many investigators of earthquake damage in substations have suspected that the interconnections between substation components by conductors have been the cause of some of the observed damage. When a massive component begins to shake violently and undergoes soil-structure interaction and foundation failure, it can pull adjacent and interconnected pieces of equipment to the point that their porcelain insulators or metal fittings break. Analytical and shaking-table studies currently underway will lead to at least an improved appreciation of the potential for such damage to occur and possibly to improved procedures for electrically connecting substation equipment so that future earthquakes do less damage.

Improved industry design practices

An essential step in managing future geohazards risk is to design practices that provide acceptable performance of facilities given their state of hazard exposure. Modern building codes have provided useful guidance in addressing geohazards for residential and commercial construction, and many of these practices have been used by electric utility personnel as a minimum design level, even for structures and facilities for which the codes are not required. For the past decade, the Federal Emergency Management Agency (FEMA) and the National Institute of Standards and Technology (NIST), with cooperation and encouragement from industry and other governmental agencies, have been acting to implement national guidelines for reducing risks to utility and transportation systems from natural hazards. For electric power systems, this process has led to two key developments:

- For the past six years, utility personnel, manufacturers, and consultants have been working to establish and improve a consensus guideline for the design and evaluation of substation equipment (IEEE, 1997). The standard, known as IEEE Std –693-1997, has standardized the ground motion criteria and qualification procedures used to procure seismically qualified substation equipment.

- In 1998, FEMA entered into a cooperative agreement with the American Society of Civil Engineers (ASCE) to carry out a project called American Lifelines Alliance (ALA). ALA's goal is to facilitate the creation of national consensus guidelines and standards that, when implemented by lifeline owners and operators, will systematically improve the performance of utility and transportation systems to acceptable levels in seismic and other natural hazard events (ALA, 2000). The resulting guidelines will enable utilities to make geohazards risk-management decisions that are readily accepted by owners, regulators, ratepayers, and public officials.

Active risk management of geohazards

New technology is enabling timely data collection on actively occurring geohazards that can be used to make better real-time decisions to manage the possible consequences of such events. For example, remote sensing technology is providing new tools, such as radar interferometry (Gas Research Institute, 1998) that can enable identification of actively moving land masses when the ground displacement is only a few centimeters. This technology could be used repeatedly after a rainstorm or large earthquake to identify moving slides. Installation and operation of accelerometers at substations is intended to provide strong-motion data to facilitate rapid and remote damage assessment at key facilities. Improved fragility data for electric power equipment can be combined with accurate measurements of ground motions at substations to enable determinations of likely damage states within ten minutes or so of an earthquake (Savage et al., 1998).

CONCLUSIONS

Societal expectations of reliability and safety of electric power demand that utility companies, power generators, power transmission operators, and their regulators establish and maintain a clear understanding of the threats posed by geohazards and of the acceptable level of performance that the services should provide. This expectation has been largely met in recent earthquakes, landslides, and other geologic hazard events in California, but the future may bring more severe events than those that have been experienced recently. Fortunately, strategic and technological developments provide multiple means to improve the safety and reliability of electric power service in geohazardous conditions in cost-effective and practical ways. Continued cooperation and collaboration among industry, academia, state and federal agencies, and public officials will likely lead to a successful realization of the societal goals for safe and reliable electric power service.

ACKNOWLEDGMENTS

The authors wish to thank and acknowledge the support of Lloyd Cluff, Norman Abrahamson, and Eric Fujisaki from the Pacific Gas and Electric Company and Robert Strand from the California Energy Commission. The material in this paper was developed through numerous discussions and projects carried out with many talented and progressive individuals involved with geohazards and electric power systems in industry, academia, and government agencies. Their contributions are gratefully acknowledged.

AUTHOR PROFILES

William Savage received his PhD. in seismology from the University of Nevada at Reno. Dr. Savage joined the Pacific Gas and Electric Company as Senior Seismologist in 1986. He is currently the National Lifelines Coordinator with the USGS. Robert Anderson is a Certified Engineering Geologist in California. Mr. Anderson worked as an Associate Engineering Geologist with the California Integrated Waste Management Board from 1990 to 1998, and with the California Energy Commission's Engineering Office from 1999 to 2001. He is currently the Senior Engineering Geologist with the California Seismic Safety Commission.

SELECTED REFERENCES

ALA (American Lifelines Alliance), 2000, Web page on the ASCE website: *www.americanlifelinesalliance.org.*

Anad, Y. (ed.), 1985, Seismic experience data - Nuclear and other plants: American Society of Civil Engineers, 81 p.

Anagnos, T., 1999, Improvement of fragilities for electrical substation equipment: *in* Elliott, W., and McDonough, P., (eds.), Optimizing post-earthquake lifeline system reliability, Technical Council on Lifeline Earthquake Engineering monograph 16, p. 673-682.

Brune, J., 1999, Precarious rocks along the Mojave section of the San Andreas fault, California: Constraints on ground motion from great earthquakes: Seismological Research Letters, v. 70, no. 1, p. 29-33.

DMG (California Division of Mines and Geology), 1975, San Fernando earthquake of 9 February 1971: California Division of Mines and Geology Bulletin 196, 463 p.

DMG (California Division of Mines and Geology), 1995, The Northridge, California, earthquake of 17 January 1994: California Division of Mines and Geology Special Publication 116, 302 p.

DMG (California Division of Mines and Geology), 1997, Guidelines for evaluating and mitigating seismic hazards in California: California Division of Mines and Geology Special Publication 117, 74 p.

California Energy Commission, 1989, Recommended seismic design criteria for non-nuclear power generating facilities in California: Consultant's report by URS/John A. Blume and Associates for the California Energy Commission, 68 p.

Der Kiureghian, A., 1999, Fragility estimates for electrical substation equipment: *in* Elliott, W., and McDonough, P. (eds.), Optimizing post-earthquake lifeline system reliability, Technical Council on Lifeline Earthquake Engineering Monograph 16, p. 643-652.

DeLisle, M.J., 2001, Seismic hazard evaluation and liquefaction zoning in the City and County of San Francisco, California: in Ferriz, H., Anderson, R., (eds.), Engineering Geology Practice in Northern California: Association of Engineering Geologists Special Publication 12 and California Division of Mines and Geology Bulletin 210

EERI (Earthquake Engineering Research Institute), 1985, Learning from earthquakes, the Morgan Hill earthquake of April 24, 1984: Earthquake Spectra, v. 1, no. 3, 293 p.

EERI (Earthquake Engineering Research Institute), 1988, Learning from earthquakes, the Whittier Narrows earthquake of October 1, 1987: Earthquake Spectra, v. 4, no. 2, 190 p.

EERI (Earthquake Engineering Research Institute), 1990, Loma Prieta earthquake reconnaissance report: Earthquake Spectra, Supplement to v. 6, May 1990, 448 p.

EERI (Earthquake Engineering Research Institute), 1996a, Scenario for a magnitude 7.0 earthquake on the Hayward fault: Earthquake Engineering Research Institute HF-96, 109 p.

EERI (Earthquake Engineering Research Institute), 1996b, Learning from earthquakes, post-earthquake investigation field guide. no. 96-1, 144 p.

EERI (Earthquake Engineering Research Institute), 1996c, Northridge earthquake reconnaissance report: v. 1 [Supplement C to Volume 11].

Fujisaki, E., Matsuda, E., Fenves, G. M, Whittaker, A., and Gilani, A., 1999, Seismic qualification and fragility testing of porcelain transformer bushings: *in* Elliott, W., and Mc Donough, P., (eds.), Optimizing post-earthquake lifeline system reliability, Technical Council on Lifeline Earthquake Engineering monograph 16, p. 663-672.

Gas Research Institute, 1998, Satellite radar interferometry to detect and characterize slope motion hazardous to gas pipeline: a demonstration study of three sites: Consultant's report by Hartford Steam Boiler Inspection and Insurance Company for the Gas Research Institute, GRI-99/0096, 50 p.

Japanese Society of Civil Engineers, 1995, Preliminary report on the great Hanshin earthquake January 17, 1995: Japanese Society of Civil Engineers, special monograph, 346 p.

Kramer, S., 1996, Geotechnical earthquake engineering: Prentice Hall, (New York, New York), 653 p.

Matsuda, E., Savage, W., Williams, K., and Laugens, G., 1991, Earthquake evaluation of a substation network: in Lifeline Earthquake Engineering, Proceedings of 3rd. U. S. Conference, TCLEE/ASCE, (Los Angeles, California), August 22-23, p. 295-317.

Munroe, T., 1998, California economic outlook and key issues, 1999 and beyond: Pacific Gas and Electric Company, (San Francisco, California), 70 p.

Petersen, M., Bryant, W., Cramer, C., Tianqing, C., Reichle, M., Frankel, A., Lienkaemper, J., McCrory, P., Schwartz, D., 1996, Probabilistic seismic hazard assessment for the state of California: Division of Mines and Geology Open-file Report 96-08, 33 p.

Petersen, M., Beeby, D., Bryant, W., Cao, C., Cramer, C., Davis, J., Reichle, M., Saucedo, G., Tan, S., Taylor, G., Toppozada, T., Treiman, J., and Willis, C., 1999, Seismic shaking hazard maps of California: Division of Mines and Geology Map Sheet 48.

Savage, W.U., 1995, Utility lifelines performance in the Northridge earthquake: *in* The Northridge, California earthquake of January 17, 1994, Division of Mines and Geology Special Publication 116. p. 153-162.

Savage, W. U., Matsuda, E. N., and Cluff, L. S., 1995, Long-term risk-management strategy for reducing earthquake vulnerability of gas and electric systems: *in* Proceedings of the 5th International Conference on Seismic Zonation, October 17-19, (Nice, France), p. 208-214.

Savage, W. U., Abrahamson, N. A., and McLaren, M. K., 1998, Gas and electric utility application of rapid earthquake information for earthquake, tsunami, and volcanic eruption hazards: Abstract *in* Proceedings of the International Conference on Modern Preparation and Response Systems for Earthquake, Tsunami, and Volcanic Hazards, (Santiago, Chile), April 27-30.

Schiff, A. (ed,), 1997, Guide to post-earthquake investigation of lifelines: Technical Council of Lifeline Earthquake Engineering, Monograph 11, American Society of Civil Engineers, (Reston, Virginia), 697 p.

Schiff, A. (ed,), 1999, Guide to improved earthquake performance of electric power systems: American Society of Civil Engineers Manuals and Reports on Engineering Practice 96, American Society of Civil Engineers, (Reston, Virginia), 341 p.

WGCEP (Working Group on California Earthquake Probabilities), 1999, Probabilities of large earthquakes in the San Francisco Bay region, California: U.S. Geological Survey Open-File Report 99-517, 60 p.

ENGINEERING GEOLOGY OVERVIEW OF MUNICIPAL SOLID WASTE LANDFILLS IN NORTHERN CALIFORNIA

SCOTT WALKER[1] AND ROBERT ANDERSON[2]

INTRODUCTION

Municipal solid waste landfills (landfills) are an extremely important and controversial part of the public infrastructure. Their performance depends to a large extent on natural geologic conditions, so engineering geology plays a key role in designing adequate controls to protect public health and the environment. As with other complex civil engineering works, the engineering geologist involved in landfill projects should be well versed in the specific geologic aspects of landfills, and in the environmental regulatory requirements that apply to them. Engineering geology is particularly important in landfill siting, design and construction, selection of earthen final covers, assessment of static and dynamic stability, environmental monitoring and control, and closure and postclosure maintenance. This paper provides an overview of these topics to assist engineering geologists new to landfill projects in northern California, and engineering geologists that desire more specific information for application to projects in northern California.

Case histories of engineering geology work in existing landfills throughout northern California (Table 1) are helpful in addressing the challenges of new projects. As of January 1, 1999, there were approximately 185 active landfills statewide, of which approximately half are in northern California (for the purposes of this paper, northern California includes counties inclusive and north of Monterey, Kings, Tulare, and Inyo Counties). In October 1991 the number of active landfills statewide was approximately 270. This paper focuses on landfills that have received municipal solid waste since October 1991. Much of the information presented can also be applied to older sites, including those that may not have accepted municipal solid waste. Approximately 2,500 solid waste disposal sites statewide closed before October 1991, based on California Integrated Waste Management Board records.

Landfills in northern California are located in a diverse range of geologic settings (Harden, 1996; 2001, this volume), including the Basin and Ranges (Great Basin), Cascade Ranges, Coast Ranges, Great Valley (Central Valley), Klamath Mountains, Modoc Plateau, and Sierra Nevada.

The following topics are listed in the order of appearance in the paper, as a quick guide for finding material on the reader's topic of interest:

- Regulatory framework
- Landfill siting
- Design and construction
- Landfill containment systems
- Alternative earthen final covers
- Foundation and slope stability
- Seismic stability
- Seismic performance of landfills
- Environmental monitoring and control

[1]California Environmental Protection Agency
Integrated Waste Management Board
Remediation, Closure and Technical Services
8800 Cal Center Drive
Sacramento, CA 95826
swalker@ciwmb.ca.gov

[2]California Seismic Safety Commission
1755 Creekside Oaks Drive, Suite 100
Sacramento, CA 95833
banderson@quiknet.com

County	Facility	Closure	Waste footprint (acres)	Geologic setting	Gas control	Ground Water monitoring & control	Liner system	Final cover system
Alameda	Tri-Cities	2002	115	Coast Ranges San Francisco Bay sediments	Active—Flare	Evaluation	UL	CCL
Alameda	Altamont	2007	206	Coast Ranges—tertiary sedimentary—(great valley sequence)	Active—Flare	Corrective Action	UL-GM/CCL	CCL-GM/CCL
Alameda	Vasco Road	2018	222	Coast Ranges—ternary sedimentary—(great valley sequence)	Active—Flare	Detection	UL-GM-geocomposite/GM	CCL-GM/CCL
Amedor	Buena Vista	2006	56	Sierra Nevada—foothills—tertiary sedimentary (Ione Fm)	None	Detection	UL-CCL-GM/CCL	CCL-GM/CCL
Butte	Neal Road	2018	87	Cascade Range—intermediate volcanic/sediments (Tuscan Fm)	None	Corrective Action	UL-CCL-GM/CCL	GM-GM/CCL or GM/CCL
Calevoras	Rock Creak	2032	57	Sierra Nevada foothills—metamorphic	None	Detection	CCL-GM/CCL-GM/GCL	GM/CCL
Colusa	Evens Road	1995	14	Great (Sacramento) Valley—(Tehame Fm.)	None	Detection	UL	CCL
Colusa	Stonyford	2059	4	Coast Ranges—alluvial	None	Detection	UL	CCL
Contra Costa	West Contra Costa	2000	160	Coast Ranges San Francisco Bay sediments	Active—Flare	Corrective Action	UL	CCL
Contre Costa	Acme Sanitary	2001	109	Coast Ranges San Francisco Bay sediments—Debris spreed failure—1978	Active—Flare	Corrective Action	UL-CCL	CCL
Contra Costa	Contra Costa Pittsburg-GBF	1992	74	Coast Ranges—tertiary sedimentary—(great valley sequence)	Active—Flare Proposed	Evaluation	UL	CCL
Contra Costa	Keller Canyon	2098	271	Coast Ranges—tertiary sedimentary—(great valley sequence)—native slope failures—1997-98	Active—Flare	Detection	GM/CCL-FM/GCL (side)-GM/GCL/GM	GM/CCL
Del Norte	Crescent City	2002	23	Coast Ranges Northern coastal zone dune sands	Passive Venting	Detection	UL	GM
El Dorado	Union Mine	2015	40	Sierra Nevada foothills—metamorphic	Active—Flare	Detection	UL-GM/GCL-GM/GCL(side)	CCL-GCL-GM/CCL
Fresno	Chateau Fresno	1996	75	Great (San Joaquin) Valley	Active—Flare	Corrective Action	UL-CCL	GM
Fresno	Clovis	2029	55	Great (San Joaquin) Valley	None (Violation 10/99)	Corrective Action	UL-CCL-GM/CCL	CCL-GM/CCL
Fresno	Coalinga	2034	52	Coast Ranges—tertiary sedimentary	None	Detection	UL	CCL
Fresno	American Ave	2028	367	Great (San Joaquin) Valley	None	Detection	UL-GM/CCL	GM/CCL
Fresno	Orange Ave	2005	29	Great (San Joaquin) Valley	Active—Flare	Evaluation	UL	CCL or GM
Fresno	Chestnut Ave	1994	32	Great (San Joaquin) Valley	Active—Flare	Corrective Action	UL	GM
Glenn	Glenn County	2021	50	Great (Sacramento) Valley	None	Detection	UL	CCL
Humboldt	Cummings Rd	2007	38	Coast Ranges—tertiary sedimentary	Active—Flare (Violation 10/99)	Corrective Action	UL-GM/CCL-GM/GCL	GM
Inyo	Lone Pine	2055	27	Basin and Ranges—alluvial	None	Evaluation	UL	CCL
Inyo	Independence	2045	21	Basin and Ranges—alluvial	None	Detection	UL	CCL
Inyo	Bishop Sunland	2097	68	Basin and Ranges—alluvial	None	Evaluation	UL	CCL
Inyo	Shoshone	2074	5	Basin and Ranges—alluvial	None	Detection	UL	CCL
Inyo	Tecopa	2019	9	Basin and Ranges—alluvial	None	Detection	UL	CCL
Inyo	Furnace Crk	1996	10	Basin and Ranges—alluvial	None	Detection	UL	Altern Earthen
Kings	Avenal	2039	51	Coast Ranges—(Tulare Fm)	None	Detection	UL	CCL
Kings	Hanford	1998	79	Great (San Joaquin) Valley	Active Flare (Violation 10/99)	Evaluation	UL	GCL
Kings	Mustang Hill-Not constructed	2040	41	Coast Ranges—(Tulare Fm)	NA	NA	GM/GCL	GM/GCL
Kings	Kettleman Hills	2025	43	Coast Ranges—tertiary sedimentary	None	Detection No beneficial use	GM/GM/CCL/GM/CCL	GM/CCL
Lake	Eastlake	2027	31	Coast Ranges—marine sedimentary—(great valley sequence)	None	Detection	UL-GM/CCL	GM-GM/GCL
Lassen	Bieber	1992	8	Cascade Ranges—volcanic/alluvial	None	Evaluation	UL	GCL
Lassen	Madeline	1997	<1	Basin and Ranges—alluvial	None	None	UL	GCL
Lassen	Ravendale	1997	<1	Basin and Ranges—alluvial	None	None	UL	GCL
Lassen	Bass Hill	2010	<10?	Basin and Ranges—alluvial	None	None	UL	No Closure Plan
Lassen	Westwood		<5?	Cascade Ranges—volcanic/alluvial	None	None	UL	No Closure Plan
Lassen	Sierra Army Depot	2032	32	Basin and Ranges—alluvial	None	Evaluation	UL	GM
Madera	Fairmead	2026	92	Great (San Joaquin) Valley	Active—Flare	Evaluation	UL-CCL-GM/CCL	CCL-GM/CCL-Altern Earthen
Marin	Redwood	2039	195	Coast Ranges San Francisco Bay sediments	Active—Flare	Corrective Action	UL-GM/CCL	GM/CCL
Marin	West Marin	1998	15	Coast Ranges—marine sedimentary (Franciscan Fm)	None	Evaluation	UL	CCL
Mariposa	Mariposa Co	2081	40	Sierra Nevada—foothills—ultramafic intrusive serpentine	None	Detection	UL-GM/CCL	GCL-GM/GCL
Mendocino	Ceeper	1995	16	Coast Range—coastal zone marine terrace/Franciscan Fm	Passive Venting	Corrective Action	UL	GM
Mendocino	Laytonville	1993	7	Coast Range—Marine Sedimentary—Franciscan Fm	No	Detection	UL	GCL

Table 1. Northern California Subtitle D landfills (UL - unlined; CCL - compacted clay liner; GCL - geosynthetic clay liner; GM - geomembrane; Altern Earthen - monofill alternative earthen cover.).

County	Facility	Closure	Waste footprint (acres)	Geologic setting	Gas control	Ground Water monitoring & control	Liner system	Final cover system
Mendocino	South Coast	2015	5	Coast Range Marine Sedimentary (Franciscan Fm.)—Site is within San Andreas Fault Zone	No	Corrective Action	UL	CCL
Mendocino	City of Ukiah	2000	42	Coast Range Marine Sedimentary (Franciscan Fm.)	See Comment	Corrective Action	UL	CCL
Mendocino	City of Willits	1997	19	Coast Ranges—Marine Sediments (Franciscan Fm.)—native slope failure 1994-95	Passive Venting	Detection	UL-GM	GM
Merced	Hwy 59	2012	110	Great (San Joaquin) Valley	None (Violation 10/99)	Detection	UL-GM/CCL	CCL
Merced	Billy Wright	2009	40	Coast Ranges—marine sedimentary—(great valley sequence)	None (Violation 10/99)	Detection	UL	CCL
Modoc	Alturus	2009	<107	Modoc Plateau—alluvial	None	Detection	UL	No Closure Plan
Modoc	Eagleville	1993	2	Basin and Ranges—alluvial	None	None	UL	GCL
Modoc	Fort Bidwell	1193	1	Basin and Ranges—alluvial	None	Detection	UL	GCL
Modoc	Lake City	1993	3	Modoc Plateau—alluvial	None	None	UL	GCL
Modoc	Cedarville	1993	2	Basin and Ranges—alluvial	None	None	UL	GCL
Mono	Walker	2260	10	Basin and Ranges—alluvial	None	Evaluation	UL	GCL
Mono	Bridgeport	2135	13	Basin and Ranges—alluvial	None	Evaluation	UL	GCL
Mono	Pumice Valley	2036	20	Basin and Ranges—alluvial	None	None	UL	CCL
Mono	Benton Crossing	2014	52	Basin and Ranges—alluvial	None	Evaluation	UL	CCL
Mono	Chalfant	2197	7	Basin and Ranges—alluvial	None	Evaluation	UL	GCL
Mono	Benton Crossing	2014	7	Basin and Ranges—alluvial	None	Detection	UL	GCL
Monterey	Lewis Rd	1999	14	Coast Ranges—tertiary sediments—dune sands	Active—Flare (Violation 10/99)	Evaluation	UL	GCL
Monterey	Johnson Canyon	2045	80	Coast Ranges—plutonic (granite)	Active—Flare (Violation 10/99)	Detection	UL-CCL-GM/GCL	GCL-GM/CCL
Monterey	Jolon Rd	2018	24	Coast Ranges—tertiary sedimentary	None	Detection	UL-GM/CCL	CCL-GM/CCL
Monterey	Crazy Horse	2008	72	Coast Ranges—tertiary sedimentary/dune sands	Active—Flare (Violation 10/99)	Corrective Action	UL-GM/CCL	CCL-GM
Monterey	Monterey Peninsula	2084	315	Coast Ranges—coastal zone dune sands	Active—Flare	Detection	GM/CCL-UL	GM/GCL
Napa	American Canyon	2000	97	Coast Ranges—San Francisco Bay sediments	Active—Flare	Corrective Action	UL	CCL
Napa	Clover Flat	2020	44	Coast Ranges—marine sedimentary	None	Detection	UL-GM/GCL	CCL-GM or GCL/CCL
Napa	Berryessa Garbage	1992	7	Coast Ranges—marine sedimentary	None	Detection	UL	CCL
Nevada	McCourtney Rd	1997	36	Sierra Nevada foothills—mafic/ultramafic intrusive	Active—Flare	Corrective Action	UL	GCL
Placer	Berry Street	1992	13	Great (Sacramento) Valley	None	None	UL	CCL
Placer	W. Regional	2016	231	Great (Sacramento) Valley	Active—Flare	Corrective Action	UL-GM/CCL	CCL-GM/CCL
Placer	Eastern Regional	1994	36	Sierra Nevada—plutonic (granodiorite)/alluvial	Active—Flare (Planned)	Detection	UL	CCL or GCL
Plumas	Portola	2022	8	Basin and Ranges—plutonic (granodiorite)	None	Detection	UL	CCL
Plumas	Gopher Hill	2016	13	Sierra Nevada—metamorphic	None	Corrective Action	UL	GM
Plumas	Chester	2045	28	Cascade Ranges—volcanic	None	Detection	UL	GM
Sacramento	Kiefer	2035	667	Great (Sacramento) Valley—tertiary sediments (Mehrten/Laguna Fms.)	Active—Flare	Corrective Action	UL-GM/CCL-GM/GCL	CCL-GM/CCL
Sacramento	Dixon Pit	1999	22	Great (Sacramento) Valley	Active—Flare (Violation 10/99)	Detection	UL	CCL
Sacramento	Sacramento City	1994	130	Great (Sacramento) Valley (ground water <5')	Active—Flare	Corrective Action	UL	CCL
Sacramento	L & D	2018	146	Great (Sacramento) Valley	Active—Venting	Corrective Action	UL-GM/CCL	CCL-GM
San Benito	John Smith Rd	2044	33	Coast Ranges—marine sedimentary—(great valley sequence)	None	Corrective Action	UL	CCL
San Joaquin	Austin Rd	2053	218	Great (Sacramento) Valley	Active—Flare	Corrective Action	UL-GM/CCL	CCL-GM/CCL
San Joaquin	French Camp	2010	60	Great (Sacramento) Valley	None	Evaluation	UL	CCL
San Joaquin	Harney Lane	1994	97	Great (Sacramento) Valley	Active—Flare	Corrective Action	UL	CCL
San Joaquin	Foothill	2054	50	Sierra Nevada—foothills—tertiary sedimentary (Mehrten Fm.)	None	Detection	UL-GM/CCL	CCL-GM/CCL
San Joaquin	Corral Hollow	1995	30	Great (Sacramento) Valley	None	Evaluation	UL	CCL
San Joaquin	Forward	2006	129	Great (Sacramento) Valley	None	Corrective Action	UL-CCL-GCL-GM/CCL	CCL-GM/GCL
San Joaquin	North County	2033	185	Great (Sacramento) Valley	None	Detection	GM-GM/GCL	CCL
San Mateo	Ox Mtn. (Connda Los Trancos)	2023	184	Coast Ranges—plutonic (granodiorite) (San Andreas Fault—3 miles)	Active—Flare	Detection	UL-CCL-GM/CCL-GM/GCL (side)	CCL-GCL or GM
San Mateo	Hillside	2001	30	Coast Ranges—marine sedimentary—(Franciscan Fm.)	Active—Flare	Evaluation	UL-CCL-GM/CCL	GM/CCL
San Mateo	Burlingham	1994	41	Coast Range San Francisco Bay sediments	Active—Flare	Evaluation	UL	GCL-GM
Santa Clara	Pacheco Pass	2004	91	Coast Ranges—marine sedimentary Holocene fault (Coyote Lake segment of Calaveras Falut) within formerly proposed expansion	Active—Flare (Violation 10/99)	Corrective Action	UL-GM/CCL	Altern. Earthen-GM/CCL
Santa Clara	Shoreline-Mtn. View (Vista)	1993	150	Coast Ranges San Francisco Bay sediments	Active—Flare	Evaluation	UL-CCL	CCL

Table 1 (cont). Northern California Subtitle D landfills (UL - unlined; CCL - compacted clay liner; GCL - geosynthetic clay liner; GM - geomembrane; Altern. Earthen - monofill alternative earthen cover.).

County	Facility	Closure	Waste footprint (acres)	Geologic setting	Gas control	Ground Water monitoring & control	Liner system	Final cover system
Santa Clara	Sunnyvale	1994	92	Coast Ranges San Francisco Bay sediments	Active—Flare	Corrective Action	UL	CCL
Santa Clara	Palo Alto	2011	126	Coast Ranges San Francisco Bay sediments	Active—Flare	Detection	UL	CCL
Santa Clara	Newby Island	2016	313	Coast Ranges San Francisco Bay sediments	Active—Flare	Detection	UL-GM/CCL	CCL-GM/CCL
Santa Clara	Kirby Canyon	2025	311	Coast Ranges—serpentine	Active—Flare	Detection	CCL-GM/CCL	GM/CCL
Santa Clara	Guadalupe	2020	115	Cascade Range—marine sedimentary-tertiary volcanic (Franciscan/Temblor Fm.)	Active—Flare	Evaluation	UL-CCL-GM/CCL	CCL-GM/CCL-CCL (side)
Santa Clara	All Purpose	1993	25	Coast Ranges San Francisco Bay sediments	Active—Flare	Detection	UL	CCL
Santa Cruz	Santa Cruz	2037	58	Coast Ranges—marine sedimentary	Active—Flare	Corrective Action	UL-GM/CCL	CCL-GM/CCL
Santa Cruz	City of Watsonville	2023	51	Coast Ranges—coastal dune sands—tertiary sediments	Active—Flare	Evaluation	UL-GM/GCL	CCL or GCL-GM/CCL
Santa Cruz	Ben Lomond	1994	24	Coast Ranges—tertiary sediments	Active—Flare	Corrective Action	UL	CCL
Santa Cruz	Buena Vista	2021	40	Coast Ranges—coastal dune sands-tertiary sediments	Active—Flare	Corrective Action	UL-GM/CCL	CCL-GM/CCL
Shasta	Redding (Benton)	1994	71	Great (Northern) Valley	Active—Flare	Detection	UL	CCL
Shasta	Anderson	2049	167	Great (Northern) Valley	Active—Venting	Detection	UL-GM/CCL	CCL-GM
Shasta	Intermountain	1993	4	Cascade Range—volcanic	None	Detection	UL	CCL
Shasta	West Central	2013	120	Great (Northern) Valley	None	Detection	UL-CCL-GM/CCL-GM/GCL	CCL-GM/CCL
Sierra	Loyalton	2032	29	Sierra Nevada—alluvial	None	Detection	UL	CCL
Siskiyou	McCloud	1995	13	Cascade Ranges—alluvial	None	Detection	UL	CCL
Siskiyou	Yreka	2109	547	Cascade Range—volcanic/alluvial	None	Detection	UL	CCL
Siskiyou	Black Butte	2002	27	Cascade Range—volcanic/alluvial	None	Detection	UL	CCL
Siskiyou	Weed	1995	6	Cascade Range—alluvial	None	Detection	UL	Altern. Earthen
Siskiyou	Happy Camp	1996	3	Klamath Mtns —metamorphic	None	Detection	UL	CCL
Siskiyou	Tulelake		9	Modoc Plateau—alluvial	None	Evaluation	UL	CCL
Siskiyou	Kelly Gulch	1994	1	Klamath Mtns —metamorphic	None	Detection	UL	Altern. Earthen
Siskiyou	Cecilville	1994	1	Klamath Mtns —metamorphic	None	Detection	UL	Altern. Earthen
Siskiyou	Lava Beds	1995	1	Modoc Plateau—volcanic	None	Detection	UL	Altern. Earthen
Siskiyou	New Tenent	1995	10	Cascade Range—volcanic	None	Detection	UL	Altern. Earthen
Siskiyou	Rogers Creek	1994	1	Klamath Mtns —metamorphic	None	Detection	UL	Altern. Earthen
Siskiyou	Hotelling	1994	3	Klamath Mtns —metamorphic	None	Detection	UL	Altern. Earthen
Solano	B & J Drop Box	2055	256	Great (Sacramento) Valley—alluvial—ground water <5'	None	Detection	UL-GM/CCL-GM/GCL (side)	CCL (side) Gm/CCL (top)
Solano	Rio Vista	1992	12	Great (Sacramento) Valley Sacramento River floodplain sediments	None	Detection	UL	CCL
Solano	Potrero Hills	2059	190	Coast Ranges—tertiary sedimentary	Active—Flare	Detection	CCL-GM/CCL-GM/GCL (side)	CCL-GM/CCL (Altern. Earthen test
Sonoma	Central	2014	172	Coast Ranges—marine sedimentary	Active—Flare	Corrective Action	UL-GM/GCL	GCL-GM/GCL
Sonoma	Annapolis	1995	5	Coast Ranges—marine sedimentary—(Franciscan Fm.)	None	Corrective Action	UL	GCL
Sonoma	Healdsburg	1993	27	Cascade Ranges—nonmarine sedimenta	None	Corrective Action	UL	CCL
Sonoma	Casa Grande	1993	9	Coast Ranges—fluvial	None	Detection	UL	CCL
Stanislaus	Fink Rd	2019	216	Coast Ranges—marine sedimentary	None	Corrective Action	UL-CCL-GM/CCL	CCL-GM/CCL
Tahama	Red Bluff	2003	33	Great (Northern) Valley—alluvial	None	Detection	UL-GM/CCL	CCL-GM/CCL
Trinity	Weaverville	2004	13	Coast Ranges—alluvial	None	Corrective Action	UL	CCL
Tulare	Earlimart	1996	16	Great (San Joaquin) Valley	None	Detection	UL	GCL
Tulare	Exeter	2004	34	Great (San Joaquin) Valley	None	Detection	UL	CCL
Tulare	Teapot Dome	2005	71	Coast Ranges	None (Violation 10/99)	Detection	UL	CCL
Tulare	Woodville	2039	271	Great (San Joaquin) Valley	Active— Flare	Evaluation	UL-GM/GCL	GM
Tulare	Visalia	2019	127	Great (San Joaquin) Valley—alluvial	Active—Flare	Evaluation	UL	CCL
Tulare	Balence Rock	1998	10	Sierra Nevada—plutonic (granite)	None	Detection	UL	CCL
Tulare	Kennedy Meadows	2002	6	Sierra Nevada—alluvial	None	Detection	UL	CCL
Tuolumne	Big Oak Flat	2001	4	Sierra Nevada—foothills—metamorphic	None	Corrective Action	UL	CCL
Tuolumne	Central (Jamestown)	1996	16	Sierra Nevada—foothills—metamorphic	None	Corrective Action	UL-CCL	CCL
Yolo	Yolo Central	2020	347	Great (Sacramento) Valley—alluvial—ground water <5	Active—Flare	Corrective Action	UL-GM/GCL-GM (side)	GM/CCL
Yolo	U C Davis	2032	53	Great (Sacramento) Valley	Active— Flare	Corrective Action	UL-CCL-GM/CCL	CCL-GM/CCL
Yuba	Beale AFB	1997	88	Great (Sacramento) Valley	Passive Venting	Detection	UL	CCL-GM
Yuba	Ponderosa	1995	10	Sierra Nevada—foothills—metamorphic	None	Corrective Action	UL	CCL
Yuba	Yuba Sutter Disposal, Inc	1997	45	Great (Sacramento) Valley Yuba River floodplain sediments	Passive/active Venting	Corrective Action	UL-GM/CCL	CCL-GM/GCL (top)-GM (side)
Yuba	Yuba Sutter Disposal Area (YSDA)	1997	12	Great (Sacramento) Valley Yuba River floodplain sediments	None	None	UL	CCL-Altern. Earthen
Yuba	Ostrom Rd	2038	221	Sierra Nevada—foothills—metamorphic	None	Detection	GM/CCL	GM/CCL

Table 1 (cont). Northern California Subtitle D landfills (UL - unlined; CCL - compacted clay liner; GCL - geosynthetic clay liner; GM - geomembrane; Altern. Earthen - monofill alternative earthen cover.).

- Groundwater monitoring and corrective action
- Corrective action and corrective action financial assurance
- Contamination of groundwater by landfill gas
- Surface water control
- Landfill gas monitoring and control
- Closure and postclosure maintenance and landuse
- Cost estimates for closure and postclosure maintenance
- Postclosure landuse
- Summary

REGULATORY FRAMEWORK

Landfills are regulated in California by a complex framework of federal, state, and local government codes and regulations (Table 2). These requirements control the application of engineering geology practice to landfill projects. Engineering geologists may also play a major role in preparing and coordinating permit applications, regulatory documents, and responses to comments from agencies and the public. An overall understanding of this regulatory framework is therefore essential in applying engineering geology practice to landfills.

National regulatory standards for landfills that operated on or after October 9, 1991 are contained in 40 CFR Part 258 (RCRA Subtitle D), promulgated by the United States Environmental Protection Agency (U.S. EPA). Implementation and enforcement of Subtitle D is primarily through approved state permit programs that must be equivalent or more stringent than Subtitle D. California is one of these approved states. U.S. EPA does not independently enforce Subtitle D where there is an approved state program. However, citizens may seek enforcement of Subtitle D independent of any state enforcement program by means of citizen suits in federal court under section 7002 of RCRA.

The California Integrated Waste Management Board (CIWMB) and State Water Resources Control Board (SWRCB) jointly implement California's Subtitle D program. The program is consolidated within California Code of Regulations Title 27 (27 CCR), Division 2. These regulations are also applicable in part to closed or inactive landfills that ceased receiving waste prior to the effective date of Subtitle D, and to solid and liquid waste disposal sites that exclude municipal solid waste. Air emission criteria for Subtitle D landfills are governed by the federal Clean Air Act New Source Performance Standards and Emission Guidelines. These requirements are implemented in California by local air districts (APCD/AQMD) and the California Air Resources Board (CARB).

In addition to the above the requirements, land use planning functions of local government can play a prominent role in the regulation of landfill projects and incorporation of public input. These functions primarily address implementation of the California Environmental Quality Act (CEQA), local codes and ordinances, and land use permits.

LANDFILL SITING

As in most areas of the country, siting new landfills in California is a daunting task because of pervasive negative public perception ("not in my backyard" or "NIMBY"). Siting projects for new landfills can expect to be legally challenged to the fullest extent and take 10 years or more and millions of dollars before waste is accepted or the project abandoned. The difficulty in siting new landfills is evidenced by the fact that only three new landfills became operational in northern California in the 1990's (Keller Canyon, Contra Costa County; North County, San Joaquin County; and Ostrom Road, Yuba County). Because of the difficulty in siting new landfills, most siting projects have focused on new regional landfills and lateral and vertical expansions of existing facilities.

New landfill design has recently concentrated on construction of regional landfills of immense capacity and proportions, called "megafills". Waste is transported to these facilities mainly by rail haul and large waste transfer trucks. Two "megafills" in southern California have recently been permitted but are not yet constructed. They include the Mesquite Regional Landfill (Imperial County) and the Eagle Mountain Landfill (Riverside County). The Mesquite Landfill has a total design capacity of 1,100,000,000 cubic yards. By contrast, the largest landfill in northern California, Kiefer Landfill (Sacramento County), was recently permitted for expansion to a total capacity of 127,000,000 cubic yards.

The Regional Water Quality Control Board (RWQCB) classifies landfill waste management units for siting purposes according to their ability to contain wastes. Class III landfill units typically allow disposal of municipal solid waste (nonhazard-

RCRA Subtitle D Program		
Description	**Regulatory citation**	**Implementing agency**
General scope and applicability	27 CCR, Chapter 1, Article 1	CIWMB & SWRCB
Waste classification	27 CCR, Chapter 3, Subchapter 2, Article 2	SWRCB
Waste unit/facility/site classification and siting	27 CCR, Chapter 3, Subchapter 2, Article 3	SWRCB & CIWMB
Waste unit construction standards	27 CCR, Chapter 3, Subchapter 2, Article 4	SWRCB
Water quality monitoring and response	27 CCR, Chapter 3, Subchapter ?, Article 1	SWRCB
Operating criteria	27 CCR, Chapter 3, Subchapter 4	CIWMB
Landfill gas monitoring and control	27 CCR, Chapter 3, Subchapter 4, Article 6	CIWMB
Closure and postclosure maintenance standards	27 CCR, Chapter 3, Subchapter 5	SWRCB & CIWMB
Waste discharge requirements (WDRs) and solid waste facilities permit (SWFP)	27 CCR, Chapter 4, Subchapter 3	SWRCB (RWQCB) & CIWMB (Local Enforcement Agency)
Closure and postclosure maintenance plans	27 CCR, Chapter 4, Subchapter 4	CIWMB & SWRCB
Financial assurances (closure, postclosure, operating liability, and corrective action)	27 CCR, Chapter 6	CIWMB & SWRCB
Air emission requirements		
New Source Performance Standards (NSPS) and Emissions Guidelines (EG) for municipal solid waste landfills	Rules adopted by individual APCD/AQMD (e.g. Regulation 8 Rule 34 of Bay Area AQMD and Rule 1150.1 of South Coast AQMD)	APCD/AQMD & CARB
Permits to construct and operate	Rules adopted by individual APCD/AQMD	APCD/AQMD
Other common requirements		
Evaluation and public notification of environmental impacts	California Environmental Quality Act (CEQA)	Local or State lead (In most cases City or County)
Local land use permits	Local codes and ordinances	City or County
Stormwater and discharges to surface waters	National Pollutant Discharge Elimination System (NPDES)	SWRCB
Wetlands protection	Federal Clean Water Act SWRCB Resolution 93-62 California Fish and Game Code	U.S. Army Corps of Engineers SWRCB & California Department of Fish and Game
Endangered plants and animals	Federal Endangered Species Act California Fish and Game Code	U. S. Fish & Wildlife Service & Cal. Department of Fish & Game

Table 2. Regulatory framework for California landfills.

ous solid waste, inert solid waste, and sludges from household, commercial, and industrial sources). Class II units allow disposal of designated wastes determined by the RWQCB to be nonhazardous wastes, but which may contain soluble pollutants that could be released in concentrations exceeding applicable water quality objectives and could cause degradation of waters of the state. Designated solid wastes are determined on a site-specific basis and typically include industrial ashes, sludges, contaminated soils, and hazardous wastes granted a variance. Depending on site-specific permit requirements, Class II units may include solely designated wastes, or a mixture of designated, nonhazardous, and municipal solid waste. Class II landfills in northern California accepting municipal solid waste include Altamont (Alameda County), B&J Drop Box (Solano County), Buena Vista (Amador County), Forward (San Joaquin County), Keller Canyon (Contra Costa County), Ostrom Road (Yuba County), Rock Creek (Calaveras County), and West Contra Costa (Contra Costa County). Class II units may also be surface impoundments for containment of liquid wastes such as landfill leachate. Each classification has separate siting standards, with Class II being more stringent than Class III. Siting criteria in California's Subtitle D program are summarized in Table 3.

Description	Class III landfills	Class II landfills
Geologic setting	Shall not be located within areas of potential rapid geologic change unless the RWQCB find that containment structures preclude failure	Same as Class III
Foundation	Shall provide support capable of withstanding hydraulic pressure gradients to prevent failure due to settlement, compression, or uplift	Same as Class III
Ground rupture	Shall not be located on known Holocene fault	200' Setback from known Holocene fault
Seismicity	Shall withstand the effects of seismic ground motions resulting from at least the Maximum Probable Earthquake (MPE)	Shall withstand the effects of seismic ground motions resulting from at least the Maximum Credible Earthquake (MCE)
Groundwater separation	Shall ensure wastes will be a minimum of 5-feet above highest anticipated elevation of groundwater unless engineered alternative exemption granted	Same as Class III
Flooding and tidal waves	Shall prevent inundation or washout due to floods with a 100-year return period and tsunamis, seiches, and surges	Same as Class III
Airport safety	Must demonstrate no bird hazard to aircraft (only municipal solid waste (MSW) landfills)	Same as Class III
Wetlands	Shall not be located in wetlands unless protected and impacts mitigated in accordance with Clean Water Act and State wetlands laws (Incorporated by reference from 40 CFR 258.12 & Section 404 of Clean Water Act)	Same as Class III

Table 3. Summary of siting criteria for California landfills (27 CCR, Chapter 3, Subchapter 2, Article 3).

The siting of new landfills and expansions involves a team of experts from multiple disciplines, including engineers, planners, environmental specialists, engineering geologists, and lawyers. Landfill siting studies typically include extensive site-specific geologic, geotechnical, and hydrogeologic exploration and characterization, not only for compliance with regulatory criteria and environmental impact analysis, but also as a basis for planning economic landfill design, construction, operation, and environmental monitoring and control. Table 4 provides a summary of engineering geology aspects of landfill siting studies.

DESIGN AND CONSTRUCTION

Design and construction of landfills involves engineers, engineering geologists, and contractors to prepare and implement landfill design plans and specifications. As part of the design and construction team, engineering geologists are primarily involved in the assessment of geologic and hydrogeologic site conditions, evaluation of soil or natural earthen material borrow sources, modeling the performance of these materials in containment system design, and in the evaluation of geologic factors for static and seismic stability analysis.

A major task of the engineering geologist is the assessment of the geologic and hydrogeologic site conditions with respect to the proposed landfill. This assessment is highly detailed and includes elements such as:

- Description and mapping of geologic units, stratigraphic units, and structural features (bedding, fractures, joints, faults) within one mile of the landfill
- In-grading geologic mapping
- Description of faulting and seismicity of the landfill site and adjacent region within 100 kilometers (62 miles) of the landfill
- Field determination of the hydraulic parameters of the soil or rock adjacent to the landfill (e.g., hydraulic conductivity, transmissivity)
- Documentation of the hydrogeology of the site, including compilation of recorded groundwater and tidal fluctuations
- Documentation of groundwater and surface water quality background
- Location of off-site landfills and other sites that may be potential sources of degraded groundwater or landfill gas

Engineering geologists routinely are in charge of locating and assessing borrow sources for soils that meet the engineer's specifications for construction and operation of the landfill.

Borrow sources may be developed for materials to be used as low permeability earthen components of

Aspect	Task description	References
Geology	Compile and evaluate existing geologic mapping data and reports for study area. Map geology in the field utilizing base maps, aerial photography, and remote sensing imagery as appropriate. Prepare geologic maps, cross sections, and reports for final presentation	California Division of Mines and Geology U. S. Geological Survey ASTM (1997) California Board of Registration for Geologists and Geophysicists
Geologic hazards	Compile and evaluate existing geologic hazard data for study area. Conduct field investigations as necessary to confirm and supplement existing data. Prepare reports for final presentation	California Division of Mines and Geology U. S. Geological Survey USEPA (1993a)
Faulting and seismicity	Conduct literature review of seismic and fault mapping studies for study area. Determine appropriate seismic parameters (MPE, MCE, ground acceleration). Evaluate potential occurrence of Holocene faults in study area or adjacent to study area if necessary by trenching, mapping, geophysical methods, and soil dating. Prepare reports for final presentation	California Division of Mines and Geology U. S. Geological Survey Richardson, et al. (1995) USEPA (1993a) California Board of Registration for Geologists and Geophysicists
Engineering properties of geologic materials	Conduct field sampling and evaluation utilizing borings, trenches, test pits, geophysical methods, and laboratory analyses to establish geologic material properties for study area (lithology, distribution, geotechnical properties, and applicability for use as construction materials). Conduct specialized studies as necessary on construction material sources and foundation and slope stability issues. Prepare reports for final presentation	ASTM (1997) TRB (1996) U. S. Department of Navy (1982) California Board of Registration for Geologists and Geophysicists
Hydrogeology	Conduct literature review and field investigation of ground water flow chacteristics and quality utilizing test borings, monitoring wells, aquifer test methods, and geophysical methods. Conduct modeling and tracer studies as necessary for specialized studies on environmental fate, transport, and hydraulic impacts. Prepare reports for final presentation	ASTM (1997) USEPA (1993a), (1993b), & (1986) U. S. Geological Survey California Department of Water Resources California Board of Registration for Geologists and Geophysicists
Baseline monitoring	Prepare and implement monitoring programs for baseline ground water and vadose zone quality and physical characteristics. Prepare reports for final presentation	ASTM (1997) USEPA (1993a), (1993b), & (1986)
Technical assistance and expert testimony	Review comments from public and agencies on engineering geology issues. Prepare responses and conduct testimony as necessary for administrative and court hearings and records	

Table 4. Engineering geology aspects of landfill siting studies.

liner and final cover systems, construction fill, rock and aggregate, and daily and intermediate cover. The availability of low cost soils can have a profound impact on the cost of building, operating and closing a landfill. If soils with properties appropriate for landfill construction or operation are not obtainable near the landfill, then other off-site sources need to be considered, or geosynthetic materials might need to be used to help replace the amount of soil needed for a particular landfill activity.

Borrow source evaluations will typically begin with the preliminary location of potential on-site and off-site sources for the specified materials. The potential on-site source is mapped and tested for the quality and quantities of soils that are being sought for use in the project. The assessment may include logging and sampling of boreholes, trenches, and test pits, in addition to testing of samples for geotechnical properties and conducting rippability seismic surveys if the soils are indurated. Borrow source evaluations also determine the types and amounts of the required materials available, and the quantity of overburden that must be removed to extract the target materials. Reclamation plans of excavations must also be implemented. Guidance for the evaluation of engineering properties of earthen materials is provided in U.S. Department of Navy (1982), U.S. EPA (1993b), TRB (1996), and ASTM (1997). Recommended guidance regarding assessment and development of borrow material sources specifically for landfills is also provided in Bolton (1995).

The role of engineering geologists regarding slope, foundation, and seismic stability aspects of design is to confirm the stability of the engineer's design in light of the specific geology of the substrate, and to propose design soil strength parameters for earthen construction materials to ensure that the containment structures are stable. Guidance for landfill seismic stability evaluations is provided in Kavazanjian (1999, 1998), Anderson (1997), Richardson et al. (1995), and U.S. EPA (1993a). Engineering geologists can also play an integral part in the earthquake preparedness planning for the site.

The engineering geologist may also be called upon to collect background data about the natural occurrence of methane and other gases (organic soils and sediments, oil or gas fields, asphalt seeps, and geothermal areas), and to establish a method to determine the differences between landfill gas and naturally occurring gases.

Landfill containment systems

The requirement for landfill liners is relatively recent, so the majority of landfills in northern California are unlined; however, active disposal areas are shifting to lined areas as existing footprints become full (Table 1). Subtitle D design criteria include performance and prescriptive requirements for landfill liner systems for new units and lateral expansions. The Subtitle D prescriptive design is a composite liner including an upper component with a minimum 30-mil thick (60-mil if HDPE) flexible geomembrane liner (GM) in direct contact with a lower component of at least two-feet of compacted earthen material (compacted clay liner or CCL). The CCL component must have a hydraulic conductivity of less than or equal to 1×10^{-7} cm/sec. Site-specific performance, or risk based alternative liner designs, are an option for approved Subtitle D programs. Engineered alternatives to prescriptive standards are allowed in California under 27 CCR section 20080(b). However, alternatives to the prescriptive composite liner design have been approved only for very few sites in California, except for side-slope liners and replacement of part, or all, of the CCL component by a geosynthetic clay liner (GCL).

The performance requirements for final cover systems are to minimize erosion and infiltration, and to have a permeability less than or equal to the permeability of any bottom liner system or natural subsoils to avoid the "bathtub effect". The "bathtub effect" refers to the concern that excessive infiltration over exfiltration at the base of the landfill would allow pollutants to concentrate in ponded leachate. The leachate would then pose a much higher threat to groundwater if a leak were to occur.

The prescriptive final cover design for an unlined landfill in California includes, from bottom to top, a minimum two feet thick foundation layer, a minimum one foot compacted clay infiltration-control layer with a hydraulic conductivity no greater than 1×10^{-6} cm/sec, and a minimum one foot earthen layer to resist erosion (this layer must be capable of sustaining plant growth). For a lined landfill, the prescriptive final cover must additionally have a geomembrane on top of the compacted clay infiltration-control layer. Although not specified in the regulations, many final covers include a drainage layer between the erosion and infiltration-control layers for slope stability purposes. A gas collection layer may also be required, especially when a geomembrane is used and there is no active gas control system. Final cover system design guidance is provided in Koerner and Daniel (1997) and U.S. EPA (1993a).

Geosynthetic materials have only recently been utilized on a widespread basis in northern California as landfill base liner and final cover components. In contrast, compacted clay liners started to be widely used in northern California in the late 1980's, and standard clay material sources (Table 5) and construction practices are now relatively well-established (Walker and Rosenbaum, 1995). GCL products are now becoming a cost-effective alternative for compacted clay liners because of lowering costs and more experience and comfort in the use of these products by engineers, regulators, and contractors.

Construction Quality Assurance (CQA) programs are required under California's Subtitle D program to ensure that construction of landfill containment systems is performed in accordance with approved design plans and specifications. The CQA plan must incorporate standard geotechnical testing of fills and field permeability testing of compacted clay components to establish correlation between index testing and the design hydraulic conductivity. Final documentation and certification must also be submitted to ensure that construction was in accordance with approved design criteria, plans, and specifications. Guidance for CQA of waste containment facilities is provided in U.S. EPA (1993c, 1994).

Alternative earthen final covers

There are increasing doubts about the performance of final cover systems using compacted clay infiltration-control layers, especially in arid and semi-arid areas where desiccation cracking is likely to occur. Clay-based final cover systems can also be expensive if borrow sources cannot be developed locally. Therefore, alternative earthen materials that use the natural moisture retention properties of soils and vegetation are rapidly gaining acceptance. Monofill alternative earthen final cover systems are constructed using a single soil type formed by a

Material source	Examples of landfills where used	Material characteristics (not for design purposes)
Ione Formation; commercial quarries; Amador County	Red Hill (Calaveras) Union Mine (El Dorado) Kiefer (Sacramento)	CL; PI =15 - 29%; ϕ = 19; c =150; K = 5.6 x 10^{-8} cm/sec (SDRI);
Commercial quarries and on-site (Ione Formation to Pleistocene); Placer County	Sacramento City (Sacramento) Western Regional (Placer)	CL; PI =12 -19%; K = <1 x 10^{-6} cm/sec (DRI);
San Francisco Bay muds; on-site and off-site sources; San Francisco Bay area	Acme (Contra Costa) American Canyon (Napa) All Purpose (Santa Clara)	CH-MH; PI 40 - 65 + %; ϕ = 8.5; c = 250; K = 3.5 x 10^{-8} cm/sec;
On-site soils Coast Ranges (Great Valley Sequence)	Altamont (Alameda) Potero Hills (Solano)	CH-CL; PI = 23 - 45%; K = <5 x 10^{-8} cm/sec (SDRI);
On-site soils (Victor Formation); Yuba County	Ostrom Rd; Ponderosa; YSDA; (Yuba)	CL; PI = 9 - 18%; ϕ =12.5; c = 890; K = 1 x 10^{-7} cm/sec;
On-site soils with admixture	Benton (Shasta) Harney Lane (San Joaquin)	Blended <5% commercial bentonite (Benton) In-place mixing of up to 30% Ione Clay (Harney Lane) Both required to achieve; K = <1 x 10^{-6} cm/sec (SDRI)

Table 5. Examples of Northern California low permeability earthen materials.

mixture of silt and sand with some clay. These final cover systems are also called evapo-transpiration (ET) covers and can include separate layers and capillary barriers. The earthen materials used are of higher hydraulic conductivity and are placed at lower density than the prescriptive standard compacted clay liners. Because of cost savings, ease of maintenance, and effectiveness, alternative earthen covers are also being considered in specific situations as a replacement for GM-based systems.

The Desert Research Institute is currently conducting an Alternative Cover Assessment Project (ACAP) funded primarily by U.S. EPA. This project will measure the field performance of alternative earthen final covers, improve numeric modeling capabilities and monitoring methods, and provide regional design guidance. Coupled with other ongoing research and pilot project efforts, this project is intended to provide performance data for alternative earthen cover options, so they can be approved where appropriate. At the present time, test pads are being required at most sites in California to demonstrate these systems on a site-specific basis. Two basic types of test pad monitoring programs are currently used. One type includes *in situ* moisture monitoring probes to measure the time distribution of moisture movement through the test pad (time domain reflectometry (TDR) or capacitance systems). The other type uses a pan lysimeter system to measure percolation through the test pad. In both cases, site-specific precipitation data is collected and the system is monitored over multiple seasons. Computer models (e.g. HELP, LEACHM, UNSAT-H) are normally used to design the test pad and to process the field data to demonstrate acceptable performance. Alternative earthen final cover test pad projects are currently being conducted in northern California at the Potrero Hills Landfill, Solano County (TDR system) and Kiefer Road Landfill, Sacramento County (pan lysimeter system). Further information on this developing technology is provided in Reynolds et al. (1997) and Lass et al. (1997).

Foundation and slope stability

Foundation and slope stability of landfills became a recent focus of concern as a result of a massive failure, in March 1996, of the Rumpke Sanitary Landfill in Ohio. Kenter et al. (1997) concluded that a combination of the height and angle of the fill slope, buildup of leachate in the waste, excavation at the toe, and possibly saturated soils and weathered shale bedrock may have led to a deep foundation failure at the bottom of the waste mass. Schmucker and Hendron (1998) and Evans and Stark (1997) provide additional information and debate on the causes and lessons learned from the Rumpke failure. The Rumpke Landfill failure should heighten awareness of potential landfill failures in northern California, especially in sites with weak foundation materials, such as the San Francisco Bay muds, and in landslide-prone soils of the Coast Ranges. Although not at the catastrophic level of the Rumpke Landfill failure, other slope and foundation failures have occurred at northern California landfill sites. A review of two of these cases may be useful as precedents for addressing future stability problems.

Figure 1. Aerial photograph of the Acme Landfill failure in 1978. Failure scarp and toe can be seen toward the left side of the photograph.

In 1978 a failure occurred within the Acme Landfill, Contra Costa County, resulting in spreading of waste and soils onto an adjacent wetlands area (Figure 1). The failure was attributed to rapid loading of waste on weak San Francisco Bay mud. The rate of loading was modified to prevent additional failures, and inclinometers were installed in order to monitor movement in the waste mass. The landfill has remained stable ever since.

During abnormally high rainfall in 1997-98, the Keller Canyon Landfill, Contra Costa County, experienced a major slope failure within Tertiary sedimentary rocks (Eocene Markley Formation) of the Coast Ranges (Figures 2 and 3). The failure was interpreted as a wedge-like failure reactivated from an ancient landslide. The failure encroached on a planned liner expansion area that had to be delayed and redesigned. The recommended remedial alternative was to partially remove the slide and construct an earthfill toe buttress. The total excavation removed nearly 2.5 million cubic yards of landslide material and the redesign project has been completed successfully. Detailed description of the geology of the failure area and resultant remediation and liner design changes is provided in BFI (1998).

Seismic stability

Under Subtitle D, seismic design may be based on either the peak horizontal ground acceleration from U.S. Geologic Survey hazard maps for seismic impact zones, or be based on a site-specific analysis. Seismic impact zones are areas with 10% or greater

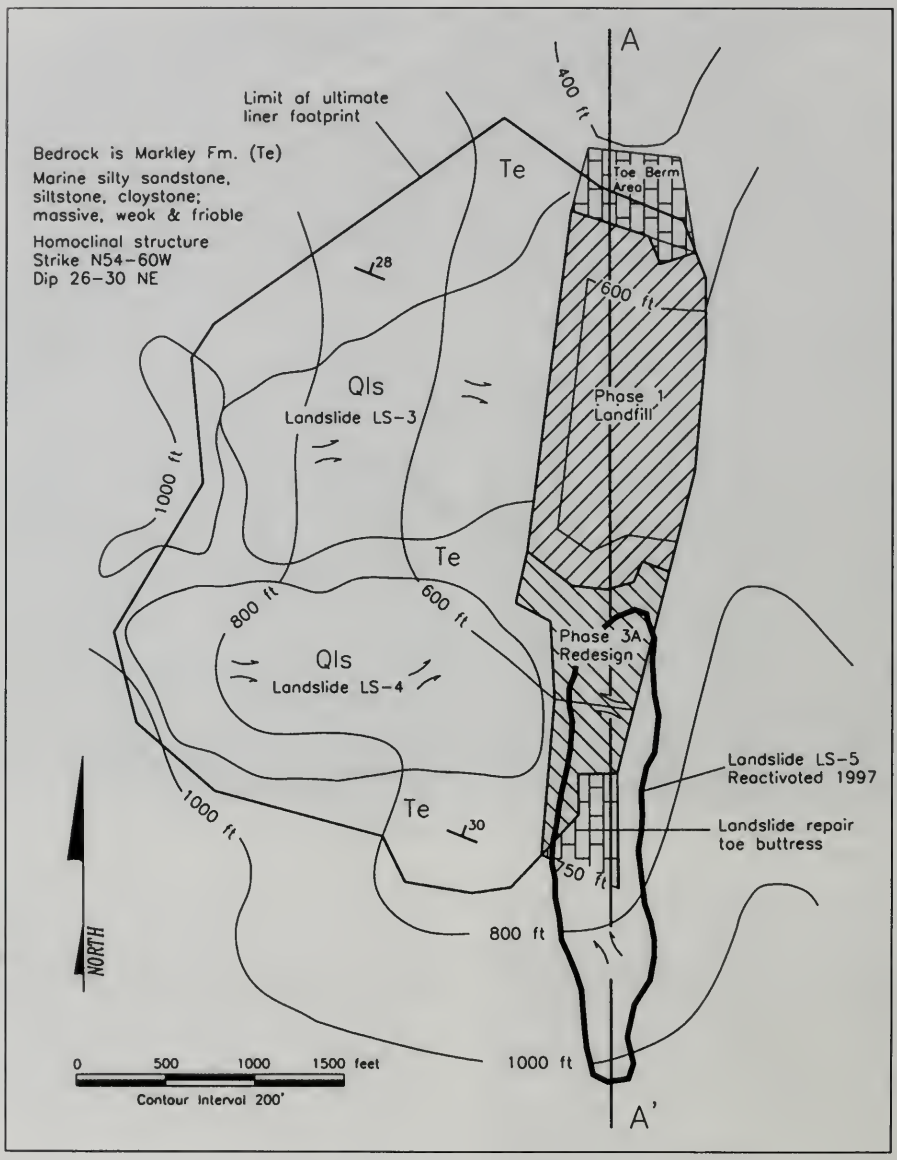

Figure 2. Engineering geology map of Keller Canyon Landfill (adapted from BFI, 1998).

probability that the peak horizontal acceleration in lithified material will exceed 0.10 g in 250 years. The hazard maps indicate design accelerations over 0.80 g in areas of northern California, which would make landfill design in these areas difficult, if not impossible. Therefore, seismic stability analysis of northern California Class III landfills is mainly based on site-specific deterministic evaluations

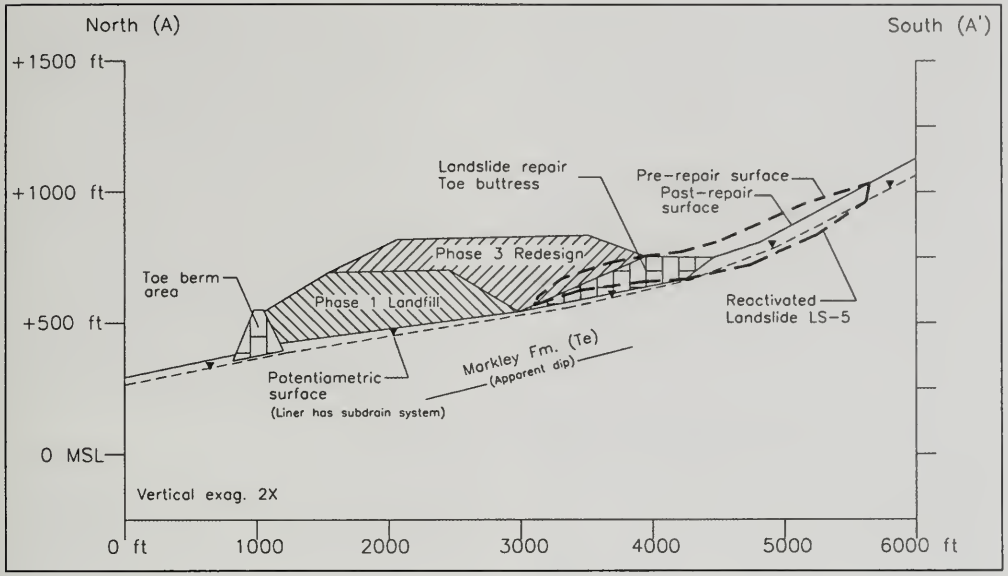

Figure 3. Section A - A' showing the toe buttress constructed for landslide repair (adapted from BFI, 1998).

based on the Maximum Probable Earthquake (MPE). The MPE is the maximum earthquake that is likely to occur during a 100-year interval, and should not be less than any historic earthquakes for the fault segment. Use of the MPE has been subject to considerable debate in California. In most cases, the peak ground accelerations from the MPE are less than those derived from hazard maps or the Maximum Credible Earthquake (MCE). However, U.S. EPA has determined that the use of the MPE in California satisfies the Subtitle D requirement for site-specific analysis (Anderson, 1997).

The state-of-practice of landfill seismic stability analysis in California is first to characterize the appropriate seismic source and then evaluate the ground motions. The engineering geologist characterizes potential seismic sources by first compiling and reviewing available information on historic earthquakes and Holocene faults in proximity to the site. Field investigations may be necessary and could include mapping, trenching, geophysical surveys, and microseismicity surveys.

Peak horizontal ground acceleration (PHGA) in lithified material is estimated using acceleration attenuation relationships that correlate earthquake magnitude, fault style, distance to source, and local site conditions. In some cases site-specific dynamic response analysis is performed using computer programs such as SHAKE. Dynamic analysis is then performed using the highest estimated PHGA. Response spectra may also be used for the dynamic analysis. The Newmark method is then applied to determine permanent seismic deformations along representative cross-sections analyzed for static and pseudo-static stability. More sophisticated site-specific analyses (e.g. finite element and three-dimensional analyses, liquefaction susceptibility assessment, vertical acceleration settlement analysis) are done on a case-by-case basis. Allowable deformations to maintain landfill containment must be demonstrated on a site-specific basis. Kavazanjian (1999) provides generic guidelines for allowable seismic displacements for landfills. Table 6 shows examples of design earthquakes and summaries of stability analyses for selected northern California landfills.

Seismic performance of landfills

Krammer (1998) defines lifeline facilities as a network of facilities that provide the services required for commerce, communication, sanitation, and care of public health, which can be found in virtually any developed area. Lifeline facilities include

Landfill & County	Design earthquake characteristics	Results of stability calculations
Altamont (Alameda)	7.0 MCE; 0.46g; Greenville fault; 4 miles	<1ft. dynamic displacement determined acceptable
Palo Alto (Santa Clara)	8.25 MPE; 0.49g; San Andreas fault; 8 miles	Minimum FS static- 1.6; 2 to 3 ft. dynamic displacement determined acceptable for final cover (unlined site) Localized potential for liquefaction
Potrero Hills (Solano)	6.4 MPE; 0.33g; Winters-Dunnigan Hills fault	Minimum FS static- 1.5; <0.5 ft. dynamic displacement (not significant)
Kiefer (Sacramento)	5.7 MPE; 0.20g; Bear Mtns. (Foothill) fault; 10 miles	Minimum FS static- 1.55; 0.25 ft.dynamic displacement (not significant)
Cummings Road (Humboldt)	7.5 MPE; 0.52g; Little Salmon fault 8.4 MPE; 0.50g; Cascadia subduction zone	Minimum FS static- 1.5; Operator determined <0.33 ft. dynamic displacement (not significant); Department of Water Resources determined dynamic displacement up to 5 ft.
Acme (Contra Costa)	6.0 MPE; 0.59g; Concord fault; <1 mile	Minimum FS static- 1.55; 0.5 to 3 ft. dynamic displacement determined acceptable for final cover (unlined to CCL-lined site); potential for liquefaction

Table 6. Selected design earthquakes for Northern California landfills.

landfills and hazardous waste landfills, and are therefore an element of seismic planning.

The standards and accepted practices for seismic design and construction of facilities, and emergency planning and response, are reevaluated after every major earthquake. The performance of landfills during earthquakes is an area of active interest and research because assessing and repairing liner damage is very difficult and because of the need for safe areas to dispose of disaster debris and waste.

In 1995 the American Society of Civil Engineering published a book entitled *Earthquake Design and Performance of Solid Waste Landfills*. This publication contains many key reference papers on landfill performance during earthquakes up to and including the Northridge earthquake of 1994. Landfill seismic performance assessment came into its own after the 1987 Whittier earthquake and investigation of the OII Landfill in Los Angeles County. The OII Landfill continues to provide valuable information on landfill seismic response from strong motion instruments installed in 1987. After the 1989 Loma Prieta earthquake, investigators reported no significant damage to landfills (Orr and Finch, 1990). This was the first large earthquake in which landfills were subsequently evaluated, although those landfills did not reflect the complex containment designs currently required. Likewise, no significant damage was reported at landfills as a result of the 1992 Landers earthquake. Landfills utilizing geosynthetic liner components were first evaluated for seismic performance and damage from strong ground motions from the Northridge earthquake of 1994 (Augello et al. 1995). After the Northridge earthquake, Matasovic et al. (1998) developed a reference chart describing the relative level of damage that a landfill had experienced. In September 1994, a large earthquake offshore of northern California (Cape Mendocino earthquake) coincided with differential settlement of a toe buttress under construction at the Cummings Road Landfill, Humboldt County. The location of the cracking and settlement was well correlated with the outer limits of the waste. The buttress was promptly repaired and no significant damage has occurred since.

The major seismic performance problem to date with landfills has been the loss of power to the landfill gas control systems and damage to gas control laterals and headers. This has occurred after each major earthquake in California with a landfill gas control system operating near the epicenter. Power to the systems was restored shortly after it was restored to the local power grid, and lateral and header piping systems have been promptly repaired. In no case was the loss of power or damage to laterals and headers the cause for shutting down a landfill for an extended period of time. Some landfills have closed temporarily after an earthquake, but only as a precautionary measure, to be reopened shortly after site inspection was completed.

In California, few composite-lined landfills, and none capped with geosynthetic components, have been subjected to high (greater than 0.3 g PHGA) ground motions. However, with the recent increase

in complex geosynthetic-based designs in landfill construction there is a continued need to evaluate the performance of landfills in future seismic events. A guide for conducting investigations after an earthquake is provided in EERI (1996).

ENVIRONMENTAL MONITORING AND CONTROL

Pollution from landfill leachate, gas, and sediment is a major concern at landfill sites. Because of the controlling influence of geologic conditions on environmental fate and transport, engineering geology is important in the design, construction, and implementation of monitoring and response programs. These programs must ensure that releases to the environment are promptly detected and controlled.

Groundwater monitoring and corrective action

Groundwater monitoring and response protocols in California's Subtitle D program include detection of a potential release (detection monitoring), assessment of any statistically significant evidence for release over background (evaluation monitoring), and evaluation and implementation of corrective action measures. Unsaturated zone monitoring is also required for early leak detection. Based on a survey conducted by SWRCB in spring 1999, groundwater monitoring programs for northern California landfills included detection monitoring at 68 sites, evaluation monitoring at 25 sites, and corrective action at 37 sites (the survey also disclosed 11 sites where no monitoring was being conducted) (Table 1).

Groundwater monitoring and response programs for individual California landfills cannot be transferred as a "boilerplate" from one site to another, but the experiences and track record of other sites can provide a basis for the design of new programs. Evaluation and corrective action programs especially need to be prepared on a site-specific basis and may require multiple phases of remedial investigation, monitoring well construction, specialized sampling and analysis, aquifer characterization, groundwater flow modeling, and engineering feasibility studies.

In addition to RWQCB file records of specific sites, a plethora of sources of information and guidance documents are available on groundwater monitoring and response programs. Selected recommended references include Hudak (1998), ASTM (1997, 1996), SWANA (1997b), and U.S. EPA (1993a, 1993b). An excellent compilation of California water quality goals and standards can be found in CVRWQCB (1998). Statistical methods in groundwater monitoring are continually evolving and subject to ongoing debate. Several recent journal articles have reevaluated the application of statistical methods to groundwater detection monitoring (Pittenger, 1998; Gibbons, 1998; Loftis et al., 1999).

Under California' Subtitle D program, the term "water quality protection standard" is used to encompass the list of constituents of concern, the concentration limits, the specified point of compliance and all monitoring points. The "water quality protection standard" is site-specific and is prescribed in permits issued by the RWQCB (e.g., waste discharge requirements [WDRs] and monitoring and reporting programs [M&RPs]). The constituents of concern (COCs) include "all waste constituents, reaction products, and hazardous constituents that are reasonably expected to be in or derived from waste contained in the unit". COCs are included as a prescribed list of contaminants for each landfill drawn from Appendices I and II of Subtitle D. COCs must be monitored at least once every five years. The default concentration limits are background levels. For detection monitoring, the operator must specify monitoring parameters for RWQCB approval that are a reliable indicator of a release from the unit. The point of compliance for groundwater is defined as "...a vertical surface located at the hydraulically downgradient limit of the waste unit that extends through the uppermost aquifer underlying the unit" (27 CCR Division 2, Subdivision 1 Chapter 2, Article 2).

Subtitle D allows groundwater monitoring to be suspended if the owner or operator demonstrates that there is no potential for migration of hazardous constituents to the uppermost aquifer ("no migration" petition). California's program in practice does not reflect the full flexibility afforded by Subtitle D and it is difficult to obtain regulatory approvals for variances from prescribed programs. For example, risk-based corrective action programs where clean-up levels are above background are of considerable nationwide interest but have not gained acceptance in California. California's Subtitle D program does allow for site-specific approval of a concentration limit greater than background, but only when the RWQCB finds that it is technologically or economically infeasible to achieve background and that the constituent will not pose a substantial pres-

ent or potential hazard to human health or the environment. In practice this approval has been difficult to obtain.

Corrective action and corrective action financial assurances

California's Subtitle D program requires financial assurances for known and "reasonably foreseeable" releases. "Reasonably foreseeable" is not defined and there are few landfills statewide with approved cost estimates. Examples where corrective action scenarios and cost estimates have been submitted to meet this requirement in northern California include Kiefer Landfill, Sacramento County ($800,000), B&J Landfill, Solano County ($869,040), and Union Mine Landfill, El Dorado County ($211,640). Corrective action measures implemented at northern California landfills include groundwater pump-and-treat systems, landfill gas control systems, leachate collection and treatment systems, and final closure.

Contamination of groundwater by landfill gas

Volatile organic compounds (VOCs) are commonly detected groundwater contaminants at landfills and are common trace components of landfill gas. Transport of VOCs from landfill gas to groundwater can occur by direct contact or indirectly as a dissolved phase in leachate or gas condensate. Landfill gas is increasingly being considered as the principal source of VOCs detected in groundwater at landfill sites, so gas control systems are commonly being used for groundwater corrective action programs. Baker (1998) reported on groundwater assessments of landfills in which 90 per cent were shown to have landfill gas as a source of VOCs. Tuchfeld et al. (1998) applied geochemical modeling methods to determine sources of groundwater VOC contamination from landfill gas. Desrocher and Lollar (1998) and Mohr et al. (1992) used isotopic methods to evaluate landfill gas and other potential sources of groundwater contamination.

In northern California extensive studies of the Kiefer Landfill concluded that landfill gas was the dominant source of VOCs (Sacramento County, 1998; Maxfield and Vanderbilt, 1997). Figure 4 is a cross section showing the extent of landfill gas migration and VOC contamination in groundwater at the Kiefer Landfill. Corrective action measures implemented at Kiefer Landfill include a groundwater pump-and-treat system, and an active landfill gas extraction and flare system. A soil vapor extraction system was planned but was not implemented because the operator contends that the landfill gas control system has successfully removed landfill gas from the unsaturated zone (Richgels, 2000).

Before landfill gas control systems are used for groundwater corrective action, site-specific demonstrations are necessary to demonstrate that landfill gas is a source of the contamination. Otherwise, a gas control system would not provide a benefit toward cleaning up the contaminated groundwater. In addition, most conventional landfill gas control systems have been constructed primarily for explosive gas control and power production, and not to remediate groundwater that has been degraded by VOCs, so they may not be effective for remediation purposes. If groundwater corrective action is to become part of the function, then the system should be reevaluated and adjusted or expanded as needed.

Surface water control

Landfills are potential sources of sediment and other pollutants that can impact surface waters. There have been several notable cases of discharges to surface water from landfills in northern California that resulted in significant environmental problems and enforcement actions. Examples include, the Gopher Hill Landfill in Plumas County, where 93,000 gallons of leachate were discharged from a breached impoundment to surface waters in 1989, and the Corinda Los Trancos (Ox Mtn.) Landfill, San Mateo County, where storm water ponds gave way during heavy rains in October 1992 resulting in a large sediment discharge to surface waters and temporary closure of State Highway 92. Case histories of other drainage and erosion problems at landfills in California are summarized in Anderson et al. (1998).

Landfill gas monitoring and control

Detection of explosive levels of landfill gas in structures, utilities, or probes beneath inhabitable off-site properties is rare but can be potentially catastrophic. There have been cases in northern California where construction workers have been injured or killed as a result of uncontrolled landfill gas migration from pre-1991 landfills. The CIWMB tracks violations and publishes an inventory of facilities in violation every 6 months. As of October 1999, there were 11 northern California landfills on the

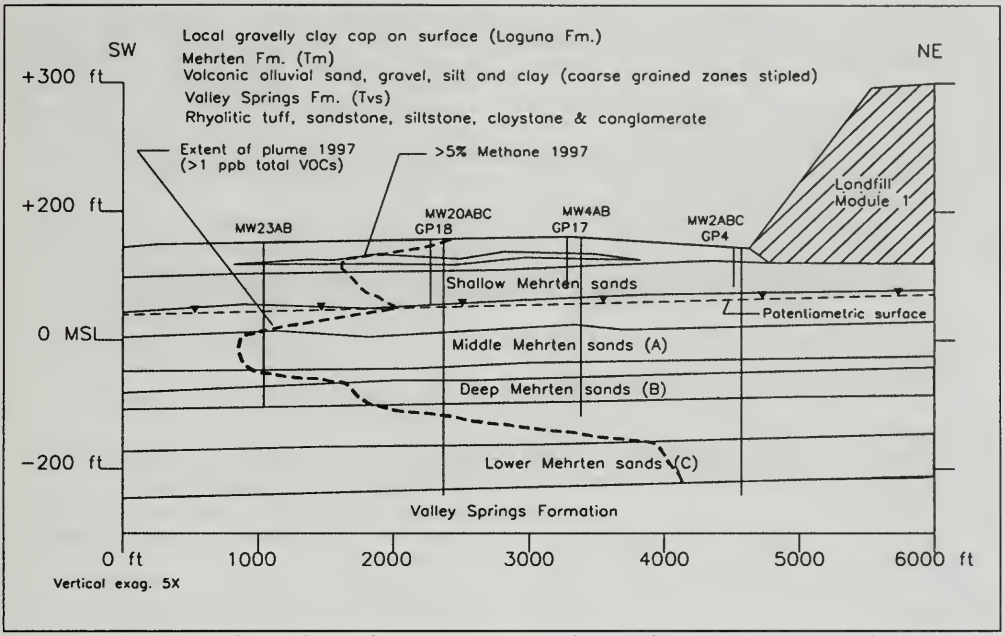

Figure 4. Geologic section of the Keifer Landfill, showing the extent of the landfill gas migration (adapted from Sacramento County, 1998).

inventory. In addition, approximately 53 landfills in northern California have installed landfill gas control systems (Table 1).

Landfill gas migrates preferentially within relatively permeable granular or fractured natural geologic materials and engineered fill. Conversely, landfill gas may be either trapped or not readily migrate through soil or rock units that have a very low permeability with respect to landfill gas, or permeable units that are saturated with water. Site-specific geologic investigations are, therefore, extremely important to ensure adequate monitoring and control. Kiefer Landfill, Sacramento County, is an example of geologic control of landfill gas migration, both for explosive gases and for trace gases that have contaminated groundwater (Figure 4).

Explosive gases require routine quarterly monitoring to ensure that methane does not exceed the lower explosive limit (5% by volume) at the property boundary, and 25% of the lower explosive limit (1.25% by volume) in any on-site structures. In addition to explosive gases, trace gases commonly found in landfill gas can pose a significant health impact to worker and public health and safety. Landfill gas criteria in California's Subtitle D program include prescriptive requirements for perimeter monitoring probe design, construction, and lateral spacing. Guidance on landfill gas monitoring and control is provided in Anderson (1998), CIWMB (1997), and SWANA (1998, 1997a). To develop a landfill gas subsurface monitoring strategy the engineering geologist needs to consider the following factors:

- Location and monitoring of sensitive receptors (e.g. structures, public use areas)
- Invert elevation and boundaries of the landfill
- Location of off-site landfills and other sites that may be potential sources of landfill gas
- Permeability of the soil or rock adjacent to the landfill, including secondary permeability due to bedding, fractures, joints, or faults
- Location and nature of utility lines and construction fills that could be a conduit for landfill gas
- Depth to groundwater
- Barometric and tidal fluctuations

- Natural occurrence of methane and other gases (e.g., organic soils and sediments, oil or gas fields, asphalt seeps, and geothermal areas)
- Likely constituents of concern for landfill gas (e.g. CH_4, CO, CO_2, H_2S, VOCs)
- Monitoring QA/QC (e.g. field and laboratory methods and equipment to be used)
- Monitoring parameters (pressure, oxygen, temperature).

CLOSURE AND POSTCLOSURE

One of the consequences of Subtitle D has been a significant increase in the number of landfills closing. Approximately 86 landfills statewide and 54 in northern California closed between October 1991 and January 1999. Of the northern California landfills, approximately half have completed closure construction and are certified as closed in accordance with current regulations.

Closure criteria in California's Subtitle D program include prescriptive and performance requirements for final cover systems, time frames for closure activities, certification, deed notation, written preliminary and final closure plans, and financial assurance. Postclosure criteria include inspection, maintenance and monitoring of the landfill during the postclosure maintenance period (minimum of 30 years), written preliminary and final postclosure plans, and financial assurance requirements. Closure and postclosure maintenance plans and the certification of closure must be signed and certified by a registered civil engineer or certified engineering geologist. Partial final closure plans may be submitted for approval for one or more individual closure activities during the active life of the landfill. Partial final closure of an active landfill, where final cover is constructed on portions of the waste fill that have reached final grade (sometimes called "rolling closure") is an increasingly common practice to enhance environmental containment of an active landfill and to reduce the set-aside funding required for financial assurance. In many cases, landfills that ceased operation have not set aside adequate funds to implement closure and postclosure. This has resulted in significant environmental and enforcement problems for California.

Landfill sites are also being closed and remediated by complete or partial removal of wastes for consolidation on-site, or disposal to an off-site facility (clean closure). In some cases, cover soil and other materials are recovered and recycled (landfill mining). The engineering geologist may be involved in development and implementation of clean closure plans, including assessment of the limits of waste and contamination, determination and confirmation of soil cleanup levels, and preparation and implementation of excavation grading plans.

At the Clovis Landfill, Fresno County, landfill mining of an older unlined cell is being conducted as a corrective action measure for groundwater contamination and explosive gas control. Soil is screened and recovered for use as daily cover for an active lined cell that is the repository for the excavated residual wastes. McCourtney Road Landfill, Nevada County, completed a clean closure project successfully where building demolition burn ash waste from an unlined cell was removed and consolidated on-site. Clean closure and on-site consolidation of older landfill sites are remedial action alternatives being implemented at several closing military bases (e.g. Mather Air Force Base, Sacramento County).

Cost estimates for closure and postclosure

Third party cost estimates for closure and postclosure maintenance must be calculated on a detailed site-specific basis. However, statewide average cost estimates based on CIWMB records (through 1998) can be summarized based on landfill footprint acreage (closure and postclosure), final cover type (only closure), and removal of outliers that reflect extreme site-specific conditions (Table 7). Cost estimates for clean closure projects can be summarized on a per-cubic-yard-removed basis.

Postclosure land use

Closed landfills are increasingly being developed for further use in northern California, especially for the older pre-Subtitle D sites in urban areas. Engineering geologists may play an integral role in the incorporation of these further use projects into final closure and postclosure maintenance plans. For example, closed landfills can be excellent sites for solid waste transfer stations and recycling facilities because of the existing solid waste infrastructure. Commercial, industrial, golf course, and park developments are also options that are being implemented successfully. CIWMB (1998) provides guidance and information on specific disposal site postclosure land use projects and applicable regulations.

Component	Final cover system	Estimate per waste footprint acre	Standard deviation and range
Postclosure maintenence (30-years)	All	$75,000	$46,000 ($20,000 - $200,000)
Closure	Alternative earthen	$50,000	$21,000 ($9,000 - $90,000)
	Compacted clay (CCL)	$65,000	$25,000 ($25,000 - $125,000)
	Geomembrane (GM) or geosynthetic clay (GCL)	$90,000	$29,000 ($50,000 - $200,000)
	Composite (GM/CCL)	$110,000	$35,000 ($50,000 - $200,000)
	Combination systems	$85,000	$34,000 ($40,000 - $200,000)
Landfill gas control systems (active-flare)	All	$15,000 - $25,000 (+15%)	NA
Clean closure	Range - $10 per cubic yard (Mather Air Force Base) to $40 per cubic yard (McCourtney Road Landfill White Metals Area)		

Table 7. Average closure and postclosure maintenance cost estimates for California landfills (1998 dollars).

SUMMARY

Municipal solid waste landfills ultimately depend on natural geologic conditions to function for their intended purpose. Therefore, engineering geology plays a fundamental role from the inception of the project, through the design and construction stages, and unto the closure and post-closure use of the land. The practice of engineering geology in Northern California on landfill projects is enhanced by knowledge and understanding of case histories and the specific aspects of engineering geology that apply to landfills. Specific engineering geology aspects of landfills summarized in this paper include the regulatory framework, landfill siting, design and construction, alternative earthen final covers, seismic performance, slope and foundation stability, landfill gas monitoring and control, surface water control, groundwater monitoring and corrective action, groundwater contamination by landfill gas, and closure and postclosure maintenance. We hope that this overview will assist engineering geologists, both experienced and new, engaged in landfill projects.

DISCLAIMER

This manuscript does not necessarily reflect the views of the State of California, the California Environmental Protection Agency, or the California Seismic Safety Commission. No official endorsement should be inferred.

ACKNOWLEDGMENTS

Grateful thanks to peer reviewers Charlene Herbst, Russel Keenan and Chief Editor Horacio Ferriz for their keen (and extensive) comments on the original draft of this paper.

AUTHOR PROFILES

Scott Walker is a California Certified Engineering Geologist (CEG) and California Registered Professional Civil Engineer (PE) currently working as Supervising Engineering Geologist for the California Integrated Waste Management Board (CIWMB). Mr. Walker has 15 years work experience as an engineering geologist for CIWMB and the Central Valley Regional Water Quality Control Board specializing in landfills, site remediation, and mines. Prior to his career with these agencies, Mr. Walker worked as a geologist for four years in consulting and mining geology. Currently Mr. Walker manages the Remediation, Closure, and Technical Services Branch of CIWMB with over twenty staff engineers, engineering geologists, and environmental specialists.

Robert Anderson is a Certified Engineering Geologist (CEG) currently working as Senior Engineering Geologist at the California Seismic Safety Commission. Mr. Anderson has 14 years work experience as an engineering geologist, specializing in landfills, fault studies, residential development, bridges, and thermal power plants.

SELECTED REFERENCES

ASTM (American Society of Testing and Materials), 1997, ASTM standards related to environmental site characterization: ASTM Publication Number PCN 03-418297-38, West Conshohocken, Pennsylvania, 1410 p.

ASTM (American Society of Testing and Materials), 1996, Provisional standard guidance for developing appropriate statistical approaches for ground-water detection monitoring programs: ASTM Publication Number PCN PS 64-96, West Conshohocken, Pennsylvania.

Anderson, R. (ed.), 1998, Proceedings of the Landfill Gas Assessment and Management Symposium, April 8-9, 1998, Ontario, California: California Integrated Waste Management Board, California Conference of Directors of Environmental Health, and Association of Engineering Geologists.

Anderson, R. (ed.), 1997, Proceedings of the Sanitary Landfill Static and Dynamic Slope Stability Conference, March 27-28, 1997, Whittier, California: Association of Engineering Geologists, American Society of Civil Engineers Geotechnical Section, and California Integrated Waste Management Board.

Anderson, R. L., Walker, S. D., and Crist, T. E., 1998, Drainage and erosion control problems at municipal solid waste landfills in heavy rains: Proceedings of the 14th Annual International Solid Waste Conference, Philadelphia.

Augello, A., Matasovic, N., Bray, J., Kavazanjian, E., Jr., and Seed, R., 1995, Evaluation of solid waste landfill performance during the Northridge earthquake: *in* M.K. Yegian and W.D.L. Finn, (eds.), Earthquake Design and Performance of Solid Waste Landfills, ASCE Geotechnical Special Publication No. 54, ASCE Annual Convention, San Diego, CA, p. 17-50.

Baker, J. A., 1998, What's in your groundwater?: Waste Age May 1998, v. 219, no. 5, p. 213-224.

Bolton, N., 1995, Handbook of landfill operations: Blue Ridge Solid Waste Consulting, Bozeman, Montana, 534 p.

BFI (Browning-Ferris Industries of California, Inc.), 1998, Joint Technical Document (JTD), Volumes 1-3, Keller Canyon Landfill, Contra Costa County: Unpublished 27 CCR permit review document submitted to Contra Costa County Local Enforcement Agency (LEA), California Integrated Waste Management Board (CIWMB), and San Francisco Regional Water Quality Control Board (RWQCB).

CIWMB (California Integrated Waste Management Board), 1998, Disposal site postclosure land use: Solid Waste Local Enforcement Agency Advisory No. 51, July 22, 1998, 9 p.

CIWMB (California Integrated Waste Management Board), 1997, Gas monitoring procedures: Solid Waste Local Enforcement Agency Advisory Amendment to No. 44, August 29, 1997, 22 p.

CVRWQCB (Central Valley Regional Water Quality Control Board), 1998, A compilation of water quality goals: Central Valley Regional Water Quality Control Board Staff report, March 1998, 92 p.

Dusrocher, S. and Lollar, B. Sherwood, 1998, Isotopic constraints on off-site migration of landfill CH_4: Ground Water, September-October 1998, v. 36, no. 5, p. 801-809.

Code of Federal Regulations (40 CFR), Part 258, Subtitle D (Subtitle D), 1991: Federal Register, U. S. Environmental Protection Agency.

EERI (Earthquake Engineering Research Institute), 1996, Post-earthquake investigation field guide Learning from earthquakes: Publication No. 96-01, 144 p.

Evans, D. W. and Stark, T. D., 1997, The Rumpke landslide: New information: Waste Age, v. 28, No. 9, p. 91.

Gibbons, R. D., 1998, False positives in groundwater statistics: Waste Age, v. 29, no. 10, p. 32.

Harden, D., 1996, California geology: Macmillan Publishing Company, 479 p.

Hudak, P. F., 1998, Configuring detection wells near landfills: Ground Water Monitoring and Remediation, v. 18, no. 2, p. 93-96.

Kavazanjian, E., Jr., 1999, Seismic design of solid waste containment facilities: 8th Canadian Conference on Earthquake Engineering, Vancouver, British Columbia, June 13-15, 18 p.

Kavazanjian, E., Jr., 1998, Current issues in seismic design of geosynthetic cover systems: Proceedings of the Sixth International Conference on Geosynthetics, Atlanta, Georgia, March 25-29, 1998, 8 p.

Kenter, R.J., Schmucker, B. O., and Miller, K. R., 1997, The day the earth didn't stand still: The Rumpke landslide: Waste Age, v. 28, no. 3, 10 p.

Koerner, R. M. and Daniel D. E., 1997, Final cover systems for solid waste landfills and abandoned dumps: The American Society of Civil Engineers (ASCE) Press, Reston, Virginia, 256 p.

Lass, G. L., Ferriz, H., Rivera, A. L., 1997, Alternative final cover demonstration project at the Milliken Landfill, San Bernardino County, California: Proceedings 2nd Annual Landfill Symposium, Solid Waste Association of North America, August 4-6, 1997, Sacramento, California, p. 69-77.

Loftis, J. C., Harniharan, K. I., Baker, H. J., 1999, Rethinking Poisson-based statistics for groundwater quality monitoring: Ground Water, v. 37, no. 2, p. 275-281.

Matasovic, N., Kavazanjian, E., and Anderson, R. L., 1998, Performance of solid waste landfills *in* earthquakes: in Earthquake Spectra, v. 14, no. 2, p. 319-334.

Maxfield, P. L. and Vanderbilt, E. S., 1997, Case study: Evolution of the groundwater contamination investigation at Kiefer Landfill: Proceedings 2nd Annual Landfill Symposium, Solid Waste Association of North America, August 4-6, Sacramento, California, p. 147-160.

Mohr, T.K.G., Davisson, M.L, Criss, R.E., Fogg, G.E., 1992, Small scale application of stable isotopes ^{18}O and deuterium to delineate migration pathways at a class III landfill.

site: *in* Proceedings of the VI National Outdoor Action Conference on Aquifer Restoration, Ground Water Monitoring and Geophysical methods, National Ground Water Association, May 11-13, 1992, Las Vegas, Nevada, p. 231-244.

Orr, W. R. and Finch, M. O., 1990, Solid waste landfill performance during the Loma Prieta earthquake: *in* Landva, A., and Knowles, G.D., (eds.), Geotechnics of Waste Fills, Theory and Practice, ASTM STP 1070, American Society for Testing and Materials, Philadelphia, p. 22-30.

Pittinger, R., 1998, How to reduce false positives in groundwater statistics: A top ten list: Waste Age, v. 29, no. 5, p. 241-254.

Reynolds, T. D. and Morris, R. C. (eds.), 1997, Landfill capping in the semi-arid west: problems, perspectives, and solutions: Conference Proceedings, Environmental Science and Research Foundation, May 21-22, 1997, Grand Teton National Park, 263 p.

Richardson, G. N. and Kavazanjian, E., Jr., April 1995, RCRA Subtitle D (258) seismic design guidance for municipal solid waste landfill facilities: EPA/600/R-95/051, 143 p.

Richgels, C., Personal communication, February, 2000.

Sacramento County (Public Works Agency, Waste Management and Recycling Division),1998, Joint Technical Document (JTD), Kiefer Landfill, Sacramento County: Unpublished 27 CCR permit review document submitted to Sacramento County Local Enforcement Agency (LEA), California Integrated Waste Management Board (CIWMB), and Central Valley Regional Water Quality Control Board (RWQCB).

Schmucker, B. O., and Hendron, D. M., 1998, Forensic analysis of the 9 March 1996 landslide at the Rumpke Sanitary Landfill, Hamilton County, Ohio: Proceedings 12th Annual Geosynthetic Research Institute Conference: Lessons Learned from Geosynthetics Case Histories, December 8-9, 1998, Geosynthetic Institute, Folsom, Pennsylvania, p. 75-95.

SWANA (Solid Waste Association of North America), 1998, Landfill gas operation and maintenance manual of practice: SWANA Technical Guidance Document.

SWANA (Solid Waste Association of North America), 1997a, Managing landfill gas at municipal solid waste landfills: SWANA Technical Guidance Document, 95 p.

SWANA (Solid Waste Association of North America), 1997b, Groundwater monitoring, sampling, analysis, and well construction: SWANA Technical Guidance Document, 115 p.

SWRCB (State Water Resources Control Board), 1993, Chapter 15 program notes, number 6 (federal MSW requirement missing from, or more stringent than, Chapter 15, September 16, 1993), number 7 (suggested laboratory methods for analyzing Appendix I and Appendix II constituents, August 2, 1993), and number 15 (statistical software packages applicable for use at MSW landfills without site-specific review and acceptance, November 10, 1994).

Title 27, California Code of Regulations (27 CCR), 1997, Environmental Protection, Volume 37: California Office of Administrative Law.

TRB (Transportation Research Board), 1996, Landslide investigation and remediation: Transportation Research Board Special Report 247: National Academy press, Washington, D.C., 673 p.

Tuchfeld, H. A., Simmons, S. P., Jesionek, K. S., and Romito, A. A., 1998, This year's model: Geochemical modeling & groundwater quality: Waste Age, v. 29, No. 7, p. 77.

U.S. Department of the Navy, 1982, Soil Mechanics, NAVFAC DM7.1: U.S. Government Printing Office, Washington, D.C., 348 p.

U.S. EPA, 1986, Test methods for evaluating for evaluating solid waste- physical/chemical methods: EPA SW-846, 3rd Edition; PB88-239-233; U.S. EPA Office of Solid Waste and Emergency Response; Washington, D.C.

U.S. EPA, 1993a, Solid waste disposal facility criteria technical manual: EPA/530/R-93/017, 349 p.

U.S. EPA, 1993b, Subsurface characterization and monitoring techniques, Desk reference guide, v. 1 & 2: EPA/625/R-93/003.

U.S. EPA, 1993c, Technical guidance document, quality assurance and quality control for waste containment facilities: EPA/600/R-93/182, 305 p.

U.S. EPA, 1994, Hydrogeologic Evaluation of Landfill Performance (HELP) Model: EPA/625/K-94/001, 205 p.

Walker, S. D. and Rosenbaum, S. E., 1995, Earthen barrier layer construction for solid waste landfills in the Sacramento area, California: Association of Engineering Geologists, 38th Annual Meeting, September 30-October 6, 1995, Sacramento, California


ASSOCIATION OF ENGINEERING
AEG
GEOLOGISTS

HYDROGEOLOGIC INVESTIGATION OF THE YUCAIPA LANDFILL, SAN BERNARDINO COUNTY, CALIFORNIA

TERRI REEDER[1], RALPH MURPHY[2] AND JAMES FINEGAN[2]

ABSTRACT

Investigations and monitoring at the Yucaipa Landfill (YLF) in San Bernardino County, California, have documented the presence of groundwater impacts beneath and down gradient of the site. The site is located in a structurally complex geologic environment, and faults underlying the landfill play a significant role in controlling groundwater flow and contaminant transport. A recent investigation focused on the distribution and orientation of faults near the site, and the hydraulic properties of aquifer materials, to help characterize the nature and extent of groundwater impacts.

Methods used in this investigation included aerial photograph lineament analysis, geologic mapping, surface geophysical surveys, drilling and installation of six new groundwater monitoring wells, and aquifer pumping tests. Although no single investigative technique provided an encompassing "picture" of site conditions, the geophysical data generated by the STING® resistivity measuring system yielded the best resolution of the subsurface structures present beneath the site. All methods, when evaluated together, enabled an improved understanding of the groundwater flow and contaminant transport conditions within the faulted and fractured bedrock and alluvial aquifers beneath the site.

INTRODUCTION

Background

The YLF is a closed, unlined municipal solid waste disposal facility that is located along the base of the Crafton Hills, on the north side of Yucaipa Valley, in southwestern San Bernardino County, California (Figure 1). During its operation from 1963 to 1980, refuse was placed within a 25-acre canyon area within the north-central portion of the County-owned 560-acre parcel. This canyon is deeply incised into bedrock northwest of the site and into older alluvium (and possibly bedrock) south and southeast of the site.

Monitoring activities indicate that the unlined landfill has released a variety of inorganic and organic constituents that threaten to impact groundwater quality down gradient of the facility, where municipal groundwater production occurs. In response to this concern, the County of San Bernardino Waste System Division implemented an Evaluation Monitoring Program (EMP) to characterize conditions governing the release, and to develop a basis for later review of alternative mitigation measures.

Geologic setting

The YLF is located along the southeastern edge of the Crafton Hills, within the San Bernardino Valley structural block. The San Bernardino Valley structural block is bounded on the northeast by the

[1]Regional Water Quality Control Board
Santa Ana Region
3737 Main Street, Suite 500
Riverside, CA 92501-3348
treeder@rb8.swrcb.ca.gov

[2]GeoLogic Associates
1831 Commercenter East
San Bernardino, CA 92408
ramurphy@geo-logic.com

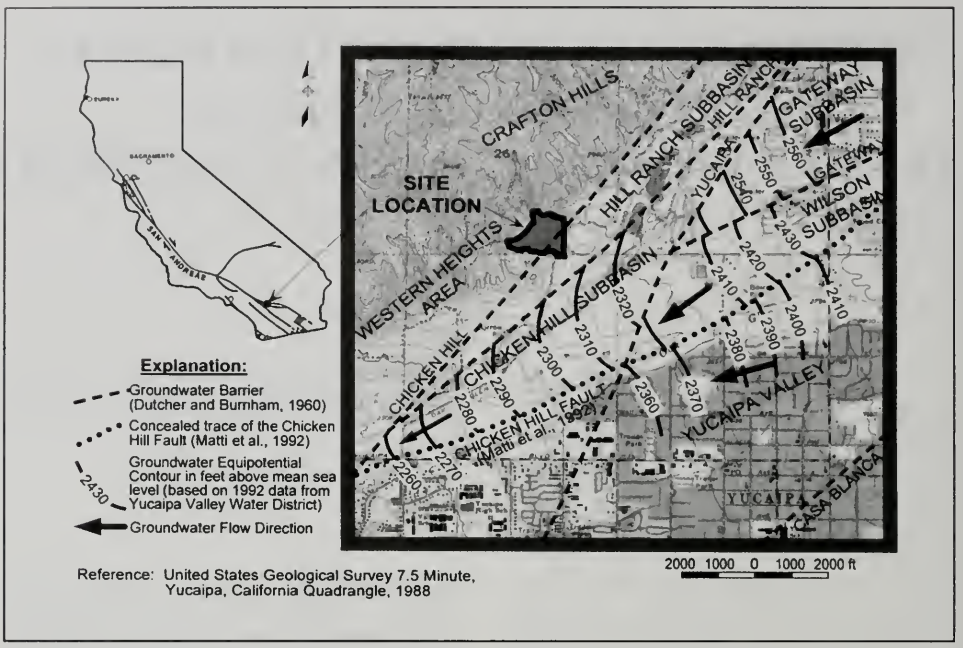

Figure 1. Site location map.

San Andreas fault (located approximately 2.5 miles northeast of the site) and on the southwest by the San Jacinto fault, which is located about 7.5 miles southwest of the site (Fife et al., 1976). Extension and rotation of the San Bernardino Valley block has occurred in response to movement on these faults, and has resulted in internal deformation of the block and formation of local fault-bounded zones of uplift (horsts) and subsidence (grabens). Along the north side of the YLF, the Crafton Hills represent the major horst on the northwest side of the Yucaipa Valley graben (Figure 1).

Matti et al. (1992) mapped two branches, or splays, of the Crafton Hills fault on the site. The main trace of the fault (north splay) forms the major break between the Crafton Hills horst and the Yucaipa Valley graben, and is exposed in drainages and a cut-slope located at the north end of the refuse prism (Figure 2). The arcuate southeastern trace splays off the main trace, just northeast of the YLF, and trends through the central and southern portions of the site before rejoining the main trace southwest of the YLF.

Geologic units near the YLF include highly fractured and metamorphosed Mesozoic granitoid rocks exposed in the upland area north of the site, Pleistocene and Recent alluvial fan sediments deposited unconformably on bedrock beneath and adjacent to the YLF, and Recent alluvial channel deposits exposed in active drainages that cross and border the site (Figure 2).

Hydrogeologic setting

The YLF is located near the northeastern limits of the Yucaipa Hydrologic Subarea (subbasin) within the San Timoteo groundwater basin (DWR, 1964). Past investigations of the Yucaipa area indicate that groundwater flow is strongly influenced by faulting and groundwater barriers. As shown in Figure 1, at least five groundwater subbasins have been identified between the Crafton Hills fault and the Chicken Hill fault (Dutcher and Burnham, 1960; California Department of Water Resources [DWR], 1964). Groundwater in the Yucaipa Valley subbasin generally occurs within alluvial deposits and flows southwest towards the Redlands Heights area (Figure 1.)

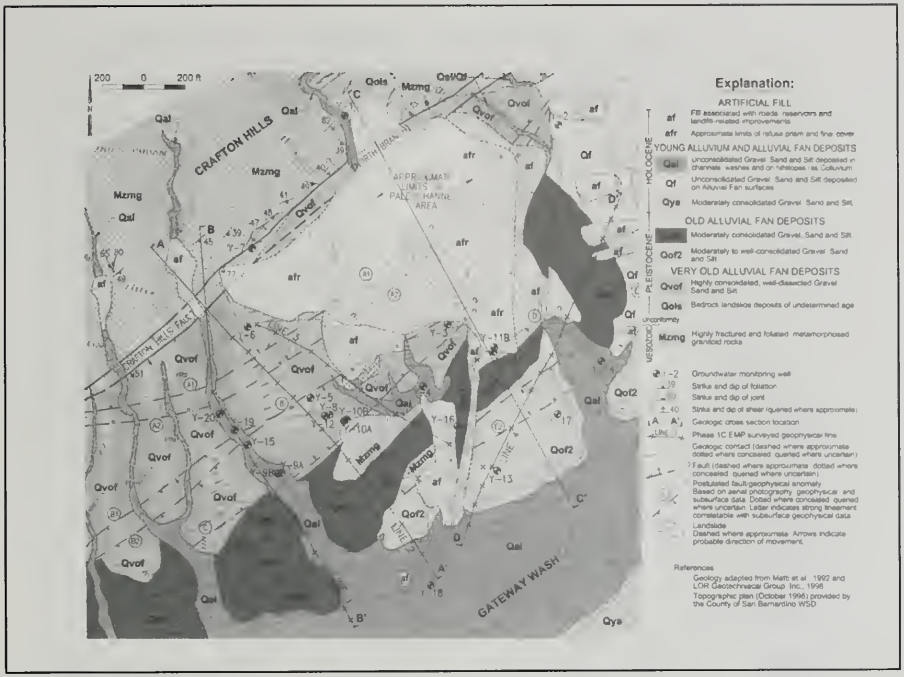

Figure 2. Geologic map.

The principal source of recharge to the Yucaipa Valley subbasin is underflow from the Chicken Hill subbasin (Dutcher and Burnham, 1960). Groundwater recharge is augmented by direct precipitation and runoff from the Crafton Hills, and by surface water flow in the Yucaipa Wash and its tributary drainages.

Groundwater near the YLF occurs at depths ranging from about 65 to 215 feet within both fractured bedrock and alluvial deposits. Beneath and north of the landfill, groundwater is typically first encountered within fractured bedrock. South and east of the YLF, groundwater is first encountered within alluvial deposits. Although faults in the area locally interrupt flow, potentiometric contours indicate that groundwater near the YLF generally flows to the south and southwest (Figure 3).

Groundwater impacts

Monitoring data collected during the facility's 12-year monitoring history indicate that tetrachloroethene (PCE) and trichloroethene (TCE) are the most commonly detected volatile organic compounds (VOCs) in groundwater near the YLF (Figures 4 and 5). Historically, the highest concentrations of PCE and TCE (47 and 134 micrograms per liter [µg/L], respectively) have been associated with wells near the downgradient (southern) border of the site (GLA, 1992-2000). Since the concentrations of these VOCs have locally exceeded the Federal Maximum Contaminant Levels (MCLs) established by the U.S. Environmental Protection Agency (CFR, 1995), they are considered the site's primary constituents of concern. The inorganic constituents that have been identified in groundwater near the site do not typically exceed MCLs (Figure 6).

Study objectives

Previous investigations of the YLF (IT, 1989; GLA, 1995; and EMCON, 1997) documented at least two major faults that traverse the site, and ground-

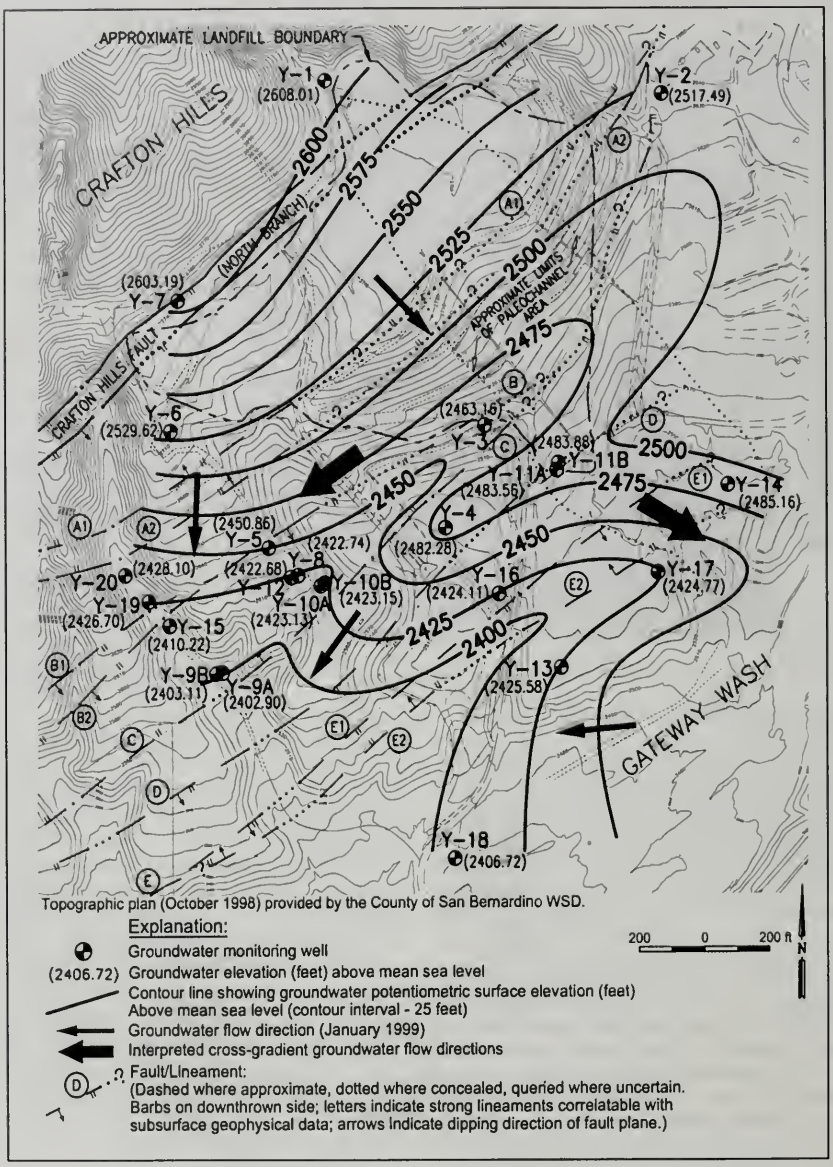

Figure 3. January 1999 groundwater equipotential contours.

water impacts that extend beyond the downgradient boundary of the YLF. However, these investigations did not sufficiently characterize the relationship between structural features, groundwater flow, and contaminant transport conditions at the site. In order to better characterize these conditions, the

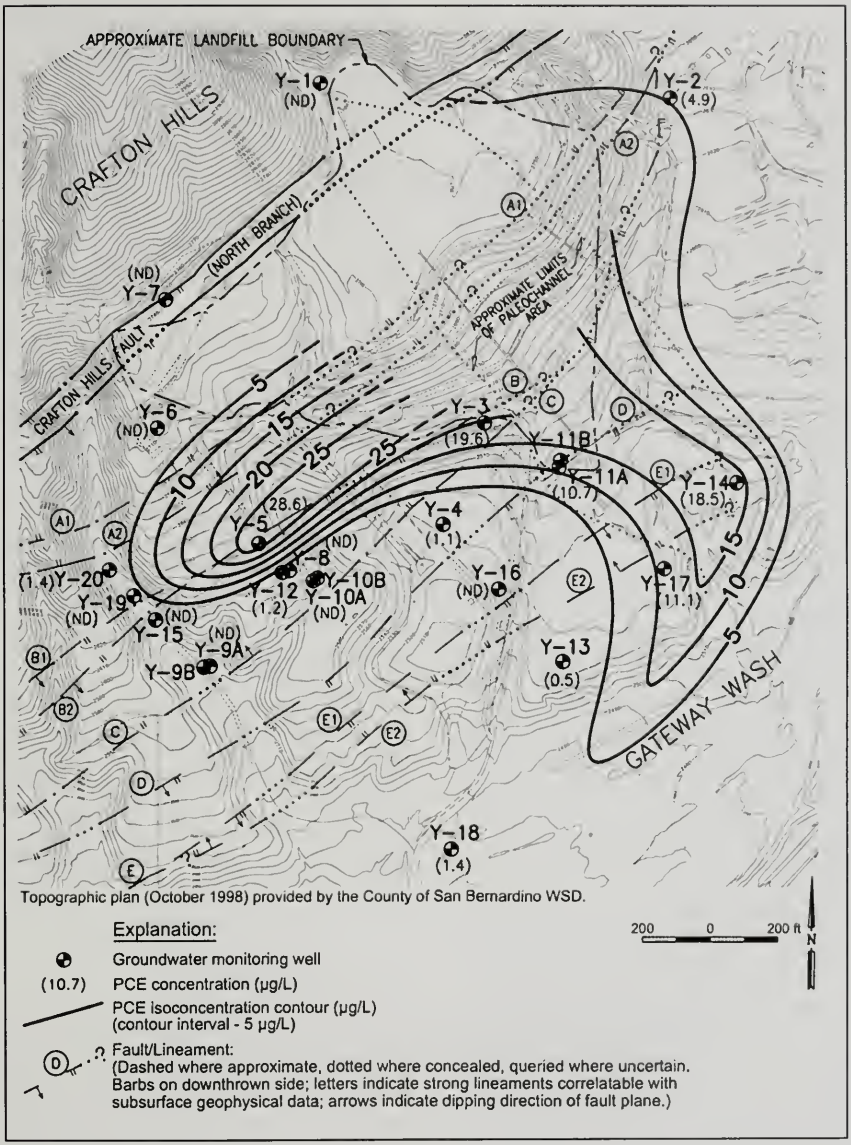

Figure 4. January 1999 PCE isoconcentration contours.

investigation described in this paper included aerial photograph (lineament) analysis, surface geophysical surveys, monitoring well installation and sampling, aquifer pumping tests, and hydrogeologic modeling.

METHODOLOGY

Aerial photograph review and lineament mapping

To evaluate faulting on the site, stereoscopic black and white aerial photographs dating from 1938 to 1997 were inspected. Lineaments were identified on the aerial photographs and were subjectively ranked according to the "intensity" of their geomorphic expression and continuity.

Geologic mapping

Geologic mapping was completed to verify and supplement earlier mapping efforts. The faults associated with the southern splay of the Crafton Hills fault were not exposed at the ground surface and, like most of the geologic contacts in the area, were obscured by thick vegetation, grading, or hydroseeding associated with landfill improvements.

Surface geophysical surveys

Geophysical surveys were performed along 4 lines within the project area (Figure 2) to determine the location and orientation of the numerous lineaments identified at the site. Although trenching methods were initially considered to evaluate faulting on the property, taking into accoung the number of lineaments that were identified, and the fact that the recency of faulting was not in question, surface geophysical survey methods were determined to be most likely to yield the data needed to characterize the geologic structures at the depths of interest (50-200 ft).

Six surface geophysical survey methods were employed for Line 1 including: STING® resistivity (SAGA Geophysics, 2000), gravity, VLF, magnetometry, spontaneous potential, and electromagnetic induction. All six methods were run on the first line, after which the geophysical results for each method were compared to one another in light of known subsurface conditions (e.g., borehole and well data). The STING® resistivity method provided the clearest picture of the subsurface structure, and in the interests of maximizing project resources, this method was used exclusively along the remaining lines. The STING® resistivity measuring system is a computer-controlled method that uses a large array of electrodes to signficantly enhance traditional roll-along dipole-dipole resistivity surveying techniques.

Monitoring well construction and sampling

Six new groundwater monitoring well locations (Y-15, Y-16, Y-17, Y-18, Y-19, and Y-20) were selected to evaluate the subsurface geologic structures indicated by the lineament and geophysical analyses, and to better characterize the spatial distribution of the release (Figure 3). Wells Y-15, Y-16, Y-17, Y-19, and Y-20 were completed in fractured bedrock, and well Y-18 was completed in the young alluvial deposits along the southern border of the property in Gateway Wash.

The groundwater samples that were obtained for the project were evaluated for the monitoring parameters that are included in the facility's quarterly monitoring program. Using criteria identified by Wiedemeier et al. (1996), an additional suite of analytes was included for select samples to evaluate the potential for natural ("intrinsic") attenuation of VOCs in groundwater near the site. Since these additional analytes assess oxidation-reduction potential and associated ion-exchange processes, they provided an indication of existing and potential degradation of PCE and TCE.

Aquifer pumping tests

Aquifer pumping tests were completed at wells Y-4, Y-15, and Y-18 to better characterize the hydraulic properties of the old alluvial fan deposits, fractured bedrock, and the young alluvial deposits, respectively. The aquifer drawdown and recovery data collected during the aquifer pumping tests were evaluated using recognized methods (e.g., Cooper-Jacob, 1946; Neuman, 1972; Theis, 1935).

FINDINGS

Geologic conditions

Based on aerial photographic review and lineament mapping, 13 lineaments were initially identified on or adjacent to the YLF, including the main trace of the Crafton Hills fault. Most of the lineaments were oriented northeast-southwest, sub-parallel to the main trace of the Crafton Hills fault. Field reconnaissance confirmed that all of the lineaments identified stereoscopically were associated with breaks in slope, and/or linear ridges and drainages, and were not related to fences or other man-made structures.

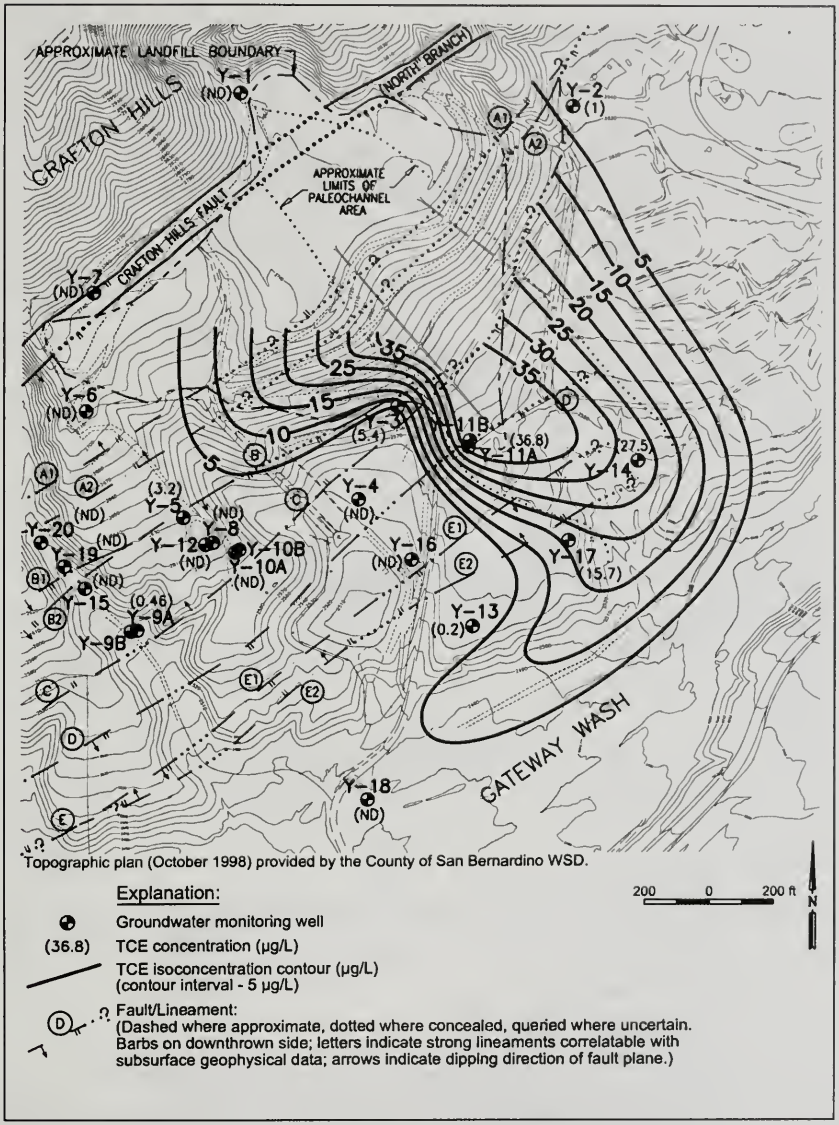

Figure 5. January 1999 TCE isoconcentration contours.

As shown on Figure 7, the STING® results depict areas of low restivity (e.g., soils, gauge zones) and high resistivity (e.g., relatively unfractured bedrock). Abrupt lateral changes, or "breaks", from high resistivity areas appear to correspond to many of the lineaments that were identified from the aerial photographs. Five lineaments, or fault zones, were identified on both the aerial photographs and in the geophysical survey data (A, B, C, D, and E; Figure 3).

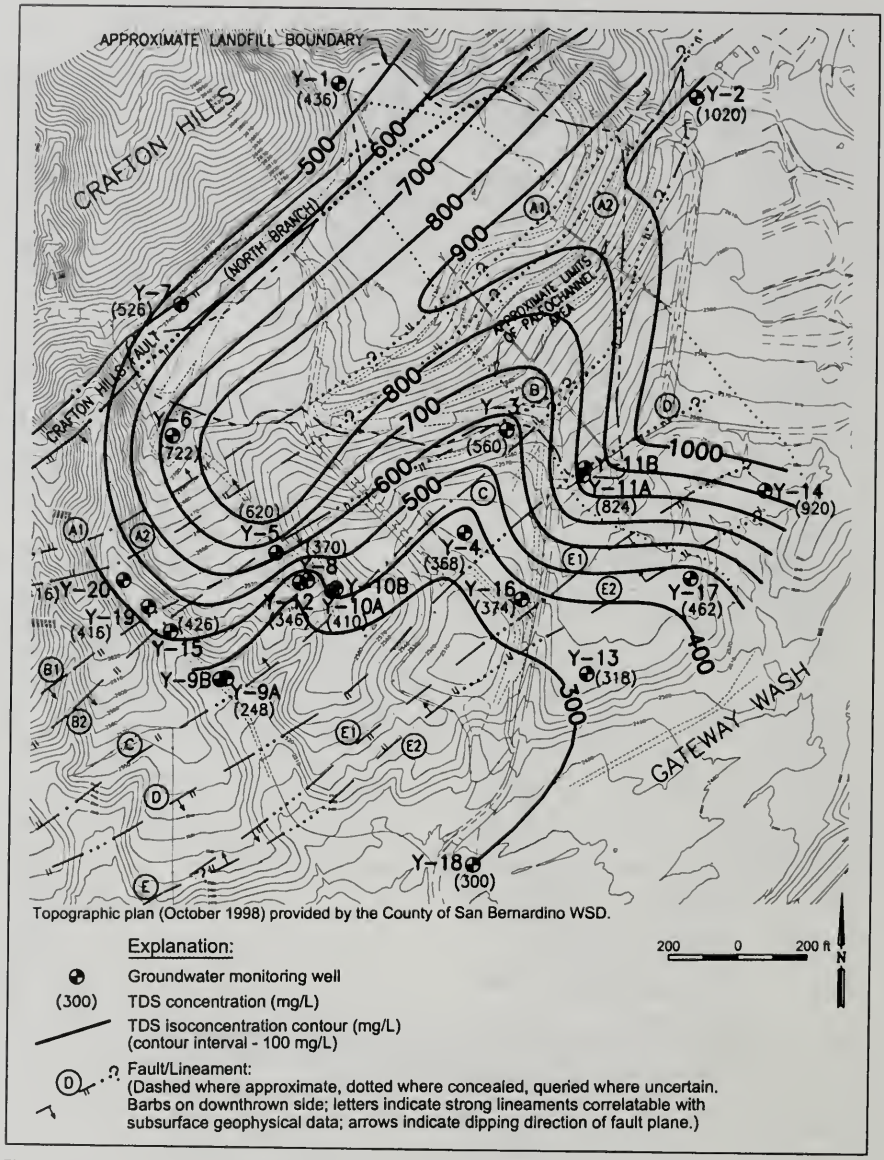

Figure 6. January 1999 TDS isoconcentration contours.

The lithologic data obtained during drilling of monitoring wells was consistent with earlier studies that indicate that the site is underlain by approximately 50 to 100 feet of well-graded alluvial deposits, that are in turn underlain by highly fractured crystalline bedrock. Groundwater is restricted to fractured bedrock in the northern and central portions of the property, but alluvial deposits are satu-

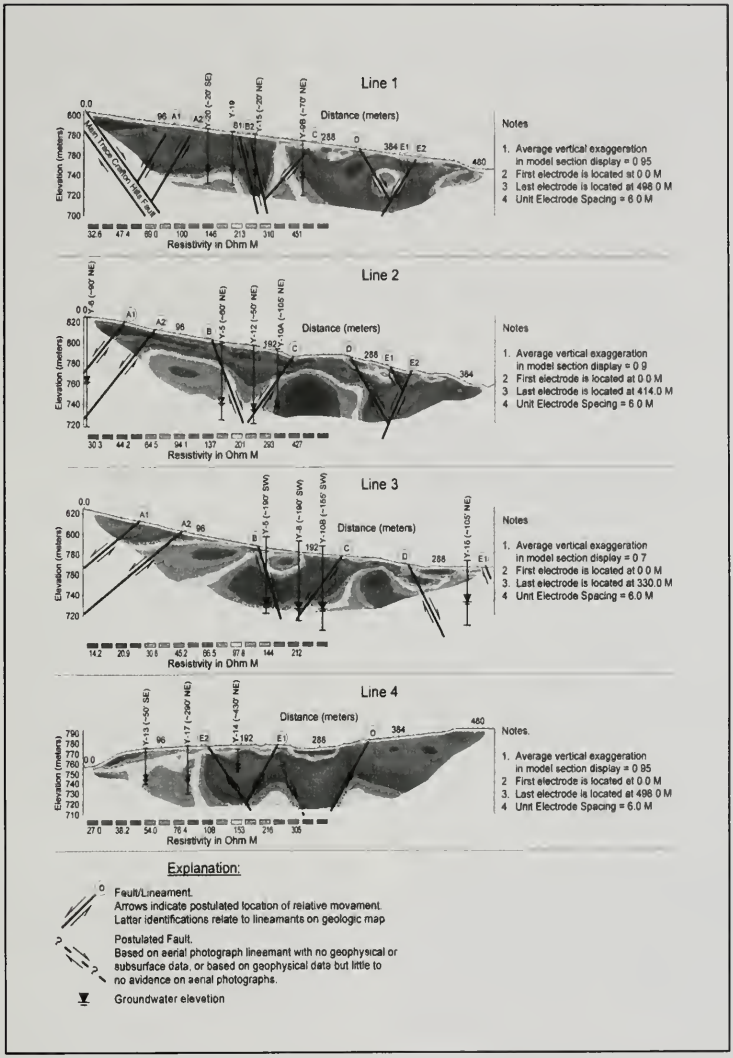

Figure 7. Interpreted STING results.

rated closer to Gateway Wash, near the southern portion of the property (Figures 2 and 3).

Aquifer hydraulic characteristics

The results of the aquifer pumping tests indicate that the hydraulic conductivity of fractured bedrock is approximately 8 feet per day (ft/day), 2 ft/day in the old alluvial fan deposits, and 20 ft/day in the young alluvial deposits. The extensive fracturing, faulting, and weathering observed in the bedrock accounts for its high hydraulic conductivity, whereas the lower hydraulic conductivity calculated for the old alluvial fan deposits is consistent with

	WELLS					
	Y-15	Y-16	Y-17	Y-18	Y-19	Y-20
GENERAL CHEMISTRY (MG/L):						
Chloride	16	12	17	18	63	55
Dissolved carbon dioxide	139	65	161	NA	NA	NA
Dissolved oxygen	8	6.2	7.7	NA	NA	NA
Nitrate (as N)	0.12	3.0	2.5	3.7	0.46	0.15
pH (units)	7.4	8.7	7.4	7.6	9.0	7.4
Sulfate	125	66	40	21	143	103
Total dissolved solids (TDS)	450	356	352	264	414	380
METALS (mg/L):						
Calcium	75	54	121	60	75	75
Magnesium	23	11	29	15	10	18
Manganese	0.010	0.14	0.42	0.038	0.030	0.12
Sodium	48	51	69	26	56	34
VOLATILE ORGANIC COMPOUNDS (µg/L):						
cis-1,2-dichloroethene	ND	ND	0.16	ND	ND	ND
Dichlorodifluormethane	ND	ND	1.9	ND	0.34	1.4
Tetrachloroethene	ND	ND	2.0	0.7	ND	1.1
Toluene	ND	ND	0.19	0.12	ND	ND
Tricloroethene	ND	ND	4.0	0.9	ND	ND
Trichlorofluormethane	ND	ND	0.7	0.32	ND	ND
MICROBIOLOGICAL ANALYSES (colony forming unit per milliliter, CFU/mL):						
Heterotrophic plate count	2.2×10^3	1.1×10^3	5.2×10^4	NA	NA	NA
Hydrocarbon plate count	NA	1.1×10^5	5.6×10^7	NA	NA	NA

Table 1. Initial water chemistry in new wells.

the well-graded grain-size distribution observed in these materials. The aquifer pumping test results obtained for well Y-15 suggest that a negative boundary condition exists in bedrock in this area and that fault planes may locally act as impediments to groundwater flow.

Analytical results

As summarized in Tables 1 and 2, the laboratory analytical results that were obtained for this investigation confirm earlier sampling programs and indicate that the most significant groundwater impacts at the site are associated with PCE and TCE. The presence of only low- or trace-levels of VOCs in samples obtained from monitoring wells along the west side of the property indicates that the release from the landfill is concentrated along the southern side of the site. High VOC concentrations associated with wells that are located near other wells where sampling has not identified significant concentrations of VOCs, confirm that groundwater flow and contaminant transport are strongly controlled by faults within bedrock.

The laboratory data indicate that reducing conditions occur in groundwater near the landfill, and that reductive dechlorination of PCE and TCE may be occurring. Factors supporting this inference include: detection of degradation products of PCE and TCE (e.g., cis-1,2-dichloroethene) down-gradient of the YLF; low dissolved oxygen and low oxidation-reduction potentials in samples obtained from wells adjacent to the YLF (reducing conditions favor biodegradation of PCE and TCE); and higher manganese and ferrous iron concentrations and lower

	Y - 3	Y - 5	Y - 6	Y - 11A	Y - 11B	Y - 17	Y - 18	Y - 20
Alkalinity	432	474	207	624	274	341	191	181
Bicarbonate	432	474	207	624	274	341	191	181
Dissolved oxygen	0.5	0.3	0.4	4.6	7.1	5.6	6.6	4.8
Fe II	0.35	ND	0.43	0.35	ND	ND	ND	ND
Redox potential (mV)	60	127	29	58	174	169	208	162
Sulfate	33	66	253	40	33	25	23	116
Total organic carbon	14	14	6.7	13	4.3	7.5	4.1	ND
Methane (mg/L)	0.639	0.103	0.028	0.009	0.010	0.009	0.009	0.009

Table 2. Water chemistry of selected VOC-impacted wells. Values in milligrams per liter unless otherwise indicated.

nitrate concentrations near highly impacted wells (indicating ion-exchange and reducing conditions).

DISCUSSION

Structural conditions

The results of the lineament analysis, geologic mapping, surface geophysical survey, and monitoring well construction were integrated to develop four geologic cross sections of the site (Figure 8). The groundwater monitoring wells that are depicted in the cross-sections were "projected" to the section lines parallel to the geologic structure (i.e., the projections do not cross structural features). As the boundary between weathered bedrock and alluvial deposits was not well defined by the geophysical data, the lithologic data generated during construction of groundwater monitoring wells were used to estimate the depth to bedrock.

As shown on Figures 2, 7, and 8, the data indicate that the site overlies a system of northeast-trending horsts and grabens. Similar fault-bounded structural blocks have been observed in clay-cake simulations of normal faulting performed by Cloos (1968). As measured in field exposures, the dip of the main trace of the Crafton Hills fault ranged from 50 to 70 degrees to the southeast, and similar inclinations were assumed for faulting elsewhere on the property.

In combination with the physiographic conditions in the area, the boring log and geophysical data also indicate that a roughly north-south oriented paleochannel may underlie the landfill (Figure 2). As discussed below, the distribution of groundwater impacts near this feature suggests that the historical channel exposed north of the site may have eroded faulted bedrock beneath the landfill, with the result that this paleochannel acts as a preferred pathway for groundwater flow and landfill constituent transport.

Groundwater flow and contaminant transport

The groundwater elevation contours that were developed for the site (Figure 3) indicate that groundwater near the landfill typically flows to the south and southwest, in general agreement with the regional groundwater flow direction. This pattern is locally modified by faults and bedrock/alluvial anisotropy that appears to promote cross-gradient flow. Two separate groundwater flow environments appear to exist near the YLF; the first is associated with faulted bedrock, and the second with old and young alluvial deposits. In the area adjacent to the YLF, old alluvial deposits are typically unsaturated. Exceptions occur near wells Y-4 and Y-11A/B, where bedrock materials have apparently been locally eroded to greater depths and the sequence of old alluvial fan deposits is thicker.

The results of the aquifer pumping tests and the distribution of groundwater impacts near wells Y-3, Y-5, Y-8, Y-10, and Y-12 indicate that, on a "macro-scale", bedrock materials appear to have significantly lower hydraulic conductivity properties in the north-south direction (perpendicular to faults) compared to the east-west direction (parallel to faults). The absence of VOCs and the relatively low inorganic constituent concentrations measured in wells located south of wells Y-3 and Y-5 indicate that faults in the area are relatively efficient barriers to groundwater flow, and that contaminant transport downgradient of the YLF locally occurs in a cross-gradient direction. The overall effect of faulting in bedrock beneath the landfill appears to be southwesterly, "stepped", groundwater flow, with westward-directed cross-gradient flow along faults, and southerly flow in areas unaffected by faulting (Figure 3).

The absence of VOC's west (cross-gradient) of well Y-5 may be related to the locally arcuate trace of

faults along the west side of the site. Alternatively, if VOCs do occur in this area, they may be restricted to discrete fracture zones that are not hydraulically connected to the five westernmost monitoring wells.

Since the Crafton Hills fault exhibits Holocene movement (Matti et al., 1992), the associated splays on the property may extend into old alluvial fan materials. However, the presence of high VOC concentrations in samples obtained in alluvial wells Y-11A/B and Y-14, downgradient and crossgradient of the landfill in the paleochannel area, suggests that fault gouge may not be well-developed in the old alluvial fan deposits. Preferred flow and transport of landfill constituents within the paleochannel is indicated by the absence of significant groundwater impacts associated with downgradient wells Y-4, Y-13 and Y-16 (directly downgradient of high VOC impacts near wells Y-3 and Y-11A/B), and by the presence of signficant groundwater impacts near crossgradient wells Y-14 and Y-17 (Figures 7 and 8).

The data indicate that groundwater impacts near the YLF are associated with both liquid- and gas-phase releases from the landfill. Landfill-gas impacts are indicated by the presence of chlorofluorocarbons (Freon 12 and Freon 11) and chlorinated ethenes/ethanes in groundwater samples obtained from both upgradient and downgradient monitoring wells. A liquid phase release is indicated by (1) higher inorganic constituent concentrations in samples from downgradient monitoring wells, (2) association of elevated inorganic constituent concentrations and high VOC impacts in samples obtained from downgradient monitoring wells, and (3) the correlation between higher inorganic constituent concentrations in samples obtained from well Y-2 at periods of high groundwater elevations.

The analytical results obtained from sampling of well pairs (e.g., wells Y-8 and Y-12; Y-9A/B; and Y-10A/B), and the data from temporary and permanent monitoring wells (e.g., wells Y-15T and Y-15), indicate that groundwater impacts are largely

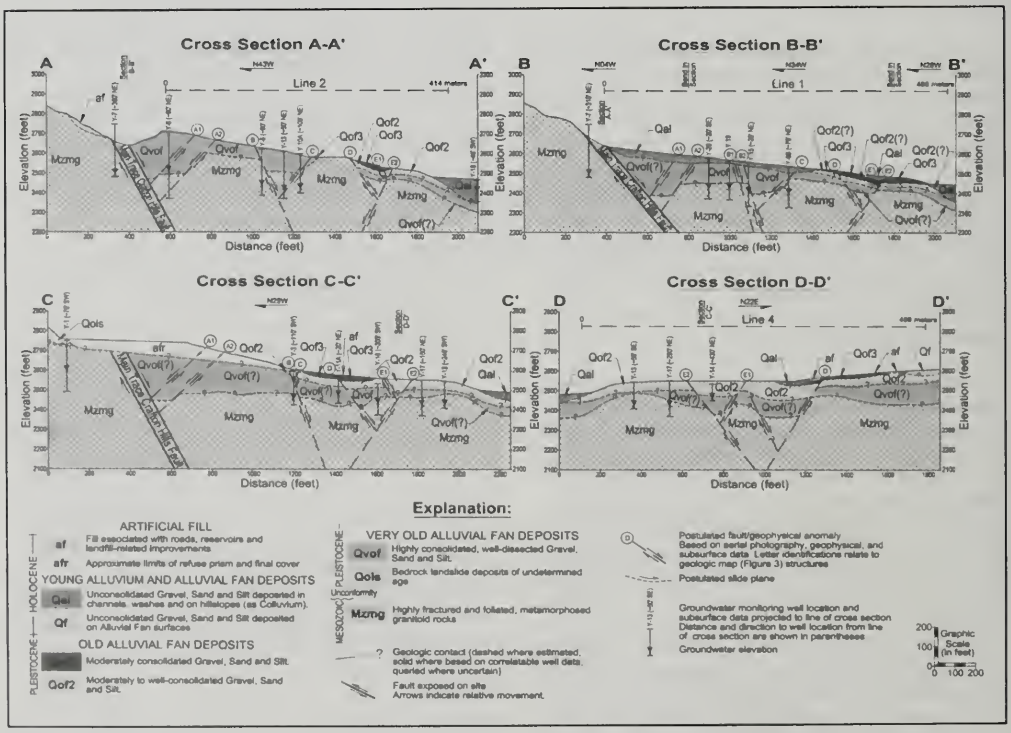

Figure 8. Geologic cross-sections.

restricted to the uppermost groundwater interval. This condition is consistent with the slight upward hydraulic gradient observed in well pairs, and the relatively low (residual) concentrations of the chlorinated VOCs identified in all well samples.

Analytical results indicate that groundwater impacts are most significant near wells Y-3, Y-5, and Y-11A/B (Figures 4, 5 and 6). Near the west end of the site, at well Y-5, PCE is the most common VOC in groundwater. TCE is most common near the southern edge of the site, at wells Y-11A/B. Approximately mid-way between wells Y-5 and Y-11A/B, PCE and TCE occur at nearly the same concentrations (e.g., in samples collected from well Y-3). Wells Y-3 and Y-5 were constructed in fractured materials north of fault B, and wells Y-11A/B were installed in saturated old alluvial fan deposits within the interpreted paleochannel. The distinction between high-PCE and high-TCE impact areas may be related to different source areas within the landfill, or possibly to reductive dechlorination (degradation) of PCE to TCE in groundwater.

The distribution of organic and inorganic constituents near the YLF indicate that inorganic constituent concentrations are attenuated (become similar to background conditions) within approximately 600 feet of the landfill (Figure 6). Organic impacts appear to decrease below MCL concentrations within about 1,100 feet of the site (Figures 4 and 5).

Intrinsic attenuation

Calculations were completed to evaluate the attenuation of VOCs that has been observed in downgradient well samples. The calculations utilized the hydraulic properties determined in the aquifer pumping tests, and typical chemical degradation coefficients (Wiedemeir et al., 1996) to estimate biodecay of chlorinated VOCs. The VOC attenuation calculations support the inference that natural attenuation processes (dispersion, mixing, and decay) result in a substantial decrease in the VOC concentrations downgradient of the landfill.

The calculations yielded a relatively good match with the monitoring well sampling data. Although the calculations indicate that some reduction (decay) and dispersion of VOCs occurs, the largest reductions in VOC concentrations appear to be related to the high hydraulic conductivity and the associated large volumes of groundwater that flows through the young alluvial deposits in Gateway Wash. In other words, substantial mixing and dilution of dissolved contaminants occurs in Gateway Wash.

CONCLUSIONS

Field and laboratory work completed for this project indicates that groundwater flow beneath and adjacent to the YLF is strongly controlled by faults and bedrock/alluvial anisotropy. The geophysical data generated by the STING® resistivity measuring system yielded the best resolution of the subsurface structures present beneath the site, and support lineament analyses that indicate that a number of subparallel faults underlie the property. The results of the aquifer pumping tests and the distribution of groundwater impacts indicate that faults on the property locally impede groundwater flow and contaminant transport. Overall, faulting appears to result in "stepped" groundwater flow with cross-gradient flow occurring parallel to faults.

Near the southern border of the YLF, the data indicate that impacted groundwater is also transported in a cross-gradient direction within a buried paleochannel that appears to extend from beneath the north end of the refuse prism, southeast to Gateway Wash.

The distribution of organic and inorganic constituents in wells indicate that inorganic groundwater impacts are attenuated within approximately 600 feet of the site, and that organic impacts decrease below MCL concentrations within about 1,100 feet of the site.

ACKNOWLEDGEMENTS

Many thanks to Russell Keenan (formerly with Norcal/San Bernardino Inc., now with Kleinfelder Associates) and Arthur Rivera of the County of San Bernardino Solid Waste Management Division for encouraging the authors to prepare this paper. Charlene Herbst, Dave Bieber and Bob Anderson generously provided peer review. Special thanks also to Chief Editor Horacio Ferriz for his patience and editorial guidance.

AUTHOR PROFILES

Terri S. Reeder is a California Certified Engineering Geologist and Hydrogeologist with over 11 years of experience in neotectonics, engineering

geology, hydrogeology, and environmental geology. Ms. Reeder is currently employed as an Associate Engineering Geologist with the California Regional Water Quality Control Board – Santa Ana Region.

Ralph Murphy is a California Certified Engineering Geologist and Hydrogeologist with 15 years of geologic, geotechnical, hydrogeologic and environmental experience. Mr. Murphy serves as a Supervising Engineering Geologist with GeoLogic Associates in San Bernardino, California. His special areas of interest and expertise include waste disposal facility siting, design, monitoring and remediation.

Dr. James Finegan is a California Certified Hydrogeologist with over 8 years of geologic, hydrogeologic and environmental experience. Dr. Finegan is a Senior Hydrogeologist with GeoLogic Associates in San Bernardino, California. His areas of expertise include hydrogeologic studies of contaminant behavior in fractured rock aquifers, as well as characterizing, evaluating, and remediating waste disposal facility impacts.

SELECTED REFERENCES

CFR (Code of Federal Regulations), 1995, Title 40, Protection of the environment, Parts 87 to 149: Office of the Federal Register, National Archives and Records Administration, distributed by Government Institutes, Inc., 1346 p.

Cloos, E., 1968, Experimental analysis of Gulf Coast fracture patterns: American Association of Petroleum Geologists Bulletin, v. 52, pp. 420-444.

Cooper, H.H. and Jacob, C.E., 1946, A generalized graphical method for evaluating formation constants and summarizing well field history, Transactions of the American Geophysical Union, v. 27, p. 526-534.

Dutcher, L.C. and Burnham, W.L., 1960, Geology and groundwater hydrology of the Redlands-Beaumont area, California, with special reference to groundwater outflow: U.S. Geological Survey Open-File Report, 352 p.

DWR (California Department of Water Resources), 1964, Location of hydrologic boundaries, Santa Ana Drainage Province, names and areal code numbers of hydrologic areas in the Southern District: Map, Scale 1:250,000.

EMCON, 1997, Phase 1B evaluation monitoring program report, Yucaipa Sanitary Landfill, San Bernardino County: Consultant's report to the County of San Bernardino Waste System Division, 39 p.

Fife, D.L., Rodgers, D.A., Chase, G.W., Chapman, R.H., and Sprotte, E.C., 1976, Geologic hazards in southwestern San Bernardino County, California: California Division of Mines and Geology Special Report 113, 40 p.

GLA (GeoLogic Associates), 1992 – 2000, Quarterly Reports: "County of San Bernardino Water Quality Monitoring Report, Yucaipa Sanitary Landfill – San Bernardino County, California": Consultant's reports to the County of San Bernardino Solid Waste Management Department (1992-1995) and the County of San Bernardino Waste System Division and NORCAL/San Bernardino, Inc. (1996-2000).

GLA (GeoLogic Associates), 1995, Phase 1A, Initial Evaluation Monitoring Program, Yucaipa Sanitary Landfill, San Bernardino County, California: Consultant's report to County of San Bernardino Solid Waste Management Department, Job no. 9436, December.

IT (IT Corporation), 1989, Solid Waste Assessment Test, Yucaipa Landfill, San Bernardino County, California: Consultant's report to San Bernardino Solid Waste Management Department.

Matti, J.C., Morton, D.M., Cox, B.F., Carson, S.E., and Yetter, T.J., 1992, Geologic setting of the Yucaipa Quadrangle, San Bernardino and Riverside Counties, California: U.S. Geological Survey, Open-File Report 92-446, Scale 1: 24,000.

Neuman, S.P., 1972, Theory of flow in unconfined aquifers considering delayed response of the watertable: Water Resources Research, v.8, p. 1031-1045.

SAGA Geophysics, 2000, STING resistivity measurement: Promotional brochure provided by Advanced Geosciences, Inc., Austin, Texas.

Theis, C.V., 1935, The relation between the lowering of the piezometric surface and the rate and duration of discharge of a well using groundwater storage: Transactions of the American Geophysical Union,, v.16, p. 519-524

Wiedemeier, T.H, Swanson, M.A., Moutoux, D.E., Gordon, E.K., Wilson, J.T., Wilson, B.H., Kampbell, D.H., Hansen, J.E., Haas, P., and Chapelle, F.H., 1996, Technical protocol for evaluating natural attenuation of chlorinated solvents in groundwater, Draft – Revision 1: Consultant's report to Air Force Center for Environmental Excellence, Technology Transfer Division, Brooks Air Force Base, San Antonio, Texas, 92 p.

ENGINEERING GEOLOGY STUDIES FOR THE NEW EAST SPAN OF THE SAN FRANCISCO-OAKLAND BAY BRIDGE, SAN FRANCISCO AND ALAMEDA COUNTIES, CALIFORNIA

REID L. BUELL[1], THOMAS W. McNEILAN[2], AND CRAIG D. PRENTICE[2]

ABSTRACT

The new east span of the San Francisco-Oakland Bay Bridge (SFOBB) will cross the portion of San Francisco Bay between Yerba Buena Island and Oakland, California, parallel to the existing bridge. The new bridge span will be 3.4 kilometers long and will become the eastern portion of the SFOBB that connects San Francisco to Oakland. Between 1994 and 1996, the California Department of Transportation (Caltrans) conducted geological engineering studies for the proposed San Francisco-Oakland East Span Seismic Safety Project as part of the seismic retrofit program in response to damage, and lessons learned, from the Loma Prieta earthquake of 1989. Subsequent to the 1997 decision to replace the SFOBB East Span, Fugro-Earth Mechanics (FEM; a joint venture of Fugro West and Earth Mechanics) was retained by Caltrans to perform an areal geological study as part of the selection process for bridge alignment and structure type. The geologic study consisted of two phases: a Phase I site characterization, and a Phase II design level study that included pier-specific subsurface exploration and geotechnical evaluation. These geologic studies have provided a detailed view of the stratigraphic units and young sediments along the alignment of the east span of the San Francisco-Oakland Bay Bridge.

INTRODUCTION

The San Francisco-Oakland Bay Bridge (SFOBB) crosses San Francisco Bay, linking San Francisco and Oakland, California (Figure 1). The original double-deck structure was built between 1933 and 1937 and currently carries 10 lanes of Interstate 80 traffic. The SFOBB consists of: (a) a west span from San Francisco to Yerba Buena Island; (b) a western viaduct, tunnel, and eastern viaduct across Yerba Buena Island; and (c) an east span from Yerba Buena Island to the Oakland Mole (a man-made extension of land west of the toll plaza).

The bridge is located between the San Andreas fault (capable of a M_W 8.4 earthquake and located approximately 8 kilometers west of the bridge) and the Hayward fault (capable of a M_W 7.1 earthquake and located approximately 18 kilometers east of the bridge). During the M_S 7.1 Loma Prieta earthquake that occurred on October 17, 1989, the bridge sustained significant damage, which included the partial collapse of a portion of the east span (Figure 2).

As repair got underway, the California Governor's Board of Inquiry noted that the SFOBB-East Span was designed for only a peak horizontal earthquake acceleration of 0.1g (10% of the value of gravity). In contrast, current practice requires that structures be designed to sustain much higher

[1]California Department of Transportation
5900 Folsom Boulevard
Sacramento, CA 95819-4612
reid_buell@dot.ca.gov

[2]Fugro West, Inc.
5855 Olivas Park Drive
Ventura, CA 93003-7672
cprentice@fugro.com

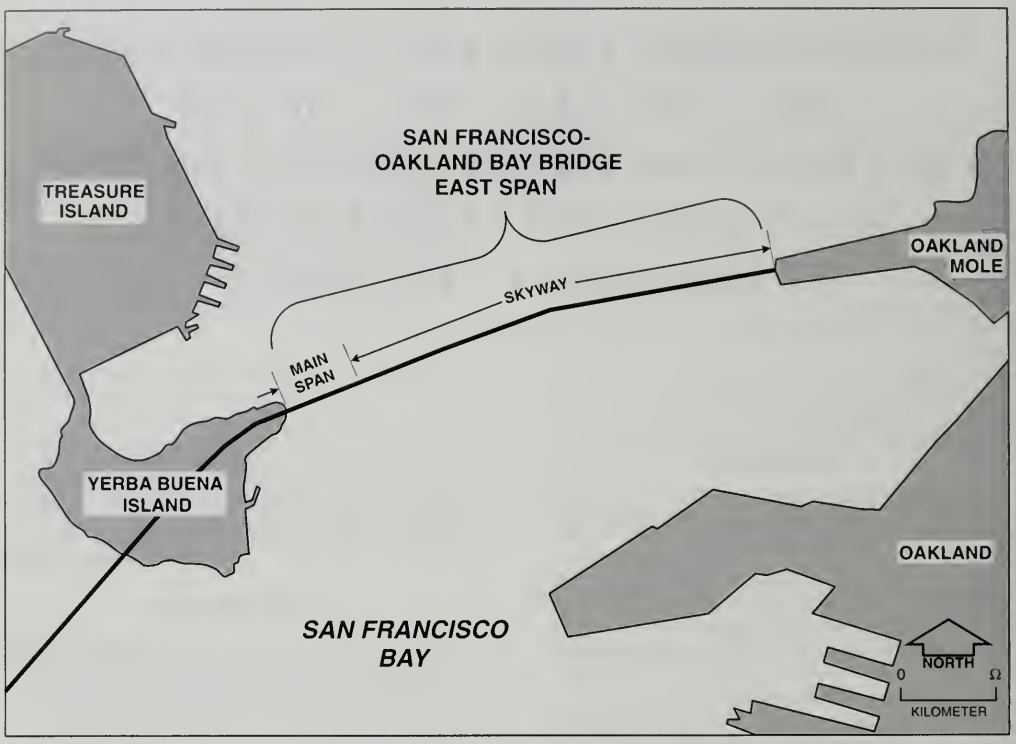

Figure 1. Vicinity map showing the proposed location of the new east span of the San Francisco-Oakland Bay Bridge.

earthquake accelerations (FEM, 1998e). As a result, Caltrans embarked on a seismic retrofit program. It was ultimately decided to retrofit the western portion of the bridge, the tunnel, and the west viaduct on the island. However, in 1997 it was decided that the eastern portion of the bridge, including the eastern transition from the tunnel on the island, should be replaced. This paper reviews the geologic and geotechnical studies and results of the exploration for the SFOBB East Span Seismic Safety Project.

PROJECT OVERVIEW

The initial geotechnical studies undertaken by Caltrans between 1989 and 1997 were directed toward a seismic retrofit of the SFOBB East Span. After deciding to replace the existing SFOBB East Span bridge, Caltrans coordinated the selection of the alignment of the replacement bridge and design evaluation with the Metropolitan Transportation Commission (MTC), the Federal Highway Administration, and the San Francisco Bay Conservation and Development Commission. Caltrans also contracted with the joint venture of TY Lin and Moffatt & Nichol (TY Lin/M&N) to prepare the bridge design, and with the joint venture of Fugro-Earth Mechanics to provide the geological/geotechnical and foundation design studies for the bridge substructure.

Phase I

In November 1997, the MTC and its Engineering Design and Advisory Panel (EDAP) task force decided the new structure should be a single-deck structure located to the north of the existing bridge. Caltrans and its consultant, Fugro-Earth Mechanics, were directed to study and evaluate the subsur-

Figure 2. Photograph of damage to the east span of the bridge from the 1989 Loma Prieta earthquake.

face geologic conditions north of the existing bridge. This Phase I study evaluated: (a) the quality and depth to suitable bedrock foundation material near Yerba Buena Island, (b) the areal distribution and character of sediments within the buried paleochannels known to exist north of the existing bridge, and (c) the physical-chemical characteristics of the bay sediments overlying bedrock (FEM, 1998a, 1998b, 1998c). The Phase I geologic database on the subsurface sediments and associated features were used by the MTC-EDAP task force to select the most suitable bridge alignment and type of structure.

In June 1998, the MTC selected a 565-meter-long, asymmetrical, single tower, self-anchored suspension bridge design with an alignment north of the existing bridge. The center pier of the main span would be located some 65 meters into the bay from Yerba Buena Island. The west pier would be founded on Yerba Buena Island and the east pier would be located 385 meters east of the center pier (Figure 4). A 2.1-kilometer-long skyway structure would complete the east span crossing to the Oakland shore.

Phase II

After receiving foundation locations from the bridge designers, the geology team began a Phase II site evaluation study to collect pier-specific information for foundation design. Specific geologic issues evaluated included: (a) the physical properties of the sloping bedrock surface that underlies the main pylon foundation, (b) the physical features of the two intersecting paleochannel systems beneath the main span east pier, (c) the location of the meandering edge of the Recent paleochannel system along the skyway alignment, and (d) the axial and lateral pile capacity for the skyway alignment.

GEOLOGIC STUDY

Phase I

The Phase I study (performed in early 1998) included development of a project-specific geographical information system (GIS) database, extensive marine and land geophysical surveys, marine drill-

ing operations from two barges, land drilling, cone penetrometer tests (CPTs), extensive in situ geotechnical sampling, and laboratory testing. The marine drilling program used sophisticated exploration equipment and techniques normally used for deep-water offshore studies, but adaptable to coastal infrastructure projects. Marine borings are usually more costly than land borings, require a greater logistical coordination effort, and require larger, more sophisticated equipment. In balance, they provide a superior quality of subsurface data.

The initial data entered in the GIS database were from subsurface data developed for: (1) the original bridge design, (2) the proposed seismic retrofit of the existing bridge, and (3) adjacent projects. GIS information was then used to help plan the subsequent exploration. The database included borehole lithology, laboratory test data, downhole compression wave (P) and shear wave (S) velocities, and historical aerial photographs. The subsurface exploration and geophysical data gathered during the Phase I and Phase II studies for the new bridge were added to the GIS database throughout the field exploration programs.

Marine geophysical surveys were performed at the beginning of the Phase I study to image the subsurface geologic structure to the north and south of the existing bridge alignment. Approximately 130 kilometers of two-dimensional (2-D) survey data were collected including: (a) navigation, (b) echo sounder, (c) side-scan sonar, (d) shallow-penetration, CHIRP high-resolution seismic reflection, and (e) deeper-penetration, 5-cubic-inch sleeve (air) gun seismic reflection data (FEM, 1998e). The preliminary geophysical data interpretations were integrated with the existing GIS database to refine the subsurface model and to aid in the selection of the locations of the Phase I borings.

The geophysical program also included a three-dimensional (3-D) survey to provide seismic reflection data at a nominal 6.25-meter spacing in the 2-square kilometer project area (FEM, 2000a, Figure 4). For the 3-D survey, the seismic source consisted of an array of three or four air-sleeve guns with data recorded on two to four 16-channel cables. The 3-D data set provided valuable correlation and continuity between exploration locations in areas underlain by sloping bedrock and complex stratigraphy (Figures 3 through 7).

The Phase 1 study included 14 marine borings drilled and cored into bedrock that lies as deep as 150 meters below the bay bottom. The borings included extensive soil sampling using downhole push and wireline sampling techniques. Between sampling intervals, in situ CPTs and vane shear tests were conducted in the upper 20 to 50 meters of the drill holes using downhole tools to provide a nearly continuous record of subsurface engineering parameters and characteristics. In addition to the downhole testing, near-surface *in situ* vane shear tests were performed concurrently with drilling (Figure 6).

Resistivity, natural gamma, caliper, spontaneous potential, P (compression) wave and S (shear) wave logs were run in each of the Phase I borings. Acoustic televiewer logs also were collected in five rock core borings in the main span area to help evaluate rock fracture orientation. Seven pressuremeter tests were performed in one of the rock core borings in the main pylon area to measure the in situ maximum and average shear modulus of the Franciscan Formation bedrock (FEM, 1998f).

Phase II

In the fall of 1998, after a preferred alignment was selected, 30 borings were drilled as part of the Phase II design-level study. The purpose of the Phase II drilling was to: (1) obtain site-specific information for the individual pier locations, (2) obtain subsurface data for unexplored areas along the proposed alignment, and (3) collect site-specific data on the proposed test pile driving locations. Adjacent to the eastern end of Yerba Buena Island, where the bedrock is shallow, the Phase II borings were cored as much as 40 meters into Franciscan Formation rock. Elsewhere along the alignment, the Phase II borings were drilled some 100 to 120 meters into the sediments overlying bedrock. The components, methods, and procedures used during the Phase II marine drilling operations were the same as described for the Phase I drilling program.

Subsurface conditions were interpreted from the geophysical data by correlating seismic reflectors imaged in the line surveys, velocity discontinuities measured in the downhole geophysical logs, and stratigraphic breaks observed in the borings. Because the geophysical survey provided relatively continuous information over a wide area, it was possible to inexpensively extrapolate or interpolate stratigraphic contacts identified in discrete, rela-

tively widespread boring locations (FEM, 2000a). An illustrative 3-D geophysical section showing prominent reflectors as well as lithology identified in a rock core boring adjacent to Yerba Buena Island is shown on Figure 3.

Most of the soil samples collected during the Phase II exploration were tested onboard the drilling barges while drilling was in progress. Laboratory soil tests included water content and unit weight measurements, fall cone testing, miniature vane testing (both undisturbed and remolded), unconsolidated-undrained triaxial (both undisturbed and remolded specimens). Representative values are reported below, in the section about stratigraphy.

Point load testing was performed on rock core samples from the Franciscan Formation (representative values are reported in a later section). Onboard testing offered more accurate measurements of the undrained shear strength of clay samples prior to stress relief and without the disturbance that occurs during sample shipment. Real time test results aid in verifying sample descriptions and in planning subsequent sampling and *in situ* testing performed as a boring is advanced.

Onshore laboratory testing was performed at Fugro's laboratories in Ventura, California, and Houston, Texas. This testing included: (a) classification tests (grain size, specific gravity, and plasticity); (b) consolidation tests (incremental and controlled rate of strain); and (c) consolidated-drained, consolidated-undrained, and K_o consolidated-undrained triaxial compression tests. A total of more than 180 consolidation tests were performed on samples recovered from the 44 marine soil borings. Special tests such as resonant column tests, cyclic direct shear tests, undrained shear strength measurements at differing strain rates, and radial consolidation tests were performed at Fugro's Houston laboratory, the University of Texas at Austin, and the University of California at Berkeley. In addition, unconfined compression and direct shear tests on rock specimens were conducted by Geo Test Unlimited of San Leandro, California.

BAY BATHYMETRY

Bathymetry collected for this study indicates that the water level beneath the bridge alignment increases in depth to the east of Yerba Buena Island and reaches a maximum depth of 30 meters about

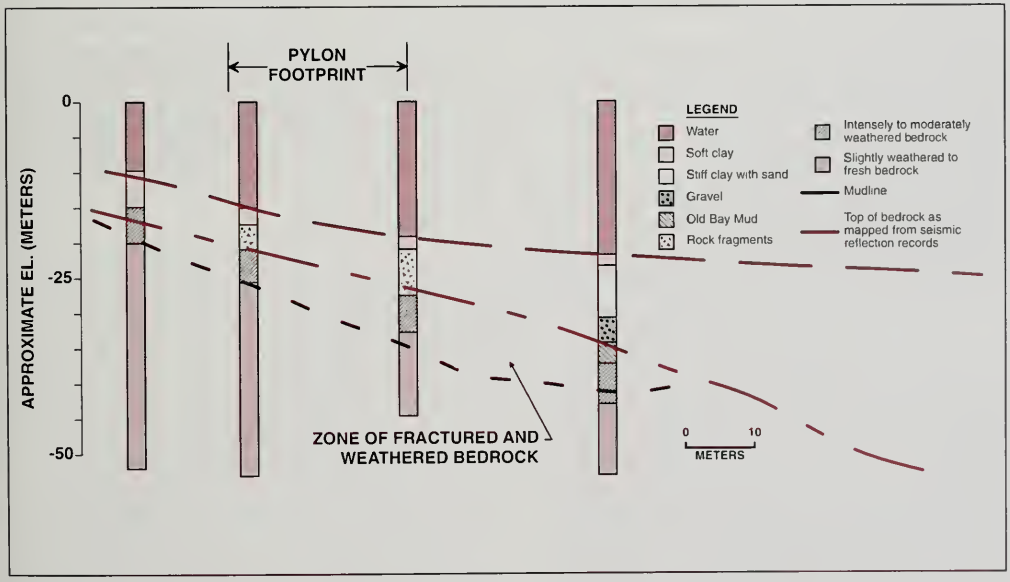

Figure 3. Example of an integrated seismic and geologic cross section.

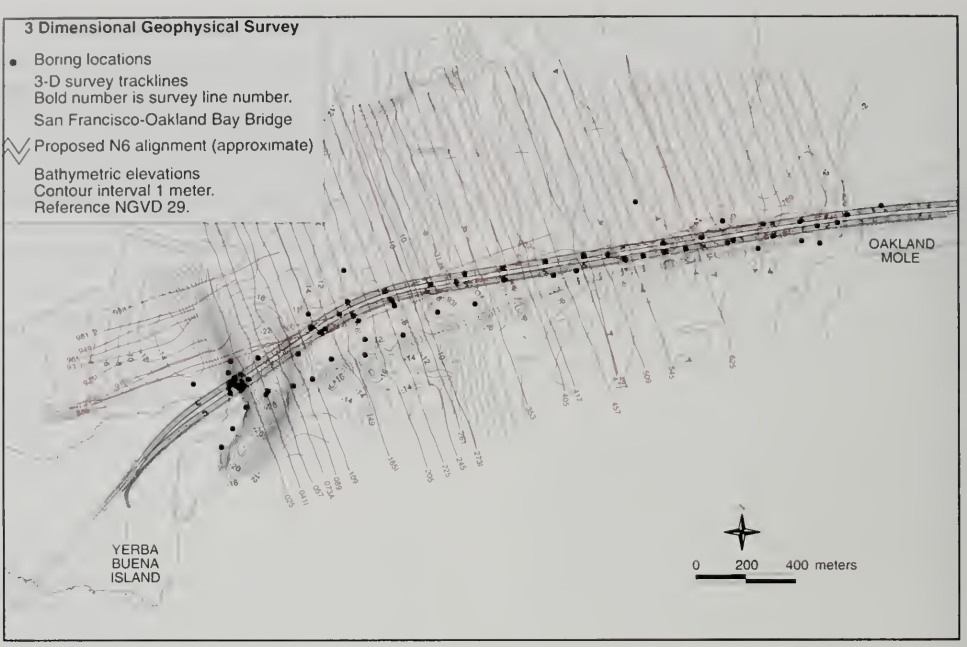

Figure 4. Bathymetry and 3-D geophysical survey database map

300 meters east of the island. The deepest water level occurs in a 15-meter-wide, enclosed depression (Figure 4). To the east of that depression, the bay bottom rises gradually toward the Oakland Mole (Figure 4). East of the depression area, the most prominent bathymetric feature is a 4-meter-high, westerly-facing slope about 800 meters east of Yerba Buena Island. The seismic sections suggest that the westerly-facing slope correlates to the westerly progressing depositional nose of the youngest sediment underlying the bay.

AREAL GEOLOGIC SETTING

Holocene and Pleistocene sediments overlying easterly-sloping bedrock underlie the SFOBB East Span alignment. The geologic conditions underlying the SFOBB East Span include: (a) easterly-sloping bedrock of the Franciscan Formation (Figures 3 and 6), (b) a westerly-thinning sequence of Pleistocene and Holocene marine and alluvial sediments, and (c) extensive paleochanneling within the Holocene and Pleistocene sediments (Figure 7). The principal geologic units identified at the site (from oldest to youngest) are: (1) Jurassic-Cretaceous Franciscan Formation, (2) lower and upper members of the Pleistocene Alameda Formation, (3) Pleistocene Old Bay Mud (also sometimes referred to as Yerba Buena Mud), (4) Pleistocene Merritt-Posey-San Antonio Formation, and (5) Holocene Young Bay Mud.

Franciscan Formation

Bedrock surface. In the study area, the Franciscan Formation consists of interbedded sandstone, siltstone, and claystone. The bedrock crops out on Yerba Buena Island and forms a prominent submerged high that rises to an elevation of -10 meters off the east tip of the island (Figure 5). From this high, the top of the bedrock slopes easterly at about 15 to 18 degrees (with occasional local areas sloping 20 to 22 degrees) down to an elevation of -95 meters (Figures 3 and 5). The toe of the steeper bedrock slope occurs about 350 meters to the east of the island. Farther to the east, the bedrock slope decreases, and the bedrock surface slopes to the east at an average slope of approximately 0.8 to 1.2 degrees, reaching an elevation of about -135 meters near the tip of the Oakland Mole (Figure 5). The

bedrock surface between the toe of the steeper slope (about 350 meters east of Yerba Buena Island) and the Oakland Mole decreases in elevation in a step-like manner, with a series of 5- to 10-meter drops separated by several hundred-meter-wide terraces.

Stratigraphy. The Jurassic-Cretaceous Franciscan Formation (Trask and Rolston, 1951) is predominantly formed by thickly-bedded-to-massive graywacke sandstone interbedded with thin siltstone and claystone layers. Overall, the fine-grained interbeds comprise less than about 10 percent of the stratigraphy, but locally as much as 30 to 40 percent of the recovered rock cores.

The upper 6 to 9 meters of bedrock are usually moderately weathered and intensely fractured, with a Rock Quality Designation (RQD) of less than 25. The weathered zone is underlain by a relatively thin, 1.5- to 3-meter-thick layer of slightly weathered rock with up to 12 millimeters of light brown, moderately weathered rock on each side of the fractures and joints.

Below the weathered zone, the fresh sandstone is hard, well indurated, and has median unconfined compressive strengths in the range of 30 to 110 megapascals (MPa). Fresh, unfractured sandstone had strengths in the range of 140 to greater than 180 MPa. The sandstone is typically moderately to slightly fractured, with three primary fracture inclinations dipping at: (a) 25 to 40 degrees (bedding), (b) 50 to 60 degrees, and (c) 75 degrees to near vertical. The fracture surfaces were typically slightly to moderately rough and moderately undulating. A majority of the fractures were filled with calcite. Zones of intensely fractured sandstone, up to 1.5 to 1.8 meters thick, were encountered in several borings.

The thinly bedded to laminated siltstone and claystone interbeds are dark gray to black, moderately hard, and typically range from about 0.1 to 0.3 meters in thickness; however, several zones of fine-grained rock up to 1.8 meters thick were encountered. The fine-grained interbeds are intensely to very intensely fractured. The siltstone/

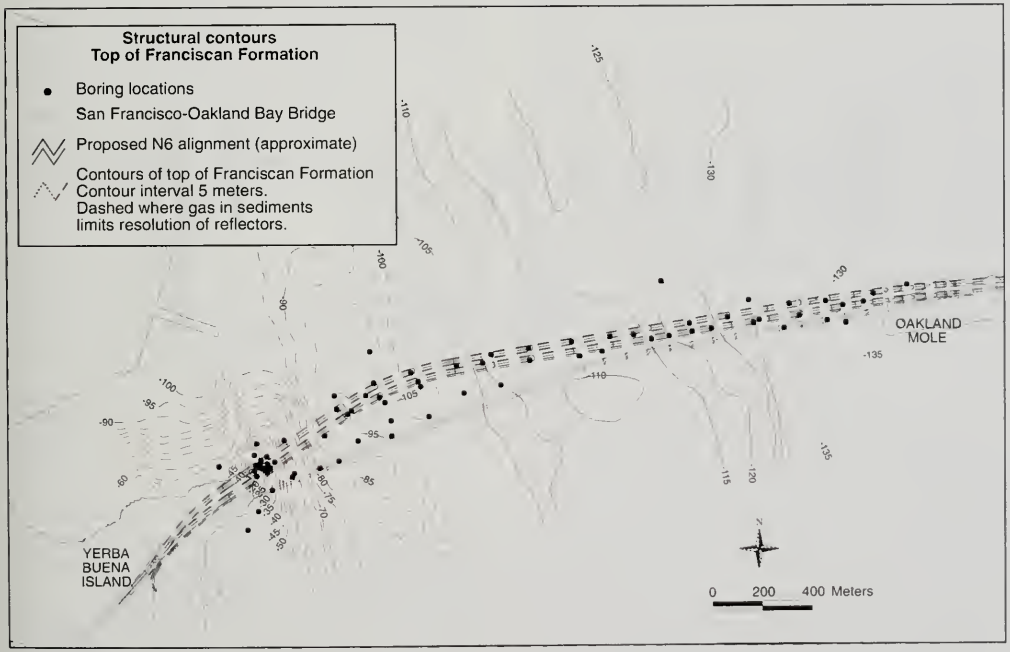

Figure 5. Structural contours of the top of the Franciscan Formation.

claystone rock in the cores generally broke along smooth, polished, bedding plane partings, the majority of which were inclined 25 to 40 degrees from the horizontal.

Pleistocene and Holocene sequence

A westerly thinning sequence of Pleistocene and Holocene marine and alluvial sediments unconformably overlies the Franciscan Formation bedrock along the bridge alignment (FEM, 1998a; Figure 6). The sediment profile appears to reflect changes in sea level that have occurred over the last several hundred thousand years. In general, the marine sediments deposited in sea-level high stands consist primarily of clays and silts, and the alluvial sediments deposited during sea-level low stands are more commonly sands. In some depth zones, however, the primarily fine-grained marine clays contain interbedded layers of sand, and the primarily granular alluvial sequences contain abundant fine-grained interbeds. Except where eroded and then backfilled by past sequences of channeling, the inclination of the sediment bedding is slight, so for practical purposes bedding can be considered to be near horizontal. However, the Holocene and Pleistocene marine and alluvial sediments are frequently interfingered and interlayered. Thus, although the stratigraphic sequences generally can be extrapolated between borings and geophysical tracklines, the lithologic and physical properties of the sedimentary units can vary significantly horizontally.

The Cenozoic geologic units described below are shown on the geologic cross section (Figure 6) that is parallel to the western end of the proposed bridge alignment. Soft sediment lithologies plotted on the cross section include stratigraphic contacts interpreted from marine geophysical records and measured with downhole CPT and drill hole testing methods. A short description of the principal units follows.

Alameda Formation

The Alameda Formation generally lies directly above the bedrock in the marine portion of the project area. The Alameda Formation is considered to be of late Pleistocene age (Sloan, 1982), and has been informally divided into a lower, primarily allu-

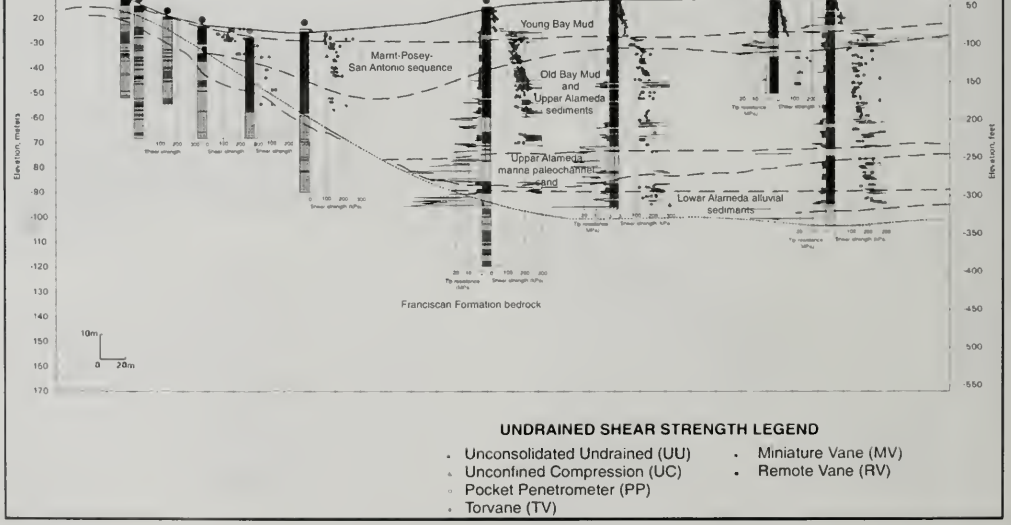

Figure 6. Subsurface cross section A1-A1' showing the stratigraphy east of Yerba Buena Island.

vial member, and an upper, primarily fine-grained marine member (Rogers and Figuers, 1992a, 1992b).

The sediments present below about -80 to -85 meters of elevation are interpreted to be the lower, primarily alluvial member of the Alameda Formation. These dense, granular sediments onlap the lower portion of the bedrock slope in the western portion of the project area, and overlie the Franciscan Formation bedrock to the east of the toe of the steep bedrock slope (Figure 6).

Although the lower member of the Alameda Formation is composed primarily of granular sediments, the top of the formation generally correlates to the top of a lean clay layer that is different in composition from the overlying clays of the upper marine member of the formation. The top of that layer correlates to a strong, generally continuous seismic reflector that correlates with a distinct increase in the primary and shear wave velocities measured in the borings (FEM, 1998a, 2000a; Figure 6).

The reflector corresponding to the top of the lower member of the Alameda Formation is typically about 5 to 15 meters above the top of the first relatively continuous dense sand layer, which is encountered between -90 and -94 meters of elevation. The sands are very dense and typically have a mean grain size of 1 to 8 millimeters. Although composed primarily of granular sediments, the sand deposits include an appreciable percentage of hard clay layers.

The lower member of the Alameda Formation is approximately 70 meters thick at the eastern boundary of the proposed alignment. To the west, the formation thins gradually to approximately 40 meters thick before pinching out (approximately 300 meters east of Yerba Buena Island) at the base of the steeply sloping Franciscan surface (Figure 6). The undrained shear strength of clay layers within the Alameda Formations typically ranges from 250 to 400 kPa.

The upper, fine-grained marine member is composed primarily of very stiff to hard, overconsolidated, plastic clay with occasional silt, clayey silt, and sand layers. Except for the increased occurrence of coarser-grained interbeds, the upper Alameda marine clays are similar to the marine clays of the overlying Old Bay Mud. The combined thickness of those marine clays, which typically extends down to an elevation of about -85 meters, is typically about 60 meters (Figure 6).

Old Bay Mud

The Old Bay Mud (sometimes locally referred to as the Yerba Buena Mud) that overlies the Alameda Formation and underlies the San Antonio Formation is considered to be an 80,000- to 130,000-year-old marine deposit (Sloan, 1982). The surface of the Old Bay Mud is extensively channeled. The Old Bay Mud typically is a very stiff to hard, overconsolidated, plastic clay that includes several, often discontinuous, crusts. Except where eroded by channeling, the Old Bay Mud is typically about 15 to 20 meters thick. The undrained shear strength of the Old Bay Mud increases in depth and typically ranges from 90 to 175 kPa at the top of the sequence to 150 to 250 kPa at the base of the sequence. The sequence also includes numerous "crust" layers with shear strengths 25 to 50 kPa higher than adjacent layers. Those crust layers are interpreted to be old soil horizons that were exposed to air during sea level changes.

Merritt-Posey-San Antonio Formation

Except where removed by erosion and channeling, a layered sequence of sand and clay is present between the Old Bay Mud and the Young Bay Mud over portions of the eastern San Francisco Bay. The seismic sections suggest that the elevation of the top of the sequence varies due to erosion and channeling. Although the base elevation of the sequence is less variable, the bottom of the sequence locally extends down into erosional channels that are cut into the underlying Old Bay Mud. The sequence is typically absent in areas of Recent channeling (Figure 7). Seismic reflections in the sequence are generally discontinuous and individual layers are often of limited lateral extent.

We have adopted the term "Merritt-Posey-San Antonio" sequence over the more simplified designation of "Merritt Sand" in recognition of the layered and interbedded characteristics of the deposits. The sequence is generally considered to be composed of late Pleistocene, non-marine sediments deposited during the late Wisconsin glacial stage (90,000 to 11,000 years ago). Rogers and Figuers (1991) report that the Merritt Formation is primarily formed by coarse-grained, aeolian sediments that were blown in from the west during low sea-level stands. In the project area, the San Antonio Formation has pre-

viously been described as a thick expanse of estuarine and alluvial sediments lying between the Alameda Formation and the Young Bay Mud (Trask and Rolston, 1951). The Posey member, typically considered the basal member of the San Antonio Formation, is reportedly of alluvial origin and was likely deposited within channels that were active during low sea-level stands. Although primarily nonmarine deposits, the late Wisconsin glacial stage also included periods of sea level fluctuations that may have produced estuarine environments. The fine-grained layers within the sequence are likely associated with those periods.

The combined sequence is from 0 to 15 meters thick and typically includes dense to very dense sand with layers of stiff to very stiff sandy clay and clay. Immediately west from the Oakland Mole, the sequence includes a distinct 3- to 4.5-meter-thick, very dense sand (Merritt) layer. To the east of Yerba Buena Island, the borings suggest that little or no sand is present within the layered sequence that infills a channel eroded into the underlying Old Bay Mud (Figure 6).

Young Bay Mud

Young Bay Mud, the youngest geologic unit in the bay, was deposited in a marine environment following the end of the last low sea-level stand, which was about 11,000 years ago (Atwater et al., 1977). Outside of the Recent paleochannels, the surface deposit of Young Bay Mud consists of a westerly thinning wedge of sediments that thins from about 8 to 10 meters thick at the end of the Oakland Mole to an average of about 4 meters at the toe of the steeper bay bottom bathymetry. The base of the deposit is typically between elevations of -12 to -18 meters. Within the paleochannels, the Young Bay Mud is as thick as 33 meters and extends down to an elevation of -45 meters (Figure 7).

The Young Bay Mud sediments are generally very soft to firm, normally to slightly overconsolidated, high plasticity clays. In the base of the Recent paleochannels, the sediments become stiff. The clays are generally greenish-gray, with shell fragments ranging from sparse to abundant. The Young Bay Mud that infills the Recent paleochannel includes sand layers and/or seams within several depth intervals that may correlate to different depositional periods. The undrained shear strength of the Young Bay Mud generally increases with depth from 2 to 4 kilopascals (kPa) at the surface to 20 to 30 kPa at the base of the sequence. At the base of deep paleochannels (21 to 24 meters in depth), the undrained shear strength typically ranges from 40 to 65 kPa.

Paleochannel systems

The SFOBB East Span Seismic Safety Project area is underlain by a series of nested, buried paleochannels. The more recent channeling (Figure 7) includes an east-west-trending channel to the north of the existing SFOBB East Span alignment (consistent with the channeling mapped by Trask and Rolston [1951]) and south-to-north tributary channels associated with the east-west channeling. The southern edge of the paleochannel meanders across both the existing and proposed bridge alignments (Figure 7). In general, the marine clays are thicker and the alluvial sands are thinner or absent within the Recent paleochannels.

Most previous interpretations of widely spaced boring data (Trask and Rolston, 1951; Goldman, 1969) have indicated that the east-west-trending channel deflects to the southwest and passes around the southern tip of Yerba Buena Island. More recent interpretations of the regional geology (Lee and Praszker, 1969; Rogers and Figuers, 1992a, 1992b) indicate that a Recent paleochannel extends northward along the eastern edge of Treasure Island. The available geological and geophysical data along the new bridge alignment indicates that outlet channels are cut into the Old Bay Mud, and the channels extend both southwest of Yerba Buena Island and westward past the eastern tip of the island.

The boring data show that along most of the east-west-trending channel, the base of the Young Bay Mud paleochannel infill generally coincides with the erosional surface cut into the Old Bay Mud. Those data suggest that the primary Young Bay Mud-filled trunk channel extends westward to the north of the eastern tip of Yerba Buena Island (and presumably under Treasure Island). In contrast, the boring data show that the clay infill in the erosional channel (which is cut into the Old Bay Mud and extends southwest past the tip of the island) is comprised of stronger and older clays. Within this channel, the Young Bay Mud infill is limited to only a thin, northerly thickening veneer at the top of the channel infill sequence.

In addition to the Recent channels described above, the site also is underlain by a number of

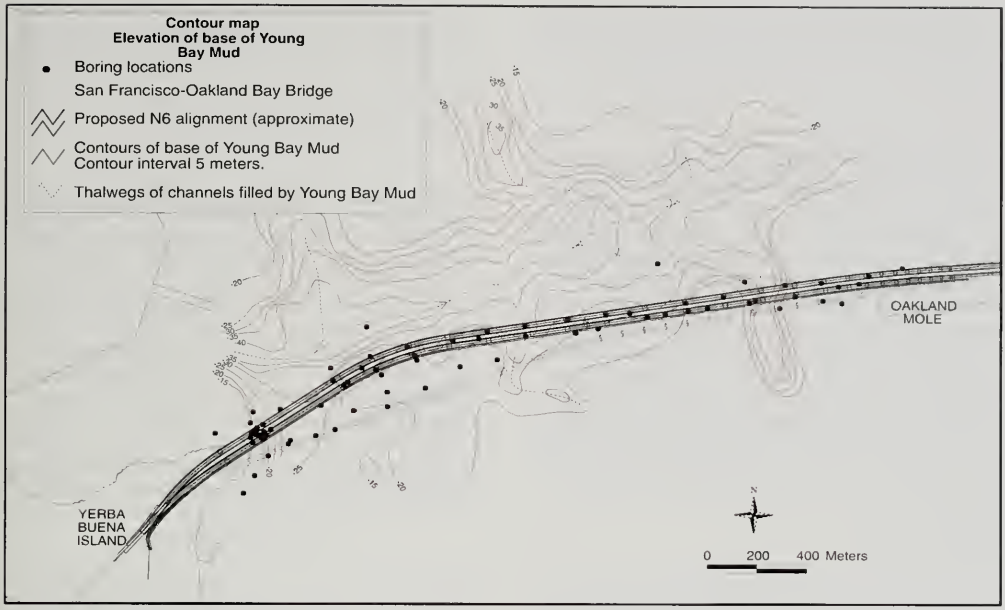

Figure 7. Structural contours of the base of Young Bay Mud.

deeper and older channels. In general, the seismic records suggest that as the channel system evolved, successive channels eroded into, along, across, and through older, deeper channels. Because the geophysical data for areas underlain by the east-west-trending Recent paleochannel are adversely affected by the pervasive presence of biogenic gas within the channel infill, it is difficult to map deeper paleochannels beneath the east-west-trending paleochannel (FEM, 1998d). However, a deeper (and older) nested series of north-south-oriented channels were clearly imaged in the western one-third of the survey area (Figure 7).

Although the Recent Young Bay Mud-filled paleochannel is interpreted to outlet to the north of Yerba Buena Island, the data suggest that flow from the east-west channel at other depths (and ages) was to the southwest of Yerba Buena Island. Two older paleochannels with southwest-trending outlets for the east-west-trending channel were mapped in the integrated geophysical study. Those channels include a stiff clay-filled channel eroded into the top of the Old Bay Mud and a predominantly sand-filled channel that was eroded into the top of the upper member of the Alameda Formation.

BRIDGE FOUNDATION CONSIDERATIONS

Main span center pier

The center pier of the proposed asymmetric main span suspension structure is located 65 meters east of Yerba Buena Island, in about 10 to 17 meters of water (Figure 4). Geologically the footprint is underlain by an eastward-thickening wedge of unconsolidated sediment that overlies the sloping Franciscan bedrock (Figure 6). In this area, the bedrock surface slopes to the east from the bedrock high at Yerba Buena Island. The east-facing bedrock surface is generally consistent with the dip of the bedrock strata observed in the marine borings.

Foundation design and construction considerations for the main span center pier include the characteristics and stability of the sediment mantle, the characteristics and uniformity of the weathered and fractured Franciscan Formation rock, the engineering parameters and characteristics of the underlying fresh rock, seismic response of the foundation, and the construction method of the drilled pier foundations (i.e., install the piles from an excavated bench or from within a surface casing). The

main span footing will consist of a 20-by-30-meter concrete mat supported by 2.5-meter-diameter piles drilled about 20 to 30 meters into fresh rock.

Main span east pier

The location proposed for the main span east pier is about 450 meters to the east of Yerba Buena Island, and overlies the edge of the nested Recent paleochannels (Figure 4). The thickness of the Young Bay Mud varies significantly beneath the 58.5-by-21.5-meter footprint of the foundation. The East Pier will be supported on steel pipe piles measuring 2.5 meters in diameter and 90 meters in length. The 16 piles for the East Pier would be driven into the first dense sand within the lower member of the Alameda Formation at an elevation of about -80 to -90 meters. The pile installation will likely encounter a variable stratigraphic column that includes sand-backfilled paleochannels that have eroded into the upper member of the Alameda Formation.

Skyway structure

The skyway structure extends from the east pier to the Oakland Mole. The skyway alignment is located along the edge of the Recent paleochannel (Figure 7). The stratigraphy and thickness of the soft Young Bay Mud, the occurrence of the dense Merritt-Posey-San Antonio sequence, and the engineering properties of the underlying Old Bay Mud and Alameda Formation vary along the skyway alignment. The inherent variability of the young sediments affects the lateral capacity and load-deflection characteristics of the foundations. The foundation design objective was to select a foundation type capable of reducing the sensitivity of the seismic lateral load response. To meet this objective, the foundation will consist of large, 2.5-meter-diameter, steel pipe piles driven on a 1:8 or 1:12 (vertical to horizontal) batter. The 2.1-kilometer-long skyway structure will be supported by 14 pairs (one pier for each of the two westbound and eastbound structures) of pile-supported piers. Six 2.5-meter-diameter, approximately 100-meter-long pipe piles will support each of the 28 piers. The static gravitational loads on each pile are on the order of 30 to 35 meganewtons.

Oakland shore approach structure

The Oakland shore approach begins about 300 meters beyond the end of the Oakland Mole. As the height of the skyway structure decreases and the spacing between piers decreases, the pier load also decreases. Vertical, 1.8-meter-diameter, driven pipe piles are planned to support those more lightly loaded piers.

ACKNOWLEDGEMENTS

Thanks and appreciation to Fugro-Earth Mechanics, TY Lin International, Moffatt & Nichols, Engineers, and the California Department of Transportation for their efforts in this project. Thanks also to John Thorne and Ronnie Gu from Caltrans, Jacob Chacko and Roger Howard of Fugro West, Inc., Po Lam, Hubert Law, Mike Kapuskar, Saverio Siciliano, and Bruce Schell of Earth Mechanics, and Diane Carlson of California State University, Sacramento, for their input into this manuscript. Acknowledgments are also extended to George A. Kiersch of Kiersch and Associates, and John W. Williams of San Jose State University for their technical review of this manuscript.

SELECTED REFERENCES

Atwater, B.F., Hedel, C.W., and Helley, E.J., 1977, Late Quaternary depositional history, Holocene sea-level changes, and vertical crustal movement, southern San Francisco Bay, California: U.S. Geological Survey Professional Paper 1014, 15 p.

FEM (Fugro-Earth Mechanics), 1998a, Preliminary marine geotechnical site characterization, San Francisco-Oakland Bay Bridge East Span Seismic Safety Project: Consultants' report to the California Department of Transportation, 4 volumes.

FEM, 1998b, Preliminary Oakland shore approach geotechnical site characterization report, San Francisco-Oakland Bay Bridge East Span Seismic Safety Project: Consultants' report to the California Department of Transportation.

FEM, 1998c, Preliminary Yerba Buena Island geotechnical site characterization report, San Francisco-Oakland Bay Bridge East Span Seismic Safety Project: Consultants' report to the California Department of Transportation.

FEM, 1998d, Final 2-D marine geophysical survey report, San Francisco-Oakland Bay Bridge East Span Seismic Safety Project: Consultants' report to the California Department of Transportation, June.

FEM, 1998e, Report on seismic ground motion for SFOBB, East Span Seismic Safety Project: Consultants' report to Caltrans, Office of Structure Foundations, December 24.

FEM, 1998f, Subcontractor reports, preliminary geotechnical site characterization, San Francisco-Oakland Bay Bridge East Span Seismic Safety Project: Consultants' report to the California Department of Transportation, 4 volumes.

FEM, 2000a, Draft of the final 3-D marine geophysical survey report, San Francisco-Oakland Bay Bridge East Span Seismic Safety Project: Consultants' report to the California Department of Transportation.

Goldman, H.B., 1969, Geology of San Francisco Bay: *in* Goldman, H.B., (ed.), Geologic and Engineering Aspects of San Francisco Bay Fill, California Division of Mines and Geology Special Report 97, p. 11-29.

Lee, C.H., and Prasker, M., 1969, Bay mud development and related structural foundation: *in* Goldman, H.B., (ed.), Geologic and Engineering Aspects of San Francisco Bay Fill, California Division of Mines and Geology Special Report 97.

McNeilan, T.W., Chacko, M.J., Dean, C.B., Rietman, J., Lam, I.P., and Buell, R., 1998, An integrated approach to the site investigation and earthquake response analysis for the San Francisco-Oakland Bay Bridge East Span replacement: XIIth European Conference on Soil Mechanics and Geotechnical Engineering (Amsterdam, The Netherlands).

Sloan, D., 1992, The Yerba Buena Mud: Record of the last interglacial predecessor of San Francisco Bay, California: Geological Society of America, v. 104, p. 716-727.

Rogers, J.D., and Figuers, S.H., 1991, Engineering geologic site characterization of the greater Oakland-Alameda area, Alameda and San Francisco Counties, California: Consultant's report to National Science Foundation, Grant No. BCS-9003785.

Rogers, J.D., and Figuers, S.H., 1992a, Engineering geologic site characterization of the Oakland-Alameda area, Alameda and San Francisco Counties, California: Consultant's report to the National Science Foundation, 52 p.

Rogers, J.D., and Figuers, S.H., 1992b, Late Quaternary stratigraphy of the East Bay plain: *in* Proceedings of the Second Conference on Earthquake Hazards in the Eastern San Francisco Bay Area, Borchardt, G. et al., (eds.), California Division of Mines and Geology.

Trask, P.D., and Rolston, J.W., 1951, Engineering geology of San Francisco Bay, California: Geological Society of America Bulletin, v. 62, p. 1079-1110.

Treasher, R.C., 1963, Geology of the sedimentary deposits of San Francisco Bay, California: California Division of Mines and Geology, Special Report 82.


ASSOCIATION OF ENGINEERING GEOLOGISTS
AEG

INTRODUCTION TO THE TUNNELS AND TRANSPORTATION SECTION

RICHARD ESCANDON[1]

This section presents three papers on engineering geology aspects of recent tunnel projects in California, and a series of papers that chronicle the development of the Bay Area Rapid Transit system (BART). The recent tunnel projects are located in the San Francisco area and involve tunnels for combined sewer and stormwater storage and transport.

Romero and Pellegrino (2001) describe how the Islais Creek tunnels were mined through weak and troublesome Bay mud using open-face shield tunneling methods. Full-face grouting techniques were successfully used for the first time ever for tunneling in soft clays.

The Richmond transport tunnel required both hard rock and soft-ground tunneling methods in ground conditions ranging from strong Franciscan Complex graywacke to saturated dune sands. As Klein et al. (2001) remind us in their paper, ground conditions were some of the most difficult and challenging in the U.S.

The third paper, by Abramson and Kobler (2001), presents a case history of the Lake Merced transport tunnel, which was mined through alluvial, beach, dune and Colma Formation sand deposits using a digger shield tunneling machine. In addition to the sand deposits, a portion of a ship's hull from the 1860's was encountered in one of the access shafts.

Of particular historical interest are the three summary papers on the BART tunnels, constructed between 1964 and 1975. In the first one, Rogers (2001a) describes various engineering geologic challenges faced in the design, construction and ongoing maintenance of BART's 3.1 mile long Berkeley Hills twin tunnels, along the Contra Costa Line, between the Rock Ridge and Orinda stations. These challenges included dealing with the unexpected failure of a highway cut, which recurred between 1966 and 1983, and how to accommodate the creep of the Hayward fault in the tunnel. From there Rogers (2001b) follows the line of BART under San Francisco Bay, describing the "floating" binocular-shaped steel tube that was designed to accommodate earthquake loads and differential settlement. Finally, Rogers (2001c) walks down memory lane describing the geologic conditions, design of ground support, and methods of excavation and dewatering used for the 5.6-mile long segment of the Bay Area Rapid Transit District's original line, between the foot of Market Street and Colonial Way in San Francisco.

SELECTED REFERENCES

Abramson, L. and Kobler, M., 2001, Lessons learned during construction of the Lake Merced stormdrain tunnel, San Francisco County, California: This volume.

Klein, S., Kobler, M., Strid, J., G., 2001, Overcoming difficult ground conditions in San Francisco - The Richmond transport tunnel, San Francisco County, California: This volume.

Rogers, D.J., 2001a, Influence of geology on BART's Orinda Station landslide and Berkeley Hills tunnels: This volume.

Rogers, D.J., 2001b, Influence of geology on the design and construction of BART's Trans-Bay tube: This volume.

Rogers, D.J., 2001c, Influence of geology on BART's San Francisco subways: This volume.

Romero, V.S. and Pellegrino, G., 2001, Engineering geology and ground improvement of the Islais Creek tunnels, San Francisco County, California: This volume.

[1]Kleinfelder, Inc.
1940 Orange Tree Lane
Redlands, CA 92374
rescandon@kleinfelder.com


ASSOCIATION OF ENGINEERING GEOLOGISTS
AEG

OVERCOMING DIFFICULT GROUND CONDITIONS IN SAN FRANCISCO - THE RICHMOND TRANSPORT TUNNEL, SAN FRANCISCO COUNTY, CALIFORNIA

STEVE KLEIN[1], MIKE KOBLER[2], AND JULIUS STRID[2]

ABSTRACT

Construction of the Richmond Transport Tunnel in San Francisco encountered extremely variable and difficult geologic conditions, ranging from strong Franciscan Complex graywacke to saturated dune sand. Successful completion of this 10,200-foot-long tunnel in 1996 was a significant achievement that required both hard-rock and soft-ground tunneling methods. An accurate understanding of the geologic conditions, based on a thorough pre-construction geologic exploration program conducted along the tunnel alignment, was critical in planning and constructing this important project. Another challenge was the need to minimize construction impacts in this sensitive urban setting. This paper describes the geologic explorations conducted for the project, the anticipated geologic and ground conditions, and the tunneling methods used to construct the tunnel.

[1]Jacobs Associates
500 Sansome St., 7th Floor
San Francisco, CA 94111
klein@jacobssf.com

[2]Underground Construction Managers
665 Davis Street
San Francisco, CA 94111
mkobler@ucm.net
jmstrid@ucm.net

INTRODUCTION

Similar to many of the older cities in the U.S., San Francisco has a combined sewer system with both sewage and stormwater being conveyed in a common pipeline system. Prior to completing this project, the capacity of the combined sewer system was exceeded in the Richmond District of the city whenever there was significant rainfall. Exceeding the capacity of this pipeline system resulted in surcharging of the sewers, which in turn caused overflows at several outfalls located along the northern coastline of San Francisco (Figure 1). The overflows discharged untreated sewage on two nearby beaches – Baker and China Beaches (Figure 1) – and ended closing them for several days following one of these events.

In the mid 1990's the California Regional Water Quality Control Board (RWQCB) required the City to reduce these overflows in order to meet Federal and State standards for the discharge of pollutants to San Francisco Bay. To comply, the City constructed the Richmond Transport Tunnel Project, which was put into operation in 1996. Now completed, this $30 million project has significantly reduced the number of overflows at Baker and China Beaches.

The main feature of the Richmond Transport Tunnel Project is a 10,200-foot-long tunnel that can both transport and store wastewater and stormwater flows. The 14-foot-diameter tunnel functions as a 10-million gallon storage facility for holding combined sewer/stormwater flows until they can be

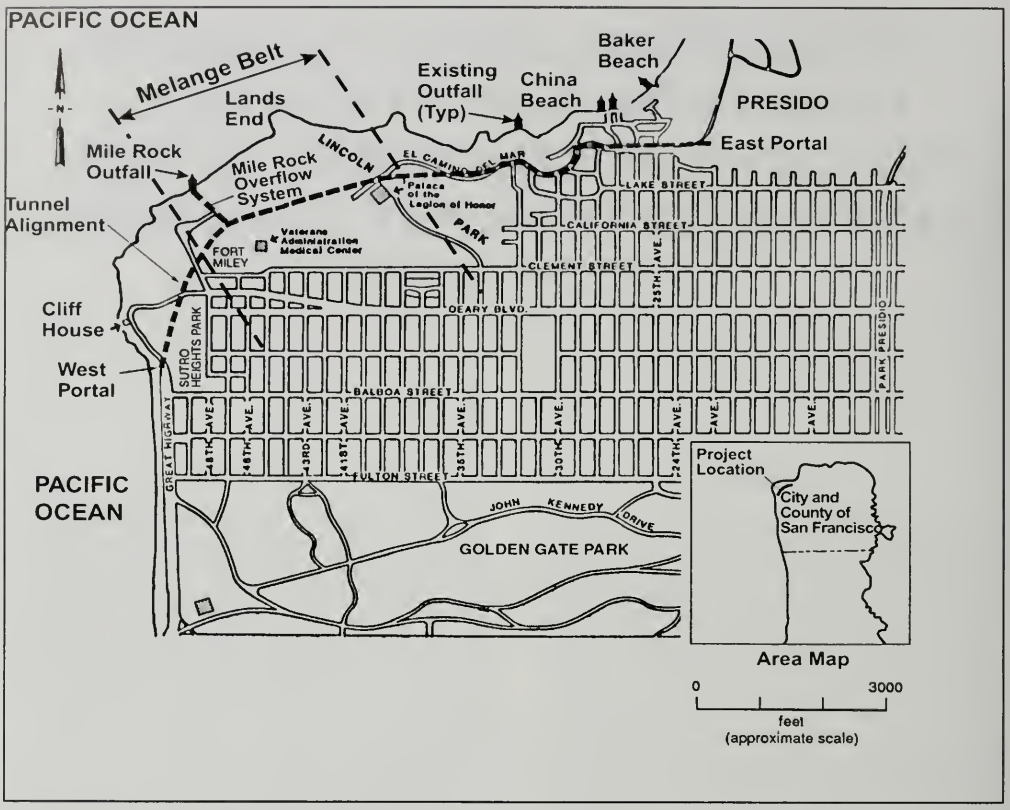

Figure 1. Alignment of the Richmond Transport Tunnel.

diverted to the Westside Transport system for treatment and disposal. Future overflows can only occur during storms that are large enough to completely fill the tunnel. These overflows will be diverted to the existing, but previously abandoned, Mile Rock Outfall Tunnel, avoiding future overflows at the Baker Beach and China Beach outfalls.

The tunnel is located in the northwest portion of San Francisco, and it traverses some the most beautiful and environmentally sensitive areas of the city, such as the Golden Gate National Recreational Area, Lincoln Park—a city park and golf course—, the exclusive Seacliff neighborhood, and the Presidio (Figure 1).

This tunnel was excavated through some of the most difficult and variable geologic conditions that have been encountered in any tunnel project in the U.S. These conditions included strong graywacke (sandstone) with a compressive strength of over 20,000 psi; weak, sheared, squeezing shale; saturated flowing dune sands; and various other soil/rock deposits. The rock tunneling conditions in the western 9,100 feet of the alignment were highly variable in terms of strength and rock quality, ranging from strong, massive sandstone to weak, sheared and crushed shale. Soft ground tunneling conditions, present in the eastern 1,100 feet of the alignment, consisted of saturated, cohesionless dune sands and weakly cemented Colma Formation sands.

This paper focuses on the results of a comprehensive pre-construction geologic exploration program, the geologic conditions anticipated in the tunnel,

and the tunneling methods utilized to successfully construct the tunnel.

GEOLOGIC SETTING

The project is located at the north end of the San Francisco Peninsula, which is in the Coast Ranges geomorphic province of California. This province is characterized by northwest-trending faults and other geologic structures. Much of the San Francisco Peninsula is underlain by the late Mesozoic rocks of the Franciscan Complex.

The Franciscan Complex is the folded, faulted, and structurally disrupted basement terrain of the Coast Ranges (Berkland et al., 1972), and is the basement rock on the San Francisco Peninsula from Shelter Cove (at Point San Pedro in San Mateo County) to the north end of the peninsula. The Franciscan Complex is typically found in northwest-trending, fault-bound lithologic belts. Rocks found in these lithologic belts include: graywacke and shale with interbedded chert and volcanic rocks; metamorphosed graywacke, chert, and volcanic rocks with varying degrees of metamorphic fabric development; and massive arkosic sandstone and shale interbedded with thin-bedded silty sandstone and shale (Norris and Webb, 1990; Harden, 2001, this volume). These lithologic belts are bound by shear zones described as melanges. The melanges are composed of inclusions of a heterogeneous assemblage of blocks and slabs of graywacke, greenstone, chert, shale, serpentinite, and other volcanic and metamorphic rocks, embedded in a pervasively sheared shale matrix. The inclusions within the melanges range from fragments a few inches across to slabs several miles long (Hsu and Ohrbom, 1969).

The melanges developed during the late Mesozoic to early Cenozoic subduction episodes and involved multiple-subducted plates (Blake and Jones, 1974). The heterogeneous nature of the melange is a result of the tectonic shearing, faulting, fragmentation, and brecciation that occurred along ancient plate boundaries.

Surficial deposits

The Franciscan Complex is overlain by post-Pliocene deposits consisting of the Colma Formation, dune sands, and man-made fills. The Colma Formation was deposited during the Pleistocene, a time of widely fluctuating sea levels related to worldwide glacial/interglacial events. Depositional regimes varied and included alluvial, aeolian, colluvial, and estuarine facies (Schlocker, 1974). The Colma Formation is a fine- to medium-grained sand deposit with minor amounts of silt and clay. It is well-bedded, friable, and often weakly cemented.

Dune sand occurs widely in San Francisco in deposits of varying thickness. The dune sand, which is derived from ocean beaches and blown landward, overlies the Colma Formation, and in places directly overlies the Franciscan Complex. The fine-grained dune sand is a cohesionless and poorly graded sand deposit.

Faults

The San Andreas fault is located offshore in the Pacific Ocean, approximately 3 miles west of the tunnel alignment. Other major active faults in the region include the Hayward fault, Calaveras fault, and the Seals Cove-San Gregorio fault.

The City College fault has been mapped as a discontinuous, northwest-trending zone of sheared rock extending from the southeast corner of San Francisco to Lands End (Schlocker, 1974; Bonilla, 1971). The fault is mapped as crossing the tunnel in the Lands End area, generally coinciding with the melange belt indicated in Figure 1. It does not appear to offset the Pleistocene Colma Formation, so it is not considered active.

GEOLOGIC EXPLORATION

Extensive geologic investigations were completed along the tunnel alignment during design, including geologic mapping, seismic refraction surveys, and 30 exploratory soil and rock core borings (WCC, 1993a). These exploration activities were the key to accurately assessing anticipated ground conditions for the tunnel. Exploratory borings were completed to depths ranging from about 25 to 340 feet below the ground surface. The exploration program also included several field tests, such as borehole permeability tests (packer tests), an aquifer pumping test, and dilatometer tests. Laboratory tests were conducted on soil and rock samples recovered from the borings. Tests performed on soil samples included grain size analyses, density measurements, and Atterberg Limits determinations. Tests performed on rock core samples included rock strength tests, swell tests, petrographic analyses, asbestos content determinations (for serpentine rocks), and X-ray diffraction analyses.

LOCAL GEOLOGIC CONDITIONS

Most of the tunnel was excavated through the Franciscan Complex rocks. Unconsolidated surficial deposits were encountered above the Franciscan Complex in the eastern portion of the tunnel alignment. These deposits included man-made fills, dune sand, and the Colma Formation. The characteristics of the various soil and rock units encountered in the tunnel are summarized below.

Fill

Man-made fill was encountered at the east end of the tunnel. The fill is a light brown to brown, poorly graded, fine- to medium-grained sand with some silt and gravel derived mainly from the dune sand and/or Colma Formation. It is generally medium-dense to dense; however, in some localized areas it is also loose.

Dune sand

Dune sand occurs extensively at the ground surface in the project area and was also encountered in the eastern portion of the tunnel alignment. The dune sand is generally light gray to brown, poorly graded, fine-grained, with grains that are subrounded to subangular. This sand deposit is cohesionless and fairly clean, with a silt and clay fines content ranging from 2% to 11%. It is also very uniform, with a mean grain size (D_{50}) generally in the range of 0.2 to 0.3 mm. The dune sand ranges from loose to dense, with the loose zones accounting for about 20% of the dune sand encountered in the borings.

Colma Formation

The Colma Formation is a medium dense to very dense sand deposit that is exposed at the ground surface locally in the project area, and was encountered in the eastern portion of the tunnel alignment. The Colma Formation is predominantly a light brown to gray, horizontally bedded, fine-to-medium-grained sand that is uncemented to weakly cemented. It is typically classified as a silty sand or clayey sand with a variable amount of silt and clay fines. Grain size analyses carried out for this project documented fines contents ranging from 3% to 30% passing the #200 sieve. In some places it contains clay beds up to about one foot in thickness.

An aquifer pump test conducted in the Colma Formation indicated a transmissivity of about 11,000 gpd/ft and a storativity of 0.076. These results correspond to a coefficient of permeability in the range of about 8 to 9 x 10^{-3} cm/sec. A radius of influence of about 400 feet was determined from the test (WCC, 1993a).

Franciscan Complex

Within the project area, the Franciscan Complex consists of thickly bedded sandstone (graywacke), interbedded sandstone and shale, and melange. Embedded within the sheared shale matrix of the melange are blocks and slabs of graywacke, serpentinite, greenstone, and chert.

Sandstone - Sandstone (graywacke), which is in some instances interbedded with shale, was encountered along several portions of the tunnel alignment. Sandstone beds exposed along the sea cliffs north of the project area are generally 3 to 10 feet thick. Petrographic descriptions of the sandstone include graywacke, silty graywacke, arkosic wacke, and brecciated sandstone. For this project, the generic term "sandstone" was used to identify the various forms of graywacke. Major constituents are 35% to 55% quartz by volume, 10% to 25% feldspar, and 5% to 15% lithic fragments.

In the tunnel the sandstone was typically slightly weathered to fresh, whereas at the surface the rock can be highly weathered. The sandstone was observed to be weak to very strong. Unconfined compressive strength tests performed on samples of intact sandstone indicated a strength ranging from about 800 pounds per square inch (psi) to over 21,000 psi, with an average value of 9,300 psi (for 44 tests).

The sandstone was typically closely fractured (spacings of one to six inches) to moderately fractured (spacings of six to twelve inches) but has zones of intensely fractured rock (spacings of one-half to one inch). Rock quality designation (RQD) ranged from zero to 100% and averaged about 60%.

Melange - Melange was encountered in a continuous section of the tunnel for about 3,500 feet, near the midpoint of the alignment (Figure 1). The melange is characterized by an extremely weak matrix of sheared and intensely fractured to crushed shale containing rock blocks of various sizes. The matrix is also highly weathered and can

exhibit the characteristics of a plastic clay. Within the melange, graywacke and other rocks occur as competent blocks embedded in the weak matrix.

A detailed evaluation of over 2,000 feet of rock core from ten of the exploratory borings in the melange belt indicated the following distribution of rock types for the blocks in the melange: 77% graywacke, 13% serpentinite, 9% greenstone, and 1% siltstone (Medley, 1994). In terms of block sizes, 27% of the blocks were determined to be larger than 10 inches and the maximum block size measured was 92 feet.

Outcrops of the melange are exposed at the sea cliffs north of the project. Consistent discontinuity orientations were not recognized during field mapping because the crushing of the matrix produces a random fracturing pattern. In addition, rock blocks embedded in the melange matrix have been subjected to rotation and translation modifying the original discontinuity orientations in an unpredictable manner.

Most of the core samples of the melange matrix were too highly fractured to obtain samples suitable for unconfined compressive strength tests. The unconfined compressive strength of two melange matrix samples were about 40 psi and 70 psi. These results seem to represent the upper bound strength for the melange matrix because most of the core samples did not hold together during the coring and recovery process.

Shale - Shale beds ranging in thickness from about 6 inches to 3 feet occur as laminae interbedded with the graywacke, shale/sandstone breccia, and as the matrix of the melange. The shale beds comprise approximately 5% to 25% of the rock mass outside of the melange belt. Petrographic descriptions of the shale include non-fissile, weakly metamorphosed claystone (argillite), mud-shale breccia, graywacke silt-shale, and silt-shale.

The shale varies from weak to strong and unconfined compressive strengths of shale samples were found to range from about 200 to 7,400 psi. The shale/sandstone breccia, which often has little or no relict rock texture, varies from extremely weak to weak in strength. The strength of the shale/sandstone breccia ranges from about 90 to 1,600 psi.

Fractures in the moderately fractured to crushed shale range from less than one fracture per foot to greater than 20 fractures per foot. The harder shale beds (argillites) are often more fractured than the weaker shale beds. The shale/sandstone breccia is typically intensely fractured to closely fractured.

Serpentinite - Serpentinite occurs as blocks in the melange and occasionally as more competent rock interbedded with shale, or with shale and sandstone, in the melange. The serpentinite is commonly intensely fractured to completely crushed. The unconfined compressive strength of the serpentinite was found to range from about 70 psi to over 15,000 psi.

Samples of serpentinite were described by petrographic analysis as hydrothermally altered dunite (a variety of peridotite) and cataclastic hydrothermally altered dunite. Petrographic analysis determined there was as much as 20% chrysotile (an asbestos mineral) present (see Sederquist et al., 2001, this volume, for a discussion of asbestiform minerals). Additional serpentinite samples were obtained and tested to determine the amount of asbestos minerals present. Results of these tests indicated that one sample had an asbestos fiber content of 1% to 5%, one sample had an asbestos content of 15% to 20%, and the other samples contained no more than a trace of asbestos. An asbestos fiber content of 1% or greater indicates a potentially hazardous material that requires special handling and disposal in order to comply with California regulations. Therefore, special requirements were incorporated into the project specifications regarding the handling, testing, stockpiling, and disposal of serpentine containing asbestos fibers, including a separate bid item for the disposal of serpentine with greater than 1% asbestos at an appropriate hazardous waste landfill.

Greenstone - Greenstone was encountered in melange in the borings. The greenstone was typically moderately to intensely fractured, with zones that are crushed. Greenstone was also mapped in several outcrops in the project area. The unconfined compressive strength of the greenstone (based on point load tests) ranges from about 1,000 psi to 17,000 psi.

Chert - Chert, which is often associated with the greenstone, is exposed locally in the cliffs north of the alignment, and was encountered interbedded with shale in one of the borings. The chert in this boring occurred as hard rock fragments interbedded with crushed shale, and was intensely fractured to crushed.

ANTICIPATED TUNNELING CONDITIONS

Approximately 90% of the tunnel was anticipated to be excavated in Franciscan Complex rocks, with the remainder expected to encounter soft ground consisting of fill, dune sand, and Colma Formation. Within the rock portion of the tunnel, about 60% was expected to encounter sandstone (graywacke), shale, and shale/sandstone breccia on each side of the melange belt (Figure 2). The quality of the rock mass, for tunneling purposes, was known to vary significantly along the alignment, ranging from good to very poor quality rock. Mixed face tunneling conditions were expected at the transition between the rock and soft ground sections of the tunnel.

Subsurface conditions along the tunnel alignment were divided into five generalized sections as indicated in Table 1 (WCC, 1993b). Anticipated ground conditions are described using Terzaghi's terms (Terzaghi, 1946; Terzaghi, 1950) for classifying ground behavior in rock and soft ground tunnels. Extremely variable ground conditions, including moderately jointed rock, blocky and seamy rock, squeezing ground, potentially flowing ground, raveling ground, and running ground were anticipated to be encountered in the tunnel. Terzaghi uses the term "blocky and seamy" to indicate a rock mass composed of intact rock fragments that are entirely separated from each other and not interconnected or interlocked. These variable ground conditions were major factors in the selection of tunneling equipment, tunnel support methods, and tunneling procedures.

ROCK TUNNELING

Selection of rock tunneling methods was limited by environmental restrictions. In order to avoid blasting vibrations in the residential areas adjacent to the tunnel, the City required a tunnel boring machine (TBM) to be used for the rock tunnel section. One key decision for the contractor was whether or not to build a TBM that could be used in both the rock and soft ground sections of the tunnel. Although it may be technically feasible to build a machine to handle this range of ground conditions, such a machine would be somewhat unprecedented. The contractor for this project elected to use two different machines for the rock and soft ground tunnel portions of the tunnel.

Considering the extremely variable geologic conditions expected along the tunnel alignment, which

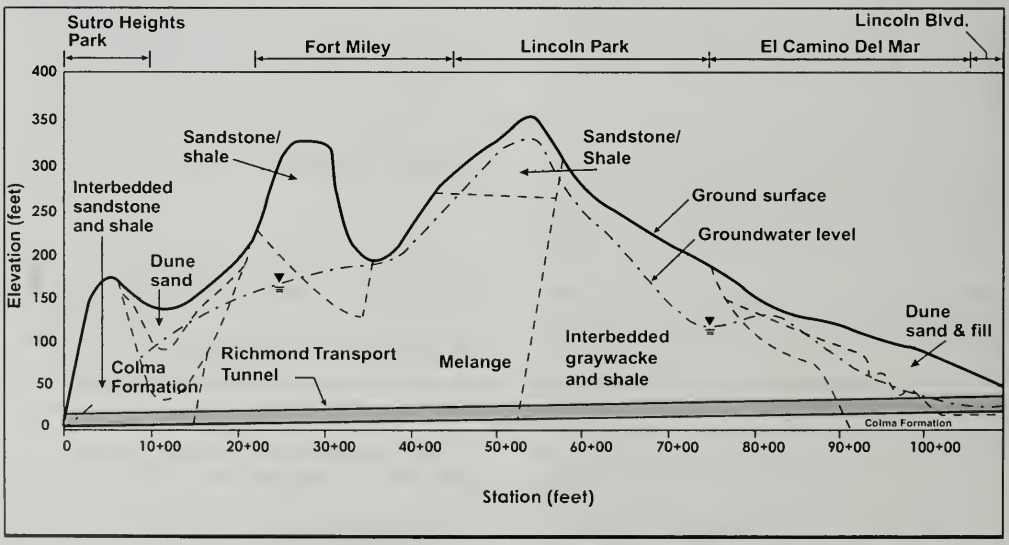

Figure 2. Generalized geologic profile along tunnel.

SECTION	STATIONS (FEET)	GEOLOGIC UNITS	ANTICIPATED GROUND CONDITIONS
I	0+00 to 14+00 (1,400 ft)	Interbedded sandstone and shale; shale/sandstone breccia	Moderately blocky to very blocky and seamy
II	14+00 to 53+00 (3,900 ft)	Melange	Moderately to very blocky and seamy; squeezing ground
III	53+00 to 89+50 (3,650 ft)	Interbedded sandstone (graywacke) and shale	Moderately jointed; moderately to very blocky and seamy
IV	89+50 to 91+50 (200 ft)	Mixed face of Colma Formation and sandstone/shale	Very blocky and seamy; raveling/running ground, potentially flowing ground
V	91+50 to 102+30 (1,080 ft)	Colma Formation; dune sand; fill	Potentially flowing ground; raveling ground; and running ground

Table 1. Summary of anticipated tunneling conditions.

included weak, sheared, and crushed rock, a fully shielded TBM was required with special features to avoid getting the TBM stuck where squeezing ground was encountered. Because of the low stand-up time and potential for face instability, the TBM cutterhead had to have rear-loading disc cutters and a cutterhead with recessed cutters. In addition, the TBM drive system was required to have multiple or variable speed drive motors in order to provide full torque at low cutterhead rotational speeds (low RPMs). This important feature allows the TBM to start mining again in blocky and squeezing ground that would otherwise jam the TBM cutterhead when mining operations were halted.

Tunnel excavation was expected to pass through alternating zones of hard rocks, such as the sandstone, and weaker materials, such as the melange. A typical hard rock TBM configured with side grippers could get stuck if it encountered hard rock at the face and weak rock at the tunnel sidewall that was not strong enough to provide the necessary support for the side grippers. For this reason the TBM was required to have a propulsion system that would advance the machine by pushing against the tunnel initial supports with hydraulic thrust jacks.

The contractor designed and custom built a fully shielded TBM (single shield TBM) to handle the anticipated ground conditions in the rock tunnel section (Figure 3). The 565-horsepower machine was fitted with 26 disc cutters (17-inch diameter) and delivered a torque of 1,320,000 ft-lbs. The TBM was advanced by pushing itself forward with twelve 50-ton hydraulic jacks (a total thrust force of 1,200,000 lbs) that thrusted against expanded precast concrete segment supports (Figure 4). This TBM was able to excavate the tunnel at reasonable advance rates of about 60 to 100 feet per shift, and the machine had no difficulty with the squeezing ground in the melange belt. The precast concrete segments provided a strong support system for the TBM to push against, which was one of the keys to avoid getting stuck in the squeezing ground. The machine was only used in the rock tunnel section, and it was abandoned underground after completing the rock tunnel drive. Electric and hydraulic components of the machine were salvaged and the cutterhead was cut into pieces and removed, leaving only the steel shield skin in the ground.

Figure 3. Fabricating TBM cutterhead on-site.

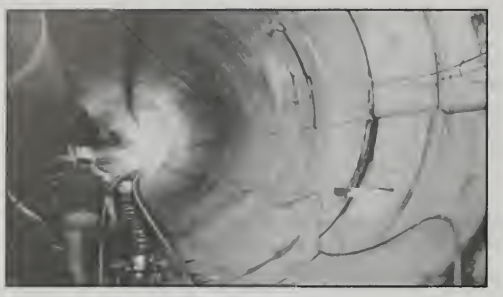

Figure 4. Expanded precast concrete segment initial supports for tunnel. Four 4-foot-wide segments were assembled to construct each ring.

SOFT GROUND TUNNELING

The saturated sand deposits in the eastern 1,200 feet of the tunnel were expected to exhibit unstable flowing ground behavior, with the potential for significant amounts of loss of ground and surface settlement. Groundwater levels ranged from about 5 to 50 feet above the tunnel invert. This section of the tunnel is located beneath El Camino Del Mar, which is bordered by expensive residences within the exclusive Seacliff neighborhood. The main concern was that the residences could be damaged by tunneling-induced ground movements and settlement. Therefore, these soils needed to be stabilized prior to tunneling or controlled with specialized tunneling equipment. Minimizing damage as a result of loss of ground and surface settlement was the key design consideration for this portion of the tunnel.

Two alternative tunneling approaches were developed for excavating this section of the tunnel, and the contractor was allowed to select either of these approaches. One approach was to utilize a pressurized-face tunneling machine, such as an earth pressure balance or slurry shield. These machines have the ability to balance the in situ soil and groundwater pressures at the face, minimizing loss of ground and avoiding the need for dewatering to lower the groundwater table. With this approach, a watertight, one-pass, bolted and gasketed precast concrete segment lining system would need to be installed behind the tunneling machine to avoid groundwater inflows.

The second approach called for dewatering the ground in advance of tunneling, injecting chemical grout ahead of the tunnel face to stabilize the unstable sand deposits, and installing either a one-pass or a two-pass (initial supports followed by a cast-in-place concrete) lining system. Chemical grouting would involve stabilizing the soils above the tunnel springline to provide a 6-foot-thick zone of stabilized soil around the tunnel perimeter. The objective of the chemical grouting was to increase the strength and stand up time of the fill, dune sand, and Colma Formation, and form a bridging layer that would minimize catastrophic loss of ground (such as running ground) that could result in large, uncontrollable surface settlements.

With either approach, compaction grouting was required concurrent with tunnel excavation to minimize surface settlement and the potential for damaging adjacent residences. Compaction grouting (Baker et al., 1983) involves injecting a thick, low-slump grout under high pressures to compensate for loss of ground at the tunnel heading (Figure 5). The contractor was required to limit the settlement of the residences along the alignment to less than ¼-inch and to control surface settlement of the street and other utilities to less than one inch.

The contractor elected to excavate the tunnel using the second approach, with an open face digger shield equipped with two breast tables to partially support the chemically grouted face (Figure 6). Twelve pumping wells, 120 feet deep, were installed along the tunnel alignment to draw the groundwater level below the tunnel invert. Chemical grouting was accomplished by drilling grout holes from the tunnel shield out about 60 feet ahead of the tunnel face, installing sleeve port grout pipes, and injecting a silicate chemical grout with a double packer system in 3-foot stages. Compaction grouting was carried out utilizing vertical holes along the tunnel centerline spaced 4 feet apart. This grouting was

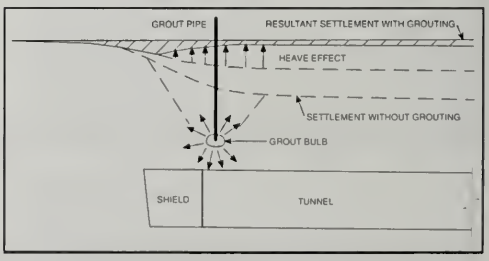

Figure 5. Compaction grouting concept. Grout is injected in bulbs above the tunnel to compensate for loss of ground.

Figure 6. Open-face shield used for soft ground tunnel section.

performed from the ground surface simultaneously with tunnel excavation to replace the volume of lost ground and minimize surface settlement from tunneling. The soft ground section of the tunnel was successfully completed without damaging any of the residences adjacent to the alignment, and surface settlement above the tunnel was generally limited to ½ inch or less. The volume of compaction grout required to control surface settlement ranged from about 5 to 22 cubic feet per foot of tunnel, averaging about 9 cubic feet. The volume of compaction grout injected ranged from about 1% to 9% of the volume of the tunnel excavation, with an overall average of approximately 3.5%.

CONCLUSIONS

Successful completion of the Richmond Transport Tunnel in these difficult and variable geologic conditions is a significant achievement that required an integrated approach to engineering geology, geotechnical engineering, and tunnel construction. Ground conditions encountered during construction were very similar to the anticipated conditions based on the results of the pre-construction geologic explorations. The importance of conducting a thorough geologic exploration program when planning a tunnel project such as this one cannot be overemphasized, particularly in difficult and variable ground conditions.

ACKNOWLEDGMENTS

The authors would like to thank the City and County of San Francisco, Department of Public Works for permission to publish this paper. We also acknowledge the important contributions of the contractor, Shank/Balfour Beatty; and the other members of the design team, including Lee Engineering Enterprises; AGS, Inc.; Don Todd Associates; Villalobos & Associates; and Hydroconsult Engineers, as well as the construction management team, Haley & Aldrich, and EPC Consultants.

SELECTED REFERENCES

Baker, W.H., Cording, E.J., and MacPherson, H.H., 1983, Compaction grouting to control ground movements during tunneling: Underground Space, v. 7, Pergamon Press Ltd., p. 205-212.

Berkland, J.O., Raymond, L.A., Kramer, J.C., Mores, E.M., and O'Day, M., 1972, What is Franciscan?: American Association of Petroleum Geologists Bulletin, v. 56, no. 12, p. 2295-2302.

Blake, M.C. Jr. and Jones, D.L., 1974, Origin of Franciscan melanges in Northern California: *in* Modern and ancient geosynclinal sedimentation, SEPM Special Publication 19, p. 345-356.

Bonilla, M.G., 1971, Preliminary geologic map of the San Francisco South Quadrangle and of the Hunters Point Quadrangle, California: U.S. Geological Survey Miscellaneous Field Studies Map MF-311, Scale 1:24,000.

Harden, D., 2001, Geologic Framework of Northern California - An overview: *in* Ferriz, H. and Andrerson, R. (eds.), Engineering Geology Practice in Northern California, Association of Engineering Geologists Special Publication 12, and California Division of Mines and Geology Bulletin 210.

Hsu, K.W. and Ohrbom, R., 1969, Melanges of San Francisco Peninsula - Geologic reinterpretation of type Franciscan: American Association of Petroleum Geologists Bulletin, v. 53, no. 7, July, p. 1348-1367.

Medley, E.W., 1994, The engineering characterization of melanges and similar block-in-matrix rocks (Bimrocks): Ph.D. Thesis, University of California at Berkeley, Civil Engineering Department, 175 p.

Norris, R.M., and Webb, R.W., 1990, Geology of California: John Wiley & Sons, Inc., 2nd Edition, p. 364-392.

Schlocker, J., 1974, Geology of the San Francisco North Quadrangle, California: U.S. Geological Survey Professional Paper 782, Plates 1 and 3.

Sederquist,D, Kroll, R., Rorem, E.J., 2001, The site specific evaluation of naturally occurring asbestos in the Central Sierra Nevada foothills of California: *in* Ferriz, H. and Andrerson, R. (eds.), Engineering Geology Practice in Northern California, Association of Engineering Geologists Special Publication 12, and California Division of Mines and Geology Bulletin 210.

Terzaghi, K., 1946, Rock defects and loads on tunnel supports: *in* Proctor, R.V., White, T.L., (eds.) Rock Tunneling with Steel Supports, Commercial Shearing (Youngstown, Ohio), 296 p.

Terzaghi, K., 1950, Geologic aspects of soft-ground tunneling: *in* Trask, P.E., (ed.), Applied Sedimentation, John Wiley and Sons (New York, N.Y.), p. 193-209.

WCC (Woodward-Clyde Consultants), 1993a, Geotechnical Data Report, Richmond Transport Project, San Francisco, CA: Consultant's report to the City and County of San Francisco, Department of Public Works, February.

WCC (Woodward-Clyde Consultants), 1993b, Geotechnical Baseline Report, Richmond Transport Project, San Francisco, CA: Consultant's report to the City and County of San Francisco, Department of Public Works, February.

ENGINEERING GEOLOGY AND GROUND IMPROVEMENT OF THE ISLAIS CREEK TUNNELS, SAN FRANCISCO COUNTY, CALIFORNIA

VICTOR S. ROMERO[1] AND GUIDO PELLEGRINO[2]

ABSTRACT

The 340-meter long Islais Creek tunnels are part of the Islais Creek transport/storage project, a series of combined sewers in southeast San Francisco designed to reduce discharges into San Francisco Bay during storms. The project involved tunneling through Bay Mud, a well-known and troublesome weak soil in San Francisco Bay. Further complicating tunnel construction was the presence of piles supporting sewers and a railroad over the tunnel. To address these challenges, jet grouting was used to pre-treat the Bay Mud to allow for open-face tunneling. Jet grouting is a form of ground modification whereby a cement grout is injected into the ground through a rotating drill bit. The soil structure is virtually obliterated by the jets and the original subsurface material is ultimately mixed with grout to form soil-cement columns. This was the first tunnel project anywhere to utilize full-face jet grouting for tunneling in soft clays. The successful completion of the project demonstrated that jet grouting for pre-treatment of soft soils is possible and compatible with open-face tunneling methods. Tunnel inflows and surface settlements above the tunnels were less than conventional theories would predict. This project also showed that ground heave is a critical issue with jet grouting under structures. Maintaining good return of cuttings during jet grouting is necessary to prevent such heave. Precutting and pretreatment of soils above the "design" zone for jet grouting was used to enhance return of jet grout cuttings.

INTRODUCTION

Between 1990 and 1997, the City of San Francisco undertook the construction of a large storm sewer system in the drainage basin of Islais Creek, called "the Islais Creek transport/storage project" (ICT/SP) (Figure 1). The ICT/SP upgraded the existing sewer system in southeast San Francisco by constructing several kilometers of subsurface box-structures and tunnels designed to store storm flows and connect various existing sewer lines (Figure 2). The box portions of the system are reinforced concrete culverts, often referred to as transport/storage (T/S) structures. Because the sanitary and storm sewers are combined in San Francisco, heavy rains overload the treatment system, requiring discharge of excess untreated sewage (storm plus sanitary) into San Francisco Bay and the Pacific Ocean. With the completion of the ICT/SP, overflow into San Francisco Bay occurs less than 5 times a year, as opposed to the previous 30 to 60 times.

[1]Jacobs Associates
500 Sansome Street, #700
San Francisco, CA 94111
romero@jacobssf.com

[2]NicholsonRodio JV
20 West Howell Street
Boston, MA 02125
gpellegrino@ibm.net

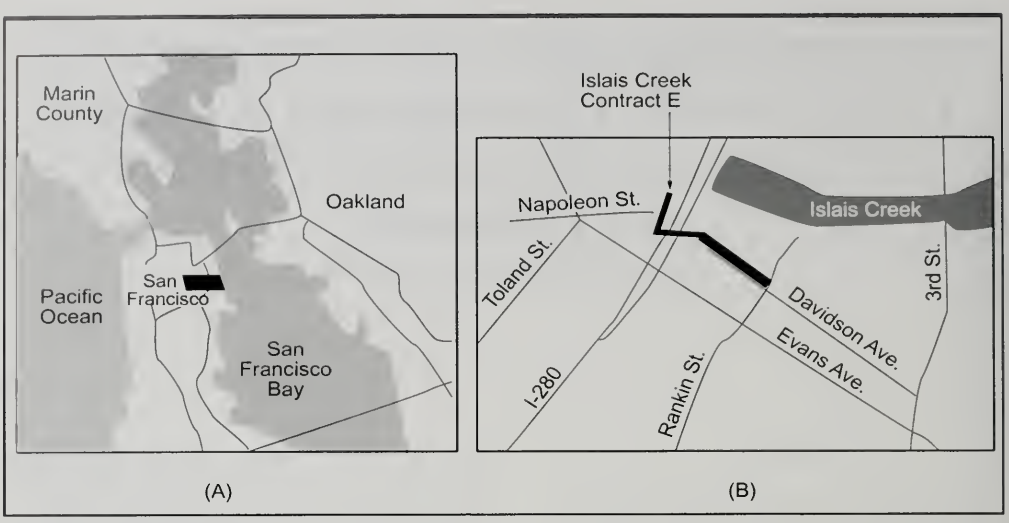

Figure 1. Project location map. (A) General location with respect to the San Francisco Peninsula. (B) Detailed location. The gray footprint shows the open-channel portion of Islais Creek.

The Islais Creek Basin is situated on the west side of San Francisco Bay, approximately 5 km south of downtown San Francisco (Figure 1). The stratigraphy of the site is generally characterized by an upper layer of rubble fill overlying a thick deposit of Bay Mud (a soft plastic clay), which, in turn, overlies marine sand, old bay clay, or bedrock. Most of the geotechnical design and construction methods for the ICT/SP were controlled by the geotechnical properties of the Bay Mud that underlies the entire project alignment. Deep excavations through these soft sediments can cause significant ground movements around the excavations. The strength, compressibility, and deformation characteristics of Bay Mud are critical in terms of base stability of the excavations, ground deformations caused by the excavations, and the response of adjacent structures to ground deformations.

Tunneling through Bay Mud presents similar problems, such as excessive settlement above the tunnels and face instability. The presence of piles that had to be removed during tunneling limited excavation to open-face methods, which substantially increases the risk of face instability. The purpose of this paper is to summarize geologic conditions on the project and describe how jet grouting was used to facilitate tunneling on one construction contract of the ICT/SP.

PROJECT DESCRIPTION

One of the construction contracts along the ICT/SP alignment, Contract E, covered two tunnels and several cut-and-cover box sewers in very difficult ground conditions (Figure 2). The alignment of Contract E is 340 meters in length and interfaces with the older sewer network. A cut-and-cover T/S structure on the west side of the Joint Powers Board (JPB) commuter railroad is connected to an east side cut-and-cover T/S structure by the Undercrossing Tunnel. This tunnel is 4.1 meters in excavated diameter, approximately 75 meters in length, and crosses under Interstate 280 and the JPB commuter railroad embankment. A second tunnel is aligned parallel to Davidson Avenue and connects the east side cut-and-cover T/S structure to a pump station. The Davidson Avenue Tunnel is 4.6 meters in excavated diameter, and approximately 155 meters in length. The east side cut-and-cover T/S structure was used as the driving shaft for both tunnels.

The nature of the soils in the area (weak Bay Mud) led the design engineer and contractor to implement jet grouting to alleviate the anticipated construction difficulties. Jet grouting is a ground modification technique in which high-pressure cement grout jets, emanating from a special drill tool, erode and mix with the soils, thereby cre-

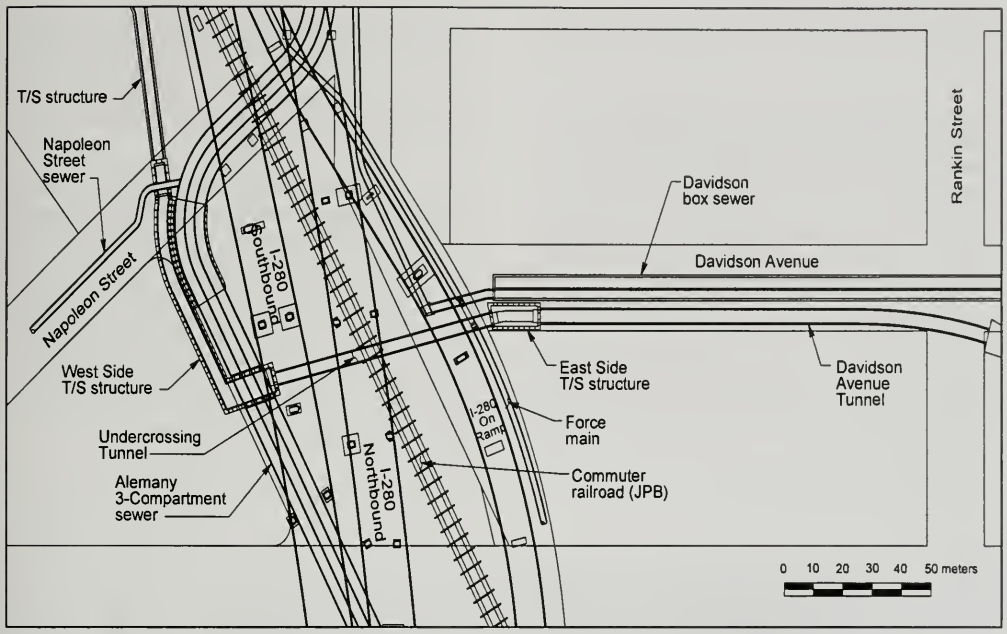

Figure 2. Site plan.

ating a soil-cement column. In the early 1990s, jet grouting was a relatively new technology in North America.

Cut-and-cover structures

Excavation support for the east and west side cut-and-cover structures was provided by diaphragm walls built with soldier piles and tremie concrete (SPTC). Piles consisted of W36x210 and W40x324 structural steel members drilled through Bay Mud into bedrock. Tremie concrete, acting as unreinforced slabs spanning horizontally between the piles, transferred lateral loads to the piles (a more detailed description of the construction and performance of the SPTC walls is given by Adams and Robison, 1996).

Because of the presence of a deep stratum of soft Bay Mud, only limited support was available for the SPTC wall below subgrade. To decrease the unsupported spans of the SPTC walls during various construction stages, a jet-grouted slab was specified below the T/S box invert. These jet-grouted kicker slabs were placed prior to excavation and effectively prestressed the support system prior to the placing of conventional internal bracing. When the jet-grouted kicker slab achieved the required strength, excavation between the walls was carried with temporary internal bracing installed as the excavation proceeded. Although not originally specified for use with the tunnels, the jet-grouting technique used for the SPTC kicker slab was also adopted for ground improvement of the tunnels.

Tunnels

Both the Undercrossing Tunnel and the Davidson Avenue Tunnel are situated in soft Bay Mud. In addition, pre-existing timber and concrete piles were present along the right-of-way available for the tunnel alignments. These piles support various structures under which the tunnels pass. Because of concerns for tunnel-face instability and the necessity to remove piles from within the tunnels, bid documents required the use of an open-face compartmentalized shield under compressed air. The specified initial tunnel support was a gasket-fitted

steel liner plate, and the final lining consisted of a steel carrier pipe.

After award of the $21.7 million contract, the general contractor and jet-grouting sub-contractor submitted a Construction Incentive Change Proposal (CICP) to use jet grouting to facilitate tunnel excavation. The CICP was a bid document clause created by the design engineer to foster innovation from the contractor. The contractor's CICP involved jet grouting to pre-treat Bay Mud within the tunnel envelope and excavation of the tunnels with an open face shield equipped with a roadheader (rotary boom excavator). Elimination of compressed air tunneling allowed for substitution of the original liner-plate support with a more economical system of steel sets, timber lagging, and steel plates at the portals. Steel carrier pipe was used for the final lining, as specified by the original design.

Previously existing structures

The JPB railroad overlies an old wood trestle that intersects the tunnel alignment. The trestle was constructed at the turn of the century and was covered by an embankment fill during land reclamation that took place during the 1920s and 1930s. Piles supporting the trestle posed significant obstructions during tunneling.

An elevated section of Interstate 280 crosses one of the tunnel alignments within the JPB corridor. At the time of construction for Contract E, portions of Interstate 280 were temporarily out of service due to the September 1989 Loma Prieta earthquake. The state transportation authority (Caltrans) conducted a seismic retrofit of the freeway concurrent with the construction of Contract E. Because large surface and subsurface ground movements could affect the integrity of these freeway structures, Caltrans required design and construction methods that would minimize these movements.

In addition to the JPB commuter railroad and Interstate 280, the project alignment crossed under several major utilities, as shown in Figure 2. Each

Figure 3. Pre-1890 shoreline. Dark lines show former channels of the Islais Creek estuary, which was filled in the 1930s (from Boults, 1990).

of these utilities required careful consideration of construction methods to minimize damage from ground movements.

GEOLOGIC AND GEOTECHNICAL CONDITIONS

The drainage basin of Islais Creek is a low plain that occupies about one square-mile in area. Prior to about 1890, the basin contained a small embayment, located mostly east of the present day commuter railroad, and a tidal marsh area on both sides of Islais Creek extending to the southwest in a gradually narrowing pattern (Figure 3). The wide meandering creek and surrounding marshlands were flanked by hills rising 75 to 100 meters above the creek. Coast and Geodetic Survey maps from 1859 and 1869 show that much of the present dry-land area of the basin was once covered with 0.3 to 5.5 meters of water at low tide. In the 1930s, most of the area was reclaimed from the bay by filling with dune sand, rock fill, miscellaneous debris, and organic waste, resulting in a ground surface that is now 3.0 to 6.1 meters above mean sea level.

The interpolated shape of the bedrock surface (Figure 4) suggests that the basin of Islais Creek is a drowned valley created by rising water of the San Francisco Bay after the Wisconsin glacial episode (Radbruch and Schlocker, 1958). Before the bay level rose, two major streams cut deep channels into the Franciscan bedrock. These streams were tributaries to an ancient northward-trending channel that discharged into the bay. One of these valleys is located below the present-day channel. A second, more extensive valley is located about 340 meters south of the present Islais Creek channel. The floor of this valley is now more than 60 meters below mean sea level. Over time, rising waters of the bay gradually flooded the streams, depositing marine soils. Early deposits consisted of interbedded sands and clays. Following periods of intermediate bay levels, the bay clays (now known collectively as

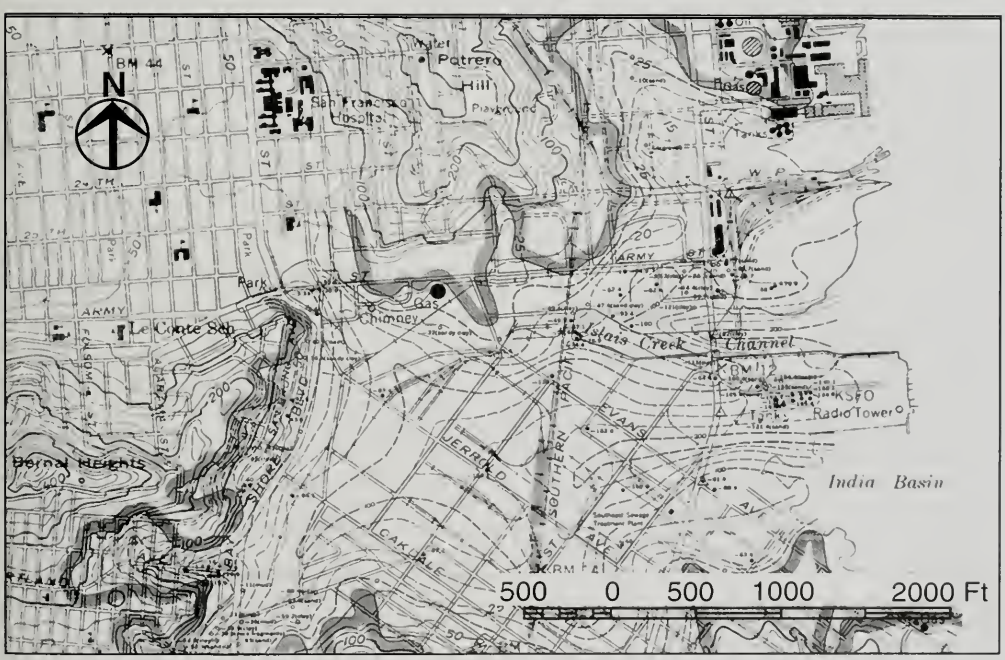

Figure 4. Bedrock map of the Islais Creek basin (from Radbruch and Schlocker, 1958).

the old bay clay) became overconsolidated due to subaerial exposure. In the past 20,000 years, new clays were deposited (young Bay Mud) on top of the old bay clay.

Detailed descriptions of stratigraphy and groundwater conditions along the project alignment are given below. The interpreted geologic profile along the project alignment is shown in Figure 5. A summary of the design properties for *in situ* soils is given in Table 1.

Artificial fill

The artificial fill in the Islais Creek basin consists of loose sand and rock excavated from the surrounding hills. As observed in excavations within the project area, some portions of the fill contain miscellaneous rubbish and organic garbage from city dumps that were formerly located in the area. Most of the fill in these dumps consists of rubble from the 1906 earthquake. Excavated material from the hills generally consists of unconsolidated sand, silt, clay, and pieces of bedrock. Old wood piles and sunken ships are often encountered in foundation work in some areas and can be troublesome for construction and excavation. As a result of these factors the character of the fill is variable. It generally consists of brown, medium dense to dense, poor to well-graded sand and gravel, clayey silt, clayey sand, and silty sand.

Bay Mud

Bay Mud is a well-known and troublesome soil deposit in the San Francisco Bay. This deposit is a soft marine clay with low shear strengths (a very comprehensive and detailed characterization of Bay Mud is given by Bonaparte and Mitchell, 1979).

Along the Islais Creek project alignment, Bay Mud is a plastic, silty clay or clayey silt with trace amounts of organic matter, shells, and sand. It is generally classified as CH or MH, according to the Unified Soil Classification System. The consistency ranges from very soft to soft in the upper portions of the deposit, and soft to medium stiff in the lower portions of the deposit. In addition to exhibiting low undisturbed strengths, Bay Mud is sensitive to disturbance, and shear strengths are reduced to about 25 percent of original strength upon remolding. The upper 6 meters of Bay Mud generally have a higher water content and a lower unit weight than the mud below a depth of 12 meters. These differences could be related to soil composition and pre-consolidation pressures.

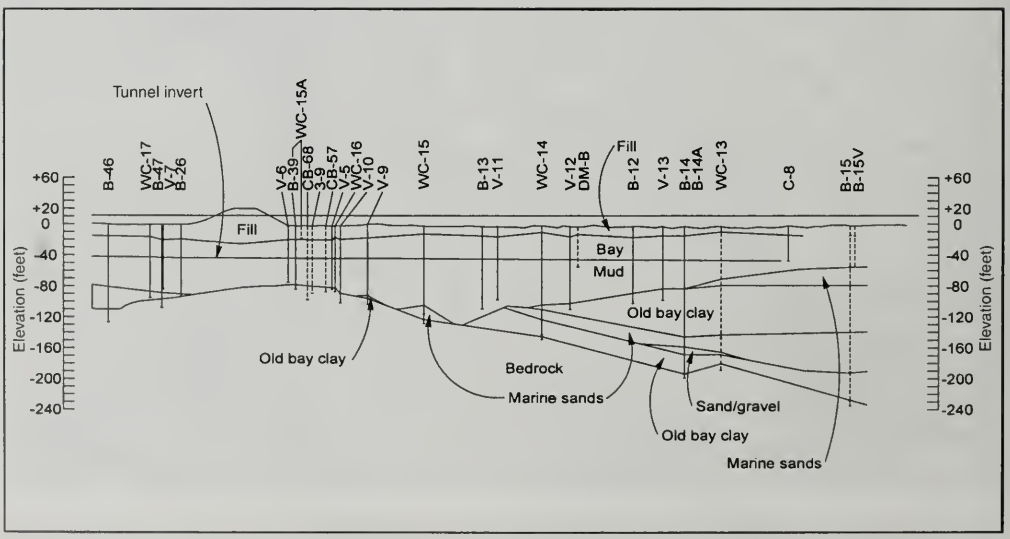

Figure 5. Geologic profile.

STRATUM	TOTAL UNIT WEIGHT, γt (kN/m^3)	BUOYANT UNIT WEIGHT γb (kN/m^3)	EFFECTIVE FRICTION ANGLE, Φ (degrees)	UNDRAINED SHEAR STRENGTH, S_u (kPa)	AT-REST LATERAL SOIL PRESSURE COEFF., K_o
Fill	19.2	9.4	35°	0	0.43
Bay Mud (West Side)	14.6	4.9	0°	24+1.2*H [1]	0.55
Bay Mud (East Side)	14.6	4.9	0°	18+1.2*H [1]	0.55
Bay Mud (Davidson Ave)	14.6	4.9	0°	13+1.1*H [1]	0.55
Old bay clay	16.3	6.4	0°	72+1.6*H [2]	0.55
Marine sands	20.6	10.8	37°	0	0.40
Alluvium/ colluvium	20.4	10.7	40°	0	NA
Bedrock	22.0	NA	30°	144	NA

[1] H = Depth (in meters) below top of Bay Mud stratum
[2] H = Depth (in meters) below top of old bay clay strata

Table 1. Soil properties assumed for design.

Test data indicate that the Bay Mud ranges from normally consolidated to slightly overconsolidated throughout the depth of the layer. Consolidation of Bay Mud in the Islais Creek area is an ongoing process. It is influenced by many factors, such as age and weight of the fill, elevation of the groundwater table, and thickness of Bay Mud. As a result, future Bay Mud settlements can be expected to vary between 150 and 200 mm over the next 50 years.

Along the Contract E alignment, undrained shear strengths in the Bay Mud increase linearly with depth below 7 meters. In addition, the Bay Mud stratum exhibits lower strengths and lower preconsolidation pressures than is typical in other parts of the bay. For example, at Islais Creek the normalized shear strength parameter, s_u/p (s_u = undrained shear strength; p = effective overburden pressure) is 0.11, which is at the low end for typical Bay Mud (Bonaparte and Mitchell, 1979). Geologic studies indicate that one of the channels mentioned previously ran roughly along Evans Street. Deep deposits of old bay clays and Bay Mud now occupy this former channel, and soils within the channel are weaker than surrounding deposits, as shown by lower undrained shear strengths and failures that occurred during construction of the Davidson Avenue sewer. These differences in strength are attributed to variations in soil composition, minimal exposure to desiccation effects, incomplete consolidation under the artificial fill, and possible artesian pressures in the lower sand layers (Mana et al., 1973).

Since Bay Mud is very sensitive to disturbance, the best method for obtaining data for undrained shear strength is an *in situ* vane shear test. In general, the Bay Mud appears to be weaker along Davidson Avenue than near the railroad embankment (Figures 6 and 7). Surcharge load from the addition of the railroad embankment has caused consolidation of the Bay Mud under the embankment, and a corresponding increase in shear strength. Because of accessibility problems, vane shear tests could not be performed under the embankment; however, data from vane shear tests adjacent to the embankment toe show this trend of increased shear strength (Figure 6). In lieu of vane shear tests, Bay Mud shear strength under the railroad was estimated from computed consolidation pressures induced by the embankment. In summary, vane shear tests performed as part of this project yielded undrained shear strengths that vary considerably. In order to allow for this variation in Bay

Mud strength, the design strengths used varied with location, as shown in Table 1.

Marine sand and old bay clay

Sand strata beneath the Bay Mud are marine sands with mollusk shells. Although the deposit ranges in grain size from gravel to clay, the bulk of it consists of fine- to medium-grained, yellowish-gray to dark yellowish-orange sand, slightly cemented with clay and silt. The marine sands are medium dense to very dense. High pile-driving resistances were encountered in this stratum. The marine sands are a separate deposit from the Colma Formation, which is sometimes found above bedrock at other locations along the San Francisco peninsula.

Also underlying the Bay Mud are old bay clays, which are dark greenish- to bluish-gray, moderately plastic, stiff, silty clay with trace amounts of sand,

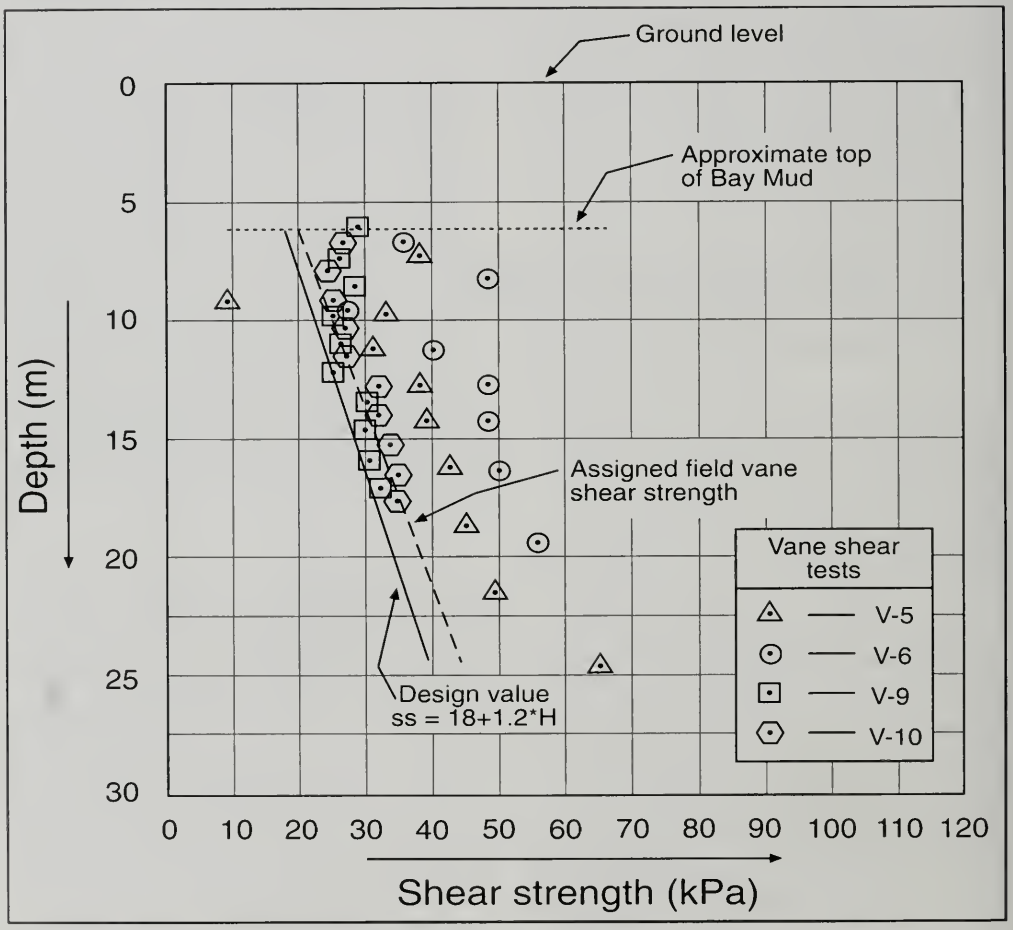

Figure 6. Bay Mud shear strength along the east side of the railroad embankment. Vane shear V-6 was located at the toe of the railroad embankment. Additional consolidation from the embankment surcharge is believed to have resulted in higher shear strengths at this location. SS = shear strength in kPa; H = depth in meters below top of Bay Mud.

and are generally classified as CL or CH, according to the Unified Soil Classification System. These over-consolidated clays are more competent than the younger Bay Mud and have substantially lower moisture contents.

Bedrock

The bedrock along the alignment is completely covered by unconsolidated sediments. Rock cores obtained from borings drilled during geotechnical investigations indicated that the project is underlain by highly weathered to hard serpentinite of the Franciscan Complex (Bailey et al., 1964), which is locally fractured and sheared and exhibits varying amounts of weathering at the soil/bedrock interface. Discontinuities are oriented at various angles, with some vein-infilling along shears. Consequently, in its weathered state, the density and strength parameters of the rock show great variability.

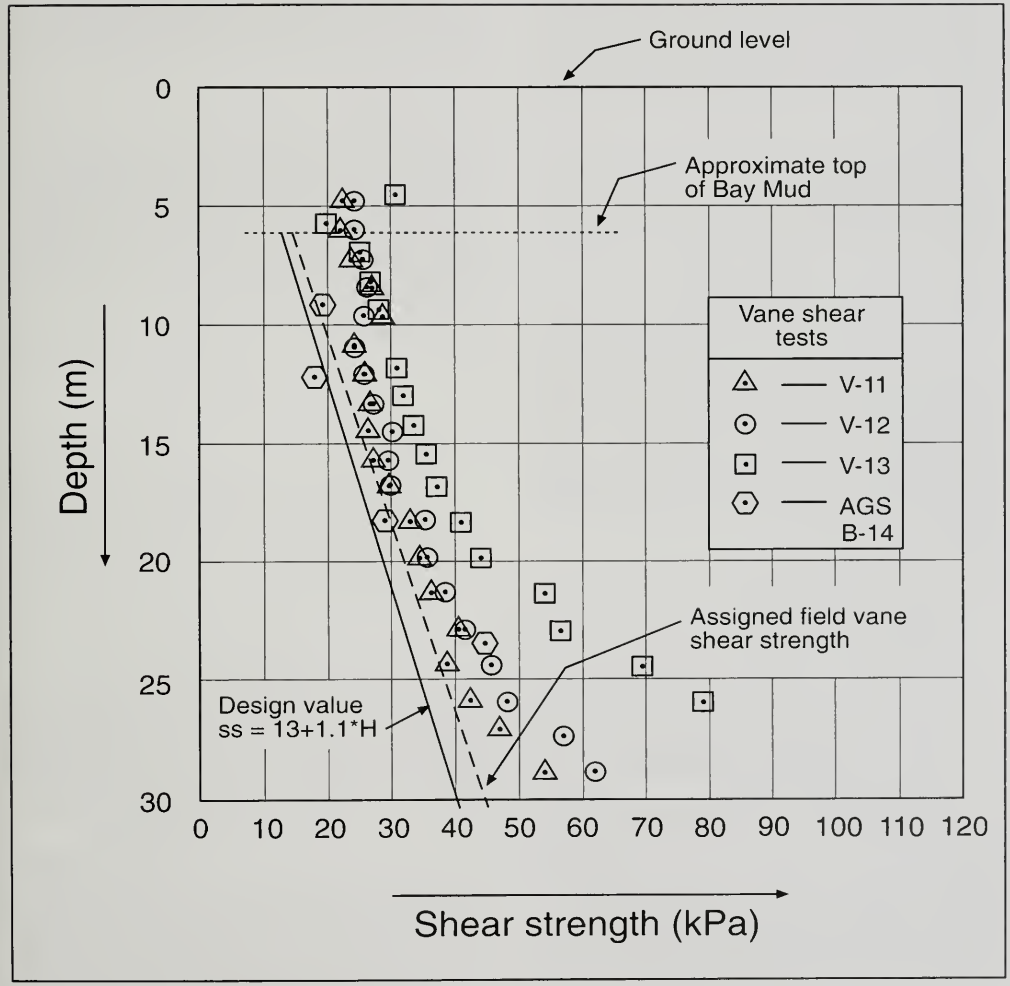

Figure 7. Bay Mud shear strength along Davidson Avenue. SS = shear strength in kPa; H = depth in meters below top of Bay Mud.

Based on test data and visual classification of core samples, rock quality at the site is generally very poor. The Rock Quality Designations (RQD) ranged from 0 percent to 66 percent (very poor to fair). Core recoveries ranged from 42 percent to 100 percent.

Groundwater

Borings indicated that the water table is at an elevation of –1.5 meters below mean sea level within the artificial fill. Because dewatering of the artificial fill would cause consolidation of the Bay Mud and result in surface settlement, project specifications prohibited the drawdown of groundwater in the area of Contract E.

In addition to the upper, unconfined aquifer, a lower, confined aquifer is present in the marine sand. This aquifer is under artesian pressure, which may be one of the causes for lower preconsolidation pressures in the overlying Bay Mud.

Geoenvironmental considerations

Three soil borings for environmental sampling were drilled along the Contract E alignment. Four samples were collected from each boring, two from the fill materials and two from the Bay Mud. The fill and Bay Mud samples were composited at each location for analysis. On the basis of the data collected for the environmental investigation, the following conclusions were made for the locations at which samples were collected:

- The fill is not a RCRA waste.
- The fill may be a California hazardous waste.
- The Bay Mud is a nonhazardous waste.
- The tunnels could be classified as "potentially gassy" by the criteria of CalOSHA.

TUNNEL DESIGN CONSIDERATIONS

Many factors are considered during design of a tunnel in soft ground. Good summaries of tunnel design considerations are given in Bickel et al. (1996), Peck (1969), and Peck et al. (1972). Design issues of particular importance include:

- Soil stabilization and groundwater control.
- Selection of tunnel excavation method.
- Initial ground support and final lining.
- Surface effects of tunnel construction.

Design of the Islais Creek tunnels involved several challenges that were somewhat unique to the geologic and geotechnical conditions anticipated. The more significant of these challenges are described below.

Face stability

Tunnel-face stability is an important issue when constructing a tunnel in soft clay such as Bay Mud. It influences excavation methods, magnitude of ground movements, and design/construction of the lining. The face stability of a tunnel in clay can be represented by the overload factor (OLF), which is defined as (Bickel et al., 1996):

$$OLF = \frac{\sigma_v - P_a}{S_u}$$

where

σ_v = overburden pressure at the tunnel mid-section depth (i.e., springline),

P_a = internal air pressure in a compressed air tunnel, and

S_u = undrained shear strength of the soil.

From the project geotechnical data, it was estimated that the overload factor for the Islais Creek tunnels (constructed without compressed air) would range between 5 and 9. A limiting value of OLF>6 represents a threshold of instability due to squeezing ground, whereas a limiting value of OLF=5 represents a practical limit below which tunneling may be carried out without unusual difficulties.

The use of compressed air was originally specified to reduce the overload factor to values of less than 5, and to resist the entry of water into the tunnel. Case studies had shown that substantial ground movements have occurred in squeezing ground conditions when compressed air was not used. However, the proposal for jet grouting to pre-treat soils within

the tunnel envelope provided an alternate means to address face-stability and ground movements.

Tunnel lining

The tunnels themselves are not directly supported by foundations such as piles. However, the tunnels tie-in to T/S structures that are founded on piles. Due to long-term consolidation of the Bay Mud, differential settlements are anticipated between the tunnels and the adjacent T/S structures. Steel pipe was, therefore, specified as a final lining in order to accommodate movements from the expected long-term differential settlement.

A minimum 75 mm spacing was required between the outside of the steel pipe and the inside of the initial tunnel support (initial support is typically designed by the contractor to suit his excavation methods). The annular space between the steel pipe and the initial lining was backfilled with cellular concrete. The design assumes that all loads are ultimately carried by the final lining. The function of the cellular backfill concrete was to fill all voids outside of the steel pipe and to provide corrosion protection for the steel.

TUNNEL CONSTRUCTION

Although jet grouting is customarily employed in the construction of underground excavations in Asia and Europe (Tornaghi et al., 1985; Stella et al., 1990; Bruce and Pellegrino, 1996; Pellegrino, 1999b), its use in the North-American tunneling industry is relatively rare. Furthermore, prior to ICT/SP Contract E, there were no recorded case histories in the literature of full-face treatment by jet grouting in soft marine clay.

Construction of the Contract E tunnels involved jet grouting for pre-treatment of Bay Mud, tunneling through the resulting soil-cement material using an open-face shield, erecting an initial support system of steel ribs and timber lagging, and installation of a steel pipe lining.

Jet grouting technique

Jet grouting is a ground modification technique based on the erosional action of high-velocity fluids, acting under nozzle pressures of up to 60 MPa (Moseley, 1993). The fluids (generally water and grout) are injected via a special drill tool called a "monitor," which is attached to the end of a steel drill string (Figure 8). As the monitor is rotated and withdrawn at controlled rates, the pressurized fluids fracture, erode, mix, and partially replace the surrounding soils with a stabilizing cementitious grout. The high velocity and pressures are obtained by pumping the water and grout with heavy-duty pumps, developed for the petroleum-drilling industry, through small-diameter nozzles located on the monitor. The soil structure is virtually obliterated by the jets and the original subsurface material is ultimately mixed with grout to form soil-cement columns. Since the grout being injected only partially replaces *in situ* soils, eroded soils and excess grout are returned to the surface as spoil.

This technique was originally conceived in Japan to overcome the limitations associated with grouting in fine-grained soils; traditionally, only coarse-grained soils had been considered groutable by techniques such as permeation grouting (Xanthakos et al., 1994).

Different jet grouting systems are commercially available, depending on the type and number of fluids injected (Pellegrino, 1999a). The single-fluid system is most common, and employs only a grout jet to fracture and mix the soil *in situ* (Figure 9). The erosional efficiency of the jet can be enhanced by shrouding the grout jet with compressed air, in the so-called double fluid system. The triple fluid system separates the erosional fluids (air and water) from the stabilizing fluids (grout).

In all three systems the monitor is generally attached at the bottom of a specific string of drill-rods and advanced in the ground to the required depth by means of a specialized drill rig (Figure 10). The monitor is then rotated and extracted in a controlled fashion while injecting fluids at high pressures. The dimensions and mechanical properties of the treated body depend on the combined effect of the type of soil, composition of the grout, grout pressure and flow, and monitor rotational and withdrawal speed. The diameter of single-fluid columns, typically in the range of 0.5 to 0.9 m, can be increased to over 4 m by using double- or triple-fluid techniques.

The drill rigs generally used in jet grouting are equipped with a controlled lift and rotation mechanism (De Paoli et al., 1991). In recent years, rig-mounted automatic monitoring devices have been

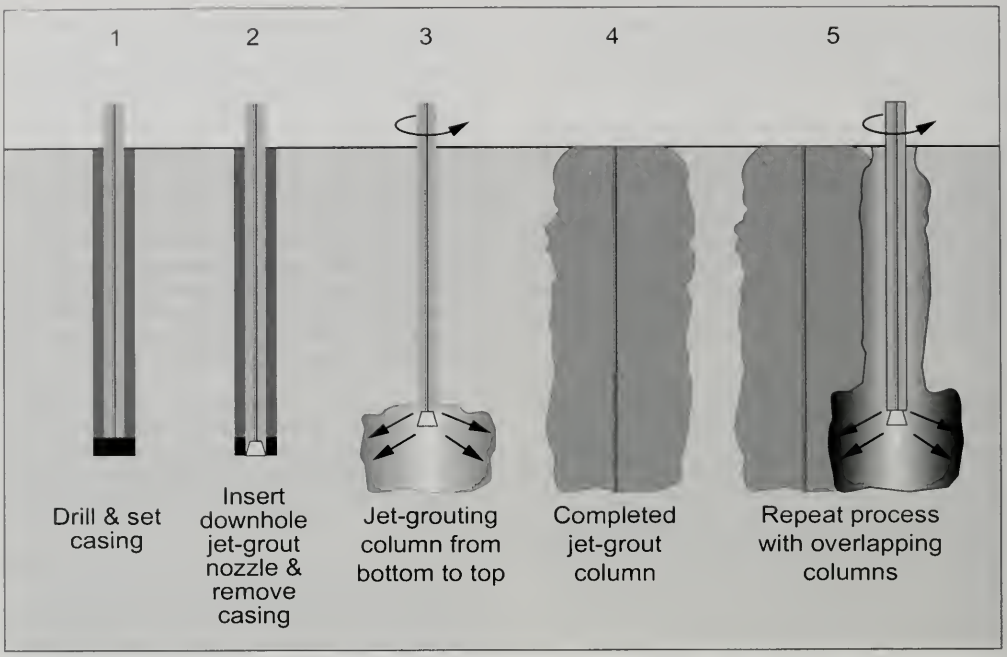

Figure 8. Jet grouting process.

developed that are capable of recording and displaying the most significant installation parameters in real time, thus allowing for enhanced quality control (Jameson et al., 1998; Fortunati et al., 1998).

The grout is prepared in high-capacity batching plants (Figure 11). Due to the large volumes of cementitious grout injected, the plants are generally fully automated, and the dry material is stored in silos.

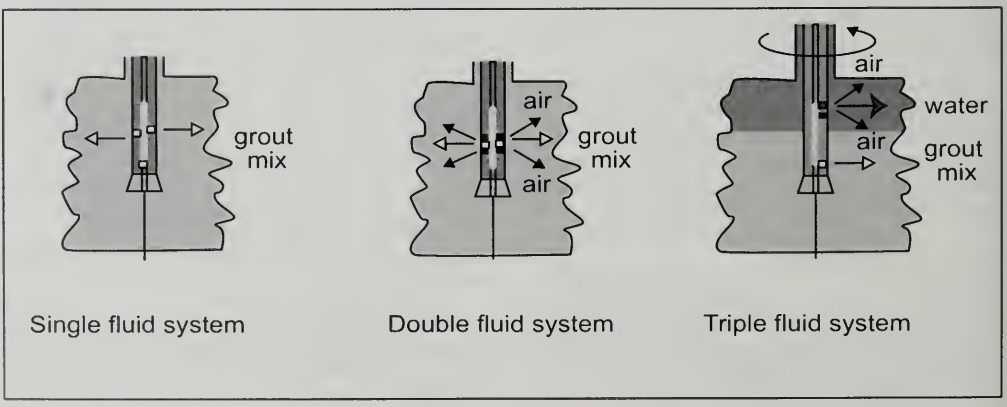

Figure 9. Jet grout injection systems.

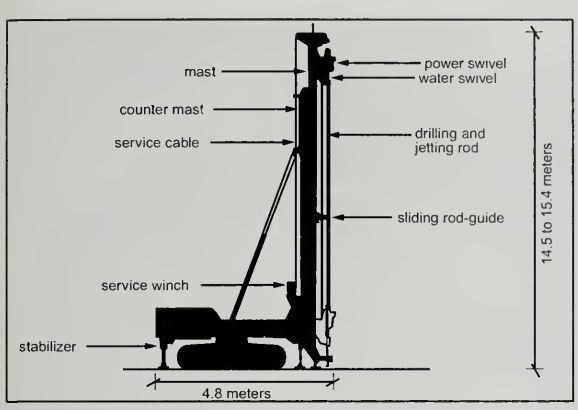

Figure 10. Jet grout rig.

Jet grouting on the Islais Creek project

Because of the presence of soft Bay Mud on Contract E, squeezing ground occurs far below subgrade during excavation. Jet grouting was specified in the bid documents as a pre-support measure for sheet pile and SPTC walls in the cut-and-cover sections. Pre-support of the sheet-pile and SPTC walls consisted of a jet-grouted kicker slab placed tight against the walls. The primary purpose of this jet-grouted kicker slab was to reduce deflections of the SPTC walls. The secondary purpose was to reduce the bracing requirements and facilitate construction activities at the bottom of the excavation by "pre-installing" a solid slab. During subsequent phases of the project, jet grouting was also used to underpin a pile-supported box sewer prior to the removal of the sewer's bearing piles during tunneling.

As noted above, the contractor proposed jet grouting for stabilization of soils within the tunnel profiles (Figures 12 and 13). By using jet grouting to modify the Bay Mud into soil-cement, the tunnel could be excavated with an open-face shield without compressed air for support of the face. The proposal for jet grouting of tunnel soils called for full-face treatment. The required mechanical characteristics of the grouted soil were determined by finite element analysis of soil stresses around the tunnel excavation, which also determined the minimum required unconfined compressive strength (U_c) of 803 kPa.

On Contract E the jet grouting contractor opted to use the double-fluid system (Figure 9) to consolidate the Bay Mud ahead of the tunnel face. The choice was made on a technical as well as a commercial basis. The single-fluid system, which yields smaller-diameter grout columns than the double-fluid system, was not selected because of the excessive number of grout column installations necessary to modify the required volume of soil. The triple-fluid system was not selected because of its higher cost and the large volume of low-density spoil typically generated by this technique.

Jet grout test program

The purpose of the jet grout test program was to demonstrate the quality of jet grouted columns in Bay Mud under field conditions. Column strength and continuity were key criteria for evaluation of the test program results. In addition, the test program was monitored to study heave and settlement of the ground that is generally associated with jet grouting.

The test consisted of 12 jet grouted columns installed using the Rodinjet techniques and equipment (Pellegrino and Adams, 1997). Six of the test columns were single-fluid, whereas the other six were double-fluid. Different combinations of grouting parameters were tested to optimize the subsequent production work. In general, the grout pressures varied from 300 to 400 bars, corresponding to

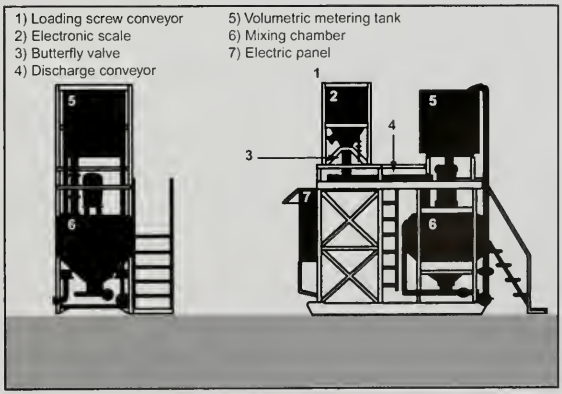

Figure 11. Jet grout batch plant.

Figure 12. Installing jet grouted columns for tunnels.

flow rates from 1.97 to 2.35 l/sec, through 2.6 mm nozzles (two nozzles per monitor). The grout was a neat mix of water and low alkali type II cement, with a water/cement ratio of 0.83 by weight. The characteristic unconfined compressive strength of the grout mix was 10.4 MPa after 7-days curing and 17.8 MPa after 28-days curing. In the double-fluid jet grouting, compressed air was utilized at a pressure of 8 bars and a flow rate of 75 l/sec. The dry cement yield (defined as the weight of dry cement injected per unit volume of soil-cement body) of the individual soil-cement columns installed by the double-fluid technique varied from 100 to 160 kg/m^3; for the single-fluid system the range was from 330 to 520 kg/m^3.

The test columns were installed below the fill level to depths ranging from 4.6 to 8.5 m in two days. At completion of jet grouting, a 9 meter by 9 meter sheet pile and bracing supported test pit was excavated to expose the top 1.2 m of each column (Figure 14). Column diameters ranged from 0.8 to 1 m for the single-fluid system and from 2.4 to 2.9 m for the two-fluid system. Before the test program there was concern that soil-cement strengths would be low in the soft Bay Mud (Fang, 1998); however, laboratory testing on core samples of the grouted soil showed an average unconfined compressive strength after 28-days curing of 3,400 kPa for the single-fluid columns and 1,400 kPa for the double-fluid columns. These values were well above the design strength of 803 kPa.

Jet grouting treatment for tunnels

Based on the test-program results, a production grouting pressure of 400 bars was selected, together with an air pressure of 9 bars and a target cement factor of 125 kg/m^3. A conservative jet grouting column spacing of 1.8 meters on a triangular pattern was chosen to account for the numerous subsurface obstructions (Figure 15). This layout resulted in 7,500 lineal meters of columns, and a cement consumption of up to 400 kg of cement per cubic meter of grouted soil.

Production started on the Davidson Avenue Tunnel in July 1994. The 156-meter stretch was grouted with 676 columns. The operation then

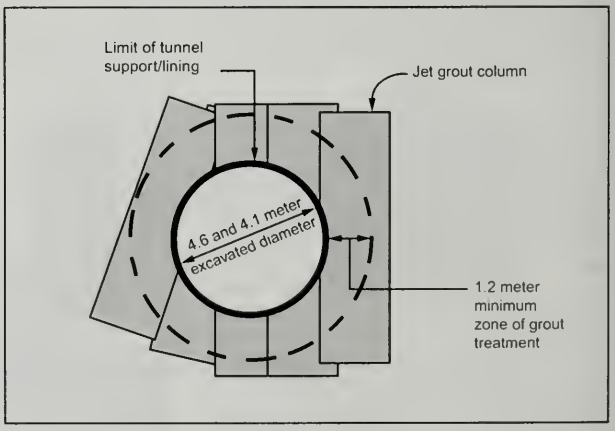

Figure 13. Tunnel cross section showing jet grout ground modification.

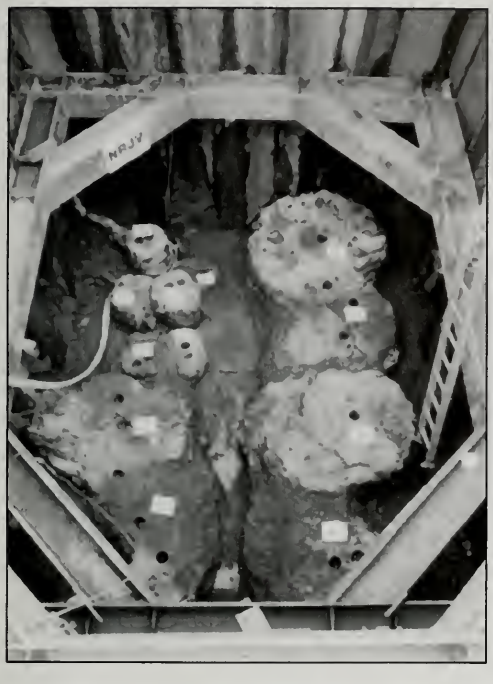

Figure 14. Jet grout test columns.

moved to the Undercrossing Tunnel, where treatment required installation of columns inclined up to 30 degrees from vertical and as deep as 24 m (Figure 16). Installation of jet grouted columns beneath the railroad embankment required the use of a temporary earth platform on both sides of the embankment (Figure 17). The inclined columns

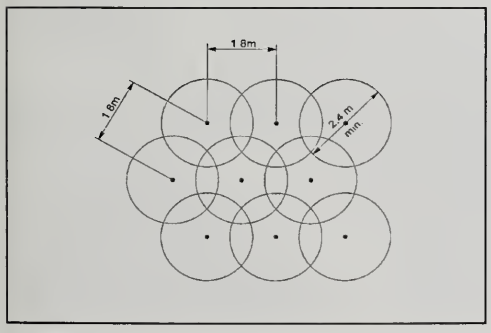

Figure 15. Layout of jet grout columns.

underneath the tracks were grouted through precased holes to prevent the washing of the embankment soils by the drilling fluids. The 76 m tunnel stretch was grouted with 306 columns, with no heave of the tracks.

Ground deformation associated with jet grouting was a significant issue during construction. In the early stages of jet grouting, the Bay Mud heave in overlying utilities was as much as 140 mm. Heave during jet grouting occurred when the drill hole annulus became clogged or reduced in area, thereby impeding the return of cuttings. To reduce heave, the jet grouting sequence was modified to include precutting and pretreatment of the fill above the Bay Mud. Precutting used increased flow and pressure of fluids during drilling to maintain an open hole while jetting. Pretreatment involved placing soil-cement to stabilize soils above the "design" jet grout zone to allow for drilling and jetting with continuous flow of spoils.

Continuous core sampling was used to verify the continuity and consistency of the grouted mass prior to starting tunnel excavation. Vertical and inclined core sampling was performed at nine different locations on both tunnels. Testing indicated an average unconfined compressive strength of 3,860 kPa at different curing ages, confirming that substantial strength increase in jet grouted clays occurs after the initial 28 days (Fang, 1998). Unconfined compressive strength test results on soil-cement cores

LOCATION	U_c (kPa) @ 28-days
Undercrossing Tunnel West	2,140
Undercrossing Tunnel East	2,430
Undercrossing Tunnel embankment	5,070
Davidson Avenue Tunnel	4,520

Table 2. Jet grout strengths

are shown in Table 2. Column continuity was very good, allowing RQD to be calculated for the cores samples taken from the surface. RQD values for the jet grouted soils averaged more than 60 percent.

Tunnel equipment

The tunnels were excavated with a Dosco/Terra Form open-faced roadheader tunneling machine

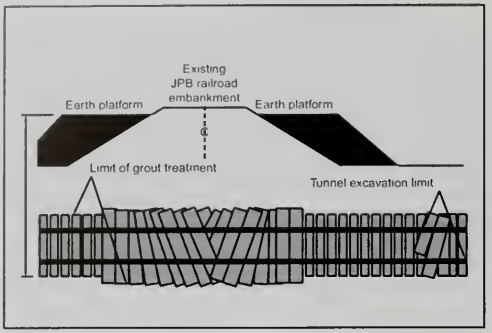

Figure 16. Profile of Undercrossing Tunnel.

(Figure 18). The machine was made of two main components: a shield and a roadheader boom cutter. The shield was equipped with a hood, boom-cutter frame, twelve 1,350 kN thrust jacks with 1.7 m of stroke, and a rib erector and expander. A 17 m long conveyor belt brought muck from the face out over the top of a trailing frame into 6 m^3 muck cars, which were transported by locomotive to the tunnel shaft.

The roadheader boom-cutter was ring mounted on a rail carriage and was powered by a 190 horsepower direct-drive hydraulic motor. It had a 118 mm cutter head with 20 drag bits located radially around it, and was capable of extending 2.3 m in front of the shield. Head rotation was 60 rpm at 32 MPa during normal operations. The torque at normal operations was 2237 kg-m, with a force of 58 kN delivered at each bit.

Shields of 4.6 m and 4.1 m diameter, equipped with the same boom cutter, were used to mine the two tunnels.

Tunnel excavation

The Davidson Tunnel excavation commenced on 14 February 1995. During the first 30 working days, the tunnel advanced an average of 0.8 m per day. After the full trailing gear was installed, the remaining 129 m of tunnel yielded an advance rate of 5 m per 10 hour shift. An average of 6.1 m per shift was achieved during the last 15 shifts, leading to hole-through on May 8, 1995.

The tunnel machine was removed from the Davidson Tunnel, and the boom cutter was reassembled within the second 4.1-m-diameter tunnel shield. Tunneling for the Undercrossing Tunnel commenced on June 22, 1995. During the first 13 work days the average advance rate was 1.5 m per 10-hour shift. After assembly of the trailing gear, the average advance rate increased to about 3.7 m per shift, with hole-through on August 3, 1995.

During excavation, the initial lining of steel ribs and wood lagging was erected within the tail section of the machine (Figure 19). As the machine was shoved forward, the primary lining was shoved out against the previous set, and then expanded.

Throughout excavation of both tunnels, the jet grouted soils in the face and crown were stable. Throughout much of the Davidson Tunnel, the jet grouted soil was completely continuous, so in most instances the initial lining did not experience soil loads. Throughout the Undercrossing Tunnel, discontinuities in jet grout treatment occurred around timber piles. During one excavation sequence, a third of the tunnel face was found to be untreated. However, the clay in these untreated areas was very stiff and uncharacteristically dry, and in no cases did instability of the face occur.

Figure 17. Jet grouting under the commuter railroad embankment.

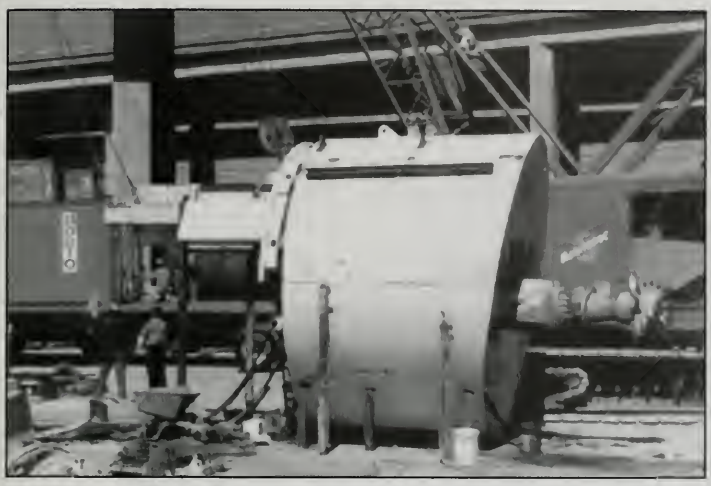

Figure 18. Tunnel shield with roadheader excavator.

Tunnel muck consisted of chips of the jet grouted clay ranging in size from 3 to 70 mm, which behaved like siltstone or mudstone chips. By comparison, untreated Bay Mud, excavated during construction of the many cut-and-cover structures, was difficult to handle and costly to dispose of.

Total groundwater seepage for the entire length of the tunnels was approximately 0.32 liters/sec at the Davidson Tunnel, and 0.12 liters/sec at the Undercrossing Tunnel.

A total of 41 old piles were encountered during both tunnel excavations. Precast concrete piles and timber piles were broken up and removed from the face with no impact on the excavation operations. However, the wood in the tunnel muck did make disposal more difficult. In addition, at several locations the remaining timber "stub" at the limits of the excavation complicated the steerage of the machine. At two different locations steel H-piles were encountered. These two piles did stop excavation, but stability of the jet grouted soil mass at the face made removal by hand relatively quick, resulting in very little impact on production.

A strong ammonia odor was typically released into the air inside the tunnels, a condition that had not been observed before in other Bay Mud excavations. It is possible that ammonia was already present in Bay Mud along the project alignment, but if so it is surprising that it was not detected during the geotechnical investigations. Alternatively, it may have formed as a by-product of the grouting process, as similar conditions have been reported on other construction projects after injecting cement grout into clays. Air monitoring during excavation found that airborne ammonia concentrations ranged from 7 to 20 mg/m^3. After excavation stopped, however, airborne concentrations of ammonia dropped quickly to less than 2.6 mg/m^3. Organic cartridge respirators were required to be worn during excavation, even though full-circulation ventilation was run continuously to the tunnel face throughout the tunnel operations.

Figure 19. Initial tunnel lining. Steel ribs and wood lagging tunnel support are clearly shown.

Figure 20. Final tunnel lining consisting of steel pipe.

On completion of the tunnels, steel carrier pipe was installed as the final lining for the tunnels (Figure 20). Individual sections of steel pipe were connected by "push-on" bell and spigot joints with gaskets, and the interior surface of the pipe was coated with flexible coal-tar epoxy. After the steel pipe was installed, the annulus between the steel pipe and the initial tunnel support (steel ribs and timber lagging) was filled with cellular concrete. Cellular concrete is a light-weight material (750 kg/m^3) composed of water, cement, and an air-entraining foam. Cellular concrete has traditionally been used for roof decks; however, the low cost and high placement volumes that can be achieved with cellular concrete have led to this material being used as a geotechnical fill or as annular backfill in tunnels.

Geotechnical instrumentation

Performance monitoring consisted of surface-settlement points, lateral-displacement reference points, inclinometers, vibrating wire strain gauges, and observation wells located across the entire project site.

Settlements as a result of tunneling were generally within the limiting response values given in the contract. During excavation of the Davidson Avenue Tunnel, most settlement points moved less than 13 mm, well within the 25 mm limiting response value. Exceptions were two points that settled approximately 25 mm during tunneling.

Settlement data for the Undercrossing Tunnel are difficult to generalize due to the use of the temporary earthen work platforms, the continuous settlement of the railroad embankment (documented prior to the start of construction), and the repeated track re-ballasting effort. Re-ballasting was required as part of a stringent settlement control program enforced jointly by the JPB and the City. Jet grouting of the Undercrossing Tunnel caused a 1.7-m force main to heave 150 to 300 mm above the tunnel centerline. After this initial heave, jet grouting procedures were modified and heave was brought under control. During excavation, settlement of the 1.7-m force main was generally within the 25 mm limiting response value, and most other reference points showed settlements of less than 13 mm. Settlements that occurred after jet grouting but before tunneling were most likely due to consolidation settlement of Bay Mud below the adjacent earthen work platforms and railroad embankment. As noted above, these temporary earthen work platforms were installed to facilitate drilling and jet grouting under the railroad embankment.

Most of the lateral displacement points showed very little movement, and where movement was documented it was within limiting response values. Two lateral displacement markers fixed to Interstate 280 piers exceeded the 16 mm limiting response value after the Undercrossing Tunnel face had passed the piers. These lateral displacement markers showed approximately 18 mm and 25 mm of total movement. These movements were attributed to the jacking of the piers, which was conducted as part of the ongoing seismic retrofit of the freeway structure.

Three inclinometers were installed within 15 feet of the tunnel centerline after jet grouting was completed. The inclinometer data were obtained daily, immediately before and after the tunneling machine passed, and then weekly when the machine was within 100 feet of the instrument. The data collected, in conjunction with observations made during tunneling, indicated that ground movements around the tunnel were negligible. Only the inclinometer installed near an Interstate 280 pier exceeded the limiting response value. At this location the maximum movement was 42 mm, attributed to outward heave of the jet grouted kicker slab installed for construction of the Davidson Diversion Sewer; in other words, this movement was not a result of tunneling.

Data from inclinometers installed within the SPTC wall demonstrated both the jet grout's ability to restrain wall movement during excavation and its impact on the walls prior to excavation. Installation of the jet grout kicker slab resulted in outward wall movement of approximately 20 to 25 mm, thus pre-stressing the excavation support system. During excavation for the T/S structure SPTC walls moved inward approximately 13 to 25 mm, mostly at the very start of the excavation. The smaller and smaller magnitudes of movement over time indicate that the jet grout kicker slab was performing very well.

LESSONS LEARNED

The following generalizations can be made based on construction experience gained on 1CT/SP Contract E:

1. Surface settlements above a tunnel being excavated in jet grouted soil-cement are less than conventional theory would predict.

2. Tunnel inflows from within a mass of jet grouted soil-cement are very low.

3. Jet grouted soil-cement with unconfined compressive strengths of 2 to 5 MPa is possible in soft marine clays.

4. Jet grouting in marine clays with a high organic content may produce ammonia vapor when tunneling through a mass of jet grouted soil-cement.

5. Ground heave is a critical issue with jet grouting under structures. Maintaining good return of cuttings during jet grouting is critical to prevent heave. Precutting and pretreatment of soils above the "design" zone for jet grouting can be used to enhance return of jet grout cuttings.

Above all, this project demonstrated that jet grouting for pre-treatment of soft soils is possible and compatible with open-face tunneling methods. It is a versatile ground modification technology that can be used in other geotechnical applications on future projects.

ACKNOWLEDGEMENTS

The authors would like to acknowledge the various parties involved in this successful project: City of San Francisco Department of Public Works, owner of the project; Jacobs Associates, design engineer for the City, Kajima Engineering and Construction, the general contractor; Nicholson-Rodio JV, the jet grouting sub-contractor; and Haley & Aldrich /EPC, the construction administrators. Our personal thanks to Manfred Wong, Norman Chan, Dan Adams, Bill Edgerton, and Mike Robison. We would also like to thank Horacio Ferriz, Richard Proctor, and Manuel Bonilla for their thoughtful peer reviews of this paper.

AUTHOR PROFILES

Victor Romero is a licensed Civil Engineer in California, Washington, Massachusetts and Puerto Rico, as well as a California Certified Engineering Geologist. He has over 10 years experience in tunnel engineering, and is currently an Associate at Jacobs Associates and a past instructor of engineering geology at San Francisco State University. His specialties include shaft design, pipe jacking, portal stabilization, slope stability, pressure tunnel design,

soft- ground tunneling methods, initial tunnel support design, final tunnel lining design, grouting, boreability (TBM) assessment, microtunneling, and geotechnical baseline reports.

Guido Pellegrino graduated in Geotechnical Engineering at Milan University, with a research thesis on "Rock Mass Classification for the Prediction of Temporary Tunnel Support." He joined the Rodio Group in 1989 and since then he has been involved in several ground improvement and ground modification projects worldwide, particularly for tunneling applications. He has been actively operating in geotechincal engineering and construction in North America since early 1994, through Nicholson Construction Company, Rodio's U.S. subsidiary.

SELECTED REFERENCES

Adams, D.N., and Robison, M.J., 1996, Construction and performance of jet grout supported soldier pile tremie concrete walls in weak clay: Boston Society of Civil Engineers, Journal of Civil Engineering Practice, Fall/Winter 1996, p. 13-34.

Bailey, E.H., Irwin, W.P., and Jones, D.L., 1964, Franciscan and related rocks, and their significance in the geology of western California: California Division of Mines and Geology, Bulletin 183, 177 p.

Bickel, J.O., Kuessel, T.R., and King, E.H., 1996, Tunnel engineering handbook, Second Edition: Chapman & Hall, (New York, New York), 544 p.

Bonaparte, R. and Mitchell, J.K., 1979, The properties of San Francisco Bay Mud at Hamilton Air Force Base, California: Report by the Department of Civil Engineering, University of California, Berkeley, April 1979, 179 p.

Boults, W., 1990, Map of historic marshland margins, San Francisco: William Boults, 1325 26th Avenue, San Francisco, CA 94122, scale 1:24,000.

Bruce, D.A. and Pellegrino, G., 1996, Jet grouting for the solution of tunneling problems in soft clays: Proceedings, Second International Conference on Ground Improvement Geosystems, Japanese Geotechnical Society and International Society for Soil Mechanics and Foundation Engineering, (Tokyo, Japan), p. 347-352.

Clough, G. W. and Reed, M. W., 1984, Measured behavior of braced wall in very soft clay: American Society of Civil Engineers, Journal of Geotechnical Engineering, v. 110, no. 1, p. 1-19.

De Paoli, B., Stella, C., and Perelli Cippo, A., 1991, A monitoring system for the quality assessment of the jet grouting process through an energy approach: Proceedings, Fourth International Conference on Piling and Deep Foundations, Deep Foundation Institute, (Stresa, Italy), p. 211-215.

Fang, Y.S. and Yu, F.J., 1998, Engineering properties of jet grouted soilcrete and slime: Proceedings, Second International Conference on Ground Improvement Techniques, Geotechnics Holland B.V., (Singapore), p. 589-596.

Fortunati, F. and Pellegrino, G., 1998, The use of electronics in the design and implementation of ground improvement works: Proceedings, Geotechnical Site Characterization, International Society of Soil Mechanics and Geotechnical Engineering, (Atlanta, Georgia), p. 357-364.

Hausman, M.R., 1990, Engineering principles of ground modification: McGraw-Hill, (New York, New York), 632 p.

Henn, R.W., 1996, Practical guide to grouting of underground structures: American Society of Civil Engineers, 191 p.

Jacobs Associates, 1992, Geotechnical design summary report, Islais Creek Transport/Storage Project, Contract 'E': Contract Documents: Consultant's report to the City and County of San Francisco, 66 p.

Jameson, R., Pellegrino, G.,and Shea, M., 1998, Instrumentation for performance monitoring of jet grouting: Proceedings, Second International Conference on Ground Improvement Techniques, Geotechnics Holland B.V., (Singapore), p. 613-620.

Kutzner, C. 1996, Grouting of rock and soil: A.A. Balkema, (Netherlands), 286 p.

Ladd, C.C. and Foot, R., 1974, New design procedures for stability of soft clays: American Society of Civil Engineers, Journal of the Geotechnical Engineering Division, v. 100, no. GT7, p. 753-786.

Mana, A.I. and Clough, G.W., 1981, Prediction of movements for braced cuts in clay: American Society of Civil Engineers, Journal of the Geotechnical Engineering Division, v. 107, no. GT6, p. 759-778.

Moseley, M.P., 1993, Ground improvement: Blackie Academic and Professional Publishers, (London, England), 218 p.

Mussger, K., Koinig, J., and St. Reischl, 1987, Jet grouting in combination with NATM: Rapid Excavation and Tunneling Conference Proceedings, American Institute of Mining, Metallurgical, and Petroleum Engineers and American Society of Civil Engineers, (New Orleans, Louisiana), v. 1, p. 292-308.

Peck, R.B., 1969, Deep excavations and tunneling in soft ground: Proceedings, Seventh International Conference on Soil Mechanics and Foundation Engineering, International Society for Soil Mechanics and Foundation Engineering, (Mexico City, Mexico), p. 225-290.

Peck, R.B., Hendron, A.J., and Mohraz, B., 1972, State of the art of soft-ground tunneling: Rapid Excavation and Tunneling Conference Proceedings, American Institute of Mining, Metallurgical, and Petroleum Engineers and American Society of Civil Engineers, (Chicago, Illinois), p. 259-286.

Pellegrino, G. and Adams, D.N., 1997, The use of jet grouting to improve soft clays for open face tunnelling: International symposium on Geotechnical Aspects of Underground Construction in Soft Ground, International Society for Soil Mechanics and Foundation Engineering, (London, England), 1996, p. 423-428.

Pellegrino, G., 1999a, Grouting technologies for soft ground tunneling: recent developments: Proceedings, Tenth Australasian Tunneling Conference, The Australian Institute of Mining and Metallurgy, (Melbourne, Australia), p. 263-268.

Pellegrino, G., 1999b, Soil improvement technologies for tunneling in soft ground: Selected case histories: State of the Art Technology in Earth and Rock Tunneling, American Society of Civil Engineers, MET Section, Geotechnical Seminar, (New York, New York), p. 1-12.

Radbruch, D.H. and Schlocker, J., 1958, Engineering geology of Islais Creek basin, San Francisco, California: U.S. Geological Survey, Map I-264, scale 1:12,000.

Stella, C., Ceppi, G., and D'Apollonia, E., 1990, Temporary tunnel support using jet-grouted cylinders: American Society of Civil Engineers, Journal of Construction Engineering and Management, v. 116, no. 1, p. 35-53.

Tornaghi, R. and Perelli Cippo, A., 1985, Soil improvement by jet grouting for the solution of tunnelling problems: Proceedings of the 4th International Symposium of Minerals and Metallurgy, Tunnelling, Brighton, (London, England), p. 265-276.

Xanthakos, P.P., Abramson, L.W., and Bruce, D.A., 1994, Ground control and improvement: John Wiley & Sons, (New York, New York), 910 p.


ASSOCIATION OF ENGINEERING
GEOLOGISTS
AEG

LESSONS LEARNED DURING CONSTRUCTION OF THE LAKE MERCED STORMDRAIN TUNNEL, SAN FRANCISCO COUNTY, CALIFORNIA

LEE ABRAMSON[1] AND MIKE KOBLER[2]

ABSTRACT

During the 1980's and 1990's, the City of San Francisco built a series of large underground structures to increase sewage treatment capacity and reduce the number of overflows into the Pacific Ocean to acceptable levels. One feature of this project was the Lake Merced Transport Tunnel, which is 2.6 km long and has an excavated diameter of 5.5 m and a finished diameter of 4.3 m. The tunnel was excavated through alluvial, beach, and dune sandy soils, and through sand deposits of the Colma Formation utilizing a digger shield tunneling machine. The tunnel lining consisted of a precast concrete segmental initial lining and a cast-in-place concrete final lining. The tunnel was anticipated to be excavated predominantly through the Colma Formation; however, builders encountered more beach/dune sands than expected. The characteristics of the beach/dune sands caused shield steering problems, slow progress, and pronounced ground settlements. This article describes how these and other challenging site conditions were resolved amicably during construction with the aid of reasonable contract clauses and cooperation among the owner, designer, construction manager, and contractor.

[1]Hatch Mott MacDonald
27 Bleeker St.
Millburn, NJ 07041
labramson@hatchmott.com

[2]Underground Construction Managers
118 Airport Drive, Suite 204
San Bernardino, CA 92408
mkobler@ucm.net

INTRODUCTION

In the early seventies, the City and County of San Francisco embarked on a program to control wet-weather storm sewage overflows. In San Francisco, urban runoff and sanitary sewage flowed in the same pipes and often caused the system to become overloaded during storms. Studies conducted in the late 1960's showed that, during major storms, significant amounts of storm water and untreated sanitary wastes bypassed the City's treatment facilities and overflowed into the bay and the Pacific Ocean. The City's Bureau of Sanitary Engineering was charged with developing a wastewater master plan to increase sewage treatment capacity and reduce the number of overflows to an acceptable level. Instead of replacing the existing network of combined sewer lines with separate systems, the City built a series of large underground structures to intercept, temporarily store, and then transport rain-swollen sewage to upgraded treatment facilities. Since the facilities came online in the 1990's, storm sewage overflows have been reduced from an annual average of 80 in the 1960's, to eight or less in the 1990's.

A major feature of the storage, conveyance, and treatment scheme was the Lake Merced transport tunnel. The tunnel is 2.6 km long, with an excavated diameter of 5.5 m and a finished diameter of 4.3 m (Abramson and Owyang, 1993). It was expected that excavation would be entirely within the Colma Formation, an alluvial deposit consisting of weakly cemented sand. Once excavation of the tunnel access and staging portal began, however, it became evident that a portion of the tunnel would be excavated through beach/dune sand. Ultimately, beach/dune sand was encountered in over 35 per-

cent of the tunnel alignment. Through cooperation between the contractor, the City, the design engineer and the construction manager, excavation proceeded with minimal delay, and the impact of the differing site conditions on the contractor's work was minimized by prompt processing of change orders.

This paper presents engineering geology work performed in support of construction for the Lake Merced transport tunnel. The paper describes the project, the contract, the Contractor's plan for construction, and a chronology of the conditions and unforeseen obstacles encountered during excavation.

PROJECT DESCRIPTION

The Lake Merced transport and storage project was planned and designed in the 1970's and 1980's to capture sewage and runoff from the extreme southwestern portion of the city. It was designed to function with the new Oceanside secondary treatment plant, the Southwest ocean outfall, the Westside pump station, the Westside transport tunnel and the Richmond transport tunnel (Figure 1). These facilities make up the west side core system of San Francisco's combined sewer overflow control facilities.

The Lake Merced transport tunnel runs beneath the right-of-way of Highway 1 from an existing pump station near the shore of Lake Merced to a point near the Pacific Ocean, where it connects with the existing Westside transport/storage tunnel (Figure 2). From there, sewage is pumped into a treatment plant, which feeds into the Southwest ocean outfall.

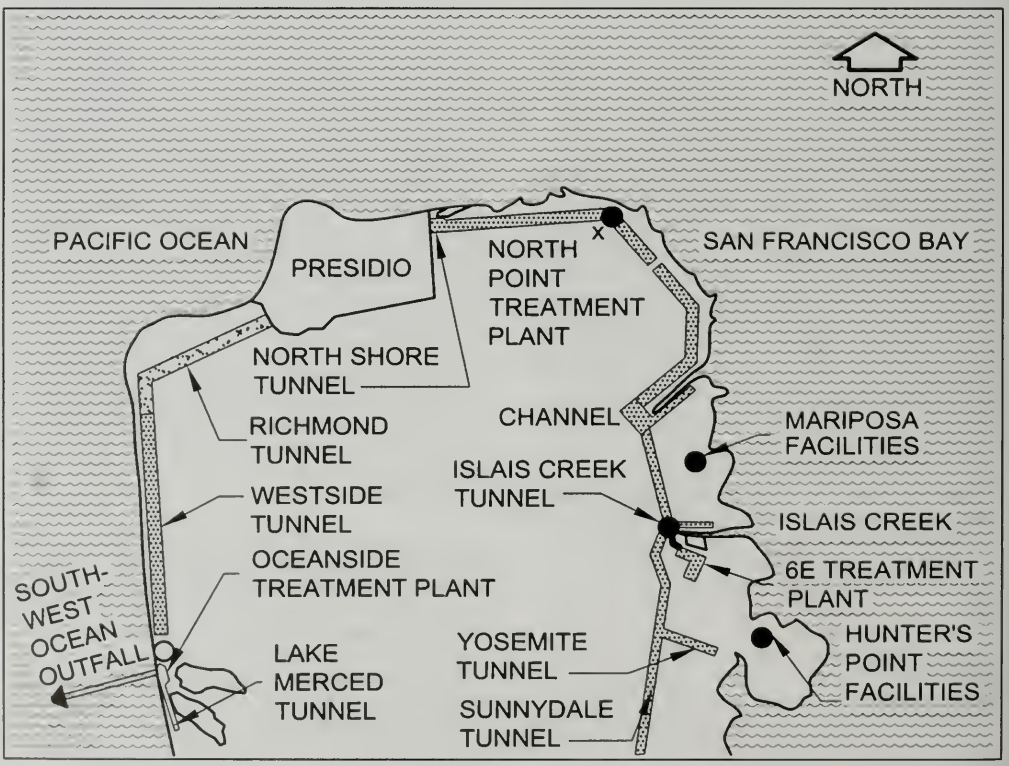

Figure 1. Project location map.

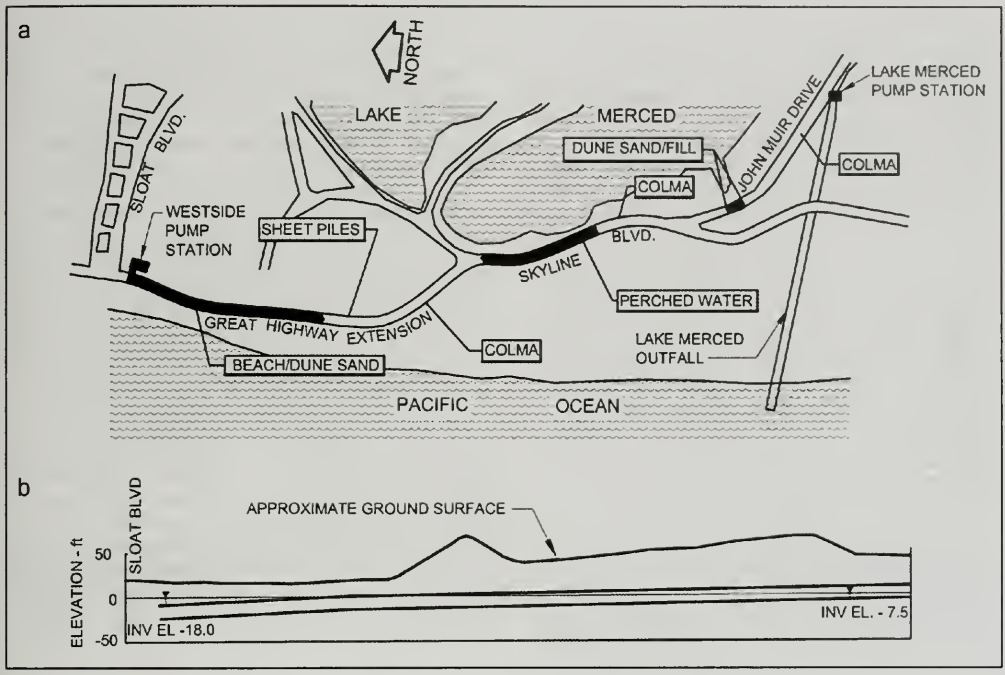

Figure 2. (a) Plan view of the project. (b) Profile view of the project.

Subsurface conditions

Near-surface soils along the tunnel alignment are dune and beach sands, loose and uniformly graded (Mamak et al., 1990). The builders encountered zones of these sands through 35% of the alignment of the tunnel; the remaining 65% of the alignment ran through sands of the Colma Formation. Colma sands typically are uniformly graded, medium to fine silty sands interbedded with some layers of silt. They are dense to very dense and possess some cohesion. Along the Pacific shore the Colma Formation is exposed in stable slopes as steep as 65 degrees. Unfortunately, it is difficult to sample the Colma sands intact. Cementation is often destroyed during sampling, making it difficult to differentiate between Colma and other sand deposit samples. The combination of uncemented and cemented zones of sand having variable horizontal and vertical extent below the water table made tunneling behavior difficult to predict.

PRE-CONSTRUCTION

Design documents

The design documents contained provisions distinctive to the tunneling industry, including a prequalification process, differing site conditions clause, escrow bid documents, and a geotechnical design summary report (Parsons Brinckerhoff, 1990). Several years before this project, in reaction to the relatively high rate of construction claims on tunneling projects, the tunnel design and construction industry in the U.S. endeavored to develop such features in tunnel construction contracts that would improve deliberations on such claims. A means was developed to better define the basis upon which contractors bid tunnel construction projects and the basis upon which claims of differing site conditions were evaluated (should such conditions be claimed by the contractor).

One major feature of this approach consists of providing the contractor with a geotechnical design summary report (GDSR) as part of the contract documents. This report establishes the baseline geotechnical conditions upon which the contractor bids the project and the baseline for claims related to differing site conditions. The contractor must demonstrate that geologic conditions were significantly different from the basis of bidding and show that variations had a negative impact on construction schedule and cost. This design report has more recently been referred to as a geotechnical baseline report (GBR) and the American Society of Civil Engineers (ASCE, 1997) has developed guidelines for its use. One key necessity for the proper preparation of this report, and consequent monitoring of geologic conditions during construction, is the involvement of experienced, knowledgeable engineering geologists and geotechnical engineers on both the owner/designer side and the contractor side.

A geotechnical baseline report has been incorporated into most tunneling projects over the past 15 to 20 years. For the most part, this disclosure of the assumptions used in design of tunnel projects has improved the level of common understanding between owners, designers, and contractors. It is generally accepted that establishing a geotechnical baseline on a tunnel project is better than leaving all of the interpretations to the contractor during bidding. Though having a baseline report has not totally eliminated construction claims related to differing site conditions on tunnel projects, it has provided a much sounder basis upon which to deliberate such claims. Without having a stated basis for bids, it is difficult to validate the contractor's assumptions during bidding.

Other contract mechanisms used on this project include a prequalification process, differing site conditions clause, and escrow bid documents. A more detailed description of these mechanisms may be found in ASCE (1991). The prequalification of bidders usually consists of contractors supplying the owner with qualifications related to the type of work stipulated in the contract. Information such as number of similar projects, miles constructed in similar tunnels, client references, equipment at hand, or number of skilled operators is required. This information is usually supplied ahead of bidding and results in a list of prequalified bidders. The owner usually conducts the prequalification process with assistance from the designer, in accordance with set specifications that the contractors receive in advance. There is an appeal process for any contractors who, for whatever reason, do not pass the prequalification process, and the contractors can take legal steps to challenge the decisions made should they feel that the process was not conducted fairly.

Escrowed bid documents are the work sheets and assumptions that formed the basis for the winning contractor's bid, written down in a sufficiently understandable form so that, if the contractor's basis for bidding were to become an issue during construction, these work sheets would not be subject to speculation and change when a dispute arises. The documents remain the property of the contractor, are placed in escrow at the beginning of construction after joint review by the owner and the contractor, and are referenced only if they relate to resolution of a dispute. The purpose of these documents is to establish, in case of dispute, the contractor's understanding and intentions at the time of the bid. The corresponding documentation of the owner's (and design engineer's) understanding and intentions is contained in the baseline report, which is the reason for including it in the contract documents.

The Lake Merced transport tunnel contract did not include a Disputes Review Board, although many tunnel projects have used this method of dispute resolution since the 1980's. A Disputes Review Board is usually composed of a three-member panel of independent third parties retained for this purpose during construction and convened to resolve disputes that arise without first resorting to legal measures. The contractor supplies one member, the owner supplies one member, and the third member is chosen by the other two.

The contract mechanisms described above have reduced the litigious nature of tunnel contract claims, but have not completely eliminated the need for a geotechnical baseline for bidding, as will be seen in the following discussion. The baseline report for the Lake Merced transport tunnel stated that the tunneling was expected to encounter only Colma Formation. It described the Colma Formation as a weakly cemented, poorly graded, medium dense material that included fine to medium grained sand, silty sand, silty clay, sandy silt, and fine gravel. A significant portion of the formation was expected to be sand or silty sand.

The baseline report also described anticipated ground behavior and construction difficulties. The report included sections on saturated Colma Formation and drained Colma Formation to account for the earth pressure balance tunneling methods and open face or closed-face tunneling methods, respectively. Also included was a section on construction dewatering. The horizontal permeability of the ground was found to range from 3.5 to 6.0 x 10^{-3} cm/sec, and vertical permeability was assumed to be 10 times smaller than the horizontal permeability. The baseline report included a section on tunneling methods, stating that open-face shields were suitable, but only if used in conjunction with a rigorous dewatering plan. Closed-face shields were also recognized as suitable, but a non-pressurized closed face shield would require a rigorous dewatering plan. The stated preference, according to the baseline report, was a pressurized shield that could be used in conjunction with bolted and gasketed precast concrete segments. With the pressurized face it would not be necessary to dewater to the same extent required by either the open-face or non-pressurized shields.

Bidding

The bid documents for the Lake Merced transport tunnel were issued on February, 1991, and allowed prospective contractors to choose one of three excavation and support methods for the project:

- Method A – Open face shield or non-pressurized closed-face tunnel boring machine with "two-pass" cast-in-place final lining.
- Method B – Earth pressure balance tunnel boring machine with "one-pass" precast final lining.
- Method C - Open face shield or non-pressurized closed-face tunnel boring machine with "one-pass" precast final lining.

The contract was originally open for bid on February 6, 1991. Of the six bids received on that date, three specified the use of method A, two specified method B and one specified method C. The low bidder specified the use of method A. However, the original bids were not accepted because they did not adequately address contract-mandated minority participation issues, and the contract was rebid on May 29, 1991. All five of the bids received on that date specified method A. The low bidder was the joint venture of Shank/Torno at $20,050,000.

CONSTRUCTION

Notice to proceed was given on November 18, 1991. The open-face shield was designed and built by the contractor (Figure 3). The skin was rolled with 2.5 cm steel plate and included a 1.3 cm overcutter (a bead of metal around the shield so that the excavated hole is slightly larger than the shield).

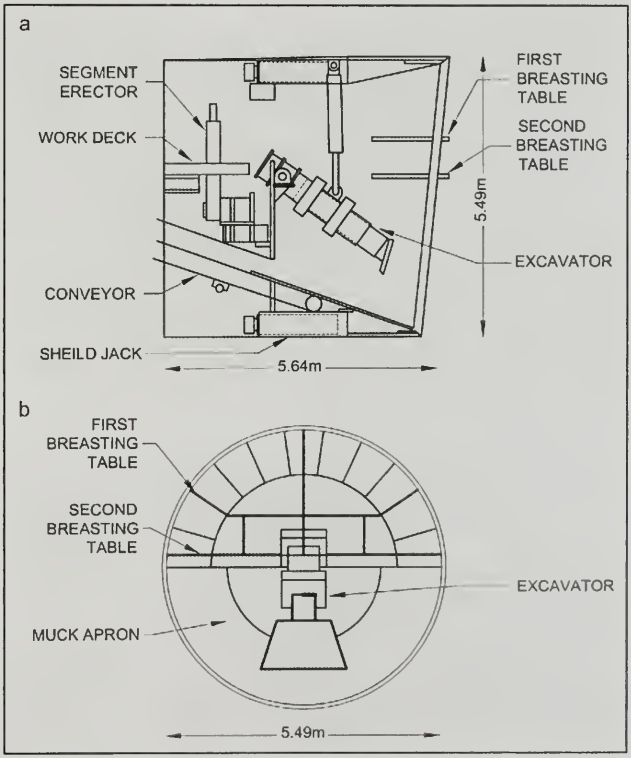

Figure 3. Digger shield tunnel boring machine. (a) Side view. (b) Front view.

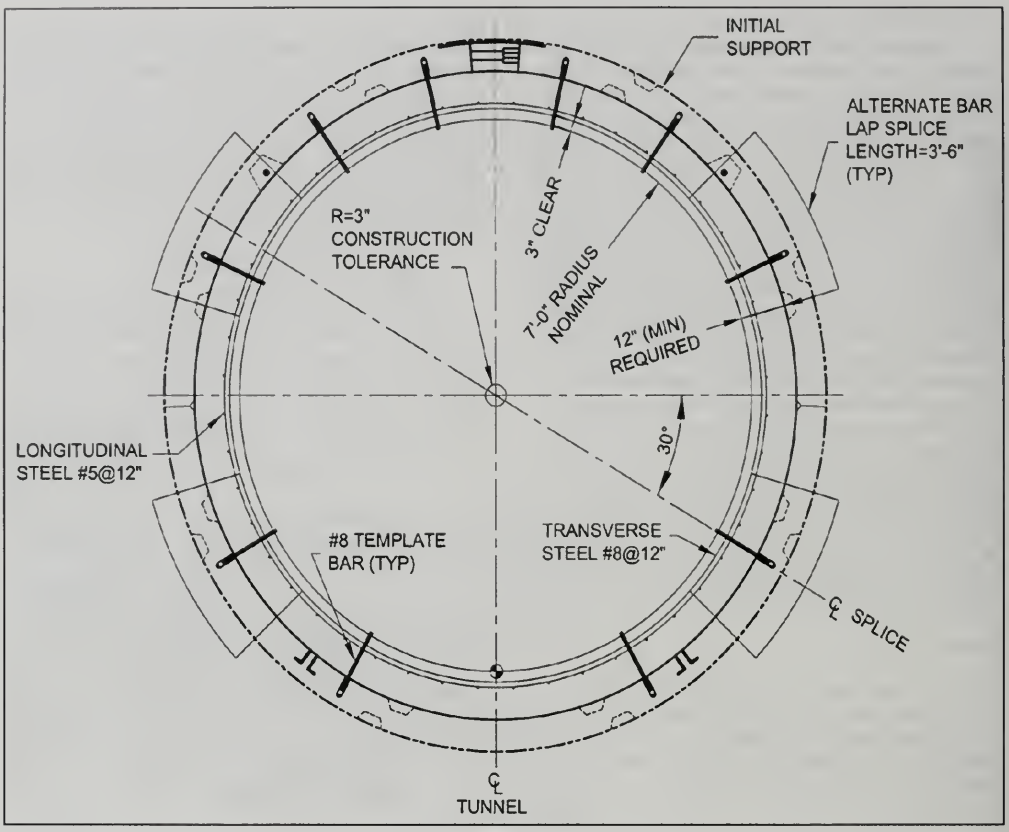

Figure 4. Cross-section view of precast concrete tunnel lining.

The shield had a total of 24 thrust cylinders with a push capacity of 145 metric tons each. The breasting table (a horizontal table within the shield for muck to pile up on) was made of 7.6 cm thick steel plate mounted 1.2 m above springline (vertical centerline of the shield). The excavator consisted of a steel paddle mounted on a sliding boom. A two-pass lining system was used with the initial lining consisting of 23-cm thick, precast concrete segments (Figure 4). The segments were erected in a four-section ring every 1.22 m. The segments had butt joints at invert (bottom of the ring) and springline and were expanded in the crown (top of the ring) by a pair of 27 metric ton jacks. Two pipe struts were installed in the crown following expansion of the ring. These precast segments were thinner than the one-pass segments in the design documents and did not require bolts and gaskets. The final lining consisted of cast-in-place concrete. The dewatering system consisted of 4 wells at both portals and 75 wells along the tunnel alignment, located at spacings ranging from 18 to 36 m.

Geologic conditions encountered

The contractor began construction of the 15.2-m diameter access shaft in February 1992 (Robison et al., 1993). Support for the shaft consisted of RZ 10 interlocking steel sheet piles driven around the perimeter to a depth of 15.2 m. Ring beams consisting of W10X60 steel sections were installed 0.5 m below surface and just above the crown of the starter tunnel at a depth of 6 m. Excavation of the shaft began in March 1992, and took 2 weeks to

reach a depth of 9.2 m. Work was interrupted in one section of the shaft, when a 6-m long by 4.5-m wide section of a ship's wooden hull was discovered. Archaeologists and maritime specialists from the National Park Service and the San Francisco Maritime Museum visited the construction site to assess the discovery. They determined that the ship was vintage 1860's. Two days after viewing the hull, the National Park Service gave permission to remove the hull section from the shaft and store it temporarily on the job site to be reburied when the shaft was backfilled at the end of the project.

Tunnel excavation

Following excavation of the shaft to 9.2 m, the contractor erected false sets (steel beam tunnel supports) within the shaft and then began excavation of the top heading of a 6-m long starter tunnel. Excavation support consisted of steel ribs and liner plate. Problems with running ground developed immediately, and it became obvious that the starter tunnel was being mined through beach/dune sand. The beach/dune sand was cohesionless and had negligible stand-up time. Timber spiles (horizontal poles driven ahead of the tunnel face) were required to complete the top heading of the starter tunnel. It was known that beach/dune sand existed along the tunnel alignment but not at this location.

Following completion of the top heading, the contractor excavated the shaft to its final depth of 12.2 m. The bottom bench of the starter tunnel was excavated and a bulkhead installed at the end of the starter tunnel. A receiving cradle was poured on the shaft bottom, and on April 8 the shield was lowered into the shaft.

On May 12, 1992, the contractor began excavation of the tunnel using a single mining shift. The contractor began by installing a false ring of segments in the shield and blocking the false ring across the shaft using pipe struts. After advancing 3.7 m, the shield was stopped for 2 days to add four additional pipe struts to prevent cracking of invert segments. Mining then continued to the 119-foot station and on May 22, a scheduled shutdown took place, to allow for installation of the trailing gear.

When mining resumed on June 4, 1992, the shield encountered a 41-cm diameter, cast iron pipe across the face at the 122-foot station. The pipe was apparently an abandoned saltwater intake to the old Fleishhacker Pool, located east of Great Highway. The crew removed the section of cast iron pipe in approximately 6 hours and mining resumed. On June 15, the contractor began mining with two 9-hour shifts.

Surface settlement in excess of 10 cm, along with several small surface voids, appeared on the southbound lanes of Great Highway. The small voids were grouted immediately upon discovery. Concern for ground loss, settlement, and steering of the shield led the contractor to stop on July 1, 1992 at the 598-foot station to install a second breasting table. The second breasting table was located below the initial breasting table at springline. At the same time, in an effort to lower the shove pressure on the shield and reduce cracking of the concrete segments, the contractor installed two air cannons in the muck apron. The second breasting table was effective in controlling the running ground condition. In addition, it reduced the ground load carried by the shield, which in combination with the air cannons significantly reduced the shove pressure on the machine and also significantly reduced cracking and spalling of the segments.

Although the shield was then mining with the face under control, it still had a strong tendency to dive in the beach/dune sand. Thus, the shield had to be operated "looking up", which resulted in plowing. This plowing resulted in a 10-cm deep settlement trough on the surface above the tunnel, although no more surface voids developed. This trough continued until a full face of Colma Formation was reached at the 1,811-foot station on July 16. On graveyard shift on July 21, at the 2,280-foot station, the shield encountered two abandoned sheet piles left from construction of the Southwest ocean outfall. From the 1,811-foot to the 4,180-foot stations, the tunnel was mined through Colma Formation. In the Colma Formation the shield was able to operate nearly level, which eliminated the plowing and reduced the surface settlement trough to 4 cm or less.

On August 4, at the 4,180-foot station, the tunnel again encountered loose, cohesionless dune sand. Again, control of the machine became difficult and the operator had to plow in order to keep the shield from diving. This zone of dune sand was encountered on the east side of the ridge along the Pacific coast, under Skyline Boulevard. In this zone, the settlement trough reached a depth of 18 cm, which led to cracking of the pavement parallel to the centerline of the tunnel.

On August 12, at the 4,946-foot station, the invert of the tunnel began seeping water. The water came from a perched lens developed in the dune sand on top of a clay layer located only 0.3 m below the invert. Because the dune sand had no cohesive strength, it washed into the bottom of the tail shield during the shove. This sand had to be removed to allow the segments to be installed.

The tunnellers encountered hard Colma Formation when they came out of the perched water section. Although the shield was able to run level and surface settlement again decreased to 4 cm or less, the hard Colma Formation caused some difficulties in mining. The second breasting table, which had been added to control running ground, was damaged in the hard Colma Formation, and the roll fins were also damaged. The contractor's progress through this section was delayed for repairs to the roll fins and the second breasting table.

One final unforeseen, non-geological problem developed during tunneling on John Muir Drive. When the shield reached the area adjacent to Oakwood Apartments, residents complained about noise and vibration, particularly throughout the night, when excavation was taking place on graveyard shift. Consequently, the City directed the contractor to limit mining to the hours of 6:00 a.m. to 10:00 p.m. After only one night of disturbance and one lost graveyard shift, the contractor changed his mining to day and swing shifts and no further complaints were received. On September 14, the shield holed-through at the 8,504-foot station into the recovery shaft at the overflow structure.

SUMMARY

Early in the project, all parties recognized that a portion of the tunnel would be driven through differing site conditions. The contractor proceeded with excavation of the starter tunnel and the beginning of shield mining. The contractor did not formally put the City on notice of the differing site condition until after shield mining had begun and it became obvious that the running condition of the beach/dune sand was impacting his operation. By this time, the City, the design engineer, and the construction manager had reviewed the geotechnical baseline report and already had several discussions about differing site conditions. All parties agreed that the dune sand/Colma Formation contact was extremely elusive to locate and it had not been identified accurately by the project engineering geologists in some locations along the tunnel alignment. The City responded to the contractor's notice by acknowledging that the material encountered in the tunnel was not Colma Formation. This acknowledgement by the City helped to prevent the letter-writing campaigns and the hard feelings that often develop between contractors and owners in such situations. As a result, the City and the contractor were able to negotiate an equitable settlement for the effects of differing site conditions and subsurface obstacles on the project.

The Lake Merced Transport was a successful tunneling project, due to cooperation among the contractor, the City, the design engineer, and the construction manager. Fortunately, the contract for the Lake Merced transport tunnel included a geotechnical baseline report. The baseline report was used effectively on this project as the baseline for evaluating differing site conditions. Through the cooperation described in this paper, the project was not significantly delayed, the contractor was compensated for his costs and delays in a timely manner, and the use of costly litigation for claims resolution was avoided.

ACKNOWLEDGEMENTS

The authors acknowledge the assistance received from the contractor, Shank/Torno J.V. and their supervising personnel Mike Shank, Jerry Stokes and Steve Wardwell; the designer, Parsons Brinckerhoff Quade & Douglas and their representative, Matt Fowler; the City and County of San Francisco's Department of Public Works Engineering and Construction Management staff, including James Chia; and the construction management personnel provided by Stone & Webster Engineering Corp., including Mike Robison and Dan McMaster, the Brierley & Lyman Division of Haley & Aldrich, Inc., and EPC Consultants, including Ben Townley and Rex Frobenius.

AUTHOR PROFILES

Lee W. Abramson is a geotechnical/tunnel engineer with extensive experience in various aspects of civil engineering in the United States and abroad. He has worked in the consulting and A/E fields as project manager, department head, deputy office manager, and regional manager for over 25 years. He has been a key participant in, or leader of, a variety of major engineering projects for transit systems, railroads, highways, water resource, and

other public infrastructure facilities. His direct responsibilities have covered all aspects of engineering including planning, analysis, design, rehabilitation, and inspection. The author of numerous articles and books, he has also assisted in the preparation of manuals on tunnel rehabilitation for the Underground Technology Research Council, shafts and tunnels in rock for the U. S. Army Corps of Engineers and on slope stability for the Federal Highway Administration. He also teaches continuing education short courses on tunnel and microtunnel construction, ground improvement, and slope stability for the American Society of Civil Engineers, University of Wisconsin - Madison, and the Colorado School of Mines.

Michael Kobler has over 20 years of experience in tunneling and underground construction as construction manager, resident engineer, cost estimator, scheduler, and consultant. He has worked on a variety of projects such as soft ground and hard rock tunnels and shafts, underground stations and powerhouses, and tunnel remediation. His extensive tunneling equipment experience includes NATM, cut and cover, tunnel boring machines, earth pressure balance machines, soft ground diggers, and drill and blast. He has experience in all aspects of construction management, including constructability evaluation, documentation of job progress, processing progress payments, negotiation of change orders, and contract administration.

SELECTED REFERENCES

Abramson, L. W. and Owyang, M. S., 1993, Lake Merced tunnel lining – Two-pass in shaky ground: *in* Bowerman, L. D. and Monsees, J. E. (eds.), Proceedings of the Rapid Excavation Tunneling Conference, (Boston, Massachusetts), Society for Mining, Metallurgy, and Exploration, p. 47-64.

ASCE (American Society of Civil Engineers), 1991, Avoiding and resolving disputes during construction: American Society of Civil Engineers, 82 p.

ASCE (American Society of Civil Engineers), 1997, Geotechnical baseline reports for underground construction: *in* Essex, R. J. (ed.), American Society of Civil Engineers, 40 p.

Mamak, A., Pickus, S., and Schmidt, B., 1990, Lake Merced transport: World Tunneling, v. 6, no. 2, June, p. 186-191.

Parsons Brinckerhoff, 1990, Lake Merced transport tunnel geotechnical design summary report: Consultant's report to the City of San Francisco Clean Water Program, p. 12-47.

Robison, M. J., Kobler, M. H., Cheung, J., and Chia, J., 1993, Lake Merced transport - Tunneling through a differing site condition: *in* Bowerman, L. D. and Monsees, J. E. (eds.), Proceedings of the Rapid Excavation Tunneling Conference, American Institute of Mining Engineers, (Boston, Massachusetts), p. 203 -221.


ENGINEERING
GEOLOGISTS

INFLUENCE OF GEOLOGY ON BART'S ORINDA STATION LANDSLIDE AND BERKELEY HILLS TUNNELS

J. DAVID ROGERS[1]

ABSTRACT

This article describes various geologic challenges faced in the design, construction and ongoing maintenance of BART's 3.1 mile long Berkeley Hills twin tunnels, along the Contra Costa line, between the Rockridge and Orinda stations. These challenges included: (1) dealing with the unexpected failure of a highway cut, which recurred between 1966 and 1983; (2) how the geologic conditions of the tunnel alignment were characterized; (3) a debate that erupted regarding the average rate of aseismic creep along the Hayward fault, and (4) how this might be accommodated in the tunnel's operational life span. Placement of timber ties to enable track shifting, and continual monitoring have been employed to mitigate ongoing right-lateral offset, which has averaged about 5.5 mm/year since the tunnel's completion in 1968. Post-construction evaluations carried out between 1979 and 1981 concluded that the Berkeley Hills tunnels are able to accommodate active creep because the offset is distributed across a 220-foot wide fault zone, and the tunnel's stiff concrete-filled inverts help spread the imposed deflection over an even greater distance.

[1]Department of Geological Engineering
129 McNutt Hall
University of Missouri-Rolla
Rolla, MO 65409-0230
jdrogers@umr.edu

INTRODUCTION

The greatest engineering challenge along BART's Contra Costa line was the excavation of the 3.1-mile long Berkeley Hills Tunnels, between the Rockridge and Orinda stations (Figure 1). The tunnels cross the active Hayward fault a short distance from their west portals, whereas the dormant Moraga thrust cuts across the line a few yards beyond the east portals, at Orinda station. At the time the tunnels were designed (1964), scant reliable information was available about rates of aseismic creep along the Hayward fault, even though it offset Berkeley's Memorial Stadium, built in 1923. Between Orinda and Walnut Creek the BART alignment was placed within a newly-created median of State Highway 24, allowing easy freeway access to all the Contra Costa stations. Several geologic surprises found during construction have required continual monitoring and maintenance.

ORINDA BART STATION LANDSLIDE

An integral part of BART's original plan was to incorporate their 90-foot wide right-of-way within the median of State Highway 24 through central Contra Costa County, between Orinda and Walnut Creek. Approximately eight million cubic yards of earth was moved to create this dual transit corridor, with BART financing relocation of the existing westbound freeway lanes and their own facilities, whereas the State paid for enlarging the freeway from 8 to 10 lanes. All the excavation and structural improvements in this segment were managed by the highway department, and a maximum grade of 3.5% was maintained, per BART requirements (Payne et al., 1968).

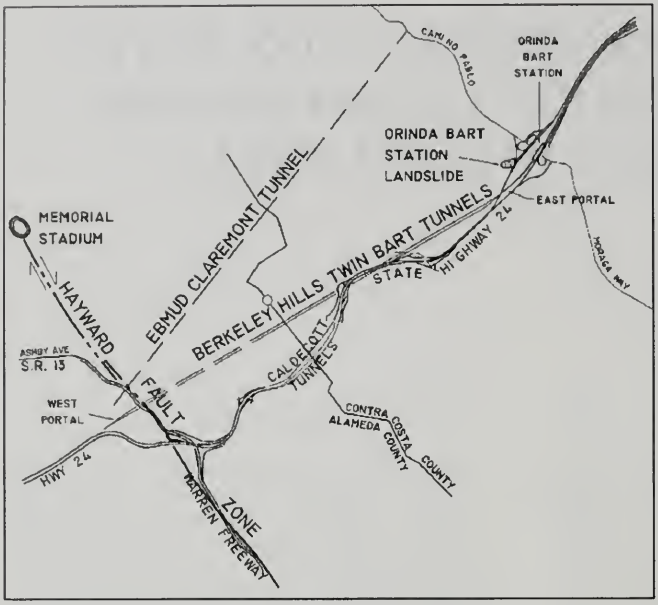

Figure 1. Vicinity map of the BART Berkeley Hills tunnels and Orinda BART station landslide, along State Route 24.

In June 1966 excavation began on a circuitous westbound alignment for Highway 24 in Orinda to create a staging area for the 3-mile long Berkeley-Oakland Hills tunnel, which was subsequently transformed into the Orinda station. By September a sizable portion of the natural hillside northwest of the staging area had been excavated at an inclination of 1.5:1. The hillside above this new cut slope began to detach and slide toward the new freeway alignment and the tunnel staging area.

During 1967-68 the State Division of Highways was forced to mitigate the slide, with BART paying the cost. A grading solution was chosen, laying the base of the slope (in the Mulholland Formation) back to a 3:1 inclination, then transitioning to a 2:1 cut in the overlying Grizzly Peak (Moraga) volcanics, exposed above the Moraga fault (Case, 1963). Groundwater flowing through the pervious volcanic rocks became perched against the fault, and the units below the fault are dragged, causing them to dip toward the BART station (out of slope), as shown in Figure 2. This creates a situation whereby high pore water pressures are developed in the hillside. The Moraga fault is believed to be an ancillary thrust, connected to the Hayward fault at depth (Borchardt and Rogers, 1991).

Although this "repair" cost BART just under $35,000, the new cut slope began to develop large tension cracks in the winter of 1972-73. An extreme frost hit the hills of the East Bay during the winter of 1972-73, followed by a heavy storm sequence during the last week of January, which caused numerous slide problems throughout the San Francisco Bay area. The 1967 cut slope began to slide onto the westbound on-ramp of Highway 24, adjacent to the Orinda BART station. A large tension crack developed in the Grizzly Peak (Moraga) volcanics, up above the Moraga thrust.

A record two-year drought occurred between 1975 and 1977. In early February 1978 the rains returned. On February 12, approximately 100,000 cubic yards of bedrock material mobilized and began to creep down onto the westbound on-ramp of Highway 24 (Figure 3). Under their original agreement, BART was obliged to reimburse Caltrans for any slope failures that occurred within 10 years of BART-related freeway realignments, but this clock had ticked its course by 1976. In 1980 Caltrans spent $500,000 to repair the 1978 slide. This repair experienced some reactivation during the winter of 1982-83, but did not encroach on the freeway. It has been relatively quiescent since.

GEOLOGY OF THE BERKELEY HILLS TUNNELS

Geologic mapping of the Berkeley Hills commenced in the 1890's under the tutelage of U.C. Berkeley Professor Andrew Lawson (Lawson and Palache, 1902). In Lawson's San Francisco Folio, released in 1914, the Hayward fault was formally recognized as existing, but not traced across the base of the East Bay Hills. During construction of Berkeley's Memorial Stadium in 1922, Buwalda (1929) tentatively identified the Hayward fault in four exploratory trenches, and summarized the evidenced for right lateral offset and formation of a shutter ridge across the mouth of Strawberry Creek.

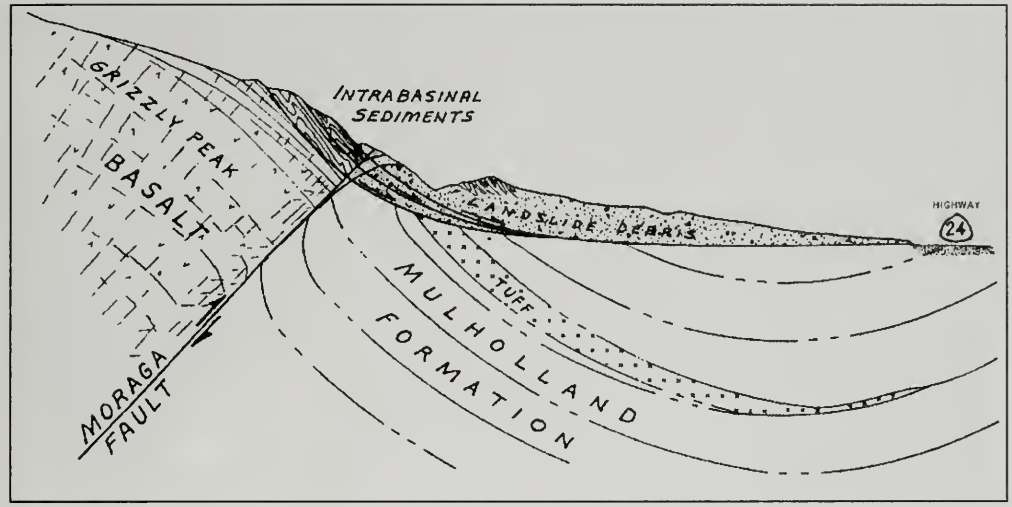

Figure 2. Geologic cross-section through the February 1978 Orinda BART station slide (from Rogers, 1979).

Shortly thereafter, Russell (1926) recognized horizontal offsets along the newly discovered fault further south. Subsurface mapping of the Berkeley Hills was initially undertaken during construction of East Bay Municipal Utility District's (EBMUD) Claremont water supply tunnel (1929), San Pablo water tunnel (1952) and the Caldecott tunnels (1930-38 and 1960-62). The geologic conditions encountered in these tunnels were described by Hulin (1926), Hall (1928), Young (1929), Louderback (1929, 1930), Page (1950), EBMUD, (1951), Bowen (1951), Radbruch (1964), and Blanchard and Laverty (1966). The west portal of EBMUD's Claremont tunnel is located about 500 feet northwest of the BART west portal.

Bechtel Corporation was given charge of carrying out the geologic exploration and design of the Berkeley Hills BART tunnels in 1963-64. The proposed alignment was 3.1 miles, between Lake Temescal and Orinda (Figure 4). Bechtel drilled 5,000 feet of NX diamond core in 32 exploratory borings along the proposed alignment, with depths up to 600 feet. Several of the holes were inclined to penetrate greater depths through inclined strata (Figure 4).

From their west portal, the twin tunnels pierce undifferentiated Franciscan assemblage rocks, the Hayward fault, Leona Rhyolite, undifferentiated Great Valley Sequence (Cretaceous age) sediments, the Sobrante and Claremont shale/chert members of the Monterey Formation, Orinda Formation conglomerate, siltstone and claystone, Grizzly Peak volcanic series, intrabasinal sediments, back into volcanics. Siesta Formation basinal lacustrine silts and clays lie within a faulted (Lawson's old "Pinole fault") syncline, whose axis crossed the tunnels near station 126, about 12,600 feet east of the west portal. The tunnels then intersect southwest-dipping Grizzly Peak volcanics and sediments, passing into finer grained Orinda Formation units caught in the axis of a tightly folded anticline (crossing the tunnel near station 156). The balance of the alignment then crosses the northeast-dipping limb of the anticline, cutting through Grizzly Peak volcanics and intrabasinal sediments at the east portal (Figure 4). A series of secondary faults truncate many of the units, approaching both portals. The tunnel cuts the dominant N40W strike of the structure at about 45 degrees.

The tunnels cross the Hayward fault zone about 900 feet in from their west portals, the Wildcat fault zone about 5,500 feet east of the west portal, Lawson's old Pinole fault (in Gateway Valley) about 12,600 feet east of the west portal, and several unnamed faults. The Moraga thrust appears to crease the tunnel's Orinda portal, and was not

Figure 3. Aerial oblique view of the 1978 Orinda BART station landslide, adjacent to the westbound lanes of State Highway 24, just west of Orinda Crossroads. The Orinda BART parking lot is seen at lower left. It cost Caltrans $550,000 to have this slide repaired in 1980.

mapped as part of the study. Succinct discussions of the tectonic evolution of the central Berkeley Hills were subsequently presented in Graham et al. (1984) and Buising (1996), among others.

DESIGN OF THE TUNNELS

The parallel tunnels were to be 3.1 miles long, on an overall 1.2% uphill grade proceeding northeasterly (rising at 2% to the tunnel mid-point, then

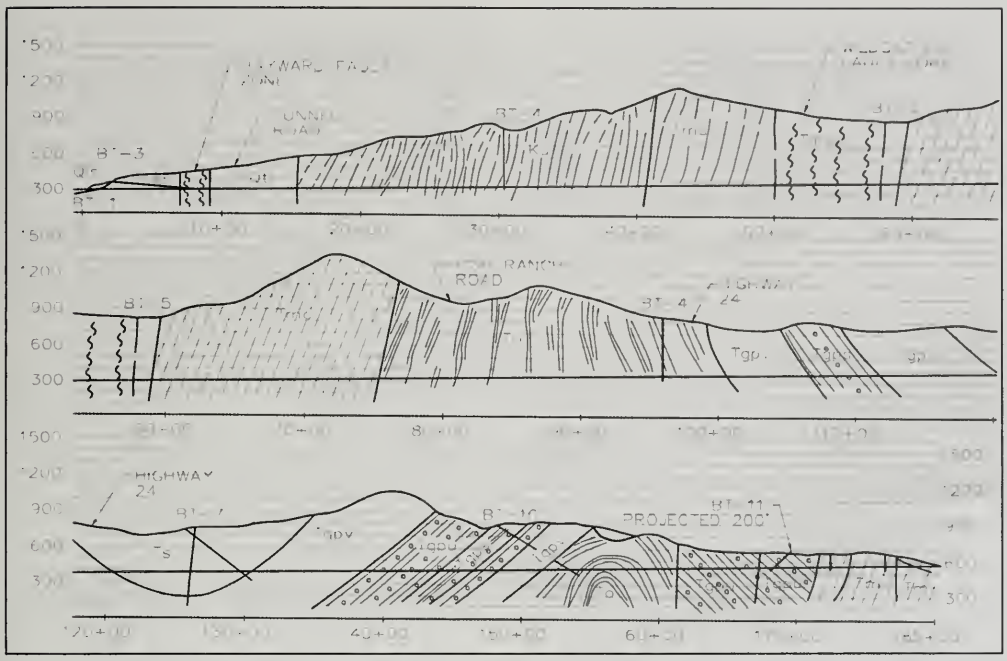

Figure 4. Geologic profile along the 3.1-mile long Berkeley Hills tunnel, which intercepts the Hayward fault about 700 feet in from the west portal. The tunnel was not designed for tectonic offset, but tracks have been continuously adjusted through the fault zone.

at +0.3 % grade to the east portal). Trending N61E, the tunnels cut the predominant strike of the folded late Tertiary strata at about 45 degrees. Nineteen load zones within prescribed segments of the tunnels were identified along the tunnel alignments, on the basis of the geologic units encountered in the exploration. Each of these were assigned a Terzaghi load factor, according to Proctor and White (1946), and different loads were estimated for the temporary sets and the permanent lining.

The BART Board of Consultants considered the Terzaghi (1946) load values to be overly conservative, and suggested lower loads could be utilized for design of the steel support sets. Bechtel engineers incorporated the load assumptions prescribed by Drucker (1943), who derived load equations from lateral passive soil pressures for cast iron-lined tunnels in soft clay. Assumed values for rock compressibility were then derived for the nineteen load zones; the resulting pressures were 30 psf acting vertically and 18 psf acting horizontally. These design assumptions were summarized in Brown et al. (1981).

The tunnels were intended to be excavated at a diameter of approximately19 feet, with an average overreach of 1.5 feet. One hundred feet of rock was to be left between the two bores, with cross cuts every 1,000 feet. The spacing between tunnels narrowed to 55 feet at each portal. The bores were braced with 8-inch WF40 steel horseshoe-shaped sets, spaced on 4-foot centers with invert struts, dropping to 2-foot centers within the Hayward fault zone (between stations 650 and 1300). Inside this bracing, the finish tunnels were lined with at least 1.75 feet of reinforced concrete, using the modified circular section shown in Figure 5. The finished inside diameter was 17.5 feet.

Because of the anticipated high loads, the completed tunnels were to be circular, formed within the excavated horseshoe-shaped section. The inside

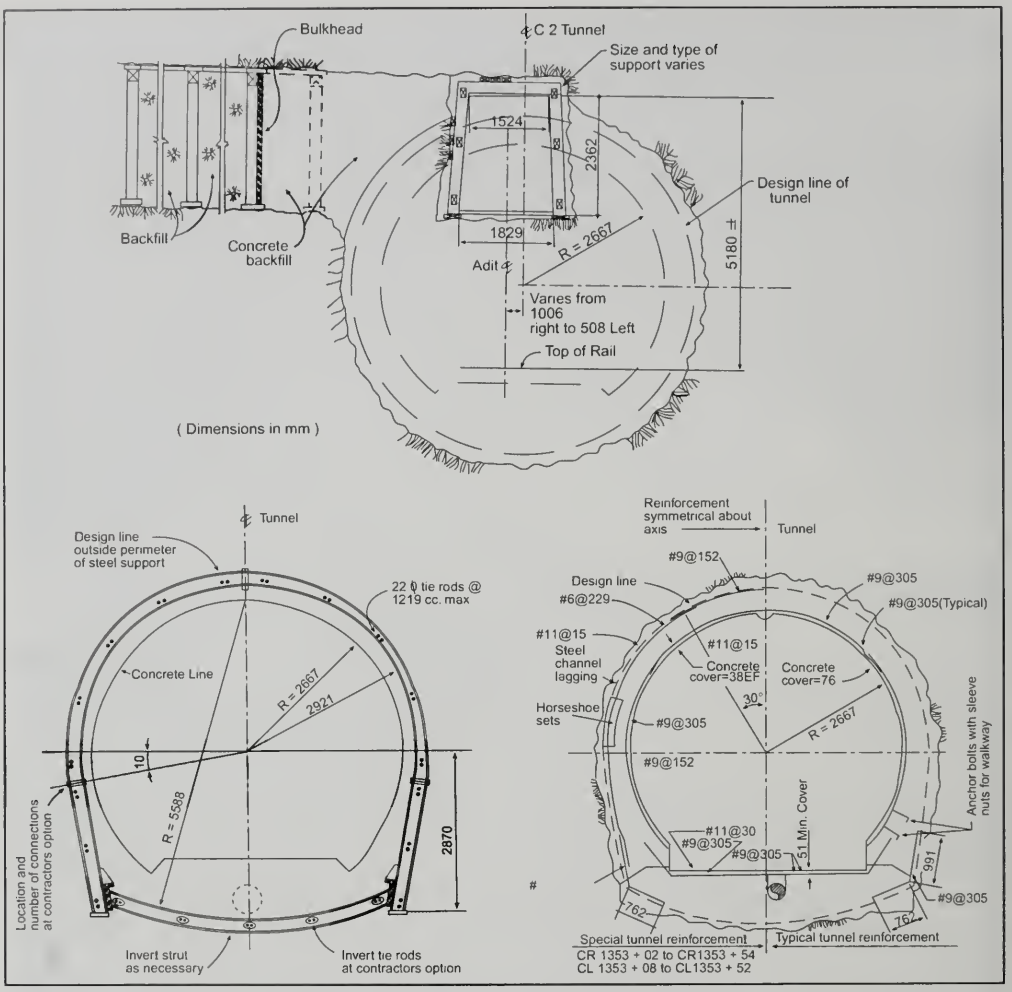

Figure 5. Comparative cross sections of the Berkeley Hills tunnels at various stages of construction, taken from Brown et al. (1981). The upper section shows the position of the exploratory adit excavated into the north tunnel, through the Hayward fault.

radius of the finished tunnels was 3 inches greater than the "standard" circular tunnels used on BART, due to uncertainties at the time about the final configuration of the BART cars. In order to retain flexibility, an 18-inch thick lining was prescribed, with extensive subdrainage. This was felt to be as thin a lining as practicable.

IN SITU TESTING

After the preliminary design values described above were agreed upon, *in situ* tests were carried out inside two 5 x 7 foot exploratory adits excavated between May and September 1964. The east adit was 1,000 feet long whereas the west one extended 1,412 feet, across the Hayward fault zone. The west

adit encountered 700 feet of fault gouge and crushed rock, mostly serpentine, 220 feet of which was thereafter termed the "Hayward fault zone" (Bechtel, 1964; Content, 1967; Brown et al., 1981). *In situ* strength and indices tests were performed in both adits, to gain an appreciation of the ground loads. Load cells were also placed in the west exploratory adit to help estimate the loads that might require support through the Hayward fault zone (load problems had plagued the nearby water supply tunnels, described by West, 1965). The load cells were installed between the rock and the tunnel supports, along with several extensometers.

The collected data suggested that within the Franciscan Formation, a relaxation zone developed within 10 feet of the 5 x 7 foot adit. Fifty to 75% of the movement occurred within 3 feet of the opening, and loads tended to stabilize within 5 to 20 days after initial excavation. However, within the Hayward fault zone, only about 25% of the movement was detected within 3 feet of the opening; the remainder of the volumetric relaxation occurring between 3 and 10 feet, and possibly further. About a quarter of the rock movement was observed to occur within 12 days of excavation, followed by a reduced rate of change.

CONSTRUCTION

Construction began in early February 1965 and the tunnels were holed through in March 1967. Construction was completed in July 1968. The tunnels were driven using conventional drill-and-blast methods, with a full face, pulling blast rounds four feet deep. They excavated the two bores simultaneously with offset, working four headings (two from each end). The contractors used a jumbo rig to drill the face, then placed conventional steel sets with maximum spacing 4 feet on center. The average rate of advance was about 19 feet per day, per heading.

Numerous springs and seeps were monitored within both test adits, as well as within the exploratory borings. Standpipe measurements in the borings suggested that as much as 850 feet potential hydraulic pressure head (equating to 368 psi) might be expected over the tunnels near the drainage divide (near station 72+50). In order to effect gravity drainage from the four working faces, the bid design was altered during construction to provide a 1.75% grade westerly, to a high point 5,100 feet from the east portals. From this drainage divide a 0.3% grade was maintained eastward, toward the east portals.

Tunnel alignments were maintained using newly developed laser survey methods (Colson, 1970). For bid purposes, the potential water inflow was estimated to be as much as 6,000 gallons per minute (gpm) initially, diminishing to about 2,000. The actual inflow during construction was about 650 gpm at both portals. Maximum inflow at the face occurred when the bores penetrated a Grizzly Peak basaltic flow breccia, where inflows reached 300 gpm. In general, seepage decreased as the headings advanced.

SQUEEZING GROUND

When the face of the north bore reached the Hayward fault, near station 1203+75 (in October 1965), cross-tunnel measurements indicated that the ground was squeezing inward at a rate of 1 inch per day for a distance extending 180 feet back from the face. Eight-foot long rockbolts were installed horizontally at the base of each post, with channel whaler anchors connecting each bolt. Excavation was halted and 6 x 8-inch timber floor spreaders were installed at each post extending 300 feet behind the face. The invert (tunnel floor) was then deepened by 2 feet, and 8-inch WF40 steel invert struts were installed to transfer load across the opening. Set spacings across the fault zones were decreased to 2 feet instead of the usual 4 feet. These efforts were described in Ayers (1969). Invert struts were placed in the Hayward and Wildcat fault zones, and within the faulted (and overturned) Siesta syncline (near station 125+80). Because of difficulties in maintaining support during construction, the arch of the finished tunnel was lowered by 2 inches within the Hayward fault zone.

Bechtel engineers noticed that the squeezing generally decreased over a period of one to two months. The squeezing was noted again during re-timbering and realigning of sets in preparation for placing the interior concrete lining. Of the 11,101 steel sets installed in the two bores, 1,597 experienced deformations that necessitated replacement or realignment. After holing through, the contractor began placing invert concrete in June 1967 and concreting of the arches commenced in December, using telescoping slip forms.

ASEISMIC CREEP OF THE HAYWARD FAULT

During design, considerable foresight and attention were drawn to the appropriate accommodation of loads that might be generated within the Hay-

ward fault zone. Bechtel geologists recognized that the fault had spawned earthquakes in 1836 and 1868, but made no mention of aseismic creep, which had been widely observed along the south side of Memorial Stadium at U.C. Berkeley, 1.25 miles from the west portal (a June 1836 quake on the northern Hayward fault was subsequently disproved by Toppozada and Borchardt, 1998) . Berkeley seismologists had been measuring aseismic creep-induced offset of a buried concrete culvert beneath Cal Memorial Stadium since mid-May 1964, but this data was not published until mid-1966, after the tunnels had been designed (Bolt and Marion, 1966).

Something of a public debate erupted on September 29, 1965 when the U.S. Geological Survey (USGS) issued a press release describing the potential for damage to structures situated along the Hayward fault, citing ongoing creep being measured along the fault, particularly at Berkeley's Memorial Stadium. On October 7 the USGS and UC Berkeley cooperatively installed a slip-meter within the 1922 concrete culvert beneath Memorial Stadium.

In mid 1966 the USGS released Circular 525, which contained five articles detailing various aspects of aseismic creep measured along the Hayward fault. In this publication, Radbruch and Lennert (1966) described the fault-induced offset they observed in June 1965 while inspecting two reinforced concrete culverts beneath and adjacent to Memorial Stadium. The oldest culvert, across Strawberry Creek, had been inspected about every ten years since being built in 1923. They noted tensile displacements correlating to an average creep rate of about 2.8 mm/year. Unfortunately, the Strawberry Creek culvert crosses the fault at an acute angle (about 20 degrees), which greatly complicates resolution of offset measurements that must be inferred from tensile separations at various joints. Several years later, Schultz (1989) noted that the Strawberry Creek creepmeter missed the active trace of the Hayward fault, and that the Stadium had actually been offset by 13 inches of aseismic creep, which would correlate to an average rate of about 5 mm/yr.

Also in Circular 525, Blanchard and Laverty (1966) reported their measurements of tectonic offset in EBMUD's Claremont tunnel, completed in 1929. They reported an average offset of 4.8 mm/year. In 1966 NOAA established a survey network at Memorial Stadium, which recorded an average creep rate of 5 mm/year between 1966-69 (Miller, 1970). These measurements were recognized to be lower bounds thresholds because the fault actually bifurcates beneath Memorial Stadium, widening northward.

BART could not ignore these indications of ongoing aseismic creep because they were made only 500 feet northwest of the BART portals.

TRACK SHIFTING TO ACCOMMODATE ASEISMIC CREEP

As the tunnels were being excavated, BART was forced to deal with the issue of accommodating active creep, even though construction contracts had been let two years earlier. The construction team felt they could accommodate creep offset through the Hayward fault by placing wood ties across the fault zone and periodically shifting the tracks. The tunnel diameter of 17.5 feet was half a foot greater than the standard diameter used throughout the BART system (Figure 5). Based on information gleaned from the October 1868 Hayward earthquake, designers had assumed 24 inches of horizontal and 12 inches of vertical movement along the Hayward fault (surface offset during the October 21, 1868 earthquake was restricted to an area south of the BART tunnels). If such offset were to occur along a single discrete surface, the tunnel's radius would need to be increased by 10 inches to accommodate track shifting. However, if such movement was distributed over the 300-foot width of the Hayward fault zone, 53 inches of horizontal movement could be accommodated within the 17.5-foot diameter of each tunnel.

In October 1966 a change order was issued allowing for the installation of load cells and extensometers at 16 locations in the north tunnel, between stations 1218+86 and 1254+25, across the Hayward fault zone. By February 1967 a total of 75 load cells were installed, 4 to 6 at each location, located at the 10 and 2 o'clock positions in the crown, between the rock and the interior concrete lining. These load cells were recorded at regular intervals until the steel sets were reblocked, just prior to placement of the concrete lining in March 1967. Three sets of cells were left in place for after-construction monitoring. In addition, sixteen 30-foot long and four 10-foot long extensometers were installed horizontally at the springline in the north bore through the Hayward fault zone, between stations 1198 and 1206+50 (BART, 1977).

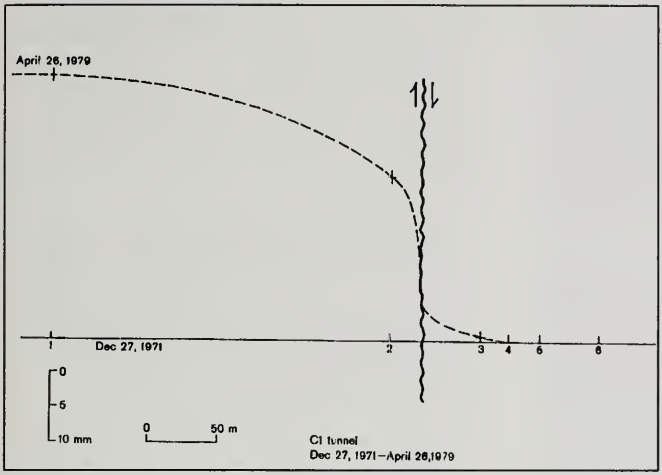

Figure 6. Aseismic creep along the Hayward fault, as measured in the south (C1) BART tunnel, between December 1971 and April 1979 (from Brown et al., 1981).

SUMMARY AND CONCLUSIONS

BART has carried out careful alignment surveys of the tunnels since their completion in 1968. Curious results recorded over the first few years caused speculations about the source of apparent surveying errors, or drift. As a result, extensometer measurements were resumed in the Hayward fault zone, and a program of horizontal alignment surveys was established in December 1971. This was continued throughout the succeeding decade. Between 1969 and 1981, an approximately 80 mm of right-lateral offset was conclusively recorded in the north tunnel, as shown in Figure 6. The average rate of creep was between 6 and 8 mm/year between 1971 and 1980 (Brown et al., 1981), distributed along a 220-foot wide zone. By 1979, the lining of the tunnels exhibited considerable cracking, with a thrust component, as sketched in Figure 7.

An extensive study of the BART tunnels through the Hayward fault was commissioned by BART and the Federal Urban Mass Transit Administration between 1979 and 1981. Brown et al. (1981) summarized the results of the study, and found that several of the load cells were still operable and indicated increased passive pressures on the northwest side of the fault, with decreased active pressures on the south. These readings were consistent with right-lateral strike-slip movement. Most of the displacement was confined within the gouge zone mapped during construction. The 1981 federal study recommended that BART continue to monitor damage to their linings and make periodic adjustments to the tracks.

The evaluation stopped short of predicting how much future realignment could be accommodated because that depends on the structural reaction of the tunnels, which behave as large reinforced concrete pipes, subject to massive lateral shear. If the imposed strain is spread over a wide zone, the tunnels could handle considerable offset. The thick concrete invert of both tunnels (lower half of Figure 5) serves to spread the imposed deformation over a slightly wider zone and, thereby, dissipate the shear strain.

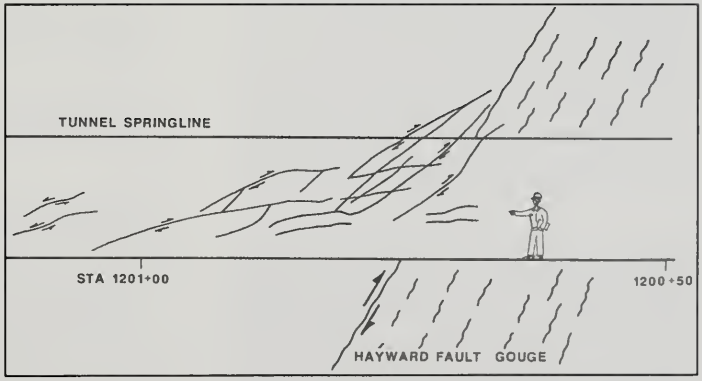

Figure 7. Fracture pattern in concrete lining of the south BART tunnel where it crosses the Hayward fault (as mapped in 1979). The low-angle fractures are suggestive of axial compression within the Berkeley Hills tectonic block (from Rogers, 1986).

After a decade of anticipation, the Contra Costa line through the Berkeley Hills Tunnels opened in February 1973. More extensive evaluations of aseismic creep and microseismicity along the Hayward fault were undertaken after completion of the Berkeley Hills tunnels, including those of Radbruch (1967, 1974), Herd (1978), Smith (1980), Brown et al. (1981), Prescott and Lisowski (1982), Taylor et al. (1982, 1992), Steinbrugge et al. (1987), Lienkaemper et al. (1991), and Lienkaemper (1992).

BART has never experienced any serious problems with train operations across the Hayward fault because the offset is accommodated across a 220-foot wide zone. BART has continued to monitor aseismic displacement of the tunnels across the fault using their in-house surveying staff. Lienkaemper et al. (1991) has reported an historic creep rate of 5.5 $\pm$ 0.5 mm/year in the vicinity of the BART tunnels. This correlates well with the rate of creep being recorded at Berkeley's Memorial Stadium. BART maintenance crews adjust the tracks about once per year.

ACKNOWLEDGEMENTS

The writer is indebted to conversations with many individuals regarding their roles in the BART station landslide, Berkeley Hills tunnels, and the Hayward fault. These include Glenn Borchardt, Earl E. Brabb, Tor L. Brekke, Ian R. Brown, James E. Case, Chuck Content, Garniss Curtis, David G. Heyes, John Lisenko, the late Benjamin M. Page, Dorothy H. Radbruch, Ed Searby, Harry Sutcliffe, Joan Van Velsor, J. Ross Wagner, and John L. Walkinshaw. Tor Brekke provided copies of all the original reports for construction of the BART tunnels. Dave Heyes provided copies of geotechnical information on the BART station landslide. Chuck Taylor, Steve Klein, Victor Romero, Steve Stryker and Bob Anderson kindly reviewed the manuscript and provided helpful suggestions.

SELECTED REFERENCES

Ayres, M.O., 1969, Case history – Berkeley Hills twin transit tunnels: Proceedings of the Second Symposium on Rapid Excavation, (Sacramento, California), p. 10-26 –10-37.

BART, 1977, BART Berkeley Hills tunnel instrumentation results and interpretations, Hayward fault zone: Unpublished report, BART Design Division, Department of Design and Construction, Bay Area Rapid Transit District, Oakland, 48 p.

Bechtel Corporation, 1964, Engineering geology of the proposed Rapid Transit Berkeley tunnels: Consultant's report to BART, June, 16 p., 2 pl.

Bechtel Corporation, 1965, Engineering geology of the Berkeley Hills tunnel, central Costa Costa line: Consultant's report to BART, 31 p., 6 pl.

Blanchard, F.B. and Laverty, C.L., 1966, Cracks in the Claremont water tunnel: U.S. Geological Survey Circular 525, p. 6.

Bolt, B.A. and Marion, W.C., 1966, Instrumental measurement of slippage on the Hayward fault: Bulletin of the Seismological Society of America, v. 56, no.2, p. 305-316.

Borchardt, G. and Rogers, J.D., 1991, Earthquake potential along the Hayward fault, California: Proceedings Second International Conference on Recent Advances in Geotechnical Earthquake Engineering and Soil Dynamics, St. Louis, March 11-15, 1991, Vol. 3, p. 2,309-2,321.

Bowen, O.E., 1951, Highways and byways of particular geologic interest: in Geologic Guidebook of the S.F. Bay Counties, California Division of Mines and Geology Bulletin 154, p. 315-379 (includes cross-section through Berkeley Hills on p. 345).

Brown, I.R., Brekke, T.L. and Korbin, G.E., 1981, Behavior of the Bay Area Rapid Transit tunnels through the Hayward fault: U.S. Department of Transportation, Urban Mass Transit Administration, Report No. UMTA-CA-06-0120-81-1, 208 p.

Buising, A.V. (ed.), 1996, Neogene paleogeographies in the greater San Francisco Bay area, 10 Ma contraction-corrected: Northern California Geological Society Field Trip Guidebook (May 4, 1996), 71 p.

Buwalda, J.P., 1929, Nature of late movements on the Hayward rift, Central California: Bulletin of the Seismological Society of America, v. 19, no. 4 (December), p. 187-199.

Case, J.E., 1963, Geology of a portion of the Berkeley and San Leandro Hills, California: Ph.D. thesis, Dept. of Geology and Geophysics, University of California, Berkeley, 216 p., 3 pl.

Chandler, R.R., 1969, Field trip 4 - Bay Area Rapid Transit system: Field Trips, National Meeting, Association of Engineering Geologists, San Francisco, October 21-25, p. D-1 – D-7.

Colson, G.P., 1970, Control of tunneling machines by "TunneLaser" system: Civil Engineering, ASCE, v. 40, no. 2 (February), p. 55-57.

Content, C., 1967, Berkeley Hills tunnel holes through: The Engineering Geologist, Engineering Geology Division, Geological Society of America, v. 2, nos. 3/4 (July,October), p. 8-9.

Drucker, M.A., 1943, Determination of lateral passive soil pressure and its effect on tunnel stresses: Journal of the Franklin Institute, v. 235, no. 5, p. 499-512

EBMUD (East Bay Municipal Utility District), 1951, Geological section along San Pablo tunnel: East Bay Municipal

Utility District, Oakland, Dwg. No. 235-P, dated Jan 29, 1951, scale 1:3,222.

ENR (Engineering News Record), 1969, Transit tunnel runs obstacle course: ENR, McGraw-Hill, v.183, no. 1 (July 3, 1969), p. 22-23.

ENR (Engineering News Record), 1969, BART tracks spur new methods: ENR, McGraw-Hill, v.183, no. 17 (October 23, 1969), p. 28-29.

Graham, S.A., McCloy, C., Hitzman, M., Ward, R., and Turner, R., 1984, Basin evolution during change from convergent to transform continental margin in central California: American Association of Petroleum Geologists Bulletin, v. 68, p. 233-249.

Hall, L.S., 1928, Preliminary report on springs in the vicinity of the Claremont tunnel: Consultant's report to EBMUD, dated Nov. 16, 1928, 16 p., with appendices.

Herd, D.G., 1978, Map of Quaternary faulting along Hayward fault zone: U.S. Geological Survey Open File Report 78-308.

Hulin, C.D., 1926, Geologic cross section of the Claremont tunnel: EBMUD Dwg. DH 2120-35, Oakland, scale 1: 4,800.

Lawson, A.C., and Palache, C., 1902, The Berkeley Hills: A detail of Coast Range geology: Bulletin of the Department of Geology, University of California, v. 2, no. 12, p. 349-450, plate 1:12,000.

Lawson, A.C., et al., 1914, Description of the San Francisco district; Tamalpais, San Francisco, Concord, San Mateo, and Hayward [15-minute] quadrangles: U.S. Geological Survey Geologic Atlas, Folio 193, 24 p., 5 pl.

Lienkaemper, J.J., Borchardt, G., and Lisowski, M., 1991, Historic creep rate and potential for seismic slip along the Hayward fault, California: Journal of Geophysical Research, v. 96, no. B11, p. 18,261-18,283.

Lienkaemper, J.J., 1992, Map of recently active traces of the Hayward Fault, Alameda and Contra Costa Counties, California: U.S. Geological Survey Miscellaneous Field Studies Map MF-2196.

Louderback, G.D., 1929, Seepage in the Claremont tunnel: Consultant's report to EBMUD, dated Mar. 11, 1929, includes geologic cross sections on EBMUD Dwg. DH 2179-1A.

Louderback, G.D., 1930, Preliminary report on the geological conditions along the line of the proposed highway tunnel between Alameda and Contra Costa Counties: Consultant's report to Joint Highway District #13, July 7, 1930, 7 p., 1 pl., scale 1:1200.

Miller, R.W., 1970, Results of triangulation for earth movement study, vicinity of Berkeley, El Cerrito, and Fremont, California: U.S. Department of Commerce, National Ocean Survey Report Supplement No. 1.

Page, B.M., 1950, Geology of the Broadway tunnel, Berkeley Hills, California: Economic Geology, v. 45, no. 2 (March-April), p. 142-166.

Payne, H.L., Russell, W.W., and Pacheco, W.A., 1968, Freeway and rapid transit share corridor: Civil Engineering, ASCE, v. 38, no. 5 (May), p. 38-41.

Prescott, W.H., and Lisowski, M., 1982, Deformation along the Hayward and Calaveras faults: Steady aseismic slip or strain accumulation: in Hart, Hirschfeld and Schulz (eds.), Proc. Earthquake Hazards Eastern S.F. Bay Area: California Division of Mines and Geology Special Publication 62, p. 231-237.

Proctor, R.V., and White, T.L., 1946, Rock tunneling with steel supports: Youngstown Printing Co., (Youngstown, Ohio), 291 p.

Radbruch, D.H., 1964, Log for field trip through Caldecott tunnel: U.S. Geological Survey Open File Report (for A.E.G. field trip, Mar. 30, 1963), 3 p.

Radbruch, D.H., 1967, Approximate location of fault traces and historic surface ruptures within the Hayward fault zone between San Pablo and Warm Springs, California: U.S. Geological Survey Miscellaneous Geologic Investigations Map I-522.

Radbruch, D.H., 1969, Areal and engineering geology of the Oakland East Quadrangle, California: U.S. Geological Survey Map GQ-769.

Radbruch-Hall, D.H., 1974, Map showing recently active breaks along the Hayward fault zone and southern part of the Calaveras fault zone, California: U.S. Geological Survey Miscellaneous Investigations Map I-813.

Radbruch, D.H. and Lennert, B.J., 1966, Damage to culvert under Memorial Stadium, University of California, Berkeley: U.S. Geological Survey Circular 525, p. 3-6.

Rogers, J.D., 1979, Shallow creep measurements in landslides: M.S. thesis, Department of Civil Engineering, University of California, Berkeley, 122 p.

Rogers, J.D., 1986, Landslide processes of the East Bay Hills: Field Trip Guidebook, 29th Annual Meeting, Association of Engineering Geologists, San Francisco, 90 p.

Russell, R.J., 1926, Recent horizontal offsets along the Hayward Fault: Journal of Geology, v. 34, p. 507-511.

Schultz, S.S., 1989, Catalog of creepmeter measurements in California from 1966 through 1988: U.S. Geological Survey Open File Report OFR 89-650, 193 p.

Smith, T.C., 1980, Fault evaluation report, Hayward fault, Oakland segment: California Division of Mines and Geology FER-102.

Steinbrugge, K.V., Bennett, J.H., Lagorio, H.J., Davis, J.F., Borchardt, G., and Toppozada, T.R., 1987, Earthquake planning scenario for a magnitude 7.5 earthquake on the Hayward fault in the San Francisco Bay area: California Division of Mines and Geology Special Publication 78, 220 p.

Taylor, C.L., and Conwell, F.R., 1981, BART - Influence of geology on construction conditions and costs: Bulletin of Association of Engineering Geologists, v. 18, no. 2, p. 195-205.

Taylor, C.L., Cluff, L., and Hirschfeld, S. (eds.), 1982, Field trip guidebook: Conference on Earthquake Hazards in the [Eastern] San Francisco Bay Area: California State University Hayward, 142 p.

Taylor, C.L, Hall, N.T., and Melody, M. (eds.), 1992, Field Trip Guidebook: Second Conference on Earthquake Hazards in the Eastern San Francisco Bay Area, Mar. 25-29, California State University Hayward, 225 p.

Terzaghi, K., 1946, Rock defects and loads on tunnel supports: in Proctor, R.V. and White, T.L. (eds.), Rock tunneling with steel supports: Youngstown Printing Co, (Youngstown, Ohio), p. 16-99.

Toppozada, T.R. and Borchardt, G., 1998, Re-evaluation of the 1836 "Hayward fault" and the 1838 San Andreas fault earthquakes: Bulletin of the Seismological Society of America, v. 88, no. 1 (February), p. 140-159.

West, L. J., 1965, Rock instrumentation and geology of the Berkeley Hills tunnel, San Francisco Bay Area Rapid Transit system: Association Engineering Geologists, Abstracts, 1965 National Convention, Association of Engineering Geologists, Denver, p. 35-36.

Western Construction, 1966, Driving the BART Berkeley Hills tunnels: Western Construction, v. 41, no. 3 (March), p. 37-40.

Western Construction, 1968, Concrete linings - BART Berkeley Hills tunnels: Western Construction, v. 43, no. 3 (March), p. 44-45.

Western Construction, 1973, Bay Area Rapid Transit – A special issue: Western Construction, v. 48, no. 4 (April), p. 27-72.

Young, G.J., 1929, Driving the Claremont tunnel: Engineering and Mining Journal, v. 127, no. 21, p. 832-834.

INFLUENCE OF GEOLOGY ON THE DESIGN AND CONSTRUCTION OF BART'S TRANS-BAY TUBE

J. DAVID ROGERS[1]

ABSTRACT

The Bay Area Rapid Transit (BART) system evolved between 1947-1962, centered on the concept of providing a high-speed commuter rail link with San Francisco and Oakland, across central San Francisco Bay. A joint-venture team of consultants was organized by BART to develop a scheme to cross beneath the bay within 3.6-mile long twin tunnels. Geotechnical exploration was carried out in the early 1960's. The environments of deposition of Quaternary sediments on either side of the bay were different, and a bedrock rise existed in the center of the bay. Because of the soft ground conditions encountered along the route, the consulting team opted to design a "floating" binocular-shaped steel tube, designed to accommodate earthquake loads and differential settlement. The binocular-shape tube sections were placed in a dredged excavation across the bay floor over a two year period, between 1966 and 1968. The tubes were sealed and placed without flooding, having been constructed with sufficient weight and ballast to maintain negative buoyancy. The tube was completed in April 1969, but not placed in operation until September 1974.

[1]Department of Geological Engineering
129 McNutt Hall
University of Missouri-Rolla
Rolla, MO 65409-0230
jdrogers@umr.edu

INTRODUCTION

The kingpin structure of the Bay Area Rapid Transit (BART) system was the 3.6-mile long Trans-Bay Tube, at the time the longest and deepest subaqueous tunnel in the world. It was also the first such structure designed to resist earthquake shaking. The geologic conditions exposed along the alignment raised concerns about navigation safety, room for future expansion, differential settlement and seismic survivability, leading to the unprecedented decision to build a flexible tube on a "floating" foundation, with sliding "earthquake joints" at either end. Unique procedures and methods of placement had to be developed during construction to install the prefabricated steel tube sections, over a two year period. The purpose of this article is to summarize the geologic conditions and their impact on the design decisions that were made, as well as to provide a brief overview of the construction practices used to complete the project. The primary sources of information are individuals associated with the project, including Thomas R. Kuesel, who headed the design team, and Ralph B. Peck, who served on the project's board of consultants.

THE ORIGIN OF BART

The origin of the Bay Area Rapid Transit system dates back to 1947, when a joint Army-Navy board suggested construction of a rapid transit tube beneath San Francisco Bay, to speed travel between Oakland and San Francisco and relieve increasing congestion on the San Francisco-Oakland Bay Bridge, completed in 1936. In 1951 legislation was enacted to create a San Francisco Bay Area Rapid Transit Commission, with directors selected from the nine Bay Area counties. Feasibility studies

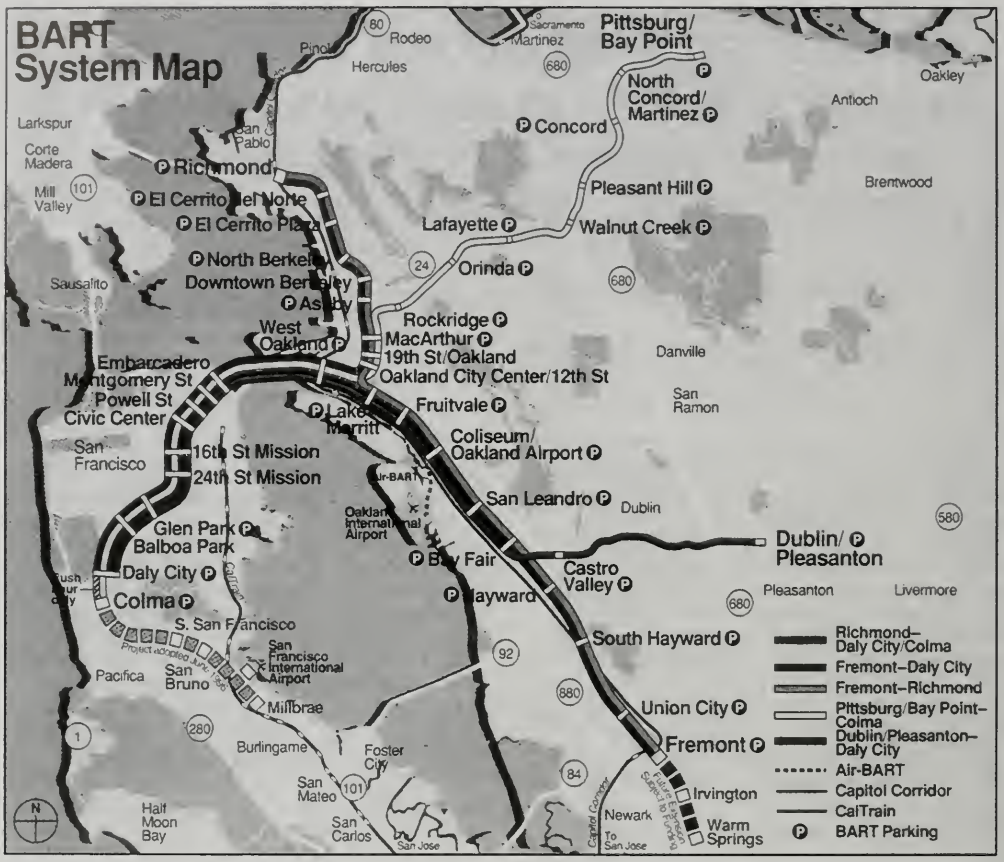

Figure 1. Map showing the existing BART system. The original system had 34 stations, with lines terminating in Daly City, Richmond, Fremont and Concord. The Pittsburg, Dublin and San Francisco Airport extensions were completed between 1992 and 2001.

for a trans-bay tube were undertaken in 1952 and submitted for review in January 1956. The original concept incorporated a 300-mile long system, drawing commuters in and out of San Francisco.

In June 1957 the Bay Area Rapid Transit District was formed, then known as "BARTD." This was subsequently shortened to the BART acronym we recognize today. Engineering studies were performed between 1957 and 1961. In early September 1961, BART released its initial plans for a five-county system, incorporating 123 miles of double track. This scaled-down plan envisioned using the Golden Gate Bridge to extend service into Marin County, south along the San Francisco Peninsula to Palo Alto (San Mateo County), to Richmond, Oakland and Fremont in Alameda County, and Walnut Creek and Concord in Contra Costa County. San Mateo and Marin Counties soon opted out of the plan.

In November 1962, 61% of the aggregate total of votes cast in San Francisco, Alameda and Contra Costa Counties approved funding for the new rapid transit system, with a $792 million construction bond. Another $133 million was to come from Bay Bridge tolls (Demoro, 1968). The 75-mile rail system would serve three counties, as shown in Figure 1. The envisioned cost of $925 million made BART

the first "billion dollar mass transit project", and attracted many contractors to the Bay Area.

GENERAL ENGINEERING CONSULTANT TEAM

Engineering expertise was brought in from across the country to deal with the many pioneering aspects of the first "from the ground up" rapid transit system to be constructed in America in almost 50 years (Bugge and Irvin, 1964). In 1952, New York-based Parsons, Brinckerhoff, Quade and Douglas (PBQD) was retained to prepare a comprehensive mass transportation study for the Bay Area (Bobrick, 1985). In 1957 San Francisco-based Bechtel Corporation sponsored a joint venture consulting team, along with Parsons-Brinckerhoff and Tudor Engineering Co. (PBTB) of San Francisco. The PBTB team served as BART's general engineering consultants for the feasibility studies conducted between 1957 and 1962, the design work performed between 1963 and 1970, and construction management between 1964 and 1975.

The original PBTB design team initially employed about 300 engineers, which swelled to nearly 8,000 engineers and technicians during construction. After wind-tunnel tests by Stanford Research Labs, PBTB selected relatively lightweight electrified cars running on 115-pound (per yard) rails. The spacing between rails was spread from the 4.7-foot standard gage to 5.5 feet, to ensure stability in San Francisco's winds on exposed aerial structures. Power would be transferred to individual running trucks (wheels) via a 1,000-volt DC third rail. The speed of the system was designed to be between 50 and 80 mph, and the right-of-way would be entirely separated from other traffic, to avoid any delays associated with rail or vehicular crossings.

Being in the seismically active San Francisco Bay region, the PBTB consulting team was expected to design an "earthquake safe" rapid transit system. After considering the requisite earthquake loads, PBTB concluded that it would be impracticable to design BART structures to "entirely resist" the forces of a maximum event earthquake. The decision was made to design structures that would be able to accept deformations induced by an earthquake with a 100-year recurrence interval without causing permanent distortion, keeping the risk to both passengers and the system "within acceptable limits" and "still make the project economically feasible" (Chandler, 1969; Kuesel, 1969).

GEOTECHNICAL EXPLORATION

The 3.6-mile long twin-track trans-bay tube was originally estimated to cost $133 million. The actual $180-million price tag was paid by Bay Bridge tolls (Godfrey, 1966). In 1960 PBQD drilled five exploratory borings in the Bay, as part of the feasibility studies (Swain, 1960), to confirm the general soil profile. The geologic conditions beneath the nearby San Francisco-Oakland Bay Bridge were already well-documented (Proctor, 1936; CDH, 1939; Trask and Rolston, 1951).

During 1964-65 PBQD (1965) drilled another 25 borings in the bay, more or less following the track of water-borne ferries that had plied the bay prior to completion of the Bay Bridge in November 1936. The locations of these borings are shown in the upper half of Figure 2. Of foremost interest to the design team were potential settlement problems, stability of the temporary excavations to be made in the bottom of the bay, and the proximity of the Franciscan Formation bedrock along the proposed alignment. This was because the design team wanted to keep the tube "floating" on the Young Bay Mud, and avoid variances in dynamic response that could be expected if portions of the tube were founded on the stiff basement rock, which protrudes from the Bay on Yerba Buena Island (Figure 3).

Settlement of the tubes was to be mitigated by employing "compensated excavations", which are intended to remove sufficient soil to compensate for the weight of the structure being placed on compressible material. The design team was concerned about future settlement in the vicinity of the east portal, where the Port of Oakland planned an extension of their existing mole (across the tube's proposed alignment). The BART alignment was subsequently shifted so it would proceed beneath the Port's new Seventh Street Terminal, built in the early 1970s. Supporting piles were placed on either side of the BART tube.

The alignment was unique in that engineers sought to avoid good foundation materials, opting to keep the tube on compressible material, so that its flexibility could distribute relatively large seismic oscillations over its length and avoid zones where bending stresses might be concentrated. Seeking to avoid the Yerba Buena rise in the Franciscan basement rock underlying central San Francisco Bay, the design profile varied both horizontally and vertically, dipping as much as 135 feet beneath the Bay.

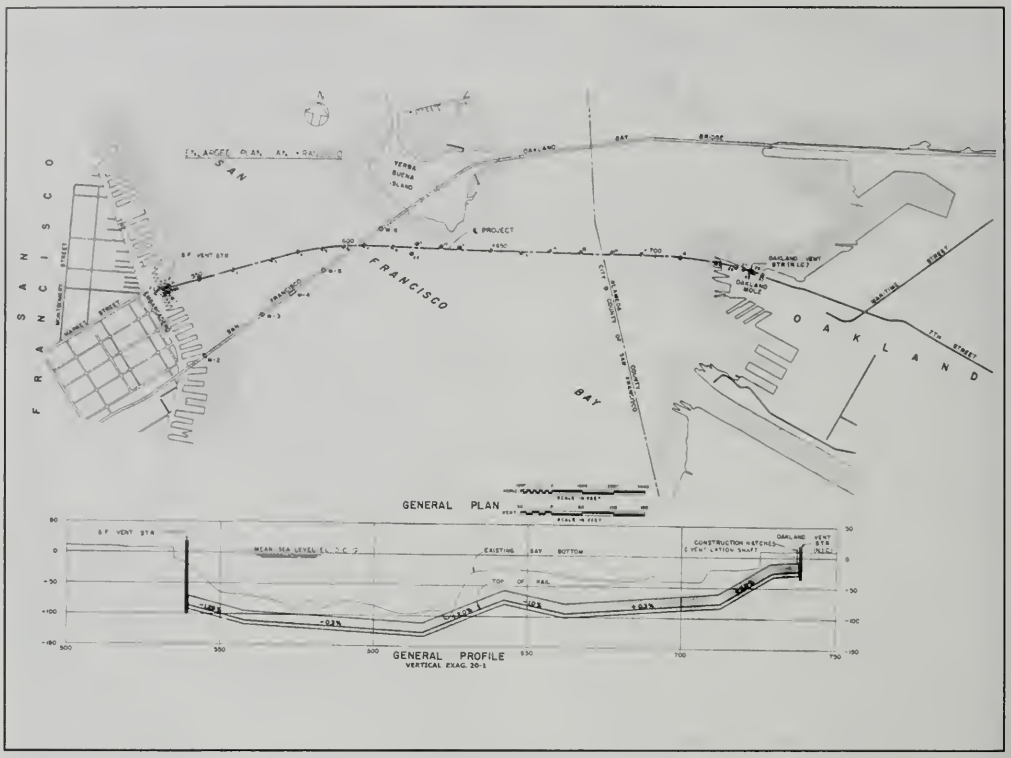

Figure 2. Plan and profile views of the BART Trans-Bay Tubes, as originally conceived in 1965. The alignment was intended to accommodate a second tube south of the first, and also allow a second Bay Bridge, south of and parallel to the existing span.

as shown in the lower portion of Figure 2. Grades were limited to a maximum of 3%, with a minimum of 0.3% to facilitate drainage.

GEOLOGY OF THE BAY CROSSING

The geologic structure beneath either side of central San Francisco Bay is different, as shown in the generalized geologic profile across this portion of the bay presented in Figure 4. The depth to Jurassic-Cretaceous Franciscan Formation basement rock between San Francisco and Yerba Buena is only 225 feet, but drops to more than 700 feet near downtown Oakland. Figure 4 presents the approximate stratigraphic relationships between various units cited in engineering geologic studies (Trask and Rolston, 1951; Louderback, 1951; Radbruch, 1957; Treasher, 1963; USACE, 1963; Schlocker, 1974; Taylor and Conwell, 1981; Rogers and Figuers, 1991a; Caltrans, 1997; Figuers, 1998). Alternative nomenclature has been proposed to describe various biostratigraphic aspects of the Quaternary and Holocene sediments (Atwater et al., 1977; Atwater, 1979; Helley and Lajoie, 1979; Sloan, 1992; Hensolt and Brabb, 1994).

The main focus of exploration in 1960 and 1964-65 was aimed at characterizing the depth and extent of the Young Bay Mud, which reaches maximum thicknesses of over 100 feet just off the San Francisco Embarcadero, at the foot of Market Street, and over 120 feet south of Yerba Buena Island (Goldman, 1969). The Young Bay Mud is a Holocene estuarine clay that progressively filled low-lying areas of San Francisco Bay as sea level rose during the past 11,000 years (Atwater, 1979).

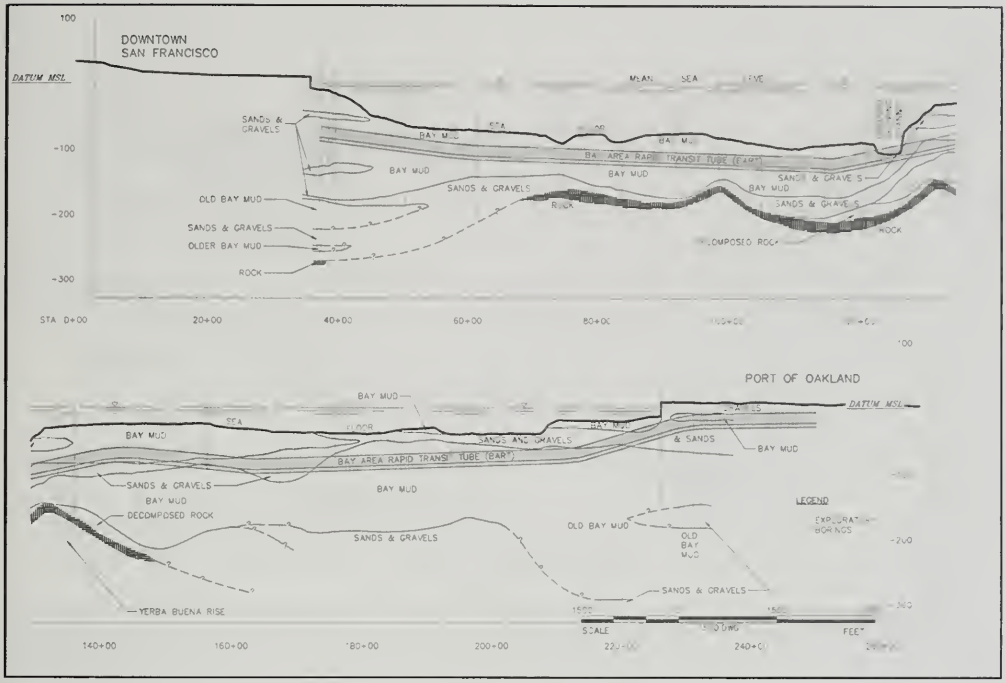

Figure 3. Geologic cross-section along the BART Trans-Bay Tunnel, prepared by Parsons- Brinkerhoff in their August 1965 geotechnical report. The focus of the design was to keep the twin tubes sitting on soft compressible soils, avoiding bedrock promontories.

On the east side of the bay, the Temescal Formation of Radbruch (1969) infills incised Holocene channels above sea level, and interfingers with the Young Bay Mud in old sloughs, estuaries and marshy areas (Rogers and Figuers, 1991a).

The stratigraphic relationships between the late Quaternary and Holocene units along the East Bay shore are illustrated in Figures 5 and 6. A pull-apart basin perturbs the Franciscan basement beneath the Fruitvale-Alameda-Bay Farm Island area (Figure 5). The combined Quaternary and Holocene cover reaches depths of over 1,300 feet in this area, south of downtown Oakland (Rogers and Figuers, 1991a). Along the east shoreline the Young Bay Mud overlies and abuts the Merritt sand, a late Pleistocene aeolian deposit analogous to the dune sands blanketing much of San Francisco (Figure 6). Along the East Bay margins the Young Bay Mud is locally absent.

Along the west side of the Bay, the Young Bay Mud is underlain by dune sands: the Colma Formation and the Posey sand member of the San Antonio Formation (Treasher, 1963; Figure 7). The Posey and San Antonio sands also locally underlie the Young Bay Mud along the eastern shore, within large depressions, such as the San Antonio Estuary, between Oakland and Alameda (Radbruch, 1957; Rogers and Figuers, 1991a; Figuers, 1998) .

The Yerba Buena mud of Sloan (1992) used to be called the "Old Bay Mud" (Trask and Rolston, 1951). It was likely deposited during the earliest estuarine deposition of the last interglacial interval (Sangamon), approximately 122 to 125 ka ago (Sloan, 1992). During this interval (isotope stage 5e) sea level was approximately 22 feet higher than at present. This appears to account for the older estuarine clay underlying much of the East Bay plain, including downtown Oakland and Hayward. South

and east of Yerba Buena Island the Yerba Buena mud reaches a thickness of over 100 feet beneath the BART alignment (Rogers and Figuers, 1991a).

The Yerba Buena mud is underlain by the marine facies of the Alameda Formation (Rogers and Figuers, 1991a; Figuers, 1998). This facies appears to contain at least three definable marine estuarine clay members across the eastern side of the San Francisco Bay (Figure 4), but may extend into western San Francisco Bay, farther south. A continental facies of the Alameda Formation underlies the marine facies, and extends to depths between 400 feet (at BART's Oakland Ventilation Structure) and as much as 700 feet (near the 880/980 freeway junction, further east). The combined thickness of the marine and continental facies of the Alameda Formation varies between 100 feet just southeast of Yerba Buena Island to over 500 feet near the 880/980 interchange.

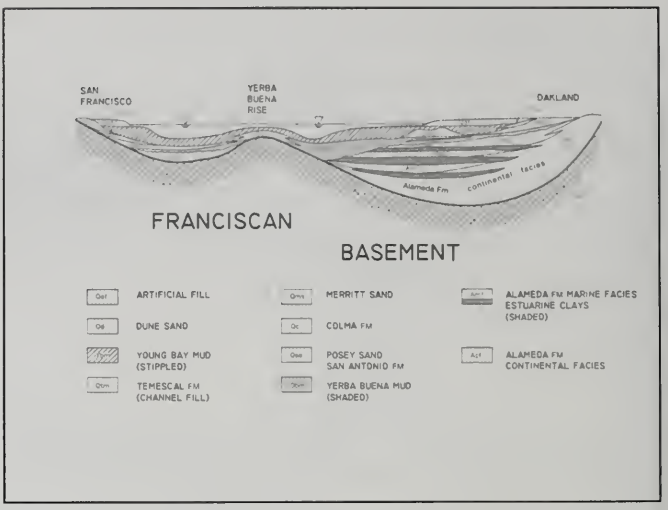

Figure 4. Stratigraphic relationships between various geologic units in the vicinity of the BART trans-bay crossing, based on the suggested nomenclature of Rogers and Figuers (1991a).

The age of the Alameda Formation is inferred from a sample of the 400 ka Rockland Tuff recovered from Hole 42 for the Southern Crossing (Trask and Rolston, 1951), about 45 to 55 feet above the base of the formation. Work by Sarna-Wojcicki et al. (1985) constrains the age of the Alameda as being slightly older than 400 ka and younger than 130 ka, and would make it roughly correlative with the Merced Formation that occupies the San Bruno/Colma channel between San Bruno Mountain and the San Andreas fault (Clifton and Hunter, 1991; Rogers and Figuers, 1991b; Figuers, 1998).

At the time the BART alignment was explored, the depth of the Franciscan basement rocks (of Jurassic-Cretaceous age) was unknown east of the Yerba Buena rise. Between San Francisco and Yerba Buena Island the depth of the basement is a maximum of 225 feet below sea level. East of Yerba Buena the Franciscan basement drops sharply, reaching a depth of 450 feet near BART's Oakland Ventilation Structure (in the Port of Oakland). The basement continues to drop easterly, reaching a maximum depth of approximately 700 feet where BART crosses by the I-880/I-980 interchange (Rogers and Figuers, 1991a; Muir, 1993; Hensolt and Brabb, 1994; Figuers, 1998).

The PBTB design team sought to avoid bedrock knobs protruding from the bay floor, at the Yerba Buena Rise and 3,500 feet to the west of Yerba Buena (Figure 3). At the Yerba Buena Rise the Franciscan basement lies at −143 feet, only 40 feet beneath the tube. Here the cushion of Yerba Buena mud (old bay mud) was only 30 feet thick. At a distance of 3,500 feet west and 500 feet north of the Bay Bridge, the basement rises to −156 feet (below sea level), within 30 feet of the tube invert. The tube lies on just 15 feet of Young Bay Mud at this location (Figure 3).

DESIGN CONSIDERATIONS

The use of immersed steel tubes for railway tunnels was actually pioneered in 1906 with the Michigan Central Railroad Tunnel beneath the Detroit River, and in New York in 1913 during construction of the 4-track Lexington Avenue Interurban Rapid Transit Line across the Harlem River. Subsequent to these successes, concrete box submersed tubes were developed in the Netherlands.

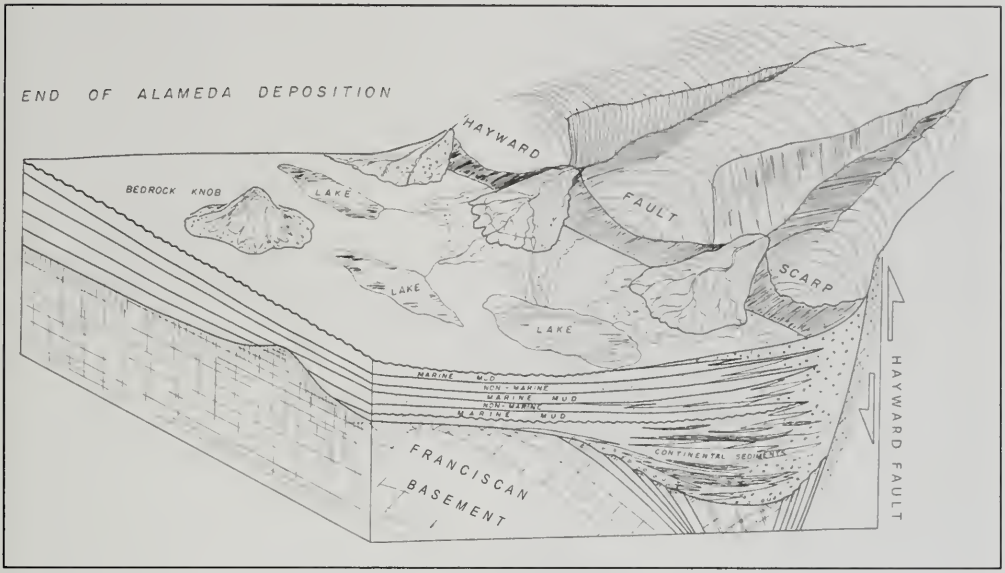

Figure 5. Block diagram depicting depositional conditions along the eastern side of central San Francisco Bay at the end of Alameda deposition, when the bay appeared much as it does today. Continental sediments of the lower Alameda Formation infilled the pull-apart basin, whereas the upper Alameda is characterized by marine facies. Taken from Rogers and Figuers (1991a).

Both steel and concrete tubes were considered for BART, but the steel shell design was selected for its superior ductility and ability to resist the distortions that could be produced by earthquakes. The design team used available recorded data on earthquake amplitude versus wavelength, scaled up to represent what could be expected in a repeat of the 1906 San Francisco earthquake. The engineers soon learned that the critical design case was for small amplitude half-waves moving through the Young Bay Mud, which caused the greatest distortion of the tube in free field excitation. The steel option had the advantage of being very tough in tension.

A steel tube could accommodate twin tracks inside a rigid box. The thickness of the tube was only 3/8 inch, but an additional 24 inches of reinforced concrete lining was placed inside the tube walls to help overcome buoyancy. The structural stresses on the tube were moderate, and all joints were arc welded to allow transmission of tensile stresses far above the levels envisioned even in an earthquake.

The designers were also concerned with out-of-phase motions between the soft bay mud and the stiffer San Antonio and Alameda Formation materials lying beneath it in San Francisco and Oakland. Due to the tube's 3.6-mile length, concerns also arose about the tube being pulled apart at its end connections. It was decided to fit the tube with special seismic joints on either side of the San Francisco ventilation structure (Douglas and Warshaw, 1971). These "universal joints" would allow up to 6 inches of movement (lengthening-shortening and/or rising-falling). They were fabricated by Kaiser Steel in Napa, and attached to the west end of Tube 1 (attached to east side of the San Francisco vent structure) and the east side of Tube 58 (attached to the west side of the vent structure). Tube 58 was a special segment built to accommodate movement between the vent structure and the shield tunnels coming off the foot of Market Street. A model of the trans-bay tube was also taken to the University of Mexico for shaking-table tests.

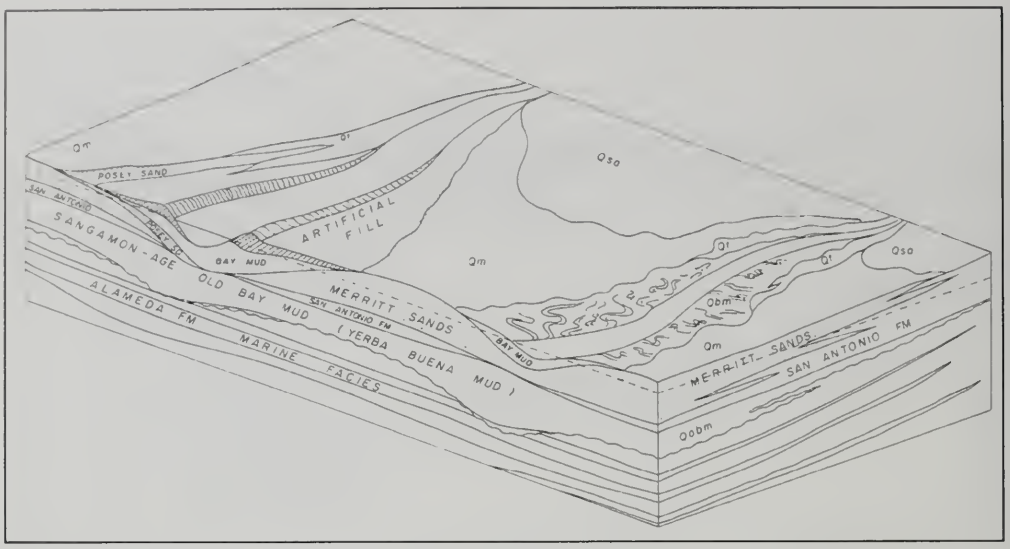

Figure 6. Schematic block diagram view looking north along the East Bay shoreline in the vicinity of Oakland, showing stratigraphic relationships between various Holocene and late Pleistocene sediments and artificial fill. Taken from Rogers and Figuers (1991a).

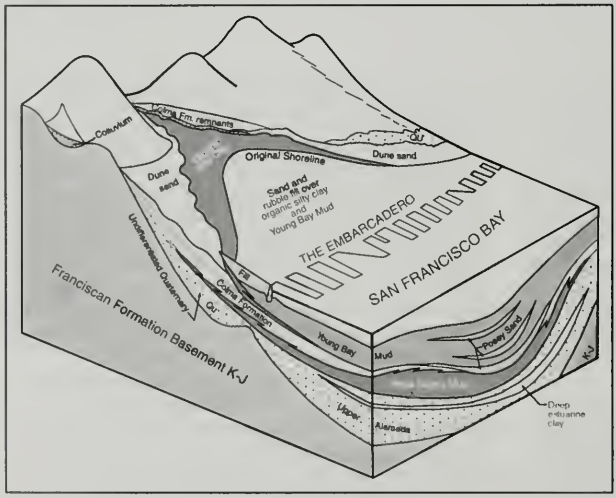

Figure 7. Schematic block diagram looking northwest along the San Francisco shoreline in the vicinity of Yerba Buena Cove, between Rincon and Telegraph Hills. This diagram presents generalized stratigraphic relationships between various units commonly encountered, but locally absent, from this area.

PLACEMENT OF THE TUBE SECTIONS

In April 1966 BART awarded the initial $90 million construction contract for the trans-bay tubes to Trans-Bay Constructors (TBC). TBC contracted with Bethlehem Steel's South San Francisco Shipyard for fabrication of the binocular-shaped shells, using 3/8 inch thick steel sheets (Figure 8). The tubes were between 273 and 366 feet long and averaged 11,000 tons apiece. They were 48 feet wide by 24 feet high, with two 17-feet diameter enclosures for the tracks. Ventilation and access galleries, as well as emergency cross-overs were fitted between the tunnels, as shown in Figure 9. After launching, the tubes were taken to an outfitting dock, where concrete was formed into 24-inch thick walls and 48-inch deep inverts, to reduce buoyancy (Figure 9). In all, 19,113 feet of twin-track tube were built in 57 tubes, and placed between the Oakland and San Francisco ventilation structures. The horizontal and vertical

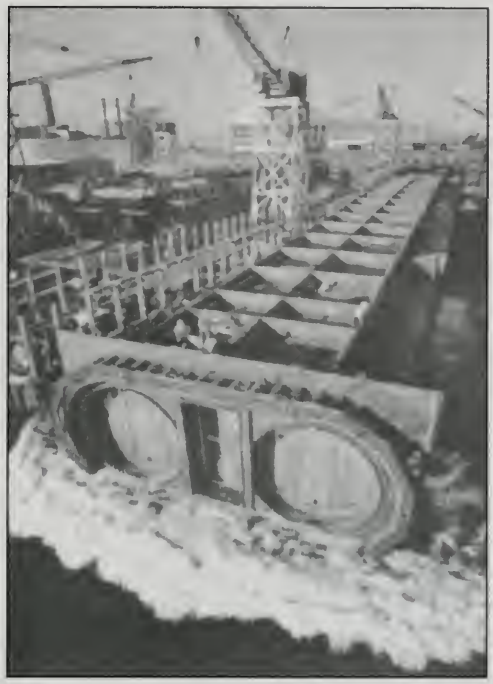

Figure 8. Fabrication of a tube section at Bethlehem Steel's South San Francisco Shipyard. The tubes were 48 feet wide, 24 feet high, and varied between 273 and 366 feet long. Their average displacement was 11,000 tons. Fifty seven tubes were constructed in this manner. Note the ballast pockets being laid out on top of the tube. Five hundred tons of gravel were poured into these pockets to sink the tube. Photo courtesy of Parsons-Brinckerhoff.

curves built into the alignment (shown in Figure 2) were at that time unique for a trench-type tunnel, which required 15 horizontally curved segments, four with vertical curves, and two with both vertical and horizontal curves.

The contractor excavated nearly 6 million cubic yards of Young Bay Mud, Merritt sand and undifferentiated organic silt encountered on the floor of the bay along the proposed alignment, using a 13-yard clamshell and hydraulic dredge. This trench was between 33 and 133 feet deep, 60 feet wide at the base, with side slopes between 1.5:1 and 3:1 (horizontal to vertical), as shown in Figure 9. Excavated material was dumped into 2,000 cubic-yard bottom dump barges, and disposed of in the tidal draw channel west of Alcatraz Island.

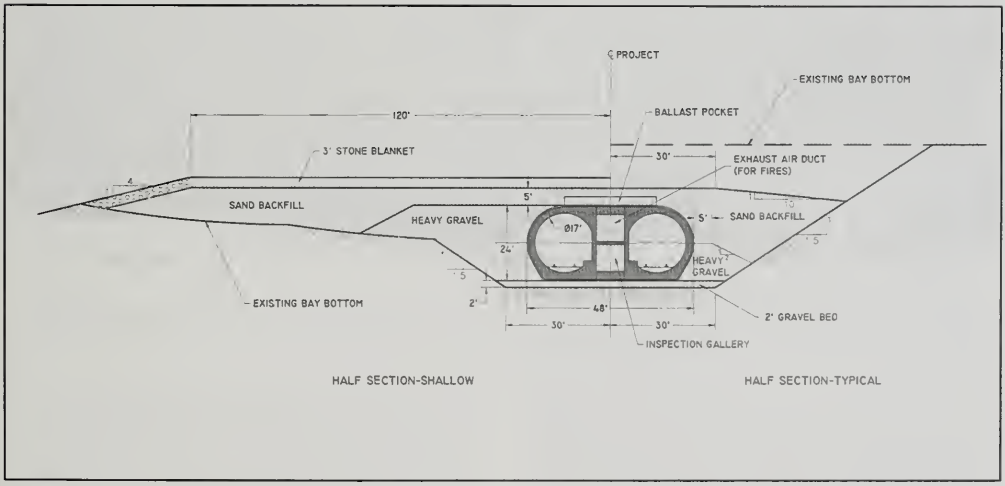

Figure 9. Typical cross-section through shallow and normal depth trenches excavated for the Trans-Bay Tube. Note the two-foot thick gravel bed that the tubes were set on, and the three-foot thick stone blanket used on the shallow half sections.

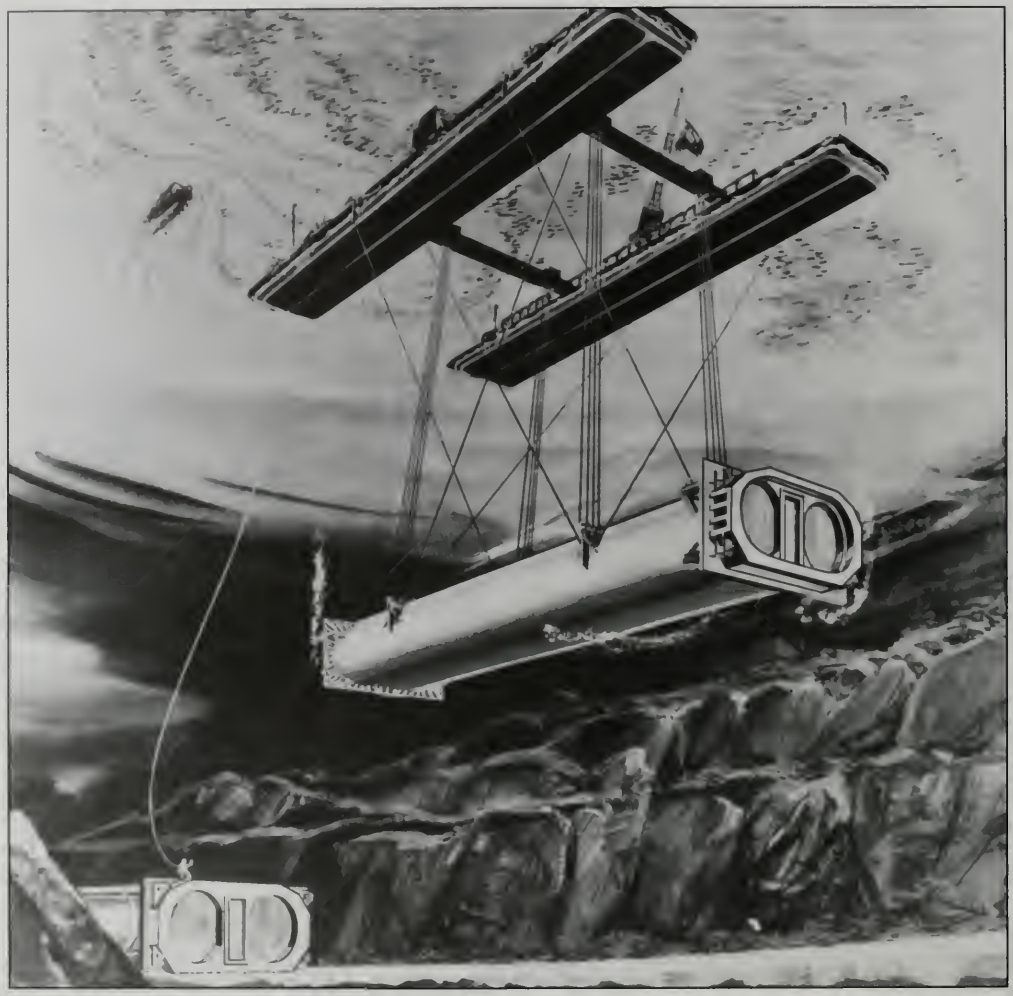

Figure 10. Artist's rendering showing the placement barge lowering one of the tube sections. The tubes remained filled with air, and were lowered by placing gravel ballast in special racks built into the tops of each section. The bulkheads were removed and reused after the ends were welded to the next adjoining segment.

After fitting out, the tube sections were temporarily sealed at either end and floated to a catamaran placing barge, from which they were suspended for lowering (Figure 10). Contrary to legend, the tubes were never filled with water; they were sunk by dumping 500 tons of gravel onto ballast pockets built atop the tubes, gradually lowering them into position (Murphy and Tanner,1966; ENR, 1967; Civil Engineering, 1967). The tubes were set on 2-foot thick gravel blankets and placed within 0.15 feet of design grade, across the floor of the dredged channel (Figure 9). The goal was to place each tube about 2 feet from the existing line of tubes, then bring them within 1 inch of design alignment using

50-ton hydraulic jacks with 39-inch strokes, connected to four railroad car couplers installed at each end.

Once positioned, water was trapped between neoprene gaskets mounted on the end bulkheads. This trapped water was bled from the joint and pumped out, creating a vacuum that brought the sections closer together. The temporary bulkheads on both sides of the new joint were then removed and reused on other sections. Liner plates were welded across the new joint from the inside to make a permanent connection. A two-foot thick concrete lining was then placed within the transition (the majority of the concrete lining having already been installed at Bethlehem's dock).

Before the catamaran barge and tube were brought into place, a gravel bed was laid to serve as foundation for the tube (Construction Methods, 1967). The gravel bed was smoothed within a tolerance of 0.15 feet. After the tubes were joined, gravel backfill was placed along both sides to stabilize them, and over the top as protection against dragging anchors or vessels that might sink onto the tube. The tube was also provided with cathodic corrosion protection.

In September 1966 the first tube was placed against the west side of the Oakland Ventilation structure. Twenty-six sections were then placed, stretching 2 miles into the Bay by April 1968. Upon completion of the more extensive San Francisco ventilation structure, work shifted to the west side of the Bay, preceding easterly. One tube section was placed approximately every two weeks, and placement of all the tubes was completed in early April 1969 (ENR, 1969). Track-laying within the tubes was completed in August 1969, and electrification and ventilation were in place by 1972.

SUMMARY AND CONCLUSIONS

The first portion of BART to begin operation was the southern portion of BART's Richmond-Fremont line in September 1972. Forty-seven miles of the 60-mile system remained unfinished, owing to political delays in completing the San Francisco subways. All of the East Bay lines were running by August 1973. However, after one fatal collision and a derailment State officials had misgivings about the reliability of the automated train control system, so permission was withheld for running trains through the Trans-Bay Tube. BART began service between Daly City and Montgomery Station in November 1973, and, after additional testing, the Public Utilities Commission finally allowed service across the bay, beginning on September 16, 1974.

At the time of its completion, the BART tube was the longest and deepest immersed tube ever built (Warshaw, 1968). The success of the BART tube led to design of similar structures for the Hong Kong Cross-Harbor Tunnel, the East River-63rd Street Tunnel in New York City, and the second Hampton Roads Bridge-Tunnel (Kuesel, 1974).

The Trans-Bay Tube came through the 1989 Loma Prieta earthquake without any serious problem, although as a precaution the tube was shut down and inspected. Soft sediments are recognized to enhance incoming energy through wave impedance (Dickenson, 1994), but the tubes are laterally confined within the backfilled trench, and the weight of water helps reduce "ground whip" effects. Some minor leaks were noted several days after the earthquake, but further study showed these to be corrosion pinholes, related to patches fitted over grout holes. These were easily repaired.

BART will likely be remembered as the prototype American urban mass-transit project of the mid-20th Century, conceived and built as a stand-alone project. The many problems experienced with funding the project led to mass-transit funding at the federal level, which has since subsidized similar projects in other parts of the United States.

ACKNOWLEDGEMENTS

The writer is indebted to interviews with Thomas R. Kuesel and Ralph B. Peck regarding the evolution of the tube concept, design, and implementation. Ralph Peck kindly provided copies of the engineering plans and geotechnical reports. In addition, Parsons-Brinkerhoff lent copies of photos from their files to include in the article. Discussions with Brian Atwater, Doc Bonilla, Earl Brabb, Reid Buell, Ed Clifton, Sandy Figuers, Walt Hensolt, Ed Margason, Jack Rolston, Doris Sloan, and the late Clyde Wahrhaftig contributed to the author's understanding of the structure and stratigraphy of central San Francisco Bay and its margins. Tom Kuesel, Dick Harlan, Reid Buell, Chuck Taylor, Steve Klein, Victor Romero, Bob Anderson and Steve Stryker kindly reviewed the manuscript and provided helpful suggestions.

SELECTED REFERENCES

Atwater, B.F., Hedel, C.W., and Helley, E.J., 1977, Late Quaternary depositional history, Holocene sea level changes, and vertical crustal movement, southern San Francisco Bay, California: U.S. Geological Survey Professional Paper 1014, 15 p., plates.

Atwater, B.F., 1979, Ancient processes at the site of southern San Francisco Bay: *in* Conomos, T.J. (ed.), Movement of the crust and changes in sea level of San Francisco Bay: American Association for the Advancement of Science, Pacific Division, p. 31-45.

Bobrick, B., 1985, Parsons Brinckerhoff: The First 100 Years: Van Nostrand Reinhold Co., (New York, New York), 276 p.

Bugge, W.A. and Irvin, L., 1964, Designing the San Francisco Bay Area rapid transit system: Civil Engineering, v. 34, no.10, p. 58-63.

Caltrans, 1997, East span of the San Francisco-Oakland Bay bridge, log of test borings: Preliminary geologic report to the Metropolitan Transportation Commissions, Engineering and Design Advisory Committee, California Dept. of Transportation, Division of Structures, April 18, 1997, 62 p.

Carlson, P.R., Alpha, T.R., and McCulloch, D.S., 1970, The floor of central San Francisco Bay: California Division of Mines and Geology Mineral Information Service, v. 23, no. 5, p. 97-107.

CDH (California Division of Highways), 1939, Geological report on foundation conditions (from reports of the consulting geologists): *in* Sixth Annual Report on the San Francisco-Oakland Bay Bridge: California Division of Highways, Department of Public Works, State Printing Office, p. 102-104.

Civil Engineering, 1967, Placing the underwater tubes for BART: Civil Engineering, American Society of Civil Engineers, v. 37, no. 9, p. 33-35

Chandler, R. R., 1969, Field trip 4 - Bay Area Rapid Transit System: Field Trips, National Meeting, Association of Engineering Geologists, San Francisco, October 21-25, p. D-1 – D-7.

Clifton, H.E. and Hunter, R.E., 1991, Depositional and other features of the Merced Formation in sea cliff exposures south of San Francisco, California: in Sloan, D. and Wagner, D.L., (eds.), Geologic excursions in Northern California: California Division of Mines and Geology Special Publication 109, p. 35-44.

Construction Methods, 1967, Underwater bay tunnel rests on barge-made gravel bed: Construction methods, v. 49:9 (September), p. 104.

Demoro, H.W., 1968, BART at mid-point: Interurbans magazine, Special issue 31, Los Angeles, v. 25, no. 3, 117 p.

Dickenson, S.E., 1994, Dynamic response of soft and deep cohesive soils during the Loma Prieta Earthquake of Oct. 17, 1994: Ph.D. dissertation, Dept of Civil and Environmental Engineering, U.C. Berkeley, p. 284-291.

Douglas, W.S. and Warshaw, R., 1971, Design of seismic joint for San Francisco Bay tunnel: Journal of the Structural Division, American Society of Civil Engineers, v.97, no. ST4, p. 1129-1141.

ENR (Engineering News Record), 1967, Barge armada makes tunnel look like a snap: ENR, McGraw-Hill, v.179, no. 20 (November 16, 1967), p. 42-44.

ENR (Engineering News Record), 1969, BARTD closes bay tube and gets rescue funds: ENR, McGraw-Hill, v.182, no. 15 (April 10, 1969), p. 62.

Figuers, S.H., 1998, Groundwater study and water supply history of the East Bay plain, Alameda and Contra Costa Counties, California: Consultant's report by Norfleet Consultants for The Friends of the San Francisco Estuary, Oakland, 90 p., 24 figs, 2 pl.

Godfrey, K. A., Jr., 1966, Rapid transit renaissance: Civil Engineering, American Society of Civil Engineers, v. 36, no. 12, p. 28-33

Goldman, H.B. (ed.), 1969, Geologic and engineering aspects of San Francisco Bay fill: California Division of Mines and Geology Special Report 97, 130 p., 4 pl.

Helley, E.J. and Lajoie, K.R., 1979, Geology and engineering properties of flatland deposits: in Helley, E.J., et al. (eds.), Flatland deposits of the San Francisco Bay region, California – Their geology and engineering properties, and their importance to comprehensive planning: U.S. Geological Survey Professional Paper 943, p. 14-68.

Hensolt, W.H. and Brabb, E.E., 1994, Maps and profiles of the upper and lower sedimentary strata in the San Francisco Bay Area, California: unpublished manuscript, 32 p, 13 figs.

Kuesel, T.R., 1968, Structural design of the Bay Area Rapid Transit System: Civil Engineering, American Society of Civil Engineers, v. 38, no. 4, p. 46-50.

Kuesel, T.R., 1969, Earthquake design criteria for subways: Journal of the Structural Division, American Society of Civil Engineers, v. 95, p. 1,213-1,231.

Kuesel, T. R., 1972, Soft ground tunnels for the BART project: Proceedings of the North American Rapid Excavation and Tunneling Conference, Chicago, v. 1, p. 287-313.

Kuesel, T. R., 1974, A tale of three tunnels: Civil Engineering, American Society of Civil Engineers, v. 44, no. 12, p. 50-55

Louderback, G.D., 1951, Geologic history of San Francisco Bay: *in* Geologic guidebook of the San Francisco Bay counties: California Division of Mines and Geology Bulletin 154, p. 75-94.

Muir, K.S., 1993, Geologic framework of the East Bay groundwater basin, Alameda County, California: Consultant's report to Alameda County Water District, Hayward, 27 p., 10 figs, 1 pl.

Murphy, G. J. and Tanner, D. N., 1966, The BART trans-bay tube: Civil Engineering, American Society of Civil Engineers, v. 36, no. 12, p. 51-55.

PBQD (Parsons, Brinkerhoff, Quade and Douglas, Inc.), 1965, Soil investigation B 7200 trans-bay tube: Consultant's report to S.F. Bay Area Rapid Transit District, August, 21 p, 8 figs.

Peck, R.B., Hendron, A.J., and Mohraz, B., 1972, State of the art of soft-ground tunneling: Proceedings of the North American Rapid Excavation and Tunneling Conference, Chicago, v. 1, p. 259-286.

Proctor, C.S., 1936, The foundations of the San Francisco-Oakland Bay Bridge: Proceedings of the International Conference on Soil Mechanics and Foundation Engineering, Harvard University, v.3, p. 183-193.

Radbruch, D.H., 1957, Areal and engineering geology of the Oakland West quadrangle, California: U.S. Geological Survey Miscellaneous Geologic Investigations Map I-239.

Radbruch, D.H., 1958, Former shoreline features along the east side of San Francisco Bay, California: U.S. Geological Survey Miscellaneous Geologic Investigations Map I-298.

Radbruch, D.H., 1969, Areal and engineering geology of the Oakland East quadrangle, California: U.S. Geological Survey Geologic Map GQ-768.

Radbruch, D.H. and Schlocker, J., 1958, Engineering geology of the Islais Creek Basin, San Francisco, California: U.S. Geological Survey Miscellaneous Geologic Investigations Map I-264.

Rogers, J.D. and Figuers, S.H., 1991a, Engineering geologic site characterization of the Greater Oakland-Alameda Area, Alameda and San Francisco Counties, California: Final report to the National Science Foundation: Grant No. BCS-9003785, 59 p., 4 plates.

Rogers, J.D. and Figuers, S.H., 1991b, Site stratigraphy and near-shore development effects on soil amplification in the Greater Oakland Area: in Baldwin, J.E. and Sitar, N. (eds.), Loma Prieta Earthquake: Engineering geologic perspectives, Association of Engineering Geologists, Special Publication No. 1, p. 123-149.

Sarna-Wojcicki, A.M., Meyer, C.E., Bowman, H.R., Hall, N.T., Russell, P.C., Woodward, M.J., and Slate, J.L., 1985, Correlation of the Rockland ash bed, a 400,000 year old stratigraphic marker in northern California and western Nevada, and implications for middle Pleistocene paleogeography of central California: Quaternary Research, v. 23, p. 236-257.

Schlocker, J., Bonilla, M.G., and Radbruch, D.H., 1958, Geology of the San Francisco North quadrangle, California: U.S. Geological Survey Miscellaneous Geologic Investigations Map I-272.

Schlocker, J., 1974, Geology of the San Francisco North quadrangle, California: U.S. Geological Survey Professional Paper 782, 109 p., 3 pl.

Sloan, D., 1992, The Yerba Buena mud: Record of the last-interglacial predecessor of San Francisco Bay, California: Geological Society of America Bulletin, v. 104, p. 716-727.

Swain, R.J., 1960, Bottom of San Francisco Bay evaluated for trans-bay tube: Civil Engineering, American Society of Civil Engineers, v. 30, no. 11, p. 66-67.

Taylor, C.L. and Conwell, F.R., 1981, BART - Influence of geology on construction conditions and costs: Bulletin of Association of Engineering Geologists, v. 18, no. 2, p. 195-205.

Trask, P.D. and Rolston, J. W., 1951, Engineering geology of the San Francisco Bay, California: Bulletin of the Geological Society of America, v. 62, p. 1,079-1,109.

Treasher, R.C., 1963, Geology of the sedimentary deposits in San Francisco Bay, California: California Division of Mines and Geology Special Report 82, p. 11-24.

USACE (U.S. Army Corps of Engineers), 1963, Comprehensive survey of San Francisco Bay and tributaries, Appendix E - Barrier plans, geology, soils and construction materials: U.S. Army Corps of Engineers San Francisco District, 144 p., 63 figs, 46 pl.

Warshaw, R., 1968, BART tube ventilation building: Civil Engineering, American Society of Civil Engineers, v. 38, no. 12, p. 28-31.

Western Construction, 1973, Bay Area Rapid Transit – A special issue: Western Construction, v. 48, no. 4, p. 27-72.


ASSOCIATION OF ENGINEERING
AEG
GEOLOGISTS

INFLUENCE OF GEOLOGY ON BART'S SAN FRANCISCO SUBWAYS

J. DAVID ROGERS[1]

ABSTRACT

The geologic conditions, design of temporary and permanent ground support, and methods of excavation and dewatering are summarized for the 5.6-mile long segment of the Bay Area Rapid Transit District's original line, between the foot of Market Street and Colonial Way in San Francisco. An overview of the stratigraphic relationships between various Quaternary sediments is presented to aid the reader in untangling the variety of terms that have historically been applied to these deposits by engineers and geologists in San Francisco. Conditions along each tunnel and station segment are then profiled, with a brief description of the methods employed and problems encountered during excavation of tunnels and cut-and-cover excavations for stations. These include shield tunneling under compressed air in soft ground and early employment of various types of tunnel boring machines (TBMs) in soft and hard ground. A variety of ground support techniques are also described, including flexible linings for the tunnels, conventional soldier piles and lagging for stations along Mission Street, and soldier pile tremie concrete (SPTC) walls for the Market Street station excavations. Brief discussions of groundwater control and differential settlements observed during construction are also included.

[1]Department of Geological Engineering
129 McNutt Hall
University of Missouri-Rolla
Rolla, MO 65409-0230
jdrogers@umr.edu

INTRODUCTION

BART's 5.6-mile long path through downtown San Francisco is entirely below ground between the Ferry Building and Colonial Way, just south of I-280 (Figure 1). The line proceeds up Market Street for two miles, then turns south at Van Ness, and heads south for two miles beneath Mission Street. Near Mission and Randall the line diverges from Mission, passing in a tunnel through the natural gap between Bernal Heights and the San Miguel Hills, to Glen Park Station and beneath I-280. Interestingly, this route parallels the City's first rail connection (San Francisco to San Jose), completed in 1864.

The problems encountered during design and construction were largely controlled by the underlying geology. Construction contracts in this zone consisted of seven cut-and-cover excavations for stations, divided by eight tunnel segments and the San Francisco Ventilation Structure (Figure 1). Construction work was completed between 1964 and 1975. Principal tunnel contracts were let between 1966 and 1970, and the station excavations were undertaken between 1967 and 1972. Most of the construction was done by different contractors (mostly joint ventures) because the work was performed concurrently.

The purpose of this article is to summarize the geologic conditions and their impact on the design methods and construction practices chosen for the project. Primary sources of information included individuals involved with most of the major geotechnical design decisions, including Thomas R. Kuesel, Ralph B. Peck, and Richard C. Harlan.

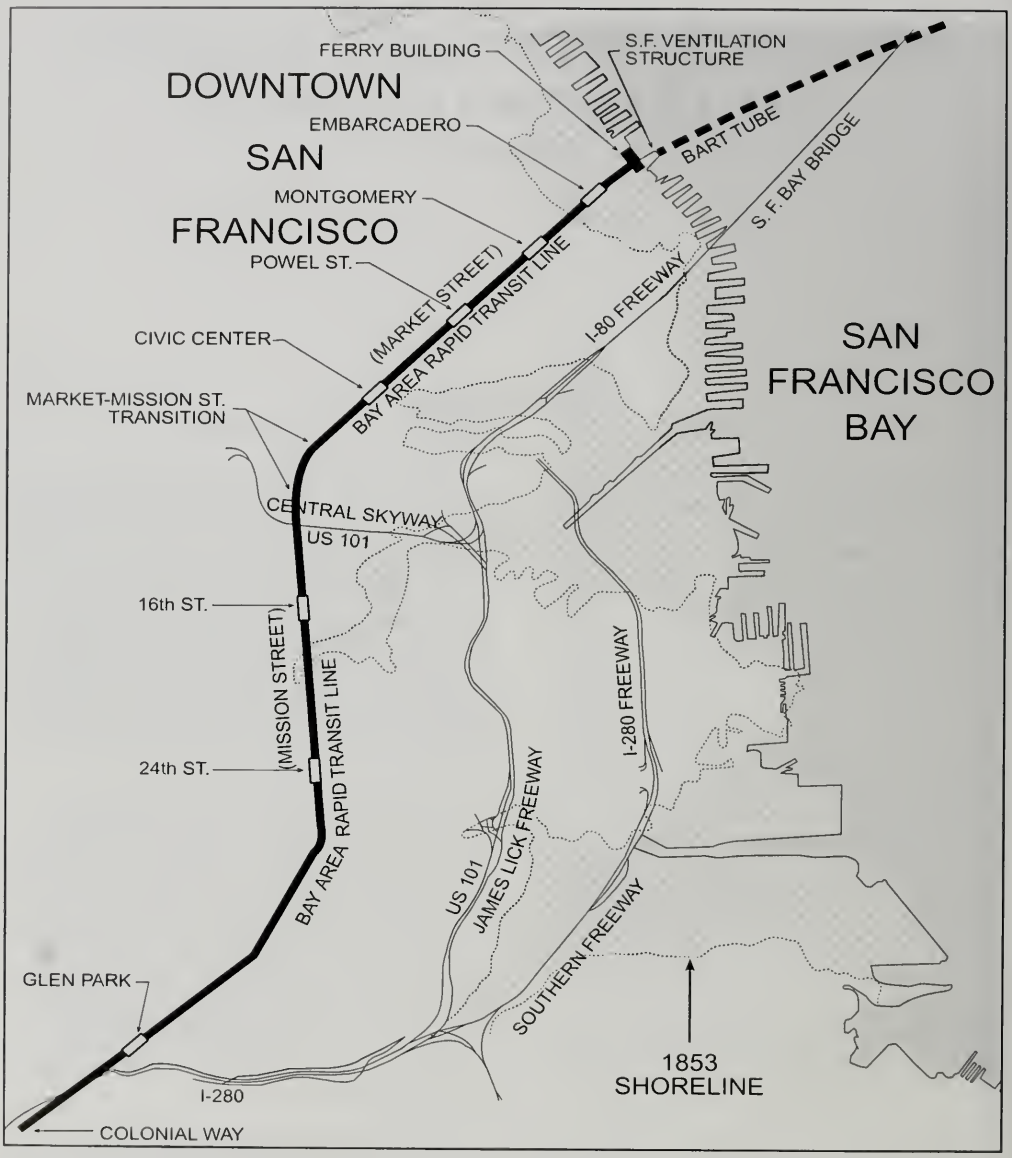

Figure 1. Simplified map of San Francisco, showing relative position of the BART alignment, BART stations, principal freeways, and original and present waterfront. The line extends 5.6 miles underground, between the San Francisco Ventilation Structure and Colonial Way, just south of I-280.

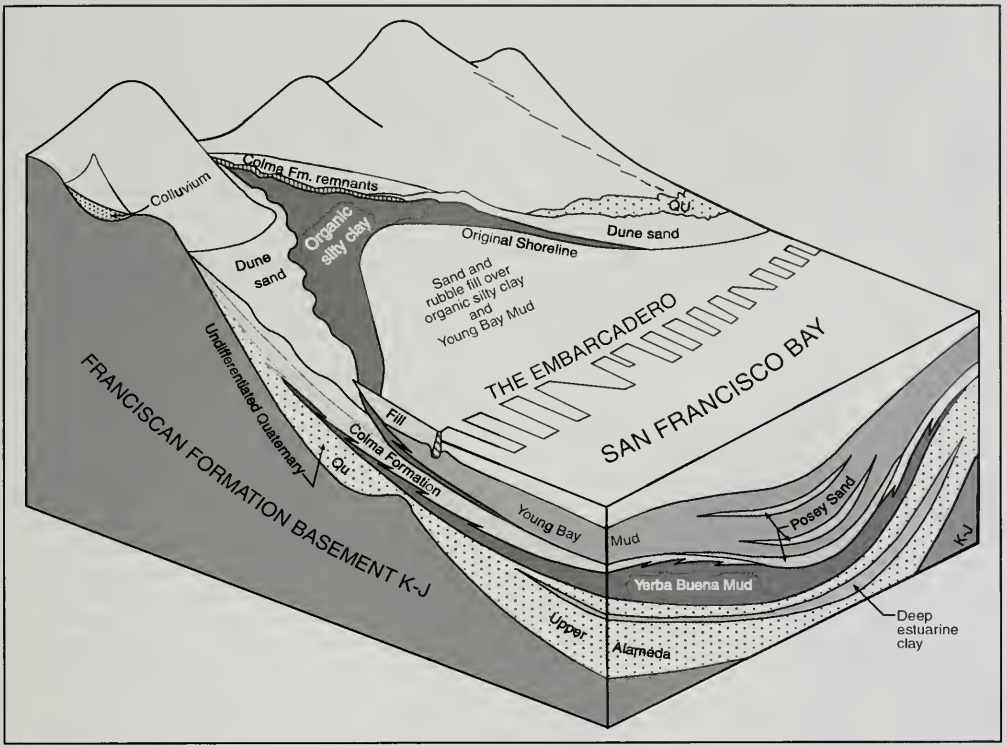

Figure 2. Schematic block diagram looking northwest along San Francisco shoreline, in the vicinity of old Yerba Buena Cove, which was filled between 1849 and 1916. This diagram presents generalized stratigraphic relationships between various units encountered in the foot of the Market Street area.

GEOLOGY OF THE BART ALIGNMENT

Geologic mapping of the area had been undertaken in the decade preceding BART by the USGS (Schlocker et al., 1954, 1958; Schlocker, 1961, 1974; Radbruch and Schlocker, 1958; Bonilla, 1964, 1971) and by CDMG for the newly formed Bay Conservation Development Commission (Goldman, 1969). The geologic conditions beneath BART's San Francisco alignment are highly variable, ranging from soft estuarine clay to massive Franciscan greenstone. Of particular concern were soft ground conditions that would be encountered in the vicinity of the San Francisco Embarcadero, at the foot of Market Street. The original shore of the bay was located at Market and First Streets, six blocks inland (U.S. Coast Survey, 1853). After 1849, shallow embayments, sloughs and inlets were progressively filled, as shown in Figures 1 and 2.

Borrow material for the fill was extracted from numerous quarries along the north and eastern sides of Telegraph Hill and Rincon Hill, a bedrock knob over 100 feet high prior to its excavation following the 1906 earthquake. The "made ground" was accommodated by randomly placing fill on compressible estuarine clay, known as the Young Bay Mud. The lower Market Street area was infamous for its settlement, locally as much as six vertical feet along lower Market Street. The average annual rate of settlement in the lower Market Street fill ranged between 0.02 and 0.8 feet per year between 1865 and 1930 (Whitworth, 1931). The average rate of settlement after 1936 appears to have progressively

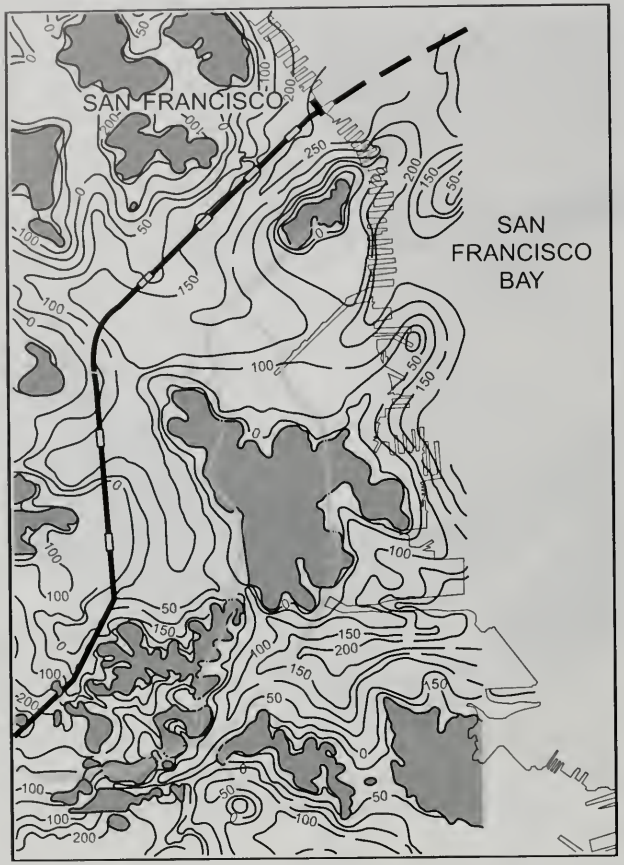

Figure 3. Combination of Schlocker (1974) and Bonilla's (1965) maps showing elevation contours of the top of Franciscan bedrock along the BART alignment between Embarcadero and Glen Park Stations. Elevations are in feet below sea level, with 50-foot contour intervals. Shaded areas are bedrock outcrops that extend above sea level.

diminished, according to data cited by Lee and Praszker (1969) and Helley et al. (1979).

The thickness of the Holocene and late Quaternary sediments infilling the San Francisco Bay depression also varies considerably across the waterfront area, as shown in Figures 3 and 4. Numerous tidal inlets (Figures 2 and 3) cut the original shoreline, many of which overlie deeper channels cut into the underlying Jurassic-Cretaceous Franciscan bedrock. These channels appear to have been excavated during lower sea stands, and extend between 60 and 200 feet beneath current sea level (Bonilla and Schlocker, 1966). A generalized bedrock surface map of eastern San Francisco is included as Figure 3. Bedrock surface maps began to appear in 1908 (Lawson, 1908), and were gradually refined as more data became available (Whitworth, 1931; Schlocker, Radbruch and Bonilla, 1954; Schlocker, 1961; Bonilla, 1965, 1971; and Schlocker, 1974).

The distribution of the late Quaternary fill lying over the Franciscan basement rock was of primary concern to BART, as their tunnels were to be excavated in these materials. Being the most compressible, the Young Bay Mud received considerable attention during the planning stages. Young Bay Mud infills low-lying valleys and ravines excavated during late Pleistocene time, around 11 ka ago. Sea level rose at a rate of 0.14 ft/year between 11 and 9.65 ka; 0.080 ft/year between 9.65 and 8.4 ka; 0.015 ft/year between 8.4 and 6 ka; and about 0.005 ft/year over the last 6 ka (Atwater et al., 1977). A simplified isopach map of the Young Bay Mud in the lower Market Street area, taken from Goldman (1969), is reproduced in Figure 4.

A prominent late Pleistocene unit blanketing much of San Francisco is the Colma Formation of Schlocker et al. (1958), a sequence of locally-derived unconsolidated sands, locally containing beds of clay (between 0.5 and 5 feet thick), that includes a basal layer of poorly sorted gravelly sand. The Colma unconformably overlies the Merced Formation, and is locally covered by dune sand and Young Bay Mud near the bay margins. The base of the formation is mapped at elevations varying between –150 feet (at The Embarcadero) to as much as 550 feet above sea level, near the San Andreas fault. Where exposed above sea level, the Colma beds appear to have accumulated in an extensive complex of shallow bays, inlets, and channels, such as might exist if sea level were 35 to 100 feet higher than present ·

(Schlocker, 1974). However, Rogers and Figuers (1991) suggested that the southwestward-increasing elevation of the Colma beds can be explained by uplift along the east side of the San Andreas fault, as shown in Figure 5. The age of the Colma beds is thought to be between 90 and 100 ka (Schlocker, 1974). Approximately 1 mm/year of vertical uplift (of the 22 mm/year average strike-slip horizontal displacement) could account for 340 feet of uplift, which could be expected to diminish with increasing distance from the fault.

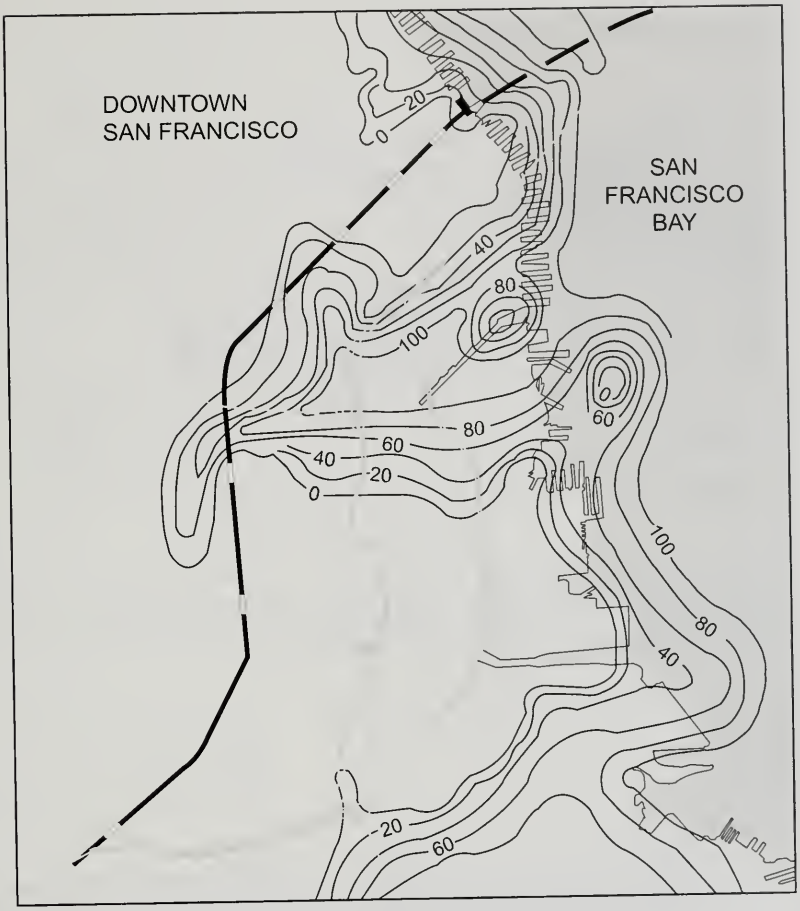

Figure 4. Isopach map of Holocene Young Bay Mud, taken from Goldman (1969). Contour intervals are 20 feet. Note the approximate correlation of lowland depressions infilled during Holocene sea level rise with underlying bedrock depressions depicted on Figure 3.

Figure 6 is taken from Schlocker (1974). It shows the stratigraphic relationships between various late Pleistocene units in the lower Market Street area, roughly parallel to the BART alignment. This can be compared with Figures 7 and 8, which show the distribution of generalized soil types along BART.

BART designers were most concerned about the high groundwater table along the proposed alignment, indicated in Figures 7, 8, and 9. The entire line was excavated below the water table through San Francisco, because of the extensive blanket of unconsolidated sand overlying relatively impervious clays.

MARKET STREET – SAN FRANCISCO TUBE APPROACH TUNNELS

The most challenging segment of the BART underground work was construction of the twin tunnels running between Montgomery Station and the San Francisco Ventilation Structure, through the foot of Market Street (see Figure 1). In this segment BART rises from 85 feet below sea level through Young Bay Mud that reaches a thickness of nearly

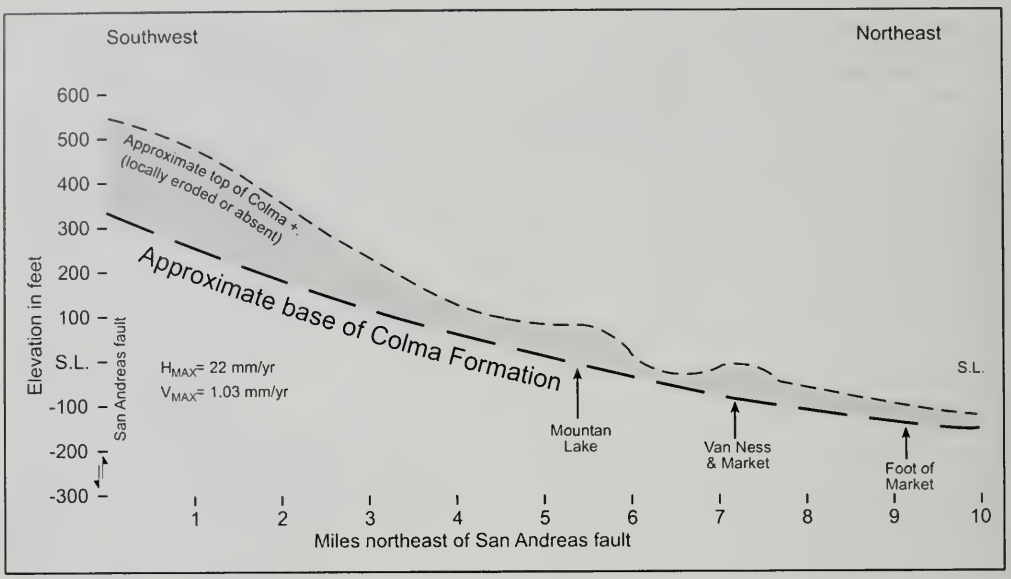

Figure 5. Elevation of Colma beds by 1.03 mm/year ancillary uplift over 100 ka, along the east side of the San Andreas fault, in San Francisco. Such a model might explain the homocline defined by the base of the Colma Formation, which reaches a maximum elevation of 550 feet adjacent to the fault, but dips below sea level in the lower Market Street area.

100 feet (Figure 8). Everyone associated with the project knew this segment would be the most challenging to design and the most expensive to construct.

In the past, tunnels in soft clay had been designed to resist the entire load of soil and water lying above them by brute force. For BART, Peck (1969, 1972) convinced the design team that significant cost savings might be realized by using flexible

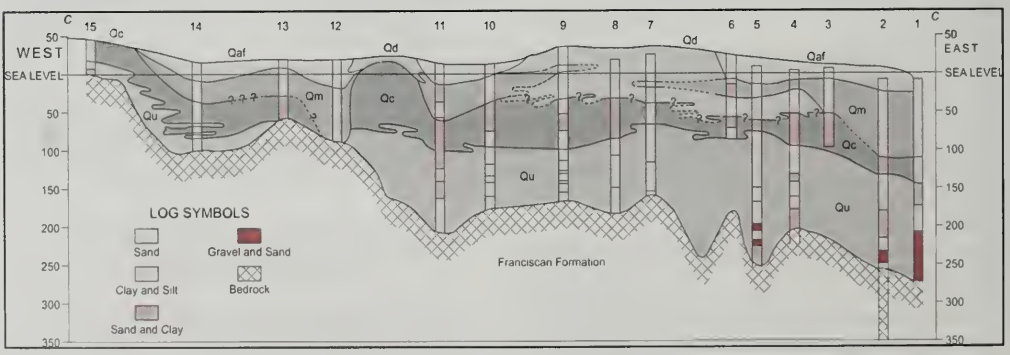

Figure 6. Stratigraphic relationships between Quaternary sediments in downtown San Francisco, taken from Schlocker (1974). This transect parallels lower Market Street as far as 6th St., then diverges southerly, re-connecting with the BART alignment at 20th and Mission St. Qaf is artificial fill; Qd is Holocene dune sand; Qm is Young Bay Mud; the dark unit is Qc, the Colma Formation; and Qu are undivided Quaternary sediments.

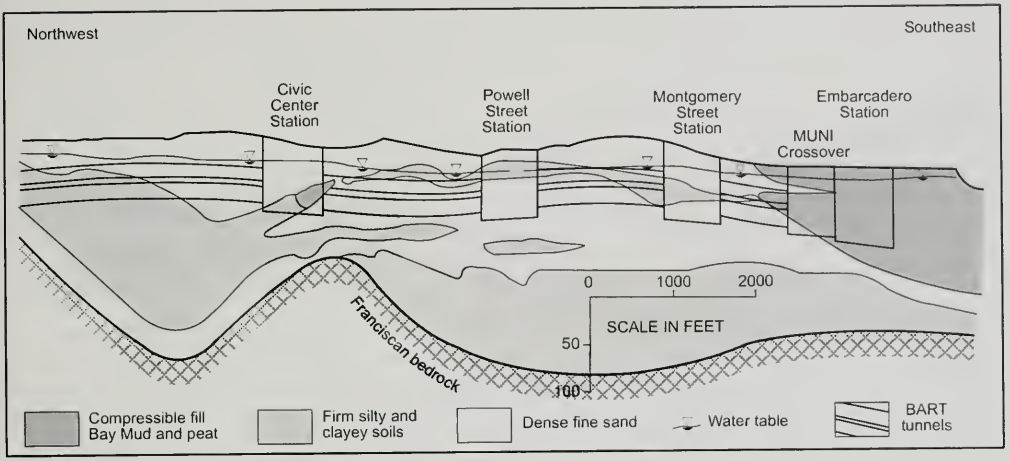

Figure 7. Soil types along the BART alignment in downtown San Francisco, as classified by BART (modified from Kuesel, 1972). Note the differences in subsurface conditions between the Montgomery and Embarcadero Stations, and the relative position of the groundwater table.

circular linings in the soft bay muds, which would distort under unequal external pressures until sufficient passive pressure was mobilized to establish equilibrium.

The prescribed route cut through a maze of timber piles supporting the Ferry Building, the Embarcadero wharf and sea wall, an active railroad, an abandoned underpass, countless utilities and

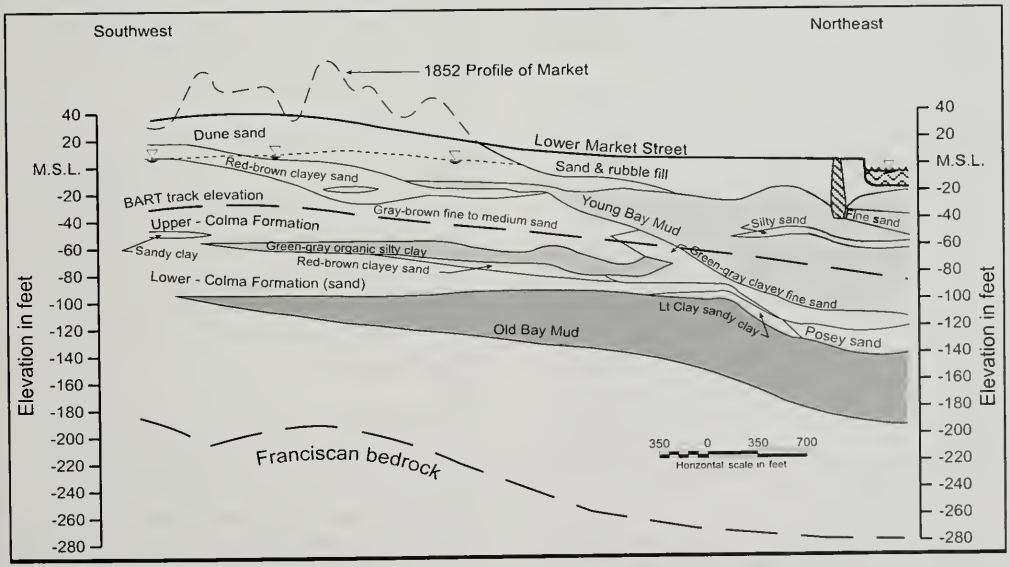

Figure 8. Geologic cross-section of the lower Market Street corridor, modified from Dames and Moore (1964). Note stratigraphic assignments, using Schlocker's (1974) nomenclature (Figure 6).

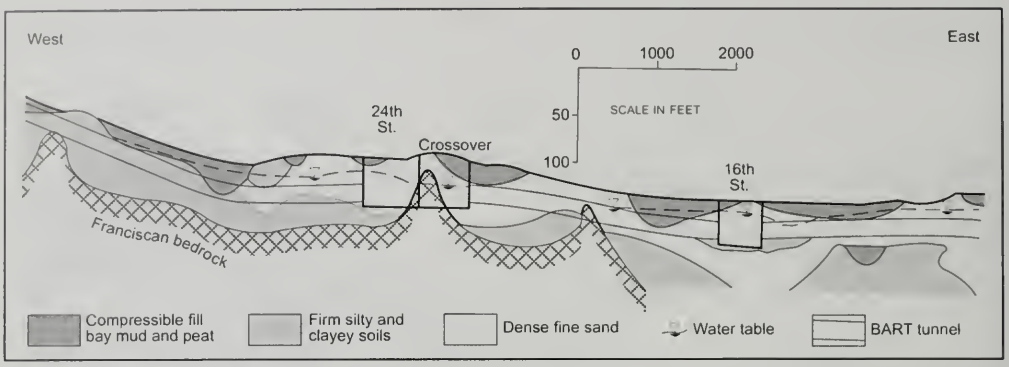

Figure 9. Soil types encountered along the Mission Street line, between Market Street and the Fairmont tunnels (modified from Harding Associates, 1964). These segments were excavated with tunnel boring machines below the water table. Note that Franciscan pinnacles were encountered at the 24th St. Station, between 20th and 21st Streets and at 30th Street. From 29th St. south, the line pierced weathered Franciscan rock, through the Fairmont Hills tunnels (left of this section).

the steel H-piles supporting the old I-480 Embarcadero Freeway (dismantled following the 1989 Loma Prieta earthquake). The 108-foot high San Francisco Ventilation Structure was constructed about 450 feet offshore from the San Francisco Ferry Building to preclude damage to this historic structure from any ground movement that might occur adjacent to the trench excavations for the Trans-Bay Tube.

The contractor used conventional soft ground tunnel shields under air pressure, maintaining a minimum spacing of 300 feet between headings (Peterson and Frobenius, 1971). Special "risk sharing" contractual clauses provided for extra payment for removal of substantial buried obstructions in this segment, such as buried gold-rush era sailing ships and a veritable forest of old timber piles (ENR, 1969b; Kuesel, 1972). The Ferry Building had been underpinned, so the piles were no longer supporting the building, but they were tied to large pedestal footings (Figure 10). These conditions proved nerve-racking for the contractor, who was forced to advance the excavation with shields while probing ahead for old piles, and then use chainsaws to sever the piles 3 to 4 inches above and several inches beneath the shields.

Although the chopped piles extended just 50 feet above the tunnels, the contractor was concerned about their developing negative skin friction in the Young Bay Mud, causing the severed piles to be dragged downward, onto the new tunnel lining. This eventually happened, causing numerous dimples in the steel lining. The contractor had to weld plates and fashion makeshift stiffeners to keep the dimples from proceeding further. The downdrag load on the linings also caused ovaling of the tunnel, which grew to 1.5 percent of the diameter over a period of 5 months. However, redistribution of internal stresses within the clay tended to equalize horizontal and vertical pressures and the ovaling ceased.

During the driving of the first shield, the contractor encountered soft ground sooner than expected, and Tunnel No.1 "holed through" into the offshore ventilation structure ahead of schedule (ENR, 1969a). On the second bore, the contractor installed new mucking equipment that doubled production and changed the excavation procedures, succeeding in sealing off the tunnel at the vent structure in half the time. As a consequence, the second bore was completed three months ahead of the 22 month schedule (ENR, 1969b).

Twenty-five years later, when the San Francisco MUNI turnaround was built across this same foot-of-Market Street area, excavations came within 4 feet of the BART tunnels, but only imperceptible movements were recorded in the tunnels themselves (Hashash et al., 1995). This stellar performance testified to the theories upon which the flexible-lining support system was based.

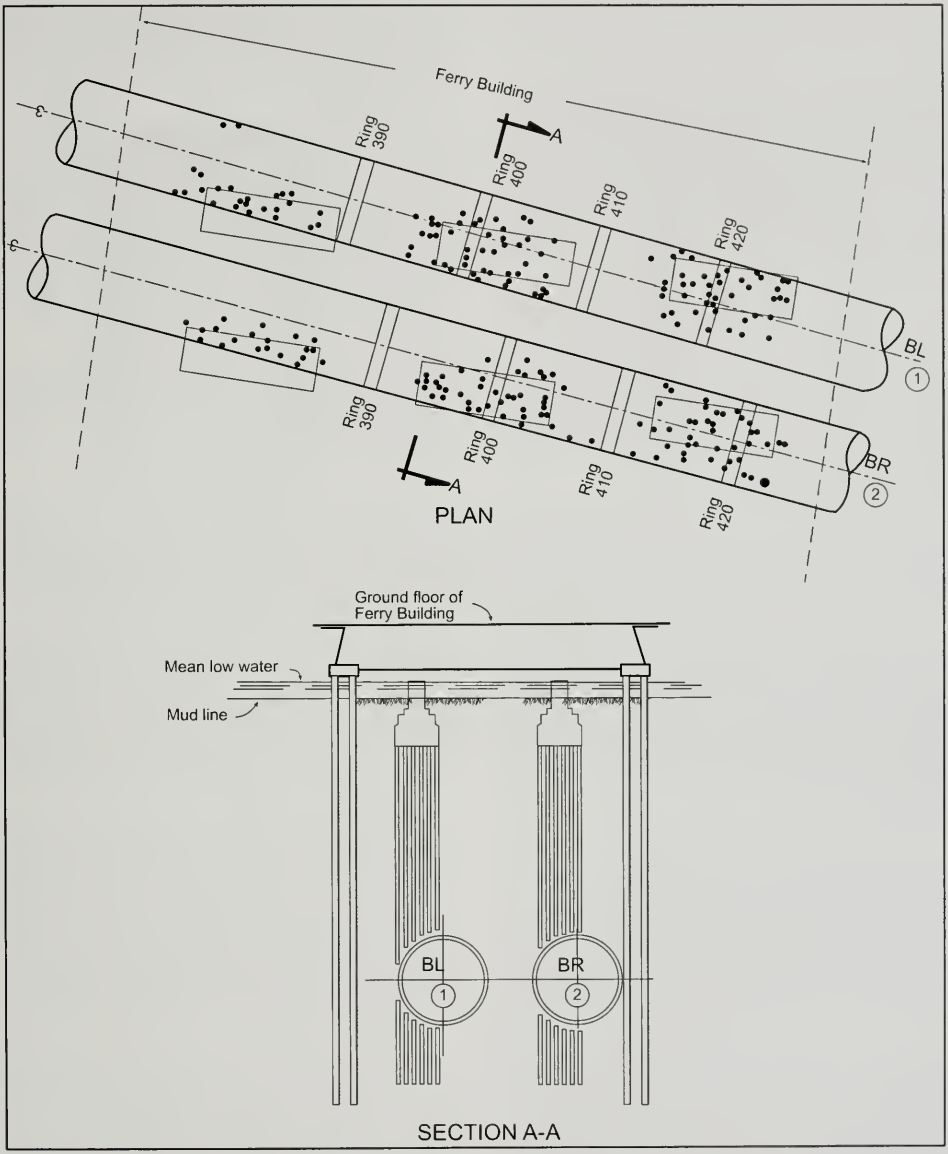

Figure 10. Tunneling conditions for BART beneath the S.F. Ferry Building and Embarcadero, taken from Kuesel (1972). The tunnel crowns were situated 50 feet beneath the base of the old pile cap foundations, shown as rectangles in the upper plan view. The Ferry Building was underpinned (long piles outboard of both tunnels), then the old piles were severed at the indicated positions (black dots).

SPTC WALLS FOR MARKET STREET STATIONS

The excavation that concerned the design team most was Montgomery Street Station, originally slated to be the lowest on the line, within old Yerba Buena Cove. The lower Market Street area had been explored and characterized for BART by Dames and Moore (1964) (Figure 8). The Market Street stations had to be sandwiched between large pile-supported structures while utilities and transportation arteries remained operating.

The Parsons Brinckerhoff-Tudor-Bechtal (PBTB) engineering and construction management joint-venture for BART designed cut-and-cover excavations up to 80 feet deep and 61 feet wide for the Montgomery, Powell and Civic Center Stations (Figures 1 and 7). The stations have double-decked track levels, to accommodate San Francisco's Municipal Railway system (MUNI).

Soldier pile tremie concrete (SPTC) technology had recently been pioneered on the Bank of California building (Gerwick, 1965, 1967). The PBTB design team was impressed by the success of the SPTC support system at the bank site, because it was very rigid and sufficiently watertight to maintain groundwater levels beneath adjacent buildings, thereby restricting construction-related settlement. In mid-1966 the decision was made to implement SPTC support systems on the Montgomery, Powell, and Civic Center Stations. These systems proved very successful.

EMBARCADERO STATION

At the time of the November 1962 bond issue, which funded construction of BART, the Embarcadero Station was not contemplated because the area below Montgomery St. was a warehouse district adjoining the waterfront. Once BART was approved, however, developers bought up the warehouses and began construction of new commercial structures. In November 1967 these interests petitioned the City to build another station, fronting $500,000 for engineering fees to reimburse BART for design of the "Davis Street Station", where the tracks would be 80 feet below street level. In April 1968 the San Francisco Board of Supervisors approved $15 million for the construction of what eventually became Embarcadero Station. Like the other Market Street stations, BART would be accommodated on a lower deck, and MUNI above (Figure 9). The Embarcadero Station would be 700 feet long and 80 feet deep, an unprecedented excavation in the confines of old Yerba Buena Cove, where the Young Bay Mud reaches a thickness of between 80 and 95 feet.

PBTB engineers struggled with the design for adequate temporary support because the safety factor for heave of the floor of the excavation was too low. Engineers debated how to proceed, faced with providing sufficient lateral support to retain 80 feet of Young Bay Mud (Figures 8 and 11). Options, such as progressive excavation, ground freezing, eggcrate slurry walls, and thick mats were discussed and evaluated (Armento, 1973). In the end, the design team opted for using thickened "heave piles", a heroic measure intended to support the adjacent ground through brute strength, because of concerns over claims for causing settlement to adjacent structures lining Market Street.

At the core of the Embarcadero SPTC wall were W36-182 soldier piles with specially fitted circular "pile tips" placed in drilled 36-inch diameter shafts extending 110 feet below grade (Figure 11). In the vertical zones supporting Young Bay Mud, the flanges of the soldier piles were upgraded to W36x300 sections, using flanges reinforced by thickened plates (Armento, 1973). They were the heaviest soldier piles ever used for shoring in San Francisco up until that time and were known as "30-ton piles"—for their individual weight, not their bearing capacity. The piles extended into old bay mud, 55 feet below station platform level (Figures 8 and 11).

The SPTC method used a bentonite mud slurry to support the sides of the caisson holes. Once excavated to the desired depth, 36-inch soldier piles were lowered into the slurry-filled holes and concrete was tremied into the annulus, displacing the bentonite slurry. Once installed, the space between caissons was also excavated with a bentonite slurry, then displaced by tremie concrete, to form walls 3 to 4 feet thick that comprised the SPTC bulkhead.

The funding for the Embarcadero Station came too late for it to be included in the initial phase of subway construction. So, the first phase was limited to constructing the SPTC walls, a concrete invert slab, and sufficient internal structure to accommodate BART trains on the lower track level, providing wooden stairs for access. The SPTC walls remained braced with pipe struts (left half of Figure 11). Two years later, the upper 28 feet of the SPTC wall were demolished to accommodate the mezzanine level of .

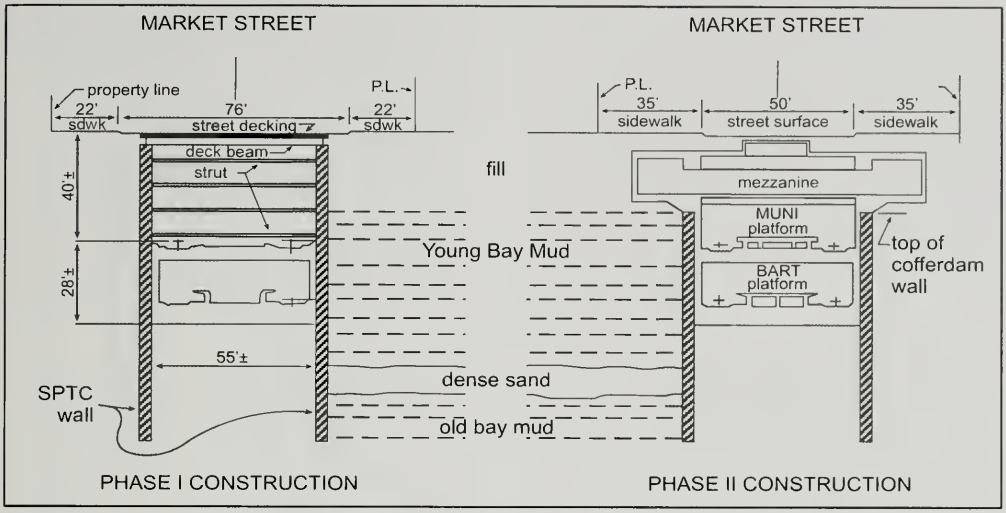

Figure 11. Transverse cross-sections through Embarcadero Station, during Phase I construction (left), which accommodated operations for the first two years, and the Phase II construction (right), when BART and MUNI were completed. This was the deepest and most challenging retained excavation in San Francisco.

the completed stations (ENR, 1974). Permanent concrete walls and floors were then built inside the SPTC structure below –28 feet (right half of Figure 11). The station's interior was constructed between May 1974 and November 1975.

The Embarcadero, Montgomery, Powell, and Civic Center Stations along Market Street were constructed in this manner, using cut-and-cover, with contractor staging on temporary platforms built atop the excavations. Only buses and trolleys were allowed on Market Street during construction, running along either curbside. The lower Market Street stations were constructed between July 1967 and April 1972. Construction staging was alternated from north to south sides of Market during that interim, and the street was re-opened to traffic in February 1973. Work on the MUNI stations began in early 1973 and was completed in 1979.

THE MARKET STREET TUNNELS

All of BART's tunnels were lined with 30-inch wide flexible segmented ring liners, using six semicircular segments and one smaller "key" segment. These segments were fabricated by Kaiser Steel at their Napa facility. This standardized support system was designed as a thin wall flexible lining system (Wolcott and Birkmyer, 1968; Thon and Amos, 1968; Kuesel, 1968, 1972; Bickel et al., 1995). The design team ended up specifying three different thicknesses for their circular steel lining, for differing overburden conditions (3/8 inch, ½ inch and 5/8 inch). The flexible linings were afforded only enough strength to hold themselves up (they could deflect as much as 3 or 4 inches under their own weight when bolted together). Sixtyfour thousand lineal feet of 18-feet diameter shield-driven tunnels were lined in this manner during construction of BART. As the mined ground relaxed behind the liner plates and deflected to spread the load, contractors had the option of packing the annulus between the plates and ground with pea gravel or cement grout (Peterson and Frobenius, 1971).

Three tunnel contracts were let along Market Street to connect the BART/MUNI stations. Each contract required excavation of four tunnels on two levels, up to 70 feet deep (Figure 12), between 720 and 1,890 feet long. In February 1969 Morrison-Knudsen was given the contract for the shortest segment and the shell excavation for Embarcadero Station. At Powell St. Station, five streets converge and the famed Powell St. cable car line terminates.

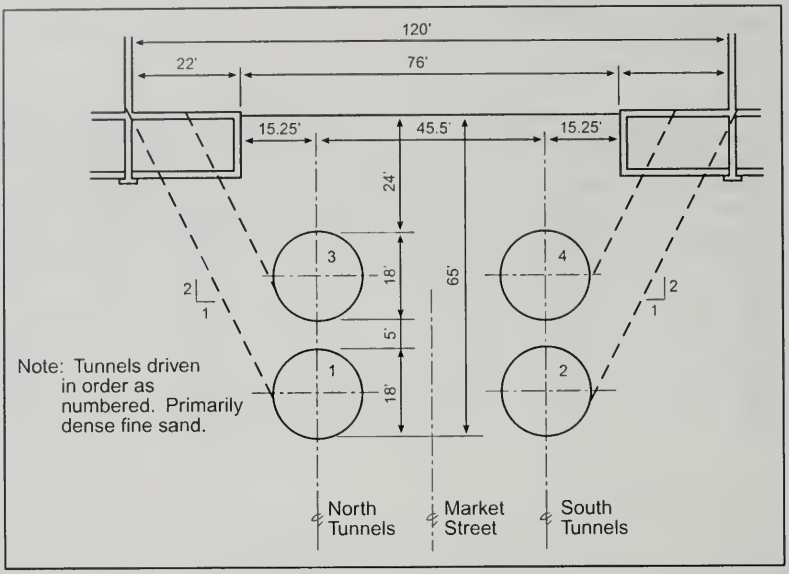

Figure 12. Spatial relationships between the twin MUNI and BART tunnels that ran two miles beneath lower Market Street, between The Embarcadero and Van Ness. Note proximity of the bores to the sidewalk basements, lining either side of Market Street.

In 1970, Delaware Vianini Memco Corporation (DVM) was awarded the contract for the 1,890-foot segment between the Powell and Civic Center Stations (Figure 7). DVM chose to employ a hydraulically operated tunnel boring machine (TBM) with a 3-foot diameter central cutting wheel and wedge-shaped blade openings, that could extend between 3 inches and 3 feet in width, depending on the softness of the ground encountered. PBTB recommended that the 17.5 feet diameter bores be driven under 10 to 12 psi air pressure because of the high groundwater table in poorly graded sand and clay (Kuesel, 1972).

Like the lower Market tunnels, working room was extremely limited, and the contractor was confined to a 50 by 75 ft shaft to service all four bores. DVM developed a specialized 60 cubic yard muck car, 41 feet long, that could be passed through an oversized air lock. The 60-yard muck car could accommodate material from two 2.5-feet advances of the TBM. The muck car dumped its load into a 60-yard capacity bottom dump hopper, situated at the base of the access shaft. For bottom dumping of the muck into dump trucks, DVM then placed a rail-mounted 200-ton gantry crane over the shaft opening, that could lift the bottom dump hopper and move 100 feet away from the shaft.

DVM's progress on these tunnels, using their TBM, was impressive, boring through 1,300 feet in 17 working days, with 107 feet in their best single day (ENR, 1971). DVM drove three of the four tunnels under air pressure, then convinced BART to share the savings by driving the last bore without air pressure. The average rate of advance under air was about 40 feet per day, and 55 to 60 feet without. When the TBM ran into soft ground, they closed the wedge-shaped blade openings down to about 3 inches, thus preventing overbreakage. Maximum overhead subsidence along Market Street above this segment was only 5/8 inch.

CIVIC CENTER STATION

The station farthest up Market Street was at Civic Center, between 7th and 8th Sts. Like the others, it was 740 feet long, 60 to 99 feet wide, and up to 78 feet deep (ENR, 1968). The buildings along either side of Market Street were 120 feet apart. The Mission Bay estuary originally extended to within 250 feet of the excavation (outline shown on Figure 1,

taken from the US Coast Survey, 1853). About 10 feet of brown compressible peat and organic silt were encountered at the east end of the excavation (Thon and Harlan, 1971).

The depth to the water table varied between 12.5 feet at the east end and 22 feet at the west end of the excavation (Figure 7). A key aspect of the station excavation would be maintaining groundwater at pre-construction levels outside the excavation in order not to trigger construction-related settlements. Several structures south of the station had registered settlements of as much as 8 feet in the old Mission Bay fill.

A comprehensive geotechnical sampling and lab testing program focused on evaluation of overconsolidation (since considerable sand had been excavated off the site in the 1850's and '60s) and special at-rest earth pressure (K_o) tests. The sands exhibited average K_o values of 0.34 and silty clays had characteristic values of 0.36 to 0.45 (Thon and Harlan, 1971). An overall average at-rest soil pressure of 0.45 with full hydrostatic pressure below the water table was assumed for design of the SPTC walls, which would be braced (restrained) excavations.

Thirtysix-inch thick SPTC walls were utilized with 36WF x160 H-beams. These were extended to a depth of approximately 103 feet below street level. Twentyfour-inch thick SPTC walls were used outside the 36-inch walls in the mezzanine area, which was 98 feet wide, 10 feet below the street. Three levels of cross-struts were provided, with a minimum vertical gap of 15 feet. The three permanent floors for the station were constructed between these struts, similar to the configuration shown in Figure 11. Strut loads measured during the excavation sequence described a trapezoidal apparent earth pressure distribution, similar to that predicted by Terzaghi and Peck (1967) from their measurements on the Chicago Subway.

A problem common to all the station excavations was groundwater control within the excavation, while maintaining pre-construction levels outside the excavation in order to avoid basal heave of the excavation floor. The outside groundwater levels were maintained through recharge wells, extending into three different sand layers. Despite these precautions, the water level dropped 15 feet in the upper (dune) sand layer during construction (Thon and Harlan, 1971). Inside the station, basal heave was controlled by pumping groundwater down to a level at least 15 feet below the floor of the excavation, with uplift relief wells being extended 30 feet below the excavation floor. The floor of the excavation was in clayey silt. The maximum settlement observed around the excavation was 0.75 inches. Of 35 benchmarks, 16 settled between 0.50 and 0.75 inches, 12 settled 0.25 to 0.50 inches, and 7 recorded drops of less than 0.25 inches. These diminutive settlements attested to the success of the watertight SPTC support system when working up to 65 feet below the water table.

CIVIC CENTER TO 16TH STREET TUNNELS

At Van Ness and Market, the BART and MUNI systems diverge, with BART turning south, along Mission Street (see "transition" in Figure 1). The 5,120-foot long segments between the Civic Center and 16th Street Stations were excavated as twin tunnels with TBMs. These 93-ton TBMs were 18 feet in diameter and capable of developing 1.7 million ft-lbs of torque on the cutting heads. They used 1-inch thick steel plates, employing a closed face, with four hydraulically operated doors. The doors had cutting edges that scraped soil off the face as the head rotated up to 4 revolutions-per-minute. The TBMs were advanced in increments of 2.5 feet, using twenty-nine 115-ton hydraulic jacks (ENR, 1967; Peterson and Frobenius, 1971).

The 16th Street tunnels were 40 to 80 feet deep, cutting through alluvial deposits dominated by fine sand, but including clayey and silty sand as well, as depicted in Figures 7 and 8. Several pockets of silty clay were avoided. The biggest concern prior to excavation was with dewatering, because the entire alignment would be below the water table (Figure 8). The contract allowed two methods of controlling groundwater: by means of deep wells or by using compressed air inside the tunnel. The contractor elected to use both methods, with varying degrees of success. Those sections excavated using 12 psi compressed air tended to record less settlement. A length of 12,841 feet of tunnel was excavated under air pressure, while a length of 6,215 feet was driven under free air.

To fill the annular space between mined ground and the tunnel lining plates, the contractor was given the choice between using a one-shot cement grout or air-blown pea gravel, followed by grouting at a later date. Neither system proved entirely successful, as grout leaked out of the liners, and the

pea gravel squeezed into the surrounding ground, requiring additional grouting later.

Of great concern to area residents was ground settlement, because the line curved beneath several blocks of existing structures (shown as the "transition" in Figure 1). Where the tunnels were driven in free air, the settlement due to dewatering was between ½ and ¾ inches, and the passing of the tunnels added another ¼ inch of movement directly over the tunnels. Where the tunnels were driven under compressed air, settlements were usually under 3/8 inch (Kuesel, 1972).

One of the problems encountered with the TBM was the inability of the operator to "see" the ground he was excavating. When the cutting head encountered moist sandy soil, the effective cohesion diminished with increasing disturbance and the overlying ground began to run into the face of the TBM, causing excessive settlements and, in some cases, sinkholes above the tunnel. This was the only location in San Francisco where caving to the ground surface actually occurred. Checks were subsequently developed to prevent over-excavation by comparing rates-of-advance to volume of mucked material. These sorts of comparisons are now commonplace. Tunneling rates of up to 70 feet advance in 24 hours were recorded on these segments, with an average rate of advance of 150 feet per 5-day work week. General aspects of construction of the north 16th Street tunnels are described in Thon and Amos (1968).

THE MISSION STREET STATIONS

The 16th and 24th Street Stations were constructed as cut-and-cover excavations because, unlike the stations on Market St., these pierced more sandy materials. This change in geology accommodated less expensive support methods. After installation of perimeter dewatering wells, the contractor pre-drilled holes for soldier piles. Steel soldier piles were then inserted in the holes and filled with lean concrete. After excavating a shallow ditch between the soldier piles, steel girders were placed between them to support a temporary deck for the street. Excavation then proceeded, beneath the timber street deck. During excavation the contractor saved time by welding anchors to the soldier piles to attach "contact lagging" (lagging is usually placed within the webs of the soldier piles). Two sets of internal pipe struts were used to brace the excavation, one at –30 feet, and another between –47 and –50 feet (below street level). At one end, tiebacks had to be used to provide construction access. The station excavations were 750 feet long, 54 feet wide and 47 to 50 feet deep (ENR, 1969c).

MISSION STREET TUNNELS SOUTH OF 16TH STREET

Twin tunnels were excavated down Mission Street, between the 16th and 24th Street Stations (3,470 feet long), and between 24th and Randall Streets (4,550 feet long) (Figures 1 and 12), with a Calweld oscillating TBM, the only such device used on BART. The oscillating TBM employed four independently activated cutter blades, each covering a quadrant of the tunnel face, sweeping back and forth, like windshield wiper blades. Each blade was powered by two rams with a 15-inch stroke. The machine was advanced by means of 20 shove jacks, moving forward in increments of 2.5 feet. These machines were designed for excavating more blocky ground, but fared very well in the loose alluvial materials (Peterson and Frobenius, 1971). One lasting conclusion from these contracts was the appreciation that TBM-excavated tunnels were advanced at a rate 60 percent faster than equivalent hand-excavated bores, even in soft soil conditions. Because of this success, TBMs gradually gained favor.

THE FAIRMONT HILLS TUNNELS

The only rock tunnel contract in San Francisco was the 3,450-foot long Fairmont Hills Tunnels, between Randall Street and Glen Park Station. The route lay beneath the sloping face of the San Miguel Hills, beneath Chenery Street and parallel to San Jose Avenue. This alignment cuts through Franciscan strata of varying hardness, including sandstone, chert, greenstone, sheared shale, serpentine and silica-carbonate rock, with up to 140 feet of cover (Bonilla, 1971). "Greenstone" was a catch-all term used at the time to describe various types of extrusive volcanic rocks that have undergone low-temperature high-pressure metamorphism along the subducting continental margin. This unit varied in consistency from light-green tuff to dark-green porphyritic basalt.

A TBM was unexpectedly used to bore these tunnels as a result of PBTB's introducing "value engineering", a concept that allows the contractor to share in the profits of alternative designs or construction procedures that reduce the estimated construction costs (Kuesel, 1969). Because of the variability of rock types and the massive nature of

the greenstone, PBTB engineers had assumed that TBMs would hamper progress of the overall project, and had specified conventional drill-and-blast methods for this contract. After considering the number of existing structures lying above the proposed alignment, the absence of any major faults, and the moderate overburden, the contractor offered a reduction of several hundred-thousand dollars for approval of a TBM, based in large part on fears of residential damage claims ascribable to blast vibrations. By reducing this potential, a sizable contingency was also reduced in terms of cost and time to completion. The excavation contractor proposed using a Jarva Mk. I TBM equipped with rock-bit cutter heads (Construction Methods, 1970), and work commenced in July 1967.

The tunnels were dug from a shaft excavated near the intersection of Randall Street and San Jose Avenue, where thin alluvial deposits overlie the Franciscan bedrock. The first 180 feet of both tunnels were excavated by conventional techniques, in order to acquire the requisite space to set up the Jarva TBM. The rough bores were circular, and 20 feet in diameter. The only problems occurred while cutting through serpentinite and silica-carbonate rocks, although the hardness of some of the greenstone also stymied the TBM rate of advance. Completely sheared and crushed serpentinite also caused some delays, because of severe overbreakage and binding.

One of the surprises were mud-filled cavities found in the silica-carbonate rocks, described by Chandler (1969). Occasionally, these cavity fillings would drop into the tunnel behind the TBM, necessitating crib support. Water inflows throughout the tunnels were low and tended to decrease with time, but a seasonal fluctuation was noted (Chandler, 1969). The more or less continuous inflow emanating from the sheared serpentinite hampered tunneling progress. Circular steel support sets were placed behind the TBM, spaced 2 to 4 feet apart throughout the tunnels. With the exception of the sheared serpentinite, no obvious loading was noted on the sets prior to lining. The TBM was able to move through differing rock types and ground conditions, encountering rock with compressive strengths between 1,000 and 40,000 psi (Construction Methods, 1970). The TBM advanced between 5 and 109 feet per day, with a maximum weekly advance of 389 feet. Overall, everyone was pleased, especially BART's insurance carrier.

GLEN PARK STATION

The Glen Park Station lies at the south end of the Fairmont Hills tunnels, adjacent to I-280 (Figure 1). Excavation for this station was extensive, measuring 750 feet long, 45 feet wide, and extending 75 feet below original ground surface. The excavation penetrated artificial fill, estuarine marine clays, colluvium, Colma Formation sands, and weathered Franciscan Formation. Toward the south end of the station, the excavation bottomed in the iron-stained Colma sands, which became increasingly indurated with depth. The remainder of the excavation floored in Franciscan units.

H-piles with wood lagging, spaced 8 feet apart, provided temporary support. The narrow character of the excavation lent itself to the use of interior bracing, using 20-inch diameter steel pipe struts. The station was excavated with ripper-equipped bulldozers. During construction, some instability of the temporary support occurred near the northern end (in sheared Franciscan material), and this was controlled by placing a concrete thrust block at the base of the opposing face, and installing raker struts. A minor slope failure also occurred towards the south end, in the Colma Formation, adjacent to Joost Avenue. Traffic vibrations were believed to have been partly responsible for the apparent loss of cohesion of the Colma beds (Chandler, 1969).

SUMMARY AND CONCLUSIONS

Eight tunnel segments and seven cut-and-cover station excavations comprised the 5.6-mile route between the San Francisco Ventilation Structure and Colonial Way, just south of I-280. All of this work was completed on time and within budget, largely because of superior management practices, including value engineering, and because most of the work was completed by late 1971, ahead of the ensuing inflation that caused BART so many financial problems between 1971 and 1975.

The successful excavation of two sets of dual tunnels up Market Street and major excavations for stations in soft ground were unprecedented at the time. BART represented the first rapid transit project in which TBMs were employed successfully, in every instance. BART began running trains between Daly City and Montgomery Street Stations in November 1973, with connecting service to the East Bay beginning in September 1974. The completion of Embarcadero Station in November 1975 was

the last segment of the original 75-mile long BART system. The BART line through downtown San Francisco has performed admirably, a testament to the foresight employed in laying out California's first rapid-transit system. Many subsequent systems have benefited from the lessons learned on BART, especially in design of flexible linings for soft ground conditions (Peck, 1969, 1972; Kuesel, 1972).

ACKNOWLEDGEMENTS

In preparing this synopsis the writer is indebted to information provided by Ben C. Gerwick, Jr., Richard C. Harlan, Thomas R. Kuesel and Ralph B. Peck. Earl Brabb, Ed Clifton, Walt Hensolt, Doris Sloan and the late Clyde Wahrhaftig provided helpful discussions regarding the geology of the bay margins. Tom Kuesel, Chuck Taylor, Steve Klein, Victor Romero, Horacio Ferriz and Steve Stryker kindly reviewed the manuscript and provided helpful suggestions.

SELECTED REFERENCES

Armento, W. J., 1973, Cofferdam for BART Embarcadero subway station: Journal of the Soil Mechanics and Foundations Division, American Society of Civil Engineers, v. 99, no. SM10 , p. 727-744.

Atwater, B.F., Hedel, C.W., and Helley, E.J., 1977, Late Quaternary depositional history, Holocene sea level changes, and vertical crustal movement, Southern San Francisco Bay, California: U.S. Geological Survey Professional Paper 1014, 15 p., plates.

Bickel, J.O., Kuesel, T.R., and King, E.H., 1995, Tunnel engineering handbook, 2nd Ed.: Chapman & Hall, 379 p.

Bonilla, M.G., 1964, Bedrock surface map of the San Francisco South quadrangle, California: U.S. Geological Survey Miscellaneous Field Studies Map MF-334 and ABAG Basic Data Contrib. 26.

Bonilla, M.G., 1971, Preliminary geologic map of the San Francisco South quadrangle and part of the Hunter's Point quadrangle, California: U.S Geological Survey Miscellaneous Field Studies Map MF-311 and ABAG Basic Data Contribution 29 (originally released as a USGS OFR in 1965 at 1:20,000).

Bonilla, M.G., and Schlocker, J., 1966, Field trip San Francisco Peninsula: *in* Bailey, E.H. (ed.), Geology of Northern California: California Division of Mines and Geology Bulletin 190, p. 441-452.

Chandler, R. R., 1969, Field trip 4 - Bay Area Rapid Transit System: Field Trips, National Meeting, Association of Engineering Geologists, San Francisco, October 21-25, p. D-1 – D-7.

Construction Methods, 1970, Tunneling rig takes on drill-and-shoot operation: Construction Methods, v. 52, no. 3, p. 76-79.

Dames and Moore, 1964, Soil investigation S702 San Francisco-Market: Consultant's report to Parsons Brinkerhoff-Tudor-Bechtel, Aug. 28, 1964, 31 p., 57 plates.

ENR (Engineering News Record), 1967, Mole pushed BARTD underground: McGraw-Hill, v. 179, no. 5 (August 3, 1967), p. 43.

ENR (Engineering News Record), 1968, Slurry walls protect subway station: McGraw-Hill, v. 181, no. 2 (July 11, 1968), p. 44-45.

ENR (Engineering News Record), 1969a, BARTD closes Bay Tube and gets rescue funds: McGraw-Hill, v.182, no. 15 (April 10, 1969), p. 62.

ENR (Engineering News Record), 1969b, Transit tunnel runs obstacle course: McGraw-Hill, v.183, no. 1 (July 3, 1969), p. 22-23.

ENR (Engineering News Record), 1969c, Struts clear way for stations: McGraw-Hill, v.183, no. 4 (July 24, 1969), p. 30-32. (16th & Mission and 24th & Mission St. Stations).

ENR (Engineering News Record), 1971, Big gear mucks bores through mini shaft: McGraw-Hill, v.186, no. 2 (January 14, 1971), p. 30.

ENR (Engineering News Record), 1974, BART demolition job damages piles: McGraw-Hill, v.192, no. 3 (January 17, 1974), p. 16.

Gerwick, B. C., Jr., 1965, Excavation is shored in a new way: Western Construction News, v. 43, no. 8, p. 47.

Gerwick, B.C., Jr., 1967, Slurry-trench techniques for diaphragm walls in deep foundation construction: Civil Engineering, v. 37, no. 12, p. 70-72.

Goldman, H.B. (ed.), 1969, Geologic and engineering aspects of San Francisco Bay fill: California Division of Mines and Geology Special Report 97, 130 p., 4 pl.

Hashash, Y.M.A., Schmidt, B., and Abramson, L.W., 1995, BART tunnel monitoring during MUNI construction: Geotechnical News, v. 13, no. 2, p. 33-36.

Helley, E.J., Lajoie, K.R., Spangle, W.E., and Blair, M.L., 1979, Flatland deposits of the San Francisco Bay region, California – Their geology and engineering properties, and their importance to comprehensive planning: U.S. Geological Survey Professional Paper 943, 88 p.

Kuesel, T. R., 1968, Structural design of the Bay Area Rapid Transit System: Civil Engineering, American Society of Civil Engineers, v. 38, no. 4, p. 46-50.

Kuesel, T.R., 1969, BART subway construction: Planning and costs: Civil Engineering, American Society of Civil Engineers, v. 39, no. 3, p. 60-65.

Kuesel, T. R., 1972, Soft ground tunnels for the BART project: Proceedings of the North American Rapid Excavation and Tunneling Conference, Chicago, v. 1, p. 287-313.

Lawson, A.C. (ed.), 1908, Atlas of maps and seismograms accompanying the report of the State Earthquake Investigation Commission upon the California earthquake of April 18, 1906: Carnegie Institute of Washington, Pub. No. 87, v. 2, Carnegie Institute, (Washington, D.C.) (reprinted 1970).

Lee, C.H., and Praszker, M., 1969, Bay mud developments and related structural foundations: *in* Goldman, H.G. (ed.), Geologic and Engineering Aspects of San Francisco Bay Fill: California Division of Mines and Geology Special Report 97, p. 41-86.

Peck, R.B., 1969, Deep excavations and tunneling in soft ground: Proceedings of the 7th International Conference on Soil Mechanics and Foundation Engineering Geology, Mexico City, State-of-the-Art volume, p. 225-290.

Peck, R.B., 1999, Six decades of subway geo-engineering: The interplay of theory and practice: *in* Fernandez, G. and Bauer, R.A. (eds.), Geo-engineering for underground facilities, American Society of Civil Engineers Geotechnical Special Publication 90, p. 1-15.

Peck, R.B., Hendron, A.J., and Mohraz, B., 1972, State of the art of soft-ground tunneling: 1972, deep excavations and tunneling in soft ground: Proceedings of the North American Rapid Excavation and Tunneling Conference, Chicago, v. 1, p. 259-286.

Peterson, E., and Frobenius, P., 1971, Soft-ground tunneling technology on the BART project: Civil Engineering, American Society of Civil Engineers, v. 41, no. 10, p. 72-76.

Radbruch, D.H., and Schlocker, J., 1958, Engineering geology of the Islais Creek Basin, San Francisco, California: U.S. Geological Survey Miscellaneous Geologic Investigations Map I-264.

Rogers, J.D., and Figuers, S.H., 1991, Site stratigraphy and near-shore development effects on soil amplification in the Greater Oakland Area: *in* Baldwin, J.E. and Sitar, N. (eds.), Loma Prieta earthquake: Engineering geologic perspectives, Association of Engineering Geologists, Special Publication No. 1, p. 123-149.

Schlocker, J., 1961, Bedrock-surface map of the San Francisco North quadrangle, California: U.S. Geological Survey Miscellaneous Field Studies Map MF-334 and ABAG Basic Data Contrib. 26.

Schlocker, J., 1974, Geology of the San Francisco North quadrangle, California: U.S. Geological Survey Prof. Paper 782, 109 p., 3 pl.

Schlocker, J., Radbruch, D.H., and Bonilla, M.G., 1954, Preliminary bedrock-surface map of the San Francisco City area, California: U.S Geological Survey Open File Report, 1:24,000.

Schlocker, J., Bonilla, M.G., and Radbruch, D.H., 1958, Geology of the San Francisco North quadrangle, California: U.S Geological Survey Miscellaneous Geologic Investigations Map I-272.

Taylor, C.L. and Conwell, F.R., 1981, BART - Influence of geology on construction conditions and costs: Bulletin of the Association of Engineering Geologists, v. 18, no. 2, p. 195-205.

Terzaghi, K. and Peck, R.B., 1967, Lateral supports in open cuts: *in* Soil Mechanics and Engineering Practice, 2nd Ed., John Wiley & Sons, (New York, New York), p. 396-403.

Thon, J. G. and Amos, M. J., 1968, Soft-ground tunnels for BART: Civil Engineering, American Society of Civil Engineers, v. 38, no. 6, p. 52-55.

Thon, J.G., and Harlan, R.C., 1971, Slurry walls for BART Civic Center Subway Station: Journal of the Soil Mechanics and Foundations Division, American Society of Civil Engineers, v. 97, no. SM9, p. 1317-1334.

U.S. Coast Survey, 1853, [Map of] City of San Francisco and its vicinity, California: [topographic map, contour interval 20 feet] scale 1:10,000.

U.S. Coast Survey, 1869, San Francisco Peninsula: [topographic map, contour interval 20 feet], scale 1:40,000, reprinted by NOAA National Ocean Service [1969], Map BiC-32.

Western Construction, 1973, Bay Area Rapid Transit – A special issue: Western Construction, v. 48, no. 4, p. 27-72.

Whitworth, G.F. (ed.), 1931, Subsidence and the foundation problem in San Francisco: Report of the Subsoil Committee, San Francisco Section, American Society of Civil Engineers, 107 p.

Wolcott, W. W. and Birkmyer, J., M., 1968, Tunnel liners for BART subways: Civil Engineering, v. 38, no. 6, p. 55-59

INTRODUCTION TO THE RESIDENTIAL SECTION

ROY C. KROLL[1]

No other aspect of engineering geology directly impacts the everyday life of John Q. Public more than residential development. Soft soils, hard rock, seismic hazard, slope stability, drainage issues, paleontological resource constraints, differential foundation conditions, frost heave, and even onsite sewage disposal in rural areas can all dramatically make the average homeowner suddenly aware of the realities of residing in the complex geologic setting of Northern California. Although many of these geologic engineering issues are addressed upfront by the developer in modern subdivisions, older homes and residential facilities built before the current codes and state-of-the-practice evolved are vulnerable to geologic impacts long after initial construction. Additionally, many master developers in hillside communities are now opting to record specific plans and put in the backbone infrastructure—roads and utility mainlines—only, leaving specific improvement details for individual lots or parcels to custom home merchant builders. Although typically well versed in the custom home construction process, many custom builders address only the minimum building code requirements in the design process. Design modifications that arise in the course of regulatory review, or remedial design instigated by home-owner complaints, are often all that motivates the custom builder to address engineering geology issues.

This section contains five papers that discuss the effects of various geologic constraints on residential development and improvement, varying in locale from the San Francisco Bay area to the Sierra foothills and beyond to the mountainous environment of the Lake Tahoe basin. As the cost of residential development continues to rise, the consequences of failing to adequately address geologic engineering issues can have enormous emotional and financial impacts on the involved parties. The goal of this set of papers is to expose the practicing engineering geologist to the various technical, logistical, regulatory, client, homeowner, and cost issues that he or she may face in the course of a residential project, and to suggest various approaches currently available for "walking the tightrope".

Until relatively recently, large-scale hillside developments in hard rock terrain were common only in the Southern California housing market due to comparatively high real estate values. As high technology companies have become established in Northern California, however, the housing needs of their work forces have brought property values up, making hard rock hillside development viable. Oliveira et al. (2001) provide a comprehensive overview of the 1,600 acre Empire Ranch project in Folsom, Sacramento County, developed on a hillside underlain by metavolcanics. Hard rock excavation was only one of many issues that had to be addressed during the design and construction phases. A teamwork approach to solutions was needed to deal with subsurface water migration through the fractured bedrock, placement of oversize rock materials, and layout of utility lines. The client, civil engineer, engineering geologist, and contractor had to coordinate their efforts and expertise at a rather high level. And of course the homebuyer had to be kept foremost in mind. Many homebuyers would no doubt be unfamiliar with hard rock terrain, so the master developer and the engineering geologist collaborated on an open "Dear Homebuyer" letter to convey to the residents, in plain language, the best way to make use of their property. This letter will be included in the homebuyer packets of the various merchant builders, and conveys the notion that grass lawns and hot-tubs will have to take the place of trees and swimming pools.

[1]Youngdahl Consulting Group
1234 Glenhaven Court
El Dorado Hills, CA 95762
mail@youngdahl.net

Sometimes the value of residential property is so high that severe engineering geologic constraints are addressed in spite of the financial consequences. Godwin and Korbay (2001) discuss such a project, in their case study of the student housing complex that was eventually built on a portion of the Berkeley campus of the University of California that is cut by the Hayward fault zone. Seismic hazards, landslide remediation, slope stability, subsurface hydrostatic conditions, ground shaking, and differential settlement all had to be addressed at a level not normally applied to typical residential development. The reader will no doubt find their solutions instructive and provocative, as the Hayward fault may someday put their project to the test.

The paper by Reynolds (2001) is a clear and useful examination of the challenge that development poses to the preservation of paleontological resources. So the contractor has just uncovered a woolly mammoth fossil during the height of earthwork on *your* very exclusive, high-profile development project? Now what do you do? This paper will be invaluable when the time comes and you need to advise your client, know who to call, or decide how to proceed. There is a happy medium between resource conservation and development, and this paper will show you, the consultant, how to balance the two.

Yes, we all know it flows downhill! Franks (2001) paper reveals, however, that much more happens to sewage in the onsite disposal process. The paper explores the roots of sewage disposal practices, and briefly chronicles how we got to where we are today in the design and regulatory process. Because of our patchwork quilt by county design ordinances for onsite sewage disposal, the process can be somewhat daunting to the engineering geologist on his or her first such project. This is one of the fields where we co-exist with the sanitary engineers and hygienists, so qualitative evaluation has given way to quantitative measurements. In addition to the basic geology, the consulting geologist must determine seasonal depth to water, thickness of the soil layer, grain size and distribution of the vadose zone soils, slope of land surface, percolation rate of the soils in the disposal area, hydraulic gradient within the aquifer, and location of nearby wells and springs. This informative paper will show you why the engineering geologist is the best professional to handle this stage of the design process.

Proper foundation design is essential to the long-term stability and functionality of a residential structure. Joslin et al. (2001) discuss the challenges of foundation design in the Sierra Nevada. Dealing with subsurface water seepage and adequately accounting for the various paths it may take in a residential development in mountainous terrain is essential to the long-term functionality of the design. The authors provide a valuable compilation of the various subsurface water conditions and pathways that need to be considered and addressed when consulting on residential development projects above the snowline. Frost heave and damming brought on by foundation improvements can lead to distress and even slope instability. The authors bring their experience to bear and summarize their solutions to these issues for the reference and use of the reader.

SELECTED REFERENCES

Franks, A.L., 2001, Sewage disposal in the geologic environment: This volume.

Godwin, W., Korbay, S., 2001, Engineering geologic input to design and construction of the Foothill Student Housing Project, University of California, Berkeley, California: This volume.

Joslin, R., Smith, D., Putnam, J., 2001, Geological engineering considerations for the Sierra Nevada: This volume.

Oliveira, L.L., Rader, D.H., Kroll, R.C., 2001, Empire Ranch: Geotechnical aspects of a large scale development in the Sierra Nevada foothills: This volume.

Reynolds, R.E., 2001, Preserving California's fossil heritage during construction excavation: This volume.

EMPIRE RANCH: GEOTECHNICAL ASPECTS OF A LARGE-SCALE DEVELOPMENT IN THE SIERRA NEVADA FOOTHILLS, SACRAMENTO COUNTY, CALIFORNIA

L. LINDA OLIVEIRA[1], DAVID H. RADER[1], AND ROY C. KROLL[1]

ABSTRACT

Large-scale hillside developments in metavolcanic terrain typically present a range of geotechnical problems; a development in the geologically complex foothills of the Sierra Nevada is a good example. The geotechnical problems and best-practice solutions associated with this metavolcanic hillside development are characterized in this article. Subsurface conditions, including weathering and fracturing of the bedrock, as well as associated hydrostatic buildup, mitigative subdrainage techniques, and rippability issues are all explored. Mitigation measures for challenges posed by placement of rocky native material are described, particularly with respect to how rock fill might affect future homeowner property improvements.

OVERVIEW

The development of a 1,600-acre master-planned hillside community within the resistant metavolcanic bedrock of the Sierra Nevada foothills is unprecedented in the Sacramento area. The geologically complex, relatively steep terrain provided a multitude of issues requiring resolution even prior to initial earthwork operations. Engineering geology and geotechnical issues associated with this hillside construction included rippability of dense bedrock, regional seismicity, generation of fine material for rocky fills, proper compaction of these fills, and persistent groundwater seepage. Substantial engineering geology evaluation was provided in the design of mitigation measures for many of these issues. Other issues were necessarily addressed during construction by interactive communication with the contractor, and field performance evaluation.

SITE DESCRIPTION

Empire Ranch is a 1,600-acre master-planned community (MPC) located along the western base of the Sierra Nevada foothills, within the City of Folsom in eastern Sacramento County, California (Figure 1). The large, irregularly-shaped parcel is typified by rolling hillside grassland with scattered oak trees and seasonal creeks, which previously supported substantial herds of cattle and horses. Small seasonal tributaries cross the Empire Ranch MPC and drain into Willow Creek. Willow Creek is a major natural drainage west of the site that flows westward toward Lake Natoma on the American River. The eastern boundary of the project area is coincident with the county line dividing Sacramento County on the west from El Dorado County east of the site. Beyond the county line is vacant undeveloped ranchland that is part of the steep topographic rise of the El Dorado Hills. The northern portion of the development is bordered by the Mormon Island Wetlands Preserve, a privately owned ranch complex, and by a newly-constructed residential subdivision. An existing residential subdivision and rolling hillside ranchland adjoin the western boundary. State Highway 50 borders the site to the south.

[1]Youngdahl Consulting Group, Inc.
1234 Glenhaven Court
El Dorado Hills, CA 95762
mail@youngdahl.net

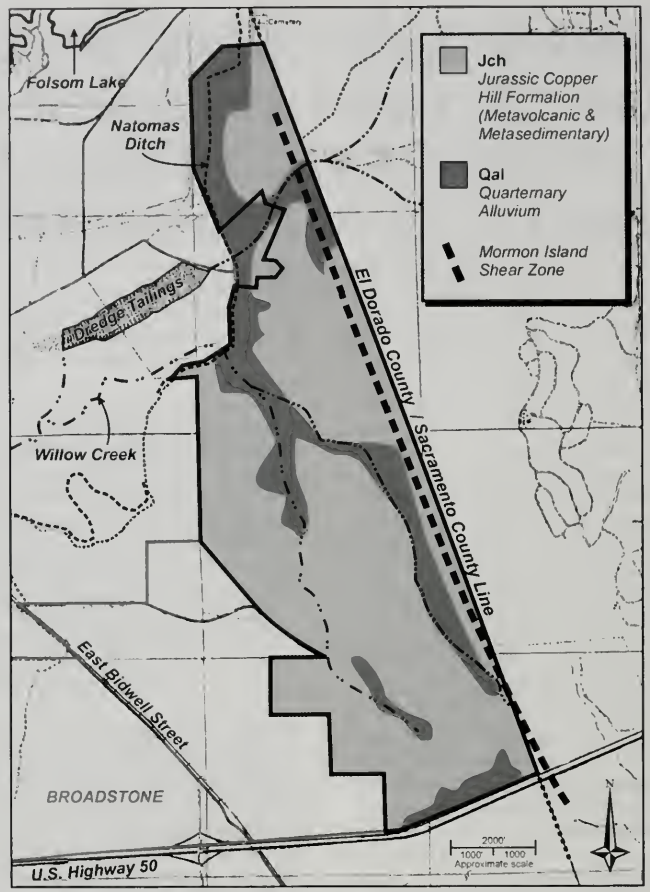

Figure 1. Empire Ranch MPC simplified geologic map (after Loyd, 1984). Some geologic features not shown due to scale.

GEOLOGIC AND SEISMIC SETTING

The site is underlain by thick accumulations of Paleozoic and Mesozoic marine sedimentary and volcanic rocks that have been deformed, intruded, and metamorphosed. The late Jurassic Copper Hill volcanics (Jch) consist of metamorphosed mafic to andesitic pyroclastic rocks, lava, and pillow lava, with subordinate felsic porphyritic and pyroclastic rocks. Also present within the site (although not included on Figure 1) are small exposures of the underlying Jurassic Salt Spring Slate (Jss), composed of metamorphosed dark gray slate, with subordinate tuff, graywacke, and conglomerate. Tertiary and Quaternary alluvium occupy the western portion of the site, along with dredge tailings located within offsite easement areas on the northwest periphery of the site. Surficial soils are derived mainly from the weathering of the underlying bedrock and consist of sands, silts, kaolinitic and sandy clays.

Faults in the vicinity of the site include the Mormon Island shear zone and the Bear Mountains and Melones fault zones. The Mormon Island shear zone is located adjacent to the eastern boundary

of the property and trends closely parallel to the Sacramento/El Dorado County line just south of Folsom Lake and the Mormon Island Dam (Figure 1). The Mormon Island shear zone has not been traced through the dam or north of it (TEC, 1983). Disturbance of surface deposits adjacent to the dam during construction and antecedent gold dredging operations have obscured the traces of any lineaments that might have existed there. The Mormon Island shear zone has screens of metasedimentary greenstone and schist. Asbestos-bearing serpentine was not encountered in this shear zone (Y&A, 1998).

The Mormon Island shear zone was trenched along the eastern margins of the site in November 1982 to determine if Quaternary sediments were displaced or offset by underlying shears. The observed soil-stratigraphic markers and related colluvial deposits were continuous throughout, indicating that any displacement of the shear zone in this area took place at least 50,000 to 70,000 years ago (TEC, 1983).

The Bear Mountains fault zone has two traces in the Sierra Nevada foothills. They are located to the east of the site approximately 1.5 miles and 8.5 miles, respectively, in the El Dorado Hills-Cameron Park area. The Melones fault zone is located approximately 17 miles east of the site, in the Placerville area.

According to the fault map of California (Jennings, 1994), and based on field evidence, it was concluded that no active faults are located within the general proximity of the subject property. The closest active faults are the Dunnigan Hills fault, situated approximately 40 miles northwesterly, and the Cleveland fault approximately 50 miles to the north.

PROJECT DESCRIPTION

The development of the Empire Ranch MPC is designed to occur in two phases. Construction of the first phase started in 1997. It comprises the north and west portions and includes twelve residential villages with a combined total of 1,035 lots for single-family hillside residences built around an eighteen-hole golf course in the flats. Cuts as deep as 45 feet in the metavolcanic hillside terrain, and engineered fills up to 28 feet thick, are planned to construct building pads and streets. Buried wet utilities will occupy trenches that at some points are as much as 25 feet in depth resulting in a total depth of 70 feet below the original ground surface. The northern portion also includes a commercial area, an elementary school, community parks, and a domestic water tank-site with associated pump stations. The southern portion, development phase 2, consists of twenty-six hillside villages, two schools, parks, and a commercial area. Proposed cuts range between 10 and 42 feet in depth.

RIPPABILITY CHARACTERIZATION

The site surface soils consist of loose to medium dense, fine-grained silty sands and sandy silts. Underlying these surface soils at highly variable depths is dense, often non-rippable metavolcanic bedrock. To ascertain the depth of non-rippable material in order to better plan building pad and buried utility main elevations, a detailed seismic refraction analysis was conducted. The planning criterion utilized for determining the need for a seismic refraction line was a design cut in excess of 10 feet. Seismic refraction surveys were conducted in a grid pattern in the designated cut areas utilizing a 60-channel Seistronic DS-6 seismograph. Blast charges or hammer impacts were set off along the lines and beyond the end points to generate deep seismic signals, and to provide high resolution of bedrock refractor boundaries based on differing velocities. Minimum and maximum design cuts along each seismic line were determined, which were then correlated against the estimated depth to non-rippable material, based on rippability charts from the Caterpillar Handbook for D-9 and D-10 bulldozers (Caterpillar, 1996). It was determined that non-rippable metavolcanic bedrock (generally having seismic velocities greater than 8,500 to 10,000 feet-per-second) would likely be encountered at depths from 17 feet to 50 feet (G&A, 1997, 1999). Based upon this information, it was concluded that non-rippable bedrock would be encountered that would require drilling and blasting in the deeper borrow areas prior to achieving design pad grade, as well as in some of the main utility trenches (Y&A, 1997).

EXCAVATION LOGISTICS

Near-surface soils were excavated using heavy earthmoving equipment. The underlying rock materials were excavated to depths of several feet using bulldozers equipped with ripping shanks. Fracturing in the metamorphosed volcanic bedrock was observed to have wider spacing and poorer development with increasing depth. The upper,

weathered portion of the bedrock, which extended 3 to 4 feet below the rock surface at most locations, was easily ripped by a Caterpillar D-9 bulldozer equipped with single or multiple shank rippers. The ripper-equipped D-9 was able to maintain penetration at most locations with moderate effort. Deeper excavations into the less weathered rock (>30') required heavier equipment, such as a ripper-equipped Caterpillar D-10 bulldozer.

Figure 2. Significant moisture being added during fill placement.

Excavation in the largest borrows had maximum cut depths of 45 feet, well into the less-weathered bedrock. Oversized resistant core stones, ledges, and ridges were encountered within the variably weathered bedrock. These areas provided for very difficult excavation that required ripping parallel to the trend of predominant joint and fracture sets, followed by perpendicular cross-ripping, but did not require blasting.

Blasting, to date, has been required in several locations where non-rippable bedrock was encountered, generally in deeper sanitary sewer trenches. In order to maintain utility line design grades where hard rock was generally encountered below 5 feet, the contractor used special rock-trenching equipment including heavy duty ripper-equipped bulldozers, large track-mounted excavators with oversize "V" buckets, and cutting wheels. The sidewall slope gradients for the "V" type trench excavated for the deeper sanitary sewer lines was 1H:1V. This provided adequate room for Caterpillar 815's to properly compact 18- to 24-inch thick lifts of backfill material in the 8 to 15 foot deep trenches.

FILL PLACEMENT PROCEDURES

Due to its great abundance, the angular rock material generated by the excavation of cut areas was utilized in fill placement. This material was transported to fill areas by Caterpillar 631 scrapers. Frequent repair or replacement of tires on earthmoving equipment was initially required due to punctures and slashes caused by the sharply fragmented rocky fill material. Monthly tire repair and replacement cost initially averaged tens of thousands of dollars. To minimize further tire damage, the contractor elected to keep angular rock lifts in a somewhat dry state just prior to further fill placement by scrapers. It was discovered that the angular rocks of the compacted fill were less likely to penetrate tire tread and sidewalls if these rocks were allowed to dry slightly. Apparently, excess residual water acted as a lubricant, thus allowing deeper incisions into tire tread and sidewalls.

Fill material composed of soil generally consisted of silty sands or sandy silts. A significant amount of material placed as fill consisted of angular rock fragments mixed with soil that, due to the composition, was not consistently testable for relative com-

paction by conventional methods. As a result, significant qualitative evaluation of the filling operations had to be performed. In general, fill materials were best compacted when placed with sufficient moisture (Figure 2) and, depending on rock size, when placed in approximately 6- to 24-inch thick lifts. An extensive amount of water was added to the rock-fill mixture during the compaction operation, which was accomplished by bulldozers with pull-along sheepsfoot rollers or Caterpillar 825's, to allow finer material to infill void areas. The rockfill material generally realigned itself internally to yield a compact, interlocking fill (Figure 3). Densification of fill materials and relative moisture uniformity were verified by pit observations prior to placement of additional materials. Oversize material was placed so as to preclude nesting and the formation of voids. Spot inspection of engineered fill material was also performed via bulldozer pits (Figure 4) to verify their in-place suitability (Y&A, 1997).

Figure 3. Interlocking fill showing finer material between large angular rock fragments.

SURFACE/SUBSURFACE DRAINAGE

The Mormon Island shear zone creates a leaky groundwater barrier that hinders the flow of subsurface water from the El Dorado Hills and contributes to localized saturated ground conditions westerly of its trace in the Empire Ranch MPC. Seasonal perched water also gives rise to intermittent artesian spring activity where water-bearing joints within the rock are oriented favorably to convey water to the surface. Because of (1) the many seasonally active drainages that pass through the project site, (2) the steep nature of the adjoining El Dorado Hills to the east, (3) the anticipated landscape irrigation from many sources, including the eighteen-hole golf course, and (4) the shallow fractured bedrock that is prone to artesian conditions during wet winter sequences, an extensive subdrain plan was needed to mitigate problems in the Empire Ranch villages (e.g., hydrostatic buildup of groundwater, differential settlement, and foundation moisture).

Based on known areas of subsurface flow and hydrostatic build-up, cut-off and canyon subdrainage systems were designed by the engineering geologist and geotechnical engineer within each residential village. The goal was to divert nuisance groundwater into the storm drain utility trenches in the streets (Y&A, 1997). Utilization of the storm drain utility trenches allowed the minimization of additional trenching. The 6-inch to 8-inch diameter canyon subdrains were excavated in square-cut trenches, parallel to and along the axis of the drainages, and were constructed to daylight along the golf course or low-lying wetlands to preclude hydrostatic build-up within the engineered fill. Where the drainage axis was broad and shallow, a cut-off subdrain system was excavated perpendicular to the drainage route and directed into the nearest planned storm drain trench (Figure 5). Filter fabric

was placed at the engineered fill and pipe cover interfaces to preclude fines from entering the subdrain system, and a sand-lean grout slurry collar was placed at the termination of the perforated pipe to direct water flow into storm drain manholes. Polyethylene sheeting was utilized within the cut-off subdrain system, the canyon subdrainage system, and within utility trenches on the down-gradient trench sidewall and bottom to control lateral migration of water onto lots.

The trenches for 12-inch to 24-inch diameter storm drains were purposely deepened where necessary to allow gravity pickup. The storm drain trenches were then backfilled with 3/4" crushed rock to provide additional mitigation of hydrostatic buildup of groundwater in the fractured bedrock. In many places, the fractured bedrock underlies the engineered fill at relatively shallow depths. This fractured bedrock can be expected to receive not only seasonal infiltration from storm run-off originating in the adjoining El Dorado Hills, but also landscape irrigation water from the residential lots themselves, the golf course, roadway landscaping, neighborhood parks, schools, and recreation fields (Y&A, 1997).

Figure 4. Dozer pit excavated for visual observation.

HOMEOWNER IMPROVEMENTS

The home buyers are the recipients of the final earthwork product. It is these consumers who will have to live with the rocky nature of the cut and fill areas, and seepage tendencies of the fractured bedrock within this hillside master-planned community. A 6-inch to 12-inch thick veneer of rock-free material was placed on the surface of building pads to provide a smooth finish grade. However, any subsurface activity performed by the homeowners will be met with the harsh reality that their lot is more conducive to having a shallow-rooted lawn than to in-ground swimming pools. Many people purchasing homes in this foothill community are from locales such as valley communities where this situation is not typically encountered. In order to adequately educate the consumers about these improvement constraints, a future homeowner letter, composed by the geotechnical consultant, will be given to the prospective buyers of any lot within this project site. This letter will provide buyers with information, in layman's terms, regarding the rocky nature of the fill, and seepage tendency of the bedrock, and give potential homeowners suggestions for properly planning, constructing, and maintaining property improvements (Y&A, 1997).

CONCLUSIONS

The engineering geologist is increasingly called upon to provide mitigation solutions for less than

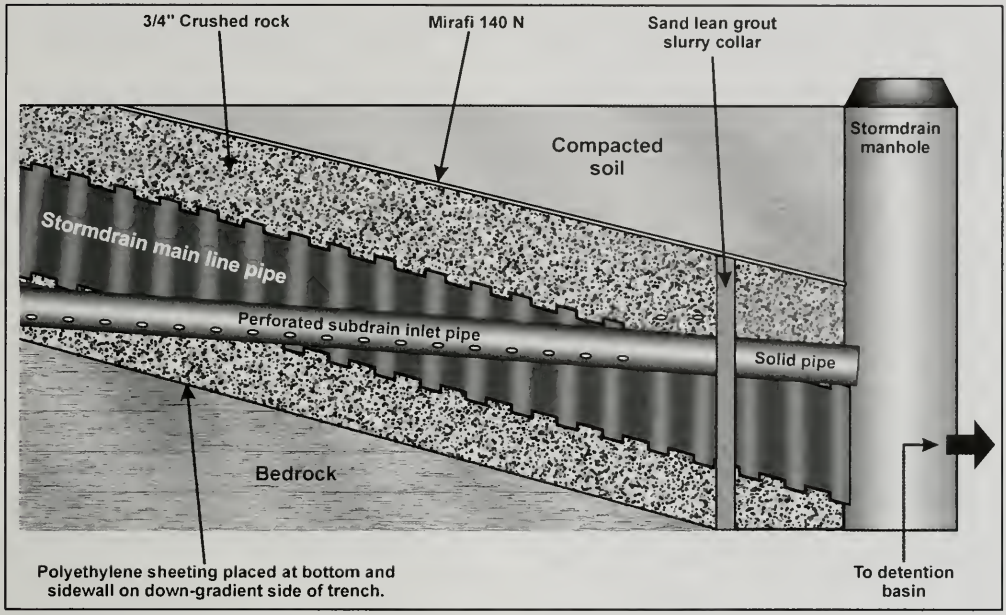

Figure 5. Cutoff subdrain inlet detail. The perforated subdrain inlet pipe can empty its water into the stormdrain inlet pipe, or convey it directly into the stormdrain manhole. (Modified from Youngdahl & Associates, Inc. Grading Handbook, copyright 1999).

optimal terrain, where remedies must be carefully integrated into the overall design plans, while remaining relatively cost-effective. By careful coordination between the engineering geologist, the contractor, and the civil engineer, constructive multidisciplinary solutions come to light that might not have been ventured, as in the case of the rock fill placement methodology and storm drain trench utilization in subdrainage infrastructure.

By far the engineering geologist's most delicate role and visible interface, as far as the home-buying public is concerned, revolves around the layman information letter supplied in the purchase documents. The letter must be carefully crafted to informally educate and constructively motivate the new hillside lot owners regarding long-term maintenance and modification of their parcels. Successfully conveying such complex technical issues in an easily understood informal format to these owners will ultimately raise the public's awareness of the engineering geologist's value, and may prove to be the greater accomplishment for our profession.

ACKNOWLEDGMENTS

Our sincere thanks to Eric Chase, David Gius Jr., Alan Kropp, and Robert Sydnor who provided invaluable advice as peer reviewers. Additional thanks to Thomas Balbierz for sharing his geotechnical engineering insight and Scott Youngdahl for his illustration wizardry.

AUTHOR PROFILES

L. Linda Oliveira is a staff geologist with Youngdahl Consulting Group, Inc. Her technical experience includes slope stability, hydrogeologic and geotechnical engineering studies, aerial photograph interpretation, and Phase 1 environmental assessments.

David H. Rader is a staff geologist with Youngdahl Consulting Group, Inc.. His technical experience includes investigative trenching, field oversight of earthwork operations, multi-parameter age estimations of fault systems, and concrete quality control and testing.

Roy C. Kroll is a California Certified Engineering Geologist and Registered Environmental Assessor with over 19 years of engineering geology, seismic, geotechnical, hydrogeologic, and environmental experience throughout California. He is the chief engineering geologist and environmental manager at Youngdahl Consulting Group, Inc..

SELECTED REFERENCES

ASCE (American Society of Civil Engineers), 1995, So your home is built on expansive soils? A discussion of how expansive soils affect buildings: American Society of Civil Engineers, 59 p.

Caterpillar, 1996, Caterpillar Performance Handbook: Caterpillar, Inc., 944 p.

G&A (Gasch & Associates), 1997, The Foothills-Refraction seismic rippability report: Consultant's report to Youngdahl & Associates, Inc., 30 p.

G&A (Gasch & Associates), 1999, Empire Ranch Development, Phase 2, Southern Portion, Rippability Study: Consultant's report to BGP-Russell Ranch L.L.C., 24 p.

Jennings, C.W., 1994, Fault activity map of California and adjacent areas: California Division of Mines and Geology, Geologic Data Map No. 6.

Loyd, R.C., 1984, Generalized geology of the Folsom 15-minute quadrangle: California Division of Mines and Geology, Open File Report 84-50, 44 p.

Petersen, M.D., 1996, Probabilistic seismic hazard assessment for the State of California: California Division of Mines and Geology in conjunction with U.S. Geological Survey, Open-File Report 96-08, 33 p.

TEC (Tierra Engineering Consultants, Inc.), 1983, Geologic and seismologic investigations of the Folsom, California area - final report: Consultant's report to U.S. Army Corps of Engineers, Sacramento District, 324 p.

Y&A (Youngdahl & Associates, Inc.), 1994, Geotechnical engineering studies review, Russell ranch development: Consultant's report to Dame Construction Company, San Ramon, California, (Y&A office at El Dorado Hills, CA), 17 p.

Y&A (Youngdahl & Associates, Inc.), 1997a, The Foothills, development phase I addendum, revisions to subdrainage evaluation report: Villages 4, 6, 7, 8, 11, 13, 16, 17, 18, 20, 29 & 41: Consultant's report to Paradigm Communities, Inc., (Y&A office at El Dorado Hills, CA), 6 p.

Y&A (Youngdahl & Associates, Inc.), 1997b, Grading factors, The Foothills, development phase I: Consultant's technical memorandum to Paradigm Communities, Inc., (Y&A office at El Dorado Hills, CA), 1 p.

Y&A (Youngdahl & Associates, Inc.), 1997c, Short-term, long-term and financial considerations with respect to "bony" fill placement: mass grading for infrastructure improvements and Villages 4, 6, 7, 8, 11, 13, 16, 17, 18, 20, 29 & 41, The Foothills, development phase I : Consultant's report to Paradigm Communities, Inc., (Y&A office at El Dorado Hills, CA), 5 p.

Y&A (Youngdahl & Associates, Inc.), 1997d, Maintenance of hillside homesites for slope stability and erosion control: Consultant's homeowner Letter, (Y&A office at El Dorado Hills, CA), 4 p.

Y&A (Youngdahl & Associates, Inc.), 1998, Lack of serpentine or serpentinite in The Foothills MPC: Consultant's report to Paradigm Communities, Inc., (Y&A office at El Dorado Hills, CA), 26 p.

GEOLOGICAL ENGINEERING OF THE FOOTHILL STUDENT HOUSING PROJECT, UNIVERSITY OF CALIFORNIA, BERKELEY, ALAMEDA COUNTY, CALIFORNIA

WILLIAM GODWIN[1] AND STEPHEN KORBAY[2]

ABSTRACT

Geological engineering input was essential to the success of a student housing project on the University of California campus in Berkeley, California. Design considerations included (1) identifying zones of active, Holocene faulting, and establishing setbacks from these zones, (2) evaluating impacts of earthquake-induced ground shaking on structures, (3) evaluating slope stability and active landsliding, (4) determining subsurface drainage and hydrostatic conditions upslope of the fault zone, and (5) predicting differential settlement under foundations.

The site is located in the Berkeley Hills area of the Coast Ranges geomorphic province of Northern California. A key geologic feature of the site is the northwest-trending Hayward fault, an active segment of the San Andreas fault system. Landslide deposits are found adjacent to the fault and immediately upslope of the planned facilities. Several geotechnical investigations have been performed in the area, and have included logging of fault trenches, excavation of test pits, description and sampling of rock and soil borings, the installation of borehole instrumentation, and geologic mapping.

During construction, the geotechnical consultant provided monitoring and testing services. Structures built included nine three-story dormitory residences founded on lateral spread footings, a 25-ft high tie-back soldier pile wall built to retain an existing roadway, and gravity-type crib retaining walls to support fills placed for the parking areas. Landslide remediation included construction of an engineered buttress fill and installation of horizontal drains. Post-construction monitoring was performed to evaluate settlement and slope stability.

INTRODUCTION

This paper describes the engineering geology of the Foothill Student Housing site (FSH), based on the information obtained during the investigative and construction phases of the project. Recent work is mentioned and presented in the reference list.

The FSH project is located on the University of California campus (UCB) in Berkeley, California. The project consists of nine buildings situated at the north end of the campus (Figure 1). Three of these buildings occupy a site at the corner of La Loma and Hearst Avenues, referred to as "the La Loma Ridge site". The remaining six buildings comprise the Hillside Commons site and are located along Cyclotron Road near Highland Avenue. Parking areas for the project are located north of The Greek Theater and Bowles Hall.

[1]Harding ESE
90 Digital Dr.
Novato, CA 94949
whgodwin@mactec.com

[2]Kleinfelder Inc.
2240 Northpoint Parkway
Santa Rosa, CA 95407
skorbay@kleinfelder.com

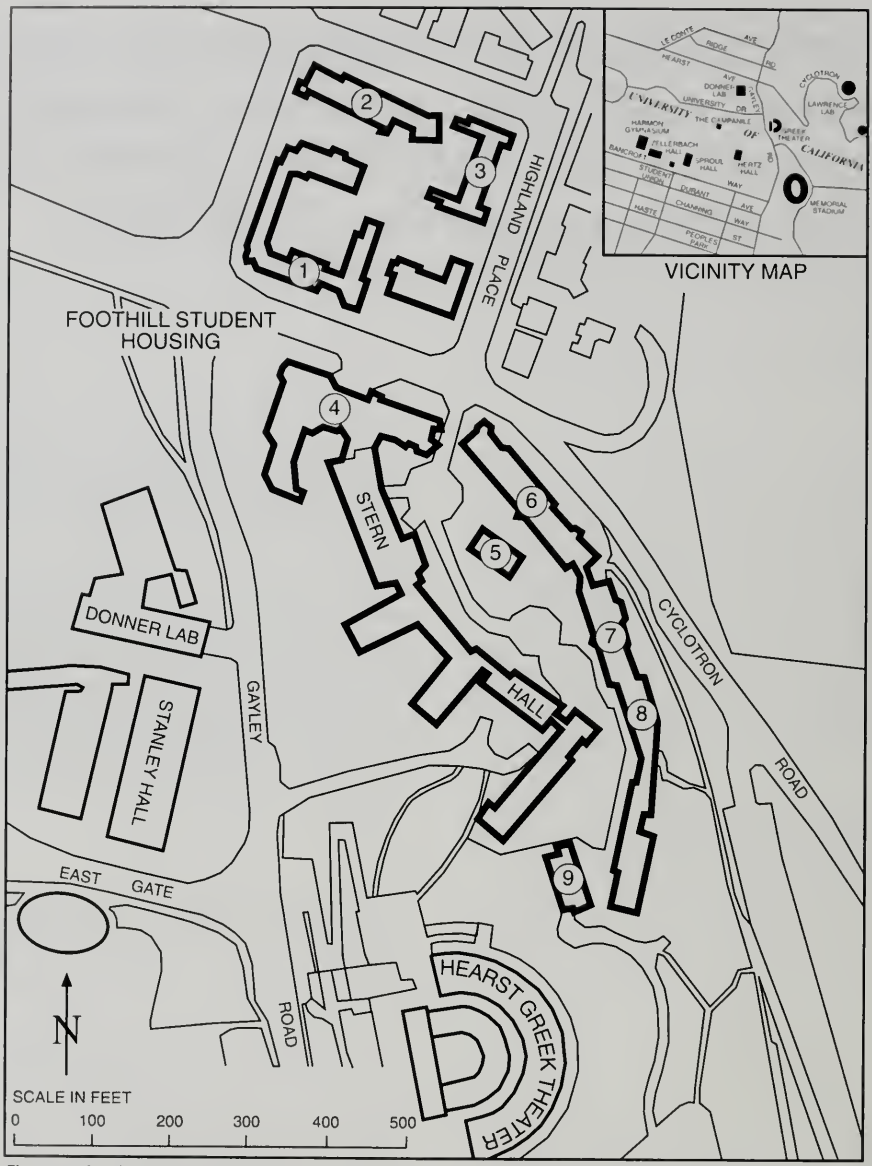

Figure 1. Site location map. Foothill Student Housing site is located on the eastern end of the University of California campus in Berkeley, California. La Loma buildings are labeled 1-3; Hillside Commons buildings are labeled 4-9.

The area surrounding the La Loma Ridge site is heavily urbanized with residential neighborhoods and the UCB campus. Lawrence Berkeley Laboratory (LBL) is located upslope and to the east. Except

for Stern Hall, the Hillside site and parking areas were undeveloped.

Harding Lawson Associates (HLA) was retained as the geotechnical and engineering geology consultant to UCB for the project. Reimer and Associates was the project civil engineer and the project architect was Ratcliff Architects. HLA conducted several investigations on the project site, beginning in 1986. HLA also provided observation and testing services during construction (1988-1990). The facilities were occupied in 1991.

UCB required that the project design be reviewed and approved by their Seismic Review Board (SRB). The SRB retained Geomatrix Consultants (GCI) for review of the geotechnical/geologic investigations. Geologists from UCB, LBL, the U.S. Geological Survey (USGS), and the California Department of Conservation, Division of Mines and Geology (DMG) were also invited to review site conditions and exploration trenches.

Investigation	Purpose	Area of study	Field exploration	Comments
HLA, 1986	Identify and evaluate geologic hazards	Hillside site and La Loma Ridge site	Research, geologic mapping, 15 borings, 7 fault trenches	
HLA, 1988a	Detailed geohazards study of tentative building locations. Preliminary design and site feasibility	Hillside site, La Loma Ridge site, and Bowles Hall	Geologic mapping, 36 borings, borehole geophysics, 8 test trenches	Installation of monitoring wells
HLA, 1988b	Geotechnical engineering conclusions and recommendations of the housing sites and the proposed parking	Hillside Housing (dormitories and parking areas); Hillside Commons; La Loma Ridge Housing	Extensive laboratory testing amd geotechnical analysis	Based on field exploration of HLA 1998a
HLA, 1988c	Evaluation of slope stability	Lower Cyclotron Road	Geologic mapping, 2 borings, laboratory testing	
HLA, 1988d	Evaluate activity level of "Louderback trace"	Stern Hall and various areas on the UC Berkeley campus	Culvert creep survey, geologic mapping, 6 new trenches, 5 borings, tunnel survey, age dating	
HLA, 1990	Reevaluation of bearing capacity of crib walls and slope stability	Lower Cyclotron Road, Hillside parking areas	6 borings; laboratory testing	Post-construction

Table 1. Summary of investigations.

GEOTECHNICAL INVESTIGATIONS

A series of investigations were performed to provide geotechnical design criteria of the housing structures and parking areas. Research included reviews of previous geologic reports related to the general area, including studies by Louderback (1937), Radbruch and Lennert (1966), Lennert and Curtis (1980, 1985). Geologists conducted the majority of the field investigations, which included logging of fault trenches, excavation of test pits, logging and sampling of soil and rock borings, geophysical borehole logging, installation of piezometers and slope inclinometers, and surface and underground geologic mapping. Trenches were excavated using track- and wheel-mounted backhoes to depths of 2 to 22 feet. Most exploratory borings for the foundation studies and landslide investigations were advanced through soils and into bedrock to depths of 70 feet using solid flight and hollow-stem augers. Deeper borings, to 150 feet, were drilled using rotary wash methods and pitcher barrel samplers. Geologic mapping of the accessible portion (255 feet) of an existing adit was performed. Table 1 presents a summary of each of these investigations.

The FSH site is located within the seismically active Hayward fault zone and within the boundary of an Earthquake Fault Zone designated by DMG in accordance to the Alquist Priolo Act of 1972, (now referred to as the Fault Hazard Act). Fault and geologic hazard investigations (HLA, 1986, 1988a, 1988d) were required to satisfy the requirements of the Act and were conducted in accordance with the fault investigation criteria outlined in DMG Notes 37 and 49.

REGIONAL GEOLOGIC SETTING

The FSH site is situated in the Berkeley Hills, which rise above the eastern San Francisco Bay area to an elevation of 1,300 feet above mean sea level. The hills were formed by Post-Pliocene compressional fault uplift and are relatively steep, with

many developed areas that have undergone extensive hillside grading.

The most significant geologic feature of the FSH site is the northwest-trending Hayward fault, an active segment of the San Andreas fault system (Lettis, 2001, this volume). The Hayward fault is a right lateral strike slip fault that trends parallel to the Berkeley Hills. It extends from east of San Jose, where it branches away from the Calaveras Fault as a left-hand stepover, to San Pablo Bay. The Hayward fault separates Cretaceous shales and sandstones of the Great Valley Sequence and Tertiary rocks on the east and the Franciscan Complex of Jurassic-Cretaceous age on the west.

Surficial materials, including Quaternary colluvium and landslide deposits, are distributed extensively across the area and tend to obscure the underlying bedrock.

LOCAL GEOLOGIC CONDITIONS

Artificial fill – Fill was encountered in several exploratory borings and trenches to depths of up to 13 feet. In general, the fill consists of clays, sandy clays, and clayey sands with occasional rock fragments. Organically rich, debris-laden fill was observed in trenches on the La Loma Ridge site.

Colluvium – Relatively thick colluvial deposits were mapped on the FSH site and were encountered in test borings and pits. These deposits consist of gravelly and sandy clays derived from sloping areas to the east and contain fragments of sandstone, shale, chert, and rhyolite. The colluvium is most abundant within and west of the Hayward fault and is intermixed with landslide debris (Figures 2a and 2b). In the vicinity of Stern Hall, the colluvium ranges in thickness from less than 10 feet to over 100 feet.

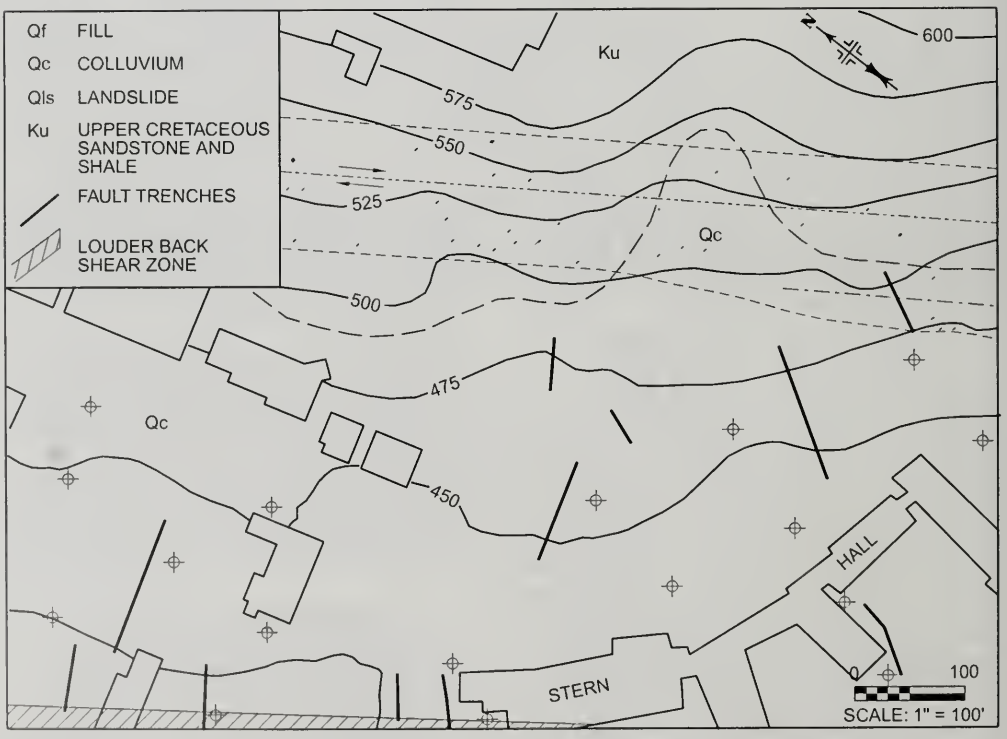

Figure 2a. Geologic map of La Loma Ridge and Hillside Commons housing areas. Figure 2b is a continuation of this map to the right.

Landslides – Landslide deposits were observed mostly in the area upslope of Bowles Hall and adjacent to the planned parking area. They included shallow (<20 feet thick) younger slides adjacent to, or overlying, older slides (up to 45 feet in depth). The slide debris consisted of a chaotic mix of clayey gravel and rock fragments of varied sizes. Test trenches excavated in 1986 and 1987 exposed several shallow landslide failure planes.

Bedrock – Bedrock east of the Hayward fault consists of sandstone and shale assigned to the Upper Cretaceous Great Valley Sequence. The rocks are intensely fractured and, in the vicinity of the Hayward fault zone, the shale is highly sheared and brecciated. Silica-carbonate boulders were encountered in the La Loma Ridge and Hillside Commons areas, but they do not represent in-place bedrock.

Faulting

Two active traces of the Hayward fault zone cross the site. The main fault trace traverses the Hillside Commons site and cuts across the parking lot. Figure 3 depicts the fault trace in Trench H adjacent to older landslide debris. The west fault trace is sub-parallel to the main trace and is separated from it by as much as 150 feet, east of The Greek Theater. The precise location of the west trace is unknown east of Bowles Hall; however, based on its trend, it most likely converges with the main trace in the vicinity of Memorial Stadium (Figure 1).

The Louderback trace is a 200-foot wide zone of sheared rock and colluvium originally identified by Louderback (1939) in the Lawson adit located

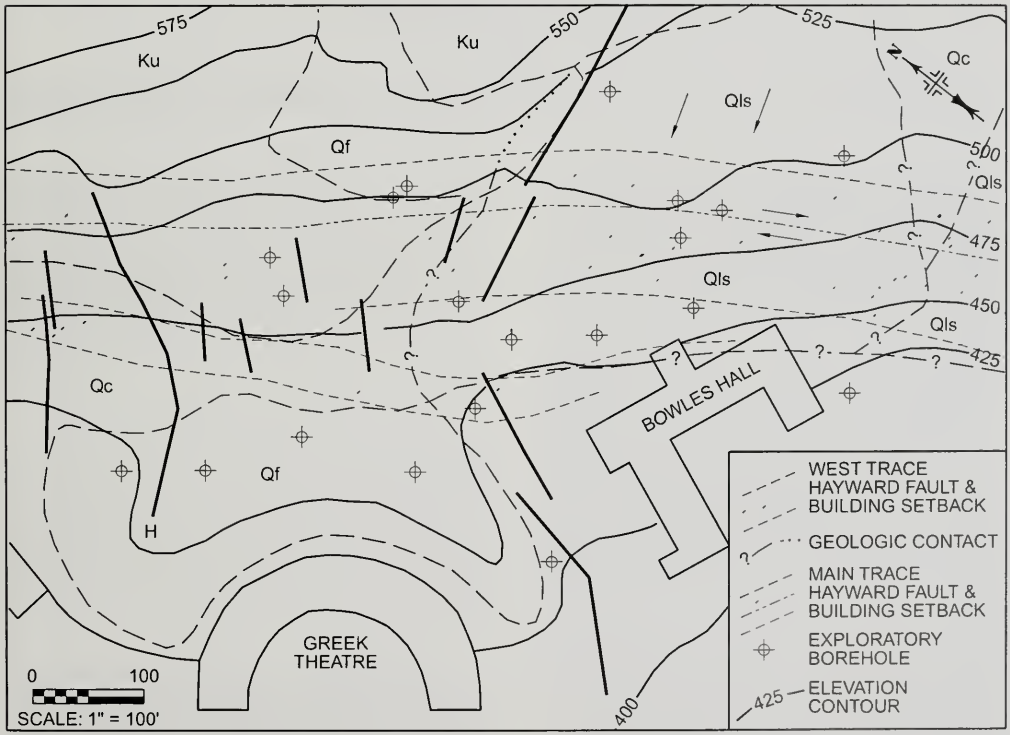

Figure 2b. Geologic map of the parking areas. Extensive trenching was conducted to satisfy the requirements of the Fault Hazard Act and to establish building setbacks. Stabilization of a landslide east of Bowles Hall required an earth buttress fill (see Figure 4).

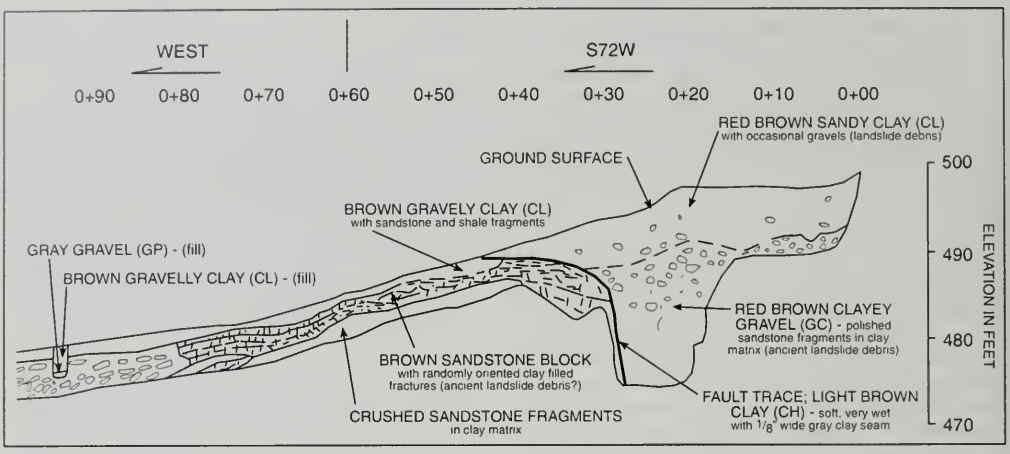

Figure 3. Fault trench H. Note fault trace depicted in trench log. See Figure 2b for trench location. Scale is approximately 1"=20'. Downslope portion of log is not shown due to scale.

beneath Stern Hall and, subsequently, investigated by Lennert and Curtis (1980). The trace trends northwest from just southwest of Stern Hall to just west of the Greek Theater. It is not considered active, based on trenching and pedochronological studies (HLA, 1988d). Studies have shown that there is little risk of secondary or triggered fault rupture at the FSH site (Hoexter, 1992).

Both the main and west Hayward fault traces are considered active based on observed displacements of Holocene material in the fault trenches and documented fault creep on the main trace under Memorial Stadium, located southeast of FSH. The Hayward fault has exhibited long-term horizontal creep of about 5 mm per year, as evidenced by noticeable crack offsets in Memorial Stadium (Radbruch and Lennert, 1966). Measured fault creep on the main trace during the mid-1980s was 2.5 mm per year as recorded by a creep meter array installed upslope of Stern Hall in 1983 by the USGS. However, the array hardware was installed at only a depth of 6 feet and may have been measuring a component of surface soil creep. The array was subsequently removed during the FSH construction. More recently, curb line surveys have been conducted to determine creep-rates (Hoexter et al., 1992); 1991 data have shown the creep-rate to be about 4 mm per year in the northern portion of Berkeley.

GEOLOGIC ENGINEERING RECOMMENDATIONS

Based on the geologic investigations, development of the site was judged geotechnically feasible. The two sub-parallel active fault traces that cross the project were located with precision, and building setbacks of 50 feet on the uphill side and 75 feet on the downhill side of the active traces were recommended for a minimum 125-foot wide building exclusion zone. Landslide mitigation and subsurface drains across the southern areas were also suggested.

Additional evaluation in 1988 redefined the boundaries of the building setbacks (50-foot minimum) with respect to the planned structures. The maximum horizontal displacement on either trace was estimated to be as much as 10 feet from a maximum credible earthquake with vertical displacement of as much as 1.5 feet. The empirical estimated maximum probable earthquake of 6.5 to 7.0 had corresponding horizontal and vertical displacements of about 3 feet and 1 foot, respectively.

Prior to development, additional investigation of the Louderback trace was required to satisfy a court injunction requiring reasonable proof that the activity level would not be a potential hazard. Based on additional surface and underground geologic mapping, logging of test trenches and test borings, laboratory age-dating, and curb offset surveys, the Lou-

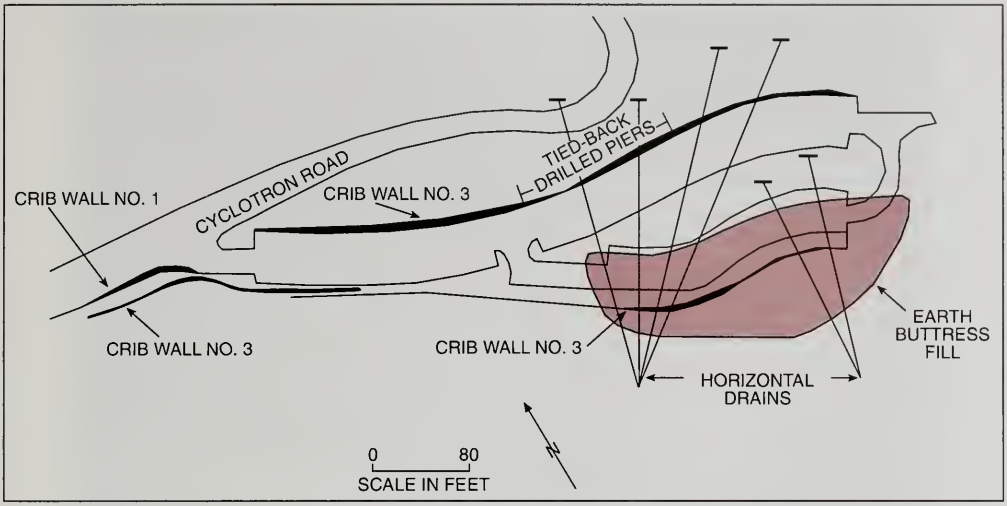

Figure 4. Drawing of engineered features. To accommodate construction of the student housing structures and parking lots, several engineered retaining and slope stabilization structures were required. These included an earth buttress fill, a tied-back soldier pile wall, four crib walls, and six horizontal drains.

derback trace was judged not seismically active. Some near vertical traces identified in test trenches were interpreted to be the result of dip-slip movement associated with ancient folding and compression uplift of the Berkeley Hills. However, lateral displacement along vertical separations during ground shaking associated with a Hayward fault seismic event was considered possible. Geologic mapping in the southeast portion of the site resulted in additional landslide mitigation measures.

Geotechnical recommendations for site development were provided by HLA in 1988. These included landslide mitigation (i.e., buttress fill), measures for site preparation and grading, design of surface and subsurface drainage, allowances for settlement, foundation support, retaining walls, concrete slabs-on-grade, and asphalt concrete pavement.

Pre-earthwork activities

Horizontal drains - Prior to construction of the parking lot, six horizontal drains were installed to reduce hydrostatic pressure beneath the landslide mass situated above the parking lot. Gently inclined boreholes, totaling 1,500 feet in length, were drilled in a radial pattern from two locations near Stern Hall, as shown in Figure 4. Slotted PVC casing, measuring 1 1/2-inch in diameter was inserted into the boreholes. Soon after completion, water began flowing out of each horizontal drain, and continued to flow at varying degrees during the period of construction. Flows were collected into piping manifolds and connected to the storm-drain system.

Monitoring points – Of major concern during design was slope stability. Earlier recommendations included installing monitoring points to identify potential slope movement of the excavation for a soldier pile wall immediately south of Cyclotron Road. This was accomplished by installing two slope indicator casings and four piezometers (monitoring wells). Survey monuments were placed along the sidewalk to allow continuous monitoring for lateral surface movement.

CONSTRUCTION MONITORING

An engineering geologist was onsite full-time to monitor the construction of several structures.

Landslide buttress – The first phase of parking lot construction included buttressing of an active landslide at the southern end of the parking area.

Figure 5. Parking lot slope retention. This photograph, taken at the completion of the project, shows the earth buttress fill above a crib wall. View is to the southeast. The main trace of the Hayward fault crosses the parking lot at the extreme lower right hand corner of the photograph.

Landslide debris at the toe of the landslide was removed and a shear key was constructed into the underlying competent material. The keyway excavation was mapped by the geologist prior to placement of a backdrain at the rear of the excavation. Complete removal of landslide debris continued upslope using a series of stepped benches that penetrated beneath the slide plane. The excavation was backfilled with compacted, engineered fill constructed to a slope of 2:1 (H:V). A keyway drain and several bench drains were installed during construction of the buttress.

Tied-back retaining wall – A soldier pile retaining wall with tied-back anchors was constructed immediately below the Cyclotron Road "horseshoe curve", (Figure 4). A geologist logged the drilling of 34 30-inch diameter cast-in-place soldier piles, drilled on 5 to 6 foot centers to minimum depths of 8 feet below the base (toe) of the wall. Each pile was anchored by 2 to 4 tied-back steel rods. Wood lagging was installed between the H-beam steel members. A backdrain was placed behind the wall.

Crib-type retaining walls - After stabilization of the area upslope of the parking lot, construction began on four gravity-crib walls around the perimeter of the parking area. The walls have a 1/4:1 (H:V) finished slope that is free-draining (Figure 5). The walls consisted of interlocking pre-cast concrete components arranged in a box or crib. The design provided for bearing of the dead weight of the wall on either engineered fill or firm soil subgrade. The crib walls ranged in height from 35 ft high in front of the tied-back soldier pile wall to less than 3 feet elsewhere. Each crib was backfilled with drain rock and capped with compacted fill.

Some concern was raised by the design team as to the allowable bearing capacity required to support these walls, and the stability of the slope above a section of the wall that was at maximum design height. A supplemental site investigation and reevaluation was performed in 1990. This work included exploratory borings, triaxial compressive strength testing, and slope stability analysis. It was concluded that the foundation soils provided suitable bearing capacity under dead and live loading with an acceptable factor of safety. However some crib walls required tied-backed anchors to compensate for earthquake loading.

Figure 6. Mapping shear features. The geologist is indicating an inclined fracture in a temporary slope adjacent to one of the housing areas. Darker horizon is top soil, lighter is colluvium. View to the east.

Hillside and La Loma Ridge dormitory sites - The dormitories consisted of 3- and 4-story steel and wood frame structures founded on lateral spread footings. In general, these structures were founded on stiff natural clays and silts. Beneath the Hillside Commons however, large boulders ("floaters") of silica-carbonate were exposed. The presence of these required substantial effort by pneumatic hammers to excavate to sufficient depth below grade to accommodate the foundations and minimize differential settlement. In addition, organic-rich fill was found in footing excavations beneath the La Loma Ridge site; this fill was excavated and replaced with clean engineered fill.

During site grading for the Hillside site, a series of discontinuous shears was observed in the excavation. These features had pronounced slickensides and *en echelon* orientations relative to the nearby Hayward fault, yet they did not offset a recent soil horizon (Figure 6). Extensive investigation and consultation among engineering geologists (GCI, 1990) concluded that these were not fault features but, instead, were stress- fractures caused by ground shaking.

POST-CONSTRUCTION MONITORING

Concerns were raised regarding some cracks observed along new curb and gutters adjacent to Cyclotron Road in the vicinity of the parking areas and retaining walls. A network of monitoring points was established, and measurements were made to assess the horizontal and vertical movement associated with these cracks. After a period of less than a year the movements stopped. It was concluded that these cracks were associated with normal yielding of the retaining walls and from backfill settlement.

SUMMARY AND CONCLUSIONS

Geologic engineering input was essential to the success of a student housing project on the University of California campus in Berkeley, California. The University's design team confronted numerous technical challenges on the project. Focused geologic engineering investigative techniques and analysis provided design engineers with the necessary information to complete the project. Mitigation of significant geologic hazards, including avoiding the highly active Hayward fault, was accomplished. Engineering geologists also provided valuable geotechnical

design input and full-time observation during construction activities.

ACKNOWLEDGEMENTS

The authors wish to thank Jeffrey Gee of UC Berkeley Facilities Management for permission to publish this paper and Keith Bergman, Project Geotechnical Engineer, who provided valuable information and background for preparation of this paper. We would also like to acknowledge the editors who reviewed the manuscript: Horacio Ferriz, Chief Editor; Roy Kroll, Section Editor; Steve Styker, English Editor; and John Juhrend, peer reviewer.

AUTHOR PROFILES

William Godwin, C.E.G., is a Senior Geologist living in Sebastopol, California. After leaving Harding Lawson in 1990 to work for a large engineering construction company he has recently returned to work in Harding ESE's Novato, California office. He has over 17 years of experience in engineering and environmental geology in California and abroad.

Stephen Korbay, C.E.G., is a Principal Engineering Geologist with Kleinfelder Associates. Prior to joining Kleinfelder, he was Principal Engineering Geologist at HLA. He currently works in Kleinfelder's Santa Rosa, California office.

SELECTED REFERENCES

Geomatrix Consultants, 1990, Observation of ground cracks, Foothill Student Housing Project, University of California, Berkeley, California: Consultant's report to University of California, Office of Facilities Management, 32 p.

HLA (Harding Lawson Associates), 1990. Supplemental report, crib wall bearing capacity re-evaluation and slope stability analysis, Foothill Student Housing, University of California: Consultant's Report to University of California, Office of Facilities Management, 15 p.

HLA (Harding Lawson Associates), 1988a, Geologic and fault hazard investigation, Phase II, proposed student housing, University of California: Consultant's Report to O'Brien-Kreitzberg & Associates, 27 p.

HLA (Harding Lawson Associates), 1988b, Geotechnical investigation, Foothill Student Housing, University of California, Berkeley, California: Consultant's Report to O'Brien-Kreitzberg & Associates, 31 p.

HLA (Harding Lawson Associates), 1988c, Slope stability reevaluation, Lower Cyclotron Road Area (Hillside Housing), Foothill Student Housing, University of California, Berkeley, California: Consultant's Report to O'Brien-Kreitzberg & Associates, 4 p.

HLA (Harding Lawson Associates), 1988d. Supplemental fault hazard investigation, "Louderback Trace", Foothill Student Housing, University of California, Berkeley, California: Consultant's Report to The Honorable Michael Ballachey, Judge of the Alameda County Superior Court, 28 p.

HLA (Harding Lawson Associates), 1986, Geologic and fault hazard investigation, Phase I, proposed student housing, University of California: Consultant's report to University of California, Office of Facilities Management. 31 p.

Hoexter, D. F., 1992, Potential for triggered slip on secondary faults in the East Bay: implications for the planning process: *in* Borchardt, G., (ed.), Proceedings of the Second Conference on Earthquake Hazards in the Eastern San Francisco Bay Area: California Department of Conservation, Division of Mines and Geology Special Publication 113, p.153-158

Hoexter, D. F., Knudsen, K., Hecht, B., Luduzinsky, D., and Fiedler, G., 1992, Creep and downslope movements in the Hayward fault zone in north Berkeley: Ten years later: *in* Borchardt, G., (ed.), Proceedings of the Second Conference on Earthquake Hazards in the Eastern San Francisco Bay Area: California Department of Conservation, Division of Mines and Geology Special Publication 113, p.121-127

Lennert, B.J. and Curtis, G.H., 1985, Final fault hazard study, Dwight-Derby project, University of California, Berkeley, California: Consultant's report to University of California, Office of Facilities Management

Lennert, B.J. and Curtis, G.H., 1980, Fault hazard study, Berkeley campus, University of California, Berkeley, California: Consultant's report to University of California, Office of Facilities Management

Lettis, W.R., 2001, Late Holocene behavior and seismogenic potential of the Hayward-Rodgers Creek fault system in the San Francisco Bay area, California: in Ferriz, H., Anderson, R. (eds.), Engineering Geology Practice in Northern California: Association of Engineering Geologists Special Publication 12 and Division of Mines and Geology Bulletin 210.

Louderback, G.D., 1939, Preliminary report on geological conditions. Proposed Stern dormitory site, University of California, Berkeley, California. 7 p.

Radbruch, D.H. and Lennert, B.J., 1966, Damage to culvert under Memorial Stadium, University of California, Berkeley, California, caused by slippage in the Hayward fault zone: Bulletin of the Seismological Society of America, v. 56, no. 2, p. 295-304.

PRESERVING CALIFORNIA'S FOSSIL HERITAGE DURING CONSTRUCTION EXCAVATION

ROBERT E. REYNOLDS[1]

ABSTRACT

Established methods for paleontologic resource impact mitigation (PRIM) can preserve California's fossil heritage without stopping excavation or construction. Federal, state, and local legislation recognizes that fossils are significant non-renewable resources that need to be protected from adverse impacts. A review of existing locality records and an on-site survey are necessary to establish the potential presence of fossils on a project site. Once this potential has been established, a project-specific PRIM program is followed that reduces adverse impacts to a low level of significance. A PRIM program generally includes monitoring and salvage, washing and specimen preparation, identification and cataloging, repository storage, and a report. With advanced planning, California's fossil heritage can be preserved as excavation for construction programs proceeds.

INTRODUCTION

As the California landscape is transformed by development, the accompanying excavations provide opportunities to recover important fossil resources and expand our knowledge of California's past biologic history. Why save fossils from excavation impacts? The reasons are important to science, to geologists, to their clients — the developers — and to society in general. The reasons include:

- Positive community relations.
- Preservation of important biostratigraphic data and irreplaceable evidence of past life.
- Planning concerns related to urbanization and population growth.
- Conformance to standards and laws regarding non-renewable resources.

Community relations

In a climate of environmental controversy, a client often benefits from a favorable, high-profile image. What better way to enhance an image than by saving a "dinosaur"? Examples abound of favorable media coverage and of high-profile technical and popular publications resulting from paleontologic resource salvage operations. Examples of some salvage operations that sparked public interest and yielded significant scientific data are given below.

- The Simi Valley Landfill and Recycling Center (Ventura County), where new vertebrate species, including numerous middle Eocene rodents and a primate, were found. New fossil localities resulted in the extension of the estimated age of the Sespe Formation (Kelly, 1990, 1992; Kelly et al., 1991; Kelly and Whistler, 1994).

[1]LSA Associates
3403 10th Street, Suite 520
Riverside, CA 92501
bob.reynolds@lso-assoc.com

- The Fairmead Landfill (Fresno County), where the salvage of Ice Age land mammal fossils was halted due to a limited budget. Subsequently, local residents lobbied for and received additional funds to preserve their prehistoric heritage (Dundas, 1994).

- Carlsbad (San Diego County), where excavation unearthed a late Cretaceous nodosaurid dinosaur—a find that was covered by the press for many years. The specimen was prepared in public view, with the developer's name prominently displayed (Coombs and Deméré, 1996).

- Pipeline trenching in North Las Vegas unearthed an Ice Age mammoth (Figure 1). This find changed a project with the perceived nuisance of fossil monitoring into a model of environmental concern (Reynolds et al., 1991).

- Eastside Reservoir (Diamond Lake), near Hemet (Riverside County), continues in the public eye as media nationwide report bigger and better Ice Age land mammal fossils salvaged during the reservoir excavation. The reservoir operator constructed a visitor center with fossil displays, and funds out-

Figure 1. The lower jaw of a 10 to 15,000 year old mammoth still sits in the matrix and plaster cast from its excavation at the site of the Kern River Gas Transmission Company pipeline in 1992. Trenching operations were temporarily halted while paleontologists surveyed the site and stabilized the skeletal material. The find also included two upper molars, a tusk, and a shoulder blade. Photograph courtesy of the Nevada State Museum and Historical Society.

reach exhibits and lectures (Springer and Scott, 1994; Springer et al., 1998).

- California Department of Transportation (CalTrans) excavations in San Diego County provided new genera and species of middle Eocene rodents (Walsh, 1997, 1998).

The public in general is fascinated by fossils, and local communities are especially proud of fossils found in their own back yards (Figure 2). The recovery of fossils often will cast a positive light on construction-related excavation.

New fossils as a valuable source of geologic data

The salvage of fossils has practical aspects for the geologist, in addition to the intrinsic value of the preservation of past life forms. Fossils are important tools used in dating sediments, and can provide information that refines or revises the ages of fossil-bearing sediments or the rates of fault movement along basin boundaries. For example:

- Highway cuts in Cajon Pass, San Bernardino County, have produced fossil rodent faunas that changed the estimated age of the Crowder Formation from 3 million years to 18.8 million years (Reynolds, 1991b, 1994)

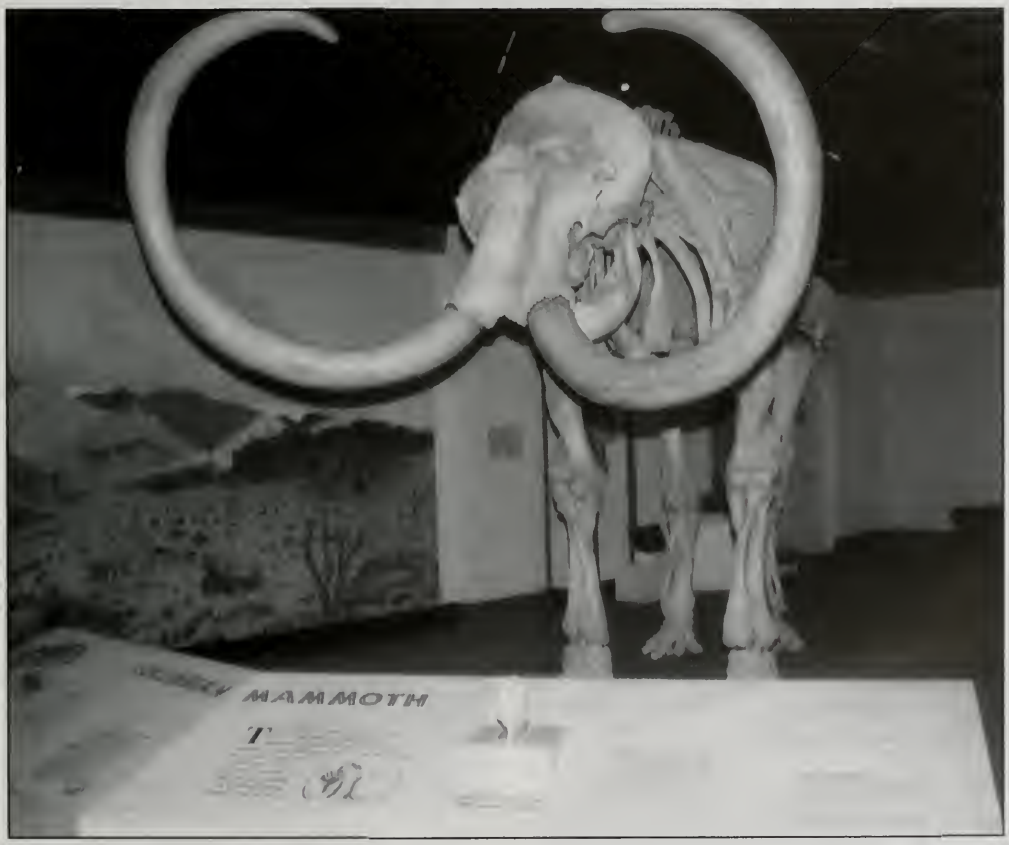

Figure 2. *Mammuthus columbi*, the Columbian mammoth, stood about 13 feet high at the shoulder and roamed a cooler southern Nevada during the Pleistocene. Photograph courtesy of the Nevada State Museum and Historical Society.

Figure 3. Jaw of the Miocene shrew, *Paradomnina relictus*, recovered during excavation monitoring. This fossil insectivore changed the age of the Crowder Formation to 18.8 million years. The small jaw is mounted on the shaft of a sewing pin with its head removed.

(Figure 3). This change prompted re-evaluation of rates of movement along the San Andreas fault (Meisling and Weldon, 1989).

- Excavation for solar energy generating sites at Daggett, San Bernardino County, uncovered fossils that suggested the Calico fault dammed the Mojave River between 12,000 and 9,000 years ago (Reynolds, 1992; Reynolds and Reynolds, 1991a). This fault now is recognized as active for the purpose of the Alquist-Priolo Special Studies Act.

- In 1982, only two isolated Late Pleistocene fossils were known from Murrieta, Riverside County. Monitoring of construction-related excavation has identified 450 paleontologic localities to date, and has shown that this portion of the Elsinore Trough was filled with continental sediments ranging in age from 3.5 million years to less than 500,000 years (Reynolds et al., 1991; Pajak et al., 1996) (Figure 4).

- The Intermountain Power Project crossed the Mojave Desert on a well-traveled utility corridor where no fossil localities had been recorded previously. Monitoring during construction of this project located 52 new fossil localities and changed the estimated ages of three formations (Reynolds, 1986a, 1986b, 1991a).

- Lassen and Modoc Counties are crossed by the Tuscarora Pipeline. Monitoring and salvage during pipeline construction located small mammals that dated the early Pliocene uplift and volcanism of the Modoc Plateau and western Cascades, and the Klamath Mountains orogeny (Wagner et al., 1997).

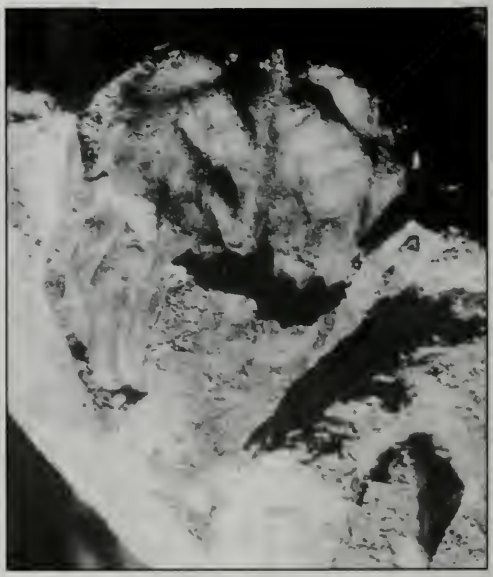

Figure 4. This brain case, an internal skull mold of the camel *Miolabis*, was unearthed by a D9 caterpillar tractor with ripping claws.

Planning

The planning of mitigation measures is greatly facilitated by paleontologic resource assessments and excavation monitoring programs. By analyzing information from paleontologic sensitivity maps and data from assessments and prior mitigation projects in a region, agency planners and paleontologists can forecast paleontologic sensitivity and determine necessary mitigation measures early in the project planning stage. Early planning allows developers to be alerted about paleontologic resources and to incorporate adequate impact mitigation measures during project planning. The mitigation measures, which include monitoring and salvage, washing and preparation, identification and curation, storage, and a report of findings, are implemented during construction and make up the paleontologic resource impact mitigation (PRIM) program. The results of some of these mitigation programs are summarized below.

- As previously noted, just two fossil localities were known from the Murrieta-Temecula area of western Riverside County (Kennedy, 1977). The area was covered by thick soils, and outcrops were not exposed until cuts by earth-moving equipment allowed paleontologists to examine the strata and discover additional fossils (Figure 5). Today, 450 localities are known from Murrieta (Reynolds et al., 1991; Pajak et al., 1996).

- In 1991, one fossil site was known about two miles from Diamond Lake. Planning concerns over nonrenewable resources required a PRIM program and today 1,700 sites have been recorded from the project (Springer, 1998).

- In 1980, prior to the Intermountain Power Project, six fossil sites were known from the Victorville area of San Bernardino County. Paleontologic mitigation led to 350 fossil localities being recorded in this portion of the southwestern Mojave Desert (Reynolds, 1986b; Scott et al., 1997).

Figure 5. D9 Caterpillar tractors use blades and rippers to develop railroad cuts. Paleontologists looking for fossils must be responsive to sudden moves.

Mitigation programs can help planning agencies develop predictive models for determining where fossils might occur. Paleontologists and planners have worked together to develop paleontologic resource sensitivity maps for the southern California counties that show the developer (or more commonly the developer's environmental planning firm), during initial scoping, what fossil-bearing formations might be encountered (Reynolds, 1988). The environmental engineer who faces the challenge of protecting both non-renewable paleontologic resources and the client's interests will find that early scoping of issues in concert with the planning agency can be very beneficial. It is far preferable to plan for the potential discovery of a major fossil resource during the design stage than to deal with the unanticipated discovery of such an occurrence during construction excavation, when there might be adverse consequences to project schedules and budgets.

STANDARDS AND LAWS

The preservation of significant fossils is supported by legislation because such fossils are recognized as non-renewable resources. Vertebrate and certain invertebrate, plant, and trace fossils are non-renewable because only on rare occasions can someone return to an outcrop and recover additional similar fossil remains.

A memorandum from Grissold E. Petty (1978), Acting Associate Director of the Bureau of Land Management, stated that there is no universally accepted definition for a significant scientific paleontologic resource. A definite determination can only be made by a qualified, trained paleontologist. A paleontologic resource is of significant scientific, and educational value if it:

1. Provides important information of the evolutionary trends among organisms, relating living inhabitants of the earth to extinct organisms.

2. Provides important information regarding development of biological communities or interaction between botanical and zoological biotas.

3. Demonstrates unusual or spectacular circumstances in the history of life.

4. Is in short supply and in danger of being depleted or destroyed by the elements, vandalism, or commercial exploitation, and is not found in other geographic locations. All vertebrate fossils have been categorized as being of significant scientific value.

More than a dozen federal and California state laws and acts apply to the preservation of nonrenewable paleontologic resources (Appendix A). For example, under the California Environmental Quality Act (CEQA), county and city agencies have implemented guidelines to protect paleontologic resources in areas under their respective jurisdictions. Some state, county and city agencies within the counties of San Diego, Orange, Los Angeles, Ventura, Riverside and San Bernardino, use guidelines (Appendix B) that conform to those recommended by the Society of Vertebrate Paleontology (SVP, 1991, 1995).

Southern California has led in the field of fossil resource recovery, following CEQA mandates for the recognition of paleontologic resources at construction sites. Northern California is beginning to recognize the vast fossil heritage that can be recovered through excavation monitoring.

PALEONTOLOGIC RESOURCE IMPACT MITIGATION PROGRAMS

What does a developer do when asked if the project will have significant impacts in paleontologic resources? Simply looking at a geologic map will not provide enough information. For example, paleontologic investigations may show that fossil localities may have been recognized in Pleistocene sediments that underlie an area mapped as Holocene alluvium, or that a Miocene conglomeratic sandstone in an otherwise fossiliferous formation has been shown by previous fieldwork to have low potential for fossils. The mitigation process to prevent negative impacts to significant non-renewable fossils thus must start with a search of paleontologic locality records through major museums and libraries, in order to determine the potential for an excavation to encounter fossiliferous sediments. In California, these institutions include the University of California Museum of Paleontology, Berkeley; the Natural History Museum of Los Angeles County; the San Bernardino County Museum in Redlands; the University of California, Riverside; and the San Diego Natural History Museum. The records search will indicate to the developer if the potential for significant paleontologic resources is high or low. If the potential cannot be determined through a records search, a field survey by a qualified paleontologist will help determine a high or low potential.

If the potential is low, no impact mitigation program is required. If the potential is high for nonrenewable paleontologic resources, standard procedures, summarized in the list below, may be recommended for impact mitigation.

1. Conduct a pre-excavation field inspection to determine whether paleontologic resources are present on the surface and develop a plan for their removal.

2. Develop a construction phase paleontologic resource impact mitigation (PRIM) program for monitoring and recovery of fossils by a qualified paleontologist during excavation. Excavation equipment may need to be temporarily diverted for short periods of time during this process.

3. Recovered specimens are prepared to a point where they can be identified and curated for the itemized compliance report.

4. Specimens are identified and itemized in accordance with the curatorial system of the repository institution.

5. Arrangements for storage of the specimens at the repository are made prior to the start of excavation. To reduce costs of storage, specimens may be preserved and prepared

to reduce size. The SVP has proposed receivership conditions to insure that museum repositories do not become "dumping grounds" for homeless non-renewable resources (SVP, 1996).

6. A final report signals compliance with the conditions of the planning agency and the repository museum. The report should be circulated to concerned agencies and groups and be made available to the public.

SUMMARY

Vertebrate and certain invertebrate fossils are protected by law. By following guidelines for mitigation of construction impacts on fossils, planners and developers can work together to preserve an irreplaceable natural resource, and foster research that has direct bearing on the practical understanding of stratigraphy and structural geology. At the same time, they can nurture a positive public attitude toward the conservation of an important aspect of our natural heritage.

ACKNOWLEDGEMENTS

The author thanks Bob Anderson, whose experience in dealing with Northern California paleontologic resources encouraged me to write this article. Thanks also to E. Bruce Lander and Richard P. Hilton for their constructive and thoughtful reviews of this manuscript.

AUTHOR PROFILE

Robert E. Reynolds is a paleontologist in the Riverside, California office of LSA Associates, Inc. As a member of the Society of Vertebrate Paleontology and as a Curator of Earth Sciences for 32 years, he was instrumental in developing guidelines for paleontologic resource management for the Society and for counties in Southern California in response to CEQA regulations.

SELECTED REFERENCES

Coombs, W.P., Jr. and Deméré, T.A., 1996, A late Cretaceous nodosaurid ankylosaur (Dinosauria: Ornithischia) from marine sediments of coastal California: Journal of Paleontology, v. 270, no. 2, p. 311-326.

Deméré, T.A.,1988, Early Arikareean (Late Oligocene) vertebrate fossils and biostratigraphic correlations of the Otay Formation at Eastlake, San Diego County: S.E.P.M. West Coast Paleogene Symposium, v. 58, p. 35-43.

Dundas, R.G., 1994, The Fairmead landfill locality: a Late Irvingtonian fauna from western Madera County, California: Geological Society of America, 90th Annual Cordilleran Section, Abstracts with Programs, v. 26, no. 2, p. 49.

Kelly, T.S., 1990, Biostratigraphy of Uintan and Duchesnean land mammal assemblages from the middle member of the Sespe Formation, Simi Valley, California: Contributions in Science, no. 419, p. 1-43.

Kelly, T.S., 1992, New Uintan and Duchesnean (middle and late Eocene) rodents from the Sespe Formation, Simi Valley, California: Bulletin of the Southern California Academy of Science, v. 91, no. 3, p. 97-120.

Kelly, T.S., Lander, E. B., Whistler, D. P., Roeder, M. A., and Reynolds, R. E., 1991, Preliminary report on a paleontologic investigation of the lower and middle members, Sespe Formation, Simi Valley Landfill, Ventura County, California: PaleoBios, v. 13, no. 50, p. 1-13.

Kelly, T.S. and D. P. Whistler, 1994, Additional Uintan and Duchesnean (middle and late Eocene) mammals from the Sespe Formation, Simi Valley, California: Contributions in Science, no. 439, p. 1-29.

Kennedy, M.P., 1977, Recency and character of faulting along the Elsinore fault zone in southern Riverside County, California: California Division of Mines and Geology, Special Report 131, p. 1-12.

Lander, E.B., 1994, Paleontologic resource impact mitigation program final report, Santiago Canyon Landfill, southeast and southwest borrows, Orange County, California: Consultant's report to County of Orange, Integrated Waste Management Department, p. 1-85.

Lander, E. B., 1997, Paleontologic resource impact mitigation program final report, Puente Hills Landfill expansion, Los Angeles County, California: Consultant's report to Solid Waste Management Department, County Sanitation Districts of Los Angeles County, Whittier, California, 112 p.

Meisling, K.E. and Weldon, R.J. III, 1989, Late Cenozoic tectonics of the northwestern San Bernardino Mountains, southern California: Geological Society of America Bulletin, v. 101, p. 106-128.

Pajak, A.F., III, Scott, E., and Bell, C.J., 1996, A review of the biostratigraphy of Pliocene and Pleistocene sediments in the Elsinore fault zone, Riverside County, California: PaleoBios, v. 17, nos. 2-4, p. 28-49.

Reynolds, R.E., 1986a, Intermountain Power Project (IPP): Coyote Ground Electrode Project, paleontological resources salvage program, final report: Consultant's report to Applied Conservation Technology, Inc., Westminster, California, 52 p.

Reynolds, R.E., 1986b, Paleontologic monitoring and salvage, Intermountain Power Project, Intermountain-Adelanto Bipole I transmission line, California section, Part I: Consultant's report to Applied Conservation Technology, Inc., Westminster, California, 275 p.

Reynolds, R.E., 1988, Paleontologic resource overview and management plan for Edwards Air Force Base, California: Consultant's report to Edwards Air Force Base, 199 p.

Reynolds, R.E., 1990, Paleontologic monitoring and salvage, Sycamore Cogeneration Project, Oildale, Kern County, California: Consultant's Report to Sycamore Cogeneration Company, Bakersfield, 222 p.

Reynolds, R.E., 1991a, Hemingfordian/Barstovian Land Mammal Age faunas in the central Mojave Desert, exclusive of the Barstow Fossil Beds: *in* Woodburne, M.O., Reynolds, R.E. and Whistler, D.P. (eds.), Inland southern California, the last 70 million years, p. 88-90: Redlands, San Bernardino County Museum Association, Quarterly v. 38 no. 3, 4, 115 p.

Reynolds, R.E., 1991b, Biostratigraphic relationships of Tertiary small vertebrates from Cajon Valley, San Bernardino County, California: *in* Woodburne, M.O., Reynolds, R.E. and Whistler, D.P., (eds.), Inland southern California, the last 70 million years, p. 54-59: Redlands, San Bernardino County Museum Association, Quarterly v. 38 no. 3, 4, 115 p.

Reynolds, R.E., 1992, Quaternary movement on the Calico fault, Mojave Desert, California: *in* Richard, S.M., (ed.), Deformation associated with the Neogene Eastern California Shear Zone, southeastern California and southwestern Arizona: Redlands, San Bernardino County Museums Special Publication, 92-1, p. 64-65.

Reynolds, R.E., 1994, Quantum leaps through time: biostratigraphic analysis of the Miocene Crowder Formation, Cajon Pass, San Bernardino County, California: Geological Society of America, 90th Annual Cordilleran section, Abstracts with Programs, v. 26, no. 2, p. 84.

Reynolds, R.E., Mead, J.I., and Reynolds, R. L., 1991, A Rancholabrean fauna from the Las Vegas Formation, North Las Vegas, Nevada: San Bernardino County Museum Association Special Publication, v. 91, no. 1, p. 140-146.

Reynolds, R.E. and Reynolds, R.L., 1991a, Structural implications of Late Pleistocene faunas from the Mojave River Valley, California: *in* Woodburne, M.O., Reynolds, R.E. and Whistler, D.P., (eds.), Inland southern California, the last 70 million years, San Bernardino County Museum Association, Quarterly v. 38, no. 3, 4, p. 100-105.

Reynolds, R.E., Reynolds, R.L., and Pajak, A.F., III, 1991, Blancan, Irvingtonian, and Rancholabrean(?) Land Mammal Age faunas from western Riverside County, California: *in* Woodburne, M.O., Reynolds, R.E. and Whistler, D.P. (eds.), Inland southern California, the last 70 million years: San Bernardino County Museum Association, Quarterly v. 38, no. 3, 4, p. 27-40.

Scott, E., Springer, K.B., and Murray, L.K., 1997, New records of early Pleistocene vertebrates from the west central Mojave Desert, San Bernardino County, California: Abstracts of Papers, Journal of Vertebrate Paleontology 57th Annual Meeting, p. 75A.

Springer, K.B. and Scott, E., 1994, First record of Late Pleistocene vertebrates from the Domenigoni Valley, Riverside County, California: Abstracts of Papers, Journal of Vertebrate Paleontology 54th Anual Meeting, p. 47A.

Springer, K. B., Scott, E., Murray, L. K., and Spaulding, W. G., 1998, Partial skeleton of a large individual of *Mammut americanum* from the Domenigoni Valley, California: Journal of Vertebrate Paleontology, Abstracts of Papers, 58th Annual Meeting, p. 79a.

Wagner, H.M., Hanson, C.B., Gustafson, E.P., Gobalet, K.W., and Whistler, D.P., 1997, Biogeography of Pliocene and Pleistocene vertebrate faunas of northeastern California and their temporal significance to the development of the Modoc Plateau and the Klamath Mountains orogeny: San Bernardino County Museum Association Quarterly, v. 44, no. 1, p. 13-22.

Walsh, S. L., 1997, New specimens of *Metanoiamys*, *Pauromys*, and *Simimys* (Rodentia, Myomorpha) from the Uintan (Middle Eocene) of San Diego County, California, and comments on the relationships of selected Paleogene Myomorpha: Proceedings of the San Diego Society of Natural History, no. 32, p. 1-20.

Walsh, S.L., 1998, Notes on the anterior dentition and skull of *Proterixoides* (Mammalia: Insectivora: Dormaaliidae), and a new dormaaliid genus from the early Uintan (Middle Eocene) of southern California: Proceedings of the San Diego Society of Natural History, no. 34, p. 1-26.

Walsh, S.L. and Deméré, T.A., 1991, Age and stratigraphy of the Sweetwater and Otay formations, San Diego County, California: Pacific Section S.E.P.M., v. 68, p. 131-148.

APPENDIX A

LEGAL OBLIGATIONS FOR THE PROTECTION OF PALEONTOLOGIC RESOURCES

Discussion

Paleontologic remains are recognized as nonrenewable resources significant to our culture, and as such are protected under provisions of the Antiquities Act of 1906 and subsequent related legislation, policies, and enacting responsibilities.

In general, significant paleontologic resources are fossils or assemblages of fossils that are unique, unusual, rare, uncommon, diagnostically or stratigraphically important, and those that add to an existing body of knowledge in specific areas, stratigraphically, taxonomically, or regionally. They include fossil remains of large to very small aquatic and terrestrial vertebrates, remains of plants and animals previously not represented in certain portions of the stratigraphy, and assemblages of fossils

that might aid stratigraphic correlations, particularly those offering data for the interpretation of tectonic events, geomorphologic evolution, paleoclimatology, and the relationships of aquatic and terrestrial species.

Summary of federal legislation

Federal Antiquities Act of 1906. Forbids and establishes criminal sanctions for disturbance of any object of antiquity on Federal lands without a permit.

1872 Mining Law, amended 1988. Operators may not knowingly disturb or destroy any scientifically important paleontological remains on Federal lands.

Mineral Leasing Act of 1920. Provides for the protection of interest of the United States. Paleontologic resources are commonly regarded as such interests.

National Natural Landmarks Program under the Historic Sites Act of 1935. A National Natural Landmark is defined as "an area of national significance . . . that contains an outstanding representative example(s) of the nation's natural heritage, including . . . geological features . . . or fossil evidence of the development of life on earth."

National Environmental Policy Act of 1969 (NEPA). Mandates evaluation of impacts to "preserve important historic, cultural, and natural aspects of our national heritage".

Executive Order 11593, May 31, 1971, Protection and Enhancement of the Cultural Environment (36 CFR 8921). Requires Federal agencies to inventory and protect properties under their jurisdiction. National Park Service regulations under 36 CFR provide that paleontologic specimens may not be disturbed or removed without a permit.

Archaeological and Historic Data Preservation Act of 1974. Provides for the survey, recovery, and preservation of significant scientific, prehistoric, historic, archaeological, or paleontological data when such data may be destroyed or irreparably lost due to a Federal, federally licensed, or federally funded project.

36 CFR Part 800: Procedures for the Protection of Historic and Cultural Properties. Establishes procedures to ensure that historic and cultural resources are given proper consideration in the preparation of environmental impact statements.

Federal Land Management and Policy Act of 1976. Provides authority for BLM to regulate lands under its jurisdiction to "protect the quality of scientific, scenic, historic, ecological, environmental . . . and archaeological values."

Surface Mining Control and Reclamation Act of 1977. Provides designation as unsuitable for surface mining if mining would " . . . result in significant damage to important cultural, scientific, and esthetic values and natural systems . . ."

Summary of California legislation

California Environmental Quality Act of 1970. Requires identification of potential adverse impacts of a project to any object or site of scientific importance.

Guidelines for the Implementation of the California Environmental Quality Act. Requires mitigation of adverse impacts to a paleontologic site from development on public land.

Guidelines for the Implementation of CEQA, 1992, Appendix G, section J (Significant effects). Defines when a project will normally have a significant effect on the environment. Paleontology is specifically mentioned as a protected resource.

California Environmental Quality Act, State of California Public Resources Code, 2100-21177 as amended January 1, 1999, Appendix G - Environmental Checklist Form. Impacts to known, important paleontological resources are specifically covered under CEQA as potentially significant effects.

Warren-Alquist Act. Requires the California Energy Commission to take into account scientific concerns when evaluating proposed energy facilities for certification.

Public Resources Code, Section 5097.5. Prohibits excavation or removal of any "vertebrate paleontological site . . . or any other archaeological, paleontological or historical feature, situated on public lands, except with the express permission of the public agency having jurisdiction over such lands."

Public Resources Code, Section 30244. Requires reasonable mitigation of adverse impacts to paleontological resources from development on public land.

APPENDIX B

GUIDELINES FOR MITIGATION OF ADVERSE IMPACTS TO PALEONTOLOGIC RESOURCES

Construction impacts to significant paleontologic resources can be mitigated as follows.

1. **Literature and records search.** Geologic and paleontologic literature and site reports must be reviewed to determine the paleontologic sensitivity of specific areas.

2. **Field survey.** A field survey should be performed to clarify the sensitivity of areas of undetermined potential. The field study will classify the areas into either high sensitivity or low sensitivity. High sensitivity includes not only the potential for abundant fossils but also the potential for production of a few significant fossils that may provide new and significant data. The field survey must be conducted by a qualified paleontologist.

3. **Adequate monitoring** to salvage specimens. Monitoring must take place during hours when excavation is underway. If excavation is in a formation with potential for fossils, a monitor must be present at least 50% of the time. If fossils are being found, the monitor must be present 100% of the time. The monitoring must include contingency for back-up monitors to assist in removal of large or abundant fossils so that delays to construction excavation can be avoided. Monitors must be qualified and experienced in paleontologic salvage, authorized to temporarily divertequipment to remove fossils, and must be provided with supplies and equipment to allow rapid removal of specimens.

4. **Storage and preparation.** Arrangements for adequate storage of significant specimens recovered during monitoring must be provided. Adequate storage includes storage in a recognized paleontologic specimen repository, such as a museum or university, with a permanent curator. Specimens must be stored in a fashion that allows retrieval by researchers in the future. Specimens must have excess matrix removed to reduce storage space and cost and to allow the significance of the specimens to be determined.

5. **Identification.** Specimens must be identified individually by family, genus and species.

6. **Report of significance.** A report must be prepared by the paleontologist, describing the significance of the specimens recovered, and their relationship to the strata from which they were recovered and to other similar fossil localities. An inventory of specimens with numbers that correspond to the recording systems used by the institution where the specimens are curated and stored must be appended to the report of significance.

SEWAGE DISPOSAL IN THE GEOLOGIC ENVIRONMENT

ALVIN L FRANKS[1]

ABSTRACT

The best and the most reliable methods available for the treatment and disposal of domestic sewage use designs and natural materials suited to the local geologic environment. Therefore, mapping and testing of the local geologic, hydrogeologic, and topographic conditions are critical to the dependability and life expectancy of disposal systems. A disposal system constructed in the wrong geologic environment can be a threat to public health and can also result in the degradation of both groundwater and surface water quality.

In the proper geologic setting, the septic tank, leach field system/seepage pit disposal systems, beneficial use of reclaimed water, or the land disposal by percolation of flows from small- to moderate-sized waste water treatment plants can work 100% of the time. Even when there is an upset in a treatment plant, the partially treated waste-water discharged to a well-designed percolation system is given sufficient treatment in the geologic environment to remove all pathogenic organisms prior to reaching the groundwater body. This can be compared to the fact that most municipal sewage treatment plants function without biological upset and discharge of partially treated sewage to surface waters only 85% of the time.

The liquid disposal portions of both the individual system and some of the treatment plants using percolation for disposal have a life expectancy of, at most, 10 to 12 years under ideal geologic conditions. At that time they have to be rehabilitated, replaced, or rested for a period of time prior to being placed back into service.

All types of sewage effluent disposal systems should avoid use of fractured rock, open gravel, or limestone for percolation of waste water. Ideally, to provide sufficient soils for full treatment of the waste, there should be at least ten feet of soil above impervious bedrock or the first clay layer, or at least three feet of unsaturated soil over fractured rock or open gravels. This soil must have sufficient permeability to carry both the sewage and the natural water away without surfacing, and contain enough fine soils to prevent transport of bacteria into the groundwater system or to the surface. In the proper geologic environment and topography, these disposal systems should outlive the buildings being served.

INTRODUCTION

The methods for proper disposal of sewage to land, and the geologic problems encountered when doing so, have been known since the early 1950s. The same geologic problems that were "solved" then are, in many instances, ignored today. This is particularly true now that prime land has become less available for development. Industry and subdivisions are being constructed in areas with less than ideal conditions for disposal of sewage and other liquid wastes. In many areas the liquid disposal systems are being constructed with little or no geologic investigation, resulting in undesirable contamination of both surface and groundwater. Many prime areas, such as the foothills and mountains, reclaimed flood plains and prime agriculture land,

[1]Engineering Geology Consultant
44 Lakeshore Circle
Sacramento, CA 95831
alfranks@prodigy.net

have had extensive residential and business development without proper geologic investigation. This has resulted in contamination of the same groundwater that is being extracted for domestic use on the overlying land or in contamination of the adjoining water ways.

Some inexperienced geologists, engineers, and contractors design liquid disposal systems based only on percolation tests, disregarding the geologic and topographic environment. They measure the rate of infiltration in a shallow pit dug in overburden soils, but ignore crucial measurements of the distance to bedrock or impervious clay layers, the surface slope, or the maximum high water table conditions. They assume that if the fluid percolates and is out of sight "the natural environment will clean it up" before it can cause a problem.

HISTORICAL BACKGROUND

Prior to about 1870, all sewage was discharged to the land, or to a stream, or was just dumped out the window. The systems used by the Greeks and Romans, and the flush toilets designed by Leonardo da Vinci (1500) in Italy and John Harington (1870s) in England, all used water to carry the raw sewage to the land or to a stream. At about the same time that the flush toilet was reinvented, a Frenchman, Jean Louis, developed the use of seepage pits/cesspools to percolate the sewage carried by pipes from individual buildings (Cotteral and Norris, 1969).

When the pits became clogged and the fluid started to come to the surface, a trench was dug to carry the fluid to the nearest stream. Jean Louis found that the fluid percolated from the trench became less odoriferous within a few tens of feet. To hide the remaining odors, he started to backfill the ditch with rock and gravel and cover it with dirt. He found that the odors disappeared, and all of the fluid would percolate if the trench was long enough. The cesspool systems, along with the gravel-filled trenches, were introduced into the United States in 1884. This was the start of the septic tank leach field/seepage pit systems used today.

Prior to the early thirties, discharge of domestic sewage from urban areas was combined with storm water, in a pipeline, and conveyed to the nearest body of water. In the 1930s a few of the larger inland cities started to remove some of the solids with primary clarification units or storage ponds before dumping the waste water into the rivers. In 1949, the federal government began to give limited matching grant funds to municipal governments for construction of treatment plants in an effort to clean up some of the polluted rivers and ocean beaches. This effort culminated with proclamation of the Federal Clean Water Act of 1977. This act, and the water quality requirements for surface water discharge permits, led to the design and construction of digesters, primary clarification units, extended aeration and liquid oxygen systems for the treatment of sewage. Federal matching funds were also used to construct separate pipelines for sewage and storm water.

NATURE OF THE WASTE FLUIDS DISCHARGED TO THE GEOLOGY SYSTEM

To better understand the role of the geologic environment in the treatment and disposal of domestic sewage, it is necessary to know the nature of the waste fluid. The fluid discharged into a septic tank or pit contains all of the materials from baths, laundries, toilets, and kitchen sinks. In a single family dwelling there is an intermittent flow of this waste material, compared to an almost continuous flow from apartments or business complexes. In either instance, the sewage passes through two steps in the septic tank that make it percolate at a faster rate into the soils in the disposal system: (1) the removal of solids by settling and breakdown to a fluid state, and (2) the anaerobic biological breakdown of much of the organic materials with formation of methane and ammonia gases. Sludge and scum remain behind in the tank (Figure 1). The clarified liquid is discharged from the septic tank to the leach field or seepage pit system. Ironically, this liquid is more unpleasant than the original waste effluent. It is an odoriferous fluid containing large quantities of anaerobic bacteria, nutrients, salts, fine suspended solids and, in many instances, pathogens (Franks, 1972).

The inflow to a treatment plant often includes commercial and industrial wastes, which contain additional chemicals. The fluid discharged from a treatment plant is variable and largely depends on the degree of treatment.

The treated fluid from the primary clarification unit is similar to that from a septic tank: an odoriferous fluid containing large quantities of anaerobic bacteria, nutrients, salts, and pathogens. The fluid from the extended aeration or liquid oxygen unit can

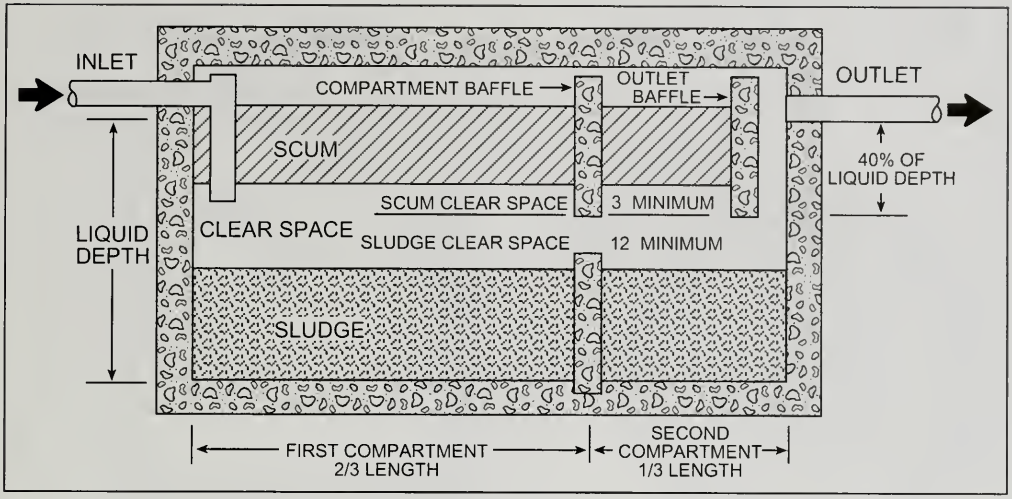

Figure 1. Typical two compartment septic tank. The sewage comes in through the inlet at the left. Solids and other non-floating matter sink to the bottom and floating scum is kept from going out the outlet by baffles. Breakdown of sewage by bacteria in a septic tank can take place only under anaerobic conditions.

be processed to rather high water standards, with the exception of the dissolved organics, nitrates, other salts, and some of the pathogens and viruses that cannot be killed or removed in the chlorination process.

TREATMENT OF THE EFFLUENT IN SOILS

The individual disposal systems usually consist of the two-compartment septic tank (Figure 1) discharging to a seepage pit or to a junction box that divides the flow into two or more trenches with gravel-packed perforated pipe buried in the trenches (Figures 2 and 3). In some cases, a single compartment tank can be used. Percolation tests are used to determine the near-surface infiltration rates which, in turn, determine the required depth and size of a leach field or the size and depth of a seepage pit. For percolation testing, a six-inch diameter hole is dug to the proposed depth of the seepage trench or pit, and a layer of gravel is placed in the bottom of the hole. The bottom portion of the hole is kept full of water for a day until saturated. The hole is then refilled and the rate of infiltration is measured in minutes per inch of drop of the water level in the hole. A rate of percolation of over 60 minutes per inch is not acceptable because the slow rate of infiltration might lead to anaerobic bacterial plugging. A rate of percolation faster than 5 minutes per inch indicates a lack of fine-grained materials, without which harmful bacteria will not be removed.

As the waste fluid moves out of the septic tank into the leach line system or the seepage pit, anaerobic bacteria continue to act on the solids within the fluid, resulting in a continued release of ammonia gas, with partial denitrification of the fluid. As the effluent percolates from the leach line into the soil, the fluid is being changed in at least seven ways: (1) soil filters it, (2) soil exchanges ions with it, (3) it is oxidized, (4) parts of it are electrostatically bonded to the soil, (5) aerobic conditions are established, (6) bacteria in the effluent are attacked by bacteria in the soil, and (7) its temperature is lowered. The last three steps destroy the harmful bacteria.

Tests and studies on the effectiveness of soils as agents for the removal and destruction of harmful bacteria use "coliform" counts as a base. Coliform bacteria are easier to detect than most other pathogenic bacteria. They are called coliform because they resemble the colon bacillus, *Escherichia coli (E. coli)*, which is found in all vertebrate intestinal tracts. Studies of percolation from sewage ponds show that at some point between 4 and 7 feet from

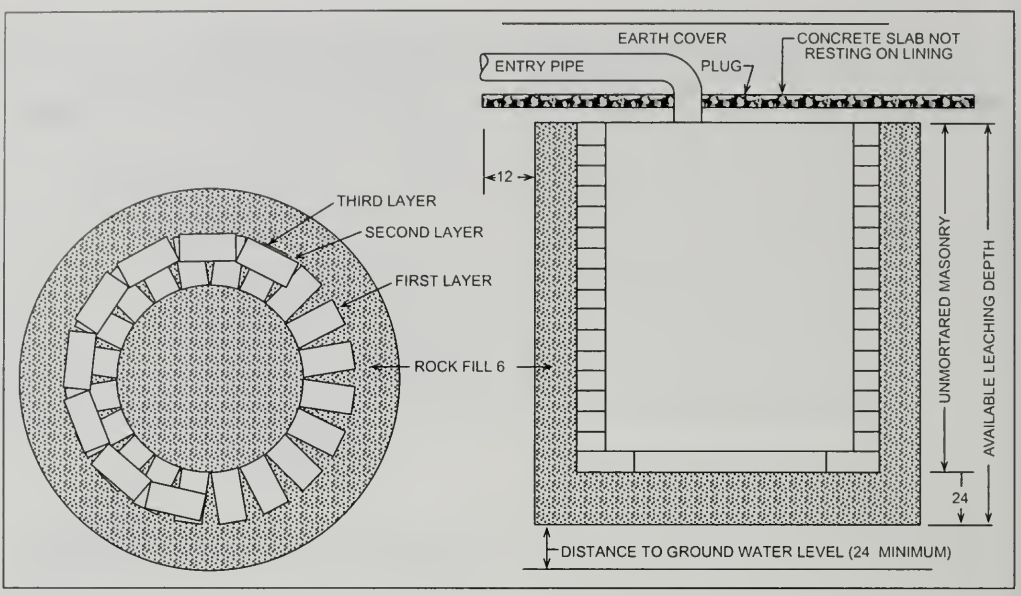

Figure 2. Conventional septic-tank seepage pit seen in plan view and cross section. One or more pits may be used, depending on anticipated disposal volume.

the bottom of the pond, in saturated sandy silt, the number of coliform bacteria declines to less than one organism per 100 milliliters of fluid (SWPCB, 1953). These same experiments also showed that the number of coliform bacteria penetrating one foot or more into the soil is essentially independent of the concentration of pollutants in the water of the infiltration pond.

The survival rates of coliform bacteria traveling through natural soils under saturated and unsaturated conditions were developed from case histories of standard leach fields and specially constructed systems. In all cases the effective grain size of the underlying soil was measured in the system being used for disposal. A summary of the results of studies on the effectiveness of soils for the removal of coliform bacteria is shown in the two graphs in Figure 4 (Franks, 1972; Romero, 1970). They show the distance that effluent must percolate through natural soils for the complete removal of bacteria as a function of particle size. Data for the shaded example on the chart were collected only out to 115 feet down gradient from the percolation trench pollution source. It took the bacteria 187 days, or about 27 weeks, to travel 115 feet through a saturated gravely sand composed of 21.6% gravel, 28.8% coarse sand, 48.4% medium sand, and 1.2% fine sand. Due to the lack of natural recharge and the high permeability of this deposit, the coliform bacteria pollutant traveled only as a thin sheet at the surface of the zone of saturation. There was no evidence that it mixed or dispersed readily downward into the groundwater body under these conditions.

The effective grain size of the soil is more important than the permeability in removal of bacteria. The effective grain size for sediments is defined as the 10th percentile of the grain size distribution (d_{10} — the size in millimeters at which 10% of the soil sample is finer and 90% is coarser). For example, ponding of effluent in a trench over a Hanford sandy loam with an effective grain size of 0.0056 mm and an infiltration rate of 0.3 foot-per-day was measured to have a coliform count of 45 organisms per 100 ml at a depth of 3 feet. Similar testing of a Yolo sandy loam with an effective grain size of 0.0155 mm and an infiltration rate of 0.3 foot per day had a coliform

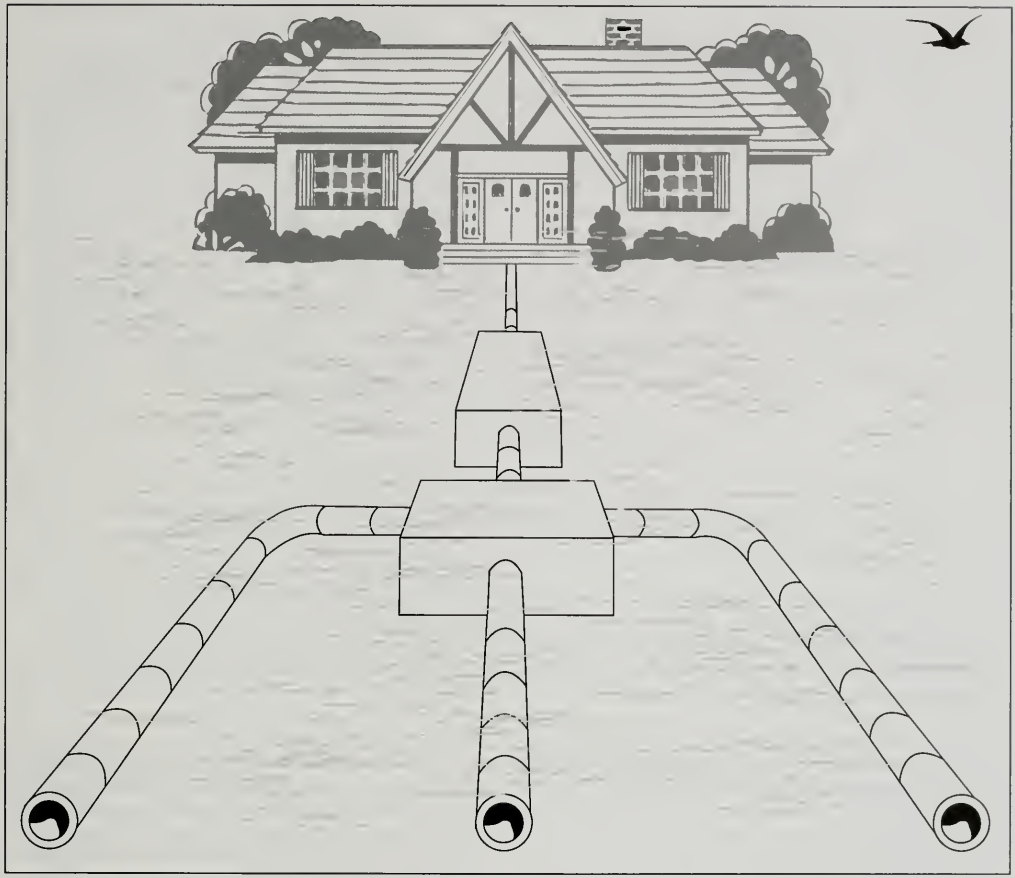

Figure 3. A typical installation of a septic tank, junction box, and leach field with three branches.

count of 24,000 organisms per 100 ml at the same depth. This comparison seems to indicate that with a 3-fold increase in effective grain size there was a 500-fold increase in coliform bacteria at the 3-feet level (Orlob and Krone, 1956). In brief, the location of a disposal system must always take into consideration the effective grain size of the receiving soil, regardless of the results from the percolation test. Materials and geologic conditions that do not provide filtration, such as fractured rock formations, solution channels, and coarse-grained soils that allow passage of pathogenic organisms and viruses over much greater distances should never be used for disposal of sewage.

SOILS AND GEOLOGIC CONDITIONS FOR ON-SITE DISPOSAL SYSTEMS

The basic geology of the bedrock or sediments below the soil horizon to be used for disposal of waste from the septic tank is critical in the design of the disposal system. In addition to the basic geology, the consulting geologist must determine (1) the minimum seasonal depth to water, (2) thickness of

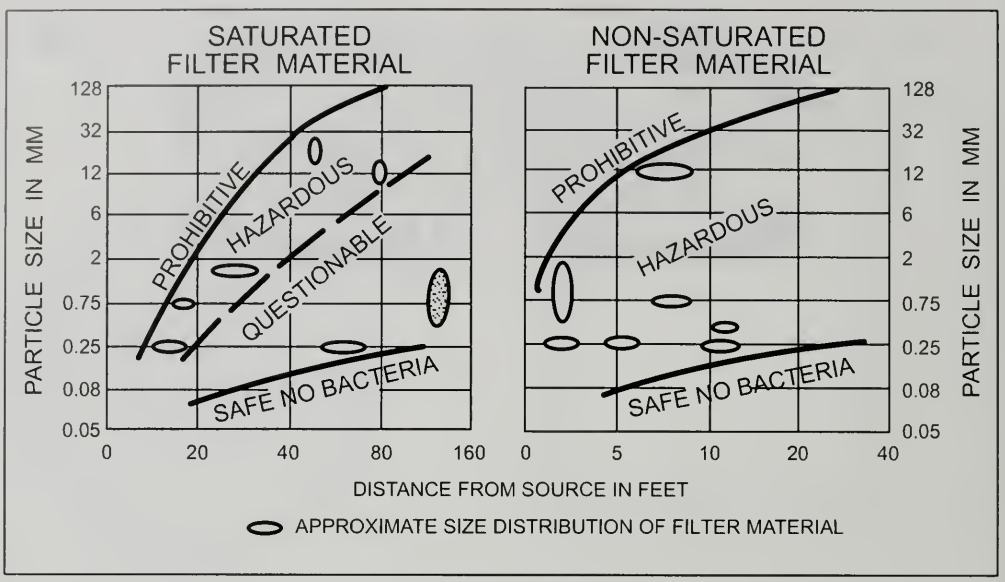

Figure 4. The graphs show the sizes of filter material particles that are effective or ineffective in treating septic tank effluent as it moves away from the leach line system. The shaded enclosed curved area on the right side of the graph for saturated filter material represents filter material that ranges in size from about 0.4 to 1.5 mm. The effective grain size of the shaded area (i.e., the size threshold at which 10 percent by weight of the sample is finer and 90 percent is coarser) is approximately 0.45 mm.

the soil layer, (3) grain size distribution of the soils in the vadose zone, (4) slope of land surface, (5) percolation rate of the soils in the disposal area, (6) hydraulic gradient within the aquifer, and (7) location of nearby wells and springs.

Open fractures or solution channels in rock do not provide filtration or treatment of effluent. Leach fields and seepage pits must have sufficient overlying soil cover to provide for full treatment when located over areas of fractured and fissured rock through which untreated sewage can flow (Figure 5). Case histories of pollution sources have shown that in fractured and cavernous rock there is free flow of contaminants, bacteria, and viruses for thousands of feet. Untreated or partially treated sewage percolating into fractured bedrock, cavernous limestone or open lava tubes has been detected miles away at springs (Franks, 1972).

Superficial pervious deposits over impervious, unfractured rocks provide a method of filtering the effluent, but can result in downstream surfacing of the partially treated fluid. In many areas of Northern California silty-sandy-gravel terrace deposits are underlain by impervious rocks. The percolation tests of these materials would seem to be satisfactory according to the guidelines in the U.S. Public Health *Manual of Septic Tank Practice* (1998). However, if the areal extent of these materials were mapped, it would be shown that they are lens-like deposits thickening toward the river or stream. Because of their limited lateral extent, it is usually found that during the winter months the water table comes up almost to the surface, with flooding of the leach fields built on them. Effluent might then flow downhill untreated and enter the stream with little or no removal of pathogenic organisms.

An example of this condition was found at the South Fork of the American River in El Dorado County, California. A study was done to provide data for a Draft Environmental Impact Report (DEIR) completed in 1999 to determine the effect that 5,000 weekend rafters may have on the quality of water in the river. The bedrock is, for the most

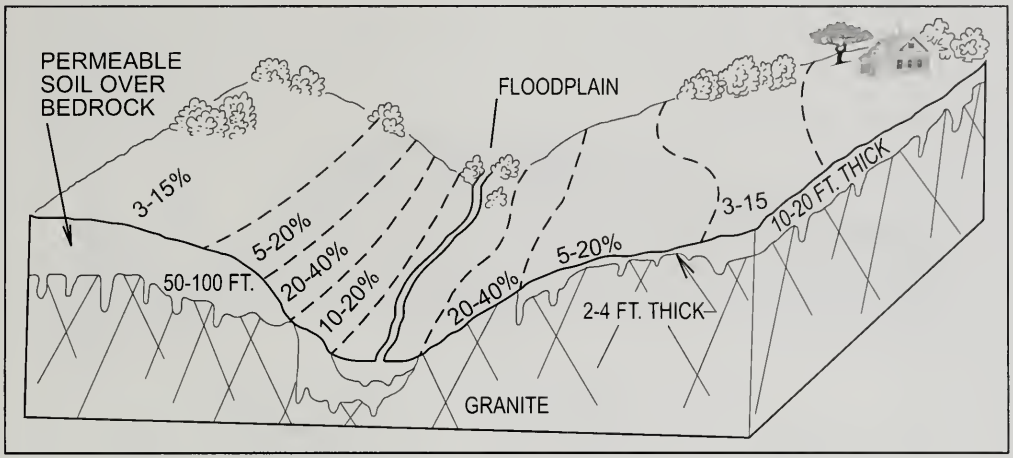

Figure 5. The deep soil over the fractured granite at the left makes this area suitable for septic tank filter fields, except for the fact that layout and construction may be difficult on the steeper slopes. The area with soil 10 to 20 feet thick, at the extreme right, is questionable for filter fields if water supplies come from wells. The shallow soil, 2 to 4 feet thick, is unsuitable for filter fields; if incompletely treated effluent were to enter one of the many fractures in the granite, the effluent might pollute water sources over a long distance.

part, impervious metamorphic rock overlain by flood plain silts and gravely sand terrace deposits. For a period of more than two years water samples were taken in the river immediately downstream from the locations that could be affected by rafters landing for rest stops. It was found that during the summer months, when the river was used by the rafters, there were no coliform bacteria. However, a few days or a week after the first heavy winter storms brought the water table up in the terrace deposits and fractured bedrock used by local residents and businesses for sewage disposal in leach fields, fecal coliform bacteria were found in the samples from the river. The high coliform bacteria count remained up until the end of the rainy season.

High water-table conditions that impact septic systems have multiple causes. The geologist should be aware of other factors that might affect the entire system. The more obvious ones are: (1) Summer/winter fluctuations in water levels as described in the previous paragraph. (2) Multiple systems may cause excessive hydraulic loading in a small area, especially if the loading is at a faster rate than the effluent can drain away. (3) Hydraulic barriers, such as near surface volcanic ash or clay layers, that can limit the ability of effluent to drain vertically or horizontally from the leach field. (4) The import of excess water. The last item is a variable that may be hard to evaluate initially due to the fact that, as the population increases, water may have to be imported and water wells may be abandoned. With the added water supply, lawns are watered, swimming pools built and more disposal systems are added. Under these conditions the water table could rise and flood out many of the leach fields.

The slope of the ground surface can also influence the performance of the disposal system. The slope and the geologic conditions upon which the leach field is constructed are critical to prevent down slope surfacing of the sewage. The standard plumbing code requires that the burial depth of the system on a slope provides at least 15 feet of soil horizontally between the ground surface and the bottom of the leaching system. In many instances, this rational will not work. Most hillside areas are not uniform and in most places there is either bedrock or reduced permeability at depth. As illustrated in Figure 6, any sewage disposed uphill from these areas will follow the same route as the natural water and might flow as a thin film on top of the saturated zone with little or no mixing.

Regardless of the type of material in which the system is constructed, the infiltration rate is

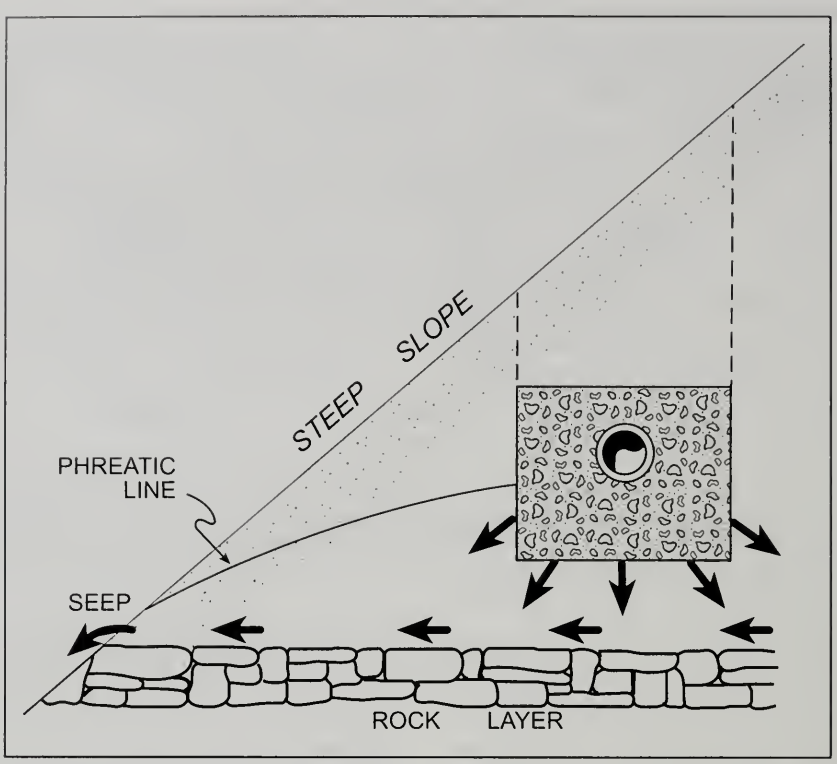

Figure 6. A leach field on a steep slope where there is a layer of dense clay, rock, or other impervious material near the surface is unsatisfactory. The effluent will flow above the impervious layer to the hillside soil surface and run unfiltered down the slope.

reduced over time by (1) plugging of the system with solids, (2) dispersion of the clay particles by exchange of sodium ions from the sewage to the soil, (3) physical breakdown of the soil by wetting and drying and (4) biological plugging. Eventually, all systems reach a minimum infiltration rate based on the extent of development of a biological mat on the trench walls. These factors all work in unison and, as conditions become favorable for one, they become more favorable for the others. Due to these factors, the expected life of a disposal system, even when constructed in the right location, is about 10 to 12 years, at which time it must be replaced. The old plugged disposal system will rehabilitate under aerobic conditions and can usually be placed back into service by the time that the replacement field starts to plug up. In many areas today, it is found to be more economic to install a duplicate system during original construction, with a flip valve to make the changes when required. In the proper geologic environment these systems should outlive the building being served.

EFFLUENT DISPOSAL SYSTEMS FOR TREATMENT PLANTS

The effluent from a plant can be disposed of in at least two types of systems. One is a percolation system into a geologic environment that can remove or destroy all pathogens. The other is the use of the "reclaimed" water in parkways, golf courses, parks, or crops. Both types of systems require a complete geologic investigation to determine the effect of disposal on surface and groundwater quality and public health.

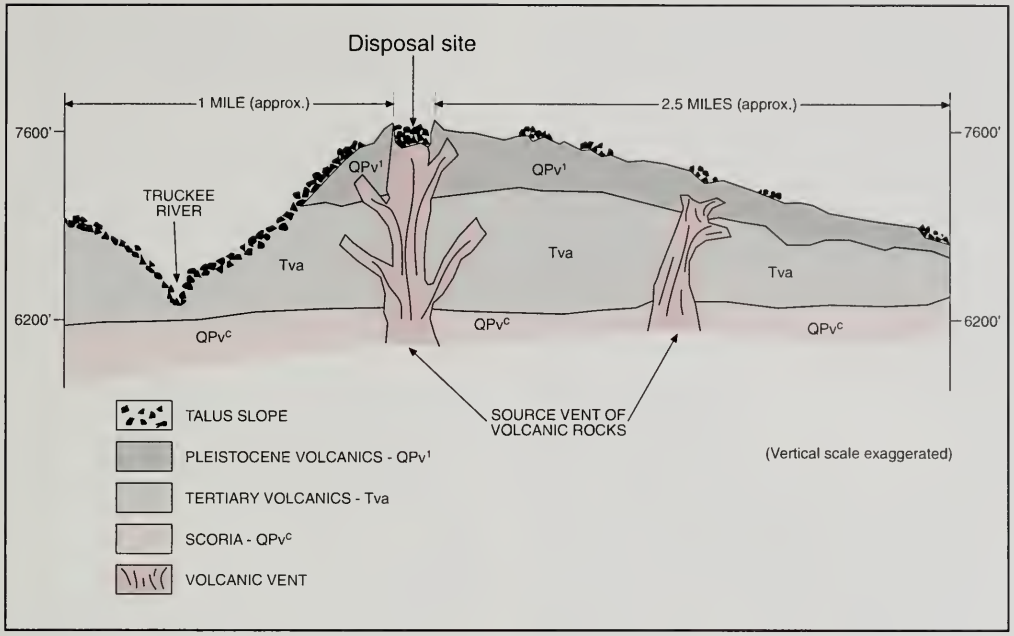

Figure 7. Diagrammatic geologic cross section of the effluent disposal site of the Tahoe City Public Utility District.

Percolation of treated waste water

The Lake Tahoe, California Case Study (Matthews and Franks, 1971). The Tahoe City Public Utility District used the pyroclastic deposits of a cinder cone as an interim disposal site for all of the waste collected at Lake Tahoe north of Emerald Bay. The pre-disposal treatment consisted of a clarifier to remove solids, a storage pond, and a pump to transport the waste two and a half miles to a disposal area about 1,300 feet in elevation above the treatment plant. The maximum flow pumped to the disposal site was about 3.2 million gallons per day, with an average flow of 2.5 million gallons per day.

The geologic exploration program of the disposal site included detailed mapping, drilling, down hole packer tests, slug permeability tests, geophysical exploration and water quality investigation of all springs and seepage areas. Figure 7 shows a diagrammatic sketch of the cinder cone structure and the related volcanic rocks. Several characteristics suggested that the system would provide sufficient treatment and divert effluent from the Lake Tahoe basin. (1) 100 to 125 feet of unsaturated volcanic scoria would act as an aerobic percolation media —similar to an aerobic trickle filter in a standard treatment plant—before the sewage could enter the underlying fractured latite. (2) Disposal water percolating into the latite would flow in a northwesterly direction to a group of existing springs, where the effectiveness of the "trickle filter" could be easily monitored. (3) The buried surface of the underlying impervious bedrock (Tertiary volcanics) sloped to the north, away from Lake Tahoe. (4) The pre-project water levels in the scoria and fractured latite showed that groundwater flows to the northwest, away from Lake Tahoe (Figure 8).

A series of percolation trenches were excavated into 17 acres of the pyroclastic deposits. Areas with high rates of infiltration, as shown by percolation tests, were mixed with fine-grained soil to decrease infiltration rates. A remote control pipe distribution system was installed to alternate the locations for discharge to the trenches during the winter months, when the site was under as much as 15 feet of

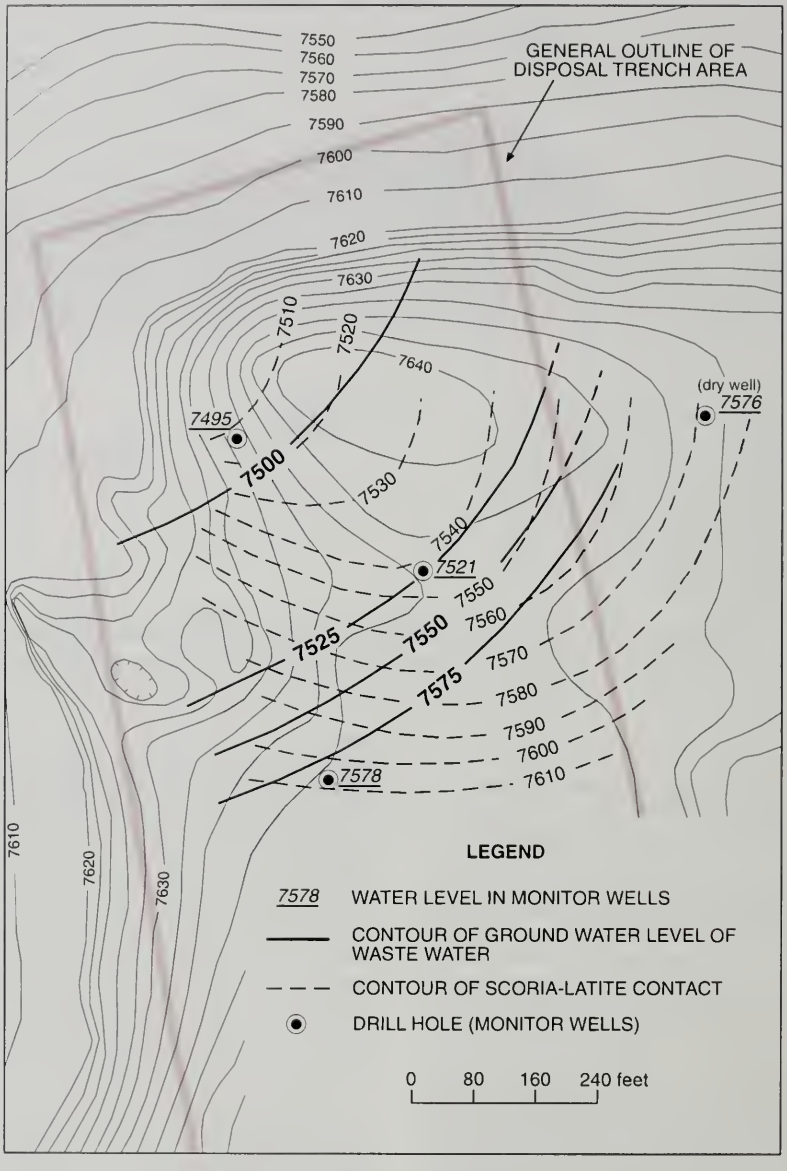

Figure 8. Contour map of ground water elevation (measured 8 June 1971) and scoria-latite contact from data derived from drill hole and seismic refraction studies of the cinder cone site.

snow. The system was placed into operation in the summer of 1970. Additional trenches were added in 1972 for backup in case of future decrease in percolation rates.

The monitoring program showed that the only springs with increases in flow were northwest of the disposal site. Water quality analysis proved that there were no coliform bacteria in any of these down-gradient springs, and that about one half of the nitrogen and all of the phosphate were removed by the percolation through the scoria. There were no changes of background historic flow rates or water quality at any of the springs in the Lake Tahoe watershed.

Martis Creek Treatment Plant, Truckee, California Case Study. The percolation of tertiary treated effluent to recharge a groundwater body is done in many areas in the state. The largest system in Northern California is the Martis Creek sewage plant, located a few miles east of Truckee, California.

Pre-construction drilling and testing showed that the glacial deposit located south of the Truckee River and west of Martis Creek had a capability for percolation of at least 10-million gallons per day. The percolated water would likely flow northeasterly and enter the Truckee River as base flow. Pump tests and calculations showed that the fluid would not surface until it reached the river (Lawrence 1974). Both the State and Federal regulatory agencies required that the treatment plant have the capability for removal of nitrogen and phosphorus to protect the downstream water quality for the city of Reno, Nevada.

The pipeline down the Truckee River to the plant was built in 1976-77, with a capacity of 11.6 million gallons per day. It was designed to pick up all of the sewage from the Tahoe City Public Utilities District system, from the existing structures along the river and tributaries, and from all future developments. Trenches were dug and perforated pipes with a gravel cover were installed along the south bank of the Truckee River and also along the west bank of Martis Creek. The extension of the trenches to Martis Creek were constructed to accommodate future increases in flow to the plant above the calculated percolation rate of 10 million gallons per day along the Truckee River.

The plant has been operating without problems since 1978. All of the water flows underground toward the Truckee River and Martis Creek, where it enters as base flow. Subsequent to the start up of the plant, it was found that the denitrification unit would not be required to meet water quality standards in the Truckee River. The unit was taken out of service with no adverse effects. However, it was found that the extension trenches along Martis Creek added nitrogen to the creek above the limits established by the Department of Fish and Game. The matter was negotiated with Fish and Game and resolved by management of flows to prevent percolation along Martis Creek when the flow in the creek was too low to provide dilution. The plant continues to operate with no problems in the disposal of this highly treated effluent.

Recycling of treated waste water

Use of water from secondary and tertiary treatment plants is a common practice in areas with limited water supply. In Northern California communities use these waters for irrigation of parks, parkways, golf courses and crops. Two examples close to Sacramento are in the communities of El Dorado Hills and Rancho Murieta. The city of Sacramento is also in the process of installing a color-coded pipeline system from the regional waste water treatment plant to parks, future parkways, and other city-controlled property. The treated effluent will be used to cut back on the use of treated drinking water for irrigation purposes.

El Dorado Hills Case Study. The El Dorado Hills planned community is located in the hills southeast of Folsom reservoir, predominately on weathered Jurassic metamorphic rocks with a thin veneer of soil. Most of the residential housing is north of Interstate 80, with the golf course located on the southern portion next to the highway. A business complex is located to the south of the highway. All waste water is collected and given secondary treatment at an on site plant.

Potable water for the El Dorado Hills subdivision and the golf course is imported. There are no municipal or community water wells in the area and the low-yield bedrock wells to the south are used exclusively for domestic water supply for single-family dwellings. Prior to getting approval for use of wastewater, a geologic investigation was made to assure the local water users that there would be no adverse effect to their wells. The investiga-

tion found that excess water applied to the thin soil mantle would be intercepted at the bedrock contact and flow downhill as underflow into existing drainage courses. Under these conditions the excess runoff and percolated water could be collected in small onsite lakes to prevent offsite flow. The project has now been fully implemented with success, and watering is done by sprinklers at night to prevent exposure to the public.

Rancho Murieta Case Study. The Rancho Murieta subdivision is located east of Sacramento, to the north of State Highway 16 in the watershed of the Cosumnes River. The geologic investigation showed that most of the area to be irrigated with reclaimed water was weathered and fractured Jurassic metamorphic rock with a thin soil mantle. Alongside the river there are some overbank river deposits. Potable water for the subdivision is imported and there are no water wells in the service area. The water of the Cosumnes River is used for irrigation downstream from the subdivision, and the underflow and winter overflow provide recharge for the near-river sands and gravels in which some wells are operated for irrigation and domestic use.

Again, prior to getting approval for use of waste water, a geologic investigation was made to assure the downstream water users that there would be no adverse water quality effects. The investigation found that excess water applied to the thin soil mantle would be intercepted at the bedrock contact and flow downhill into the existing drainage courses. This water, along with excess applied irrigation water, is now collected and stored in shallow lakes. The treated wastewater is now used to irrigate parkways, common community property and the golf course with no adverse water quality effects.

City of Fresno Case Study. Water from the city of Fresno secondary treatment plant is used to irrigate raisin grape vines grown on Quaternary sediments that overlie the Central Valley aquifer system. Prior to approval, a geologic investigation was made of the soil types in the vineyard, the depth to the water table, and the existing groundwater quality.

The treated water is chlorinated and pumped to the fields, where it is distributed to ditches for furrow irrigation. Monitoring of the groundwater shows no coliform bacteria and a slight increase in nitrate levels down-gradient from the fields. The increase in nitrate is not a problem since water from the aquifer at this location is used exclusively for irrigation.

SUMMARY AND CONCLUSIONS

The determination of the proper location and design for the land disposal or use of sewage is not a difficult task. Still, many projects fail because little regard was given to the geologic environment. A case in point is the failure of many disposal systems along the American River in El Dorado County due to high water table conditions during the winter months. The case histories outlined in this paper are "success stories" for which thorough geologic investigations were made and a proper disposal or reclamation system was constructed to fit the geologic conditions.

The practicing geologist should be aware that there are many published books and papers by non-geologists that ignore the geologic environment and the capability of the soils for removal of pathogenic organisms and other harmful substances. In many cases these publications set forth specifications that do not follow the local or state statutory requirements. The Uniform Building Code and the U.S. Department of Health's *Manual of Septic Tank Practice* are a good starting point to identify the data that geologists need to provide to the engineer who is designing a wastewater disposal system. However, lest we fall into the fallacy that engineering geology is a cookbook discipline, it is well to remember that these manuals do not tell us how to keep wastewater underground, or how to stop it from causing pollution of surface and groundwater. The construction of a system that is well suited to existing geologic or groundwater conditions remains a challenging technical and scientific endeavor.

Most counties in California have ordinances with specific minimum standards for land disposal, based on State and Federal guidelines. Unfortunately many have not been updated since 1982 and either do not incorporate the latest technology or are not enforced due to political pressure to develop additional taxable property. It is up to the geologic and engineering professions to provide the information and know-how for construction of safe and dependable systems.

ACKNOWELDGMENTS

Grateful thanks are due to David Sederquist, Roy Kroll, and Horacio Ferriz for their thoughtful peer reviews of the manuscript.

AUTHOR PROFILE

Dr. Alvin Franks is a consulting Engineering/ Environmental Geologist. He has over forty years of combined experience, including work with the California Division of Highways, the Water Rights Board, the Water Resources Control Board and as a consultant. He was the author of Chapter 15- Waste Disposal to Land, of the State guideline for on site sewage disposal, and of many other regulatory measures for the protection of groundwater. He received his Ph.D. in geology from the University of California at Davis in 1980. He has been National Membership Chair, Treasure, and Secretary for the Association of Engineering Geology and Chair for the AEG Sacramento Section. After taking the written examination, the Board of Registration, honored him with CHG license #1.

SELECTED REFERENCES

Cotteral, H.A. and Norris, D.P., 1969, Septic tank systems: American society of Civil Engineers, Journal of the Sanitary Engineering Division. S.A. 4-6735.

Franks, A. L., 1972, Geology for individual sewage disposal systems: California Geology, California Division of Mines and Geology. September, v. 25. no. 9, p. 193-203.

Franks, A. L., 1975, Update of sewage disposal at the north Tahoe cinder cone: Association of Engineering Geologists, Field Trip Guide Book, 18th Annual Meeting, Lake Tahoe, California

Franks, A. L., 1993, Hybrid disposal systems and nitrogen removal in individual sewage disposal systems: Bulletin of the Association of Engineering Geologists, v.30. no.2, p. 181- 208.

Lawrence, D. A., Dorratcaque, D. E., Mitchell, S. J., 1974, Hydrogeological investigation of land disposal of reclaimed wastewater near Truckee, California: Unpublished consultant's report.

Matthews, R. A. and Franks, A. L.,1971, Cinder cone sewage disposal site at North Lake Tahoe: California Geology, California Division of Mines and Geology, October, v. 24, no. 10. p. 183-194.

Orlob, G.T. and Krone, R.B., 1956, Movement of coliform bacteria through porous media: Sanitary Engineering Research Laboratory, University of California, Final Report, U.S. Public Health Service Grant No.4286.

Romero, J. C., 1970, The movement of bacteria and viruses through porous media: Groundwater, April 1970, v. 8, no. 4.

RWQCB (Regional Water Quality Control Board), 1970, Waste discharge requirements and monitoring files on El Dorado Hills and Rancho Murieta sewage disposal systems: California Water Quality Control Board, Central Valley Region

RWQCB (Regional Water Quality Control Board), 1999, Waste discharge requirements and monitoring files on El Dorado Hills and Rancho Murieta sewage disposal systems: California Water Quality Control Board, Central Valley Region

RWQCB (Regional Water Quality Control Board), 1974, Waste discharge requirements and monitoring files for Martis Creek plant, Tahoe-Truckee Sanitation Agency: California Water Quality Control Board, Lahontan Region

RWQCB (Regional Water Quality Control Board), 1999, Waste discharge requirements and monitoring files for Martis Creek plant, Tahoe-Truckee Sanitation Agency: California Water Quality Control Board, Lahontan Region

RWQCB (Regional Water Quality Control Board), 1970, Waste discharge requirements and monitoring files for the Cinder Cone disposal area, Tahoe City Public Utility District: California Water Quality Control Board, Lahontan Region

SWPCB (State Water Pollution Control Board), 1953, Field investigation of waste water reclamation in relation to groundwater pollution: California, State Water Pollution Control Board Publication No.6.

U.S. Department of Health, Education and Welfare, 1998, Manual of septic tank practice: Public Health Service Publication No. 526.


ASSOCIATION OF ENGINEERING GEOLOGISTS
AEG

SHALLOW SOILS AND SUBSURFACE DRAINAGE SYSTEMS IN THE SIERRA NEVADA OF CALIFORNIA: A REVIEW OF CONDITIONS, POTENTIAL PROBLEMS, AND MITIGATION METHODS

ROBERT JOSLIN[1], DOUGLAS SMITH[2], AND JAMES PUTNAM[3]

ABSTRACT

Problems associated with spread foundations on shallow soils in the Sierra Nevada include ground freezing and associated frost heave, damming of water flowing along the soil/bedrock interface behind foundations, water seepage into crawl spaces, slope instability and backfill settlement as soils become saturated, and formation of mudflows.

Predicting if and where groundwater will surface is difficult. Where a good cross-section is exposed, it is highly advisable to evaluate the exposed soil profile for evidence of past water flow and any other indicators of potential problems. Foundations or other site improvements placed perpendicular to the fall line should be designed and constructed with an eye towards potential groundwater flow. Subdrains or curtain drains, both upslope and adjacent to site improvements, are far easier (and less expensive) to place during initial construction than after a problem arises. Other methods of controlling shallow soil drainage may include an upslope surface-water diversion, cutoff walls and drain outlets in utility trenches, and, quite simply, proper compaction of all backfill. Additional moisture protection may include waterproof membranes applied to the outside or underside of structures.

Shallow soils over steeply sloping bedrock, especially where groundwater seepage may be concentrated, lead to increased mudflow risk. Preliminary evidence indicates that the presence of even minor surface swales in a shallow sloping soil situated above a proposed project further raises the risk factor. This is due to the potential for channeling. The combination of these factors immediately on or above a project site may be cause to notify the client of potential risk and take appropriate measures.

A well-executed geologic site evaluation will consider local and regional bedrock, soil mantle and drainage conditions, as well as site-specific exposures. Time spent up front—on the initial site evaluation, for design of subsurface drainage systems, and during construction—can pay dividends in avoiding the hazard mitigation process and potential litigation.

[1]Joslin Geotechnical
P.O. Box 193
Dutch Flat, CA 95714
Joslingo@foothill.net

[2]California Regional Water
Quality Control Board
2501 Lake Tahoe Blvd.
South Lake Tahoe, CA 96150
smitd@rb6s.swrcb.ca.gov

[3]Putnam and Associates
6991 Horseshoe Bar Rd.
Loomis, CA 95650
jputnam@jps.net

INTRODUCTION

Problems associated with spread foundations on shallow soils are often found in the Sierra Nevada province. Some of these potential problems have often been unrecognized or under-considered in preliminary design. This is exacerbated when engineers and designers use codes to design structures without regard for the specific geologic setting. The geologic engineer or engineering geologist is then contacted to resolve a problem that should have been identified at the design stage. Solutions vary, but all start with identification of the potential problems. Overall, it is easier and more economical to either avoid the problems or resolve them during initial site earthwork phases than it is to attempt to snake subdrains or other water control measures around existing buildings and utilities.

The following sections provide an overview of some of the geologic problems and risks that our experience indicates are routinely under-considered during site investigations and project design in the Sierra Nevada.

GENERAL CONDITIONS

Geographically, the area addressed by this review covers much of the central Sierra Nevada in California, ranging from about 4,500 feet in elevation on the western slope, to the base of the Sierra on the eastern side. However, the general problem of shallow permeable soils atop essentially impermeable soil or bedrock often exists in other locations. In some cases, the potential for subsurface water problems may be obvious, but in others it is less so.

In the Sierra Nevada range, in addition to the geologic considerations, severe climatic conditions often interact with geologic and topographic conditions to challenge site development. Winter tends to be the "main" problematic season, with coldest temperatures routinely in the +10 to -5 degree Fahrenheit range and occasionally in the -5 to -15 degree range. Harsh winter conditions, followed by wet spring and early summer snowmelt periods, lead to complications. This is true of both surface and subsurface geologic conditions. Although it could be expected that an insulating cover of snow would keep ground-based engineered structures from assuming the same temperature as the very cold air, this is not always the case. In late February 1991, many areas of the Sierra were completely lacking of any snow cover and freezing temperatures prevailed for many days. The lack of snow cover caused many shallow, underground water pipes to burst because the frost depth extended deeper than normal into the ground. Even with the insulating snow cover, the frost depth in most Sierran soils can extend to a couple of feet. Although frost penetration is not addressed further in this discussion, it may be assumed that, where groundwater seepage problems are encountered, ground freezing and associated frost heave may not be far behind.

Soil depth in the Sierra Nevada is generally shallow, especially on the flanks and crests of mountains or ridges, and soil is, in many instances, absent over large glaciated areas. In other areas, it is common to have a relatively shallow soil depth of 2 to 6 feet overlying relatively unweathered bedrock (USDA, 1974). The bedrock may be deeply weathered in places with large sections of grus. Wagner (1991) describes grus as in-place, decomposed granite that has weathered into a soft granular material that is easily eroded. Deeply developed grus is permeable and can become saturated with water, which under the wrong conditions could cause the pore water pressure to exceed the strength of the rock and lead to slope failures. However, it is our experience that grus is very dense when it retains the original granitic mineral structure and, therefore, does not readily transmit water even when saturated.

High groundwater in the overlying soil mantle originates seasonally with the spring snowmelt. Water enters the soil as a result of snowmelt or moderate to heavy rainfall. As the water migrates through the soil, it intercepts either grus or less weathered bedrock. The rock usually has significantly lower permeability than the soil, and thus becomes an aquitard. Cracks in the bedrock then become filled with water and soil, causing the aquitard to gradually accept little or no additional groundwater, thus behaving like an aquiclude. The excess groundwater then generally flows along the soil-rock interface. The heaviest flows are typically in April through early July. In times of heavy winters or late snowmelt, seasonal high groundwater conditions may remain into late summer. Conversely, early thaws can bring about flows in March.

FOUNDATION "DAMS"

Where foundations contact or approach the shallow bedrock, especially where the foundations are roughly perpendicular to the direction of groundwater flow, partial "dams" can form. The backup of

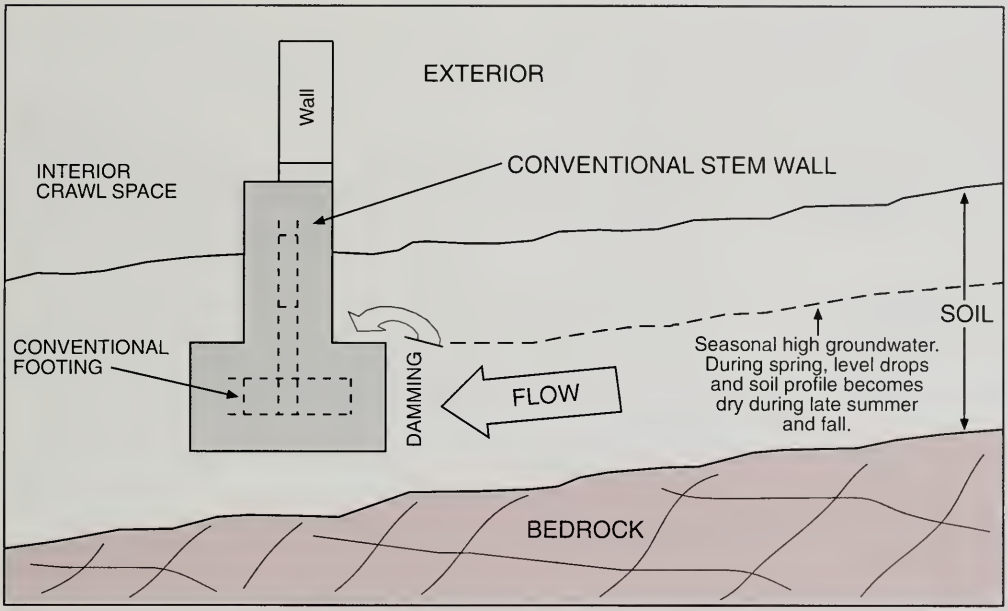

Figure 1. Foundation "damming" effect. As the snow melts during spring, the groundwater level rises and can backup at the foundation. This "damming" effect can reduce the subgrade soil strength and can permit excess moisture to enter the interior crawl space. The "damming" condition reduces in severity as the groundwater level drops during the summer, and the soils can commonly dry completely during fall.

water flow in the soil can potentially lead to slope instability or seepage at unforeseen locations. One simple example may be where subgrade soils are well compacted for foundation support, but footing or stem wall backfill is poorly compacted. Here groundwater will readily follow the more permeable path of the loosely compacted soil, resulting in settlement problems or seepage at unforeseen locations. Figure 1 illustrates an example of this foundation damming action.

Fill embankments placed roughly perpendicular to the fall line may also experience similar problems. In this case, a well-compacted, less-permeable fill may be keyed into the underlying grus or less weathered bedrock, resulting in the damming or diversion phenomenon. This may again lead to slope instability or seepage. When improvements such as building footings or fill embankments are planned, consideration should be given in the planning phase for subdrain placement and outlets.

BEDROCK FRACTURES AND DRAINAGE PROBLEMS

Granitic rocks, such as those common in the high Sierra, are usually cut by fractures (Norris and Webb, 1990; Spittler and Wagner, 1998; Wagner, 1991). Fractures in the bedrock can be connected downslope as well-developed, recurrent, joint sets. This may result in a pressure head developing in lower-elevation, fractured and jointed bedrock. Water can then enter otherwise "protected" sites by flow through the bedrock fissures. Water problems have been observed in building crawl spaces via this mechanism, as shown in Figure 2.

This problem is very difficult to predict and even more difficult to resolve after the fact. Drainage of crawl spaces and similar areas should be considered in the design of structures. Careful evaluation and measurement of bedrock features, such as joint sets and fracture patterns, should be accomplished prior to construction of the foundation. Particular atten-

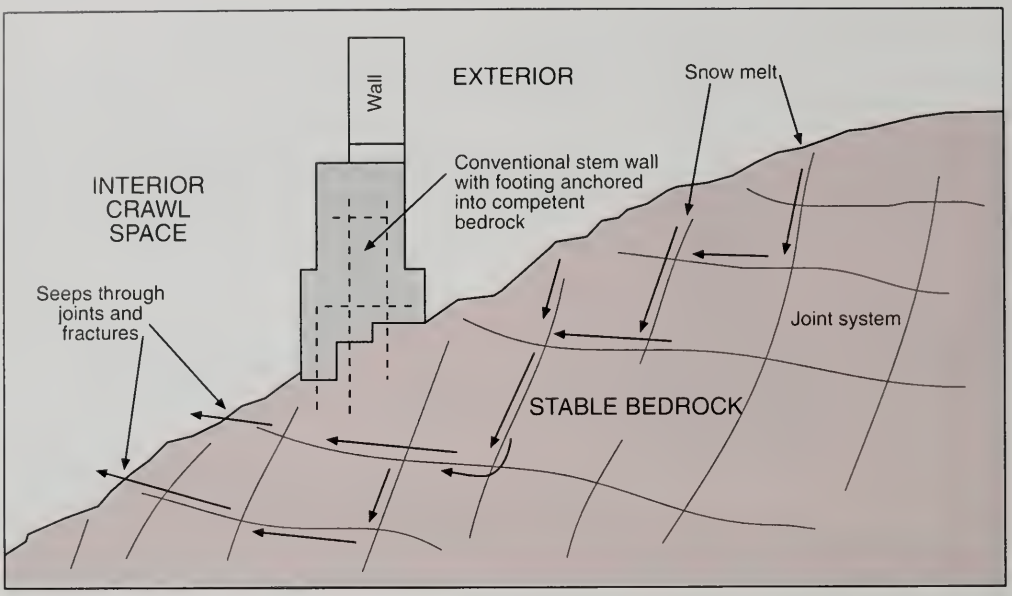

Figure 2. Bedrock seep. As snow melts during spring, or because the structure radiates heat outward during winter, the snowmelt water can seep into bedrock joints and exit in basements. Although the bedrock may be stable, joint patterns within the rock can yield groundwater in undesired places.

tion should be paid to the degree of weathering of granitic bedrock underlying any soils on site. Birkeland (1980) has documented that the rate of subsurface weathering of granitic clasts exceeds the rate of subaerial weathering, which means that hard, granitic outcrops may be underlain by softer, grussified bedrock at depth.

Predicting if and where groundwater in fractures will surface is difficult. A good joint and fracture mapping program is beneficial, but there are no clear-cut means of non-destructively determining whether the bedrock discontinuities are infilled with relatively impermeable joint gouge or other similar material, or if they are clear "pipes" into an area to be developed. Where a good cross-section is exposed, it is highly advisable to evaluate the exposed fractures and joints for joint width and spacing, infill, evidence of past water flow, and any other indicators of potential problems.

SEASONAL SEEPS AND SPRINGS

Where foundation, lot grading, road, or other cuts intersect the soil-bedrock interface, at least some seasonal "spring" activity should be expected. Since water will flow along the soil-bedrock interface, as previously discussed, cuts that intersect this water flow will result in seeps of water surfacing and flowing out of the cut. Such seeps may also result when cuts intersect the water flowing along rock discontinuities. Even in the dry season, seasonal springs can be located by noting the presence of certain hydrophilic vegetation. In the Sierras, the most common vegetation seen in these areas are willows, horsetails, rushes, sedges, cottonwoods, blackwoods, alders, quaking aspen, and sometimes lodgepole pine.

UTILITY TRENCH GROUNDWATER FLOW

Where utility trenches intersect the bedrock or have been blasted to a level below the rock surface, some "perched" groundwater will typically flow into the trenches. Utilities are usually bedded in sand or sand and gravel, both relatively permeable materials. Water flow is therefore probable in the trench bedding and backfill. This is the beginning of the

classic "piping" engineering problem and, even when the water is not moving soil particles, serious water-related problems can occur. Where trench orientation, invert grading elevation, site elevations, and other factors are unfavorable, it becomes possible for intercepted groundwater flowing within the utility trench soils to enter unwanted areas such as crawl spaces, beneath (and through) concrete slabs, and into poorly sealed manholes and utility boxes. This often results in moisture problems affecting crawl spaces or slabs, or backfill settlement.

Even if the trench bottom grading were not conducive to transporting groundwater beneath the structure, trenches excavated into the bedrock might allow significant groundwater flow within the trench backfill to downslope areas. Infiltration and inflow into sewer lines, and piping and erosion within buried trenches, are potential consequences. These potential problems should be anticipated and addressed by the geotechnical professional. Cut-off walls, proper compaction of trench backfill, diversion berms, impermeable caps, and possibly outlets to remove collected water from trenches are all mitigation measures that may be considered. Sometimes, when groundwater seepage is such that other mitigation methods will not suffice, it may be appropriate to add "French drains" upslope from the development

MUDFLOW POTENTIAL

When groundwater saturates shallow soil over bedrock, it can adversely affect slope stability due to the weight of the water, the seepage force of the water, and the decreased soil strength. The combination of these factors may lead to the formation of mudflows.

In at least two cases, we have observed the formation of mudflow slides on relatively steep slopes (20 degrees or greater), when the bedrock was between 3 and 8 feet below the soil surface. Both of these occurred in December-January of 1996-97, a very wet period in the Sierra Nevada. Precipitation occurred as rainfall on an existing moderate snow pack, and runoff was intense. Subsurface soil moisture was probably near 100 percent saturation, and mudflows were reported at various locations in the Sierra Nevada (e.g., DeGraff, 2001). At one location in the Truckee River drainage, the subsurface bedrock topography formed a trough or swale. The mudflow mechanism was very easy to explain after the flow occurred. However, apparently it was either a very slight swale, or was not visibly different at the surface from nearby areas that did not develop mudflows. There was no microtopography available for this area prior to the mudflow. As such, ground-penetrating radar or seismic geophysical surveys would have been required to "see" the subsurface trough. Such work would be well beyond the scope of almost all geologic investigations, unless a contract was specifically developed to check for these features.

The field conditions that became apparent after the flow occurred included a steeply sloping bedrock ridge flank, underlain by an indurated volcanic mudflow. Apparently the volcanic mudflow had developed a sloping swale that was eventually infilled with colluvial soil. As the colluvial soil became saturated, water apparently flowed along the bedrock surface, became concentrated in the swale, and developed conditions that mobilized the overlying soil. The resulting flow and subsequent runoff were such that the upper portion of the newly exposed bedrock looked like it had been pressure-washed.

Although it is beyond the scope of this discussion to address prediction of mudflows in the Sierra Nevada, it is important to realize that they do occur. Shallow soils over steeply sloping bedrock, especially where groundwater seepage may be concentrated, lead to increased mudflow risk. Preliminary evidence indicates that the presence of even minor surface swales in a shallow sloping soil situated above a proposed project further raises the risk factor. This is due to the potential for channeling. The combination of these factors immediately on or above a project site may be cause to notify the client of potential risk and take appropriate measures.

SITE EVALUATION

Due to site access issues, equipment availability, shallowness of soil cover, and presence of numerous cobbles and boulders, test pits are often used for site evaluation rather than boreholes. The ubiquitous presence of granitic, volcanic, and metamorphic bedrock in the Sierra Nevada often results in a relatively shallow refusal of the backhoe bucket. It is sometimes possible to observe signs of at least seasonal groundwater immediately atop the bedrock. Such signs include seepage at time of excavation, mottling of the soil, and occasionally gleying, which indicates long-term wetting.

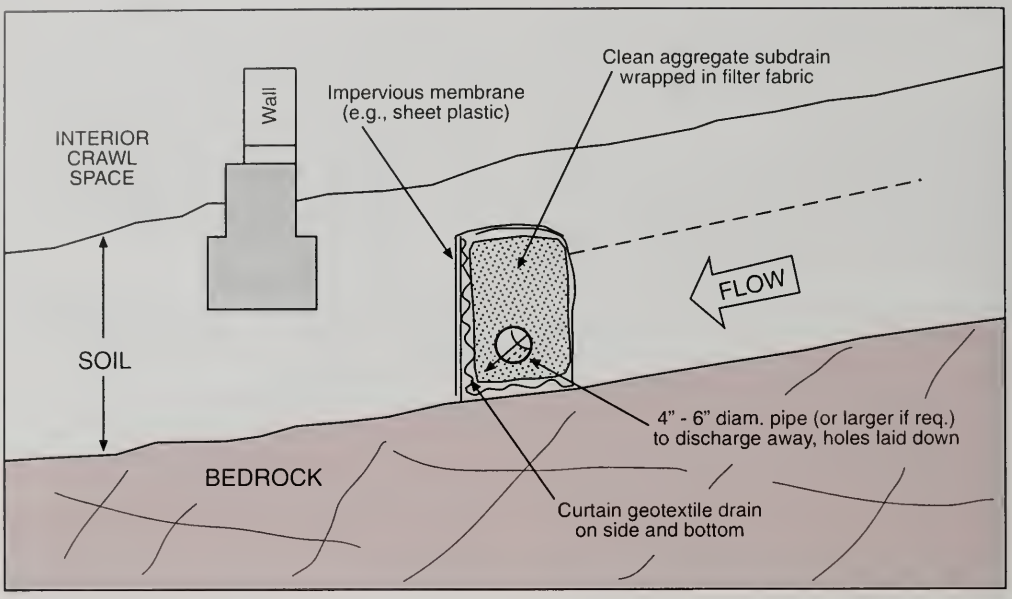

Figure 3. To mitigate for "damming" effect, one can install a subdrain to collect the high groundwater and convey it to an appropriate location away from the foundation. This mitigation measure prevents moisture from entering the crawl space and keeps the supporting soils relatively dry under the footings.

In our experience, shallow soil gleying is relatively rare, but mottling is common. However, mottling alone should not be relied upon to indicate periodic wetting, as mottling can also develop from the long-duration moistening caused by snowmelt. Careful observation can sometimes discern gradation with mottling: More mottling near the ground surface, lessening vertically downward, may indicate development due to snowmelt. Conversely, heavy mottling near an aquitard or aquiclude, lessening vertically upward, is more likely due to seasonal high moisture and probable flow atop the rock. Abundant, low chroma mottles, clay depletions, iron and manganese accumulations, pore linings, and reduced matrices in the soil strata may indicate the level of highest seasonal groundwater levels (Verpraskas, 1995). Careful attention should be paid to discerning the specific redoximorphic features in the soil. Because many of the soils in the Sierra are coarse and granular, the redoximorphic features are not always present. Concentric, low chroma, gleyed, or reduced areas around tree roots that are exposed in the test pit also indicate seasonal high groundwater situations.

Observation of the bedrock surface exposed in test pits or other recent exposures, such as road or drainage cuts, is also helpful. Instead of just noting that a bedrock surface has been found at shallow depth, it is useful, where practical, to determine if the rock is highly fractured and/or sloping, and what is upslope. Does it appear that a pressure head can develop, either in the shallow soil or in fractures within the bedrock?

The orientation of the bedrock surface is also an indicator of flow potential. There are very few areas in the Sierra Nevada range where the underlying bedrock is flat. Moderately sloping surfaces with large upslope areas appear to be more prone to developing shallow subsurface flow in the overlying soils than do steeply dipping surfaces. Rainfall and some snowmelt tend to flow over the ground surface as runoff on steeper slopes, whereas water may infiltrate the soil more on a flatter slope. Our experience is that natural slopes of 20 degrees, or about 3:1 (horizontal to vertical), and steeper tend to have the surficial runoff described, whereas shallower slopes typically exhibit the infiltration and saturation con-

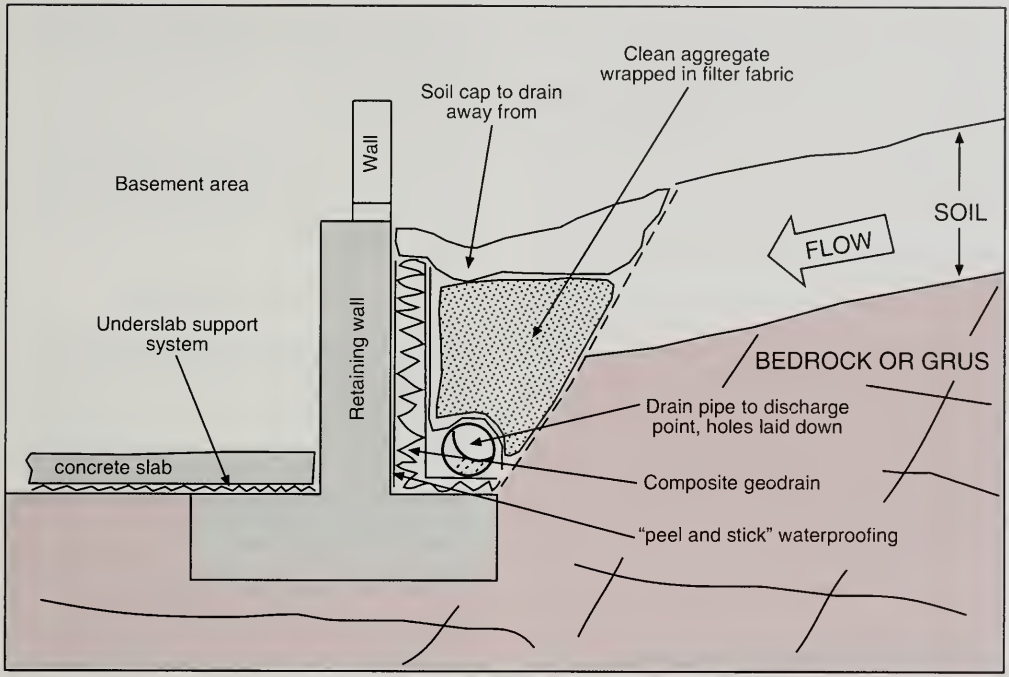

Figure 4. To mitigate basement seeps one can cut back an area suitable for fitting a backdrain, as shown. It is best to wrap the foundation with waterproofing membrane, attach a composite geodrain that is connected to a drain pipe, and extend the drain pipe to exit away from the foundation to keep the area dry.

dition. However, this can vary considerably depending on the permeability of the soil profile. Also, rapidly melting snow, long-duration rain on snow, or high-intensity short-duration thundershowers may release water in volumes that can exceed infiltration rates of soils on even the shallower slopes.

CONCLUSION

The combination of shallow soils overlying sloping bedrock with seasonal subsurface groundwater movement provides special problems in site development. Subsurface drainage, whether natural or manmade, can significantly alter the performance of a project, whether by slope instability, nuisance moisture, or water seepage from unforeseen locations. Thus, time spent up front—on the initial site evaluation, for design of subsurface drainage systems, and during construction—can pay dividends in avoiding the hazard mitigation process and potential litigation.

A well-executed geologic site evaluation will consider local and regional bedrock, soil mantle, and drainage conditions, as well as site-specific exposures. An investigator should look for indications of highest previous groundwater and the ability of the soil and bedrock (and bedrock joint system) to transmit water. Even in the drier parts of the year, much can be learned about the groundwater conditions at a site by observing the following:

- Types of vegetation
- Soil subsurface characteristics, such as mottling and gleying
- Bedrock characteristics, such as depth and degree of weathering
- Joint characteristics, such as joint width, continuity, spacing, infill, and evidence of past water flow.

Since the probable life of a structure is at least 50 to 100 years, redundancy in subsurface drainage systems is considered to be a good thing. Foundations or other site improvements placed perpendicular to the fall line should be designed and constructed with an eye towards potential groundwater flow. Subdrains or curtain drains, both upslope and adjacent to site improvements, are far easier (and less expensive) to place during initial construction than after a problem arises (Figure 3). Other methods of controlling shallow soil drainage may include an upslope surface-water diversion, cutoff walls and drain outlets in utility trenches, and, quite simply, proper compaction of all backfill. Additional moisture protection may include waterproof membranes applied to the outside or underside of structures (Figure 4). Finally, permeability-reducing concrete admixtures and high-cement-content concrete, such as a 7-sack mix, can be used. Although a higher cement content will produce stronger concrete, the more desirable characteristics in this case are the increased density, and corresponding decreased permeability.

ACKNOWLEDGEMENTS

Our sincere thanks to John Bonell, who has worked with us extensively over the past 25 years developing the expertise that only comes from hands-on experience. Also thanks to Deborah Putnam for her tireless review, constructive comments, and technical editing.

AUTHOR PROFILES

Robert Joslin is a California-registered civil engineer with over 25 years of geotechnical, geologic, and mining engineering experience, specialized in the Sierra Nevada of Northern California. Mr. Joslin is the owner and principal engineer of Joslin Geotechnical, a 16-year-old firm in Dutch Flat, California.

Douglas Smith is a California-registered geologist with 15 years of geologic and geotechnical experience. Mr. Smith is an associate engineering geologist for the California Regional Water Quality Control Board, Lahontan Region. He was formerly the agency geologist for the Tahoe Regional Planning Agency.

Jim Putnam is a California-registered geotechnical engineer with over 25 years of geotechnical engineering experience throughout Northern and Southern California. Mr. Putnam is the owner and principal engineer of Putnam and Associates in Loomis, California.

SELECTED REFERENCES

Birkeland, P.W., 1980, Pedology, weathering, and geomorphological research: Department of Geological Sciences, University of Colorado, Boulder, Colorado. Oxford University Press, New York.

DeGraff, J.V., 2001, Sourgrass debris flow: A landslide triggered in the Sierra Nevada by The 1997 New Year storm: *in* Ferriz, H., Anderson, R., (eds.), Engineering Geology Practice in Northern California: Association of Engineering Geologists Special Publication 12 and California Division of Mines and Geology Bulletin 210

Hurt, G.W., Whited, P.M., and Pringle, R.F., (eds.), 1998, Field indicators of hydric soils in the United States, Version 4.0: U.S. Department of Agriculture, Natural Resources Conservation Service, Ft. Worth, Texas.

Norris, R.M. and Webb, R.W., 1990, Geology of California: John Wiley & Sons, (New York, New York), Second Edition.

Schweickert, R.A., Lahren, M.M., Smith, K., Karlin, R., 1999, Preliminary fault map of the Lake Tahoe Basin, California and Nevada: Seismological Research Letters, v. 70, no. 3, p. 306-313.

Spittler, T.E. and Wagner, D.L., 1998, Geology and slope stability along Highway 50: California Geology, California Department of Conservation, v. 51, no. 3, p. 3-16.

USDA (U. S. Department of Agriculture), 1974, Soil Survey – Tahoe Basin area, California and Nevada: U. S. Department of Agriculture, Map sheet no. 6, Glenbrook Quadrangle.

Verpraskas, M.J., 1995, Redoximorphic features for identifying aquic conditions:, North Carolina State University, (Raleigh, North Carolina), Technical Bulletin 301.

Wagner, D.L., 1991, Decomposed granite: California Geology, California Department of Conservation, Division of Mines and Geology, v. 44, no. 11, p. 243-249.

AN ENGINEERING GEOLOGY KALEIDOSCOPE

HORACIO FERRIZ[1]

This section includes those papers for which the editors could not find a pre-fabricated home. But please do not feel sorry for these "orphans", for they are wonderful examples of the ingenuity and commitment to problem solving that has made engineering geology such a special discipline. They show that we, as a profession, are committed to keep pushing the technical cutting edge, dealing with problems as they are brought to the table by our ever changing society. The papers in this section deal with liquefaction, forensic geology, coastal engineering geology, asbestos, environmental geology, and volcanic hazards, and yet are but an appetizer of what we can do when we put our nose to the ground (quite literally in some cases).

LIQUEFACTION

Liquefaction is the loss of strength that loose cohesionless soils that are saturated with water experience when subjected to strong seismic shaking. The potential for liquefaction is of great concern in California, where major alluvial basins with shallow water tables have undergone extensive urban development; thus, many young engineering geologists will no doubt be involved in liquefaction susceptibility studies sometime in the course of their professional careers. The brief paper by Ferriz (2001) gives an overview of the standard procedure that is most often used to evaluate liquefaction susceptibility, and the paper by DeLisle (2001) discusses some of the applications of the method developed to identify susceptible areas at a regional level. This latter paper entices us with a sample of the ambitious project of the California Division of Mines and Geology to produce liquefaction susceptibility maps for the major urban areas of the Golden State. These maps are not to be taken as identifying *de facto* hazardous zones, but rather as delimiting areas where site-specific investigations by a qualified engineering geologist or geotechnical engineer are required before a building permit can be granted.

FORENSIC GEOLOGY

The term forensic geology makes me shudder, because it often connotes disaster, lawsuits, and angry people. Then again, this may well be why some of our number seem to find a special challenge in doing these types of investigations. For example, join "Sherlock" Shlemon and his associate, Dr. Van Houten, as they inquire into the strange case of the short freeway fence, that led to the untimely demise of "Cisco" the horse (Shlemon and Van Houten, 2001). Not only will you have a chuckle or two, but I think you will find that a combination of common sense and basic sedimentologic mapping can go a long way toward solving some tough problems.

For those of you who have not yet met Roy Shlemon, I will take the liberty to introduce you to a highly regarded member of our profession, and a very nice fellow as well. Roy does fine work in Quaternary geology using detailed soil mapping, and he often can see paleo-meandering rivers and rising shorelines where most of us would only see small hillocks of dirt. I, for one, have always enjoyed

[1]HF Geologic Engineering
1416 Oakdale-Waterford Hwy.
Waterford, CA 95386

Department of Physics and Geology
California State University, Stanislaus
Turlock, CA 95382
hferriz@geology.csustan.edu

seeing him at work, or philosophizing about geologic education. For example, he wonders, why is it that young geologists are prone to use non-quantitative color names—such as sienna, fuchsia and periwinkle—instead of Munsell designations when logging trenches? Could it be, perhaps, that the geologist is truly an artist at heart?

COASTAL ENGINEERING

As part of my introduction to the very interesting paper by Sayre et al. (2001), about mitigating the sea cliff failures caused by the 1998 El Niño storms, I cannot resist the temptation to share the following story, heard at an oceanographic conference:

> In history one reads of man's interferences with nature and of the disastrous results that follow. One such interference has been the building of harbors and breakwaters along the coastlines of the world. These structures interfere with wave action and with the drifting of beach sands, so nature crushes the structures or fills the harbor with sand and seeks new equilibrium. Man, struggling as he may, never quite succeeds with his meddling.
>
> Take, for example, the small sport and fishing harbor at Redondo Beach, and see the similarities between its history and that of Carthaginian generals and their fascination with elephants. . . *By the time of Hamilcar (275 B.C.), history had taught us never to use elephants in war. Hamilcar, however, stuck to his elephants to the end, and encouraged them to rush forward and trample the Romans, only to see them panic and rush backward trampling the Carthaginians. Still, Hamilcar always felt that his elephants would have won the First Punic War if it hadn't developed into a naval affair. . .*
>
> At Redondo Beach, a rubble breakwater was constructed 1,000 feet perpendicular to the beach and was attached to an 800-foot leg parallel with the beach to the south. Sand was trapped on the north side of the breakwater and the south shore eroded. The erosion was one of the finest ever. All the sand disappeared, the boardwalk with its hot-dog stands and shooting galleries fell into the sea, a road collapsed, and one by one the houses disappeared. No telling how great the erosion might have been if the property owners hadn't insisted on a retaining wall to protect their land. The sand then flowed around the end of the breakwater and was deposited in the boat anchorage. Naturally, the sand wouldn't deposit in the denuded southerly beach until the boat anchorage was filled.
>
> A similar harbor was soon built at Santa Barbara. . . *Hamilcar was drowned in 228 B.C. while crossing a stream with a herd of elephants, but not before his son, Hannibal, was well versed in the strategy of elephant warfare. Hannibal crossed the Alps in 218 B.C. with a large army and 37 elephants to start the Second Punic War, but everything went badly until all 37 had died. Hannibal then defeated the Romans in the Battle of Trasimene. Again at Cannae, fresh out of elephants, another great victory was won. He lost the chance of complete victory, however, through his inactivity for the next few years: he was waiting for more elephants. . .* The property damage along the southerly beach was much less than at Redondo Beach because there wasn't as much property to be damaged. Sand again was deposited on the northerly side of the harbor and this made a fine beach until it started drifting around the end of the dog-legged breakwater to accumulate inside the harbor. . . *The final showdown of the Second Punic War, fought near Carthage in 203 B.C., ended when Hannibal's 80 front-line elephants turned and trampled his army. Hannibal tried to stir up another war with a scheme involving elephants, but no one seemed interested. . .* The sand deposit became so extensive that the entire harbor was threatened, which led the late Will Rogers to remark that "The harbor will not be of much value unless we can devise a way of irrigating it". Santa Barbara harbor has been called by some "the prototype sand-trap."
>
> With the knowledge gained at Santa Barbara and Redondo Beach, a harbor was built at Santa Monica. The harbor comprised only a 1,000-foot breakwater parallel to the beach, behind which small boats could seek shelter in heavy seas. Eliminating

> the section perpendicular to the beach was intended to allow the sand drifting along the coast to continue without interruption. Again, the sand was deposited behind the breakwater in the anchorage area. . . *Many say that Hannibal's greatness was in his strategy of drawing his enemy into a trap. If only his elephants would have cooperated he might have been even able to kill the enemy once inside the trap. . .* Boats were found high on the beach following each storm after being torn from their anchors by waves refracted from the breakwater into the harbor. The breakwater itself was never affected by the waves. . . *When Hannibal crossed the Alps many of his men died of hunger and cold, but he encouraged those that survived by saying "Cheer up, the elephants are all right."...*
>
> ...Since those early days the problem of harbor design has been studied with more vigor than ever. No telling what may be accomplished in the years to come. The trend is toward bigger and better breakwaves. . . *To the end, Hannibal knew everything would still come out right if he just had a few more dozens of you-know-whats.*

But alas, engineering geologists are not the ones who make the decision as to whether it makes sense to build on coastal cliffs, and until natural geologic processes change we are there to help mitigate the consequences. So, if you are called upon to do battle with the incessant pounding of the waves, you will no doubt find useful the experience of the Pacifica sea cliff mitigation project, described by Sayre et al. (2001) *(and yes, forget the elephants).* In their article, Ted and his co-workers present a thorough summary of the steps taken to design the mitigation measures, and provide useful references to engineering geology work in coastal environments.

ASBESTOS

In early 1965 it was pretty quiet around the State legislature, so to stir things up Senator Luther E. Gibson and Assemblyman Pearce Young introduced Senate Bill 265 to designate the official state rock. For lack of something better to do, the legislature debated lustily the merits of granite, sandstone and schist as potential symbols of the Golden State, but, in the end, the honor landed on serpentinite. In signing the legislation on April 23, Governor E.G. Brown honored the state rock by remarking that serpentinite was of great economic importance to California as the host for the state's newest mineral industry—asbestos—, which now produces about 10,000 tons per year of the fire-resistant fibers.

Little did the honorable legislators know that the golden child of the 60's and 70's would become the villain of the 90's! Whereas in the early years land developers would proudly boast outcrops of the "state rock" on their properties, by the turn of the millennium serpentinite had lost its appeal and was considered an unmitigated nuisance. The reason for this change of heart was mass hysteria regarding carcinogenic asbestos, triggered by a series of newspaper articles that claimed that asbestos fibers were being churned into the air by grading activities. Sederquist et al. (2001) pick up the story at this point, and briefly summarize how the public perception of this hazard has changed geotechnical practice in the foothills of the Sierra Nevada. Their paper includes a useful discussion of the geology and mineralogy of asbestos, and gives practical recommendations regarding property evaluation, sampling, and design of mitigation measures. These activities may be the bread and butter of the next generation of engineering geologists working in this region, so keep this reference handy.

ENVIRONMENTAL GEOLOGY

Environmental geology is a very important part of what we do, and if it does not figure more prominently in this volume it is only because many other books have already been dedicated to the subject. Nevertheless, this volume would not be complete without at least a sample of the environmental work that a good many of our number do for a living. Of the papers submitted, the one by Smelser and Whyte (2001) about environmental restoration of the Gambonini mercury mine, in Marin County, caught our attention because it covered a wide spectrum of issues. The reclamation and remediation of abandoned mines involve tasks such as development of mine closure plans, site characterization (including analysis of historic aerial photographs, detailed field mapping, and subsurface investigations), development of conceptual alternatives, stabilization of tailings deposits, mitigation of sediment discharge, restoration of stream channels, and revegetation of slopes. In addition, the engineering geologist often becomes involved in negotiations for project funding, coordination with government agencies, and public

relations—a refreshing departure from "yank-a-tank" projects!

VOLCANIC HAZARD ANALYSIS

California has it all! Fossil subduction zones, active faults and earthquakes, batholiths, gold and mercury mines, thick sedimentary sequences, and volcanoes. The latter have been rather subdued over the last 100 years, with only the modest 1914-1917 eruption of Mt. Lassen to break the monotony, but every California geologist should know that some of our volcanoes are very much alive, and that they are capable of inflicting great damage to life and property.

As history shows, there are several ways in which volcanic hazard may be mitigated. The first recorded attempt occurred in 1669, when a lava flow from Mount Etna, Sicily, threatened to destroy the city of Catania. Armed with iron bars, several dozen Catanians covered themselves with wet cowhides and managed to dig a hole through one of the levees of the flow, high in the mountain. Lava started oozing from the breach, and the relief in pressure slowed down the movement of the main flow toward Catania. Unfortunately the new lava flow started heading for the town of Palermo, so several hundred angry Palermoans climbed the mountainand drove away the Catanians from the man-made breach in the levee. Left unattended the breach soon clogged, the main flow was reactivated, and a good portion of Catania was destroyed. Ever since, volcanologists have been faced with the ethical dilemma of whether to interfere with an Act of God or not. The decision must take into account local conditions and the nature of the hazard, so the first step is to know the nature of the hazard. Hopson (2001) tackles this task for the volcanic centers of the Owens Valley, with special emphasis on the risks that volcanic activity poses to the water supply of the City of Los Angeles. In this volcanic province one finds the Long Valley caldera (by far the most significant volcanic hazard in California), the Mono-Inyo domes, and a number of basaltic cinder cones; thus, in one paper we get a discussion of many different types of volcanic hazards.

SELECTED REFERENCES

DeLisle, M.J., 2001, Seismic hazard evaluation and liquefaction zoning in the City and County of San Francisco, California: This volume.

Ferriz, H., 2001, The basics of liquefaction analysis: This volume.

Hopson, R.F., 2001, Potential impact on water resources from eruptions near Mammoth Lakes, Mono County, California: This volume.

Sayre, T., Shires, P.O., Skelly, D.W., 2001, Mitigation of a 1998 El Niño seacliff failure, Pacifica, California: This volume.

Sederquist, D.C., Kroll, R.C., 2001, Evaluation of naturally occurring asbestos in the Central Sierra Nevada Foothills of California: This volume.

Shlemon, R.J., Van Houten, G.E., 2001, The use of sedimentation rates in forensic geology: The case of the short freeway fence at Petaluma, California: This volume.

Smelser, M.G., Whyte, D.C., 2001, The role of engineering geology in remediating abandoned mine sites - The case of the Gambonini mercury mine, Marine County, California: This volume.

THE BASICS OF LIQUEFACTION ANALYSIS

HORACIO FERRIZ[1]

INTRODUCTION

Liquefaction is the loss of strength that loose cohesionless soils that are saturated with water experience when subject to strong seismic shaking. In cohesionless granular material that has a low relative density (for example, loose sandy sediment), seismic vibration can disturb the particle framework, leading to increased compaction of the material and reduction of pore space between the framework grains. With continued shaking, transfer of intergranular stress to pore water can generate pore pressures great enough to cause the sediment to lose its strength and change from a solid state to a liquefied state. This phenomenon has been well known for many years, and the procedure for evaluating liquefaction resistance of soils continues to be refined as more field examples become available. The initial work was summarized by Seed and Idriss (1982), but the database of case histories has been revisited several times since (e.g., NRC, 1985; Ishihara, 1993; Youd and Idriss, 1997; Bardet et al., 2000). Recent reviews of the state-of-the-practice have been summarized by Youd et al. (2001) and Lew (2001).

[1]HF Geologic Engineering
1416 Oakdale-Waterford Hwy.
Waterford, CA 95386

Department of Physics and Geology
California State University, Stanislaus
Turlock, CA 95382
hferriz@geology.csustan.edu

LIQUEFACTION SUSCEPTIBILITY

The basic procedure used to determine liquefaction susceptibility of a site is based on the empirical correlations established by Seed and Idriss (1982); based on field observations, they concluded that liquefaction typically occurs at depths less than 50 ft below ground surface (bgs), with the most susceptible conditions occurring at depths shallower than 30 ft bgs, in loose, saturated sandy soils with less than 15% silt and clay. (Liquefaction may occur at greater depths in the case of soils that are near a free face, such as near a coastal cliff or the sides of an earth dam.) Diminished susceptibility as depth increases is apparently due to the increased firmness of deeper sedimentary materials, which results from increased overburden pressure and increased geologic age.

As summarized by Matti and Carson (1991), the analytical procedure described by Seed and Idriss (1982) requires (1) a measure of the penetration resistance of the soils, as measured by the Standard Penetration Test (SPT), (2) estimates of peak horizontal ground acceleration resulting from each scenario earthquake, (3) data on depth to ground water, (4) values for the median grain size and fines content of tested materials (Matti and Carson, 1991; Seed et al., 1985), and (5) estimates of overburden pressure and effective stress. These data are then used to calculate two parameters (cyclic-stress ratios) that determine liquefaction susceptibility.

A cyclic stress ratio (τ_{av}/σ'_o) is the ratio between average shear stress (τ_{av}) induced by the ground shaking and the effective overburden pressure (σ'_o) affecting a saturated sediment at a given subsurface depth. Cyclic-stress ratios are unitless parameters that characterize the response of a given sediment type, at a particular subsurface depth, to ground-shaking conditions of specified strength

and duration. The seismic cyclic-stress ratio [$(\tau_{av}/\sigma'_o)_{dem}$, referred to hereafter as CSR] describes the cyclic-loading conditions expected to develop at a location during a given earthquake. The liquefaction resistance cyclic-stress ratio [$(\tau_{av}/\sigma'_o)_{liq}$, referred to hereafter as CRR] describes the loading conditions required at the location for liquefaction to occur.

DETERMINATION OF CSR

According to Seed and Idriss (1982), the seismic cyclic-stress ratio that can be expected to develop at the location of each SPT as the result of a given earthquake can be determined by

$$CSR = 0.65*(\sigma_o/\sigma'_o)*(A_{max}/g)*R_d$$

The ratio of total overburden stress to effective overburden stress (σ_o/σ'_o) quantifies the inherent resistance to deformation of a particular sediment at a particular subsurface depth below the water table. σ_o and σ'_o are calculated using standard engineering relations. The ratio of maximum horizontal ground-surface acceleration to gravitational acceleration (A_{max}/g) quantifies the strength of ground shaking expected at a particular site during a specified earthquake (today there are two basic approaches for calculating A_{max}, deterministic and probabilistic, as described by Martin et al., 1999). The parameter R_d is a stress-reduction coefficient that compensates for the fact that the shear stress affecting a sediment mass at a given subsurface depth during an earthquake is less than the maximum value because the overlying sediment column is flexible rather than rigid. Values for R_d can be obtained from the nomogram presented in Youd et al. (2001, fig. 1), or from the equations presented in Youd et al. (2001).

DETERMINATION OF CRR

Derivation of CRR relies mainly on penetration resistance (N) determined at specific sites. The raw penetration data must be modified to compensate for several factors, including (1) a numerical compensation for SPT tests conducted at shallow subsurface depths, (2) normalization of N to an overburden pressure of 2,000 lb/ft^2 to compensate for the effect of overburden pressure, and (3) a numerical compensation applied to N for SPT determinations in silty or partly silty materials. The corrections for these factors are described by Seed and Idriss (1982), NRC (1985), Matti and Carson (1991), Youd and Idriss (1997), and Youd et al. (2001). These adjustments to N yield a modified penetration resistance, N*, that can be used to determine CRR values for specific earthquakes by using empirical curves proposed by Seed and Idriss (1982; fig. 57), NRC (1985), Youd and Idriss (1997), and Youd et al. (2001; fig. 2).

OTHER EXPLORATION TECHNIQUES

Youd et al. (2001) discuss current advances in the use of other exploration techniques for evaluation of the liquefaction resistance of soils. These include cone penetrometer testing (CPT), measurements of seismic shear wave velocity, and Becker penetration testing (BPT). CPT has been used extensively over the last 15 years, and is particularly well suited for non-gravelly, thinly interbedded soils. Measurement of seismic shear-wave velocity has not been used as extensively, but holds much promise because (Youd et al, 2001; Andrus and Stokoe, 2000): (1) shear-wave velocity measurements can be made in gravelly soils, or in sites where borings or soundings may not be feasible, and (2) shear-wave velocity is a basic mechanical property of soils, directly related to small-strain shear modulus (albeit liquefaction is related to medium- to high-strain phenomena). Becker penetration testing is best suited for investigation of sites underlain by gravelly soils.

SUSCEPTIBILITY EVALUATION

Susceptibility ratios and factors of safety

To determine liquefaction susceptibility the two cyclic-stress ratios, CRR and CSR, are compared as the ratio FS, where:

$$FS = CRR/CSR$$

The ratio FS defines a factor of safety against liquefaction. If CRR is equal to or greater than CSR, then the factor of safety is greater than 1.0, and the materials evaluated by the penetration test have a margin of safety against liquefaction that increases as the ratio FS increases. Where CRR is less than CSR, the factor of safety is 1.0 or less, and the materials evaluated by the penetration test have no margin of safety against liquefaction during the specified earthquake.

No appropriate margin of safety is widely agreed upon as a standard for liquefaction-hazard recognition, "...primarily because the degree of conservatism thought desirable at this point depends upon the extent of the conservatism already introduced in assigning the design earthquake" (NRC, 1985,

p. 96). If the specified ground-shaking conditions are deemed reasonable, factors of safety of about 1.35 are generally acceptable. If the ground-shaking conditions are deemed very conservative to begin with, or if the sands have more than 15% fines, factors of safety only slightly above 1.0 may be acceptable.

LIQUEFACTION HAZARDS

If a certain layer of unconsolidated sediment is susceptible to liquefaction, what are the possible consequences? Some of the most common are (SMGB, 1997):

- Flow slides, or slope failures due to low strengths of liquefied soil layers
- Limited lateral spreads
- Ground settlement
- Ground heaving
- Loss of bearing capacity for shallow foundations
- Additional loading on deep foundations

MITIGATION MEASURES

And what can we do to mitigate these hazards? The three major structural solutions are (SMGB, 1997):

- Soil densification (e.g., vibrocompaction, explosives, wicks, deep dynamic compaction)
- Hardening/mixing (e.g., permeation grouting, soil mixing, jet grouting)
- Structural options (e.g., post-tensioned slab foundations, continuous spread footings). Note that structural options do not attempt to reduce the likelihood of liquefaction itself, but rather aim to increase the performance of a structure in the event of liquefaction-induced settlement.

EPILOGUE

This brief paper stemmed from an overgrown introduction to the Kaleidoscope section of this volume, and my personal dislike for "black box" approaches to engineering geology. My intent with it is to provide a starting point for young engineering geologists who may need to sift through the literature on the subject (my personal recommendation would be to start with Youd et al., 2001). Many new papers have appeared over the last few years, and more are sure to follow once the data from the recent earthquakes in Japan and Turkey are processed, and I hope the basics discussed here will make reading them a little easier.

SELECTED REFERENCES

Andrus, R.D., Stokoe, K.H., 2000, Liquefaction resistance of soils from shear-wave velocity: Journal of Geotechnical and Geoenvironmental Engineering, v. 126, p. 1,015-1,025.

Bardet, J.-P., Hu, J., Tobita, T., Mace, N., 1999, Database of case histories on liquefaction-induced ground deformation: Consultant's report to the Pacific Engineering Research Center and Pacific Gas and Electric, Department of Civil Engineering, University of Southern California, (Los Angeles, California), 95 p.

Ishihara, K., 1993, Liquefaction and flow failure during earthquakes: Geotechnique, v.43, p. 351-415.

Lew, M., 2001, Liquefaction evaluation guidelines for practicing engineering and geological professionals and regulators: Environmental & Engineering Geoscience, v. 7, p. 301-320.

Martin, G.R., Lew, M., Arulmoli, K., Baez, J., Blake, T., Earnest, J., Gharib, F., Goldhammer, J., Hsu, D., Kupferman, S., O'Tousa, J., Real, C., Simantob, E., Youd, T.L., 1999, Recommended procedures for implementation of DMG SP117 "Guidelines for evaluating and mitigating seismic hazards in California": Southern California Earthquake Center, University of Southern California, (Los Angeles, California), 63 p.

Matti, J.C., Carson, S.E., 1991, Liquefaction susceptibility in the San Bernardino Valley and vicinity, Southern California - A regional evaluation: U.S. Geological Survey Bulletin 1898, 53 p.

NRC (National Research Council), 1985, Liquefaction of sands during earthquakes: National Academy Press (Washington, D.C.), 240 p.

Seed, H.B., Idriss, I.M., 1982, Ground motions and soil liquefaction during earthquakes: Earthquake Engineering Research Center, University of California, Berkeley, 134p.

Seed, H.B., Tokimatsu, K., Harder, L.F., Chung, R.M., 1985, Influence of SPT procedures in soil liquefaction resistance evaluations: Journal of Geotechnical Engineering, v.111, p.1,425-1,445.

Seed, H.B., Wong, R.T., Idriss, I.M. and Tokimatsu, K., 1986, Moduli and damping factors for dynamic analyses of cohesionless soils: Journal of the Geotechnical Engi-

neering Division, ASCE, v.112, No. GTI1, November, p.1,016-1,032.

SMGB (State Mining and Geology Board), 1997, Guidelines for evaluating and mitigating seismic hazards in California: California Department of Conservation, Division of Mines and Geology, Special Publication 117, 74 p.

Youd, T.L., and Idriss, I.M., (eds.), 1997, Proceedings of the NCEER workshop on evaluation of liquefaction resistance of soils: Technical report NCEER-97-0022, 277 p.

Youd, T.L., Idriss, I.M., Andrus, R.D., Arango, I., Castro, G., Christian, J.T., Dobry, R., Finn, W.D.L., Harder, L.F., Hynes, M.E., Ishihara, K., Koester, J.P., Liao, S.S.C., Marcuson, W.F., Martin, G.R., Mitchell, J.K., Moriwaki, Y., Power, M.S., Robertson, P.K., Seed, R.B., Stokoe, K.H., 2001, Liquefaction resistance of soils: Summary report from the 1996 NCEER and 1998 NCEER/NSF workshops on evaluation of liquefaction resistance of soils: Journal of Geotechnical and Geoenvironmental Engineering, v. 127, p. 817-833.

SEISMIC HAZARD EVALUATION AND LIQUEFACTION ZONING IN THE CITY AND COUNTY OF SAN FRANCISCO, CALIFORNIA

MARK J. DeLISLE[1]

ABSTRACT

The Seismic Hazard Mapping Project of the California Department of Conservation, Division of Mines and Geology (DMG), evaluates seismic hazards and designates zones of required seismic investigation. Within these zones, state law requires that site-specific geotechnical investigations be performed to determine if higher standards of design are needed prior to granting a permit for redevelopment or new construction for human occupancy. These zones include areas likely to contain geologic materials susceptible to liquefaction or landsliding during earthquakes. Since the implementation of the Seismic Hazards Mapping Act, DMG has designated zones of required seismic investigation for over 100 jurisdictions within California.

Liquefaction zones are based on the presence of cohesionless soils that are, or could become, saturated. The criteria for liquefaction zone delineation were established by the Seismic Hazards Mapping Act Advisory Committee. The method of liquefaction evaluation applied by DMG combines geotechnical data analyses, and geologic and hydrogeologic mapping.

DMG conducted a liquefaction susceptibility evaluation for the County of San Francisco using regional geology and site-specific geotechnical data collected from more than 600 sites at which one or more geotechnical boreholes had been drilled. High, moderate, or low susceptibility was assigned depending on the site-specific conditions and the ratings became the basis for determining the zone boundaries. Depth to groundwater, age and type of material, and historical liquefaction during the 1906 and 1989 earthquakes largely controlled the size and shape of the zones of required seismic investigation. The highest susceptibility was found in areas where dune sand was saturated at depths of less than 10 feet, and areas that contained artificial fill and beach deposits.

INTRODUCTION

Prompted by damaging earthquakes in northern and southern California, in 1990 the State Legislature passed the Seismic Hazards Mapping Act (the Act). The Act became operative on April 1, 1991, and directs the California Department of Conservation, Division of Mines and Geology (DMG), to delineate seismic hazard zones. The purpose of this delineation is to reduce the threat to public health and safety, and to minimize the loss of life and property, by identifying and mitigating seismic hazards. Cities, counties, and state agencies are directed to use the seismic hazard zone maps in their land-use planning and permitting processes. The Act requires that site-specific geotechnical investigations be performed prior to permitting most urban development projects within the hazard zones. Evaluation and mitigation of seismic hazards are to be conducted

[1]California Department of Conservation
Division of Mines and Geology
801 K Street, MS 12-31
Sacramento, CA 95814
mjdelisle@jps.net

under criteria established by the California State Mining and Geology Board (the Board) (SMGB, 1997). The Board appoints and consults the Seismic Hazards Mapping Act Advisory Committee in developing criteria for the preparation of the seismic hazard zone maps. This advisory committee consists of geologists, seismologists, civil and structural engineers, representatives of city and county governments, the state insurance commissioner, and representatives of the insurance industry. In 1991, the Board adopted initial criteria for delineating seismic hazard zones to promote uniform and effective statewide implementation of the Act. These initial criteria include procedures for mapping regional liquefaction hazards and direct DMG to develop a set of probabilistic seismic maps for California.

The criteria for mapping regional liquefaction hazards were developed by a working group of the advisory committee consisting of geologists and civil engineers from academia, the government, and the geotechnical industry. The working group also reviewed the resultant DMG maps.

The first objective of this paper is to present information that will be useful in understanding the nature of seismic hazard zones, how they are used, and how liquefaction hazards are assessed. The seismic hazard zones are not *de facto* hazardous areas, but are regions that may contain hazardous areas that must be identified by site-specific investigations. One intent of this paper is to encourage the use of established analysis methods, using up-to-date advances in hazard evaluation.

The second objective is to present the assessment of liquefaction potential for the city and county of San Francisco. It is the combination of the work completed for the liquefaction zoning pilot project and zoning work (DeLisle, 1997, 2000), and follow-up work encompassing the whole of the County of San Francisco.

THE SETTING OF THE PILOT STUDY

The city of San Francisco is a large urban area that lies within a region of high seismic potential. Within the city, liquefaction-induced ground failure has historically been a major cause of earthquake damage. Many residential, commercial, and industrial developments are in areas underlain by susceptible soils, and further development of these areas continues. The pilot liquefaction study undertaken by DMG for the city of San Francisco evaluated the methods used to assess liquefaction potential over a large geographic area and produced the prototype maps.

The area selected for the pilot study includes the northern part of the city, which is covered by the southern portion of the San Francisco North quadrangle and western portion of the Oakland West 7.5-minute quadrangle. This area was selected because detailed geologic and geotechnical information was readily available, and high seismicity and historical liquefaction occurrences were well-documented. The pilot study was conducted between 1992 to 1994, and the prototype maps were released in 1996.

In 1996, technical working groups established by the advisory committee reviewed the prototype maps and the techniques used to create them. The reviews resulted in endorsement of the methods used for liquefaction zoning and recommendation to apply them in the preparation of new quadrangle maps. Criteria for delineating seismic hazard zones were prepared from recommendations by the advisory committee and the technical-working groups (SMGB, 1999). Further DMG investigations were conducted according to these specified criteria. The resultant Official Seismic Hazard Zones are the products of a three-dimensional integration of geotechnical and geological data.

EVALUATING LIQUEFACTION POTENTIAL

Liquefaction occurs in water saturated sediments subject to the ground shaking that accompanies moderate to strong earthquakes. Liquefied sediments lose their strength, potentially causing damage to man-made structures. A number of methods for mapping liquefaction hazard have been proposed, as summarized by Youd (1991). Youd and Perkins (1978) demonstrate the use of geologic criteria for the qualitative discrimination of susceptibility units, and introduce the mapping technique of combining a liquefaction susceptibility map and a liquefaction opportunity map to evaluate liquefaction potential (liquefaction susceptibility is a function of the capacity of sediments to resist liquefaction, and liquefaction opportunity is a function of the seismic ground shaking intensity). Tinsley et al. (1985) applied a combination of the techniques used by Seed et al. (1983) and Youd and Perkins (1978) for mapping liquefaction hazards in the Los Angeles region. Tinsley et al. (1985) determined areal variations in liquefaction potential by considering a lique-

faction susceptibility map together with a liquefaction opportunity map. A liquefaction susceptibility map delineates areas where liquefiable materials are likely to be present based on local geology and hydrogeology. A liquefaction opportunity map reflects the frequency of earthquake occurrence and intensity of ground shaking produced by those events. The application of the Seed simplified procedure (Seed et al., 1985; see also the introduction to this section) for evaluating liquefaction potential allows a quantitative characterization of susceptibility of geologic units (a procedure updated in the series of papers edited by Youd and Idriss, 1997). The method applied in this study is similar to that described by Tinsley et al. (1985), which combines geotechnical data analysis, and geologic and hydrologic mapping.

LIQUEFACTION SUSCEPTIBILITY

Liquefaction susceptibility is a function of the relative resistance of soils to loss of strength when subjected to ground shaking. The degree of resistance is governed by the physical properties and condition of the soil, such as sediment grain-size distribution, compaction, cementation, and depth to the water table. Some of these properties and conditions are significantly correlated to geologic age and environment of deposition. With increasing age, the relative density of a deposit may increase through cementation of the particles or the increase in thickness of the overburden sediments. Grain-size characteristics of a soil also influence susceptibility to liquefaction. Higher soil densities generally result in higher penetration resistances to a penetration sampler (different blow count corrections are used for silty sand and nonplastic silt than for clean sand; Seed et al., 1985). Therefore, blow count or cone penetrometer values are useful indicators of liquefaction susceptibility. Sands are more susceptible than silts or gravels, although silts of low plasticity are treated as liquefiable in this investigation. Cohesive soils are generally not considered susceptible to liquefaction. Such soils may be vulnerable to strength loss with remolding and represent a hazard that is not addressed in this investigation. Finally, saturation is required for liquefaction; consequently liquefaction susceptibility increases as the depth to groundwater decreases.

In summary, soils that lack resistance (susceptible soils) are typically saturated, loose sandy sediments. Soils resistant to liquefaction include all soil types that are dry or sufficiently dense.

DMG's inventory of areas containing soils susceptible to liquefaction begins with evaluation of geologic maps, cross sections, geotechnical test data, geomorphology, and groundwater hydrology. Soil condition factors such as type, age, texture, color, and consistency, along with historical depths to groundwater, are used to identify, characterize, and correlate susceptible soils. Because Quaternary geologic mapping is based on similar soil observations, findings can be related in terms of the map units.

GEOLOGIC CONDITIONS

Stratigraphy

The city and county of San Francisco are covered by the San Francisco North, Oakland West, San Francisco South and Hunters Point 7.5-minute quadrangles. These quadrangles have been mapped in detail by Radbruch (1957), Bonilla (1971), Schlocker (1974), Helley et al. (1979), Helley and Graymer (1997) and Knudsen et al. (1997). Figure 1 shows the Quaternary geologic map modified from Knudsen et al. (1997) for a portion of the study area.

For the purpose of liquefaction analysis, the geologic formations can be divided into three groups: Mesozoic bedrock, Tertiary deposits, and Quaternary deposits. The older bedrock consists of Franciscan Complex sedimentary rocks, greenstone, other metamorphic and sheared rocks, and associated serpentinite and gabbro-diabase intrusions. Tertiary rocks of the Merced Formation (QTm) crop out in the sea cliffs in the southwestern part of the county. These tilted marine rocks of Plio-Pleistocene age (Clifton and Hunter, 1987) are covered unconformably by the Pleistocene Colma Formation and by late Pleistocene and Holocene dune sand deposits and colluvium in the hills. Unconsolidated late Pleistocene and Holocene deposits are primarily sands that are grouped in various units (beach, dune sand, undifferentiated Quaternary, old beach, and Colma), but also include bay mud, landslides, rubbly slope debris, and ravine fill (colluvium). These units were deposited on the old topographic surface of Franciscan Complex rocks. Artificial fill is also widespread in the area.

Yerba Buena Island is a natural island composed of sandstone, reworked colluvium, and artificial fill. Treasure Island is made entirely of sandy and silty artificial fill.

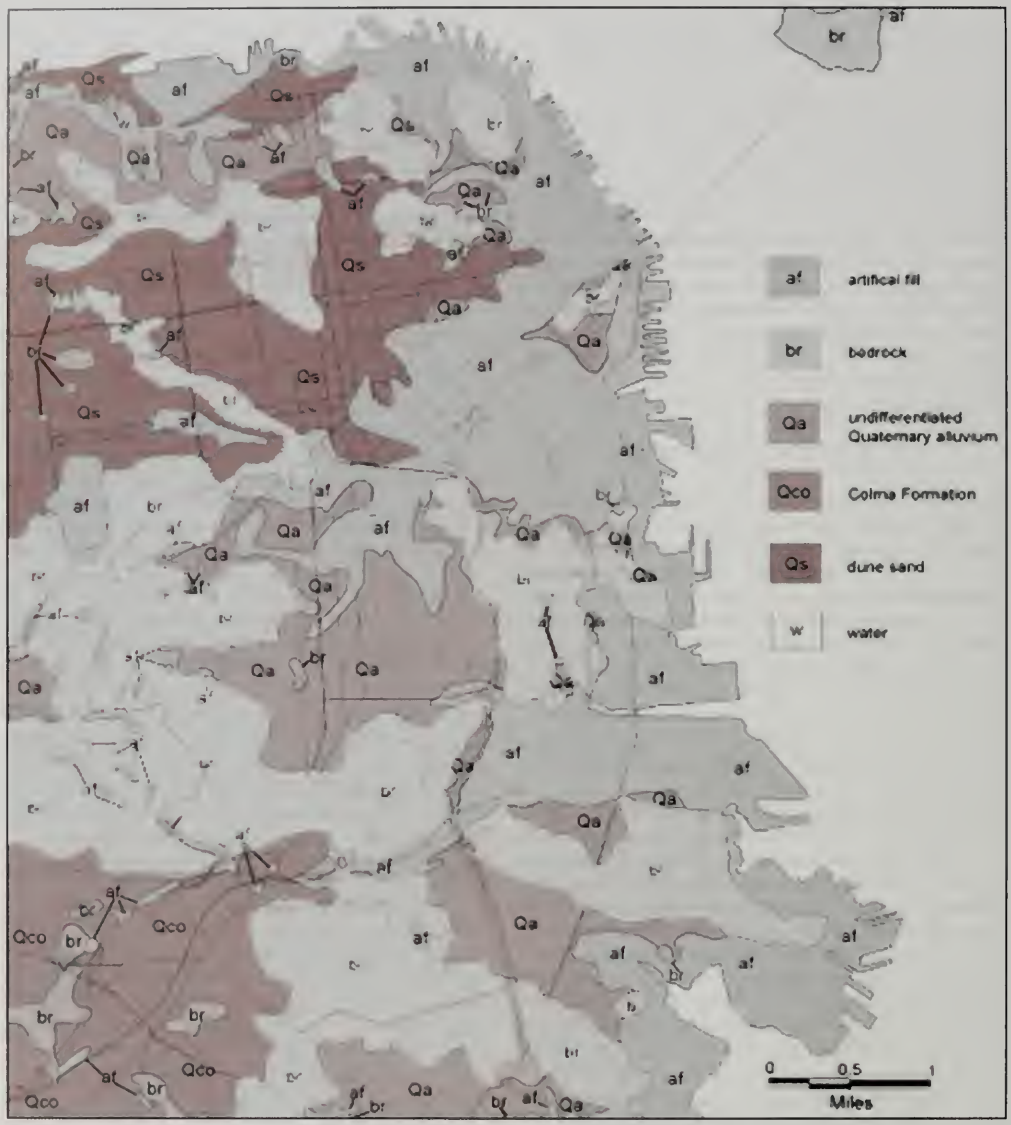

Figure 1. Quaternary geologic map of a portion of San Francisco. Geology modified from Knudsen et al. (1997).

The Quaternary geology was compiled from published geologic maps of Radbruch (1957), Radbruch and Schlocker (1958), Bonilla (1971), Schlocker (1974), Helley et al. (1979) and Knudsen et al. (1997). Slight modifications to the boundaries of some Quaternary units were made based on examination of old U.S. Coast Survey (1851, 1857a, 1857b, 1867) topographic maps, which are particularly useful in determining areas of artificial fill. These modifications were accomplished by convert-

ing paper prints of these historical maps to a digital raster format using a scanner. The raster images were geo-referenced to current maps, using the proper coordinate system, and previously unknown fills were identified by comparing the pre-existing coastline and old drainage patterns with present-day topography.

The Quaternary deposits evaluated for liquefaction zoning consist of artificial fills, bay mud, modern beach deposits, dune sand, and undifferentiated alluvial deposits of sand, silt and clay. The bay mud, where present onshore, is always covered by artificial fill.

Subsurface geology

Borehole information was used to determine general subsurface conditions. Water depths, local site stratigraphy, and standard penetration test (SPT) results or converted blow counts were used to characterize the geotechnical properties of each stratigraphic unit. Geotechnical data were collected from more than 600 sites, where one or more holes had been drilled. Borehole logs from these sites were collected after inspecting several thousand files from the California Department of Transportation (Caltrans), and the city of San Francisco's Bureau of Building Inspection, Clean Water Program, Bureau of Engineering, and Department of City Planning. An advanced, geotechnically-oriented, geographic information system capable of subsurface stratigraphic correlation was used for data integration and spatial analysis. Figure 2 shows the locations of boreholes used in this study.

Several geologic cross sections were constructed across the study area using the available geologic mapping and borehole lithology information to make subsurface stratigraphic correlations.

On the western side of the peninsula, the dune sand overlies the Pleistocene Colma Formation. Thickness of the dune sand ranges from zero to nearly 100 feet; its relative density grades from loose near the surface, to dense and very dense with depth. The dune sand is Holocene to possibly Pleistocene. The Colma Formation, which originated in shallow marine, estuarine, and alluvial environments, consists of interbedded dense sand, silty sand, clayey sand, and stiff clay. The Colma Formation rests unconformably on Franciscan Complex rocks or on the Merced Formation.

On the eastern side of the peninsula, the dune sand deposits extend from the bay on the north to an area south of Market Street. Toward the north, the dune sand overlies probable Colma Formation, whereas toward the south it overlies undifferentiated Quaternary deposits and interfingers with the Holocene bay mud. The undifferentiated deposits overlie the Colma Formation and consist of stiff clay, clayey sand, silty sand, and sand. These deposits appear to be late Pleistocene to Holocene alluvial, estuarine, and, possibly, eolian deposits. Bay mud underlies areas of artificial fill along fringes of the bay. One boring near China Basin, between 4th and 5th Streets, penetrated 125 feet of bay mud. Artificial fill is recorded at 60 feet below the surface in a boring south of Market Street along the Embarcadero.

Geotechnical properties of unconsolidated deposits

From a geotechnical perspective, dune sand is fine- to medium-grained and well-sorted, with less than 5% fines by weight. Normalized blow count values, $(N_1)_{60}$, for 597 dune sand samples have a mean value of 29 (Table 1). Where the ground is saturated, less than 1% of the samples have values less than 15, and the mean $(N_1)_{60}$ is 39, indicating that this sand may densify rapidly when saturated. Samples of undifferentiated Quaternary deposits were grouped into two categories: sand (SP in the Unified Soil Classification) and silty sand (SM). The 129 well-sorted sand (SP) samples have a mean $(N_1)_{60}$ value of 43, and the 134 samples of silty sand (SM) have a mean $(N_1)_{60}$ of 40. A summary of the geotechnical properties of the Quaternary units is shown in Table 1.

GROUNDWATER CONDITIONS

Soils below a permanent or perched groundwater table are usually saturated, whereas soils above the water table are usually not saturated (although such soils may become saturated temporarily during or after storms). For this investigation, evaluation of the distribution of the shallowest water levels throughout the mapped area was required, and a groundwater surface map showing the historically highest known groundwater was prepared. DMG uses the historically highest known groundwater levels because water levels during any earthquakes are unknown due to the unpredictable fluctuations caused by natural variations and human activities. Soils above the mapped water surface are consid-

Figure 2. Location of borehole sites used in this study.

ered non-liquefiable. Data used in preparation of the map include water depths recorded on log from Caltrans boreholes, U.S. Geological Survey (USGS) monitoring wells (Phillips et al., 1993), California Department of Water Resources water-wells, soils reports and other geotechnical investigations from 1955 to 1992, and approximately 700 water wells recorded in a study by Bartell (1913). Data were plotted and tabulated, and depths of groundwater were contoured (Figure 3). Such a map differs from

GEOLOGIC DATA		DRY UNIT WEIGHT (PCF)			STANDARD PENETRATION RESISTANCE (blows/foot)*		
Geologic unit	Soil class	Minimum range (lowest 10%)	Average (40-60%)	High range (lowest 10%)	Low range (lowest 10%)	Most common range (40-60%)	High range (upper 10%)
Dune sand	SP	92-98	105	112-124	3-9	20-28	54-128
Undiff. Quat.	SP	93-101	107	115-123	6-14	33-48	77-136
Undiff. Quat.	SM	97-104	110	118-124	6-11	30-38	75-133

*Where the sampler diameter, hammer size or drop distance differed from those specified for an SPT, recorded blow counts were converted to the equivalent of SPT blow counts. The actual and converted SPT blow counts were normalized using a common effective overburden pressure and adjusted for equipment and operational procedures using a method described by Seed and Idriss (1982) and Seed et al. (1985). This normalized blow count, $(N_1)_{60}$, is used in Table 1.

Table 1. Summary of geotechnical characteristics for Quaternary geological units evaluated for liquefaction zoning in the city and county of San Francisco.

most groundwater maps, which show the actual water table at a particular time, in that this map depicts a hypothetical "high" water table based on data acquired over widely differing times. These unpublished groundwater maps have been used during the liquefaction analysis.

GEOTECHNICAL DATA ANALYSIS

Liquefaction opportunity

According to the criteria adopted by SMGB (1999), liquefaction opportunity is a measure, expressed in probabilistic terms, of the potential for ground shaking to be strong enough to generate liquefaction. Analyses of *in situ* liquefaction resistance require assessment of liquefaction opportunity. According to the criteria, the minimum level of seismic excitation to be used for such purposes is that level of peak ground acceleration with a 10% probability of exceedance over a 50-year period. Earthquakes that could produce ground-shaking levels great enough to trigger liquefaction within the project area are likely to be associated with the San Andreas fault, which intersects the coast approximately 5.5 miles south of the study area, or with the Hayward fault, which lies 10 miles east of San Francisco. The Working Group on California Earthquake Probabilities (1999), estimates about a 70% chance for at least one magnitude 6.7 or greater earthquake occurring in the San Francisco Bay region in the next 30 years.

For the San Francisco County area, peak ground acceleration values of 0.52 to 0.86 g, resulting from earthquakes of magnitude 7.9, were used for liquefaction analysis. Because of this overall high shaking hazard, the liquefaction potential maps are essentially the same as the susceptibility maps. The peak ground acceleration and magnitude values were based on de-aggregation of the probabilistic hazard at the 10%-in-50 years hazard level (Petersen et al., 1996). Figure 4 shows the hazard for peak ground acceleration at 10% probability of exceedance in 50 years assuming the entire map area has alluvial conditions. The sites where the hazard is calculated are represented as dots and ground-motion contour intervals as shaded regions. Estimated ground shaking shown on this map only applies to sites underlain by alluvium.

Quantitative liquefaction analysis

Unpublished liquefaction susceptibility maps made during the pilot study show the areal distribution of sediments calculated to be liquefiable under given ground-motion parameters.

DMG performs quantitative analyses of geotechnical data to evaluate liquefaction potential using the Seed simplified procedure (Seed et al., 1985; National Research Council, 1985; Youd and Idriss, 1997) (see also the introduction to this section). This procedure calculates soil resistance to liquefaction, expressed in terms of cyclic resistance ratio (CRR), based on SPT results, depth to groundwater, soil density, soil type, content of fines by weight, and sample depth. CRR values are then compared to calculated earthquake-generated normalized shear stresses expressed in terms of cyclic stress ratio (CSR). The certainty with which CSR can be calculated decreases with depth using this simplified procedure (Seed and Idriss, 1982; Youd and Idriss, 1997) and a depth of 40 feet is the practical limit used for the evaluation of liquefaction. The factor of safety relative to liquefaction is determined by the ratio CRR/CSR. Therefore, the factor of safety is a quantitative measure of liquefaction potential. DMG uses a factor of safety of 1.0 or less, where CSR equals or exceeds CRR, to indicate the presence of potentially liquefiable soil. Although a factor of

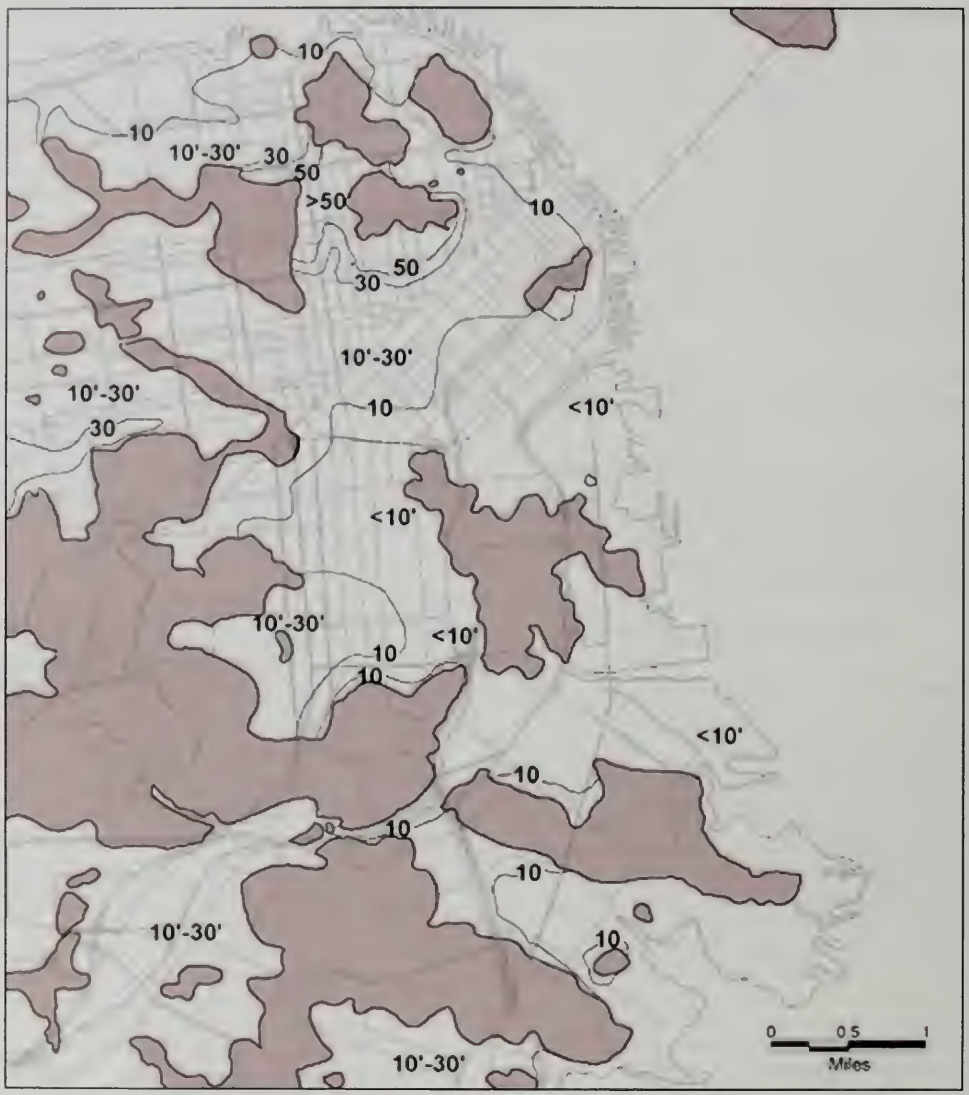

Figure 3. Depths to near-surface groundwater for a portion of San Francisco. Isobaths are in feet.

safety of 1.0 is considered the "trigger" for liquefaction, a factor of safety of as much as 1.5 may be appropriate when conducting a site specific analysis depending on the vulnerability of the site structures.

The DMG liquefaction analysis program calculates the factor of safety at each sample location that has blow counts. This calculation normally yields a range of factors of safety. The lowest factor of safety

Figure 4. Portions of the San Francisco North and South 7.5 minute quadrangles (from Petersen et al., 1996), showing 10% exceedance in 50 years peak ground acceleration (as a fraction of g) assuming all alluvium conditions. Base map modified from MapInfo Street Works.

in the range is used for that location. The factors of safety vary in reliability according to the quality of the geotechnical data. The factor of safety, as well as other considerations such as slope, free-face conditions, and thickness and depth of potentially liquefiable soil are evaluated in order to construct liquefaction potential maps, which then directly translate to zones of required investigation.

More than 450 of the borehole logs collected in San Francisco County include blow count data from SPTs or from penetration tests that allow reasonable blow count translations to SPT-equivalent values. Non-SPT values, such as those resulting from the use of 2-inch or 2.5-inch inside diameter ring samplers, were translated to SPT-equivalent values if reasonable factors could be used in conversion calculations. SPT-equivalent values vary in reliability so generally they were used in a more qualitative manner. Few borehole logs, however, include the information required for an ideal Seed simplified analysis.

During the pilot project, liquefaction opportunity maps were not available and the liquefaction analyses were completed for only selected sites. In each case, the analysis was repeated after changing one of three variables: magnitude of the earthquake, peak ground acceleration at the site, and depth to groundwater. The magnitudes varied from 6.0 to 8.3, the peak ground acceleration varied from 0.1 to 0.5 g, and the depth to groundwater varied from 3 to 30 feet. Results from the liquefaction analyses indicate that sites where saturated units have a penetration resistance $(N_1)_{60}$ of less than 25 to 30 will liquefy at levels of shaking exceeding 0.35 to 0.45 g. Units with a high susceptibility to liquefaction in the study area included all artificial fills (except where proper engineering practices were employed in placing the fill) and some areas underlain by late Holocene dune sand. The results of the pilot study and the later, systematic investigation (DeLisle 1997, 2000) are in agreement.

Due to the proximity of the San Andreas and Hayward faults, acceleration estimates are high, and their effect on soft, low shear-strength soils is subject to some debate. Observations made after the 1906 San Francisco earthquake ($M \approx 7.9$) indicate a surprising lack of liquefaction in the undifferentiated Quaternary and the dune sand, where the depth to water was more than 10 feet, with the exception of the reported occurrence of ground failure on 48th Avenue, between K and N Streets (currently 48th Avenue between Kirkham and Noriega Streets) (Lawson et al., 1908). The area was developed prior to 1906; consequently, it may have been underlain by loose fill material that failed. It appears that the high peak ground acceleration renders the Seed simplified procedure problematic for this area. Using available documentation of ground failures for the 1906 San Francisco earthquake (Lawson et al., 1908; Youd and Hoose, 1976, 1978), it was decided to emphasize past performance for determining liquefaction susceptibility.

Overall liquefaction susceptibility

The propensity for a deposit to fail was characterized by grouping deposits into high, moderate, low, and very low susceptibility categories (Table 2) based on depth to groundwater, type of sediment, texture, and stiffness, as determined by blow counts. The highest susceptibility was found in areas where dune sand is saturated at depths of less than 10 feet, areas of artificial fill, and beach deposits.

Water depth	High	Moderate	Low	Very low
<10 ft	Artificial fill, beach sand, dune sand	Undiff. Quaternary		Colluvium, bedrock
10-30 ft	Artificial fill	Dune sand	Undiff. Quaternary	Colluvium, bedrock
30-40 ft	Artificial fill	Dune sand	Undiff. Quaternary	Colluvium, bedrock

Table 2. Liquefaction susceptibility.

LIQUEFACTION ZONES

Criteria for zoning

The areas underlain by late Quaternary geologic units were included in liquefaction zones using the criteria developed by the Seismic Hazards Mapping Act Advisory Committee and adopted by the California State Mining and Geology Board (SMGB, in press). Under those criteria, liquefaction zones are defined for areas meeting one or more of the following:

1. Areas known to have experienced liquefaction during historic earthquakes

2. All areas of uncompacted fills containing liquefaction-susceptible materials that are saturated, nearly saturated, or may be expected to become saturated

3. Areas where sufficient existing geotechnical data and analyses indicate that the soils are potentially liquefiable

4. Areas where existing geotechnical data are insufficient. In areas of limited or no geo-

technical data, susceptibility zones may be identified by geologic criteria as follows:

(a) Areas containing soil deposits of late Holocene age (current river channels and their historic floodplains, marshes and estuaries), where the M7.5-weighted peak acceleration that has a 10% probability of being exceeded in 50 years is greater than or equal to 0.10 g, and the historic high water table is less than 40 feet below the ground surface; or

(b) Areas containing soil deposits of Holocene age (less than 11,000 years), where the M7.5-weighted peak acceleration that has a 10% probability of being exceeded in 50 years is greater than or equal to 0.20 g, and the historic high water table is less than or equal to 30 feet below the ground surface; or

(c) Areas containing soil deposits of latest Pleistocene age (between 11,000 years and 15,000 years), where the M7.5-weighted peak acceleration that has a 10% probability of being exceeded in 50 years is greater than or equal to 0.30 g, and the historic high water table is less than or equal to 20 feet below the ground surface.

The criteria 4a through 4c reflect the fact that at low degrees of consolidation, liquefaction may be triggered even at low peak ground acceleration values or when the water table is deep. For more consolidated sediments, the historical water table must be higher and the peak ground acceleration must be larger for liquefaction to occur. A flow chart summarizing the criteria for delineating zones of required investigation for liquefaction used in the city and county of San Francisco is shown in Figure 5.

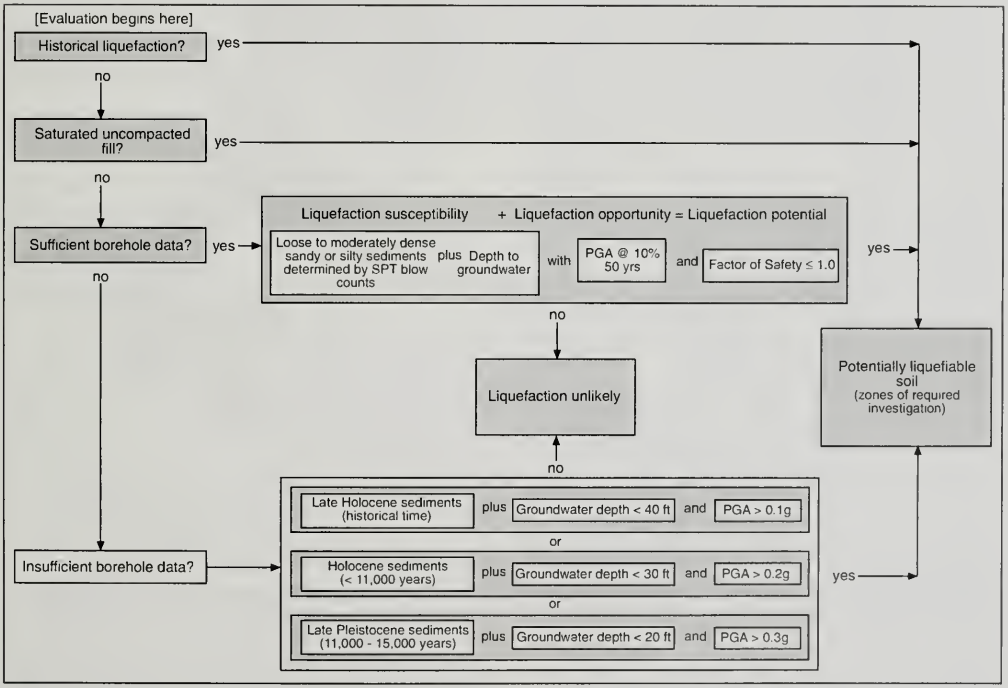

Figure 5. Flow chart summarizing SMGB criteria for delineating zones of required investigation in the city and county of San Francisco.

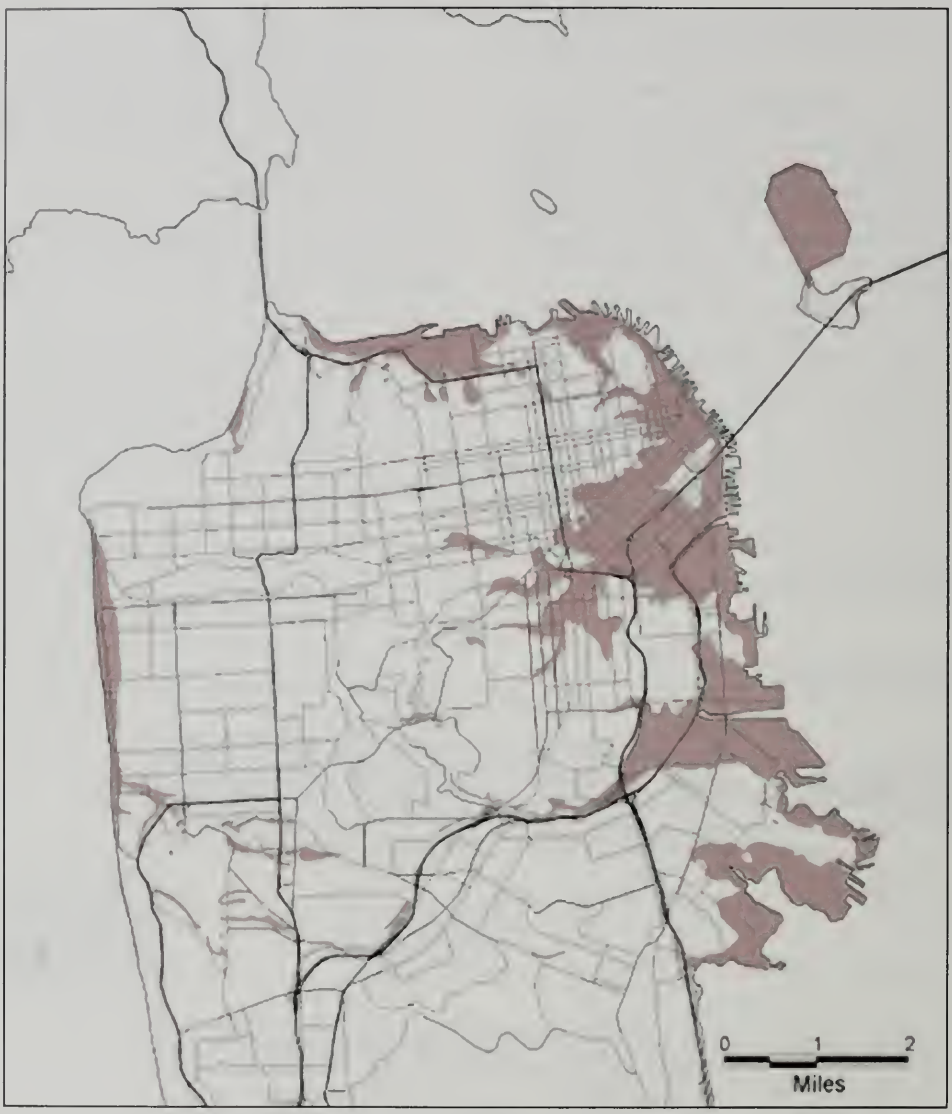

Figure 6. Seismic Hazard Zones for the city and county of San Francisco showing zones of required investigation for liquefaction (shaded area).

Zones of required investigation for potentially liquefiable soils within the city and county of San Francisco are presented as shaded areas on the Seismic Hazard Zones Map (Figure 6). Areas zoned as containing potentially liquefiable soils, and the criteria applied in the development of the hazard zones, are discussed below.

Areas of past liquefaction

In the study area, historical occurrences of liquefaction have been documented by Lawson et al. (1908), Youd and Hoose (1976, 1978), Bennett (1990), Seed et al. (1990), HLA et al. (1991a, 1991b), Pease et al. (1992), Bardet and Kapuskar (1993), Pease and O'Rourke (1993) and Tinsley et al. (1998). All areas of historic liquefaction are included in the hazard zone shown in Figure 6.

Artificial fills

Artificial fill has been placed at many localities during the development of San Francisco. Many of the historical occurrences of ground failure related to liquefaction are associated with artificial fill. These fills are composed of various materials compacted to varying densities. Pease et al. (1992), in a study of the Marina District using borehole and SPT information, found hydraulic fill has a mean $(N_1)_{60}$ of 6, land-tipped fill has a mean $(N_1)_{60}$ of 14, and natural sand deposits have a mean $(N_1)_{60}$ of 26. Due to the variability of the material and the haphazard distribution of that material in artificial fill deposits, a site-specific investigation is necessary to determine if a hazard exists. Consequently, all fill material that is saturated or may become saturated is included within the hazard zone.

Areas with sufficient geotechnical data

Geotechnical data were collected from more than 600 sites where one or more boreholes were drilled (Figure 2). These data were used to develop the liquefaction zone in most areas.

The undifferentiated Quaternary deposits and the dune sand deposits were analyzed and characterized, as discussed previously. The hazard zone boundary is defined by the high susceptibility category. There is no modification by ground shaking because over the entire area it exceeds the critical level necessary to induce liquefaction.

Areas with insufficient geotechnical data

No geotechnical borehole information was found for the former Presidio Military Reservation or the area containing the modern beach deposits. Zoning of these areas was accomplished in accordance with item 4 of the Advisory Committee's criteria for zoning.

CONCLUSIONS

This paper has reported the results of two studies conducted as part of the DMG Seismic Hazard Mapping Program. Zones of required seismic investigation for San Francisco included areas likely to contain geologic conditions susceptible to liquefaction during earthquakes, and are based on the geologic age of cohesionless deposits, their geotechnical properties, depth to saturation using historical high groundwater levels, and the 10% in 50-year peak acceleration expected in the area. In addition to the city and county of San Francisco, the DMG Seismic Hazard Mapping Program has designated zones of required seismic investigation for over 100 jurisdictions in Alameda, Los Angeles, Orange and Ventura counties, California. Additional work is ongoing throughout southern California and the San Francisco Bay area.

ACKNOWLEDGMENTS

Thanks are due to Catherine Bauman, of the San Francisco Department of City Planning; Larry Litchfield, Laurence Kornfield, and Zan Turner, of the San Francisco Bureau of Building Inspection; and Robert Darragh, James Gamble, Tom Holzer, Keith Kelson, Faiz Makdisi, Lelio Mejia, Frank Rollo, Dick Tait and Henry Taylor for providing peer review for the pilot program.

I wish to thank Julie Monet for collecting much of the borehole data for the southern part of the city; Tim McCrink and Chuck Real, of DMG for assisting in the assessment of hazard for the pilot project, and Teri McGuire for helping with the database and preparation of the figures.

AUTHOR PROFILE

Mark J. DeLisle recently retired from his position as Senior Engineering Geologist with the Division of Mines and Geology, and supervisor of the liquefaction mapping unit of the Seismic Hazard Mapping Program. He was with DMG for 12 years and with this program from its inception. Before joining DMG, he worked as an exploration geologist for over 25 years in the petroleum industry. Mark DeLisle holds A.B. and M.S. degrees in Geology from San Diego State University.

SELECTED REFERENCES

Atwater, B.F., Hedel, C.W., and Helley, E.J., 1977, Late Quaternary depositional history, Holocene sea-level changes, and vertical crustal movement, southern San Francisco Bay, California: U.S. Geological Survey Professional Paper 1014, 15 p.

Bardet, J.P. and Kapuskar, M., 1993, Liquefaction sand boils in San Francisco during 1989 Loma Prieta earthquake: Journal of Geotechnical Engineering, v. 119, no. 3, p. 543-562.

Bartell, M.J., 1913, Report on the underground water supply of San Francisco County: San Francisco Department of Public Works, 157 p.

Bartlett, S.F. and Youd, T.L., 1992, Empirical analysis of horizontal ground displacement generated by liquefaction-induced lateral spreads: National Center for Earthquake Engineering Research, State University of New York at Buffalo, New York, Technical Report NCEER-92-0021.

Bennett, M.J., 1990, Ground deformation and liquefaction of soil in the Marina District: U.S. Geological Survey Open-File Report 90-253, p. 44-79.

Bonilla, M.G., 1964, Bedrock-surface map of the San Francisco South Quadrangle, California: U.S. Geological Survey Miscellaneous Field Studies Map MF-334, scale 1: 31,680.

Bonilla, M.G., 1971, Preliminary geologic map of the San Francisco South Quadrangle and part of the Hunter's Point Quadrangle, California: U.S. Geological Survey Miscellaneous Field Studies Map MF-311, 2 sheets, scale 1:24,000.

Bonilla, M.G., 1990, Natural and artificial deposits in the Marina District: U.S. Geological Survey Open-File Report 90-253, p. 8-32.

Carlson, P.R. and McCulloch, D.S., 1970, Bedrock-surface map of central San Francisco Bay: U.S. Geological Survey Open-File Map, scale 1:15,840.

Clifton, H.E. and Hunter, R.E., 1987, The Merced Formation and related beds: a mile-thick succession of late Cenozoic coastal and shelf deposits in the sea cliffs of San Francisco, California: Geological Society of America Centennial Field Guide-Cordilleran Section, p. 257-262.

Cooper, W.S., 1967, Coastal dunes of California: Geological Society of America, Memoir 104, 131 p.

DeLisle, M.J., 1997, Seismic hazard evaluation of the south half of the San Francisco North and part of the Oakland West 7.5-minute quadrangles, San Francisco County, California: California Department of Conservation, Division of Mines and Geology, Open-File Report 97-05, 19 p.

DeLisle, M.J., 2000, Liquefaction zones in the city and county of San Francisco, California: California Department of Conservation, Division of Mines and Geology, Open File Report 00-09, 15p.

Goldman, H.B., 1969, Geology of San Francisco Bay: *in* Geologic and engineering aspects of San Francisco Bay fill, California Division of Mines and Geology Special Report 97, p. 9-29.

HLA (Harding-Lawson Associates), Dames and Moore, Kennedy, Jenks, Chilton, and EQE Engineering, 1991a, Li-quefaction Study, North Beach, Embarcadero Waterfront, South Beach, and Upper Mission Creek Area, San Francisco, California: Harding Lawson Associates, San Francisco, California, Report No. 17592.041.04.

HLA (Harding-Lawson Associates), Dames and Moore, Kennedy, Jenks, Chilton, and EQE Engineering, 1991b, Marina District and Sullivan Marsh Liquefaction Study, San Francisco, California: Harding Lawson Associates, San Francisco, California, Report No. 17592.041.04.

Helley, E.J. and Graymer, R.W., 1997, Quaternary geology of Alameda County, and parts of Contra Costa, Santa Clara, San Mateo, San Francisco, Stanislaus and San Joaquin counties, California: A Digital Database: U.S. Geological Survey Open File Report 97-97.

Helley, E.J., Lajoie, K.R., Spangle, W.E., and Blair, M.L., 1979, Flatland deposits of the San Francisco Bay region, California- their geology and engineering properties, and their importance to comprehensive planning: U.S. Geological Survey Professional Paper 943, 88 p.

Joyner, W.B., 1982, Map showing the 200-foot thickness contour of surficial deposits and the landward limit of bay mud deposits of San Francisco, California: U.S. Geological Survey Miscellaneous Field Studies Map MF-1376, scale 1:24,000.

Kayen, R.E., Liu, H.P., Fumal, T.E., Westerlund, R.E., Warrick, R.E., Gibbs, J.F., and Lee, H.J., 1990, Engineering and seismic properties of the soil column at Winfield Scott School, San Francisco: U.S. Geological Survey Open-File Report 90-253, Menlo Park, California, p. 112-129.

Knudsen, K.L., Noller, J.S., Sowers, J.M. and Lettis, W.R., 1997, Map showing Quaternary geology and liquefaction susceptibility, San Francisco, California, 1:100,000 Sheet: Final Technical Report: National Earthquake Hazards Reduction Program, U. S. Geological Survey, FY95 Award Number 1434-94-G-2499, p. 1-20.

Lajoie, K.R. and Helley, E.J., 1975, Differentiation of sedimentary deposits for purposes of seismic zonation: *in* Borcherdt, R.D. (ed.), Studies for seismic zonation of the San Francisco Bay Region: U.S. Geological Survey Professional Paper 941-A, p. A39-A51.

Lawson, A.C. and others, 1908, The California earthquake of April 18, 1906: Report of the State Investigative Commission, Carnegie Institute, Washington, D.C., 451 p.

Lee, C.H. and Praszker, Michael, 1969, Bay mud developments and related structural foundations: *in* Goldman, H.B. (ed.) Geologic and engineering aspects of San Francisco Bay fill: California Department of Conservation, Division of Mines and Geology Special Report 97, p. 41-85.

National Research Council, 1985, Liquefaction of soils during earthquakes: National Research Council Special Publication, Committee on Earthquake Engineering, National Academy Press, Washington, D.C., 240 p.

Pease, J.W., O'Rourke, T.D., and Stewart, H.E., 1992, Post-liquefaction consolidation and lifeline damage in the Marina District after the 1989 Loma Prieta earthquake: *in* Hamada, Masanori and O'Rourke, T.D. (eds), Proceedings from the Fourth Japan-U.S. Workshop on Earthquake Resistant Design of Lifeline Facilities and Countermeasures for Soil Liquefaction, v. 1, National Center for Earthquake Engineering Research, State University of New York at Buffalo, New York, Technical Report NCEER-92-0019, p. 395-412.

Petersen, M.D., Bryant, W.A., Cramer, C.H., Cao. T., Reichle, M.S., Frankel, A.D., Lienkaemper, J.J., McCrory, P.A., and Schwartz, D.P., 1996, Probabilistic seismic hazard assessment for the State of California: California Department of Conservation, Division of Mines and Geology, Open-File Report 96-08; U.S. Geological Survey Open File Report 96-706, 33 p.

Phillips, S.P., Hamlin, S.N., and Yates, E.B., 1993, Geohydrology, water quality, and estimation of ground-water recharge in San Francisco, California, 1987-92: U.S. Geological Survey Water-Resources Investigations Report 93-4019, 69 p.

Radbruch, D.H., 1957, Areal and engineering geology of the Oakland West Quadrangle, California: U.S. Geological Survey Miscellaneous Geologic Investigations Map I-239, scale 1:24,000.

Radbruch, D.H. and Schlocker, Julius, 1958, Engineering geology of Islais Creek basin, San Francisco, California: U.S. Geological Survey Miscellaneous Geologic Investigations Map I-264, scale 1:12,000.

Roth, R.A. and Kavazanjian, E.J., 1984, Liquefaction susceptibility mapping for San Francisco, California: Bulletin of Association of Engineering Geologists, v. 21, no. 4, p. 459-478.

Schlocker, J., 1974, Geology of the San Francisco North Quadrangle, California: U.S. Geological Survey Professional Paper 782, 109 p.

Seed, H.B. and De Alba, P., 1986, Use of SPT and CPT tests for evaluating the liquefaction resistance of sands: *in* Clemence, S.P., (ed.), Use of in situ tests in geotechnical engineering: ASCE-Geotechnical Special Publication No. 6: p. 281-302.

Seed, R.B., Dickenson, S.E., Riemer, M.F., Bray, J.D., Sitar, N., Mitchell, J.K., Idriss, I.M., Kayen, R.E., Kropp, A., Harder, L.F., Jr., and Power, M.S., 1990, Preliminary report on the principal geotechnical aspects of the October 17, 1989 Loma Prieta earthquake: Earthquake Engineering Research Center, College of Engineering, University of California, Berkeley, Report No. UCB/EERC-90/05.

Seed, R.B. and Harder, L.F., 1990, SPT-based analysis of cyclic pore pressure generation and undrained residual strength: Proceedings of the H. Bolton Seed Memorial Symposium, v. 2, p. 351-376.

Seed, H.B. and Idriss, I.M., 1971, Simplified procedure for evaluating liquefaction potential: Journal of the Soil Mechanics and Foundations Division, ASCE, v. 97, no. SM9, p. 1,249-1,273.

Seed, H.B. and Idriss, I.M.,1982, Ground motions and soil liquefaction during earthquakes: Monograph Series, Earthquake Engineering Research Institute, Berkeley, California, 134 p.

Seed, H.B., Idriss, I.M., and Arango, I., 1983, Evaluation of liquefaction potential using field performance data: Journal of Geotechnical Engineering, v. 109, p. 458-482.

Seed, H.B. and Sun, J.I., 1989, Implications of effects in the Mexico City earthquake of September 19, 1985 for earthquake-resistant design criteria in the San Francisco Bay area of California: UCB/EERC Report No. 89/03, 124 p.

Seed, H.B., Tokimatsu, Kohji, Harder, L.F., and Chung, R.M., 1985, Influence of SPT procedures in soil liquefaction resistance evaluations: Journal of Geotechnical Engineering, ASCE, v. 111, no. 12, p. 1,425-1,445.

Sloan, D., 1992, The Yerba Buena mud: record of the last interglacial predecessor of San Francisco Bay, California: Bulletin of the Geological Society of America, v. 104, no. 6, p. 716-727.

Smith, T.C., 1996, Preliminary maps of seismic hazard zones and draft guidelines for evaluating and mitigating seismic hazards: California Geology, v. 49, no. 6, p. 147-150.

State Mining and Geology Board, 1997, Guidelines for evaluating and mitigating seismic hazards in California: California Department of Conservation, Division of Mines and Geology, Special Publication 117, 74 p.

State Mining and Geology Board, 1999, Criteria for delineating seismic hazard zones: California Department of Conservation, Division of Mines and Geology, Special Publication 118, 21 p.

Tinsley, J.C. and Dupre', W.R., 1992, Liquefaction hazard mapping, depositional facies, and lateral spreading ground failure in the Monterey Bay area, central California, during the October 17, 1989 Loma Prieta earthquake: *in* Hamada, Masanori and O'Rourke, T.D. (eds.), Proceedings from the Fourth Japan-U.S. Workshop on earthquake resistant design of lifeline facilities and countermeasures for soil liquefaction, v. 1, Technical Report NCEER-92-0019, National Center for Earthquake Engineering Research, State University of New York at Buffalo, New York, p. 71-86.

Tinsley, J.C., Egan J.A., Kayen, R.E., Bennett, M.J., Kropp, A., and Holzer, T.L.., 1998, Appendix: Maps and descriptions of liquefaction and associated effects: *in* Holzer, T.L. (ed.), The Loma Prieta, California, earthquake of October 17,1989, U.S. Geological Survey Professional Paper 1551-B60, p. B287-314.

Tinsley, J.C., Youd, T.L., Perkins, D.M., and Chen, A.T.F., 1985, Evaluating liquefaction potential: *in* Ziony, J.I. (ed.), Evaluating earthquake hazards in the Los Angeles region—an earth science perspective, U.S. Geological Survey Professional Paper 1360, p. 263-316.

Trask, P.D. and Rolston, J.W., 1951, Engineering geology of San Francisco Bay, California: Bulletin of the Geological Society of America, v. 62, no. 9, p. 1,079-1,110.

U.S. Coast Survey, 1851, South shore Golden Gate from Point Lobos to San Francisco, California: Surveyed by R.J. Cutts, scale 1:10,000.

U.S. Coast Survey, 1857a, City of San Francisco and its vicinity, California: Register No. 687, scale 1:10,000.

U.S. Coast Survey, 1857b, Revisionary survey for the determination of the light houses and defense works of the harbor of San Francisco, California: Register No. 663, scale 1:10,000.

U.S. Coast Survey, 1867, Map showing part of land approaches to city of San Francisco, California for use of Engineering Department U.S. Army: Register No. 1059, scale 1:10,000.

WGCEP (Working Group on California Earthquake Probabilities), 1999, Understanding earthquake hazards in the San Francisco Bay region, California: U.S. Geological Fact Sheet-152-99, U.S. Government Printing Office, Washington, D.C., 4 p.

Yates, E.B., Hamlin, S.N., and McCann, L.H., 1990, Geohydrology, water quality, and water budgets of Golden Gate Park and the Lake Merced area in the western part of San Francisco, California: U.S. Geological Survey Water-Resources Investigations Report 90-4080, 45 p.

Youd, T.L., 1978, Major cause of earthquake damage is ground failure: Civil Engineering, ASCE, v. 48, no. 4, p. 47-51.

Youd, T.L., 1984, Geologic effects-liquefaction and associated ground failure: *in* Williams, M.E. (ed.), Proceedings of the geologic and hydrologic hazards training program, U.S. Geological Survey, Menlo Park, Open-File Report 84-760, p. 210-232.

Youd, T.L., 1991, Mapping of earthquake-induced liquefaction for seismic zonation: *in* Proceedings of the Fourth International Conference on Seismic Zonation, v. 1, p. 111-147.

Youd, T.L. and Hoose, S.N., 1976, Liquefaction during the 1906 San Francisco earthquake: Journal of the Geotechnical Engineering Division, v. 102, no. GT5, p. 425-440.

Youd, T.L. and Hoose, S.N., 1977, Liquefaction susceptibility and geologic setting: *in* Proceedings of the Sixth World Conference on Earthquake Engineering, Prentice-Hall, (Englewood Cliffs, New Jersey), v. 3, p. 2,189-2,194.

Youd, T.L. and Hoose, S.N., 1978, Historic ground failures in northern California triggered by earthquakes: U.S. Geological Survey Professional Paper 993, 171 p.

Youd, T.L. and Idriss, I.M. (eds.), 1997, Proceedings of the NCEER workshop on evaluation of liquefaction resistance of soils: Technical Report NCEER-97-0022, 277 p.

Youd, T.L., Nichols, D.R., Helley, E.J., and Lajoie, K.R., 1975, Liquefaction potential: *in* Borcherdt, R.D. (ed.), Studies for seismic zonation of the San Francisco Bay region: U.S. Geological Survey Professional Paper 941-A, p. A68-A74.

Youd, T.L. and Perkins, D.M., 1978, Mapping liquefaction-induced ground failure potential: Journal of the Geotechnical Engineering Division, ASCE, v. 104, no. GT4, p. 433-446.

THE USE OF SEDIMENTATION RATES IN FORENSIC GEOLOGY: THE CASE OF THE SHORT FREEWAY FENCE AT PETALUMA, SONOMA COUNTY, CALIFORNIA

ROY J. SHLEMON[1] AND GARY E. VAN HOUTEN[2]

ABSTRACT

In 1985 a Volkswagen sedan traveling north on Highway 101 at Petaluma collided with a horse. The horse ("Cisco") was killed, the young male driver became a paraplegic, and litigation ensued. The horse apparently broke through or stepped over a fence that was about 1.5 ft shorter than design specifications. But no obvious modification to the fence had taken place during the 40 years since construction. Questions as to how and why such an accident could have happened led to the use of forensic geology.

Based on trench exposures, soil-stratigraphic assessments and radiocarbon dates, we determined that late Holocene natural sedimentation rates were ~1.5 ft/500 years. In contrast, ~1.5 ft of sediments had accumulated on the "broken fence" side of the freeway during the 40 years since the fence was constructed (1954). The cause of this accelerated sedimentation and partial burying of the freeway fence was ultimately found to be the unintentional "damming" of the natural drainage. Thus, during those 40 years the freeway fence was imperceptibly shortened. Consequently, lacking horse sense, Cisco stepped over the partially buried fence and onto the freeway, therefore precipitating his own demise and physical and financial damage to others. By using sedimentation rates, forensic geology helped solve "the mystery of the short fence" at Petaluma. The case eventually was settled.

INTRODUCTION

We present this "short fence" article as a case study of a rather unusual application of sedimentation rates to forensic geology. Most geologists get an initial taste of "forensic work" when retained by a lawyer in the course of litigation. In reality, almost every geological investigation, whether driven by litigation or not, involves good detective work: collecting bits and pieces of information from readily available sources, interpreting the data, and arriving at a reasonable conclusion. In academic parlance this is called the "scientific method" – the procedure through which one ultimately arrives at a working hypothesis to explain a collection of facts.

Forensic geology is traditionally applied to landslide, subsidence and construction defect cases (e.g., Kiersch and Cleaves, 1969; Dunn, 1991; Patton, 1992; Leighton, 1992; Shuirman and Slosson, 1992). However, forensic geology also played a very important role in determining the cause of an automobile accident that occurred near Petaluma, California in 1985. In this paper we present the background of the litigation, our investigative procedures, and results of a forensic geology investigation that helped resolve the mystery of the "short freeway fence at Petaluma, California." Retained by attor-

[1]Roy J. Shlemon & Associates, Inc.
P.O. Box 3066
Newport Beach, CA 92659-0620
rshlemon@jps.net

[2]Van Houten Consultants, Inc.
P.O. Box 932
Petaluma, CA 94953-0922

neys for the plaintiffs, we obtained most of our technical data from site mapping, trench logging, sample collection and laboratory analysis of geotechnical properties, and sediment dating using radiocarbon and soil-stratigraphic techniques.

BACKGROUND OF THE LITIGATION

In 1985, a 25-yr old male was driving his 1969 Volkswagen sedan north on the Highway 101 freeway several hundred feet north of the city limits of Petaluma, in an unincorporated area of Sonoma County (Figure 1). About 9:00 pm the sedan collided with a horse that had wandered into the northbound lanes. The horse, described by investigating officers as "large and brown, and named Cisco," was killed. A clean-up crew took the remains to the local tallow works. The driver sustained severe head injuries and was transported to a hospital in nearby Santa Rosa. Unfortunately, the driver's injuries were so severe that he never completely recovered. He became a paraplegic and, according to medical testimony, would likely be so for the rest of his life. The victim's guardians brought suit, seeking financial redress from the property owner, the lessee of the land from which the horse had wandered, and the California Department of Transportation (Caltrans), which had designed and built the freeway and its bordering fences in 1954.

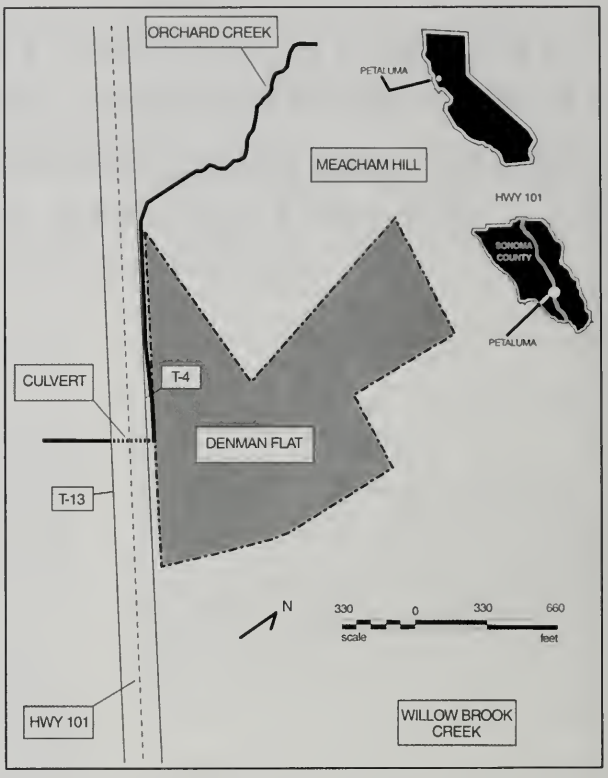

Figure 1. Maps showing the location of Petaluma in Sonoma County, and place names referred to in the text. The heavy dashed lines enclose the "horse" property; the solid line shows the 1954 southward redirection of Orchard Creek, parallel to Highway 101, and its passage under the freeway via a culvert to the southwest. Logs and photo-documentation of trenches T-4 and T-13 are shown in Figures 4, 5 and 6.

Police officers investigating the accident scene, by observation and interview, determined that Cisco apparently "walked through" the freeway fence. Furthermore, they noted that the now-broken fence had been only "two to three feet" high at time of the accident, substantially shorter than the 4.5-ft height originally specified by Caltrans. Fundamental questions were then raised: Why was the fence so short? Was it a result of poor construction or poor maintenance? Perhaps accelerated sedimentation had occurred? And, if such sedimentation took place, was the cause wholly natural or induced by man? The answers to these questions required regional and site-specific geologic investigations and a good dose of common sense.

GEOLOGIC FRAMEWORK

The short-fence accident occurred in the northwest part of Denman Flat, a poorly drained floodplain between Willow Brook on the east, the Highway 101 freeway on the southwest, and Meacham Hill on the northeast (Figure 1). The regional geology is typical for this part of the Northern Coast Ranges; namely, Tertiary sediments and volcanics unconformably overlying the Jurassic-Cretaceous Franciscan Group (Wagner and Bortugno, 1982). Bordering the site, and contributing particularly to the Willow Brook catchment, are Pliocene sediments of the

Petaluma and Wilson Grove Formations and the Sonoma Volcanic Group. Nearby Quaternary deposits range from numerous landslides and debris flows mantling adjacent hills, to interfingering alluvial fan and fluvial terrace deposits along the major drainage. There are no unusual geological conditions, such as fault scarps or sag ponds that may have contributed to on-site accelerated sedimentation. Rather, trench exposures showed that late Holocene colluviation was very slow, resulting in formation of thick, accretionary (cumulic) soil organic horizons (Table 1). The investigation area extended to both sides of the freeway (Figures 1 and 2), which are mainly underlain by floodplain silt and basin clay (Brown and Jackson, 1974; Huffman and Armstrong, 1980).

GEOMORPHIC AND HYDROLOGIC SETTING

Orchard Creek and Willow Brook once traversed southwestward across Denman Flat as tributaries to the Petaluma River. However, with freeway construction in 1954, Orchard Creek was diverted about 800 ft to the southwest, parallel to the freeway, before being redirected via a culvert to the west (Figure 1).

Historically, both Orchard Creek and Willow Brook impacted the short-fence area only during infrequent floods. After freeway construction, however, water often "dammed up" at upstream culverts and, almost annually, backed up onto the northwest part of Denman Flat. Under natural conditions, the adjacent Meacham Hill contributed only minor colluvial deposits to Denman Flat.

No major on-site or nearby grading has taken place that may have accelerated local sedimentation. However, with local land-use change, including operation of a large, 1950's "chicken ranch," accelerated deposition has occurred, particularly along Orchard Creek (Figures 1 and 2).

INVESTIGATION PROCEDURES

Initial reconnaissance showed that the Caltrans-constructed fence, bordering the north lanes of the freeway at the accident scene, was indeed short, confirming the investigating officer's observations. However, the posts supporting the fence along the southbound lanes proved to be 54-inches high, conforming to 1954 Caltrans specifications. It thus

Depth (ft)	Horizon	Description
0.0 — 0.3	A1p	Very dark gray (10YR 3/1) to very dark grayish brown (10YR 3/2) when moist silty clay; moderate fine subangular blocky structure; very hard, very firm, slightly sticky and slightly plastic; common fine roots; abrupt wavy to abrupt smooth boundary.
0.3 — 1.4	A2	Black (2.5Y 2/0) to very dark brown (10YR 2/2) when moist clay loam; moderate very coarse angular blocky structure; very hard, very firm, sticky and plastic; few fine vertical roots; few fine root holes; few discontinuous pressure faces; gradual wavy boundary.
1.4 — 3.9	A3	Black (2.5Y 2/0) dry and moist clay loam; moderate to strong very coarse angular blocky structure to weak coarse prismatic structure; very hard, very firm, sticky and plastic; few fine medium vertical roots; many pressure faces (slickensides) to 5 inches length on basal ped faces in lower part of horizon; gradual to abrupt wavy boundary.
3.9 — 4.4	A4k	Black (10YR 2/1) to very dark gray (10YR 3/1) when moist clay loam; massive, hard, firm, sticky and very plastic; few fine vertical roots; common pressure faces dipping ~35 degrees; few to common carbonate nodules and filaments; effervesces violently; gradual wavy boundary.
4.4 — 5.1	C	Black (5Y 2.5/2) to dark gray (5Y 4/1) when moist silty clay; massive; soft, friable, slightly sticky and very plastic; few disseminated charcoal fragments; few fine carbonate nodules to 2-inches diameter; base of trench.

Notes:
1. Measurement by RJS, 6 June 1991.
2. Profile is a cumulic mollic epipedon (A/C) with surface plowpan (Ap horizon).
3. Deposition in poorly drained basin giving rise to organic-rich, smectitic clay.
4. No post-1954 accretion apparent in profile.

Table 1. Soil stratigraphic measurement and description — Trench 13

Figure 2. Aerial-photograph of the accident scene. Orchard Creek (upper center) now parallels the northeast side of Highway 101 to a culvert and into a drainage ditch across the freeway bordering the tree line (lower left). The "short fence" is on northeast or "upstream" side of the freeway; the horse "Cisco" entered the roadway near the two trees (lower center).

appeared, and was alleged in the litigation, that "fence-shortening" was caused by accelerated sedimentation, resulting in burial of several fence strands, in loss of height and, ultimately, in the ability of the horse, Cisco, to gain entry to the freeway.

As called for in Caltrans specifications, the 1954 freeway, "Type B" fence posts were wood, 6 x 6-inches square, and emplaced on 12-ft centers. The posts were set 30 inches into the ground, and strung with 10-strand wire mesh (Figure 3).

To determine the extent, thickness and possible cause of the alleged accelerated sedimentation, we undertook several investigative tasks. These included: (1) excavating and logging trenches at and near the accident scene; (2) surveying fence-post height on both sides of the freeway; (3) preparing a site-specific topographic map with contour intervals of one-half and one foot, respectively; (4) interpreting aerial photographs to assess land-use change and morphology before and after freeway construction; and (5) measuring and describing soils (pedogenic profiles) following procedures and terminology of the U. S. Natural Resources Conservation Service (Shlemon, 1985; Birkeland, 1999). The trench exposures, and the samples collected from them, proved to be particularly instructive, for they provided data about the extent, thickness, age, and rate of sedimentation, both in the "short" and "normal" fence areas.

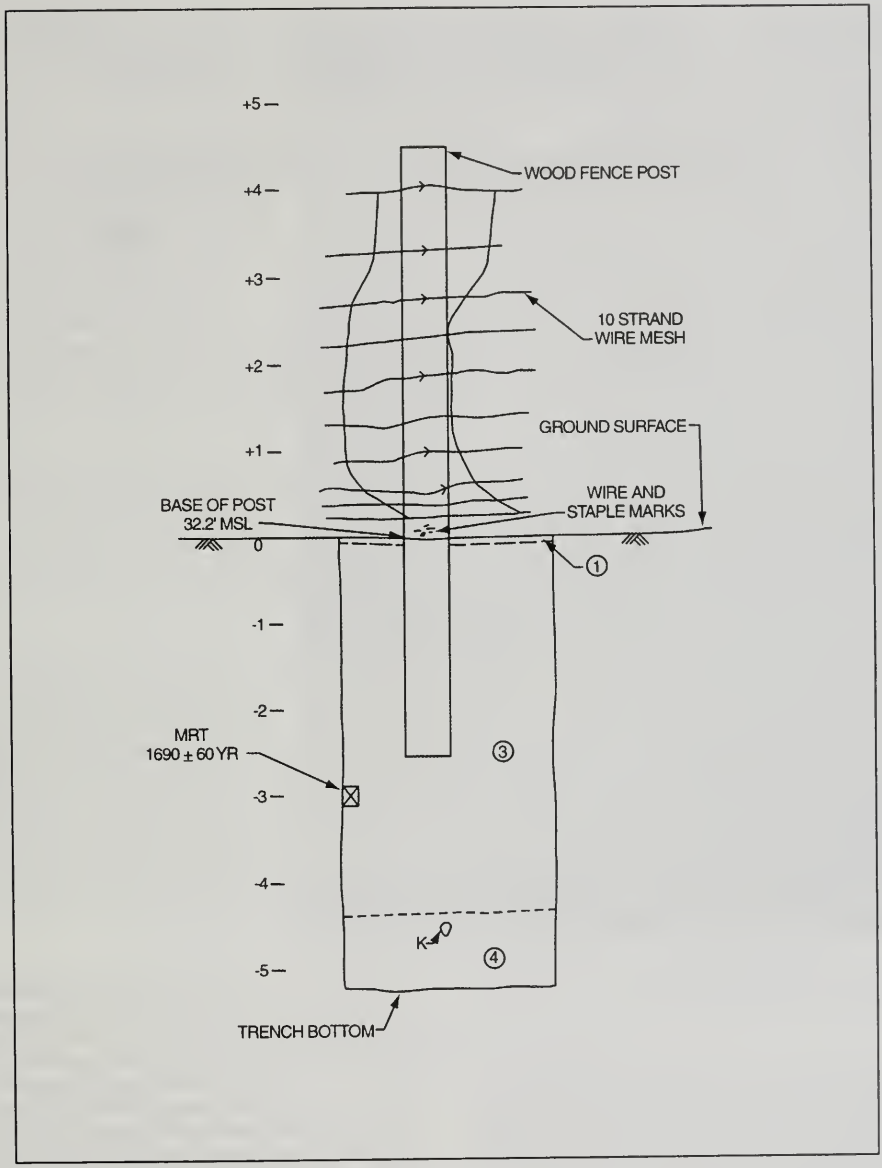

Figure 3. A typical 1954 Caltrans freeway, type B fence post as observed in T-13 (Figures 1 and 7): 54-inches high, 6 x 6-inches square, and strung with 10-strand wire mesh. Apparent mean-resident-time (MRT) radiocarbon date shown for native sediments at 3.0-ft depth. Marker 1=1954 ground surface; 3=Clear Lake clay; 4=sandy silt; K=krotovinas (filled rodent burrow). Elevations in feet.

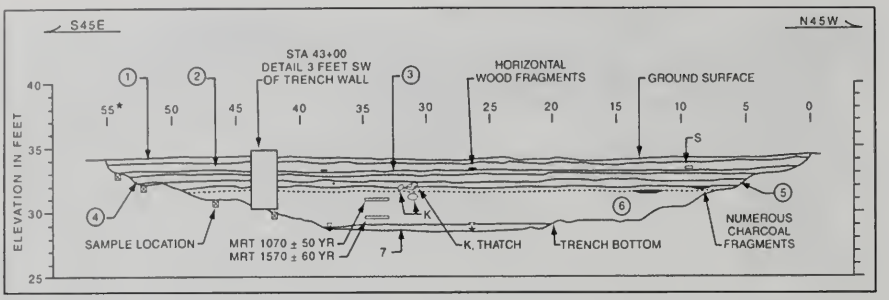

Figure 4. Log of Trench T-4 showing fence post (station 43+00, figs. 5 and 6) buried by post-1954 interbedded fine- to coarse-sand (units 1 through 5), and location of samples collected for analysis of engineering properties and for radiocarbon (MRT) dating. Dotted line shows the base of anthropic sediments; units 6 and 7 are brown to dark grayish brown clay loam and silty clay, respectively, parent material for the Clear Lake soil series (Miller, 1972). K=krotovina.

THE TRENCHES

A total of 14 trenches were excavated on both sides of the freeway by a backhoe with a 30-inch bucket. Most trenches were 5 to 6-ft deep. Particularly relevant were trenches T-4 and T-13, which exposed the bases of "short" and "normal" fence posts located adjacent to the accident scene on opposite sides of the freeway (Figure 1).

Trench T-4

Trench T-4, approximately 55-ft long and 6-ft deep, exposed the "short fence" post nearest the accident. As documented on the log (Figure 4), the pre-historic ground surface was identified 2.6 ft below the modern surface (1992) at the base of unit 5. The pre-historic sediments were readily distinguished as the dark-gray, highly expandable "Clear Lake Clay," a soil series typical of poorly drained basins in the Petaluma area (Miller, 1972). The five overlying stratigraphic units all proved to be anthropic in origin, caused by historic sedimentation emanating mainly from Orchard Creek.

At T-4 we found historic, but pre-1954, sediments at a depth of 2.3 ft. These sediments bore only a relatively undeveloped soil profile (A/E/Cb horizons). In contrast to the underlying Clear Lake Clay, they were typically brown to dark grayish brown in color (Munsell 10YR 4/3-4/2) and silty clay to fine sand in grain size. Thus, about 1.3 ft of anthropically accelerated sedimentation occurred in the area prior to construction of the freeway and culverts, and to the diversion of Orchard Creek (Figure 4).

Our investigations also showed that, since 1954, another 1.3 ft of sediments accumulated in the short-fence area. This approximately 40-yr sedimentation process resulted in burial of the lower part of the fence post and its 5 lowermost strands (Figure 5). The "short fence" proved to be about 2.8 ft high, substantially less than its specified 4.5-ft height (Figure 6).

We compared natural and accelerated sedimentation rates at T-4 by obtaining radiocarbon dates for two samples taken from the Clear Lake Clay. These samples, vertically separated by 1.5 ft (Figure 4), produced apparent mean-residence-time (MRT) dates of approximately 1070 and 1570 yr. BP, respectively (Beta-45241 and -45242). Thus, about 500 years of natural sedimentation produced the same thickness of deposits laid down in the approximately 40-yr period since construction of the freeway!

Trench T-13

Adjacent to the southbound lanes, the freeway fence appeared to be intact. No signs of "shortening" or inadequate maintenance were obvious. We therefore tested the hypothesis that man-accelerated sedimentation took place only next to the northbound lanes, ostensibly caused by land-use change, channel redirection, or partial blockage of Orchard Creek, which now passed through a culvert under Highway 101. Accordingly, we excavated Trench T-13 on the southwest or "downstream" side of the freeway and thereby specifically exposed a 1954 fence post (Figures 1 and 3). Trench exposures and soil-stratigraphic measurements showed that neg-

ligible sedimentation had occurred since 1954, that the post was still 4.5-ft high, and that the 10-strand wire mesh was intact (Figures 3 and 7; Table 1).

We also collected a bulk soil sample from the Clear Lake Clay, in this case from the A_3 horizon at a depth of 3 feet (Table 1). This sample yielded a radiocarbon MRT date of about 1690 yrs bp (Beta-47309). Ironically, and perhaps fortuitously, this date indicated that the rate of pre-historic "natural sedimentation" was about 1.5 ft/500 years, quite comparable to that measured on the opposite side of the freeway in T-4. This comparison of sedimentation rates clearly showed that accelerated deposition had indeed "shortened" the fence along the northbound lanes of the freeway.

SUMMARY AND CONCLUSIONS

Litigation usually brings out many allegations as to the cause of a problem. In this case, based on the geological investigations, there was little doubt that accelerated sedimentation "shortened" the northbound, freeway fence. Ultimately, the fence became too short to restrain a horse in the adjacent pasture, and his resultant passage through the fence led to the fateful collision and to serious injury of a young man.

But what caused, or at least substantially contributed, to the sedimentation? We were able to document that rapid sedimentation, even before freeway construction, was occurring adjacent to the natural channel of Orchard Creek. Trenches in this area (Figure 4) exposed old bottles and other pre-1954 debris. Yet, from changes in surface morphology, it became apparent that the 1954 redirection of Orchard Creek into an unlined channel parallel to the freeway, and into the area of high sedimentation, was certainly a major contributor. Caltrans records indicated that the culvert through which the redirected Orchard Creek passed was, at times, at least partially filled with sediment (Figure 8). Allegations were then made that culvert maintenance was insufficient. Apparently, when the culvert was either partially or wholly blocked, the freeway acted as a drainage barrier, resulting in "upstream" sedimentation that slowly buried the bordering fence.

Figure 5. Exposure showing accretion of 1.3 ft of sediments on "upstream" side of Highway 101 at T-4 (Figures 1 and 4), and the now-buried five lower wires of the 10-strand mesh. The 1954 ground surface is shown by the light-colored line in the lower part of the photograph.

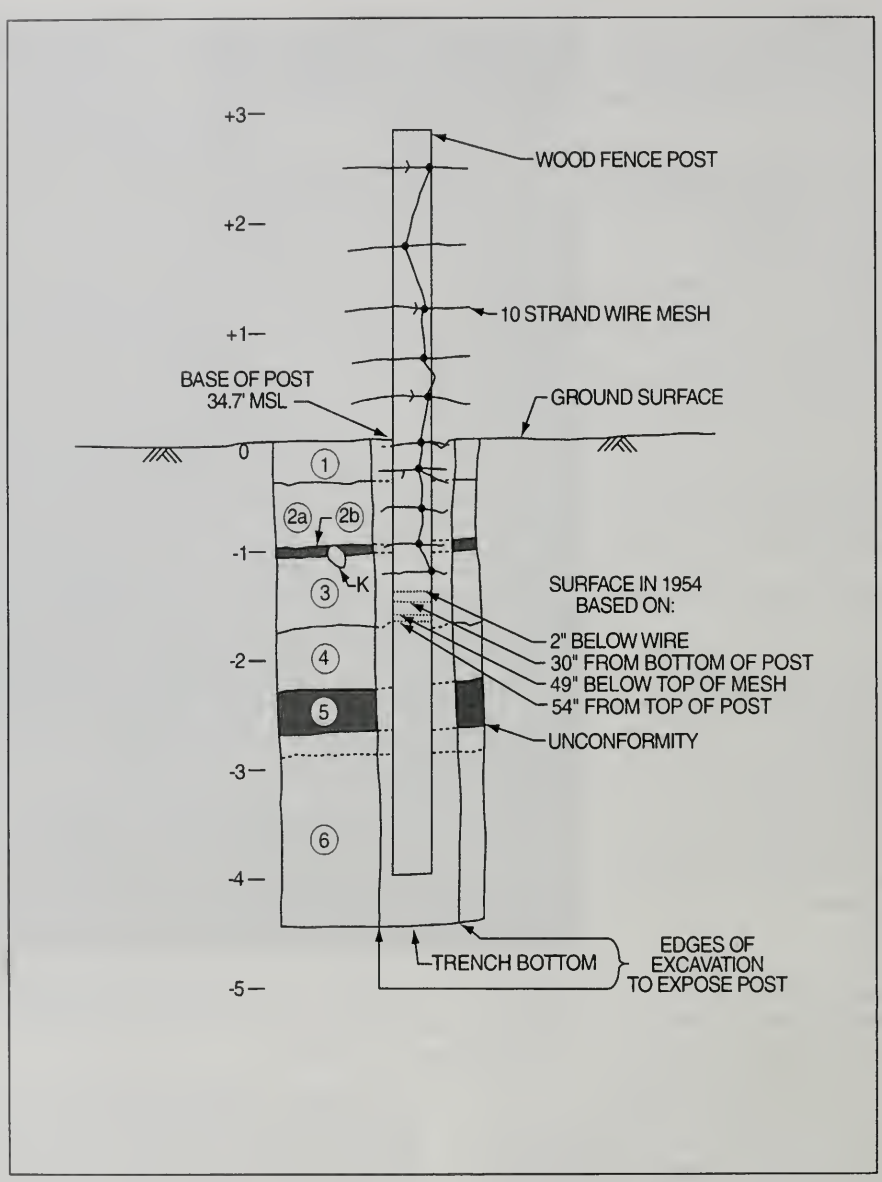

Figure 6. Log of exhumed freeway fence post showing the modern (1992) surface and burial of five, wire-mesh strands. Units 1 through 5 are post-1954 sediments; unit 6 is the "native" Clear Lake clay with dotted line depicting original near-surface organic (A) horizon. Elevations in feet.

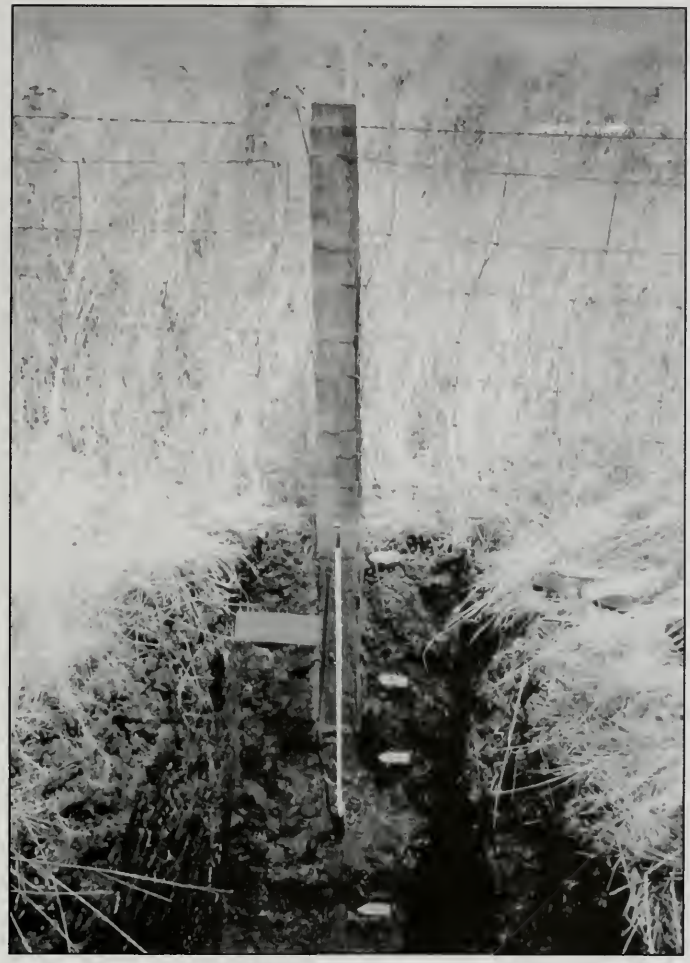

Figure 7. Essentially intact fence post and 10-strand wire mesh on "downstream" side of Highway 101 (Trench 13, Figures 1 and 3). The 1954 ground surface coincides with the modern grass line; arrows indicate base of the four, uppermost organic horizons (cumulic mollic epipedon; Table 1).

As expert witnesses, retained on behalf of the plaintiff, we presented our data and interpretations during depositions. All these, and many other non-technical issues, were discussed and debated in the lengthy and costly manner typical of American jurisprudence. The fundamental conclusions of our geologic investigations were ultimately accepted. Accordingly, the case was settled without going to a likely lengthy and expensive trial, and the plaintiffs received undisclosed financial redress from Caltrans and other defendants. In retrospect, this rather unusual use of sedimentation rates in forensic geology—in reality, the application of the scientific method and common sense—played a major role in

Figure 8. The upstream (northeast) side of the 1954 Freeway culvert almost completely plugged with Orchard Creek sediments.

this automobile-accident litigation and thus helped to solve "the case of the short fence at Petaluma."

ACKNOWLEDGMENTS

We gratefully acknowledge critiques of a draft manuscript by Chief Editor H. Ferriz, by Professor S. B. Stryker, and by peer reviewers F. Kresse and E. Winterhalder.

AUTHOR PROFILES

Roy J. Shlemon is a Consulting Geologist based in Newport Beach, California. His specialties are Quaternary geology, geomorphology and soil stratigraphy, particularly as applied to engineering-geology practice.

Gary E. Van Houten is the President of Van Houten Consultants, Inc. based in Petaluma, Cali-

fornia. The firm provides consulting services in forensic geology, engineering geology, and geotechnical engineering, particularly in the San Francisco Bay area.

SELECTED REFERENCES

Birkeland, P. W., 1999, Soils and geomorphology: third edition, Oxford University Press, New York, 430 p.

Brown, W. M. and Jackson, L. E., Jr., 1974, Sediment source and deposition sites, and erosional and depositional provinces, Marin and Sonoma counties, California: U.S. Geological Survey Miscellaneous Field Studies Map, MF-625, pamphlet and maps, various scales.

Cardwell, G. T., 1958, Geology and ground water in the Santa Rosa and Petaluma Valley areas, Sonoma County, California: U. S. Geological Survey Water Supply Paper 1427, 273 p., plates.

Dunn, J. R., 1991, Forensic geoscience for engineering works; litigation, hearings and testimony: in Kiersch, G. A. (ed.), The heritage of engineering geology, the first hundred years: Geological Society of America Centennial Special Volume 3, chapter 25, p. 575-588.

Huffman, M. E. and Armstrong, C. F., 1980, Geology for planning in Sonoma County: California Division of Mines and Geology Special Report 120, pamphlet and maps, various scales.

Kiersch, G. A. and Cleaves, A. B. (eds.), 1969, Legal aspects of geology in engineering practice: Geological Society of America, Engineering Geology Case Histories, v. 7, 93 p.

Leighton, F. B., 1992, Mitigation of geotechnical litigation in California: Munson Book Associates, Huntington Beach, CA, 274 p.

Miller, V. C., 1972, Soil survey, Sonoma County, California: U.S. Department of Agriculture, Forest Service and Soil Conservation Service, U.S. Government Printing Office, Washington, DC, 187 p., appendices, plates.

Patton, J. H., Jr., 1992, The nuts and bolts of litigation: in Pipkin, B. W. and Proctor, R. J. (eds.), Engineering geology practice in southern California, Star Publishing Company, (Belmont, California), p. 339-359.

Shlemon, R. J., 1985, Application of soil-stratigraphic techniques to engineering geology: Bulletin, Association of Engineering Geologists, v. XXII, no. 2, p. 129-142.

Shuirman, G. and Slosson, J. E., 1992, Forensic engineering: Academic Press, San Diego, 296 p.

Sonoma County Water Agency, 1986, Petaluma River watershed master drainage plan, Petaluma Basin Flood Control Zone 2a: City of Petaluma, plates.

Wagner, D. L. and Bortugno, E. J., 1982, Geologic map of the Santa Rosa Quadrangle: California Division of Mines and Geology Regional Geologic Map Series, Map No. 2A, scale: 1:24,000.


ASSOCIATION OF ENGINEERING
AEG
GEOLOGISTS

MITIGATION OF THE 1998 EL NIÑO SEA CLIFF FAILURE, PACIFICA, CALIFORNIA

TED SAYRE[1], PATRICK O. SHIRES[1], AND DAVID W. SKELLY[1]

ABSTRACT

Erosion of sea cliffs along the central California coastline has become a major concern for public and private improvements constructed in harm's way. Stability of the local sea cliff is adversely affected by young, poorly consolidated sediments comprising the bluff, vulnerability to wave attack under combined high-wave and high-tide conditions, and elevated groundwater levels resulting in seepage at the cliff face. Coastal geologic mapping and geomorphic analysis completed by the U.S. Geological Survey, after extensive local shoreline damage from the 1982-83 El Niño event, correctly identified critical erosion-prone and unstable bluff areas. However, mitigation of identified hazards is often initiated only shortly after catastrophic failures occur, when public interest is sufficiently aroused to initiate Federal/State relief efforts.

Along Esplanade Avenue, within the City of Pacifica, seven homes were lost or damaged beyond repair during the 1998 El Niño event because of rapid sea cliff retreat. At the same time, the public road, which provides access to 21 local residential properties, was recognized by city, state, and federal governments as being vulnerable to active coastal erosion processes. The recognition of local hazards (aided by daily television footage of homes perched at the edge of a retreating cliff) resulted in funding for the design and construction of a rock revetment (seawall) intended to guard against damage to, or loss of, the public roadway. This paper presents a summary of geologic, geotechnical, oceanographic, and practical factors taken into consideration during the design of the subject rock revetment.

INTRODUCTION

In February 1998, several residences on the seaward side of Esplanade Avenue were in immediate danger of collapse due to failure of the steep sea cliff (Figure 1). Parts of some of the houses had already fallen over the bluff, others were overhanging the bluff, and a few were intact near the edge of the bluff. House-site stability at the top of the bluff is adversely affected by the weak nature of the oversteepened alluvial sediments comprising the lower to middle bluff, the steepness of the bluff, groundwater seeping from the bluff face, and a 10-foot thick layer of uncemented dune sand at the top of the bluff, upon which the houses were built. In addition, rapid bluff retreat represented a threat to Esplanade Avenue; consequently it was essential to implement appropriate coastal protection measures if loss of this public road and associated utilities was to be prevented.

The northern Pacifica coastline has been undergoing progressive sea cliff retreat with a long-term average erosion rate of approximately 2 feet per year (Lajoie and Mathieson, 1998). It is not unusual for several years to pass with little noticeable erosion, only to be followed by several feet of bluff retreat within a single day. The segment of bluff

[1]Cotton, Shires & Associates
330 Village Lane
Los Gatos, CA 95030
losgatos@cottonshires.com

Figure 1. Residences along Esplanade Avenue, Pacifica, in danger of collapse in February, 1998.

along Esplanade Avenue was placed in the most unstable category by the USGS in their Coastal Stability and Critical Erosion maps as early as 1985 (Griggs and Savory,1985; Lajoie and Mathieson, 1998). When this area was subdivided in 1949, the length of bluff-top back yards (west of the house sites) was approximately 50 feet. Figure 2 illustrates local retreat of the sea cliff between 1956 and 1998 based on aerial photographs.

Increased rates of bluff erosion in early 1998 resulted from severe winter waves, high tides, and El Niño ocean water thermal expansion effects, coupled with a diminishing natural supply of sand to the shoreline. Some bluff segments retreated over 30 feet during two weeks in February 1998. Erosion at the base of the bluffs and landsliding of the undermined upper parts of the bluffs were the primary processes of sea cliff retreat. In addition, increased water seepage from the bluff face softened and loosened bluff sediments, contributing to instability and retreat.

Past efforts to stabilize the bluff were largely unsuccessful. In response to rapid local bluff retreat that occurred during the 1982 El Niño event, a homeowners group, in cooperation with the City of Pacifica, funded construction of a rock revetment. The lack of adequate maintenance, coupled with adverse design aspects (rock size was relatively small and apparently not keyed into bedrock materials), resulted in a short life-span for this structure. Although relatively intact sections of this revetment were still visible in 1996, by March 1998 the earlier revetment had been reduced to an irregular scattering of boulders across the narrow sandy beach (Figure 3).

SITE GEOLOGY

The site is located along the California coastline (Figure 4), approximately 1.3 miles south of Mussel Rock where the San Andreas fault enters the Pacific Ocean. Steep bluffs fronted by narrow, sandy beaches characterize this section of the coastline. Bluff height increases from approximately 70 feet along Esplanade Avenue to greater than 300 feet north of Mussel Rock. A terrace surface to the northeast of the bluff is clearly warped as a result of geologically active uplift along the tectonic plate boundary.

Conspicuous within the City of Pacifica are several broad, relatively flat-floored valleys that open to the ocean, suggesting periods of channel incision into bedrock followed by fluvial deposition. During the last major ice age, sea level was more than 100 feet lower than it is at present. Upon final melting of the large continental glaciers (initiated approximately 15,000 years ago), sea level rose, changing the base levels of coastal drainage channels. Consequent reductions in stream gradients resulted in lower flow-velocities and burial of eroded channels with alluvial deposits. Near Esplanade Avenue, subsequent tectonic uplift and coastal erosion notched sea cliffs into these alluvial deposits. This recent geologic history has resulted in the deposition and exposure of the relatively young, poorly consolidated sediments that form the local bluffs. Periods of rapid bluff retreat can be seen as one consequence of this dynamic geologic setting.

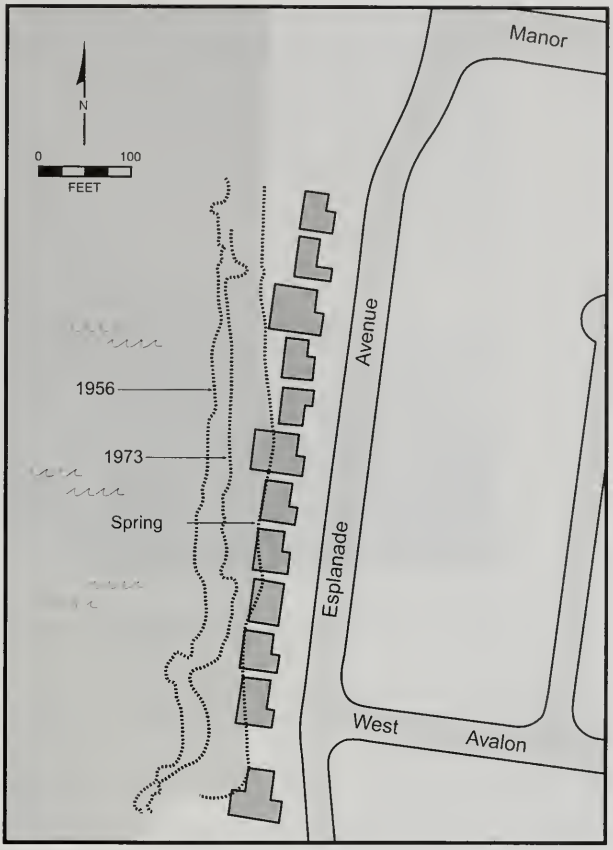

Figure 2. Top of bluff retreat from 1956 to Spring 1998 (modified from Lajoie and Mathieson, 1998).

In the area under study, "greenstone" bedrock of the Franciscan Complex lies below the base of the bluff. This rock is a relatively firm to hard, altered, submarine basaltic assemblage composed of pillow lavas, flows, and breccias. It is overlain partially by beach sand in the tidal zone, and by an approximately 50-foot thick section of poorly lithified Quaternary alluvial fan deposits (coarse basal breccia, intervals of poorly indurated silts, and fine- to medium-grained sands and gravels) exposed in the lower portion of the bluff. The alluvial deposits are overlain by a clayey, dark brown soil horizon, approximately 5 feet thick. Capping the soil horizon, and extending to the current ground surface, is a 10-foot thick layer of dune sand. Figure 5 illustrates the stratigraphy of the sea cliff and position of the rock revetment.

The uncemented dune sand is very weak when unconfined, especially when it loses moisture-related interstitial tensile forces (Figure 6). House loads provide some confinement pressure that helps contain this sand when it is moist. When it becomes dry, it seeks its natural angle of repose at approximately 30 degrees (or approximately 1.7 horizontal to 1 vertical). In addition to the weak dune sand,

Figure 3. Remnants of previous rock revetment scattered across the beach after the 1998 El Niño event.

the underlying soil and alluvial deposits, although stronger than the dune sand, are prone to sloughing and larger-scale slumping.

REVETMENT DESIGN

The following section summarizes the methodology utilized for the design of a quarry stone revetment (seawall) intended to reduce the potential for future rapid sea cliff erosion and provide protection for Esplanade Avenue.

Oceanographic design considerations

The recommended coastal structure design criteria reflect consideration of nearshore bathymetry, water level, wave height, maximum scour elevation, beach slope, and bedrock material properties. The design methods used in our analysis are described in Chapter 7 of the *Shore Protection Manual* (U.S. Army Corps of Engineers, 1984). With this method, design criteria are developed for a set of recurrence interval oceanographic conditions. Both 50-year and 100-year recurrence interval oceanographic conditions were evaluated in our analysis.

The offshore bathymetry is characterized by ridges and valleys aligned perpendicular to the shoreline. An approximate nearshore slope of 0.2% was assumed. The beach slope varies across the proposed revetment site from as steep as 30% to less than 18%.

The "*design water level*" is the maximum possible still-water elevation. During storm conditions, the sea surface rises along the shoreline (super-elevation) and allows waves to break just before, or at, the revetment structure. In this study, super-elevation of the sea surface was accounted for by wave set-up (1.0 to 2.5 feet), wind set-up and inverse barometer (0.5 to 1.5 feet), wave group effects (1.0 to 2.5 feet), and El Niño thermal water expansion effects (0.5 to 1.0 feet). The 50-year recurrence interval maximum high tide elevation is +5.4 feet amsl (above mean sea level), which, when combined with the effects of super-elevation, yields a 50-year recurrence interval water level of +7.0 feet amsl. The 100-year recurrence interval maximum tide elevation is +5.9 feet, which could result in a maximum water level of +7.5 feet amsl.

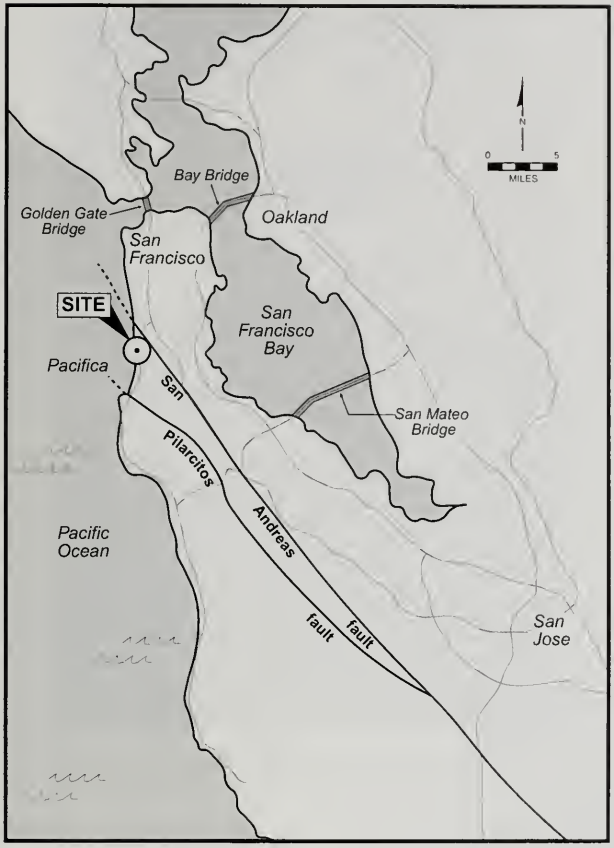

Figure 4. Location of the Esplanade Avenue site within the City of Pacifica.

The "*maximum scour depth*" is determined by the rate at which the bedrock that the revetment structure is founded upon wears down. The lower formational material at this site is greenstone bedrock of the Franciscan Complex, a firm but erodible material. The down-wearing rate was estimated to be approximately 1 inch per year for the purposes of project design (the actual rate of abrasion would be expected to diminish at depths significantly below mean sea level). The elevation of the existing grade at the toe of the lowest segment of the revetment is approximately 3 feet below mean sea level. Accounting for bedrock down-wearing, and using maximum still-water levels, the design water depth (i.e., elevation difference between the revetment toe and maximum still-water level) at the revetment, for the 50-year recurrence interval conditions, is approximately 12 feet. The design water depth for the 100-year recurrence interval is approximately 15 feet. These static submergence depths are utilized in the following section for the calculation of wave run-up.

In general, high waves in combination with high water levels locally result in erosion of beaches and wave attack at the base of the coastal bluffs (Figure 7). At this site, offshore wave heights exceeding 20 feet are not uncommon during winter storms. However, the design wave condition for a shoreline structure is generally not the largest wave, because

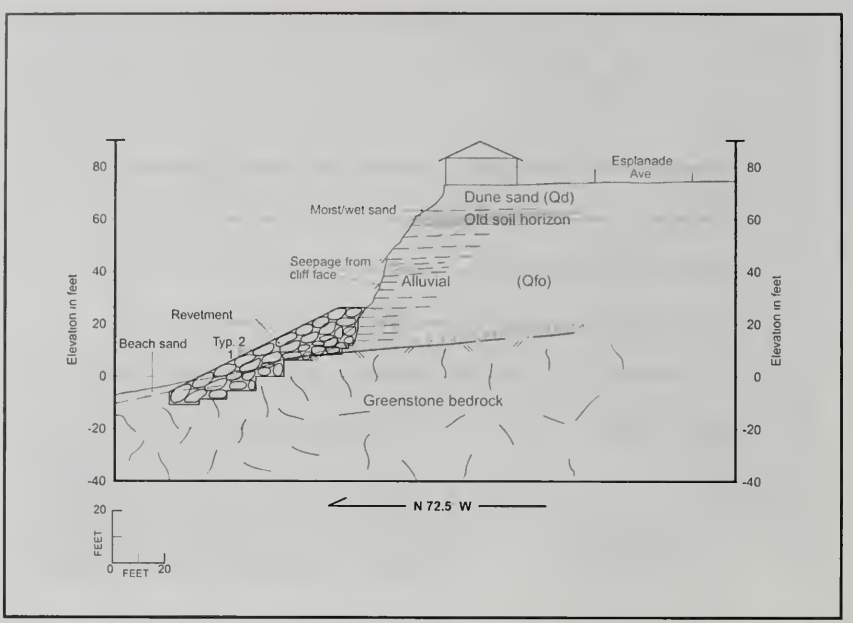

Figure 5. Stratigraphy of the sea cliff and rock revetment position near the southern terminus of Esplanade Avenue.

the largest waves break offshore in water depths approximately equal to the wave's height. The largest "*design wave force*" will occur when a wave breaks directly on the shoreline structure. The largest wave that can break on the revetment is determined by the depth of water at the toe of the structure. Using the water depths defined earlier, the resulting design wave heights are 10.0 feet for the 50-year recurrence interval and 12.0 feet for the 100-year recurrence interval. Incoming wave periods vary from 9 to 20 seconds. A design period of 20 seconds was selected because this period wave would produce the highest run-up.

Wave run-up

As waves encounter a revetment, they break and the water rushes up the face of the structure. Often, wave run-up and overtopping strongly influence the design and cost of coastal projects (Weggel, 1976). "*Wave run-up*" is defined as the vertical height above the still water level to which a wave will rise on a structure of infinite height. "*Overtopping*" is the flow rate of water over the top of a revetment as a result of wave run-up. The run-up analysis is performed to determine the design height of the revetment so that no overtopping can occur. Overtopping of the structure would exacerbate erosion of the alluvial deposits comprising the middle of the bluff.

Wave run-up and overtopping for the revetment were calculated using the U.S. Army Corps of Engineers Automated Coastal Engineering System, (ACES). ACES is an interactive, computer-based design and analysis system commonly used in the field of coastal engineering. The methods to calculate run-up and overtopping implemented within this ACES application are discussed in greater detail in Chapter 7 of the *Shore Protection Manual* (SPM) (U.S. Army Corps of Engineers, 1984). The run-up estimates calculated herein are corrected for the effect of onshore winds (i.e., wind direction from sea to land).

The empirical expression for the monochromatic-wave overtopping rate is:

$$Q = C_w (g\, Q_0^* H_0^3)^{1/2} [(R+F)/(R-F)]^{-0.1085/\infty}$$ where:

Figure 6. Loose dune sand exposed in the upper cliff face, immediately beneath the residence.

Q = overtopping rate per unit length of structure ($ft^3/sec\ ft$)

C_w = wind correction factor

g = gravitational acceleration (32.2 ft/sec^2)

Q_0*, $\propto$ = empirical coefficients (see SPM figure 7-27)

H_0 = unrefracted deepwater wave height (ft)

R = run-up (ft)

$F = h_s - d_s$ = freeboard (ft)

h_s = height of structure (ft)

d_s = water depth at structure (ft)

The correction for onshore winds is:

$C_w = 1 + W_f (F/R + 0.1) \sin(\theta)$ where:

$W_f = U^2/1800$

U = onshore wind speed (mph)

$F = h_s - d_s$ = freeboard (ft)

R = run-up (ft)

θ = angle of the ocean-facing revetment slope, measured from the horizontal in degrees.

The severity of storm impacts to the local coast is partially dependent on the direction of wave approach and the local shoreline orientation (Fulton-Bennet and Griggs, 1987). The ACES analysis was performed on two sets of local oceanographic

conditions that represent typical 50- and 100-year storms. The onshore wind speed was chosen to be 60 knots (52 mph) for each case.

The output from the ACES analysis indicates that the maximum wave run-up for the 50-year recurrence interval oceanographic conditions is approximately +17 feet amsl, and for the 100-year recurrence conditions, approximately +19 feet amsl. Based upon this analysis, the height of the revetment for a "no overtopping" condition should be a minimum of +20 feet amsl. A top of revetment elevation of +26 feet amsl was selected to buttress a lower sand lens on the bluff face, to allow for future settling of the revetment, and to increase the factor-of-safety in project design. Site observations during storm conditions and engineering judgement also influenced the selection of final revetment height.

Revetment geometry and stone weight considerations

For initial design purposes, an armor stone unit weight of 165 pcf and a 50% slope for the face of the structure were selected. The primary factor in determining the design stone weight is the incident wave energy, which is proportional to the wave height. The output of the ACES analysis includes the stone weight and revetment crest width. The weight of the stone required to withstand the design wave conditions is given by the following formula:

$$W = W_r H^3/[(K_D(S_r-1)^3\cot(\theta)] \quad \text{where:}$$

W = Weight of the individual armor stone in the primary cover unit (lbs)

W_r = Unit weight of the armor stone (pcf)

H = Design wave height (ft)

S_r = Specific gravity of the armor stone relative to water ($S_r = W_r/W_w$)

W_w = The unit weight of water (62.4 pcf)

θ = Angle of the structure slope, measured from horizontal in degrees

K_D = Stability coefficient that depends on the shape of the armor stone

The calculated individual armor stone weight for the 50-year oceanographic conditions is approximately 5 tons. The crest width is approximately 12 feet, with approximately 80 armor stones per 1,000 square-feet for 50-year recurrence conditions. The individual armor stone weight for the 100-year wave conditions is approximately 10 tons, with a crest width of approximately 14 feet. This results in approximately 50 armor stones per 1,000 square feet. Ultimately, an armor stone weight of 8 to 10 tons was selected for project design, considering several years of performance observations by the Pacifica Public Works Department, available funding, and the restricted availability of rocks in the 10 ton range.

Figure 7. Offshore wave height may exceed 20 feet and wave surge from shore break attacks the base of coastal bluffs during high tides.

Quarry stone selection and placement

Two weight ranges of stone are generally selected for revetment construction: armor stone and core stone. The armor stone weight ranged from 8 to 10

tons, whereas the core stone weight ranged from 100 pounds to 5 tons. The smaller weight fraction of the core stones was placed deepest within the revetment. All the stone material was examined to verify that the rock was free of undesirable qualities that might contribute to crumbling or breaking during handling. The armor stone consisted of select quarry rock, free of open fissures and apparent planes of weakness. Ideally, armor stone should be rough and angular in shape, with the shortest principal dimension not less than one-third the longest dimension to improve interlocking qualities.

The qualitative evaluation of rock durability relates to the geological origin of the rock, and specific tests evaluate rock properties important to longevity as a revetment component. Rock evaluation should include consideration of the following:

1. Petrographic make-up of the rock.

2. Performance of the candidate rock type in other marine structures.

3. Test results that address the Standard Practice for Evaluation of Rock to be Used for Erosion Control (ASTM D 4992-94). Testing may include:

   a. C 88—Test methods for soundness of aggregates by use of sodium sulfate or magnesium sulfate

   b. C 127—Test method for specific gravity and absorption of coarse aggregate

   c. C 294—Descriptive nomenclature of constituents of natural mineral aggregates

   d. C 295—Practice for petrographic examination of aggregates for concrete

   e. C 535—Test method for resistance to degradation of large-size coarse aggregate by abrasion and impact in the Los Angeles machine

   f. D 5313—Test method for evaluation of durability of rock for erosion control under wetting and drying conditions.

CONSTRUCTION CHALLENGES

Suitable large armor stones in the 8- to 10-ton weight range were difficult to obtain because significant demands for large rock had been placed on local quarries during El Niño conditions. Rock samples from four quarries, with haul distances of approximately 40 to 100 miles to the site, were delivered for detailed examination. Samples included limestone, graywacke sandstone, welded volcanic tuff and a metaconglomerate. Submitted samples, other than the limestone, generally had favorable density and durability properties. Due to the scarcity of large rock, favorable rock types available from three quarries were utilized for project construction.

Trucks delivering armor stones to the site would typically accommodate only two large stones per load, with possibly room for a few smaller core stones. Because the keyway for the revetment was to extend into Franciscan bedrock located below mean sea level, stone placement was possible only during periods of low tide (Figures 8 and 9). Sufficient stone for the construction of a 100-foot segment of the revetment was delivered to a staging area high on the beach, and placement of rock into the keyway (excavated the previous day) occurred during low tide.

Rock was placed in conformance with the following guidelines, with the guiding principle that good craftmanship during stone placement is essential to structural integrity: 1) rock-to-rock contact was maximized (at least three points of contact per stone) and the voids were minimized; 2) stones that were flat in one dimension were preferred and round stones were avoided; 3) stones that had one particularly long dimension were placed with the longer dimension perpendicular to the shoreline to prevent rolling down slope; and 4) "chink" armor stones (smaller than 3 feet in their longest dimension) were not used to support the larger armor stones.

MAINTENANCE

Any large engineered structure placed along the base of a sea cliff will interact with dynamic shoreline erosional processes. Consequently, such structures require periodic inspection and maintenance. Inspections should be performed by an engineer with experience in coastal structures. In addition, coastal structures should be inspected by the property owners after any major storm for damage caused by wave attack. When damage is observed, an engineer should be consulted to determine the nature and extent of necessary maintenance. Maintenance on a quarry stone revetment would include

Figure 8. Filter fabric is being placed in the keyway and along the base of the revetment prior to stone placement.

re-shaping the revetment to the design profile through addition or repositioning of stones. Maintenance of the revetment should be undertaken in a manner that will improve the quality of the profile, as well as the contact and orientation of the individual stones. The rehabilitation of a revetment should be supervised by a coastal engineer. The City of Pacifica has reportedly taken steps toward establishing a maintenance assessment district to ensure that funding is available for periodic upkeep of the revetment.

SUMMARY/COMMENTARY

Key aspects of revetment design included selection of adequate armor stones, keying of imported stone below beach and alluvial deposits well into firm bedrock, and selection of an appropriate revetment face-slope and height. Design parameters were based on oceanographic analysis—including consideration of maximum possible still-water levels, wave run-up, the design wave force, and anticipated scour depth. Final quarry stone selection included consideration of constituent mineralogy, rock density, and anticipated durability in a dynamic marine environment.

Even though the design intent of the revetment is to help protect the nearby public roadway from coastal erosion, there may be pressures to redevelop what remains of the top lots on the bluff. Landsliding along the precipitous bluffs is a significant potential hazard to adjacent residential development. One limitation for the placement of a revetment at the base of the bluff is that it will not significantly improve stability of the slope above the revetment crest (i.e., above an elevation of 26 feet amsl). Although dewatering measures may improve slope stability by reducing adverse groundwater seepage from the face of the bluff, the viability of the bluff lots for redevelopment will depend on the outcome of detailed geotechnical studies. In addition, revetments have design-life limitations and maintenance requirements that must be considered during redevelopment evaluations.

Figure 9. Keyway excavation below mean sea level required strategic construction timing with respect to tidal conditions.

Engineering efforts to arrest coastal erosion processes should be viewed as temporary solutions that are often not free of collateral impacts (Griggs et al., 1992). In the case of engineered revetments or seawalls, these structures are typically constructed at locations that already have inadequate protective beach or dune buffer zones. The sand-deficient beaches may become narrower and steeper with time after the protective structure is installed. These changes may result from increased rebound energy of waves reflected off relatively hard, fixed engineered structures, and the reduction of cliff detritus descending to the beach. Consequent alteration to the beach and near-shore profiles can ultimately undermine foundation support of the protective structure. It is also possible that erosion of adjacent vulnerable coastal bluffs may result in gradual outflanking of the protective structure. With the best revetment or seawall designs, protective success over the time period of a human life span can occasionally be achieved. From a long-term geologic perspective, however, protective revetments placed within wave impact zones will eventually face inevitable consequences. Utilization of protective design alternatives in dynamic coastal zones should follow full consideration of a cost-and-benefit analysis, impacts to beaches and adjacent properties, and alternative hazard avoidance/relocation options.

ACKNOWLEDGMENTS

The authors thank Gary Griggs of U. C. Santa Cruz and Kenneth Lajoie of the U. S. Geological Survey for their tireless efforts to characterize California coastal hazards and to educate the public about consequent risks of living in this dynamic environment. We also express gratitude to our peer

reviewers and Chief Editor, who greatly enhanced the quality of the final manuscript.

AUTHOR PROFILES

Mr. Ted Sayre is a Certified Engineering Geologist with 19 years of local experience. Mr. Patrick O. Shires is the Principal Geotechnical Engineer of Cotton, Shires & Associates, with 28 years of experience addressing complex geotechnical problems in the western United States. Mr. David W. Skelly is a Professional Engineer with expertise in coastal engineering who works with Cotton, Shires and Associates on special projects. Cotton, Shires & Associates, Inc. is a geotechnical consulting firm established in 1974 with offices in Los Gatos and Carlsbad, California. The firm offers geotechnical expertise to engineers, designers and local governments with regard to development, hazard analysis and mitigation, commercial and municipal construction, and failure analysis. The authors also provide expert witness testimony for litigation and arbitration related to geotechnical engineering and engineering geology.

SELECTED REFERENCES

Aherns, J. P., 1997, Prediction of irregular wave overtopping: U.S. Army Corps of Engineers Waterways Experiment Station, Vicksburg, MS

Aherns, J. P. and Mc Cartney, B. L., 1975, Wave period effects on the stability of rip rap: Proceedings of Civil Engineering in the Oceans/III, American Society of Civil Engineers, p. 1019-1034

Douglass, S. L. and Smith, O. P., 1986, Cost-effective optimization of rubble-mound breakwater cross sections: U.S. Army Corps of Engineers Waterways Experiment Station, Vicksburg, MS, p. 45-53

Ewing, L. and Sherman, D. (Editors), 1998, California's coastal natural hazards: Sea Grant Program, University of Southern California, 162 p.

Fulton-Bennet, K. and Griggs, G. B., 1987, Coastal protection structures and their effectiveness: California Department of Boating and Waterways, 48 p.

Griggs, G. B., Pepper, J. E. and Jordan, M. E., 1992, California's coastal hazards: A critical assessment of existing land-use policies and practices: California Policy Seminar, University of California, 224 p.

Griggs, G. B. and Savoy, L. E. (Editors), 1985, Living with the California coast: Duke Univ. Press, Durham, N.C., 393 p.

Lajoie, K. R. and Mathieson, S. A., 1998, 1982-83 El Niño coastal erosion, San Mateo County, California: U. S. Geological Survey Open-File Report. 98-41, 61 p.

Lajoie, K. R. and Mathieson, S. A., 1985, San Francisco to Ano Nuevo coastal segment *in* Griggs, G. B., and Savoy, L. E. (eds.), Living with the California coast: Duke Univ. Press, Durham, N.C., p. 140-177

Markel, D. G. and Davidson, D. D., 1979, Placed stone stability tests, Tillamook, Oregon; hydraulic model investigation: U.S. Army Corps of Engineers Waterways Experiment Station, Vicksburg, MS

National Research Council, 1990, Managing coastal erosion: National Academy Press, Washington, D.C., 182 p.

National Research Council, 1987, Responding to changes in sea level - Engineering implications: National Academy Press, Washington, D.C., 148 p.

Norris, R., 1990, Seacliff erosion: A major dilemma: California Geology, v. 43, no. 8, p. 171-177

U.S. Army Corps of Engineers,1996, Shoreline protection and beach erosion control study: Corps of Engineers, Institute for Water Resources, Alexandria, VA, 226 p.

U.S. Army Corps of Engineers, 1984, Shore protection manual: U.S. Army Corps of Engineers, Coastal Engineering Research Center, Waterways Experiment Station, Vicksburg, MS, 2 Volumes

Weggel, J. R., 1972, Maximum breaker height: Journal of Waterways, Harbors and Coastal Engineering Division, American Society of Civil Engineers, v. 98, no. WW4, p. 529-548

Weggel, J. R., 1976, Wave overtopping equation: Proceedings of the 15th Coastal Engineering Conference, American Society of Civil Engineers, Honolulu, HI, p. 2,737-2,755

EVALUATION OF NATURALLY OCCURRING ASBESTOS IN THE CENTRAL SIERRA NEVADA FOOTHILLS OF CALIFORNIA

DAVID C. SEDERQUIST[1] AND ROY C. KROLL[1]

ABSTRACT

Health officials of the State of California and the U.S. Environmental Protection Agency have identified potential health hazards from naturally occurring asbestos in most counties of the Sierra Nevada and Klamath Mountains. Asbestos minerals are a class A carcinogen. The asbestiform minerals identified include chrysotile and amphibole asbestos such as tremolite. Potential sources of exposure to asbestos include dust from earthwork and from some gravel surfaced roads. New ordinances have been developed to reduce exposure to dust containing asbestos. Besides strengthening previously existing fugitive dust rules, stricter controls on activities that may generate asbestos dust have been implemented.

The foothills asbestos occurrences are associated with ultramafic zones and fault/shear zones, many of which contain serpentinites of complex mineralogy and genesis. Metamorphic carbonates and some hydrothermal deposits may also contain asbestiform minerals. Field geologists need to be able to recognize potential asbestos occurrences so that disturbance activities, such as earthwork construction, can be appropriately managed to reduce the potential for adverse health effects from dust exposure. The mapping of potential asbestos deposits requires a thorough understanding of the regional geology. Mapping should include the use of road cuts or excavations to expose rock otherwise covered by soil. Appropriate sampling methods and laboratory analysis techniques need to be selected to address the specific data needs for an assessment. The findings should be communicated in a clear manner useful to those who will make decisions based on the assessment. Continuing monitoring for occurrences of asbestos may be recommended, even if an initial assessment fails to identify asbestos.

INTRODUCTION

In the spring of 1998, *The Sacramento Bee* published a front-page article that fingered naturally occurring asbestos as a health risk (Bowman, 1998). The article focused on western El Dorado County, an area east of Sacramento experiencing significant growth and development. It also included a map showing the locations of ultramafic rocks and serpentinites associated with asbestos, and identified tremolite as the asbestiform mineral in one of the localities (Tennant, 1998). The article made a strong impact and a mild public hysteria enveloped the residents of western El Dorado County.

The public concern resulted in the implementation of new regulations in El Dorado County regarding health and safety issues triggered by construction in areas that contain naturally occurring asbestos. The purpose of this paper is to describe a methodology in the identification of asbestos-bearing rock, in preparation for and during earthwork.

[1]Youngdahl Consulting Group, Inc.
1234 Glenhaven Court
El Dorado Hills, CA 95762
mail@youngdahl.net

HEALTH RISKS OF ASBESTOS EXPOSURE

The U.S. EPA regulates six asbestiform minerals: chrysotile, anthophyllite, amosite, crocidolite, tremolite, and actinolite (CFR, 1998). Except for chrysotile, all of the others are amphiboles, and all have non-asbestiform analogues. In the foothills of the Sierra Nevada, the concern has been mainly focused on chrysotile and the asbestos of the tremolite-actinolite series.

The health effects of exposure to asbestos are generally asbestosis, lung cancer, and mesothelioma, a cancer of the pleural lining (ATSDR, 1990). The U.S. EPA has classified asbestos as a group A human carcinogen (U.S. EPA, 1993b), and estimates an inhalation unit risk of 2.3×10^{-1} per fiber per ml of air. This translates to a risk of one case of asbestos-triggered cancer in 10,000 people for lifetime exposures (70 years for 24 hours per day) of 4×10^{-4} fibers per ml of air. The standard regulatory risk threshold number of one case of cancer in population of one million is estimated after a lifetime of exposure to 4×10^{-6} fibers per ml of air. There is evidence that different types of asbestos fibers vary in carcinogenic potency relative to one another; amphibole asbestos fibers may be more carcinogenic than chrysotile fibers.

Differences in fiber size distribution may also contribute to variations in risk (U.S. EPA, 1993b). The effects of sizes, shapes, and mineralogy of asbestos fibers on health risks were explored in the study reported by Berman et al. (1995).

The California Air Resources Board (CARB, 1990) concluded that risks associated with exposures to miners and millers from asbestos in dust generated from naturally occurring asbestos may be 50-fold less than that of textile workers. More recently, Nolan (1999) completed a study for miners incidentally exposed to asbestiform amosite that suggests that the cancer risk from short-term exposures (0.05 fibers per ml for 8 hours per day for 22 days) may be very minimal. Nolan (1999) estimated the lifetime risk for this short-term exposure to be less than one case of cancer per one million individuals. Because earthwork construction often generates dust in a similar manner to mining activities, the dust exposures during earthwork can be inferred to be similar to mining exposure.

Gravel roads surfaced with asbestos containing rock, such as serpentinites, can also provide dust exposure pathways for asbestos. Using data obtained when developing the California Serpentine Covered Roadway Asbestos Model (CALSCRAM) for dust emissions (CARB, 1992), CARB estimated that, for lifetime exposures 5 feet from a road containing 1% asbestos, an estimated 94 cases of mesothelioma and 54 cases of lung cancer would occur in a population of one million (lifetime exposure equals 24 hours per day for 70 years: CARB, 2000). In 1991, CARB set the maximum allowable level of asbestos in serpentinite at 5% (by number of particles) for materials used in road surfacing, not including aggregate encased in asphalt or concrete (CARB, 1991). Most recently, CARB voted to completely ban the use of serpentinites for road surfacing in California, with only a few permissible exceptions.

THE DEVELOPMENT OF A NEW COUNTY ORDINANCE

The identification of a potential health risk from exposure to asbestos quickly impacted earthwork in western El Dorado County, an area with lithologies, such as serpentinite, where asbestos minerals are relatively common. Additionally, tremolite—an asbestiform amphibole—is a common mineral in the Bear Mountains fault zone.

Similar concerns about exposure to naturally occurring asbestos associated with serpentinite had previously occurred in other counties of California. Lake County, for example, has adopted special regulations regarding serpentinite and construction (Lake County AQMD, 1992). The Lake County regulations prohibit the use of serpentinite containing more than 1% asbestos (as measured by California Air Resources Board Method 435) for road or parking area surfacing, and establish guidelines for dust minimization for disturbance by construction activities. Additionally, construction projects in serpentinite areas must file and receive approval of an asbestos dust hazard mitigation plan prior to any construction activity. The guidelines suggest the use of water to dampen soil to control dust, or limiting construction to the wet weather season. Spoils piles are to be covered, kept damp, or treated with dust palliatives.

Lake County and CARB regulations addressed dust inhalation as the primary route of exposure, and provided a framework to reduce dust generation by best management practices, such as wetting. The CARB regulations provided additional control by limiting the quantities of asbestos that could be

placed onto road surfaces, thus limiting the quantities of asbestos-bearing source material that could potentially generate dust.

Existing regulations were all considered in establishing new El Dorado County regulations to protect human health during construction projects in areas that may contain naturally occurring asbestos. One area of weakness present in all the regulations discussed above was the definition of the potential sources of asbestos fibers; all of these regulations focus on serpentinite as being the primary source of asbestos fibers and ignore other potential sources.

El Dorado County has mandated strict fugitive dust control measures for several years as required by CARB. Although not always heavily enforced, the regulations require best management practices for dust control for all dust sources, not just for projects with a potential for asbestos release. In response to asbestos exposure concerns, however, El Dorado County developed an ordinance for additional control measures on construction projects in serpentinite.

The El Dorado County Naturally Occurring Asbestos and Dust Protection ordinance applies to the use of asbestos-containing materials for unpaved road surfacing; grading, excavation, and construction activities in areas where naturally occurring asbestos may be present; and mining of mineral deposits that may contain naturally occurring asbestos. The ordinance requires that grading permit applications in areas with a potential to contain asbestos include an asbestos hazard dust mitigation plan. Specific requirements for dust mitigation include wetting (Figure 1), limitations on vehicle access and speed in construction areas, the covering of materials containing asbestos, the maintenance of a high soil moisture content in areas of disturbance, the covering or wetting of materials stockpiles, employee notification of health risks, worker safety precautions, and air monitoring as needed. The ordinance specifies penalties of up to $25,000 per day for violations.

This new ordinance was written to apply to areas underlain by serpentinite, as defined by soil maps in the Soil Survey of El Dorado County (Rogers, 1974). Unfortunately, the soils approach to mapping fails to fully account for the relationship of asbestos occurrences with the underlying geology. Administrative difficulties in implementing a map-specific ordinance has led to the requirement for the submission of an Asbestos Hazard Dust Mitigation Plan for all activities that require building or grading permits.

The ordinance expresses a spirit of concern for risks associated with asbestos exposure, but applies mostly to areas underlain by serpentinite. The county ordinance fell into the trap of equating serpentinites with asbestos. Consulting geologists performing site evaluations quickly recognized that not all serpentinite contains asbestos, and not all asbestos is associated with serpentinite. Fortunately, the ordinance is also triggered whenever asbestos is tentatively identified, regardless of whether serpentinite is present or not. A standard-of-practice is correspondingly evolving, in which geologists tailor their evaluations to address the occurrence of naturally occurring asbestos, and not just for serpentinite, in order to comply with the spirit of the ordinance and to best protect the public.

THE GEOLOGY OF NATURALLY OCCURRING ASBESTOS

The field identification of asbestos-bearing rock requires an understanding of the rock assemblages and structures where it can be found. Asbestos are primarily metamorphic minerals that occur in areas with complex geology. In the Sierra Nevada Foothills, they are most commonly found in metamorphosed ultramafic rock assemblages and fault zones.

Western El Dorado County is transected by a northwest trending belt of metamorphic rocks that underlies the western slope of the Sierra Nevada between Mariposa and Lake Almanor (Churchill et al., 2000). This belt, known as the western Sierra Nevada metamorphic belt, is divided into three major fault-bounded lithologic terranes (Harden, 2001, this volume). These terranes are composed of thick accumulations of Paleozoic and Mesozoic marine sedimentary and volcanic rocks that have been deformed, intruded by igneous rocks, and metamorphosed. The bedding, foliation, and structures generally trend north to northwest and dip steeply to the east. Ultramafic rocks that have been altered to serpentinite are common in the central portion of the western Sierra Nevada metamorphic belt, and along major faults within the belt.

Geologists currently interpret the overall stratigraphic and structural framework of the western Sierra Nevada metamorphic belt in terms of plate tectonic concepts. Most geologists generally agree

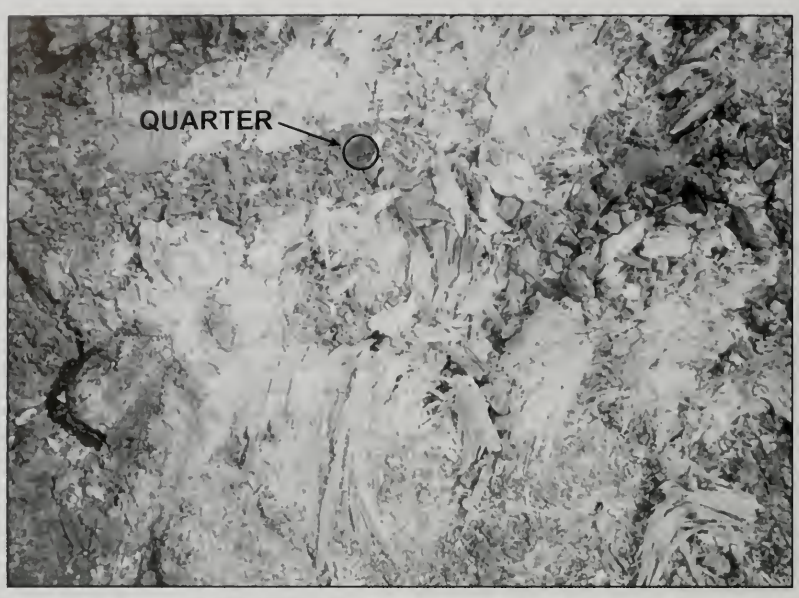

Figure 1. Cut face exposure of long curving masses of actinolite asbestos. Coin in upper center for scale.

that convergent plate tectonism governed the Early Paleozoic to Late Jurassic development of the belt, and the fault-bounded terranes collectively represent tectonically accreted blocks emplaced along the western margin of the North American continent (Churchill et al., 2000; Harden, 2001, this volume). Many of these terranes are portions of ophiolites (oceanic crust).

Massive serpentinite, which is formed by metasomatism of ultramafic rocks such as peridotites, pyroxenites, and dunite, is very ductile and is very easily squeezed tectonically away from its site of origin. Serpentinite has a lower density than most other rocks, enhancing a tendency for massive bodies to rise diapirically in the crust. Common serpentinite minerals are lizardite, chrysotile, and antigorite, but in many instances also contain talc, brucite, tremolite-actinolite, carbonates, and magnetite (Coleman, 1971). Chrysotile and picrolite (columnar antigorite) are often present in slip or cross fiber veins, as asbestiform fibers. Tremolite asbestos commonly occurs as slip fiber veins associated with fault or shear zones in serpentinite.

Talc schists can form lenses and streaks within serpentinite rocks (Williams, 1954). Talc schists form at temperatures above 500°C, whereas crystallization of serpentine minerals spans the temperature range between 100°C (lizardite and chrysotile formation) and 500°C (antigorite) (Shelly, 1993). When silica and carbon dioxide are present in aqueous fluid streaming through intergranular pores as deformation proceeds at low temperatures, the chemical composition of the rock may be profoundly altered. Any one of several alternative mineral assemblages may develop, ranging from antigorite schists to quartz-carbonate schists to actinolite-chlorite schists (Williams, 1954).

The field geologist locating areas with a potential for deposits of asbestos is probably going to be most concerned with serpentinite bodies. O'Hanley (1996) provides a detailed discussion of the occurrence of serpentinites in ophiolites, melanges, and faults, and of the conditions that lead to their formation in the course of thrust faulting, subducted slab-mantle interactions, diapiric intrusion, and hydrothermal activity. He further describes massive serpentinites,

foliated serpentinites, antigorite mylonites, antigorite schists, and lizardite-chrysotile cataclastites. Partly serpentinized peridotites exhibit zones of green to black weathering serpentinite surrounding cores of partially serpentinized peridotite, known as kernal patterns, which are found adjacent to shear zones defined by serpentine cataclastite. Another variant is completely serpentinized peridotites and dunites in association with lenses of chrysotile in bastite.

The process of active tectonism and the presence of mineralizing fluids may provide the environment for the growth of asbestiform minerals. As the rocks shear, microscopic tension fractures form and are filled with asbestiform minerals across the fracture. In some ultramafic bodies, the asbestiform minerals can be observed forming abundant, fine anastomosing veinlets. In others, massive asbestos veins can be found.

Published observations on the occurrence of tremolite asbestos suggest that it is associated with both altered limestones and serpentinites (Chidester, 1962). Coleman (1971) suggests that tremolite/actinolite asbestos may develop from calcium liberated from pyroxene minerals during ultramafic rock serpentinization combining with silica from the wall rocks. Rice (1957) describes tremolite veins occurring along serpentinite contacts with amphibolite, slate, and schist in the Sierra Nevada Foothills. O'Hanley (1996) suggests that tremolite and chrysotile asbestos occur together only where a tectonic inclusion or rodingitized gabbro is present in a shear zone adjacent to an ore zone of chrysotile asbestos.

The terranes in Western El Dorado County are bounded by faults and shear zones. Hydrothermal quartz veins are frequently associated with these shear zones. Where hydrothermal fluids come into contact with low grade magnesian marbles, talc and tremolite can form (Williams, 1954). It is not uncommon to find talc schists associated with carbonates. Where the formation of such minerals is associated with active tectonism, it is reasonable to expect the potential occurrence of asbestiform minerals. A limited amount of such amphibole asbestos minerals in association with carbonates have been identified in El Dorado County (Churchill et al., 2000).

Lode-gold deposits are characterized by ore either in quartz-rich veins or altered rock, with the vein and alteration assemblages indicative of greenschist-facies metamorphism, although a few deposits form as amphibolite-facies (Roberts, 1987). On a regional scale, the deposits cluster along major faults. Such deposits can be found throughout Western El Dorado County, but especially along the Melones fault zone in the well-known Mother Lode. O'Hanley (1996) indicates that, on a regional scale, asbestos deposits also cluster along major faults, such as the Melones fault, but convincingly argues that, geochemically, lode-gold and asbestos have very little in common. In fact, at a local scale lode-gold and asbestos manifest an antithetic relationship.

Amphibole asbestos can often be observed in fault zones in close association with serpentinites. The shear zones in some instances contain anastomosing lenses that individually can be several inches in thickness, and as a zone may be 10 to 40 feet in thickness. Talc schists in these shear zones will sometimes grade into zones of amphibole asbestos. Tectonic fractures that contain cross fiber amphibole asbestos have been observed in rocks up to 1,000 feet away from faults. These veins have been observed to grade in and out of quartz veins.

Weathered serpentinites that contain white calcite, hydromagnesite, and chalcedony are common in the Sierra Nevada Foothills. Weathered serpentinites are often light brown to light gray in color, and result in blocky outcrops with rounded corners. Often, the structures of the serpentinites weather in relief and are even highlighted by varying growths of lichens. Serpentinite zones in the Sierra Nevada Foothills are often marked by flora, such as the gray pine, which preferentially grow in magnesium-rich soils. The light gray foliage provides a marked contrast with other nearby conifers, and assists in the mapping of serpentinites.

In summary, it is reasonable to find naturally occurring asbestos in the Sierra Nevada Foothills within metamorphosed ultramafic rock complexes and within fault/shear zones. Asbestos is often associated with serpentinites within these complexes. There are numerous ways that serpentinite can form and therefore a wide diversity of potential serpentinite structures are possible. Other areas with the potential to contain asbestiform minerals may include carbonate deposits. The consulting geologist should become familiar with the lithology of the potential asbestos bearing zones in his area of investigation.

THE FIELD IDENTIFICATION OF NATURALLY OCCURRING ASBESTOS

The first task that a consulting geologist undertakes in performing an asbestos-occurrence field study is to develop a solid geologic map of the study area. This requires a thorough understanding of the regional geology as discussed above. The consultant in the Central Sierra Nevada Foothills should become thoroughly familiar with the resources offered by the California Division of Mines and Geology (CDMG). Besides the open-file mineral resource reports that include geologic maps of 15-minute quadrangles at 1:48,000 scale (e.g., Loyd et al., 1983; Loyd, 1984), the Regional Geologic Map Series includes separate maps that reference the specific field studies used by the CDMG to develop the maps (e.g., Wagner, 1981). Most recently, the CDMG has completed a pilot study open-file report and map that identifies areas of western El Dorado County that have a significant potential to contain asbestos (Churchill et al., 2000). The CDMG plans to prepare similar open-file reports for other areas of California.

After completing a review of regional maps, the consultant should conduct a detailed review of existing geologic maps for the project area and a preliminary field reconnaissance. The latter may be as simple as the collection of hand specimens from existing road cuts. Every effort should be made to identify these specimens and the geologic history of their formation.

The next step would be to plan basic large scale geologic mapping for the area of concern. The preliminary field reconnaissance should have provided some perspective on the availability of rock exposures. The consulting geologist will most likely initially evaluate the potential for asbestos from examination of outcrops protruding through the soil mantle or road cuts. Mapping should then utilize a series of test pits excavated to fresh rock in addition to natural outcrops. Asbestiform minerals are often associated with zones of alteration that are highly susceptible to weathering, so a geologic map based solely on natural exposures might miss these zones.

There are typically three questions to be asked by the geologic mapping of asbestiform mineral occurrences. Are the rocks exposed in the area potentially asbestos-bearing? If the answer is yes, are there asbestiform minerals present? If so, how pervasive are they? To answer these questions requires a sampling plan.

Field inspection of hand specimens should indicate to the geologist whether "suspect" lithologies are present in the project area. As described in the previous section these include serpentinites, magnesian schists, metamorphosed carbonates, and cataclastites. If these lithologies are found the second question should be addressed. Alternatively, the geologist might determine that the bedrock is composed of granites, volcanic rocks, or quartz-feldspathic metamorphic rocks, and that no nearby shear or fault zones are present, in which case the inquiry on asbestos minerals can be brought to an end.

To ascertain the presence of asbestiform minerals when "suspect" lithologies are present simply requires the identification of such. The field geologist should have a keen eye trained to identify any specimens containing visible fibers. Specimens containing visible fibers should be collected for laboratory analyses. A simple field test is to scrape a potential asbestos sample with the blade of a pocket knife. If fibers can easily be generated then the sample should be considered for laboratory analysis. However, the lack of fibers does not mean that it does not contain asbestos. It should be understood that it may be possible, especially with fine grained schists, for asbestiform minerals to be present in a size undetectable to the naked eye, so inevitably a few samples may need to be sent to the laboratory for either standard asbestos analysis or for petrographic analysis.

The collection of samples based solely on hand specimen appearance cannot be used to characterize the asbestos content of an area. In order to establish the extent of asbestiform minerals, some sort of decision rule-based sampling is necessary. This may include grid sampling, random sampling or a stratified random sampling plan, coupled with appropriate laboratory analyses. The geologist preparing a sampling plan should be well versed in environmental statistics. U.S. EPA (1989, 1996) and Berman (1998a, 1998b) provide useful discussions on the design of sampling plans and selection of analytical methods, along with some of the pitfalls of the common approaches.

Systematic sampling often requires the development of a grid. Oftentimes a project will have some survey control that can be used for the purpose. For example, the stationing for a grading plan can often be used to establish a grid. A grid does not have to be rectangular, nor does it have to be sampled

at every grid point. For example, in the random sampling approach, the sampling points are selected using a random-number algorithm.

The sampling of test pits for asbestiform minerals is usually not truly random. Although the location of the pit may be randomly selected, the collection of a specific rock sample from the pit may be highly selective. If the most likely asbestiform specimens are authoritatively collected from the test pit, then the overall evaluation is biased and very conservative, which may or may not be a desirable outcome. Ultimately, the goal of sampling and analyses is to allow the estimation of an upper confidence level for the average concentration of asbestos in materials disturbed by earthwork. This does not necessarily directly address risk from the inhalation of dust containing asbestos, but is an important early step. The only way to ensure that a sampling plan will produce reliable data, and that it is cost effective, is to tailor each plan to the specific conditions of the site and the specific problem to be solved.

On large projects that straddle fault zones or narrow bands of ultramafic rock, trenching should cut across the zone, to document the mineralogy across the zone of interest. For example, a sampling plan could be set up based on the trench length and depths of material. A series of test pits oriented across the zone might provide some of the same function. However, neither of these may be able to fully address the potential for disturbing asbestiform minerals during earthwork.

Visible asbestiform minerals are usually found in fibrous masses (Figure 1). Sometimes they can be found as a fibrous mat on a fracture surface. Often, a translucent vein filling may be found that, when scratched by a knife blade, generates fine fibers (Figure 2). It is common to find these in thin anastomosing veinlets within asbestos-bearing ultramafic rocks and within fault zones. In sounder rocks, veins may be found following existing fractures.

Field identification can best be calibrated by laboratory confirmation methods. The U.S. EPA bulk method using polarized light microscopy is relatively inexpensive and can provide detection limits as low as 1 percent (U.S. EPA, 1993). The CARB 435 method gives the relative percentage of asbestos fibers released by grinding, as measured by point counting under polarized light microscopy (CARB, 1991), but the EPA bulk method is simpler and quicker. However, both of these methods may not be able to detect smaller, more respirable fibers. If a risk analysis is to be performed, then other, more costly methods, such as the superfund method developed by Berman (1998), may be appropriate. The superfund method generates dust by gently tumbling rocks, followed by extraction of the dust onto filters and the identification and measurement of asbestos by transmission electron microscopy. This is the only method by which asbestos contained in the rock can be related to potential airborne asbestos, but is the slowest and most costly method currently available. Ultimately, feedback from laboratory testing will allow the refinement of a conceptual model and a better understanding of the association of asbestiform minerals with project specific rock assemblages.

Field identification should continue during construction in areas with known deposits of asbestos, and in areas with a high potential for asbestos. The consultant often will be asked to identify asbestos deposits as they are found so that mitigation measures, such as wetting, can be employed. Figure 3 shows a water stream being applied to asbestos-containing soil during removal. Figure 1 shows the same deposit between passes by the earthmoving equipment. The asbestos vein is visible in Figure 3 as a white streak below the person holding the water hose.

DATA ANALYSIS AND REPORTING

An evaluation for asbestos will generate results that need to be communicated to a client and regulatory officials. These individuals can be expected to use the information provided in the report to make decisions about activities or conditions that may generate asbestos-containing dust and pose a human health risk. Therefore, it is important early in the evaluation process to clearly state the questions that form the purpose and scope of the investigation.

The simplest scope may be a brief site reconnaissance to see if rocks that potentially contain asbestos are present. The deliverable may be a single page field report. In even this simplest case, the purpose of the evaluation, the observations, the findings, and the recommendations should be clearly stated for the report to be useful.

Figure 2. Vein of cross fiber asbestos in serpentinite.

The consulting geologist evaluating naturally occurring asbestos should become familiar with U.S. EPA and California Department of Toxic Substances Control (DTSC) guidance documents. U.S. EPA (1994) provides guidance on using data quality objectives, U.S. EPA (1996) presents generic information on developing sampling plans and methods of data analysis, and U.S. EPA (1998) addresses data quality assessment. All of these documents can be downloaded from the U.S. EPA web site.

The DTSC (1994) provides guidance for preliminary endangerment assessment. This document outlines a suggested approach for the entire preliminary endangerment assessment, including reporting.

Consulting geologists planning an investigation following the U.S. EPA or DTSC guidelines must remember that the only available method for quantifying asbestos exposure risk from rock or soil is the superfund method (Berman, 1998a). All other methods can give, at best, only a relative assessment of the presence of asbestos.

The simple identification of the presence or absence of asbestos still provides valuable information. The understanding of the geologic occurrence allows measures to be taken to minimize exposure. Report recommendations may include measures that minimize asbestos dust generation, such as wetting (Figure 1) and/or covering with clean soil. The identification of zones of asbestos within a project allows planning that may route roads or utilities so as to avoid excavating known deposits of asbestos, and geologic observation to monitor for asbestos during earthwork. The identification of asbestos deposits allows land users and regulators to make decisions that can protect human health.

Figure 3. Excavation in progress at cut face shown in Figure 1. Asbestos deposit is the white band below the worker holding the water hose. Water is here being used to ensure that no asbestos-bearing dust is generated.

ACKNOWLEDGMENTS

Our sincere thanks to David Bieber both as a peer reviewer, and for being a driving force in the implementation of better geologic techniques to assess asbestos hazards. Peer reviewer Eric Hubbard and Chief Editor Horacio Ferriz deserve our gratitude for guiding us through insightful editorial suggestions to produce a useful paper for the practicing engineering geologist.

AUTHOR PROFILES

David C. Sederquist is a Senior Engineering Geologist and Hydrogeologist with Youngdahl Consulting Group. David heads the asbestos-assessment team of the company. His technical experience also includes slope stability, hydrogeologic and geotechnical engineering studies, groundwater resources studies, onsite sewage disposal design, and environmental assessments.

Roy C. Kroll is the Chief Engineering Geologist and environmental manager at Youngdahl Consulting Group. He has performed engineering geology, fault hazard, geotechnical, hydrogeologic, and environmental studies throughout both northern and southern California since 1981. His experience also includes extensive forensic and litigation studies of distress and defects resulting from geologic conditions.

SELECTED REFERENCES

CFR (Code of Federal Regulations), 1998, Title 40, Part 763-Asbestos, Subpart E - Asbestos containing materials in schools: Office of the Federal Register National Archives and Records Administration.

ATDSR (Agency for Toxic Substances and Disease Registry), 1990, Asbestos, public health statement.

Barker, D.S., 1983, Igneous rocks: Prentice Hall, (Englewood Cliffs, New Jersey), 417 p.

Berman, D.W., 1998a, Asbestos measurement in soils and bulk materials: Sensitivity, precision, and interpretation - you can have it all: *in* Beard, M.E., Rook, H.L., (eds), Advances in environmental measurement methods for asbestos, ASTM STP 1342, American Society for Testing and Materials, 20 p.

Berman, D.W., 1998b, Addressing data quality issues throughout the site characterization process to minimize

decision errors: *in* First international symposium on integrated technical approaches to site characterization, Proceedings of an Argonne National Laboratory conference on expedited site characterization, (Chicago, Illinois), p. 13-29.

Berman, D.W., Crump, K.S., Chatfield, E.J., Davis. J.M., and Jones. A.D., 1995, The sizes, shapes, and mineralogy of asbestos structures that induce lung tumors or mesothelioma in AF/HAN rats following inhalation: Risk Analysis, v. 15, no. 2, 14 p.

Bowman, C., 1998, Projects in El Dorado churning up asbestos: Potential cancer hazard in unearthed bedrock: Sacramento Bee, p. 1, 29 March 1998.

CARB (California Air Resources Board), 1990, Proposed control measure for asbestos containing serpentine rock in surfacing applications, Technical Support Document: CARB Stationary Source Division, 43 p.

CARB (California Air Resources Board), 1991, Method 435 determination of asbestos content of serpentine aggregate, 18 p.

CARB (California Air Resources Board), 1992, Development of a technique to estimate ambient asbestos downwind from serpentine covered roadways, 86 p.

CARB (California Air Resources Board), 1998, Naturally occurring asbestos in El Dorado County: CARB website, 5 p.

CARB (California Air Resources Board), 2000, Initial statement of reasons for the proposed amendments to the asbestos airborne toxic control measure for surfacing applications, 38 p.

CCR (California Code of Regulations), 1998, Title 8 Register 96, Construction safety orders: California Office of Administrative Law, 47 p.

Chidester, A.H., and Shride, A.F., 1962, Asbestos in the United States: U.S. Geological Survey, Map MR-17.

Churchill, R.K., Higgins, C.T., and Hill B., 2000, Areas more likely to contain natural occurrences of asbestos in western El Dorado County, California: California Department of Conservation, Division of Mines and Geology, Open-File Report 2000-002, 66 p.

Coleman, R.G., 1971, Petrologic and geophysical nature of serpentinites: Geological Society of America Bulletin, v. 82, p. 887-918.

Dame, H.A., and Wheeldon, G.A., 1999, A critical look at the asbestos issue, 21 p. (unpublished paper).

DTSC (Department of Toxic Substances Control), 1994, Preliminary endangerment assessment guidance manual: California Environmental Protection Agency, Department of Toxic Substances Control, 52 p.

Harden, D. R., 2001, Geology of Northern California - an overview: *in* Ferriz, H., Anderson, R., (eds.), Engineering Geology Practice in Northern California: Association of Engineering Geologists Special Publication 12 and California Division of Mines and Geology Bulletin 210

Lake County AQMD (Air Quality Management District), 1992, District rules sections 467 - Asbestos Airborne Toxic Control Measure, 8 p.

Loyd, R.C., 1984, Mineral land classification of the Folsom 15' Quadrangle, Sacramento, El Dorado, Placer, and Amador Counties, California: California Department of Conservation, Division of Mines and Geology, Open File Report 84-50SAC, 44 p.

Loyd, R.C., Anderson, T.P., and Bushnell, M.M., 1983, Mineral land classification of the Placerville 15' Quadrangle, El Dorado and Amador Counties, California: California Department of Conservation, Division of Mines and Geology, Open File Report 84-29SAC, 45 p.

O'Hanley, D.S., 1996, Serpentinites, records of tectonic and petrological history: in Charnock, H. et al., (eds), Oxford Monographs on Geology and Geophysics No. 34, Oxford University Press, (New York and Oxford), 277 p.

Rice, S.J., 1957, Asbestos: in California Division of Mines and Geology Bulletin 176, Mineral Commodities of California, p. 49-58.

Roberts, R.G., 1987, Ore deposits models No. 11. Archean lode gold deposits: Geoscience Canada v. 14, p. 37-52.

Rogers, J.H., 1974, Soil Survey of El Dorado Area, California: U.S. Department of Agriculture, Soil Conservation Service, 89 p.

Schweikert, R.A.,1981, Tectonic evolution of the Sierra Nevada Range: *in* Ernst, W.G., (ed.), The geotectonic development of California, Volume I, Prentice-Hall, (Englewood Cliffs, New Jersey), p. 133-181.

Shelly D., 1993, Igneous and metamorphic rocks under the microscope: Chapman & Hall, (London, England), 445 p.

REMEDIATION OF THE GAMBONINI MERCURY MINE, MARIN COUNTY, CALIFORNIA

MARK G. SMELSER[1] AND DYAN C. WHYTE[2]

ABSTRACT

Between 1964 and 1969 cinnabar was mined from the Gambonini mercury mine in northern California. The ore was extracted from an open pit, and approximately 275,000 cubic yards of overburden and other mine waste were dumped onto steep slopes adjacent to the pit. Following mine closure, the mine waste deposit settled, suffered a deep-seated rotational failure, and was dissected by numerous rills and gullies, resulting in the discharge of mercury-contaminated sediment into Tomales Bay, one of California's pristine estuary/marine ecosystems.

In 1998, the U.S. Environmental Protection Agency and the State of California implemented remediation efforts at the Gambonini mine through a joint funding agreement. The goal of the remediation project was to stabilize the primary mine waste deposit and reduce the discharge of mercury-laden sediment. The project entailed constructing a gravity buttress with drainage terraces and a surface drainage system that included V-ditches and drop-inlets connected to stormdrain pipelines. A stream channel was reconstructed on top of the buttress to convey water draining the upper watershed and the stabilized waste pile out of the remediated area. An extensive native-plant revegetation program is currently underway to reduce erosion on the recontoured landscape and promote long-term stability.

Since mine closure in 1969, engineering geologists have worked at the Gambonini mine in various capacities, ranging from the development of mine closure plans to the quantification of the toxic sediment discharge. Engineering geologists were involved in legal proceedings against the former mine owners and negotiations for project funding, and were instrumental in the development of mitigation alternatives and the final remediation plan. In addition, engineering geologists provided technical input during all phases of the project, including grading and post-grading revegetation.

At the Gambonini mine, problem identification, funding negotiations, remediation plan development, and construction required approximately 13 years, the involvement of four government agencies, and the collected work of engineering geologists from six different consulting firms. The development and implementation of an appropriate remediation plan required a highly accurate topographic base map, analysis of historic aerial photographs, detailed field mapping, and subsurface investigations.

[1]California Department of Conservation
Division of Mines and Geology
1330 Bayshore Way
Eureka, CA 95501
msmelser@consrv.ca.gov

[2]California Regional Water Quality Control Board
San Francisco Bay Region
1515 Clay Street, Suite 1400
Oakland, CA 94612
dwc@rb2.swrcb.ca.gov

INTRODUCTION

The reclamation and remediation of abandoned mines involves a variety of engineering geology and geotechnical tasks that include problem identification, site characterization, development of conceptual alternatives, stabilization of tailings deposits, mitigation of sediment discharge, restoration of stream channels, and revegetation of slopes. In this article we describe the history of the Gambonini mercury mine and the professional involvement of engineering geologists in the remediation of the environmental problems caused by this abandoned mine (Table 1). The Gambonini mercury mine is located in Marin County, California approximately 35 miles north of San Francisco. The principal sources of information for this article are the project files maintained by Cotton, Shires, and Associates, Inc. and the California Regional Water Quality Control Board.

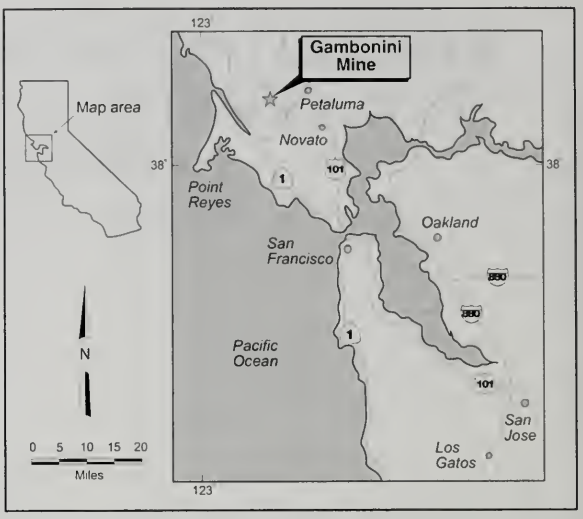

Figure 1. Map showing the location of the Gambonini mercury mine in northern California.

BACKGROUND

Regional setting and geology

The Gambonini mercury mine is located in the steep headwaters region of the Tomales Bay watershed, approximately 10 miles west of Petaluma, California (Figures 1 and 2). In this region, the steep, rugged mountainous areas are typically covered with native shrubs and oak trees, and the gentler sloping areas are used for cattle grazing. Average annual rainfall is approximately 35 inches, and torrential winter rainstorms with intensities of two inches per hour have been measured.

- Problem identification
- Problem characterization
- Expert witness testimony
- Development of preliminary remediation alternatives
- Funding negotiations
- Superfund classification
- Project planning and setting of goals and objectives
- Feasibility studies
- Design level engineering geology investigation
- Final remediation plan design
- Final plan selection
- Project construction
- As-built reporting
- Erosion control and slope revegetation
- Post-project monitoring

Table 1. Professional involvement of engineering geologists in the remediation of the Gambonini mercury mine.

The mine area is drained by a narrow, incised, and steep-gradient ephemeral creek known as Gambonini Ranch Creek. This creek drains into Walker Creek, which in turn flows into Tomales Bay (located approximately 13 miles downstream from the mine). The bay is renowned for its sport fishery and commercial oyster beds. The bay also provides winter habitat for hundreds of migratory waterfowl, and is part of the Gulf of the Farallones National Marine Sanctuary.

The Gambonini mine lies approximately 6 miles east of the San Andreas fault (Figure 2) and is underlain by Franciscan Complex rocks (Bailey et al., 1964; Blake et al., 1974; Wagner and Bortugno, 1982). Shallow and deep-seated landslides are common features in this region (Wentworth and Frizzell, 1975). Mercury ore (cinnabar) was found concentrated along a prominent north-trending shear zone that apparently trapped ore-rich gases and fluids. The rocks in this zone consist of a tightly folded graywacke sandstone and shale unit, intensely sheared and altered black siltstone, and serpentinite. Spectacular occurrences of high-grade ore, assaying 200 to 300 pounds of mercury per ton, were reportedly

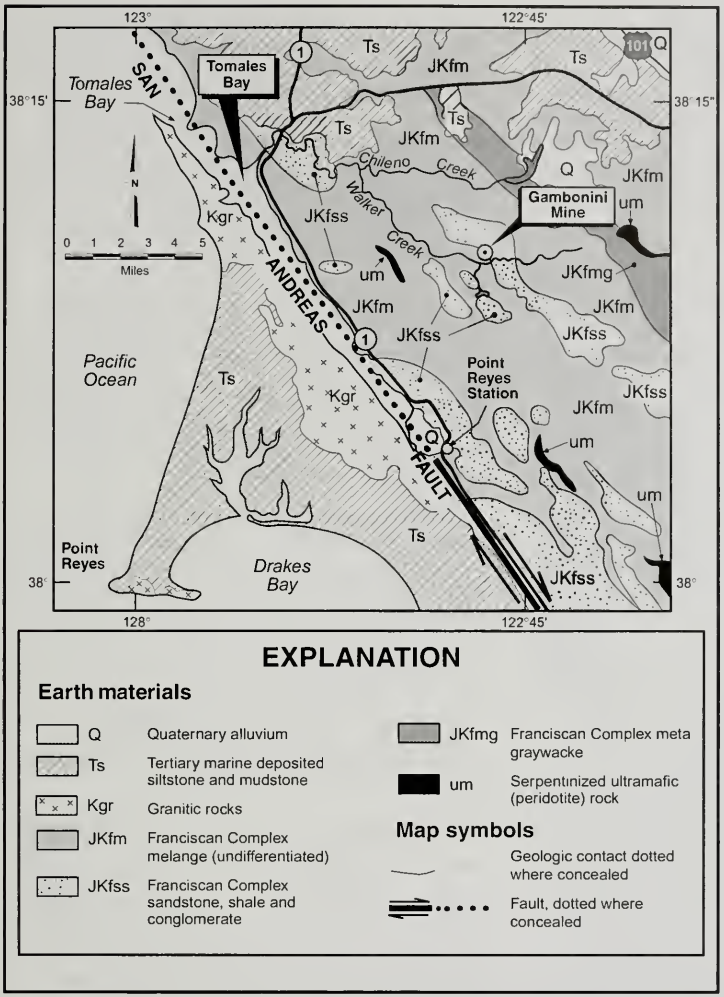

Figure 2. Regional geologic map of the Marin County area (after Blake et al., 1974).

uncovered during mining activities. This deposit is similar to other mercury deposits found in the Coast Ranges of California as described by Bailey and Everhardt (1964) and Rytuba and Enderlin (1999).

Mine history

Cinnabar was discovered on the Gambonini property in 1943, but it was not until 1964 that Buttes Gas and Oil Company developed the mine and conducted a nearly continuous open-pit mining operation until mine closure in 1969. By mining cinnabar from benches in an open pit, they produced approximately 4,000 flasks of mercury. In the process, the mine operators dumped overburden and other mine waste into nearby ravines and onto steep slopes immediately east of the pit.

Mercury was extracted from the cinnabar by roasting the ore at temperatures between 500 to 600 degrees centigrade. The most efficient roasting systems recover between 90 and 95 percent of the mercury in cinnabar (Rytuba and Enderlin, 1999). The residue (roasted ore-rock) from the roasting process is known as clinker or calcines. The clinker at the Gambonini site has a distinctive grayish red-brown color and is a poorly sorted mixture of gravel, sand, and silt-size particles.

PROBLEM RECOGNITION, ASSESSMENTS, AND ACTIONS

In 1987, approximately 18 years after the mine had closed, the Marin County Resource Conservation District identified the Gambonini mine as a critical erosion site. In 1990 the San Francisco Bay Regional Water Quality Control Board (Regional Board), under a newly established mine identification and cleanup program, listed the mine site as a potential source of mercury and sediment that could adversely affect Tomales Bay. In 1994 the Regional Board secured funding to evaluate the water quality threat posed by the mine. From 1994 to 1998

engineering geologists monitored discharge from the mine, examined historic aerial photographs, developed topographic maps from the historic photographs, performed a petrographic analysis of the wall rocks in the mine pit, examined mercury levels in sediment and biota in Tomales Bay, and reconnoitered the Tomales Bay watershed for other mercury sources. This multi-year monitoring and investigation program confirmed that the mine was a significant environmental problem (Whyte, 1998).

The Regional Board's investigation revealed that the primary mine waste deposit contained approximately 200,000 cubic yards of overburden, waste rock from the gravity separation and crushing mills, and clinker. The average mercury concentrations in two sediment cores drilled near the base of the waste pile were 260 and 500 parts per million (for comparison, the mercury concentration in the average grade ore rock was approximately 2,250 ppm). The State considers material with more than 20 ppm mercury hazardous waste. The silt, clay, and fine sand size fractions of the samples contained the highest mercury concentrations and are a source of concern because particles of this size are readily transported off-site during runoff events.

Whyte and Kirchner (1999) installed a continuous monitoring system in Gambonini Creek below the mine, and estimated that over 180 pounds of mercury were discharged during January and February of 1998. Total mercury concentrations in the creek were highly variable, ranging from 0.485 to 1,040 parts per billion (ppb); significantly exceeding the State's water quality objective of 0.012 ppb at all times. The majority of that mercury was in the particulate phase and was released during brief, intense storm events. Most likely, the particles were inorganic mercury complexes such as cinnabar, metacinnabar, or a mercury chloride (Kim et al., 1999). Once released from a site and discharged into aquatic environments, these inorganic mercury particles may be transformed (methylated) to toxic, organic mercury complexes that are known to bioaccumulate in the food chain. Methylation is biologically mediated and occurs in aquatic bottom sediments (Rytuba and Enderlin, 1999).

An investigation of downstream environmental conditions revealed watershed-wide impacts (Whyte, 1998). Stream samples taken 3 miles downstream from the mine and at the mouth of Walker Creek in Tomales Bay (13 miles downstream) contained high concentrations of mercury (ranging from 0.25 to 7.07 ppb) and exceeded the water quality objective at all times. Native clams collected along the shoreline near the Walker Creek estuary contained elevated levels of mercury (up to 0.67 ppm). Mercury concentrations up to 23 ppm were measured in bay sediment samples from the same area. Hoffman et al. (1998) investigated hepatic mercury concentrations in diving ducks from Tomales Bay and discovered that the concentrations were high enough (up to 19 ppm) to threaten overwinter survival and reproductive success.

Faced with elevated concentrations of mercury in the aquatic ecosystem, the Regional Board began investigating remediation alternatives and contacted the U.S. Environmental Protection Agency's (EPA) Emergency Response Unit for assistance. In May of 1998 the Gambonini mine area was declared an emergency Superfund Site, and funds were allocated for remediation work.

The EPA and Regional Board established two primary project goals. First, to significantly reduce the discharge of mercury-laden sediment, and second, to complete the remediation effort within two construction seasons. Before a final remediation plan could be developed, the agencies identified the need to (1) better define the project area and map the distribution of mine waste, (2) re-estimate the volume of the primary mine waste deposit, and (3) characterize the landslide in the primary mine waste deposit. To fulfill these needs, a design-level engineering geologic investigation was undertaken.

RESULTS OF THE DESIGN-LEVEL ENGINEERING GEOLOGY INVESTIGATION

Mine waste was distributed around the 40-acre mine area in various deposits, stored as canyon fill downstream of the mine area, and was present in the active stream channel. The primary waste deposit covered approximately ten acres, contained approximately 275,000 cubic yards of material, and was located north of the old separator mill (Figures 3 and 4). We estimate that the primary mine waste deposit contained approximately 90% overburden and 10% processing waste. Compositionally, the deposit was a well-graded mixture of clay and silt (30%), sand (35%), gravel (30%), and blocks and boulders (5%), derived from graywacke and arkosic sandstones, and sheared black siltstone. The primary waste deposit was loose to medium-dense, uncemented, friable, and dissected by numerous erosional rills and deep gullies. Surface water

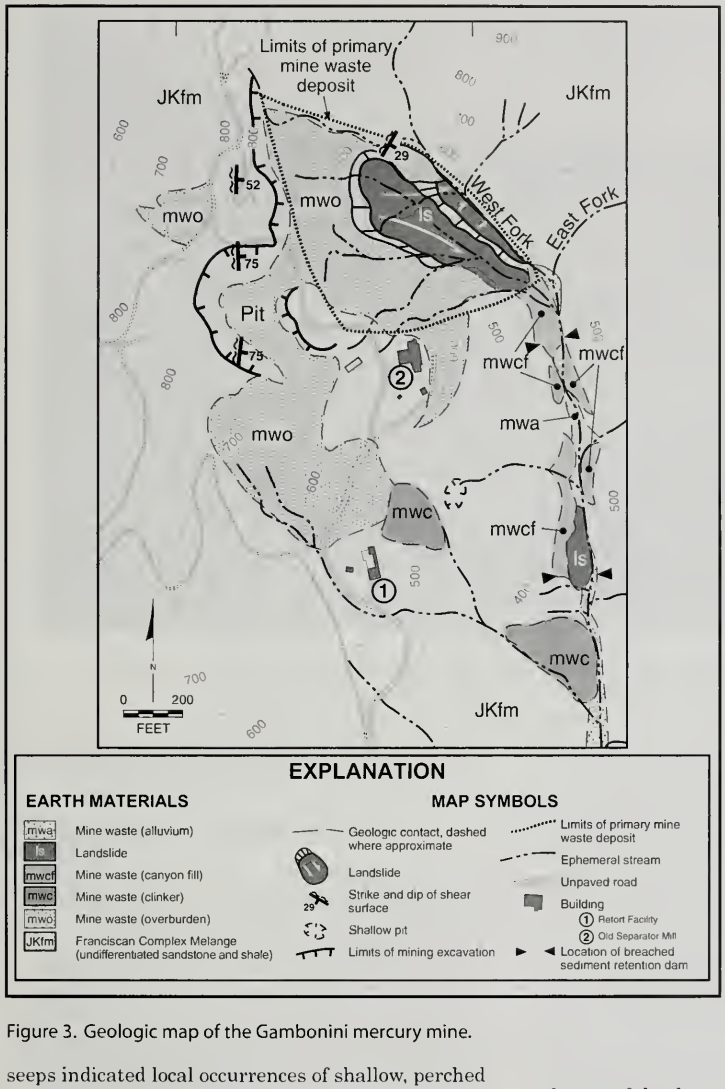

Figure 3. Geologic map of the Gambonini mercury mine.

seeps indicated local occurrences of shallow, perched ground water within the primary mine waste deposit.

Historic maps and aerial photographs suggested that the primary mine waste deposit had buried steep and undulating topography (adjacent ravines). Similarly, the borehole data indicated that the waste material varied in thickness from 13 feet to 43 feet. Borehole data and outcrops in the deeper gullies, showed that the mine waste was deposited on a buff-yellow clayey colluvium overlying a deeply weathered sandstone unit. Collectively, the colluvium and sandstone were approximately 20 feet thick and were underlain by black siltstone and shale. Groundwater in the boreholes was between 40 and 50 feet below the surface, near the contact between the deeply weathered sandstone and underlying black siltstone.

Rotational slumping of the waste material resulted in a near-vertical arcuate scarp that was 30 to 50 feet high in the northern portion of the primary mine waste deposit (Figures 3 and 4). Tension cracks and grabens (showing up to one foot of separation) were observed throughout the body of the landslide, indicating that the slide was still active. Downslope movement was nearly due-east (S83E) into the narrow canyon bottom and the West Fork of Gambonini Ranch Creek (Figure 3). The toe of the landslide had filled-in approximately 550 feet of stream channel length with loose and friable landslide debris, including mercury-laden mine waste.

In one of the deep erosional gullies we observed a prominent shear zone cutting through the siltstone bedrock underlying the active landslide. This shear zone was distinctly planar, approximately 6 inches thick, seeping with water, and composed of highly plastic stiff clay. The dip direction (S61E) of this shear zone was nearly parallel to that of the downslope movement direction of the active landslide. This prominent shear zone in the bedrock, its

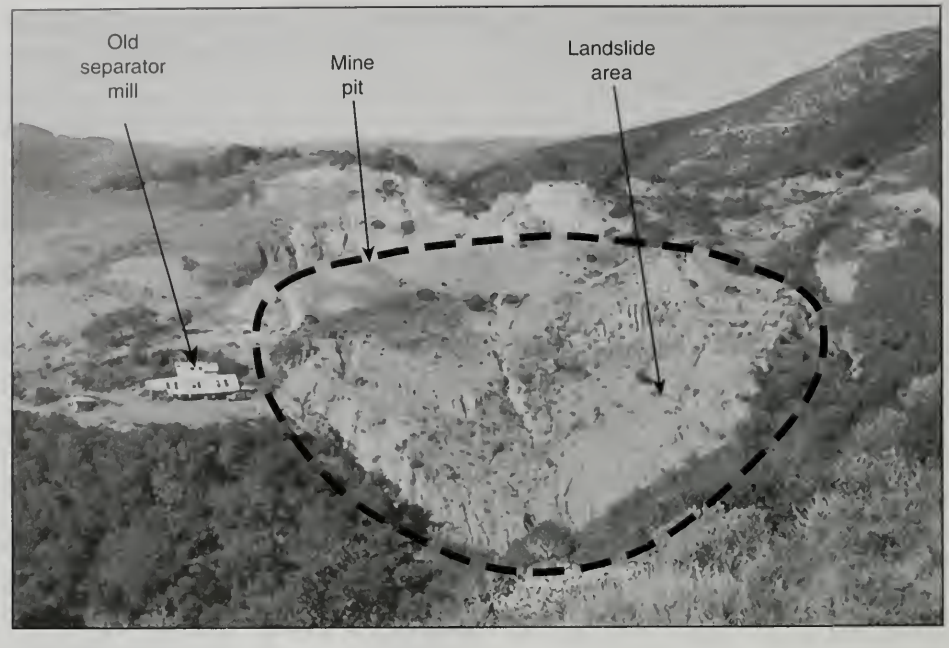

Figure 4. Photograph of the Gambonini mercury mine in 1997 prior to remediation. The primary mine waste deposit is delineated by the heavy dashed line.

orientation, and the substantial height of the landslide headscarp, led us to conclude that the active landsliding probably extended into the bedrock and was not confined to the mine waste deposit. Consequently, any remediation plan designed to control surface water runoff and reduce sediment discharge from the primary mine waste would have to include stabilization of this bedrock landslide.

REMEDIATION ALTERNATIVES AND PROJECT SELECTION

The EPA and Regional Board limited the project area to the ten-acre primary mine waste deposit, and evaluated three remediation alternatives: (1) removing all mine waste from the slope area and placing it into the pit, (2) stabilizing the waste material in place using a gravity buttress, and (3) stabilizing the waste material in place by building a large retaining wall. The relative merits and implementation constraints for each alternative are outlined in Table 2. Following the evaluation, the agencies chose to construct a gravity buttress.

PROJECT CONSTRUCTION

The emergency nature of this project mandated that both design and construction efforts begin immediately following selection of a final plan. Thus, construction of the gravity buttress began in August 1998, with clearing and grubbing of the lower portion of the waste pile and existing channel area. The remediation team worked on a number of tasks simultaneously. Supplementary topographic surveying, slope stability analysis, and engineering design were performed during the middle part of August. Excavation and grading continued through September and October. By late October, the buttress and drainage terraces, drop inlets, and the stormdrain pipeline system had all been constructed. In early November, V-ditch construction was postponed due to weather. Erosion control, soil conditioning, and hydroseeding efforts continued through the winter.

	REMEDIATION ALTERNATIVES		
	RETAINING WALL	**GRAVITY BUTTRESS**	**REMOVE AND PLACE IN PIT**
PRIMARY CONSTRUCTION TASKS	1. Drill and construct 108 shear pins 30 feet deep 2. Construct concrete wall and install double tie-backs 3. Remove uppermost portion of mine waste (60,000 cubic yards) and fill in major gullies 4. Install surface drainage system on existing mine waste deposit 5. Revegetate slopes	1. Construct butress using on-site materials 2. Construct subdrain system 3. Compact butress fill and terrace the fill slopes 4. Reconstruct the stream channels, or route stream through culvert beneath the butress 5. Install surface drainage system on cutslopes and compacted fill slopes 6. Revegetate slopes	1. Remove existing fill in pit and construct a subdrain system in the pit 2. Remove mine waste from slopes and transport up to pit area 3. Compact fill in pit and terrace fill slopes 4. Install surface drainage system on compacted fill slopes 5. Terrace, shape, and reconfigure exhumed slopes 6. Revegetate fill slopes 7. Revegetate exhumed slopes
ADVANTAGES	1. Minimal grading	1. Simple construction 2. Easier grading, i.e. mine waste moved downslope 3. One month required to complete design 4. Proposed cut and fill volumes well estimated 5. Moderate to low probability of "surprises" during construction	1. Mine waste isolated
DISADVANTAGES	1. Mercury-laden mine waste exposed at the surface 2. Minimum of 2 months required to complete investigation and design 3. Upon completion of final design, construction costs could be much higher	1. Mercury-laden mine waste exposed at the surface	1. Mercury-laden mine waste exposed at the surface 2. Minimum of 2 months required to complete investigation and design 3. Depending on actual amount to be removed and extent of slope reconstruction, construction costs could be significantly greater 4. Difficult and lengthy construction, e.g. mine waste hauled upslope 5. Volume of fill expected to significantly exceed the volume of the pit 6. High probability of "surprises" during construction (e.g. landslide could move) 7. Does not stabilize bedrock landslide
DESIGN REQUIREMENTS	1. Detailed subsurface investigation along wall alignment and toe of landslide 2. Slope stability analysis 3. Sophisticated geotechnical design	1. Slope stability analysis	1. Detailed subsurface investigation to plan out simultaneous excavation and slope reconstruction 2. Slope stability analysis
ESTIMATES OF CONSTRUCTION COSTS	$2.9 to 3.5 million	$3.0 to 3.6 million	$4.5 to 5.0 million

Table 2. Comparison of conceptual remediation alternatives.

The project required the removal of approximately 213,000 cubic yards of mine waste and weathered bedrock from five acres in the upper half of the project area (between grid sections A and D, and 2 and 5 on the reference grid shown on the as-built map in Figure 5). Excavation and grading in the upslope area were necessary to (1) construct the gravity buttress to stabilize the bedrock landslide, (2) remove the driving forces surcharging the bedrock landslide, (3) remove loose and saturated materials from steep areas, (4) blend the graded area into the adjacent native topography, and (5) provide controlled surface drainage paths.

The gravity buttress was constructed within a 3.5-acre triangular area in the lower half of the project area (between grid sections E to G and 2 to 4 in Figure 5). Prior to buttress construction, approximately 1,430 feet of subdrains were placed along the largest pre-existing drainage routes. An additional 1,200 feet of subdrains were constructed within the engineered fill. Engineered fill for the buttress was benched into the pre-existing ground surface, placed in 8- to 12-inch lifts, and compacted to 90 percent of maximum dry density. The buttress was constructed with approximately 146,000 cubic yards and has a maximum thickness of 50 feet (Figure 6). Finished fill slopes ranged from 2:1 to 5.5:1 (H:V).

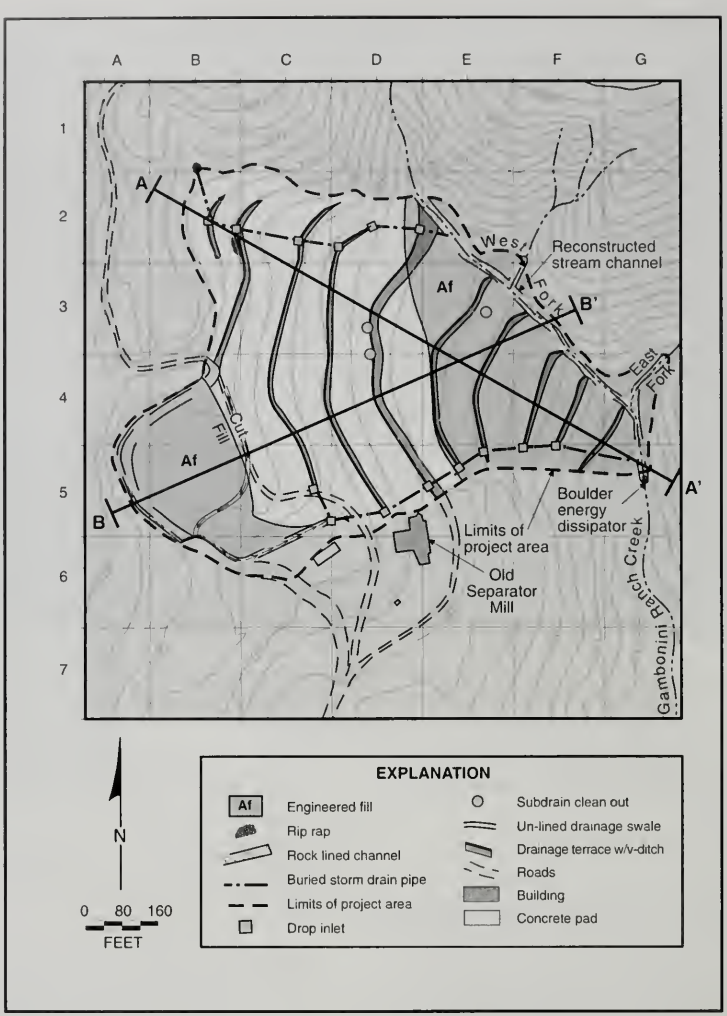

Figure 5. As-built map of the remediated primary mine waste deposit.

The key elements of the surface drainage system are drainage terraces and a reconstructed stream channel. Ten drainage terraces were constructed along slope contours in conjunction with the excavation in the upper project area and buttress construction in the lower project area. These terraces are separated by an average elevation interval of 40 feet and they all contain concrete V-ditches that drain to either drop inlets or the reconstructed stream channel (Figures 5 and 7). The reconstructed stream channel is approximately 1,000 feet long, lined with angular blocks greater than 18 inches in size, and follows the grade of the gravity buttress. This channel is up to 40 feet higher in elevation than the pre-remediation channel and is designed to convey water out of the upper watershed, and off the stabilized waste pile without contacting mine waste. At the downstream end of the reconstructed channel, an energy dissipator made of large boulders marks the transition point to the pre-existing channel.

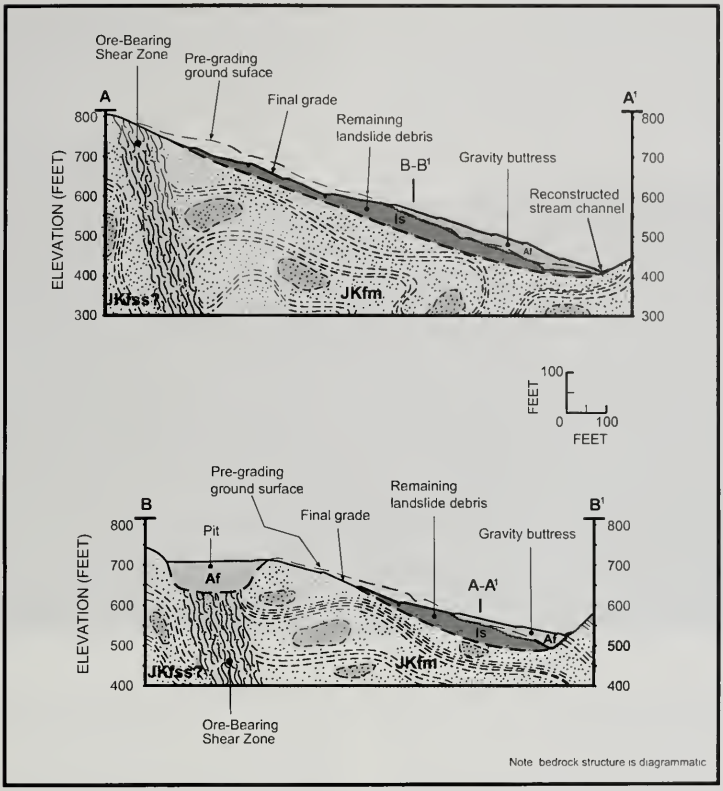

Figure 6. Geologic cross sections showing the as-built conditions. Af stands for engineered fill.

Over 67,000 cubic yards of excavated earth materials were determined to be unsuitable for use as engineered fill in the gravity buttress and were consequently placed in the abandoned mine pit. These materials included saturated mine waste, colluvium, and ravine-bottom sediments mixed with organic detritus. Thus, the total thickness of fill in the pit is approximately 70 feet, and the pit is essentially filled. The resultant fill slopes are approximately 40 feet high and are protected from sheetflow erosion by drainage swales and vegetation.

The final phase of the project included implementing bioengineering erosion control methods and revegetating the site with indigenous native plants. Previous revegetation studies at the Gambonini mine had demonstrated that native plants can be grown successfully in mine waste that has been treated with compost and nutrients. Consequently, compost was incorporated into the outboard edge of the engineered fill slope during grading and the typical surficial slough generated during grading was allowed to remain on the slopes. Thus, a mixture of organic compost and loose fill, approximately 6-inches thick, was left on the slope as rooting material for native plants.

The site was hydroseeded with indigenous native seeds, and straw mulch was applied to the slopes to promote germination and reduce surface erosion. In addition to the hydroseeding, willow wattles were planted at known water seeps. Other plants, such as native shrubs and oaks, are being grown at a local nursery; these one-to-three-year-old shrub and oak seedlings will be planted at the site over the next two years (2001 to 2002). To further protect

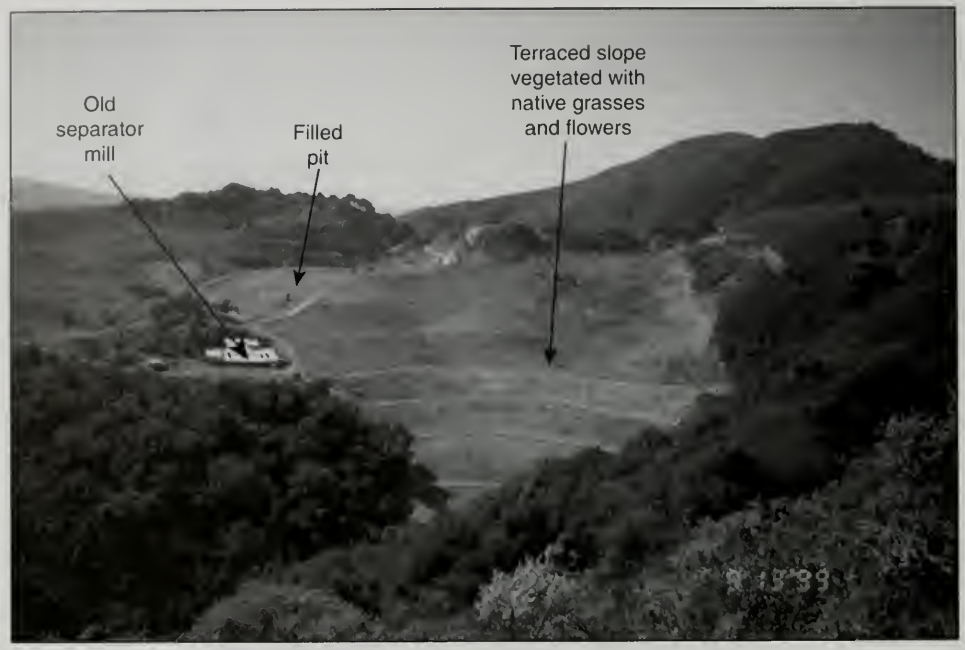

Figure 7. Post remediation photograph of the mercury mine waste deposit taken in September, 1999. The reconstructed stream channel is obscured by vegetation but lies along the right-hand side of the graded slope.

the slopes from erosion, approximately 2,000 feet of straw wattles were installed along slope contours, and erosion-control blankets have been installed on the steepest cut-slopes.

As of January 2000, the remediation at the Gambonini mine appeared to be a success. The primary mine-waste deposit was stabilized, the surface-water drainage system was functioning as planned, and construction was completed in under two years and within budget ($3 million). The vegetation is flourishing and over the next five years the Regional Board will be monitoring water quality to quantify the effectiveness of the remediation plan.

CONCLUDING REMARKS

Whether it is mineral exploration, mineral extraction, or mining reclamation, mines are the domain of geologists, and engineering geologists are well qualified for characterizing abandoned mine sites. In keeping with the spirit of this volume as "a tool for practitioners", we offer some technical advice and recommendations for geological and geotechnical professionals who are involved, or desire to be involved, in the remediation and reclamation of mined lands.

Mined areas are severely disturbed landscapes that typically include steep slopes, vertical cuts, underground adits, large deposits of non-engineered fill, ravines filled with trash, and myriad drainage paths. At the Gambonini mine, a detailed geologic site characterization was the key to developing appropriate remediation measures, accurate cost estimates, and efficient project implementation. Such a characterization can only come from a detailed engineering geologic map, measured geologic profiles, and subsurface investigations.

Detailed mapping, slope stability analyses, efficient plan design, and project construction require highly accurate topographic base maps. With the increased usage of photogrammetric techniques

and remotely sensed survey data, detailed ground surveying is often minimized. At the Gambonini mine, the axis of Gambonini Ranch Creek was not surveyed because of dense overstory and understory vegetation. Consequently, the axis of the channel was laterally mislocated by approximately 40 feet with coincident elevational errors in the range of 10 feet. At a reconnaissance level such discrepancies are hardly noticed. However, at the detailed levels of investigation, design, and construction, such discrepancies cause analysis and plan design errors, and substantial frustration for contractors and project surveyors. Consequently, it is our recommendation that project base maps be developed from topographic surveys that are "ground-controlled" through all densely vegetated areas, especially stream channels.

Mined landscapes are formed by dynamite, excavators, and dozers. Consequently, the topography of these landscapes can be highly irregular. In planning a subsurface exploration program, geologists and engineers should keep in mind that if truck-mounted drill rigs are used, substantial grading may be required to provide access to key borehole locations. Instead, we recommend track-mounted drill rigs that are better suited for moving through irregular terrain.

Aerial photographs have proven to be of great value in deciphering the evolution of the mining operation, locating cut and fill areas, and interpreting truncated or partially buried landforms mapped in the field. Furthermore, one of the more important tools used in quantifying the volume of mine waste at the Gambonini mine was the construction of topographic maps from historic aerial photographs and contemporary ground surveys.

Perhaps most importantly, it should be recognized that remediation of abandoned mine sites requires much more time than typical geotechnical projects. At abandoned mine sites, time is required to identify and quantify the mine-related environmental problem, develop mitigation alternatives, undertake legal action, secure funding, and implement remediation measures. At the Gambonini mine, this process required approximately 13 years, the involvement of four government agencies, and the collected work of engineering geologists and geotechnical engineers from six different consulting firms.

ACKNOWLEDGMENTS

First, we wish to recognize the organizations and several individuals that contributed, over the years, to the environmental assessment and remediation efforts at the Gambonini Mine. These organizations include the U.S. Environmental Protection Agency, the San Francisco Bay Regional Water Quality Control Board, the California Department of Conservation, the California Conservation Corps, the Marin County Resource Conservation District, Cotton, Shires and Associates, Inc., Robert S. Miller and Associates, Prunuske and Chatham Engineers, Ninyo & Moore Geotechnical and Environmental Science Consultants, Ecology and Environment, Inc., and CET Environmental Services, Inc. Tom Dunkleman with the U.S. EPA was instrumental in securing funding for the project and coordinating the remediation effort. Gail Newton and Karen Weise with the California Department of Conservation developed the revegetation plan. Secondly, we wish to acknowledge the reviewers of this manuscript who improved the readability of this paper: John H. Dilles, Robert Joslin, and Steve Stryker. Finally, we wish to thank Chief Editor Horacio Ferriz for his hard work and leadership in bringing this publication together.

AUTHOR PROFILES

Mark Smelser is a Fluvial Geomorphologist/ Senior Engineering Geologist with DMG (formerly with Cotton, Shires and Associates, Inc.) He is a Certified Engineering Geologist in the State of California and has over 10 years of experience in the fields of engineering geology, fluvial geomorphology, and watershed science. Mr. Smelser specializes in characterizing landslides and the contemporary and historical behavior of stream channels.

Dyan Whyte is an Associate Engineering Geologist with the California Regional Water Quality Control Board, San Francisco Bay Region. She has over 10 years of experience working on water quality issues, and clean-up of abandoned mines in the San Francisco Bay region. In recent years, Ms. Whyte has been involved in detailed studies to quantify the bioaccumulation of mercury in the Tomales Bay ecosystem and its impacts to humans.

SELECTED REFERENCES

Bailey, E.H. and Everhardt, D.L., 1964, Geology and quicksilver deposits of the New Almaden District, Santa Clara, County, California: U.S. Geological Survey Professional Paper 360, 206 p.

Bailey, E.H., Irwin, W.P., and Jones, D.L., 1964, Franciscan and related rocks, and their significance in the geology of western California: California Division of Mines and Geology, Bulletin 183, 177 p.

Blake, M.C., Jr., Bartow, J.A., Frizzell, V.A., Jr., Scholocker, J.S.D.H., Wentworth, C.M., and Wright, R.H., 1974, Preliminary geologic map of Marin and San Francisco Counties and parts of Alameda, Contra Costa and Sonoma Counties, California: U.S. Geological Survey Miscellaneous Field Studies map MF-574, scale 1:62,500.

Hoffman, D.J., Ohlendorf, H.M., Marn, C.M., and Pendleton, G.W., 1998, Association of mercury and selenium with altered glutathione metabolism and oxidative stress in diving ducks from San Francisco Bay Region, USA: Environmental Toxicology and Chemistry, v. 12, no. 2, p. 167-172.

Kim, C.S., Rytuba, J.J., and Brown, G.E., 1999, Utility of EXAFS in characterization and speciation of mercury-bearing mine wastes: Journal of Synchrotron Radiation: Proceedings from Tenth International XAFS Meeting, Chicago, IL, August 1998.

Rytuba, J.J. and D.A. Enderlin, 1999, Geology and environmental geochemistry of mercury and gold deposits in the northern part of the California Coast Range mercury belt: In Wagner, D.L. and S.A. Graham (ed.), Geologic Field Trips in Northern California Centennial Meeting of the Cordilleran Section of the Geological Society of America, Special Publication 119, p. 214-235.

Taylor, K., 1998, Defining the mercury problem in the northern reaches of San Francisco Bay and designing appropriate regulatory approaches: Staff Report San Francisco Bay Regional Water Quality Control Board, 104 p.

Wagner, D.L. and E.J. Bortugno, 1982, Geologic map of the Santa Rosa quadrangle: California Division of Mines and Geology, Regional Geologic Map 2A, scale 1:250,000.

Wentworth, C.M. and Frizzell, V.A., 1975, Reconnaissance landslide map of parts of Marin and Sonoma Counties, California: U.S. Geological Survey Open-File Report OFR-75-281, scale 1:24,000.

Whyte, D.C., 1998, The Gambonini mercury mine – water quality threats and remediation alternatives: California Regional Water Quality Control Board, San Francisco Bay Region, Staff Summary Report, 25p.

Whyte, D.C. and J.W. Kirchner, 2000, Assessing water quality impacts and cleanup effectiveness in streams dominated by episodic mercury discharges: Science of the Total Environment, v. 260, p. 1-9.

POTENTIAL IMPACT ON WATER RESOURCES FROM ERUPTIONS NEAR MAMMOTH LAKES, MONO COUNTY, CALIFORNIA

R. FORREST HOPSON[1]

ABSTRACT

Small to moderate eruptions that have occurred near the resort community of Mammoth Lakes, eastern California, along the Mono-Inyo Craters volcanic chain over the past 5,000 years can be anticipated to recur in the future. Such eruptions have produced phreatic blasts, lava domes and flows, fallout ash, and pyroclastic flows and surges. Locally destructive flooding and lahars may result if eruptions were to recur during times of heavy rainfall or when the ground is covered with heavy snowpack. Volcanic activity could cause temporary disruptions in water conveyance lasting from a few days to weeks after an eruption.

Renewed volcanism near Mammoth Lakes could impact the quality of water resources in the eastern Sierra Nevada in a number of ways: (1) Streams could be displaced from their channels by advancing lava flows. (2) Volcanic ash, lahars, or debris avalanches could cause increased turbidity and acidity. (3) Voluminous pyroclastic flows, lahars, and debris avalanches might impound stream channels and cause changes in stream channel morphology; subsequent failure of debris dams could result in disastrous floods downstream. (4) Minor compositional changes in water would be possible due to leaching of volcanic ash or sediment from lahars or debris avalanches. (5) Change in snowmelt runoff rates might occur. (6) Large pyroclastic flows, lahars, and debris avalanches could cause clogging and burial of water intake structures, ditches, and pipelines along the Los Angeles-Owens River Aqueduct.

INTRODUCTION

The Mammoth Lakes region has been identified by the U.S. Geological Survey as having potential for renewed volcanic activity (Miller et al., 1982). Increased seismicity beneath the south-central moat of Long Valley caldera, uplift of the caldera floor, emission of carbon dioxide gas, and increased hot spring activity, have all prompted concerns of possible renewed volcanic activity at Long Valley caldera (Hill et al., 1985; Farrar et al., 1995).

The purpose of this paper is to assess the potential impact of small- to moderate-size volcanic eruptions on water resources in the vicinity of Mammoth Lakes, specifically, the impact on surface water quality and water distribution systems, including the Los Angeles-Owens River Aqueduct. This paper reviews eruption scenarios, hazards associated with such eruptions, and potential impact on water quality. The release of volcanic gases (e.g., carbon dioxide, hydrogen sulfide, sulfur dioxide) should be anticipated but will not be discussed, because volcanic gases generally do not pose a serious threat to water supply, although high concentrations of volcanic gases could endanger human lives downwind from a vent. Examples from the May 18, 1980 erup-

[1]Consulting Geologist
2930 Salem Place, #608
Reno, NV 89509
fhopson@worldnet.att.net

tion of Mount St. Helens, Washington and the 1953 eruptions of Mount Spurr, Alaska are discussed. A previous paper (Hopson, 1991) concluded that the introduction of microorganisms and the decomposition of organic detritus contained in volcanic deposits such as lahars might lead to degradation of water quality. This paper, instead, focuses more directly on the volcanologic impact. Major sources for this paper are Bailey (1989), Bailey et al. (1976), Blong (1984), Hill et al. (1997), Hopson (1991), Miller et al. (1982), Miller (1985, 1989), Major and Newhall (1989), Whetstone (1955), and Wood (1977).

Renewed volcanic activity in the Long Valley-Mono Lake region is of major concern to people living in this area. Furthermore, water from this region and northern Owens Valley is the source of approximately 65% of the drinking water for the City of Los Angeles, 300 miles to the south. Of particular concern is how volcanic activity might impact the Los Angeles-Owens River Aqueduct, which carries water to Los Angeles. The Long Valley-Mono Lake region is a popular recreation area in the eastern Sierra Nevada (Hopson, 1991); thus, a volcanic eruption could also have significant negative consequences for the nearby communities of Mammoth Lakes, June Lake, and Lee Vining.

GEOGRAPHIC SETTING

This paper focuses in the area of recent volcanism of the Long Valley-Mono Lake region. This region lies at the base of the Sierra Nevada at the western boundary of the Basin and Range Province. It is just north of Owens Valley, a fault-bound graben between the Sierra Nevada on the west and the White Mountains on the east.

The Los Angeles-Owens River Aqueduct (Figure 1) transports water via a series of pipelines, ditches, tunnels, storage reservoirs, and the Owens River. Water is temporarily stored in Grant Lake, Lake Crowley, and Pleasant Valley Reservoir. Water is gathered from the Lee Vining, Walker and Parker Creek intake structures, the Lee Vining conduit, and Grant Lake reservoir, where it is transported through the Mono Craters tunnel into the Owens River, which flows into Lake Crowley. From Lake Crowley, water is carried through tunnels, conduits, and penstocks via three hydroelectric plants on a 730 m drop into Pleasant Valley Reservoir. Water from Pleasant Valley Reservoir flows down the Owens River about 48 km, at which point it enters the intake of the Los Angeles Aqueduct.

The resort community of Mammoth Lakes (Figure 1), Mono County, California, is at the base of the eastern Sierra Nevada escarpment in the southwestern part of Long Valley caldera, approximately 50 km northwest of Bishop. Mono Lake, contained within Mono Basin, is approximately 30 km north of Mammoth Lakes. The Sierra Nevada rises to over 3,200 m above Mammoth Lakes.

The Long Valley caldera is an elliptical, east-west-trending volcanogenic depression that measures 17 x 32 km (Bailey, 1989; Bailey et al., 1976), with a resurgent dome that is surrounded by an annular moat. Long Valley proper is in the eastern part of the caldera and contains Lake Crowley. Mammoth Mountain rises above the caldera's southwest rim.

The Mono-Inyo Craters volcanic chain (Figure 2) forms a north-trending string of volcanic domes 45 km long, extending southward from the south shore of Mono Lake to the west moat of Long Valley caldera (Bailey, 1989). Mono Craters forms a barren, arcuate ridge 17-km-long between Mono Lake and June Lake. It rises 610 m above the surrounding plains to a maximum elevation of about 2,800 m. The Inyo Craters define an 18-km-long, discontinuous chain of low domes, extending from Wilson Butte, about 10 km south of Mono Craters, to the west moat of Long Valley caldera. The two Inyo Craters are the largest of four aligned phreatic explosion craters at the south end of the Mono-Inyo Craters chain (Mastin and Pollard, 1988; Figure 3). Several other such craters lie within a 1-km^2-area near Inyo Craters (Mastin and Pollard, 1988; Mastin, 1991).

PREVIOUS INVESTIGATIONS

The impact of volcanic eruptions on surface waters and municipal water supplies has been discussed by Hopson (1991) and Blong (1984). Water quality data for the Mammoth Lakes area can be found in DWR (1967, 1973), Abresch and Ghorbonzadeh (1979), and Setmire (1984). The possibility of renewed volcanism near Mammoth Lakes is now well accepted. Volcanic hazard zones have been delineated for the Mammoth Lakes area, and the Los Angeles Department of Water and Power has written a contingency plan for mitigating the impact of volcanic eruptions (Miller, 1989; Miller et al. 1982; LADWP, 1998). For an example of a watershed degraded by microorganisms and the decomposition of organic detritus, the interested reader may want

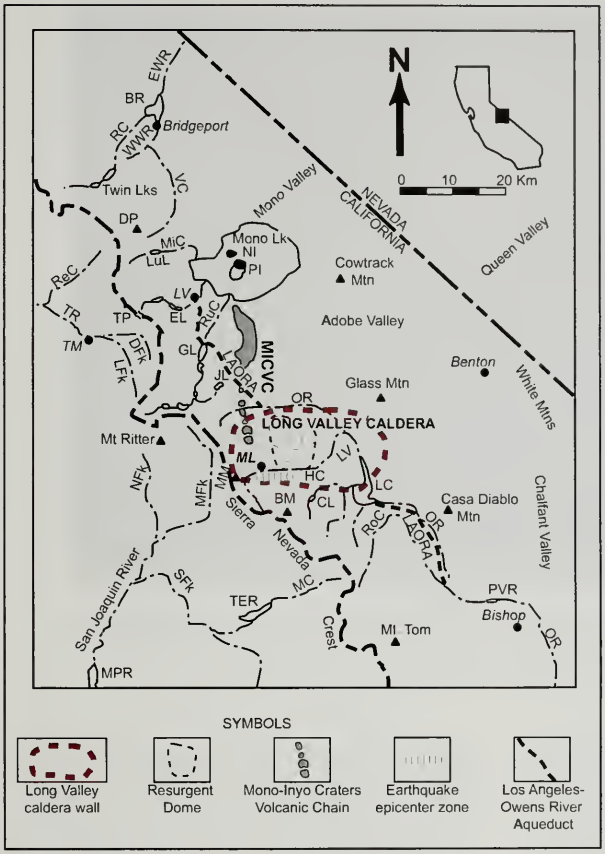

Figure 1. Generalized map of Mammoth Lakes region showing the Owens River Aqueduct, and selected lakes and streams likely to be impacted by volcanic activity. Note that the Owens River Aqueduct flows through the Mono Craters tunnel, denoted by the dashed line, and empties into the Owens River just west of Long Valley. Hatchured line pattern denotes zone of earthquake epicenters that may mark the location of the next eruption near Mammoth lakes. MICVC denotes Mono-Inyo Craters volcanic chain; NI, Negit Island; PI Paoha Island; ML, Mammoth Lakes; EWR, East Walker River; WWR, West Walker River; BR, Bridgeport Reservoir; RC, Robinson Creek; VC, Virginia Creek; DP, Dunderberg Peak; ReC, Return Creek; MiC, Mill Creek; LuL, Lundy Lake; TR, Tuolumne River; DFk, Dana Fork Tuolumne River; LFk, Lyle Fork Tuolumne River; TM, Tuolumne Meadows; TP, Tioga pass; LV, Lee Vining; EL, Ellery Lake; RuC, Rush Creek; GL, Grant Lake; JL, June Lake; MM, Mammoth Mountain; NFk, North Fork San Joaquin River; MFk, Middle Fork San Joaquin River; SFk, South Fork San Joaquin River; OR, Owens River; LAORA, Los Angeles-Owens River Aqueduct; HC, Hot Creek; LV, Long Valley; LC, Lake Crowley; CL, Convict Lake; RoC, Rock Creek; PVR, Pleasant Valley Reservoir; MC; Mono Creek; TER, Thomas Edison Reservoir; and MPR, Mammoth Pool Reservoir.

to consult Larson (1993) and references therein for studies of the biological impact and recovery of Spirit Lake after the May 18, 1980 eruption of Mount St. Helens.

The geology of Long Valley caldera has been studied by Bailey (1989), Bailey et al. (1976), and Hill et al. (1985). Overviews of the tectonics and recent unrest of the Long Valley magmatic system can be found in Hill et al. (1985) and Rundle and Hill (1988). Studies focusing on the age and origin of Mono-Inyo Craters chain and associated deposits are discussed in Sieh and Bursik (1986), Mastin and Pollard (1988), Mastin (1991), and Wood (1977, 1983). The origin, chemical, and physical aspects of the hydrothermal system have been studied by Smith (1976), Sorey et al. (1978), Sorey (1985), and Farrar et al. (1985).

GEOLOGIC HISTORY

The prevolcanic basement in the Mammoth Lakes vicinity consists mainly of Mesozoic granitic rocks of the Sierra Nevada batholith, with pendants of Paleozoic metasedimentary and Mesozoic metavolcanic rocks (Bailey, 1989; Bailey et al., 1976). The Long Valley caldera fill, up to 1,500 m thick, is mostly Bishop Tuff and is overlain by lacustrine deposits and alluvium eroded from the caldera walls. Late Pleistocene glacial till and outwash occur along the Sierra Nevada front (Bailey,

Figure 2. The Mono-Inyo Craters volcanic chain from the summit of Deer Mountain. The prominent domes in the middle distance are South Glass Creek and North Glass Creek domes. Mono Craters proper form the high, barren ridge on the right side of the photograph. View is to the north. Photo by R. Forrest Hopson.

1989). Quaternary normal faults, frontal faults to the Sierra Nevada, transect the area (Bailey, 1989).

Volcanism along the east flank of the central Sierra Nevada has recurred over the past 3.6 million years (Bailey, 1989) with many silicic eruptions occurring in the last 2,000 years (Sieh and Bursik, 1986). Volcanism in this region climaxed at 0.76 Ma, with catastrophic Plinian eruptions and associated collapse that formed the Long Valley caldera (Izett and Obradovich, 1991; Bailey, 1989; Bailey et al., 1976). Explosive eruptions resulted in the partial emptying of the magma chamber as 600 km^3 of rhyolite magma was expelled as hot, pumiceous pyroclastic flows, which formed the Bishop Tuff. The Bishop Tuff buried 1,500 km^2 of the surrounding countryside and accumulated locally to about 200 m.

The Long Valley caldera forms a prominent reentrant in the Sierran escarpment, at the north end of the Owens Valley rift, and possibly formed in a pull-apart basin (Bursik and Sieh, 1989). The Long Valley magma chamber has erupted lava about every 0.2 million years for the past 0.9 million years (Hill et al., 1985). Active hot springs and fumaroles issue from vents in the southern and southeastern parts of the caldera.

The Mono-Inyo Craters volcanic chain constitutes a Quaternary volcanic complex, with rocks ranging in composition from basalt to rhyolite. This complex includes Mammoth Mountain, a cumulovolcano made up of twelve quartz latite and low silica rhyolite domes and flows (Bailey, 1989).

Small to moderate eruptions from the Mono-Inyo Craters chain have had a recurrence interval of about 500 years for the past 2,000-3,000 years. The last eruption along the Mono-Inyo Craters chain occurred about 250 years ago at Pahoa Island, in Mono Lake, suggesting the possibility of renewed volcanism along the Mono-Inyo Craters chain in the next 250 years.

Figure 3. Inyo Craters proper from the summit of Deer Mountain. View is to the southwest. Photograph by R. Forrest Hopson.

POSSIBLE ERUPTION SCENARIOS

The most likely scenarios for future eruptions in the Mammoth Lakes area are small- to moderate-size eruptions (0.1 to 1 km^3 of magma), comparable to those that have occurred along the Inyo volcanic chain during the past 5,000 years (Miller, 1985; Hill et al., 1997). Such eruptions typically involve three eruptive phases: 1) a phreatic phase, 2) explosive magmatic phase, and 3) an effusive phase (Hill et al., 1997). Phreatic eruptions, also called steam-blast eruptions, usually mark the opening of eruptive activity, and occur when rising magma makes contact with groundwater (the phreatic zone) causing the groundwater to flash to steam. An excess of hydrostatic pressure builds to produce a violent explosion of vaporized water and brecciated rock leaving circular craters tens of meters deep, such as the Inyo Craters (Williams and McBirney, 1979; Sheridan and Wohletz, 1983). The explosive magmatic phase is marked by explosive outbursts that can blast volcanic ash and pumice more than 10 km above the volcano, and produce occasional pyroclastic flows and surges. The final stage involves the non-explosive extrusion of viscous magma, typically rhyolite or rhyodacite, which piles up over a volcanic vent to form a lava dome. Such dome-building eruptions have built the domes along the Inyo-Mono Craters chain (Williams and McBirney, 1979; Hill et al., 1997).

Another type of effusive volcanic activity that has occurred in the Mammoth Lakes area has built cinder cones and led to emissions of basaltic lava that commonly have flowed several kilometers from their source (Hill et al., 1997). Such basaltic eruptions produced flows around the base of Mammoth Mountain and in the west moat of Long Valley caldera between 60,000 and 400,000 years ago; they also built Red Cones, located approximately 3 kilometers south-southwest of Mammoth Mountain, about 5,000 years ago (Hill et al., 1997).

Potentially hazardous volcanic events

It is unknown if the current unrest at Long Valley will culminate in an eruption. Earthquakes commonly precede volcanic activity, so if an eruption does occur the most likely site for volcanic activity

would be in the south-central part of the caldera, where the most recent earthquakes have occurred (Miller et al., 1982). Although not as likely, future volcanic activity need not necessarily be restricted to that area, and eruptions could occur in other places that have been volcanically active in the geologically-recent past, such as at Mono and Inyo Craters (Miller et al., 1982).

From the standpoint of impact to surface water resources, much can be learned by perusal of aerial photographs and maps, studying the volcanic history of the Long Valley region, determining the character of eruptions, and mapping the extent of their ejecta (e.g., ash deposits, lava flows). By overlapping volcanic hazard and watershed maps one can identify water resources likely to be threatened by volcanic activity.

The past history of volcanic activity can also shed light on the character of eruptive activity that may be anticipated in the future. For example, Inyo Craters volcanic chain is visible on aerial photographs and maps as a north-trending zone of domes and phreatic eruption craters. Geological field studies demonstrate that the Inyo Craters volcanic chain has erupted airfall ash, pyroclastic flows, and rhyolite lava for the past 5,000 years. Dome and phreatic eruptions along the Inyo Craters volcanic chain 650-550 years ago were the result of emplacement of a shallow silicic dike (Miller, 1985). By analogy to the events of 650-550 years ago, an incipient dike-like intrusion may explain the seismic activity beneath the south moat and provides a model for future eruptive events (Miller, 1985). If the south moat seismic activity were to develop into phreatic and dome eruptions like those along the Inyo Craters volcanic chain 650-550 years ago, the following volcanic events might be expected.

Lava domes and flows

Lava domes and flows have erupted sporadically in the Mammoth Lakes area for over 3 Ma (Metz and Mahood, 1985; Bailey, 1989), therefore it is reasonable to expect the eruption of lava in any future volcanic event. Quaternary lava domes and flows occur in the west half of Long Valley caldera; the youngest domes and flows make up the Mono-Inyo volcanic chain. Basalt flows generally travel farther than rhyolite because basalt is more fluid; rhyolite forms thick, stubby flows because of higher viscosity. If lava domes and flows were erupted from new vents at the loci of the most recent earthquakes in the south moat of the caldera, they could flow into Hot Creek Gorge and dam the creek, but would probably not affect areas much beyond.

Volcanic ash

The impact of volcanic ash on surface water depends on whether the ash is airborne or is a pyroclastic flow or surge, the volume of ash expelled, and prevailing wind velocity and direction (Hopson, 1991). Pyroclastic flows and pyroclastic surges behave similarly, differing only in mode of emplacement (Miller, 1989).

Airfall ash. The eruption of airfall ash typically marks the opening phase of volcanic activity. Clouds of airfall ash are blown by wind away from the vent, and the thickness of ash deposits diminishes away from the source. The central and southern Sierra Nevada was blanketed by ash from eruptions at Mono and Inyo Craters, although the predominate transport direction was to the south. An eruption at Mono Craters approximately 1,200 years ago deposited a layer of ash up to 2 cm thick and roughly 0.2 km^3 in volume (Wood, 1977). Measurable ash – 0.14 cm thick – from the Mono Craters eruption was detected approximately 150 km to the south. An eruption from Inyo Craters, about 750 years ago, deposited a layer of ash up to 3 cm thick and involved about 0.1 km^3 of magma. The Inyo Craters eruption deposited an ash lobe approximately 190 km long to the south, where it measured approximately 0.1 cm in thickness (Wood, 1977).

Pyroclastic flows and surges. Pyroclastic flows and surges result from phreatomagmatic or magmatic eruptions, or from dome eruptions, when pent-up gas is explosively released. Pyroclastic flows and surges will be restricted to stream valleys as density flows. However, very large, fast moving pyroclastic flows and surges can ride over topographic barriers in their paths. Clouds of ash commonly accompany pyroclastic flows and can be deposited mantling topography in areas surrounding the pyroclastic flow.

Pyroclastic flows from new vents along the Inyo Craters chain or the elongate zone of earthquake epicenters in the caldera's south moat could send pyroclastic flows to Mammoth Lakes, the Owens River or even to Lake Crowley. A pyroclastic flow from the outburst at Inyo Craters 750 years ago was emplaced over a 5.5-km^2-area (Wood, 1977). Pyroclastic flows discharged from vents from the north end of the Mono-Inyo Craters volcanic chain could be expected to reach Mono Lake and nearby Rush Creek.

Lahars and floods

Lahars and floods can be anticipated from future eruptions in the Mammoth Lakes area, especially during periods of heavy rainfall and during winter months when there is heavy snowpack (Miller et al., 1982; Hill et al, 1997). Lahars are poorly sorted, high-density slurries of mud and rock mixed with water that originate on the slopes of a volcano (Scott, 1989). Floods resulting from volcanic activity are heavily sediment-laden relative to nonvolcanic floods (Miller, 1989; Scott, 1989).

Lahars can develop when pyroclastic flows and surges follow stream channels and mix with water. They also develop during periods of volcanic quiescence, many decades or centuries after the most recent eruption, by remobilization of loose volcanic debris during heavy rains (Pierson, 1989; Pringle, 1990). Lahars and floods could be generated in the Mammoth lakes area in several ways: 1) pyroclastic flows mixing with streams and/or snow, 2) basal melting of snowpack induced by volcanic or geothermal activity, 3) tephra, loose rocks, glacial sediments and other unconsolidated surficial deposits mixing with snow meltwater, and 4) eruptions beneath a lake (Miller et al., 1982; Major and Newhall, 1989).

Lahars stemming from eruptions at the zone of recent earthquake epicenters in the south moat, or from Inyo Craters, could become channeled in one of the local streams, such as Hot Creek or the Owens River, and flow as far as Lake Crowley. Lahars related to eruptions at Mono Craters would only impact surface water in Mono Basin.

Debris avalanches

Debris avalanches are fast-flowing or sliding chaotic mixtures of wet or dry soil and rock that form when the weakened flanks of a large volcano collapse (Miller, 1989). They can travel many kilometers before coming to rest and can transform to lahars if they flow into a stream channel (Miller, 1989; Scott, 1989). A small debris avalanche from Mammoth Mountain in the late Pleistocene traveled about 6 km (Lipshie, 1976; Miller, 1989). Debris avalanches are a potential hazard from Mammoth Mountain but not from other volcanoes near Mammoth Lakes (Miller, 1989). If a debris avalanche were to occur, it could affect areas within 10 km of its source (Miller, 1989).

ASSESSMENT OF POSSIBLE IMPACT ON WATER RESOURCES

Lava domes and flows

Generally, lava domes and flows have little impact on the quality of surface waters. Fresh lava is insoluble so contamination would be minimal (Hopson, 1991), although water pipelines within the path of an oncoming lava flow would be destroyed (Blong, 1984). However, lava flows can impede stream flow by damming the channel, and create large lakes such as Butte and Snag lakes at Lassen Volcanic National Park in northern California. The greatest danger from domes is pyroclastic flows or debris avalanches, which originate when the steep sides of the growing dome fail under the force of gravity or as pent-up gas is explosively released. The potential impact of pyroclastic flows and debris avalanches on water supplies is discussed below.

Volcanic ash

Volcanic ash, either from pyroclastic flows or airfall deposits, can have several effects on the quality of surface water. One effect would be a temporary increase in turbidity. For example, an increase in turbidity of the public water supply for Anchorage, Alaska, was reported following a 3-6 mm ash fall resulting from the 1953 eruption of Mount Spurr (Whetstone, 1955; Wilcox, 1959). Klein (1981) also reported increased turbidity in surface waters northeast of Mount St. Helens following the May 18, 1980 eruption. Furthermore, a large increase in turbidity may temporarily increase a stream's erosive power, as happened to the Rio Itzicuaro during ash eruptions from Paricutin, Mexico (Foshag and Gonzalez, 1956). Turbidity levels in these waters returned to normal levels after a few days as fine ash particles settled out of suspension.

Acidity of water may increase depending on the volume of ash released. For example, the ash fall from the 1953 Mount Spurr eruption caused pH levels in the public water supply to decrease to 4.5 before returning to normal levels of 7.9 a few hours later in response to natural buffering and dilution (Blong, 1984).

Large volumes of ash could trigger short-term chemical changes from leaching of newly-erupted ash washed by rains or deposited in water (Klein, 1984; Smith et al., 1983). Leaching of newly erupted

ash from Mount St. Helens and Mount Spurr on nearby watersheds was well documented by Klein (1981, 1984), Smith et al. (1983), and Wilcox (1959), who reported short-term chemical changes. The toxicity of the resulting leachate is governed by ash composition and water/ash concentrations. However, the toxicity of the leachate is expected to decrease away from the vent because ash concentrations would decrease in that direction.

Ash layers overlying snowpack may result in a change in ablation rates. Thick layers would slow ablation rates, whereas thin ash layers would increase ablation rates (Davis et al., 1982; Driedger, 1981; Major and Newhall, 1989). Reduced ablation rates lowers melt runoff because ash insulates snow from solar radiation (Davis et al., 1982). Driedger (1981) found that ablation was deterred when ash layers were thicker than 24 mm. At 20 mm ash thickness, ablation rates were similar to snow without ash. Ablation was at a maximum when ash layers were 3 mm, owing to a lower albedo and greater heat absorption (Driedger, 1981).

Pyroclastic flows and surges generally travel down stream canyons for several tens of kilometers before terminating, clogging the actual stream channel along the way. They may melt snow and ice and trigger lahars, debris flows, and floods (Tilling et al., 1990; Major and Newhall, 1989). A significant amount of volcanic ash, especially from pyroclastic flows, would clog filters, pumps, and pipes in water intake and reticulation systems along the Los Angeles-Owens River Aqueduct (Blong, 1984). Ash would also damage turbines for power plants.

Lahars, floods, and debris avalanches

Lahars, floods, and debris avalanches can travel many kilometers from their source, causing changes in water chemistry and physically damaging the stream channel. Secondary effects from erosion and sedimentation may continue for several years after the eruption (Pringle, 1990).

Lahars, floods, and debris avalanches can affect the water supply in at least three ways.

(1) Lahars can block and change the morphology of stream channels and deposit massive volumes of volcanic sediment (Costa and Schuster, 1988; Pierson, 1989). Several streams were blocked by large lahars following the May 18, 1980 eruption of Mount St. Helens, which resulted in the formation of new lakes (Tilling et al., 1990). In Long Valley caldera, the Owens River and Hot Creek might be prone to impoundment by large lahars. Impoundment of the San Joaquin River east of Mammoth Pool reservoir and Owens River Gorge would also be possible if large lahars were to enter them, thus creating potential hazards of lake breakouts, which could in turn cause flooding downstream (Pringle, 1990). Reservoirs in the paths of large lahars, such as Lake Crowley and Mammoth Pool Reservoir, are at risk from flooding. If such a lahar were to enter a reservoir, it might cause the water to overtop the dam resulting in massive flooding downstream and possible damage to the dam (Miller, 1989; Scott, 1989). Therefore, if an eruption were imminent, Lake Crowley and other reservoirs on the Owens and San Joaquin Rivers should be lowered to accommodate lahar deposits and prevent overtopping and possible dam failure.

(2) Public water supply systems can be especially vulnerable to lahars and floods. For example, flooding from the massive lahar from the May 18, 1980 eruption of Mount St. Helens either heavily damaged or destroyed intake systems for several cities as far as 70 km from the volcano, owing to burial by several meters of mud (Schuster, 1981; Blong, 1984). Water intake and reticulation systems along the Los Angeles-Owens River Aqueduct might thus be susceptible to clogging by mud and silt (Blong, 1984).

(3) Changes in water chemistry from the leaching of mud and sediment would be inevitable. Klein (1981) showed that levels of sulfate, total nitrogen, total organic nitrogen, total iron, manganese and aluminum rose drastically in the Toutle and Cowlitz Rivers following the 1980 eruption of Mount St. Helens. Furthermore, very high levels of turbidity might render water virtually untreatable.

DISCUSSION AND CONCLUSIONS

By analogy to the experience of the 1953 Mount Spurr and catastrophic 1980 Mount St. Helens eruptions, potential volcanic events could clearly affect the quality of surface water near Mammoth Lakes. The Mount St. Helens eruption devastated lakes and watersheds near the volcano by the combined effects of massive debris avalanche and pyroclastic flows, lahars, airfall ash, and thousands of downed trees deposited into lakes and streams. In addition, leachate from the blast-pyrolitized timber and foliage dramatically altered the water chemistry. Fortu-

nately, the impact on water quality of creeks, rivers, and lakes following the 1980 eruption of Mount St. Helens was temporary (Tilling et al., 1990; Larson, 1993).

If eruptive activity such as that which occurred along the Mono-Inyo Craters volcanic chain during the past 5,000 years were to recur, the following impacts on nearby surface waters and the Los Angeles-Owens River Aqueduct might be anticipated (Hopson, 1991): (1) Streams might be displaced from their channels by advancing lava flows from growing cones and domes. (2) An increase in acidity and turbidity from volcanic ash, lahars, or debris avalanches would occur. (3) Voluminous pyroclastic flows, lahars, and debris avalanches might impound stream channels as water backs up behind the debris dams, causing changes in stream-channel morphology. Failure of debris dam could result in disastrous floods and heavy sedimentation downstream. (4) Minor changes in the composition of waters may result from leaching of volcanic ash or sediment from lahars or debris avalanches. (5) Less runoff if thick ash layers were to accumulate over snow, insulate it from solar radiation, and reduce snowmelt rates. (6) Water-intake structures along the Los Angeles-Owens River Aqueduct could get clogged and buried by large pyroclastic flows, lahars, and debris avalanches.

ACKNOWLEDGEMENTS

I am grateful to Robert Tilling and Dan Miller (both of the U.S. Geological Survey), Clifford Plumb and Gary Stolarik (both of the Los Angeles Department of Water & Power), and Richard Fisher (UC Santa Barbara) for reading the manuscript and making helpful suggestions. Additional comments and discussions with Steve Lipshie (Los Angeles County Department of Public Works), Clifford Hopson (UC Santa Barbara), and Chief Editor Horacio Ferriz were very helpful. Robert Stull (CSU Los Angeles) critiqued an earlier version of the manuscript.

AUTHOR PROFILE

R. Forrest Hopson is a consulting geologist in Reno. He has a Master of Science Degree in Geology. His professional interests include engineering geology, volcanology, tectonic geomorphology, active tectonics, and geotectonic development of the Mojave Desert. He has had papers published in peer-reviewed journals and field trip volumes, and has given presentations at meetings of the Geological Society of America and American Geophysical Union.

SELECTED REFERENCES

Abresch, R.T. and Ghorbonzadeh, A., 1979, Water quality overview: in Strojan, C.L., and Romney, D.M. (eds.), An environmental overview of the Mono-Long Valley KGRA: Laboratory of Nuclear Medicine and Radiation Biology, UCLA, p. 96-128.

Bailey, R.A., 1989, Geologic map of the Long Valley caldera, Mono-Inyo Craters volcanic chain, and vicinity, eastern California: U.S. Geological Survey Map I-1933, scale 1: 62,500.

Bailey, R.A., Dalrymple, G.B., and Lanphere, M.A., 1976, Volcanism, structure, and geochronology of Long Valley caldera, Mono County, California: Journal of Geophysical Research, v. 81, no. B5, p. 725-744.

Blong, R.J., 1984, Volcanic hazards: Academic Press Australia, North Ryde, N.S.W., 424 p.

Bursick, M. and Sieh, K., 1989, Range front faulting and volcanism in the Mono Basin, eastern California: Journal of Geophysical Research, v. 94, no. B11, p. 15, 587-15,609.

Costa, J.E. and Schuster, R.L., 1988, The formation and failure of natural dams: Geological Society of America Bulletin, v. 100, p. 1054-1068.

DWR (Department of Water Resources), 1967, Investigation of geothermal waters in the Long Valley area, Mono County: California Department of Water Resources, Sacramento, CA, 141 p.

DWR (Department of Water Resources), 1973, Mammoth basin water resources environmental study (final report): California Department of Water Resources, Sacramento, CA, 70 p.

Davis, R.T., Marron, J.K., and Crook, A.G., 1982, Effects of Mt. St. Helens eruptions on snowpack: *in* Mt. St. Helens effects on water resources, Report No. 41: U.S. Department of Agriculture Forest Service, p. 138-148.

Driedger, C.L., 1981, Effect of ash thickness on snow ablation: *in* Lipman, P.W. and Mullineaux, D.R. (eds.), The 1980 eruptions of Mount St. Helens, Washington: U.S. Geological Survey Professional Paper 1250, p. 757-760.

Farrar, C.D., Sorey, M.L., Rojstaczer, S.A., Janik, C.J., Mariner, R.H., Winnet, T.L., and Clark, M.D., 1985, Hydrologic and geochemical monitoring in Long Valley caldera, Mono County, California: U.S. Geological Survey Water Resources Investigation Report 85-4183, 137 p.

Farrar, C.D., Sorey, M.L., Evans, W.C., Howle, J.F., Kerr, B.D., Kennedy, B.M., King, C.-Y., Southon, J.R., 1995, Forest-killing diffuse CO_2 emission at Mammoth Mountain as a sign of magmatic unrest: Nature, v. 376, p. 675-678.

Foshag, W.F. and Gonzalez, J., 1956, Birth and development of Paricutin volcano: U.S. Geological Survey Bulletin 965-D, p. 355-489.

Hill, D.P., Bailey, R.A., and Ryall, A.S., 1985, Active tectonic and magma processes beneath Long Valley caldera, eastern California — an overview: Journal of Geophysical Research, v. 90, no. B13, p. 11,111-11,120.

Hill, D.P., Bailey, R.A., Miller, C.D., Hendley, J.W. II, and Stauffer, P.H., 1997, Future eruptions in California's Long Valley area — What's likely?: U.S. Geological Survey Fact Sheet 073-97.

Hopson, R.F., 1991, Potential impact on water resources from future volcanic eruptions at Long Valley, Mono County, California: Environmental Geology and Water Sciences, v. 18, p. 49-55.

Izett, G.A. and Obradovich, J.D., 1991, Dating of the Matuyama-Brunhes boundary based on $^{40}Ar/^{39}Ar$ ages of the Bishop Tuff and Cerro San Luis rhyolite: Geological Society of America Abstracts with Programs: v. 23, p. A106.

Klein, J.M., 1981, Some effects of the May 18, 1980 eruption of Mount St. Helens on river water quality: in Lipman, P.W., and Mullineaux, D.R. (eds.), The 1980 eruptions of Mount St. Helens, Washington: U.S. Geological Survey Professional Paper 1250, p. 719-731.

Klein, J.M., 1984, Some chemical effects of the Mt. St. Helens eruption on selected streams in the State of Washington: U.S. Geological Survey Circular 850-E, 26 p.

Larson, D., 1993, The recovery of Spirit Lake: American Scientist, v. 81, p. 166-177.

Lipshie, S.R., 1976, Geological guidebook to the Long Valley-Mono Craters region of eastern California: Geological Society of the University of California, Los Angeles, 184 p.

LADWP, (Los Angeles Department of Water and Power) 1998, Contingency plan for Long Valley eruptions: City of Los Angeles, Los Angeles Department of Water and Power, 46 p.

Major, J.J. and Newhall, C.G., 1989, Snow and ice perturbation during historical volcanic eruptions and the formation of lahars and floods: Bulletin of Volcanology, v. 52, p. 1-27.

Mastin, L.G., 1991, The roles of magma and groundwater in the phreatic eruptions at Inyo Craters, Long Valley caldera, California: Bulletin of Volcanology, v. 53, p. 579-596.

Mastin, L.G. and Pollard, D.D., 1988, Surface deformation and shallow dike intrusion processes at Inyo Craters, Long Valley, California: Journal of Geophysical Research, v. 94, no. B11, p. 13,221-13,235.

Metz, J.M. and Mahood, G.A., 1985, Precursors to the Bishop Tuff eruption: Glass Mountain, Long Valley, California: Journal of Geophysical Research, v. 90, p. 11,111-11,126.

Miller, C.D., 1985, Holocene eruptions along the Inyo volcanic chain, California: Implications for possible eruptions in Long Valley caldera: Geology, v. 13, p. 14-17.

Miller, C.D., 1989, Potential hazards from future volcanic eruptions in California: U.S. Geological Survey Bulletin 1847, 17 p.

Miller, C.D., Mullineaux, D.R., Crandell, D.R., and Bailey, R.A., 1982, Potential hazards from future eruptions in the Long Valley-Mono Lake area, east-central California and southwest Nevada—a preliminary assessment: U.S. Geological Survey Circular 877, 10 p.

Pierson, T.C., 1989, Hazardous hydrologic consequences of volcanic eruptions and goals for mitigative action: An overview: *in* Starosolszky, O., and Melder, O.M., (eds.), Hydrology of disasters: James & James, London, p. 220-236.

Pringle, P., 1990, Mount St. Helens—a ten-year summary: Washington Geologic Newsletter, v. 18, p. 2-10.

Rundle, J.B. and Whitcomb, J.H., 1984, A model for deformation in Long Valley, California: Journal of Geophysical Research, v. 89, no. B11, p. 9,371-9,380.

Schuster, R.L., 1981, Effects of the eruptions on civil works and operations in the Pacific Northwest: in Lipman, P.W., and Mullineaux, D.R., (eds.), The 1980 eruptions of Mount St. Helens, Washington: U.S. Geological Survey Professional Paper 1250, p. 701-718.

Scott, W.E., 1989, Volcanic and related hazards: *in* Tilling, R.I., (ed.), Volcanic hazards: American Geophysical Union, p. 9-23.

Setmire, J.G., 1984, Water quality appraisal of Mammoth Creek and Hot Creek, Mono County, California: U.S. Geological Survey Water Investigation Report 84-4060, 50 p.

Sheridan, M.F. and Wohletz, K.H., 1983, Hydrovolcanism: basic considerations and review: in Sheridan, M.F. and Barberi, F., (eds.), Explosive volcanism: Journal of Volcanology and Geothermal Research, v. 17, p. 1-17.

Sieh, K. and Bursik, M., 1986, Most recent eruption of the Mono Craters, eastern central California: Journal of Geophysical Research, v. 91, no. B12, p. 12,539-12,571.

Smith, G.I., 1976, Origin of lithium deposits and other components in the Searles Lake evaporites, California: *in* Vine, J.D., (ed.), Lithium resources and requirements by the year 2000: U.S. Geological Survey Professional Paper 1005, p. 785-791.

Smith, D.B., Zielinski, R.A., Taylor, H.E., Sawyer, M.B., 1983, Leaching characteristics of ash from the May 18, 1980 eruption of Mt. St. Helens volcano, Washington: Bulletin of Volcanology, v. 46-2, p. 103-124.

Sorey, M.L., 1985, Evolution and present state of the hydrothermal system in Long Valley caldera, California: Journal of Geophysical Research, v. 90, p. 11,219-11,228.

Sorey, M.L., Lewis, R.E., and Olmsted, F.H., 1978, The hydrothermal system in Long Valley caldera, California: U.S. Geological Survey Professional Paper 1044-A, 60 p.

Tilling, R.I., Topinka, L., and Swanson, D.A., 1990, Eruptions of Mt. St. Helens: past, present, future: U.S. Geological Survey General Interest Publications, 57 p.

Whetstone, G.W., 1955, The effects of volcanic ash from Mt. Spurr on the chemical character of surface waters near Anchorage, Alaska: Geological Society of America Bulletin, v. 66, p. 1709.

Wilcox, R.E., 1959, Some effects of recent volcanic ash falls with especial reference to Alaska: U.S. Geological Survey Bulletin 1028-N, p. 409-476.

Williams, H. and McBirney, A.R., 1979, Volcanology: Freeman, Cooper and Company, (San Franciso, California), 397 p.

Wood, S.H., 1977, Distribution, correlation, and radiocarbon dating of late Holocene tephra, Mono and Inyo Craters, eastern Cailfornia: Geological Society of America Bulletin, v. 88, p. 89-95.

Wood, S.H., 1983, Chronology of Late Pleistocene and Holocene volcanics, Long Valley and Mono Basin geothermal areas, eastern California: U.S. Geological Survey Open-File Report 83-747, 76 p.


ASSOCIATION OF ENGINEERING
GEOLOGISTS
AEG

SUBJECT INDEX